MACQUARIE UNIVERSITY

HIGHER DEGREE THESIS
AUTHOR'S CONSENT
DOCTORATE DEGREE

This is to certify that I, ALPESH RAMANLAL PATEL being a candidate for the degree of Doctor of PHILOSOPHY am aware of the policy of the University relating to the retention and use of higher degree theses as contained in the University's Higher Degree Research Thesis Preparation, Submission and Examination Policy.

In the light of this policy, I agree to allow a copy of my thesis to be deposited in the University Library for consultation, loan and photocopying forthwith.

Fei Liu

Signature of Candidate
Date: 21/10/2013

Full Name & Signature of Witness
Date:

MACQUARIE University
SYDNEY·AUSTRALIA

The Academic Senate on 27 March 2014 resolved that Mr Alpesh Ramanlal Patel satisfied the requirements for admission to the degree of PhD.

This thesis represents a major part of the prescribed program of study

ARC THESIS
QP
606
.P76
P38
2014

USE OF THESES

This volume is the property of Macquarie University, but the literary rights of the author must be respected. Passages must not be copied or closely paraphrased without the written consent of the author. If the reader obtains any assistance from this volume, he/she must give proper credit in his/her own work.

This thesis by A. R Patel has been used by the following persons, whose signatures attest their acceptance of the above restrictions.

NAME	DATE	NAME	DATE

Synthesis and Conformational Investigations of Bioactive Natural Products and Fluorinated Analogues

A thesis by publications submitted in partial fulfillment of the requirements for the degree of

Doctor of Philosophy

by

Alpesh Ramanlal Patel

M.Tech. (Pharm.)

Department of Chemistry and Biomolecular Sciences

Macquarie University

October 2013

Table of Contents

Abstract..... vi

Declaration..... vii

Acknowledgements..... viii

Publications..... x

List of Abbreviations and symbols..... xi

List of Figures..... xv

List of Schemes..... xviii

List of Tables..... xix

Chapter 1 Introduction 1

1.1 Protein Kinases in Drug Discovery..... 2

1.1.1 Introduction to Protein Kinases..... 2

1.1.2 AGC Protein Kinase Family and Therapeutic Role..... 3

1.1.3 The PKC Isozymes: Structure, Regulation and Implications..... 4

1.1.4 Kinase Drug Discovery: Gleevec with Conformational Specificity..... 7

1.1.5 Current PKC Drug Developments and Challenges..... 9

1.2 Balanol as an ATP mimic in PKC Inhibition..... 12

1.2.1 Discovery and Structure Elucidation of Balanol..... 12

1.2.2 Synthetic Protocols for Balanol..... 14

1.2.2.1 Total Syntheses of Balanol..... 14

1.2.2.2 Formal Syntheses of Balanol..... 22

1.2.3 Biological Activity of Balanol..... 23

1.2.4 Balanoids – Chemical Diversity and SARs..... 24

1.2.4.1 Modifications of the Benzophenone Fragment..... 24

1.2.4.2 Modifications of the Perhydroazepane Moiety..... 27

1.2.4.3 Modifications of the Ester/Amide Linkages..... 28

1.3 Fluorine: A Tool for Conformation Coupled Chemical Diversity..... 29

1.3.1 Stereoelectronic Effects of Fluorine..... 30

1.3.2 C–F bond Formation Methodology..... 34

1.3.3 Key Examples of Fluorination in Biological Activity Tuning..... 37

1.4 Project Outline..... 41
1.5 References..... 43
Chapter 2 Diastereospecific Fluorination of Substituted Azepanes..... 64
2.1 Relevance of Study..... 65
2.2 Results and Discussion..... 66
2.3 Cross Reference of Compounds in Chapter 2..... 76
2.4 Experimental..... 78
2.4.1 Structure Elucidation of the Key Intermediates..... 78
2.4.1.1 (3*R*,4*R*,5*S*)–3–Azido–4–benzyloxyazepane–5–ol (**2.9b**)..... 78
2.4.1.2 (3*R*,4*R*,6*S*)–3–Azido–4–benzyloxyazepane–6–ol (**2.9c**)..... 82
2.4.1.3 (3*R*,4*R*,6*R*)–3–Azido–4–benzyloxyazepane–6–ol (**2.9d**)..... 85
2.4.1.4 (3*R*,4*R*,5*S*)–3–Azido–4–benzyloxy–5–fluoroazepane (**2.11b**)..... 89
2.4.1.5 (3*R*,4*R*,6*S*)–3–Azido–4–benzyloxy–6–fluoroazepane (**2.11c**)..... 93
2.4.1.6 (3*R*,4*R*,6*R*)–3–Azido–4–benzyloxy–6–fluoroazepane (**2.11d**)..... 97
Chapter 3 Conformational Regulation of Substituted Azepanes through Selective Monofluorination..... 101
3.1 Relevance of Study..... 102
3.2 Results and Discussion..... 103
3.3 Cross Reference of Compounds in Chapter 3..... 110
3.4 Experimental..... 111
3.4.1 General Methods..... 111
3.4.2 Synthetic Procedures and Characterization of Intermediates..... 112
3.4.2.1 (3*S*,4*R*)–4–benzyloxy–3–hydroxyazepane–1–carboxylic acid–*tert*–butyl ester (**3.2**)..... 112
3.4.2.2 (3*R*,4*R*)–3–azido–4–benzyloxyazepane–1–carboxylic acid–*tert*–butyl ester (**3.3**)..... 113
3.4.2.3 (3*R*,4*R*)–3–Azido–4–benzyloxyazepane (**3.1**)..... 114
3.4.3 Structure Elucidation of the Azepane **3.3** ($(CD_3)_2CO$)..... 115
3.4.4 Structure Elucidation of the Azepane **3.1**..... 119

Chapter 4 Conformational Regulation of Substituted Azepanes through Fluorination 122
4.1 Relevance of Study 123
4.2 Results and Discussion 124
4.3 Cross Reference of Compounds in Chapter 4 136
4.4 Experimental 138
4.4.1 Structure Elucidation of the Azepane **4.1** 138
4.4.2 Structure Elucidation of the Azepane **4.2** 142
4.4.3 Structure Elucidation of the Azepane **4.3** 146
Chapter 5 Cascade Neighbouring Group Effect: Potentially Fluoronium–assisted Aziridinium Opening in Solution 150
5.1 Introduction 151
5.2 Results and Discussion 153
5.2.1 Synthesis of Fluorohydroxyazepanes **5.4** and **4.10** 153
5.2.2 Structure Elucidation of **5.4** and **4.10** 155
5.2.2.1 Structure Elucidation of **4.10** 155
5.2.2.2 Structure Elucidation of **5.5** 157
5.2.3 Synthesis of Difluoroazepanes **5.6** and **5.12** 159
5.2.3.1 Structure Elucidation of **5.8** 159
5.2.3.2 Structure Elucidation of **5.14** 160
5.2.4 Effect of the *N*–tosyl Protecting Group on Fluorination Outcomes 161
5.2.5 Structure Elucidation of *N*–tosyl Fluoroazepanes 163
5.2.5.1 Structure Elucidation of **5.19** 163
5.2.5.2 Structure Elucidation of **5.23** 164
5.2.5.3 Structure Elucidation of **5.24** 165
5.2.6 A Proposed Fluoronium–Aziridinium Neighbouring Group Effect 166
5.2.7 Preliminary Computational Studies on Potential Fluoronium–Aziridinium Intermediates 173
5.3 Experimental 175
5.3.1 General Methods 175

5.3.2 Synthetic Procedures and Characterization of Intermediates..... 175
5.3.3 Structure Elucidation of Key Azepanes..... 189
5.4 Conclusions..... 217
5.5 References..... 218
Chapter 6 Synthesis and Activity of Fluorinated Balanol Analogues 220
6.1 Introduction..... 221
6.2 Results and Discussion..... 222
6.2.1 Total Synthesis of (−)–Balanol (**1.1**)..... 222
6.2.1.1 Synthesis of the Benzophenone Fragment (**1.28**)..... 222
6.2.1.2 Synthesis and Coupling of the Azepane Core (**1.10**) with the Benzophenone (**1.28**)..... 224
6.2.2 Synthesis of Fluorinated Balanol Analogues 225
6.2.3 Binding Studies of Compounds **6.27**–**6.32** against Protein Kinases 226
6.3 Experimental..... 232
6.3.1 General Methods..... 232
6.3.2 Synthetic Procedures and Characterization of Intermediates..... 233
6.4 Conclusions..... 254
6.5 References..... 255
Chapter 7 Conclusions and Future Directions 257
Appendix A 262
Appendix B 346
Appendix C 388
Appendix D 480
Appendix E 643

Abstract

(−)–Balanol, a fungal metabolite from *Verticillium balanoides*, is a potent protein kinase C (PKC) inhibitor and has potential as an antitumor agent. However, it competitively inhibits other AGC protein kinases and lacks PKC isozyme specificity. The success from the first kinase drug, Gleevec, suggests that conformationally biased small molecules can lead to selective inhibition of tyrosine protein kinases. Fluorination has recently been utilized as a tool to conformationally tune the shape of molecules. The aim was to synthesize conformationally biased fluorinated balanol analogues and examine their PKA/PKC affinity and selectivity profiles (Figure 1). The structure activity relationship from this study may help understand conformational control in molecular recognition in general.

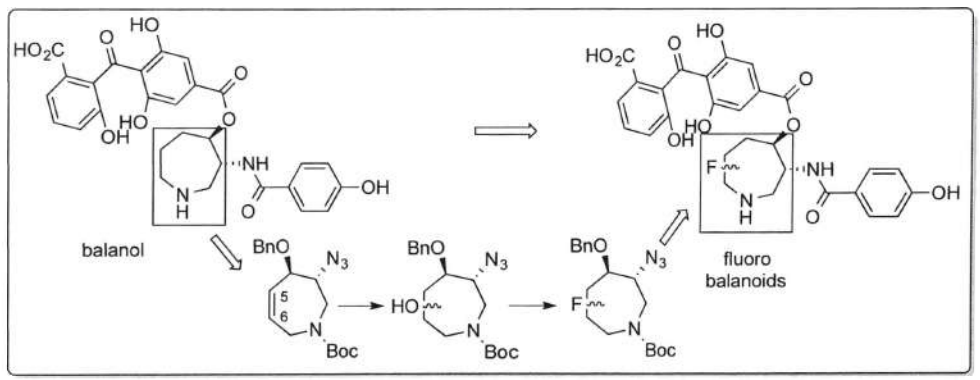


Figure 1. Design of fluorinated balanol analogues

The synthesis of mono–, di– and trifluoroazepanes was accomplished with unusual stereochemical outcomes due to neighbouring group participation. The conformational preferences of the mono–, di– and trifluoro azepanes were investigated using computational methods and *J* based analysis after detailed 2D NMR structure elucidations. The parent (−)–balanol and fluorinated balanol analogues were synthesized, and the analogues were subjected to binding affinity measurements with selected PKC isozymes and PKA.

Declaration

I certify that the work in this thesis entitled "Synthesis and Conformational Investigations of Bioactive Natural Products and Fluorinated Analogues" has not previously been submitted for a degree nor has it been submitted as part of requirements for a degree to any other university or institution other than Macquarie University. I also certify that the thesis is an original piece of research and it has been written by me. Any help and assistance that I have received in my research work and the preparation of the thesis itself have been appropriately acknowledged. In addition, I certify that all information sources and literature used are indicated in the thesis.

Alpesh Ramanlal Patel

(SN: 41948270)

20/10/2013

Acknowledgements

I would like to acknowledge the following people, without whom this thesis would not have been submitted within the stipulated deadline.

My supervisor Dr. Fei Liu for always providing guidance, feedback, encouragement and a good working environment. For developing my skills in communication, organization and perseverance.

Dr. Luke Hunter (UNSW) for his expert advice, guidance and encouragement especially training on NMR simulations and conformational analysis.

Prof. Peter Karuso who was always available to offer me advice and assistance, particularly regarding the NMR experiments presented herein.

Past and present members of the Liu and Karuso group: In particular Christopher Anstiss and Mark Richardson for helping me in my organic chemistry infancy. Benjamin Stephens for helping me start up in the lab and training me on NMR. Michael Gotsbacher for training me on HPLC and providing the intermediates for biotin-probe synthesis. Wendy Loa-Kum for training me on LCMS and always available for emergency help. Dr. James Webb for his suggestions and friendly conversations regarding chemistry. Herold Spedding for his synthetic and purification assistance. All the summer scholarship and French scholarship students for lively conversations and assistance. Rajesh, Wendy, Soumit, Michael and Girish for discussion on my project and the enjoyable social moments that we shared in lunch time

The researchers at UNSW: Dr. Graham Ball, Dr. Samuel Kutty, Raju, Xiang-Guo Hu and Dr. Mohan Bhadbhade for their availability and technical support.

The academics at their group members at CBMS: in particular Dr Andrew Try, A/Prof Joanne Jamie and Dr Christopher McRae for his ongoing and efficient IT and technical support. The

support staff at CBMS: in particular, Maria Hyland, Michelle Kang, Catherine Wong and Jenny Minard for their continuous assistance.

The academics back in India who shaped my carrier and life, particularly Mr. Manibhai Patel, Dr. Anita Lalwani and Prof. A. K. Chakraborti.

The laboratory technical staff, Keith, Tony, Mark, Hong and Thulasy for their training on various instruments and the provision of emergency chemicals.

HDR Macquarie University for providing information and support throughout the program.

My parents Ramanbhai and Leelaben for their blessings, care and encouragement. My sisters Nayana and Kalpana and their families for continual physical and emotional support. The family here in Sydney Kalpana, Falgun, Utkal, Risidhdhi, Mitesh and Vineshwari (including loving kids Joel and Nyasa) for providing love, care and support which made me never feel homesick. The friends at Jethalal volleyball club for refilling me with joy and energy to continue work.

There is simply no way to express gratitude to my loving and caring wife **Mittal**, for kindly accepting this three way relationship with my thesis and I. For listening to all my frustrations and excitements with patience and more importantly for always keeping my back free of everyday issues.

Finally, I am grateful to the Lord Swaminarayana for all his blessings.

Publications

1. **Patel, A. R.**; Liu, F. Diastereospecific Fluorination of Substituted Azepanes. *Tetrahedron* **2013**, *69*, 744–752.

The candidate ARP synthesized all the compounds for this study, acquired and analyzed all data and wrote the article under the guidance of FL.

2. **Patel, A. R.**; Ball, G.; Hunter, L.; Liu, F. Conformational Regulation of Substituted Azepanes through Selective Monofluorination. *Org. Biomol. Chem.* **2013**, *11*, 3781–3785.

The candidate ARP synthesized all the compounds for this study and acquired all the NMR data. The computational studies were accomplished by FL and GB. The NMR simulations and weighted fits were calculated by LH. The data analysis and manuscript writing was contributed by all the authors.

3. **Patel, A. R.**; Hunter, L.; Bhadbhade, M. M.; Liu, F. Conformational Regulation of Substituted Azepanes through Fluorination. *Eur. J. Org. Chem.* (accepted manuscript on 31st January 2014).

The candidate ARP synthesized all the compounds for this study and acquired all the NMR data. The computational studies were contributed by FL. The NMR simulations and weighted fits were calculated by ARP under the guidance of LH. MMB contributed the X–ray crystallography data. The data analysis and manuscript writing was contributed by ARP, FL and LH.

List of Abbreviations and Symbols

°	degrees
$[\alpha]^{20}_{D}$	specific rotation at 20 °C and wavelength of sodium D line
Å	angstrom
Ac	acetyl
AcO	acetate
aq.	Aqueous
AKT/PKB	protein kinase B
Ar	aryl
ATP	adenosine triphosphate
9–BBN	9–borabicyclo[3.3.1]nonane
Bn	benzyl
Boc	N–*tert*-Butoxycarbonyl
br	broard
Bu	butyl
BzO	benzoate
CBz	carboxybenzyl
COSY	correlation spectroscopy
CAM kinase	calcium/calmodulin–dependent kinase
CK1	casein kinase 1
CDK	cyclin–dependent kinase
cAMP	cyclic adenosine monophosphate
°C	degrees celsius
δ	NMR chemical shift in parts per million
d	doublet
DMPK	Myotonic dystrophy protein kinase
DAG	1,2–diacylglycerol
DABCO	1,4-diazabicyclo[2.2.2]octane
DCE	dichloroethane
DCM	dichloromethane

DFT	density functional theory
DMAP	*N*,*N*-dimethylaminopyridine
DMF	*N*,*N*-dimethylformamide
DMSO	dimethylsulfoxide
DAST	diethylaminosulfur trifluoride
Deoxofluor®	diisopropylaminosulfur trifluoride
dppb	1,4-diphenylphosphino butane
dr	diastereomeric ratio
ER	endoplasmic reticulum
ee	enantiomeric excess
ESI-MS	electrospray ionisation-mass spectroscopy
Et	ethyl
g	gram
GABA	γ–aminobutyric acid
GRK	G–protein coupled receptor kinase
GSK3	glycogen synthase kinases
h	hour
HSQC	heteronuclear single bond correlation spectroscopy
HMBC	heteronuclear multiple bond correlation spectroscopy
Hz	hertz
i-Pr	isopropyl
J	coupling constant
K_d	binding constant
LAH	lithium aluminium hydride
Me	methyl
MAST3	microtubule–associated serine–threonine kinase 3
MRCK	myotonic dystrophy related CDC42–binding kinase
MSK	mitogen– and stress–activated protein kinase
MAPK	mitogen–activated protein kinase
mg	milligram
min	minute

mmol	millimol
MMPP	magnesium monoperoxy phthalate hexahydrate
μ	micro
MS3Å	molecular sieve 3 angstrom
MS4Å	molecular sieve 4 angstrom
Nu	nucleophile
NOESY	nuclear overhauser effect spectroscopy
n	nano
PLC	phospholipase C
PIP2	phosphoinositol–4,5–biphosphate
PCC	pyridinium chlorochromate
Ph	phenyl
ppm	parts per million
PKA or PKAC	protein kinase A
PKC	protein kinase C
PKG or CGK1α	protein kinase G
PKN	protein kinase N
q	quartet
r	correlation coefficient
ROESY	rotating frame nuclear overhauser effect spectroscopy
RACK	receptor for activated C–kinase
R	any functional group
r.t.	room temperature
ROCK	Rho–associated kinase
RSK	ribosomal s6 kinase
S6K	analogous to RSK
s	singlet
SAR	structure activity relationship
Ser	serine
STE kinase	sterile kinase
SGK	serum/glucocorticoid regulated kinase

t	triplet
t-Bu	tertiary butyl
TEMPO	(2,2,6,6–tetramethyl–piperidine–1–yl)oxyl
TBDMS or TBS	tertiary butyl dimethyl silyl
THF	tetrahydrofuran
TP	triphenylphosphine
Ts	toluene sulfonyl
TKL	tyrosine kinase like group
TK	tyrosine kinase
TFA	trifluoroacetic acid
USFDA	United States food and drug administration

List of Figures

Figure 1.1: Protein kinase super family: A dendrogram representation..... 2
Figure 1.2: Roles of AGC kinases in various diseases..... 4
Figure 1.3: Structure of PKC isozymes..... 5
Figure 1.4: Structural mechanism of the Imatinib for Abl inhibition 8
Figure 1.5: Structure of balanol (**1.1**) and ophiocordin (**1.2**)..... 12
Figure 1.6: X–ray crystal structure of *p*–bromobenzoyl balanol derivative..... 13
Figure 1.7: Balanol: retrosynthetic analysis..... 14
Figure 1.8: Balanol and ATP superposition: ATP (black stick) and balanol (ball and stick model)..... 24
Figure 1.9: Top selling fluorinated drugs 30
Figure 1.10: Conformational effects of fluorine: (A) dipole–dipole interactions, (B) charge–dipole interactions, (C) hyperconjugation effects 32
Figure 1.11: X–ray crystal structures of fluoroalkanes diastereomers **1.85** and **1.86**..... 33
Figure 1.12: Most commonly used commercially available fluorinating reagents 34
Figure 1.13: Chiral *N*–fluorosultams 36
Figure 1.14: Recent deoxyfluorinating reagents..... 37
Figure 1.15: HIV protease inhibitor Indinavir (**1.96**) and fluorinated analogues **1.97** and **1.98**..... 38
Figure 1.16: (A) Neurotransmitter GABA (**1.99**) and fluorinated analogues (*R*)–**1.100** and (*S*)–**1.100**; (B) Hunter's GABA analogues 38
Figure 1.17: Effects of monofluorination on proline residue strengthening collagen 40
Figure 1.18: Conformational tuning of proline by stereospecific monofluorination 40
Figure 2.1: Relevance of monofluoro azepane synthesis 65
Figure 2.2: Neighbouring group participation 66
Figure 2.3: ^{1}H–^{13}C HSQC 2D NMR correlations of the azepane ring in **2.9b** 78
Figure 2.4: ^{1}H–^{13}C HMBC 2D NMR correlations of the azepane ring in **2.9b** 79
Figure 2.5: ^{1}H–^{1}H COSY 2D NMR correlations of the azepane ring in **2.9b**..... 80
Figure 2.6: ^{1}H–^{1}H NOESY 2D NMR correlations of the azepane ring in **2.9b** 81
Figure 2.7: ^{1}H–^{13}C HSQC 2D NMR correlations of the azepane ring in **2.9c** 82
Figure 2.8: ^{1}H–^{13}C HMBC 2D NMR correlations of the azepane ring in **2.9c** 83
Figure 2.9: ^{1}H–^{1}H COSY 2D NMR correlations of the azepane ring in **2.9c** 84
Figure 2.10: ^{1}H–^{13}C HSQC 2D NMR correlations of the azepane ring in **2.9d**..... 85
Figure 2.11: ^{1}H–^{13}C HMBC 2D NMR correlations of the azepane ring in **2.9d** 86
Figure 2.12: ^{1}H–^{1}H COSY 2D NMR correlations of the azepane ring in **2.9d** 87
Figure 2.13: ^{1}H–^{1}H NOESY 2D NMR correlations comparison in **2.9c** and **2.9d** 88
Figure 2.14: ^{1}H–^{13}C HSQC 2D NMR correlations of the azepane ring in **2.11b** 89
Figure 2.15: ^{1}H–^{13}C HMBC 2D NMR correlations of the azepane ring in **2.11b** 90
Figure 2.16: ^{1}H–^{1}H COSY 2D NMR correlations of the azepane ring in **2.11b** 91

Figure 2.17: ^{1}H–^{1}H NOESY 2D NMR correlations of the azepane ring in **2.11b** 92
Figure 2.18: ^{1}H–^{13}C HSQC 2D NMR correlations of the azepane ring in **2.11c** 93
Figure 2.19: ^{1}H–^{13}C HMBC 2D NMR correlations of the azepane ring in **2.11c** 94
Figure 2.20: ^{1}H–^{1}H COSY 2D NMR correlations of the azepane ring in **2.11c** 95
Figure 2.21: ^{1}H–^{1}H NOESY 2D NMR correlations of the azepane ring in **2.11c** 96
Figure 2.22: ^{1}H–^{13}C HSQC 2D NMR correlations of the azepane ring in **2.11d** 97
Figure 2.23: ^{1}H–^{13}C HMBC 2D NMR correlations of the azepane ring in **2.11d** 98
Figure 2.24: ^{1}H–^{1}H COSY 2D NMR correlations of the azepane ring in **2.11d** 99
Figure 2.25: ^{1}H–^{1}H NOESY 2D NMR correlations of the azepane ring in **2.11d** 100
Figure 3.1: Conformational preferences in contributing geometries of **2.11c** and **2.11d**. 104
Figure 3.2: ^{1}H–^{13}C HSQC 2D NMR correlations of the azepane ring in **3.3**..... 115
Figure 3.3: ^{1}H–^{13}C HMBC 2D NMR correlations of the azepane ring in **3.3**..... 116
Figure 3.4: ^{1}H–^{1}H COSY 2D NMR correlations of the azepane ring in **3.3**..... 117
Figure 3.5: ^{1}H–^{1}H NOESY 2D NMR correlations of the azepane ring in **3.3**.....118
Figure 3.6: ^{1}H–^{13}C HSQC 2D NMR correlations of the azepane ring in **3.1**..... 119
Figure 3.7: ^{1}H–^{13}C HMBC 2D NMR correlations of the azepane ring in **3.1**..... 120
Figure 3.8: ^{1}H–^{1}H COSY 2D NMR correlations of the azepane ring in **3.1**..... 121
Figure 4.1: Schematic representation of the conformations analysis results 125
Figure 4.2: ^{1}H–^{13}C HSQC 2D NMR correlations of the azepane ring in **4.1**..... 138
Figure 4.3: ^{1}H–^{13}C HMBC 2D NMR correlations of the azepane ring in **4.1**..... 139
Figure 4.4: ^{1}H–^{1}H COSY 2D NMR correlations of the azepane ring in **4.1**..... 140
Figure 4.5: ^{1}H–^{1}H NOESY 2D NMR correlations of the azepane ring in **4.1**.....141
Figure 4.6: ^{1}H–^{13}C HSQC 2D NMR correlations of the azepane ring in **4.2**..... 142
Figure 4.7: ^{1}H–^{13}C HMBC 2D NMR correlations of the azepane ring in **4.2**..... 143
Figure 4.8: ^{1}H–^{1}H COSY 2D NMR correlations of the azepane ring in **4.2**..... 144
Figure 4.9: ^{1}H–^{1}H NOESY 2D NMR correlations of the azepane ring in **4.2**.....145
Figure 4.10: ^{1}H–^{13}C HSQC 2D NMR correlations of the azepane ring in **4.3**..... 146
Figure 4.11: ^{1}H–^{13}C HMBC 2D NMR correlations of the azepane ring in **4.3**..... 147
Figure 4.12: ^{1}H–^{1}H COSY 2D NMR correlations of the azepane ring in **4.3**..... 148
Figure 4.13: ^{1}H–^{1}H NOESY 2D NMR correlations of the azepane ring in **4.3**.....149
Figure 5.1: Olah's computational studies on fluoronium and chloronium ions 152
Figure 5.2: X–ray crystal structure of **4.11**.....156
Figure 5.3: Proposed fluoronium structure for the fluorination of **5.4**..... 173
Figure 5.4: ^{1}H–^{13}C HSQC 2D NMR correlations of the azepane ring in **4.10**..... 189
Figure 5.5: ^{1}H–^{13}C HMBC 2D NMR correlations of the azepane ring in **4.10**..... 190
Figure 5.6: ^{1}H–^{1}H COSY 2D NMR correlations of the azepane ring in **4.10**..... 191
Figure 5.7: ^{1}H–^{1}H NOESY correlations of the azepane ring in **4.10**.....192
Figure 5.8: ^{1}H–^{13}C HSQC 2D NMR correlations of the azepane ring in **5.5**..... 193
Figure 5.9: ^{1}H–^{13}C HMBC 2D NMR correlations of the azepane ring in **5.5**..... 194
Figure 5.10: ^{1}H–^{1}H COSY 2D NMR correlations of the azepane ring in **5.5**..... 195

Figure 5.11: ^{1}H–^{1}H NOESY correlations of the azepane ring in **5.5**.....196
Figure 5.12: ^{1}H–^{13}C HSQC 2D NMR correlations of the azepane ring in **5.8**..... 197
Figure 5.13: ^{1}H–^{13}C HMBC 2D NMR correlations of the azepane ring in **5.8**..... 198
Figure 5.14: ^{1}H–^{1}H COSY 2D NMR correlations of the azepane ring in **5.8**..... 199
Figure 5.15: ^{1}H–^{1}H NOESY correlations of the azepane ring in **5.8**.....200
Figure 5.16: ^{1}H–^{13}C HSQC 2D NMR correlations of the azepane ring in **5.14**..... 201
Figure 5.17: ^{1}H–^{13}C HMBC 2D NMR correlations of the azepane ring in **5.14**..... 202
Figure 5.18: ^{1}H–^{1}H COSY 2D NMR correlations of the azepane ring in **5.14**..... 203
Figure 5.19: ^{1}H–^{1}H NOESY correlations of the azepane ring in **5.14**.....204
Figure 5.20: ^{1}H–^{13}C HSQC 2D NMR correlations of the azepane ring in **5.19**..... 205
Figure 5.21: ^{1}H–^{13}C HMBC 2D NMR correlations of the azepane ring in **5.19**.....206
Figure 5.22: ^{1}H–^{1}H COSY 2D NMR correlations of the azepane ring in **5.19**..... 207
Figure 5.23: ^{1}H–^{1}H NOESY correlations of the azepane ring in **5.19**.....208
Figure 5.24: ^{1}H–^{13}C HSQC 2D NMR correlations of the azepane ring in **5.23**..... 209
Figure 5.25: ^{1}H–^{13}C HMBC 2D NMR correlations of the azepane ring in **5.23**..... 210
Figure 5.26: ^{1}H–^{1}H COSY 2D NMR correlations of the azepane ring in **5.23**..... 211
Figure 5.27: ^{1}H–^{1}H NOESY correlations of the azepane ring in **5.23**.....212
Figure 5.28: ^{1}H–^{13}C HSQC 2D NMR correlations of the azepane ring in **5.24**..... 213
Figure 5.29: ^{1}H–^{13}C HMBC 2D NMR correlations of the azepane ring in **5.24**..... 214
Figure 5.30: ^{1}H–^{1}H COSY 2D NMR correlations of the azepane ring in **5.24**..... 215
Figure 5.31: ^{1}H–^{1}H NOESY correlations of the azepane ring in **5.24**.....216
Figure 6.1: Azepanes for fluorinated balanol analogues synthesis 225
Figure 6.2: KINOME*scan*™ assay schematic representation 227
Figure 6.3: Comparison of major conformer of azepane **2.11b** (corresponding to **6.29**) with balanol active form conformation..... 229

List of Schemes

Scheme 1.1: Hughes' synthesis of azepane core **1.10**..... 15
Scheme 1.2: Lampe and Hughes' synthesis of balanol (**1.1**)..... 16
Scheme 1.3: Nicolaou's synthesis of azepane core **1.25**..... 17
Scheme 1.4: Nicolaou's synthesis of balanol (**1.1**)..... 17
Scheme 1.5: Vicker's synthesis of azepane core **1.25**..... 18
Scheme 1.6: Vicker's synthesis of balanol (**1.1**)..... 19
Scheme 1.7: Tanner's synthesis of azepane core **1.44**..... 19
Scheme 1.8: Tanner's synthesis of balanol (**1.1**)..... 20
Scheme 1.9: Barbier's synthesis of azepane core **1.53**..... 20
Scheme 1.10: Barbier's synthesis of balanol (**1.1**)..... 21
Scheme 1.11: Naito's synthesis of azepane core **1.25**..... 21
Scheme 1.12: Naito's synthesis of balanol (**1.1**)..... 22
Scheme 1.13: Single electron transfer mechanism for electrophilic fluorination..... 35
Scheme 1.14: S_N2 mechanism for nucleophilic deoxyfluorination 37
Scheme 3.1: Synthesis of the azepane **3.1**..... 112
Scheme 5.1: First evidence of fluoronium ion in solution 151
Scheme 5.2: Synthesis of *syn*–dihydroxyazepanes **4.6** and **4.7**..... 154
Scheme 5.3: Synthesis of fluorohydroxyazepanes **5.4** and **4.10**..... 155
Scheme 5.4: Synthetic evidence for structure assignments of **5.5**..... 158
Scheme 5.5: Synthesis of vicinal difluoroazepanes **5.6** and **5.12** with C5–F epimerization 159
Scheme 5.6: Synthesis of **5.19**: Effect of *N*–tosyl protecting group in monofluorination . 162
Scheme 5.7: Mechanism for the monofluorination outcomes in **2.9c** and **5.18**..... 163
Scheme 5.8: Synthesis of *N*–tosyl difluoroazepanes **5.23** and **5.24**..... 163
Scheme 5.9: Possible pathways for the fluorination of **5.4** and **5.21**..... 168
Scheme 5.10: Possible pathways for the fluorination of **4.10**..... 172
Scheme 6.1: Synthesis of the key fragments **6.5** and **1.14**..... 223
Scheme 6.2: Synthesis of the benzophenone fragment **1.28**..... 224
Scheme 6.3: Synthesis of the azepane core **1.10**..... 224
Scheme 6.4: Synthesis of the balanol **1.1**..... 225
Scheme 6.5: Synthesis of the balanol analogues **6.27–6.32**..... 226

List of Tables

Table 1.1: Role of PKC isozymes in human diseases 6
Table 1.2: Main classes of PKC inhibitors studied: Highlight 10
Table 1.3: Summary of Heerding and Crane's modifications in benzophenone fragment... 25
Table 1.4: Summary of Nicolaou's modifications in benzophenone fragment 26
Table 1.5: Highlight of Lai's modifications in azepane moiety 27
Table 1.6: Summary of Jagdmann's modifications in ester/amide linkages 28
Table 2.1: Cross reference of compound nomenclature from the thesis and *Tetrahedron*, **2013**, *69*, 744..... 76
Table 3.1: Cross reference of compound nomenclature from the thesis and *Org. Biomol. Chem.*, **2013**, *11*, 3781..... 110
Table 4.1: Cross reference of compound nomenclature from the thesis and *Org. Biomol. Chem.* article submitted for publication 136
Table 5.1: 2D NMR structure elucidation of the azepane **4.10**..... 156
Table 5.2: 2D NMR structure elucidation of the azepane **5.5**..... 157
Table 5.3: 2D NMR structure elucidation of the azepane **5.8**..... 160
Table 5.4: 2D NMR structure elucidation of the azepane **5.14**..... 161
Table 5.5: 2D NMR structure elucidation of the azepane **5.19**..... 164
Table 5.6: 2D NMR structure elucidation of the azepane **5.23**..... 165
Table 5.7: 2D NMR structure elucidation of the azepane **5.24**..... 166
Table 6.1: K_d's of compounds **6.27–6.32**..... 228

CHAPTER 1

Introduction

1.1 Protein Kinases in Drug Discovery

1.1.1 Introduction to Protein Kinases

Protein kinases are enzymes that chemically transfer a phosphate group from nucleoside triphosphates (usually ATP) to amino acids with a free hydroxyl group. This phosphorylation of proteins usually directs their enzyme activity, cellular location or associations with other proteins. Protein kinases can modify up to 30% of all human proteins and constitute about 2% of all human genes.[1] As one of the largest and most functionally diverse gene families, protein kinases play a central role in cell regulation.

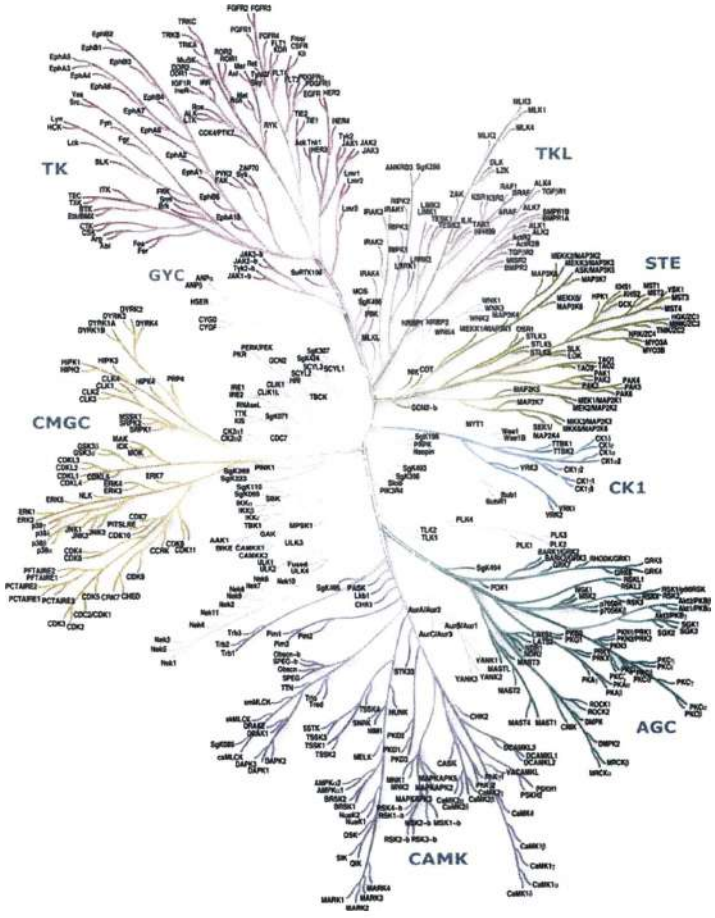


Figure 1.1. Protein kinase super family: A dendrogram representation.[2]

Protein kinases are subdivided mainly into serine/threonine kinases and tyrosine kinases based on their substrate specificity. There are also protein kinases that act on other amino acids such as histidine kinases. There are in total 518 human protein kinases identified to date, of which 478 have catalytic domain sequence homology and belong to a single superfamily.[2] These can be clustered into groups, families and sub–families, of increasing similarity in sequence and biochemical function. The human protein kinase superfamily is divided into the following seven groups based on the structure and biological functions (Figure 1.1).[2] (i) AGC kinases – containing PKA (protein kinase A), PKG (protein kinase G) and PKC (protein kinase C) (ii) CaM kinases – containing the calcium/calmodulin–dependent protein kinases (iii) CK1 – containing the casein kinase 1 group (iv) CMGC – containing CDK (cyclin–dependent kinase), MAPK (mitogen–activated protein kinases), GSK3 (glycogen synthase kinases) and CLK kinases (CDC–like kinases) (v) STE – containing the homologs of yeast Sterile 7, Sterile 11, and Sterile 20 kinases (vi) TK – containing the tyrosine kinases (vii) TKL – containing the tyrosine–kinase like group of kinases.

1.1.2 AGC Protein Kinase Family and Therapeutic Role

AGC kinase, a subgroup of serine/threonine kinases, was first named by Hanks and Hunter[3] in 1995. In total 60 AGC kinases have been grouped into 21 subfamilies based on their homology outside the catalytic domain.[4] The AGC kinases based on sequence homology in the catalytic domain are most closely related to cAMP–dependent protein kinase 1 (PKA; also known as PKAC), cGMP–dependent protein kinase (PKG; also known as CGK1α) and protein kinase C (PKC). 42 out of 60 AGC kinases feature additional functional domains along with the kinase core, which regulate kinase activity and localization. Moreover, multiple isoforms and splice variants add on to the complexity of this family.[4]

Understandably, as AGC kinases control vital cellular processes it is inevitable that their dysregulation is implicated in many human diseases (Figure 1.2), most noticeably in cancer[5] and diabetes.[6] In addition, specific mutations in other AGC kinases (DMPK, GRK1, GRK4, MAST3, MASTL, PKCγ and RSK2) have been shown to cause various inherited syndromes due to neurological, cardiovascular, haematological, immunological, and chromosomal aberrations.[7]

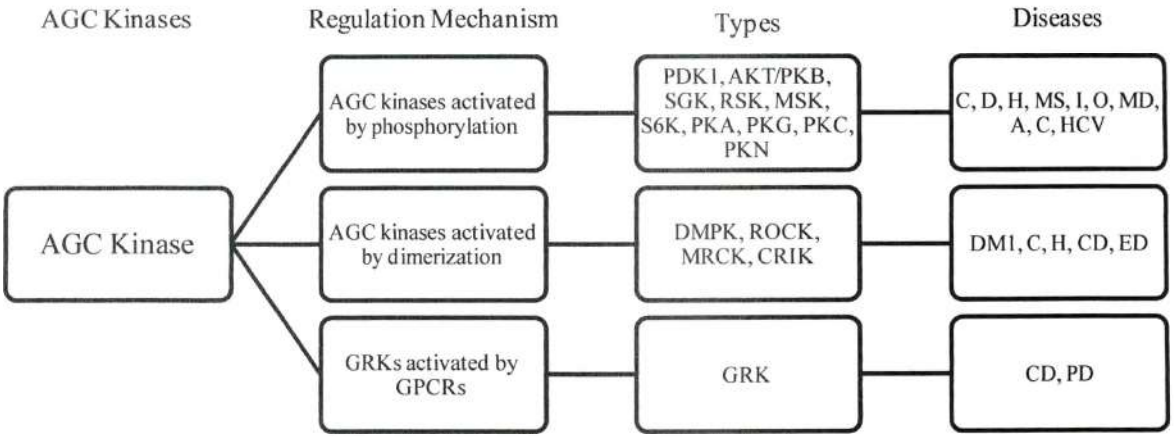


Figure 1.2. Roles of AGC kinases in various diseases.[4,8] C, cancer; D, diabetes; H, hypertension; MS, metabolic syndrome; I, inflammation; O, obesity; MD, metabolic disorders; A, allergy; HCV, hepatitis C; DM1, myotonic dystrophy type 1; CD, cardiovascular disease; ED, erectile dysfunction; PD, Parkinson's disease. PDK, pyruvate dehydrogenase kinase; AKT/PKB, protein kinase B; SGK, serum/glucocorticoid regulated kinase; RSK, ribosomal s6 kinase; MSK, mitogen– and stress–activated protein kinase; S6K, analogous to RSK; PKN, protein kinase N; DMPK, Myotonic dystrophy protein kinase; ROCK, Rho–associated kinase; MRCK, Myotonic dystrophy related CDC42–binding kinase; GRK, G–protein coupled receptor kinase; MAST3, microtubule–associated serine–threonine kinase 3.

In most cases, precisely how these mutations cause disease is unclear. Despite over 100,000 research articles on AGC kinases,[4] much work is still required to uncover the molecular mechanisms behind their functions.

1.1.3 The PKC Isozymes: Structure, Regulation and Implications

Nishizuka and coworkers[9] (1977) discovered a new calcium dependent phosphorylating enzyme, which was termed protein kinase C (PKC). After 36 years, exhaustive genetic

screening has defined a superfamily of mammalian PKC isotypes consisting of at least 10 distinct isozymes,[10] with one PKC isoform present in almost every cell type in the human body.[11] Based on their secondary messenger mode of regulation, PKC family is subdivided into three groups: (i) cPKCs: conventional (PKCα, PKCβI, PKCβII, PKCγ), (ii) nPKCs: novel (PKCδ, PKCε, PKCη, PKCθ), and (iii) aPKCs: atypical (PKCζ, PKCλ/ι).[12] PKC isozymes differ in structure, cellular location, co–factor requirements, and substrate specificity. All PKC family members share conserved domain architecture, consisting of a C–terminal kinase core (catalytic domain) and an N–terminal regulatory moiety[13] (Figure 1.3).[14] Each catalytic domain contains an ATP and a substrate-binding region, while the regulatory domains are far more varied in structure and function. The regulatory domain is where signaling molecules upstream bind to and activate PKC.[10]

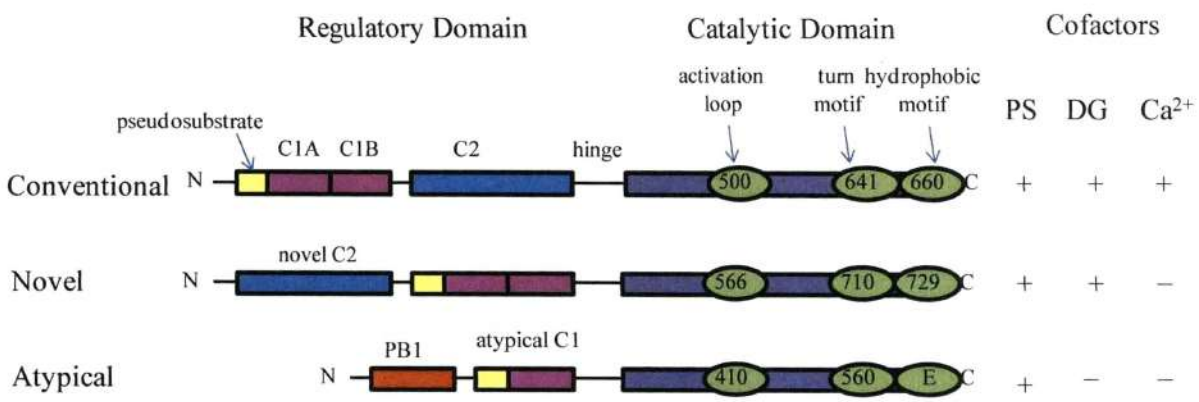


Figure 1.3. Structure of PKC isozymes.[14] The primary structure of the three classes of PKC isozymes: conventional, novel, and atypical. The regulatory moiety contains the cofactor–binding modules: the pseudosubstrate (yellow); the C1A and C1B domains (pink) that bind phosphatidylserine for all PKCs and diacylglycerol/phorbol esters for conventional and novel PKCs; the C2 domain (blue) that binds anionic lipids and Ca^{2+} for conventional PKCs; and a PB1 domain (red) that serves as a protein–protein interaction module for atypical PKCs. The requirements for cofactor binding are shown to the right: PS, phosphatidylserine; DG, diacylglycerol; and Ca^{2+}. The catalytic moiety contains the conserved kinase domain (violet) with the activation loop phosphorylation site (green circle) and a C–terminal tail that contains two conserved phosphorylation sites: the turn motif and the hydrophobic motif (green circles; note that for atypical PKCs a glutamate occupies the phosphoacceptor position of the hydrophobic motif). The numbering of the phosphorylation sites is representative of the PKC isozyme underlined to the left.

Generally, PKCs are activated by releasing the pseudosubstrate from the catalytic site.[12,15] For example, cPKC enzymes initially are located in the cytoplasm of a cell in the inactive state with pseudo–substrate bound to the catalytic domain preventing phosphorylation. External stimuli such as hormones or neurotransmitters bind to and initiate a G–protein–coupled receptor (GPCR) signaling which activates phospholipase C (PLC).[16] PLC cleaves a membrane bound phosphoinositol–4,5–bisphosphate (PIP2) molecule into 1,2–diacylglycerol (DAG), which remains attached to the membrane while PIP2 relocates to the endoplasmic reticulum (ER) where it stimulates an ion channel to release Ca^{2+}. This prompts cPKC to translocate to the plasma membrane where it associates with DAG. It is has been demonstrated that calcium greatly increases cPKC's affinity for DAG.[17] The interactions with DAG facilitate the dissociation of the pseudo–substrate and activate the kinase activity.

The role of PKC isozymes in a particular disease has been investigated with both genetic and pharmacological tools. Table 1.1 lists some of the diseases and the related PKCs likely involved in these pathologies.[18]

Table 1.1. Role of PKC isozymes in human diseases.[18]

Disease	PKC isozyme implicated	Role of PKCs in pathology
Cancer	PKCα	Proliferation, intravasation and metastasis[19]
	PKCβ	Vasculogenesis and cancer cell invasion[20]
	PKCδ	Angiogenesis[21]
	PKCε	Proliferation, tumour survival, metastasis and resistance to chemotherapy[22]
	PKCθ	Gastrointestinal stromal cell proliferation[23]
	PKCη	Glioblastomal cancer; increased proliferation and resistance to radiation[24]
Diabetic complications	PKCβII	Vascular complications[25]
	PKCβ	Knockout attenuates obesity and increased glucose transport (potentially PKCβI)[26]
	PKCδ	Stimulation of islet cell function[27]
Ischaemic heart disease	PKCδ	(mediates injury) Increased ROS production, decreased ATP generation and increased apoptosis and necrosis[28]
	PKCε	(protective effect; useful for predictive ischaemia such as in surgery or organ transplantation) Protection of mitochondrial functions and proteasomal activity, activation of ALDH2 and reduction of aldehydic load[29]
Heart failure	PKCα	Decreased cardiac contractility, force of myofilaments, uncoupling of β–adrenergic receptors[30]

	PKCβII	In rats: decreased proteasomal activity, removal of misfolded proteins in several models and disregulation of calcium handling[31]
	PKCβII	Conflicting data in mice: overexpression either results in hypertrophy or it is not required for hypertrophy; PKCβII has also been shown to decrease or increase contractility[32]
	PKCε	Increased fibrosis, fibroblast proliferation and inflammation[29]
Psoriasis	PKCδ	Increased inflammation, increased proliferation and disregulation of angiogenesis[33]
Pain	PKCγ	Key mediator of pain in dorsal root ganglia[34]
	PKCε	Key mediator of pain in spinal cord[34]
Autoimmunity, inflammation	PKCδ	B cell development and inflammation[35]
	PKCθ	Involved in many T cell responses[36]
Stroke	PKCδ	Increased mitochondrial fission, ROS production and dysfunction of blood–brain barrier[37]
	PKCε	Cytoprotective effect; increased cerebral blood flow[38]
Bipolar disorders	PKCα	Altered gene expression[39]
	PKCε	Altered neuronal transmission[40]
Asthma and other lung diseases	PKCθ	Inflammation and airway hyper–responsiveness[41]
	PKCδ	(loss of other isozymes may also contribute to disease pathology) Eosinophil activation[42]
Parkinson's disease	PKCδ	Inflammation and neuronal cell death[43]

1.1.4 Kinase Drug Discovery: Gleevec with Conformational Specificity

Protein kinases are now validated drug targets although their drugability was once in question given the high homology observed in the ATP–site of its kinase domain.[44] In the early 1980s, isoquinolinesulphonamides were developed by Hiroyoshi Hidaka[45] as the first protein–kinase inhibitors targeting the ATP–binding pocket with good cell permeability. However, low potency and lack of selectivity of these inhibitors amongst kinases limited their use. AT877 (fasudil hydrochloride) was approved in Japan as early as in 1995 for the treatment of cerebral vasospasm after surgery for subarachnoid haemorrhage and associated cerebral ischaemic symptoms, even though it was not clear that the drug activity was targeted to kinases.[46] The discovery of a bacterial metabolite staurosporine, as a nanomolar inhibitor of PKC,[47] raised interest in the pharmaceutical industry for kinase–targeted drug development. Following this, several bisindolyl maleimide compounds were developed and used in cell–based assays.[48]

However, these bisindolyl maleimides were later shown to lack specificity, and inhibited many other protein kinases *in vitro*.[49] Nevertheless, a few bisindolyl maleimides have progressed to human clinical trials, although it is unclear whether their efficacy stems from the inhibition of a PKC or the combined inhibition of several protein kinases.[50]

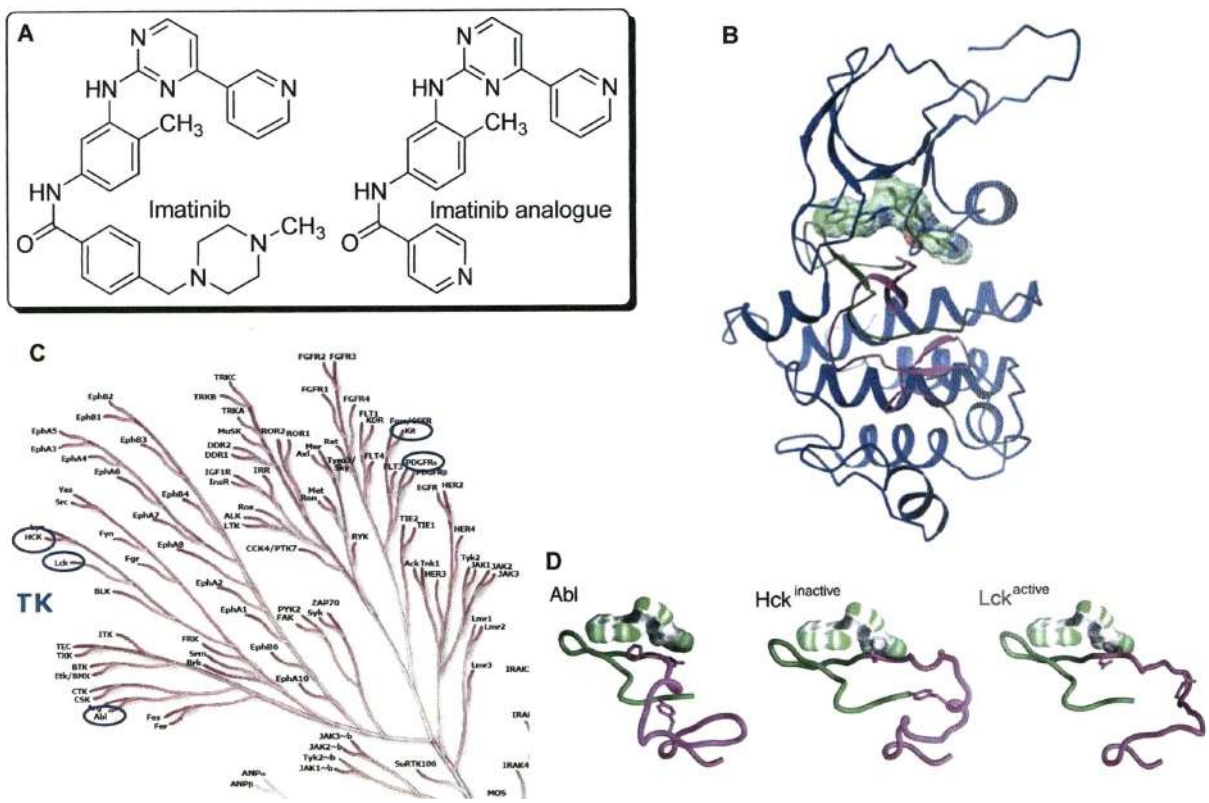


Figure 1.4. Structural mechanism of Imatinib for Abl inhibition.[51] (A) Chemical structure of Imatinib and its analogue. (B) X–ray crystal structure of Abl kinase in complex with imatinib analogue. (C) Places of c–kit and PDGF in comparison with HCK, LCK and Abl kinases within TK family tree based on homology. (D) Imatinib exploits the unique conformation of the activation loop in the down–regulated form of Abl. The activation loop is magenta, the catalytic segment is green and the conserved side–chains of Asp–Phe–Gly motif along with tyrosine residue are shown in ball–stick model.

The first relatively specific kinase drug, targeting the Abelson (Abl) tyrosine kinase, was approved for clinical treatment of chronic myelogenous leukaemia (CML) in May 2001 as Gleevec[52] (STI–571; or Imatinib), marking the start of a very active field focused on protein kinase drug discovery (Figure 1.4). The most interesting aspect of imatinib is that its Abl

specificity in the ATP pocket extends much beyond simple homology requirements.[51] This fact is clearly demonstrated by (i) virtually no inhibition of highly homologous Src–family tyrosine kinases; (ii) inhibition of c–kit and PDGF receptor kinases with much less homology and significantly different chemical structure in the activation loop.[53] As shown by the landmark structural work by the Kuriyan group (Figure 1.4B and D), imatinib achieves its high specificity by recognizing the catalytic site of a protein kinase in a drug–matched conformation. This induced–conformational specificity is the basis to imatinib's success as a multi–billion dollar drug.[51] The case of imatinib is now followed by 24 protein kinase drugs that are approved by USFDA till date and about 150 under development.[54]

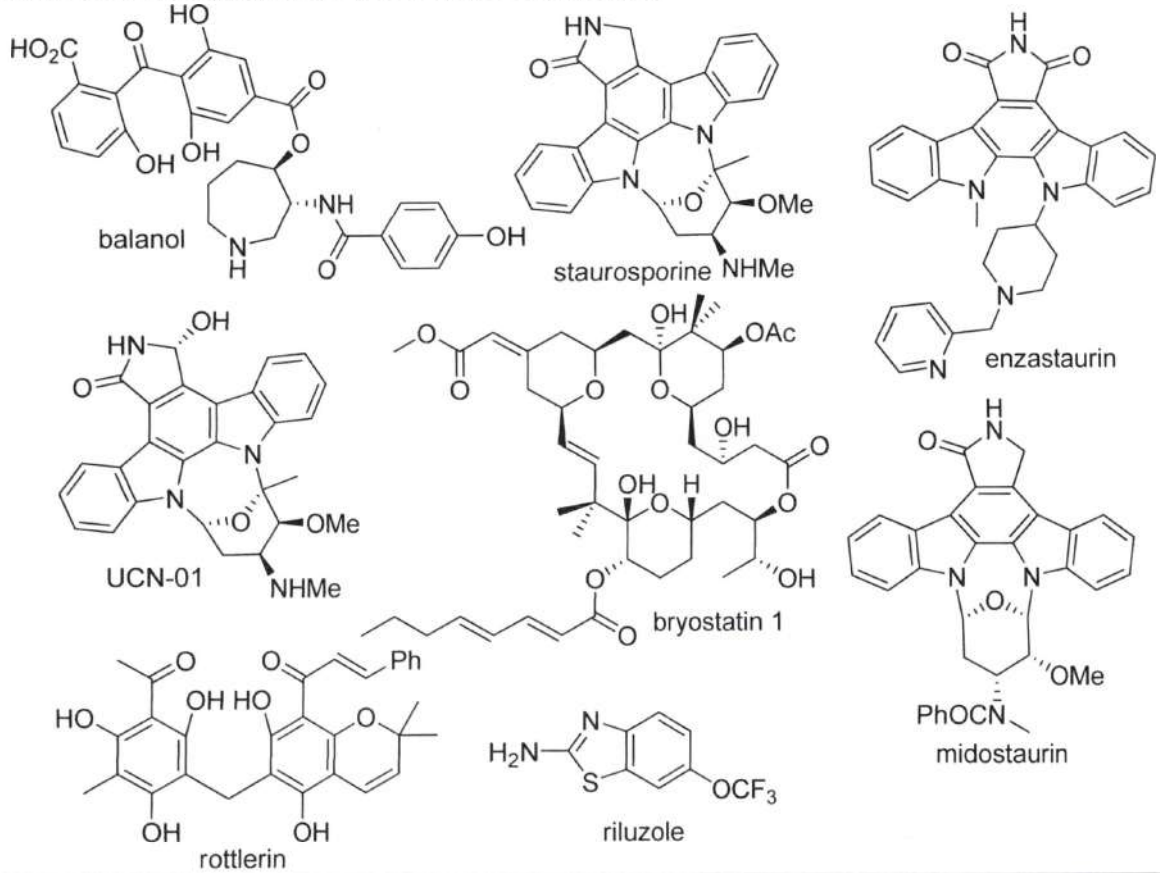
1.1.5 Current PKC Drug Developments and Challenges

PKC has proven to be an elusive drug target since 1982,[55] when it was first identified as the receptor for the tumour promoter phorbol ester.[18] Unfortunately, both academic and pharmaceutical efforts have yet to result in the approval of a single new drug that specifically targets PKC. One exception, Ruboxistaurin, is an investigational drug from Eli Lilly and currently used to treat diabetic peripheral retinopathy as a PKCβ inhibitor. In August 2006, USFDA declared it "approvable" with a request for additional clinical trials. Why does PKC remain a tantalizing drug target? There is evidence that PKC has a crucial role in many important human diseases, including diabetes,[25] cancer,[56] ischaemic heart disease[29] and heart failure,[31] autoimmune diseases,[57] Parkinson's disease,[58] Alzheimer's disease,[59] bipolar disorder[39] and psoriasis.[60] However, determining which and how a PKC isozyme contributes to the pathology of a given disease has been severely hindered by the general lack of PKC isozyme–specific molecular tools due to the substantial homology among protein kinases in general and PKC isozymes in particular. As selective regulators of PKC isozymes have not

been used in many studies, the main questions in the PKC field remain controversial and unresolved.

Efforts to identify selective modulators of PKC have taken disparate approaches[18] including (i) development of ATP–competitive small–molecule inhibitors; (ii) phorbol esters and derivatives activators and inhibitors that bind to the C1 domain, mimicking the binding of diacylglycerol; and (iii) peptides that disrupt protein–protein interactions between PKC and RACK (receptor for activated C–kinase). The following is a list of the main classes of PKC modulators developed in the last 20 years. (Table 1.2)[18]

Table 1.2. Main classes of PKC inhibitors studied: Highlight.[18]



Drug	Selective to	Order of isozyme selectivity
Balanol[61]	PKC and PKA inhibitor (ATP–binding site)	PKCβII>PKCβI>PKCη>PKCδ>PKCα>PKCε>>>PKA
Riluzole[62]	Inhibits other serine/threonine kinases (ATP–binding site)	Preferential inhibitor of PKCα
Staurosporine[63]	ATP–binding site	Non–selective PKC inhibitor

Enzastaurin[64]	ATP–binding site	Three– to five fold selectivity for PKCβ inhibition
Midostaurin[65] (PKC412)	ATP–binding site	Inhibitor of various protein kinases, including PKC
UCN–01(7–hydroxy staurosporine)[66]	ATP–binding site	Inhibitor of various protein kinases, including tyrosine kinases and classical PKC, at a similar IC50 (25–50 nM)
Rottlerin[65,67]	PKCδ inhibitor (ATP–binding site)	Selective for PKCδ, but also targets calcium/calmodulin–dependent protein kinase VI at a similar IC50 (5 μM)
Bryostatin 1[68]	C1 domain of PKC	Twofold selectivity for PKCε over PKCα and PKCδ
δV1–1(KAI9803 or delcasertib)[69]	PKCδ inhibitor (RACK–binding site)	>1,000–fold selectivity over other isozymes
εV1–2(KAI–1678)[70]	PKCε inhibitor (RACK–binding site)	>100–fold selectivity over other isozymes
ψεRACK (KAI–1455)	PKCε activator (intramolecular interaction in PKC)	>100–fold selectivity over other isozymes
Aprinocarsen[71]	PKCα inhibitor (expression)	Selectivity for PKCα

Moreover, the following drugs have reached clinical trials as PKC modulators.[18] (i) flosequinan[72] (non–selective PKC inhibitor) – congestive heart failure; (ii) volatile anaesthetics,[73] adenosine,[74] acadesine[75] (PKCε activator) – coronary bypass grafting; (iii) adenosine[76] (PKCε activator), delcasertib (PKCδ activator) – AMI salvage; (iv) tamoxifen[77] (non–selective PKC inhibitor) – bipolar mania; (v) bryostatin[78] (non–selective PKC activator), aprinocarsen[79] (PKCα inhibitor), enzastaurin[80] (PKCβ inhibitor), tamoxifen[81] (non–selective PKC inhibitor), midastaurin[82] (non–selective PKC inhibitor), UCN–01[83] (non–selective PKC inhibitor) – oncology; (vi) ruboxistaurin (PKCβ inhibitor) – diabetic retinopathy,[84] nephropathy[85] and neuropathy;[86] and (vii) sotrastaurin[87] (non–selective PKC inhibitor) – transplant rejection.

The challenges in the development of isozyme specific PKC inhibitors according to the targeted domain are as follows: (i) Competitive inhibitors of ATP: PKC catalytic region within PKC family is ~70% homologous, and the ATP–binding site in all protein kinases is highly conserved. Therefore, generating a drug that selectively inhibits one kinase has been a great challenge.[88] (ii) Mimetics of DAG binding: The C1 domain and DAG–binding site are highly

homologous among isozymes (60–80%), again. Furthermore, other non–PKC proteins also have C1 domains that bind DAG.[89] However, Blumberg *et al.*[90] and Wender and colleagues[91] have identified some selective C1–binding molecules. (iii) Competitive inhibitors of RACK: RACK anchor proteins that bind activated PKC, (through C2 domain) have not been identified for all the PKC isozymes.[92] However, the C2 domain homology amongst PKC isozymes is only 8–50%.

1.2 Balanol as an ATP mimic in PKC Inhibition

1.2.1 Discovery and Structure Elucidation of Balanol

In 1977, Kneifel and coworkers isolated and characterized a fungal metabolite from *Cordyceps ophioglossoides* which they named as 'ophiocordin'.[93] Ophiocordin (**1.2**) recorded potent antibiotic activity against fungi such as Zygomycetes, Ascomycetes, and Deuteromycetes. In 1980, Kneifel and coworkers proposed the structure of ophiocordin (**1.2**) from extensive derivatization and decomposition studies (Figure 1.5).[94]

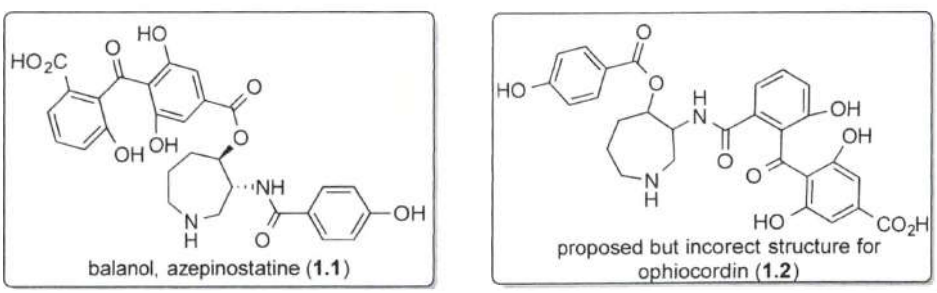


Figure 1.5. Structure of balanol (**1.1**) and ophiocordin (**1.2**).

In 1993, Kulanthaivel and coworkers[95] from Sphinx Pharmaceuticals, USA (now part of Eli Lilly) isolated a metabolite with IC_{50} values of 4–9 nM against human PKC from *Verticillium balanoides* fungal species. This compound was characterized as 2–[2,6–dihydroxy–4–[(3*R*,4*R*)–3–[(4–hydroxybenzoyl)amino]azepan–4–yl]oxycarbonylbenzoyl]–3–hydroxybenzoic acid (**1.1**), a structural isomer of ophiocordin and was named 'balanol' after

its source. Balanol (**1.1**) differs from the proposed structure of ophiocordin (**1.2**) in two aspects: (i) the benzophenone and 4–hydroxybenzamide moieties are swapped; and (ii) the benzophenone moiety is attached with different carboxylic acid groups. After a few months in their quest for novel PKC inhibitors, researchers at the Nippon Roche Research Center, Japan isolated a novel compound called 'azepinostatin' from two species, *Fusarium merismoides* Corda and *Fusarium aquaeductuum* Lagh.[96] However, structure elucidation revealed that it was identical to 'balanol'.

Kulanthaivel and coworkers accomplished the structure elucidation of balanol (**1.1**) using ^{1}H, ^{13}C, and 2D NMR (COSY, NOESY, TOCSY, HMQC, and HMBC) experiments. The absolute

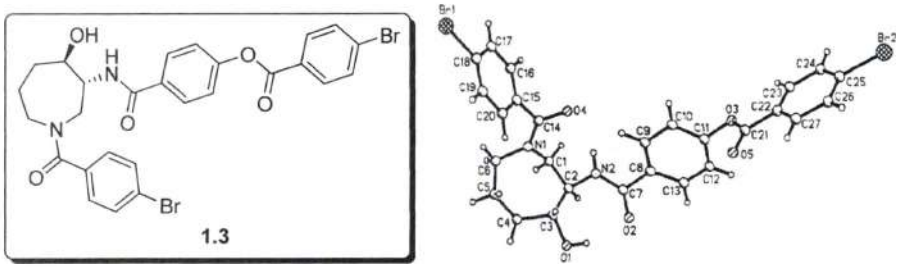


Figure 1.6. X–ray crystal structure of *p*–bromobenzoyl balanol derivative (**1.3**).[95]

stereochemistry was determined to be *R* at both the stereocentres by X–ray analysis of a derivative **1.3** synthesized from an authentic sample of **1.1** (Figure 1.6). The stereochemistry of ophiocordin was yet to be assigned. Studies were carried out to clarify structural differences of balanol (**1.1**) and ophiocordin (**1.2**). Authentic samples of both were collected and compared. An NMR experiment of a mixture of these samples confirmed that they were the same compound, with the correct structure being the one proposed by Kulanthaivel and coworkers.[97]

In summary, **1.1** was first isolated and reported to be antibiotic by Kneifel and coworkers, whereas Kulanthaivel and coworkers elucidated the correct structure of **1.1** as a potent PKC inhibitor.

1.2.2 Synthetic Protocols for Balanol

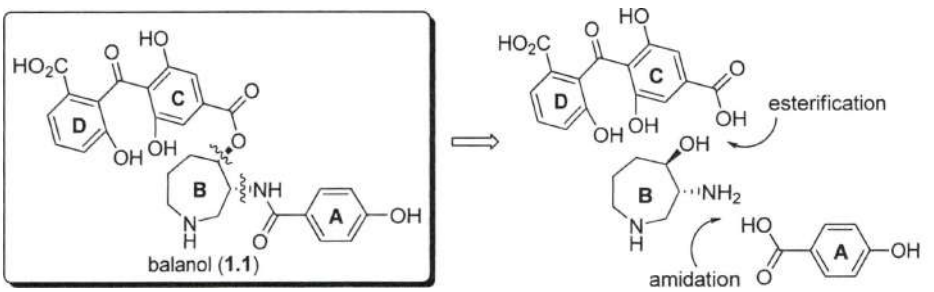


Figure 1.7. Balanol: retrosynthetic analysis.

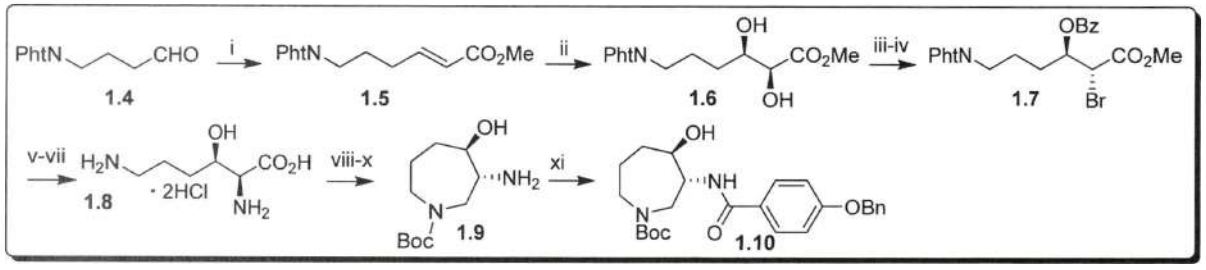
There are about 50 total and formal syntheses of balanol (**1.1**) published to date. Balanol molecule is comprised of three major fragments: a tetra–*ortho*–substituted benzophenone (ring C and D), a perhydroazepane (ring B), and a *p*–hydroxybenzamide (ring A) moiety. These three fragments are connected by an ester and an amide linkage. Thus, the retrosynthetic analysis invariably involves disconnections at these ester and amide linkages (Figure 1.7).

The 1,2–*trans* aminohydroxyazepane core has been of particular interest amongst synthetic chemists because of its stereochemical challenges. All of the balanol (**1.1**) total syntheses reported so far addressed three main synthetic hurdles; (1) installation of the correct 1,2–*trans*–aminohydroxy stereocentres; (2) formation of the seven–membered azepane ring; and (3) benzophenone synthesis. The following summarizes the six total syntheses of balanol chronologically to highlight the different strategies and identify the ones most appropriate for new diversification of the azepane ring.

1.2.2.1. Total Syntheses of Balanol

The first total synthesis of balanol (**1.1**) was accomplished by Lampe and Hughes[98] in 1994 shortly after its structure elucidation.[95]

Lampe and Hughes (1994)[98]

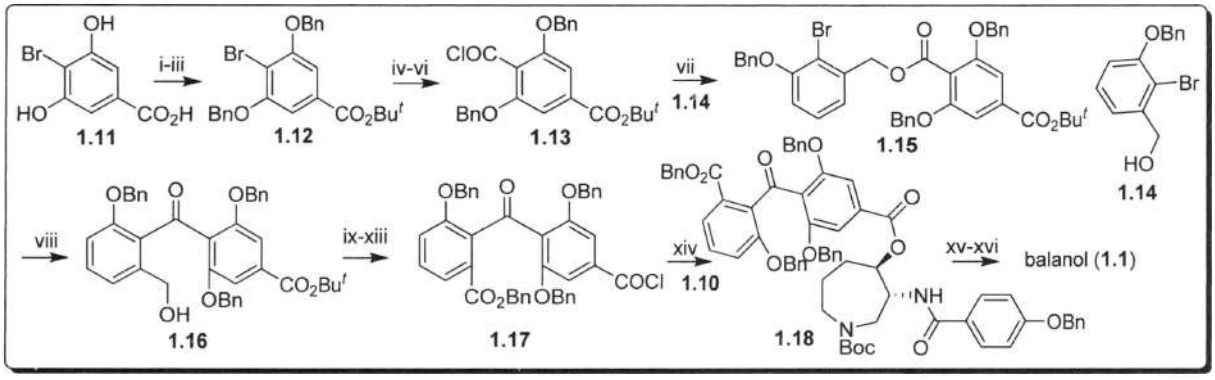


Scheme 1.1. Hughes' synthesis of azepane core **1.10**.[99] *Reactions and conditions*: (i) $Ph_3P{=}CHCO_2CH_3$, CH_2Cl_2; (ii) $K_3Fe(CN)_6$, K_2CO_3, $(DHQD)_2$–PHAL, $K_2Os(OH)_3$, H_2O, $(CH_3)_3COH$; (iii) $C_6H_5C(OCH_3)_3$, $BF_3{\cdot}OEt_2$; (iv) CH_3COBr, NEt_3; (v) NaN_3, DMSO; (vi) H_2, 10% Pd on carbon, EtOAc, $(Boc)_2O$, EtOH; (vii) 6 *N* HCl, reflux; (viii) $(TMS)_2NH$, xylenes, reflux; isopropanol; (ix) BH_3, THF; (x) $(Boc)_2O$, NaOH; (xi) *p*–$BnOC_6H_4COCl$, NaOH, DCM.

The desired (2*S*,3*R*) amino–hydroxy stereochemistry in **1.8** was secured from a (2*S*,3*R*) dihydroxy precursor **1.6** by formation of bromohydrin **1.7** followed by S_N2 displacement of Br with NaN_3 (Scheme 1.1).[99] The diol **1.6** was prepared from 4–phthalimidobutanal (**1.4**) by triphenylphosphine mediated addition of α–olefinic ester moiety to furnish **1.5** which then underwent enantioselective *cis*–dihydroxylation to afford **1.6** with the desired stereochemistry in 96% yield. The (2*S*,3*R*)–3–hydroxylysine **1.8** underwent activation by hexamethyldisilazane (HMDS) followed by intramolecular coupling to yield cyclized caprolactam which was then reduced with borane and Boc protected to furnish key azepane **1.9** (Scheme 1.1). In brief, azepane moiety **1.10** was synthesized in eleven linear steps in 19% overall yield.

Synthesis of the benzophenone moiety was achieved in thirteen synthetic steps starting from a tetra–substituted 4–bromo–3,5–dihydroxybenzoic acid (**1.11**) to yield **1.12** in three steps by using standard protecting groups (Scheme 1.2). The functionalized bromobenzene **1.12** then underwent lithium–halogen exchange, nucleophilic addition, and acid activation to give acid chloride **1.13**. In the presence of a substituted alcohol **1.14**, **1.13** was converted to the highly

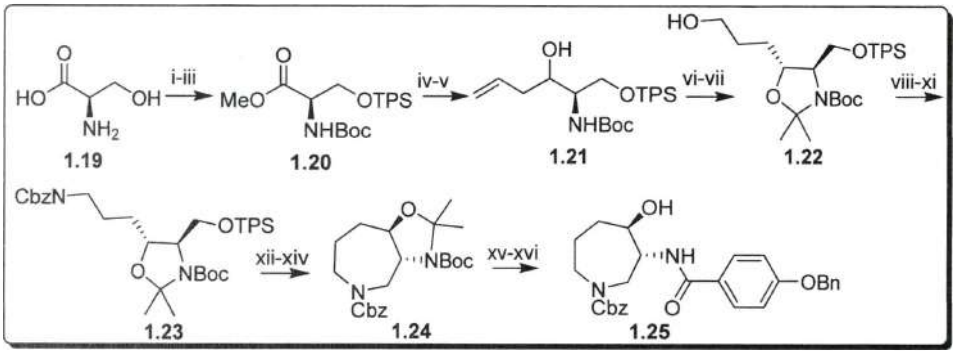
functionalized ester **1.15** that then underwent homo–Fries rearrangement using *n*–BuLi to result in the tetra–*ortho*–substituted benzophenone **1.16** (Scheme 1.2). **1.16** was then converted readily to the fully protected acid chloride **1.17** to couple with **1.10**. Overall, (−)–Balanol (**1.1**) was synthesized in 16 linear steps in 3% yield.



Scheme 1.2. Lampe and Hughes' synthesis of balanol (**1.1**).[98] *Reactions and conditions*: (i) BnBr, K_2CO_3; (ii) NaOH; (iii) CDI, *t*–BuOH, DBU; (iv) *n*–BuLi, −78 °C; (v) CO_2; (vi) $(COCl)_2$; (vii) *t*–BuOK, THF; (viii) *n*–BuLi, THF, −78 °C; (ix) PDC, DMF; (x) Bu_4NMnO_4, pyr; (xi) BnBr, K_2CO_3; (xii) quinoline, 205 °C; (xiii) $(COCl)_2$, DMF; (xiv) Et_3N, DCM; (xv) H_2, $Pd(OH)_2/C$; (xvi) TFA.

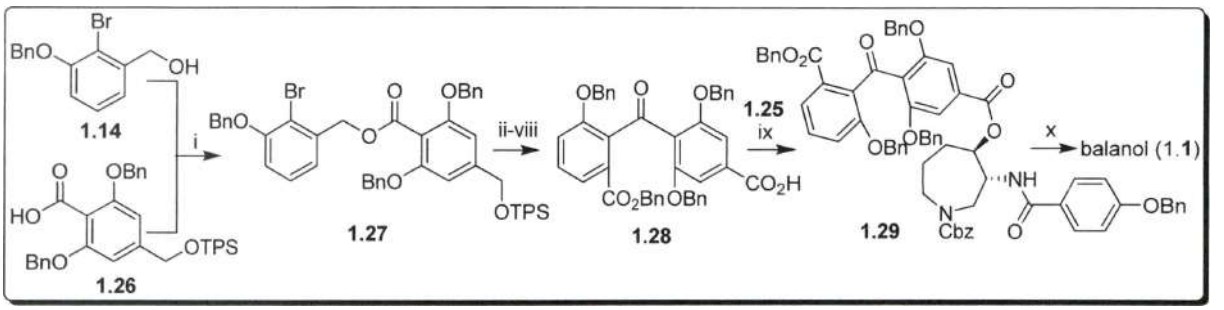
Nicolaou (1994)[100]

The approach by Nicolaou and coworkers secured the amino–hydroxy stereocentres via a diastereoselective nucleophilic addition, starting from homochiral amino acid D–serine (**1.19**). D–serine **1.19** was first protected and transformed to its *α*–amino ketone via **1.20**, followed by the addition of Brown's allyl borane to furnish the amino–hydroxy **1.21** in five steps and 68% yield (Scheme 1.3; steps i–v). **1.21** was then converted to **1.23** in six steps via standard functional group transformation and protection for the intramolecular S_N2 cyclization to furnish the key intermediate **1.24** which was treated with TFA to produce the primary amine followed by amidation with 4–(benzyloxy) benzoyl chloride to achieve the hexahydroazepane core **1.25**.



Scheme 1.3. Nicolaou's synthesis of azepane core **1.25**.[100] *Reactions and conditions*: (i) $(Boc)_2O$, NaOH, 1,4–dioxane, H_2O, 0–25 °C; (ii) K_2CO_3, MeI, DMF, 0–25 °C; (iii) TPSCl, imidazole, DMF, 25 °C; (iv) DIBALH, toluene, −78 °C; (v) Allyl–B(^{i}Ipc)$_2$, Et_2O, −78 °C, ethanolamine; (vi) 2,2–dimethoxypropane, CSA, CH_2Cl_2, 25 °C; (vii) a) 9–BBN, THF; b) NaOH, H_2O_2; (viii) MsCl, Et_3N, CH_2Cl_2, 0 °C; (ix) NaN_3, DMF, 25 °C; (x) H_2, Pd/C, THF; (xi) Benzyl chlorocarbonate, NaOH, 1,4–dioxane, H_2O, 0 °C; (xii) TBAF, THF, 25 °C; (xiii) MsCl, Et_3N, CH_2Cl_2, 0 °C; (xiv) KO^{t}Bu, THF, 25 °C; (xv)TFA, CH_2Cl_2, 25 °C; (xvi) *p*–(benzyloxy) benzoyl chloride, Et_3N, 0–25 °C.

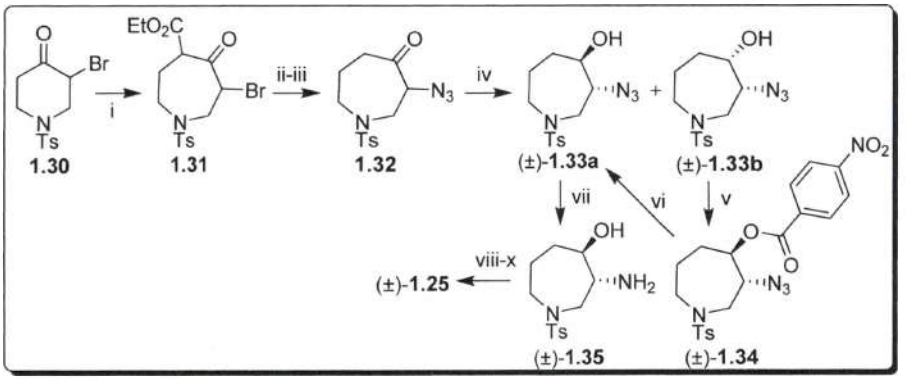
The benzophenone moiety was synthesized using a protocol similar to that of Lampe and Hughes with only minor modifications (Scheme 1.4), the key one being the coupling of alcohol **1.14** and carboxylic acid **1.26** using Mitsunobu esterification. Benzophenone **1.28** and azepane **1.25** were coupled using Mukaiyama esterification[101] with 2–chloro–1–methylpyridinium iodide to yield fully protected balanol **1.29** and finally balanol (**1.1**) after hydrogenolysis in 15 linear steps and 20% yield.



Scheme 1.4. Nicolaou's synthesis of balanol (**1.1**).[100] *Reactions and conditions*: (i) DEAD, PPh_3, THF; (ii) *n*–BuLi, THF, −78 °C, NH_4Cl (aqueous); (iii) NMO, TPAP, MeCN; (iv) $NaClO_2$, NaH_2PO_4, 2–methyl–2–butene, THF, *t*–BuOH, H_2O; (v) BnBr, K_2CO_3, DMF; (vi) TBAF, THF; (vii) NMO, TPAP, MeCN; (viii) $NaClO_2$, NaH_2PO_4, 2–methyl–2–butene, THF, *t*–BuOH, H_2O; (ix) **1.25**, 2–chloro–1–methylpyridinium iodide, DMAP, NEt_3, DCM; (x) H_2, Pd black, THF, H_2O, AcOH.

Vicker (1995)[102]

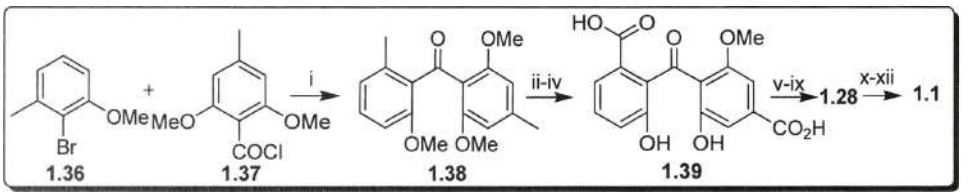
Vicker and coworkers synthesized a mixture of *cis/trans* amino–hydroxy azepanes after first the regiospecific homologation of 3–bromopiperidine–4–one (**1.30**) under Lewis acidic condition in 71% yield (Scheme 1.5), followed by non–selective ketone reduction. The undesired *cis* diastereomer **1.33b** underwent Mitsunobu inversion and hydrolysis to furnish the desired *trans* stereochemistry. **1.25** was synthesized in ten steps with 14% overall yield as a racemic mixture and resolved subsequently by forming its Mosher's ester.



Scheme 1.5. Vicker's synthesis of azepane core **1.25**.[102] *Reactions and conditions*: (i) N_2CHCO_2Et, $BF_3{\cdot}OEt_2$, DCM; (ii) HCl, dioxane; (iii) NaN_3, AcOH, DMF; (iv) $NaBH_4$, EtOH; (v) PPh_3, DIAD, THF, *p*–nitrobenzoic acid; (vi) NaOH (aq.), MeOH, dioxane; (vii) $LiAlH_4$, THF; (viii) HBr (aq.); (ix) NEt_3, DCM, 18–crown–6, benzyl chloroformate; (x) *p*–(benzyloxy) benzoyl chloride, Et_3N, DCM.

The benzophenone fragment was synthesized by a key Grignard reaction of **1.36** with 2,6–dimethoxy–4–methylbenzoyl chloride (**1.37**) to obtain tetra–*ortho*–substituted benzophenone **1.38** (Scheme 1.6). The methyl groups on benzophenone **1.38** were oxidized using $KMnO_4$ to furnish diacid **1.39**. The residual methoxy group was removed by universal deprotection with BBr_3, followed by conversion to Nicolaou's benzophenone fragment[100] **1.28** via benzyl protection and selective mono–benzyl ester hydrolysis. Finally, the synthesis of (+) and (−)–balanol was accomplished by coupling of **1.28** and (±)–**1.25** reproducing Nicolaou's work.[100]

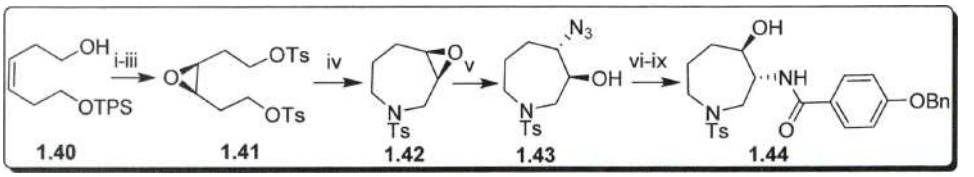
Vicker's synthesis has comparatively less chemical steps, however it involves a few low yielding reactions.



Scheme 1.6. Vicker's synthesis of balanol (**1.1**).[102] *Reactions and conditions*: (i) Mg, THF; (ii) $KMnO_4$, pyridine (aq.); (iii) $SOCl_2$, MeOH; (iv) BBr_3, DCM; (v) $SOCl_2$, MeOH; (vi) NaH, BnBr, DMF; (vii) BBr_3, DCM; (viii) NaH, BnBr, DMF; (ix) Na_2CO_3 (aq.), EtOH; (x) **1.25**, 2–chloro–1–methylpyridinium iodide, DMAP, NEt_3, DCM; (xi) H_2, Pd black, EtOAc, H_2O, AcOH; (xii) HPLC separation.

Tanner (1995)[103]

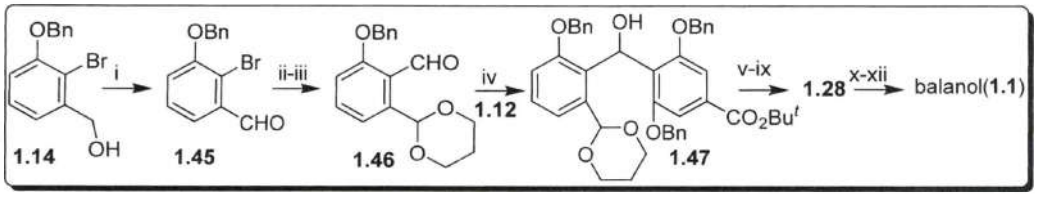
Tanner and coworkers secured the (3*R*,4*R*)–aminohydroxy stereochemistry by asymmetric epoxidation[104] and epoxide ring opening with nucleophilic azide. The regiochemistry of azido–hydroxy was corrected by aziridine formation followed by regioselective ring opening with *p*–toluenesulfonic acid hydrate (Scheme 1.7, steps vi–ix). The azepane ring was synthesized by ring closure of *cis*–tosyloxy intermediate **1.41** with *p*–toluenesulfonamide. Overall, the azepane core **1.44** was synthesized in nine steps with 27% yield.



Scheme 1.7. Tanner's synthesis of azepane core **1.44**.[103] *Reactions and conditions*: (i) $Ti(O^iPr)_4$, (+)–DET, *t*–BuOOH, DCM; (ii) *p*–TsCl, NEt_3, DMAP, DCM; (iii) *N*–tosylimidazole, Bu_4NF, THF; (iv) *p*–$TolSO_2NH_2$, CS_2CO_3, DMF, r.t.; (v) LiN_3, DMF, 90 °C; (vi) MsCl, NEt_3, DCM; (vii) $LiAlH_4$, THF, 50 °C; (viii) *p*–$BnOC_6H_4COCl$, NEt_3, DCM; (ix) *p*–TsOH, H_2O, THF.

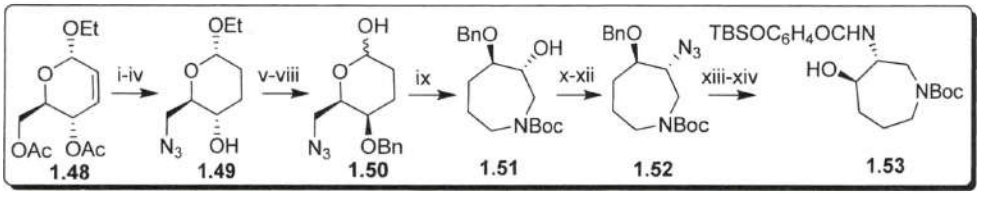
The benzophenone fragment was produced by a modified Hollinshead's procedure.[105] The primary alcohol **1.14** was oxidized using TEMPO and sodium hypochlorite to the corresponding aldehyde **1.45** which was protected as cyclic ketal and readily converted to

aldehyde **1.46** by lithium–halogen exchange with *n*–butyllithium and DMF. Aldehyde **1.46** and functionalized aryl bromide **1.12** were coupled by similar lithiation chemistry to afford secondary alcohol **1.47** which by reported protocols[98] was converted to **1.28** (Scheme 1.8). Overall, (−)–balanol was synthesized in twelve steps in 4% yield.



Scheme 1.8. Tanner's synthesis of balanol (**1.1**).[103] *Reactions and conditions*: (i) TEMPO, THF, NaBr, NaOCl, 0 °C; (ii) $HO(CH_2)_3OH$, *p*–TSA, PhMe, reflux; (iii) *n*–BuLi, THF, −78 °C, DMF; (iv) **1.12**, *n*–BuLi, THF, −110 °C; (v) TPAP, NMO, DCM; (vi) *p*–TSA, acetone, H_2O, reflux; (vii) $NaClO_2$, H_2NSO_3H, MeCN, H_2O; (viii) BnBr, K_2CO_3, DMF; (ix) quinoline, 205 °C; (x) **1.44**, 2–chloro–1–methylpyridinium iodide, DMAP, NEt_3, DCM; (xi) Na(Hg), Na_2HPO_4, MeOH; (xii) Pd black, HCO_2H.

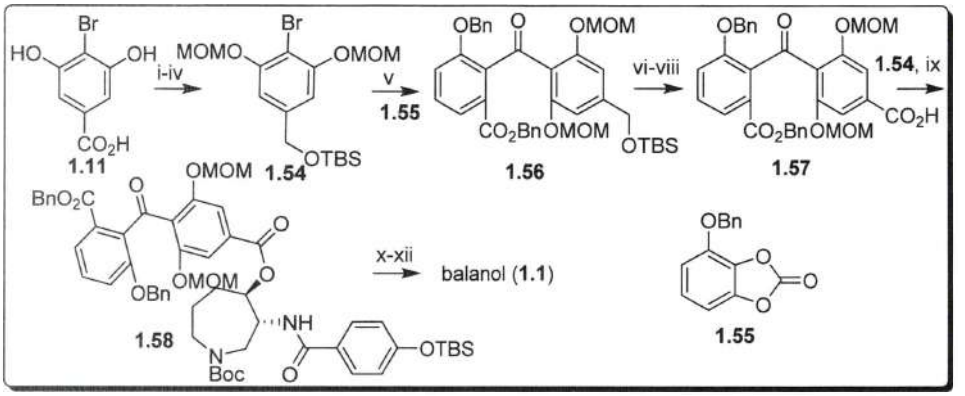
Barbier (1996)[106]



Scheme 1.9. Barbier's synthesis of azepane core **1.53**.[106] *Reactions and conditions*: (i) H_2, PtO_2, AcOEt; (ii) NaOEt, EtOH; (iii) p–TsCl, pyridine; (iv) NaN_3, TBAHS, DMF; (v) 4–O_2N–C_6H_4–CO_2H, PPh_3, DEAD, THF; (vi) KOH, EtOH; (vii) a) NaH, THF; b) BnBr, Bu_4NI, THF; (viii) 1 *N* H_2SO_4, acetone; (ix) a) H_2, Pd/C, THF; b) $(Boc)_2O$, dioxane; (x) 4–O_2N–C_6H_4–CO_2H, PPh_3, DEAD, THF; (xi) KOH, EtOH; (xii) HN_3, PPh_3, DEAD, THF, PhH; (xiii) H_2, Pd/C, THF; (xiv) *p*–TBSO–C_6H_4–CO_2H, EDC, DMAP, DCM.

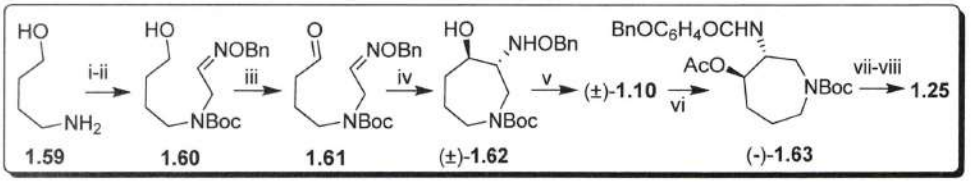
Barbier and coworkers secured the desired 1,2–*trans*–aminohydroxy stereochemistry from the chiral dihydropyran **1.49**. The synthesis of azepane ring from **1.50** was initiated by azido reduction, followed by reductive cyclization and protection to furnish **1.51** as the key azepane for the synthesis of azepane core **1.53** (Scheme 1.9).

The benzophenone fragment was synthesized using previous methods (Nicolaou, Lampe and Hughes)[98,100] with minor modifications such as different protecting groups and oxidation conditions.



Scheme 1.10. Barbier's synthesis of balanol (**1.1**).[106] *Reactions and conditions*: (i) MeOH, HCl (g); (ii) a) NaH, THF, DMF; b) MOMCl; (iii) $LiAlH_4$, THF; (iv) TBDMSCl, imidazole, DMF; (v) a) *n*–BuLi, THF; b) **1.55**; c) BnBr; (vi) Bu_4NF, THF; (vii) MnO_2, DCM; (viii) MMPP, DMF; (ix) **1.53**, *p*–TsOH, DMAP, DCM; (x) TBAF, THF; (xi) H_2, Pd/C, THF; (xii) *i*–PrOH, DME.

Naito (1997)[107]

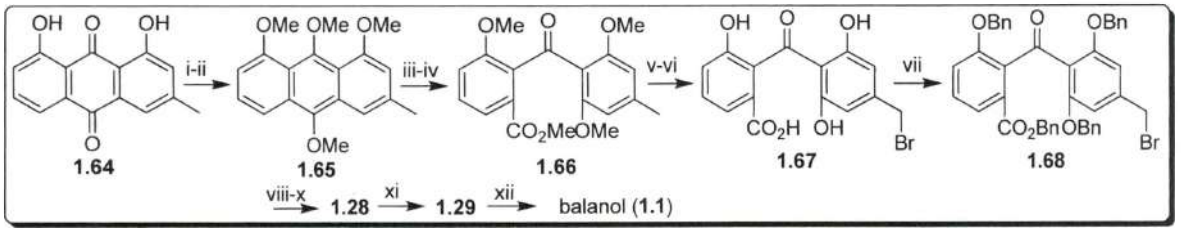


Scheme 1.11. Naito's synthesis of azepane core **1.25**.[107] *Reactions and conditions*: (i) *α*–chloroacetaldoxime benzyl ether, Et_2O, H_2O; (ii) $(Boc)_2O$, $NaHCO_3$, $(CH_3)_2CO$; (iii) CrO_3–pyridine, DCM; (iv) SmI_2, HMPA, *t*–BuOH, –78 °C; (v) a) H_2, PtO_2, MeOH; b) *p*–(benzyloxy) benzoyl chloride, $NaHCO_3$, H_2O, DCM; (vi) immobilized lipase, vinyl acetate, *t*–BuOMe, 45 °C; (vii) a) TFA, DCM; b) CBzCl, Na_2CO_3, H_2O, acetone; (viii) KOH, MeOH, r.t..

Naito and coworkers synthesized the azepane ring with the desired (3*R*,4*R*)–aminohydroxy moiety by SmI_2 mediated radical cyclization of the oxime ether **1.61** (46% yield with 7% *cis* product) using HMPA (hexamethylphosphoramide) as a ligand. **1.61** was synthesized from 4–aminobutanol (**1.59**) by alkylation with *α*–chloroacetaldoxime benzyl ether followed by Boc

protection to get alcohol **1.60** and then oxidation to give oxime ether **1.61** (Scheme 1.11). In summary, the azepane core **1.25** was synthesized in eight steps with 5% yield.

Naito composed benzophenone **1.28** from naturally available chrysophanic acid **1.64**. The anthracene **1.65** was synthesized by methylation. Following Berger–Lohr's protocol,[108] anthracene **1.65** was radically oxidized in the presence of UV light and reacted with sulfuric acid to form benzophenone regioisomers. The desired isomer **1.66** was separated after methyl esterification, which underwent radical bromination and benzyl protection to form benzophenone **1.68** (Scheme 1.12). Overall, balanol was synthesized in twelve steps in 8% overall yield.



Scheme 1.12. Naito's synthesis of balanol (**1.1**).[107] *Reactions and conditions*: (i) Me_2SO_4, K_2CO_3, $(CH_3)_2CO$, reflux; (ii) a) $Na_2S_2O_4$, Bu_4NBr, THF, H_2O; b) 6 *N* KOH, Me_2SO_4, r.t.; (iii) O_2/ *hv*, Et_2O, H_2SO_4, acetone; (iv) NaH, MeI, DMF; (v) NBS, AIBN, CCl_4, reflux; (vi) BBr_3, DCM, r.t.; (vii) BnBr, K_2CO_3, DMF; (viii) $CaCO_3$, H_2O, dioxane, reflux; (ix) Pr_4NRuO_4, NMO, MeCN; (x) $NaClO_2$, NaH_2PO_4, 2–methyl–2–butene, THF, *t*–BuOH, H_2O; (ix) **25**,2–chloro–1–methylpyridinium iodide, DMAP, NEt_3, DCM; (x) H_2, Pd black, HCO_2H, r.t.

1.2.2.2. Formal Syntheses of Balanol

In addition to the aforementioned total syntheses, many formal syntheses (especially the azepane core) for balanol (**1.1**) were reported. The majority of these formal syntheses produced the azepane core comprising the *p*–(benzyloxy)benzoyl group (ring A) and azepane ring with either *N*–Boc, (**1.10**)[98] *N*–Cbz (**1.25**)[100a] or *N*–Ts (**1.44**)[103a] protection. The syntheses of the azepane core can be enlisted as Mueller (1993);[109] Lampe, Hughes and Hu (1996);[110] Le Merrer (1996);[111] Pollini (1996);[112] Jacobsen (1997);[113] Kato (1998);[114] Cook (1999);[115]

Herdeis (1999);[116] Fürstner (2000);[117] Genêt (2000);[118] Panek (2000);[119] Skrydstrup (2000);[120] Yadav (2002);[121] Raghavan (2006);[122] Aggarwal (2006);[123] Trost (2007);[124] Chattopadhyay (2008);[125] Panda (2008);[126] Hudlicky (2009);[127] Muthyala (2010);[128] Pérez–Luna (2011);[129] Sutherland (2012);[130] Kang (2012)[131] and Kumar (2013).[132] The formal syntheses of benzophenone moiety are diverse and can be enlisted as Hollinshead (1994);[105] Foglesong (1997);[133] Andersson (1999);[134] Skrydstrup (1999) [135] and Borate (2004).[136]

From these literature procedures available for balanol synthesis, Nicolaou's protocol for the benzophenone fragment and coupling it with azepane appears to be the most reproducible for the total synthesis of balanol and potential analogues, since it involves the well-established and high yielding reactions, in spite of a slightly longer reaction sequence. For the azepane core synthesis, Fürstner's protocol, in essence related to Tanner's synthesis, seems the most efficient since it establishes the desired *trans*–aminohydroxy stereochemistry in the first step with catalytic asymmetric epoxidation, which is followed by well-established high yielding reactions. Further, it enables access to the key azepane **2.7** with a functionalizable olefin. The Fürstner's protocol was followed with minor modifications in Sharpless epoxidation procedure. The synthetic route here involved asymmetric epoxidation of divinylcarbinol using cumene hydroperoxide instead of *tert*–butyl hydroperoxide, followed by benzyl protection of secondary alcohol. The epoxide ring was next opened by allylamine followed by Boc protection of secondary amine. The Boc protected diene intermediate was then cyclized-using ring closing metathesis followed by Mitsunobu reaction to get azepane **2.7**.

1.2.3 Biological Activity of Balanol

In 1995, Koide et al. investigated the biological activity of balanol and its analogues. The results indicated that along with PKCs, balanol is also a potent inhibitor of cyclic AMP–

dependent protein kinase (PKA).[137] It was shown that the balanol competes with ATP for binding to PKA or PKC while the inhibition could be overcome by higher concentrations of ATP. Furthermore, the comparison between an X–ray crystal structure of balanol (**1.1**) or ATP bound to PKA clearly demonstrated that balanol acts as an ATP mimic.[138] In particular, the *p*–hydroxybenzamide group (A–ring) replaces the adenine ring in the ATP pocket, the hexahydroazepine ring (B–ring) occupies the ribose–binding sub–site, and the benzophenone group (C– and D–rings) mimics the triphosphate portion of ATP, although it occupies a slightly different region in this part of the ATP pocket that is highly flexible and partly solvent exposed (Figure 1.8). Compared to ATP, balanol is a stronger binder to the ATP site by 3000 fold.[137]

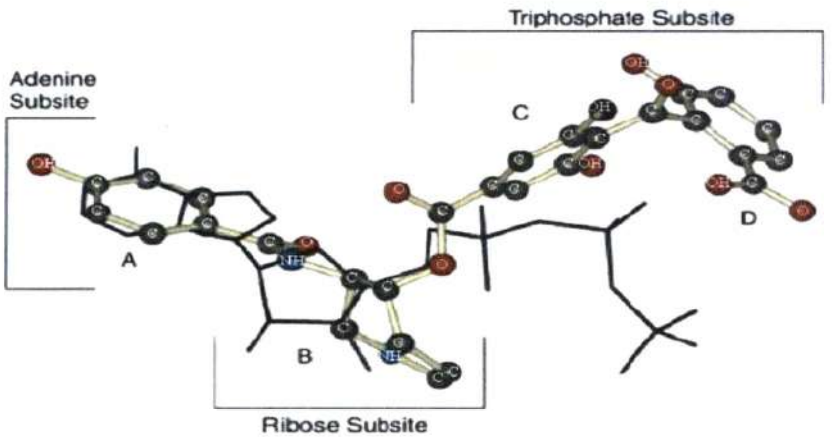


Figure 1.8. Balanol and ATP superposition: ATP (black stick) and balanol (ball and stick model).[138]

1.2.4 Balanoids – Chemical Diversity and SARs

Many balanol analogues have been designed not only to achieve PKC selectivity (or even PKC isozyme selectivity) but also to improve physical properties resulting in better cellular activity and bioavailability.[139] Modifications mostly occur in the benzophenone part (ring C and D), azepane moiety (ring A and B) or in the ester and amide linkages.

1.2.4.1 Modifications of the Benzophenone Fragment

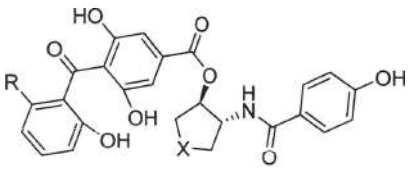


Table 1.3. Summary of Heerding and Crane's modifications in benzophenone fragment.[140]

Entry	X	R	Kinase enzyme assays IC_{50} (μM)					
			PKA	α	βII	δ	ε	η
1	$(CH_2)_2NH$	COOH	na	0.074	0.044	0.032	0.049	0.022
2	CH_2	COOH	na	0.04	0.05	0.0009	0.05	0.0006
3	CH_2	COOMe	na	0.21	0.04	0.005	0.3	0.004
4	CH_2	COOEt	na	0.92	1.6	0.067	0.66	0.0052
5	NH	COOH	na	0.022	0.033	0.005	0.01	0.004
6	NH	COOMe	na	0.25	0.29	0.018	0.17	0.016
7	CH_2	CF_3SO_2NH	4.6	0.1	0.05	<0.05	0.31	na
8	CH_2	CH_3SO_2NH	4.3	0.45	0.15	0.03	2.0	na

na = not tested.

Crane *et al.*,[140b] (1995) in an effort to enhance the cellular activity of balanol, prepared and evaluated a series of benzophenone ester analogues of varying steric size and hydrolytic stability. The results suggested that small alkyl esters and the pivaloyloxymethyl ester analogues improved cellular PKC inhibition. However, PKC selectivity over PKA was unclear since no PKA inhibition data were reported in this study. It was demonstrated that balanol analogue with cyclopentane replacement has comparable inhibitory activity against PKC isozymes (entry 1–6; Table 1.3).

Heerding and coworkers[140a] (1995) designed the first balanol analogues bearing carboxylic acid replacements (ring D) (amides, sulfonamide and tetrazoles) and evaluated them for PKC inhibitory activity (entry 7–8; Table 1.3). The replacement of carboxylic acid group with proton and hydroxyl group reduced activity, whereas analogues with acidic proton ($pKa \leq 7.6$) retained PKC inhibitory activity with better selectivity over PKA. This study highlighted importance of acidic proton on the benzophenone fragment. The replacement with

sulfonamide resulted in retention of inhibitory activity against only PKCδ comparable to that of balanol (entry 8; Table 1.3) while reducing the inhibition of the other isozymes. Heerding and Cranes' analogues had the azepane ring replaced with a five–membered ring to overcome synthetic difficulties and improve physical properties.[140]

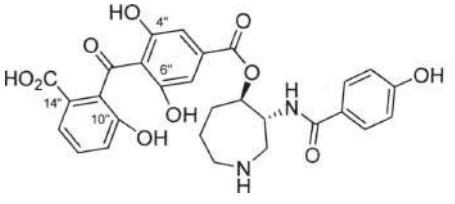


Table 1.4. Summary of Nicolaou's modifications in benzophenone fragment.[100b,137,141]

Kinase(K_i nM)	Balanol	10"–deoxy	14"–decarboxy	4",6"–dideoxy
PKA	4.7 ± 1.3	3.9	11	3.4
PKC	5.3 ± 1.8	640	5000	80

Nicolaou and coworkers[100b,137,141] (1995) also reported synthesis and activity of deoxy– and decarboxybalanol analogues, which resulted in higher PKA selectivity over PKC (Table 1.4). More recently, Lampe and coworkers[142] (2002) reported a series of more than 40 balanol analogues with modified benzophenone substituents in order to reduce the polarity of balanol. The modifications included planer benzophenone, cyclohexane or naphthalene ring instead of phenyl ring and amide linkage between two phenyl rings. The results suggested that the benzophenone moiety is important for obtaining potent PKC inhibition and modifications on this lead to selective PKA inhibitors. In particular, and in agreement with earlier proposals, it was found that replacement of the benzophenone carboxylate with bioisosteric equivalents could lead to potent analogues.[140] Moreover, it was uncovered that lipophilic substituents on the ring D are well tolerated. None of the designed analogues[142] was more potent than balanol,

although several of them were, for the first time, selective over PKCα, PKCβII and PKCε isozymes.

1.2.4.2 Modifications of the Perhydroazepane Moiety

Lai and coworkers[143] (1995) had reported several modifications of the perhydroazepane ring (Table 1.5). Firstly, in a series of seven balanol analogues the perhydroazepine ring was replaced by a pyrrolidine or substituted cyclopentane ring was studied[143a] as shown earlier by Heerding and Crane.[140]

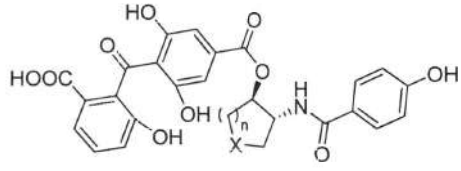


Table 1.5. Highlight of Lai's modifications in azepane moiety.[143a,143d]

Entry	X	n	PKC IC_{50} (μM)							
			α	βI	βII	γ	δ	ε	η	ζ
1	CH_2	3	0.27	0.22	0.43	0.06	0.09	0.28	0.06	>150
2	NH	2	5.1	2.2	4.7	2.2	0.05	1.8	0.08	>150
3	NH	1	0.022	0.017	0.033	0.013	0.005	0.01	0.004	>0.15
4	CH_2	1	0.04	0.04	0.05	0.01	0.0009	0.05	0.0006	22
5	O	3	6.7	2.5	3.3	1.0	0.09	16	0.01	>150
6	S	3	3.3	3.8	2.4	1.0	0.09	5.9	0.10	121
7	SO_2	3	9.6	5.2	3.6	4.3	4.0	45	0.83	>150
8	CH_2	3	0.27	0.22	0.43	0.06	0.09	0.28	0.06	>150

Interestingly, these cyclopentane–based analogues were found to be, in general, more potent PKC inhibitors than balanol itself. However, the isozyme selectivity was also better than balanol with more potency for PKCδ and PKCη (entry 4, Table 1.5). Unfortunately, again the PKA inhibitory profile was not presented. Subsequently, Lai and Stamper[143d] (1995) focused on perhydroazepine N atom replacement with other heteroatoms such as O, S, or C. The analogues with O and S atoms demonstrated enhanced PKC isozyme selectivity, despite the

general trend of being less potent relative to balanol. These studies concluded that the size and nature of the ring at the perhydroazepine position were crucial for potency. Moreover, a five–membered ring is favored over a seven–membered ring for the PKC inhibitory activity in the balanol series. A related publication by Lai et al.[143c] (1997) further showed that the perhydroazepine ring can be replaced by its surrogate that can hold the two aromatic side chains in a stereochemically correct manner. Mendoza[144] and Defauw[145] replaced the azepane ring with conformationally constrained bi–/tricyclic heterocycles and acyclic moieties, respectively. In general, these analogues retained PKC inhibitory potency and improved PKC inhibition over PKA. However, the PKC isozyme selectivity remained limited, although some analogues showed selectivity for PKCδ and PKCη (entry 4, Table 1.5).

Hu and coworkers[146] (1996) replaced the perhydroazepine ring with an indane scaffold which improved PKC inhibition and also showed excellent selectivity for PKC over PKA. In the subsequent publication,[147] the authors synthesized and evaluated analogues with varying substitution on *p*–hydroxybenzamide moiety. In general, these inhibitors were found to be less potent than balanol, but a number of analogues were identified with improved isozyme selectivity. This study concluded that the 4–hydroxy group, amide linkage and the conformation associated with the benzamide moiety appear to have a profound effect on PKC inhibition.

1.2.4.3 Modifications of the Ester/Amide Linkages

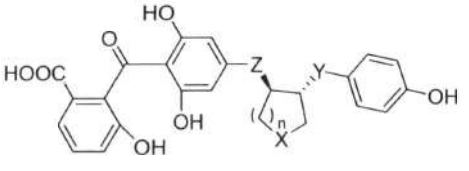


Table 1.6. Summary of Jagdmann's modifications in ester/amide linkages.[148]

Entry	X	n	Y	Z	PKC IC_{50} (μM)						
					α	βI	βII	γ	δ	ε	η
1	NH	3	NHCO	C(O)NH	3.2	0.63	1.2	0.42	0.22	0.67	0.05
2	NH	3	NHCO	$C(O)N(CH_3)$	>50	>50	>50	>50	42	>50	31
3	NH	1	NHCO	C(O)NH	0.92	0.22	0.33	0.33	0.012	0.08	0.003
4	CH_2	1	NHCO	CH_2O	0.46	0.43	0.29	1.1	0.02	0.37	0.03
5	CH_2	1	NHCO	$C(O)OCH_2$	0.04	0.04	0.03	0.3	0.02	0.34	0.02
6	CH_2	1	NHCO	$C(O)NHCH_2$	35	17	4.9	46	0.33	>50	2.3
7	NH	1	CH_2	C(O)O	0.26	0.01	0.03	0.04	0.005	1.8	0.02
8	CH_2	1	O	C(O)O	0.22	0.02	0.02	0.25	0.02	0.24	0.01
9	CH_2	1	CH_2	C(O)O	0.03	0.004	0.003	0.04	0.005	0.12	0.003

Jagdmann and coworkers[148a] (1995) concentrated on the ester and amide linkages of balanol (Table 1.6). They replaced the ester linkage (between ring B and C) with amide, methylene or methylenoxy groups. Although these analogues displayed lower activity, they were more stable to serum esterases. Additional analogues[148b] with replacement of the carboxamide linkage (between ring A and B) by a single atom bridging unit suggested that the methylene linker in concert with a cyclopentane skeleton improves PKC isozyme inhibition and selectivity for PKC over PKA (entry 4, Table 1.6). Moreover, these analogues also displayed good cellular activity, which was further enhanced when the carboxylate moiety was masked as a methyl ester.

To sum up, extensive chemical diversification of balanol molecule has revealed that the benzophenone fragment (especially the acidic COOH proton) and 4–hydroxybenzamide moieties are essential for the PKC inhibitory activity and are sensitive to the diversification. However, the central azepane core can tolerate a wide variety of chemical modifications. Few analogues to date exhibited single isozyme selectivity. This suggests the necessity of development of new chemical diversity space to address the question of isozyme selectivity.

1.3 Fluorine: A Tool for Conformation Coupled Chemical Diversity

Amongst naturally occurring organohalides, fluorinated compounds are the least abundant[149] and fluorine is virtually absent in natural molecules of medicinal interest.[150] In 1957, the first fluorinated drug 5–fluorouracil was discovered. Since then, over 150 fluorinated drugs have been approved and now fluorinated drugs make up ~20% of pharmaceuticals[151] and up to 30% of agrochemicals.[151b] Noticeably, 1/3rd of top selling drugs contain at least one fluorine atom(s).[152] The structures of top selling fluorinated drugs such as the anti–depressant fluoxetine (Prozac),[153] the cholesterol lowering drug atorvastatin (Lipitor),[154] and the antibacterial ciprofloxacin (Ciprobay)[155] are presented in the Figure 1.9.

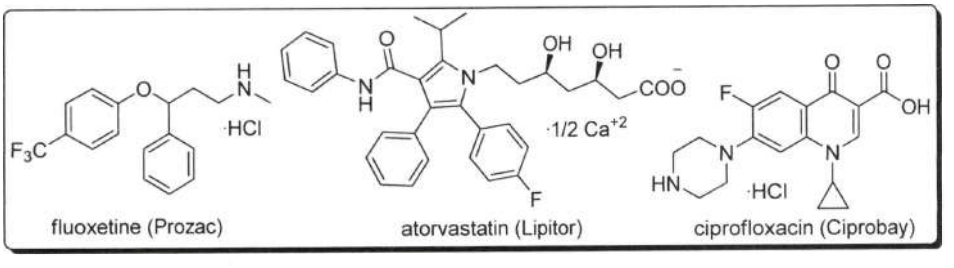


Figure 1.9. Top selling fluorinated drugs.

1.3.1 Stereoelectonic Effects of Fluorine

The success of organofluorine compounds in chemical industries ranging from pharmaceuticals and agrochemicals to polymers and fine chemicals is striking. It has been recognized for many years that hydrogen substitution with fluorine can lead to profound changes in physical, chemical and biological properties.[156] More recently the influence of fluorine substitution on conformation is gaining interest amongst organofluorine chemists.[156j] Fluorine has an atomic size (1.47 Å) intermediate between hydrogen (1.20 Å) and oxygen (1.52 Å) meaning that hydrogen replacement with fluorine should not dramatically affect the overall molecular size.[157] However, being the most electronegative element, fluorine makes the C–F bond highly polarized and significantly different from the C–H bond.[157a,158] C–F bond

is short and strong bond with significant ionic character imparted by attraction of partial positive and partial negative charges on carbon and fluorine atoms, respectively.[156j] This polarized C–F bond results in unique conformational effects because of (i) dipole–dipole interactions, (ii) charge–dipole interactions, and (iii) hyperconjugation effects.

(i) Dipole–dipole interactions:

The polarized C–F bond is anticipated to electrostatically interact with its environment. Such interactions have been observed in fluorinated drug–receptor interactions (Figure 1.10A). For instance, fluorinated drugs can bind their receptors with the orientation favoring the interaction of fluorine with a partially positive amide carbon (**1.69**) or acidic hydrogen (**1.70**).[156a,156b] However, such intermolecular electrostatic interactions are quite weak.[157a] Significantly stronger electrostatic dipole effects can also occur intramolecularly. For example, α–fluorocarbonyl compounds (**1.71–1.74**) show strong preference for the conformation with the C–F bond antiparallel to C=O bond.[157a] Along with stabilizing some conformations, the dipole–dipole interactions can also destabilize some other conformations. For instance, 1,3–difluoroalkanes (**1.75b**) prefer to twist to avoid a parallel alignment (repulsion) of two C–F bonds.[159]

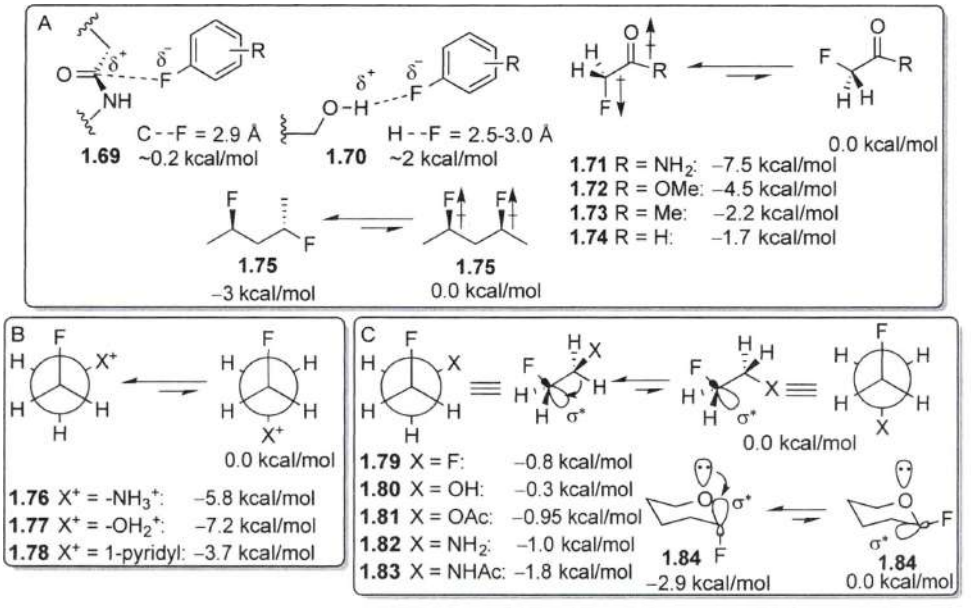


Figure 1.10. Conformational effects of fluorine: (A) dipole–dipole interactions, (B) charge–dipole interactions, (C) hyperconjugation effects.[156j]

(ii) Charge–dipole interactions:

The presence of a formally charged neighbouring group enhances C–F electrostatic interactions (Figure 1.10B).[160] The C–F bond allows the molecule to prefer the conformation in which $F^{\delta-}$ is in close proximity to the formal positive charge. For example, in the cases of 2–fluoroethyl ammonium ion (**1.76**), protonated 2–fluoroethanol (**1.77**) and 2–fluoroethylpyridinium ion (**1.78**), the *gauche* conformers are strongly preferred because in such conformations $F^{\delta-}$ is in close proximity to N^{+}.[161]

(iii) Hyperconjugation effects:

This effect can clearly be explained by the simple example of 1,2–difluoroethane (**1.79**). NMR and molecular modeling studies suggest that the *gauche* conformer is more stable than the *anti* which is contrary to an explanation by electron repulsion that fluorine atoms should repel each other to prefer the *anti* conformer. What effect overrides the difluoro repulsion and stabilizes the *gauche* conformer? In the *gauche* conformer of **1.79**, both of the vacant low–energy σ^*_{CF}

orbitals are aligned with adjacent C–H bonds for hyperconjugation.[157a,158] Such effect renders the C–F bond longer and less covalent. There are other explanations for the *gauche* preference such as the "bent bond" theory[162]; however hyperconjugation is widely accepted.[157a] The *gauche* effect is very general and applicable to a variety of systems (Figure 1.10C, **1.80–1.83**) such as F–C–C–O and F–C–C–N groups.[161–163] The hyperconjugation effect is also applicable to lone pairs (**1.84**)[158,164] and π–systems[165] along with σ bonds.

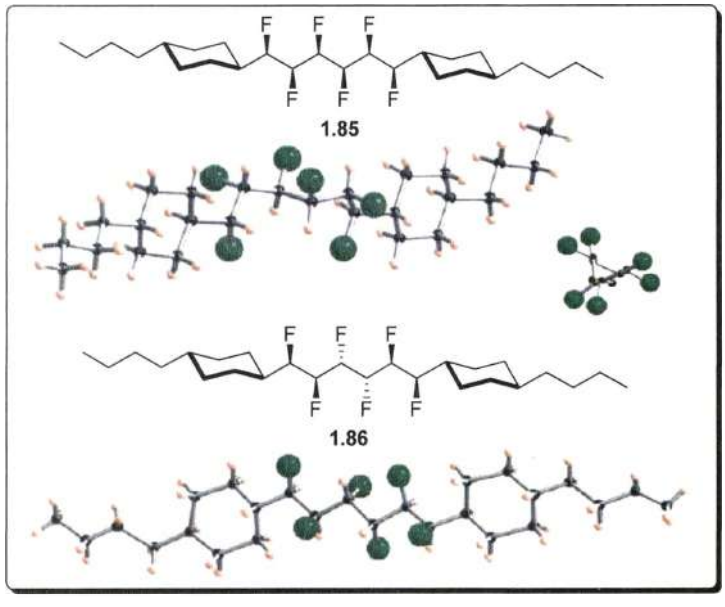


Figure 1.11. X–ray crystal structures of fluoroalkanes diastereomers **1.85** and **1.86**.[166]

O'Hagan and coworkers have pioneered work on the synthesis and stereoelectronic effects (*gauche* effect) in multi–vicinal fluoroalkanes.[166–167] The complex stereochemical effects have been explored with compounds containing up to six vicinal fluorines and the results suggests two main preferences in general. (i) parallel 1,3–C–F bonds are avoided and (ii) *gauche* 1,2–C–F bonds are favored. For instance, *syn*–hexafluoroalkane **1.85** adopts the helical shape with *gauche* alignment of each vicinal fluorines and without parallel 1,3–C–F bonds to avoid difluoro repulsion.[166] In contrast, the diastereomer **1.86** acquires the zigzag conformation with three out of five possible *gauche* alignments and no 1,3–difluoro repulsions.

1.3.2 C–F bond Formation Methodology

The increasing demand of enantiomerically pure fluorinated bioactive molecules presents significant challenges in making a stereogenic C–F bond.[158,168] Such C–F bond formation can be achieved mainly in two ways: (i) Electrophilic fluorination, utilizing F^+ reagents; and (ii) Nucleophilic fluorination involving a negatively charged fluoride ion. The overview of most

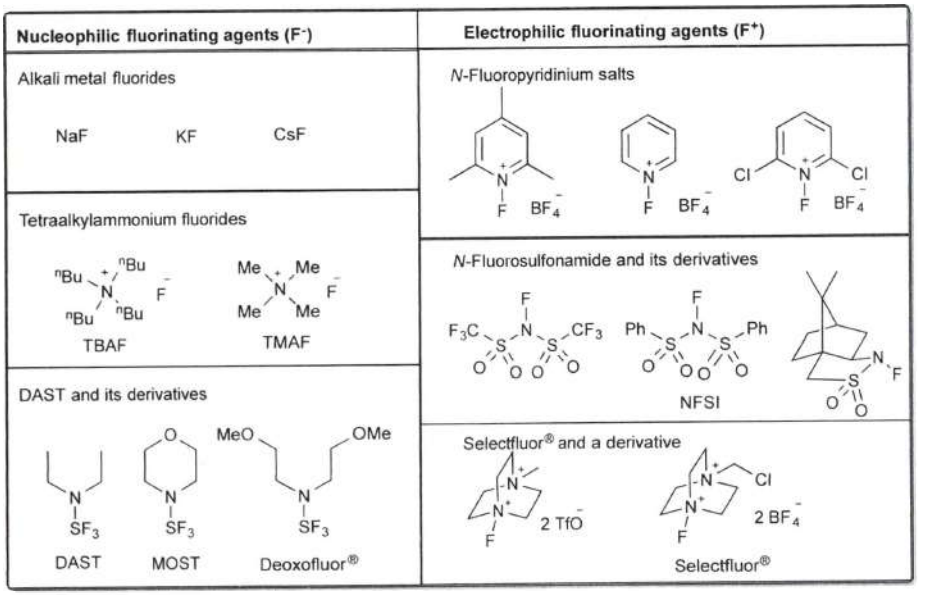


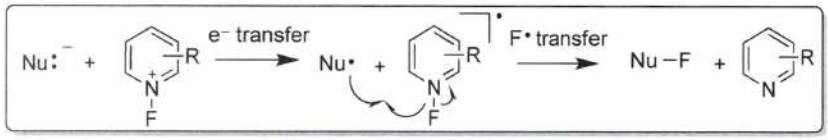
Figure 1.12. Most commonly used commercially available fluorinating reagents.[172]

commonly used commercially available fluorinating agents is presented in Figure 1.12.

(i) Electrophilic fluorination:

Elemental fluorine is essentially an electrophilic fluorinating agent. However, its high reactivity, lack of selectivity and toxicity limits its use.[169] Nevertheless diluted F_2 in an inert gas such as N_2 or argon under controlled conditions has been successfully used in the synthesis of 5–fluorouracil.[170] In 1970s, organofluoroxy reagents (RO–F) such as acetyl hypofluorite[171] were used for aromatic ring fluorination,[173] addition to double bonds,[174] α–fluorination of carboxylic acids[175] and lithium enolates fluorinations.[176] The electrophilic

fluorination grew rapidly with the development of *N*–F reagents offering the advantages of improved selectivity and ease of handling. The *N*–F reagents can be categorized in mainly 3 subgroups:



Scheme 1.13. Single electron transfer mechanism for electrophilic fluorination.

(a) *N*–fluoropyridinium triflates and derivatives: mostly developed by Umemoto and coworkers (1980s).[177] They have been employed in fluorination of aromatic rings, carbanions, enol ethers and their derivatives. Their reactivity and selectivity largely depends on the type of ring substituents and counter ions.[177] The substituents that decrease electron density in the N^+–F bond enhances the fluorinating power. Several counter ions have also been explored and triflate resulted in the best reactivity.[177c] One potential mechanism for fluorination with *N*–fluoropyridinium salts involves a single–electron transfer process (Scheme 1.13).[172]

(b) The sulfonyl derivatives $RSO_2N(F)R'$: studied extensively by Barnette *et al.* (1984).[178] In contrast to other electrophilic fluorinating agents, *N*–fluorosulfonimides are neutral and are easy to handle.

(c) Selectfluor® and its derivatives (Figure 1.12) developed by Banks and coworkers (1988).[179] Though air sensitive, this group of compounds, with tunable reactivity, has been extensively utilized for fluorination of aryl groups, nucleosides,[180] steroids,[181] other building blocks and diverse organic substrates.[182]

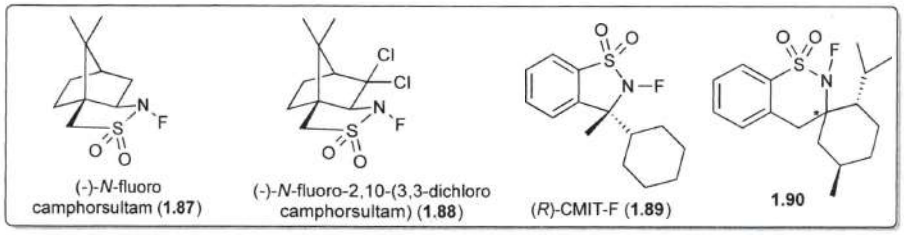


Figure 1.13. Chiral *N*–fluorosultams.

Following the development of highly efficient electrophilic fluorinating reagents the next challenge was asymmetric fluorination. Differing *et al.*[183] (1988) (**1.87**) described the first enantio–selective fluorination reaction, followed by Davis[184] (**1.88**) and Takeuchi[185] (**1.89**, **1.90**), using chiral *N*–fluorosultams (Figure 1.13). Several other chiral Selectfluor® derivatives have been developed and explored mainly by Banks,[186] Shibata,[187] Cahard[188] and Gouverneur.[189]

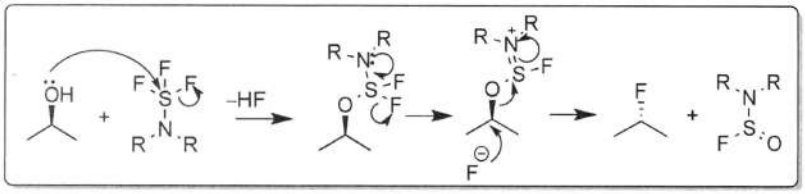
(ii) Nucleophilic fluorination:

A wide variety of inorganic and organic fluorides are available such as LiF,[190] CsF,[191] NaF,[192] KF,[193] and TBAF.[194] These fluorides however suffer from interactions with solvents. In protic solvents they are strongly solvated; whereas tight ion pair formation limits their use in aprotic solvents.

Another class of reagents is HF and derivatives such as $Et_3N{\cdot}HF$ and Olah's reagent (pyridine·9HF).[195] Such derivatives have been widely employed for the nucleophilic fluorinations; however these require activated substrates as the nucleophilicity is compromised by the presence of base.

Nucleophilic fluorination was widely developed after the appearance of diethylaminosulfur trifluoride (DAST) (Figure 1.12), developed by Middleton *et al.* (1975).[196] DAST has emerged as an efficient deoxyfluorinating agent for mono and difluorination of alcohols, ketones, aldehydes and carboxylic acids under mild conditions. Lal and coworkers[197] developed

Deoxofluor® as an alternative to DAST with similar use and the advantage of being nonexplosive. The deoxyfluorination mechanism follows the S_N2 pathway with inversion of stereochemistry at the participating stereo–center. First the nucleophilic oxygen (hydroxyl group) attacks on the DAST sulfur and liberates fluoride ion. Subsequently, this fluoride attacks the carbon bearing the X–S–O^+ group and displaces it (Scheme 1.14).



Scheme 1.14. S_N2 mechanism for nucleophilic deoxyfluorination.

Several other deoxyfluorinating agents have also been developed recently (Figure 1.14) such as perfluoro–1–butanesulfonyl fluoride (PBSF) (**1.91**),[198] 2,2–difluoro–1,3–dimethyl–imidazolidine (DFI) (**1.92**), tetrafluoroethyldimethylamine (TFEDMA) (**1.93**),[199] Ishikava's reagent (**1.94**),[200] and Fluolead™ (**1.95**).

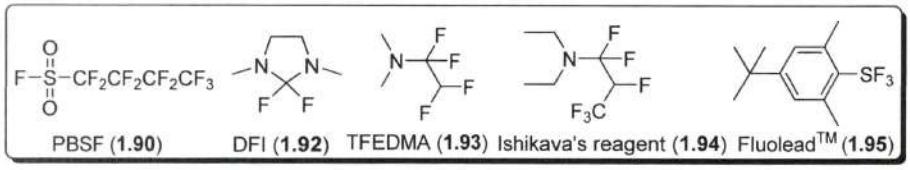


Figure 1.14. Recent deoxyfluorinating agents.

1.3.3 Key Examples of Fluorination in Biological Activity Tuning

It is known that if a ligand is pre–organized into the correct conformation, its binding affinity is enhanced and the fluorine atom can be used to impart conformational preferences in such molecules.[156a,201] Recently, stereogenic C–F bonds have been used for conformational tuning of biologically active compounds. For example, Merck's HIV protease inhibitor Indinavir (**1.96**) is a functionalized pseudopeptide with a central hydroxyethylene moiety. X–ray

crystallography studies of **1.96** in a bound form with its HIV protease target revealed that this central hydroxyethylene moiety acquired an extended zigzag conformation.[202] To investigate further, Myers *et al.* synthesized and screened monofluoro analogues **1.97** and **1.98** (Figure 1.15).[203] The results suggested analogue **1.97** was equipotent to Indinavir (**1.96**) while its diastereomer **1.98** was 14–fold less active. These results can be explained by inherent conformational preferences due to the F–C–C–O *gauche* effect in both the analogues. In **1.97**, this *gauche* effect reinforces

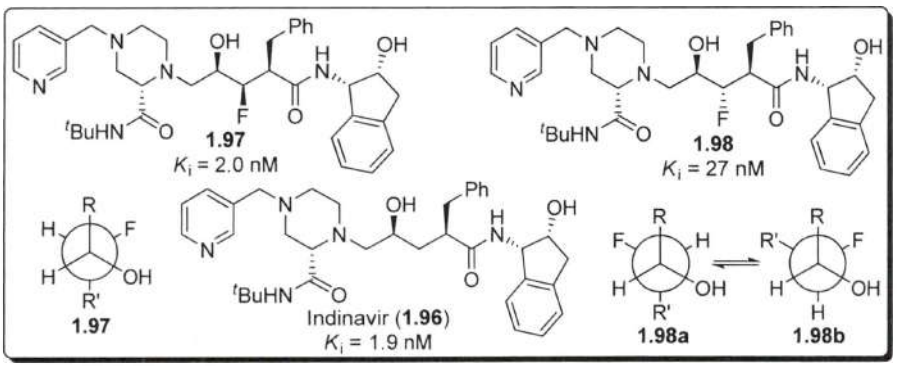


Figure 1.15. HIV protease inhibitor Indinavir (**1.96**) and fluorinated analogues **1.97** and **1.98**.[156j]

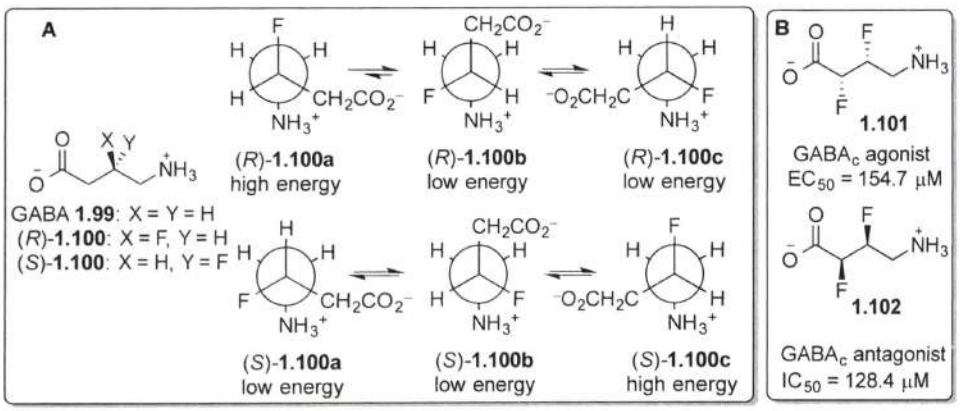


Figure 1.16. (A) Neurotransmitter GABA (**1.99**) and fluorinated analogues (*R*)–**1.100** and (*S*)–**1.100**; (B) Hunter's GABA analogues.[156j,204]

the desired zigzag conformation while the zigzag conformation is destabilized by *gauche* effect in **1.98** (Figure 1.15).

GABA (γ–aminobutyric acid, **1.99**, Figure 1.16) is an important neurotransmitter with three freely rotatable C–C bonds. Because of its flexibility GABA binds to several protein targets. Fluorine substitution on GABA was used as a tool to uncover the binding conformations of GABA by O'Hagan and coworkers.[205] In general the GABA molecule can have three staggered conformations around the C3–C4 bond. In the monofluoro analogues (*R*)–**1.100** and (*S*)–**1.100** there would be preference for conformations supporting charge–dipole interactions between F and N^+. The biological activity data of **1.100** was then used to identify the correct binding conformation of the parent molecule GABA. For instance, both the enantiomeric analogues bound to $GABA_A$ synaptic receptor with equal potency[205a] meaning the extended conformer **b** (Figure 1.16A) is the binding conformation. As in both the enantiomers (*R*)–**1.100** and (*S*)–**1.100** conformer **b** gains about the same energy by the *gauche* F–C–C–N^+ alignment. In contrast, (*R*)–**1.100** enantiomer bound to GABA–aminotransferase enzyme with 10–fold higher affinity than (*S*)–**1.100**.[205b] These results suggest the involvement of a bent conformer **c** (Figure 1.16A) as binding mode, because in (*R*)–**1.100**, conformer **c** is favored because of stabilizing *gauche* F–C–C–N^+ alignment while conformer **c** is not favorable in (*S*)–**1.100**. Hunter et al.[204] extended this work by describing conformational behavior and GABA receptor activity of all stereoisomers of 2,3–difluoro–4–aminobutyric acid. The *syn*–enantiomers **1.101** and **1.102** (Figure 1.16B) were inactive against $GABA_A$ and $GABA_B$ while found to be agonist and antagonist of $GABA_C$ receptors, respectively.

Raines and coworkers have used fluorinated proline to synthesize shape–controlled collagen. Surprisingly, the replacement of the 4–(*R*)–hydroxyproline (**1.104**) residue by 4–(*R*)–fluoroproline (**1.105**)[206] increased the strength of the collagen triple helix (Figure 1.17). There were two main explanations for this observation: (i) inductive pull of fluorine lowers the

C(O)–N bond order[207] and reduces the energy barrier for *cis/trans* isomerization, which allows the peptide strand to align in the desired all–*trans* conformations favoring triple helix formation; (ii) in proline residues (**1.103**) the pyrrolidine moiety adopts a Cγ–*endo* ring pucker, while 4–(*R*)–fluoroproline (**1.105**) confers the Cγ–*exo* ring pucker benefitting from *gauche* F–C–C–N^+ alignment (Figure 1.17).[208] As a consequence, the *trans* amide is stabilized[209] and more importantly the C–F bond is projected antiparallel to three proximal C=O dipoles in triple helix which offers an extra strength to the helix.[208]

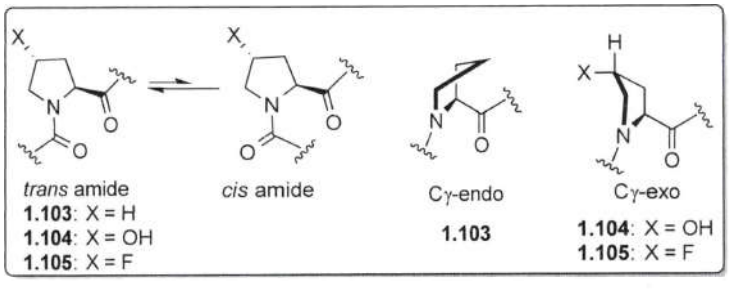


Figure 1.17. Effects of monofluorination on proline residue strengthening collagen.[156j]

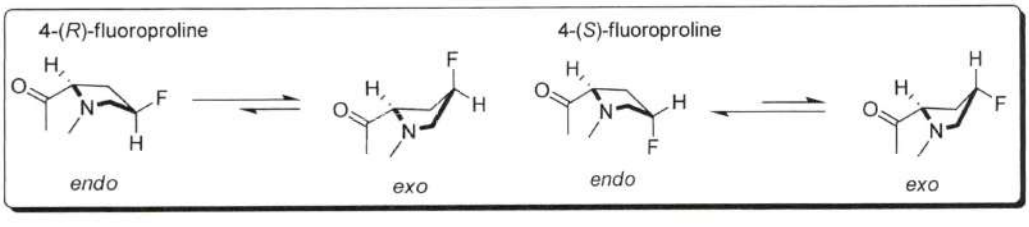


Figure 1.18. Conformational tuning of proline by stereospecific monofluorination.[210]

Zondlo and coworkers[210] have recently reported conformational tuning of proline by stereospecific monofluorination (Figure 1.18). The five–membered proline ring prefers the *exo* ring pucker in 4–(*R*)–fluoroproline while the 4–(*S*)–fluoroproline favors the *endo* ring pucker. The *exo/endo* conformational preference is conferred by the hyperconjugation effects.

In addition to the representative examples above, other important examples of fluorine–based activity tuning include fluorinated cholesteryl ester transfer protein,[211] nucleosides,[212]

dihydroquinidine,[213] insect pheromone,[214] amino acids,[215] opioid receptor binding peptides,[216] β–peptides[217] and capsaicin.[218] Fluorine–based activity tuning has also been demonstrated in organocatalysis[219] and liquid crystals.[166,220]

1.4 Project Outline

There is a current lack of PKC isozyme specific molecules to understand the roles of individual PKC isozymes in normal and diseased conditions and their ligand–receptor interactions. Several investigations have been carried out for isozyme specific PKC inhibitors with chemical modifications. However, there are only few PKC isozyme specific analogues available suggesting the need to examine new chemical diversity space.

The success story of Gleevec suggests that the potency and specificity of a ligand–receptor interaction depends on the interplay of conformations of the bioactive epitope and the target protein. Thus, it would be of interest to investigate means to conformationally control analogues of bioactive natural products such as (−)–balanol. Recently, fluorination has been developed as a tool to conformationally tune the molecular shapes and in turn their biological activity. This raises some possible questions: (i) can fluorination be used as a tool to generate conformation–coupled chemical diversity from (−)–balanol? (ii) what effects would fluorination have on balanol's activity profile against PKA/PKC isozymes?

The azepane moiety of balanol is a highly flexible ring structure, and previous modifications of balanol's azepane ring have led to analogues with altered activity profiles against PKA/PKC isozymes. There is no report available on the stereogenic fluorination on azepane rings. In addition, the highly substituted azepane ring may have unusual fluorination outcomes by neighbouring group effects. Moreover, the conformational effects of fluorination on

azepane ring are unknown. The fluorinated azepanes can be utilized as synthones for generating conformation–coupled chemical diversity.

To address these questions fluorinated balanol analogues were synthesized and subjected to biological activity screening. First, methodology for azepane monofluorination was established (chapter 2). The conformational flexibility of the azepane ring of (−)–balanol was investigated (chapter 3 and 4), and method for multiple fluorine installation on the azepane ring was also investigated (chapter 4 and 5). The synthesized fluoroazepanes were then transformed into fluorinated balanol analogues and tested for their activity against PKA/PKC isozymes (chapter 6).

1.5 References

(1) Manning, G.; Whyte, D. B.; Martinez, R.; Hunter, T.; Sudarsanam, S. *Science* **2002**, *298*, 1912.

(2) (a) Kinome Project, http://kinase.com/human/kinome/ (Accessed August 2013); (b) Cell Signaling Technology, http://www.cellsignal.com/reference/kinase/ (Accessed August 2013).

(3) Hanks, S. K.; Hunter, T. *FASEB J.* **1995**, *9*, 576.

(4) Pearce, L. R.; Komander, D.; Alessi, D. R. *Nat. Rev. Mol. Cell Biol.* **2010**, *11*, 9.

(5) (a) Carpten, J. D.; Faber, A. L.; Horn, C.; Donoho, G. P.; Briggs, S. L.; Robbins, C. M.; Hostetter, G.; Boguslawski, S.; Moses, T. Y.; Savage, S.; Uhlik, M.; Lin, A.; Du, J.; Qian, Y.–W.; Zeckner, D. J.; Tucker–Kellogg, G.; Touchman, J.; Patel, K.; Mousses, S.; Bittner, M.; Schevitz, R.; Lai, M.–H. T.; Blanchard, K. L.; Thomas, J. E. *Nature* **2007**, *448*, 439; (b) Manning, B. D.; Cantley, L. C. *Cell* **2007**, *129*, 1261; (c) Meek, D. W.; Knippschild, U. *Mol. Cancer Res.* **2003**, *1*, 1017; (d) Lin, H.–K.; Wang, G.; Chen, Z.; Teruya–Feldstein, J.; Liu, Y.; Chan, C.–H.; Yang, W.–L.; Erdjument–Bromage, H.; Nakayama, K. I.; Nimer, S.; Tempst, P.; Pandolfi, P. P. *Nat. Cell Biol.* **2009**, *11*, 420; (e) DeBerardinis, R. J.; Sayed, N.; Ditsworth, D.; Thompson, C. B. *Curr. Opin. Genet. Dev.* **2008**, *18*, 54.

(6) (a) Sano, H.; Kane, S.; Sano, E.; Miinea, C. P.; Asara, J. M.; Lane, W. S.; Garner, C. W.; Lienhard, G. E. *J. Biol. Chem.* **2003**, *278*, 14599; (b) Sakamoto, K.; Holman, G. D. *Am. J. Physiol.* **2008**, *295*, E29; (c) McManus, E. J.; Sakamoto, K.; Armit, L. J.; Ronaldson, L.; Shpiro, N.; Marquez, R.; Alessi, D. R. *EMBO J.* **2005**, *24*, 1571; (d) Li, X.; Monks, B.; Ge, Q.; Birnbaum, M. J. *Nature* **2007**, *447*, 1012; (e) Cho, H.; Mu, J.;

Kim, J. K.; Thorvaldsen, J. L.; Chu, Q.; Crenshaw, E. B., III; Kaestner, K. H.; Bartolomei, M. S.; Shulman, G. I.; Birnbaum, M. J. *Science* **2001**, *292*, 1728.

(7) (a) Yamamoto, S.; Sippel, K. C.; Berson, E. L.; Dryja, T. P. *Nat. Genet.* **1997**, *15*, 175; (b) Cideciyan, A. V.; Zhao, X.; Nielsen, L.; Khani, S. C.; Jacobson, S. G.; Palczewski, K. *Proc. Natl. Acad. Sci. U. S. A.* **1998**, *95*, 328; (c) Schiebel, K.; Winkelmann, M.; Mertz, A.; Xu, S.; Page, D. C.; Weil, D.; Petit, C.; Rappold, G. A. *Hum. Mol. Genet.* **1997**, *6*, 1985; (d) Trivier, E.; De, C. D.; Jacquot, S.; Pannetier, S.; Zackai, E.; Young, I.; Mandel, J.–L.; Sassone–Corsi, P.; Hanauer, A. *Nature* **1996**, *384*, 567.

(8) Arencibia, J. M.; Pastor–Flores, D.; Bauer, A. F.; Schulze, J. O.; Biondi, R. M. *Biochimica et Biophysica Acta (BBA) – Proteins and Proteomics* **2013**, *1834*, 1302.

(9) Inoue, M.; Kishimoto, A.; Takai, Y.; Nishizuka, Y. *J. Biol. Chem.* **1977**, *252*, 7610.

(10) Jaken, S. *Curr. Opin. Cell Biol.* **1996**, *8*, 168.

(11) Yoshida, Y.; Huang, F. L.; Nakabayashi, H.; Huang, K. P. *J. Biol. Chem.* **1988**, *263*, 9868.

(12) Jaken, S. *BioEssays* **2000**, *22*, 245.

(13) Newton, A. C. *J. Biol. Chem.* **1995**, *270*, 28495.

(14) Gould, C. M.; Newton, A. C. *Curr. Drug Targets* **2008**, *9*, 614.

(15) Kikkawa, U.; Nishizuka, Y. *Ann. Rev. Cell Biol.* **1986**, *2*, 149.

(16) Nishizuka, Y. *Science* **1992**, *258*, 607.

(17) Grandy, S.; Czernik, A. J.; Greengard, P. *Proc. Natl. Acad. Sci. USA* **1988**, *85*, 6218.

(18) Mochly–Rosen, D.; Das, K.; Grimes, K. V. *Nat. Rev. Drug Discovery* **2012**, *11*, 937.

(19) Konopatskaya, O.; Poole, A. W. *Trends Pharmacol. Sci.* **2010**, *31*, 8.

(20) Sledge, G. W., Jr.; Gokmen–Polar, Y. *Semin. Oncol.* **2006**, *33*, S15.

(21) Basu, A.; Pal, D. *TheScientificWorldJOURNAL* **2010**, *10*, 2272.

(22) Gorin, M. A.; Pan, Q. *Mol. Cancer* **2009**, *8*, 9.

(23) Kim, K.–M.; Kang, D. W.; Moon, W. S.; Park, J. B.; Park, C. K.; Sohn, J. H.; Jeong, J. S.; Cho, M.–Y.; Jin, S.–Y.; Choi, J. S.; Kang, D. Y. *Mod. Pathol.* **2006**, *19*, 1480.

(24) Kraft, A. S.; Anderson, W. B.; Cooper, H. L.; Sando, J. J. *J. Biol. Chem.* **1982**, *257*, 3193.

(25) Geraldes, P.; King, G. L. *Circ. Res.* **2010**, *106*, 1319.

(26) Lee, S. K.; Chung, J. I.; Park, M. S.; Joo, H. K.; Lee, E. J.; Cho, E. J.; Park, J. B.; Ryoo, S.; Irani, K.; Jeon, B. H. *Cardiovasc. Res.* **2011**, *91*, 502.

(27) Bezy, O.; Tran, T. T.; Pihlajamaki, J.; Suzuki, R.; Emanuelli, B.; Winnay, J.; Mori, M. A.; Haas, J.; Biddinger, S. B.; Leitges, M.; Goldfine, A. B.; Patti, M. E.; King, G. L.; Kahn, C. R. *J. Clin. Invest.* **2011**, *121*, 2504.

(28) Inagaki, K.; Hahn, H. S.; Dorn, G. W.; Mochly–Rosen, D. *Circulation* **2003**, *108*, 869.

(29) Inagaki, K.; Churchill, E.; Mochly–Rosen, D. *Cardiovasc. Res.* **2006**, *70*, 222.

(30) Liu, Q.; Molkentin, J. D. *J. Mol. Cell. Cardiol.* **2011**, *51*, 474.

(31) Ferreira, J. C. B.; Brum, P. C.; Mochly–Rosen, D. *J. Mol. Cell. Cardiol.* **2011**, *51*, 479.

(32) Bowman, J. C.; Steinberg, S. F.; Jiang, T.; Geenen, D. L.; Fishman, G. I.; Buttrick, P. M. *J. Clin. Invest.* **1997**, *100*, 2189.

(33) Sadeh, J. S.; Rudikoff, D.; Gordon, M. L.; Bowden, J.; Goldman, B. D.; Lebwohl, M. *Arch. Dermatol.* **1997**, *133*, 747.

(34) Sweitzer, S. M.; Wong, S. M. E.; Peters, M. C.; Mochly–Rosen, D.; Yeomans, D. C.; Kendig, J. J. *J. Pharmacol. Exp. Ther.* **2004**, *309*, 616.

(35) Limnander, A.; Depeille, P.; Freedman, T. S.; Liou, J.; Leitges, M.; Kurosaki, T.; Roose, J. P.; Weiss, A. *Nat. Immunol.* **2011**, *12*, 425.

(36) Boschelli, D. H. *Curr. Top. Med. Chem.* **2009**, *9*, 640.

(37) Bright, R.; Steinberg, G. K.; Mochly–Rosen, D. *Brain Res.* **2007**, *1144*, 146.

(38) Bright, R.; Sun, G.–H.; Yenari, M. A.; Steinberg, G. K.; Mochly–Rosen, D. *Neurosci. Lett.* **2008**, *441*, 120.

(39) Zarate, C. A.; Manji, H. K. *CNS Drugs* **2009**, *23*, 569.

(40) Einat, H.; Yuan, P.; Szabo, S. T.; Dogra, S.; Manji, H. K. *Neuropsychobiology* **2007**, *55*, 123.

(41) Cole, D. C.; Asselin, M.; Brennan, A.; Czerwinski, R.; Ellingboe, J. W.; Fitz, L.; Greco, R.; Huang, X.; Joseph–McCarthy, D.; Kelly, M. F.; Kirisits, M.; Lee, J.; Li, Y.; Morgan, P.; Stock, J. R.; Tsao, D. H. H.; Wissner, A.; Yang, X.; Chaudhary, D. *J. Med. Chem.* **2008**, *51*, 5958.

(42) Langlois, A.; Chouinard, F.; Flamand, N.; Ferland, C.; Rola–Pleszczynski, M.; Laviolette, M. *J. Leukocyte Biol.* **2009**, *85*, 656.

(43) Kanthasamy, A. G.; Anantharam, V.; Zhang, D.; Latchoumycandane, C.; Jin, H.; Kaul, S.; Kanthasamy, A. *Free Radical Biol. Med.* **2006**, *41*, 1578.

(44) Bradshaw, D.; Hill, C. H.; Nixon, J. S.; Wilkinson, S. E. *Agents Actions* **1993**, *38*, 135.

(45) Hidaka, H.; Inagaki, M.; Kawamoto, S.; Sasaki, Y. *Biochemistry* **1984**, *23*, 5036.

(46) (a) Kimura, K.; Ito, M.; Amano, M.; Chihara, K.; Fukata, Y.; Nakafuku, M.; Yamamori, B.; Feng, J.; Nakano, T.; et, a. *Science* **1996**, *273*, 245; (b) Uehata, M.; Ishizaki, T.; Satoh, M.; Ono, T.; Kawahara, T.; Morishita, T.; Tamakawa, H.; Yamagami, K.; Inui, J.; Maekawa, M.; Narumiya, S. *Nature* **1997**, *389*, 990.

(47) Cohen, P.; Frame, S. *Nat. Rev. Mol. Cell Biol.* **2001**, *2*, 769.

(48) Toullec, D.; Pianetti, P.; Coste, H.; Bellevergue, P.; Grand–Perret, T.; Ajakane, M.; Baudet, V.; Boissin, P.; Boursier, E.; et, a. *J. Biol. Chem.* **1991**, *266*, 15771.

(49) (a) Alessi, D. R. *FEBS Lett.* **1997**, *402*, 121; (b) Davies, S. P.; Reddy, H.; Caivano, M.; Cohen, P. *Biochem. J.* **2000**, *351*, 95.

(50) Cohen, P. *Nat. Rev. Drug Discovery* **2002**, *1*, 309.

(51) Schindler, T.; Bornmann, W.; Pellicena, P.; Miller, W. T.; Clarkson, B.; Kuriyan, J. *Science* **2000**, *289*, 1938.

(52) (a) Buchdunger, E.; Zimmermann, J.; Mett, H.; Meyer, T.; Mueller, M.; Druker, B. J.; Lydon, N. B. *Cancer Res.* **1996**, *56*, 100; (b) Druker, B. J.; Tamura, S.; Buchdunger, E.; Ohno, S.; Segal, G. M.; Fanning, S.; Zimmermann, J.; Lydon, N. B. *Nat. Med.* **1996**, *2*, 561; (c) Druker, B. J.; Talpaz, M.; Resta, D. J.; Peng, B.; Buchdunger, E.; Ford, J. M.; Lydon, N. B.; Kantarjian, H.; Capdeville, R.; Ohno–Jones, S.; Sawyers, C. L. *N. Engl. J. Med.* **2001**, *344*, 1031; (d) Druker, B. J.; Lydon, N. B. *J. Clin. Invest.* **2000**, *105*, 3; (e) Morin, M. J. *Oncogene* **2000**, *19*, 6574.

(53) Buchdunger, E.; Cioffi, C. L.; Law, N.; Stover, D.; Ohno–Jones, S.; Druker, B. J.; Lydon, N. B. *J. Pharmacol. Exp. Ther.* **2000**, *295*, 139.

(54) Fabbro, D.; Cowan–Jacob, S.; Möbitz, H.; Martiny–Baron, G. In *Kinase Inhibitors*; Kuster, B., Ed.; Humana Press: 2012; Vol. 795, p 1.

(55) Castagna, M.; Takai, Y.; Kaibuchi, K.; Sano, K.; Kikkawa, U.; Nishizuka, Y. *J. Biol. Chem.* **1982**, *257*, 7847.

(56) Toton, E.; Ignatowicz, E.; Skrzeczkowska, K.; Rybczynska, M. *Pharmacol. Rep.* **2011**, *63*, 19.

(57) Zanin–Zhorov, A.; Dustin, M. L.; Blazar, B. R. *Trends Immunol.* **2011**, *32*, 358.

(58) (a) Burguillos, M. A.; Deierborg, T.; Kavanagh, E.; Persson, A.; Hajji, N.; Garcia–Quintanilla, A.; Cano, J.; Brundin, P.; Englund, E.; Venero, J. L.; Joseph, B. *Nature* **2011**, *472*, 319; (b) Zhang, D.; Anantharam, V.; Kanthasamy, A.; Kanthasamy, A. G. *J. Pharmacol. Exp. Ther.* **2007**, *322*, 913.

(59) Garrido, J. L.; Godoy, J.; Alvarez, A.; Bronfmian, M.; Inestrosa, N. C. *FASEB J.* **2002**, *16*, 1982.

(60) Maioli, E.; Valacchi, G. *Curr. Drug Metab.* **2010**, *11*, 425.

(61) (a) Defauw, J. M.; Murphy, M. M.; Jagdmann, G. E., Jr.; Hu, H.; Lampe, J. W.; Hollinshead, S. P.; Mitchell, T. J.; Crane, H. M.; Heerding, J. M.; et, a. *J. Med. Chem.* **1996**, *39*, 5215; (b) Pande, V.; Ramos, M. J.; Gago, F. *Anti–Cancer Agents Med. Chem.* **2008**, *8*, 638.

(62) Noh, K.–M.; Hwang, J.–Y.; Shin, H.–C.; Koh, J.–Y. *Neurobiol. Dis.* **2000**, *7*, 375.

(63) Swannie, H. C.; Kaye, S. B. *Curr. Oncol. Rep.* **2002**, *4*, 37.

(64) Lee, K.–W.; Kim, S. G.; Kim, H.–P.; Kwon, E.; You, J.; Choi, H.–J.; Park, J.–H.; Kang, B.–C.; Im, S.–A.; Kim, T.–Y.; Kim, W. H.; Bang, Y.–J. *Cancer Res.* **2008**, *68*, 1916.

(65) Goekjian, P. G.; Jirousek, M. R. *Expert Opin. Invest. Drugs* **2001**, *10*, 2117.

(66) Tamaoki, T. *Methods Enzymol.* **1991**, *201*, 340.

(67) Gschwendt, M.; Mueller, H. J.; Kielbassa, K.; Zang, R.; Kittstein, W.; Rincke, G.; Marks, F. *Biochem. Biophys. Res. Commun.* **1994**, *199*, 93.

(68) Szallasi, Z.; Denning, M. F.; Smith, C. B.; Dlugosz, A. A.; Yuspa, S. H.; Pettit, G. R.; Blumberg, P. M. *Mol. Pharmacol.* **1994**, *46*, 840.

(69) Chen, L.; Hahn, H.; Wu, G.; Chen, C.–H.; Liron, T.; Schechtman, D.; Cavallaro, G.; Banci, L.; Guo, Y.; Bolli, R.; Dorn, G. W., II; Mochly–Rosen, D. *Proc. Natl. Acad. Sci. U. S. A.* **2001**, *98*, 11114.

(70) Gray, M. O.; Karliner, J. S.; Mochly–Rosen, D. *J. Biol. Chem.* **1997**, *272*, 30945.

(71) Lahn, M.; Sundell, K.; Moore, S. *Ann. N. Y. Acad. Sci.* **2003**, *1002*, 263.

(72) Packer, M.; Narahara, K. A.; Elkayam, U.; Sullivan, J. M.; Pearle, D. L.; Massie, B. M.; Creager, M. A. *J. Am. Coll. Cardiol.* **1993**, *22*, 65.

(73) Julier, K.; da, S. R.; Garcia, C.; Bestmann, L.; Frascarolo, P.; Zollinger, A.; Chassot, P.–G.; Schmid, E. R.; Turina, M. I.; von, S. L. K.; Pasch, T.; Spahn, D. R.; Zaugg, M. *Anesthesiology* **2003**, *98*, 1315.

(74) Belhomme, D.; Peynet, J.; Florens, E.; Tibourtine, O.; Kitakaze, M.; Menasche, P. *Ann. Thorac. Surg.* **2000**, *70*, 590.

(75) Newman, M. F.; Ferguson, T. B.; White, J. A.; Ambrosio, G.; Koglin, J.; Nussmeier, N. A.; Pearl, R. G.; Pitt, B.; Wechsler, A. S.; Weisel, R. D.; Reece, T. L.; Lira, A.; Harrington, R. A. *JAMA, J. Am. Med. Assoc.* **2012**, *308*, 157.

(76) Ross, A. M.; Gibbons, R. J.; Stone, G. W.; Kloner, R. A.; Alexander, R. W. *J. Am. Coll. Cardiol.* **2005**, *45*, 1775.

(77) Bebchuk, J. M.; Arfken, C. L.; Dolan–Manji, S.; Murphy, J.; Hasanat, K.; Manji, H. K. *Arch. Gen. Psychiatry* **2000**, *57*, 95.

(78) Madhusudan, S.; Protheroe, A.; Propper, D.; Han, C.; Corrie, P.; Earl, H.; Hancock, B.; Vasey, P.; Turner, A.; Balkwill, F.; Hoare, S.; Harris, A. L. *Br. J. Cancer* **2003**, *89*, 1418.

(79) Cripps, M. C.; Figueredo, A. T.; Oza, A. M.; Taylor, M. J.; Fields, A. L.; Holmlund, J. T.; McIntosh, L. W.; Geary, R. S.; Eisenhauer, E. A. *Clin. Cancer Res.* **2002**, *8*, 2188.

(80) Robertson, M. J.; Kahl, B. S.; Vose, J. M.; de, V. S.; Laughlin, M.; Flynn, P. J.; Rowland, K.; Cruz, J. C.; Goldberg, S. L.; Musib, L.; Darstein, C.; Enas, N.; Kutok, J. L.; Aster, J. C.; Neuberg, D.; Savage, K. J.; LaCasce, A.; Thornton, D.; Slapak, C. A.; Shipp, M. A. *J. Clin. Oncol.* **2007**, *25*, 1741.

(81) Couldwell, W. T.; Hinton, D. R.; Surnock, A. A.; DeGiorgio, C. M.; Weiner, L. P.; Apuzzo, M. L. J.; Masri, L.; Law, R. E.; Weiss, M. H. *Clin. Cancer Res.* **1996**, *2*, 619.

(82) Millward, M. J.; House, C.; Bowtell, D.; Webster, L.; Olver, I. N.; Gore, M.; Copeman, M.; Lynch, K.; Yap, A.; Wang, Y.; Cohen, P. S.; Zalcberg, J. *Br. J. Cancer* **2006**, *95*, 829.

(83) Rini, B. I.; Weinberg, V.; Shaw, V.; Scott, J.; Bok, R.; Park, J. W.; Small, E. J. *Cancer* **2004**, *101*, 90.

(84) Aiello, L. P.; Vignati, L.; Sheetz, M. J.; Zhi, X.; Girach, A.; Davis, M. D.; Wolka, A. M.; Shahri, N.; Milton, R. C. *Retina* **2011**, *31*, 2084.

(85) Tuttle, K. R.; Bakris, G. L.; Toto, R. D.; McGill, J. B.; Hu, K.; Anderson, P. W. *Diabetes Care* **2005**, *28*, 2686.

(86) Vinik, A. I.; Bril, V.; Kempler, P.; Litchy, W. J.; Tesfaye, S.; Price, K. L.; Bastyr, E. J., III *Clin. Ther.* **2005**, *27*, 1164.

(87) Budde, K.; Sommerer, C.; Becker, T.; Asderakis, A.; Pietruck, F.; Grinyo, J. M.; Rigottig, P.; Dantal, J.; Ng, J.; Barten, M. J.; Weber, M. *Am. J. Transplant.* **2010**, *10*, 571.

(88) Karaman, M. W.; Herrgard, S.; Treiber, D. K.; Gallant, P.; Atteridge, C. E.; Campbell, B. T.; Chan, K. W.; Ciceri, P.; Davis, M. I.; Edeen, P. T.; Faraoni, R.; Floyd, M.; Hunt, J. P.; Lockhart, D. J.; Milanov, Z. V.; Morrison, M. J.; Pallares, G.; Patel, H. K.; Pritchard, S.; Wodicka, L. M.; Zarrinkar, P. P. *Nature Biotech.* **2008**, *26*, 127.

(89) Griner, E. M.; Kazanietz, M. G. *Nat. Rev. Cancer* **2007**, *7*, 281.

(90) Blumberg, P. M.; Delclos, K. B.; Dunphy, W. G.; Jaken, S. *Carcinog. – Compr. Surv.* **1982**, *7*, 519.

(91) Wender, P. A.; Baryza, J. L.; Brenner, S. E.; DeChristopher, B. A.; Loy, B. A.; Schrier, A. J.; Verma, V. A. *Proc. Natl. Acad. Sci. U. S. A.* **2011**, *108*, 6721.

(92) Mochly–Rosen, D. *Science* **1995**, *268*, 247.

(93) Kneifel, H.; König, W. A.; Loeffler, W.; Miiller, R. *Arch. Microbiol.* **1977**, *113*, 121.

(94) König, W. A.; Sinnwell, V.; Witt, S.; Kneifel, H. K. *Chem. Ber.* **1980**, *113*, 2221.

(95) Kulanthaivel, P.; Hallock, Y. F.; Boros, C.; Hamilton, S. M.; Janzen, W. P.; Ballas, L. M.; Loomis, C. R.; Jiang, J. B. *J. Am. Chem. Soc.* **1993**, *115*, 6452.

(96) Ohshima, S. Y., M.; Katoh, A.; Fujii, T.; Sano, T.; Matsukuma, S.; Furumai, T.; Fujiu, M.; Watanabe, K.; Yokose, K.; Arisawa, M.; Okuda, T. *J. Antibiot.* **1994**, *47*, 639.

(97) Boros, C.; Hamilton, S. M.; Katz, B.; Kulanthaivel, P. *J. Antibiot.* **1994**, *47*, 1010.

(98) Lampe, J. W.; Hughes, P. F.; Biggers, C. K.; Smith, S. H.; Hu, H. *J. Org. Chem.* **1994**, *59*, 5147.

(99) Hughes, P. F.; Smith, S. H.; Olson, J. T. *J. Org. Chem.* **1994**, *59*, 5799.

(100) (a) Nicolaou, K. C.; Bunnage, M. E.; Koide, K. *J. Am. Chem. Soc.* **1994**, *116*, 8402; (b) Nicolaou, K. C.; Koide, K.; Bunnage, M. E. *Chem. –Eur. J.* **1995**, *1*, 454.

(101) Mukaiyama, T. *Angew. Chem. Int. Ed. Engl.* **1979**, *18*, 707.

(102) Adams, C. P.; Fairway, S. M.; Hardy, C. J.; Hibbs, D. E.; Hursthouse, M. B.; Morley, A. D.; Sharp, B. W.; Vicker, N.; Warner, I. *J. Chem. Soc., Perkin Trans. 1* **1995**, 2355.

(103) (a) Tanner, D.; Almario, A.; Hoegberg, T. *Tetrahedron* **1995**, *51*, 6061; (b) Tanner, D.; Tedenborg, l.; Almario, A.; Pettersson, I.; Csoeregh, I.; Kelly, N. M.; Andersson, P. G.; Hoegberg, T. *Tetrahedron* **1997**, *53*, 4857.

(104) Suzuki, T.; Sato, O.; Hirama, M.; Yamamoto, Y.; Murata, M.; Yasumoto, T.; Harada, N. *Tetrahedron Lett.* **1991**, *32*, 4505.

(105) Hollinshead, S. P.; Nichols, J. B.; Wilson, J. W. *J. Org. Chem.* **1994**, *59*, 6703.

(106) Barbier, P.; Stadlwieser, J. *Chimia* **1996**, *50*, 530.

(107) (a) Naito, T.; Torieda, M.; Tajiri, K.; Ninomiya, I.; Kiguchi, T. *Chem. Pharm. Bull.* **1996**, *44*, 624; (b) Miyabe, H.; Torieda, M.; Kiguchi, T.; Naito, T. *Synlett* **1997**, 580; (c) Miyabe, H.; Torieda, M.; Inoue, K.; Tajiri, K.; Kiguchi, T.; Naito, T. *J. Org. Chem.* **1998**, *63*, 4397.

(108) Franck, B.; Berger–Lohr, B. *Angew. Chem. Int. Ed. Engl.* **1975**, *14*, 818.

(109) Müller, A.; Takyar, D. K.; Witt, S.; König, W. A. *Liebigs Ann. Chem.* **1993**, *6*, 651.

(110) (a) Lampe, J. W.; Hughes, P. F.; Biggers, C. K.; Smith, S. H.; Hu, H. *J. Org. Chem.* **1996**, *61*, 4572; (b) Hu, H.; Jagdmann, G. E., Jr.; Hughes, P. F.; Nichols, J. B. *Tetrahedron Lett.* **1995**, *36*, 3659.

(111) Tuch, A.; Saniere, M.; Le, M. Y.; Depezay, J.–C. *Tetrahedron: Asymmetry* **1996**, *7*, 2901.

(112) (a) Albertini, E.; Barco, A.; Benetti, S.; De, R. C.; Pollini, G. P.; Zanirato, V. *Synlett* **1996**, 29; (b) Albertini, E.; Barco, A.; Benetti, S.; De, R. C.; Pollini, G. P.; Zanirato, V. *Tetrahedron* **1997**, *53*, 17177.

(113) Wu, M. H.; Jacobesen, E. N. *Tetrahedron Lett.* **1997**, *38*, 1693.

(114) Morie, T.; Kato, S. *Heterocycles* **1998**, *48*, 427.

(115) Cook, G. R.; Shanker, P. S.; Peterson, S. L. *Org. Lett.* **1999**, *1*, 615.

(116) Herdeis, C.; Mohareb, R. M.; Neder, R. B.; Schwabenlander, F.; Telser, J. *Tetrahedron: Asymmetry* **1999**, *10*, 4521.

(117) Fürstner, A.; Thiel, O. R. *J. Org. Chem.* **2000**, *65*, 1738.

(118) Phansavath, P.; De, P. S. D.; Ratovelomanana–Vidal, V.; Genet, J.–P. *Eur. J. Org. Chem.* **2000**, 3903.

(119) Masse, C. E.; Morgan, A. J.; Panek, J. S. *Org. Lett.* **2000**, *2*, 2571.

(120) Riber, D.; Hazell, R.; Skrydstrup, T. *J. Org. Chem.* **2000**, *65*, 5382.

(121) (a) Yadav, J. S.; Srinivas, C. *Tetrahedron Lett.* **2002**, *43*, 3837; (b) Yadav, J. S.; Srinivas, C. *Tetrahedron* **2003**, *59*, 10325.

(122) Raghavan, S.; Kumar, C. N. *Tetrahedron Lett.* **2006**, *47*, 1585.

(123) Unthank, M. G.; Hussain, N.; Aggarwal, V. K. *Angew. Chem., Int. Ed.* **2006**, *45*, 7066.

(124) Trost, B. M.; Fandrick, D. R.; Brodmann, T.; Stiles, D. T. *Angew. Chem., Int. Ed.* **2007**, *46*, 6123.

(125) Roy, S. P.; Chattopadhyay, S. K. *Tetrahedron Lett.* **2008**, *49*, 5498.

(126) Srivastava, A. K.; Panda, G. *Chem. – Eur. J.* **2008**, *14*, 4675.

(127) (a) Sullivan, B.; Gilmet, J.; Leisch, H.; Hudlicky, T. *J. Nat. Prod.* **2008**, *71*, 346; (b) Sullivan, B.; Hudlicky, T. *Tetrahedron Lett.* **2008**, *49*, 5211; (c) Hudlicky, T. *Pure Appl. Chem.* **2010**, *82*, 1785.

(128) Yaragorla, S.; Muthyala, R. *Tetrahedron Lett.* **2010**, *51*, 467.

(129) Louvel, J.; Chemla, F.; Demont, E.; Ferreira, F.; Pérez–Luna, A.; Voituriez, A. *Adv. Synth. Catal.* **2011**, *353*, 2137.

(130) Ahmad, S.; Sutherland, A. *Org. Biomol. Chem.* **2012**, *10*, 8251.

(131) Oh, H.–S.; Kang, H.–Y. *Bull. Korean Chem. Soc.* **2012**, *33*, 3895.

(132) Kumar, K. S. A. *Bioorg. Med. Chem.* **2013**, *21*, 3609.

(133) Johnson, M. G.; Foglesong, R. J. *Tetrahedron Lett.* **1997**, *38*, 7001.

(134) (a) Nilsson, J. P.; Anderson, C.–M. *Tetrahedron Lett.* **1997**, *38*, 4635; (b) Storm, J. P.; Andersson, C.–M. *Org. Lett.* **1999**, *1*, 1451; (c) Storm, J. P.; Andersson, C.–M. *J. Org. Chem.* **2000**, *65*, 5264.

(135) (a) Denieul, M.–P.; Skrydstrup, T. *Tetrahedron Lett.* **1999**, *40*, 4901; (b) Denieul, M.–P.; Laursen, B.; Hazell, R.; Skrydstrup, T. *J. Org. Chem.* **2000**, *65*, 6052; (c) Laursen, B.; Denieul, M.–P.; Skrydstrup, T. *Tetrahedron* **2002**, *58*, 2231.

(136) Patil, M. L.; Deshpande, V. H.; Ramlingam, S.; Borate, H. B. *Tetrahedron* **2004**, *60*, 1869.

(137) Koide, K.; Bunnage, M. E.; Gomez–Paloma, L.; Kanter, J. R.; Taylor, S. S.; Brunton, L. L.; Nicolaou, K. C. *Chem. Biol.* **1995**, *2*, 601.

(138) Akamine, P.; Brunton, L. L.; Ou, H. D.; Canaves, J. M.; Xuong, N.–h.; Taylor, S. S. *Biochemistry* **2004**, *43*, 85.

(139) Pande, V.; Ramos, M. J.; Gago, F. *Anti–Cancer Agents Med. Chem.* **2008**, *8*, 638.

(140) (a) Heerding, J. M.; Lampe, J. W.; Darges, J. W.; Stamper, M. L. *Bioorg. Med. Chem. Lett.* **1995**, *5*, 1839; (b) Crane, H. M.; Menaldino, D. S.; Jagdmann, G. E., Jr.; Darges, J. W.; Buben, J. A. *Bioorg. Med. Chem. Lett.* **1995**, *5*, 2133.

(141) Setyawan, J.; Koide, K.; Diller, T. C.; Bunnage, M. E.; Taylor, S. S.; Nicolaou, K. C.; Brunton, L. L. *Mol. Pharmacol.* **1999**, *56*, 370.

(142) Lampe, J. W.; Biggers, C. K.; Defauw, J. M.; Foglesong, R. J.; Hall, S. E.; Heerding, J. M.; Hollinshead, S. P.; Hu, H.; Hughes, P. F.; Jagdmann, G. E., Jr.; Johnson, M. G.; Lai, Y.–S.; Lowden, C. T.; Lynch, M. P.; Mendoza, J. S.; Murphy, M. M.; Wilson, J. W.; Ballas, L. M.; Carter, K.; Darges, J. W.; Davis, J. E.; Hubbard, F. R.; Stamper, M. L. *J. Med. Chem.* **2002**, *45*, 2624.

(143) (a) Lai, Y.–S.; Menaldino, D. S.; Nichols, J. B.; Jagdmann, G. E., Jr.; Mylott, F.; Gillespie, J.; Hall, S. E. *Bioorg. Med. Chem. Lett.* **1995**, *5*, 2151; (b) Lai, Y.–S.; Mendoza, J. S.; Hubbard, F.; Kalter, K. *Bioorg. Med. Chem. Lett.* **1995**, *5*, 2155; (c) Lai, Y.–S.; Mendoza, J. S.; Jagdmann, G. E., Jr.; Menaldino, D. S.; Biggers, C. K.; Heerding, J. M.; Wilson, J. W.; Hall, S. E.; Jiang, J. B.; et, a. *J. Med. Chem.* **1997**, *40*, 226; (d) Lai, Y.–S.; Stamper, M. *Bioorg. Med. Chem. Lett.* **1995**, *5*, 2147.

(144) Mendoza, J. S.; Jagdmann, G. E., Jr.; Gosnell, P. A. *Bioorg. Med. Chem. Lett.* **1995**, *5*, 2211.

(145) Defauw, J. M.; Murphy, M. M.; Jagdmann, G. E., Jr.; Hu, H.; Lampe, J. W.; Hollinshead, S. P.; Mitchell, T. J.; Crane, H. M.; Heerding, J. M.; et, a. *J. Med. Chem.* **1996**, *39*, 5215.

(146) Hu, H.; Hollinshead, S. P.; Hall, S. E.; Kalter, K.; Ballas, L. M. *Bioorg. Med. Chem. Lett.* **1996**, *6*, 973.

(147) Hu, H.; Mendoza, J. S.; Lowden, C. T.; Ballas, L. M.; Janzen, W. P. *Bioorg. Med. Chem.* **1997**, *5*, 1873.

(148) (a) Jagdmann, G. E., Jr.; Defauw, J. M.; Lai, Y.–S.; Crane, H. M.; Hall, S. E.; Buben, J. A.; Hu, H.; Gosnell, P. A. *Bioorg. Med. Chem. Lett.* **1995**, *5*, 2015; (b) Jagdmann, G. E., Jr.; Defauw, J. M.; Lampe, J. W.; Darges, J. W.; Kalter, K. *Bioorg. Med. Chem. Lett.* **1996**, *6*, 1759.

(149) Harper, D. B.; O'Hagan, D.; Murphy, C. D. In *The handbook of Environmental Chemistry*; Gribble, G. W., Ed.; Springer: Heidelberg, Germany, 2003; Vol. 3P, p 141.

(150) Deng, H.; O'Hagan, D.; Schaffrath, C. *Nat. Prod. Rep.* **2004**, *21*, 773.

(151) (a) Bégué, J.–P.; Bonnet–Delpon, D. *J. Fluorine Chem.* **2006**, *127*, 992; (b) Isanbor, C.; O'Hagan, D. *J. Fluorine Chem.* **2006**, *127*, 303; (c) Kirk, K. L. *J. Fluorine Chem.* **2006**, *127*, 1013.

(152) Ritter, S. K. *Chemical & Engineering News Archive* **2012**, *90*, 10.

(153) Wong, D. T.; Bymaster, F. P.; Engleman, E. A. *Life Sci.* **1995**, *57*, 411.

(154) Roth, B. D. In *Prog. Med. Chem.*; King, F. D., Oxford, A. W., Eds.; Elsevier: Amsterdam, 2002; Vol. 40, p 1.

(155) Drlica, K.; Malik, M. *Curr. Top. Med. Chem.* **2003**, *3*, 249.

(156) (a) Müller, K.; Faeh, C.; Diederich, F. *Science* **2007**, *317*, 1881; (b) Böhm, H.–J.; Banner, D.; Bendels, S.; Kansy, M.; Kuhn, B.; Müller, K.; Obst–Sander, U.; Stahl, M. *ChemBioChem* **2004**, *5*, 637; (c) Gerebtzoff, G.; Li–Blatter, X.; Fischer, H.; Frentzel, A.; Seelig, A. *ChemBioChem* **2004**, *5*, 676; (d) Jeschke, P. *ChemBioChem* **2004**, *5*, 570; (e) Kirk, K. L. *Org. Process Res. Dev.* **2008**, *12*, 305; (f) Lipinski, C. A.; Lombardo, F.; Dominy, B. W.; Feeney, P. J. *Adv. Drug Delivery Rev.* **1997**, *23*, 3; (g) Park, B. K.; Kitteringham, N. R.; O'Neill, P. M. *Annu. Rev. Pharmacol. Toxicol.* **2001**, *41*, 443; (h) Paulini, R.; Müller, K.; Diederich, F. *Angew. Chem. Int. Ed.* **2005**, *44*,

1788; (i) Smart, B. E. *J. Fluorine Chem.* **2001**, *109*, 3; (j) Hunter, L. *Beilstein J. Org. Chem.* **2010**, *6*, 38.

(157) (a) O'Hagan, D. *Chem. Soc. Rev.* **2008**, *37*, 308; (b) Smith, M. B.; March, J. *March's Advanced Organic Chemistry: Reactions, Mechanisms, and Structure*; 5th ed.; Wiley–Interscience: New York, USA, 2001.

(158) Kirsch, P. *Modern Fluoroorganic Chemistry: Synthesis, Reactivity, Applications*; Wiely–VCH: Weinheim, Germany, 2004.

(159) (a) Wu, D.; Tian, A.; Sun, H. *J. Phys. Chem. A* **1998**, *102*, 9901; (b) Hunter, L.; Slawin, A. M. Z.; Kirsch, P.; O'Hagan, D. *Angew. Chem., Int. Ed.* **2007**, *46*, 7887.

(160) Sun, A.; Lankin, D. C.; Hardcastle, K.; Snyder, J. P. *Chem. – Eur. J.* **2005**, *11*, 1579.

(161) Briggs, C. R. S.; Allen, M. J.; O'Hagan, D.; Tozer, D. J.; Slawin, A. M. Z.; Goeta, A. E.; Howard, J. A. K. *Org. Biomol. Chem.* **2004**, *2*, 732.

(162) Wiberg, K. B.; Murcko, M. A.; Laidig, K. E.; MacDougall, P. J. *J. Phys. Chem.* **1990**, *94*, 6956.

(163) (a) Briggs, C. R. S.; O'Hagan, D.; Rzepa, H. S.; Slawin, A. M. Z. *J. Fluorine Chem.* **2004**, *125*, 19; (b) O'Hagan, D.; Bilton, C.; Howard, J. A. K.; Knight, L.; Tozer, D. J. *Perkin 2* **2000**, 605.

(164) Juaristi, E.; Cuevas, G. *Tetrahedron* **1992**, *48*, 5019.

(165) Tozer, D. J. *Chem. Phys. Lett.* **1999**, *308*, 160.

(166) Hunter, L.; Kirsch, P.; Slawin, A. M. Z.; O'Hagan, D. *Angew. Chem., Int. Ed.* **2009**, *48*, 5457.

(167) (a) Hunter, L.; O'Hagan, D. *Org. Biomol. Chem.* **2008**, *6*, 2843; (b) Farran, D.; Slawin, A. M. Z.; Kirsch, P.; O'Hagan, D. *J. Org. Chem.* **2009**, *74*, 7168.

(168) Brunet, V. A.; O'Hagan, D. *Angew. Chem., Int. Ed.* **2008**, *47*, 1179.

(169) Merritt, R. F. *J. Org. Chem.* **1966**, *31*, 3871.

(170) (a) Purrington, S. T.; Kagen, B. S.; Patric, T. B. *Chem. Rev.* **1986**, *86*, 997; (b) Cech, D.; Holy, A. *Collect. Czech. Chem. Commun.* **1976**, *41*, 3335.

(171) Ladan, G.; Satyamurthy, N.; Barrio, J. R. *J. Fluorine Chem.* **1995**, *74*, 211.

(172) Furuya, T.; Kutruff, C. A.; Ritter, T. *Curr. Opin. Drug Discovery Dev.* **2008**, *11*, 803.

(173) (a) Lerman, O.; Tor, Y.; Rozen, S. *J. Org. Chem.* **1981**, *46*, 4629; (b) Lerman, O.; Tor, Y.; Hebel, D.; Rozen, S. *J. Org. Chem.* **1984**, *49*, 806.

(174) Rozen, S.; Lerman, O.; Kol, M.; Hebel, D. *J. Org. Chem.* **1985**, *50*, 4753.

(175) Rozen, S.; Hagooly, A.; Harduf, R. *J. Org. Chem.* **2001**, *66*, 7464.

(176) Rozen, S.; Brand, M. *Synthesis* **1985**, 665.

(177) (a) Umemoto, T.; Fukami, S.; Tomizawa, G.; Harasawa, K.; Kawada, K.; Tomita, K. *J. Am. Chem. Soc.* **1990**, *112*, 8563; (b) Umemoto, T. *Chem. Rev.* **1996**, *96*, 1757; (c) Umemoto, T.; Kawada, K.; Tomita, K. *Tetrahedron Lett.* **1986**, *27*, 4465; (d) Umemoto, T.; Tomizawa, G. *J. Org. Chem.* **1995**, *60*, 6563.

(178) Barnette, W. E. *J. Am. Chem. Soc.* **1984**, *106*, 452.

(179) (a) Banks, R. E.; Boisson, R. A. D.; Morton, W. D.; Tsiliopoulos, E. *J. Chem. Soc. Perkin Trans. 1* **1988**, 2805; (b) Banks, R. E.; Besheesh, M. K.; Mohialdin–Khaffaf, S. N.; Sharif, I. *J. Chem. Soc. Perkin Trans. 1* **1996**, 2069.

(180) (a) Kumamoto, H.; Haraguchi, K.; Ida, M.; Tanaka, H.; Hamasaki, T.; Baba, M. *Nucleic Acids Symp. Ser.* **2008**, *52*, 609; (b) Lal, G. S.; Pastore, W.; Pesaresi, R. *J. Org. Chem.* **1995**, *60*, 7340; (c) Lal, G. S. *Synth. Commun.* **1995**, *25*, 725.

(181) Lal, G. S. *J. Org. Chem.* **1993**, *58*, 2791.

(182) Banks, R. E. *J. Fluorine Chem.* **1998**, *87*, 1.

(183) Differding, E.; Lang, R. W. *Tetrahedron Lett.* **1988**, *29*, 6087.

(184) Davis, F. A.; Zhou, P.; Murphy, C. K.; Sundarababu, G.; Qi, H.; Han, W.; Przeslawski, R. M.; Chen, B.–C.; Carroll, P. J. *J. Org. Chem.* **1998**, *63*, 2273.

(185) Takeuchi, Y.; Suzuki, T.; Satoh, A.; Shiragami, T.; Shibata, N. *J. Org. Chem.* **1999**, *64*, 5708.

(186) Abdul–Ghani, M.; Banks, R. E.; Besheesh, M. K.; Sharif, I.; Syvret, R. G. *J. Fluorine Chem.* **1995**, *73*, 255.

(187) (a) Shibata, N.; Suzuki, E.; Takeuchi, Y. *J. Am. Chem. Soc.* **2000**, *122*, 10728; (b) Shibata, N.; Ishimaru, T.; Nagai, T.; Kohno, J.; Toru, T. *Synlett* **2004**, 1703; (c) Shibata, N.; Ishimaru, T.; Nakamura, M.; Toru, T. *Synlett* **2004**, 2509; (d) Shibata, N.; Kohno, J.; Takai, K.; Ishimaru, T.; Nakamura, S.; Toru, T.; Kanemasa, S. *Angew. Chem., Int. Ed.* **2005**, *44*, 4204; (e) Shibata, N.; Yasui, H.; Nakamura, S.; Toru, T. *Synlett* **2007**, 1153.

(188) (a) Cahard, D.; Audouard, C.; Baudoux, J.; Mohar, B.; Plaquevent, J.–C.; Molecular Diversity Preservation International: 2000, p 1052; (b) Cahard, D.; Audouard, C.; Plaquevent, J.–C.; Roques, N. *Org. Lett.* **2000**, *2*, 3699; (c) Cahard, D.; Plaquevent, J. C.; Baudoux, J.; Baudequin, C.; Rhodia Chimie, Fr. . 2004, p 35 pp.

(189) (a) Greedy, B.; Paris, J.–M.; Vidal, T.; Gouverneur, V. *Angew. Chem. Int. Ed.* **2003**, *42*, 3291; (b) Bobbio, C.; Gouverneur, V. *Org. Biomol. Chem.* **2006**, *4*, 2065; (c) Carroll, L.; McCullough, S.; Rees, T.; Claridge, T. D. W.; Gouverneur, V. *Org. Biomol. Chem.* **2008**, *6*, 1731; (d) Lam, Y.–h.; Bobbio, C.; Cooper, I. R.; Gouverneur,

V. *Angew. Chem., Int. Ed.* **2007**, *46*, 5106; (e) Tredwell, M.; Gouverneur, V. *Org. Biomol. Chem.* **2006**, *4*, 26.

(190) Manna, S.; Falck, J. R.; Mioskowski, C. *Synth. Commun.* **1985**, *15*, 663.

(191) Bram, G.; Loupy, A.; Pigeon, P. *Synth. Commun.* **1988**, *18*, 1661.

(192) Tullock, C. W.; Coffman, D. D. *J. Org. Chem.* **1960**, *25*, 2016.

(193) Shahak, I.; Bergmann, E. D. *J. Chem. Soc. C* **1967**, 319.

(194) Sharma, R. K.; Fry, J. L. *J. Org. Chem.* **1983**, *48*, 2112.

(195) Olah, G. A.; Welch, J. T.; Vankar, Y. D.; Nojima, M.; Kerekes, I.; Olah, J. A. *J. Org. Chem.* **1979**, *44*, 3872.

(196) Middleton, W. J. *J. Org. Chem.* **1975**, *40*, 574.

(197) (a) Lal, G. S.; Pez, G. P.; Pesaresi, R. J.; Prozonic, F. M. *Chem. Commun.* **1999**, 215; (b) Lal, G. S.; Pez, G. P.; Pesaresi, R. J.; Prozonic, F. M.; Cheng, H. *J. Org. Chem.* **1999**, *64*, 7048.

(198) Yin, J.; Zarkowsky, D. S.; Thomas, D. W.; Zhao, M. M.; Huffman, M. A. *Org. Lett.* **2004**, *6*, 1465.

(199) Petrov, V. A.; Swearingen, S.; Hong, W.; Chris Petersen, W. *J. Fluorine Chem.* **2001**, *109*, 25.

(200) Takaoka, A.; Iwakiri, H.; Ishikawa, N. *Bull. Chem. Soc. Jpn.* **1979**, *52*, 3377.

(201) Purser, S.; Moore, P. R.; Swallow, S.; Gouverneur, V. *Chem. Soc. Rev.* **2008**, *37*, 320.

(202) Chen, Z.; Li, Y.; Chen, E.; Hall, D.; Darke, P.; Culberson, C.; Shafer, J. A.; Kuo, L. A. *J. Biol. Chem.* **1994**, *269*, 26344.

(203) Myers, A. G.; Barbay, J. K.; Zhong, B. *J. Am. Chem. Soc.* **2001**, *123*, 7207.

(204) Yamamoto, I.; Jordan, M. J. T.; Gavande, N.; Doddareddy, M. R.; Chebib, M.; Hunter, L. *Chem. Commun.* **2012**, *48*, 829.

(205) (a) Deniau, G.; Slawin, A. M. Z.; Lebl, T.; Chorki, F.; Issberner, J. P.; van, M. T.; Heygate, J. M.; Lambert, J. J.; Etherington, L.–A.; Sillar, K. T.; O'Hagan, D. *ChemBioChem* **2007**, *8*, 2265; (b) Clift, M. D.; Ji, H.; Deniau, G. P.; O'Hagan, D.; Silverman, R. B. *Biochemistry* **2007**, *46*, 13819.

(206) Holmgren, S. K.; Taylor, K. M.; Bretscher, L. E.; Raines, R. T. *Nature* **1998**, *392*, 666.

(207) Eberhardt, E. S.; Panisik, N., Jr.; Raines, R. T. *J. Am. Chem. Soc.* **1996**, *118*, 12261.

(208) Holmgren, S. K.; Bretscher, L. E.; Taylor, K. M.; Raines, R. T. *Chem. Biol.* **1999**, *6*, 63.

(209) (a) Bretscher, L. E.; Jenkins, C. L.; Taylor, K. M.; DeRider, M. L.; Raines, R. T. *J. Am. Chem. Soc.* **2001**, *123*, 777; (b) Panasik, N., Jr.; Eberhardt, E. S.; Edison, A. S.; Powell, D. R.; Raines, R. T. *Int. J. Pept. Protein Res.* **1994**, *44*, 262.

(210) Pandey, A. K.; Naduthambi, D.; Thomas, K. M.; Zondlo, N. J. *J. Am. Chem. Soc.* **2013**, *135*, 4333.

(211) Massa, M. A.; Spangler, D. P.; Durley, R. C.; Hickory, B. S.; Connolly, D. T.; Witherbee, B. J.; Smith, M. E.; Sikorski, J. A. *Bioorg. Med. Chem. Lett.* **2001**, *11*, 1625.

(212) (a) Pankiewicz, K. W. *Carbohydr. Res.* **2000**, *327*, 87; (b) Meng, W.–D.; Qing, F.–L. *Curr. Top. Med. Chem.* **2006**, *6*, 1499; (c) Marquez, V. E.; Tseng, C. K. H.; Mitsuya, H.; Aoki, S.; Kelley, J. A.; Ford, H., Jr.; Roth, J. S.; Broder, S.; Johns, D. G.; Driscoll, J. S. *J. Med. Chem.* **1990**, *33*, 978; (d) Barchi, J. J., Jr.; Karki, R. G.; Nicklaus, M. C.; Siddiqui, M. A.; George, C.; Mikhailopulo, I. A.; Marquez, V. E. *J. Am. Chem. Soc.*

2008, *130*, 9048; (e) Van, R. P.; Salerno, J. M.; Chu, C. K.; Schinazi, R. F. *Proc. Natl. Acad. Sci. U. S. A.* **1989**, *86*, 3929; (f) Mikhailopulo, I. A.; Pricota, T. I.; Sivets, G. G.; Altona, C. *J. Org. Chem.* **2003**, *68*, 5897.

(213) Bucher, C.; Sparr, C.; Schweizer, W. B.; Gilmour, R. *Chem. – Eur. J.* **2009**, *15*, 7637.

(214) Khrimian, A. P.; Oliver, J. E.; Waters, R. M.; Panicker, S.; Nicholson, J. M.; Klun, J. A. *Tetrahedron: Asymmetry* **1996**, *7*, 37.

(215) O'Hagan, D.; Rzepa, H. S.; Schüler, M.; Slawin, A. M. Z. *Beilstein J. Org. Chem.* **2006**, *2*, 19

(216) (a) Marcotte, I.; Separovic, F.; Auger, M.; Gagne, S. M. *Biophys. J.* **2004**, *86*, 1587; (b) Kitamoto, T.; Marubayashi, S.; Yamazaki, T. *Chem. Lett.* **2006**, *35*, 1264; (c) Kitamoto, T.; Marubayashi, S.; Yamazaki, T. *Tetrahedron* **2008**, *64*, 1888.

(217) (a) Seebach, D.; Hook, D. F.; Glattli, A. *Biopolymers* **2006**, *84*, 23; (b) Seebach, D.; Gardiner, J. *Acc. Chem. Res.* **2008**, *41*, 1366; (c) Hook, D. F.; Gessier, F.; Noti, C.; Kast, P.; Seebach, D. *ChemBioChem* **2004**, *5*, 691; (d) Mathad, R. I.; Gessier, F.; Seebach, D.; Jaun, B. *Helv. Chim. Acta* **2005**, *88*, 266; (e) Mathad, R. I.; Jaun, B.; Flogel, O.; Gardiner, J.; Loweneck, M.; Codee, J. D. C.; Seeberger, P. H.; Seebach, D.; Edmonds, M. K.; Graichen, F. H. M.; Abell, A. D. *Helv. Chim. Acta* **2007**, *90*, 2251.

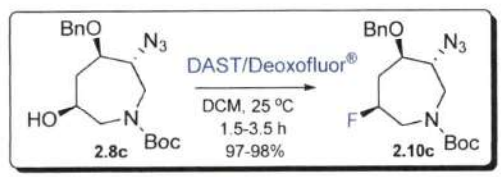
(218) (a) Winkler, M.; Moraux, T.; Khairy, H. A.; Scott, R. H.; Slawin, A. M. Z.; O'Hagan, D. *ChemBioChem* **2009**, *10*, 823; (b) Jordt, S.–E.; Julius, D. *Cell* **2002**, *108*, 421.

(219) (a) Sparr, C.; Schweizer, W. B.; Senn, H. M.; Gilmour, R. *Angew. Chem., Int. Ed.* **2009**, *48*, 3065; (b) MacMillan, D. W. C. *Nature* **2008**, *455*, 304; (c) Chandler, C. L.; List, B. *J. Am. Chem. Soc.* **2008**, *130*, 6737; (d) DiRocco, D. A.; Oberg, K. M.; Dalton, D. M.; Rovis, T. *J. Am. Chem. Soc.* **2009**, *131*, 10872.

(220) (a) Hird, M. *Chem. Soc. Rev.* **2007**, *36*, 2070; (b) Kirsch, P.; Hahn, A.; Froehlich, R.; Haufe, G. *Eur. J. Org. Chem.* **2006**, 4819; (c) Nicoletti, M.; Bremer, M.; Kirsch, P.; O'Hagan, D. *Chem. Commun.* **2007**, 5075.

CHAPTER 2

Diastereospecific Fluorination of Substituted Azepanes



2.1. Relevance of the Study

Fluorine substitution can lead to interesting conformational effects in addition to profound changes in the physical, chemical and biological properties of the molecules. The effect of fluorination has been extensively studied in acyclic systems, carbocycles and fused heterocycles.[2–3] However, such studies are absent for seven–membered heterocycles such as azepanes. Given that substituted azepane rings are prevalent in many bioactive natural products including (−)–balanol, methods for fluorination of azepanes need to be developed first. Fluorinated azepanes are not only chemically diversified but also conformationally modified. Consequently, (−)–balanol analogues containing fluorinated azepanes may present very different specificity profiles in the active site of proteins.

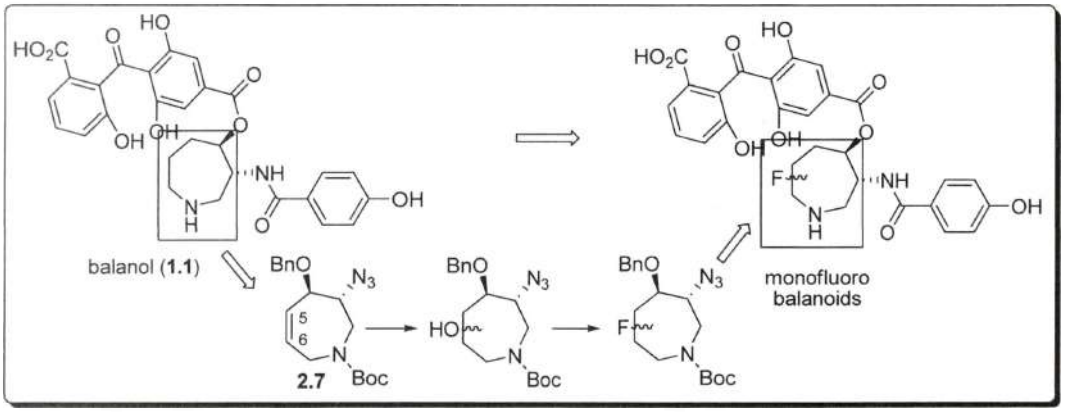


Figure 2.1. Relevance of monofluoro azepane synthesis.

In this chapter, the methods for installing fluorine atom(s) in a selective manner onto the azepane core of balanol were investigated in order to generate conformation–coupled chemical diversity (Figure 2.1).

The monofluoroazepanes were synthesized from the key tetrahydroazepine intermediate (**2.7**) previously used in balanol synthesis. The tetrahydroazepine **2.7** enabled entry to fluorination since it has a functionalizable C5–C6 double bond. This double bond underwent asymmetric

hydroboration to afford hydroxyazepane intermediates. The conditions for this reaction were optimized in order to achieve diastereoselectivity in hydroboration. The hydroxyazepanes were then deoxyfluorinated diastereospecifically to achieve the desired monofluoroazepanes in excellent yields. Usually, such deoxyfluorination follows a S_N2 pathway, especially in six–membered ring systems,[5a,21] and results in the inversion of stereochemistry. Interestingly, the azepane deoxyfluorination here was found to deviate from prior observations and resulted in retention of stereochemistry at the participating stereocentres C5 and C6. This retention can be best explained by neighbouring group participation by the azepane nitrogen or carbamate oxygen (Figure 2.2).

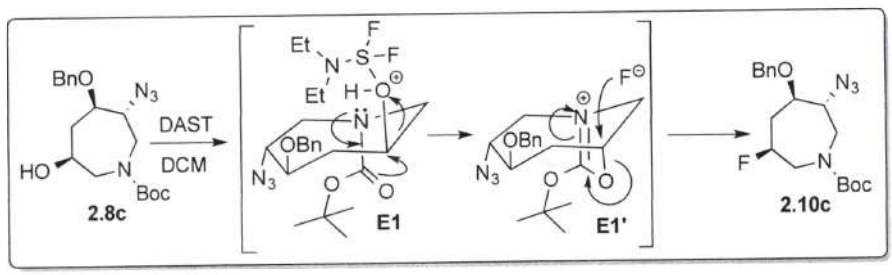


Figure 2.2. Neighbouring group participation.

Synthesis and 2D NMR structure elucidation of the substituted monofluoroazepanes are discussed in this chapter. In Chapter 3 the conformational properties of these model monofluoroazepanes are discussed, followed by a more extensive analysis in Chapter 4 that also includes di– and trifluorinated azepanes. In Chapter 5 the scope of the fluorination methodology in Chapter 2 is further expanded for the more challenging vicinal difluorination. Finally, in Chapter 6 the fluorinated azepanes are advanced further into fluorinated balanols for testing their biological activities. The model development here in this chapter serves as a foundation that extends into all of the following chapters.

2.2. Results and Discussion

The results of this chapter have been published and will be presented mostly in the published form. To summarize, key disubstituted tetrahydroazepine starting material (**2.7**) was synthesized following the protocol reported previously by Fürstner and Thiel.[24] The functionalized azepine **2.7** was then subjected to hydroboration using BH_3·DMS as the hydroborating agent to give all four possible monohydroxyazepanes diastereomers (**2.8a–d**). These diastereomers were separated using reverse phase HPLC and the structure elucidation was secured using 2D NMR experiments (HSQC, HMBC, COSY and NOESY). The detailed NMR structure elucidation is explained in the experimental section of this chapter. Various parameters for hydroboration reaction conditions were optimized. Firstly, different hydroborating agents were utilized at different temperatures and BH_3·DMS was found to work best at 25 °C. Secondly, different solvents were screened and THF was found to be an ideal reaction solvent. Finally, various Rh, Ir and Cu catalysts-ligand conditions were screened for better diastereoselectivity using PinBH and CatBH as hydroborating agents. The Cu catalysed PinBH hydroboration in the presence of Tangphos ligand and NaO^{t}Bu in toluene at 70 °C resulted in the best diastereoselectivity.

The hydroxyazepanes (**2.8b–d**) then underwent deoxyfluorination in excellent yields to provide the desired monofluoroazepanes (**2.10b–d**). The reaction parameters such as solvent and temperature for deoxyfluorination of azepanes were optimized. Boc–deprotected derivatives of all the key intermediates were synthesized for clearer structure elucidations without the presence of *cis/trans* geometric isomers of the Boc group. The deoxyfluorination resulted in the complete retention of stereochemistry at the participating carbon center. This stereochemical outcome suggests neighbouring group participation of the azepane nitrogen or carbamate oxygen. There are a few reports available for neighbouring group participation

from electron–rich *N*–Bn nitrogen in deoxyfluorination via an aziridinium intermediate.[37–38] However, there has not been a report on participation from *N*-Boc nitrogen or carbamate participation. It was interesting to observe such aziridinium/carbamate participation from relatively non-nucleophilic *N*-Boc nitrogen especially in the case of C5 fluorination.

Following is the published research article presented as a main part of the results and discussion of this chapter. The details of the structure elucidation of all key intermediates, which were not shown in the manuscript, are presented in the experimental section here and all of the relevant NMR spectra are included in the appendix A (pages 262–345) at the end of the thesis.

The numbering of all the compounds in the research article (**1–14**) has been referred in the thesis with the prefix "**2**". The detailed cross–referencing table is presented in the following section to make the compounds numbering unambiguous.

Tetrahedron 69 (2013) 744–752

Contents lists available at SciVerse ScienceDirect

Tetrahedron

journal homepage: www.elsevier.com/locate/tet

Diastereospecific fluorination of substituted azepanes

Alpesh Ramanlal Patel, Fei Liu *

Department of Chemistry and Biomolecular Sciences, Macquarie University, Sydney, NSW 2109, Australia

ARTICLE INFO

Article history:
Received 28 August 2012
Received in revised form 11 October 2012
Accepted 29 October 2012
Available online 6 November 2012

Keywords:
Hydroboration
Deoxyfluorination
Azepanes
Neighboring group effect
Diastereospecificity

ABSTRACT

Fluorination of bioactive compounds is an important step in drug discovery and development. Fluorination has been extensively studied in acyclic systems, carbocycles, and fused heterocycles. However, there is no report on fluorination of azepanes. As azepanes are components of many biologically active substances and natural products. We herein present the first fluorination examples of substituted azepanes. Fluoroazepanes were prepared by deoxyfluorination diastereospecifically in excellent yields. The absolute configuration at the fluorination site was unambiguously assigned by 2D NMR spectroscopy.

© 2012 Elsevier Ltd. All rights reserved.

1. Introduction

Fluorine is virtually absent in bioactive natural molecules. However, 20% of all drugs approved and 3 of the top 10 best selling drugs in 2011 contain fluorine atom(s).[1] In general, more than 1/5th of all pharmaceuticals and 1/3rd of agrochemicals have at least one fluorine atom.[2] Because fluorine is the most electronegative atom, is small and forms very strong C–F bonds, hydrogen replacement by its bioisosteric fluorine in compounds can lead to profound changes in their physical, chemical, and biological properties.[2d,3] For example, the fluorine *gauche* effect is known to influence the conformation of molecules as a complex function of steric, electrostatic, and stereoelectronic contributors.[4] Thus, fluorination reactions continue to be of interest to organic, medicinal, and agro chemists as evidenced by a growing number of publications in this area.[5] In particular, fluorinated building blocks represent the most efficient entry into diverse structures of fluorinated compounds.[1] Herein, we report the first examples of fluorinated azepanes as new building blocks for diversity generation.

Substituted azepane rings are prevalent in many bioactive natural compounds.[6] Recently, polysubstituted azepane rings and related compounds (iminocyclitols or iminosugars) have attracted considerable attention of medicinal chemists and biologists as they have demonstrated great potential[7] as glycosidase inhibitors and antidiabetics,[8] anticancer,[9] antivirals[10] including HIV,[11] and DNA minor groove binding agents (MGBLs).[12] The added flexibility of a seven membered ring allows functional groups (for instance hydroxyl groups) to adopt a variety of H-bonding positions for protein binding.[13] Unfortunately, despite the important role of azepanes in bioactive molecules[14] and the large potential of fluorinated azepanes in diversity-oriented bioactivity discovery, their preparation has not been reported.

We chose a substituted tetrahydroazepine **7** as our starting model for investigation. The 1,2-*trans*-benzyloxyazido substitution motif in **7** can be easily reduced to 1,2-*trans*-hydroxylamino motif found in many bioactive natural products.[15] The 3-aminoazepane motif is also seen in antitumor *cis*-platin analogs[16] and somatostatin mimics.[17] Therefore fluorinated azepane building blocks from **7** will have wide utility in diversity-oriented synthesis of fluorinated bioactive leads. Many approaches, such as substitution of oxygen with fluorine(s) in carbonyls and replacement of amides with vinyl fluoride[18] have been achieved successfully. Replacement of a hydroxyl group with fluorine has also gained increasing popularity recently, and an increasing number of natural products and bioactive molecules have been synthesized using deoxyfluorination.[19] This strategy was therefore investigated in this study.

The most commonly used nucleophilic fluorinating agents for substituting hydroxyl group with fluorine are diethylaminosulfur trifluoride (DAST),[20] bis(2-methoxyethyl)aminosulfur trifluoride (Deoxofluor®),[21] Fluorinox, 2,2-difluoro-1,3-dimethyl-imidazolidine (DFI),[22] and perfluoro-1-butanesulfonyl fluoride (PBSF).[23] However, DFI and PBSF being milder reagents require harsher reaction conditions and longer reaction times than DAST and Deoxofluor®. So, we focused our attention on fluorination using

* Corresponding author. Tel.: +61 2 9850 8312; fax: +61 2 9850 8313; e-mail address: fei.liu@mq.edu.au (F. Liu).

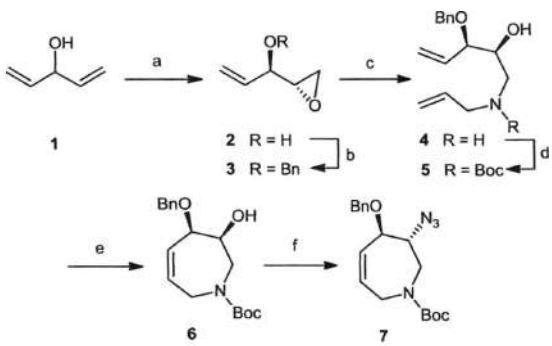
0040-4020/$ – see front matter © 2012 Elsevier Ltd. All rights reserved.
http://dx.doi.org/10.1016/j.tet.2012.10.078

DAST and Deoxofluor®. The general reactivity trend in nucleophilic deoxyfluorination reactions follows the S_N2 pathway with inversion of stereochemistry at the participating stereo-center. However, there are some reports of racemization mainly due to S_N1 competition.[19a,19b] Fluorination reactions of fused heterocycles have been reported before[19d,19e] with S_N2 outcomes. The stereochemical outcomes of deoxyfluorination of substituted azepanes were thus investigated, and we report here deoxyfluorination with retention of stereochemistry due to neighboring group participation.

2. Results and discussion

2.1. Synthesis of tetrahydroazepine 7

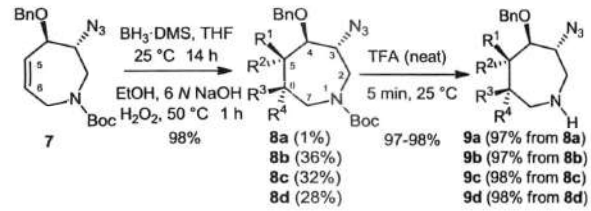
Our investigation started with the preparation of the hydroxyazepanes for use in deoxyfluorination. Disubstituted azepine **7** was synthesized first as the precursor to hydroxyazepanes. The concise six-step protocol (Scheme 1) by Fürstner and Thiel[24] was adopted, starting from divinylcarbinol **1**. Sharpless epoxidation of **1** was performed as described previously[25] and furnished epoxide **2** in excellent optical purity and yield. O-Benzylation was achieved using benzyl bromide before regioselective opening of the oxirane ring of **3** with allylamine to provide diene **4** in 88% yield over two steps. *tert*-Butyloxycarbonyl (Boc) protection of the secondary amine readily provided diene **5**, which served as the precursor for the following ring closing metathesis. Metathesis reaction of **5** was performed by refluxing 0.02 M solution of diene **5** in CH_2Cl_2 in the presence of Grubbs catalyst (5+3 mol %) to afford the desired cycloalkene **6** in 86% yield. Secondary alcohol functionality of **6** was subsequently converted into an azido group with $(PhO)_2P(O)N_3$, diethyl azodicarboxylate, and triphenylphosphine (PPh_3) in THF at room temperature to provide **7** in an overall yield of 54% in six steps.



Scheme 1. Synthesis of tetrahydroazepine **7**. Reagents and conditions: (a) (D)-(−)-DIPT, cumene hydroperoxide, $Ti(O^iPr)_4$, CH_2Cl_2, −35 °C, 83%, >99% ee; (b) NaH, BnBr, THF, 14 h, rt, 93%; (c) Allylamine (neat), 40 h, 70 °C, 95%; (d) Boc_2O, Et_3N, CH_2Cl_2, 16 h, rt, 96%; (e) Grubbs catalyst, CH_2Cl_2, 42 h, 86%; (f) PPh_3, DEAD, $(PhO)_2P(O)N_3$, THF, 2 h, rt, 89%.

2.2. Hydroboration–oxidation of tetrahydroazepine 7

Tetrahydroazepine **7** then underwent hydroboration (Scheme 2) with borane dimethylsulfide ($BH_3 \cdot SMe_2$) as the boronating agent in THF at 25 °C to furnish hydroxyazepanes **8a–d** in 98% overall yield with 2:1 regioselectivity. The mixture of compounds **8a–d** was separated by reverse phase HPLC using acetonitrile:water:trifluoroacetic acid (TFA) (from 30:70:0.1 to 60:40:0.1 over 85 min; flow rate: 8.8 mL/min) as a mobile phase to give **8a** (1%), **8b** (36%), **8c** (32%), and **8d** (28%) as colorless oils. The hydroboration exhibited a mild level of regioselectivity (**8a**+**8b**:**8c**+**8d** at 38:62) and a moderate level of diastereofacial selectivity (**8a**+**8c**:**8b**+**8d** at 30:70). It is noteworthy that the diastereoselectivity (1:37 at C5; *cis*:*trans* to C4 substitution) and regioselectivity (C5 to C6 at 1:1.63)



Scheme 2. **8a** and **9a**: R^1=OH, R^2, R^3, R^4=H; **8b** and **9b**: R^2=OH, R^1, R^3, R^4=H; **8c** and **9c**: R^3=OH, R^1, R^2, R^4=H; **8d** and **9d**: R^4=OH, R^1, R^2, R^3=H.

pattern observed is significantly different from the monosubstituted azepine reported previously (diastereoselectivity: 2:1 at C4; *cis*:*trans* to C3 substitution; and regioselectivity: C4 to C5 at 3:1) by Trost et al.[26] The observed difference in selectivity may potentially be due to the *O*-benzyl directing group (at C4) here instead of *N*-Cbz (at C3) used by Trost.

Detailed analysis of ^1H, ^{13}C, and 2D NMR (HSQC, HMBC, COSY, and NOESY) enabled us to unambiguously elucidate the structures of compounds **8a–d** (Supplementary data).

The key correlations of **8c** and **8d** are shown in Fig 1 as a representative for the absolute configuration assignment. In **8c**, HMBC and HSQC couplings with C1′ (δ_C 71.7 ppm) and C4 (δ_C 78.7 ppm), respectively, identified H4 at 3.37 ppm. H4 further showed COSY correlations with H5a (δ_H 1.74 ppm) and H5b (δ_H 2.30 ppm), both of which showed correlations to H6 (δ_H 3.97 ppm). Moreover, H4 showed NOE to H6 in its NOESY spectra. However, in **8d** H6 (δ_H 4.14 ppm) did not show any detectable NOE to H4 (δ_H 3.80 ppm), but showed strong NOE to H3 (δ_H 3.70 ppm). Thus, the absolute configuration assignments at C6 in **8c** and **8d** were confirmed to be *S* and *R*, respectively. The same process enabled the assignment at C5 in **8a** and **8b** to be *R* and *S*, respectively. The stereochemistry was further confirmed by *N*-Boc deprotection using neat TFA to furnish compounds **9a–d** in quantitative yields (Scheme 2). In the absence of geometric isomers (*cis* and *trans*) of the *N*-Boc group, the assignments of **9a–d** were secured by 2D NMR spectroscopy and confirmed the assignment of **8a–d** (Supplementary data).

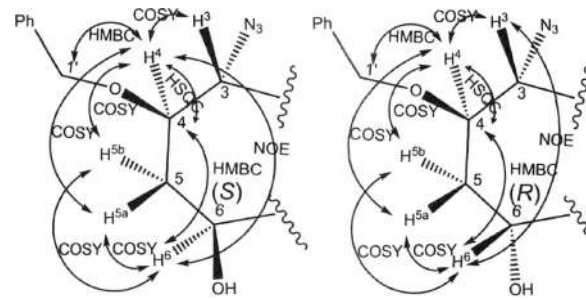


Fig. 1. Key 2D NMR correlations for compound **8c** and **8d**.

2.3. Optimization of hydroboration of 7

While hydroboration of **7** using $BH_3 \cdot SMe_2$ furnished an excellent overall yield of **8a–d**, reaction conditions were investigated to examine the regio- and diastereoselectivity of this reaction (Table 1). The conventional condition with borane tetrahydrofuran complex (Table 1, entry 2) gave excellent yield but unsurprisingly, poor diastereoselectivity. On the other hand 9-BBN (Table 1, entry 6) furnished excellent diastereoselectivity but poor yield even after reflux for 48 h. $BH_3 \cdot NMe_3$ after reflux for 48 h (Table 1, entry 4) gave

Table 1
Screening of different hydroborating agents[a]

Entry	Conditions	Yield[b] (%)	Ratio[c]			
			8a	**8b**	**8c**	**8d**
1	BH_3·DMS, 25 °C, 14 h	98	1	37	33	29
2	BH_3·THF, 25 °C, 14 h	81	0	34	31	35
3	BH_3·NMe_3, 25 °C, 24 h	0	0	0	0	0
4	BH_3·NMe_3, 66 °C, 48 h	20	0	49	0	51
5[a]	BH_3·NMe_3, 101 °C, 48 h	0	0	0	0	0
6[a]	BH_3·NMe_3, 110 °C, 48 h	0	0	0	0	0
7	9-BBN, 25 °C, 24 h	0	0	0	0	0
8	9-BBN, 66 °C, 48 h	12	0	1	0	99
9	CatBH, 25 °C, 24 h	0	0	0	0	0
10	CatBH, 66 °C, 48 h	42	0	37	27	36
11[d]	CatBH, 25 °C, 24 h	0	0	0	0	0
12[d]	CatBH, 66 °C, 48 h	14	0	1	51	48
13	PinBH, 25 °C, 24 h	0	0	0	0	0
14	PinBH, 66 °C, 48 h	0	0	0	0	0

[a] All the reactions were carried out in THF except entry 5 (in dioxane) and 6 (in toluene).
[b] Isolated yield of **8** after column chromatography; unreacted **7** was recovered.
[c] Ratio was calculated on the basis of HPLC traces.
[d] 10 mol % $(PPh_3)_3RhCl$ was used.

diastereofacial selectivity but poor yield. Utilization of dioxane and toluene as solvents for BH_3·NMe_3 condition gave only starting material **7** back. More stable hydroborating agents, such as CatBH and PinBH were also employed. As anticipated, at room temperature only starting materials were recovered. However, refluxing in THF after 48 h with CatBH (Table 1, entry 10) furnished a mixture of diastereomers **8b–d** in low yield but no improvement in diastereoselectivity.

The addition of rhodium catalyst (Table 1, entry 12) improved regioselectivity, which was consistent with prior studies by Evans et al.[27] but the yield remained low. In the case of PinBH, only starting azepine **7** was recovered (Table 1, entries 13, 14).

With BH_3·SMe_2 as the hydroborating agent, solvents were screened for optimization (Table 2). In non-polar solvents, such as benzene, diethyl ether, chloroform, methylene chloride, and dioxane under reflux for 48 h, only starting materials were recovered. However, toluene (Table 2, entry 2) furnished **8b–d** in 19% yield with no significant change in diastereoselectivity to that of THF (Table 2, entry 1). DCE resulted in excellent yields (Table 2, entries 3) with significantly different regioselectivity (C6:C5 at 20:1) compared to 1.63:1 in the case of THF. In acetonitrile, only **7** was recovered (Table 2, entry 4). Overall polar aprotic solvents, such as THF and DCE are the best for this hydroboration reaction, which is in accordance with previous reports on diverse range of substrates, such as styrene, acyclic, carbocyclic, and heterocyclic olefins.[28]

Table 2
Solvent effects in hydroboration of **7**[a]

Entry	Conditions	Yield[b] (%)	Ratio[c]			
			8a	**8b**	**8c**	**8d**
1	THF, 25 °C, 14 h	98	1	37	33	29
2	Toluene, 110 °C, 48 h	19	0	35	30	35
3	DCE, 25 °C, 14 h	98	0	5	40	55
4	MeCN, 82 °C, 48 h	0	0	0	0	0

[a] All reactions were carried out using BH_3·SMe_2 as hydroborating agent.
[b] Isolated yield of **8a–d** after column chromatography; unreacted **7** was recovered.
[c] Ratio was calculated on the basis of HPLC traces.

Stabilized boranes, such as CatBH and PinBH with less Lewis-acidity, offer an advantage of better functional group tolerance and ease for storage and handling. However, hydroboration with stabilized boranes usually requires catalytic activation. As such the course of the reaction can be tuned by a catalytic additive. Transition metal-catalyzed addition of CatBH/PinBH to alkenes and alkynes has shown remarkable chemo-,[29] regio-,[27,30] diastereo-,[27,30,31] and enantioselectivities for acyclic, carbocyclic, and heterocyclic substrates.[28a,32] We employed different metal–ligand combinations for hydroboration of azepine **7** to examine their effects on diastereoselectivity. $[Rh(COD)_2Cl]_2$,[33] Ir(COD)(PCy_3)(Py)PF_6,[34] Rh(COD)(DPPB) BF_4,[33b] and Rh(COD)(PPh_3)BF_4[33b] have demonstrated excellent selectivity in styrene hydroboration and were thus investigated in the hydroboration of **7**. In the case of CatBH, $[Rh(COD)_2Cl]_2$, and Ir(COD)(PCy_3)(Py)PF_6 furnished a regioselectivity ratio of (C6:C5) of 13.3:1 in moderate yields (Table 3, entries 1–2). Ir(COD)(PCy_3)(Py)PF_6 under reflux resulted in higher yield but lower (8:1) regioselectivity (Table 3, entry 3). In the case of PinBH, Rh(COD)(DPPB)BF_4, and Rh(COD)(PPh_3)BF_4 furnished 10:1 regioselectivity and moderate yields. Recently, Lata and Crudden[28b] have reported the use of Lewis acid additives, such as Sc(OTf)$_3$ and tris(pentafluorophenyl) borone (FAB) for Rh catalyzed hydroboration of acyclic olefins. Sc(OTf)$_3$ and FAB were therefore employed with Rh(COD)(DPPB)BF_4 and DCE as solvent. In the case with Sc(OTf)$_3$, **7** was recovered (Table 3, entry 6) while FAB alone furnished 10:1 regioselectivity in good yield with heating (Table 3, entry 8). The best diastereoselectivity (**8d**:**8a–c**) obtained in our study (Table 3, entries 1–8) with Rh and Ir catalysts is 2.2:1. Noh et al.[35] have reported excellent enantio- and regioselectivity with the use of ligands (*R*)-DTMB-Segphos and (*S,S,R,R*)-Tangphos in copper(I)-catalyzed hydroboration of styrene and β-substituted vinyl arenes. We investigated these ligands for CuCl catalyzed hydroboration of azepine **7** with PinBH in toluene. (*R*)-DTMB-Segphos furnished **8b–d** in 78% yield with 11.5 to 1 regioselectivity (C6:C5) at 70 °C in toluene (Table 3, entry 10) while (*S,S,R,R*)-Tangphos demonstrated 24:1 regioselectivity and 82% yield (Table 3, entry 12). Solvent effects were investigated for this copper-(*S,S,R,R*)-Tangphos catalyzed condition. THF, DCE and $CHCl_3$ did not result in better yield or selectivity. It is noteworthy that although transition metal catalyzed hydroboration has been extensively studied, reports on complex heterocyclic substrates are rare. To our best knowledge, this is the first study of transition metal catalyzed hydroboration of a substituted azepane ring.

2.4. Deoxyfluorination of azepanes 8b–d

Compounds **8b–d** were subjected to fluorination reactions (Scheme 3) in the presence of DAST or Deoxofluor® in DCM at 25 °C to provide fluoroazepanes **10b–d**, respectively (Table 4, entries 3, 13, and 15). The stereochemical assignments of C5 and C6 in **10b–d** were secured by 2D NMR experiments. Furthermore, **10b–d** were Boc deprotected to give **11b–d** (Scheme 3) to further confirm the stereochemistry at C5 and C6 without *cis*/*trans* isomerism due to the Boc group.

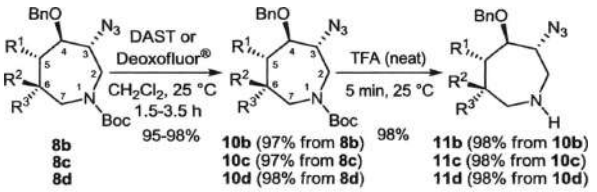
Fluorination using nucleophilic agents, such as DAST is expected to give inversion of stereochemistry at the participating chiral carbon center.[36] However, in our case retention of stereochemistry at C5 and C6 of **10b–d** was observed as revealed by 2D NMR data (Supplementary data).

Retention of stereochemistry in such fluorination cases is possible with the assistance of neighboring group participation.[37] In the case of cyclitol derivatives, there are a few reports for retention of stereochemistry explained by double inversion through participation of adjacent 2-methoxyethoxymethyl,[37a] benzyl,[37e] methoxy[37d] groups containing nucleophilic centers or bromomethyl[37d] via bromine anchimeric assistance. Electron rich nitrogen or sulfur containing heterocyclic substrates also demonstrates retention of stereochemistry through formation of aziridinium or episulfonium intermediates.[37c,38] For example, retention of stereochemistry in fluorination of benzyl protected piperidine **12** by hydroxy

Table 3
Catalyst screening in hydroboration of **7**[a]

Entry	Conditions	Yield[a] (%)	Ratio[b]			
			8a	**8b**	**8c**	**8d**
1	CatBH, 1 mol % $[Rh(COD)_2Cl]_2$, THF, 25 °C, 24 h	43	0	7	52	41
2	CatBH, 5 mol % $Ir(COD)(PCy_3)(Py)PF_6$, THF, 25 °C, 24 h	38	0	7	24	69
3	CatBH, 5 mol % $Ir(COD)(PCy_3)(Py)PF_6$, THF, 66 °C, 14 h	72(70)	0	11	27	62
4	PinBH, 1 mol % $Rh(COD)(PPh_3)BF_4$, DCE, 25 °C, 24 h	40	0	9	33	58
5	PinBH, 1 mol % Rh(COD)(DPPB)BF_4, DCE, 25 °C, 24 h	41	0	9	32	59
6	PinBH, 1 mol % Rh(COD)(DPPB)BF_4, 2 mol % $Sc(OTf)_3$, DCE, 25 °C, 24 h	0	0	0	0	0
7	PinBH, 1 mol % Rh(COD)(DPPB)BF_4, 2 mol % FAB, DCE, 25 °C, 24 h	36	0	12	21	67
8	PinBH, 1 mol % Rh(COD)(DPPB)BF_4, 2 mol % FAB, DCE, 70 °C, 14 h	67(63)	0	9	24	67
9	PinBH, 3 mol % CuCl, 3.3 mol % Segphos, 6 mol % NaO^tBu, toluene, 25 °C, 24 h	26	0	5	49	46
10	PinBH, 3 mol % CuCl, 3.3 mol % Segphos, 6 mol % NaO^tBu, toluene, 70 °C, 14 h	78(72)	0	8	38	54
11	PinBH, 3 mol % CuCl, 3.3 mol % Tangphos, 6 mol % NaO^tBu, toluene, 25 °C, 24 h	53	0	4	31	65
12	**PinBH, 3 mol % CuCl, 3.3 mol % Tangphos, 6 mol % NaO^tBu, toluene, 70 °C, 14 h**	**82(80)**	**0**	**4**	**31**	**65**
13	PinBH, 3 mol % CuCl, 3.3 mol % Tangphos, 6 mol % NaO^tBu, toluene, 110 °C, 14 h	86	0	7	35	58
14	PinBH, 3 mol % CuCl, 3.3 mol % Tangphos, 6 mol % NaO^tBu, $CHCl_3$, 61 °C, 14 h	0	0	0	0	0
15	PinBH, 3 mol % CuCl, 3.3 mol % Tangphos, 6 mol % NaO^tBu, DCE, 70 °C, 14 h	14	0	18	40	42
16	PinBH, 3 mol % CuCl, 3.3 mol % Tangphos, 6 mol % NaO^tBu, THF, 66 °C, 14 h	60	0	9	36	55

The entries in bold indicate the most optimal reactions conditions.
[a] 1.5 equiv CatBH or PinBH were used; % conversion based on crude ^1H NMR; number in parentheses is isolated yield of **8a–d** after column chromatography; unreacted **7** was recovered.
[b] Ratio was calculated on the basis of HPLC traces.

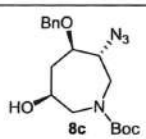
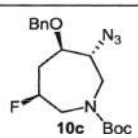
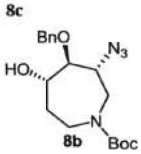
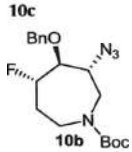
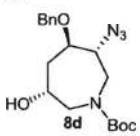
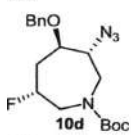


Scheme 3. **8b**: R^1=OH, R^2, R^3=H; **8c**: R^2=OH, R^1, R^3=H; **8d**: R^3=OH, R^1, R^2=H; **10b** and **11b**: R^1=F, R^2, R^3=H; **10c** and **11c**: R^2=F, R^1, R^3=H; **10d** and **11d**: R^3=F, R^1, R^2=H.

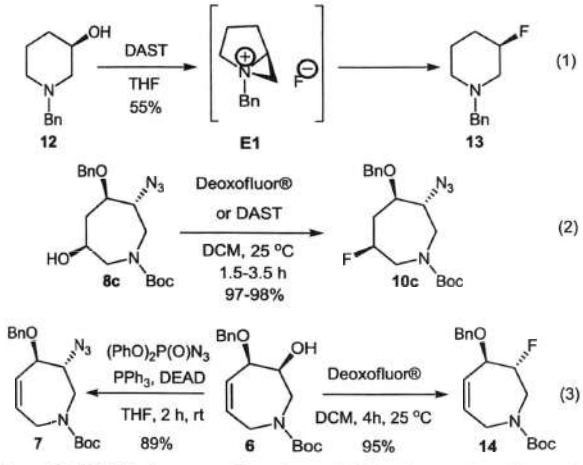
replacement was conferred via an aziridinium intermediate[38] (Scheme 4, Eq. 1) to give **13**. This neighboring group effect from an electron rich nitrogen center by aziridinium formation is not possible in our azepanes **8b–d**, given the presence of the *N*-Boc protecting group.

In the case of **8b–d**, the retention of stereochemistry can best be explained by the neighboring group effect of the carbamate oxygen (Scheme 4, Eq. 2) via formation of a five (**8c–d**) or six (**8b**) membered ring. This would be in accordance with prior examples

Table 4
Deoxyfluorination of compounds **8b–d**

Entry	Fluorinating agent	Substrate	Product[a]	Solvent	Temperature (°C)	Time (h)	Yield (%)[b]
1	DAST			CH_2Cl_2	−78	6.5	92
2	DAST	**8c**	**10c**	CH_2Cl_2	0	6.5	89
3	**DAST**	**8c**	**10c**	**CH_2Cl_2**	**25**	**3.5**	**>99(97)**
4	DAST	**8c**	**10c**	Toluene	25	14	48[c]
5	DAST	**8c**	**10c**	$CHCl_3$	25	14	5
6	DAST	**8c**	**10c**	*n*-Pentane	25	14	90
7	Deoxofluor®	**8c**	**10c**	CH_2Cl_2	−78	6.5	94
8	Deoxofluor®	**8c**	**10c**	CH_2Cl_2	0	6.5	96
9	**Deoxofluor®**	**8c**	**10c**	**CH_2Cl_2**	**25**	**1.5**	**>99(98)**
10	Deoxofluor®	**8c**	**10c**	Toluene	25	14	76[c]
11	Deoxofluor®	**8c**	**10c**	$CHCl_3$	25	14	91
12	Deoxofluor®	**8c**	**10c**	*n*-Pentane	25	14	88
13	**DAST**			**CH_2Cl_2**	**25**	**3.5**	**96(95)**
14	**Deoxofluor®**	**8b**	**10b**	**CH_2Cl_2**	**25**	**1.5**	**>99(97)**
15	**DAST**			**CH_2Cl_2**	**25**	**4**	**97(95)**
16	**Deoxofluor®**	**8d**	**10d**	**CH_2Cl_2**	**25**	**1.5**	**>99(97)**

The entries in bold indicate the most optimal reactions conditions.
[a] Only one diastereomer was formed.
[b] Yield was calculated on the basis of HPLC traces; number in parentheses represents isolated yield.
[c] Diastereomeric ratio (**10c**:**10d**) was 98:2.



Scheme 4. (1) Neighboring group effect via an aziridinium intermediate; (2) retention of stereochemistry in deoxyfluorination; (3) inversion of stereochemistry in **6** via S_N2 pathway.

of amide oxygen participation.[37b] Sekar et al.[39] investigated the effect of nitrogen protecting groups for chlorination reaction using PPh_3 and *N*-chorosuccinimide (NCS), which also follows a S_N2 pathway. Their study showed that protecting groups like phenyl, substituted phenyl, and amide exhibit neighboring group participation resulting in retention of stereochemistry from double inversion. However, in their system protecting groups, such as *N*-tosyl or Cbz did not show any neighboring group effect and inversion of stereochemistry was observed. In their study, the substrate used was 2-hydroxy cyclohexylamine, which is quite different from the azepanes here. To test if ring rigidity may influence such neighboring group participation, alcohol **6** was subjected to deoxyfluorination using Deoxofluor® in DCM. Compared to **8c**, **6** may undergo deoxyfluorination with retention of stereochemistry, given that the hydroxyl group is equal distance to the carbamate group as is the case of **8c**. However, due to the presence of the double bond between C5 and C6, the seven-membered ring in **6** is more rigid. The resulting fluoroazepane **14** from **6** was obtained in excellent yield with inversion of stereochemistry (Scheme 4, Eq. 3). It is also noteworthy that alcohol **6** undergoes inversion of stereochemistry to form tetrahydroazepine **7** under mitsunobu conditions following an S_N2 pathway (Scheme 4, Eq. 3). Thus, in spite of being at equicarbon distance to the nitrogen center, the center of substitution in **6** (C3) and **8b–d** (C5 or C6) presented different neighboring group effects potentially because of the rigidity of **6** compared to **8b–d**. This suggests that retention of stereochemistry in **8b–d** deoxyfluorination is dependent on ring rigidity. To the best of our knowledge, this is the first example of carbamate oxygen neighboring group effect for retention of stereochemistry in deoxyfluorination. Given this neighboring group effect, the yields and diastereomeric ratios under other fluorination conditions were examined using **8b–d** (Table 4). The deoxyfluorination at lower temperatures resulted in longer reaction times as expected (Table 4, entries 1–3). The diastereospecific conversion was maintained in all cases while different solvents only affected yields. As Deoxofluor®[21,40] is considered a better fluorinating agent than DAST in terms of thermal stability[40b] and reactivity,[40e] deoxyfluorination of **8b–d** was also examined using Deoxofluor® (Table 4, entries 7–12, 14, and 16). The yields of fluorination observed in these cases were slightly better than those of DAST.

Significant differences in yields however were observed in toluene and $CHCl_3$ where Deoxofluor® compared to DAST led to much better yields (Table 4, entries 4, 5, 10, and 11). On the other hand, slight racemization (98:2) was observed in the case of toluene with DAST and Deoxofluor® (Table 4, entries 4 and 10).

3. Conclusion

In conclusion, we report here the first practical and efficient diastereospecific fluorination of substituted azepanes in two steps with an overall yield of>95% from a starting tetrahydroazepine **7**. The approach of deoxyfluorination using DAST or Deoxofluor® gave diastereospecific fluorination with retention of stereochemistry, most likely by neighboring group participation from a carbamate. As fluorinated azepanes are important pharmacophores, these fluorinated azepanes should serve as new fluorinated building blocks in drug discovery.

4. Experimental section

4.1. General

All reactions were conducted under N_2 atmosphere. Unless otherwise specified, all reagents were purchased from Sigma–Aldrich and used without further purification. CH_2Cl_2 was obtained from a solvent purification system (Innovative Technology SPS400) and stored over MS 4 Å beads. Ethyl acetate and petroleum ether were distilled before use and the later refers to the fraction collected between 60 °C and 80 °C. THF and toluene were distilled from Na–benzophenone and stored over MS 4 Å beads. $CHCl_3$ was distilled from $CaCl_2$ and stored over MS 4 Å beads in the dark. Anhydrous *n*-pentane was obtained from Sigma–Aldrich and used without further purification. ^1H NMR spectra were recorded at 25 °C on either a Bruker DRX600K or DPX400 NMR Spectrometer and are reported in parts per million using the specified solvent as the internal standard ($CDCl_3$ at 7.26 ppm). ^{13}C NMR spectra are reported in ppm using the specified solvent as the internal standard ($CDCl_3$ at 77.16 ppm).

4.2. (2*S*,3*R*)-1,2-Epoxy-4-penten-3-ol (2)

A crushed 4 Å molecular sieves (400 mg) in CH_2Cl_2 (12 mL) was cooled to −35 °C. Pre-cooled (−35 °C) titanium tetraisopropoxide (350 μL, 1.19 mmol) and (*R*,*R*)-(−)-diisopropyl tartrate (330 μL, 1.55 mmol) were added drop wise via syringe. Pre-cooled (−35 °C) divinylcarbinol (1.00 g, 11.9 mmol) and cumene hydroperoxide (3.50 mL, 23.8 mmol) were added drop wise via glass syringe after 30 min. The reaction mixture was allowed to stir at −35 °C for 36 h. Aqueous saturated Na_2SO_4 (1 mL) was added after warming up to room temperature and the mixture was diluted with Et_2O (10 mL). The mixture was then stirred at ambient temperature for 3 h, the resulting slurry was vacuum filtered through a pad of Celite and the resulting yellow solution was concentrated under vacuum at 0 °C to furnish the crude residue, which was subjected to flash chromatography (petroleum ether/EtOAc, 4/1 then 100% Et_2O) to give **2** (990 mg, 83%) as a colorless oil with optical rotation and ^1H NMR spectral data matching those reported previously.[25] $[\alpha]_D^{20}$ −50 (*c* 0.73, $CHCl_3$). ^1H NMR ($CDCl_3$, 400 MHz): δ 5.90–5.83 (m, 1H), 5.39 (br d, *J*=17.3 Hz, 1H), 5.26 (d, *J*=10.5 Hz, 1H), 4.34 (br s, 1H), 3.09 (dd, *J*=6.4, 3.0 Hz, 1H), 2.84–2.74 (m, 2H), 2.08 (br, s, 1H).

4.3. (*S*)-2-((*R*)-1-Benzyloxy-allyl)-oxirane (3)

NaH (260 mg, 10.9 mmol) was added slowly to a solution of epoxyalcohol **2** (990 mg, 9.90 mmol) and $(n\text{-}Bu)_4NI$ (370 mg, 990 μmol) in THF (22 mL). Benzyl bromide (3.39 g, 19.8 mmol) was added drop wise via syringe after 5 min and the resulting suspension was stirred at ambient temperature for 14 h. The reaction was quenched by drop wise addition of aqueous saturated $NaHCO_3$

(10 mL) and the aqueous layer was extracted with Et_2O (2×20 mL). The combined organic phases were dried (Na_2SO_4) before solvent was evaporated to get the residue, which was purified by flash chromatography (petroleum ether/EtOAc, 9/1) to give **3** (1.75 g, 93%) as a colorless oil with optical rotation and ^1H NMR spectral data matching those reported previously.[24] $[\alpha]_D^{20}$ −31.6 (*c* 1.4, $CHCl_3$); ^1H NMR ($CDCl_3$, 400 MHz): δ 7.34–7.24 (m, 5H), 5.88–5.77 (m, 1H), 5.38–5.31 (m, 2 H), 4.63 (d, *J*=12.0 Hz, 1H), 4.47 (d, *J*=12.0 Hz, 1H), 3.80 (dd, *J*=7.3, 4.2 Hz, 1H), 3.10–3.06 (m, 1H), 2.76 (dd, *J*=5.2, 4.0 Hz, 1H), 2.67 (dd, *J*=5.2, 2.6 Hz, 1H).

4.4. (2*S*,3*R*)-1-Allylamino-3-benzyloxy-pent-4-en-2-ol (4)

An epoxide **3** (790 mg, 4.15 mmol) was refluxed in freshly distilled allylamine (6.25 mL, 83.0 mmol) for 40 h. Excess allylamine was removed under reduced pressure. The remaining pale yellow oil was amine **4** (980 mg, 95%) with optical rotation and ^1H NMR spectral data matching those reported previously[24] and was pure enough to be used in the next step without further purification. $[\alpha]_D^{20}$ −36.6 (*c* 2.0, $CHCl_3$); ^1H NMR ($CDCl_3$, 400 MHz): δ 7.35–7.22 (m, 5H), 5.96–5.75 (m, 2H), 5.36–5.31 (m, 2H), 5.18–5.02 (m, 2H), 4.59 (d, *J*=11.8 Hz, 1H), 4.35 (d, *J*=11.8 Hz, 1H), 3.82–3.73 (m, 2H), 3.30–3.22 (m, 2H), 3.14 (br s, 2H), 2.77 (dd, *J*=12.3, 3.7 Hz, 1H), 2.70–2.63 (m, 1H).

4.5. (2*S*,3*R*)-Allyl-(3-benzyloxy-2-hydroxy-pent-4-enyl)-carbamic acid-*tert*-butyl ester (5)

Di-*tert*-butyl dicarbonate (48.8 mg, 220 μmol) in CH_2Cl_2 (2 mL) was added to a mixture of amine **4** (49.5 mg, 200 μmol) and Et_3N (39.0 μL, 280 μmol) in CH_2Cl_2 (2 mL) at 0 °C and the resulting mixture was stirred at ambient temperature for 2 h. The reaction mixture was quenched by addition of water (2 mL) before the extraction of the aqueous phase with EtOAc (2×5 mL). Successive washing of the combined organic layers with aqueous 2 N HCl (5 mL) and brine (5 mL) followed by drying (Na_2SO_4), evaporation of the solvents and flash chromatography of the residue (petroleum ether/EtOAc, 6/1) gave compound **5** (66.8 mg, 96%) as a colorless oil with optical rotation and ^1H NMR spectral data matching those reported previously.[24] $[\alpha]_D^{20}$ −28.8 (*c* 2.0, $CHCl_3$); ^1H NMR ($CDCl_3$, 400 MHz): δ 7.34–7.23 (m, 5H), 5.89–5.68 (m, 2H), 5.39–5.29 (m, 2H), 5.12–5.02 (m, 2H), 4.62 (d, *J*=12.0 Hz, 1H), 4.35 (d, *J*=12.0 Hz, 1H), 3.88–3.67 (m, 4H), 3.41–3.35 (m, 2H), 1.42 (s, 9H).

4.6. (3*S*,4*R*)-4-Benzyloxy-3-hydroxy-2,3,4,7-tetrahydroazepine-1-carboxylic acid-*tert*-butyl ester (6)

Grubbs catalyst (generation I) (11.6 mg, 14.1 μmol, 5 mol %) was added to a solution of diene **5** (98.0 mg, 280 μmol) in CH_2Cl_2 (30 mL). The reaction mixture was refluxed for 20 h when additional Grubbs catalyst (7.00 mg, 8.50 μmol, 3 mol %) was added and solution was refluxed for additional 22 h. Solvent was then evaporated and the residue was subjected to flash chromatography (petroleum ether/EtOAc, 5/1 to 2/1) to provide tetrahydroazepine **6** (77.8 mg, 86%) as a yellow oil with optical rotation and ^1H NMR spectral data matching those reported previously.[24] $[\alpha]_D^{20}$ −78 (*c* 1.5, $CHCl_3$); ^1H NMR ($CDCl_3$, 400 MHz): δ 7.38–7.27 (m, 5H), 5.79–5.65 (m, 2H), 4.74–4.61 (m, 1H), 4.58–4.46 (m, 1H), 4.45–4.10 (m, 3H), 4.03–3.90 (m, 1H), 3.82–3.63 (m, 1H), 3.31–3.11 (m, 1H), 2.51 (br s, 1H), 1.41 (s, 9H).

4.7. (3*R*,4*R*)-3-Azido-4-benzyloxy-2,3,4,7-tetrahydroazepine-1-carboxylic acid-*tert*-butyl ester (7)

To a well stirred solution of (3*S*,4*R*)-4-benzyloxy-3-hydroxy-2,3,4,7-tetrahydroazepine-1-carboxylic acid-*tert*-butyl ester **6** (95.8 mg, 300 μmol), PPh_3 (314 mg, 1.20 mmol), and $(PhO)_2P(O)N_3$ (258 μL, 1.20 mmol) in dry THF (7.5 mL) under N_2 atmosphere at 25 °C, diethyl azodicarboxylate (DEAD, 189 μL, 1.20 mmol) was added drop wise via syringe and the resulting mixture was stirred at same temperature until the completion of reaction (monitored by TLC, 4.5 h). The residue obtained by evaporation of reaction mixture under reduced pressure was suspended in EtOAc (15 mL), followed by filtration through a short pad of silica. The filtrate was washed with aqueous 2 N HCl (15 mL), brine (15 mL), and dried over $MgSO_4$. The solvent was evaporated, and the crude was purified by flash chromatography (pentane/*tert*-butylmethylether, 20/1) to afford compound **7** (91.3 mg, 89%) as a pale yellow syrup with optical rotation and ^1H NMR spectral data matching those reported previously.[24] $[\alpha]_D^{20}$ +38 (*c* 8.8, $CHCl_3$); ^1H NMR ($CDCl_3$, 400 MHz): δ 7.39–7.20 (m, 5H), 5.74 (br s, 2H), 4.68–4.55 (m, 2H), 4.25–4.23 (m, 2H), 3.90–3.49 (m, 4H), 1.47 (s, 9H).

4.8. General procedure for hydroboration–oxidation

Borane dimethylsulfide ($BH_3{\cdot}SMe_2$) 2 M solution in THF (78.0 μL, 156 μmol) was added drop wise via syringe to a well stirred solution of olefin **7** (50.0 mg, 145 μmol) in dry THF (150 μL) under N_2 atmosphere at 25 °C. The reaction mixture was allowed to stir at same temperature for 14 h before the addition of EtOH (900 μL), 6 N NaOH (600 μL), and 30% H_2O_2 (300 μL). The mixture was heated at 50 °C for 1 h to ensure complete oxidation. The aqueous layer was saturated with K_2CO_3 to effect the separation of the organic layer. The aqueous layer was then washed with EtOAc (2×2 mL) and the combined organic layers were dried over $MgSO_4$ before evaporation to furnish the crude residue. The crude was subjected to flash chromatography (petroleum ether/EtOAc, 3/1) to give a mixture of diastereomers **8a**–**d** (51.6 mg, 98%). The mixture was then chromatographed on a Phenomenex Gemini C18 column (150×21.20 mm) eluting with MeCN/water/TFA (from 30:70:0.1 to 60:40:0.1 over 85 min; flow rate: 8.80 mL/min; retention time 44.4, 42.0, 37.2, and 40.7 min for **8a**, **8b**, **8c**, and **8d**, respectively) to give **8a** (500 μg, 1%), **8b** (19.1 mg, 36%), **8c** (17.0 mg, 32%), and **8d** (15.0 mg, 28%) as colorless oils in a ratio of 1:37:33:29. It is noteworthy that **8a**–**d** were observed to have rotamers because of *N*-Boc group.

*4.8.1. (3R,4S,5R)-3-Azido-4-benzyloxy-5-hydroxyazepane-1-carboxylic acid-tert-butyl ester (**8a**).* $[\alpha]_D^{20}$ −53 (*c* 0.9, CH_2Cl_2); IR (film) ν_{max} (cm^{-1}): 3600–3100 (br), 2977, 2930, 2361, 2104, 1684, 1416, 1157, 1088, 1045; ^1H NMR (600 MHz, $CDCl_3$) δ 7.41–7.35 (m, 5H), 5.09–5.08 (t, *J*=10.4 Hz, 1H), 4.69–4.67 (t, *J*=10.6 Hz, 1H), 4.12–4.05 (m, 1H), 3.99–3.80 (m, 2H), 3.60–3.54 (m, 1H), 3.45–3.36 (m, 1H), 3.23–3.09 (m, 2H), 2.16–2.05 (m, 1H), 1.92–1.80 (m, 1H), 1.46 (s, 9H); ^{13}C NMR (150 MHz, $CDCl_3$) δ 155.1, 137.7, 128.9, 128.5, 128.4, 90.6, 80.6, 76.4, 71.1, 60.6, 48.1, 42.1, 30.3, 28.5; HRMS (ESI): $[M+H]^+$, *m/z* calcd for $C_{18}H_{27}N_4O_4$ 363.2039, found 363.2034.

*4.8.2. (3R,4S,5S)-3-Azido-4-benzyloxy-5-hydroxyazepane-1-carboxylic acid-tert-butyl ester (**8b**).* $[\alpha]_D^{20}$ +51.2 (*c* 0.8, CH_2Cl_2); IR (film) ν_{max} (cm^{-1}): 3600–3100 (br), 2977, 2930, 2361, 2105, 1684, 1416, 1157, 1088, 1045; ^1H NMR (600 MHz, $CDCl_3$) δ 7.41–7.36 (m, 5H), 5.00–4.96 (dd, *J*=11.0, 4.6 Hz, 1H), 4.67–4.63 (t, *J*=10.6 Hz, 1H), 3.80–3.51 (m, 4H), 3.28–3.12 (m, 2H), 3.10–2.96 (m, 1H), 2.48 (br s, 1H), 2.13–2.04 (m, 1H), 1.85–1.72 (m, 1H), 1.48 (s, 9H); ^{13}C NMR (150 MHz, $CDCl_3$) δ 154.9, 137.6, 128.9, 128.5, 128.4, 87.9, 80.9, 75.9, 70.7, 64.8, 45.0, 42.2, 30.6, 28.5; HRMS (ESI): $[M+H]^+$, *m/z* calcd for $C_{18}H_{27}N_4O_4$ 363.2039, found 363.2046.

*4.8.3. (3R,4R,6S)-3-Azido-4-benzyloxy-6-hydroxyazepane-1-carboxylic acid-tert-butyl ester (**8c**).* $[\alpha]_D^{20}$ −49.2 (*c* 0.8, CH_2Cl_2); IR (film) ν_{max} (cm^{-1}): 3600–3100 (br), 2977, 2930, 2361, 2105, 1684,

1416, 1157, 1088, 1045; ^{1}H NMR (600 MHz, $CDCl_3$) δ 7.40–7.34 (m, 5H), 4.68–4.56 (m, 2H), 4.0–3.94 (m, 1H), 3.87–3.78 (m, 1H), 3.69–3.61 (m, 2H), 3.37 (t, J=9.0 Hz, 1H), 3.30 (dd, J=14.9, 5.9 Hz, 1H), 2.90 (q, J=14.9, 8.8 Hz, 1H), 2.54 (br s, 1H), 2.34–2.28 (dd, J=14.8, 5.0 Hz, 1H), 1.79–1.71 (m, 1H), 1.48 (s, 9H); ^{13}C NMR (150 MHz, $CDCl_3$) δ 156.5, 137.2, 128.6, 128.1, 128.0, 81.2, 78.7, 71.7, 68.3, 64.5, 54.9, 49.7, 37.0, 28.3; HRMS (ESI): $[M+H]^+$, m/z calcd for $C_{18}H_{27}N_4O_4$ 363.2039, found 363.2044.

*4.8.4. (3R,4R,6R)-3-Azido-4-benzyloxy-6-hydroxyazepane-1-carboxylic acid-tert-butyl ester (**8d**).* $[\alpha]_D^{20}$ +48.8 (c 0.8, CH_2Cl_2); IR (film) ν_{max} (cm^{-1}): 3600–3100 (br), 2977, 2930, 2361, 2105, 1684, 1416, 1157, 1088, 1045; ^{1}H NMR (600 MHz, $CDCl_3$) δ 7.38–7.33 (m, 5H), 4.64–4.52 (m, 2H), 4.21–4.12 (m, 1H), 3.82–3.68 (m, 4H), 3.44–3.33 (m, 2H), 2.08–1.98 (m, 1H), 1.87 (br s, 1H), 1.48 (s, 9H); ^{13}C NMR (150 MHz, $CDCl_3$) δ 157.2, 137.8, 128.7, 128.1, 128.0, 81.2, 76.1, 71.9, 68.1, 64.9, 55.4, 49.0, 34.6, 28.4; HRMS (ESI): $[M+H]^+$, m/z calcd for $C_{18}H_{27}N_4O_4$ 363.2039, found 363.2032.

4.9. Typical procedure for Boc deprotection of 8

(3*R*,4*R*,6*R*)-3-Azido-4-benzyloxy-6-hydroxyazepane-1-carboxylic acid-*tert*-butyl ester **8d** (9.60 mg, 26.5 μmol) was dissolved in TFA (500 μL) at 25 °C. The solution was allowed to stir for 5 min before TFA was vacuum evaporated. The reaction flask was kept under high vacuum (0.005 Torr, 25 °C) for 3 h to remove traces of TFA, and the colorless oil obtained was characterized as (3*R*,4*R*,6*R*)-3-azido-4-benzyloxy-azepane-6-ol **9d** (6.80 mg, 98%).

*4.9.1. (3R,4S,5R)-3-Azido-4-benzyloxyazepane-5-ol (**9a**).* Colorless oil, yield 97%; $[\alpha]_D^{20}$ −57.6 (c 1.0, CH_2Cl_2); IR (film) ν_{max} (cm^{-1}): 3587, 2341, 1698, 1683, 1636, 1558, 1199, 1132; ^{1}H NMR (600 MHz, $CDCl_3$) δ 7.40–7.31 (m, 5H), 4.77 (d, J=11.5 Hz, 1H), 4.64 (d, J=11.5 Hz, 1H), 4.33 (q, J=4.3 Hz, 1H), 4.14 (t, J=6.8 Hz, 1H), 3.83 (t, J=5.0 Hz, 1H), 3.56–3.47 (m, 3H), 3.22–3.15 (m, 1H), 2.30–2.22 (m, 1H), 2.13–2.04 (m, 1H); ^{13}C NMR (150 MHz, $CDCl_3$) δ 137.0, 128.9, 128.6, 128.2, 84.9, 73.8, 70.1, 56.6, 47.0, 42.1, 25.7; HRMS (ESI): $[M+H]^+$, m/z calcd for $C_{13}H_{19}N_4O_2$ 263.1508, found 263.1505.

*4.9.2. (3R,4S,5S)-3-Azido-4-benzyloxyazepane-5-ol (**9b**).* Colorless oil, yield 97%; $[\alpha]_D^{20}$ +56.4 (c 1.0, CH_2Cl_2); IR (film) ν_{max} (cm^{-1}): 3587, 2341, 1698, 1683, 1636, 1558, 1456, 1199, 1132; ^{1}H NMR (600 MHz, $CDCl_3$) δ 7.40–7.31 (m, 5H), 4.67 (q, J=21.4, 8.2 Hz, 2H), 4.19–4.13 (q, J=3 Hz, 1H), 3.98–3.93 (m, 1H), 3.71 (t, J=8.2 Hz, 1H), 3.51–3.42 (m, 1H), 3.33–3.20 (m, 2H), 3.18–3.09 (m, 1H), 2.80 (br s, 1H), 2.25–2.18(m, 1H), 2.07–1.99 (m, 1H); ^{13}C NMR (150 MHz, $CDCl_3$) δ 137.0, 128.9, 128.6, 128.2, 82.4, 73.5, 69.3, 60.3, 44.1, 41.4, 25.6; HRMS (ESI): $[M+H]^+$, m/z calcd for $C_{13}H_{19}N_4O_2$ 263.1508, found 263.1503.

*4.9.3. (3R,4R,6S)-3-Azido-4-benzyloxyazepane-6-ol (**9c**).* Colorless oil, yield 98%; $[\alpha]_D^{20}$ −55.4 (c 0.9, CH_2Cl_2); IR (film) ν_{max} (cm^{-1}): 3587, 2341, 1698, 1683, 1636, 1558, 1456, 1199, 1132; ^{1}H NMR (600 MHz, $CDCl_3$) δ 7.40–7.29 (m, 5H), 4.70 (d, J=11.5 Hz, 1H), 4.53 (d, J=11.5 Hz, 1H), 4.21 (br s, 1H), 4.14–4.09 (m, 1H), 3.83 (m, 1H), 3.51 (dd, J=14.2, 3.9 Hz, 1H), 3.43 (dd, J=13.8, 5.2 Hz, 1H), 3.10 (d, J=13.0 Hz, 1H), 3.04 (dd, J=14.2, 5.9 Hz, 1H), 2.26 (dt, J=15.7, 5.9 Hz, 1H), 2.12 (dt, J=15.7, 3.7 Hz, 1H); ^{13}C NMR (150 MHz, $CDCl_3$) δ 137.0, 128.8, 128.5, 128.3, 77.4, 72.0, 64.6, 61.0, 51.6, 47.2, 34.0; HRMS (ESI): $[M+H]^+$, m/z calcd for $C_{13}H_{19}N_4O_2$ 263.1508, found 263.1507.

*4.9.4. (3R,4R,6R)-3-Azido-4-benzyloxyazepane-6-ol (**9d**).* $[\alpha]_D^{20}$ +53.6 (c 1.0, CH_2Cl_2); IR (film) ν_{max} (cm^{-1}): 3587, 2341, 1698, 1683, 1636, 1558, 1456, 1199, 1132; ^{1}H NMR (600 MHz, $CDCl_3$) δ 7.39–7.36 (m, 5H), 5.00–4.96 (m, 1H), 4.67–4.63 (m, 1H), 3.79–3.51 (m, 4H), 3.26–3.13 (m, 2H), 3.08–2.97 (m, 1H), 2.48 (br s, 1H), 2.12–2.05 (m, 1H), 1.72–1.84 (br m, 1H), 1.48 (s, 9H); ^{13}C NMR (150 MHz, $CDCl_3$) δ 137.1, 128.8, 128.4, 128.1, 75.5, 72.2, 63.6, 60.8, 54.1, 47.6, 34.2; HRMS (ESI): $[M+H]^+$, m/z calcd for $C_{13}H_{19}N_4O_2$ 263.1508, found 263.1509.

4.10. General procedure for deoxyfluorination of 10

A solution of bis(2-methoxyethyl)aminosulfur trifluoride (Deoxofluor®) (13.4 mg, 60.7 μmol) or diethylaminosulfur trifluoride (DAST) (9.80 mg, 60.7 μmol) in dry DCM (100 μL) was added drop wise via a syringe to a well stirred solution of **8c** (20.0 mg, 55.2 μmol) in dry DCM (100 μL) under N_2 atmosphere at 25 °C. The reaction mixture was allowed to stir at the same temperature until the completion of reaction (monitored by TLC). The reaction mixture was quenched by ice cooled water before the crude was extracted with EtOAc and washed with water and brine. The organic phase was evaporated under reduced pressure after drying over $MgSO_4$ to give the crude product, which was subjected to flash chromatography (petroleum ether/EtOAc, 9/1) to give **10c** (19.5 mg, 97%, using DAST; 19.7 mg, 98%, using Deoxofluor®) as colorless oil.

*4.10.1. (3R,4S,5S)-3-Azido-4-benzyloxy-5-fluoroazepane-1-carboxylic acid-tert-butyl ester (**10b**).* Colorless oil, yield 95% (DAST), 97% (Deoxofluor®); R_f (petroleum ether/EtOAc, 9/1) 0.5; $[\alpha]_D^{20}$ +55.9 (c 1.0, CH_2Cl_2); IR (film) ν_{max} (cm^{-1}): 2362, 2342, 2109, 1716, 1698, 1541, 1522, 1474, 1457, 1418; ^{1}H NMR (600 MHz, $CDCl_3$) δ 7.41–7.28 (m, 5H), 4.83–4.60 (m, 3H), 3.97–3.84 (m, 1H), 3.80–3.47 (m, 3H), 3.25–3.11 (m, 1H), 3.01–2.87 (m, 1H), 2.23–1.99 (m, 2H), 1.46 (s, 9H); ^{13}C NMR (150 MHz, $CDCl_3$) δ 155.1, 137.6, 128.6, 128.5, 128.2, 93.6 (d, $^1J_{CF}$=173.1 Hz), 85.2 (d, $^2J_{CF}$=21.2 Hz), 80.9, 75.2, 63.7 (d, $^3J_{CF}$=6.2 Hz), 45.0, 40.9 (d, $^3J_{CF}$=11.4 Hz), 29.7 (d, $^2J_{CF}$=22.4 Hz), 28.5; HRMS (ESI): $[M+H]^+$, m/z calcd for $C_{18}H_{26}FN_4O_3$ 365.1989, found 365.2002.

*4.10.2. (3R,4R,6S)-3-Azido-4-benzyloxy-6-fluoroazepane-1-carboxylic acid-tert-butyl ester (**10c**).* R_f (petroleum ether/EtOAc, 9/1) 0.51; $[\alpha]_D^{20}$ −54.1 (c 1.0, CH_2Cl_2); IR (film) ν_{max} (cm^{-1}): 2361, 2341, 2109, 1716, 1541, 1521, 1473, 1456, 1418; ^{1}H NMR (600 MHz, $CDCl_3$) δ 7.39–7.34 (m, 5H), 4.93–4.78 (d, $^1J_{HF}$=54.0 Hz, 1H), 4.73 (t, J=11.7 Hz, 1H), 4.60–4.50 (m, 1H), 3.95–3.88 (m, 1H), 3.78–3.38 (m, 5H), 2.40–2.27 (m, 1H), 2.16–1.98 (m, 1H), 1.48 (s, 9H); ^{13}C NMR (150 MHz, $CDCl_3$) δ 155.1, 137.5, 128.7, 128.2, 88.3 (d, $^1J_{CF}$=171.0 Hz), 81.0, 77.3, 71.7, 64.7, 50.8 (d, $^2J_{CF}$=34.5 Hz), 48.4, 33.1 (d, $^2J_{CF}$=21.0 Hz), 28.4; HRMS (ESI): $[M+H]^+$, m/z calcd for $C_{18}H_{26}FN_4O_3$ 365.1989, found 365.1996.

*4.10.3. (3R,4R,6R)-3-Azido-4-benzyloxy-6-fluoroazepane-1-carboxylic acid-tert-butyl ester (**10d**).* R_f (petroleum ether/EtOAc, 9/1) 0.45; $[\alpha]_D^{20}$ +53.4 (c 0.9, CH_2Cl_2); colorless oil, yield 95% (DAST), 97% (Deoxofluor®); IR (film) ν_{max} (cm^{-1}): 2361, 2341, 2109, 1716, 1541, 1521, 1473, 1456, 1418; ^{1}H NMR (600 MHz, $CDCl_3$) δ 7.40–7.34 (m, 5H), 5.13–5.00 (d, $^1J_{HF}$=48.7 Hz, 1H), 4.62 (s, 2H), 4.15–4.04 (m, 1H), 3.81–3.68 (m, 2H), 3.63–3.57 (m, 1H), 3.32–3.23 (m, 1H), 2.99–2.93 (m, 1H), 2.49–2.42 (m, 1H), 1.85–1.73 (m, 1H), 1.48 (s, 9H); ^{13}C NMR (150 MHz, $CDCl_3$) δ 154.9, 137.6, 128.7, 128.3, 128.2, 88.5 (d, $^1J_{CF}$=169.7 Hz), 81.1, 77.2, 72.4, 65.1, 51.2 (d, $^2J_{CF}$=25.9 Hz), 47.8, 33.1 (d, $^2J_{CF}$=20.1 Hz), 28.4; HRMS (ESI): $[M+H]^+$, m/z calcd for $C_{18}H_{26}FN_4O_3$ 365.1989, found 365.1994.

4.11. General procedure for Boc deprotection

10b (9.60 mg, 26.3 μmol) was dissolved in TFA (500 μL) at 25 °C. The solution was allowed to stir for 5 min before TFA was vacuum evaporated. The reaction flask was kept under high vacuum (0.005 Torr, 25 °C) for 3 h to remove traces of TFA, and the colorless oily residue obtained was characterized as **11b** (9.20 mg, 98%).

*4.11.1. (3R,4S,5S)-3-Azido-4-benzyloxy-5-fluoroazepane (**11b**).* $[\alpha]_D^{20}$ +60.6 (c 0.8, CH_2Cl_2); IR (film) ν_{max} (cm^{-1}): 2362, 2341, 2112, 1716,

1698, 1684, 1671, 1558, 1541, 1521, 1456, 1199; ^{1}H NMR (600 MHz, $CDCl_3$) δ 7.41–7.30 (m, 5H), 4.88 (d, $^1J_{HF}$=45.2 Hz, 1H), 4.72 (q, J=14.8, 11.4 Hz, 2H), 4.04 (t, J=7.7 Hz, 1H), 3.84–3.78 (m, 1H), 3.39–3.08 (m, 4H), 2.35–2.22 (m, 2H); ^{13}C NMR (150 MHz, $CDCl_3$) δ 136.5, 128.8, 128.6, 128.3, 90.6 (d, $^1J_{CF}$=177.0 Hz), 82.2 (d, $^2J_{CF}$=25.5 Hz), 73.6, 59.9 (d, $^3J_{CF}$=3.0 Hz), 44.7, 40.0 (d, $^3J_{CF}$=9.0 Hz), 26.1 (d, $^2J_{CF}$=22.5 Hz); HRMS (ESI): $[M+H]^+$, m/z calcd for $C_{13}H_{18}FN_4O$ 265.1465, found 265.1463.

*4.11.2. (3R,4R,6S)-3-Azido-4-benzyloxy-6-fluoroazepane (**11c**).* $[\alpha]_D^{20}$ +59.9 (c 1.0, CH_2Cl_2); IR (film) ν_{max} (cm^{-1}): 2361, 2341, 2111, 1716, 1684, 1671, 1558, 1541, 1521, 1456, 1199; ^{1}H NMR (600 MHz, $CDCl_3$) δ 7.41–7.30 (m, 5H), 5.08 (d, $^1J_{HF}$=44.0 Hz, 1H), 4.76 (d, J=11.6 Hz, 1H), 4.52 (d, J=11.6 Hz, 1H), 4.12 (br s, 1H), 3.96 (br s, 1H), 3.67–3.58 (m, 2H), 3.56–3.44 (m, 1H), 3.42–3.33 (m, 1H), 2.54–2.44 (m, 1H), 2.42–2.30 (m, 1H); ^{13}C NMR (150 MHz, $CDCl_3$) δ 136.6, 128.9, 128.6, 128.2, 87.5 (d, $^1J_{CF}$=173.1 Hz), 74.9, 71.9, 60.1, 49.5 (d, $^2J_{CF}$=27.4 Hz), 48.2, 31.6 (d, $^2J_{CF}$=20.8 Hz); HRMS (ESI): $[M+H]^+$, m/z calcd for $C_{13}H_{18}FN_4O$ 265.1465, found 265.1471.

*4.11.3. (3R,4R,6R)-3-Azido-4-benzyloxy-6-fluoroazepane (**11d**).* $[\alpha]_D^{20}$ +58.7 (c 0.9, CH_2Cl_2); IR (film) ν_{max} (cm^{-1}): 2362, 2341, 2112, 1698, 1684, 1671, 1558, 1541, 1521, 1456, 1199; ^{1}H NMR (600 MHz, $CDCl_3$) δ 7.41–7.30 (m, 5H), 5.04 (d, $^1J_{HF}$=46.4 Hz, 1H), 4.63 (q, J=11.6, 6.0 Hz, 2H), 4.00–3.93 (m, 1H), 3.93–3.87 (m, 1H), 3.54–3.28 (m, 3H), 3.19–3.12 (q, J=14.4, 6.9 Hz, 1H), 2.54–2.46 (m, 1H), 2.34–2.23 (m, 1H); ^{13}C NMR (150 MHz, $CDCl_3$) δ 137.0, 128.8, 128.5, 128.2, 85.8 (d, $^1J_{CF}$=171.7 Hz), 75.4 (d, $^3J_{CF}$=9.0 Hz), 72.4, 61.7, 50.9 (d, $^2J_{CF}$=26.6 Hz), 46.4, 31.9 (d, $^2J_{CF}$=21.5 Hz); HRMS (ESI): $[M+H]^+$, m/z calcd for $C_{13}H_{18}FN_4O$ 265.1465, found 265.1469.

4.12. (3*R*,4*R*)-4-Benzyloxy-3-fluoro-2,3,4,7-tetrahydroazepine-1-carboxylic acid-*tert*-butyl (14)

$[\alpha]_D^{20}$ +29.3 (c 1.7, $CHCl_3$); IR (film) ν_{max} (cm^{-1}): 2360, 2345, 2111, 1715, 1699, 1651, 1541, 1522, 1474, 1457, 1418; ^{1}H NMR (600 MHz, $CDCl_3$) δ 7.38–7.29 (m, 5H), 5.89–5.73 (m, 2H), 5.04 (d, $^1J_{HF}$=66.1 Hz, 1H), 4.91 (d, J=11.9, 1H), 4.64 (q, J=17.5, 11.6 Hz, 1H), 4.04–3.35 (m, 4H), 2.70–2.53 (m, 1H), 1.46 (s, 9H); ^{13}C NMR (150 MHz, $CDCl_3$) δ 154.9, 136.7, 128.7, 128.2, 128.0, 126.8, 123.6, 112.2 (d, $^1J_{CF}$=219.0 Hz), 80.0, 71.5, 43.5, 41.5 (d, $^2J_{CF}$=17.3 Hz), 40.3 (d, $^2J_{CF}$=21.8 Hz), 28.6; HRMS (ESI): $[M+Na]^+$, m/z calcd for $C_{18}H_{24}FNO_3Na$ 344.1638, found 344.1646.

Acknowledgements

This research was being supported by an iMQRES scholarship to ARP from Macquarie University. We thank Peter Karuso for assisting with 2D NMR spectroscopy.

Supplementary data

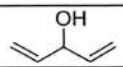
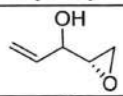
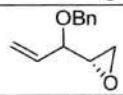
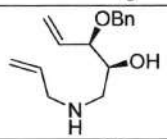
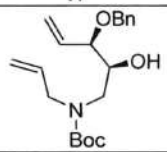
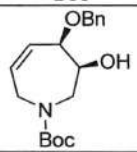
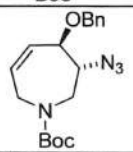
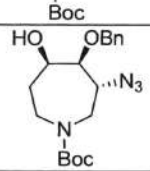
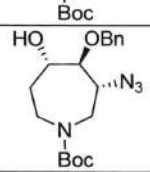
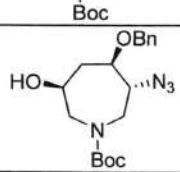
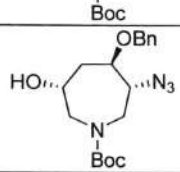
Supplementary data related to this article can be found at http://dx.doi.org/10.1016/j.tet.2012.10.078.

References and notes

1. Ritter, S. K. *Chem. Eng. News* **2012**, *90*, 10.
2. (a) Bégué, J.-P.; Bonnet-Delpon, D. *J. Fluorine Chem.* **2006**, *127*, 992; (b) Isanbor, C.; O'Hagan, D. *J. Fluorine Chem.* **2006**, *127*, 303; (c) Kirk, K. L. *J. Fluorine Chem.* **2006**, *127*, 1013; (d) Müller, K.; Faeh, C.; Diederich, F. *Science* **2007**, *317*, 1881.
3. (a) Böhm, H.-J.; Banner, D.; Bendels, S.; Kansy, M.; Kuhn, B.; Müller, K.; Obst-Sander, U.; Stahl, M. *ChemBioChem* **2004**, *5*, 637; (b) Gerebtzoff, G.; Li-Blatter, X.; Fischer, H.; Frentzel, A.; Seelig, A. *ChemBioChem* **2004**, *5*, 676; (c) Jeschke, P. *ChemBioChem* **2004**, *5*, 570; (d) Kirk, K. L. *Org. Process Res. Dev.* **2008**, *12*, 305; (e) Lipinski, C. A.; Lombardo, F.; Dominy, B. W.; Feeney, P. J. *Adv. Drug Delivery Rev.* **1997**, *23*, 3; (f) Park, B. K.; Kitteringham, N. R.; O'Neill, P. M. *Annu. Rev. Pharmacol. Toxicol.* **2001**, *41*, 443; (g) Paulini, R.; Müller, K.; Diederich, F. *Angew. Chem., Int. Ed.* **2005**, *44*, 1788; (h) Smart, B. E. *J. Fluorine Chem.* **2001**, *109*, 3.
4. (a) Craig, N. C.; Chen, A.; Suh, K. H.; Klee, S.; Mellau, G. C.; Winnewisser, B. P.; Winnewisser, M. *J. Am. Chem. Soc.* **1997**, *119*, 4789; (b) Leroux, F.; Jeschke, P.; Schlosser, M. *Chem. Rev.* **2005**, *105*, 827; (c) Muller, N. *J. Pharm. Sci.* **1986**, *75*, 987; (d) Myers, A. G.; Barbay, J. K.; Zhong, B. *J. Am. Chem. Soc.* **2001**, *123*, 7207; (e) Purser, S.; Moore, P. R.; Swallow, S.; Gouverneur, V. *Chem. Soc. Rev.* **2008**, *37*, 320; (f) Buissonneaud, D. Y.; van Mourik, T.; O'Hagan, D. *Tetrahedron* **2010**, *66*, 2196.
5. (a) Lal, G. S.; Pez, G. P.; Syvret, R. G. *Chem. Rev.* **1996**, *96*, 1737; (b) Prakash, G. K. S.; Yudin, A. K. *Chem. Rev.* **1997**, *97*, 757; (c) Umemoto, T. *Chem. Rev.* **1996**, *96*, 1757; (d) Hagmann, W. K. *J. Med. Chem.* **2008**, *51*, 4359; (e) Singh, R. P.; Shreeve, J. M. *Tetrahedron* **2000**, *56*, 7613; (f) Taylor, S. D.; Kotoris, C. C.; Hum, G. *Tetrahedron* **1999**, *55*, 12431; (g) Ametamey, S. M.; Honer, M.; Schubiger, P. A. *Chem. Rev.* **2008**, *108*, 1501.
6. (a) Núñez-Villanueva, D.; Bonache, M. A.; Infantes, L.; García-López, M. T.; Martín-Martínez, M.; González-Muñiz, R. *J. Org. Chem.* **2011**, *76*, 6592; (b) Jacobi, P. A.; Lee, K. *J. Am. Chem. Soc.* **2000**, *122*, 4295; (c) Wipf, P.; Spencer, S. R. *J. Am. Chem. Soc.* **2005**, *127*, 225; (d) Boeckman, R. K.; Clark, T. J.; Shook, B. C. *Org. Lett.* **2002**, *4*, 2109; (e) Zhu, L.; Lauchli, R.; Loo, M.; Shea, K. J. *Org. Lett.* **2007**, *9*, 2269; (f) Smith, A. B., III; Cho, Y. S.; Pettit, G. R.; Hirschmann, R. *Tetrahedron* **2003**, *59*, 6991.
7. (a) Stütz, A. E. *Iminosugars as Glycosidase Inhibitors: Nojirimycin and Beyond*; Wiley-VCH: Weinheim, 1999; (b) Martin, O. R.; Compain, P. *Iminosugars: From Synthesis to Therapeutic Applications*; Wiley-VCH: Weinheim, 2007; (c) Asano, N. In *Glycoscience: Chemistry and Chemical Biology*; Fraser-Reid, B. O., Tatsuta, K., Thiem, J., Coté, G. L., Flitsch, S., Ito, Y., Kondo, H., Nishimura, S.-i., Yu, B., Eds.; Springer: Heidelberg, 2008.
8. (a) Painter, G. F.; Eldridge, P. J.; Falshaw, A. *Bioorg. Med. Chem.* **2004**, *12*, 225; (b) Luo, B.; Marcelo, F.; Désiré, J.; Zhang, Y.; Sollogoub, M.; Kato, A.; Adachi, I.; Cañada, F. J.; Jiménez-Barbero, J.; Blériot, Y. *J. Carbohydr. Chem.* **2011**, *30*, 641; (c) Liu, P. S. *J. Org. Chem.* **1987**, *52*, 4717; (d) Jacob, G. S. *Curr. Opin. Struct. Biol.* **1995**, *5*, 605.
9. (a) Zitzmann, N.; Mehta, A. S.; Carrouée, S.; Butters, T. D.; Platt, F. M.; McCauley, J.; Blumberg, B. S.; Dwek, R. A.; Block, T. M. *Proc. Natl. Acad. Sci. U.S.A.* **1999**, *96*, 11878; (b) Nishimura, Y. *Curr. Top. Med. Chem.* **2003**, *3*, 575; (c) Fiaux, H.; Popowycz, F.; Favre, S.; Schütz, C.; Vogel, P.; Gerber-Lemaire, S.; Juillerat-Jeanneret, L. *J. Med. Chem.* **2005**, *48*, 4237.
10. (a) Laver, W. G.; Bischofberger, N.; Webster, R. G. *Sci. Am.* **1999**, *280*, 78; (b) Wu, S.-F.; Lee, C.-J.; Liao, C.-L.; Dwek, R. A.; Zitzmann, N.; Lin, Y.-L. *J. Virol.* **2002**, *76*, 3596; (c) Block, T. M.; Jordan, R. *Antiviral Chem. Chemother.* **2002**, *12*, 317; (d) Greimel, P.; Spreitz, J.; Stütz, A. E. *Curr. Top. Med. Chem.* **2003**, *3*, 513; (e) Nash, R. J.; Carroll, M.W.; Watson, A.A.; Fleet, G.W.J.; Horn, G. Vol. WO 2007010266, 2007.
11. (a) Sinnott, M. L. *Chem. Rev.* **1990**, *90*, 1171; (b) Groopman, J. E. *Rev. Infect. Dis.* **1990**, *12*, 908; (c) Robina, I.; Moreno-Vargas, A. J.; Carmona, A. T.; Vogel, P. *Curr. Drug Metab.* **2004**, *5*, 329.
12. (a) Johnson, H. A.; Thomas, N. R. *Bioorg. Med. Chem. Lett.* **2002**, *12*, 237; (b) Xuereb, H.; Maletic, M.; Gildersleeve, J.; Pelczer, I.; Kahne, D. *J. Am. Chem. Soc.* **2000**, *122*, 1883.
13. Andreana, P. R.; Sanders, T.; Janczuk, A.; Warrick, J. I.; Wang, P. G. *Tetrahedron Lett.* **2002**, *43*, 6525.
14. Lee, S. J.; Beak, P. *J. Am. Chem. Soc.* **2006**, *128*, 2178 and references therein.
15. Kulanthaivel, P.; Hallock, Y. F.; Boros, C.; Hamilton, S. M.; Janzen, W. P.; Ballas, L. M.; Loomis, C. R.; Jiang, J. B.; Katz, B. *J. Am. Chem. Soc.* **1993**, *115*, 6452.
16. Rezler, E. M.; Fenton, R. R.; Esdale, W. J.; McKeage, M. J.; Russell, P. J.; Hambley, T. W. *J. Med. Chem.* **1997**, *40*, 3508.
17. Damour, D.; Barreau, M.; Blanchard, J.-C.; Burgevin, M.-C.; Doble, A.; Herman, F.; Pantel, G.; James-Surcouf, E.; Vuilhorgne, M.; Mignani, S.; Poitout, L.; Merrer, Y. L.; Depezay, J.-C. *Bioorg. Med. Chem. Lett.* **1996**, *6*, 1667.
18. Furuya, T.; Kutruff, C. A.; Ritter, T. *Curr. Opin. Drug Discovery Dev.* **2008**, *11*, 803.
19. (a) Bio, M. M.; Waters, M.; Javadi, G.; Song, Z. J.; Zhang, F.; Thomas, D. *Synthesis* **2008**, 891; (b) Kiss, L.; Forró, E.; Fustero, S.; Fülöp, F. *Eur. J. Org. Chem.* **2011**, 4993; (c) Nemoto, H.; Nishiyama, T.; Akai, S. *Org. Lett.* **2011**, *13*, 2714; (d) Cedrón, J. C.; Estévez-Braun, A.; Ravelo, A. n. G.; Gutiérrez, D.; Flores, N.; Bucio, M. A.; Pérez-Hernández, N.; Joseph-Nathan, P. *Org. Lett.* **2009**, *11*, 1491; (e) Xia, Y.; Chackalamannil, S.; Greenlee, W. J.; Jayne, C.; Neustadt, B.; Stamford, A.; Vaccaro, H.; Xu, X.; Baker, H.; O'Neill, K.; Woods, M.; Hawes, B.; Kowalski, T. *Bioorg. Med. Chem. Lett.* **2011**, *21*, 3290.
20. Middleton, W. J. *J. Org. Chem.* **1975**, *40*, 574.
21. Lal, G. S.; Pez, G. P.; Pesaresi, R. J.; Prozonic, F. M.; Cheng, H. *J. Org. Chem.* **1999**, *64*, 7048.
22. Hayashi, H.; Sonoda, H.; Fukumura, K.; Nagata, T. *Chem. Commun.* **2002**, 1618.
23. Yin, J.; Zarkowsky, D. S.; Thomas, D. W.; Zhao, M. M.; Huffman, M. A. *Org. Lett.* **2004**, *6*, 1465.
24. Fürstner, A.; Thiel, O. R. *J. Org. Chem.* **2000**, *65*, 1738.
25. Romero, A.; Wong, C.-H. *J. Org. Chem.* **2000**, *65*, 8264.
26. Trost, B. M.; Fandrick, D. R.; Brodmann, T.; Stiles, D. T. *Angew. Chem., Int. Ed.* **2007**, *46*, 6123.
27. Evans, D. A.; Fu, G. C.; Hoveyda, A. H. *J. Am. Chem. Soc.* **1988**, *110*, 6917.
28. (a) Beletskaya, I.; Pelter, A. *Tetrahedron* **1997**, *53*, 4957; (b) Lata, C. J.; Crudden, C. M. *J. Am. Chem. Soc.* **2010**, *132*, 131.
29. Männig, D.; Nöth, H. *Angew. Chem., Int. Ed. Engl.* **1985**, *24*, 878.
30. (a) Westcott, S. A.; Blom, H. P.; Marder, T. B.; Baker, R. T. *J. Am. Chem. Soc.* **1992**, *114*, 8863; (b) Evans, D. A.; Fu, G. C.; Hoveyda, A. H. *J. Am. Chem. Soc.* **1992**, *114*, 6671.
31. (a) Burgess, K.; Cassidy, J.; Ohlmeyer, M. J. *J. Org. Chem.* **1991**, *56*, 1020; (b) Burgess, K.; Ohlmeyer, M. J. *J. Org. Chem.* **1991**, *56*, 1027; (c) Burgess, K.; Ohlmeyer, M. J. *Tetrahedron Lett.* **1989**, *30*, 395.
32. (a) Crudden, C. M.; Edwards, D. *Eur. J. Org. Chem.* **2003**, *2003*, 4695; (b) Harder, S.; Spielmann, J. *J. Organomet. Chem.* **2012**, *698*, 7; (c) Burgess, K.; Ohlmeyer, M. J. *Chem. Rev.* **1991**, *91*, 1179.

33. (a) Murata, M.; Watanabe, S.; Masuda, Y. *Tetrahedron Lett.* **1999**, *40*, 2585; (b) Hayashi, T.; Matsumoto, Y.; Ito, Y. *Tetrahedron: Asymmetry* **1991**, *2*, 601.
34. (a) Evans, D. A.; Fu, G. C. *J. Am. Chem. Soc.* **1991**, *113*, 4042; (b) Brinkman, J. A.; Nguyen, T. T.; Sowa, J. R. *Org. Lett.* **2000**, *2*, 981; (c) Knorr, J. R.; Merola, J. S. *Organometallics* **1990**, *9*, 3008.
35. (a) Noh, D.; Yoon, S. K.; Won, J.; Lee, J. Y.; Yun, J. *Chem.—Asian J.* **2011**, *6*, 1967; (b) Noh, D.; Chea, H.; Ju, J.; Yun, J. *Angew. Chem., Int. Ed.* **2009**, *48*, 6062.
36. Leroy, J.; Hebert, E.; Wakselman, C. *J. Org. Chem.* **1979**, *44*, 3406.
37. (a) Carless, H. A. J.; Busia, K. *Carbohydr. Res.* **1992**, *234*, 207; (b) Jenkins, C. L.; Lin, G.; Duo, J.; Rapolu, D.; Guzei, I. A.; Raines, R. T.; Krow, G. R. *J. Org. Chem.* **2004**, *69*, 8565; (c) Yoshimura, Y.; Endo, M.; Kitano, K.; Yamada, K.; Sakata, S.; Miura, S.; Machida, H. *Nucleosides Nucleotides* **1999**, *18*, 815; (d) Yang, S. S.; Chiang, Y.-c. P.; Beattie, T. R. *Carbohydr. Res.* **1993**, *249*, 259; (e) Ballereau, S.; Guédat, P.; Spiess, B.; Rehnberg, N.; Schlewer, G. *Tetrahedron Lett.* **1995**, *36*, 7449; (f) Jeong, L. S.; Lee, J. E.; Kim, H. O.; Chun, M. W. *Arch. Pharm. Res.* **1998**, *21*, 338.
38. Déchamps, I.; Gomez Pardo, D.; Cossy, J. *Eur. J. Org. Chem.* **2007**, 4224.
39. Jaseer, E. A.; Naidu, A. B.; Kumar, S. S.; Rao, R. K.; Thakur, K. G.; Sekar, G. *Chem. Commun.* **2007**, 867.
40. (a) Lal, G.S.; Pez, G.P. US Patent 6,080,886, 2000. (b) Lal, G. S.; Pez, G. P.; Pesaresi, R. J.; Prozonic, F. M. *Chem. Commun.* **1999**, 215; (c) Singh, R. P.; Chakraborty, D.; Shreeve, J. M. *J. Fluorine Chem.* **2001**, *111*, 153; (d) Lal, G. S.; Lobach, E.; Evans, A. *J. Org. Chem.* **2000**, *65*, 4830; (e) Singh, R. P.; Majumder, U.; Shreeve, J. M. *J. Org. Chem.* **2001**, *66*, 6263.

2.3. Cross Reference of Compounds in Chapter 2

Structure	Nomenclature in Thesis	Nomenclature in *Tetrahedron*, 2013, *69*, 744
	**2.1**	**1**
	**2.2**	**2**
	**2.3**	**3**
	**2.4**	**4**
	**2.5**	**5**
	**2.6**	**6**
	**2.7**	**7**
	**2.8a**	**8a**
	**2.8b**	**8b**
	**2.8c**	**8c**
	**2.8d**	**8d**

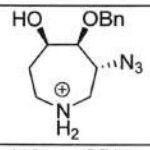
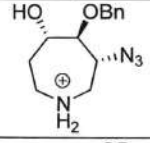
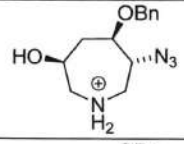
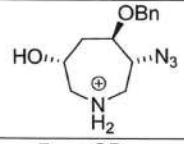
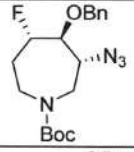
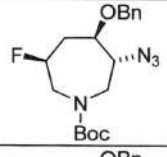
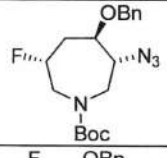
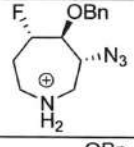
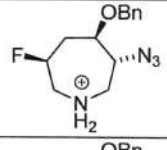
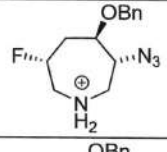
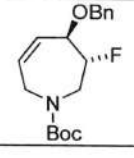
	**2.9a**	**9a**
	**2.9b**	**9b**
	**2.9c**	**9c**
	**2.9d**	**9d**
	**2.10b**	**10b**
	**2.10c**	**10c**
	**2.10d**	**10d**
	**2.11b**	**11b**
	**2.11c**	**11c**
	**2.11d**	**11d**
	**2.14**	**14**

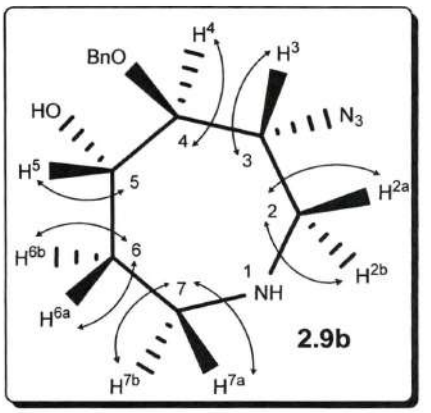
Table 2.1. Cross reference of compound nomenclature from the thesis and *Tetrahedron*, **2013**, *69*, 744.

2.4. Experimental

2.4.1. Structure Elucidation of the Key Intermediates

2.4.1.1. (3*R*,4*R*,5*S*)–3–Azido–4–benzyloxyazepane–5–ol (2.9b)

^{1}H–^{13}C HSQC 2D NMR correlations:



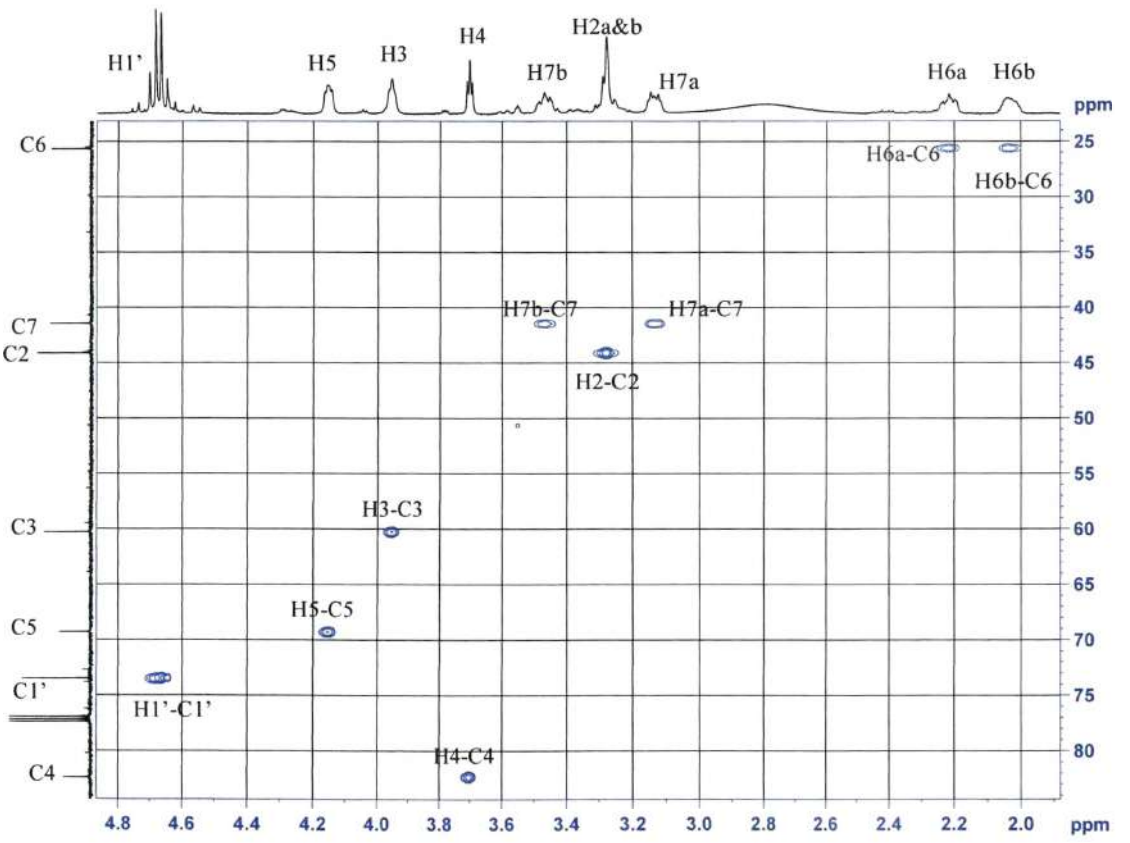
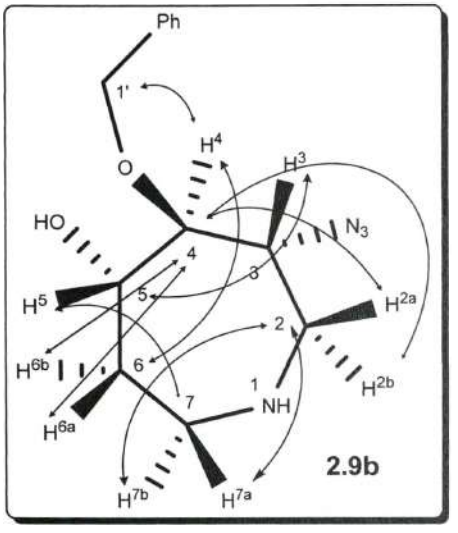


Figure 2.3. ^{1}H–^{13}C HSQC 2D NMR correlations of the azepane ring in **2.9b**.

$^{1}H–^{13}C$ HMBC 2D NMR correlations:



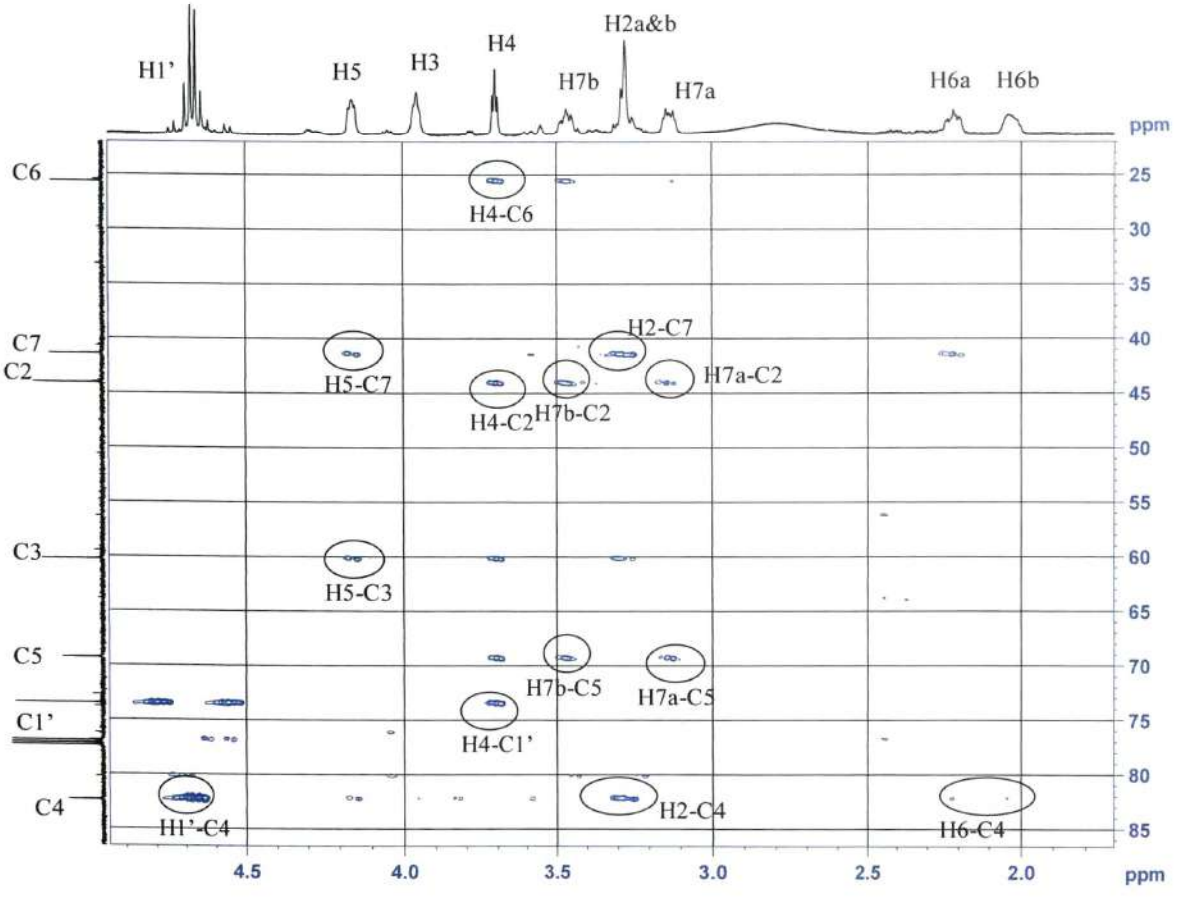
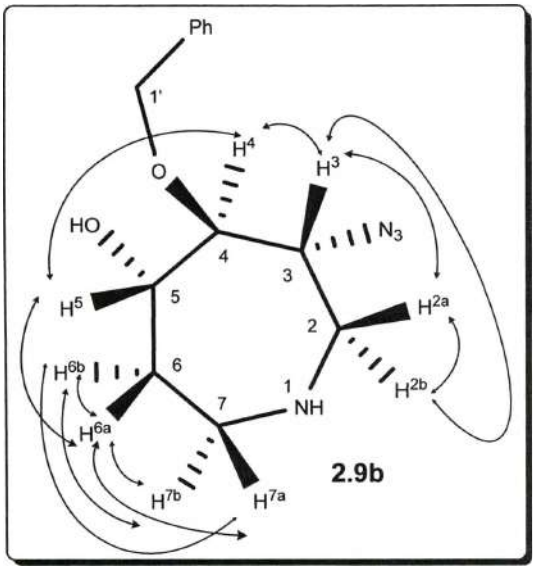


Figure 2.4. $^{1}H–^{13}C$ HMBC 2D NMR correlations of the azepane ring in **2.9b**.

^{1}H–^{1}H COSY 2D NMR correlations:



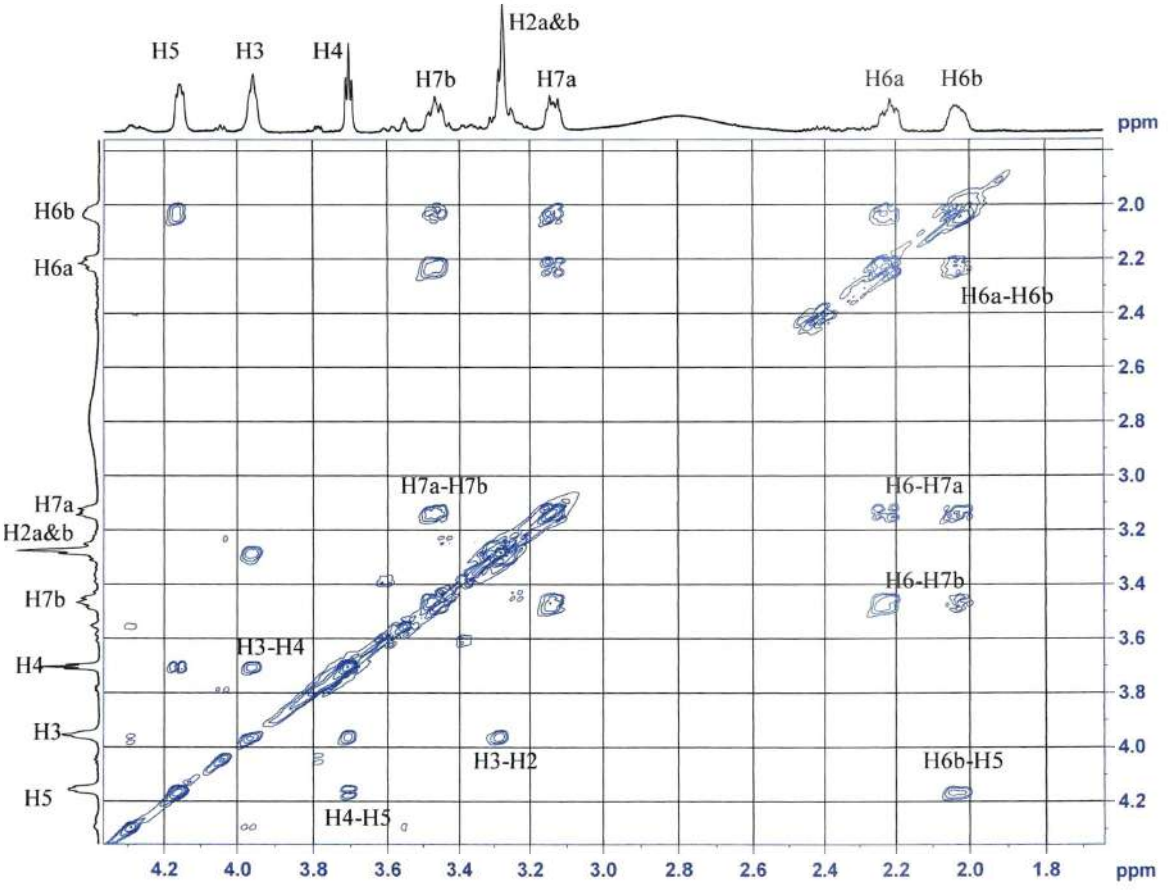
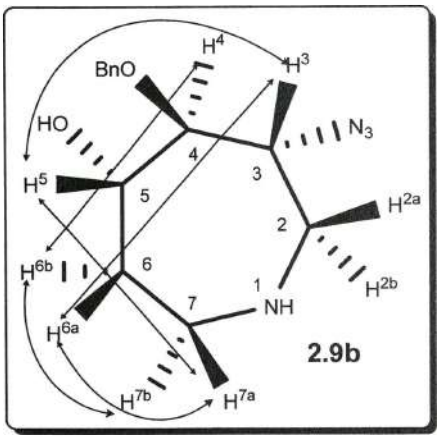


Figure 2.5. ^{1}H–^{1}H COSY 2D NMR correlations of the azepane ring in **2.9b**.

^{1}H–^{1}H NOESY 2D NMR correlations:



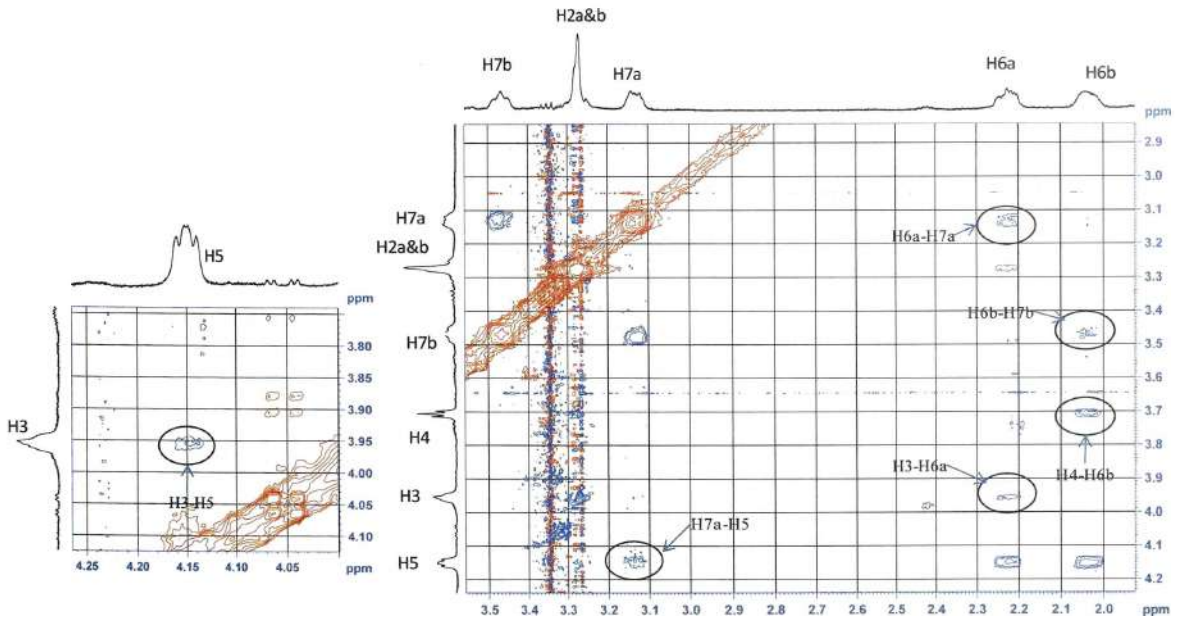
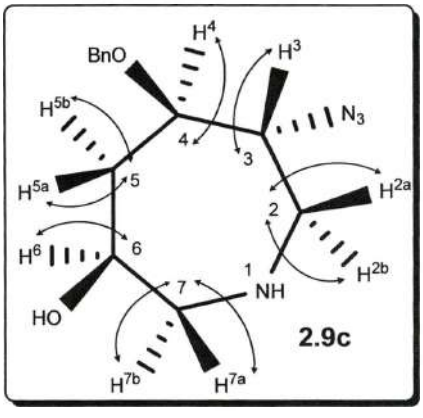


Figure 2.6. ^{1}H–^{1}H NOESY 2D NMR correlations of the azepane ring in **2.9b**.

Compound **2.9b** has two stereocentres (C3 and C4) with known stereochemistry. H3 showed NOE to H6a, with no detectable NOE to H6b, and also showed NOE to H4. H6a further showed NOE to H7a, and H6b showed NOE to H7b. H5 showed NOE to H3 and H7a, but not to H7b suggesting that C5 has the *S* configuration.

2.4.1.2. (3*R*,4*R*,6*S*)–3–Azido–4–benzyloxyazepane–6–ol (2.9c)

^{1}H–^{13}C HSQC 2D NMR correlations:



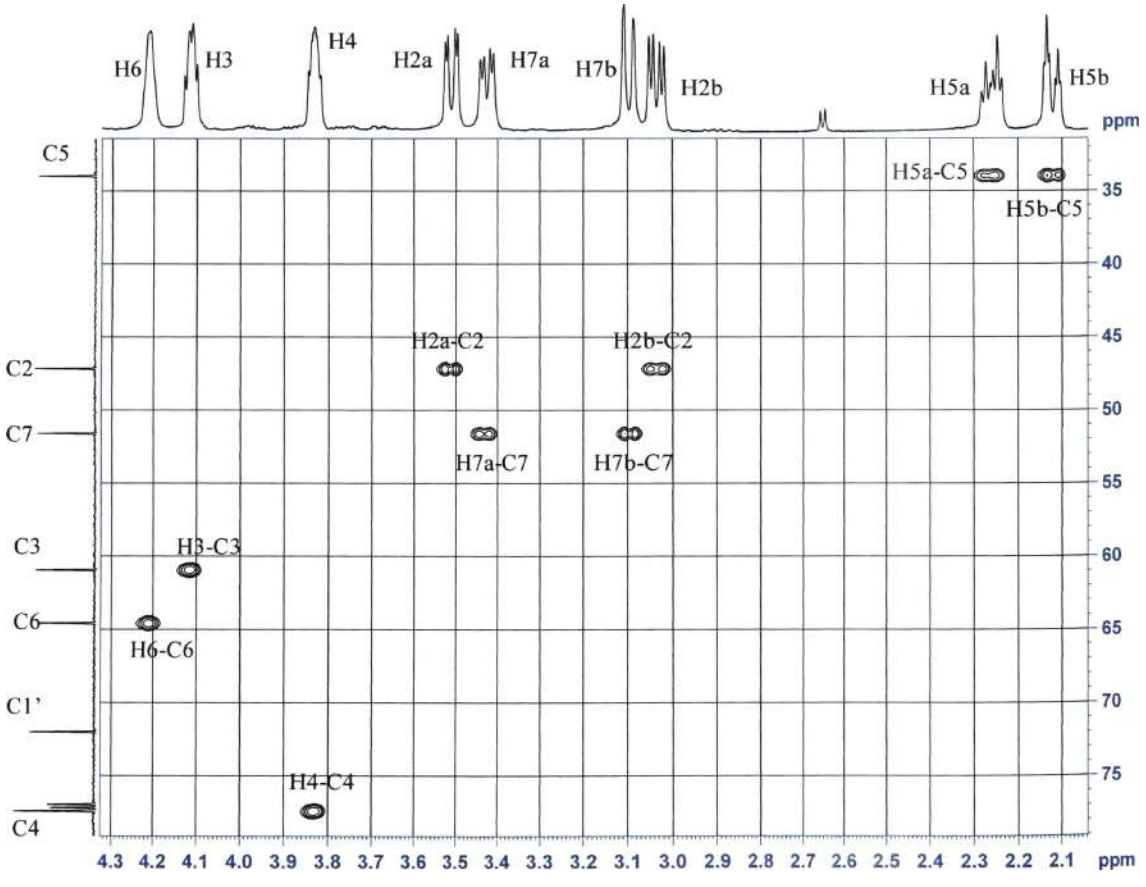


Figure 2.7. ^{1}H–^{13}C HSQC 2D NMR correlations of the azepane ring in **2.9c**.

$^{1}H–^{13}C$ HMBC 2D NMR correlations:

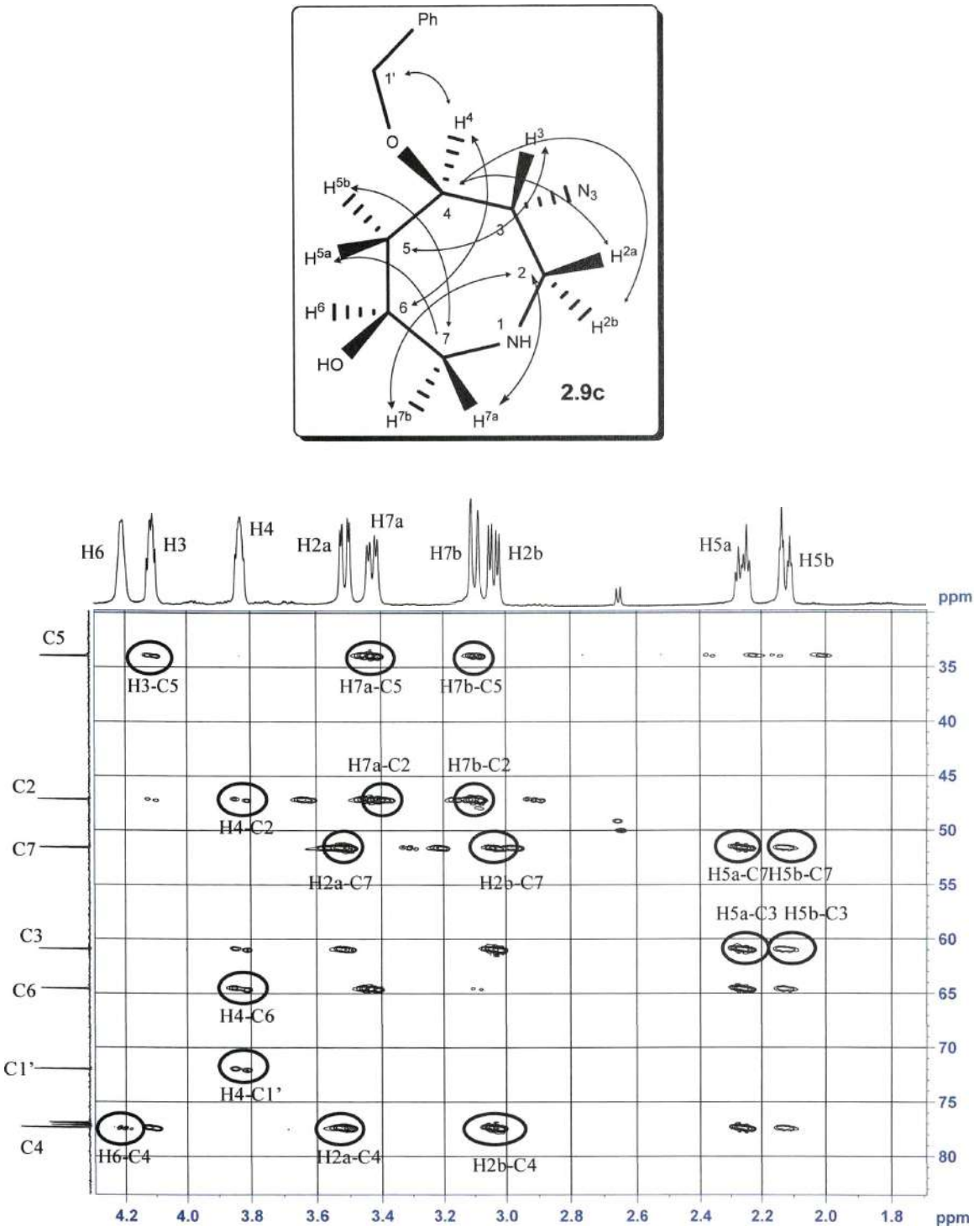
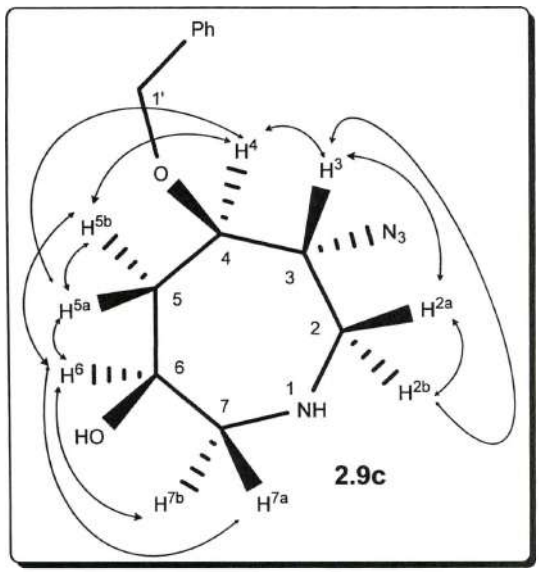


Figure 2.8. $^{1}H–^{13}C$ HMBC 2D NMR correlations of the azepane ring in **2.9c**.

^{1}H–^{1}H COSY 2D NMR correlations:



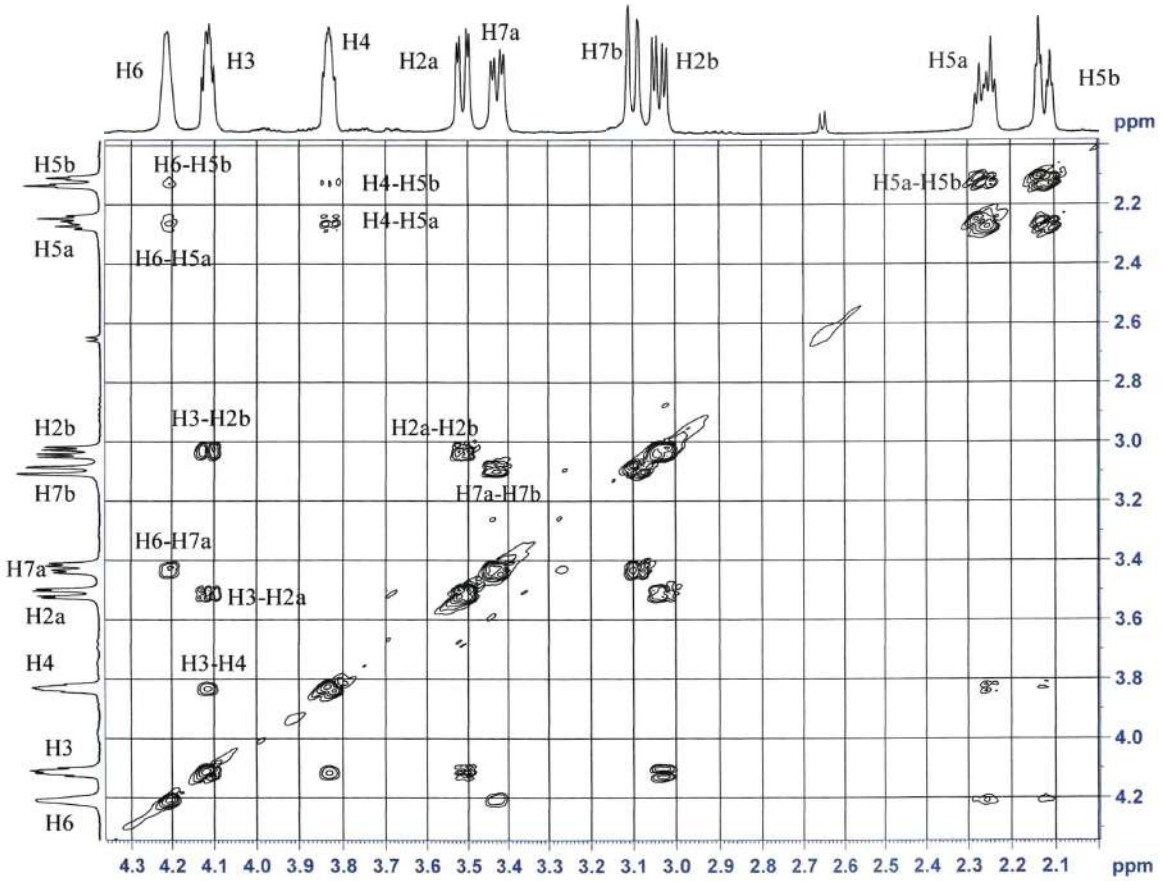
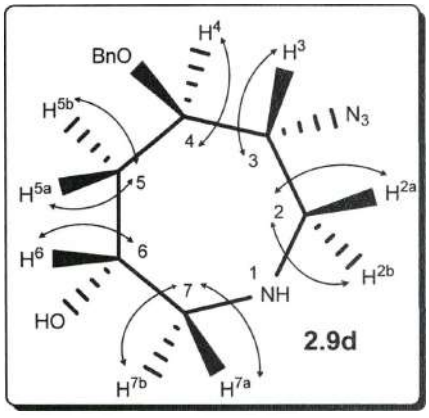


Figure 2.9. ^{1}H–^{1}H COSY 2D NMR correlations of the azepane ring in **2.9c**.

2.4.1.3. (3*R*,4*R*,6*R*)–3–Azido–4–benzyloxyazepane–6–ol (2.9d)

^{1}H–^{13}C HSQC 2D NMR correlations:



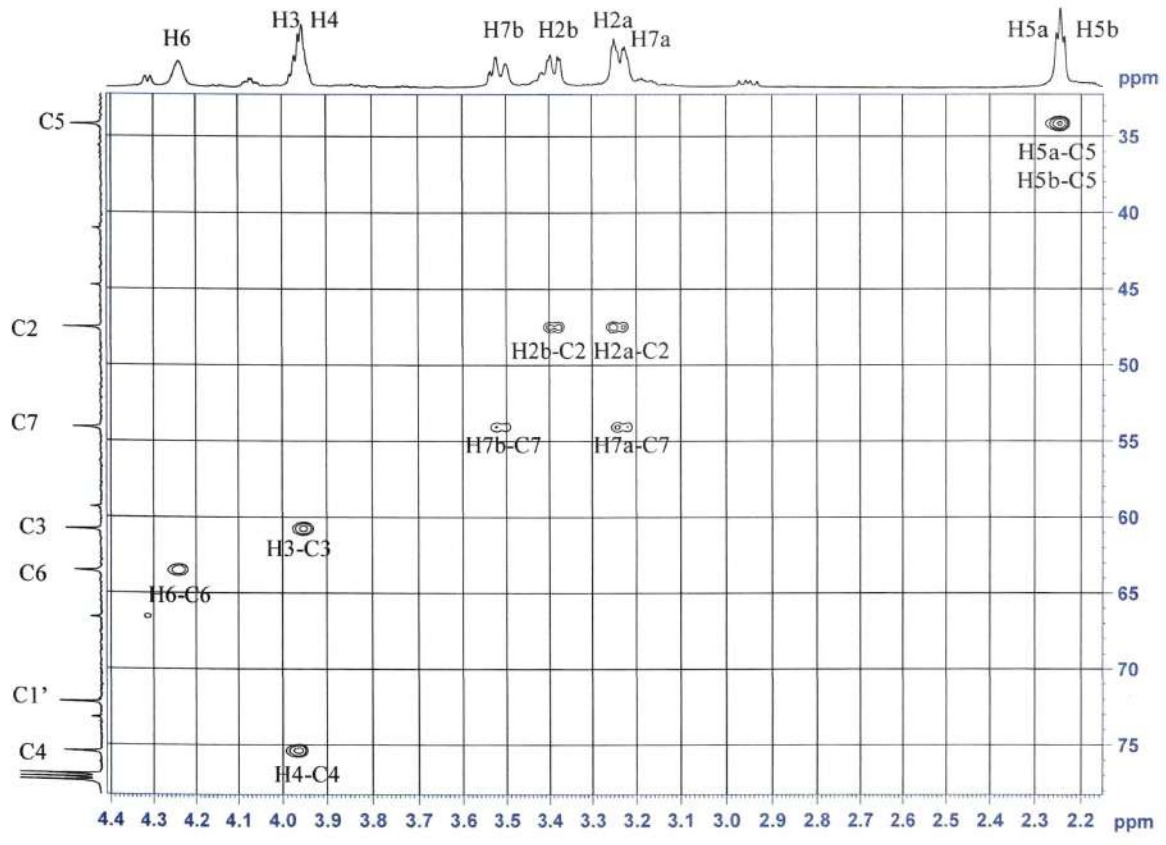
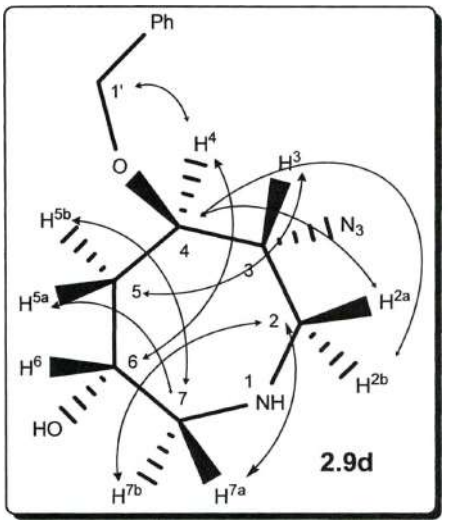


Figure 2.10. ^{1}H–^{13}C HSQC 2D NMR correlations of the azepane ring in **2.9d**.

$^{1}H–^{13}C$ HMBC 2D NMR correlations:



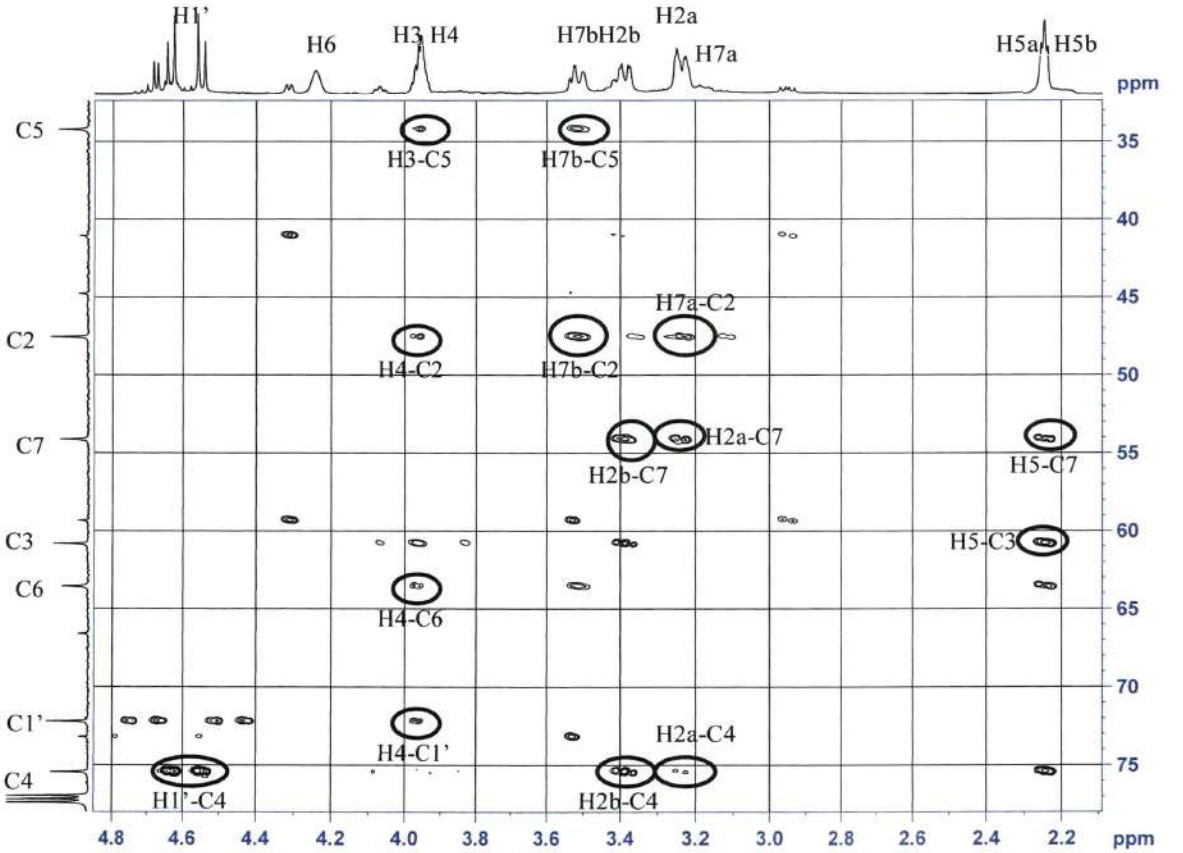
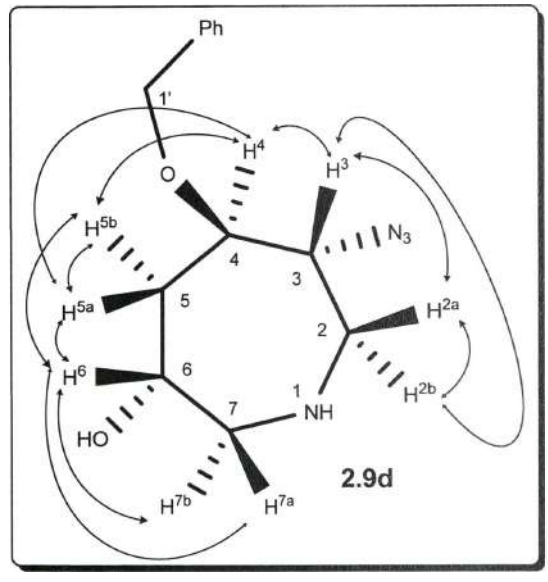


Figure 2.11. $^{1}H–^{13}C$ HMBC 2D NMR correlations of the azepane ring in **2.9d**.

^{1}H–^{1}H COSY 2D NMR correlations:



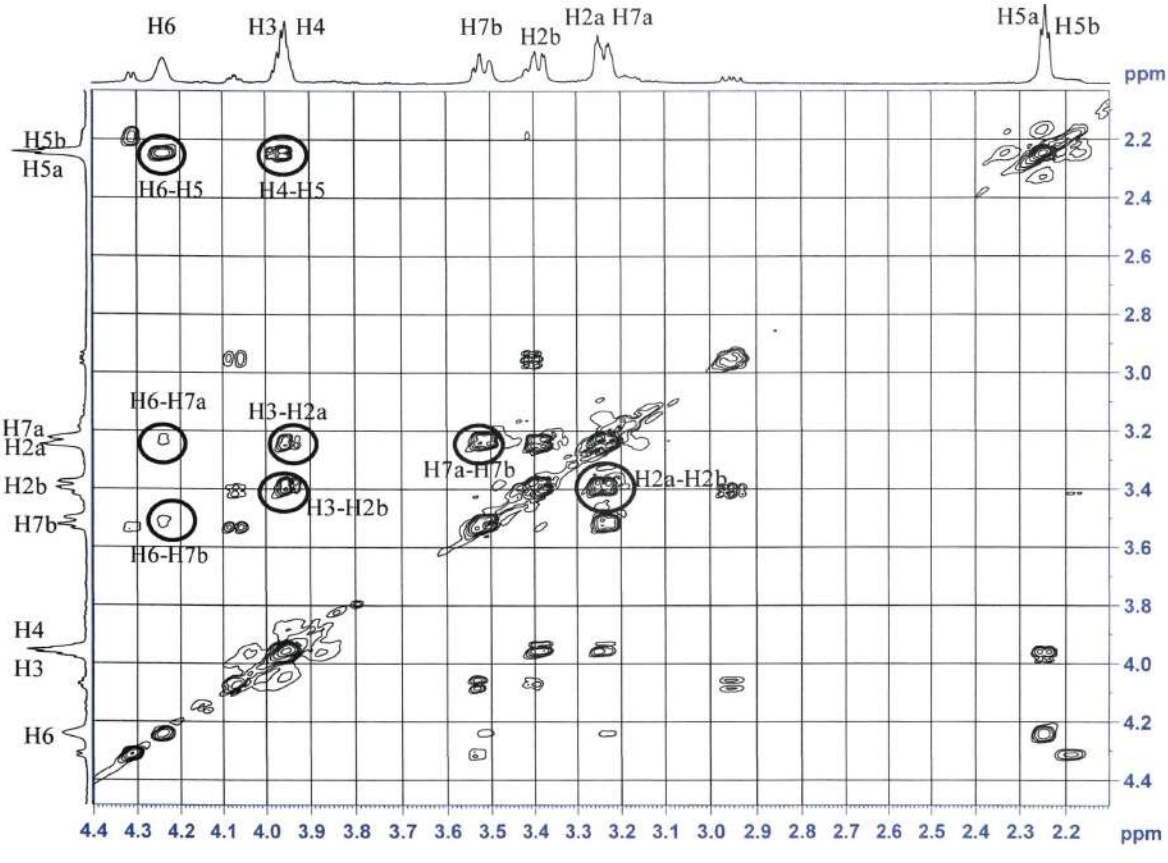


Figure 2.12. ^{1}H–^{1}H COSY 2D NMR correlations of the azepane ring in **2.9d**.

^{1}H–^{1}H NOESY 2D NMR correlations comparison 2.9c and 2.9d:

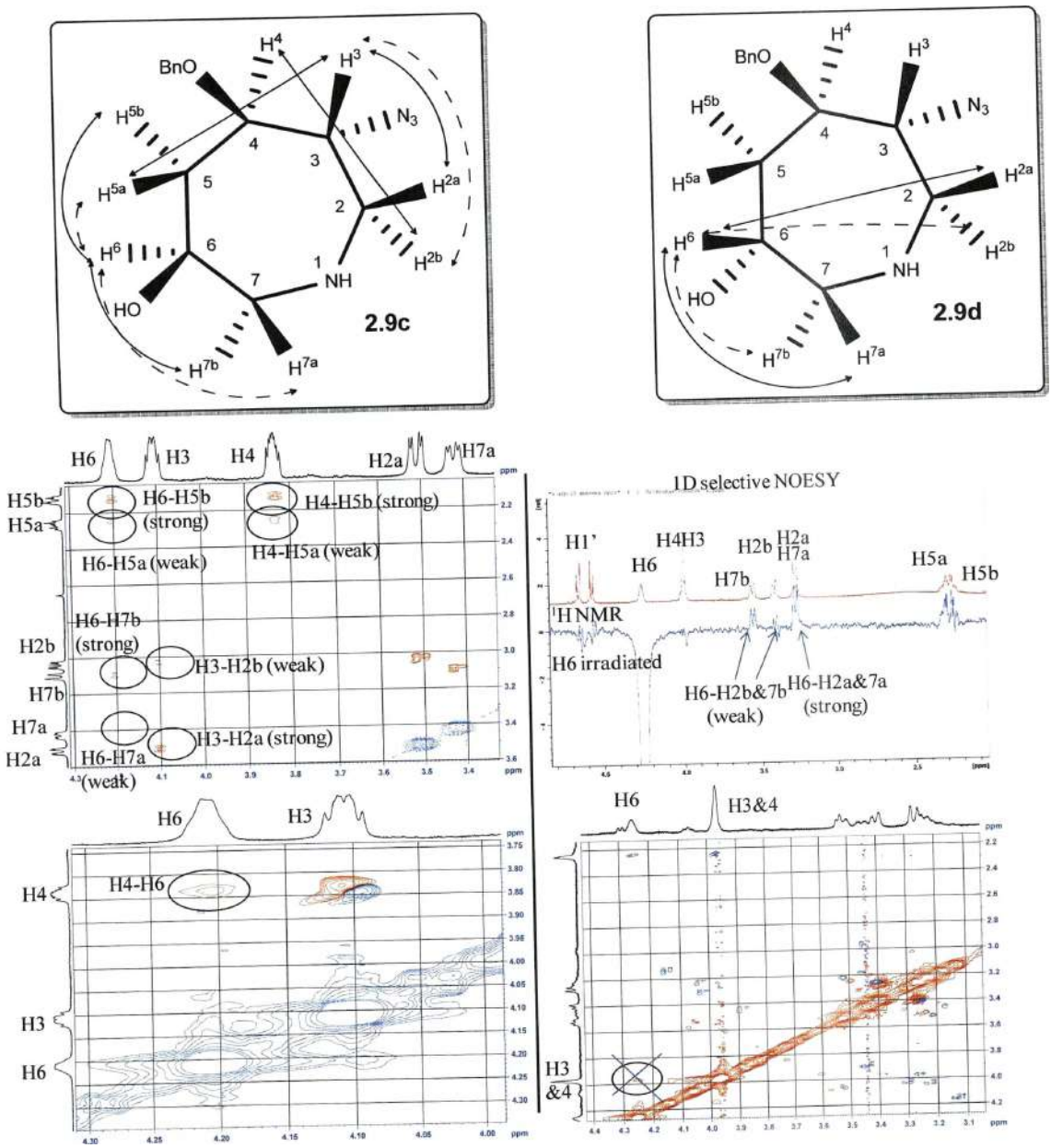
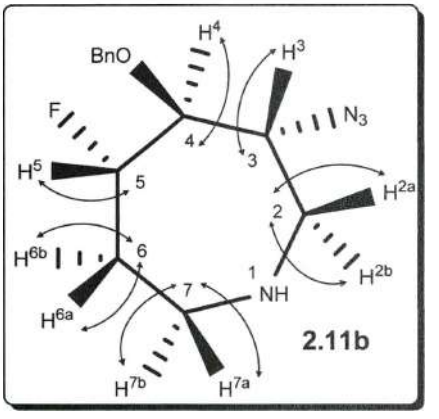


Figure 2.13. ^{1}H–^{1}H NOESY 2D NMR correlations comparison in **2.9c** and **2.9d**.

In the case of **2.9c**, H6 showed stronger NOEs to H5b and H7b compared to that of H5a and H7a. In the case of **2.9d**, H6 showed stronger NOEs to H2a and H7a compared to that of H2b and H7b. H6 showed NOE to H4 in **2.9c** but there was no detectable NOE to H4 in **2.9d**.

2.4.1.4. (3*R*,4*R*,5*S*)–3–Azido–4–benzyloxy–5–fluoroazepane (2.11b)

^{1}H–^{13}C HSQC 2D NMR correlations:



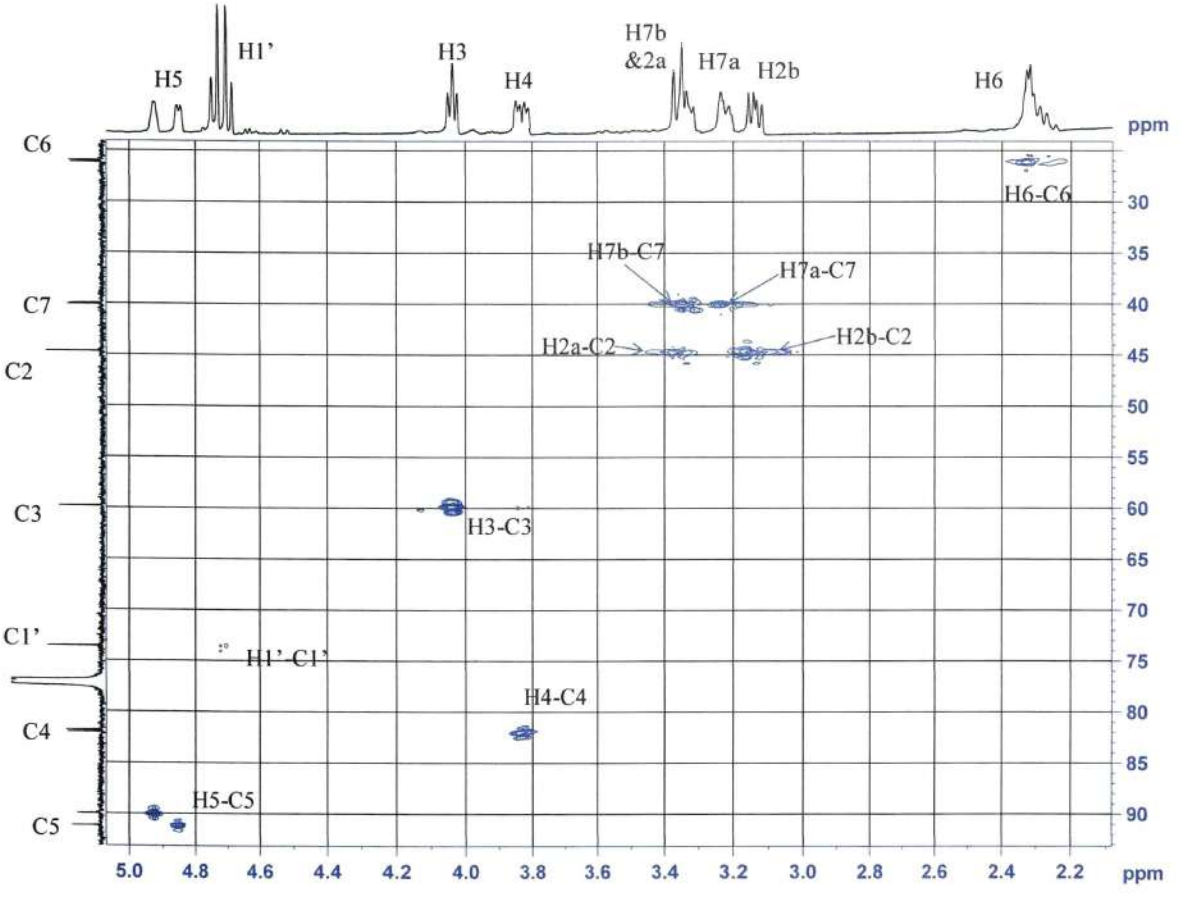
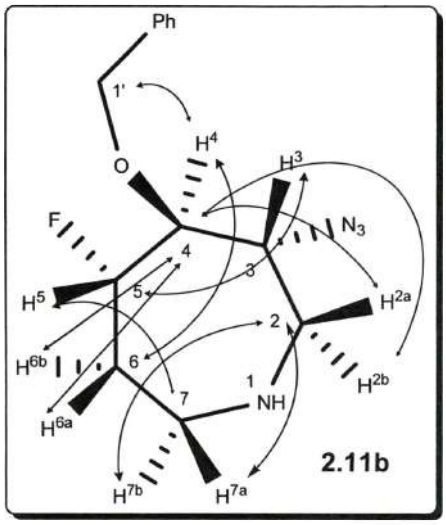


Figure 2.14. ^{1}H–^{13}C HSQC 2D NMR correlations of the azepane ring in **2.11b**.

$^{1}H–^{13}C$ HMBC 2D NMR correlations:



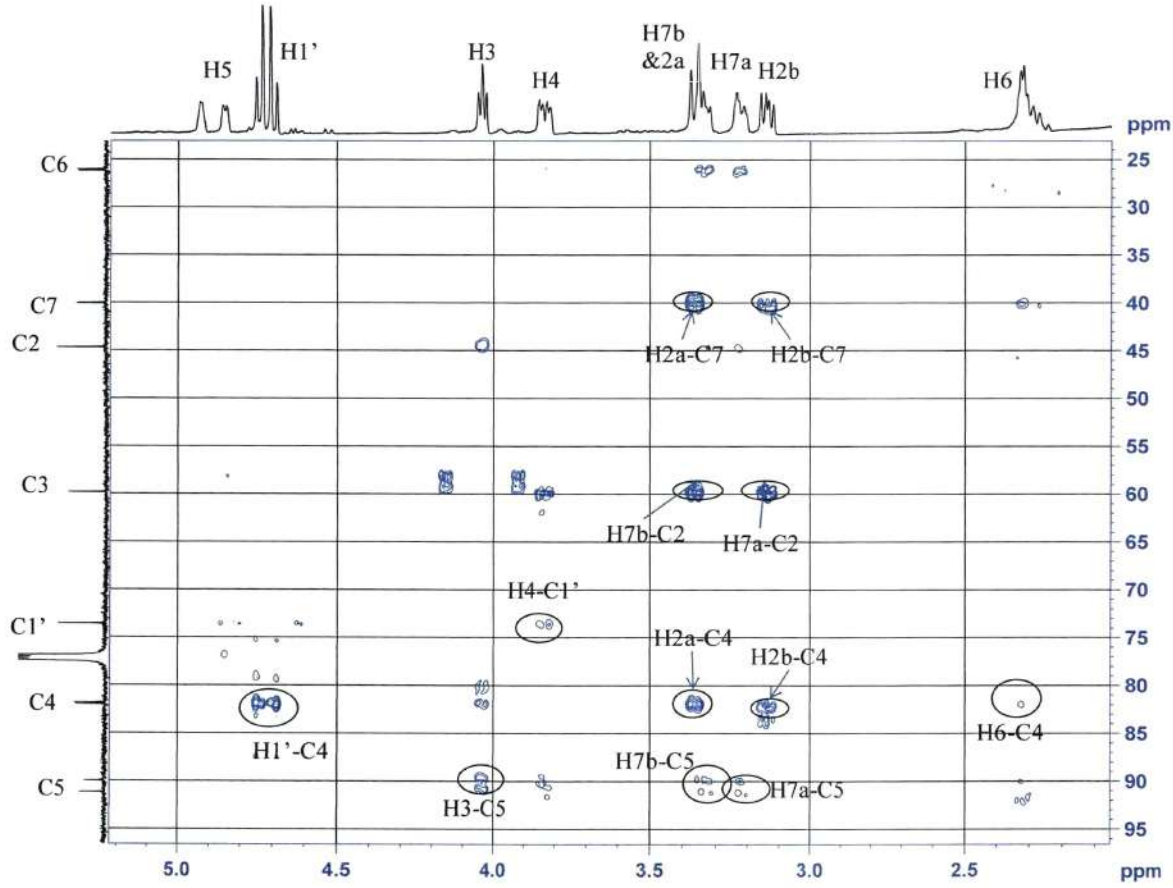
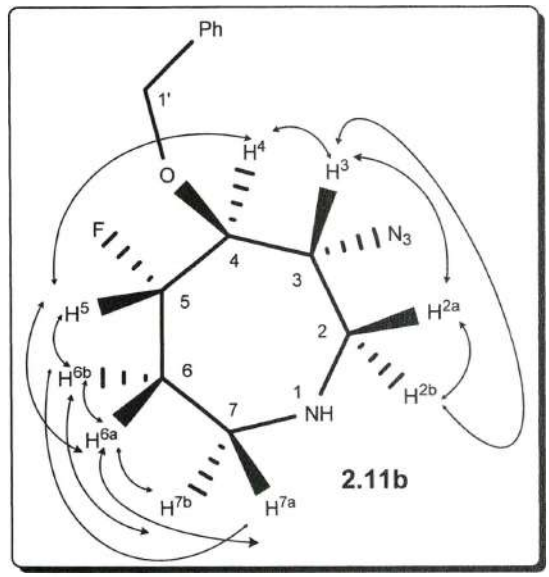


Figure 2.15. $^{1}H–^{13}C$ HMBC 2D NMR correlations of the azepane ring in **2.11b**.

^{1}H–^{1}H COSY 2D NMR correlations:



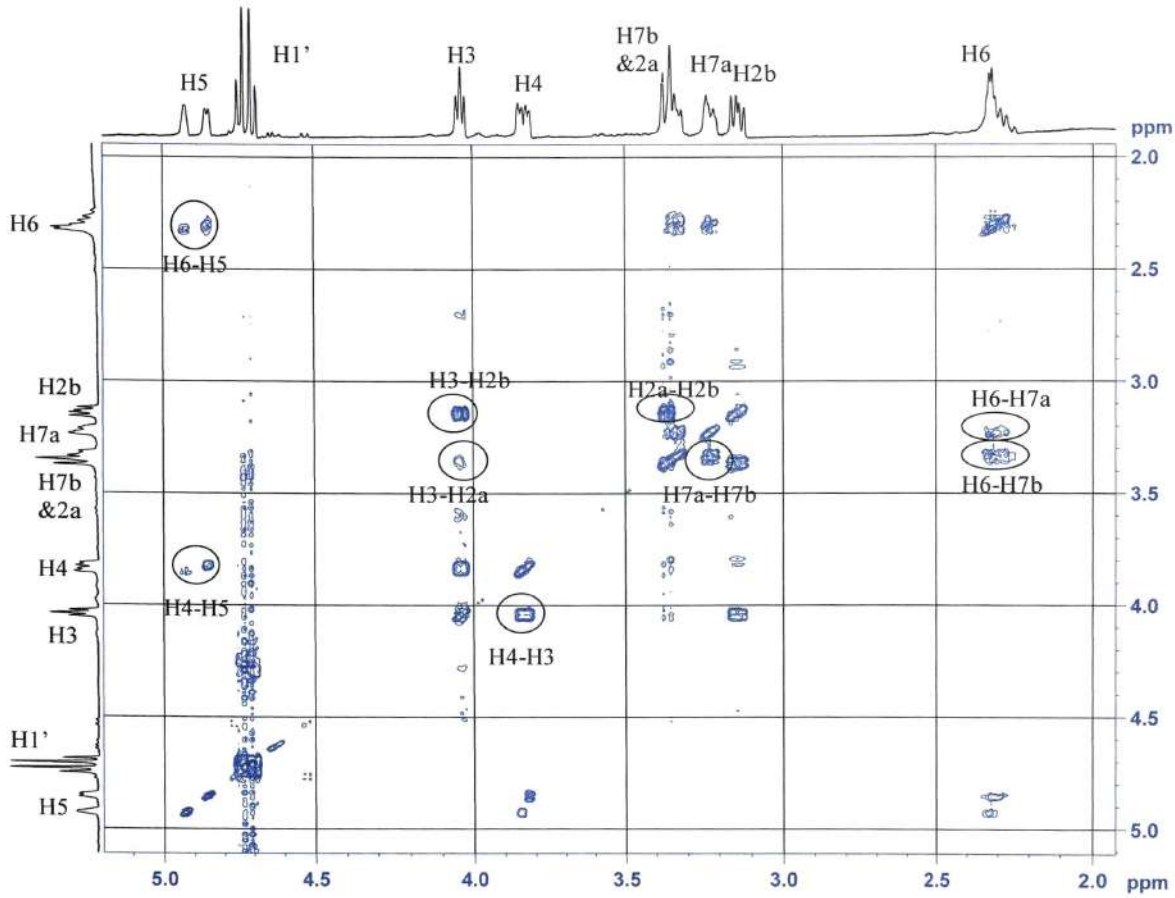


Figure 2.16. ^{1}H–^{1}H COSY 2D NMR correlations of the azepane ring in **2.11b**.

^{1}H–^{1}H NOESY 2D NMR correlations:

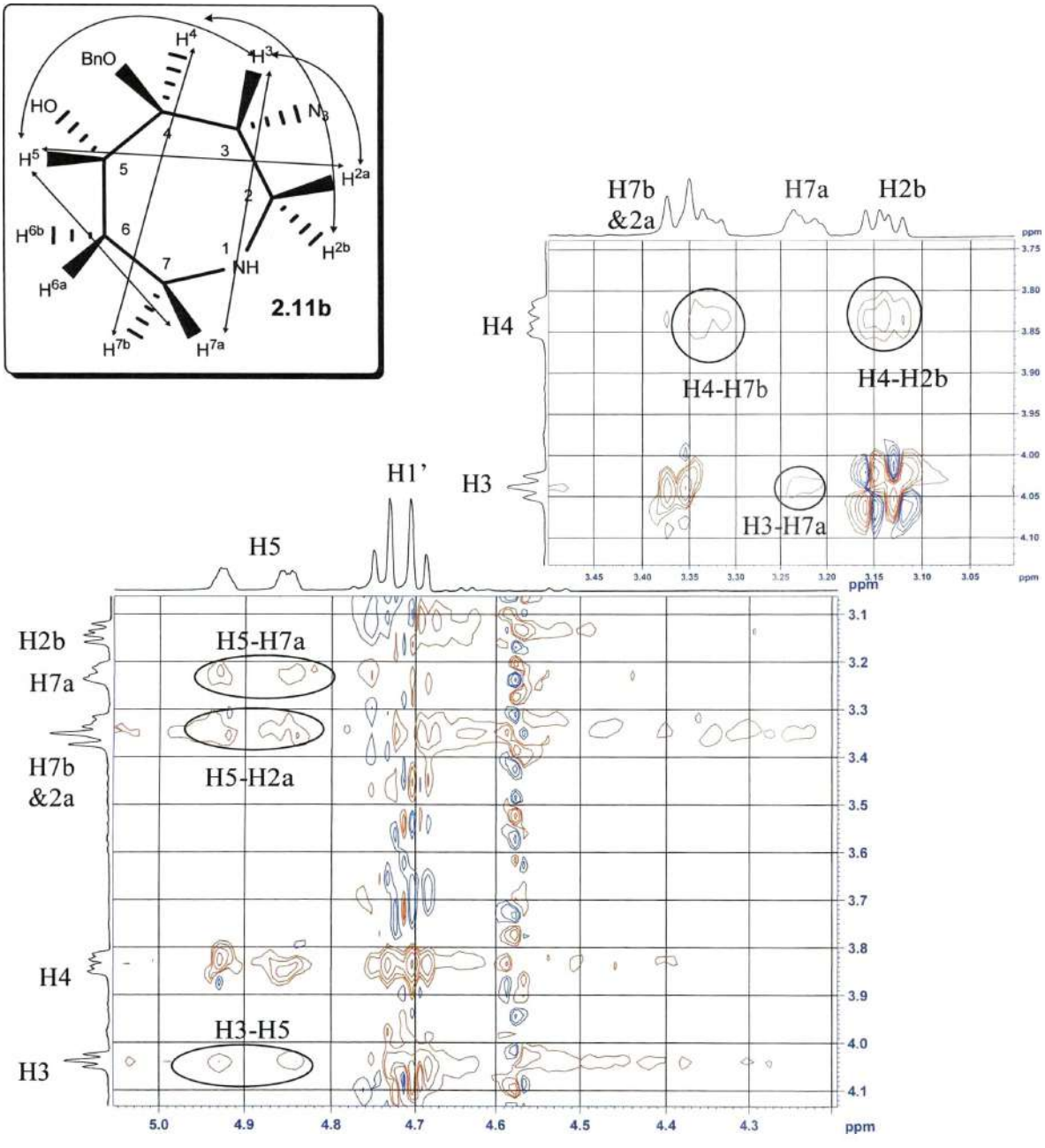
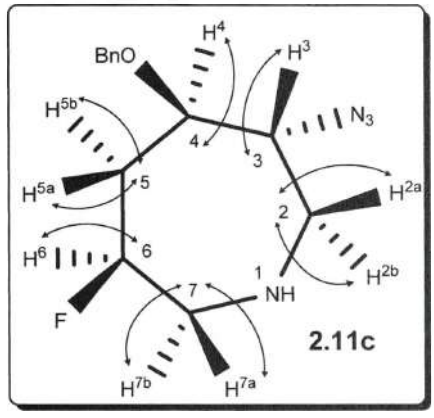


Figure 2.17. ^{1}H–^{1}H NOESY 2D NMR correlations of the azepane ring in **2.11b**.

In Compound **2.11b**, H2a, H7a and H2b, H7b showed NOEs to H3 and H4, respectively. H5 showed NOE to H3, H2a and H7a, meaning the absolute configuration at C5 is *S*.

2.4.1.5. (3*R*,4*R*,6*S*)–3–Azido–4–benzyloxy–6–fluoroazepane (2.11c)

^{1}H–^{13}C HSQC 2D NMR correlations:



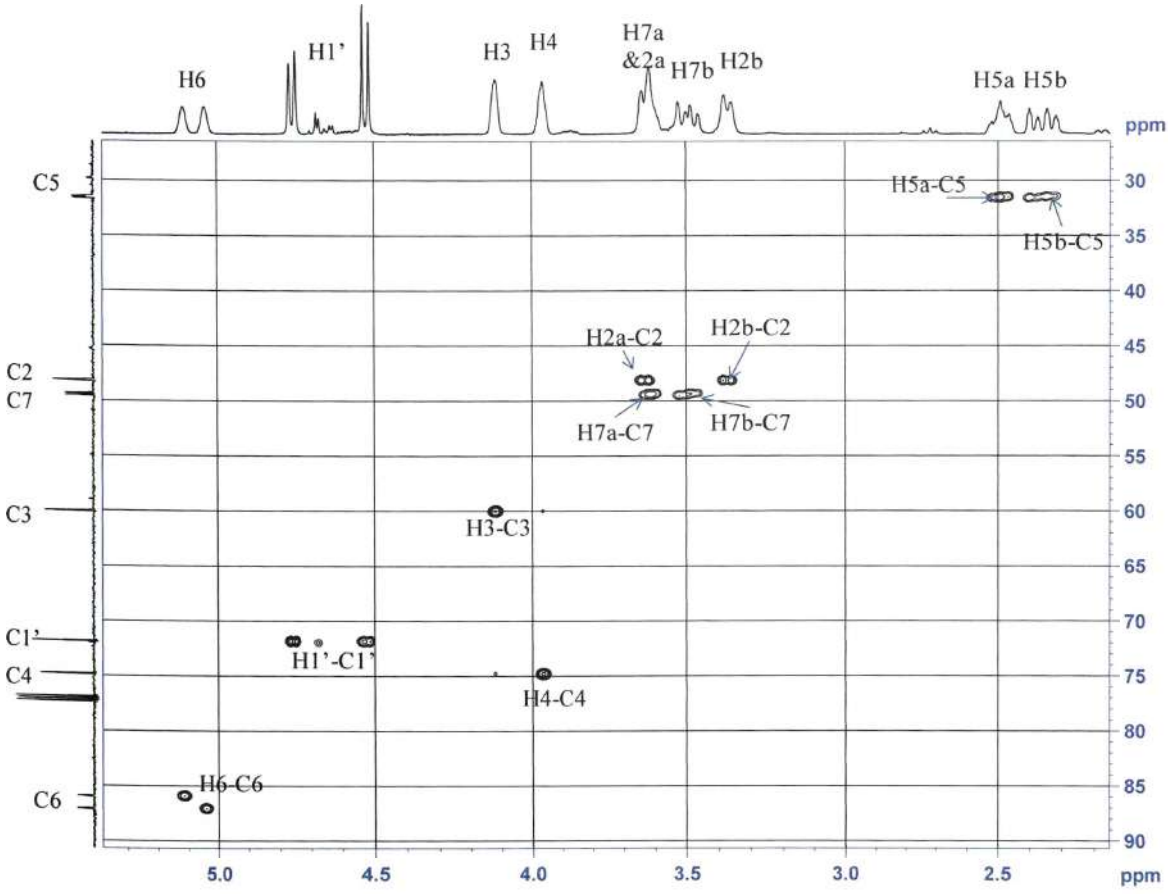


Figure 2.18. ^{1}H–^{13}C HSQC 2D NMR correlations of the azepane ring in **2.11c**.

$^{1}H–^{13}C$ HMBC 2D NMR correlations:

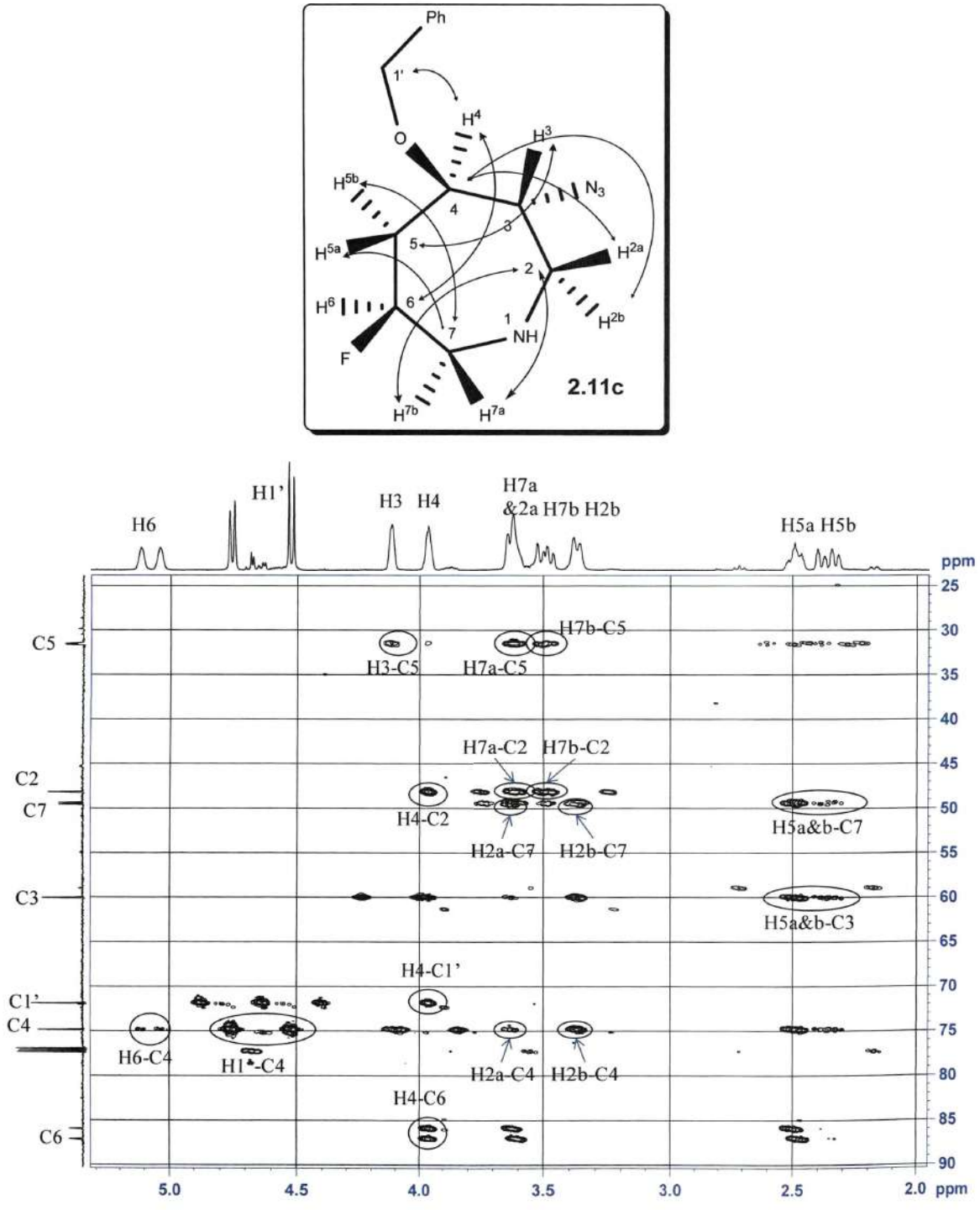


Figure 2.19. $^{1}H–^{13}C$ HMBC 2D NMR correlations of the azepane ring in **2.11c**.

^{1}H–^{1}H COSY 2D NMR correlations:

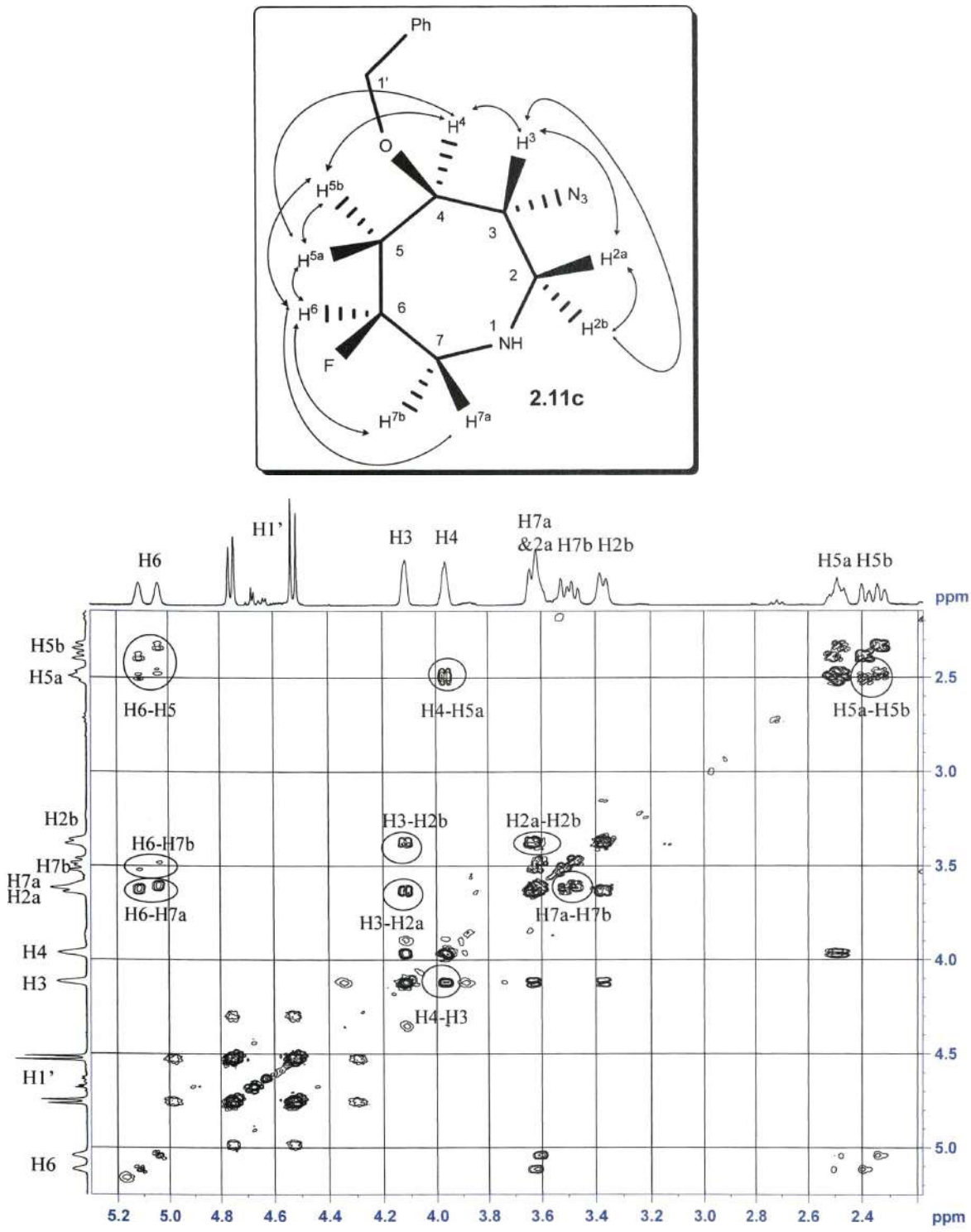


Figure 2.20. ^{1}H–^{1}H COSY 2D NMR correlations of the azepane ring in **2.11c**.

^{1}H–^{1}H NOESY 2D NMR correlations:

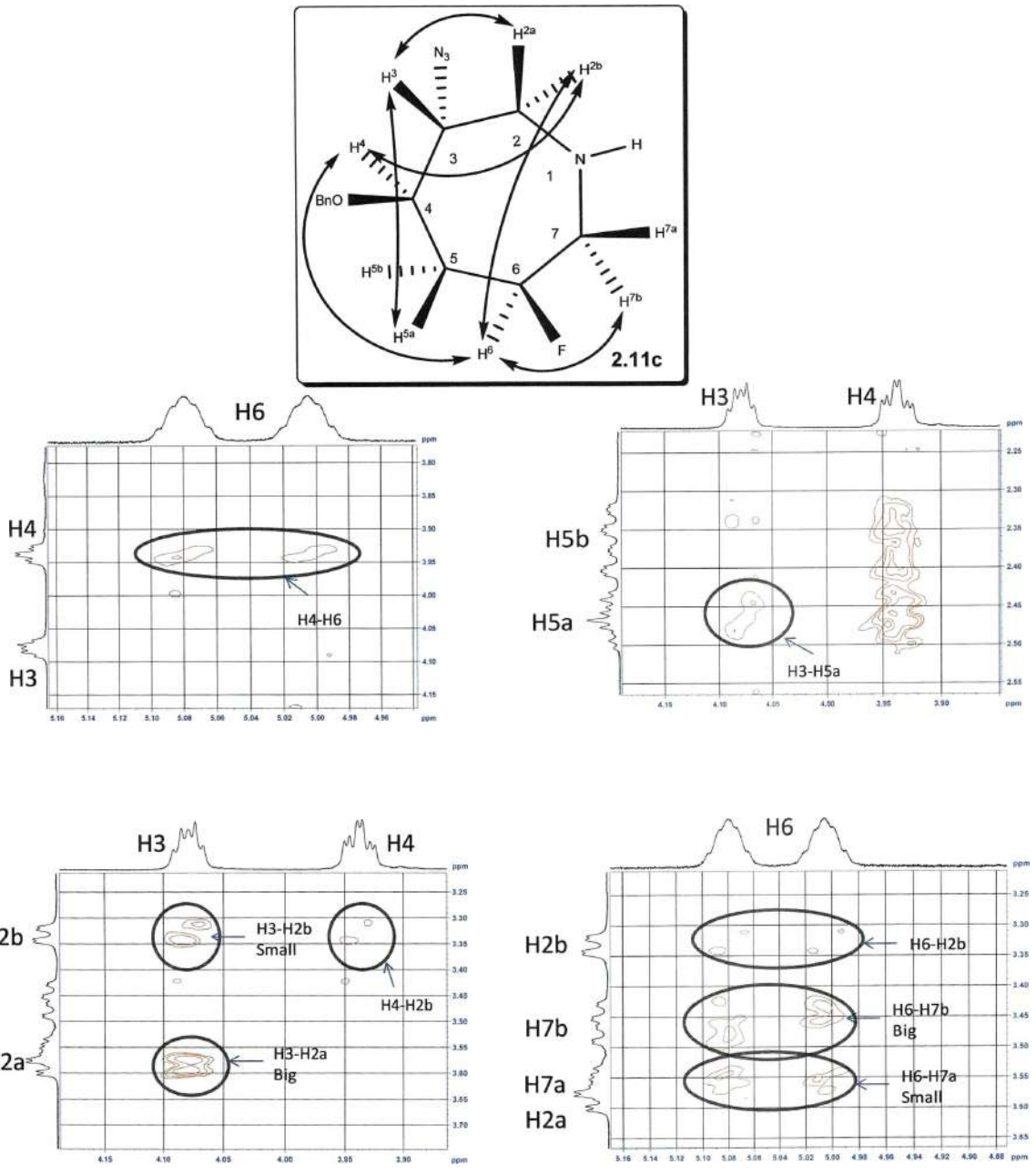
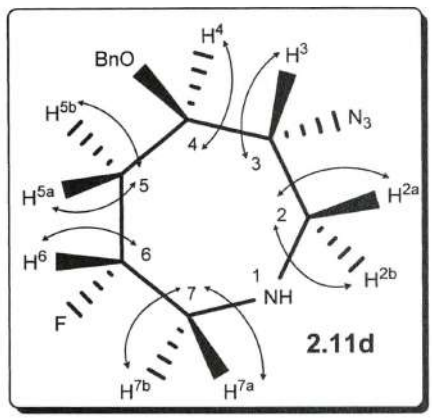


Figure 2.21. ^{1}H–^{1}H NOESY 2D NMR correlations of the azepane ring in **2.11c**.

The absolute configuration at C6 was elucidated based on known stereocentres C3 and C4. H2a, H5a, H2b, and H5b showed NOEs to H3 and H4, respectively. H6 showed NOEs to H4 and H2b, while no detectable NOE to H2a showing the C6 configuration is *S*.

2.4.1.6. (3*R*,4*R*,6*R*)–3–Azido–4–benzyloxy–6–fluoroazepane (2.11d)

^{1}H–^{13}C HSQC 2D NMR correlations:



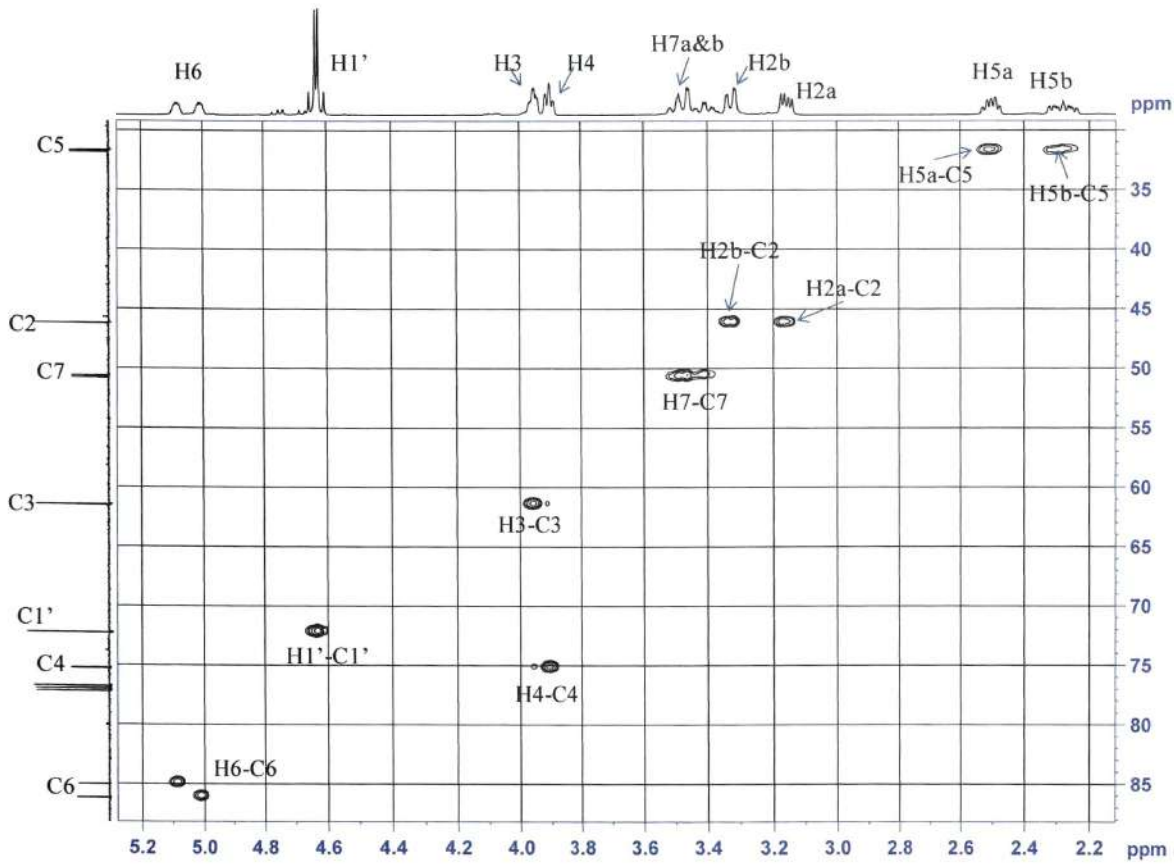


Figure 2.22. ^{1}H–^{13}C HSQC 2D NMR correlations of the azepane ring in **2.11d**.

$^{1}H–^{13}C$ HMBC 2D NMR correlations:

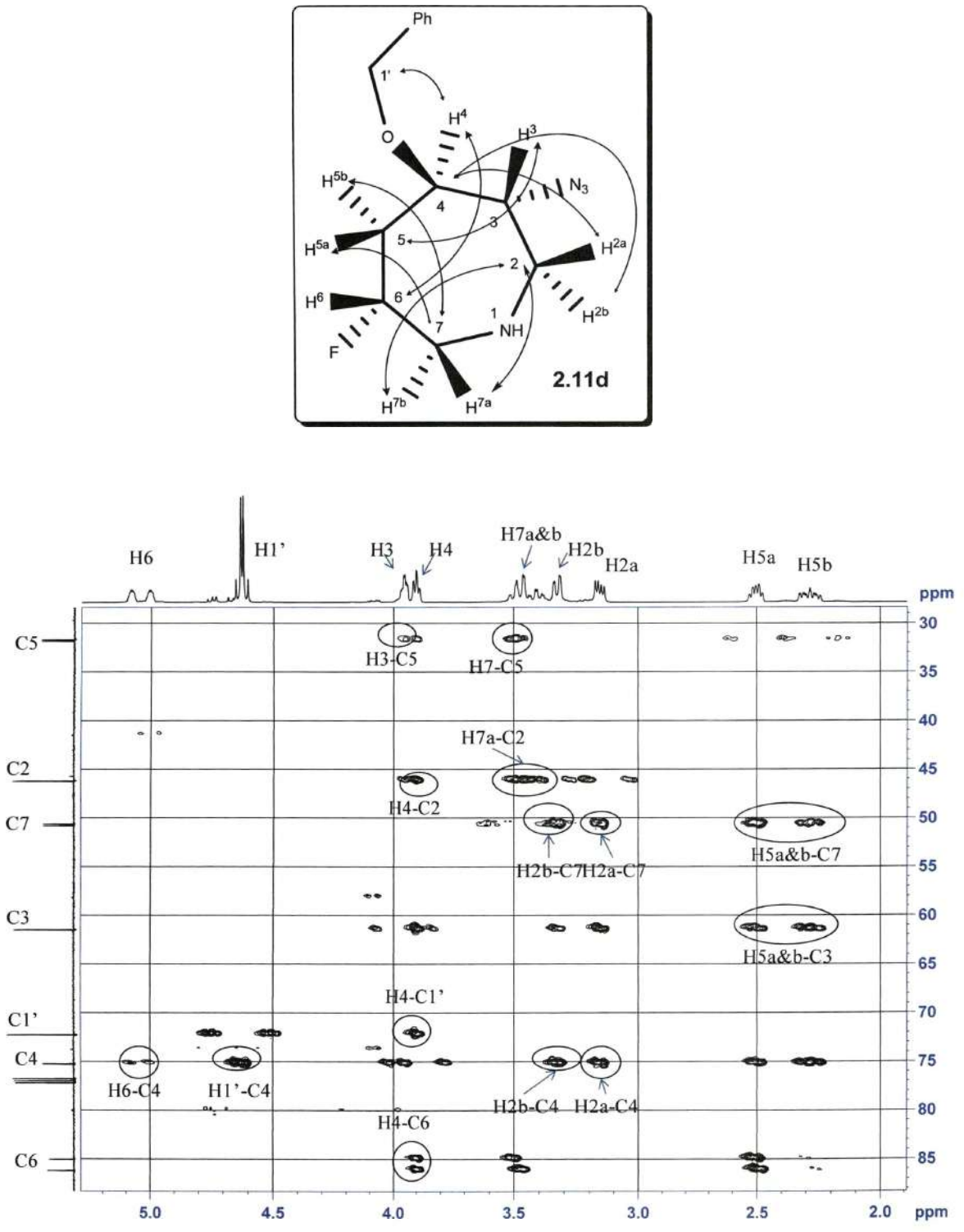


Figure 2.23. $^{1}H–^{13}C$ HMBC 2D NMR correlations of the azepane ring in **2.11d**.

^{1}H–^{1}H COSY 2D NMR correlations:

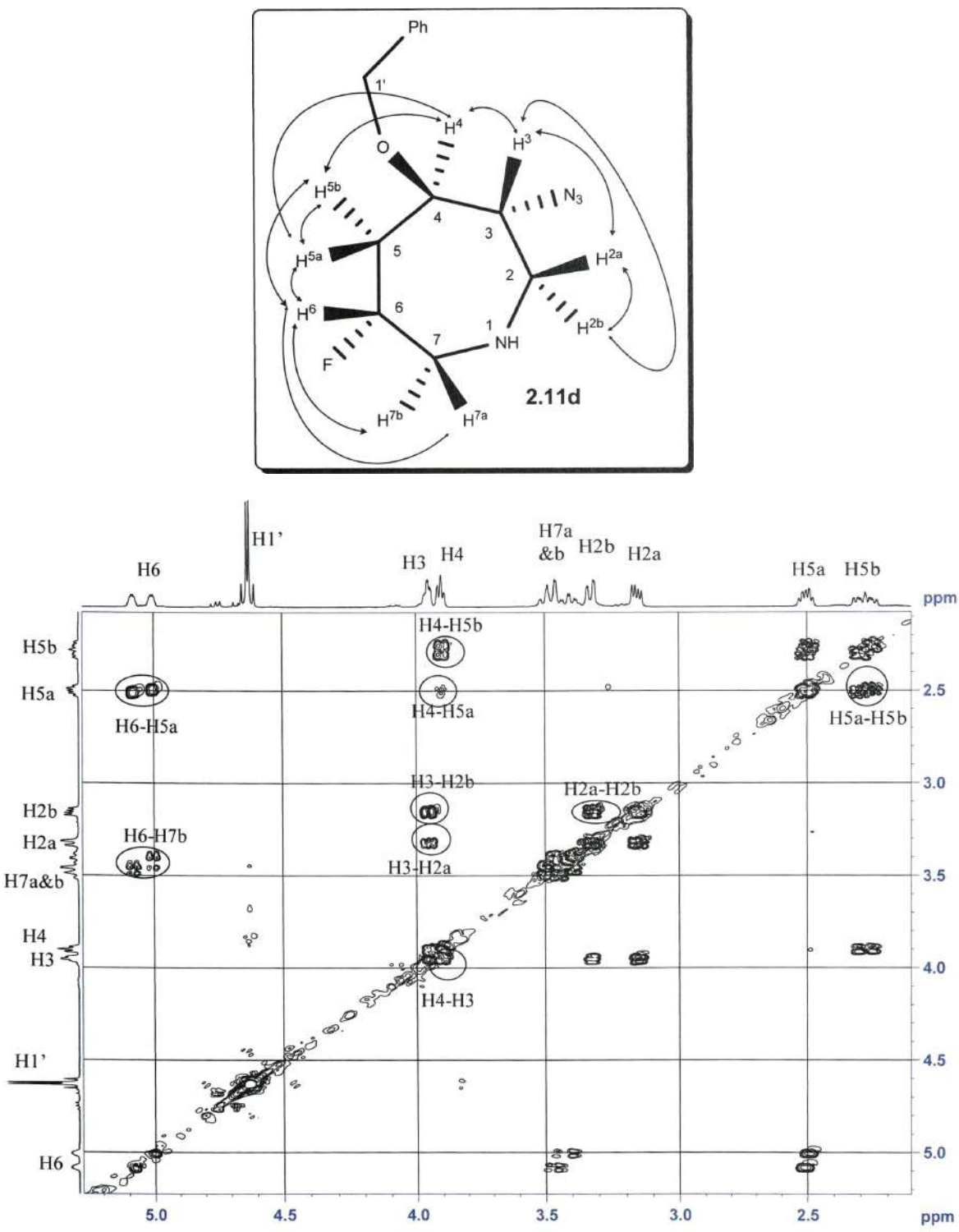


Figure 2.24. ^{1}H–^{1}H COSY 2D NMR correlations of the azepane ring in **2.11d**.

^{1}H–^{1}H NOESY 2D NMR correlations:

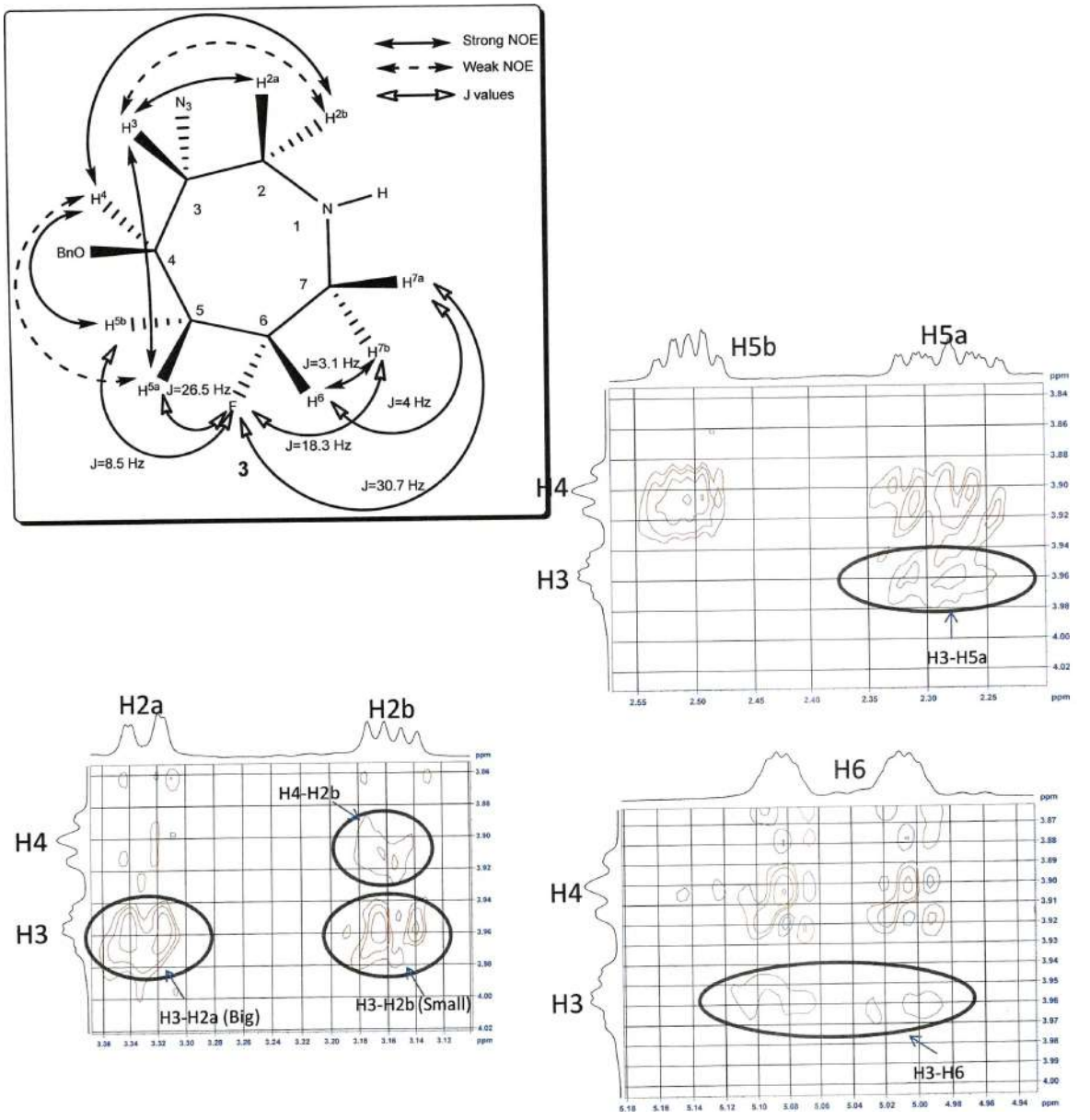


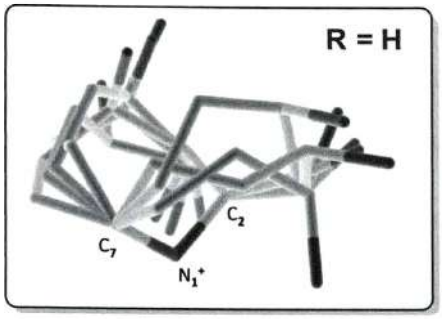
Figure 2.25. ^{1}H–^{1}H NOESY 2D NMR correlations of the azepane ring in **2.11d**.

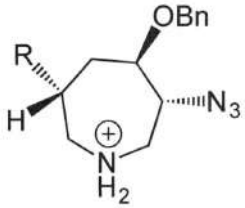
In **2.11d**, H2a, H5a and H2b, H5b had NOEs to H3 and H4, respectively while H6 showed NOE to H3 meaning the C6 stereocenter has the *R* configuration. $^3J_{HF}$ coupling constants also support this elucidation, especially with $^3J_{H5a–F}$ coupling being 26.5 Hz, suggesting the *anti* configuration.

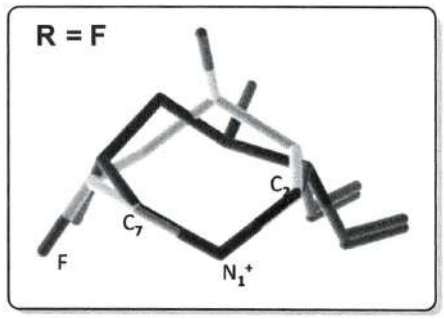
CHAPTER 3

Conformational Regulation of Substituted Azepanes through Selective Monofluorination

Stereoselective fluorination can impose conformational bias in an otherwise highly flexible seven-membered ring.







3.1. Relevance of the Study

Ligand–receptor interactions often involve conformational changes that affect potency and specificity. It is important to understand the conformational synergy of drug–target interactions for structure–based drug design. However, conformational dynamics of most of such interactions are not well understood. The utilization of fluorine atom(s) as a handle for conformational control of bioactive epitopes is an active field. Previous work has elucidated the fluorine conformational effects in four–, five–, six– and eight– membered nitrogen heterocycles. However, fluorine conformational effects in seven membered nitrogen heterocycles have not been studied. In order to fill this knowledge gap, the monofluorinated substituted azepanes in Chapter 2 were subjected to a conformational analysis as the first model system of monofluoroazepanes.

The 6*S*–F (**2.11c**) and 6*R*–F (**2.11d**) monofluoroazepanes were compared with the parent nonfluorinated azepane **3.1** to understand the conformational effects due to fluorine substitution. The synthetic challenges for the synthesis of **3.1** were overcome and the structure elucidation was secured using 2D NMR experiments. Conformational analysis of these model azepanes was then carried out using ^{1}H NMR *J* based analysis and computational modeling. A single fluorine atom, installed diastereoselectively, was found to bias the azepane ring to one major conformation for one of the two diastereomers **2.11c** and **2.11d**.

Based on these conformational analysis results in Chapter 3, a more expanded analysis is presented in Chapter 4 for di– and tri– fluoroazepanes and with polar hydroxy group instead of fluorine to examine if these effects are unique to fluorine. The expanded methodology for multiple fluorination reaction is discussed in Chapter 5.

3.2. Results and Discussion

In this chapter, the conformational effects of monofluorination on substituted azepane rings are discussed. For this study, azepane **3.1** was selected as the nonfluorinated, parent molecule for comparison to monofluoroazepanes **2.11c** and **2.11d**. Azepane **3.1** is a dihydro analogue of azepine **2.7**. However, **3.1** was inaccessible by hydrogenation of **2.7** given the presence of the azido group. The synthesis of **3.1** was accomplished from the tetrahydroazepine **2.6** instead. Tetrahydroazepine **2.6** underwent Pd (0.5 mol%) catalysed hydrogenation to selectively reduce the C5–C6 double bond without benzyl deprotection to provide **3.2**, which was then converted to the azido analogue **3.3** using Mitsunobu conditions. It is noteworthy that the participating carbons (C3 and C6) are equidistant to the azepane nitrogen with the comparable likelihood of neighbouring group participation. However, the structure elucidation with NOESY experiments revealed the desired inversion of stereochemistry at C3 from Mitsunobu reaction.

The fluorinated azepanes both have multiple factors for the conformational control of the ring structure (Figure 1; *Org. Biomol. Chem.*, **2013**, *11*, 3781;). (i) a diequatorial preference of the benzyloxy/azido groups; (b) the azido *gauche* effect; (c) the fluorine *gauche* effect. The experimental ^{1}H NMR spectra of the model azepanes were subjected to *in silico* simulations using DAISY (Topspin 3.1) to extract experimental *J* values accurately. The conformational searches were then carried out for each azepane followed by DFT energy minimization of each representative azepane ring conformation within 3 kcal/mol. Due to the conformational energy contribution of the OBn and azido groups, the calculated energies could not be reliably used to rank the ring conformers. Therefore the ring conformations were extrapolated by experimental *J* values. The *J* values were calculated for these conformers using Gaussian 09 and the

population ratios of each conformer were calculated by comparison with experimental J values.

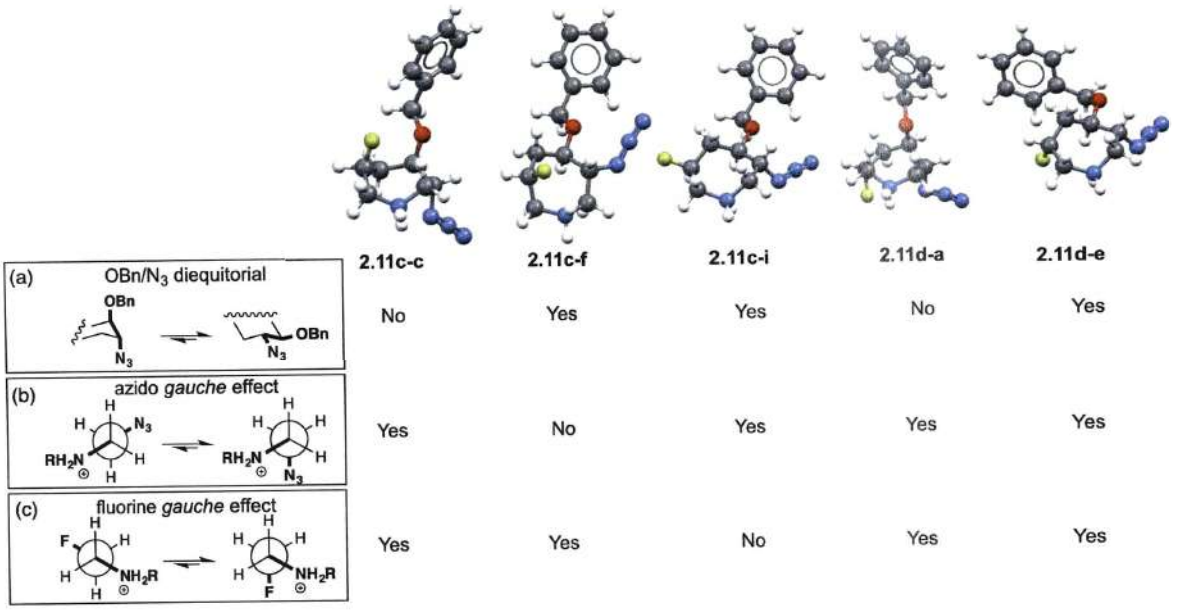


Figure 3.1. Conformational preferences in contributing geometries of **2.11c** and **2.11d**: Geometries **2.11c–c**, **2.11c–f** and **2.11c–i** were found to contribute in 1:1:1 ratio in **2.11c**. Whereas in **2.11d**, geometry **2.11d–e** and **2.11c–a** were found to contribute in 4:1 ratio.

The parent azepane **3.1** was found to be highly flexible with at least 7 distinct ring conformations within 3 kcal/mol of the global minimum, as anticipated. In the case of azepane **2.11c**, the fluorine competes with the existing conformational preferences (the azido gauche effect and a benzyloxy/azido diequatorial preference), and results in the considerable averaging on NMR time scale. There was three different ring conformers found to contribute in a 1:1:1 (Figure 3.1). In the case of azepane **2.11d**, fluorine acts in synergy with these existing preferences. Consequentially, **2.11d** exhibits less conformational disorder than **2.11c** and one conformer (**2.11d–e**) was identified as a major contributor. In conclusion, this study has demonstrated that a single C–F bond, installed diastereospecifically, can significantly regulate the conformations of substituted azepane derivatives. The extent of conformational

biasing is found to depend on both the fluorine stereochemistry and that of the other groups present.

Following is the published research communication (*Org. Biomol. Chem.*, **2013**, *11*, 3781) presented as a main part of the results and discussion for this chapter. Synthesis methods, experimental data and structure elucidation of all new compounds have been discussed in the experimental section. All of the relevant NMR spectra are included in the appendix B (pages 346–387) at the end of the thesis.

Reproduced from A. R. Patel, G. Ball, L. Hunter and F. Liu. (2013) Conformational regulation of substituted azepanes through selective monofluorination, *Organic and Biomolecular Chemistry*, vol. 23, no. 11, pp. 3781-3785. DOI: 10.1039/C3OB40391B with permission from The Royal Society of Chemistry.

Organic & Biomolecular Chemistry

RSC Publishing

COMMUNICATION

View Article Online
View Journal | View Issue

Conformational regulation of substituted azepanes through selective monofluorination†

Cite this: *Org. Biomol. Chem.*, 2013, **11**, 3781

Received 22nd February 2013,
Accepted 23rd April 2013

DOI: 10.1039/c3ob40391b

www.rsc.org/obc

Alpesh Ramanlal Patel,[a] Graham Ball,[b] Luke Hunter[b] and Fei Liu*[a]

Published on 24 April 2013. Downloaded by Macquarie University on 17/09/2013 01:01:57.

Substituted azepanes are common bioactive epitopes with flexible ring structures. The conformational effects of monofluorination in model azepane rings were investigated by ^{1}H NMR spectroscopy and computational modelling. A single fluorine atom, installed diastereoselectively, was found to bias the azepane ring to one major conformation for one diastereomer.

Ligand–receptor interactions frequently require conformational changes in both entities.[1] Such a conformational "induced-fit" confers specificity in molecular recognition that selects for a particular reaction or binding outcome.[2] Understanding conformational synergy is critical to the rational discovery of chemical function in structure-based drug design or molecular assembly; however, the details of conformational dynamics in most ligand–receptor interactions are not well understood.[3,4]

Recent examples illustrate the principle of entropy control, where conformational tuning of ligands or receptors regulates binding specificity and affinity.[5–9] Methods for controlled conformational manipulation of ligands are needed for the rational design and discovery of bioactive epitopes,[3] and one such method is selective fluorination. The C–F bond is known to present profound conformational effects,[10] and has been shown to moderate binding specificity and affinity in a variety of ligand–receptor systems including protease inhibition, GABA receptor ligands, antivirals, insect pheromones, and antimalarials.[11]

In this context of entropy control, conformational tuning of substituted azepanes represents a challenging case study due to the flexibility of such ring systems. Substituted azepanes are common moieties in bioactive natural products, DNA binders, helix inducers, and iminosugar mimics as glycosidase inhibitors.[12] Their conformational regulation is key to the potency and specificity of their bioactivity, suggesting that the introduction of fluorine into these systems may offer attractive benefits through entropy control. Previous work has elucidated the conformational effects of incorporating fluorine atoms into four-,[13] five-,[14] six-[15] and eight-[13]membered nitrogen heterocycles, but the effect of fluorine substitution in highly flexible, heterocyclic seven-membered ring systems is unknown. In order to address this knowledge gap we recently reported methods for the stereospecific fluorination of substituted azepanes,[16a] and here we report the conformational effects of monofluorination in model azepanes **1–3** (Fig. 1). Azepane **1** bears two substituents, a C-3 azido group and a C-4 benzyloxy group, while azepanes **2** and **3** also feature a diastereospecific fluorine substitution at the C-6 position.

In azepane **1**, multiple factors exist to give rise to its complex conformational properties. For example, the mutually *trans* benzyloxy and azido groups might be expected to prefer a

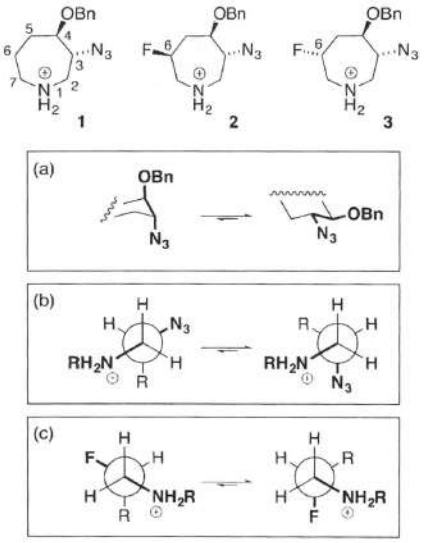


Fig. 1 The conformations of azepanes **1–3** are expected to be influenced by: (a) a diequatorial preference of the benzyloxy/azido groups; (b) the azido *gauche* effect; and (c) the fluorine *gauche* effect (*e.g.* azepane **3**).

[a]*Department of Chemistry and Biomolecular Sciences, Macquarie University, Sydney NSW 2109, Australia. E-mail: fei.liu@mq.edu.au*
[b]*School of Chemistry, The University of New South Wales, Sydney NSW 2052, Australia*

†Electronic supplementary information (ESI) available: Synthetic procedures, computational details and NMR spectra. See DOI: 10.1039/c3ob40391b

Published on 24 April 2013. Downloaded by Macquarie University on 17/09/2013 01:01:57.

diequatorial over a diaxial position in a twisted chair azepane conformation (Fig. 1a), but this would compete with the additional preference of the azido group to align *gauche* to the ring nitrogen[17] (Fig. 1b). Further, the presence of three contiguous unsubstituted methylene groups would be expected to amplify the conformational disorder in the system. In each of the fluorinated targets **2** and **3**, the expected preference of the C–F bond to align *gauche* to the ring nitrogen (Fig. 1c) would be an additional influence on the azepane conformation.[18] Comparison of the diastereoisomers **2** and **3** would allow us to explore whether an appropriately oriented C–F bond can successfully reduce or eliminate the conformational disorder inherent in substituted azepanes. A related question would be whether the C–F bond acts in synergy or in competition with the other conformational influences in the molecule. By exploring these questions, we anticipated that the general principles for entropy control in substituted azepanes might be extrapolated.

Azepane **1** was prepared from a key Boc-protected tetrahydroazepine intermediate,[19] which also gave rise to the fluorinated compounds **2** and **3** as described previously.[16a] The final Boc-deprotection in trifluoroacetic acid afforded targets **1–3** as the trifluoroacetate salt in quantitative yield in each case. The NMR spectra of **1–3** were recorded in $CDCl_3$ which gave well resolved signals, and all resonances were unambiguously assigned using appropriate two-dimensional experiments (COSY, NOESY, HSQC, and HMBC) and by accurate simulation of the spectra *in silico*.[19]

The coupling constants extracted from the ^{1}H NMR spectrum of **1** confirm that this molecule exhibits extensive conformational disorder at room temperature (Fig. 2a).[20] A single set of resonances is observed, but most of the three-bond proton–proton coupling constants are intermediate in magnitude (5–6 Hz), suggesting that significant conformational averaging is occurring on the NMR timescale. Notably, this includes H-3 and H-4 next to the benzyloxy and azido substituents, which experience a coupling of 5.4 Hz (Fig. 2a); this intermediate value agrees with our hypothesis that the benzyloxy/azido diequatorial preference and the azido *gauche* effect would compete with each other, leading to conformational disorder. The western portion of the molecule also exhibits extensive conformational mobility, as is clearly demonstrated by the intermediate magnitude of the proton–proton coupling constants, and by the appearance of the methylene hydrogens, H-7a and H-7b, as an apparent triplet (J = 5.9 Hz) rather than two doublet of doublets. A computational analysis[19] identified seven clusters of distinctly different azepane ring conformations within 3 kcal mol^{-1} of the global minimum (Fig. 2a, overlay image of the possible conformers of **1**). Overall, azepane **1** is found to be a highly flexible and disordered molecule, and as such, is an excellent but challenging starting point for the production of conformationally biased fluorinated analogues.

For the 6*S*-fluorinated azepane **2**, an initial qualitative J-based analysis suggested that this molecule still exhibits considerable conformational disorder at room temperature

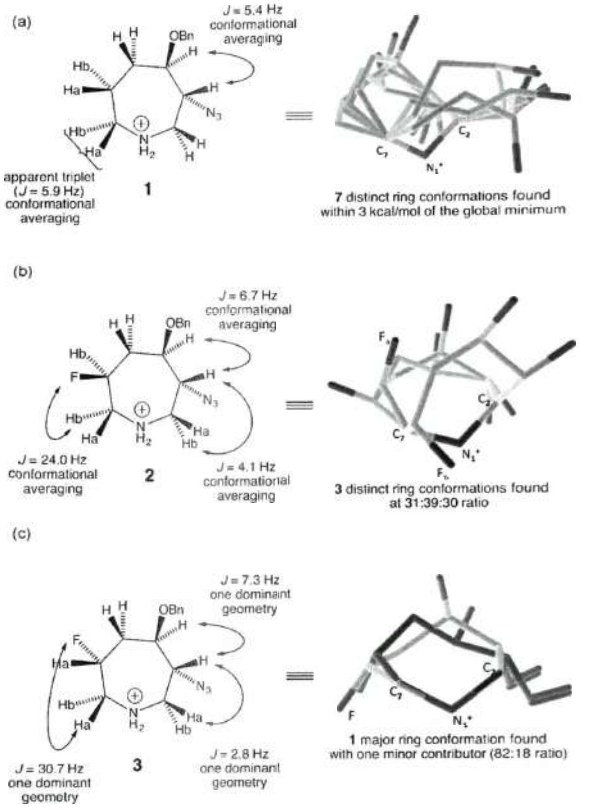


Fig. 2 A combined NMR/computational analysis reveals that azepanes **1** and **2** exhibit considerable conformational disorder, while azepane **3** has one dominant geometry. The low-energy geometries of **1–3** are displayed in the overlay images on the right; these overlays are anchored by three ring atoms (C-7, N$^+$, and C-2), and the benzyloxy and azido side chains are omitted for clarity. The major conformer of **3** is black. See the ESI† for full details of all low-energy geometries of **1–3**.

(Fig. 2b). As described above, three conformational effects were expected to be in operation: the diequatorial preference of the benzyloxy/azido groups; the azido *gauche* effect; and the fluorine *gauche* effect (Fig. 1). It seems that each of these preferences is only partially satisfied in azepane **2**. This is demonstrated by, respectively, a key J_{H3H4} value of 6.7 Hz; a key J_{H2bH3} value of 4.1 Hz; and a key J_{FH7b} value of 24.0 Hz (Fig. 2b), all of which are intermediate in magnitude[20] and hence suggestive of conformational averaging.

Computational analysis of **2** identified several azepane ring geometries that may possibly contribute to the observed NMR characteristics.[19] In order to identify the major geometries, the energy of each geometry candidate was subjected to DFT calculations at several different levels of theory, but it was not possible to reliably rank the geometries because of the uncertainties inherent to the calculations and the side chain rotations that tended to obscure the native preferences of the azepane ring itself.[19] Given the limited reliability of the computational methods alone, it was therefore necessary to perform J-based conformational analysis to assist in ranking the candidate geometries. Spin–spin coupling constants were

 This journal is © The Royal Society of Chemistry 2013

Published on 24 April 2013. Downloaded by Macquarie University on 17/09/2013 01:01:57.

calculated for each geometry using the program Gaussian09,[19] and the calculated J values were compared with the experimental values. As expected, no individual geometry of **2** matched the experimental J values perfectly, but a reasonably good agreement between calculated and experimental J values was obtained when three candidate geometries were selected and a weighted average was created in the ratio of 39 : 31 : 30 (Fig. 2b, overlay image of the probable major geometries of **2**). This population ratio corresponds to relative energies of 0.00, 0.12 and 0.13 kcal mol^{-1}, which are too close to one another to have been reliably predicted by energy calculations alone. The three lowest-energy geometries thus identified all satisfy two of the three conformational preferences described in Fig. 1. Overall, introducing a single fluorine atom into azepane **2** does not reduce the conformational disorder enough to achieve one dominant ring geometry in solution.

Our attention was next turned to azepane **3** (Fig. 2c), in which the diastereospecific fluorination gives the *R* configuration at C-6. A qualitative J-based analysis[20] of the ^{1}H NMR spectrum of **3** reveals that, in contrast to azepanes **1** and **2**, a single geometry of **3** seems to strongly dominate in solution. The benzyloxy/azido diequatorial preference is reasonably clearly satisfied, as demonstrated by a J_{H3H4} value of 7.3 Hz; the azido *gauche* effect is reasonably clearly satisfied, as demonstrated by a J_{H2aH3} value of 2.8 Hz; and the fluorine *gauche* effect is clearly satisfied, as demonstrated by a key J_{FH7a} value of 30.7 Hz (Fig. 2).

In order to acquire theoretical confirmation of the predicted ring geometry of **3**, a computational sequence was performed similar to that already described for **2**. A ring geometry of **3** consistent with the above description was readily identified amongst the low-energy candidates from a conformational analysis followed by DFT optimisation (Fig. 2c), and the calculated coupling constants for this geometry matched the experimental values reasonably well.[19] In addition, a second closely related conformer of **3** was identified which, when included as the minor component of an 82 : 18 weighted average mixture, provided a still closer match with the experimental J values. This population ratio corresponds to relative energies of 0.00 and 0.77 kcal mol^{-1}. The two low-energy geometries of **3** thus identified (Fig. 2c) differ only in a slight twist about the C3–C4 dihedral angle, with the lowest-energy geometry better satisfying the benzyloxy/azido diequatorial preference, and the next higher-energy geometry better satisfying the azido *gauche* effect.[19] Overall, introducing the fluorine atom into azepane **3**, with the *R* configuration at C-6, is found to greatly reduce the conformational disorder relative to the non-fluorinated parent structure **1**, to the extent that a single geometry strongly dominates in solution.

In conclusion, this study has demonstrated that a single C–F bond, installed diastereospecifically, can significantly regulate the conformations of substituted azepane derivatives.[21] The extent of conformational biasing is found to depend on both the fluorine stereochemistry and that of the other groups present: if the fluorine acts in synergy with the other groups (*i.e.* azepane **3**) a single ring conformation can be reinforced, whereas if the fluorine acts in competition with existing groups (*i.e.* azepane **2**), such a loss of synergy results in reduced conformational bias.[22] This finding has wider significance for future efforts to optimise host–guest interactions involving flexible heterocyclic ligands.

Acknowledgements

The authors thank Prof. Peter Karuso and Dr Douglas Lawes for NMR assistance.

Notes and references

1 S. Llabrés, J. Juárez, F. Forti, R. Pouplana and F. J. Luque, Recognition of ligands by macromolecular targets, in *Physico-Chemical and Computational Approaches to Drug Discovery*, The Royal Society of Chemistry, 2012, ch. 1.
2 Y. Savir and T. Tlusty, *PLoS ONE*, 2007, **2**, e468.
3 C. E. Chang, W. Chen and M. K. Gilson, *Proc. Natl. Acad. Sci. U. S. A.*, 2007, **104**, 1534–1539.
4 L. Skjaerven, N. Reuter and A. Martinez, *Future Med. Chem.*, 2011, **3**, 2079–2100.
5 C. Diehl, O. Engström, T. Delaine, M. Håkansson, S. Genheden, K. Modig, H. Leffler, U. Ryde, U. J. Nilsson and M. Akke, *J. Am. Chem. Soc.*, 2010, **132**, 14577–14589.
6 C. Cabezas, M. Varela, I. Pena, S. Mata, J. C. Lopez and J. L. Alonso, *Chem. Commun.*, 2012, **48**, 5934–5936.
7 G. R. Stockwell and J. M. Thornton, *J. Mol. Biol.*, 2006, **356**, 928–944.
8 N. Sturm, J. Desaphy, R. J. Quinn, D. Rognan and E. Kellenberger, *J. Chem. Inf. Model.*, 2012, **52**, 2410–2421.
9 C. S. Leung, S. S. F. Leung, J. Tirado-Rives and W. L. Jorgensen, *J. Med. Chem.*, 2012, **55**, 4489–4500.
10 (*a*) L. Hunter, *Beilstein J. Org. Chem.*, 2010, **6**, 38; (*b*) D. O'Hagan, *Chem. Soc. Rev.*, 2008, **37**, 308–319.
11 (*a*) I. Yamamoto, M. J. T. Jordan, N. Gavande, M. R. Doddareddy, M. Chebib and L. Hunter, *Chem. Commun.*, 2012, **48**, 829–831; (*b*) P. W. Chia, M. R. Livesey, A. M. Slawin, T. van Mourik, D. J. Wyllie and D. O'Hagan, *Chem.–Eur. J.*, 2012, **18**, 8813–8819; (*c*) L. Hunter, *Chim. Oggi*, 2012, **30**, 20; (*d*) M. Winkler and D. O'Hagan, *Mol. Med. Med. Chem.*, 2012, **6**, 299–331; (*e*) I. Yamamoto, G. P. Deniau, N. Gavande, M. Chebib, G. A. Johnston and D. O'Hagan, *Chem. Commun.*, 2011, **47**, 7956–7958; (*f*) N. H. Campbell, D. L. Smith, A. P. Reszka, S. Neidle and D. O'Hagan, *Org. Biomol. Chem.*, 2011, **9**, 1328–1331; (*g*) D. O'Hagan, *Future Med. Chem.*, 2011, **3**, 189–195; (*h*) C. Bucher, C. Sparr, W. B. Schweizer and R. Gilmour, *Chem.–Eur. J.*, 2009, **15**, 7637–7647; (*i*) J. J. Barchi, R. G. Karki, M. C. Nicklaus, M. A. Siddiqui, C. George, I. A. Mikhailopulo and V. E. Marquez, *J. Am. Chem. Soc.*, 2008, **130**, 9048–9057; (*j*) G. Deniau, A. M. Slawin, T. Lebl, F. Chorki, J. P. Issberner, T. van Mourik, J. M. Heygate, J. J. Lambert, L. A. Etherington, K. T. Sillar and

Published on 24 April 2013. Downloaded by Macquarie University on 17/09/2013 01:01:57.

D. O'Hagan, *ChemBioChem*, 2007, **8**, 2265–2274; (*k*) M. D. Clift, H. Ji, G. P. Deniau, D. O'Hagan and R. B. Silverman, *Biochemistry*, 2007, **46**, 13819–13828; (*l*) A. G. A. Myers, J. K. J. Barbay and B. B. Zhong, *J. Am. Chem. Soc.*, 2001, **123**, 7207–7219; (*m*) A. P. Khrimian, J. E. Oliver, R. M. Waters, S. Panicker, J. M. Nicholson and J. A. Klun, *Tetrahedron: Asymmetry*, 1996, **7**, 37–40; (*n*) P. Van Roey, J. M. Salerno, C. K. Chu and R. F. Schinazi, *Proc. Natl. Acad. Sci. U. S. A.*, 1989, **86**, 3929–3933.

12 For recent and representative examples see: (*a*) P.-L. Yeh, C.-K. Tai, T.-L. Shih, H.-L. Hsiao and B.-C. Wang, *J. Mol. Struct.*, 2012, **1018**, 64–71; (*b*) S. Goumain, H. Taghzouti, C. Portella, J.-B. Behr and R. Plantier-Royon, *Tetrahedron Lett.*, 2012, **53**, 4440–4443; (*c*) J. Perez-Castells, M. Fontanella, A. Arda, F. J. Canada, M. Sollogoub, Y. Bleriot and J. Jimenez-Barbero, *New J. Chem.*, 2012, **36**, 1008–1013; (*d*) L. J. Parker, H. Watanabe, K. Tsuganezawa, Y. Tomabechi, N. Handa, M. Shirouzu, H. Yuki, T. Honma, N. Ogawa, T. Nagano, S. Yokoyama and A. Tanaka, *Acta Crystallogr., Sect. F: Struct. Biol. Cryst. Commun.*, 2012, **68**, 860–866; (*e*) D. Nunez-Villanueva, L. Infantes, M. T. Garcia-Lopez, R. Gonzalez-Muniz and M. Martin-Martinez, *J. Org. Chem.*, 2012, **77**, 9833–9839; (*f*) J. Sardinha, A. P. Rauter, M. Sollogoub and Y. Bleriot, *Carbohydr. Chem.: Proven Synth. Methods*, 2012, **1**, 129–135; (*g*) E. Wojaczynska, I. Turowska-Tyrk and J. Skarzewski, *Tetrahedron*, 2012, **68**, 7848–7854; (*h*) J. Deschamp, M. Mondon, S. Nakagawa, A. Kato, D. S. Alonzi, T. D. Butters, Y. Zhang, M. Sollogoub and Y. Bleriot, *Bioorg. Med. Chem.*, 2012, **20**, 641–649; (*i*) E. Cini, G. Bifulco, G. Menchi, M. Rodriquez and M. Taddei, *Eur. J. Org. Chem.*, 2012, 2133–2141; (*j*) T.-L. Shih, M.-T. Liang, K.-D. Wu and C.-H. Lin, *Carbohydr. Res.*, 2011, **346**, 183–190; (*k*) S. D. Orwig, Y. L. Tan, N. P. Grimster, Z. Yu, E. T. Powers, J. W. Kelly and R. L. Lieberman, *Biochemistry*, 2011, **50**, 10647–10657; (*l*) D. Nunez-Villanueva, M. A. Bonache, L. Infantes, M. T. Garcia-Lopez, M. Martin-Martinez and R. Gonzalez-Muniz, *J. Org. Chem.*, 2011, **76**, 6592–6603; (*m*) B. Luo, F. Marcelo, J. Desire, Y. Zhang, M. Sollogoub, A. Kato, I. Adachi, F. J. Canada, J. Jimenez-Barbero and Y. Bleriot, *J. Carbohydr. Chem.*, 2011, **30**, 641–654; (*n*) F. Marcelo, Y. He, S. A. Yuzwa, L. Nieto, J. Jimenez-Barbero, M. Sollogoub, D. J. Vocadlo, G. D. Davies and Y. Bleriot, *J. Am. Chem. Soc.*, 2009, **131**, 5390–5392; (*o*) H. Li, F. Marcelo, C. Bello, P. Vogel, T. D. Butters, A. P. Rauter, Y. Zhang, M. Sollogoub and Y. Bleriot, *Bioorg. Med. Chem.*, 2009, **17**, 5598–5604; (*p*) H. Li, T. Liu, Y. Zhang, S. Favre, C. Bello, P. Vogel, T. D. Butters, N. G. Oikonomakos, J. Marrot and Y. Bleriot, *ChemBioChem*, 2008, **9**, 253–260; (*q*) T.-L. Shih, R.-Y. Yang, S.-T. Li, C.-F. Chiang and C.-H. Lin, *J. Org. Chem.*, 2007, **72**, 4258–4261; (*r*) H. Li, C. Schuetz, S. Favre, Y. Zhang, P. Vogel, P. Sinay and Y. Bleriot, *Org. Biomol. Chem.*, 2006, **4**, 1653–1662; (*s*) Y. Bleriot, M. I. Simone, M. R. Wormald, R. A. Dwek, D. J. Watkin and G. W. J. Fleet, *Tetrahedron: Asymmetry*, 2006, **17**, 2276–2286; (*t*) P. Wipf and S. R. Spencer, *J. Am. Chem. Soc.*, 2005, **127**, 225–235; (*u*) H. Li, Y. Bleriot, J.-M. Mallet, E. Rodriguez-Garcia, P. Vogel, Y. Zhang and P. Sinay, *Tetrahedron: Asymmetry*, 2005, **16**, 313–319; (*v*) K. Martinez-Mayorga, J. L. Medina-Franco, S. Mari, F. J. Canada, E. Rodriguez-Garcia, P. Vogel, H. Li, Y. Bleriot, P. Sinay and J. Jimenez-Barbero, *Eur. J. Org. Chem.*, 2004, 4119–4129; (*w*) H. Li, Y. Bleriot, J.-M. Mallet, Y. Zhang, E. Rodriguez-Garcia, P. Vogel, S. Mari, J. Jimenez-Barbero and P. Sinay, *Heterocycles*, 2004, **64**, 65–74; (*x*) D. D. Dhavale, S. D. Markad, N. S. Karanjule and J. PrakashaReddy, *J. Org. Chem.*, 2004, **69**, 4760–4766; (*y*) C. B. Breitenlechner, T. Wegge, L. Berillon, K. Graul, K. Marzenell, W.-G. Friebe, U. Thomas, R. Schumacher, R. Huber, R. A. Engh and B. Masjost, *J. Med. Chem.*, 2004, **47**, 1375–1390; (*z*) S. Barluenga, K. B. Simonsen, E. S. Littlefield, B. K. Ayida, D. Vourloumis, G. C. Winters, M. Takahashi, S. Shandrick, Q. Zhao, Q. Han and T. Hermann, *Bioorg. Med. Chem. Lett.*, 2004, **14**, 713–718; (*aa*) M. Y. Le, L. Poitout, J.-C. Depezay, I. Dosbaa, S. Geoffroy and M.-J. Foglietti, *Bioorg. Med. Chem.*, 1997, **5**, 519–533.

13 N. E. Gooseman, D. O'Hagan, A. M. Slawin, A. M. Teale, D. J. Tozer and R. J. Young, *Chem. Commun.*, 2006, 3190–3192.

14 (*a*) L. E. Combettes, P. Clausen-Thue, M. A. King, B. Odell, A. L. Thompson, V. Gouverneur and T. D. W. Claridge, *Chem.–Eur. J.*, 2012, **18**, 13133–13141; (*b*) D. D. Staas, K. L. Savage, V. L. Sherman, H. L. Shimp, T. A. Lyle, L. O. Tran, C. M. Wiscount, D. R. McMasters, P. E. J. Sanderson, P. D. Williams, B. J. Lucas, J. A. Krueger, S. D. Lewis, R. B. White, S. Yu, B. K. Wong, C. J. Kochansky, M. R. Anari, Y. Yan and J. P. Vacca, *Bioorg. Med. Chem.*, 2006, **14**, 6900–6916; (*c*) L. E. Combettes, P. Clausen-Thue, M. A. King, B. Odell, A. L. Thompson, V. Gouverneur and T. D. W. Claridge, *Chem.–Eur. J.*, 2012, **18**, 13133–13141; (*d*) J. A. Hodges and R. T. Raines, *J. Am. Chem. Soc.*, 2003, **125**, 9262–9263; (*e*) J. T. Gerig and R. S. McLeod, *J. Am. Chem. Soc.*, 1973, **95**, 5725–5729.

15 (*a*) R. Surmont, G. Verniest, A. De Groot, J. W. Thuring and N. De Kimpe, *Adv. Synth. Catal.*, 2010, **352**, 2751–2756; (*b*) S. Singh, C.-M. Martinez, S. Calvet-Vitale, A. K. Prasad, T. Prangé, P. I. Dalko and H. Dhimane, *Synlett*, 2012, 2421–2425.

16 (*a*) A. R. Patel and F. Liu, *Tetrahedron*, 2013, **69**, 744–752. For another example of azepane fluorination, see: (*b*) M. Mondon, N. Fontelle, J. Desire, F. Lecornue, J. Guillard, J. Marrot and Y. Bleriot, *Org. Lett.*, 2012, **14**, 870–873.

17 A *gauche* preference of 1–3 kcal mol^{-1} is observed in uncharged molecules containing the N–C–C–N_3 motif; see: L.-S. Sonntag, S. Schweizer, C. Ochsenfeld and H. Wennemers, *J. Am. Chem. Soc.*, 2006, **128**, 14697–14703.

18 A *gauche* preference of 5.7 kcal mol^{-1} is observed in $FCH_2CH_2NH_3^+$; see: C. R. Briggs, M. J. Allen, D. O'Hagan, D. J. Tozer, A. M. Z. Slawin, A. E. Goeta and J. A. K. Howard, *Org. Biomol. Chem.*, 2004, **2**, 732–740.

This journal is © The Royal Society of Chemistry 2013

Published on 24 April 2013. Downloaded by Macquarie University on 17/09/2013 01:01:57.

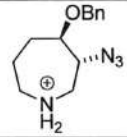
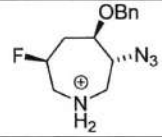
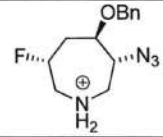
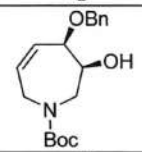
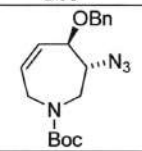
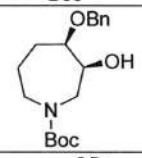
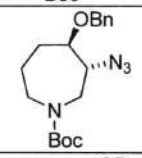
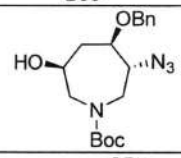
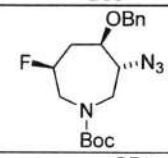
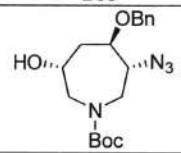
19 See ESI.†

20 Three-bond H–H and H–F coupling constants obey Karplus relationships with the corresponding H–C–C–H and H–C–C–F dihedral angles: "typical" $^{3}J_{HH}$ values are 1–3 Hz for *gauche* alignments and 6–9 Hz for *anti* alignments; see: (*a*) A. M. Ihrig and S. L. Smith, *J. Am. Chem. Soc.*, 1970, **92**, 759–763. "Typical" $^{3}J_{HF}$ values are 5–15 Hz for *gauche* alignments and 25–35 Hz for *anti* alignments; see: (*b*) C. Thibaudeau, J. Plavec and J. Chattopadhyaya, *J. Org. Chem.*, 1998, **63**, 4967–4984. For an example of conformational analysis by NMR and DFT methods, see: (*c*) P. Tähtinen, A. Bagno, K. D. Klika and K. Pihlaja, *J. Am. Chem. Soc.*, 2003, **125**, 4609–4618.

21 For comparison, analogues of **2** and **3** in which the fluorine substituents were replaced with hydroxyl groups were also examined. The similarities and differences observed between these two polar substituents are presented in preliminary form in the ESI,† and will be described more fully in a forthcoming publication.

22 For examples of conformational synergy/competition in fluorinated peptides, see: R. I. Mathad, F. Gessier and D. Seebach, *Helv. Chim. Acta*, 2005, **88**, 266–280.

3.3. Cross Reference of Compounds in Chapter 3

Structure	Nomenclature in Thesis	Nomenclature in *Org. Biomol. Chem.*, 2013, *11*, 3781.
	**3.1**	**1**
	**2.11c**	**2**
	**2.11d**	**3**
	**2.6**	**4**
	**2.7**	**5**
	**3.2**	**6**
	**3.3**	**7**
	**2.8c**	**8**
	**2.10c**	**9**
	**2.8d**	**10**

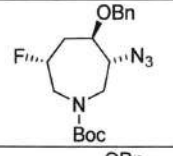
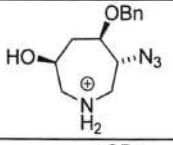
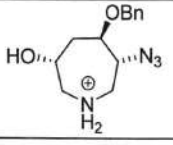
	**2.10d**	**11**
	**2.9c**	**12**
	**2.9d**	**13**

Table 3.1. Cross reference of compound nomenclature from the thesis and *Org. Biomol. Chem.*, **2013**, *11*, 3781.

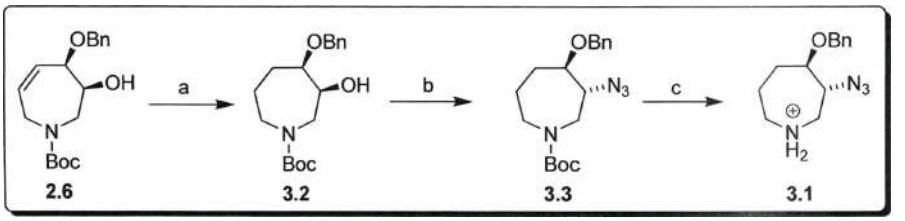
3.4. Experimental

3.4.1. General Methods

All reactions were conducted under N_2 atmosphere. Unless otherwise specified, all reagents were purchased from Sigma–Aldrich and used without further purification. Deoxofluor® was obtained from Matrix Scientific and used without further purification. CH_2Cl_2 was obtained from a solvent purification system (Innovative Technology SPS400) and stored over MS 4Å beads. Ethyl acetate and petroleum ether were distilled before use. Petroleum ether refers to the fraction collected between 60 °C and 80 °C. THF was distilled from Na–benzophenone and stored over MS 4Å beads. Anhydrous MeOH was obtained from Sigma–Aldrich and used without further purification. ^1H NMR spectra were recorded at 25 °C on either a BrukerDRX600K or DPX400 NMR spectrometer and are reported in parts per million (ppm) using the specified solvent as the internal standard ($CDCl_3$ at 7.26 ppm and $(CD_3)_2CO$ at 2.05 ppm). ^{13}C NMR spectra are reported in ppm using the specified solvent as the internal standard ($CDCl_3$ at 77.16 ppm and $(CD_3)_2CO$ at 29.84 ppm). Computational investigations

were performed using programs MOE (Molecular Operating Environment 2011.10; Chemical Computing Group), Turbomole (version 6.3), and Gaussian 09.

3.4.2. Synthetic Procedures and Characterization of Intermediates



Scheme 3.1. Synthesis of the azepane **3.1**. *Reagents and conditions*: a) H_2 (1 atm), 5% w/w Pd/C (0.5 mol%), MeOH, rt, 8 h, 95 %; b) PPh_3, DEAD, $(PhO)_2P(O)N_3$, THF, 2.5 h, rt, 91%; c) TFA (neat), 5 min, rt, quant.

Fluoroazepanes **2.11c** and **2.11d** were synthesized from **2.7** using the methods described in Chapter 2. Azepane **3.1** was synthesized from azepane **2.6** using a two-step protocol (Scheme 1). Azepanes **3.1** and **2.11c–d** were subjected to reverse phase chromatography to remove traces of impurities on a Phenomenex Gemini C18 column (150×21.20 mm) eluting with MeCN/water/TFA from 15:85:0.1 to 50:50:0.1 over 25 min; flow rate:8.80 mL/min; retention time 13.4, 14.5, and 14.4 min for **3.1**, **2.11c**, and **2.11d**, respectively.

3.4.2.1. (3*S*,4*R*)–4–Benzyloxy–3–hydroxyazepane–1–carboxylic acid–*tert*–butyl ester (3.2)

5% w/w Pd/C (3.32 mg, 1.57 μmol, 0.5 mol%) was added to a solution of **2.6** (100 mg, 313.1 μmol) in MeOH, and the resulting suspension was stirred under H_2 (1 atm) at room temperature for 8 h after TLC monitoring confirmed complete conversion. The catalyst was filtered off through a pad of Celite which was carefully rinsed with MeOH. The solvent was rotary evaporated to isolate azepane **3.2** as a colorless oil (98.6 mg, 98%). $[\alpha]^{20}_D = -68.8$ (*c* 0.8, CH_2Cl_2); IR (film) ν_{max} (cm^{-1}): 3600–3100 (br), 2988, 2937, 2115, 1688, 1419, 1153,

1076, 1049; ^{1}H NMR (400 MHz, $CDCl_3$) δ 7.39–7.27 (m, 5H), 4.65 (d, J = 11.76 Hz, 1H), 4.62 (d, J = 11.76 Hz, 1H), 3.89–3.43 (m, 3H), 3.27–3.09 (m, 1H), 3.08–2.92 (m, 1H), 2.77–2.46 (m, 1H), 2.15–2.00 (m, 1H), 1.97–1.77 (m, 1H), 1.74–1.34 (m, 3H), 1.44 (s, 9H); ^{13}C NMR (150 MHz, $CDCl_3$) δ 155.5, 138.1, 128.6, 128.0, 127.8, 80.1, 79.7, 71.2, 71.1, 48.5, 46.9, 28.5, 24.8, 21.3; HRMS (ESI): $[M + H]^+$, *m/z* calcd for $C_{18}H_{28}NO_4$ 322.2018, found 322.2021.

3.4.2.2. (3*R*,4*R*)–3–Azido–4–benzyloxyazepane–1–carboxylic acid–*tert*–butyl ester (3.3)

To a well stirred solution of ester **3.2** (20.7 mg, 64.4 μmol), PPh_3 (67.6 mg, 257.6 μmol), and $(PhO)_2P(O)N_3$ (70.9 mg, 257.6 μmol) in dry THF (1.4 mL) under N_2 atmosphere at 25 °C, diethyl azodicarboxylate (DEAD, 44.9 mg, 257.6 μmol) was added dropwise via a syringe and the resulting mixture was stirred at the same temperature until the completion of reaction (monitored by TLC, 2.5 h). The residue obtained by evaporation of the reaction mixture under reduced pressure was suspended in EtOAc (1.7 mL), followed by filtration through a short pad of silica gel. The filtrate was washed with aqueous 2 *N* HCl (1.7 mL), brine (1.7 mL), and dried over $MgSO_4$. The solvent was evaporated, and the crude mixture was purified by flash chromatography (pentane/*tert*–butylmethylether, 20/1) to afford compound **3.3** as a colorless oil (20.3 mg, 91%). R_f (petroleum ether/EtOAc, 4/1) 0.58; $[\alpha]^{20}_D$ = −38.5 (*c* 1.9, CH_2Cl_2); yield 91%; IR (film) ν_{max} (cm^{-1}): 2971, 2910, 2378, 2125, 1686, 1414, 1151, 1088, 1049; ^{1}H NMR (600 MHz, $(CD_3)_2CO$) δ 7.39 (d, J = 7.56 Hz, 2H), 7.33 (t, J = 7.39 Hz, 2H), 7.27 (t, J = 7.73 Hz, 1H), 4.69 (d, J = 11.75 Hz, 1H), 4.57 (dd, J = 11.75, 6.87 Hz, 1H), 3.64–3.39 (m, 4H), 3.22–3.15 (m, 2H), 2.09–2.01 (m, 2H), 1.93–1.85 (m, 1H), 1.66–1.58 (m, 1H), 1.46 (s, 9H); ^{13}C NMR (150 MHz, $(CD_3)_2CO$) δ 155.5, 139.6, 129.0, 128.6, 128.3, 83.3, 79.9, 71.6,

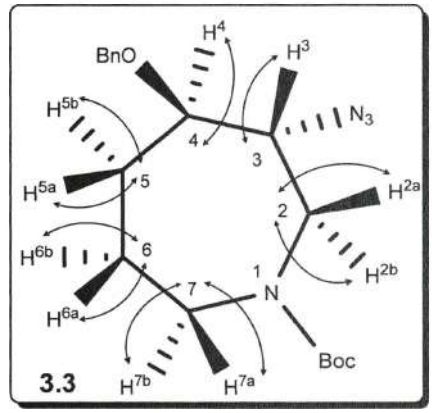
66.3, 46.29, 46.31, 28.5, 27.9, 22.5; HRMS (ESI): $[M + H]^+$, *m/z* calcd for $C_{18}H_{27}N_4O_3$ 347.2083, found 347.2081.

3.4.2.3. (3*R*,4*R*)–3–Azido–4–benzyloxyazepane (3.1)

The azepane **3.3** (15 mg, 43.3 μmol) was dissolved in TFA (500 μL) at 25 °C. The solution was allowed to stir for 5 min before TFA was evaporated under nitrogen. The reaction flask was kept under high vacuum (0.005 torr, 25 °C) for 3 h to remove traces of TFA, and the colorless oily residue obtained was characterized as **3.1** (10.5 mg, 98%). $[\alpha]^{20}_D = -44.7$ (*c* 1.5, $CHCl_3$); yield 98%; IR (film) ν_{max} (cm^{-1}): 2391, 2357, 2100, 1667, 1657, 1650, 1576, 1548, 1498, 1432; ^1H NMR (600 MHz, $CDCl_3$) δ 7.39–7.29 (m, 5H), 4.64 (d, *J* = 11.22 Hz, 2H), 4.55 (d, *J* = 11.22 Hz, 2H), 4.01–3.97 (m, 1H), 3.79–3.75 (m, 1H), 3.36 (d, *J* = 14.45 Hz, 1H), 3.22 (t, *J* = 6.06 Hz, 2H), 3.19 (dd, *J* = 14.81, 6.77 Hz, 1H), 2.07–1.92 (m, 3H), 1.83–1.76 (m, 1H); ^{13}C NMR (150 MHz, $CDCl_3$) δ 137.3, 128.8, 128.3, 128.0, 78.4, 71.6, 61.2, 46.4, 44.2, 26.9, 19.1; HRMS (ESI): $[M + H]^+$, *m/z* calcd for $C_{13}H_{19}N_4O$ 247.1559, found 247.1558.

3.4.3. Structure Elucidation of the Azepane 3.3 ($(CD_3)_2CO$)

^1H–^{13}C HSQC 2D NMR correlations:



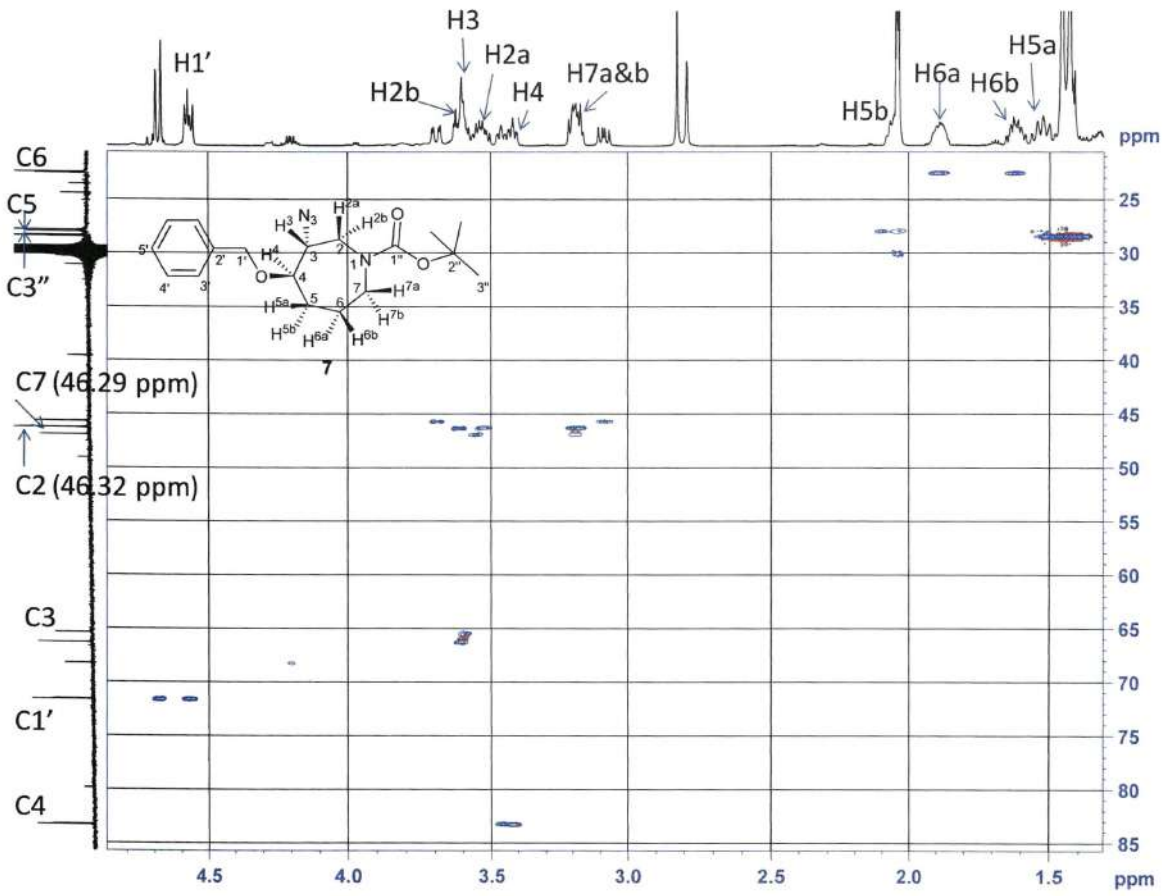
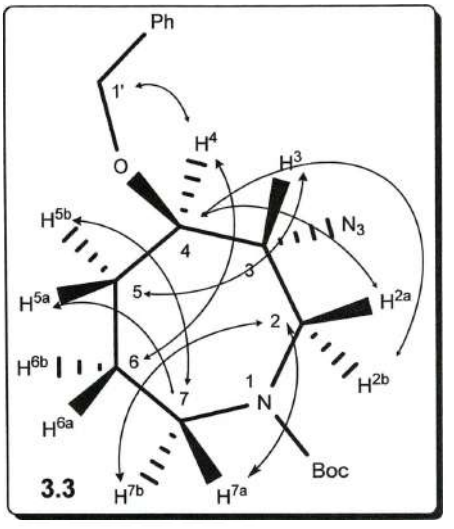


Figure 3.2. ^1H–^{13}C HSQC 2D NMR correlations of the azepane ring in **3.3**.

$^{1}H–^{13}C$ HMBC 2D NMR correlations:



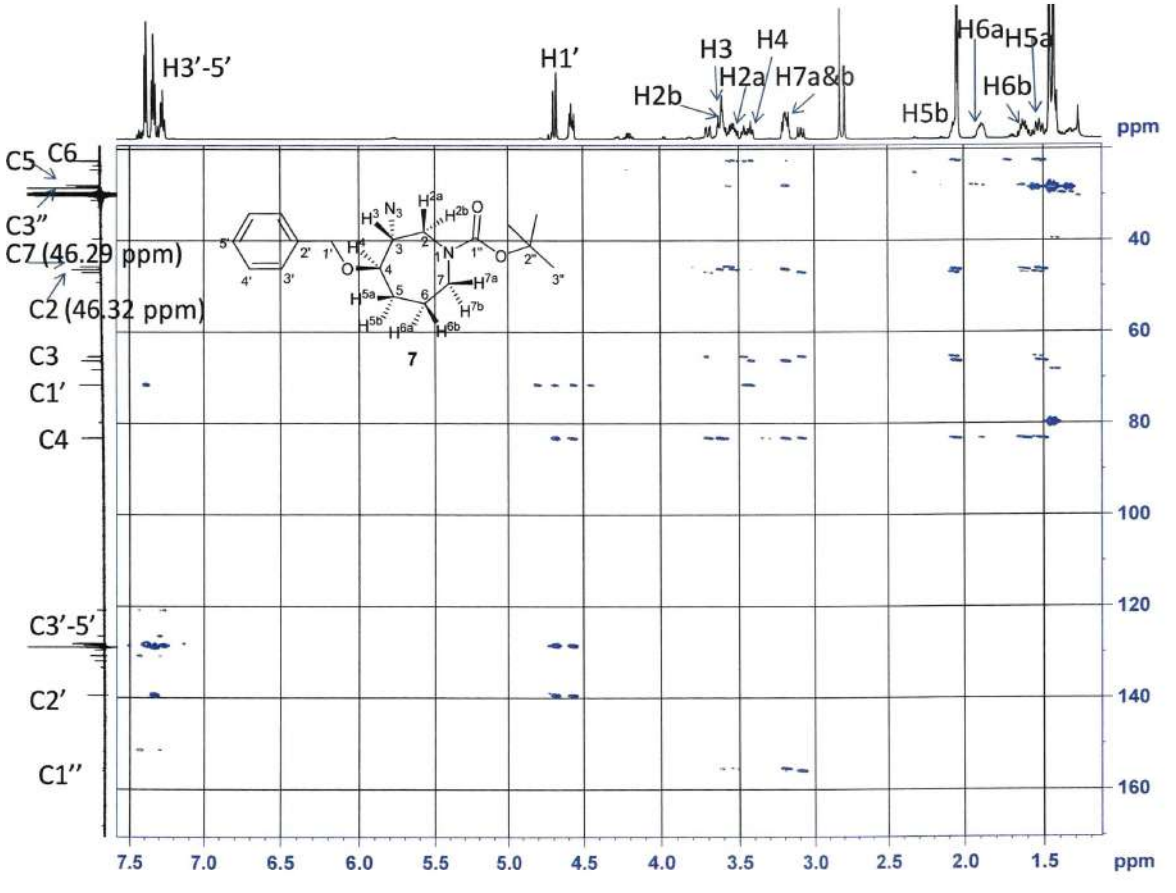
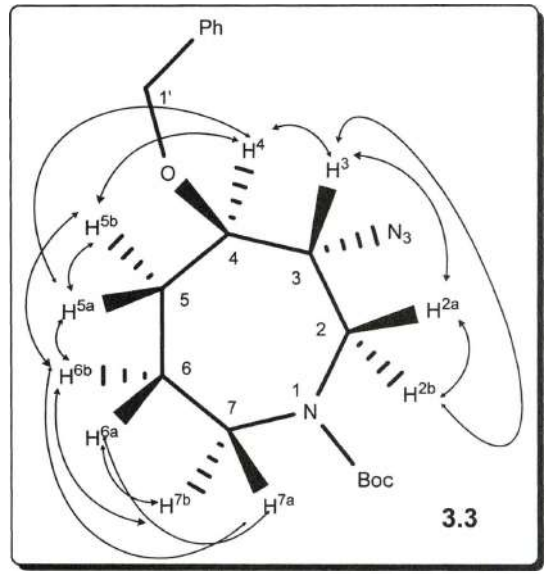


Figure 3.3. $^{1}H–^{13}C$ HMBC 2D NMR correlations of the azepane ring in **3.3**.

^{1}H–^{1}H COSY 2D NMR correlations:



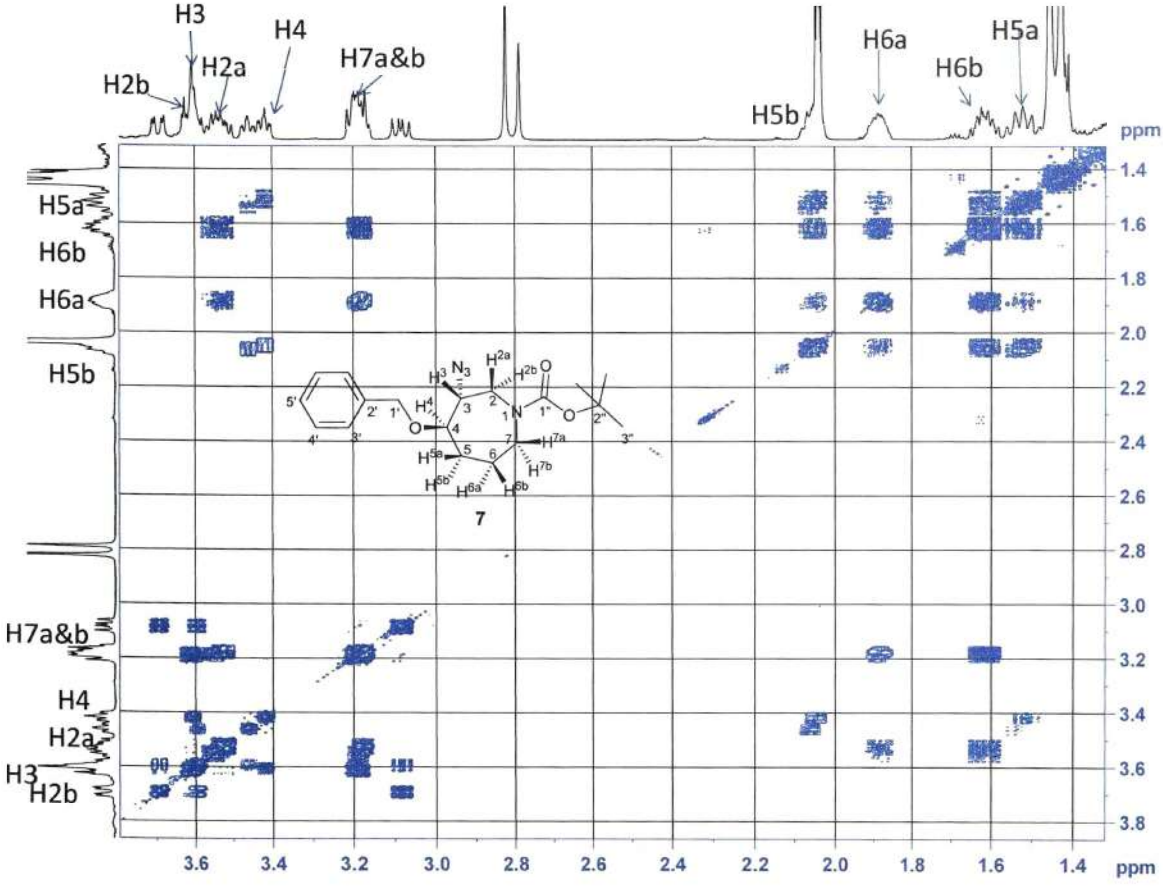
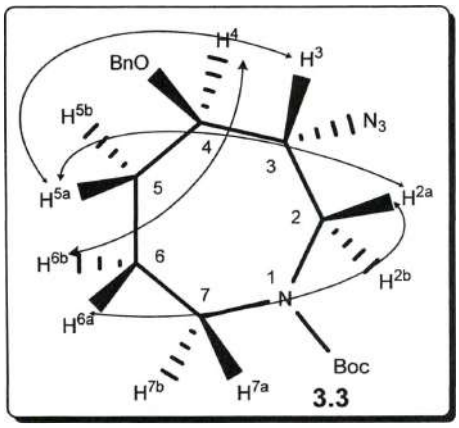


Figure 3.4. ^{1}H–^{1}H COSY 2D NMR correlations of the azepane ring in **3.3**.

^{1}H–^{1}H NOESY 2D NMR correlations:



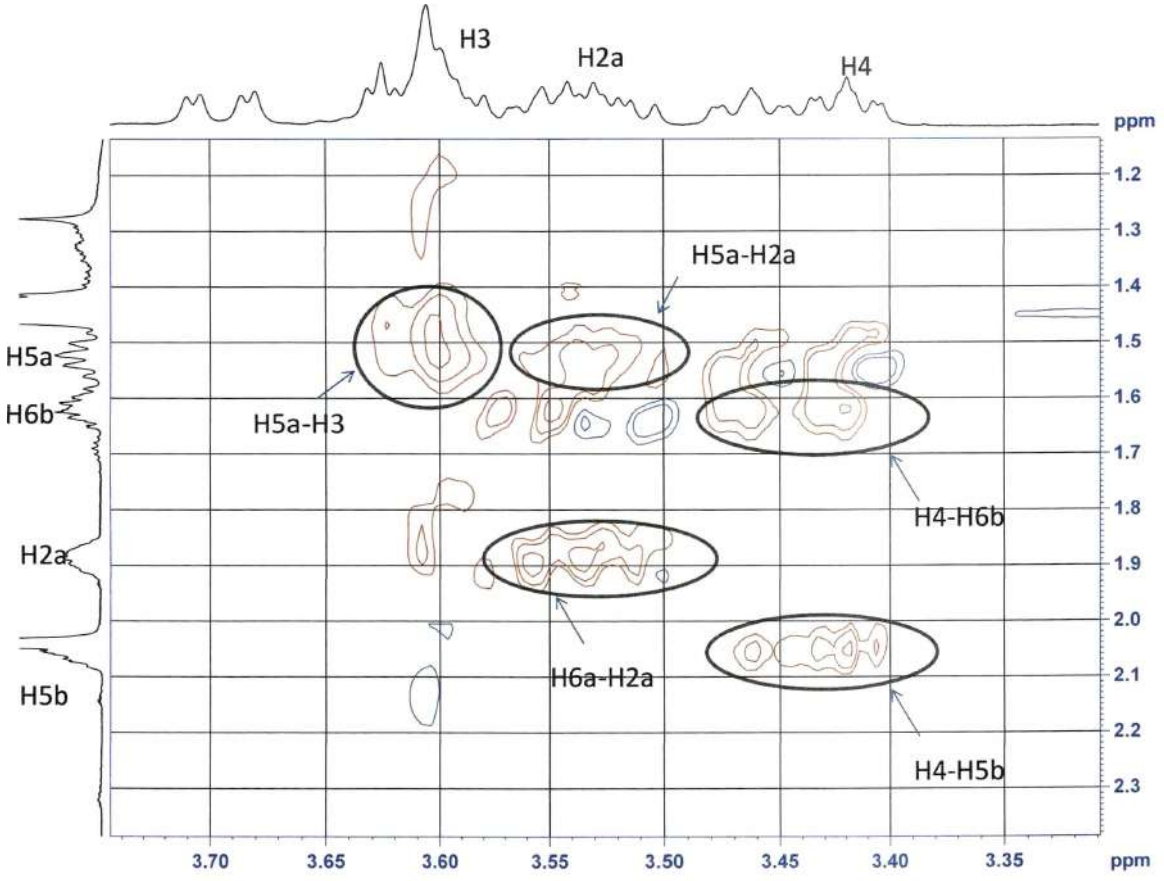
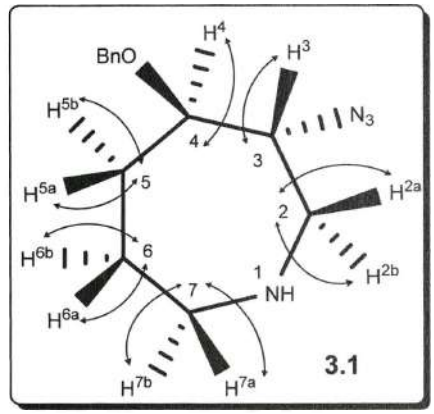


Figure 3.5. ^{1}H–^{1}H NOESY 2D NMR correlations of the azepane ring in **3.3**.

In **3.3**, H5a, H6a and H5b, H6b showed NOEs to H4 and H2a. Further, H5a also showed NOE to H3 suggesting the absolute configuration at C3 is *R*.

3.4.4. Structure Elucidation of the Azepane 3.1

$^{1}H–^{13}C$ HSQC 2D NMR correlations:



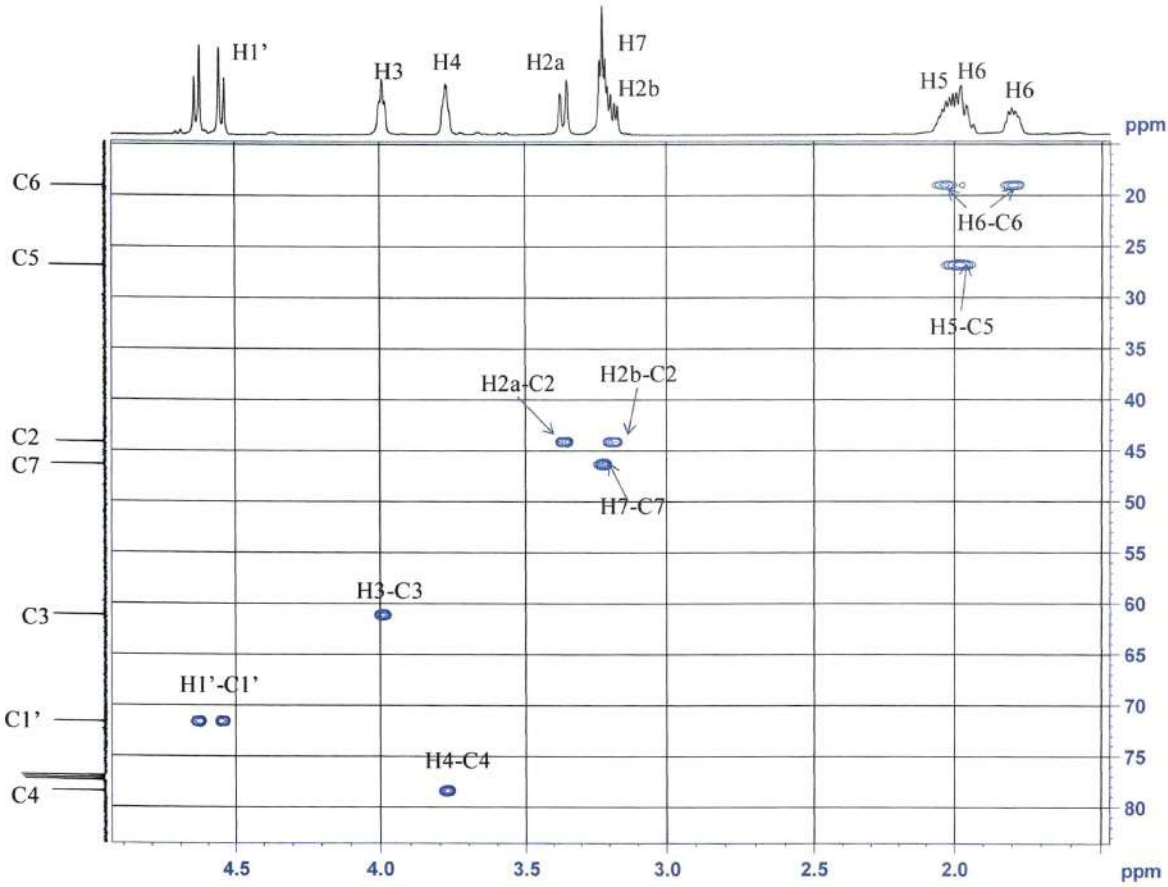
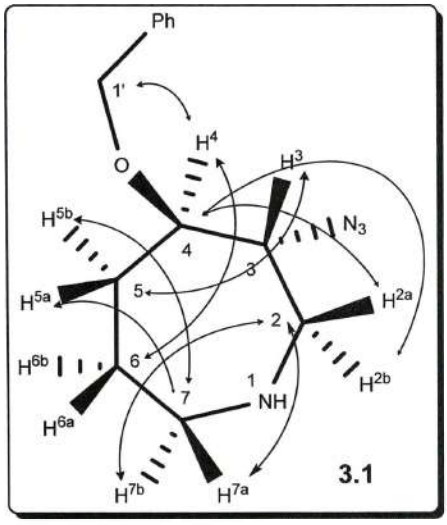


Figure 3.6. $^{1}H–^{13}C$ HSQC 2D NMR correlations of the azepane ring in **3.1**.

$^{1}H–^{13}C$ HMBC 2D NMR correlations:



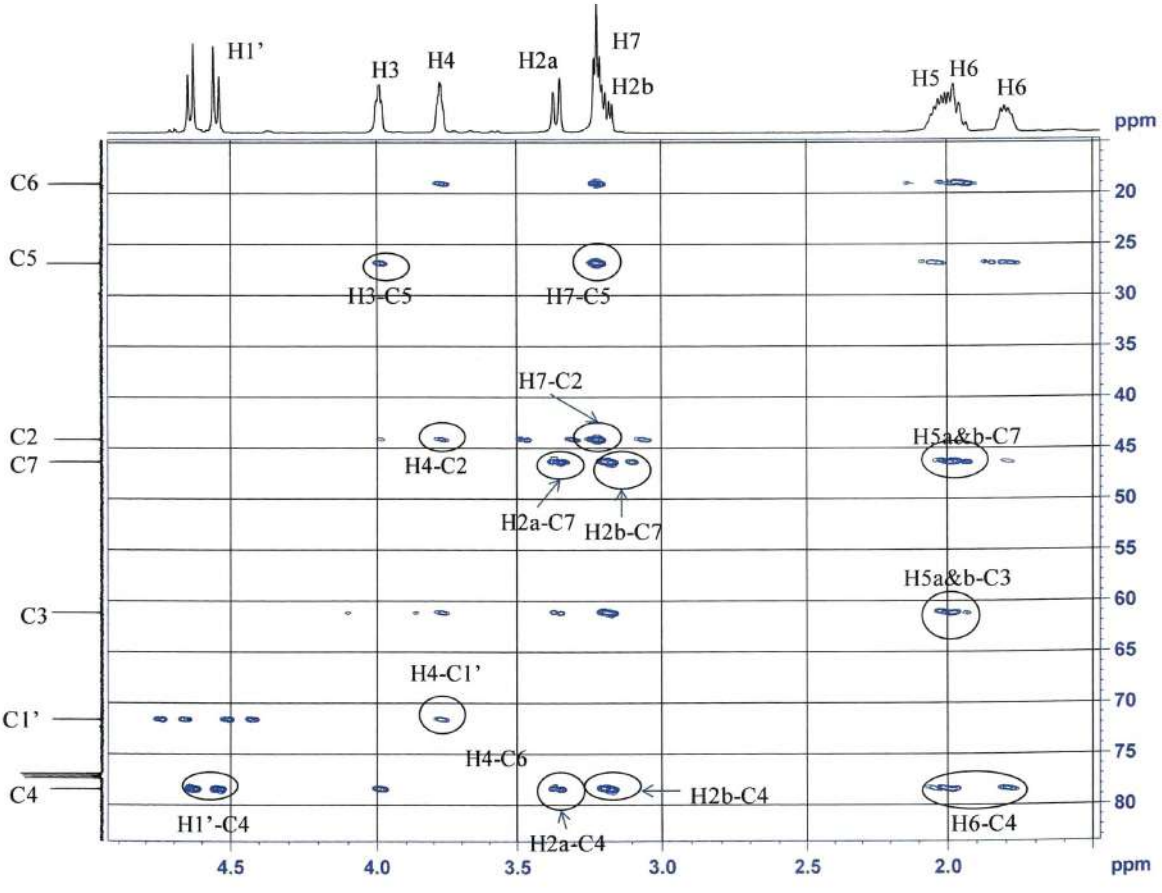
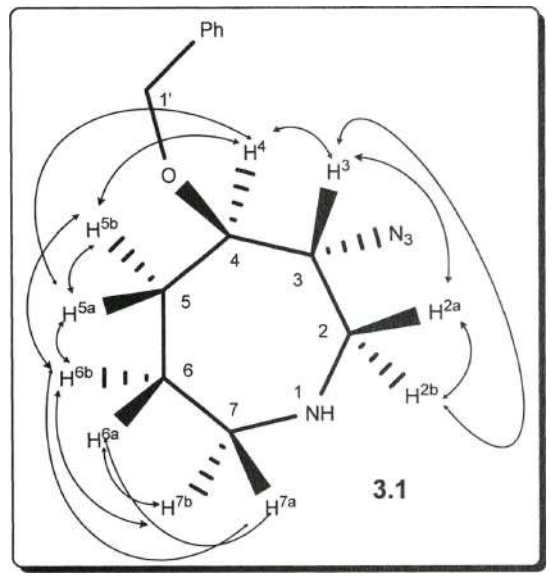


Figure 3.7. $^{1}H–^{13}C$ HMBC 2D NMR correlations of the azepane ring in **3.1**.

^{1}H–^{1}H COSY 2D NMR correlations:



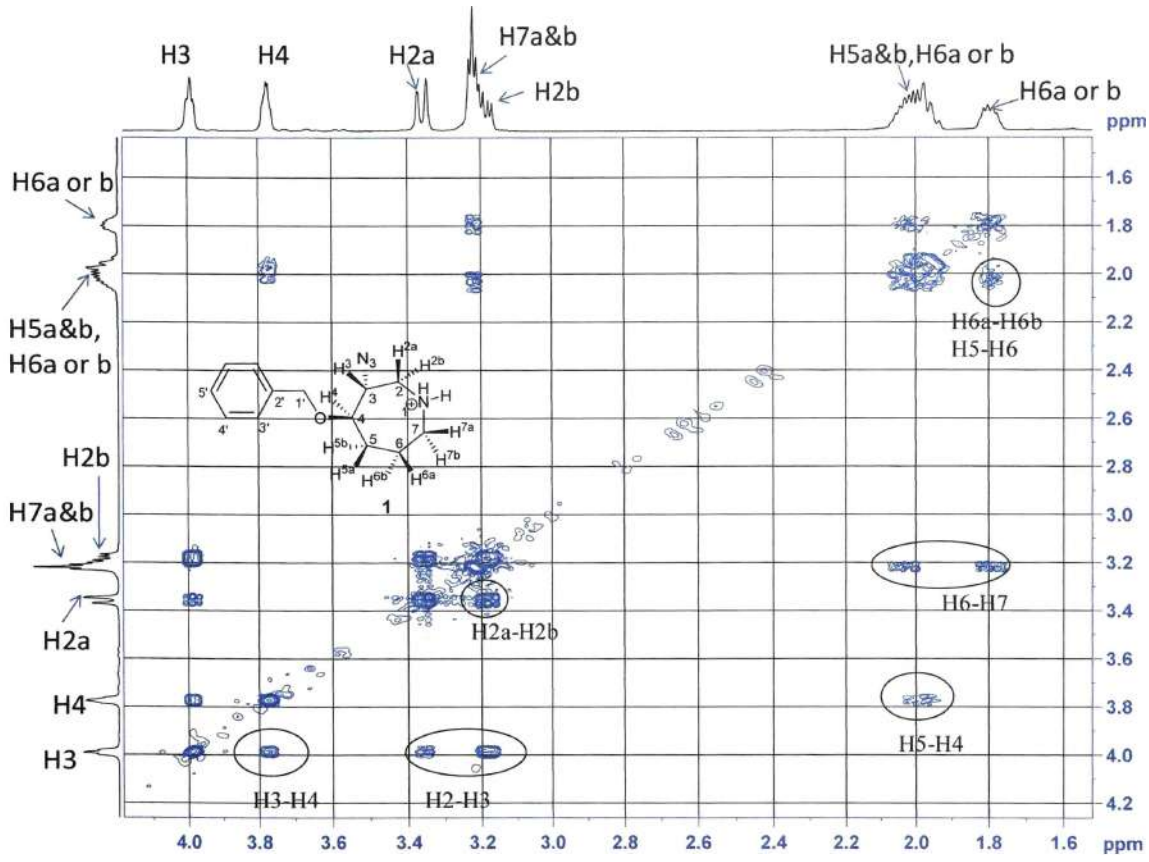
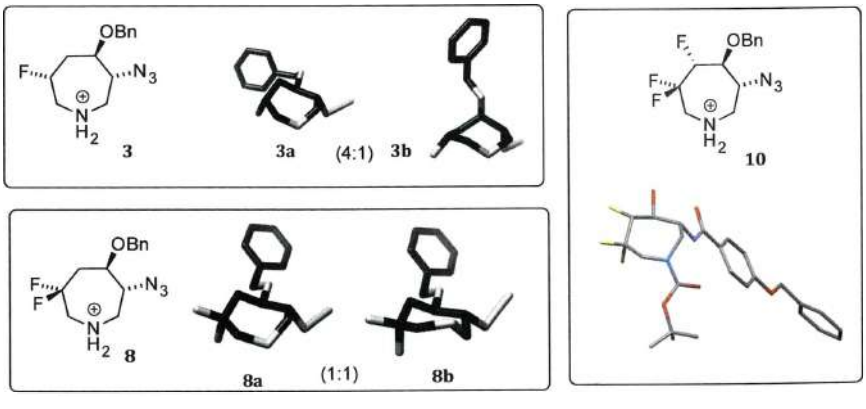


Figure 3.8. ^{1}H–^{1}H COSY 2D NMR correlations of the azepane ring in **3.1**.

CHAPTER 4

Conformational Regulation of Substituted Azepanes through Fluorination

Multiple fluorination exhibits complex conformational effects on the ring structure of substituted azepanes.



4.1. Relevance of the Study

The understanding of complex conformational changes in receptor–ligand interactions is important for drug design. However, most of such receptor–ligand interactions are poorly understood, as the experimental approaches that allow controlled conformational space sampling or manipulation are still in its infancy. Such experimental handles are highly desirable for rational discovery of specific ligand–receptor interactions. Several strategies, such as steric directing, electronic attraction and repulsion, stereoelectronic control, and H–bonding, have been developed for tuning the conformation of a ligand molecule. More recently, selective fluorination has become an important tool in conformational control, due to the strong and unusual stereoelectronic effects resulting from the C–F bond.

Substituted azepanes have been extensively studied as prevalent bioactive epitopes. The regulatory effects of selective monofluorination on substituted azepanes have been discussed in the previous chapter (Chapter 3). This was the first study of fluorine conformational regulation of a seven–membered *N*–heterocycle. For this model system, parameters for potentially synergistic conformational regulation were investigated and revealed that monofluorination was able to reduce the ring conformational disorder of the parent azepane **3.1**. However, only azepane **2.11d** with the 6*R* configuration was able to furnish one major conformation in which the pseudo–diequatorial preference, the azido *gauche* effect, and the fluorine *gauche* effect were all satisfied concurrently. This established the diastereospecificity requirement for synergistic conformational control in these azepanes.

The results of the preliminary examination posed new questions: (i) Is the conformational biasing effect unique to fluorine? (ii) What is the effect of moving the fluorine atom to a different position on the ring? (iii) Can the introduction of multiple fluorines result in

additional conformational bias? Several new comparisons were examined to address these questions important to further understand the complex conformational properties of this azepane system.

4.2. Results and Discussion

In this chapter, the conformational effects of monofluorination on substituted azepane (**2.11b–d**) rings have been further extended. Azepane **2.11b**, in which the fluorine atom is moved from C6 to C5 while maintained in the configuration *trans* to C4–OBn, is controlled by a different combination of conformational factors. The C3/C4 pseudo–diequatorial vs. pseudo–diaxial preference is now operating in close proximity to the C5–F substitution and potentially moderated by the C5–F/C4–OBn *gauche* effect. Azepanes **2.9c**, **2.9d**, and **2.9b** are the hydroxy counterparts of **2.11c**, **2.11d** and **2.11b**, respectively, where an OH group is in place of the fluorine and may answer the question if the conformational effects of fluorine at C6 are unique. Azepane **4.1** is difluorinated at C6 in order to examine if an additional fluorine at C6 would maintain or disrupt the diastereospecific conformational bias of azepane **2.11d**. Azepane **4.2** is the C6(=O) counterpart of azepane **4.1** and intended to offer a different, achiral conformational handle at C6 for comparison to **4.1**. Finally, azepane **4.3**, the C6*S*, C6*R*, and C5*R* trifluoroazepane was examined to understand the potential limits of conformational bias by multiple fluorination. Together, these substituted azepanes describe further characteristics of the intricate conformational landscape controlled by selective fluorination.

All the azepanes (**2.9b–d**, **2.11b–d**, **3.1** and **4.1–4.3**) were synthesized, and the $^{3}J_{HH}$ values were extracted from their ^{1}H NMR spectra. The ^{1}H NMR spectra were simulated to extract accurately the experimental $^{3}J_{HH}$ values. All the azepanes then underwent conformational analysis as described in the previous chapter to identify the geometries matched to

experimental $^3J_{HH}$ values. In the case of **4.3** where the $^3J_{HH}$ and $^3J_{HF}$ were difficult to extract, the solid state X–ray structure of its derivative was solved to understand the conformational effects. Additionally, variant temperature studies revealed shallow barriers for conformational inter–conversion in all these azepanes.

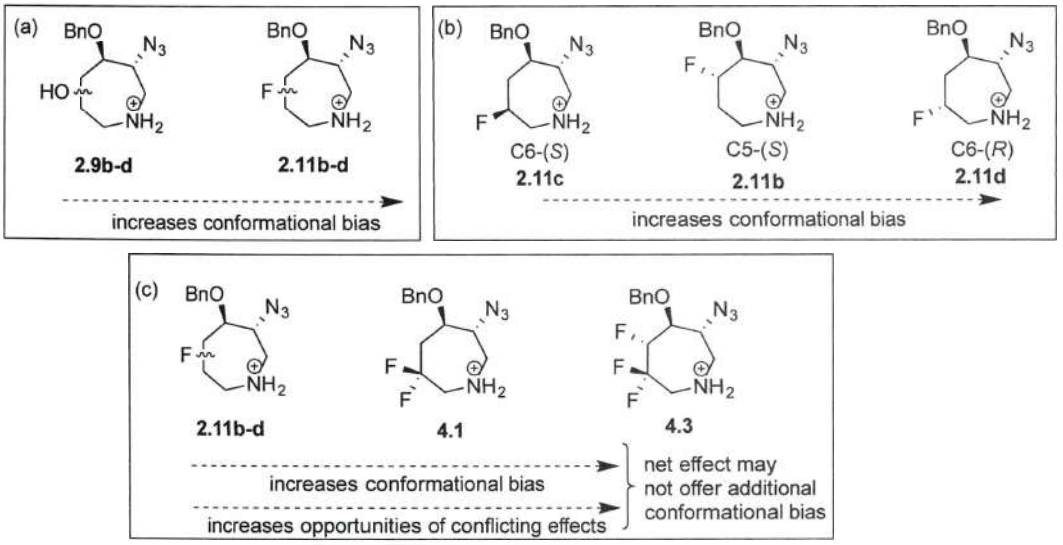


Figure 4.1. Schematic representation of the conformations analysis results:

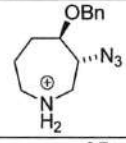
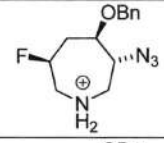
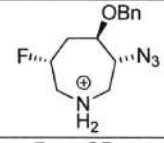
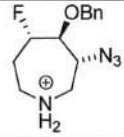
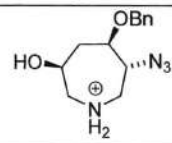
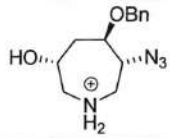
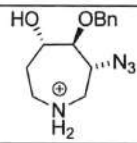
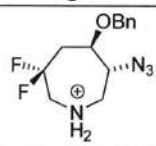
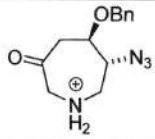
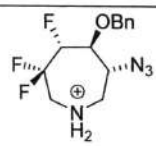
Overall, the results revealed that (i) fluorine has a better ability to impart the conformational bias than a hydroxy group; (ii) position C6–*R* in the azepane presents the best substitution for conformational bias; (iii) multiple fluorine substitutions may not offer additional conformational bias, as it also increases the opportunities of conflicting conformational effects (Figure 4.1).

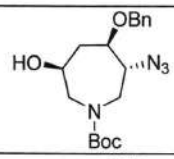
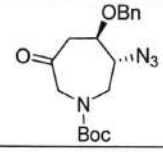
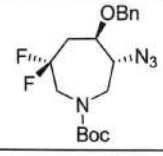
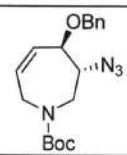
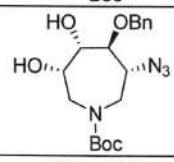
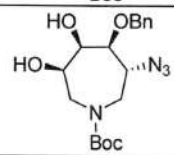
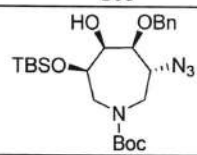
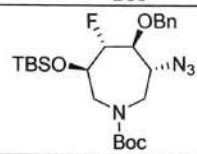
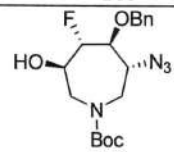
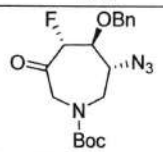
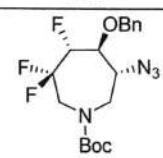
Following is the research article (*Eur. J. Org. Chem., in press, date accepted 31st January 2014*) presented as a main part of the results and discussion for this chapter. The details of the structure elucidation for all new compounds have been discussed in the experimental section. All of the relevant NMR spectra and conformational analysis details are included in the appendix C (pages 388–479) at the end of the thesis.

Pages 126-135 of this thesis have been removed as they contain published material under copyright. Removed contents published as:

Patel, A. R., Hunter, L., Bhadbhade, M. M. and Liu, F. (2014), Conformational Regulation of Substituted Azepanes through Mono-, Di-, and Trifluorination. *European Journal of Organic Chemistry*, vol. 2014, no. 12, pp. 2584-2593. https://doi.org/10.1002/ejoc.201301811

4.3. Cross Reference of Compounds in Chapter 4

Structure	Nomenclature in Thesis	Nomenclature in *Org. Biomol. Chem.*, article.
	**3.1**	**1**
	**2.11c**	**2**
	**2.11d**	**3**
	**2.11b**	**4**
	**2.9c**	**5**
	**2.9d**	**6**
	**2.9b**	**7**
	**4.1**	**8**
	**4.2**	**9**
	**4.3**	**10**

	**2.8c**	**11**
	**4.4**	**12**
	**4.5**	**13**
	**2.7**	**14**
	**4.6**	**15**
	**4.7**	**16**
	**4.8**	**17**
	**4.9**	**18**
	**4.10**	**19**
	**4.11**	**20**
	**4.12**	**21**

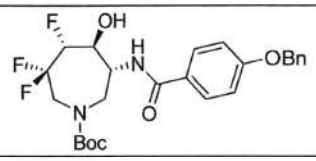
	**4.13**	**22**

Table 4.1. Cross reference of compound nomenclature from the thesis and *Org. Biomol. Chem.* article submitted for publication.

4.4. Experimental

4.4.1. Structure Elucidation of the Azepane 4.1

$^{1}H–^{13}C$ HSQC 2D NMR correlations:

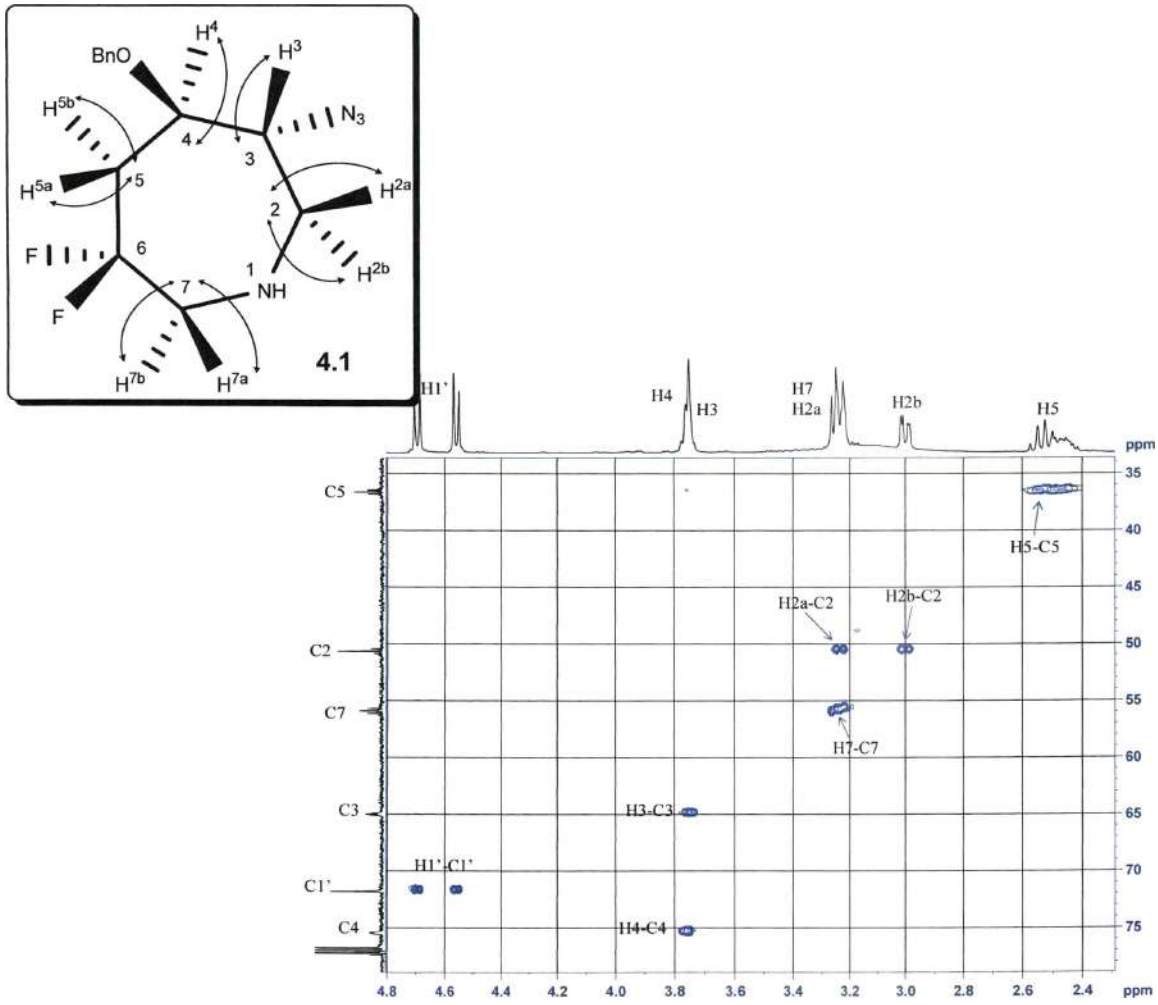
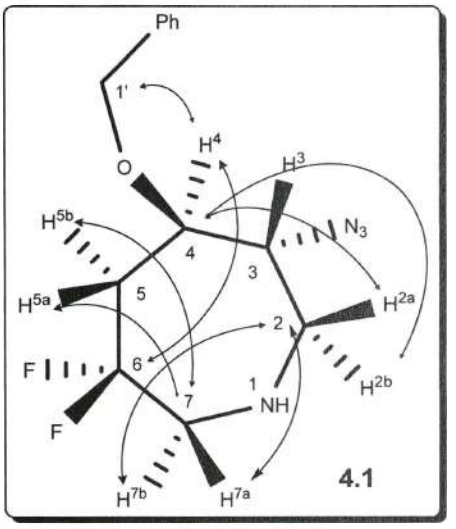


Figure 4.2. $^{1}H–^{13}C$ HSQC 2D NMR correlations of the azepane ring in **4.1**.

$^{1}H–^{13}C$ HMBC 2D NMR correlations:



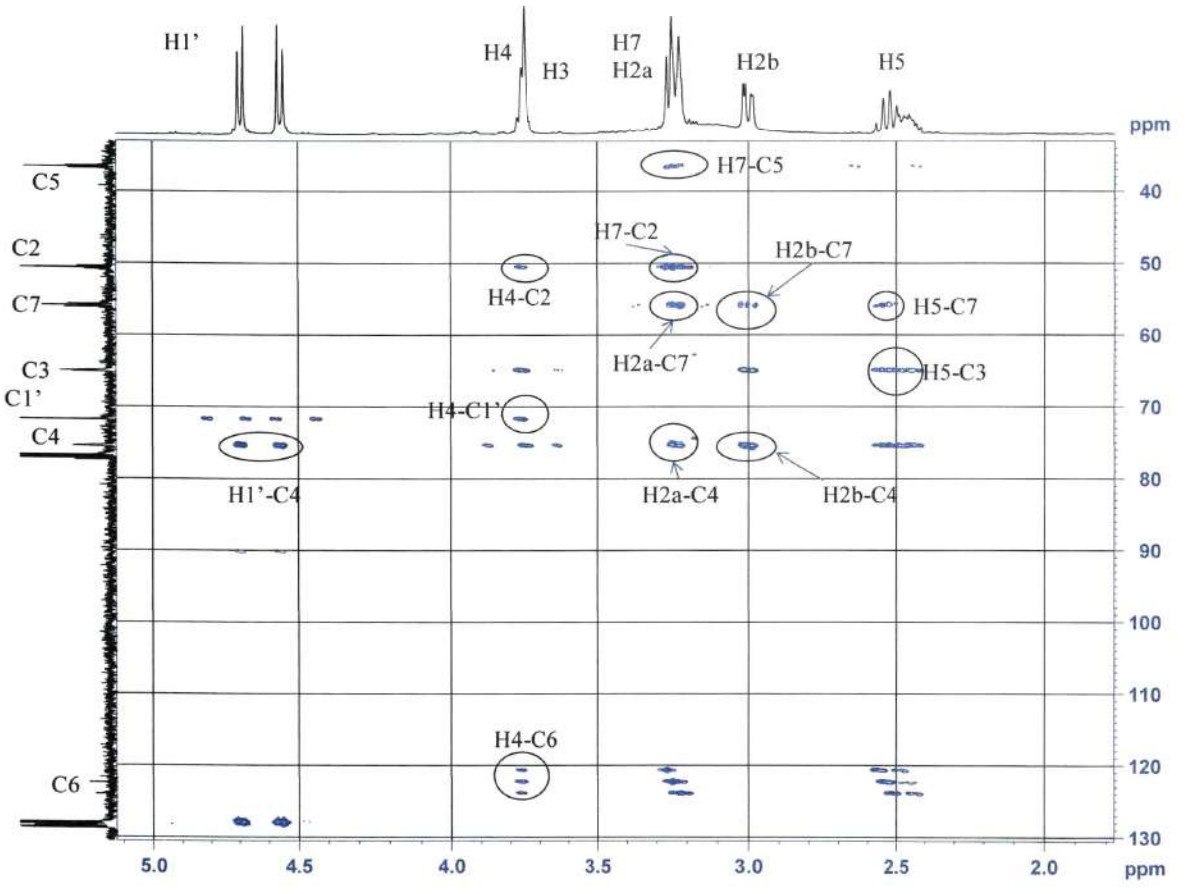


Figure 4.3. $^{1}H–^{13}C$ HMBC 2D NMR correlations of the azepane ring in **4.1**.

$^{1}H–^{1}H$ COSY 2D NMR correlations:

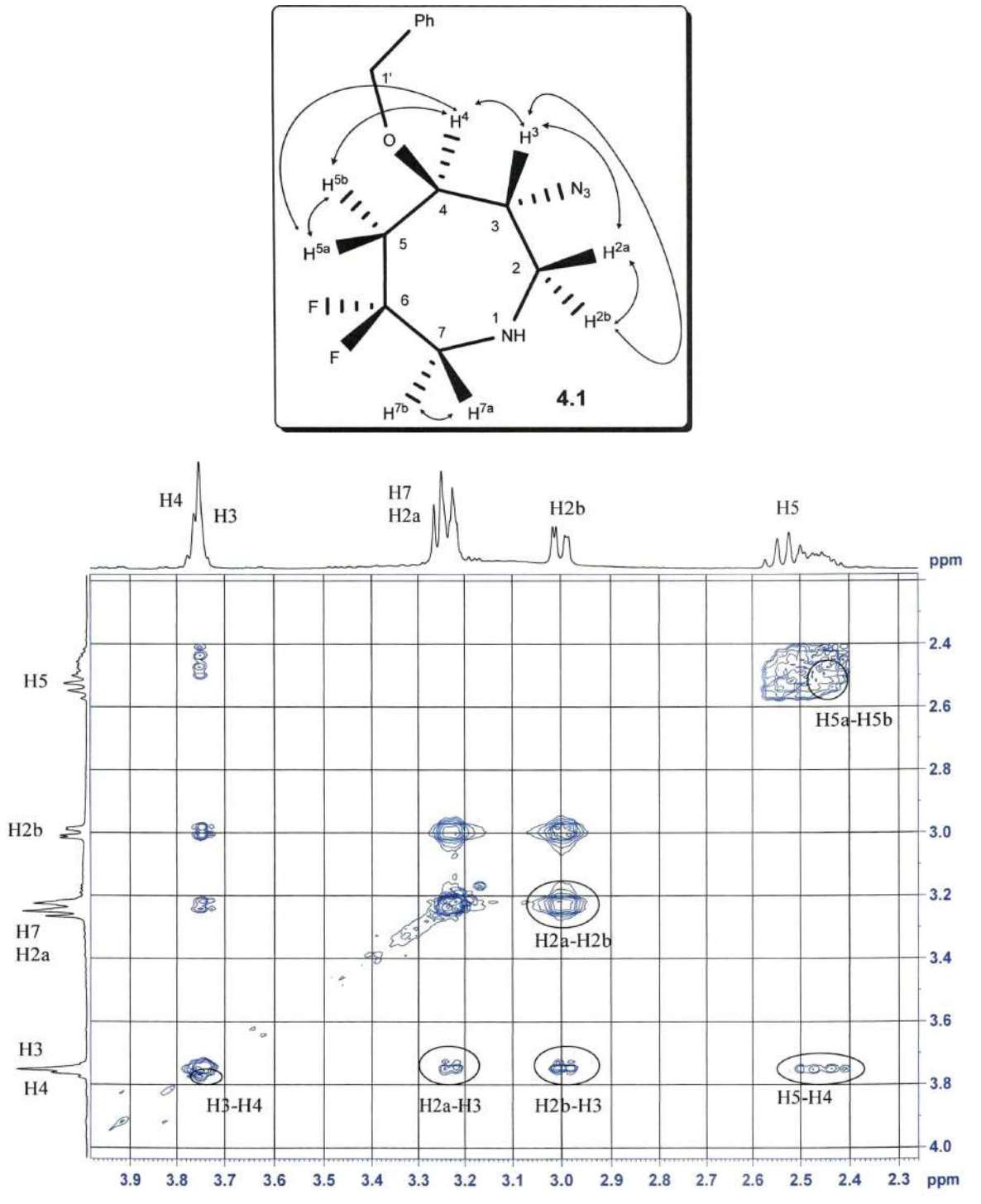
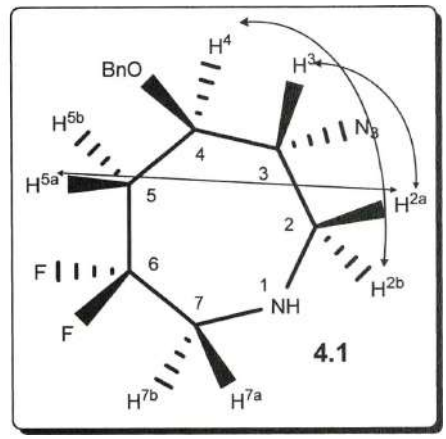


Figure 4.4. $^{1}H–^{1}H$ COSY 2D NMR correlations of the azepane ring in **4.1**.

^{1}H–^{1}H NOESY 2D NMR correlations:



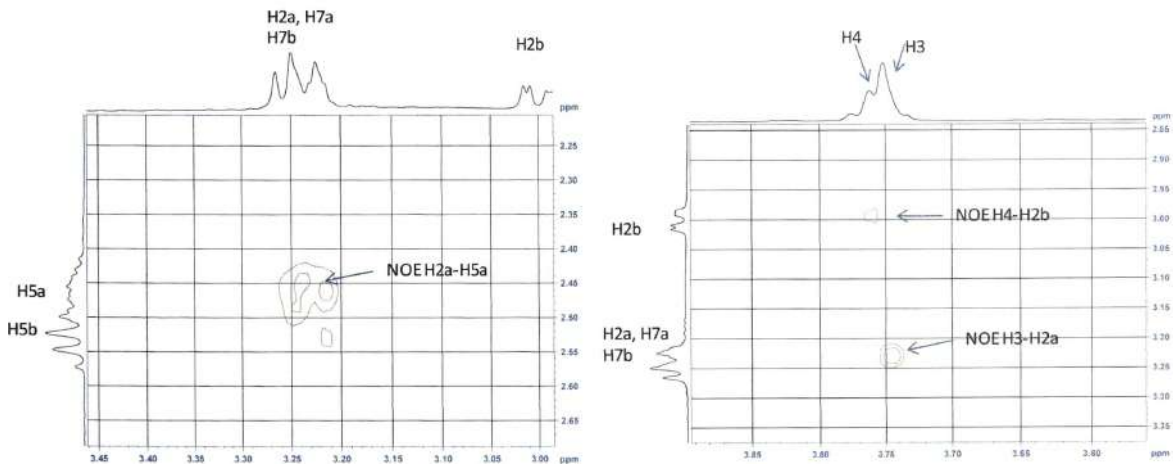
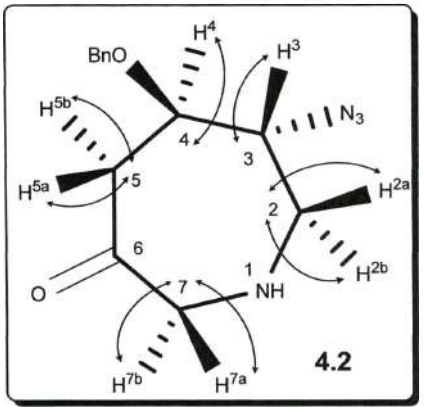


Figure 4.5. ^{1}H–^{1}H NOESY 2D NMR correlations of the azepane ring in **4.1**.

In **4.1**, H2a and H2b showed NOEs to H3 and H4, respectively. H5a showed NOE to H2a while no measurable NOE to H2b. H7a and H7b showed identical chemical shifts. This assignment was further confirmed by ^{1}H NMR spectra *in silico* simulation.

4.4.2. Structure Elucidation of Azepane 4.2

$^{1}H–^{13}C$ HSQC 2D NMR correlations:



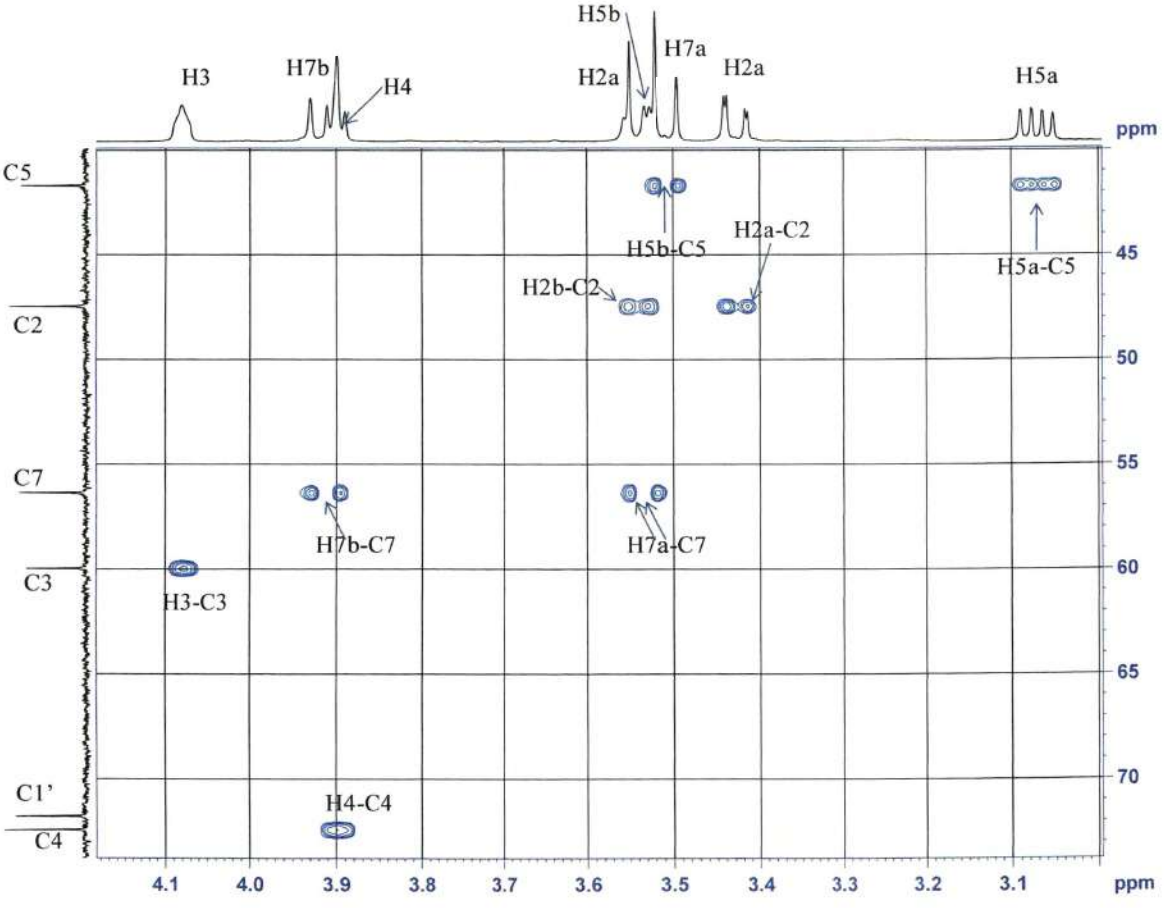


Figure 4.6. $^{1}H–^{13}C$ HSQC 2D NMR correlations of the azepane ring in **4.2**.

$^{1}H–^{13}C$ HMBC 2D NMR correlations:

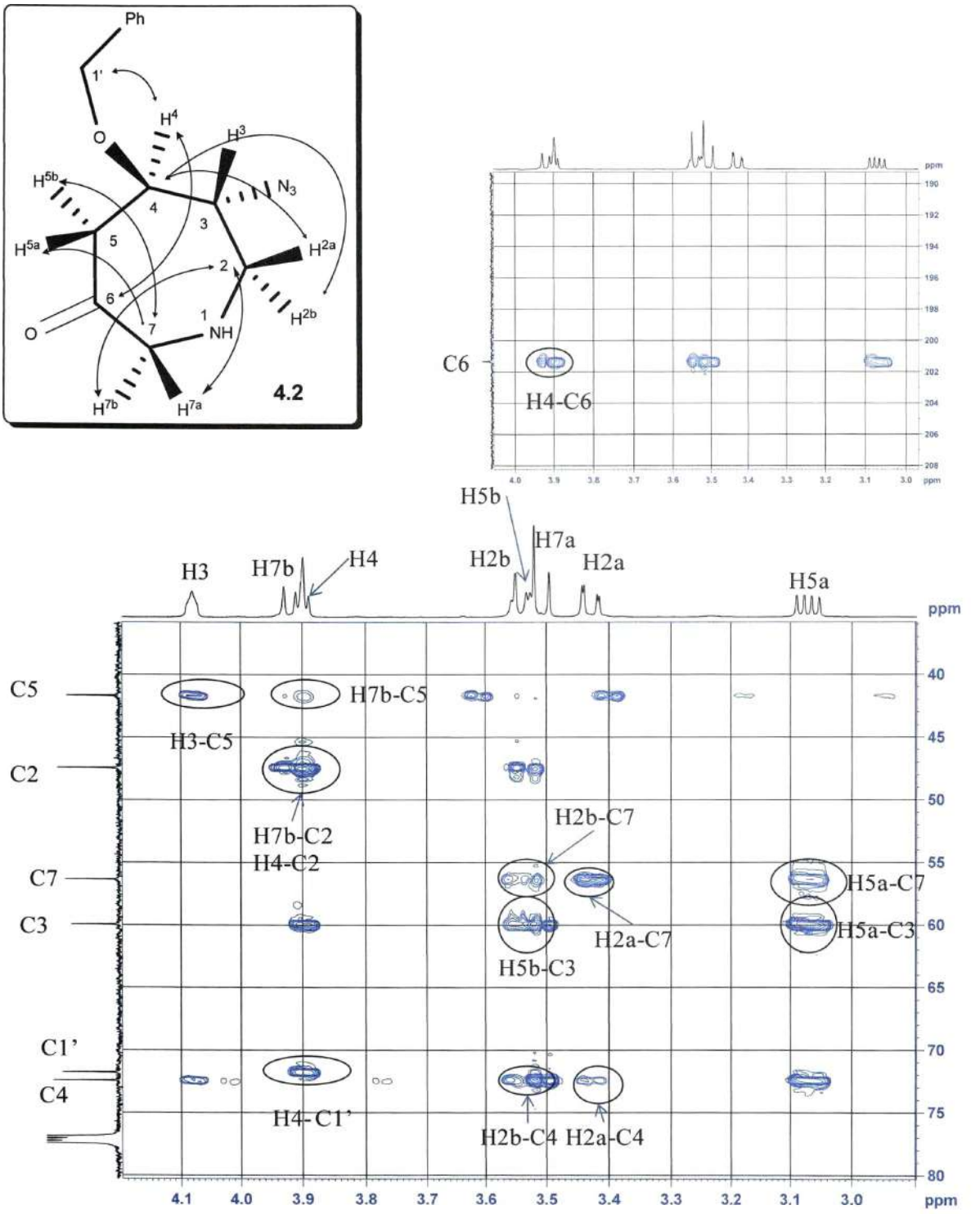
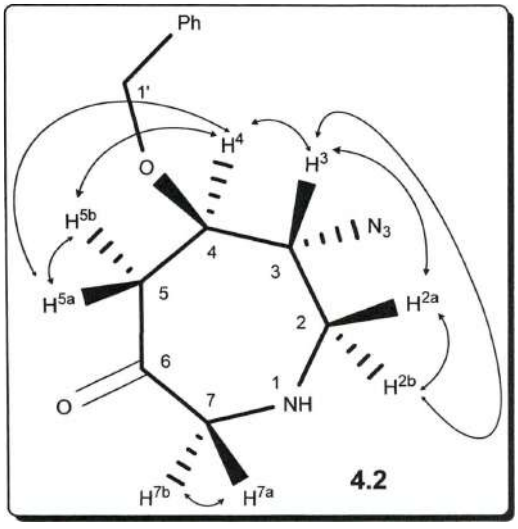


Figure 4.7. $^{1}H–^{13}C$ HMBC 2D NMR correlations of the azepane ring in **4.2**.

$^{1}H–^{1}H$ COSY 2D NMR correlations:



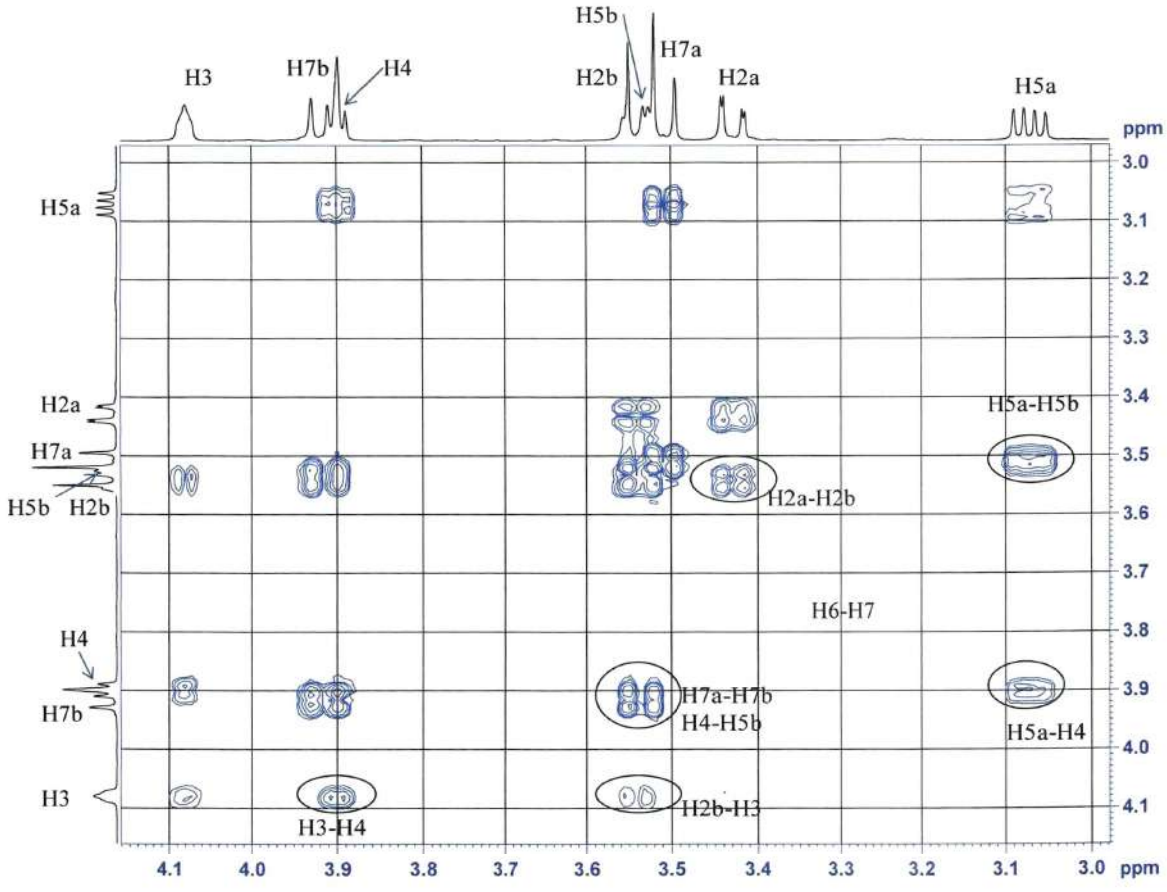
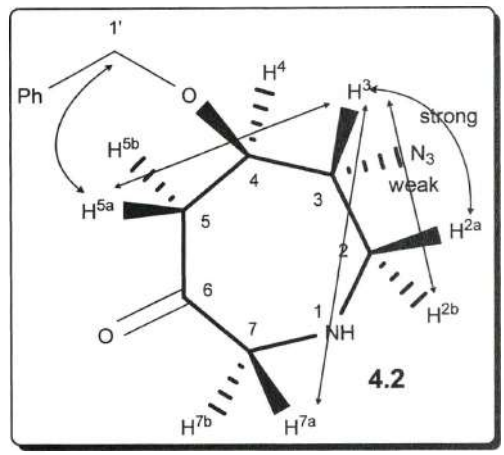


Figure 4.8. $^{1}H–^{1}H$ COSY 2D NMR correlations of the azepane ring in **4.2**.

^{1}H–^{1}H NOESY 2D NMR correlations:



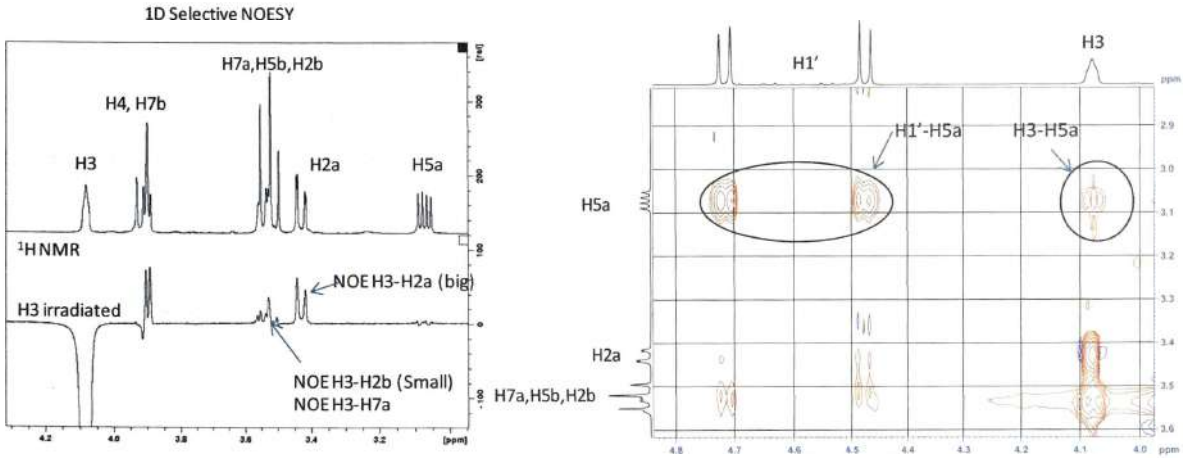
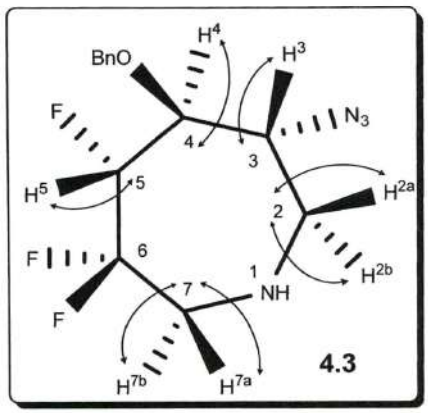


Figure 4.9. ^{1}H–^{1}H NOESY 2D NMR correlations of the azepane ring in **4.2**.

In **4.2**, H3 showed stronger NOE to H2a compared to H2b. H5a showed NOE to H1' and H3 that further showed NOE to H7a. This assignment was supported by ^{1}H NMR spectra *in silico* simulation.

4.4.3. Structure Elucidation of Azepane 4.3

$^{1}H–^{13}C$ HSQC 2D NMR correlations:



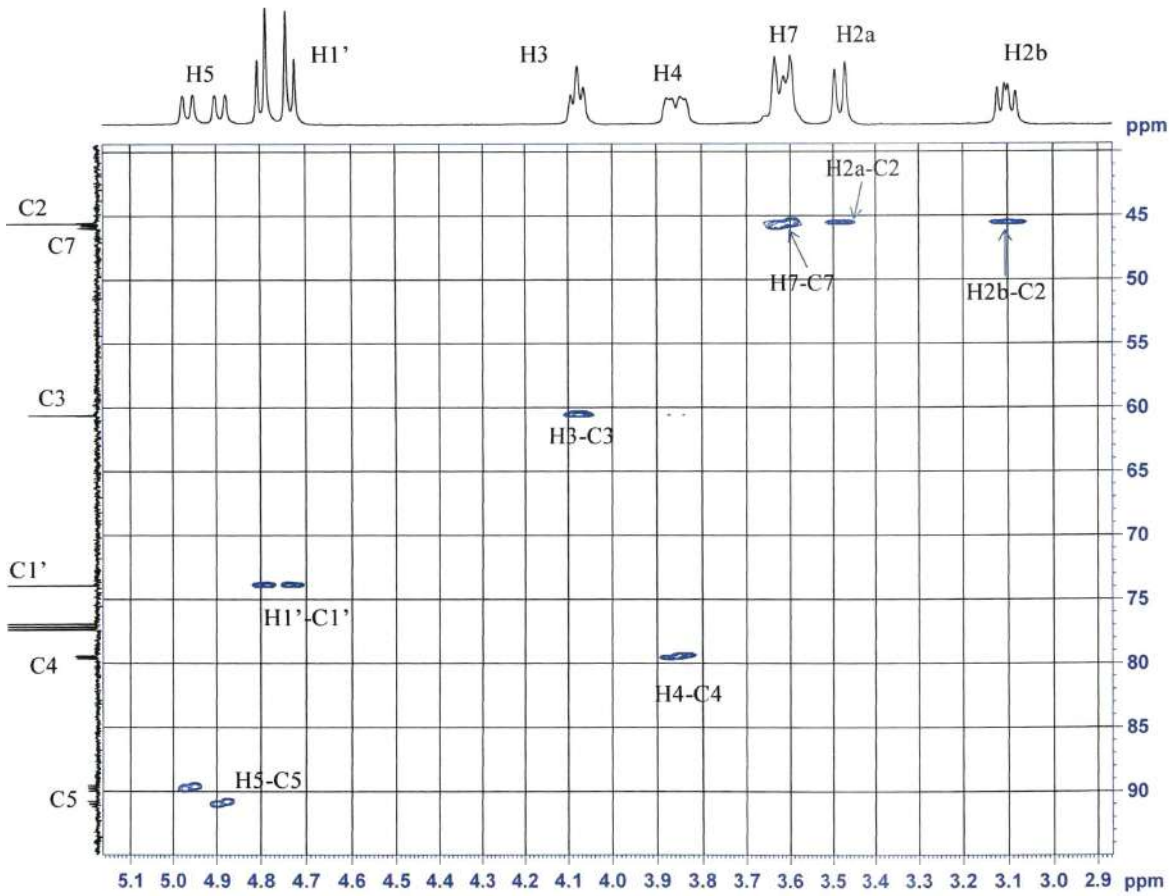


Figure 4.10. $^{1}H–^{13}C$ HSQC 2D NMR correlations of the azepane ring in **4.3**.

$^{1}H–^{13}C$ HMBC 2D NMR correlations:

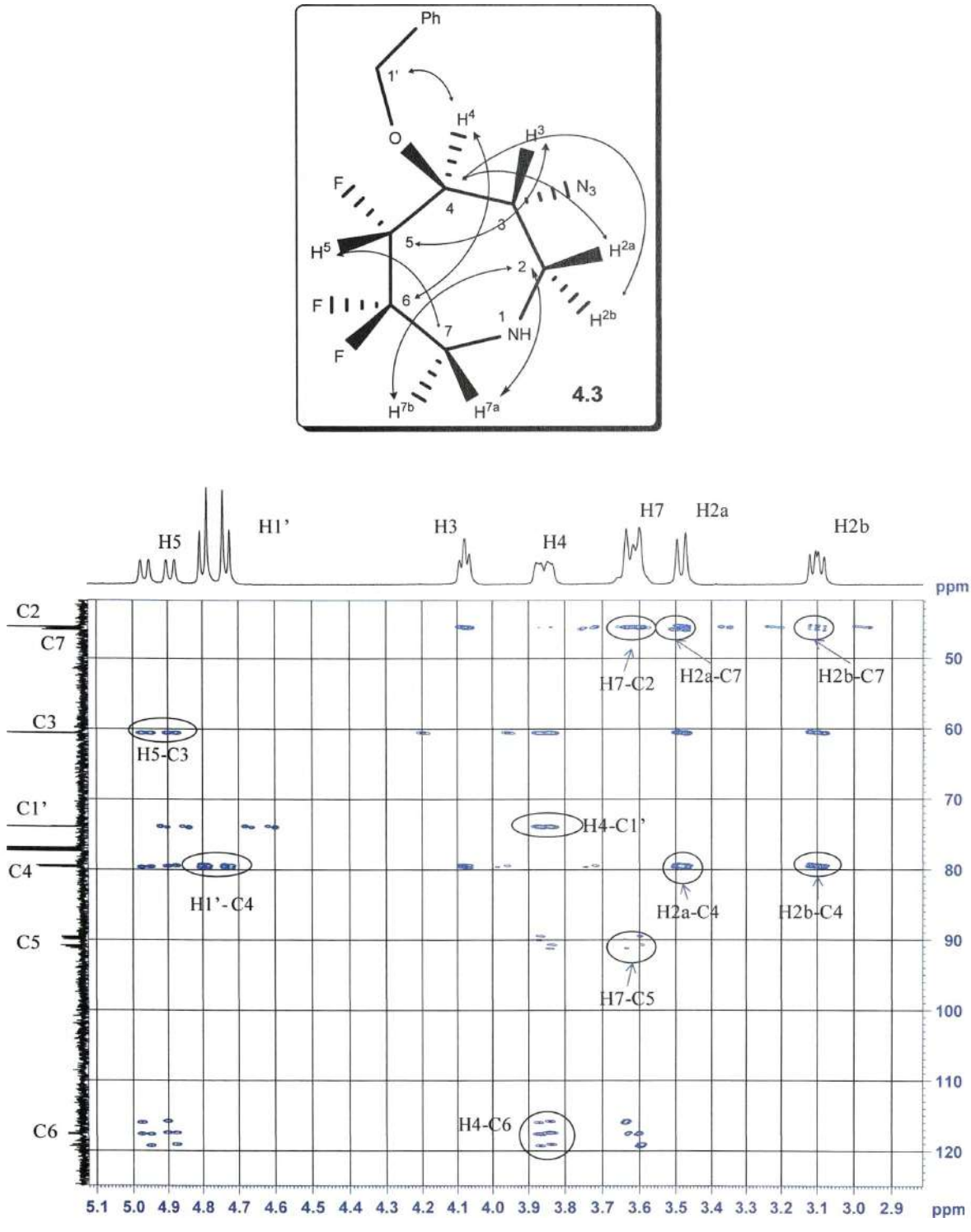
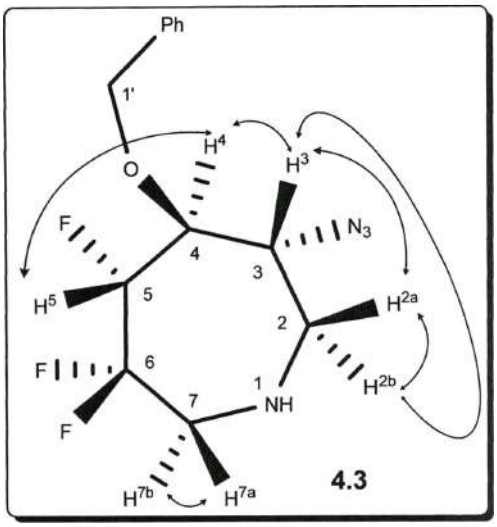


Figure 4.11. $^{1}H–^{13}C$ HMBC 2D NMR correlations of the azepane ring in **4.3**.

$^{1}H–^{1}H$ COSY 2D NMR correlations:



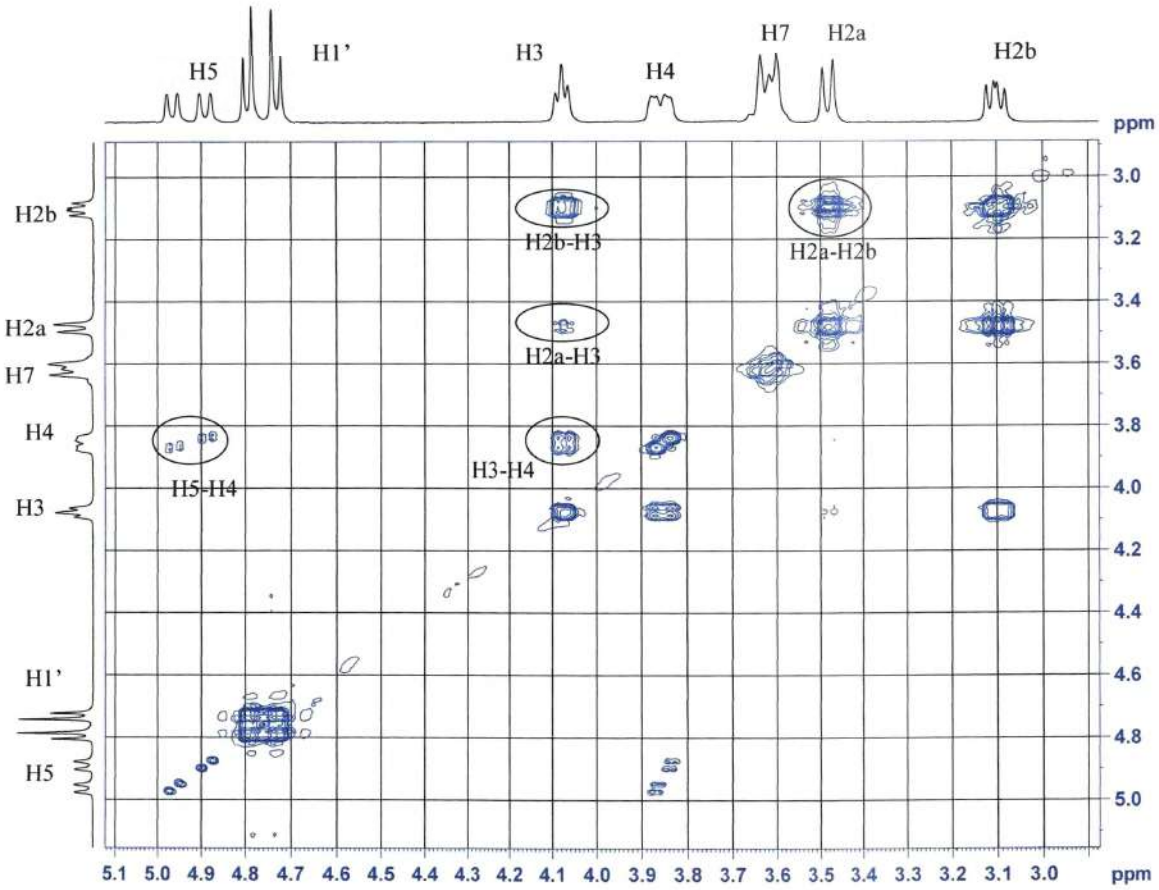
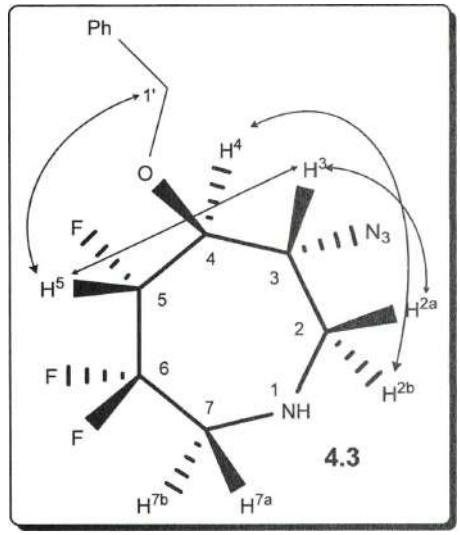
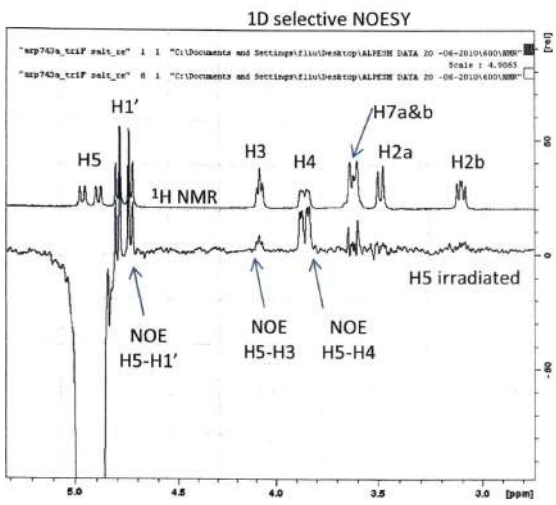


Figure 4.12. $^{1}H–^{1}H$ COSY 2D NMR correlations of the azepane ring in **4.3**.

^{1}H–^{1}H NOESY 2D NMR correlations:





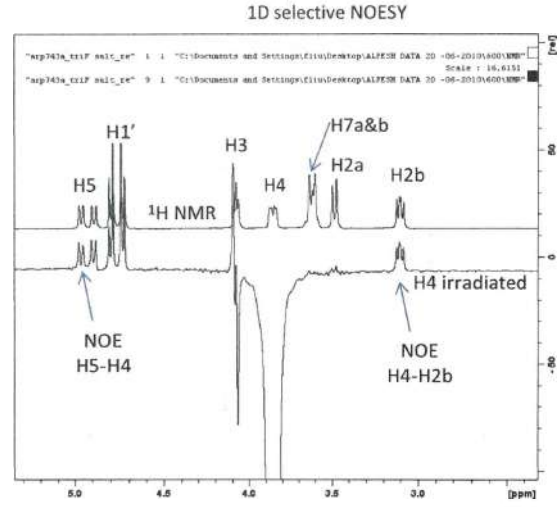


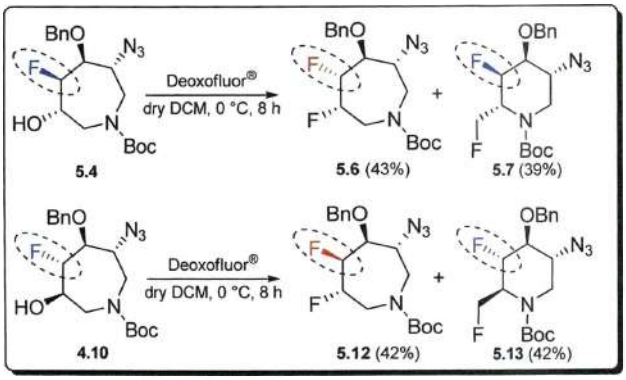
Figure 4.13. ^{1}H–^{1}H NOESY 2D NMR correlations of the azepane ring in **4.3**.

In **4.3**, H4 showed NOE to H2b while no detectable NOE to H2a. H5 had NOE to H1' and H3 suggesting the absolute configuration at C4 stereocenter is *R*. H7a and H7b showed identical chemical shifts. This assignment was further confirmed by ^{1}H NMR spectra *in silico* simulation and the X–ray crystal structure of derivative **4.13**.

CHAPTER 5

Cascade Neighbouring Group Effect: Potentially Fluoronium–assisted Aziridinium Opening in Solution

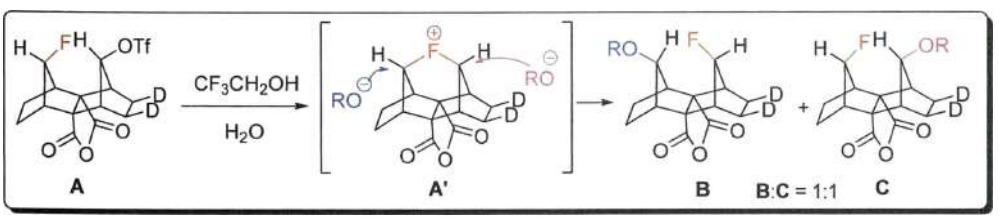
Nucleophilic fluorination of fluorohydroxyazepanes resulted in the epimerization of C–F bonds. A fluorination mechanism via cascade aziridinium–fluoronium neighbouring group participation was investigated and proposed.



5.1. Introduction

Halonium ions (chlorine, bromine, and iodine) have been investigated for about a century. Their existence has equipped design and understanding of numerous stereogenic synthesis and mechanistic investigations.[1] The propensity of halonium ion formation and stability (I>Br>Cl>F) decreases with increase in electronegativity and halonium ion bridges have been described for I, Br, and Cl. The first evidence for a fluoronium ion has been obtained in the gas phase in a mass spectrometry experiment which showed conclusively a fluorine shift.[2] New experimental evidence for the existence of a symmetrical fluoronium ion bridge in solution has recently been described,[1b] although there has been no experimental evidence for a three–membered fluoronium formation in solution.

In the recent report of Lectka et al. regarding a symmetrical fluoronium ion in solution, both chemical and theoretical evidence were presented for the formation of **A'** (Scheme 5.1).[1b] The hydrolysis of a deuterium-labeled triflate isomer **A** with trifluoroethanol/water resulted in a 1:1 mixture of isomers **B** and **C** by trapping the fluoronium ion **A'** with water. The results suggested that the reaction proceeded via the symmetrical fluoronium intermediate **A'**.



Scheme 5.1. First evidence of fluoronium ion in solution.[1b]

Lectka et al. concluded that the work "pointed out fluorine's potential role as an anchimeric assistor to open up possibilities for new reactions that can capitalize on a fluoronium intermediate to control regioselectivity, diastereoselectivity, and overall reactivity of organofluorinated molecules".

More recently, Olah and coworkers[3] investigated the properties of fluoro– and chlorodimethylbutyl cations by *ab initio* methods. Bridged fluoronium ion **D**, carbenium ion **E**, and fluorocarbenium ion **F** were found to be local minima on the potential energy surface. However, **D** was found to be less stable by 12.8 kcal/mol than **F**. While in the chloro analogue, the chloronium ion **G** was more stable compared to ions **H** and **I** by 9.0 kcal/mol and 7.4 kcal/mol, respectively (Figure 5.1).

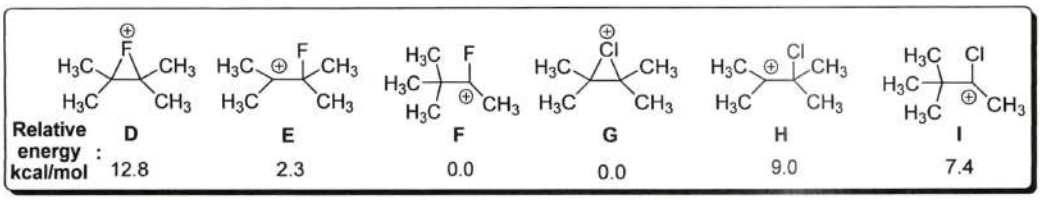
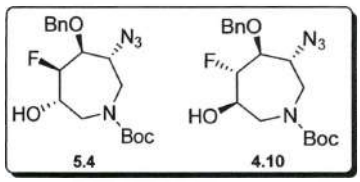


Figure 5.1. Olah's computational studies on fluoronium and chloronium ions.[3]



In this chapter, the fluorination reactions of fluorohydroxy azepanes, such as **5.4** and **4.10**, were investigated in order to understand the influence of a residential fluorine on the stereochemical outcomes of the reaction. The vicinal difluoroazepanes synthesis via potentially a fluoronium–aziridinium cascade was investigated as well. This chapter serves as an extension of the fluorination methodology (Chapter 2) and conformational analysis (Chapters 3,4) of mono–, germinal di– and tri–fluoroazepanes, and aims to understand the potentially complex neighbouring group participation in vicinal fluorination of a heterocyclic model system. The synthesis of fluorinated balanol analogues utilizing these fluoroazepanes will be discussed in the next chapter.

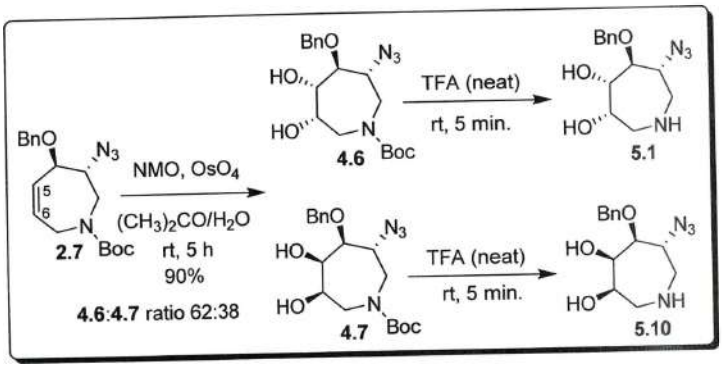
In Chapter 2 the first examples of fluorination on substituted azepanes (**2.8b–d**) was

presented with exclusive *retention* of stereochemistry at the participating carbon, possibly because of azepane nitrogen/carbamate oxygen neighbouring group participation. However, in the TBS protected azepane **4.8** (discussd in Chapter 4) the C5 monofluorination resulted in *inversion* of stereochemistry as the S_N2 outcome. The difficulty in predicting for the neighbouring group effect in this ring system may be due to the delicate interplay between electronic factors and ring conformational constraints. The neighbouring group effects in the presence of a residential fluorine in the synthesis of vicinal difluoroazepanes, therefore, was not predictable *a priori*. O'Hagan and coworkers[4] have developed vicinal fluorination of linear alkanes using epoxide and cyclic sulphate ring opening with fluoride. However, such tandem fluorination from vicinal hydroxyl groups in a heterocyclic ring system has not been investigated, and can exhibit complex neighboring group effects.

5.2. Results and Discussion

5.2.1. Synthesis of Fluorohydroxyazepanes 5.4 and 4.10

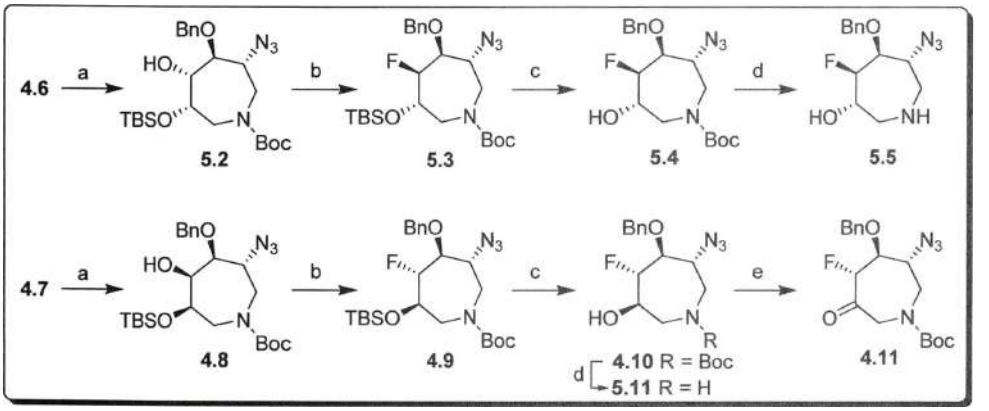
Substituted tetrahydroazepine **2.7** was synthesized following a literature procedure.[5] The synthesis of *syn*–dihydroxyazepanes **4.6** and **4.7** was achieved in a 62:38 ratio by treatment of **2.7** with *N*–methylmorpholine–*N*–oxide and catalytic OsO_4 (Scheme 5.2). The absolute stereochemistry at C5 and C6 stereo centers was secured using NOESY two–dimensional NMR experiments (see experimental section). *N*–*tert*–Butoxycarbonyl (Boc) deprotected derivatives **5.1** and **5.10** were synthesized using neat trifluoroacetic acid (TFA) from **4.6** and **4.7**, respectively (Scheme 5.2) to remove the geometric isomers (*cis* and *trans*) due to the *N*–Boc group for clearer structure elucidation.



Scheme 5.2. Synthesis of *syn*–dihydroxyazepanes **4.6** and **4.7**.

In contrast to mono–deoxyfluorination, direct reaction of vicinal diols with two equivalents of Deoxofluor® or DAST often results in sulfite esters.[6] The routes for vicinal difluorination can be enlisted as, (i) formation of cyclic sulfate and ring opening with nucleophilic fluorine,[7] (ii) formation of epoxide and ring opening with nucleophilic fluorine,[8] (iii) formation of ditriflate from diol followed by difluorination,[9] and (iv) selective monoprotection–deprotection approach.[10] The epoxidation and cyclic sulfite routes are most widely used since they are rapid and high yielding. However, they often involve vigorous reaction conditions such as strong acids and high temperature,[11] which were proven to be unsuitable for **4.6** and **4.7** given the presence of the Boc group. Moreover, the ditriflation route resulted in poor yields due to side reactions.[9] Therefore, a monoprotection–deprotection strategy was utilized for difluorination in this case. *tert*–Butyldimethylsilylether (TBS) was the protecting group of choice, which would later be selectively deprotected in the presence of OBn and Boc groups in **4.6** and **4.7**. The C6 regioselective TBS protection was achieved on compounds **4.6** and **4.7** to give **5.2** and **4.8**, respectively. Nucleophilic fluorination at C5 using Deoxofluor® was then performed on **5.2** and **4.8** to obtain **5.3** and **4.9**, respectively in good yields (Scheme 5.3) with *inversion* of stereochemistry at C5. The observed stereochemical outcome was contrary to our previous report[12] (azepane **2.8b**, Chapter 2) in which complete *retention* of

stereochemistry was observed at the C5 center because of neighboring group participation. However, the presence of a sterically bulky OTBS group in **5.2** and **4.8** may render this azepane nitrogen participation unfavorable leading to the S_N2 outcome. TBS deprotection from **5.3** and **4.9**, furnished in good yields fluoroazepanes **5.4** and **4.10**, respectively.



Scheme 5.3. Synthesis of fluorohydroxyazepanes **5.4** and **4.10**. *Reagents and conditions*: (a) Imidazole, TBSCl, dry DMF, 25 °C, 10 h, 67–70%; (b) Deoxofluor®, dry DCM, 0 °C, 8 h, 65–84%; (c) TBAF, dry THF, 45 min, 75–77%; (d) TFA, neat, 5 min, quant.; (e) PCC (1.1 equiv.), MS4Å, dry DCM, 25 °C, 1.5 h, 92%.

5.2.2. Structure Elucidation of 5.4 and 4.10

The deprotected derivatives **5.5** and **5.11** were synthesized from **5.4** and **4.10**, respectively to ensure structure elucidation without the presence of geometric isomers (*cis* and *trans*) of *N*–Boc group (Scheme 5.3). The detailed structure elucidation of **5.5** and **5.11** using 2D NMR and X–ray crystallography is discussed in this section.

5.2.2.1. Structure elucidation of 4.10

The carbons and protons assignments were secured using HSQC and COSY 2D NMR spectra; and were further confirmed by HMBC correlations. The absolute stereochemical assignments were secured using NOESY NMR experiments. Furthermore, the crystaline oxidised derivative **4.11** was synthesized from **4.10**. The X–ray crystal structure of **4.11** (Figure 5.2) also supported the 5*S*–F configuration assigned by the 2D NMR experiments

on **4.10**.

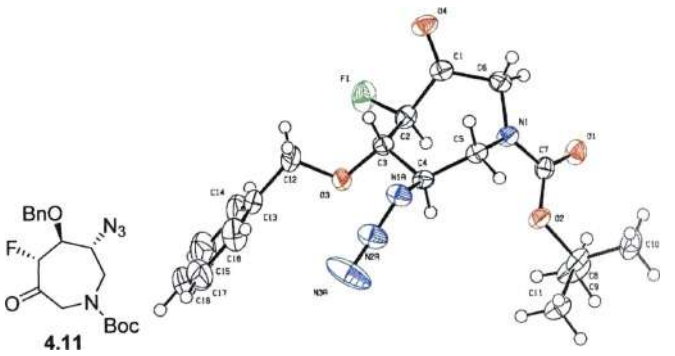


Figure 5.2. X–ray crystal structure of **4.11**.

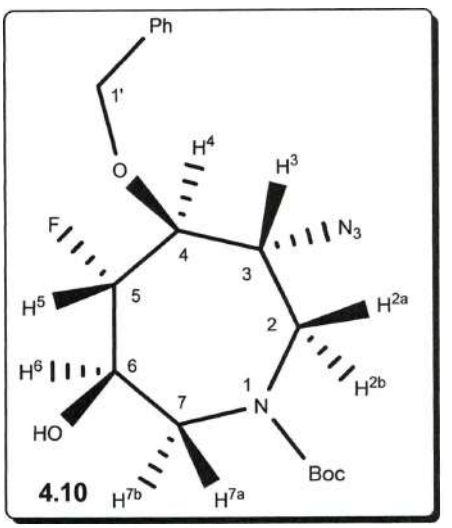


Table 5.1. 2D NMR structure elucidation of the azepane **4.10**.

No	Protons	HSQC	HMBC	COSY	NOESY
1	H2a	C2	C4, C7	H2b, H3	H3
2	H2b	C2	C4, C7	H2a, H3	H3, H4, H6
3	H3	C3	C5	H2a, H2b, H4	H2a, H5
4	H4	C4	C1', C2, C6	H3, H5	H2b, H6
5	H5	C5	C3, C7	H4, H6	H2a, H3, H7a
6	H6	C6	–	H5, H7a, H7b	H2b, H7b
7	H7a	C7	C2, C5	H6, H7b	H5
8	H7b	C7	C2, C5	H6, H7a	H6

In **4.10**, HMBC and HSQC couplings with C1' (δ_c 74.9 ppm) and C4 (δ_c 81.6 ppm), respectively identified H4 at 3.62 ppm. H4 further showed COSY correlations with H5 (δ_H 4.56 ppm) and H3 (δ_H 3.73 ppm) which had COSY correlations with H2a (δ_H 3.75 ppm) and H2b (δ_H 3.09 ppm) (Table 5.1). The assignment of H5 was also confirmed from germinal fluorine coupling ($^1J_{HF}$ = 47.43 Hz) that showed COSY correlation with H6 (δ_H 4.08 ppm) and so did H6 to H7a (δ_H 3.71 ppm) and H7b (δ_H 3.44 ppm). The fluorine couplings in the carbon spectrum further validated the proposed structure elucidation. After securing the regiochemistry, NOESY experiments were used to identify the absolute configuration at C5. Azepane **4.10** has three centres with known absolute stereochemistry: C3, C4 and C5. H2a, H2b, H7a and H7b were identified from NOEs to H3, H4 and H6. H5 showed NOE to H3, H7a and H2a while no detectable NOE to H2b and H7b. Thus, the absolute configuration assignments at C5 in **4.10** was confirmed to be *S*.

5.2.2.2. Structure Elucidation of 5.5

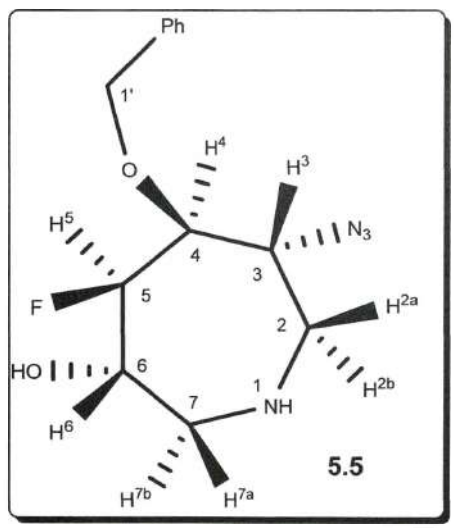


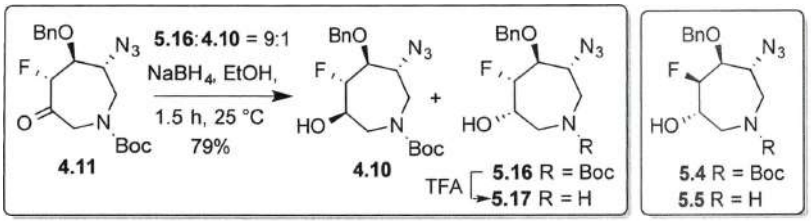
Table 5.2. 2D NMR structure elucidation of the azepane **5.5**.

No	Protons	HSQC	HMBC	COSY	NOESY[a]
1	H2a	C2	C4, C7	H2b, H3	H3

2	H2b	C2	C4, C7	H2a, H3	H3, H4, H5
3	H3	C3	–	H2a, H2b, H4	H2a
4	H4	C4	C1', C2, C6	H3, H5	H1', H2b, H5
5	H5	C5	C3, C7	H4, H6	H1', H2b&H7b (s), H2a&H7a (w)
6	H6	C6	–	H5, H7a, H7b	H7a (s), H7b(w)
7	H7a	C7	C2, C5	H6, H7b	H6 (s)
8	H7b	C7	C2, C5	H6, H7a	H5, H6 (w)

[a]s = strong, w = weak

The key 2D NMR correlations of **5.5** are presented in Table 5.2. In **5.5**, C3, C4 and C5 were the stereocenters with known absolute stereochemistry. H2a, and H2b were identified from NOEs to H3, H4, respectively. H6 showed significantly stronger NOE to H7a than H7b. H5 showed NOEs to H7a, H7b, H2a and H2b; however, the quantification of NOE signals revealed NOE to H7b was stronger than to H7a. Additionally, H5 showed strong NOE to H4. Thus, the absolute configuration assignments at C5 in **5.5** was confirmed as *R*.

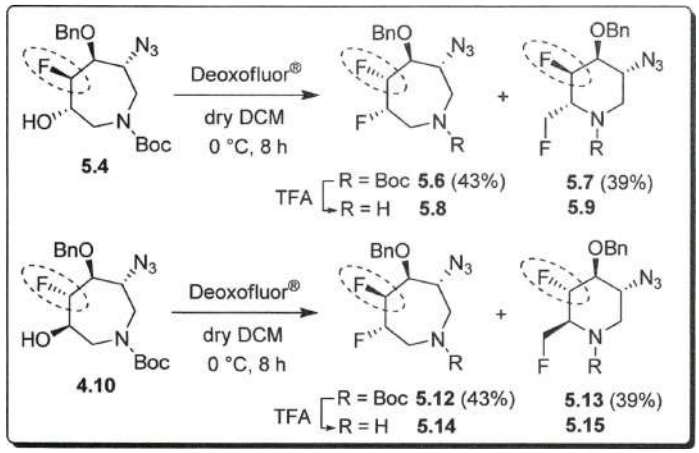


Scheme 5.4. Synthetic evidence for structure assignments of **5.5**.

The structure elucidation of **5.5** was also supported by further experimental evidence. The 5–fluoro–6–oxoazepane **4.11** was reduced using sodiumborohydride to obtain diastereomeric (C6–OH) mixture of both possible fluorohydroxyazepanes **4.10** and **5.16** in a ratio of 1:9 as a pair of diastereomers (Scheme 5.4). The X–ray structure of **4.11** proved the absolute configuration in **5.16** at C5 is *S* which means **5.4** (and the deprotected analogue **5.5**) must have *R* configuration at C5. This further validated the stereochemical assignments in **5.5**.

5.2.3. Synthesis of Difluoroazepanes 5.6 and 5.12

Nucleophilic deoxyfluorination of fluorohydroxy azepanes **5.4** and **4.10** using Deoxofluor® at 0 °C resulted in difluoroazepanes **5.6** and **5.12** along with ring contracted products difluoropiperidines **5.7** and **5.13**, respectively in about 1:1 ratio (Scheme 5.5). The deoxyfluorination of **4.10** at −20 °C resulted in low (70%) conversion with 1:1 ratio of **5.12** and **5.13**. The course of reaction was monitored using quantitative reverse phase HPLC on the reaction mixture after Boc deprotection. The azepanes **5.11**, **5.14** and **5.15** were found to have retention time of 24.6, 29.8 and 28.2 min using phenomenex Gemini analytical column (250 × 2.1 mm) and 15–50% acetonitrile in water with flow rate 0.8 mL/min over 50 min. Deprotected analogues **5.8**, **5.9**, **5.14**, **5.15**, from **5.6**, **5.7**, **5.12** and **5.13**, respectively were subjected to 2D–NMR analysis for structure elucidation and revealed the epimerization of the C–F bond at C5 for both **5.6** and **5.12**. The 2D–NMR structure elucidation details for **5.8** and **5.14** are discussed here.



Scheme 5.5. Synthesis of vicinal difluoroazepanes **5.6** and **5.12** with C5–F epimerization.

5.2.3.1. Structure Elucidation of 5.8

The key 2D NMR correlations of **5.8** are presented in Table 5.3. Assignment of the

absolute stereochemistry of **5.8** at C5 and C6 as *R* and *S*, respectively, was supported by H6 and H5 both showing NOE to H3 and H2a with no measureable NOE to H2b.

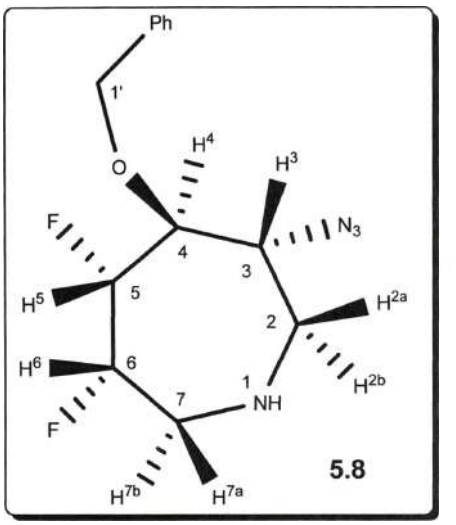


Table 5.3. 2D NMR structure elucidation of the azepane **5.8**.

No	Protons	HSQC	HMBC	COSY	NOESY
1	H2a	C2	C4, C7	H2b, H3	H3, H5, H6
2	H2b	C2	C4, C7	H2a, H3	H3, H4
3	H3	C3	C5	H2a, H2b, H4	H2a
4	H4	C4	C1', C2, C6	H3, H5	H1', H2b, H5
5	H5	C5	C3, C7	H4	H1', H2a, H3, H6
6	H6	C6	C4	H7a, H7b	H2a, H3, H5
7	H7a	C7	C2, C5	H6, H7b	–
8	H7b	C7	C2, C5	H6, H7a	–

5.2.3.2. Structure elucidation of 5.14

The key 2D NMR correlations of **5.14** are presented in Table 5.4. In the case of **5.14**, H5 showed NOE to H7b and H4 while no detactable NOE with H7a. Whereas, H6 showed NOE to H2a and H7a while no measurable NOE to H2b. These results suggested that the absolute stereochemistry at both C5 and C6 is *S*.

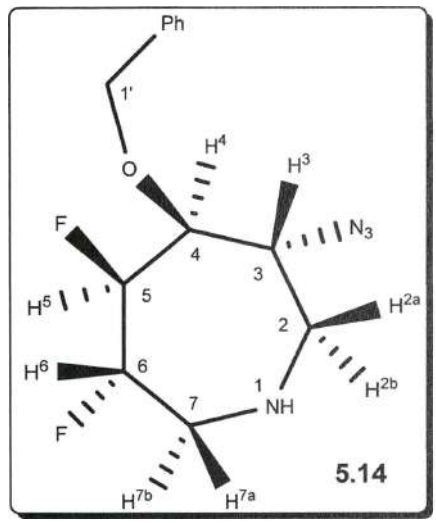


Table 5.4. 2D NMR structure elucidation of the azepane **5.14**.

No	Protons	HSQC	HMBC	COSY	NOESY
1	H2a	C2	C4, C7	H2b, H3	H3, H6
2	H2b	C2	C4, C7	H2a, H3	H3, H4
3	H3	C3	C5	H2a, H2b, H4	H2a
4	H4	C4	C1', C2, C6	H3, H5	H1', H2b, H5
5	H5	C5	–	H4, H6	H1', H4, H7b
6	H6	C6	–	H5, H7a, H7b	H7a, H2a
7	H7a	C7	C2, C5	H6, H7b	H6
8	H7b	C7	C2, C5	H6, H7a	H5

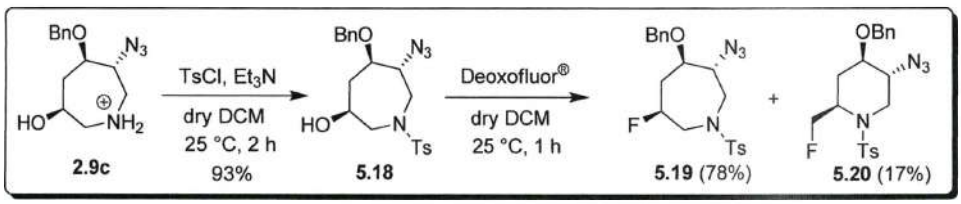
5.2.4. Effect of the *N*–tosyl Protecting Group on the Fluorination Outcomes

The structure elucidation shows that the C5–F is epimerized in both **5.6** and **5.12**; and the reaction requires an aziridinium intermediate for the formation of the piperidines **5.7** and **5.13**. Such ring contractions have also been observed in fluorination reactions with *N*–benzyl protected azepanes.[13] However, this stereospecific C5–F epimerization can not be explained by aziridinium formation alone. The next question became, would the C5–F stereospecific epimerization depend on the reactivity of the aziridinium?

The *N*–tosyl fluorohydroxyazepanes were then synthesized, given previous studies[14] showing the absence of aziridinium formation with the *N*–tosyl protecting group in

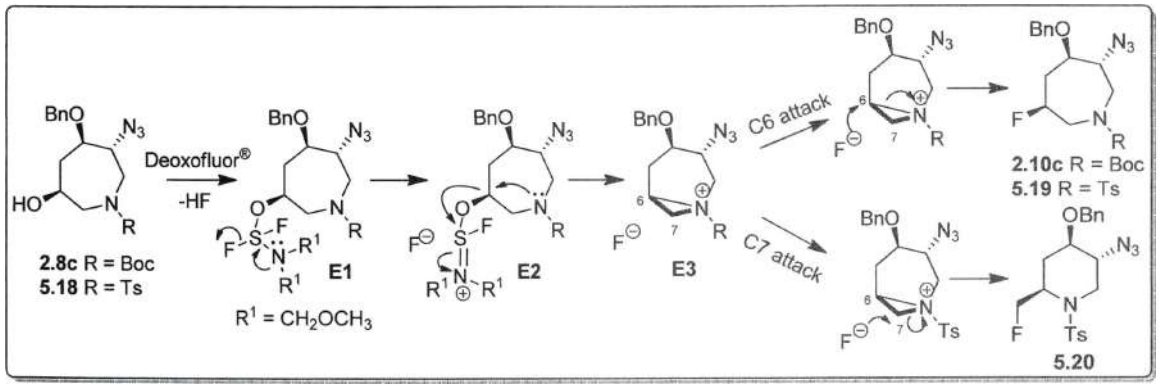
cyclohexyl alcohol chlorination. The question here became if this C5–F epimerization event would be unique to *N*–Boc protected aziridinium intermediate.

The investigation started with the case of a simple monofluorination as a control to confirm if the reaction would follow the S_N2 pathway; assuming the aziridinium intermediate would be absent as was in the case of cyclohexyl alcohol chlorination. Further more, *N*–tosyl protected azepanes are crystaline in general which may help with subsequent structure elucidation.



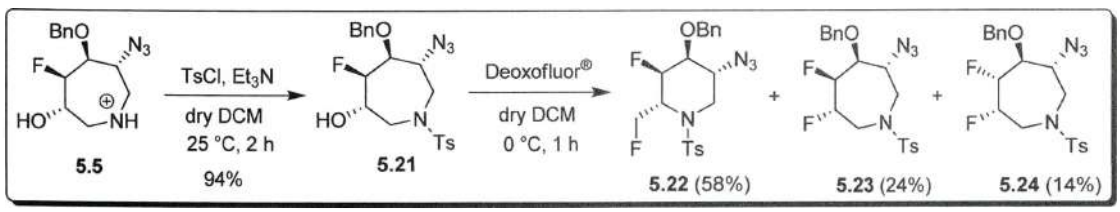
Scheme 5.6. Synthesis of **5.19**: Effect of *N*–tosyl protecting group in monofluorination.

The *N*–tosyl protection of **2.9c** was carried out using standard conditions to afford **5.18** in excellent yield (Scheme 5.6). Then azepane **5.18** was subjected to deoxyfluorination and gave monofluoroazepane **5.19** with, surprisingly, *retention* of stereochemistry and the piperidine product **5.20** in a ratio of 82:18. In hindsight, a more flexible seven-membered ring may allow the formation of the aziridinium. However, it is interesting that in the case of **2.8c** (*N*–Boc) (Chapter 2), monofluoroazepane **2.10c** was produced exclusively without the ring contracted piperidine product. These results suggest that C6 fluoride attack is preferred in the *N*–Boc aziridinium **E3** while in the *N*–tosyl aziridinium **E3**, such preference is reduced (Scheme 5.7).



Scheme 5.7. Mechanism for the monofluorination outcomes in **2.9c** and **5.18**.

The *N*–tosyl protected analogues fluorohydroxyazepane **5.21** was next synthesized from **5.5** in excellent yield (Scheme 5.8). Deoxyfluorination of **5.21** resulted in a mixture of difluoropiperidine **5.22** (58%), difluoroazepane **5.23** (24%, no C5–F epimerization) and difluoroazepane **5.24** (14%, C5–F epimerized).



Scheme 5.8. Synthesis of *N*–tosyl difluoroazepanes **5.23** and **5.24**.

These results further confirmed the C5–F epimerization event, although in the case of **5.5**, the C5–F epimerization was significantly supressed and accompanied by the nonepimerized azepane product **5.23** as the major azepane product normally expected from aziridinium ring opening at C6 with *inversion* of stereochemistry.

5.2.5. Structure Elucidation of *N*–tosyl Fluoroazepanes

5.2.5.1. Structure Elucidation of 5.19

The key 2D NMR correlations of **5.19** are presented in Table 5.5. Assignment of the absolute stereochemistry of **5.19** at C6 as *S* was supported by strong NOE of H6 to H4 and

H5b while no detactable NOE to H5a. H5a showed NOE to H3 while H5b showed NOE to H4. These results suggested *retention* of stereochemistry (*S*) at C6 in **5.19**.

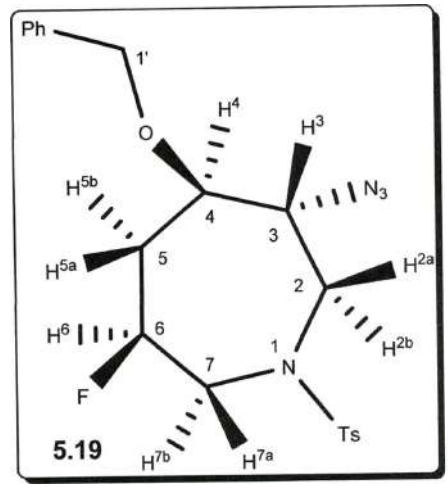


Table 5.5. 2D NMR structure elucidation of the azepane **5.19**.

No	Protons	HSQC	HMBC	COSY	NOESY[a]
1	H2a	C2	C4, C7	H2b, H3	–
2	H2b	C2	C4, C7	H2a, H3	–
3	H3	C3	C5	H2a, H2b, H4	H5a
4	H4	C4	C1', C2, C6	H3, H5a&b	H1', H5b
5	H5a	C5	C3, C7	H4, H5b, H6	H1', H7a
6	H5b	C5	C3, C7	H4, H5a, H6	H1', H7b
7	H6	C6	C4	H5a&b, H7a &b	H4, H5b
8	H7a	C7	C2, C5	H6, H7b	H6
9	H7b	C7	C2, C5	H6, H7a	H6

[a]s = stronge, w = weak

5.2.5.2. Structure Elucidation of 5.23

The key 2D NMR correlations of **5.23** are presented in Table 5.6. H2a and H2b were identified from the NOEs to H3. H2a had strong NOE to H7a while no detectable NOE to H7b. The $^{3}J_{H7aF6}$ coupling (36.8 Hz) clearly suggested the *anti* relationship with the absolute stereochemistry as *S* at C6, which was further supported by stronger H7a–H6 NOE than that of H7b–H6. The $^{3}J_{H5H6}$ coupling (7 Hz) suggested the *anti* relationship which was further

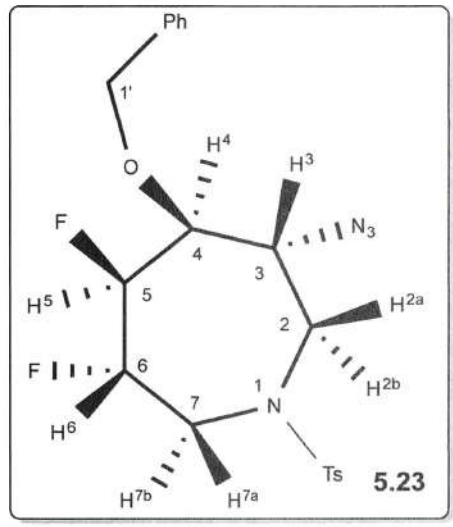


Table 5.6. 2D NMR structure elucidation of the azepane **5.23**.

No	Protons	HSQC	HMBC	COSY	NOESY[a]
1	H2a	C2	C7	H2b, H3	H3 (s)
2	H2b	C2	C4, C7	H2a, H3	H3 (w)
3	H3	C3	–	H2a, H2b, H4	H2a (s), H2b (w)
4	H4	C4	C1', C2, C6	H3, H5	H1', H5
5	H5	C5	–	H4, H6	H5
6	H6	C6	–	H5, H7a, H7b	H7a (s), H7b(w)
7	H7a	C7	C2	H6, H7b	H6 (s)
8	H7b	C7	C2, C5	H6, H7a	H6 (w)

[a]s = stronge, w = weak

supported by (i) $^{3}J_{H5F6}$ and $^{3}J_{H6F5}$ couplings (16.0 Hz) showing the *gauche* relationships; (ii) strong H4–H5 NOE while no measurable H5–H6 NOE; (iii) no measurable H3–H5 and H5–H1' NOEs. Thus, the absolute stereochemistry at C5 was confirmed as *S*.

5.2.5.3. Structure Elucidation of 5.24

The key 2D NMR correlations of **5.24** are presented in Table 5.7. In **5.24**, H4 showed NOE to H2b while no detectable NOE to H2a. H2b further had NOE to H7b while no measurable NOE to H7a. H5 showed NOE to H3, H6, and H7a while H6 showed NOE to H1' and

stronger NOE to H7a compared to H7b. This NOE data suggested the absolute stereochemistry at C5 and C6 is *R* and *S*, respectively.

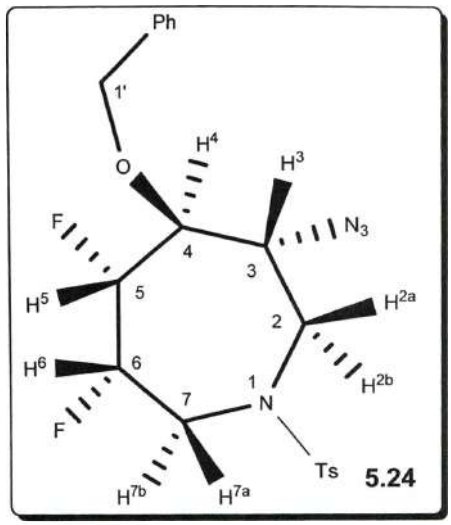


Table 5.7. 2D NMR structure elucidation of azepane **5.24**.

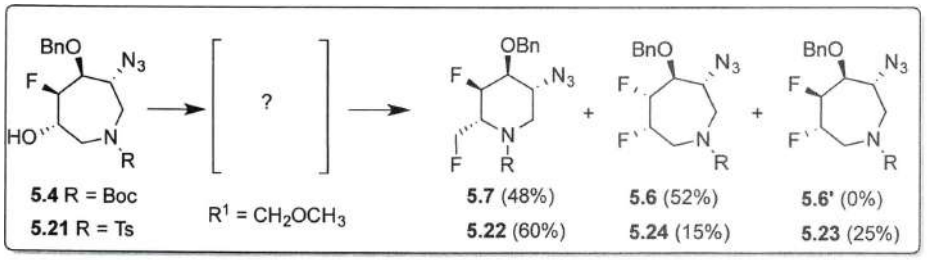
No	Protons	HSQC	HMBC	COSY	NOESY[a]
1	H2a	C2	C4, C7	H2b, H3	H3
2	H2b	C2	C4, C7	H2a, H3	H3, H4, H7b
3	H3	C3	–	H2a, H2b, H4	H2a, H5
4	H4	C4	C1', C2, C6	H3, H5	H1', H2b
5	H5	C5	C3, C7	H4	H1', H3, H6, H7a
6	H6	C6	C4	H7a, H7b	H1', H5, H7a (s), H7b (w)
7	H7a	C7	C2, C5	H6, H7b	H5, H6
8	H7b	C7	C2, C5	H6, H7a	H2b, H6

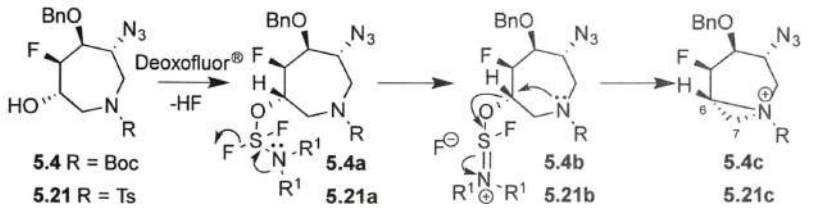
[a]s = stronge, w = weak

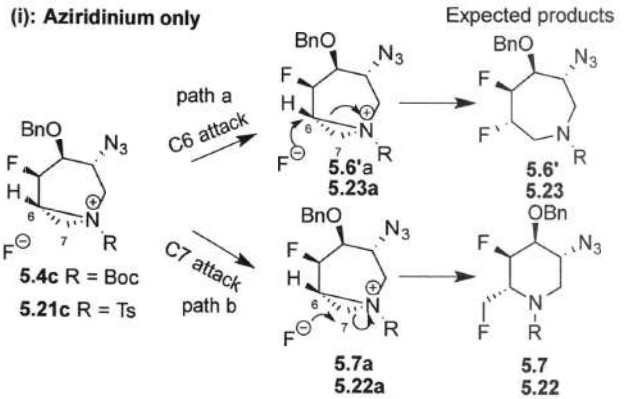
5.2.6. A Proposed Fluoronium–Aziridinium Neighbouring Group Effect

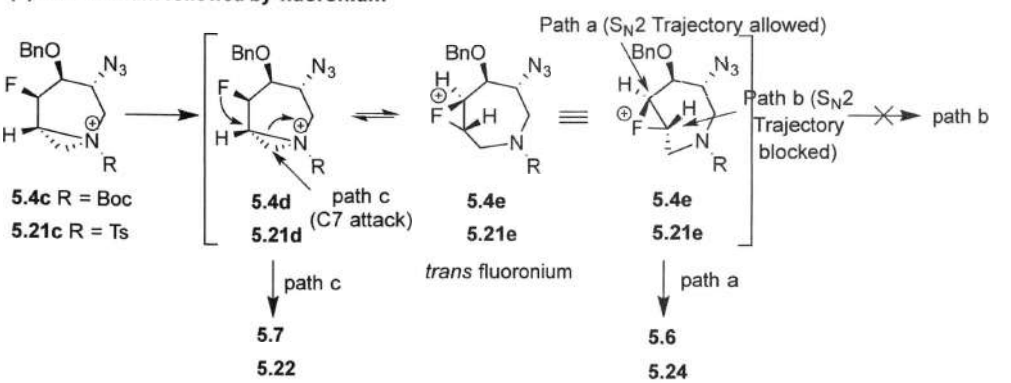
The fluorination of azepanes **5.4**, **5.21** and **4.10** resulted in products with epimerization of the C5–F bond (**5.6**, **5.24** and **5.12**, respectively) along with ring contracted products (**5.7**, **5.22** and **5.13**, respectively) in different proportions (Scheme 5.9 and 5.10). These fluorination outcomes can be explained by exploring several potential pathways: (i) aziridinium only pathway; (ii) aziridinium followed by fluoronium formation; (iii) a hybrid

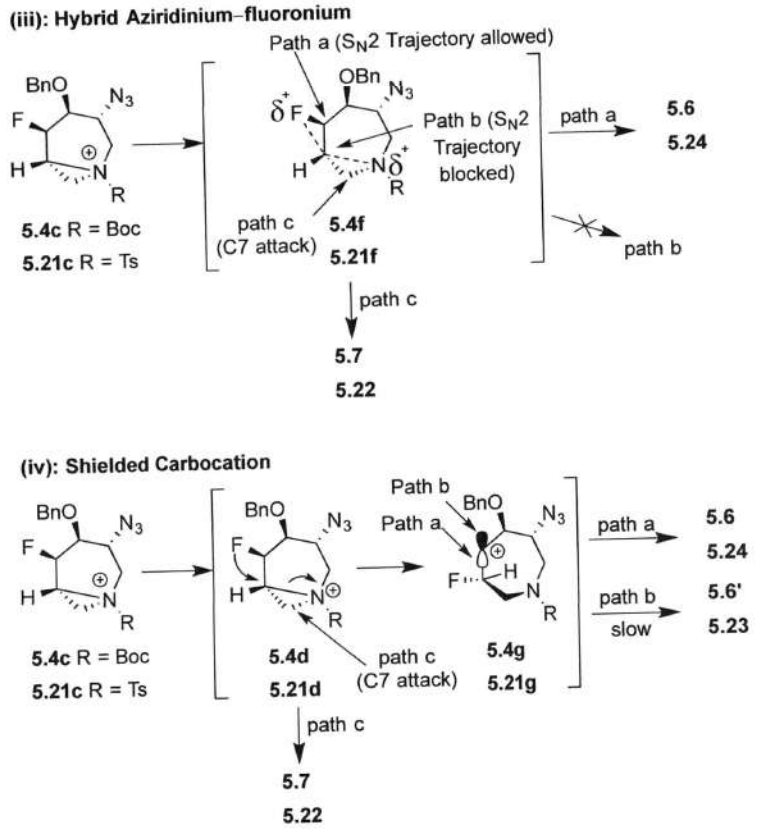
aziridinium–fluoronium formation; and (iv) shielded carbocation formation (Scheme 5.9 and 5.10).











Scheme 5.9. Possible pathways for the fluorination of **5.4** and **5.21**.

Fluorination of azepane 5.4 (with *N*–Boc):

(i) Aziridinium only (Scheme 5.9): In azepane **5.4** the epimerized azepane **5.6** and piperidine **5.7** were obtained in nearly a 1:1 ratio. The formation of piperidine **5.7** suggests the reaction route via an aziridinium intermediate (**5.4c**). However, the formation of azepane **5.6** can not be explained by aziridinium formation alone. In addition, if the reaction conferred only via an aziridinium intermediate azepane **5.6'** should form instead of **5.6**. This suggests an intermediate additional to the aziridinium must be involved.

(ii) and (iii) Fluoronium–aziridinium pathways (Scheme 5.9): The formation of epimerized azepane **5.6** can be explained by these pathways. These two pathways vary in formation sequence and type of fluoronium: in pathway (ii) a symmetrical *trans*

fluoronium (**5.4e**) forms following aziridinium ring opening; while in pathway (iii) an asymmetrical *trans* fluoronium–aziridinium hybrid intermediate (**5.4f**) forms.

Pathway (ii): After the formation of aziridinium intermediate **5.4c** the C5 fluorine can open the aziridine ring by attacking the adjacent carbon C6 (structure **5.4d**) to form the symmetrical *trans* fluoronium intermediate **5.4e**. In **5.4e** the incoming fluoride nucleophile can only open the three-membered fluoronium by attack on C5 (path a, route ii, Scheme 5.9) as the C6 position is sterically blocked by the ring (path b, route ii, Scheme 5.9). The C5 S_N2 displacement outcome would result in the observed C5 epimerized product with *retention* of stereochemistry at C6 (azepane **5.6**). It is possible that the conversion of **5.4c** to **5.4e** can be reversible. Thus, the formation of piperidine **5.7** can be explained by C7 fluoride attack to open the aziridinium without fluoronium formation in **5.4d** (path c, route ii, Scheme 5.9).

Pathway (iii): In aziridinium **5.4c**, the C5 fluorine can attack on C6 to form an asymmetrical *trans* fluoronium–aziridinium hybrid intermediate (**5.4f**, two-electron, 3-center intermediate) which can undergo path a and c similar to those in pathway (ii) (Scheme 5.9) to obtain epimerized azepane **5.6** and piperidine **5.7**.

(iv) Shielded carbocation pathway (Scheme 5.9):

The C5 fluorine in aziridinium intermediate **5.4c** can attack and shift to C6 to form a shielded carbocation at C5 (**5.4g**) which can then be trapped stereospecifically by fluoride to provide the epimerized azepane **5.6** (path a, route iv, Scheme 5.9). The stereospecific attack on the carbocation **5.4g** can be explained by the OBn group blocking the top phase of **5.4g**. The formation piperidine **5.7** may again be explained by C7 fluoride attack on the aziridinium **5.4d** before formation of the carbocation (path c, route iv, Scheme 5.9).

Overall, the experimental results suggest the need for new intermediates in fluorination of **5.4**: aziridinium followed by fluoronium (pathway ii, Scheme 5.9) or hybrid fluoronium–aziridinium (pathway iii, Scheme 5.9) or a carbocation by fluorine shift (pathway iv, Scheme 5.9). Attempts were made to trap the potential carbocation with nucleophiles such as chloride and iodide, however only the starting material was recovered from the reaction mixture.

Fluorination of azepane 5.21 (with *N*–Ts):

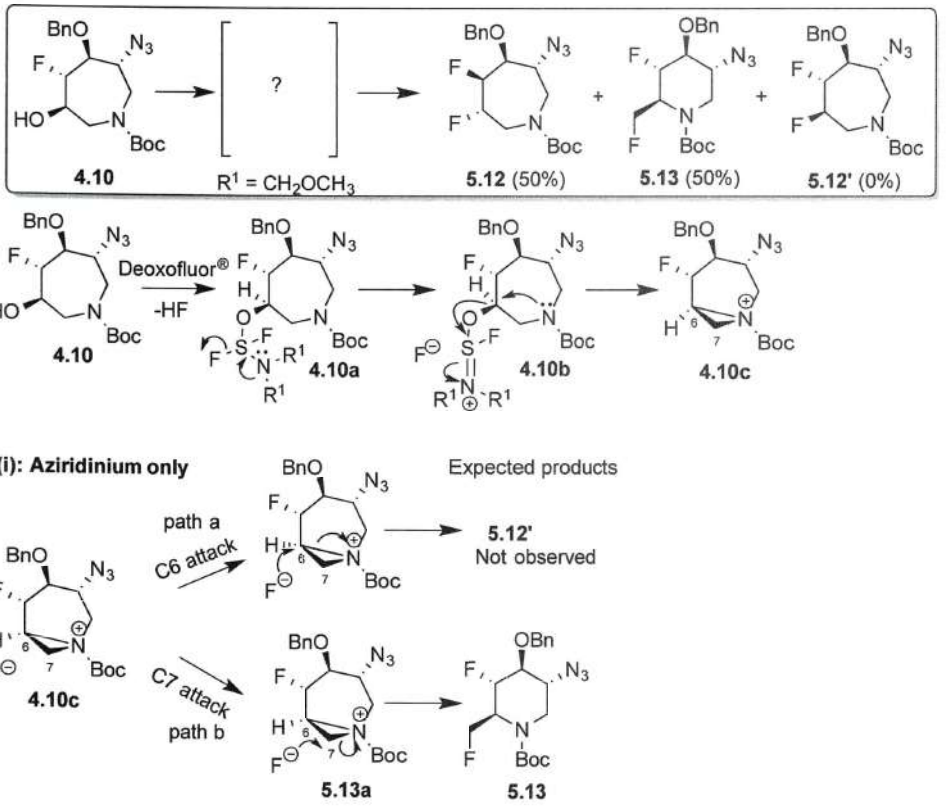
In the case of azepane **5.21**, the formation of piperidine **5.22** and non–epimerized azepane **5.23** as major products clearly suggests the major reaction path via the aziridinium (**5.21c**) (pathway i, Schem 5.9). However, the formation of minor epimerized azepane **5.24** suggests the fluoronium or carbocation pathways (ii–iv, Scheme 5.9) are supressed but still operational, showing that the C5–F epimerization is not unique to the *N*–Boc group. These results suggest that the formation of fluoronium intermediates depends on the stereo–electronics of the aziridinium intermediate directed by the *N*–protecting group.

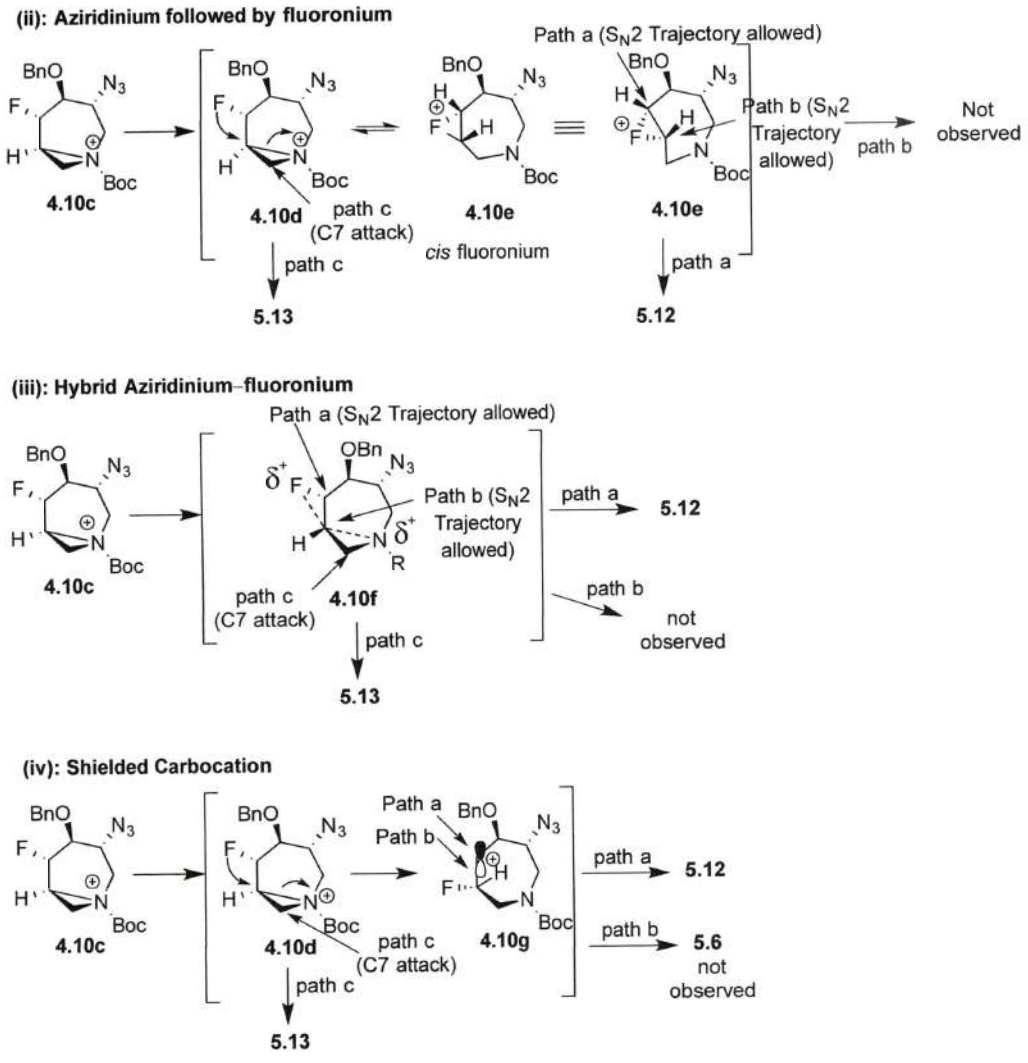
Fluorination of azepane 4.10 (with *N*–Boc):

To further understand the proposed pathways in Scheme 5.9 (i–iv), the fluorination of azepane **4.10** was carried out in a way identical to azepane **5.4**. The results obtained are comparable to that from azepane **5.4**, indicating similar fluorination mechanistic trends except for two main differences: (i) the proposed fluoronium intermediate **4.10e** is a *cis* symmetrical fluoronium; and (ii) the S_N2 fluoride attack is allowed on both C5 and C6 in **4.10e** and **4.10f** (Scheme 5.10). However, the C6 fluride attack product from **4.10e** and **4.10f** are never observed.

Overall, in the fluorination of **4.10**, the aziridinium only pathway (pathway i, Scheme

5.10) again can not explain the formation of the C5–F epimerized azepane **5.12**. The fluorination of **4.10** can be explained by either an aziridinium followed by fluoronium (pathway ii, Scheme 5.10) or a hybrid fluoronium–aziridinium (pathway iii, Scheme 5.10). The reaction may confer via a carbocation as well. However, if the OBn shielding applied in the same fashion, azepane **5.6** should be obtained instead, but it was not observed experimentally. This suggests this carbocation may not be an intermediate, at least in the case of **4.10** fluorination.





Scheme 5.10. Possible pathways for the fluorination of **4.10**.

5.2.7. Preliminary Computational Studies on Potential Fluoronium–Aziridinium Intermediates

These studies were performed by Dr. Fei Liu as a preliminary assessment of the proposed fluoronium–aziridinium intermediates and summarized here only to assist in illustrating the potential fluoronium–aziridinium structures.[1b,2b,15] Further computational investigations are ongoing but beyond the scope of this thesis.

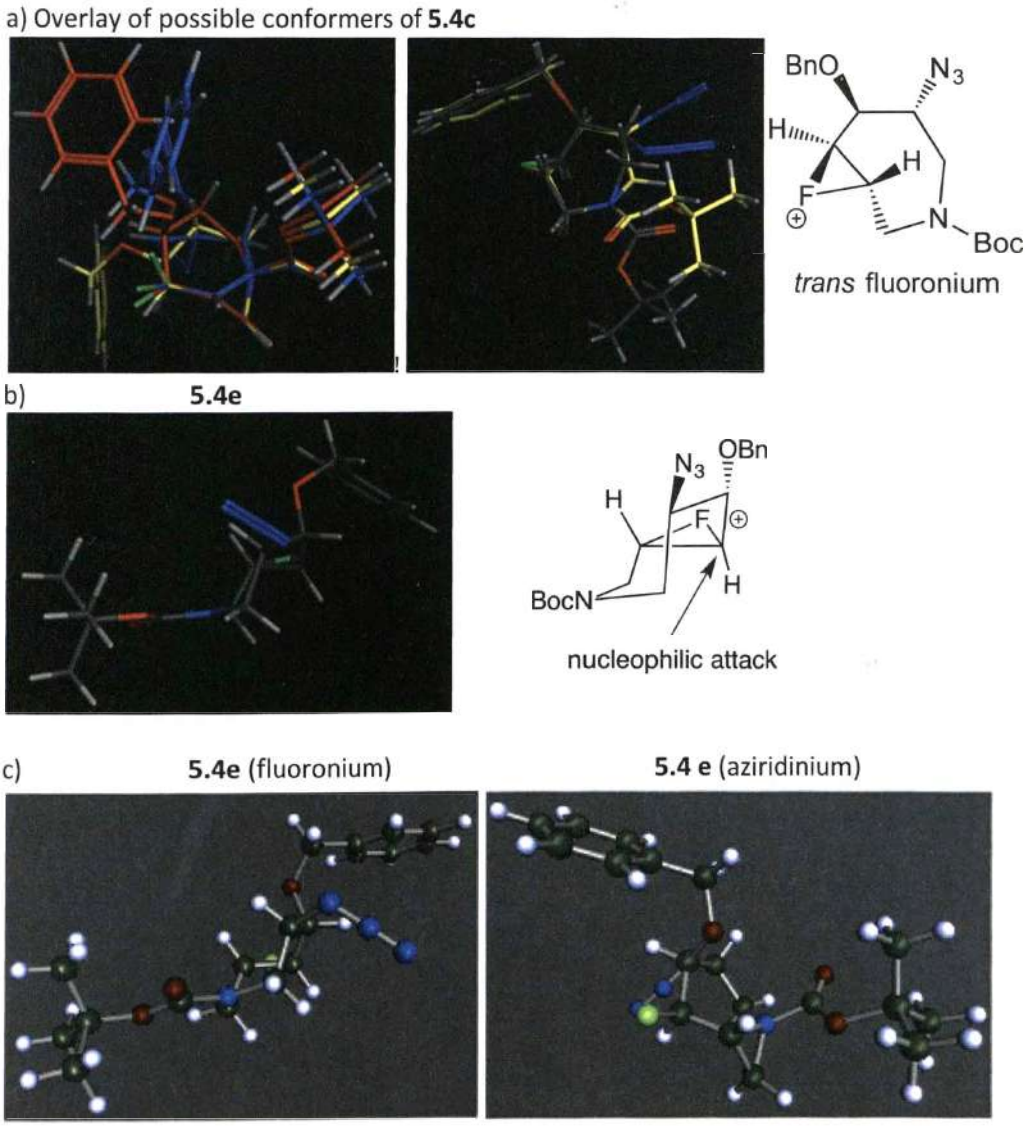


Figure 5.3. Preliminary theoretical studies of **5.4c** and **5.4e**.

Azepane **5.4** was used to model (as implemented in MOE/MMFF94x forcefield) the aziridium and fluoronium intermediates proposed in Scheme 5.9 path i and ii. A conformational search was performed for azridinium **5.4c** to identify eligible ring conformations conducive to potential fluoronium formation, in which the fluorine atom at C5 would be positioned approximately *anti* to the C6-N^+ bond for aziridium ring opening (Figure 5.3, a). Three clusters of conformations were found for **5.4c** (overlay in Figure 5.3, a, left picture), and one conformation was identified (conformation in red) as eligible for fluoronium formation. A starting fluoronium geometry for **5.4e** was then generated from this eligible **5.4c** conformation and minimized in the MMFF94x force field to give fluoronium **5.4e** as a symmetrical, *trans* fluoronium ion (Figure 5.3, a, right picture). The conformational analysis of **5.4e** identified two main clusters of conformation (overlay in Figure 5.3, a). The conformation of **5.4e** amenable for fluoronium ring opening is coloured yellow. In this conformation, the ring conformation is *pseudo*-boat, leaving C5 open for nucleophilic attack with inversion of stereochemistry (Figure 5.3, b).

Computational methods have been reported for geometry optimisation of fluoroniums, and the recent methods by Olah and Lectka are currently being investigated.[1b, 15d] The methods at the HF/ccpVTZ or B3LYP/6-311++G** level were found to be the most efficient as implemented by Turbomol 6.3. A fluoronium geometry calculated by MP2/ccpVTZ appeared comparable to the structure from the molecular mechanics calculations (Figure 5.3, c, left picture), while at the B3LYP/6-311++G** level, the fluoronium reverted back to the aziridnium (Figure 5.3, c, right picture). Further studies are ongoing to optimize these geometries and search for transitions structures.

5.3. Experimental

Synthesis methods, characterization and key structure elucidation spectral data of all new compounds have been discussed in the following experimental section. All the relevant NMR spectra are included in the appendix D (pages 480–642) at the end of the thesis.

5.3.1. General Methods

All reactions were conducted under N_2 atmosphere. Unless otherwise specified, all reagents were purchased from Sigma–Aldrich and used without further purification. CH_2Cl_2 was obtained from a solvent purification system (Innovative Technology SPS400) and stored over MS 4Å beads. Acetone, EtOAc and petroleum ether were distilled before use. Petroleum ether refers to the fraction collected between 60 °C and 80 °C. THF was distilled from Na–benzophenone and stored over MS 4Å beads. Anhydrous dimethylformamide (DMF) was obtained from Sigma–Aldrich and used without further purification. ^{1}H NMR spectra were recorded at 25 °C on either a Bruker DRX600K or DPX400 NMR Spectrometer and are reported in ppm using the specified solvent as the internal standard ($CDCl_3$ at 7.26 ppm). ^{13}C NMR spectra are reported in ppm using the specified solvent as the internal standard ($CDCl_3$ at 77.16 ppm).

5.3.2. Synthetic Procedures and Characterization of Intermediates

(3*R*,4*S*,5*S*,6*S*)–3–azido–4–benzyloxy–5,6–dihydroxyazepane (5.1)

The azepane **4.6** (13.60 mg, 35.9 μmol) was dissolved in trifluoroacetic acid (TFA, 500 μL) at 25 °C. The solution was allowed to stir for 5 min before TFA was evaporated under N_2 flow. The reaction flask was kept under high vacuum (0.005 torr, 25 °C) for 3 h to remove traces of TFA and colorless oily residue obtained was characterized as **5.1** (9.70 mg, 97%).

$[\alpha]^{20}_D$ = +32.3 (*c* 0.8, CH_2Cl_2); IR (film) ν_{max} (cm^{-1}): 3581, 2349, 1690, 1673, 1646, 1551, 1167, 1130; ^1H NMR (600 MHz, $CDCl_3$) δ 7.39–7.28 (m, 5H), 4.65 (d, *J* = 10.10 Hz, 1H), 4.57 (d, *J* = 10.10 Hz, 1H), 4.34–4.28 (m, 1H), 4.07–3.95 (m, 2H), 3.62–3.53 (m, 1H), 3.38–3.13 (m, 3H), 2.83–2.71 (m, 1H); ^{13}C NMR (150 MHz, $CDCl_3$) δ 136.8, 128.9, 128.6, 128.4, 80.6, 74.6, 73.9, 66.1, 59.9, 46.3, 45.1; HRMS (ESI): $[M + H]^+$, *m/z* calcd for $C_{13}H_{19}N_4O_3$ 279.1457, found 279.1451.

(3*R*,4*S*,5*R*,6*S*)–3–azido–4–benzyloxy–6–(tert–butyldimethylsilyl)oxy–5–hydroxyazepane–1–carboxylic acid–tert–butyl ester (5.2)

A solution of *tert*–butyldimethylsilyl chloride (96.5 mg, 0.641 mmol) in DMF (3.25 mL) was added dropwise via a syringe to a well stirred solution of **4.6** (220 mg, 0.583 mmol) and imidazole (43.6 mg, 0.641 mmol) in DMF (3.25 mL) at 25 °C under N_2 atmosphere. The reaction mixture was allowed to stir at same temperature for 10 h. The reaction mixture was quenched by addition of water (5 mL) and was extracted with EtOAc (10 mL×3). The combined organic layer was washed with water (5 mL×2) and brine (5 mL) to remove DMF residues and dried ($MgSO_4$) before evaporation under reduced pressure to obtain the crude product, which was subjected to flash chromatography (petroleum ether/EtOAc, 9/1) to give **5.2** (192.4 mg, 67%, R_f 0.33) as colorless oil. It is noteworthy that **5.2** was obtained exclusively and unreacted **4.6** was recovered. $[\alpha]^{20}_D$ = +15.1 (*c* 1.0, CH_2Cl_2); IR (film) ν_{max} (cm^{-1}): 3600–3130 (br), 2997, 2933, 2365, 2114, 1680, 1411, 1157, 1088, 1045, 990; ^1H NMR (600 MHz, $CDCl_3$) δ 7.39–7.33 (m, 5H), 4.93 (d, *J* = 11.11 Hz, 1H), 4.60 (d, *J* = 11.11 Hz, 1H), 4.28–4.25 (m, 1H), 4.02 (dd, *J* = 14.28, 5.32 Hz, 1H), 3.82–3.70 (m, 2H), 3.62 (br s, 1H), 3.58–3.53 (m, 1H), 3.31 (dd, *J* = 14.17, 10.88 Hz, 1H), 3.01 (ddd, *J* = 13.70, 4.69, 2.86 Hz, 1H), 2.60 (br s, 1H), 1.47 (s, 9H), 0.92 (s, 9H), 0.1 (s, 6H); ^{13}C NMR (150 MHz, $CDCl_3$) δ

154.7, 137.6, 128.9, 128.4, 128.3, 81.7, 80.7, 75.4, 73.4, 71.4, 64.4, 50.5, 46.0, 28.5, 26.0, −4.53, −4.85; HRMS (ESI): $[M + H]^+$, *m/z* calcd for $C_{24}H_{41}N_4O_5Si$ 493.2846, found 493.2844.

(3*R*,4*S*,5*S*,6*S*)–3–azido–4–benzyloxy–6–(tert–butyldimethylsilyl)oxy–5–fluoroazepane–1–carboxylic acid–tert–butyl ester (5.3)

A solution of bis(2–methoxyethyl)aminosulfur trifluoride (Deoxofluor®) (89.8 mg, 0.406 mmol) in dry DCM (5.5 mL) was added dropwise via a syringe to a well stirred solution of **5.2** (200.0 mg, 0.406 mmol) in dry DCM (5.5 mL) under N_2 atmosphere at 0 °C. The reaction mixture was allowed to stir at same temperature for 8 h. The reaction mixture was quenched by ice–cooled water before the crude was extracted with EtOAc and washed with water and brine. The organic phase was evaporated under reduced pressure after drying over $MgSO_4$ to obtain the crude product, which was subjected to flash chromatography (petroleum ether/EtOAc, 9/1) to give **5.3** (130.5 mg, 65%, R_f 0.52) as colorless oil. $[\alpha]^{20}_D$ = +55.1 (*c* 0.9, CH_2Cl_2); IR (film) ν_{max} (cm^{-1}): 2997, 2933, 2365, 2114, 1680, 1521, 1473, 1456, 1411, 1157, 1088, 1045, 990; ^1H NMR (600 MHz, $CDCl_3$) δ 7.44–7.28 (m, 5H), 4.80 (d, *J* = 10.29 Hz, 1H), 4.71 (d, *J* = 10.29 Hz, 1H), 4.55 (dd, *J* = 46.56 ($^1J_{HF}$), 8.47 Hz, 1H), 4.43–4.36 (m, 1H), 4.11 (dd, *J* = 14.01, 4.75 Hz, 1H), 4.01–3.90 (m, 1H), 3.75 (dd, *J* = 14.30, 2.45 Hz, 1H), 3.53–3.47 (m, 1H), 3.25 (dd, *J* = 14.30, 11.33 Hz, 1H), 3.02 (dd, *J* = 14.01, 12.36 Hz, 1H), 1.45 (s, 9H), 0.93 (s, 1H), 0.13 (d, *J* = 23.66 Hz, 6H); ^{13}C NMR (150 MHz, $CDCl_3$) δ 154.6, 137.8, 128.7, 128.6, 128.2, 95.6 (d, $^1J_{CF}$ = 177.79 Hz), 81.1, 80.8 (d, $^2J_{CF}$ = 19.18 Hz), 75.8, 71.6 (d, $^2J_{CF}$ = 28.23 Hz), 63.5 (d, $^3J_{CF}$ = 10.16 Hz), 49.4 (d, $^3J_{CF}$ = 12.65 Hz), 45.3, 28.5, 25.9, −4.61, −4.83; HRMS (ESI): $[M + H]^+$, *m/z* calcd for $C_{24}H_{40}FN_4OSi$ 495.2803, found 495.2798.

(3*R*,4*S*,5*R*,6*S*)–3–azido–4–benzyloxy–5–fluoro–6–hydroxyazepane–1–carboxylic acid–tert–butyl ester (5.4)

Solution of tetrabutylammonium fluoride (TBAF, 1 M solution in THF, 80 μL, 80.1 μmol) was added dropwise via a syringe to a well stirred solution of **5.3** (36.0 mg, 72.8 μmol) in dry THF (1 mL) under N_2 atmosphere at 25 °C. The reaction mixture was allowed to stir at same temperature until completion (45 min, TLC). The reaction mixture was evaporated to dryness and crude obtained was subjected to flash chromatography (petroleum ether/EtOAc, 4/1) to give **5.4** (21.3 mg, 77%, R_f 0.24) as colorless oil. $[\alpha]^{20}_D$ = +36.7 (*c* 0.9, CH_2Cl_2); IR (film) ν_{max} (cm^{-1}): 3600–3130 (br), 2990, 2963, 2365, 2134, 1684, 1526, 1479, 1466, 1419, 1167, 1081, 1042; ^{1}H NMR (600 MHz, $CDCl_3$) δ 7.39–7.30 (m, 5H), 4.78 (d, *J* = 11.80 Hz, 1H), 4.74 (br d, $^1J_{HF}$ = 45.70 Hz, 1H), 4.62 (d, *J* = 11.80 Hz, 1H), 4.16–4.08 (m, 1H), 4.01 (br d, *J* = 15.22 Hz, 1H), 3.98 (br d, *J* = 17.69 Hz, 1H), 3.95 (dd, *J* = 14.59, 4.09 Hz, 1H), 3.78 (br s, 1H), 3.39 (dd, *J* = 15.31, 4.32 Hz, 1H), 3.24 (dd, *J* = 15.22, 3.72 Hz, 1H), 1.48 (s, 9H); ^{13}C NMR (150 MHz, $CDCl_3$) δ 157.8, 137.3, 128.7, 128.3, 128.1, 96.5 (d, $^1J_{CF}$ = 176.11 Hz), 81.8, 79.5 (d, $^2J_{CF}$ = 22.61 Hz), 73.9, 72.6 (d, $^2J_{CF}$ = 24.36 Hz), 61.4 (d, $^3J_{CF}$ = 12.05 Hz), 52.1 (d, $^3J_{CF}$ = 9.44 Hz), 48.8, 28.3; HRMS (ESI): $[M + H]^+$, *m/z* calcd for $C_{18}H_{26}FN_4O_4$ 381.1938, found 381.1938.

(3*R*,4*S*,5*R*,6*S*)–3–azido–4–benzyloxy–5–fluoro–6–hydroxyazepane (5.5)

The procedure for the synthesis of **5.1** was followed. colorless oil, yield 96% from **5.4**; $[\alpha]^{20}_D$ = +43.2 (*c* 0.7, CH_2Cl_2); IR (film) ν_{max} (cm^{-1}): 3610–3160 (br), 2999, 2939, 2369, 2134, 1482, 1442, 1410, 1143, 1089, 1012; ^{1}H NMR (600 MHz, $CDCl_3$) δ 7.40–7.30 (m, 5H), 5.02 (dd, $^1J_{HF}$ = 46.02, 5.69 Hz, 1H), 4.75 (d, *J* = 11.86 Hz, 1H), 4.65 (d, *J* = 11.86 Hz, 1H), 4.33–4.26 (m, 1H), 4.16 (dd, *J* = 24.30, 6.78 Hz, 1H), 3.99–3.95 (m, 1H), 3.52 (d, *J* = 14.60 Hz, 1H), 3.40 (d, *J* = 14.09 Hz, 1H), 3.42–3.22 (m, 2H); ^{13}C NMR (150 MHz, $CDCl_3$) δ 136.5, 128.9, 128.6, 128.3, 93.0 (d, $^1J_{CF}$ = 178.86 Hz), 78.0 (d, $^2J_{CF}$ = 19.98 Hz), 74.0, 66.6 (d, $^2J_{CF}$ = 26.97

Hz), 57.6 (d, $^{3}J_{CF}$ = 9.21 Hz), 50.1 (d, $^{3}J_{CF}$ = 5.58 Hz), 48.2; HRMS (ESI): $[M + H]^{+}$, *m/z* calcd for $C_{13}H_{18}FN_4O_2$ 281.1408, found 281.1410.

(3*R*,4*S*,5*R*,6*S*)–3–azido–4–benzyloxy–5,6–difluoroazepane–1–carboxylic acid–tert–butyl ester (5.6)

The procedure for the synthesis of **5.3** was followed. colorless oil, yield 43% from **5.4**, R_f 0.48 (petroleum ether/EtOAc, 9/1); $[\alpha]^{20}_{D}$ = +8.7 (*c* 0.9, CH_2Cl_2); IR (film) ν_{max} (cm^{-1}): 2363, 2347, 2109, 1716, 1533, 1520, 1478, 1450, 1419, 1109; ^{1}H NMR (600 MHz, $CDCl_3$) δ 7.43–7.30 (m, 5H), 5.22–5.08 (m, 1H), 4.83 (d, *J* = 10.77 Hz, 1H), 4.74 (d, *J* = 10.77 Hz, 1H), 4.71–4.60 (m, 1H), 4.34 (ddd, *J* = 34.84 ($^{2}J_{HF}$), 15.91, 5.44 Hz, 1H), 3.91 (ddd, *J* = 9.01, 8.40, 8.32 Hz, 1H), 3.84 (br d, *J* = 14.56 Hz, 1H), 3.59–3.54 (m, 1H), 3.35–3.26 (m, 1H), 2.97 (dd, *J* = 14.10, 11.70 Hz, 1H), 1.47 (s, 9H); ^{13}C NMR (150 MHz, $CDCl_3$) δ 154.3, 137.4, 128.7, 128.7, 128.4, 93.4 (dd, $^{1}J_{CF}$ = 179.77, $^{2}J_{CF}$ = 21.74 Hz), 91.6 (dd, $^{1}J_{CF}$ = 177.26, $^{2}J_{CF}$ = 24.25 Hz), 81.6, 80.0 (dd, $^{2}J_{CF}$ = 18.92, $^{3}J_{CF}$ = 6.72 Hz), 75.9, 63.4 (d, $^{3}J_{CF}$ = 9.18 Hz), 46.6 (dd, $^{2}J_{CF}$ = 23.87, $^{3}J_{CF}$ = 11.02 Hz), 45.7, 28.4; HRMS (ESI): $[M + H]^{+}$, *m/z* calcd for $C_{18}H_{24}F_2N_4NaO_3$ 405.1714, found 405.1712.

(2*R*,3*R*,4*S*,5*R*)–5–azido–4–benzyloxy–3–fluoro–2–(fluoromethyl)piperidine–1–carboxylic acid–tert–butyl ester (5.7)

The procedure for the synthesis of **5.3** was followed. colorless oil, yield 39% from **5.4**, R_f 0.47 (petroleum ether/EtOAc, 9/1); $[\alpha]^{20}_{D}$ = −12.2 (*c* 0.9, CH_2Cl_2); IR (film) ν_{max} (cm^{-1}): 2361, 2341, 2109, 1716, 1541, 1521, 1473, 1456, 1418, 1100; ^{1}H NMR (600 MHz, $CDCl_3$) δ 7.43–7.31 (m, 5H), 5.01–3.28 (m, 9H), 2.86–2.62 (m, 1H), 1.46 (s, 9H); ^{13}C NMR (150 MHz, $CDCl_3$) δ 154.6, 137.2, 128.8, 128.4, 128.3, 86.8 (d, $^{1}J_{CF}$ = 182.15 Hz), 83.6 (d, $^{1}J_{CF}$ = 166.18

Hz), 81.6, 78.9 (br s), 72.6, 57.0, 47.5 (br s), 43.5, 28.4; HRMS (ESI): $[M + H]^+$, *m/z* calcd for $C_{18}H_{24}F_2N_4NaO_3$ 405.1714, found 405.1708.

(3*R*,4*S*,5*R*,6*S*)–3–azido–4–benzyloxy–5,6–difluoroazepane (5.8)

The procedure for the synthesis of **5.1** was followed. colorless oil, yield 95% from **5.6**; $[\alpha]^{20}_D$ = +25.5 (*c* 1.3, CH_2Cl_2); IR (film) ν_{max} (cm^{-1}): 2392, 2331, 2110, 1700, 1681, 1678, 1550, 1544, 1511, 1486, 1190; ^1H NMR (600 MHz, $CDCl_3$) δ 7.42–7.35 (m, 5H), 5.19 (ddddd, *J* = 44.09 ($^1J_{HF}$), 24.72 ($^2J_{HF}$), 6.18, 4.94, 2.06 Hz, 1H), 5.02 (dddd, *J* = 45.74 ($^1J_{HF}$), 23.49 ($^2J_{HF}$), 4.53, 1.55 Hz, 1H), 4.81 (d, *J* = 11.40 Hz, 1H), 4.74 (d, *J* = 11.40 Hz, 1H), 3.99–3.93 (m, 2H), 3.62–3.50 (m, 2H), 3.39 (br d, *J* = 14.12 Hz, 1H), 3.22 (dd, *J* = 14.12, 8.97 Hz, 1H); ^{13}C NMR (150 MHz, $CDCl_3$) δ 136.1, 128.9, 128.9, 128.6, 92.2 (dd, $^1J_{CF}$ = 184.58, $^2J_{CF}$ = 21.72 Hz), 86.6 (dd, $^1J_{CF}$ = 179.15, $^2J_{CF}$ = 21.72 Hz), 78.0 (dd, $^2J_{CF}$ = 23.60, $^3J_{CF}$ = 8.17 Hz), 74.6, 59.8, 44.9 (dd, $^2J_{CF}$ = 31.80, $^3J_{CF}$ = 8.93 Hz), 43.8; HRMS (ESI): $[M + H]^+$, *m/z* calcd for $C_{13}H_{17}F_2N_4O$ 283.1370, found 283.1371.

(2*R*,3*R*,4*S*,5*R*)–5–azido–4–benzyloxy–3–fluoro–2–(fluoromethyl)piperidine (5.9)

The procedure for the synthesis of **5.1** was followed. colorless oil, yield 96% from **5.7**; $[\alpha]^{20}_D$ = −33.7 (*c* 0.5, CH_2Cl_2); 2366, 2337, 2116, 1690, 1681, 1671, 1559, 1522, 1520, 1460, 1180; ^1H NMR (600 MHz, $CDCl_3$) δ 7.43–7.30 (m, 5H), 4.92 (dd, *J* = 45.30 ($^1J_{HF}$), 10.40 Hz, 1H), 4.87–4.74 (m, 3H), 4.65 (d, *J* = 11.07 Hz, 1H), 4.13–4.07 (m, 1H), 3.94–3.90 (m, 1H), 3.83–3.73 (m, 1H), 3.45 (br d, *J* = 14.10 Hz, 1H), 3.24 (br d, *J* = 14.10 Hz, 1H); ^{13}C NMR (150 MHz, $CDCl_3$) δ 136.8, 128.9, 128.7, 128.1, 84.4 (d, $^1J_{CF}$ = 184.22 Hz), 79.6 (d, $^1J_{CF}$ = 172.33 Hz), 74.5, 72.9 (d, $^2J_{CF}$ = 17.09 Hz), 58.2 (d, $^3J_{CF}$ = 6.29 Hz), 53.2 (dd, $^2J_{CF}$ = 26.07, $^3J_{CF}$ = 19.78 Hz), 42.4; HRMS (ESI): $[M + H]^+$, *m/z* calcd for $C_{13}H_{17}F_2N_4O$ 283.1370, found 283.1368.

(3*R*,4*S*,5*R*,6*R*)–3–azido–4–benzyloxy–5,6–dihydroxyazepane (5.10)

The procedure for the synthesis of **5.1** was followed. colorless oil, yield 96% from **4.7**; $[\alpha]^{20}_{D}$ = −18.2 (*c* 0.8, CH_2Cl_2); IR (film) ν_{max} (cm^{-1}): 3581, 2349, 1690, 1673, 1646, 1551, 1167, 1130; ^1H NMR (600 MHz, $CDCl_3$) δ 7.42–7.29 (m, 5H), 4.65 (d, 2H), 4.29–4.23 (m, 1H), 4.06–4.00 (m, 1H), 3.87–3.80 (m, 1H), 3.74–3.69 (m, 1H), 3.48–3.40 (m, 1H), 3.28–3.15 (m, 3H); ^{13}C NMR (150 MHz, $CDCl_3$) δ 136.6, 128.9, 128.7, 128.7, 81.8, 73.1, 72.5, 66.3, 58.9, 47.6, 46.6; HRMS (ESI): $[M + H]^+$, *m/z* calcd for $C_{13}H_{19}N_4O_3$ 279.1457, found 279.1459.

(3*R*,4*S*,5*S*,6*R*)–3–azido–4–benzyloxy–5–fluoro–6–hydroxyazepane (5.11)

The procedure for the synthesis of **5.1** was followed. colorless oil, yield 97% from **4.10**; $[\alpha]^{20}_{D}$ = −22.1 (*c* 0.7, CH_2Cl_2); IR (film) ν_{max} (cm^{-1}): 3610–3160 (br), 2999, 2939, 2369, 2134, 1482, 1442, 1410, 1143, 1089, 1012; ^1H NMR (600 MHz, $CDCl_3$) δ 7.41–7.34 (m, 5H), 4.85 (dd, $^1J_{HF}$ = 44.09, 6.07 Hz, 1H), 4.77 (d, J = 11.33 Hz, 1H), 4.67 (d, J = 11.33 Hz, 1H), 4.42–4.37 (m, 1H), 4.24 (dd, J = 9.01, 8.37 Hz, 1H), 3.78 (dd, J = 21.34, 8.48 Hz, 1H), 3.40 (dd, J = 14.06, 6.03 Hz, 1H), 3.36 (d, J = 14.08 Hz, 1H), 3.14 (d, J = 13.58 Hz, 1H), 2.85 (dd, J = 13.96, 9.50 Hz, 1H); ^{13}C NMR (150 MHz, $CDCl_3$) δ 136.2, 128.9, 128.9, 128.7, 92.1 (d, $^1J_{CF}$ = 173.7 Hz), 82.7 (d, $^2J_{CF}$ = 21.7 Hz), 73.8, 66.4 (d, $^2J_{CF}$ = 28.33 Hz), 59.5, 46.3, 46.0; HRMS (ESI): $[M + H]^+$, *m/z* calcd for $C_{13}H_{18}FN_4O_2$ 281.1408, found 281.1411.

(3*R*,4*S*,5*S*,6*S*)–3–azido–4–benzyloxy–5,6–difluoroazepane–1–carboxylic acid–tert–butyl ester (5.12)

The procedure for the synthesis of **5.3** was followed. colorless oil, yield 42% from **4.10**, R_f 0.48 (petroleum ether/EtOAc, 9/1); $[\alpha]^{20}_{D}$ = +38.1 (*c* 1.4, CH_2Cl_2); IR (film) ν_{max} (cm^{-1}): 2363, 2347, 2109, 1716, 1533, 1520, 1478, 1450, 1419, 1109; ^1H NMR (600 MHz, $CDCl_3$) δ 7.40–7.31 (m, 5H), 4.91–4.62 (m, 4H), 3.95–3.43 (m, 6H), 1.49 (s, 9H); ^{13}C NMR (150 MHz,

$CDCl_3$) δ 154.9, 136.9, 128.8, 128.5, 128.3, 95.1 (dd, $^1J_{CF}$ = 180.94, $^2J_{CF}$ = 23.38 Hz), 91.4 (dd, $^1J_{CF}$ = 180.76, $^2J_{CF}$ = 24.48 Hz), 81.4, 79.1 (dd, $^2J_{CF}$ = 20.43, $^3J_{CF}$ = 7.49 Hz), 74.1, 61.6, 46.8 (dd, $^2J_{CF}$ = 28.69, $^3J_{CF}$ = 8.83 Hz), 46.0, 28.4; HRMS (ESI): $[M + H]^+$, *m/z* calcd for $C_{18}H_{24}F_2N_4NaO_3$ 405.1714, found 405.1706.

(2*S*,3*S*,4*S*,5*R*)–5–azido–4–benzyloxy–3–fluoro–2–(fluoromethyl)piperidine–1–carboxylic acid–tert–butyl ester (5.13)

The procedure for the synthesis of **5.3** was followed. colorless oil, yield 42% from **4.10**, R_f 0.49 (petroleum ether/EtOAc, 9/1); $[\alpha]^{20}_D$ = +31.7 (*c* 1.1, CH_2Cl_2); IR (film) ν_{max} (cm^{-1}): 2361, 2341, 2109, 1716, 1541, 1521, 1473, 1456, 1418, 1100; ^1H NMR (600 MHz, $CDCl_3$) δ 7.43–7.31 (m, 5H), 4.76 (ddd, *J* = 46.63 ($^1J_{HF}$), 4.29, 4.03 Hz, 1H), 4.71 (d, *J* = 11.96 Hz, 1H), 4.66 (d, *J* = 11.96 Hz, 1H), 4.64–4.50 (m, 3H), 4.01 (dd, *J* = 14.87, 3.25 Hz, 1H), 3.75 (ddd, *J* = 10.22, 5.02, 4.52 Hz, 1H), 3.61 (ddd, *J* = 3.82, 3.64, 3.46 Hz, 1H), 3.37 (dd, *J* = 14.78, 3.45 Hz, 1H), 1.48 (s, 9H); ^{13}C NMR (150 MHz, $CDCl_3$) δ 154.8, 136.9, 128.8, 128.5, 128.1, 86.0 (d, $^1J_{CF}$ = 180.00 Hz), 81.5, 79.9 (dd, $^1J_{CF}$ = 173.39, $^2J_{CF}$ = 9.17 Hz), 76.0 (d, $^2J_{CF}$ = 24.92 Hz), 73.6, 57.9, 54.7 (d, $^2J_{CF}$ = 23.65 Hz), 40.3, 28.3; HRMS (ESI): $[M + H]^+$, *m/z* calcd for $C_{18}H_{24}F_2N_4NaO_3$ 405.1714, found 405.1710.

(3*R*,4*S*,5*S*,6*S*)–3–azido–4–benzyloxy–5,6–difluoroazepane (5.14)

The procedure for the synthesis of **5.1** was followed. colorless oil, yield 97% from **5.12**; $[\alpha]^{20}_D$ = +22.5 (*c* 0.9, CH_2Cl_2); IR (film) ν_{max} (cm^{-1}): 2392, 2331, 2110, 1700, 1681, 1678, 1550, 1544, 1511, 1486, 1190; ^1H NMR (600 MHz, $CDCl_3$) δ 7.42–7.33 (m, 5H), 5.20–5.05 (m, 1H), 4.95–4.79 (m, 1H), 4.81 (d, *J* = 11.65 Hz, 1H), 4.66 (d, *J* = 11.65 Hz, 1H), 3.96–3.89 (m, 2H), 3.39–3.26 (m, 3H), 3.05 (dd, *J* = 14.37, 6.02 Hz, 1H); ^{13}C NMR (150 MHz, $CDCl_3$) δ 136.3, 129.0, 128.8, 128.4, 94.1 (dd, $^1J_{CF}$ = 183.48, $^2J_{CF}$ = 23.04 Hz), 90.2 (dd, $^1J_{CF}$ = 178.52,

$^2J_{CF}$ = 27.27 Hz), 77.9 (dd, $^2J_{CF}$ = 25.22, $^3J_{CF}$ = 8.29 Hz), 73.9, 60.2, 46.3, 46.0 (dd, $^2J_{CF}$ = 28.92, $^3J_{CF}$ = 7.45 Hz); HRMS (ESI): $[M + H]^+$, *m/z* calcd for $C_{13}H_{17}F_2N_4O$ 283.1370, found 283.1364.

(2*S*,3*S*,4*S*,5*R*)–5–azido–4–benzyloxy–3–fluoro–2–(fluoromethyl)piperidine (5.15)

The procedure for the synthesis of **5.1** was followed. colorless oil, yield 96% from **5.13**; $[\alpha]^{20}_D$ = +39.2 (*c* 1.2, CH_2Cl_2); IR (film) ν_{max} (cm^{-1}): 2366, 2337, 2116, 1690, 1681, 1671, 1559, 1522, 1520, 1460, 1180; ^1H NMR (600 MHz, $CDCl_3$) δ 7.43–7.31 (m, 5H), 4.91 (d, *J* = 10.64 Hz, 1H), 4.80 (d, *J* = 10.64 Hz, 1H), 4.77–4.64 (m, 2H), 4.57 (ddd, *J* = 49.31 ($^1J_{HF}$), 9.25, 9.19 Hz, 1H), 3.69–3.62 (m, 1H), 3.62–3.54 (m, 1H), 3.35–3.29 (m, 1H), 3.13–3.03 (m, 1H), 2.57 (dd, *J* = 12.74, 11.99 Hz, 1H); ^{13}C NMR (150 MHz, $CDCl_3$) δ 137.2, 128.7, 128.5, 128.3, 90.1 (d, $^1J_{CF}$ = 181.21 Hz), 82.5 (d, $^2J_{CF}$ = 16.58 Hz), 80.8 (d, $^1J_{CF}$ = 170.82 Hz), 75.2, 60.3 (d, $^3J_{CF}$ = 7.41 Hz), 57.9 (d, $^2J_{CF}$ = 19.05 Hz), 46.7; HRMS (ESI): $[M + H]^+$, *m/z* calcd for $C_{13}H_{17}F_2N_4O$ 283.1370, found 283.1369.

(3*R*,4*S*,5*S*,6*S*)–3–azido–4–benzyloxy–5–fluoro–6–hydroxyazepane–1–carboxylic acid–tert–butyl ester (5.16)

To a solution of azepane **4.11** (14.6 mg, 38.7 μmol) in EtOH (0.12 mL) was added sodium borohydride (1.5 mg, 38.7 μmol) and the solution was allowed to stir at room temperature for 1.5 h before addition of EtOAc (5 mL) and brine (2 mL). The organic layer was separated and aqueous layer was extracted with EtOAc (5 mL × 2). The combined organic layer was rotary evaporated to obtain the crude mixture, which was subjected to flash column chromatography using 25% EtOAc/petroleum ether to get **5.16** (10.4 mg, 71%, R_f 0.24) and **4.10** (1.2 mg, 8%, R_f 0.25) as colorless oils. **5.16**: $[\alpha]^{20}_D$ = +15.5 (*c* 1.1, CH_2Cl_2); IR (film) ν_{max} (cm^{-1}): 3600–3130 (br), 2990, 2963, 2365, 2134, 1684, 1526, 1479, 1466, 1419, 1167, 1081, 1042; ^1H NMR

(400 MHz, $CDCl_3$) δ 7.44–7.30 (m, 5H), 4.82–4.67 (m, 3H), 4.44–4.26 (m, 1H), 4.04–3.91 (m, 2H), 3.76 (br d, J = 13.85 Hz, 1H), 3.62–3.53 (m, 1H), 3.24–3.13 (m, 2H), 2.29 (d, J = 4.98 Hz, 1H), 1.46 (s, 9H); ^{13}C NMR (100 MHz, $CDCl_3$) δ 154.8, 137.5, 128.7, 128.6, 128.3, 95.6 (d, $^1J_{CF}$ = 176.57 Hz), 81.2, 80.3 (d, $^2J_{CF}$ = 21.01 Hz), 75.3, 70.2 (d, $^2J_{CF}$ = 22.97 Hz), 63.6 (d, $^3J_{CF}$ = 7.24 Hz), 48.5 (d, $^3J_{CF}$ = 10.28 Hz), 46.4, 28.5; HRMS (ESI): $[M + H]^+$, *m/z* calcd for $C_{18}H_{26}FN_4O_4$ 381.1938, found 381.1941.

(3*R*,4*S*,5*S*,6*S*)–3–azido–4–benzyloxy–5–fluoro–6–hydroxyazepane (5.17)

The procedure for the synthesis of **5.1** was followed. colorless oil, yield 96% from **5.16**; $[\alpha]^{20}_D$ = +24.5 (*c* 0.8, CH_2Cl_2); IR (film) ν_{max} (cm^{-1}): 3610–3160 (br), 2999, 2939, 2369, 2134, 1482, 1442, 1410, 1143, 1089, 1012; ^{1}H NMR (600 MHz, $CDCl_3$) δ 7.42–7.35 (m, 5H), 4.81 (ddd, $^1J_{HF}$ = 44.79, 5.78, 177 Hz, 1H), 4.79 (d, J = 11.33 Hz, 1H), 4.72 (d, J = 11.33 Hz, 1H), 4.52 (dd, J = 19.41, 7.08 Hz, 1H), 4.02 (dt, J = 12.77, 5.73 Hz, 1H), 3.97 (ddd, J = 6.75, 5.73, 2.35 Hz, 1H), 3.61 (ddd, J = 14.00, 7.54, 2.06 Hz, 1H), 3.43–3.39 (m, 2H), 3.34 (d, J = 13.49 Hz, 1H); ^{13}C NMR (150 MHz, $CDCl_3$) δ 136.5, 128.9, 128.6, 128.3, 93.0 (d, $^1J_{CF}$ = 178.86 Hz), 78.0 (d, $^2J_{CF}$ = 19.98 Hz), 74.0, 66.6 (d, $^2J_{CF}$ = 26.97 Hz), 57.6 (d, $^3J_{CF}$ = 9.21 Hz), 50.1 (d, $^3J_{CF}$ = 5.58 Hz), 48.2; HRMS (ESI): $[M + H]^+$, *m/z* calcd for $C_{13}H_{18}FN_4O_2$ 281.1408, found 281.1410.

(3*S*,5*R*,6*R*)–6–azido–5–benzyloxy–1–tosylazepan–3–ol (5.18)

To a solution of azepane **2.9c** (10.0 mg, 38.1 μmol) and Et_3N (5.3 μL, 38.1 μmol) in dry DCM (0.38 mL) was added tosyl chloride (7.3 mg, 38.1 μmol) and the solution was allowed to stir at 25 °C for 2 h before addition of EtOAc (5 mL) and brine (2 mL). The organic layer was separated and aqueous layer was extracted with EtOAc (5 mL × 2). The combined organic layer was rotary evaporated to obtain the crude mixture, which was subjected to flash column

chromatography using 30% EtOAc/petroleum ether to get **5.18** (14.7 mg, 93%, R_f 0.12) as colorless oil. $[\alpha]^{20}_D$ = −50.5 (*c* 1.2, CH_2Cl_2); IR (film) ν_{max} (cm^{-1}): 3610–3143 (br), 2996, 2954, 2369, 2136, 1689, 1529, 1471, 1469, 1425, 1167, 1081, 1055, 1042; ^{1}H NMR (400 MHz, $CDCl_3$) δ 7.68 (d, J = 8.21 Hz, 2H), 7.40–7.28 (m, 7H), 4.66 (d, J = 11.49 Hz, 1H), 4.59 (d, J = 11.49 Hz, 1H), 4.02–3.89 (m, 1H), 3.62 (dd, J = 14.85, 4.95 Hz, 1H), 3.52 (t, J = 8.53 Hz, 1H), 3.35 (dd, J = 14.30, 5.78 Hz, 1H), 3.23 (dd, J = 14.68, 5.18 Hz, 1H), 3.03 (dd, J = 14.68, 7.49 Hz, 1H), 2.64 (d, J = 9.08 Hz, 1H), 2.43 (s, 3H), 2.31 (dd, J = 14.60, 4.87 Hz, 1H), 2.03 (dt, J = 14.79, 8.91, 5.88 Hz, 1H); ^{13}C NMR (100 MHz, $CDCl_3$) δ 144.0, 137.3, 136.0, 130.4, 130.1, 128.7, 128.2, 128.1, 127.2, 127.1, 79.0, 72.0, 68.0, 64.7, 56.4, 51.1, 46.0, 36.5, 21.7; HRMS (ESI): $[M + Na]^+$, *m/z* calcd for $C_{20}H_{24}N_4O_4SNa$ 439.1416, found 439.1415.

(3*R*,4*R*,6*S*)–3–azido–4–benzyloxy–6–fluoro–1–tosylazepane (5.19)

The procedure for the synthesis of **5.3** was followed. colorless oil, yield 78% from **5.18**, R_f 0.23 (petroleum ether/EtOAc, 7/3); $[\alpha]^{20}_D$ = −44.7 (*c* 0.9, CH_2Cl_2); IR (film) ν_{max} (cm^{-1}): 2369, 2134, 2119, 1756, 1587, 1482, 1446, 1410, 1149, 1089, 1012; ^{1}H NMR (600 MHz, $CDCl_3$) δ 7.69 (d, J = 8.29 Hz, 2H), 7.37–7.30 (m, 7H), 4.81 (m, $^1J_{HF}$ = 47.71 Hz, 1H), 4.70 (d, J = 11.20 Hz, 1H), 4.52 (d, J = 11.20 Hz, 1H), 3.76 (dt, J = 7.20, 4.82, 2.63 Hz, 1H), 3.67 (ddd, J = 14.18, 7.16, 7.02 Hz, 1H), 3.57 (t, J = 8.43, 7.98 Hz, 1H), 3.42–3.35 (m, 2H), 3.26 (ddd, J = 14.49, 14.27, 8.0 Hz, 1H), 2.43 (s, 3H), 2.42 (dddd, J = 23.41, 15.19, 4.93, 1.23 Hz, 1H), 2.18 (dddd, J = 16.0, 8.21, 7.80, 7.39 Hz, 1H); ^{13}C NMR (150 MHz, $CDCl_3$) δ 144.1, 137.4, 135.8, 130.1, 128.7, 128.2, 128.2, 127.3, 88.6 (d, $^1J_{CF}$ = 174.60 Hz), 77.1, 71.8, 64.2, 52.7 (d, $^2J_{CF}$ = 34.58 Hz), 50.7, 33.0 (d, $^2J_{CF}$ = 20.39 Hz), 21.7; HRMS (ESI): $[M + H]^+$, *m/z* calcd for $C_{20}H_{24}FN_4O_3S$ 419.1561, found 419.1553.

(2*R*,4*R*,5*R*)–5–azido–4–benzyloxy–2–fluoromethyl–1–tosylpiperidine (5.20)

The procedure for the synthesis of **5.3** was followed. colorless oil, yield 17% from **5.18**, R_f 0.24 (petroleum ether/EtOAc, 7/3); $[\alpha]^{20}_D = -24.5$ (*c* 0.4, CH_2Cl_2); IR (film) ν_{max} (cm^{-1}): 2375, 2139, 2123, 1747, 1580, 1482, 1441, 1423, 1149, 1078, 1017; ^1H NMR (600 MHz, $CDCl_3$) δ 7.74 (d, J = 8.29 Hz, 2H), 7.36–7.28 (m, 7H), 4.63 (ddd, J = 47.71 ($^1J_{HF}$), 9.25, 7.40 Hz, 1H), 4.59 (d, J = 11.76 Hz, 1H), 4.49 (ddd, J = 45.50 ($^1J_{HF}$), 9.25, 7.03 Hz, 1H), 4.48 (d, J = 11.76 Hz, 1H), 4.28–4.21 (m, 1H), 3.79 (dd, J = 14.70, 2.73 Hz, 1H), 3.68–3.65 (m, 1H), 3.58–3.55 (m, 1H), 3.49 (dd, J = 14.60, 2.40 Hz, 1H), 2.43 (s, 3H), 1.94–1.92 (m, 1H); ^{13}C NMR (150 MHz, $CDCl_3$) δ 143.6, 137.4, 136.5, 129.6, 128.8, 128.3, 127.8, 127.5, 81.9 (d, $^1J_{CF}$ = 164.70 Hz), 77.8, 71.9, 57.6, 51.2 (d, $^2J_{CF}$ = 28.04 Hz), 40.3, 24.5, 21.6; HRMS (ESI): $[M + Na]^+$, *m/z* calcd for $C_{20}H_{23}FN_4O_3SNa$ 441.1388, found 441.1373.

(3*S*,4*R*,5*S*,6*R*)–6–azido–5–benzyloxy–4–fluoro–1–tosylazepan–3–ol (5.21)

The procedure for the synthesis of **5.18** was followed. colorless oil, yield 94% from **5.5**, R_f 0.16 (petroleum ether/EtOAc, 7/3); $[\alpha]^{20}_D$ = +34.5 (*c* 0.6, CH_2Cl_2); IR (film) ν_{max} (cm^{-1}): 3600–3190 (br), 2990, 2939, 2365, 2134, 1526, 1482, 1465, 1417, 1123, 1089, 1044, 1027; ^1H NMR (400 MHz, $CDCl_3$) δ 7.69 (d, J = 8.09 Hz, 2H), 7.42–7.27 (m, 7H), 4.95 (dd, J = 46.08 ($^1J_{HF}$), 6.44 Hz, 1H), 4.74 (d, J = 11.6 Hz, 1H), 4.64 (d, J = 11.6 Hz, 1H), 4.14–3.91 (m, 3H), 3.85–3.78 (m, 1H), 3.63 (br d, J = 15.69 Hz, 1H), 3.26 (dd, J = 15.95, 4.15 Hz, 1H), 3.16 (dd, J = 14.67, 3.19 Hz, 1H), 3.07 (d, J = 8.29 Hz, 1H), 2.43 (s, 3H), 2.31 (dd, J = 14.60, 4.87 Hz, 1H), 2.03 (dt, J = 14.79, 8.91, 5.88 Hz, 1H); ^{13}C NMR (100 MHz, $CDCl_3$) δ 144.2, 137.2, 135.7, 130.2, 128.5, 128.2, 127.9, 127.2, 96.1 (d, $^1J_{CF}$ = 175.21 Hz), 79.6 (d, $^2J_{CF}$ = 26.78 Hz), 74.1, 71.0 (d, $^2J_{CF}$ = 37.49 Hz), 60.3, 53.2, 51.1 (d, $^3J_{CF}$ = 9.92 Hz); HRMS (ESI): $[M + Na]^+$, *m/z* calcd for $C_{20}H_{23}FN_4O_4SNa$ 457.1321, found 457.1322.

(2*R*,3*R*,4*S*,5*R*)-5-azido-4-(benzyloxy)-3-fluoro-2-(fluoromethyl)-1-tosylpiperidine (5.22)

The procedure for the synthesis of **5.3** was followed. white powder, yield 58% from **5.21**, R_f 0.31 (petroleum ether/EtOAc, 7/3); $[\alpha]^{20}_D = -14.2$ (*c* 0.6, CH_2Cl_2); IR (film) ν_{max} (cm^{-1}): 2363, 2347, 2109, 1716, 1533, 1520, 1478, 1450, 1419, 1109, 1089, 1047, 1012; ^1H NMR (600 MHz, $CDCl_3$) δ 7.71 (d, J = 8.25 Hz, 2H), 7.37–7.29 (m, 7H), 4.81 (ddd, J = 47.61 ($^1J_{HF}$), 2.30, 2.30 Hz, 1H), 4.71 (d, J = 11.63 Hz, 1H), 4.67 (d, J = 11.63 Hz, 1H), 4.67–4.46 (m, 3H), 3.88 (dd, J = 14.32, 5.50 Hz, 1H), 3.59 (ddt, J = 28.41 ($^2J_{HF}$), 9.99, 1.88 Hz, 1H), 3.48 (ddd, J = 10.52, 10.52, 5.52 Hz, 1H), 2.99 (dd, J = 14.12, 11.63, 1H), 2.43 (s, 3H); ^{13}C NMR (150 MHz, $CDCl_3$) δ 144.3, 136.9, 136.1, 130.0, 128.8, 128.4, 127.4, 86.6 (d, $^1J_{CF}$ = 183.49 Hz), 84.1 (dd, J = 175.32 ($^1J_{CF}$), 10.68 ($^3J_{CF}$), Hz), 78.5 (d, $^2J_{CF}$ = 18.84 Hz), 72.7, 57.2 (t, $^2J_{CF}$ = 20.96 Hz), 56.0, 45.4, 21.7; HRMS (ESI): $[M + Na]^+$, *m/z* calcd for $C_{20}H_{22}F_2N_4O_3SNa$ 459.1278, found 459.1276.

(3*R*,4*S*,5*S*,6*S*)–3–azido–4–benzyloxy–5,6–difluoro–1–tosylazepane (5.23)

The procedure for the synthesis of **5.3** was followed. white powder, yield 24% from **5.21**, R_f 0.31 (petroleum ether/EtOAc, 7/3); $[\alpha]^{20}_D = +30.2$ (*c* 0.5, CH_2Cl_2); IR (film) ν_{max} (cm^{-1}): 2363, 2347, 2109, 1716, 1533, 1520, 1478, 1450, 1419, 1109, 1089, 1047, 1012; ^1H NMR (600 MHz, $CDCl_3$) δ 7.73 (d, J = 8.41 Hz, 2H), 7.38–7.27 (m, 7H), 4.98 (ddd, J = 47.02 ($^1J_{HF}$), 17.67 ($^2J_{HF}$), 6.52 Hz, 1H), 4.83 (m, J = 50.01 ($^1J_{HF}$), 15.76 ($^2J_{HF}$) Hz, 1H), 4.72 (d, J = 11.71 Hz, 1H), 4.61 (d, J = 11.71 Hz, 1H), 4.16 (dd, J = 20.26 ($^2J_{HF}$), 17.27 Hz, 1H), 4.00 (ddd, J = 27.34 ($^2J_{HF}$), 5.64, 4.18 Hz, 1H), 4.02 (br d, J = 14.83 Hz, 1H), 3.78–3.72 (m, 2H), 3.21 (ddd, J = 36.70 ($^2J_{HF}$), 16.18, 3.84 Hz, 1H), 3.07 (dd, J = 14.91, 2.56 Hz, 1H), 2.43 (s, 3H); ^{13}C NMR (150 MHz, $CDCl_3$) δ 144.1, 136.8, 136.7, 139.9, 128.8, 128.0, 127.6, 127.2, 93.1 (dd, J = 186.81 ($^1J_{CF}$), 24.72 ($^2J_{CF}$), Hz), 91.9 (dd, J = 178.17 ($^1J_{CF}$), 24.72 ($^2J_{CF}$), Hz), 79.1 (dd, J = 21.52 ($^2J_{CF}$), 10.59 ($^3J_{CF}$), Hz), 74.3, 59.7 (d, $^3J_{CF}$ = 11.76 Hz), 50.4, 51.8 (dd, J = 25.74 ($^2J_{CF}$),

9.65 ($^3J_{CF}$), Hz), 21.7; HRMS (ESI): $[M + Na]^+$, *m/z* calcd for $C_{20}H_{22}F_2N_4O_3SNa$ 459.1278, found 459.1272.

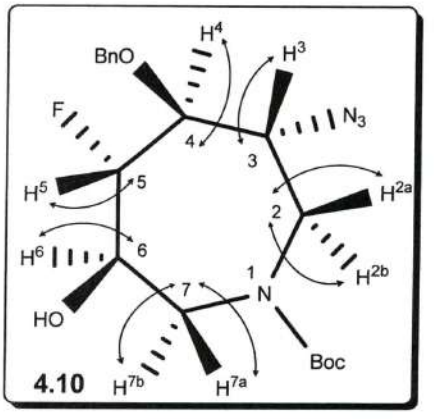
(3*R*,4*S*,5*R*,6*S*)–3–azido–4–benzyloxy–5,6–difluoro–1–tosylazepane (5.24)

The procedure for the synthesis of **5.3** was followed. white powder, yield 14% from **5.21**, R_f 0.32 (petroleum ether/EtOAc, 7/3); $[\alpha]^{20}_D$ = +4.2 (*c* 0.4, CH_2Cl_2); IR (film) ν_{max} (cm^{-1}): 2363, 2347, 2109, 1716, 1533, 1520, 1478, 1450, 1419, 1109, 1089, 1047, 1012; ^1H NMR (600 MHz, $CDCl_3$) δ 7.66 (d, *J* = 8.19 Hz, 2H), 7.42–7.30 (m, 7H), 5.20 (dddd, *J* = 48.43 ($^1J_{HF}$), 22.80 ($^2J_{HF}$), 5.21, 2.3 Hz, 1H), 4.91 (ddd, *J* = 46.78 ($^1J_{HF}$), 26.76 ($^2J_{HF}$), 8.37 Hz, 1H), 4.84 (d, *J* = 10.69 Hz, 1H), 4.75 (d, *J* = 10.69 Hz, 1H), 4.04 (ddd, *J* = 33.48 ($^2J_{HF}$), 14.35, 5.54 Hz, 1H), 3.93 (ddd, *J* = 17.36, 8.54, 8.54 Hz, 1H), 3.83–3.78 (m, 1H), 3.70 (br d, *J* = 14.97 Hz, 1H), 3.12 (ddt, *J* = 21.93 ($^2J_{HF}$), 14.65, 2.66 Hz, 1H), 2.71 (ddd, *J* = 14.65, 11.25, 2.30 Hz, 1H), 2.44 (s, 3H); ^{13}C NMR (150 MHz, $CDCl_3$) δ 144.5, 137.4, 134.9, 130.3, 128.6, 128.5, 128.2, 127.2, 93.2 (dd, *J* = 179.42 ($^1J_{CF}$), 22.63 ($^2J_{CF}$), Hz), 91.3 (dd, *J* = 177.81 ($^1J_{CF}$), 24.25 ($^2J_{CF}$), Hz), 80.3 (dd, *J* = 20.28 ($^2J_{CF}$), 7.72 ($^3J_{CF}$), Hz), 75.6, 64.4 (d, $^3J_{CF}$ = 8.33 Hz), 48.7 (dd, *J* = 24.35 ($^2J_{CF}$), 12.18 ($^3J_{CF}$), Hz), 46.9, 21.7; HRMS (ESI): $[M + Na]^+$, *m/z* calcd for $C_{20}H_{22}F_2N_4O_3SNa$ 459.1278, found 459.1285.

5.3.3. Structure Elucidation of Key Azepanes

Structure elucidation of 4.10

^{1}H–^{13}C HSQC 2D NMR correlations:



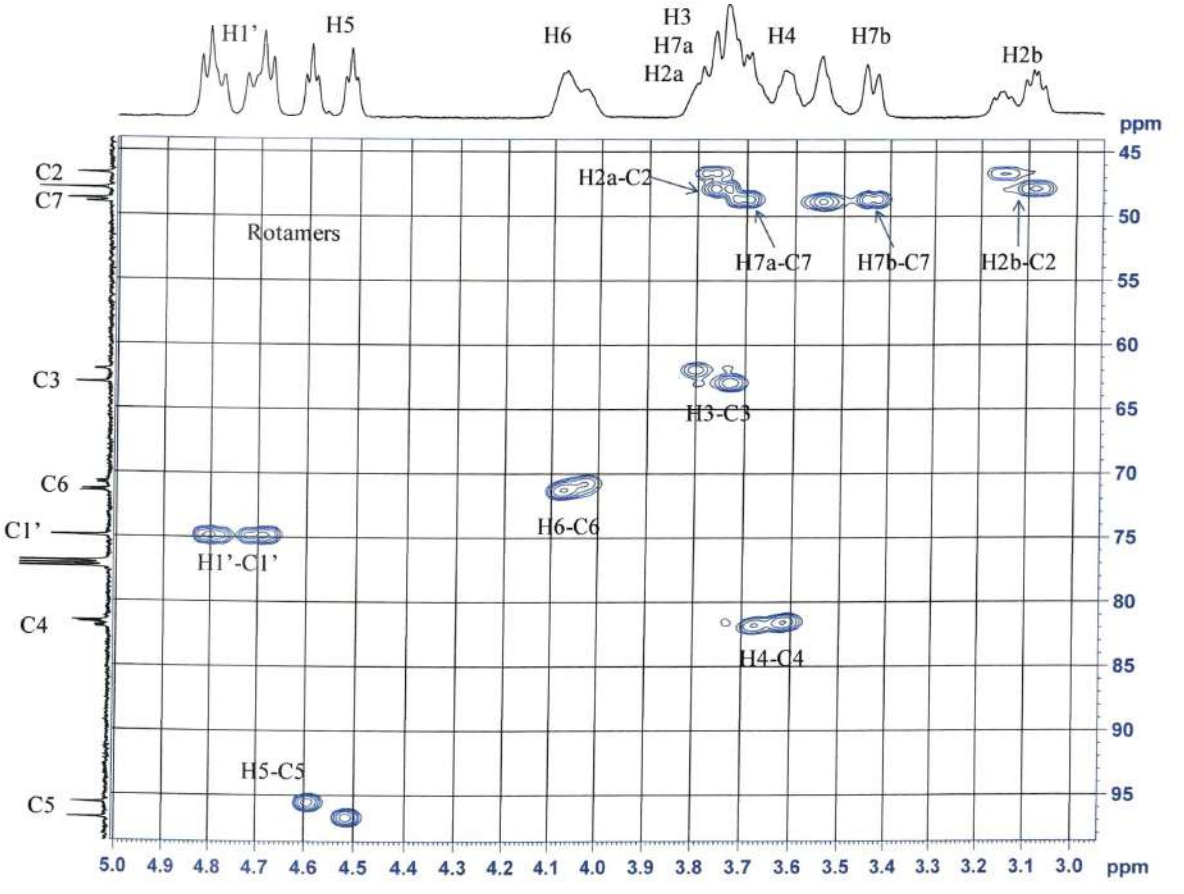
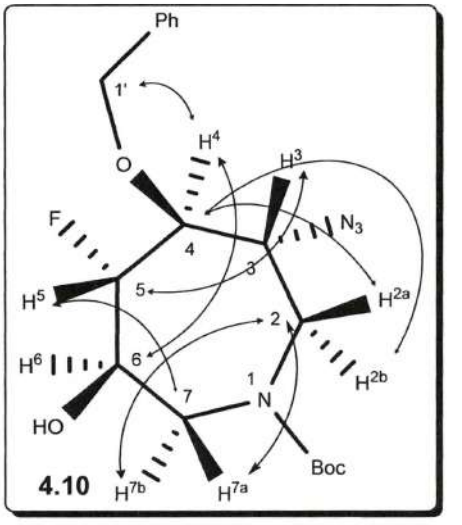


Figure 5.4. ^{1}H–^{13}C HSQC 2D NMR correlations of the azepane ring in **4.10**.

$^{1}H–^{13}C$ HMBC 2D NMR correlations:



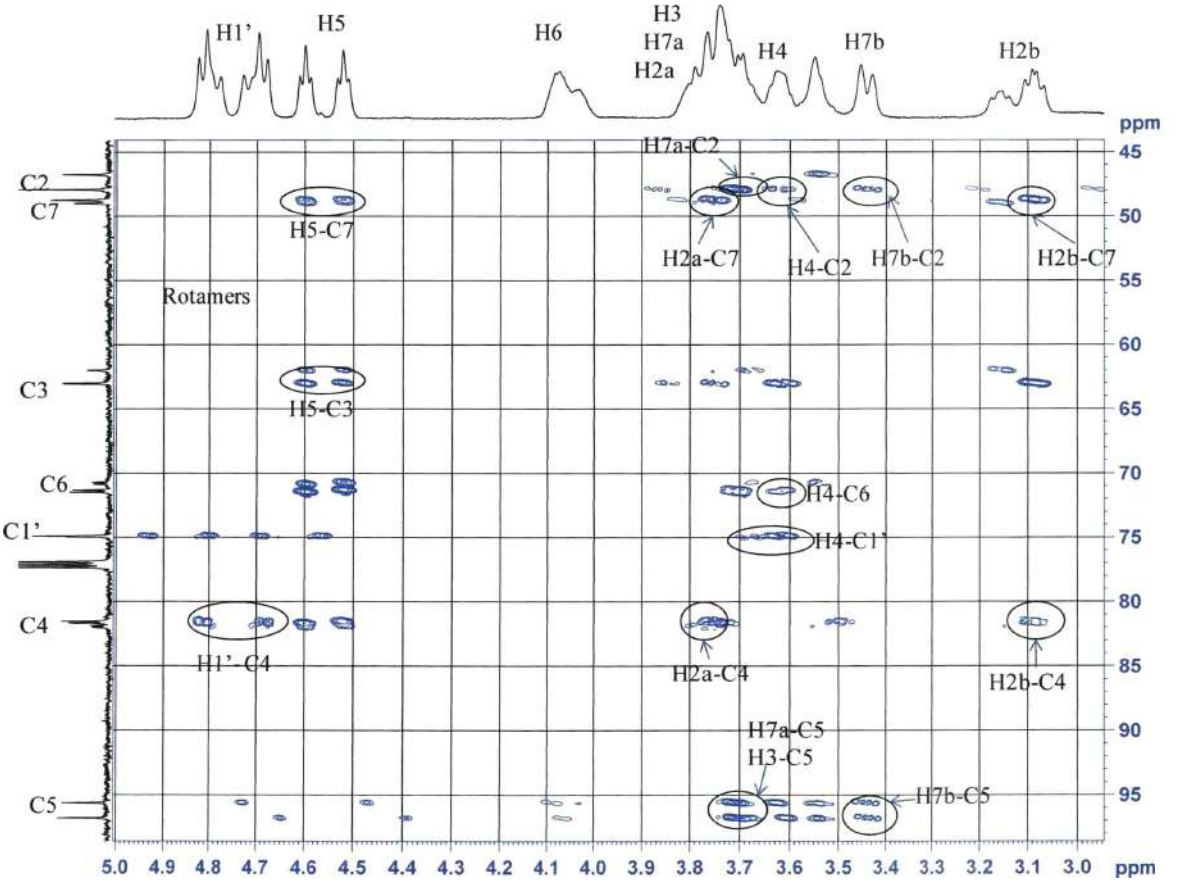
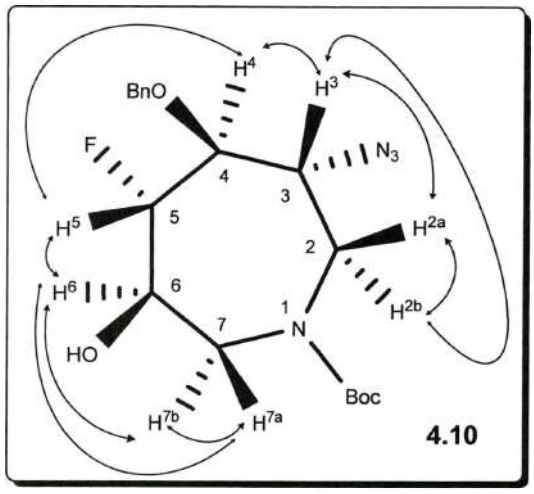


Figure 5.5. $^{1}H–^{13}C$ HMBC 2D NMR correlations of the azepane ring in **4.10**.

^1H–^1H COSY 2D NMR correlations:



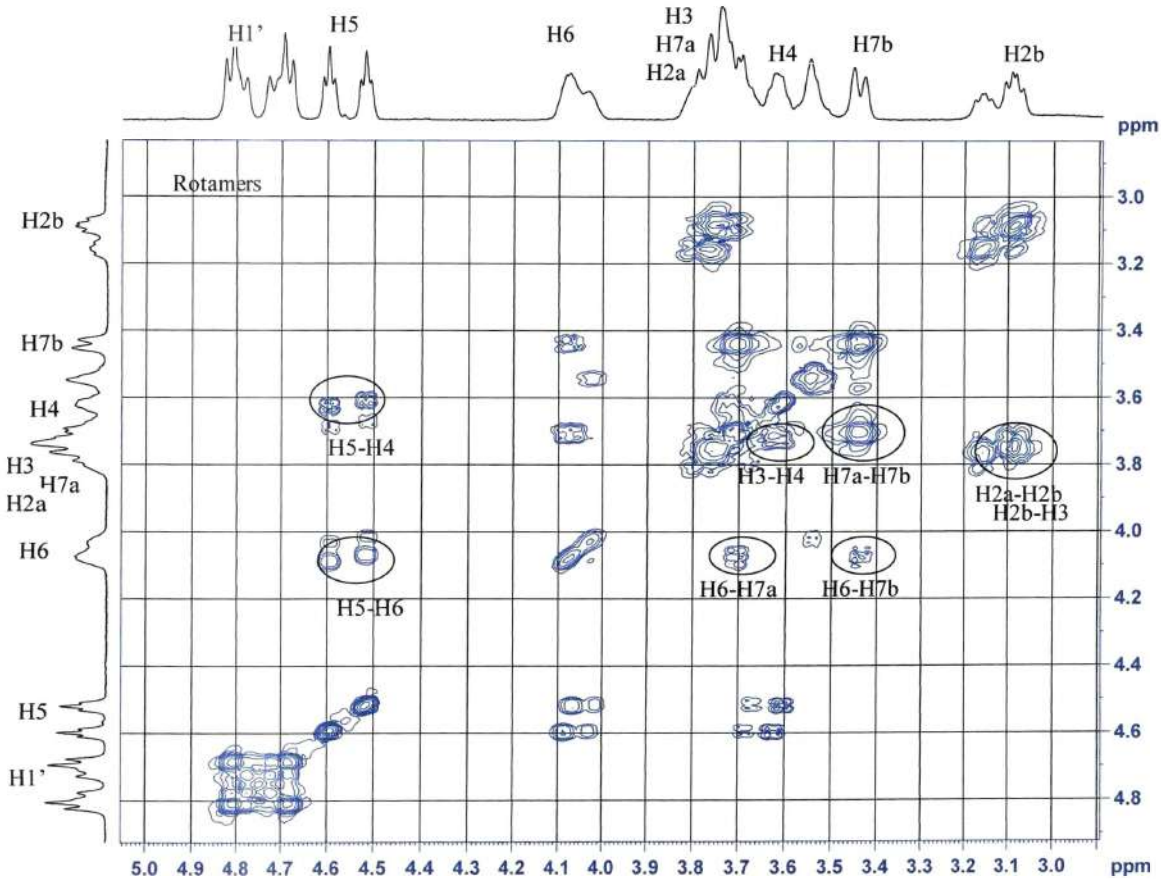
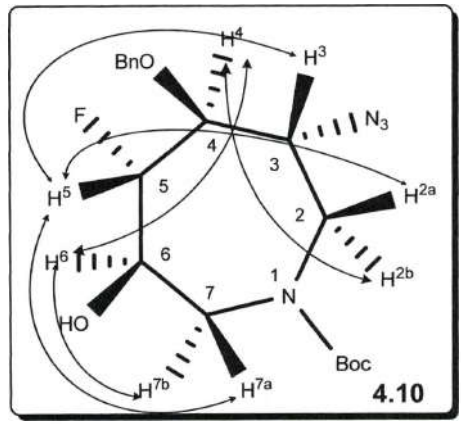


Figure 5.6. ^1H–^1H COSY 2D NMR correlations of the azepane ring in **4.10**.

^{1}H–^{1}H NOESY NMR correlations:



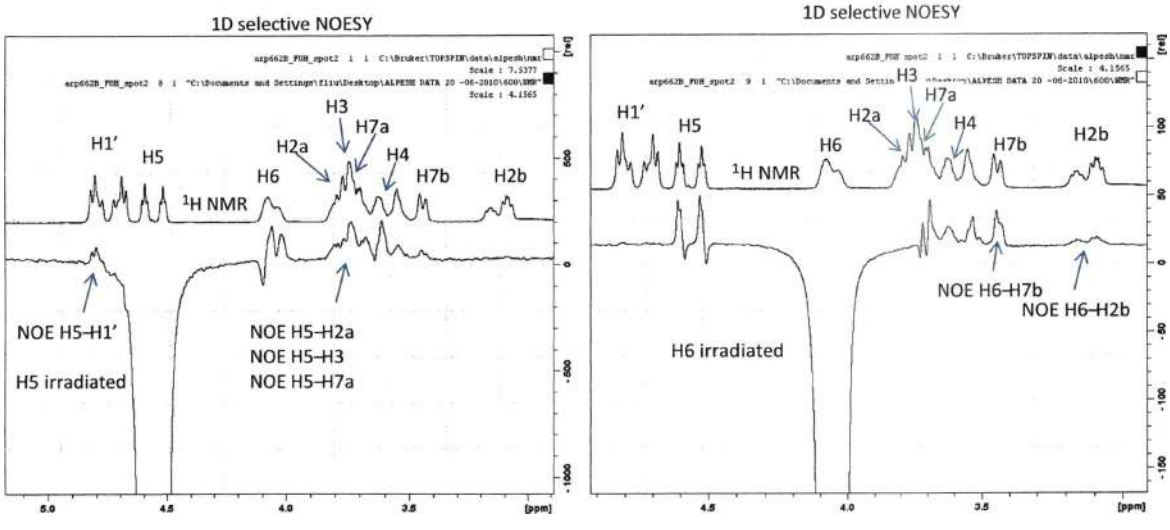
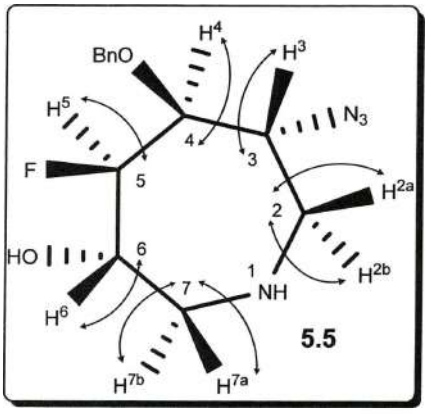


Figure 5.7. ^{1}H–^{1}H NOESY correlations of the azepane ring in **4.10**.

Structure elucidation of 5.5

$^{1}H–^{13}C$ HSQC 2D NMR correlations:



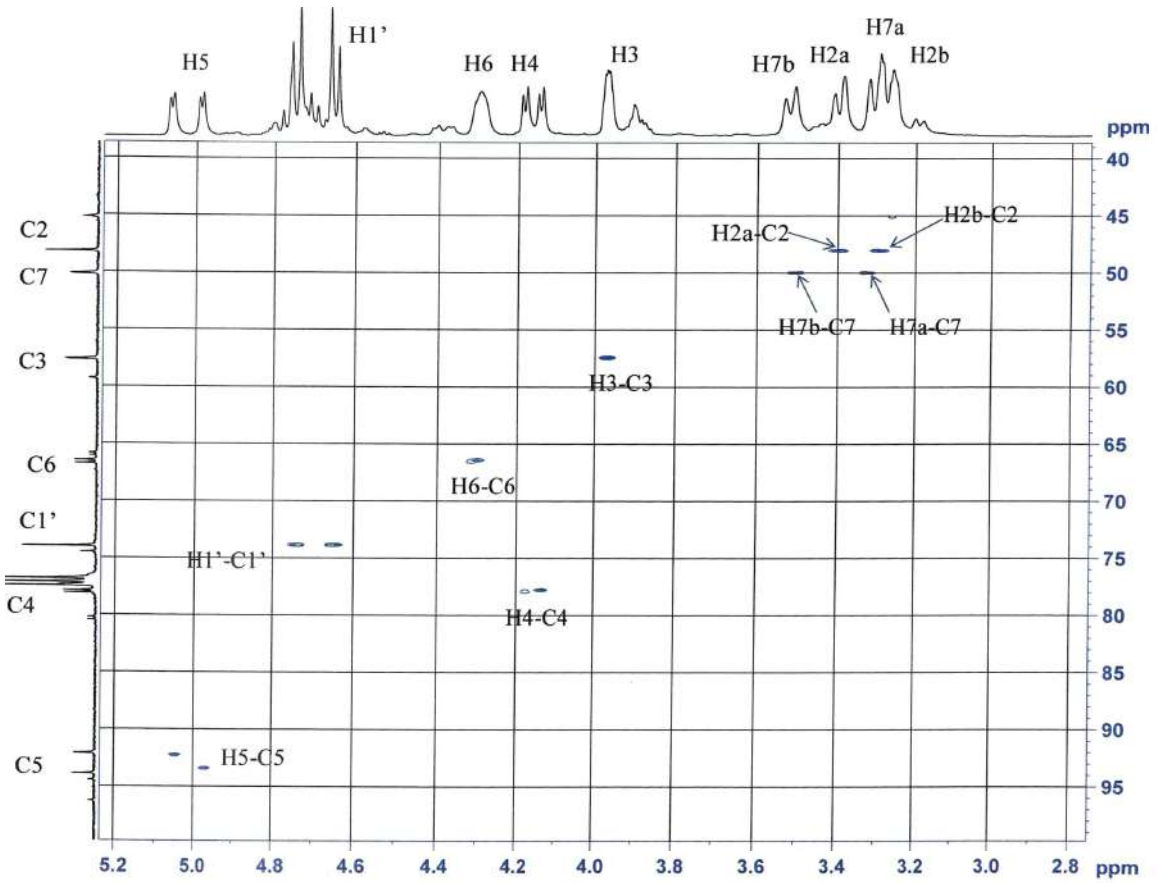
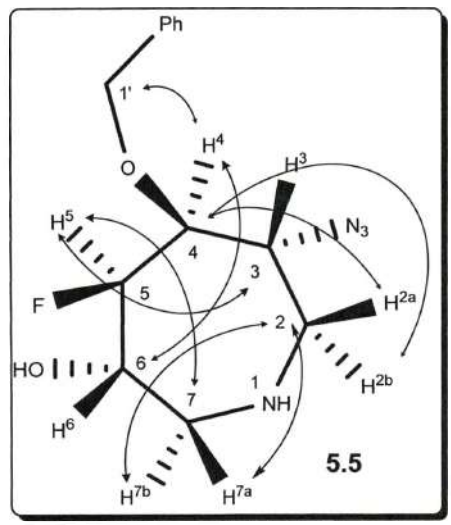


Figure 5.8. $^{1}H–^{13}C$ HSQC 2D NMR correlations of the azepane ring in **5.5**.

$^{1}H–^{13}C$ HMBC 2D NMR correlations:



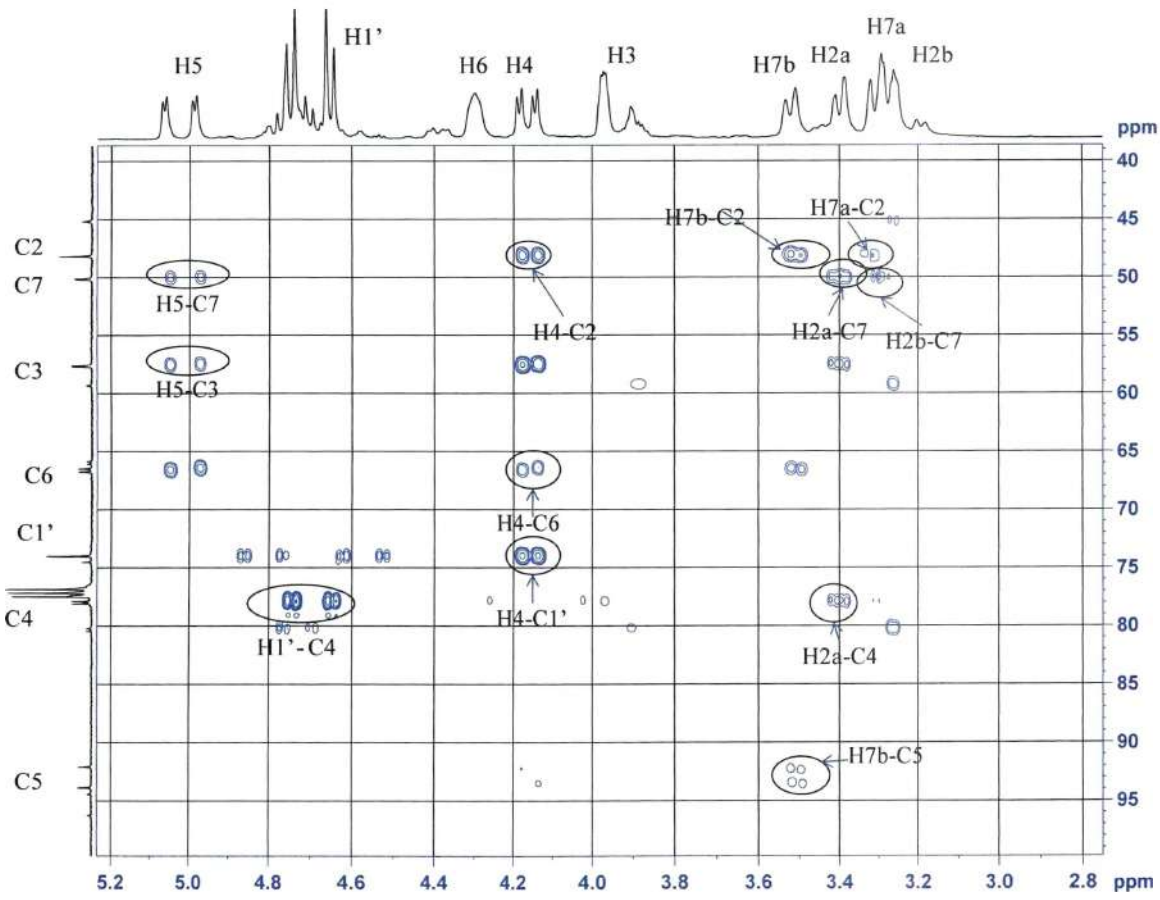
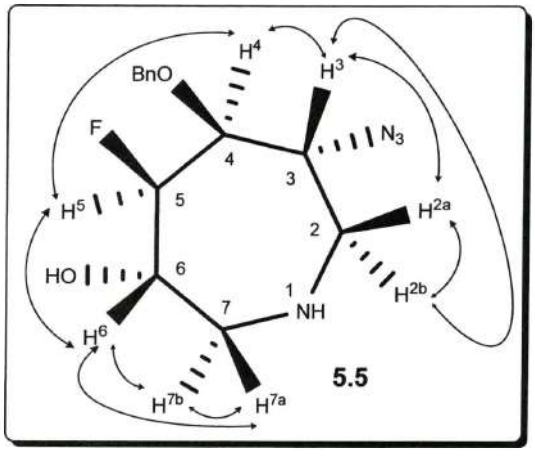


Figure 5.9. $^{1}H–^{13}C$ HMBC 2D NMR correlations of the azepane ring in **5.5**.

$^{1}H–^{1}H$ COSY 2D NMR correlations:



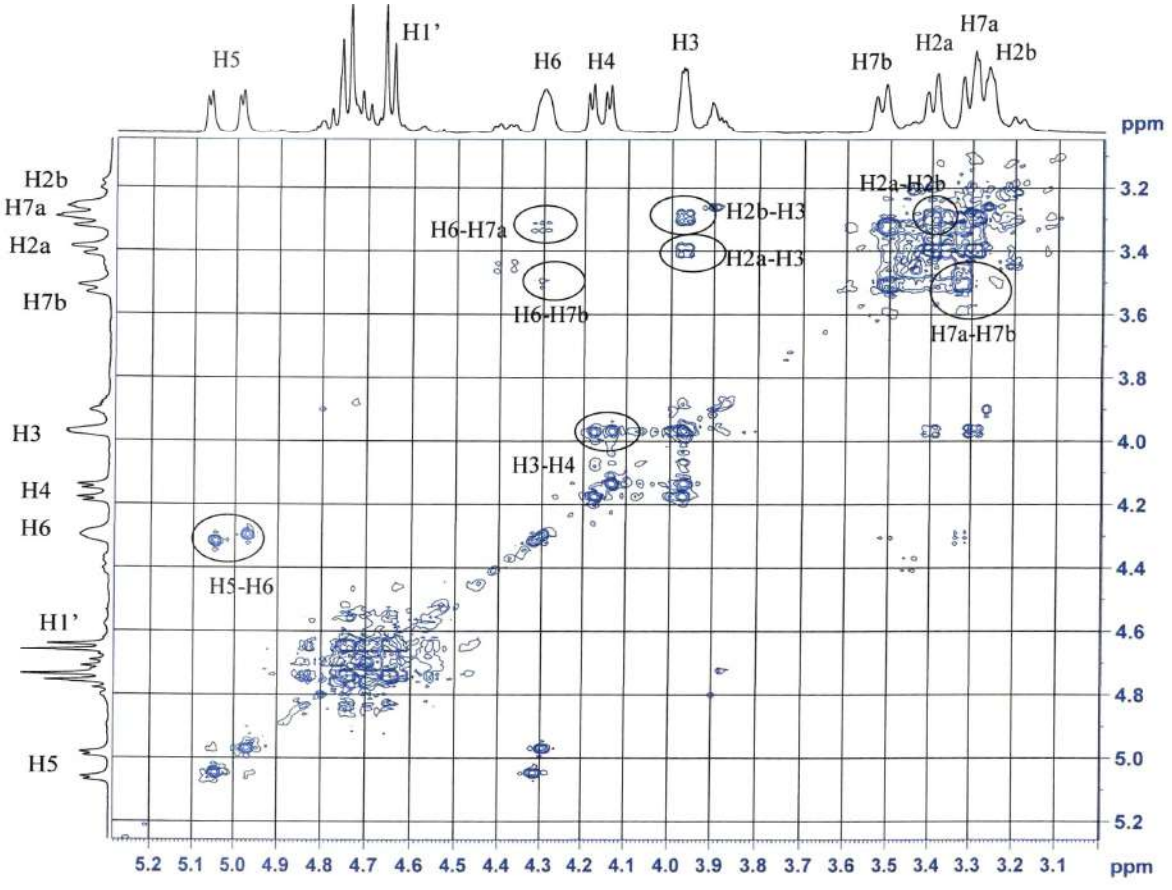


Figure 5.10. $^{1}H–^{1}H$ COSY 2D NMR correlations of the azepane ring in **5.5**.

^1H–^1H NOESY NMR correlations:

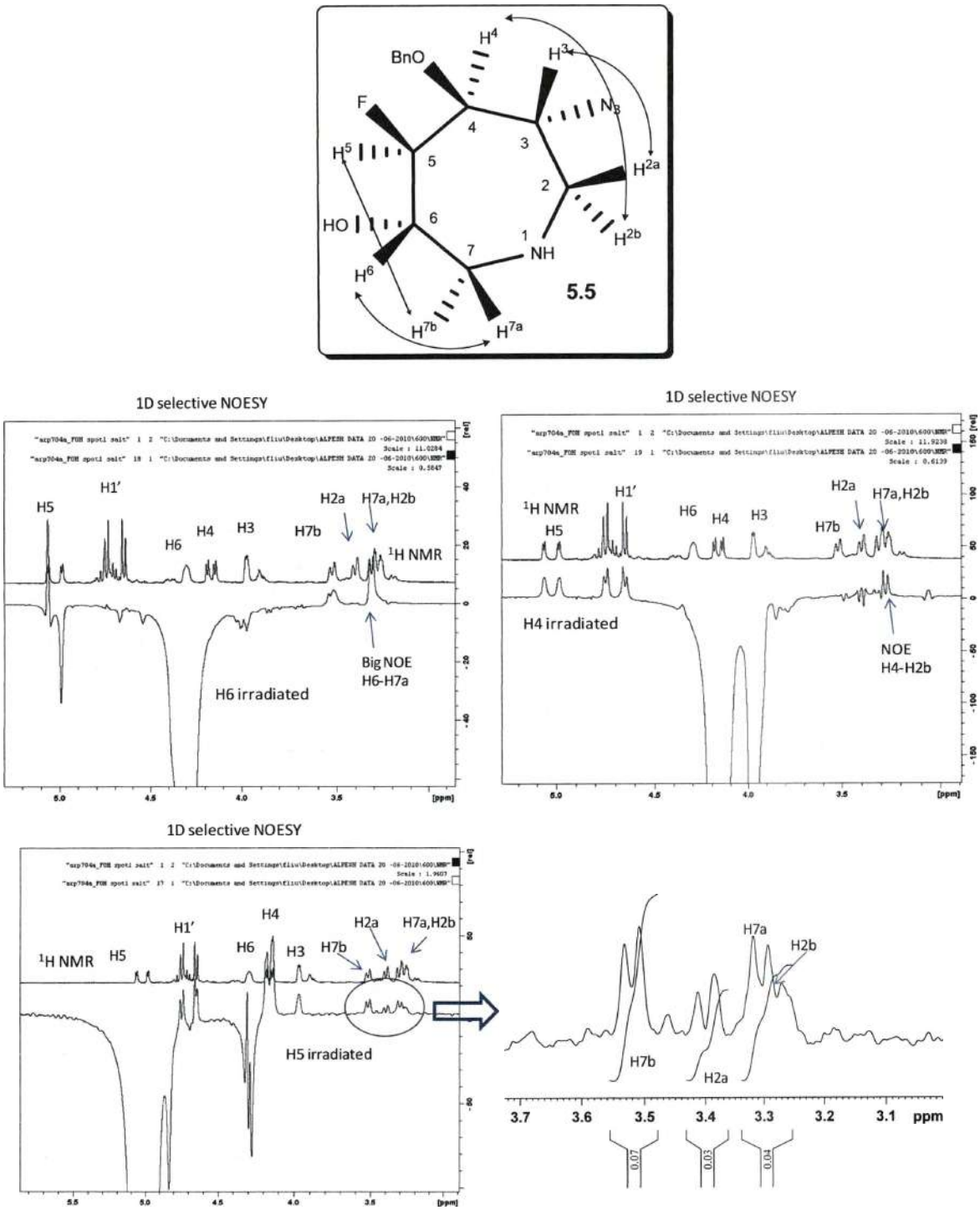
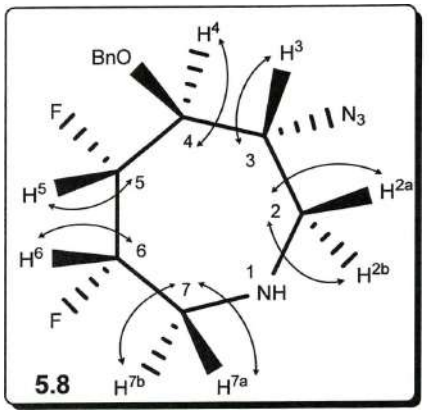


Figure 5.11. ^1H–^1H NOESY correlations of the azepane ring in **5.5**.

Structure elucidation of difluoroazepane 5.8

^{1}H–^{13}C HSQC 2D NMR correlations:



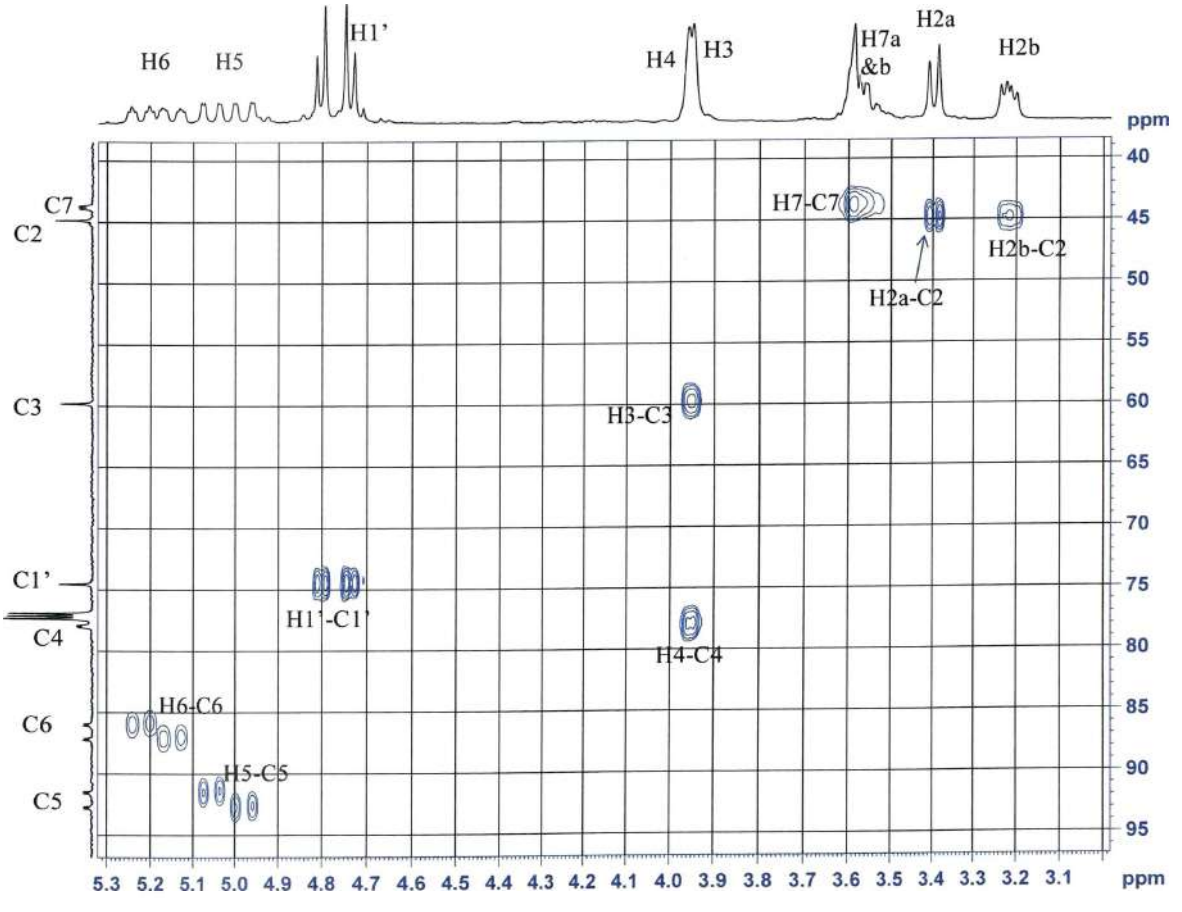
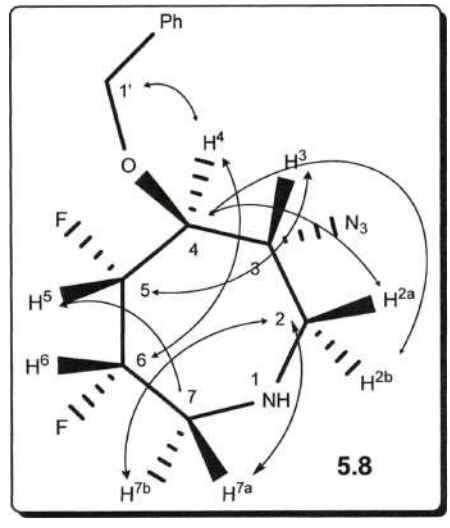


Figure 5.12. ^{1}H–^{13}C HSQC 2D NMR correlations of the azepane ring in **5.8**.

$^{1}H–^{13}C$ HMBC 2D NMR correlations:



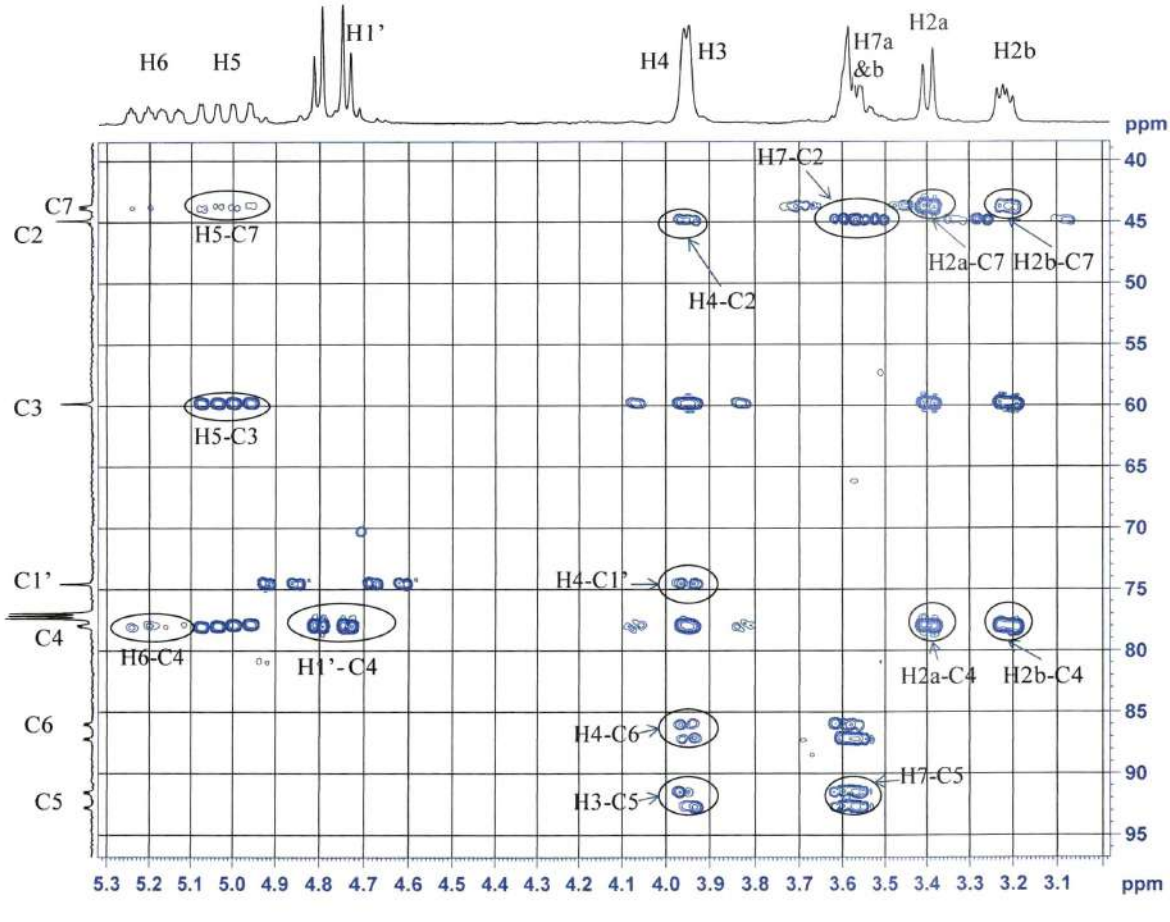
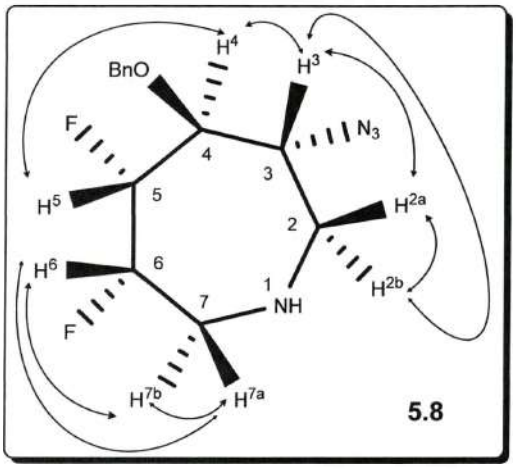


Figure 5.13. $^{1}H–^{13}C$ HMBC 2D NMR correlations of the azepane ring in **5.8**.

^{1}H–^{1}H COSY 2D NMR correlations:



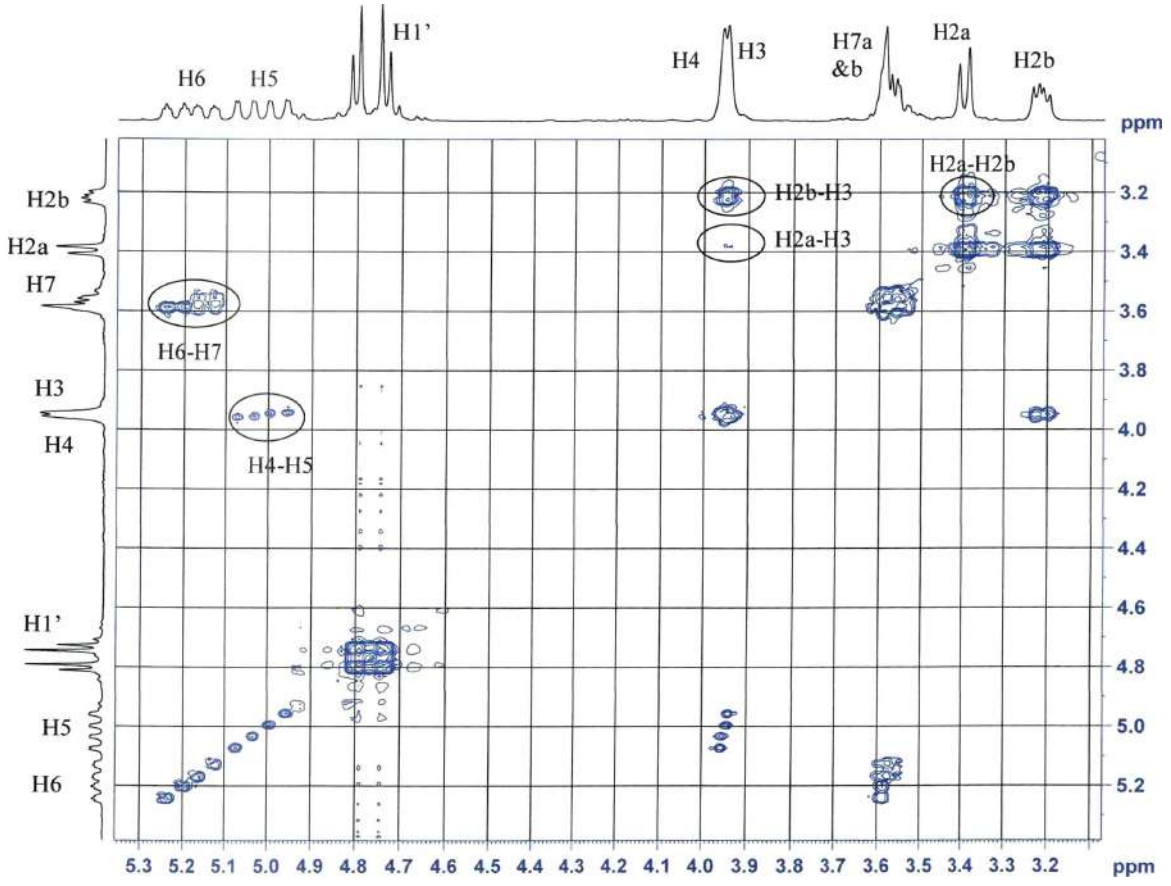


Figure 5.14. ^{1}H–^{1}H COSY 2D NMR correlations of the azepane ring in **5.8**.

^{1}H–^{1}H NOESY NMR correlations:

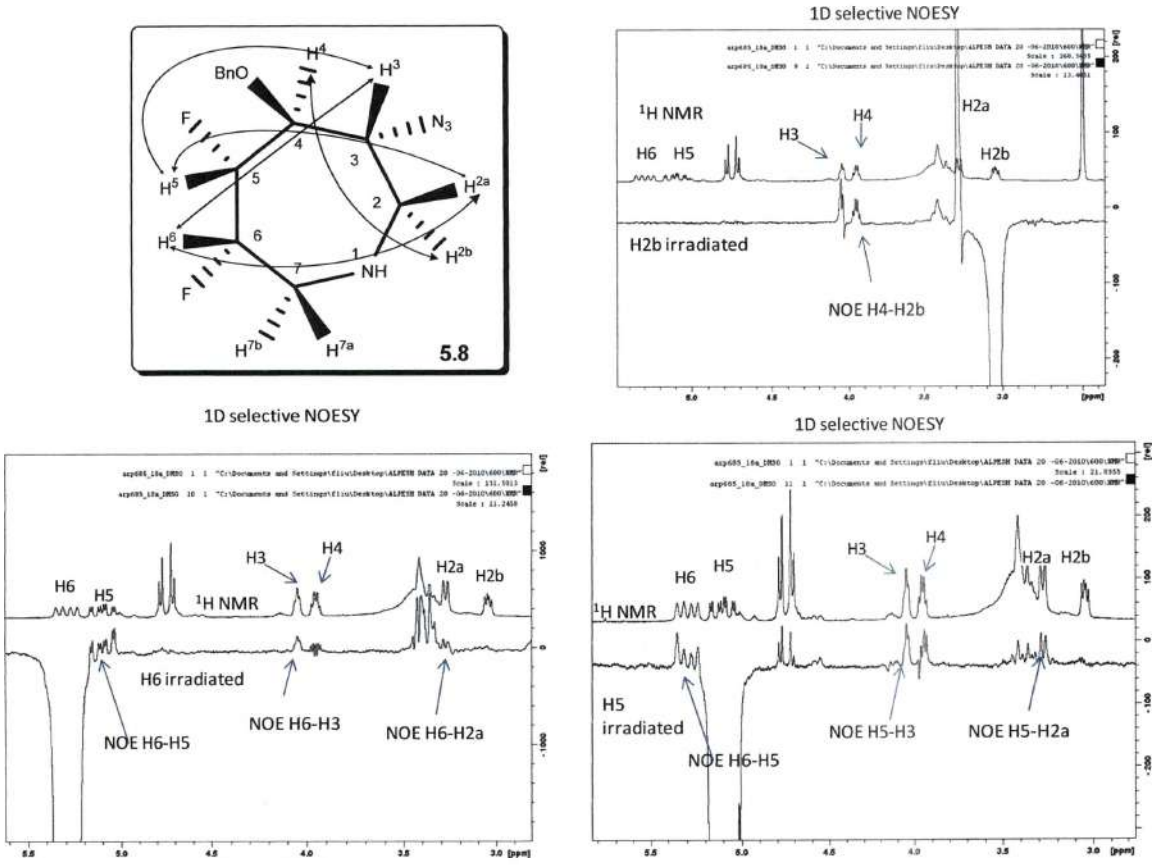
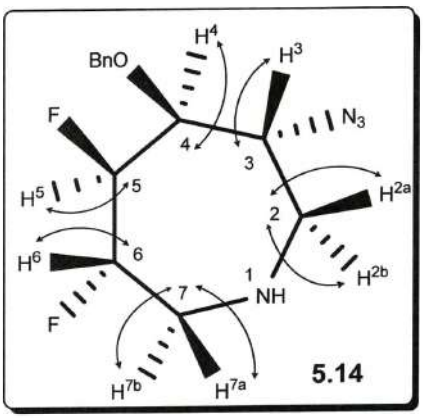


Figure 5.15. ^{1}H–^{1}H NOESY correlations of the azepane ring in **5.8**. These spectra were recorded in $(CD_3)_2SO$. Assignment of absolute stereochemistry of **5.8** at C5 and C6 as *R* and *S*, respectively was supported by H6 and H5 both showing NOE to H3 and H2a with no measureable NOE to H2b.

Structure elucidation of difluoroazepane 5.14

^{1}H–^{13}C HSQC 2D NMR correlations:



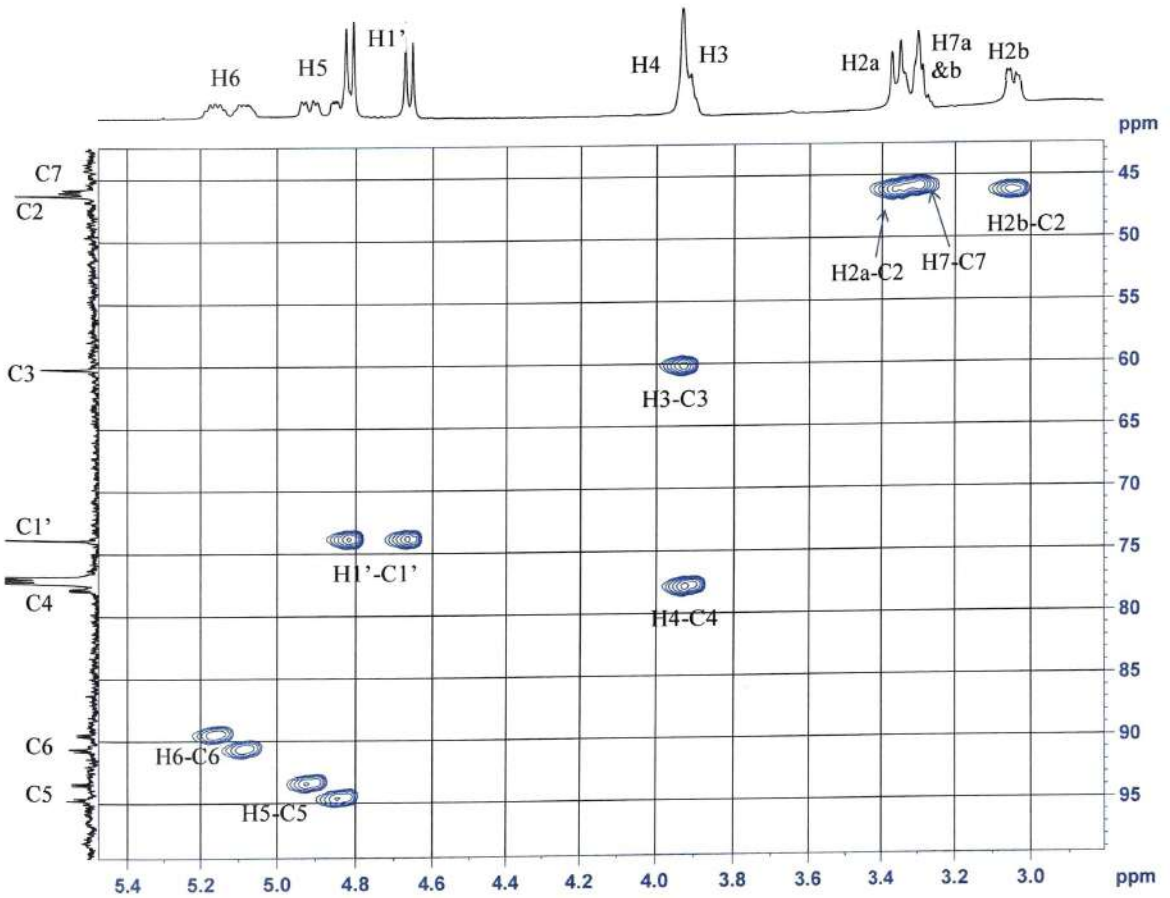
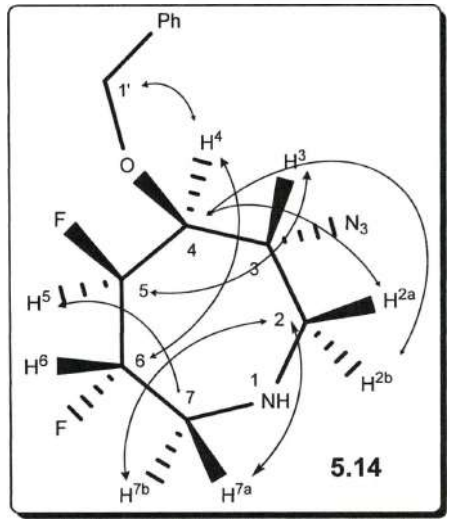


Figure 5.16. ^{1}H–^{13}C HSQC 2D NMR correlations of the azepane ring in **5.14**.

$^{1}H–^{13}C$ HMBC 2D NMR correlations:



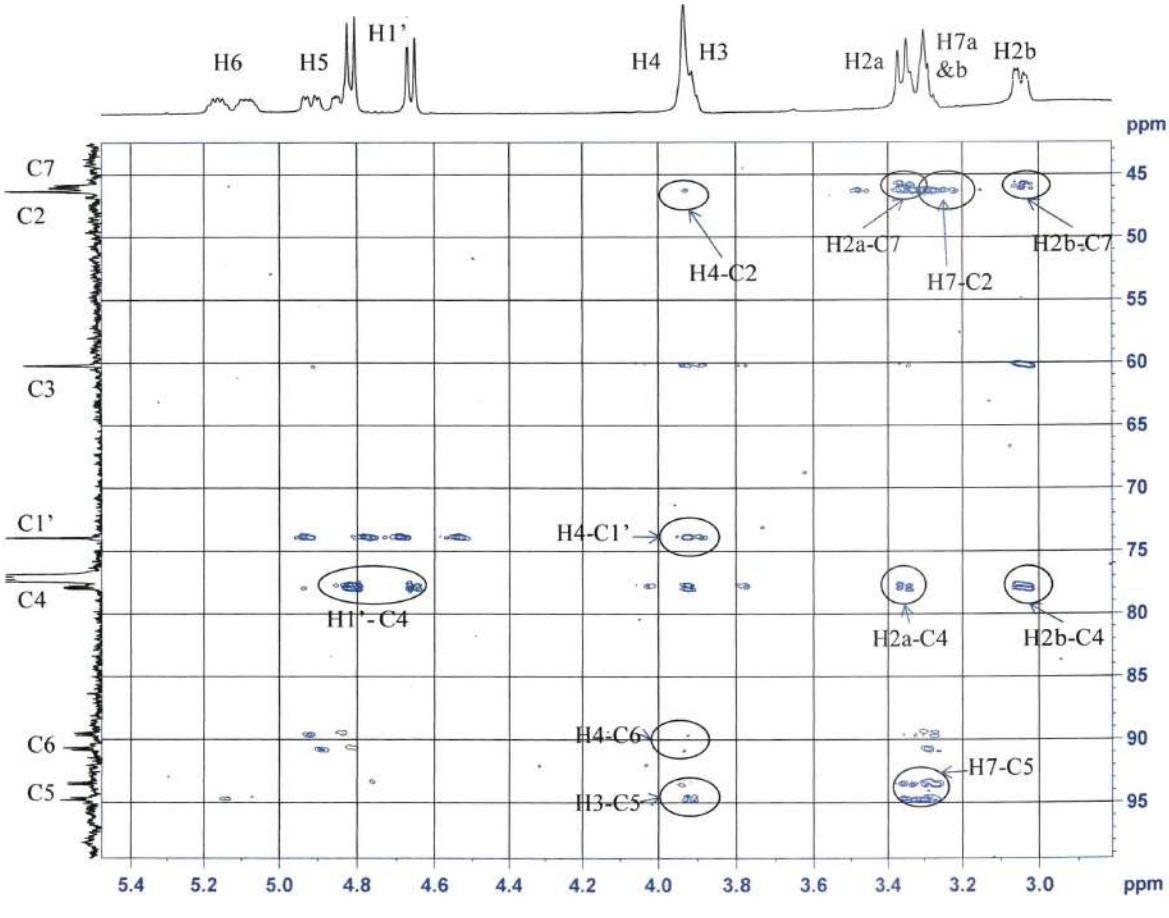
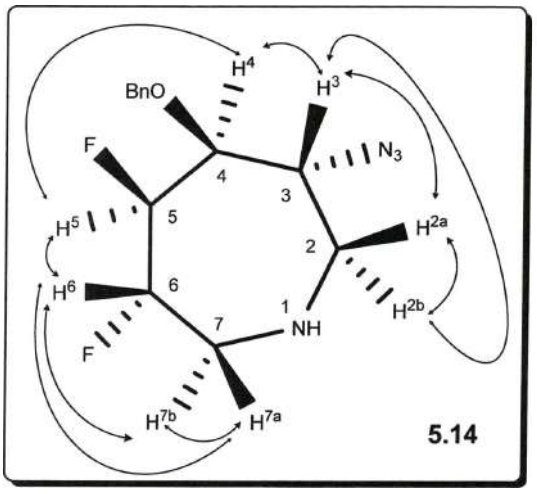


Figure 5.17. $^{1}H–^{13}C$ HMBC 2D NMR correlations of the azepane ring in **5.14**.

^{1}H–^{1}H COSY 2D NMR correlations:



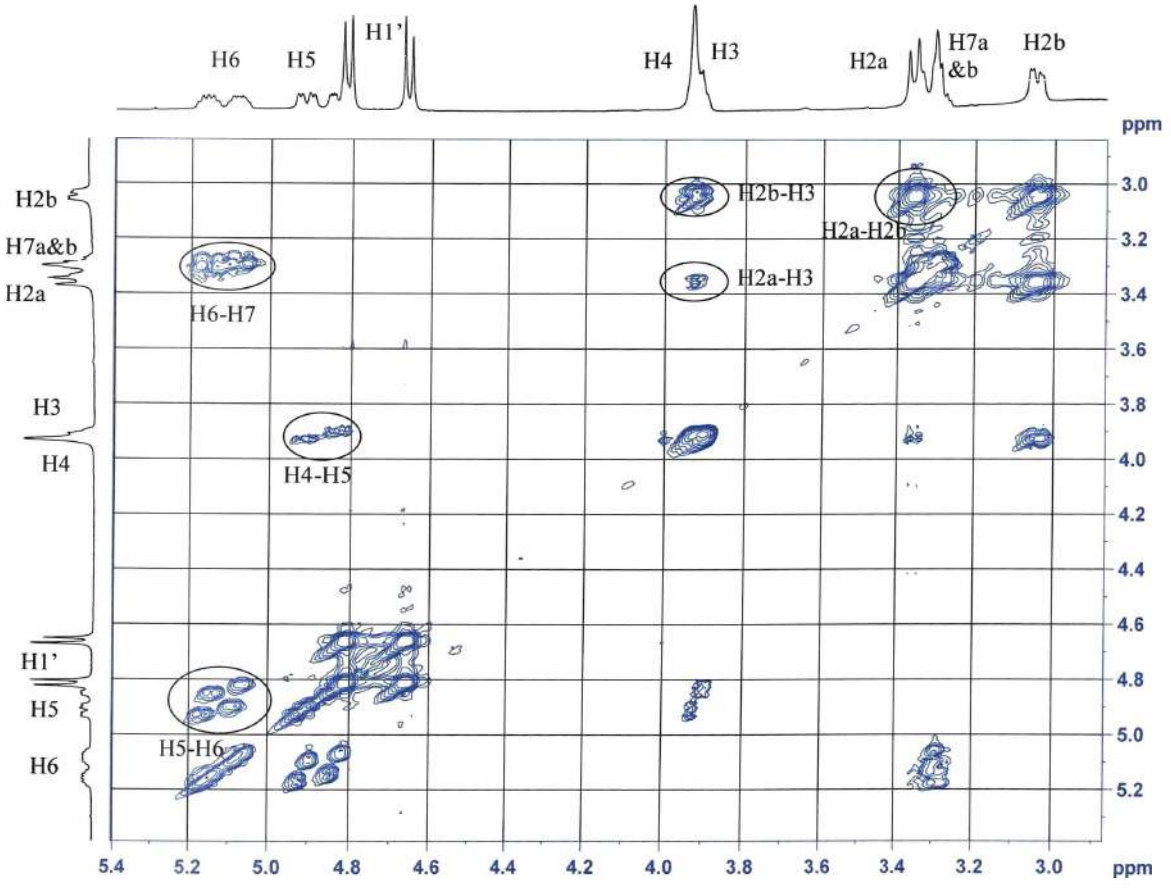


Figure 5.18. ^{1}H–^{1}H COSY 2D NMR correlations of the azepane ring in **5.14**.

^{1}H–^{1}H NOESY NMR correlations:

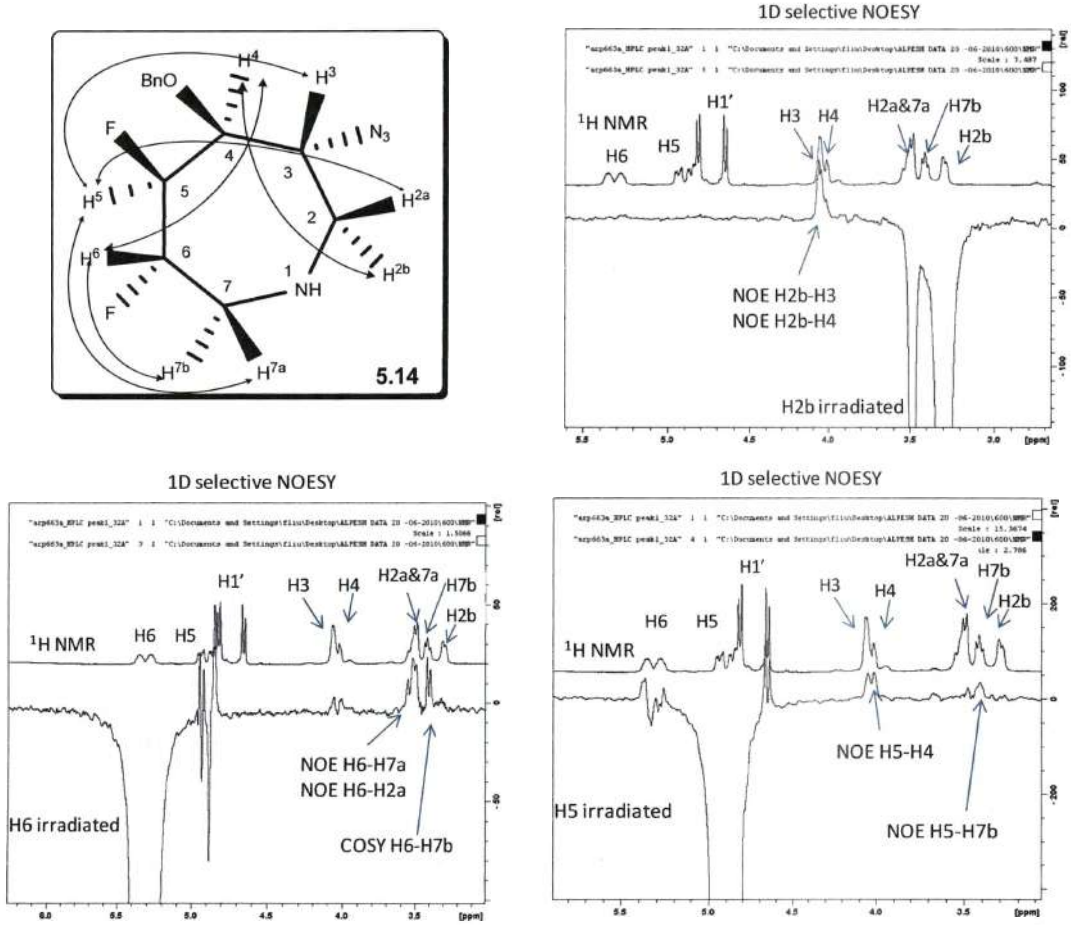
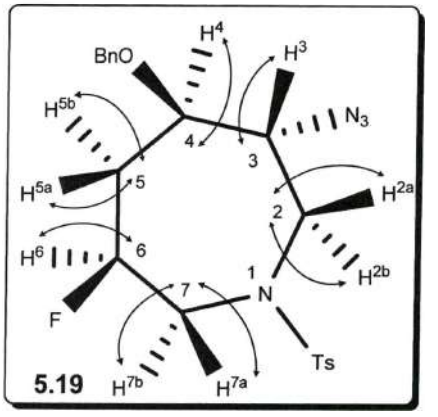


Figure 5.19. ^{1}H–^{1}H NOESY correlations of the azepane ring in **5.14**.

In the case of **5.14**, H5 showed NOE to H7b and H4 while no detactable NOE with H7a. Whereas, H6 showed NOE to H2a and H7a while no measurable NOE to H2b. These results suggested that the absolute stereochemistry at both C5 and C6 is *S*.

Structure elucidation of monofluoroazepane 5.19

$^{1}H–^{13}C$ HSQC 2D NMR correlations:



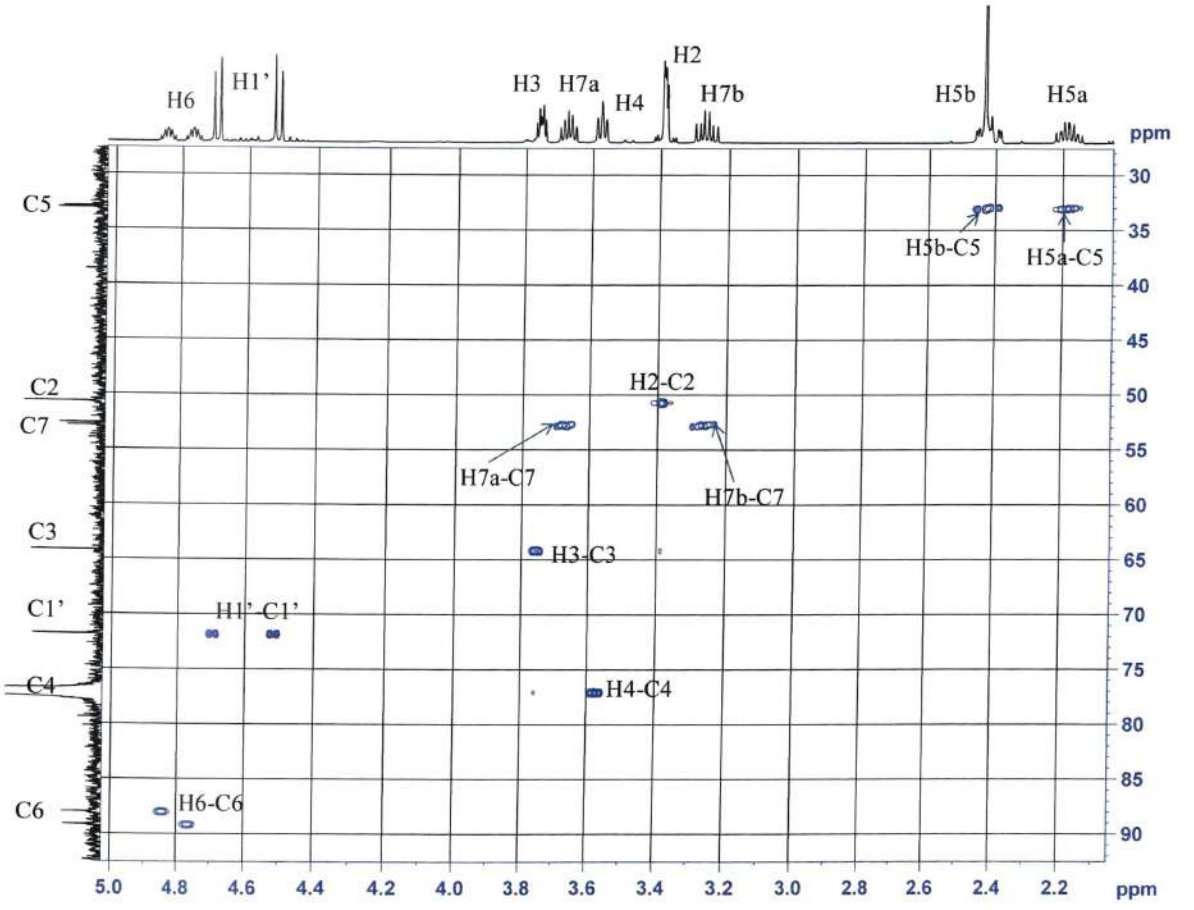
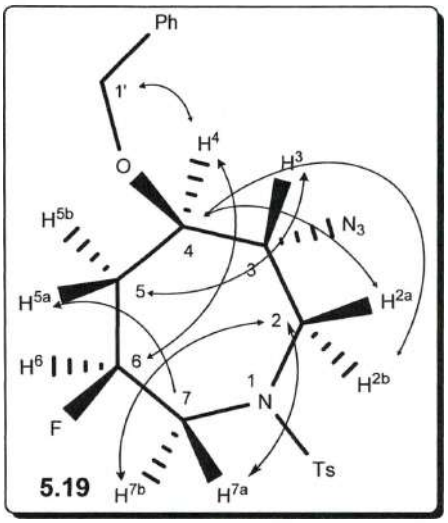


Figure 5.20. $^{1}H–^{13}C$ HSQC 2D NMR correlations of the azepane ring in **5.19**.

$^{1}H–^{13}C$ HMBC 2D NMR correlations:



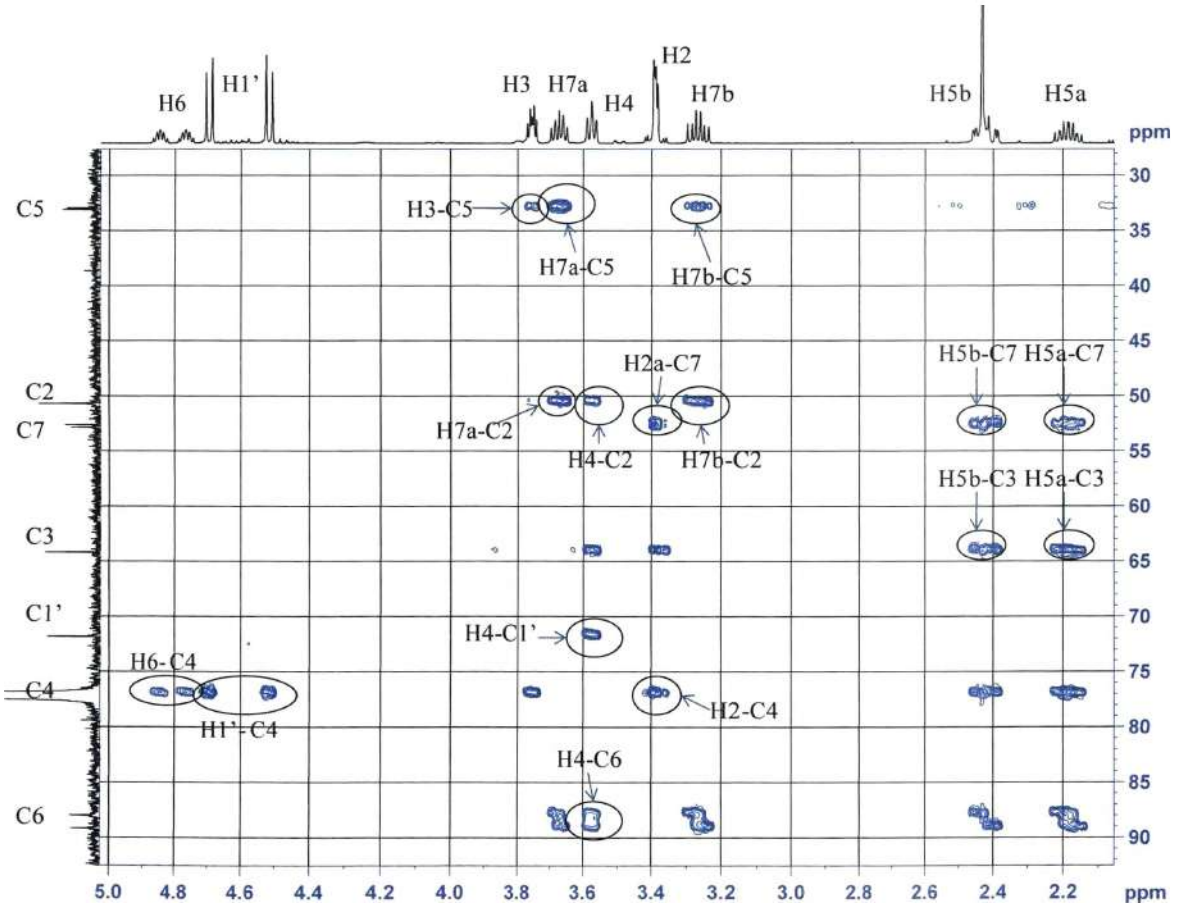
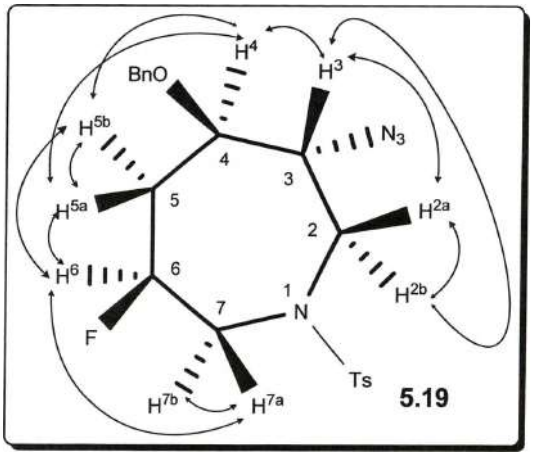


Figure 5.21. $^{1}H–^{13}C$ HMBC 2D NMR correlations of the azepane ring in **5.19**.

^1H–^1H COSY 2D NMR correlations:



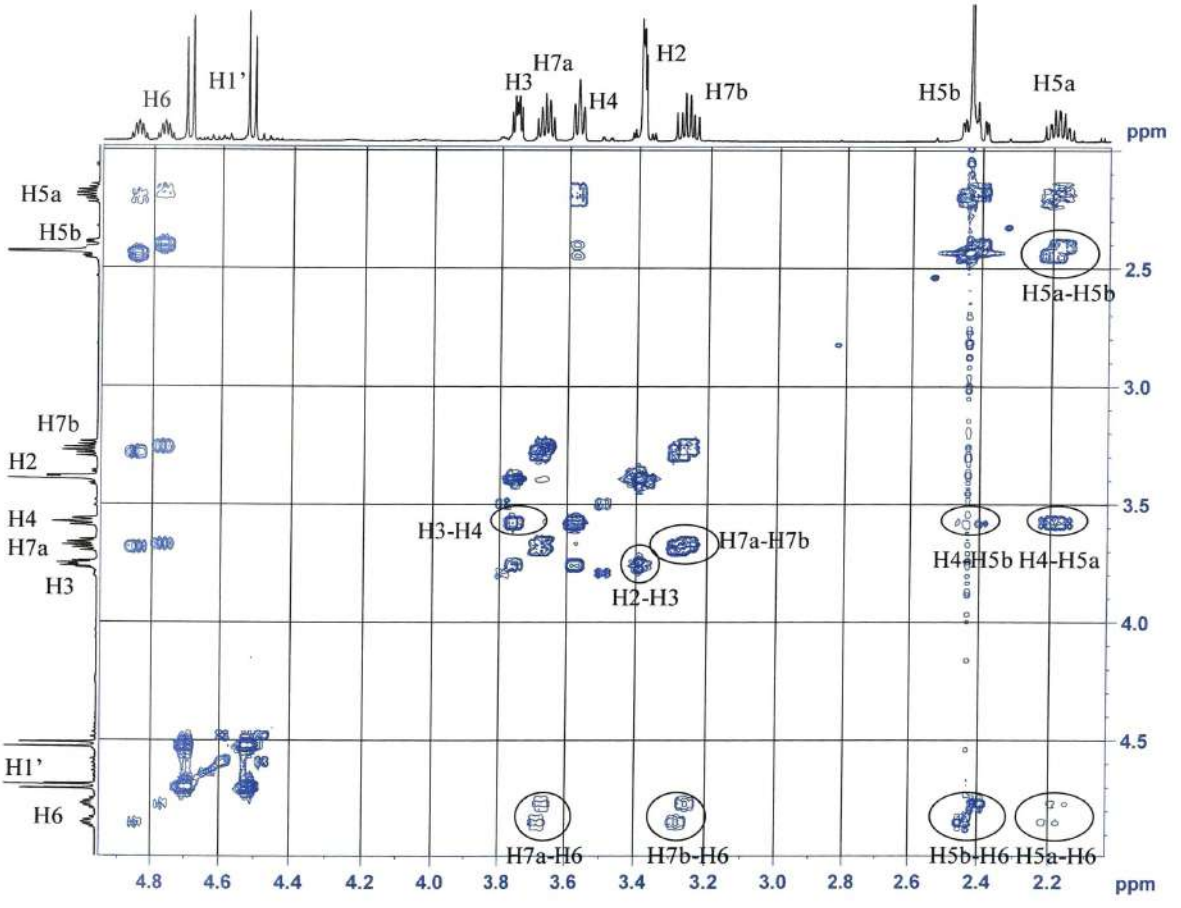


Figure 5.22. ^1H–^1H COSY 2D NMR correlations of the azepane ring in **5.19**.

^{1}H–^{1}H NOESY NMR correlations:

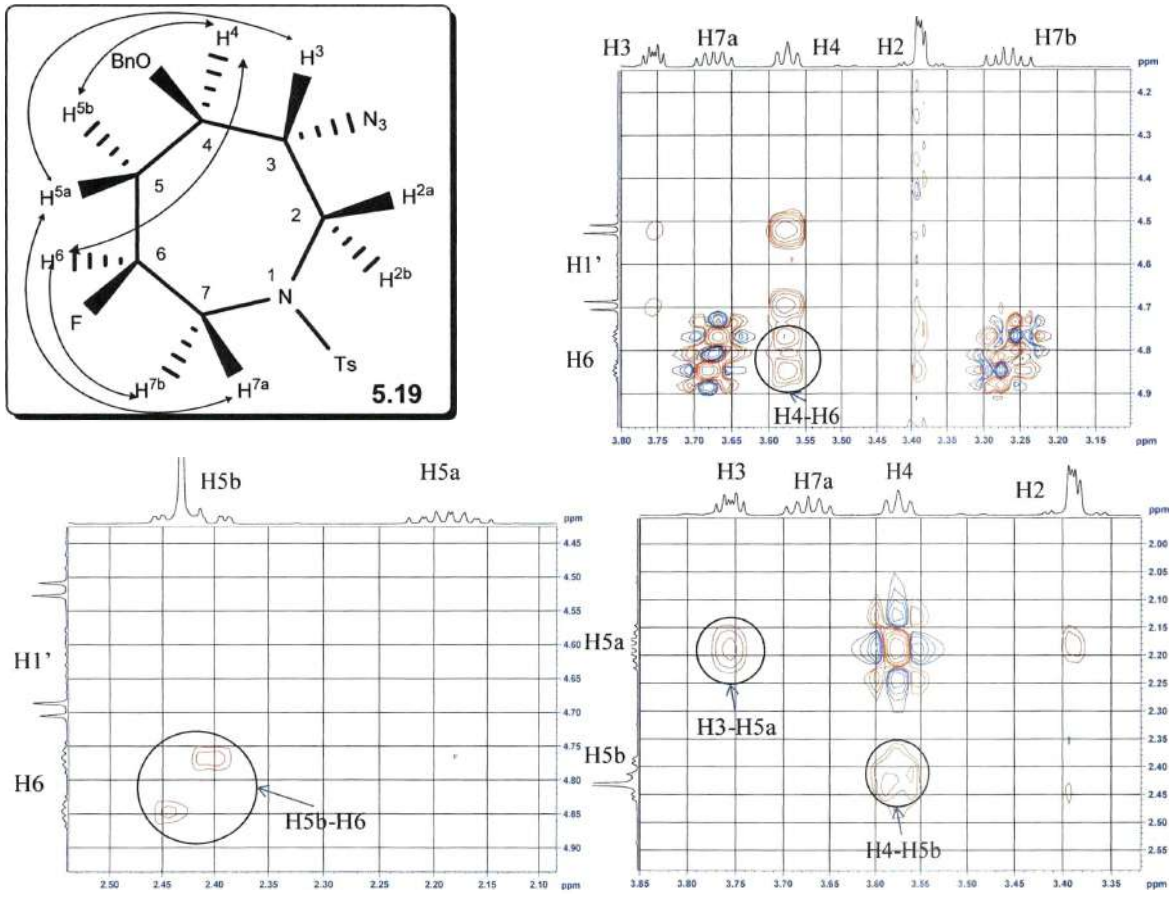
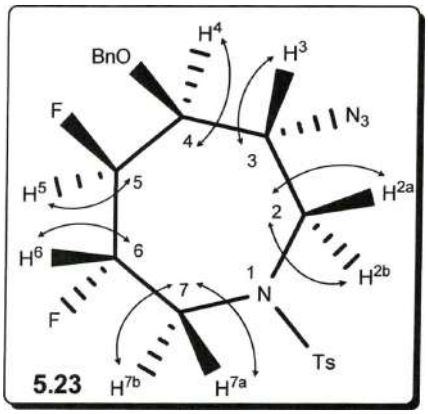


Figure 5.23. ^{1}H–^{1}H NOESY correlations of the azepane ring in **5.19**.

Assignment of the absolute stereochemistry of **5.19** at C6 as *S* was supported by strong NOE of H6 to H4 and H5b while no detactable NOE to H5a. H5a showed NOE to H3 while H5b showed NOE to H4. These results suggested the fluorination proceeded with *retention* of stereochemistry (*S*) at C6 in **5.19**.

Structure elucidation of difluoroazepane 5.23

^{1}H–^{13}C HSQC 2D NMR correlations:



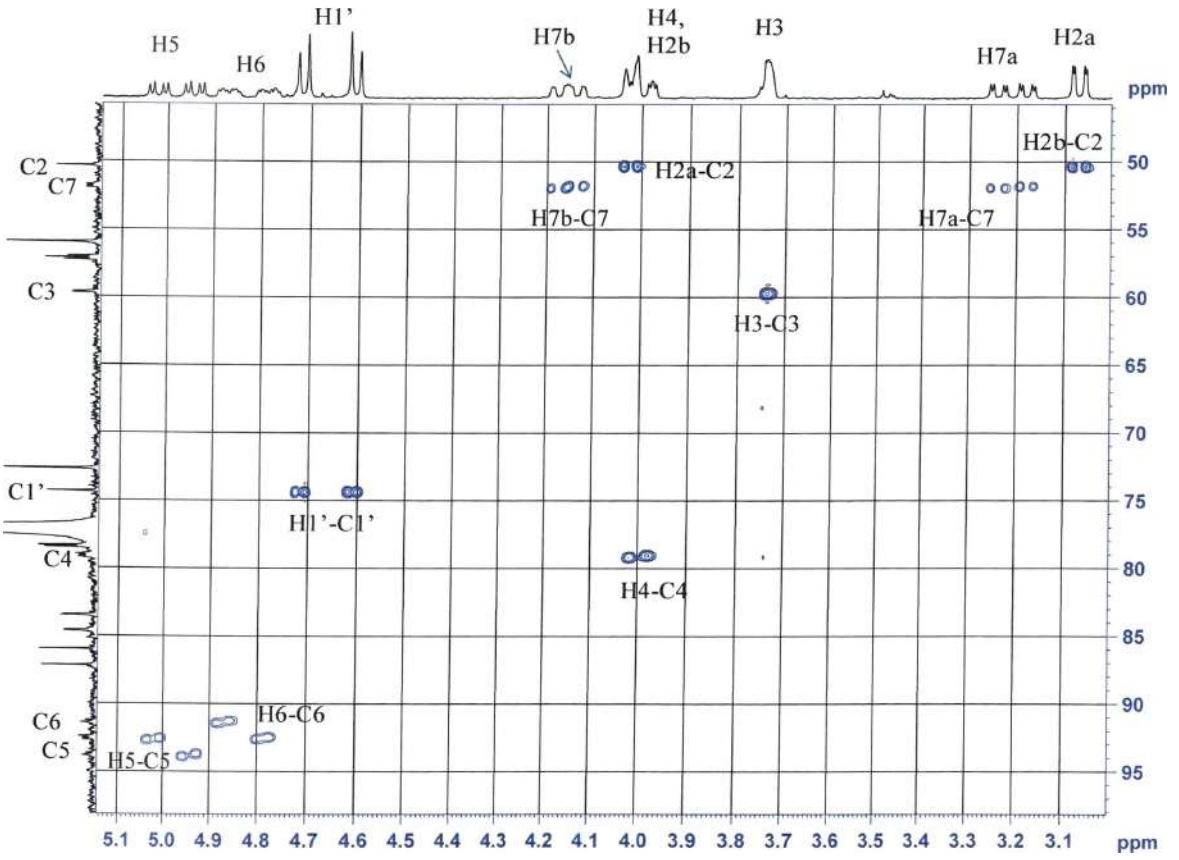
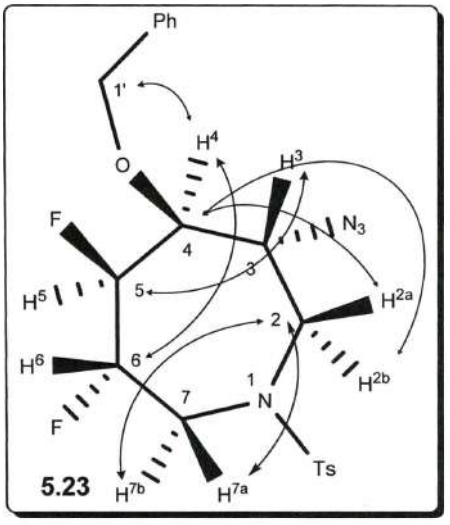


Figure 5.24. ^{1}H–^{13}C HSQC 2D NMR correlations of the azepane ring in **5.23**.

$^{1}H–^{13}C$ HMBC 2D NMR correlations:



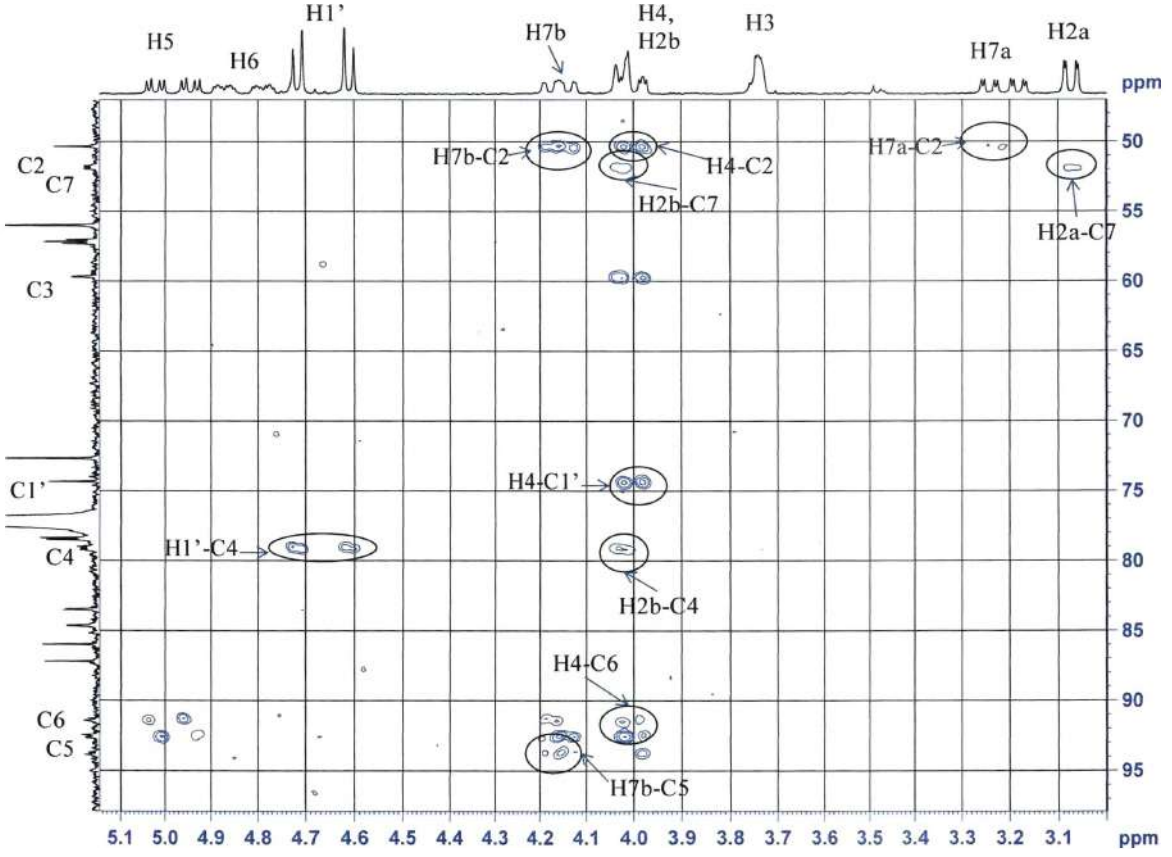
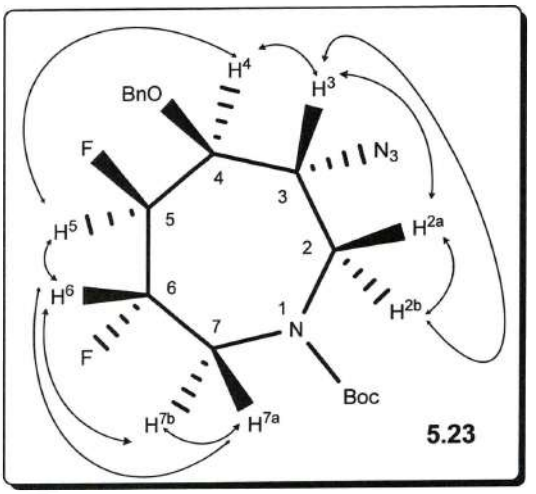


Figure 5.25. $^{1}H–^{13}C$ HMBC 2D NMR correlations of the azepane ring in **5.23**.

^{1}H–^{1}H COSY 2D NMR correlations:



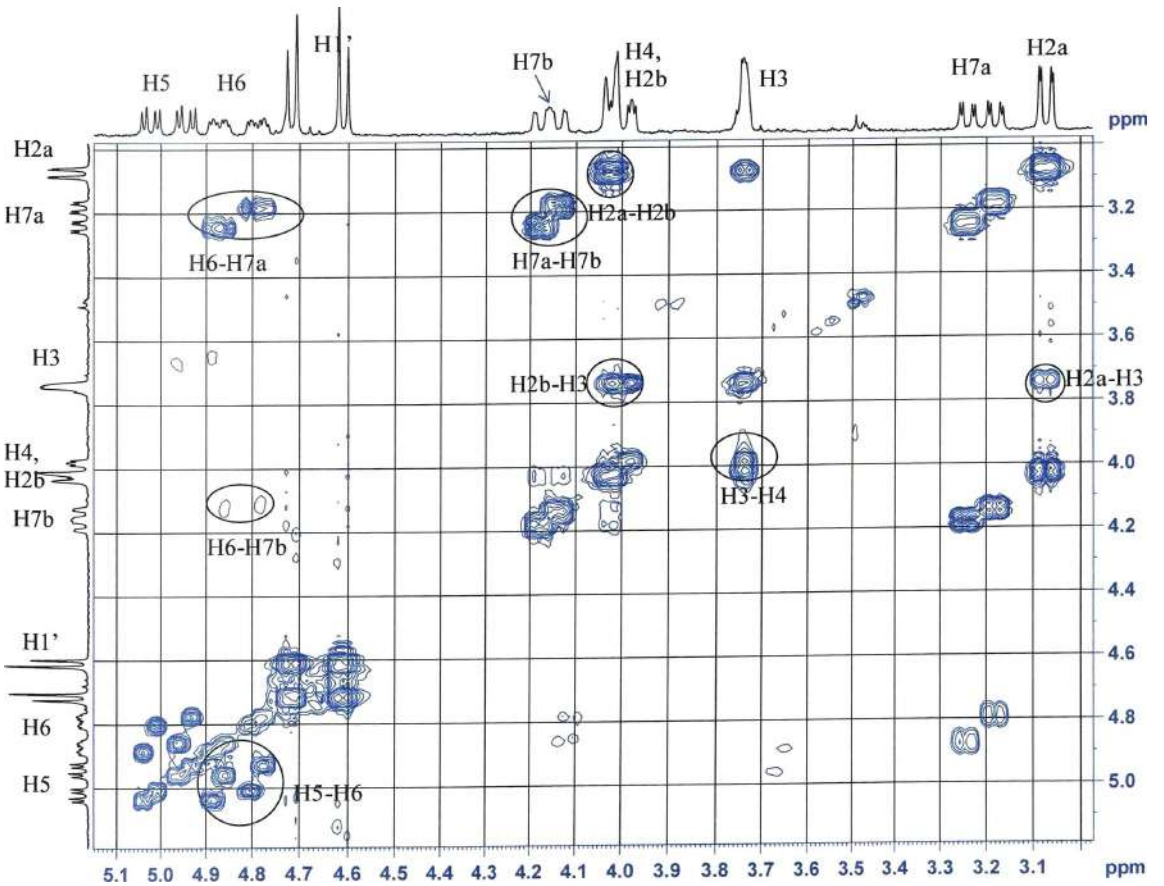
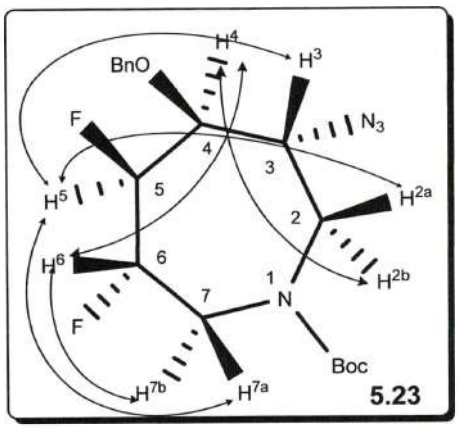


Figure 5.26. ^{1}H–^{1}H COSY 2D NMR correlations of the azepane ring in **5.23**.

^{1}H–^{1}H NOESY NMR correlations:



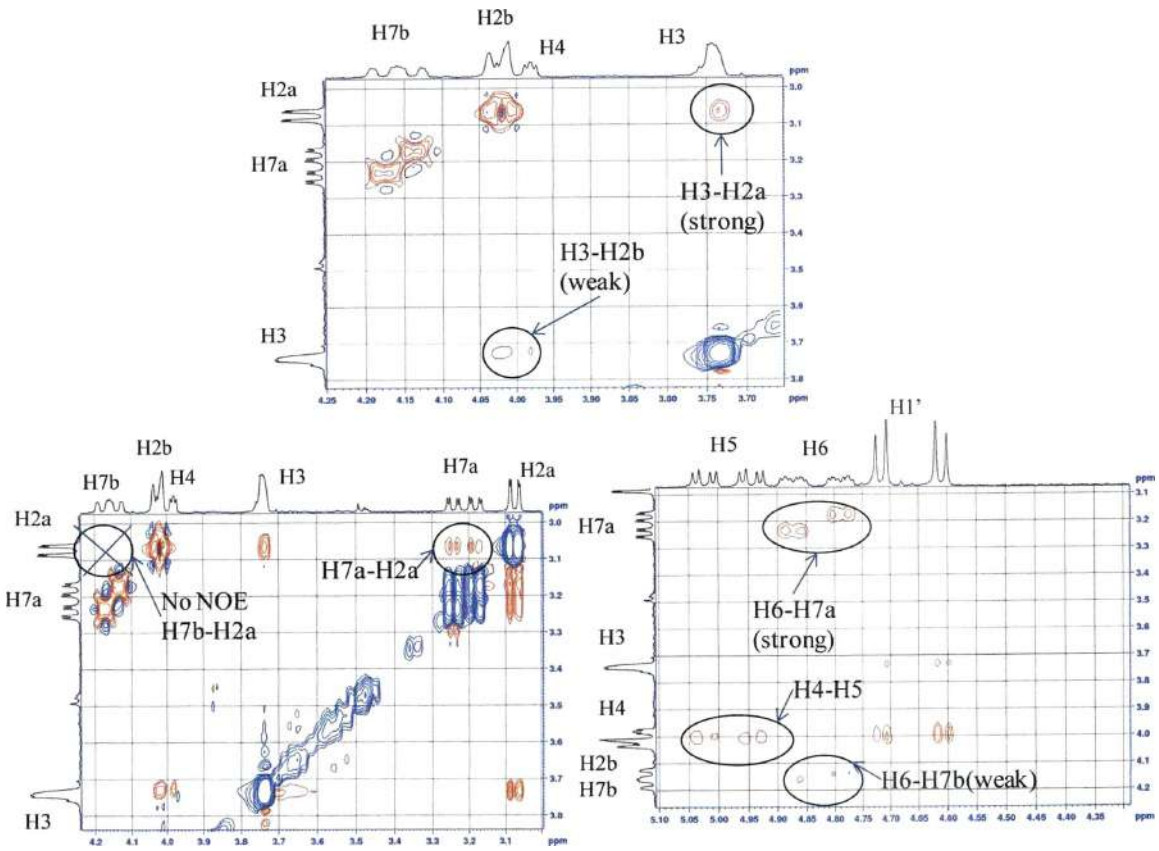


Figure 5.27. ^{1}H–^{1}H NOESY correlations of the azepane ring in **5.23**.

Structure elucidation of difluoroazepane 5.24

^{1}H–^{13}C HSQC 2D NMR correlations:

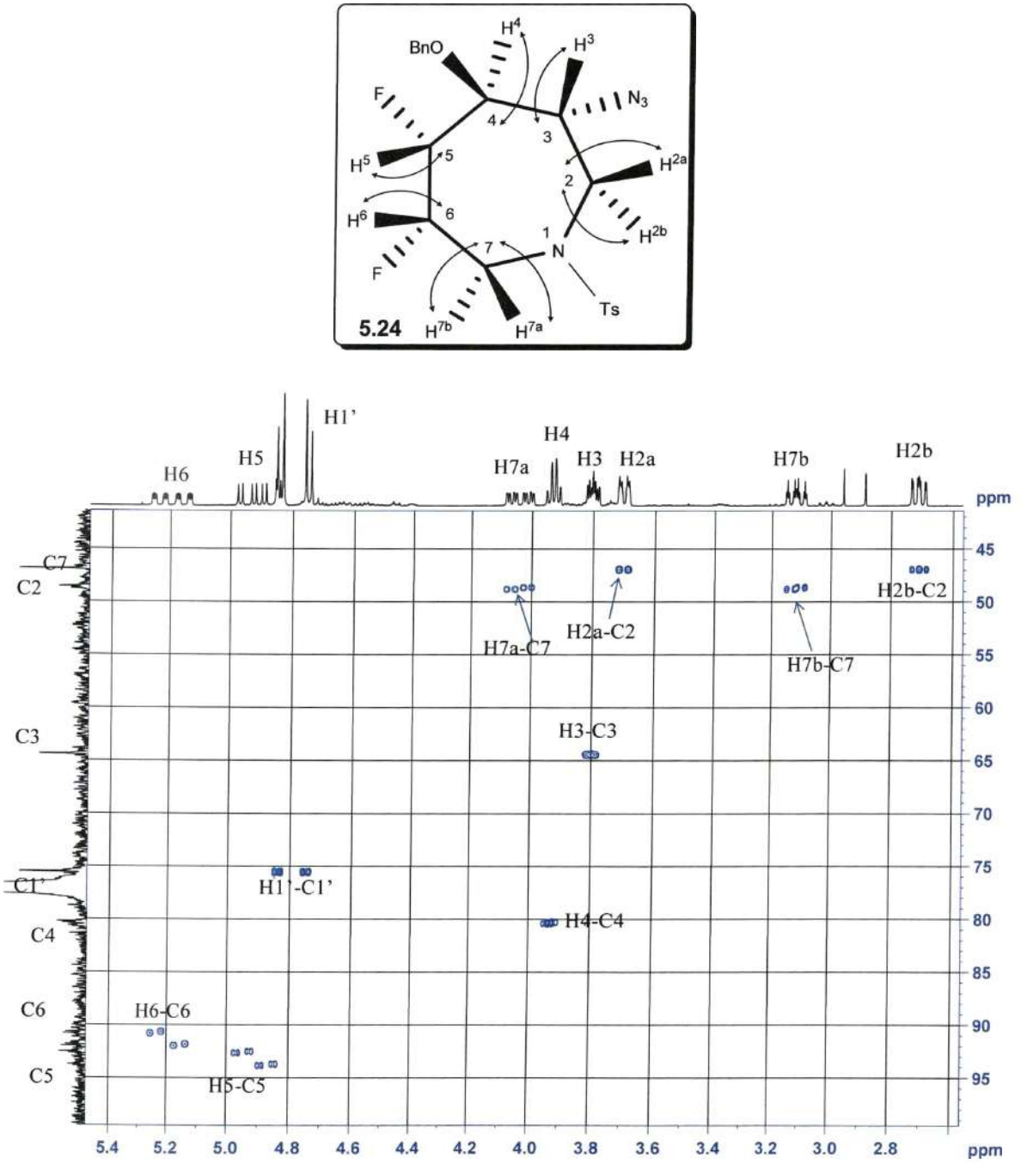


Figure 5.28. ^{1}H–^{13}C HSQC 2D NMR correlations of the azepane ring in **5.24**.

$^{1}H–^{13}C$ HMBC 2D NMR correlations:

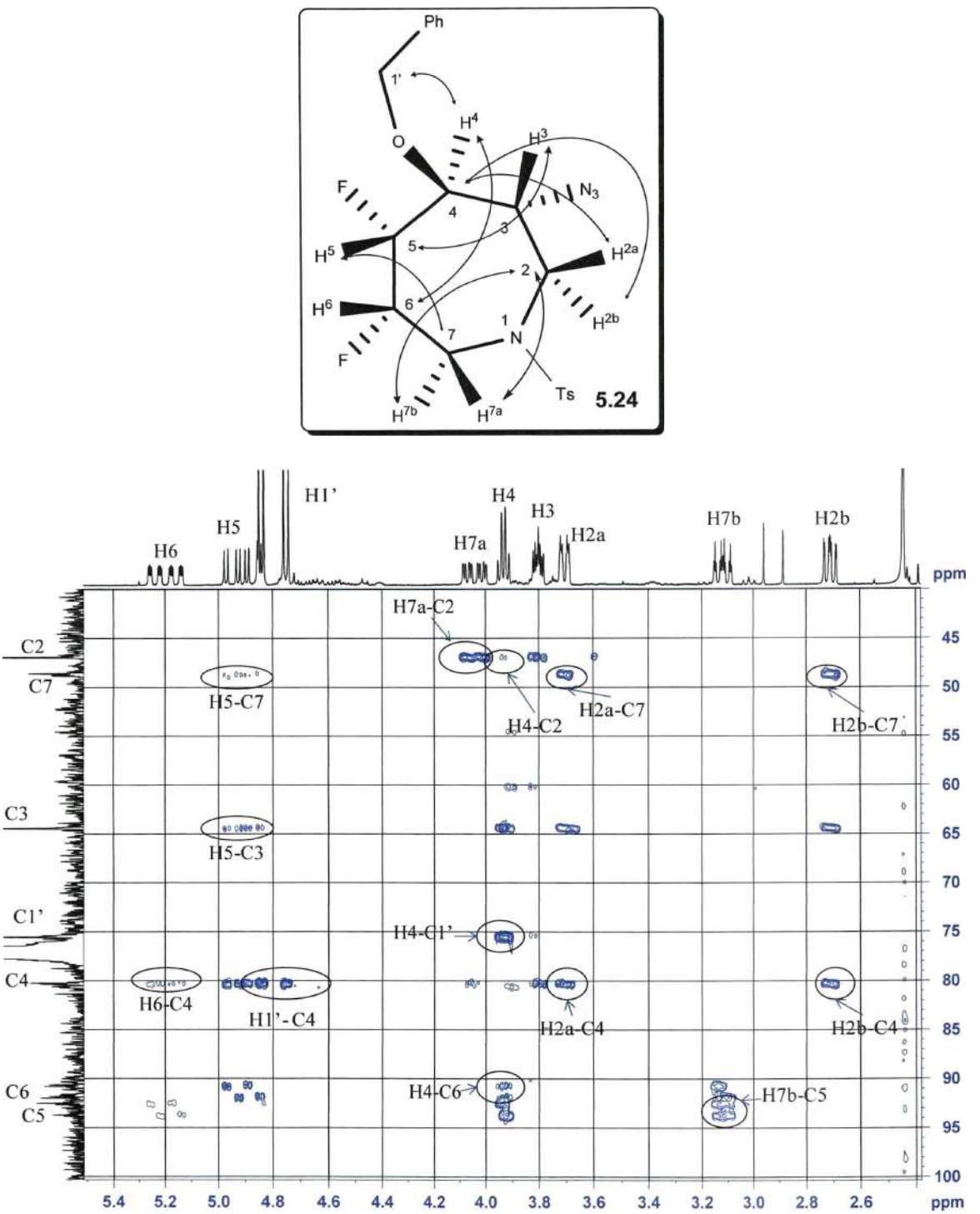
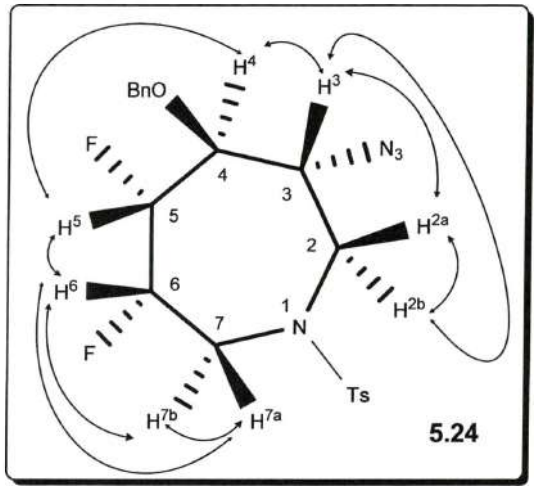


Figure 5.29. $^{1}H–^{13}C$ HMBC 2D NMR correlations of the azepane ring in **5.24**.

^{1}H–^{1}H COSY 2D NMR correlations:



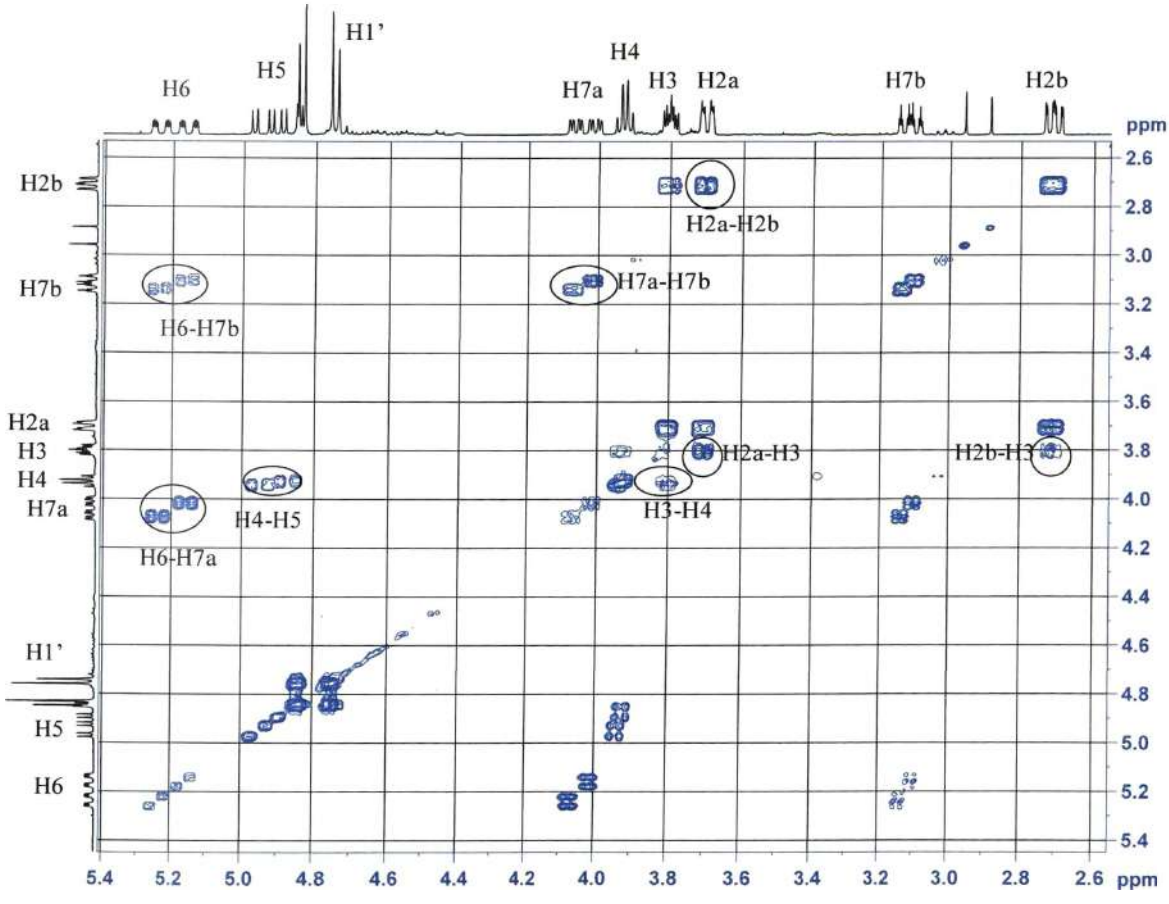


Figure 5.30. ^{1}H–^{1}H COSY 2D NMR correlations of the azepane ring in **5.24**.

^{1}H–^{1}H NOESY NMR correlations:

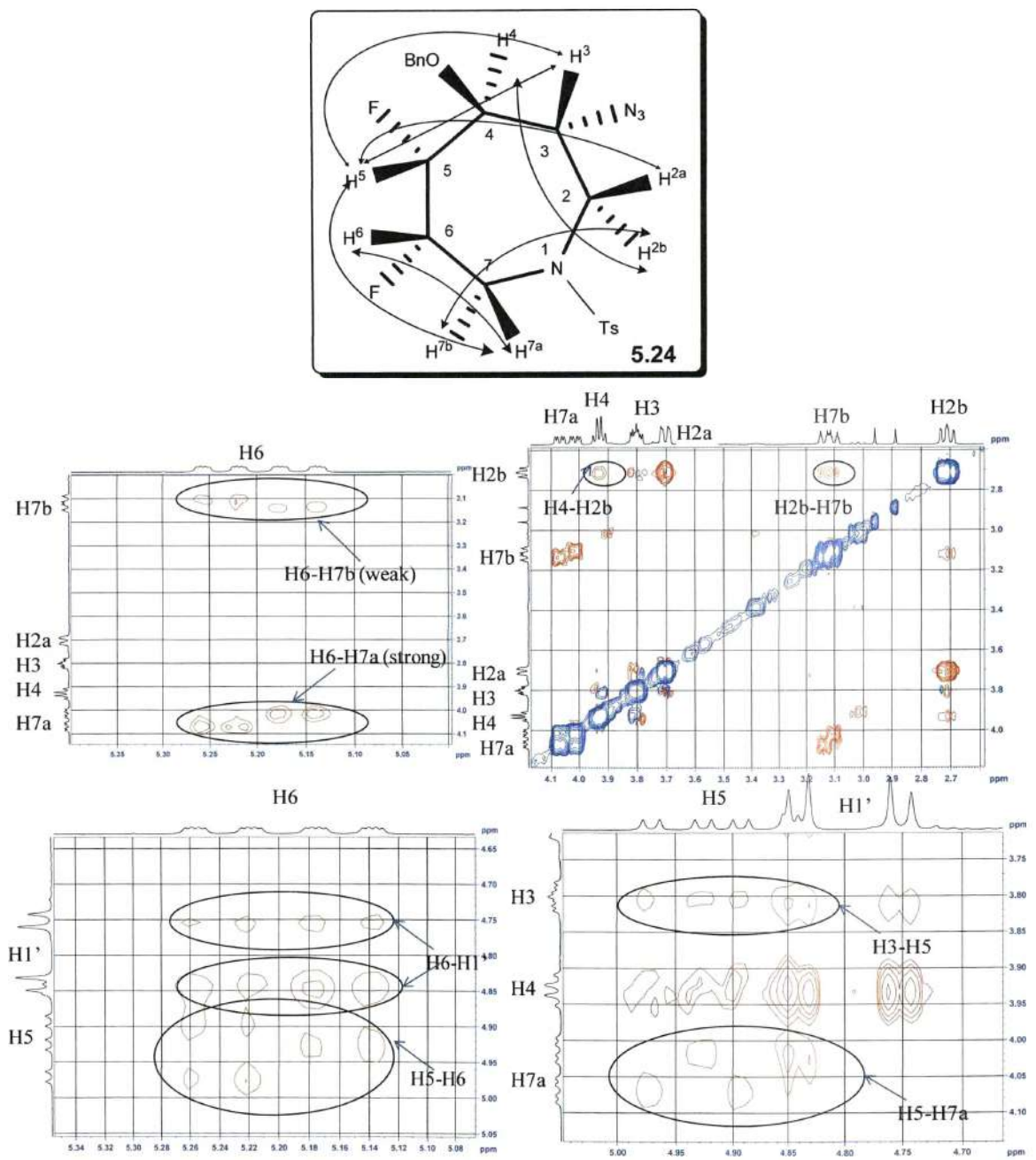


Figure 5.31. ^{1}H–^{1}H NOESY correlations of the azepane ring in **5.24**.

In **5.24**, H4 showed NOE to H2b while no detectable NOE to H2a. H2b showed NOE to H7b while no measurable NOE to H7a. H5 showed NOE to H3, H6, and H7a while H6 had NOE to

H1' and stronger NOE to H7a compared to H7b. This NOE data suggested the absolute configurations at C5 and C6 are *R* and *S*, respectively.

5.4. Conclusions

The fluoro–hydroxyazepanes **5.4** and **4.10** were synthesized from key tetrahydroazepine intermediate **2.7** in multiple steps. In **5.4** and **4.10**, it was anticipated that C6 deoxyfluorination would result in *retention* of stereochemistry without affecting the C5 fluorine. However, the results revealed that the C5–F bond was epimerized in both along with the formation of the ring contracted piperidine products confirming involvement of an aziridinium intermediate. The *N*–tosyl protected fluorohydroxyazepane **5.21** was synthesized to investigate the role of *N*–protecting group in the neighbouring group effect. The results showed that the C5 epimerization was supressed but not eliminated, and the piperidine derivative was isolated as the major product. The structure elucidations were secured unamiguously by two–diamentional NMR spectroscopy and X–ray crystallgraphy. Preliminary comutational studies furnished possible structures of fluoronium–aziridinium intermediates in solution and may account for the observed stereochemical lability.

5.5. References

(1) (a) Roberts, I.; Kimball, G. E. *J. Am. Chem. Soc.* **1937**, *59*, 947; (b) Struble, M. D.; Scerba, M. T.; Siegler, M.; Lectka, T. *Science* **2013**, *340*, 57; (c) Olah, G. A. *Halonium Ions*; Wiley: New York, 1975.

(2) (a) Nguyen, V.; Cheng, X.; Morton, T. H. *J. Am. Chem. Soc.* **1992**, *114*, 7127; (b) Wang, H.; Webster, C. E.; Perez, L. M.; Hall, M. B.; Gabbaie, F. P. *J. Am. Chem. Soc.* **2004**, *126*, 8189.

(3) Olah, G. A.; Surya, P. G. K.; Rasul, G. *Proc. Natl. Acad. Sci. U. S. A., Early Ed.* **2013**, 1.

(4) (a) Hunter, L.; Slawin, A. M. Z.; Kirsch, P.; O'Hagan, D. *Angew. Chem., Int. Ed.* **2007**, *46*, 7887; (b) Hunter, L.; Kirsch, P.; Slawin, A. M. Z.; O'Hagan, D. *Angew. Chem., Int. Ed.* **2009**, *48*, 5457.

(5) Fürstner, A.; Thiel, O. R. *J. Org. Chem.* **2000**, *65*, 1738.

(6) Shellhamer, D. F.; Anstine, D. T.; Gallego, K. M.; Ganesh, B. R.; Hanson, A. A.; Hanson, K. A.; Henderson, R. D.; Prince, J. M.; Heasley, V. L. *J. Chem. Soc., Perkin Trans. 2* **1995**, 861.

(7) Gao, Y.; Sharpless, K. B. *J. Am. Chem. Soc.* **1988**, *110*, 7538.

(8) Hamatani, T.; Matsubara, S.; Matsuda, H.; Schlosser, M. *Tetrahedron* **1988**, *44*, 2875.

(9) Marson, C. M.; Melling, R. C. *J. Org. Chem.* **2005**, *70*, 9771.

(10) Alves Benicio, A. A.; Da Silva, A. D.; De Almeida, M. V.; Da Silva, M. M.; Dov Gero, S. *Tetrahedron* **2001**, *57*, 1161.

(11) Hunter, L.; Jolliffe, K. A.; Jordan, M. J. T.; Jensen, P.; MacQuart, R. B. *Chem. - Eur. J.* **2011**, *17*, 2340.

(12) Patel, A. R.; Liu, F. *Tetrahedron* **2013**, *69*, 744.

(13) (a) Ferret, H.; Dechamps, I.; Gomez, P. D.; Van, H. L.; Cossy, J. *ARKIVOC* **2010**, 126; (b) Dechamps, I.; Pardo, D. G.; Cossy, J. *Synlett* **2007**, 263; (c) Dechamps, I.; Gomez, P. D.; Cossy, J. *Eur. J. Org. Chem.* **2007**, 4224; (d) Anxionnat, B.; Robert, B.; George, P.; Ricci, G.; Perrin, M.-A.; Gomez, P. D.; Cossy, J. *J. Org. Chem.* **2012**, *77*, 6087.

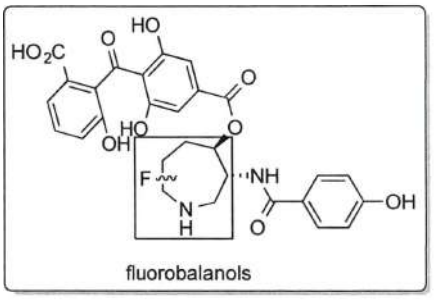
(14) Jaseer, E. A.; Naidu, A. B.; Kumar, S. S.; Rao, R. K.; Thakur, K. G.; Sekar, G. *Chem. Commun.* **2007**, 867.

(15) (a) Olah, G. A.; Rasul, G.; Hachoumy, M.; Burrichter, A.; Prakash, G. K. S. *J. Am. Chem. Soc.* **2000**, *122*, 2737; (b) DeFrees, D. J.; McLean, A. D. *J. Chem. Phys.* **1985**, *82*, 333; (c) McAllister, M.; Tidwell, T. T.; Peterson, M. R.; Csizmadia, I. G. *J. Org. Chem.* **1991**, *56*, 575; (d) Olah, G. A.; Prakash, G. K. S.; Rasul, G. *Proc. Natl. Acad. Sci. U. S. A.* **2013**, *110*, 8427; (e) Stams, D. A.; Thomas, T. D.; MacLaren, D. C.; Ji, D.; Morton, T. H. *J. Am. Chem. Soc.* **1990**, *112*, 1427; (f) Krow, G. R.; Lin, G.; Rapolu, D.; Fang, Y.; Lester, W. S.; Herzon, S. B.; Sonnet, P. E. *J. Org. Chem.* **2003**, *68*, 5292; (g) Ohta, B. K.; Scupp, T. M.; Dudley, T. J. *J. Org. Chem.* **2008**, *73*, 7052; (h) Ford, G. P.; Raghuveer, K. S. *Tetrahedron* **1988**, *44*, 7489.

CHAPTER 6

Synthesis and Activity of Fluorinated Balanol Analogues

Six mono–, di–, and tri–fluoroazepanes were utilized to synthesize balanol analogues using reported protocols for balanol synthesis. The binding affinities (K_d's) of analogues to PKC isozymes and PKA were compared to those of (−)–balanol.



fluorobalanols

6.1. Introduction

Several structure activity relationship studies have been accomplished for balanol analogues with better protein kinase C isozymes pecificity and cellular activity (Chapter 1, Section 1.2.4). Particularly, balanol analgoues with modified perhydroazepane moiety have shown that the activity and the kinase/isozyme selectivity of these compounds are largely dependent on the perhydroazepane moiety.[1] Several chemical modifications, such as different ring sizes, different heteroatoms and different nitrogen substitution have been investigated.[1-2] However, balanol analogues with single PKC isozyme selectivity have not been found till date. The example of Gleevec demonstrated that an ATP mimicking small molecule can recognise a unique conformation of a kinase active site. Here, fluorinated balanol analgoues were synthesized as an attempt to understand the potential chemical/conformational effects of fluorine substitution on the azepane ring in terms of altering the affinity and specificity profile of balanol for PKA/PKC isozymes.

The synthesis of (−)–balanol was accomplished using Nicolaou's[3] and Fürstner's[4] methods. The synthesis and conformational analysis of mono–, di–, and trifluoroazepanes is discussed in previous chapters (Chapter 2–5). These azepanes were utilized for the synthesis of fluorinated balanol analogues (Figure 6.1). The fluorinated analogues were then subjected to a competitive binding kinase assays (KINOME*scan*™, performed by DiscoveRx, San Diego). The binding profiles (K_d's) of these analogues were compared with those from the parent (−)–balanol (**1.1**) (Table 6.1).

6.2. Results and Discussion

6.2.1. Total Synthesis of (−)–Balanol (1.1)

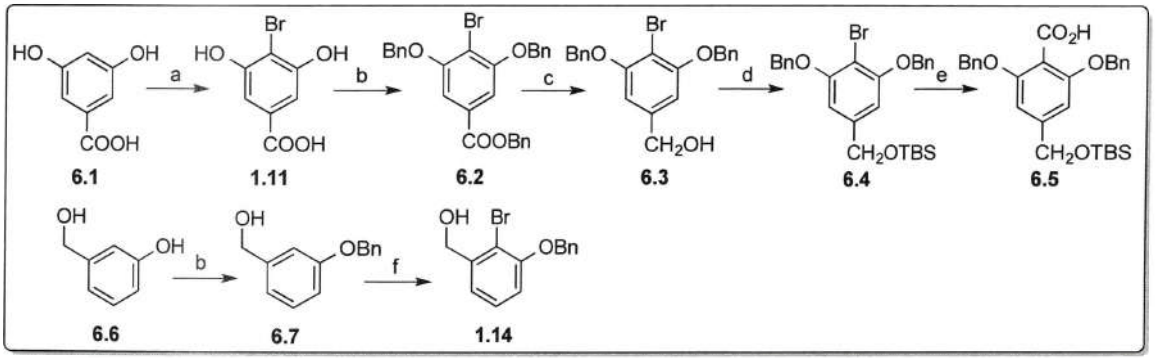
The literature protocols were reproduced with minor modifications to synthesize (−)–balanol (**1.1**). Fürstner's protocol[4] was used for the synthesis of hexahydroazepane core (**1.10**) of balanol. The benzophenone fragment was synthesized using Nicolaou's methods[3] with minor modifications. The coupling of the azepane core to the benzophenone fragment was furnished again following Nicolaou's protocol[3a] to afford (−)–balanol (**1.1**) in 70% yield after universal deprotection.

6.2.1.1. Synthesis of the Benzophenone Fragment (1.28)

The benzophenone fragment was synthesized by coupling the aromatic fragments **1.14** and **6.5** using Mitsunobu esterification[5] followed by lithium–halogen exchange to obtain the key benzophenone intermediate **6.9** in good yield (Scheme 6.2).

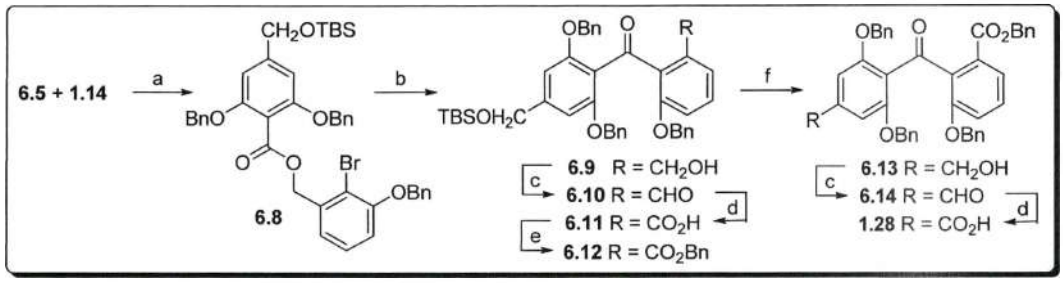
The necessary alcohol fragment **1.14** was synthesized in two steps: (i) benzylation of phenolic OH of commercially available 3–hydroxybenzyl alcohol (**6.6**) using benzyl bromide/K_2CO_3 in DMF to provide **6.7** in 88% yield; (ii) regiospecific lithiation by Comins' protocol[6], and this aryllithium species was trapped with 1,2–dibromotetrafluoroethane[7] to afford the bromide **1.14** as a single regioisomer in 50% yield (Scheme 6.1). The carboxylic acid counterpart **6.5** was synthesized using a five–step sequence commencing with regioselective nucleophilic aromatic bromination of commercially available carboxylic acid **6.1** using bromine in acidic conditions to provide **1.11** in quantitative yield. **1.11** was tribenzylated readily using standard benzyl protection protocol to furnish benzyl ester **6.2**, which was next reduced, with DIBALH to the corresponding primary alcohol **6.3** in 96% yield. The alcohol **6.3** then was protected as a silyl ether (TBS) for conversion to the functionalized aryl bromide **6.4** in excellent yield, which

was next subjected to lithium–halogen exchange with *n*–butyllithium, and the resulting aryllithium species was trapped with carbon dioxide to provide the desired carboxylic acid **6.5** in fair yield (55% overall) (Scheme 6.1).



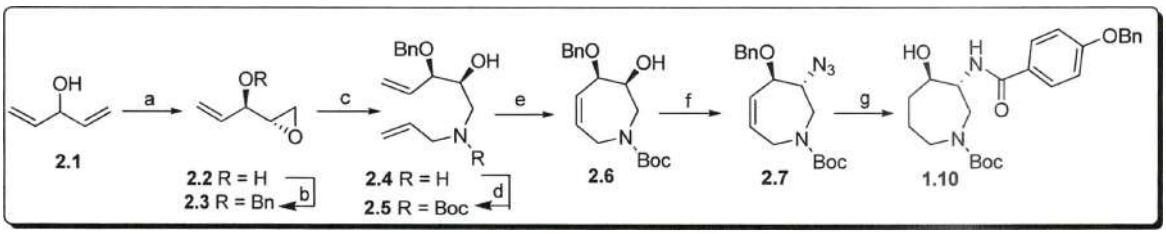
Scheme 6.1. Synthesis of the key fragments **6.5** and **1.14**. *Reactions and conditions*: (a) Br_2, HCl, reflux, 2 h, 98%; (b) BnBr, K_2CO_3, DMF, 25 °C, 12–14 h, 88–94%; (c) DIBALH, DCM, −78 °C, 0 °C, 1.5 h, 96%; (d) TBSCl, imidazole, DCM, 0 °C, 1.5 h, 91%; (e) i) *n*–BuLi, THF, −78 °C; ii) CO_2; iii) $KHSO_4$; (f) i) *n*–BuLi, toluene, −10 °C, 6 h; ii) $BrCF_2CF_2Br$, −78 °C→25 °C, 16 h; iii) NH_4Cl, 50 %.

The coupling of **1.14** and **6.5** was achieved by the Mitsunobu esterification[5] to afford the key ester intermediate **6.8** in 88% yield. The aryllithium species resulting from the low temperature (−98 °C) treatment of **6.8** with *n*–butyllithium successfully underwent the desired Fries rearrangement to afford the primary alcohol **6.9** upon protic workup in 84% yield (Scheme 6.2). This alcohol was oxidized readily to the corresponding aldehyde **6.10** in 95% yield with TPAP/NMO.[8] The sodium chlorite oxidation[9] was employed to furnish the carboxylic acid **6.11**, which was benzylated to afford **6.12** in 95 % yield. Subsequent TBAF–mediated desilylation of **6.12** provided alcohol **6.13** (92% yield), which was further subjected to similar oxidation protocols to furnish the final benzophenone component **1.28** in 61% yield over two steps. The above approach (Scheme 6.1 and 6.2) thus furnished targeted benzophenone fragment **1.28** from **6.1** in 13% overall yield in 15 steps, which is comparable with the literature report.



Scheme 6.2. Synthesis of the benzophenone fragment **1.28**. *Reactions and conditions*: (a) DEAD, PPh_3, THF, 25 °C, 1 h, 88%; (b) *n*–BuLi, THF, −98 °C, 45 min, 84%; (c) NMO, TPAP, MeCN, 30 min, 25 °C, 67–95%; (d) $NaClO_2$, NaH_2PO_4, 2–methyl–2–butene, THF, *t*–BuOH, H_2O, 14 h, 25 °C, 88–91%; (e) BnBr, K_2CO_3, DMF, 1.5 h, 25 °C, 95%; (f) TBAF, THF, 15 min, 25 °C, 92%.

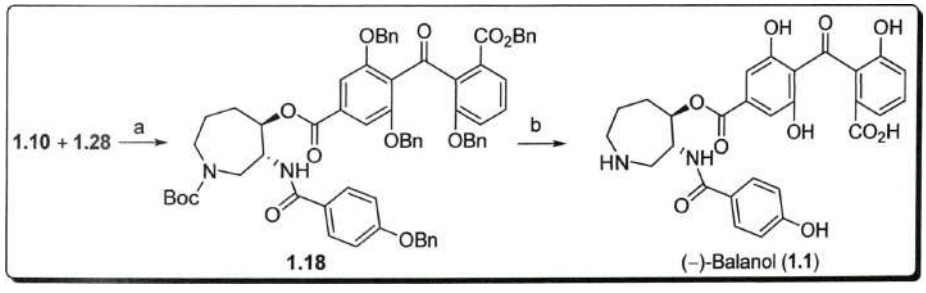
6.2.1.2. Synthesis and Coupling of the Azepane Core (1.10) with Benzophenone (1.28)



Scheme 6.3. Synthesis of the azepane core **1.10**. *Reactions and conditions*: (a) (D)–(−)–DIPT, cumene hydroperoxide, $Ti(O^iPr)_4$, CH_2Cl_2, −35 °C, 83%, >99% *ee*; (b) NaH, BnBr, THF, 14 h, 25 °C, 93%.; (c) Allyl amine (neat), 40 h, 70 °C, 95%; (d) Boc_2O, Et_3N, CH_2Cl_2, 16 h, 25 °C, 96%; (e) Grubbs catalyst, CH_2Cl_2, 42 h, 86%; (f) PPh_3, DEAD, $(PhO)_2P(O)N_3$, THF, 2 h, 25 °C, 89%; (g) i) H_2, Pd/C, triflic acid, MeOH, 14 h, 25 °C; ii) Et_3N, 4–benzyloxybenzoyl chloride, 2 h, 25 °C, 52% (over two steps).

The synthesis of key azepane **2.7** following Fürstner's formal synthesis[5] has already been described in Chapter 2 and is presented in Scheme 6.3. The tetrahydroazepine **2.7** was subjected to palladium catalyzed hydrogenation under acidic conditions (1 equiv. triflic acid) to reduce the azide and double bond with concurrent debenzylation to provide the primary amine **1.9**. The amine was immediately utilized for the amidation reaction with 4–benzyloxybenzoyl chloride to furnish the target azepane core **1.10** of balanol in 52% yield (from **2.7**) (Scheme 6.3). Overall, the synthesis of **1.10** was successfully reproduced with yields comparable to that in the literature report.

The coupling of benzophenone (**1.28**) and azepane (**1.10**) fragments was successfully accomplished via esterification using the Mukaiyama procedure to afford the fully protected balanol progenitor **1.18** in 75% yield (Scheme 6.4). The universal benzyl deprotection was achieved by mild palladium–catalyzed hydrogenolysis of **1.18** in acidic media to obtain the Boc protected balanol as a yellow solid, which was subjected to purification by reverse phase HPLC. The Boc deprotection was readily achieved by treatment with neat TFA to furnish balanol (**1.1**) in 70% yield, which exhibited characterization data consistent with the proposed structure and a ^{1}H NMR spectrum of an authentic sample.



Scheme 6.4. Synthesis of the balanol **1.1**. *Reactions and conditions*: (a) 2–chloro–1–methylpyridinium iodide, DMAP, NEt_3, DCM, 8 h, 25 °C, 75%; (b) i) H_2, Pd/C, THF, H_2O, AcOH, 25 °C, 10 h; ii) TFA, neat, 5 min., 25 °C, 70%.

6.2.2. Synthesis of Fluorinated Balanol Analogues

The following fluoroazepanes were utilized for the synthesis of fluorinated balanol analogues (Figure 6.1).

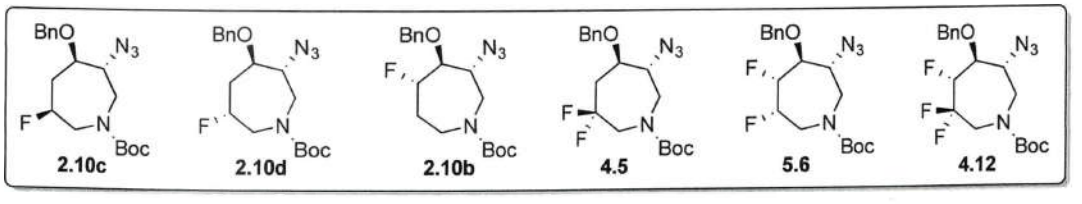
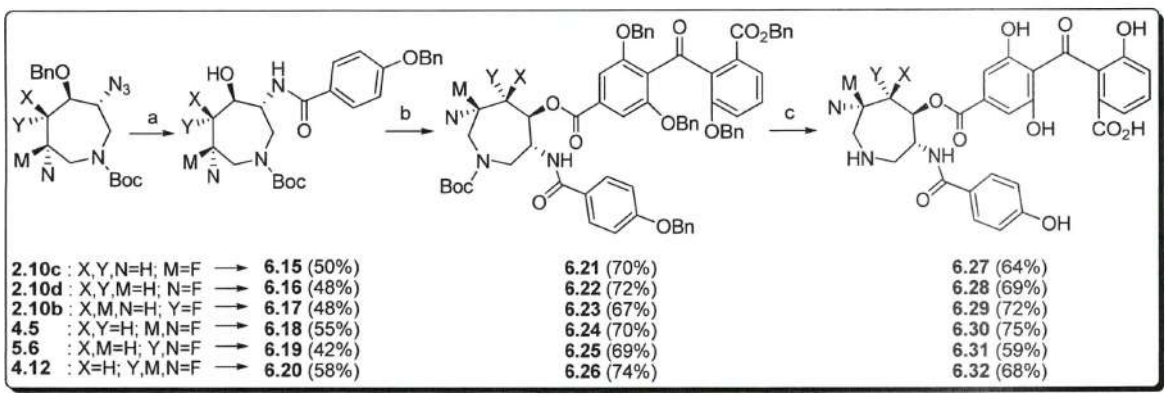


Figure 6.1. Azepanes for fluorinated balanol analogues synthesis.

These azepanes were subjected to the coupling protocol identical to that used in the total synthesis of (−)–balanol (**1.1**). The palladium catalyzed hydrogenation in acidic conditions followed by amidation afforded 3,4–*trans*–aminohydroxy azepanes (**6.15–6.20**) which were coupled with benzophenone (**1.28**) to furnish fluorinated, fully protected balanol analogues (**6.21–6.26**). Finally, the universal deprotection reaction furnished the fluorinated balanol analogues (**6.27–6.32**) in fair yields (Scheme 6.5) after purification by reverse phase HPLC.



Scheme 6.5. Synthesis of balanol analogues **6.27–6.32**. *Reactions and conditions*: (a) i) H_2, Pd/C, triflic acid, MeOH, 14 h, 25 °C; ii) Et_3N, 4–benzyloxybenzoyl chloride, 2 h, 25 °C; (b) 2–chloro–1–methylpyridinium iodide, DMAP, NEt_3, DCM, 8 h, 25 °C; (c) i) H_2, Pd/C, THF, H_2O, AcOH, 25 °C, 10 h; ii) TFA, neat, 5 min., 25 °C.

6.2.3. Binding Studies of Compounds 6.27–6.32 against Protein Kinases[10]

The biological studies on the compounds **6.27–6.32** were carried out by DiscoverRx, USA using the assay KINOME*scan*™.[10] KINOME*scan*™ is a competition–binding assay with quantitative measurement of the ability of a compound to compete with an immobilized, active–site directed ligand. The assay utilizes three components: a DNA–tagged kinase; an immobilized ligand; and a test compound. The ability of the test compound to compete with the immobilized ligand is measured via quantitative PCR of the DNA tag.

KINOME*scan*™ Assay Principle

Compounds that bind the kinase active site and directly (sterically) or indirectly (allosterically) prevent kinase binding to the immobilized ligand and consequently reduce the amount of kinase captured on the solid support (A & B). Conversely, test molecules that do not bind the kinase have no effect on the amount of kinase captured on the solid support (C) (Figure 6.2). The dissociation constants (K_d's) for test compound–kinase interactions are calculated by measuring the amount of kinase captured on the solid support as a function of the test compound concentration by using a quantitative, precise and ultra–sensitive qPCR method that detects the associated DNA label (D).

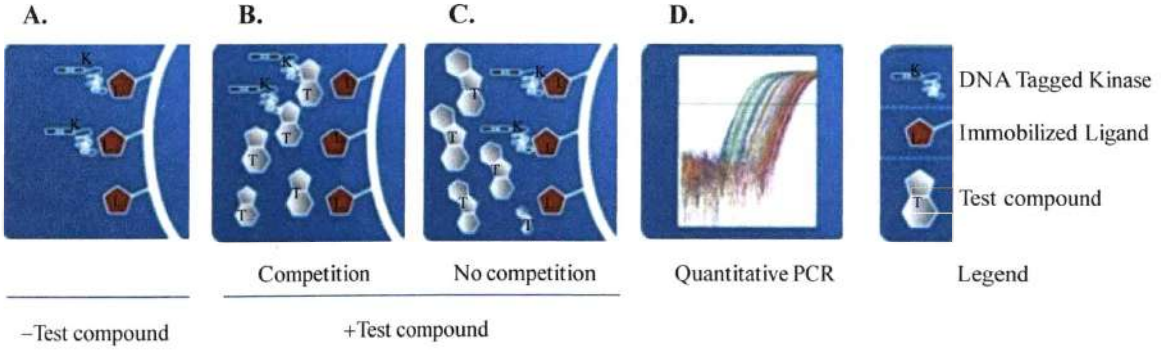


Figure 6.2. KINOME*scan*™ assay schematic representation.[10]

Binding Affinities (K_d's)

The binding constants (K_d's) were calculated with a standard dose–response curve using the Hill equation:

$$\text{Response} = \frac{\text{Signal - Background}}{1 + (K_d^{\text{Hill Slope}}/\text{Dose}^{\text{Hill Slope}})}$$

The Hill Slope was set to −1. Curves were fitted using a non–linear least square fit with the Levenberg–Marquardt algorithm.

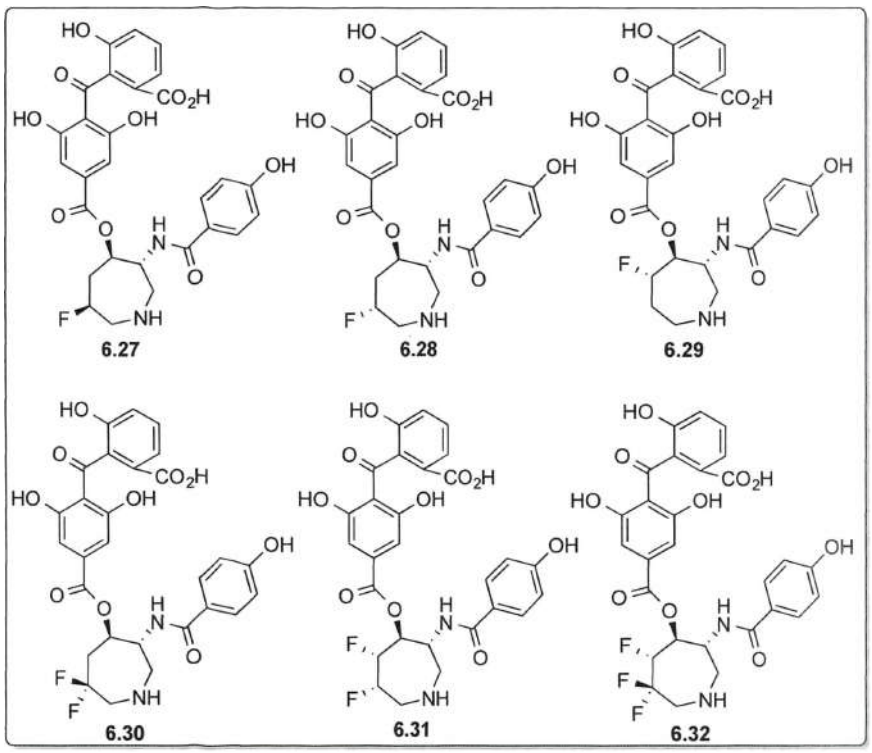


Table 6.1. K_d's of compounds **6.27–6.32**

Target	K_d (nM)						
Gene Symbol	**1.1**	**6.27**	**6.28**	**6.29**	**6.30**	**6.31**	**6.32**
PKAC–alpha	5.9	7.9	6.9	6.4	9.2	41	43
PRKCD (delta)	4.5	17	15	4.9	19	24	18
PRKCE (epsilon)	0.73	19	24	0.4	110	26	38
PRKCH (eta)	14	38	16	13	19	36	12
PRKCQ (theta)	25	120	140	24	580	480	850
PRKCI (iota)	nd	nd	nd	nd	40000	40000	40000

nd = K_d's for PKCι were not determined as the initial screen at 10mM concentration showed low activity.

The K_d values measured for the analogues **6.27–6.32** are presented in the Table 6.1. All of the PKC isozymes available at DiscoveRx were screened. The conventional PKCs were not tested; however PKA was included, which is highly homologous to conventional PKC isozymes. All of the novel PKCs were included in the study and PKCι was chosen as a

representative of atypical PKCs. However, it displayed low affinity for all the molecules tested and hence not included in the discussion.

The kinase binding assays revealed that most of the K_d values remained in the nM range showing that fluorination can be tolerated for PKA and most PKCs. The parent molecule (−)–balanol (**1.1**) was found to have the highest binding affinity to PKCε and lowest to PKCθ. The PKCε affinity was higher by 6, 8, 19 and 34 fold than that to PKCδ, PKA–α, PKCη, and PKCθ, respectively (column 2, Table 6.1) (PKCε > PKCδ > PKA–α > PKCη > PKCθ). Thus, balanol showed some limited isozyme selectivity.

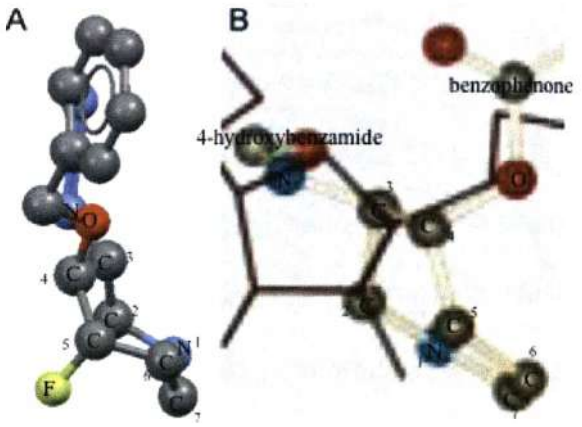


Figure 6.3. Comparison of major conformer of azepane **2.11b** (corresponding to **6.29**) with balanol active form conformation. a) major conformer of azepane **2.11b**; b) azepane ring conformation in X–ray crystal structure of PKA bound (−)–balanol (PDB code:1BX6).[11]

The monofluoro analogue **6.29** (5*S*–F) was well tolerated with improvement in affinity for PKCε. The overall affinity trend for other isozymes followed the same sequence (PKCε > PKCδ > PKA–α > PKCη > PKCθ) as that of (−)–balanol (columns 2&5, Table 6.1). The selectivity amongst PKC isozymes was improved, although not dramatic. The affinity to PKCε was higher by 12, 16, 32 and 60 fold compared to PKCδ, PKA–α, PKCη, and PKCθ, respectively (column 5, Table 6.1). This profile suggested that analogue **6.29** most likely reproduces the ligand–receptor interactions similar to those of (−)–balanol. Interestingly, the

major conformer of azepane **2.11b** (the azepane in **6.29**) identified in the conformational analysis earlier (Chapter 4) was found to resemble the conformation of the azepane ring of (−)–balanol in the ATPsite of PKA (Figure 6.3).[11] The **2.11b** conformer has a boat-chair conformation with a bent C6–C7–N^+ region, and this region is flat in the PKA-bound azepane ring conformation. This similarity in the conformation suggests that **6.29** potentially retains the azepane conformation in the protein active site. Amongst all of the low energy conformers found for the fluoroazepanes **2.11b–d**, **4.1** and **4.3** only this conformer (conformer **4a** in Chapter 4, Figure 6.3) was found to closely resemble the azepane conformation of (−)–balanol bound in the PKA ATPsite.

Conversely, monofluoroanalogues **6.27** (6*S*–F) and **6.28** (6*R*–F) were only tolerated in PKA and exhibited reduction of PKC affinity (except for PKCη with **6.28**). Both **6.27** and **6.28** displayed the highest affinity to PKA–α and lowest to PKCθ (column 3&4, Table 6.1). The selectivity amongst the PKC isozymes was overall reduced compared to that of balanol. Interestingly, in both **6.27** and **6.28**, the fold of affinity reduction, compared to that of (−)–balanol was in an identical order: PKCε (26, 33 fold reduction for **6.27** and **6.28**, respectively) > PKCθ (5, 6 fold reduction) > PKCδ (4, 3 fold reduction) > PKCη and PKA–α (3, <1 fold reduction) (column 2–4, Table 6.1). This reduction in PKCs affinities irrespective of C6–F stereochemistry suggests that the electronegativity of fluorine at C6 position most likely the source of unfavourable interactions for the PKC isozymes while tolerated by PKA. In summary, the C6–F analogues **6.27** and **6.28** showed lower affinity to PKCs but retained affinity to PKA–α. The PKC isozyme selectivity in **6.27** and **6.28** was reduced compared to that of (−)–balanol.

In the case of C6–difluoro analogue **6.30**, the binding affinities compared to (−)–balanol was again reduced for all the PKC isozymes tested and also for PKA. More specifically, the fold of affinity reduction, compared to balanol followed a similar trend as that from **6.27** and **6.28** (PKCε (151 fold) > PKCθ (23 fold) > PKCδ (4 fold) > PKA–α (2 fold) > PKCη (<1 fold)) (column 2&6, Table 6.1). The affinities to isozymes PKCδ, PKCη and PKA–α were very close to those of **6.28** whereas, the PKCε and PKCθ affinities were reduced dramatically. To sum up, **6.30** retained affinity to PKA–α and PKCη comparable to that of (−)–balanol. The drastic reduction in affinities for PKCε and PKCθ suggests their sensitivity towards possibly electronegative atoms at C6.

The vicinal difluoro analogue **6.31** was the worst as all of affinities for PKA/PKCs were worse with also reduced selectivity. Compared to **6.29**, the introduction of one more fluorine at C6 resulted in up to 65 fold reduction in affinity. The analogue **6.31** was best tolerated by PKCε and PKCδ with 3–5 fold reduction in affinity.

The trifluoro–balanol analogue **6.32** was found to retain affinity only to PKCη, while the binding affinity to all other PKA/PKC isozymes was reduced up to 52fold (column 2&8, Table 6.1). It is interesting that **6.32** has only one extra fluorine at C6 than **6.31**, and the affinity to PKCη was improved (3 fold) with comparable affinities to other isozymes. This suggests that in the case of PKCη, other factors can balance the unfavourable interactions from mono– and di–fluorination. Overall, the affinity to PKCη was comparable to that of (−)–balanol while affinities for isozymes PKCθ and PKCε have been reduced more drastically.

The analogues **6.28**, **6.30** and **6.32** were found to be best tolerated by PKCη and PKCδ. Noticeably, the conformational analysis of their corresponding azepanes (**2.11d**, **4.1** and **4.3**,

respectively) suggested that all three have a similar major conformational geometry. This raises the interesting question if they potentially have similar binding conformations.

PKA–α was tolerant to monofluorination at C5 and C6 and difluorination at C6. However, the affinities reduced significantly in the case of **6.31** and **6.32** (7 fold). PKCδ and PKCη were most tolerant to fluorination since, the affinity was reduced by around 3 fold. Conversely, PKCε (except for **6.29**) and PKCθ were most sensitive to fluorination. The order for the tolerance towards fluorination for PKC isozymes is as follows:

$$PKC\eta > PKA\text{–}\alpha, PKC\delta > PKC\theta > PKC\varepsilon$$

6.3. Experimental

Synthetic methods and characterization data of all new compounds are provided in the following experimental section. All of the relevant NMR spectra are included in the appendix E (pages 643–733) at the end of the thesis.

6.3.1. General Methods

All reactions were conducted under N_2 atmosphere. Unless otherwise specified, all reagents were purchased from Sigma–Aldrich and used without further purification. CH_2Cl_2 was obtained from a solvent purification system (Innovative Technology SPS400) and stored over MS 4Å beads. Acetone, EtOAc and petroleum ether were distilled before use. Petroleum ether refers to the fraction collected between 60 °C and 80 °C. THF was distilled from Na–benzophenone and stored over MS 4Å beads. ^1H NMR spectra were recorded at 25 °C on either a Bruker DRX600K or DPX400 NMR spectrometer and are reported in ppm using the specified solvent as the internal standard ($CDCl_3$ at 7.26 ppm, $(CD_3)_2SO$ at 2.50 ppm, CD_3CN at 1.94 ppm). ^{13}C NMR spectra are reported in ppm using the specified solvent as the internal standard ($CDCl_3$ at 77.16 ppm, $(CD_3)_2SO$ at 39.52 ppm, CD_3CN at 1.32 and 118.26 ppm).

6.3.2. Synthetic Procedures and Characterisation of Intermediates

4–bromo–3,5–dihydroxybenzoic acid (1.11)

Bromine (103.6 mg, 0.649 mmol) was added dropwise to the suspension of 3,5–dihydroxybenzoic acid (**6.1**) (100 mg, 0.649 mmol) in 20% hydrochloric acid (1.1 mL). The reaction mixture was allowed to reflux until completion. It is noteworthy that during the course of reaction, 3,5–dihydroxybenzoic acid became soluble and then formed white precipitates towards the end. The aqueous reaction mixture was then extracted with diethyl ether (3×5 mL) and the combined organic phase was dried (Na_2SO_4) before vacuum evaporation to yield **1.11** (148.2 mg, 0.636 mmol, 98%) as a white solid with mass and ^1H NMR spectra matching to those reported previously.[12] ^1H NMR (400 MHz, $(CD_3)CO$) δ 7.20 (s, 2H); MS (ESI): *m/z*, 254.94 [M^+ + Na].

Benzyl–3,5–bis(benzyloxy)–4–bromobenzoate (6.2)

Potassium carbonate (6.85 g, 49.56 mmol) and benzyl bromide (3.88 mL, 32.7 mmol) was added to a solution of 4–bromo–3,5–dihydroxybenzoic acid (**1.11**) (2.31 g, 9.91 mmol) in DMF (20 mL) under N_2 atmosphere and allowed to stir for 12 h at 25 °C. The reaction mixture was quenched with water (200 mL) and vacuum filtered. The precipitates were rinsed with cold water (100 mL × 2) and chilled EtOH (100 mL). The solid residue was then recrystallized from toluene to afford **6.2** (4.69 g, 94%) as white crystals with ^1H NMR and mass spectra matching to those reported previously.[3b] ^1H NMR (400 MHz, $CDCl_3$) δ 7.50 (d, J = 7.5 Hz, 4H), 7.44–7.30 (m, 13H), 5.35 (s, 2H), 5.20 (s, 4H); MS (ESI): *m/z*, 526.07 [M^+ + Na].

3,5–bis(benzyloxy)–4–bromobenzyl alcohol (6.3)

DIBALH (19.0 mL, 1.0 M in CH_2Cl_2, 19 mmol) was added to a solution of benzyl ester **6.2** (3.99 g, 7.93 mmol) in CH_2Cl_2 (40mL) at −78 °C under N_2 atmosphere. The reaction mixture

was stirred at 0 °C for 1.5 h before quenching with saturated aqueous NH_4Cl (5.5 mL) and dilution with Et_2O (33 mL). The mixture was further stirred for 4 h at 25 °C. $MgSO_4$ was added and the suspension was filtered through Celite followed by vacuum evaporation to obtain the crude mixture. The crude was recrystallized from EtOAc/petroleum ether to afford **6.3** (3.04 g, 96%) as a white solid with ^{1}H NMR and mass spectra matching to those reported previously.[3b] ^{1}H NMR (400 MHz, $CDCl_3$) δ 7.52–7.47 (m, 4H), 7.42–7.37 (m, 4H), 7.35–7.30 (m, 2H), 6.64 (s, 2H), 5.16 (s, 4H), 4.60 (s, 2H), 1.78 (s, 1H); MS (ESI): *m/z*, 399.05 [M^+ + H].

(3,5–bis(benzyloxy)–4–bromobenzyloxy)(*tert*–butyl)dimethylsilane (6.4)

TBSCl (1.16 g, 7.71 mmol) was added to a solution of benzyl alcohol **6.3** (2.08 g, 7.01 mmol) and imidazole (0.524 g. 7.71 mmol) in DCM (67 mL) at 0 °C under N_2 atmosphere. The reaction mixture was then stirred at 25 °C for 1.5 h before quenching with saturated $CuSO_4$ solution (50 mL). The aqueous layer was extracted with Et_2O (100 mL × 2) and then dried ($MgSO_4$), filtered and concentrated. The crude product was recrystallized from Et_2O/*n*–hexane to afford **6.4** (3.10 g, 91%) as white crystals with ^{1}H NMR and mass spectra matching to those reported previously.[3b] ^{1}H NMR (400 MHz, $CDCl_3$) δ 7.49 (d, J = 7.3 Hz, 4H), 7.42–7.36 (m, 4H), 7.34–7.29 (m, 2H), 6.61 (s, 2H), 5.17 (s, 4H), 4.64 (s, 2H), 0.93 (s, 9H), 0.06 (s, 6H); MS (ESI): *m/z*, 535.12 [M^+ + Na].

2,6–bis(benzyloxy)–4–((*tert*–butyldimethylsilyloxy)methyl)benzoic acid (6.5)

n–BuLi (3.44 mL, 2.5 M in hexanes) was added dropwise to a solution of silyl ether **6.4** (4.98 g, 7.82 mmol) in dry THF (50 mL) at −78 °C under N_2 atmosphere and stirred for 30 min. Excess of crushed dry ice was added to the reaction mixture before it was warmed up to 25 °C over 30 min. THF was vacuum evaporated followed by addition of 1 *N* $KHSO_4$ (18 mL) and

CH_2Cl_2 (50 mL). The layers were separated and the aqueous layer was extracted with CH_2Cl_2 (36 mL × 2). The combined CH_2Cl_2 layers were washed with brine (75 mL) and then dried ($MgSO_4$), filtered and vacuum evaporated to obtain the crude mixture, which was subjected to flash chromatography (2–7% MeOH in CH_2Cl_2) to afford **6.5** (2.59 g, 55%) as white crystals with ^{1}H NMR and mass spectra matching to those reported previously.[3b] R_f = 0.22 (5% MeOH in CH_2Cl_2); ^{1}H NMR (400 MHz, $CDCl_3$) δ 7.42 (d, J = 7.5 Hz, 4H), 7.34 (t, J = 7.5 Hz, 4H), 7.27 (t, J = 7.3 Hz, 2H), 6.63 (s, 2H), 5.16 (s, 4H), 4.66 (s, 2H), 0.92 (s, 9H), 0.05 (s, 6H); MS (ESI): *m/z*, 501.21 [M^+ + Na].

3–benzyloxybenzyl alcohol (6.7)

Potassium carbonate (6.22 g, 45.0 mmol) and benzyl bromide (3.59 mL, 30.0 mmol) was added to a solution of 3–hydroxybenzyl alcohol (**6.6**) (3.72 g, 30.0 mmol) in DMF (114 mL) under N_2 atmosphere and allowed to stirred for 14 h at 25 °C. The reaction mixture was quenched with cold water (200 mL) and extracted with EtOAc (100 mL × 3). The combined organic layer was back extracted with water (50 mL × 3), dried ($MgSO_4$) and vacuum evaporated to obtain the crude mixture, which was then recrystallized from toluene to afford **6.7** (5.83 g, 88%) as white crystals with ^{1}H NMR and mass spectra matching to those reported previously.[13] ^{1}H NMR (400 MHz, $CDCl_3$) δ 7.49–7.31 (m, 5H), 7.27 (t, J = 7.91 Hz, 1H), 7.01 (s, 1H), 6.93 (t, J = 7.91 Hz, 2H), 5.05 (s, 2H), 4.61 (s, 2H), 2.60 (br s, 1H); MS (ESI): *m/z*, 214.10 [M^+ + H].

3–benzyloxy–2–bromobenzyl alcohol (1.14)

A 2.5 M solution of *n*–butyllithium in hexanes (2.25 mL, 5.61 mmol) was added to a solution of **6.7** (0.50 g, 2.33 mmol) in dry toluene (7.32 mL) at −10 °C under N_2 atmosphere over 15 min. The reaction mixture was allowed to stir at −5 °C for 6 h, before it was cooled to −78 °C

and treated with 1,2–dibromo–1,1,2,2–tetrafluoroethane (1.22 g, 6.93 mmol). The solution was allowed to stir at room temperature for 16 h, after which it was poured onto 2:1 mixture (225 mL) of ether and aqueous saturated NH_4Cl. The organic layer was dried ($MgSO_4$) after washing with brine (50 mL) and vacuum evaporated. The crude mixture obtained was recrystallized from EtOAc/hexane to afford **1.14** (0.34 g. 50%) as white crystals with ^{1}H NMR and mass spectra matching to those reported previously.[3b] ^{1}H NMR (400 MHz, $(CD_3)CO$) δ 7.53 (d, J = 7.61 Hz, 2H), 7.40 (dd, J = 7.15, 6.84 Hz, 2H), 7.32 (t, J = 7.91 Hz, 2H), 7.25–7.22 (m, 1H), 7.06 (d, J = 8.28 Hz. 1H), 5.22 (s, 2H), 4.69 (d, J = 6.05 Hz, 2H), 4.41 (t, J = 6.05 Hz, 1H); MS (ESI): *m/z*, 293.00 [M^+ + H].

3–(benzyloxy)–2–bromobenzyl–2,6–bis(benzyloxy)–4–((*tert*–butyldimethylsilyloxy) methyl)benzoate (6.8)

A solution of benzyl alcohol **1.14** (61.2 mg, 0.209 mmol) and triphenylphosphine (59.3 mg, 0.230 mmol) in dry THF (0.3 mL) was added dropwise to a solution of carboxylic acid **6.5** (100 mg, 0.209 mmol) and diethyl azodicarboxylate (40.0 mg, 0.209 mmol) in THF (0.3 mL) at 0 °C. The reaction mixture was then allowed to stir at 25 °C for 1 h before vacuum evaporation to obtain the crude mixture. The crude was subjected to flash chromatography using 5% EtOAc in hexane to afford **6.8** (138.6 mg, 88% of carboxylic acid **6.5**) as a colourless oil with ^{1}H NMR and mass spectra matching to those reported previously.[3b] R_f = 0.33 (12% EtOAc in hexane); ^{1}H NMR (400 MHz, $CDCl_3$) δ 7.48 (d, J = 7.30 Hz, 2H), 7.43–7.27 (m, 13H), 7.09 (d, J = 7.90 Hz, 1H), 6.93 (t, J = 7.90 Hz, 1H), 6.83 (d, J = 8.21 Hz, 1H), 6.62 (s, 2H), 5.50 (s, 2H), 5.14 (s, 6H), 4.68 (s, 2H), 0.95 (s, 9H), 0.08 (s, 6H); MS (ESI): *m/z*, 775.21 [M^+ + Na].

(2–(benzyloxy)–6–(hydroxymethyl)phenyl)(2,6–bis(benzyloxy)–4–((*tert*–butyldimethyl–silyloxy)methyl)phenyl)methanone (6.9)

n–BuLi (0.349 mL, 2.5 M in hexane) was added dropwise to a solution of ester **6.8** (548.8 mg, 0.728 mmol) in THF (0.73 mL) at −98 °C under N_2 atmosphere. The reaction mixture was warmed to −78 °C and stirred until all the starting material reacted (45 min, TLC). The reaction mixture was then quenched with saturated aqueous $NaHCO_3$ (5 mL). The crude mixture was extracted with EtOAc (10 mL × 2) and the organic layer was dried ($MgSO_4$) and vacuum evaporated to obtain the crude mixture, which was subjected to flash chromatography (20% EtOAc in hexane) to afford **6.9** (412.8 mg, 84%) as a white foam with ^{1}H NMR and mass spectra matching to those reported previously.[3b] R_f = 0.13 (20% EtOAc in hexane); ^{1}H NMR (400 MHz, $CDCl_3$) δ 7.31 (t, J = 8.0 Hz, 1H), 7.26–7.21 (m, 7H), 7.17 (t, J = 7.36 Hz, 2H), 7.07–7.03 (m, 4H), 6.89 (t, J = 8.0 Hz, 4H), 6.47 (s, 2H), 4.76 (s, 2H), 4.71 (br s, 4H), 4.69 (s, 2H), 4.25 (d, J = 7.05 Hz, 2H), 3.30 (d, J = 7.05 Hz, 1H), 0.96 (s, 9H), 0.11 (s, 6H); MS (ESI): *m/z*, 675.31 [M^+ + H].

3–(benzyloxy)–2–(2,6–bis(benzyloxy)–4–((*tert*–butyldimethylsilyloxy)methyl)benzoyl) benzaldehyde (6.10)

To a solution of benzyl alcohol **6.9** (715.4 mg, 1.06 mmol) in dry acetonitrile (5 mL) under N_2 at 25 °C was added 4–methylmorpholine–*N*–oxide (186.9 mg, 1.6 mmol) and tetrapropyl–ammonium perruthenate (VII) (37.3 mg, 0.11 mmol). The reaction mixture was allowed to stir for 30 min before vacuum evaporation to obtain the crude mixture. The crude mixture was then purified by flash chromatography to afford **6.10** (677.6 mg, 95 %) as white powder with ^{1}H NMR and mass spectra matching to those reported previously.[3b] R_f = 0.30 (20% EtOAc in hexane); ^{1}H NMR (400 MHz, $CDCl_3$) δ 9.93 (s, 1H), 7.37–7.30 (m, 2H), 7.24–7.14 (m, 9H),

7.08–7.02 (m, 5H), 6.92–6.89 (m, 2H), 6.52 (s, 2H), 4.78 (s, 2H), 4.77 (s, 4H), 4.69 (s, 2H), 0.96 (s, 9H), 0.10 (s, 6H); MS (ESI): *m/z*, 673.30 [M^+ + H].

3–(benzyloxy)–2–(2,6–bis(benzyloxy)–4–((*tert*–butyldimethylsilyloxy)methyl)benzoyl) benzoic acid (6.11)

2–methyl–2–butene (561.0 mg, 8 mmol), NaH_2PO_4 (3.0 mL, 1.0 M in water) and 80% $NaClO_2$ (339 mg, 3.0 mmol) was added to a solution of the aldehyde **6.10** (672.9 mg, 1 mmol) in THF (4.5 mL), *t*–BuOH (4.5 mL) and water (1.5 mL). The reaction mixture was allowed to stir at room temperature until completion (14 h, TLC). The volatiles were vacuum evaporated and the residue obtained was treated with $KHSO_4$ followed by extraction with EtOAc (10 mL × 2). The combined organic layers were then washed with water (10 mL), saturated aqueous Na_2SO_3 (5 mL) and brine (10 mL); dried ($MgSO_4$); and evaporated to obtain the crude mixture. The residue was purified by flash chromatography using 1–5% MeOH in CH_2Cl_2 to afford the desired carboxylic acid **6.11** (606.2 mg, 88%) as white powder with ^1H NMR and mass spectra matching to those reported previously.[3b] R_f = 0.24 (10% MeOH in CH_2Cl_2); ^1H NMR (400 MHz, $CDCl_3$) δ 8.64 (s, 1H), 7.51–6.70 (m, 18H), 6.61 (s, 2H), 4.91–4.68 (m, 8H), 0.99 (s, 9H), 0.13 (s, 6H); MS (ESI): *m/z*, 689.29 [M^+ + H].

Benzyl–3–(benzyloxy)–2–(2,6–bis(benzyloxy)–4–((tert–butyldimethylsilyloxy)methyl) benzoyl)benzoate (6.12)

Benzyl bromide (0.27 mL, 2.28 mmol) was added to a suspension of carboxylic acid **6.11** (925 mg, 1.14 mmol) and K_2CO_3 (472.5 mg, 3.41 mmol) in dry DMF (10 mL) under N_2 atmosphere at 25 °C. The reaction mixture was stirred until completion (TLC, 1.5 h) before it was quenched with water (88 mL). The aqueous residue was then extracted with EtOAc (20 mL × 2) and the combined organic layers were washed with water (20 mL × 2); dried ($MgSO_4$) and

vacuum evaporated to obtain the crude mixture. Purification of the crude mixture by flash chromatography using 12% EtOAc in hexane afforded **6.12** (976.7 mg, 95%) as white foam with ^{1}H NMR and mass spectra matching to those reported previously.[3b] R_f = 0.39 (20% EtOAc in hexane); ^{1}H NMR (400 MHz, $CDCl_3$) δ 7.42 (dd, J = 1.85, 8.04 Hz, 2H), 7.32–7.11 (m, 17H), 7.00–6.92 (m, 4H), 6.88–6.84 (m, 2H), 5.17 (s, 2H), 4.87 (s, 2H), 4.81 (s, 2H), 4.77 (s, 2H), 4.69 (s, 2H), 0.99 (s, 9H), 0.16 (s, 6H); MS (ESI): *m/z*, 818.10 [M^+ + K].

Benzyl–3–(benzyloxy)–2–(2,6–bis(benzyloxy)–4–(hydroxymethyl)benzoyl)benzoate (6.13)

Tetrabutylammonium fluoride (1.10 mL, 1.0 M in THF) was added to a solution of the *tert*–butyldimethylsilylether **6.12** (557 mg, 0.715 mmol) in dry THF (7 mL) under N_2 atmosphere at 25 °C. The reaction mixture was stirred until completion (15 min, TLC) before vacuum evaporation to obtain the crude mixture. The crude mixture then was purified by flash chromatography using 25% EtOAc in hexane to afford benzyl alcohol **6.13** (437.3 mg, 92%) as white powder with ^{1}H NMR and mass spectra matching to those reported previously.[3b] R_f = 0.21 (20% EtOAc in hexane); ^{1}H NMR (400 MHz, $CDCl_3$) δ 7.38–7.34 (m, 2H), 7.30–7.08 (m, 17H), 6.94–6.89 (m, 4H), 6.86–6.81 (m, 2H), 5.16 (s, 2H), 4.81 (s, 2H), 4.76 (s, 2H), 4.69 (s, 4H), 2.17 (br s, 1H); MS (ESI): *m/z*, 665.25 [M^+ + H].

Benzyl–3–(benzyloxy)–2–(2,6–bis(benzyloxy)–4–formylbenzoyl)benzoate (6.14)

The procedure for the synthesis of **6.10** was followed. Yield 67% from **6.13**; White foam with ^{1}H NMR and mass spectra matching to those reported previously.[3b] R_f = 0.41 (25% EtOAc in hexane); ^{1}H NMR (400 MHz, $CDCl_3$) δ 10.34 (s, 1H), 7.39–7.10 (m, 19H), 7.06 (s, 1H), 6.97 (d, J = 7.94 Hz, 1H), 6.93–6.89 (m, 2H), 6.86–6.82 (m, 2H), 5.20 (s, 2H), 4.86 (s, 2H), 4.76 (s, 2H), 4.70 (s, 2H); MS (ESI): *m/z*, 663.23 [M^+ + H].

3,5–bis(benzyloxy)–4–(2–(benzyloxy)–6–(benzyloxycarbonyl)benzoyl)benzoic acid (1.28)

The procedure for the synthesis of **6.11** was followed. Yield 91% from **6.14**; White foam with ^{1}H NMR and mass spectra matching to those reported previously.[3b] R_f = 0.36 (7% MeOH in CH_2Cl_2); ^{1}H NMR (400 MHz, $CDCl_3$) δ 7.29 (dd, J = 8.0, 8.0 Hz, 1H), 7.25–7.17 (m, 15H), 7.12 (t, J = 7.94 Hz, 2H), 7.08–7.04 (m, 4H), 6.95 (d, J = 8.38 Hz, 1H), 6.84 (d, J = 7.62 Hz, 2H), 5.13 (s, 2H), 4.79 (s, 4H), 4.70 (s, 2H); MS (ESI): *m/z*, 679.23 [M^+ + H].

(3*R*,4*R*)–3–(4–(benzyloxy)benzamido)–4–hydroxyazepane–1–carboxylic acid–*tert*–butyl ester (1.10)

A solution of compound **2.7** (20 mg, 58.1 μmol) and trifluoromethanesulfonic acid (4 μL, 58.1 μmol) in MeOH (1.21 mL) was treated with Pd/C (5% w/w). The resulting suspension was stirred under H_2 (1 atm) for 14 h. The reaction mixture was then filtered through a pad of Celite which was rinsed with MeOH (1 mL × 5). The solvent was evaporated under reduced pressure to yield the desired amine **1.9** which was used in the next step without further purification. 4–benzyloxybenzoyl chloride (15.6 mg, 68.1 μmol) was added to the solution of amine **1.9** and Et_3N (64 μL, 681 μmol) in CH_2Cl_2 (0.81 mL) under N_2 atmosphere. The reaction mixture was stirred for 2 h at 25 °C before it was quenched by the addition of MeOH (0.15 mL) and pyridine (0.15 mL). The volatiles were evaporated under vacuum and the residue was dissolved in EtOAc. The organic phase was successively washed with aqueous 2 *N* HCl, water, aqueous saturated $NaHCO_3$, and brine. The organic layer was then dried (Na_2SO_4) before vacuum evaporation to obtain the crude mixture, which was purified by flash chromatography (petroleum ether/ethyl acetate, 1/1) to afford azepane **1.10** (15.6 mg, 52% over two steps) as a colourless oil with NMR, optical rotation and mass spectra matching to those reported previously.[4] R_f (petroleum ether/EtOAc, 1/1) 0.33; $[\alpha]^{20}_D$ = −4.1 (*c* 0.8, CH_2Cl_2); ^{1}H NMR (400 MHz, CD_2Cl_2) δ 8.96 (d, J = 4.98 Hz, 1H), 7.90 (d, J = 8.71 Hz, 2H),

7.51–7.36 (m, 5H), 7.08 (d, J = 8.71 Hz, 2H), 5.17 (s, 2H), 4.11–4.02 (m, 3H), 3.82–3.75 (m, 1H), 3.33 (dd, J = 15.46, 4.90 Hz, 1H), 2.79 (ddd, J = 13.88, 12.30, 3.50 Hz, 1H), 1.95–1.63 (m, 4H), 1.54 (s, 9H); ^{13}C NMR (100 MHz, CD_2Cl_2) δ 168.5, 162.0, 157.7, 137.0, 129.4, 129.0, 128.5, 128.0, 126.5, 115.0, 81.0, 78.0, 70.5, 61.2, 50.7, 50.1, 33.1, 28.5, 27.5; MS (ESI): *m/z*, 441.23 [M^+ + H].

(3*R*,4*R*)–*tert*–butyl–3–(4–(benzyloxy)benzamido)–4–(3,5–bis(benzyloxy)–4–(2–(benzyloxy)–6–(benzyloxycarbonyl)benzoyl)benzoyloxy)azepane–1–carboxylate (1.18)

A suspension of hydroxyazepane **1.10** (15.6 mg, 35.4 μmol), benzophenone **1.28** (24.0 mg, 35.4 μmol) and 2–chloro–1–methylpyridinium iodide (11.8 mg, 46.0 μmol) in CH_2Cl_2 (0.35 mL) was treated with Et_3N (9.9 μL, 70.8 μmol) and allowed to stir for 30 min at 25 °C. The reaction mixture was then reacted with 4–dimethylaminopyridine (2.2 mg, 17.7 μmol) and was allowed to stir for 8 h at 25 °C before vacuum evaporation to obtain the crude mixture for purification by flash chromatography (petroleum ether/ethyl acetate, 3/2) to afford the fully protected balanol **1.18** (29.2 mg, 75%) as a colourless oil with NMR, optical rotation and mass spectra matching to those reported previously.[14] R_f (petroleum ether/EtOAc, 3/2) 0.31; $[\alpha]^{20}_D$ = −61.1 (*c* 0.7, CH_2Cl_2); ^{1}H NMR (400 MHz, $CDCl_3$) δ 8.03 (d, J = 7.60 Hz, 1H), 7.77 (d, J = 8.56 Hz, 2H), 7.42–7.03 (m, 27H), 6.93 (brd, J = 8.82 Hz, 3H), 6.82 (d, J = 7.92 Hz, 2H), 5.11 (s, 2H), 5.05 (s, 2H), 4.84 (s, 4H), 4.67 (s, 2H), 4.13–3.94 (m, 2H), 3.35 (dd, J = 15.66, 5.77 Hz, 1H), 2.89–2.79 (m, 1H), 2.09–1.69 (m, 6H), 1.57 (s, 9H); ^{13}C NMR (100 MHz, $CDCl_3$) δ 191.7, 167.5, 166.4, 165.8, 161.4, 158.1, 156.4, 136.5, 135.9, 135.8, 132.9, 130.6, 129.0, 128.8, 128.4, 128.3, 128.0, 127.9, 127.6, 127.5, 127.4, 122.1, 115.5, 114.7, 107.1, 81.0, 77.9, 70.6, 70.1, 67.2, 53.7, 50.3, 49.8, 28.6; MS (ESI): *m/z*, 1101.24 [M^+ + H].

2–(2,6–dihydroxy–4–(((3*R*,4*R*)–3–(4–hydroxybenzamido)azepan–4–yloxy)carbonyl) benzoyl)–3–hydroxybenzoic acid (1.1)

A solution of fully protected balanol **1.18** (20.0 mg, 18.2 μmol) in THF/AcOH/Water (16/4/1) at 25 °C was treated with Pd/C (10% w/w) and stirred under H_2 atmosphere (1 atm) for 10 h at 25 °C before it was filtered through a pad of celite and vacuum evaporated to obtain the crude mixture. The crude was then chromatographed on a Phenomenex Gemini C18 column (150 × 21.20 mm) eluting with MeCN/water/TFA (from 35:65:0.1 to 39:61:0.1 over 25 min; flow rate: 8.80 mL/min; retention time 19.5 min) to provide boc–protected balanol as a pale yellow solid powder. The compound was treated with TFA (1 mL) at 25 °C for 5 min before TFA was vacuum evaporated. The reaction flask was kept under high vacuum (0.005 Torr, 25 °C) for 3 h to remove traces of TFA, and the pale yellow film obtained was characterized as balanol (**1.1**) (7.0 mg, 70%) with NMR, optical rotation and mass spectra matching to those reported previously.[3b] $[\alpha]^{20}_{D} = -109.3$ (*c* 0.12, MeOH); ^{1}H NMR (400 MHz, $(CD_3)_2SO$) δ 11.67 (s, 2H), 9.88 (brs, 1H), 9.06 (brs, 1H), 8.98 (brs, 1H), 8.51 (d, J = 7.91 Hz, 1H), 7.64 (d, J = 8.87 Hz, 2H), 7.37 (dd, J = 7.78, 1.01 Hz, 1H), 7.27 (t, J = 7.90 Hz, 1H), 7.05 (dd, J = 8.00, 1.01 Hz, 1H), 6.78 (d, J = 8.66 Hz, 2H), 6.78 (s, 2H), 5.29–5.23 (m, 1H), 4.53–4.45 (m, 1H), 3.39–3.25 (m, 2H), 3.20–3.11 (brs, 2H), 2.17–2.08 (m, 1H), 2.03–1.79 (m, 3H); ^{13}C NMR (100 MHz, $(CD_3)_2SO$) δ 201.6, 166.9, 166.2, 164.2, 161.5, 160.5, 153.3, 135.5, 132.5, 129.3, 129.0, 128.9, 124.4, 120.0, 119.7, 114.9, 113.5, 107.3, 75.9, 50.8, 46.0, 45.9, 28.2; MS (ESI): *m/z*, 551.17 $[M^+ + H]$.

(3*R*,4*R*,6*S*)–3–(4–(benzyloxy)benzamido)–6–fluoro–4–hydroxyazepane–1–carboxylic acid–*tert*–butyl ester (6.15)

The procedure for the synthesis of **1.10** was followed. yield 50% over two steps; colourless oil; R_f (petroleum ether/EtOAc, 1/1) 0.34; $[\alpha]^{20}_D$ = +19.7 (*c* 1.4, CH_2Cl_2); IR (film) ν_{max} (cm^{-1}): 3500–3100 (br), 1673, 1634, 1607, 1508, 1243, 1200, 1178, 1134, 1049, 849, 799, 721; ^1H NMR (400 MHz, $CDCl_3$) δ 8.76 (d, *J* = 5.34 Hz, 1H), 7.84 (d, *J* = 8.78 Hz, 2H), 7.45–7.31 (m, 5H), 7.02 (d, *J* = 8.76 Hz, 2H), 5.52 (brs,1H), 5.12 (s, 2H), 4.70–4.50 (m, $^1J_{HF}$ = 45.93 Hz, 1H), 4.37 (dd, *J* = 13.54, 5.55 Hz, 1H), 4.18–4.09 (m, 2H), 3.79 (dd, *J* = 11.03, 6.67 Hz, 1H), 3.33 (dd, *J* = 15.74, 5.47 Hz, 1H), 2.88–2.78 (m, 1H), 2.37 (dd, *J* = 15.24, 15.15 Hz, 1H), 2.23–2.12 (m, 1H), 1.49 (s, 9H); ^{13}C NMR (100 MHz, $CDCl_3$) δ 168.8, 161.9, 157.2, 136.5, 129.3, 128.8, 128.3, 127.6, 125.6, 114.9, 87.6 (d, $^1J_{CF}$ = 176.82 Hz), 82.0, 73.7 (d, $^3J_{CF}$ = 14.86 Hz), 70.3, 60.2, 53.3 (d, $^2J_{CF}$ = 34.19 Hz), 50.4, 39.5 (d, $^2J_{CF}$ = 19.96 Hz), 28.4; HRMS (ESI): $[M + H]^+$, *m/z* calcd for $C_{25}H_{32}FN_2O_5$ 459.2295, found 459.2299.

(3*R*,4*R*,6*R*)–3–(4–(benzyloxy)benzamido)–6–fluoro–4–hydroxyazepane–1–carboxylic acid–*tert*–butyl ester (6.16)

The procedure for the synthesis of **1.10** was followed. yield 48% over two steps; colourless oil; R_f (petroleum ether/EtOAc, 1/1) 0.35; $[\alpha]^{20}_D$ = −38.8 (*c* 0.9, CH_2Cl_2); IR (film) ν_{max} (cm^{-1}): 3500–3100 (br), 1673, 1634, 1607, 1508, 1243, 1200, 1178, 1134, 1049, 849, 799, 721; ^1H NMR (400 MHz, $CDCl_3$) δ 8.99 (d, *J* = 4.88 Hz, 1H), 7.85 (d, *J* = 8.79 Hz, 2H), 7.44–7.30 (m, 5H), 7.01 (d, *J* = 8.83 Hz, 2H), 5.11 (s, 2H), 4.87–4.72 (m, $^1J_{HF}$ = 45.06 Hz, 1H), 4.43 (dd, *J* = 15.94, 15.28 Hz, 1H), 4.27–4.06 (m, 3H), 3.21 (dd, *J* = 15.48, 5.38 Hz, 1H), 2.98 (dd, *J* = 15.81, 2.02 Hz, 1H), 2.39–1.97 (m, 2H), 1.47 (s, 9H); ^{13}C NMR (100 MHz, $CDCl_3$) δ 168.8, 161.9, 157.8, 135.8, 129.3, 128.8, 128.3, 127.6, 125.8, 114.8, 88.7 (d, $^1J_{CF}$ = 178.54 Hz), 81.7, 72.0 (d, $^3J_{CF}$ = 6.67 Hz), 70.2, 60.2, 54.4 (d, $^2J_{CF}$ = 22.99 Hz), 50.1, 37.4 (d, $^2J_{CF}$ = 20.06 Hz), 28.4; HRMS (ESI): $[M + H]^+$, *m/z* calcd for $C_{25}H_{32}FN_2O_5$ 459.2295, found 459.2300.

(3*R*,4*S*,5*S*)–3–(4–(benzyloxy)benzamido)–5–fluoro–4–hydroxyazepane–1–carboxylic acid–*tert*–butyl ester (6.17)

The procedure for the synthesis of **1.10** was followed. yield 48% over two steps; colourless oil; R_f (petroleum ether/EtOAc, 1/1) 0.34; $[\alpha]^{20}_D$ = +44.5 (*c* 1.2, CH_2Cl_2); IR (film) ν_{max} (cm^{-1}): 3500–3100 (br), 1673, 1634, 1607, 1508, 1243, 1200, 1178, 1134, 1049, 849, 799, 721; ^1H NMR (400 MHz, $CDCl_3$) δ 8.36 (d, J = 4.83 Hz, 1H), 7.79 (d, J = 8.28 Hz, 2H), 7.43–7.30 (m, 5H), 6.99 (d, J = 8.93 Hz, 2H), 5.10 (s, 2H), 4.81–4.62 (dt, J = 45.88 ($^1J_{HF}$), 9.43, 9.0 Hz, 1H), 4.20–3.89 (m, 3H), 3.28–3.20 (m, 1H), 3.06–2.95 (m, 2H), 2.28–2.14 (m, 1H), 2.07–1.93 (m, 1H), 1.48 (s, 9H); ^{13}C NMR (100 MHz, $CDCl_3$) δ 168.8, 162.2, 157.3, 136.7, 129.6, 129.1, 128.6, 127.9, 125.8, 115.1, 92.2 (d, $^1J_{CF}$ = 172.0 Hz), 81.8, 78.6 (d, $^2J_{CF}$ = 20.9 Hz), 70.5, 57.7 (d, $^3J_{CF}$ = 7.41 Hz), 47.8, 44.7 (d, $^3J_{CF}$ = 14.77 Hz), 33.1 (d, $^2J_{CF}$ = 21.8 Hz), 28.7; HRMS (ESI): $[M + H]^+$, *m/z* calcd for $C_{25}H_{32}FN_2O_5$ 459.2295, found 459.2297.

(5*R*,6*R*)–6–(4–(benzyloxy)benzamido)–3,3–difluoro–5–hydroxyazepane–1–carboxylic acid–*tert*–butyl ester (6.18)

The procedure for the synthesis of **1.10** was followed. yield 55% over two steps; colourless oil; R_f (petroleum ether/EtOAc, 1/1) 0.34; $[\alpha]^{20}_D$ = −27.4 (*c* 1.0, $CHCl_3$); IR (film) ν_{max} (cm^{-1}): 3500–3100 (br), 2360, 1716, 1683, 1652, 1630, 1613, 1518, 1249, 1210, 1171, 1139, 1049, 840, 793, 726, 608; ^1H NMR (400 MHz, $CDCl_3$) δ 8.84 (d, J = 5.25 Hz, 1H), 7.85 (d, J = 8.70 Hz, 2H), 7.45–7.31 (m, 5H), 7.03 (d, J = 8.58 Hz, 2H), 5.38 (brs,1H), 5.13 (s, 2H), 4.43 (dd, J = 14.99, 13.34 Hz, 1H), 4.21–4.09 (m, 2H), 4.03 (dd, J = 9.97, 7.34 Hz, 1H), 3.32 (dd, J = 15.78, 5.26 Hz, 1H), 3.09 (dd, J = 31.99, 14.94 Hz, 1H), 2.49–2.24 (m, 2H), 1.51 (s, 9H); ^{13}C NMR (100 MHz, $CDCl_3$) δ 168.8, 161.9, 157.2, 136.5, 129.3, 128.8, 128.3, 127.6, 125.6, 121.7 (d, $^1J_{CF}$ = 238.33 Hz), 114.9, 82.5, 72.1 (dd, J = 11.18 ($^2J_{CF}$), 3.82 ($^3J_{CF}$) Hz), 70.3, 60.0,

55.7 (dd, J = 41.22 ($^2J_{CF}$), 28.80 ($^3J_{CF}$) Hz), 50.1, 41.2 (t, $^2J_{CF}$ = 23.80 Hz), 28.3; HRMS (ESI): $[M + H]^+$, *m/z* calcd for $C_{25}H_{31}F_2N_2O_5$ 477.2201, found 477.2203.

(3*R*,4*S*,5*R*,6*S*)–3–(4–(benzyloxy)benzamido)–5,6–difluoro–4–hydroxyazepane–1–carboxylic acid–*tert*–butyl ester (6.19)

The procedure for the synthesis of **1.10** was followed. yield 42% over two steps; colourless oil; R_f (petroleum ether/EtOAc, 1/1) 0.36; $[\alpha]^{20}_D$ = −13.5 (*c* 0.9, $CHCl_3$); IR (film) ν_{max} (cm^{-1}): 3500–3100 (br), 1675, 1630, 1613, 1518, 1249, 1210, 1171, 1139, 1049, 840, 793, 726; ^1H NMR (400 MHz, $CDCl_3$) δ 8.54 (d, J = 4.75 Hz, 1H), 7.84 (d, J = 8.82 Hz, 2H), 7.45–7.32 (m, 5H), 7.02 (d, J = 8.66 Hz, 2H), 5.12 (s, 2H), 5.03–4.77 (m, 2H), 4.65–4.35 (m, 2H), 4.32–4.24 (m, 1H), 4.16–4.05 (m, 1H), 3.40 (dd, J = 15.61, 2.97 Hz, 1H), 3.31 (dd, J = 16.36, 2.73 Hz, 1H), 1.51 (s, 9H); ^{13}C NMR (100 MHz, $CDCl_3$) δ 168.1, 161.9, 156.6, 136.5, 129.3, 128.8, 128.3, 127.6, 125.8, 114.9, 94.1 (dd, J = 177.16 ($^1J_{CF}$), 27.26 ($^2J_{CF}$) Hz), 90.2 (dd, J = 182.89 ($^1J_{CF}$), 29.96 ($^2J_{CF}$) Hz), 81.9, 73.3 (d, $^2J_{CF}$ = 21.92 Hz), 70.3, 56.0 (d, $^3J_{CF}$ = 7.08 Hz), 50.5 (d, $^2J_{CF}$ = 22.65 Hz), 49.3, 28.4; HRMS (ESI): $[M + H]^+$, *m/z* calcd for $C_{25}H_{31}F_2N_2O_5$ 477.2201, found 477.2207.

(4*R*,5*S*,6*R*)–6–(4–(benzyloxy)benzamido)–3,3,4–trifluoro–5–hydroxyazepane–1–carboxylic acid–*tert*–butyl ester (6.20)

The procedure for the synthesis of **1.10** was followed. yield 58% over two steps; white crystals; R_f (petroleum ether/EtOAc, 1/1) 0.37; $[\alpha]^{20}_D$ = −11.4 (*c* 1.0, $CHCl_3$); IR (film) ν_{max} (cm^{-1}): 3500–3100 (br), 2360, 1716, 1683, 1652, 1630, 1613, 1518, 1249, 1210, 1171, 1139, 1049, 840, 793, 726, 608; ^1H NMR (600 MHz, $CDCl_3$) δ 8.44 (d, J = 4.87 Hz, 1H), 7.82 (d, J = 8.66 Hz, 2H), 7.45–7.32 (m, 5H), 7.03 (d, J = 8.59 Hz, 2H), 5.45 (s,1H), 5.12 (s, 2H), 4.68 (dddd, J = 46.57 ($^1J_{HF}$), 18.31, 9.42, 1.57 Hz, 1H), 4.47–4.39 (m, 1H), 4.30–4.24 (m, 1H),

4.21–4.10 (m, 2H), 4.34–4.23 (m, 2H), 1.51 (s, 9H); ^{13}C NMR (150 MHz, $CDCl_3$) δ 168.6, 162.0, 156.7, 136.4, 129.3, 128.8, 128.4, 127.6, 125.4, 121.7 (dd, J = 252.11 ($^1J_{CF}$), 18.99 ($^3J_{CF}$) Hz), 114.9, 90.3 (dt, J = 193.17 ($^1J_{CF}$), 22.29 ($^2J_{CF}$) Hz), 82.9, 73.2 (d, $^2J_{CF}$ = 16.55 Hz), 70.3, 57.6 (d, $^3J_{CF}$ = 5.71 Hz), 52.4 (dd, J = 37.68 ($^2J_{CF}$), 27.76 ($^2J_{CF}$) Hz), 48.9, 28.3; HRMS (ESI): $[M + H]^+$, *m/z* calcd for $C_{25}H_{30}F_3N_2O_5$ 495.2107, found 495.2104.

(3*R*,4*R*,6*S*)–3–(4–(benzyloxy)benzamido)–4–(3,5–bis(benzyloxy)–4–(2–(benzyloxy)–6–(benzyloxycarbonyl)benzoyl)benzoyloxy)–6–fluoroazepane–1–carboxylic acid–*tert*–butyl ester (6.21)

The procedure for the synthesis of **1.18** was followed. yield 70%; colourless oil; R_f (petroleum ether/EtOAc, 3/2) 0.33; $[\alpha]^{20}_D$ = +34.3 (*c* 0.9, CH_2Cl_2); IR (film) ν_{max} (cm^{-1}): 3365, 2390, 2324, 2288, 1715, 1688, 1666, 1652, 1638, 1585, 1493, 1129, 978, 919, 613; ^{1}H NMR (400 MHz, $CDCl_3$) δ 7.90 (d, J = 7.08 Hz, 1H), 7.75 (d, J = 8.56 Hz, 2H), 7.43–7.30 (m, 7H), 7.26–7.14 (m, 15H), 7.09–7.02 (m, 5H), 6.98–6.89 (m, 3H), 6.81 (d, J = 7.55 Hz, 2H), 5.09 (s, 2H), 5.05 (s, 2H), 4.95–4.77 (m, 1H), 4.81 (s, 2H), 4.80 (s, 2H), 4.67 (s, 2H), 4.32 (dd, J = 14.63, 6.70 Hz, 1H), 4.15 (d, J = 15.24 Hz, 1H), 3.54–3.44 (m, 1H), 3.39 (dd, J = 15.67, 4.98 Hz, 1H), 2.89 (dd, J = 24.21, 11.39 Hz, 1H), 2.46–2.30 (m, 2H), 1.55 (s, 9H); ^{13}C NMR (100 MHz, $CDCl_3$) δ 192.0, 167.8, 166.5, 165.8, 161.9, 158.4, 157.4, 156.7, 136.7, 136.6, 136.2, 136.1, 133.2, 132.9, 132.7, 130.9, 129.3, 129.1, 128.8, 128.7, 128.6, 128.3, 128.2, 127.9, 127.8, 127.6, 127.5, 126.8, 122.4, 115.7, 115.1, 107.4, 104.3, 87.8 (d, $^1J_{CF}$ = 177.72 Hz), 82.2, 72.6 (d, $^3J_{CF}$ = 7.78 Hz), 70.9, 70.5, 67.5, 67.3, 53.5, 53.1 (d, $^2J_{CF}$ = 34.37 Hz), 51.6, 34.4 (d, $^2J_{CF}$ = 20.91 Hz), 28.7; HRMS (ESI): $[M + H]^+$, *m/z* calcd for $C_{68}H_{64}FN_2O_{12}$ 1119.4443, found 1119.4413.

(3*R*,4*R*,6*R*)–3–(4–(benzyloxy)benzamido)–4–(3,5–bis(benzyloxy)–4–(2–(benzyloxy)–6–(benzyloxycarbonyl)benzoyl)benzoyloxy)–6–fluoroazepane–1–carboxylic acid–*tert*–butyl ester (6.22)

The procedure for the synthesis of **1.18** was followed. yield 72%; colourless oil; R_f (petroleum ether/EtOAc, 3/2) 0.31; $[\alpha]^{20}_D$ = −67.5 (*c* 0.6, CH_2Cl_2); IR (film) ν_{max} (cm^{-1}): 3365, 2390, 2324, 2288, 1715, 1688, 1666, 1652, 1638, 1585, 1493, 1129, 978, 919, 613; ^1H NMR (400 MHz, $CDCl_3$) δ 8.21–7.62 (m, 3H), 7.57–7.67 (m, 32H), 5.24–2.76 (m, 16H), 2.70–1.93 (m, 3H), 1.51 (s, 9H); ^{13}C NMR (150 MHz, $(CD_3)_2CO$) δ 190.8, 168.2, 167.0, 166.0, 162.6, 162.3, 162.2, 157.6, 155.6, 138.0, 137.9, 136.8, 132.6, 132.5, 130.0, 130.0, 129.8, 129.3, 129.1, 129.0, 128.9, 128.8, 128.5, 122.6, 116.2, 115.3, 115.2, 92.2 (d, $^1J_{CF}$ = 169.37 Hz), 81.6, 80.6, 76.3, 71.8, 71.5, 70.7, 70.6, 67.5, 60.0, 54.0, 53.2, 50.5, 46.7, 46.1, 39.7 (d, $^2J_{CF}$ = 21.27 Hz), 28.6, 28.4; HRMS (ESI): $[M + H]^+$, *m/z* calcd for $C_{68}H_{64}FN_2O_{12}$ 1119.4443, found 1119.4447.

(3*R*,4*S*,5*S*)–3–(4–(benzyloxy)benzamido)–4–(3,5–bis(benzyloxy)–4–(2–(benzyloxy)–6–(benzyloxycarbonyl)benzoyl)benzoyloxy)–5–fluoroazepane–1–carboxylic acid–*tert*–butyl ester (6.23)

The procedure for the synthesis of **1.18** was followed. yield 67%; colourless oil; R_f (petroleum ether/EtOAc, 3/2) 0.34; $[\alpha]^{20}_D$ = +54.9 (*c* 1.0, CH_2Cl_2); IR (film) ν_{max} (cm^{-1}): 3365, 2390, 2324, 2288, 1715, 1688, 1666, 1652, 1638, 1585, 1493, 1129, 978, 919, 613; ^1H NMR (600 MHz, $CDCl_3$) δ 7.76–7.66 (m, 2H), 7.42–6.79 (m, 32H), 5.17–4.87 (m, 5H), 4.81–4.56 (m, 6H), 4.00–3.12 (m, 6H), 2.32–2.16 (m, 2H), 1.56 (s, 9H); ^{13}C NMR (150 MHz, $CDCl_3$) δ 192.3, 167.5, 166.2, 165.7, 161.9, 158.1, 156.6, 155.1, 136.4, 135.9, 135.7, 132.2, 131.1, 130.7, 129.0, 128.8, 128.6, 128.5, 128.4, 128.1, 128.0, 127.8, 127.7, 127.6, 127.4, 122.2, 115.4, 115.2, 114.9, 114.8, 107.2, 103.9, 91.1 (d, $^1J_{CF}$ = 175.6 Hz), 81.8, 81.3 (d, $^2J_{CF}$ = 16.36

Hz), 76.1, 70.9, 70.7, 70.2, 51.2, 47.8, 46.3, 41.5, 37.3, 32.1, 28.5; HRMS (ESI): $[M + H]^+$, *m/z* calcd for $C_{68}H_{64}FN_2O_{12}$ 1119.4443, found 1119.4425.

(5*R*,6*R*)–6–(4–(benzyloxy)benzamido)–5–((3,5–bis(benzyloxy)–4–(2–(benzyloxy)–6–((benzyloxy) carbonyl)benzoyl)benzoyl)oxy)–3,3–difluoroazepane–1–carboxylic acid–*tert*–butyl ester (6.24)

The procedure for the synthesis of **1.18** was followed. yield 70%; colourless oil; R_f (petroleum ether/EtOAc, 3/2) 0.33; $[\alpha]^{20}_D = -74.9$ (*c* 0.6, CH_2Cl_2); IR (film) ν_{max} (cm^{-1}): 3370, 2383, 2322, 2282, 1711, 1687, 1652, 1649, 1631, 1581, 1484, 1122, 999, 921, 627; ^1H NMR (400 MHz, $CDCl_3$) δ 8.03–7.94 (m, 1H), 7.84–7.76 (m, 2H), 7.46–6.82 (m, 32 H), 5.50 (t, J = 7.42 Hz, 1H), 5.13 (s, 2H), 5.09 (s, 4H), 4.81 (s, 4H), 4.68–4.58 (m, 1H), 4.50–4.34 (m, 1H), 4.19 (d, J = 14.98 Hz, 1H), 3.44 (dd, J = 15.13, 4.88 Hz, 1H), 3.30 (dd, J = 15.12, 4.22 Hz, 1H), 2.76–2.47 (m, 2H), 1.56 (s, 9H); ^{13}C NMR (100 MHz, $CDCl_3$) δ 191.7, 167.5, 166.5, 161.7, 158.1, 157.1, 136.5, 135.9, 135.8, 132.3, 130.7, 129.1, 128.8, 128.6, 128.4, 127.8, 127.6, 127.2, 126.3, 122.2, 115.4, 114.9, 107.2, 82.4, 76.1, 70.7, 70.6, 70.2, 67.2, 55.7 (d, $^2J_{CF}$ = 27.60 Hz), 53.4, 50.6, 36.3 (d, $^2J_{CF}$ = 27.70 Hz), 28.3; HRMS (ESI): $[M + H]^+$, *m/z* calcd for $C_{68}H_{63}F_2N_2O_{12}$ 1137.4349, found 1137.4318.

(3*R*,4*S*,5*R*,6*S*)–3–(4–(benzyloxy)benzamido)–4–((3,5–bis(benzyloxy)–4–(2–(benzyloxy)–6–((benzyloxy)carbonyl)benzoyl)benzoyl)oxy)–5,6–difluoroazepane–1–carboxylic acid–*tert*–butyl ester (6.25)

The procedure for the synthesis of **1.18** was followed. yield 69%; colourless oil; R_f (petroleum ether/EtOAc, 3/2) 0.35; $[\alpha]^{20}_D = -39.8$ (*c* 0.7, CH_2Cl_2); IR (film) ν_{max} (cm^{-1}): 3370, 2383, 2322, 2282, 1711, 1687, 1657, 1649, 1631, 1581, 1484, 1122, 993, 921, 623; ^1H NMR (400 MHz, $CDCl_3$) δ 8.04 (d, J = 8.43 Hz, 1H), 7.82–7.59 (m, 2H), 7.47–6.76 (m, 32H), 5.14 (s,

2H), 5.10 (s, 2H), 5.09 (s, 2H), 4.88–2.99 (m, 12H), 1.52 (s, 9H); ^{13}C NMR (150 MHz, $CDCl_3$) δ 191.6, 167.6, 166.3, 161.7, 159.6, 155.1, 136.3, 135.7, 132.3, 128.8, 128.4, 127.6, 122.2, 114.8, 107.3, 91.6 (d, $^1J_{CF}$ = 182.37 Hz), 90.6 (d, $^1J_{CF}$ = 199.73 Hz), 81.9, 72.0, 70.7, 70.2, 69.5, 67.3, 63.8, 51.7, 48.7, 46.8, 43.7, 42.7, 28.4; HRMS (ESI): $[M + H]^+$, *m/z* calcd for $C_{68}H_{63}F_2N_2O_{12}$ 1137.4349, found 1137.4312.

(4*R*,5*S*,6*R*)–6–(4–(benzyloxy)benzamido)–5–((3,5–bis(benzyloxy)–4–(2–(benzyloxy)–6–((benzyloxy)carbonyl)benzoyl)benzoyl)oxy)–3,3,4–trifluoroazepane–1–carboxylic acid–*tert*–butyl ester (6.26)

The procedure for the synthesis of **1.18** was followed. yield 74%; colourless oil; R_f (petroleum ether/EtOAc, 3/2) 0.36; $[\alpha]^{20}_D$ = −57.1 (*c* 0.9, CH_2Cl_2); IR (film) ν_{max} (cm^{-1}): 3378, 2388, 2343, 2267, 1721, 1689, 1659, 1641, 1639, 1587, 1489, 1129, 987, 926, 607; ^{1}H NMR (400 MHz, $CDCl_3$) δ 7.78–7.64 (m, 2H), 7.43–6.76 (m, 32H), 5.74–5.60 (m, 1H), 5.11 (s, 2H), 5.06 (s, 2H), 4.97–4.75 (m, 1H), 4.76 (s, 4H), 4.74 (s, 2H), 4.45–4.30 (m, 1H), 4.06 (brd, *J* = 14.54 Hz, 1H), 4.00–3.82 (m, 1H), 3.58–3.34 (m, 2H), 1.56 (s, 9H); ^{13}C NMR (100 MHz, $CDCl_3$) δ 191.8, 167.6, 166.3, 161.8, 158.1, 156.2, 136.4, 135.9, 129.0, 128.8, 128.6, 128.4, 128.1, 127.9, 127.8, 127.6, 127.3, 126.4, 122.2, 115.2, 114.9, 107.3, 89.4 (d, $^1J_{CF}$ = 217.71 Hz), 82.6 (d, $^2J_{CF}$ = 24.57 Hz), 78.3, 70.9, 70.6, 70.2, 67.4, 67.3, 51.8 (d, $^3J_{CF}$ = 9.44 Hz), 30.4, 28.3; HRMS (ESI): $[M + H]^+$, *m/z* calcd for $C_{68}H_{62}F_3N_2O_{12}$ 1155.4255, found 1155.4226.

2–(4–((((3*R*,4*R*,6*S*)–6–fluoro–3–(4–hydroxybenzamido)azepan–4–yl)oxy)carbonyl)–2,6–dihydroxybenzoyl)–3–hydroxybenzoic acid (6.27)

The procedure for the synthesis of **1.1** was followed. yield 64%; yellow film; retention time 20.0 min (Phenomenex Gemini C18 column (150 × 21.20 mm); MeCN/water/TFA (from 35:65:0.1 to 44:56:0.1 over 30 min; flow rate: 8.80 mL/min); $[\alpha]^{20}_D$ = +82.1 (*c* 0.5, MeOH); IR

(film) ν_{max} (cm^{-1}): 3400–2800 (br), 2360, 2340, 1717, 1683, 1652, 1646, 1635, 1489, 1102, 991, 922, 632; ^1H NMR (600 MHz, $(CD_3)_2SO$) δ 11.63 (s, 2H), 10.00 (s, 1H), 9.83 (s, 1H), 9.24 (brs, 1H), 8.46 (d, J = 8.00 Hz, 1H), 7.62 (d, J = 8.74 Hz, 2H), 7.35 (d, J = 7.80 Hz, 1H), 7.26 (t, J = 7.90 Hz, 1H), 7.04 (d, J = 8.13 Hz, 1H), 6.77 (d, J = 8.60 Hz, 2H), 6.76 (s, 2H), 5.36–5.31 (m, 1H), 5.29–5.17 (m, $^1J_{HF}$ = 44.09 Hz, 1H), 4.57–4.51 (m, 1H), 3.50–3.31 (m, 4H), 2.57–2.42 (m, 2H); ^{13}C NMR (150 MHz, $(CD_3)_2SO$) δ 201.5, 166.9, 166.1, 164.1, 161.4, 160.4, 153.2, 135.3, 132.4, 129.2, 128.9, 128.8, 124.5, 120.0, 119.6, 114.8, 113.5, 107.3, 86.2 (d, $^1J_{CF}$ = 172.92 Hz), 71.5, 50.8, 49.2 (d, $^2J_{CF}$ = 25.48 Hz), 47.7, 33.9 (d, $^2J_{CF}$ = 22.28 Hz); HRMS (ESI): $[M + H]^+$, *m/z* calcd for $C_{28}H_{26}FN_2O_{10}$ 569.1571, found 569.1575.

2–(4–((((3*R*,4*R*,6*R*)–6–fluoro–3–(4–hydroxybenzamido)azepan–4–yl)oxy)carbonyl)–2,6–dihydroxybenzoyl)–3–hydroxybenzoic acid (6.28)

The procedure for the synthesis of **1.1** was followed. yield 69%; yellow film; retention time 27.4 min (Phenomenex Gemini C18 column (150 × 21.20 mm); MeCN/water/TFA (from 5:95:0.1 to 55:45:0.1 over 30 min; flow rate: 8.80 mL/min); $[\alpha]^{20}_D$ = −77.9 (*c* 0.4, MeOH); IR (film) ν_{max} (cm^{-1}): 3400–2800 (br), 2360, 2340, 1717, 1683, 1652, 1646, 1635, 1489, 1102, 991, 922, 632; ^1H NMR (600 MHz, $(CD_3)_2SO$) δ 11.67 (s, 2H), 10.07 (brs, 1H), 9.87 (s, 1H), 9.34 (brs, 2H), 8.55 (d, J = 8.47 Hz, 1H), 7.61 (d, J = 8.69 Hz, 2H), 7.36 (d, J = 7.61 Hz, 1H), 7.27 (t, J = 8.01 Hz, 1H), 7.04 (d, J = 8.01 Hz, 1H), 6.78 (d, J = 8.66 Hz, 2H), 6.76 (s, 2H), 5.55 (ddd, J = 10.33, 9.93, 2.02 Hz, 1H), 5.33–5.21 (m, $^1J_{HF}$ = 47.37 Hz, 1H), 4.59–4.53 (m, 1H), 3.58 (dd, J = 17.42, 15.96 Hz, 1H), 3.52–3.40 (m, 2H), 3.30 (dd, J = 14.14, 7.39 Hz, 1H), 2.57–2.52 (m, 1H), 2.39–2.27 (m, 1H); ^{13}C NMR (150 MHz, $(CD_3)_2SO$) δ 201.6, 166.9, 166.3, 164.0, 161.5, 160.6, 153.2, 135.3, 132.4, 129.2, 128.9, 128.8, 124.2, 120.0, 119.6, 114.9, 113.5, 107.4, 86.0 (d, $^1J_{CF}$ = 169.84 Hz), 70.1, 50.5, 50.3 (d, $^2J_{CF}$ = 24.68 Hz), 47.1, 32.3 (d,

$^2J_{CF}$ = 19.15 Hz); HRMS (ESI): $[M + H]^+$, *m/z* calcd for $C_{28}H_{26}FN_2O_{10}$ 569.1571, found 569.1577.

2–(4–(((3*R*,4*S*,5*S*)–5–fluoro–3–(4–hydroxybenzamido)azepan–4–yloxy)carbonyl)–2,6–dihydroxybenzoyl)–3–hydroxybenzoic acid (6.29)

The procedure for the synthesis of **1.1** was followed. yield 72%; yellow film; retention time 21.2 min (Phenomenex Gemini C18 column (150 × 21.20 mm); MeCN/water/TFA (from 35:65:0.1 to 44:56:0.1 over 30 min; flow rate: 8.80 mL/min); $[\alpha]^{20}_D$ = +58.7 (*c* 0.2, MeOH); IR (film) ν_{max} (cm^{-1}): 3400–2800 (br), 2360, 2340, 1717, 1683, 1652, 1646, 1635, 1489, 1102, 991, 922, 632; ^{1}H NMR (600 MHz, (CD_3CN) δ 10.69 (brs, 1H), 8.00 (d, *J* = 6.91 Hz, 1H), 7.68 (d, *J* = 8.06 Hz, 2H), 7.51 (d, *J* = 7.62 Hz, 1H), 7.33 (t, *J* = 7.95 Hz, 1H), 7.11 (d, *J* = 7.62 Hz, 1H), 7.02 (s, 2H), 6.83 (d, *J* = 8.06 Hz, 2H), 5.49 (t, *J* = 7.98 Hz, 1H), 5.29–5.16 (m, $^1J_{HF}$ = 43.56 Hz, 1H), 4.41 (brs, 1H), 3.71–3.64 (m, 2H), 3.59–3.54 (m, 1H), 3.42–3.34 (m, 1H), 2.63–2.46 (m, 2H); ^{13}C NMR (150 MHz, $(CD_3)_2SO$) δ 202.5, 169.5, 167.5, 162.5, 161.6, 160.5, 153.7, 137.1, 130.6, 130.6, 130.4, 125.5, 122.3, 121.2, 116.1, 109.2, 103.7, 86.9 (d, $^1J_{CF}$ = 167.92 Hz), 71.2 (d, $^2J_{CF}$ = 19.71 Hz), 53.0, 50.6, 50.3, 35.3 (d, $^2J_{CF}$ = 24.12 Hz); HRMS (ESI): $[M + H]^+$, *m/z* calcd for $C_{28}H_{26}FN_2O_{10}$ 569.1571, found 569.1567.

2–(4–((((3*R*,4*R*)–6,6–difluoro–3–(4–hydroxybenzamido)azepan–4–yl)oxy)carbonyl)–2,6–dihydroxybenzoyl)–3–hydroxybenzoic acid (6.30)

The procedure for the synthesis of **1.1** was followed. yield 75%; yellow film; retention time 27.5 min (Phenomenex Gemini C18 column (150 × 21.20 mm); MeCN/water/TFA (from 30:70:0.1 to 70:30:0.1 over 50 min; flow rate: 8.80 mL/min); $[\alpha]^{20}_D$ = −98.4 (*c* 0.7, MeOH); IR (film) ν_{max} (cm^{-1}): 3400–2800 (br), 2363, 2341, 1711, 1687, 1652, 1649, 1631, 1484, 1122, 999, 921, 627; ^{1}H NMR (600 MHz, $(CD_3)_2SO$) δ 11.68 (s, 2H), 10.09 (brs, 1H), 9.89 (s, 1H),

8.54 (d, J = 8.13 Hz, 1H), 7.63 (d, J = 8.58 Hz, 2H), 7.37 (d, J = 7.63 Hz, 1H), 7.28 (t, J = 7.99 Hz, 1H), 7.05 (d, J = 8.16 Hz, 1H), 6.78 (d, J = 8.64 Hz, 2H), 6.78 (s, 2H), 5.45–5.41 (m, 1H), 4.59–4.54 (m, 1H), 3.77–3.68 (m, 2H), 3.52–3.47 (m, 1H), 3.39–3.33 (m, 1H), 2.83–2.74 (m, 2H); ^{13}C NMR (150 MHz, $(CD_3)_2SO$) δ 201.6, 167.0, 166.3, 164.0, 161.5, 160.6, 153.3, 135.1, 132.5, 129.3, 129.0, 128.9, 124.3, 121.8 (d, $^1J_{CF}$ = 243.01 Hz), 120.0, 119.7, 115.0, 113.6, 107.5, 69.4, 51.7 (t, $^2J_{CF}$ = 38.37 Hz), 50.6, 48.1, 37.1 (t, $^2J_{CF}$ = 25.41 Hz); HRMS (ESI): $[M + H]^+$, m/z calcd for $C_{28}H_{25}F_2N_2O_{10}$ 587.1477, found 587.1467.

2–(4–(((3*R*,4*S*,5*R*,6*S*)–5,6–difluoro–3–(4–hydroxybenzamido)azepan–4–yloxy)carbonyl)–2,6–dihydroxybenzoyl)–3–hydroxybenzoic acid (6.31)

The procedure for the synthesis of **1.1** was followed. yield 59%; yellow film; retention time 24.8 min (Phenomenex Gemini C18 column (150 × 21.20 mm); MeCN/water/TFA (from 30:70:0.1 to 70:30:0.1 over 50 min; flow rate: 8.80 mL/min); $[\alpha]^{20}_D$ = −44.8 (c 0.1, MeOH); IR (film) ν_{max} (cm^{-1}): 3400–2800 (br), 2363, 2341, 1711, 1687, 1652, 1649, 1631, 1484, 1122, 999, 921, 627; ^{1}H NMR (600 MHz, $(CD_3)_2SO$) δ 11.69 (s, 2H), 10.05 (s, 1H), 9.86 (s, 1H), 9.29 (brs, 1H), 8.58 (d, J = 8.65 Hz, 1H), 7.56 (d, J = 8.49 Hz, 2H), 7.37 (d, J = 7.93 Hz, 1H), 7.28 (t, J = 7.93 Hz, 1H), 7.05 (d, J = 7.93 Hz, 1H), 6.77 (d, J = 8.63 Hz, 2H), 6.75 (s, 2H), 5.79 (dd, J = 19.05, 9.22 Hz, 1H), 5.49 (dd, J = 46.47 ($^1J_{HF}$), 20.23 ($^2J_{HF}$) Hz, 1H), 5.22 (ddd, J = 45.33 ($^1J_{HF}$), 28.29 ($^2J_{HF}$), 9.0 Hz, 1H), 4.71–4.57 (m, 1H), 3.66–3.17 (m, 4H); ^{13}C NMR (150 MHz, $(CD_3)_2SO$) δ 201.5, 166.9, 166.1, 164.2, 161.5, 160.5, 153.3, 134.8, 132.4, 129.2, 129.0, 128.9, 124.2, 120.0, 119.7, 114.9, 113.6, 107.4, 90.0 (dd, J = 180.67 ($^1J_{CF}$), 17.21 ($^2J_{CF}$) Hz), 89.2 (dd, J = 189.27 ($^1J_{CF}$), 20.23 ($^2J_{CF}$) Hz), 72.1 (brs), 47.2, 44.8, 45.4; HRMS (ESI): $[M + H]^+$, m/z calcd for $C_{28}H_{25}F_2N_2O_{10}$ 587.1477, found 587.1467.

2–(2,6–dihydroxy–4–((((3*R*,4*S*,5*R*)–5,6,6–trifluoro–3–(4–hydroxybenzamido)azepan–4–yl)oxy)carbonyl)benzoyl)–3–hydroxybenzoic acid (6.32)

The procedure for the synthesis of **1.1** was followed. yield 68%; yellow film; retention time 27.6 min (Phenomenex Gemini C18 column (150 × 21.20 mm); MeCN/water/TFA (from 30:70:0.1 to 70:30:0.1 over 50 min; flow rate: 8.80 mL/min); $[\alpha]^{20}_{D} = -64.6$ (*c* 0.4, MeOH); IR (film) ν_{max} (cm^{-1}): 3400–2800 (br), 2360, 2346, 1719, 1667, 1659, 1640, 1639, 1480, 1129, 987, 946, 607; ^{1}H NMR (600 MHz, $(CD_3)_2SO$) δ 11.68 (s, 2H), 10.01 (brs, 1H), 9.86 (s, 1H), 8.48 (d, J = 8.05 Hz, 1H), 7.57 (d, J = 8.46 Hz, 2H), 7.36 (d, J = 7.80 Hz, 1H), 7.28 (t, J = 7.97 Hz, 1H), 7.05 (d, J = 7.95 Hz, 1H), 6.76 (d, J = 8.59 Hz, 2H), 6.76 (s, 2H), 5.67–5.60 (m, 1H), 5.48–5.35 (m, $^{1}J_{HF}$ = 45.30 Hz, 1H), 4.58–4.52 (m, 1H), 3.38–3.34 (m, 1H), 3.30–3.20 (m, 2H), 3.19–3.10 (m, 1H); ^{13}C NMR (150 MHz, $(CD_3)_2SO$) δ 201.5, 166.9, 165.9, 164.1, 161.5, 160.4, 153.3, 134.7, 132.4, 129.1, 129.0, 128.9, 124.5, 121.8 (d, $^{1}J_{CF}$ = 251.98 Hz), 120.0, 119.7, 114.9, 113.7, 107.4, 89.4 (dd, J = 186.95 ($^{1}J_{CF}$), 25.49 ($^{2}J_{CF}$) Hz), 72.0 (d, $^{2}J_{CF}$ = 22.64 Hz), 63.0 (d, $^{2}J_{CF}$ = 34.43 Hz), 49.5, 48.4; HRMS (ESI): $[M + H]^{+}$, *m/z* calcd for $C_{28}H_{24}F_3N_2O_{10}$ 605.1383, found 605.1389.

6.4. Conclusions

A series of fluorinated balanol analogues was synthesized. The total synthesis of (−)–balanol was also accomplished using reported protocols. The analogues were characterized and examined for their kinase binding profiles. The results revealed that fluorine substitution can alter the isozyme selectivity profile of the parent (−)–balanol. The binding profiles varied with regio– and stereochemistry of fluorine substitution. In one incidence, **6.29** improved affinity to PKCε and retained affinity to the other PKA/PKC isozymes tested. The affinity of trifluoro balanoid (**6.32**), to the isozyme PKCη was comparable to balanol whereas the affinity to other isozymes was reduced.

6.5. References

(1) Lai, Y.-S.; Mendoza, J. S.; Jagdmann, G. E., Jr.; Menaldino, D. S.; Biggers, C. K.; Heerding, J. M.; Wilson, J. W.; Hall, S. E.; Jiang, J. B.; et, a. *J. Med. Chem.* **1997**, *40*, 226.

(2) (a) Lai, Y.-S.; Menaldino, D. S.; Nichols, J. B.; Jagdmann, G. E., Jr.; Mylott, F.; Gillespie, J.; Hall, S. E. *Bioorg. Med. Chem. Lett.* **1995**, *5*, 2151; (b) Lai, Y.-S.; Stamper, M. *Bioorg. Med. Chem. Lett.* **1995**, *5*, 2147; (c) Hu, H.; Hollinshead, S. P.; Hall, S. E.; Kalter, K.; Ballas, L. M. *Bioorg. Med. Chem. Lett.* **1996**, *6*, 973; (d) Lai, Y.-S.; Mendoza, J. S.; Hubbard, F.; Kalter, K. *Bioorg. Med. Chem. Lett.* **1995**, *5*, 2155; (e) Mendoza, J. S.; Jagdmann, G. E., Jr.; Gosnell, P. A. *Bioorg. Med. Chem. Lett.* **1995**, *5*, 2211; (f) Defauw, J. M.; Murphy, M. M.; Jagdmann, G. E., Jr.; Hu, H.; Lampe, J. W.; Hollinshead, S. P.; Mitchell, T. J.; Crane, H. M.; Heerding, J. M.; et, a. *J. Med. Chem.* **1996**, *39*, 5215.

(3) (a) Nicolaou, K. C.; Bunnage, M. E.; Koide, K. *J. Am. Chem. Soc.* **1994**, *116*, 8402; (b) Nicolaou, K. C.; Koide, K.; Bunnage, M. E. *Chem. –Eur. J.* **1995**, *1*, 454.

(4) Fürstner, A.; Thiel, O. R. *J. Org. Chem.* **2000**, *65*, 1738.

(5) Mitsunobu, O. *Synthesis* **1981**, 1.

(6) Comins, D. L.; Brown, J. D. *J. Org. Chem.* **1989**, *54*, 3730.

(7) Moorlag, H.; Meyers, A. I. *Tetrahedron Lett.* **1993**, *34*, 6993.

(8) Griffith, W. P.; Ley, S. V. *Aldrichim. Acta* **1990**, *23*, 13.

(9) Bal, B. S.; Childers, W. E., Jr.; Pinnick, H. W. *Tetrahedron* **1981**, *37*, 2091.

(10) Fabian, M. A.; Biggs, W. H.; Treiber, D. K.; Atteridge, C. E.; Azimioara, M. D.; Benedetti, M. G.; Carter, T. A.; Ciceri, P.; Edeen, P. T.; Floyd, M.; Ford, J. M.; Galvin,

M.; Gerlach, J. L.; Grotzfeld, R. M.; Herrgard, S.; Insko, D. E.; Insko, M. A.; Lai, A. G.; Lelias, J.-M.; Mehta, S. A.; Milanov, Z. V.; Velasco, A. M.; Wodicka, L. M.; Patel, H. K.; Zarrinkar, P. P.; Lockhart, D. J. *Nat Biotech* **2005**, *23*, 329.

(11) Narayana, N.; Diller, T. C.; Koide, K.; Bunnage, M. E.; Nicolaou, K. C.; Brunton, L. L.; Xuong, N.-H.; Ten, E. L. F.; Taylor, S. S. *Biochemistry* **1999**, *38*, 2367.

(12) Durola, F.; Hanss, D.; Roesel, P.; Sauvage, J.-P.; Wenger, O. S. *Eur. J. Org. Chem.* **2007**, 125.

(13) Lee, J.; Lee, J.-H.; Kim, S. Y.; Perry, N. A.; Lewin, N. E.; Ayres, J. A.; Blumberg, P. M. *Bioorg. Med. Chem.* **2006**, *14*, 2022.

(14) Lampe, J. W.; Hughes, P. F.; Biggers, C. K.; Smith, S. H.; Hu, H. *J. Org. Chem.* **1994**, *59*, 5147.

CHAPTER 7

Conclusions and Future Directions

7.1. conclusions

An attempt has been made to fulfill the knowledge gap by answering the following questions posed in the project outline: (i) What are the reaction characteristics in the fluorination of substituted azepanes? (ii) What are the conformational effects from fluorine substitution on substituted azepanes? (iii) Can fluorination be used as a tool to generate conformation–coupled chemical diversity in (−)–balanol? and (iv) Can fluorine substituion lead to different PKC/PKA kinase/isozyme specificity profile?

In **Chapter two**, the first systematic study on the synthesis of monofluoroazepanes was presented. The methodologies for hydroboration and nucleophilic fluorination of substituted azepanes were investigated. The unusual *N*–Boc neighbouring group participation was observed for the first time in the nucleophilic fluorination, which unexpectedly resulted in retention of stereochemistry. As azepanes are important pharmacophores in general, these fluorinated azepanes may serve as new synthones.

Chapter three describes the preliminary conformational study on three model azepanes. The azepanes were analyzed by ^{1}H NMR spectroscopy and computational modelling. The results suggested that introduction of a diastereospecific C–F bond can significantly regulate the conformations of the substituted azepanes. The extent of conformational bias depends on the interplay of fluorine stereoelctronic effects and effects of existing substituents.

Chapter four further expands the scope of fluorination and conformational analysis on the azepane model system. The effects of multiple fluorines and other polar groups on the azepane ring were studied. As the interplay between fluorine stereoelectronic effects and other substituent effects changed with the regioposition of fluorine substitution, the

conformational bias changed with the fluorine position. Multiple fluorination may not offer additional conformational bias as it also brought more opportunities for conflicting conformational effects. The fluorine substitution showed stronger conformational control compared to the hydroxy group in this azepane ring system. Finally, the varient temperature studies showed shallow barriers for the conformational mobility of these azepanes.

In **Chapter five**, the fluorination methodology for vicinal fluorination on substituted azepanes was investigated. The structure elucidation revealed epimerization of a residential C–F bond and formation of ring contracted piperidines during the nucelophilic fluorination. The fluorination outcomes could be explained by a potential fluoronium–aziridinium cascade neighbouring group effect.

In **Chapter 6**, fluoroazepanes were transformed to fluorinated (−)–balanol anaogues. The total synthesis of the parent compound, (−)–balanol, was accomplished using reported methods. The analogues were examined for their binding profiles to PKA/PKC isozymes. The results revealed that the fluorinated balanol analogues can retain or improve binding.

7.2. Future Directions

Fluorination results in significant conformational bias in susbstituted azepanes. It would be interesting to further investigate the chemistry and conformational effects of vicinal difluorination and the combination of fluorine with other polar functional groups in these azepanes. The hydroxy and fluorohydroxy azepanes can be utilized to produce new series of (−)–balanol analogues to investigate PKA/PKC isozyme selectivity profiles. In addition, other AGC kinases can be profiled with these balanoids, in conjuction with homology modelling to understand the role of combined chemical and conformational diversity in designing better inhibitors with improved selectivity.

Appendices

Table of contents:

Appendix A: Full NMR spectra of compounds discussed in chapter 2……..……262

Appendix B: Full NMR spectra and conformational details of compounds discussed in chapter 3……...……..…… 346

Appendix C: Full NMR spectra, variant temperature study and conformational details of compounds discussed in chapter 4……...……..……388

Appendix D: Full NMR spectra of compounds discussed in chapter 5……..……480

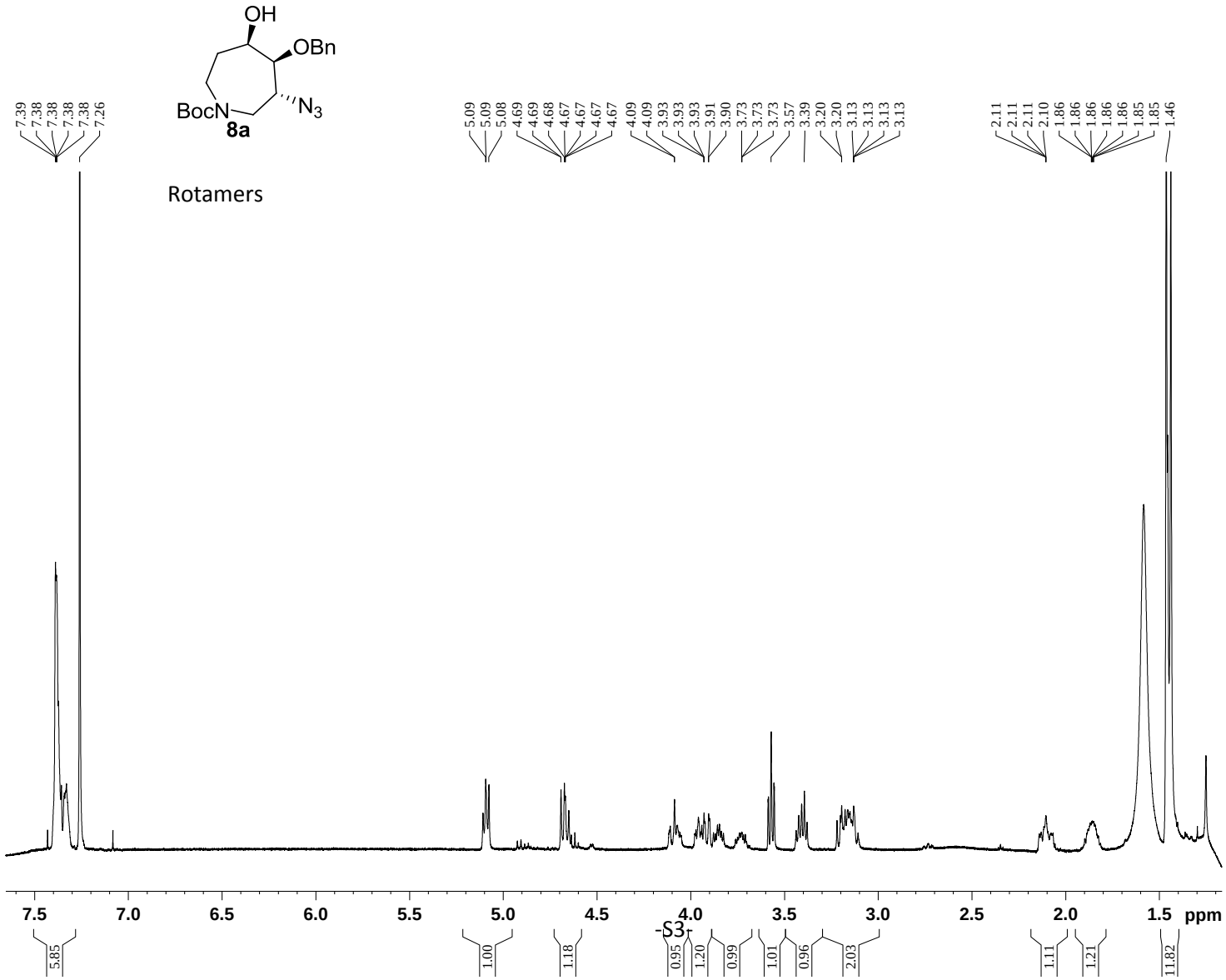
Appendix E: Full NMR spectra and binding study details of compounds discussed in chapter 6……...……..…… 643

Appendix A

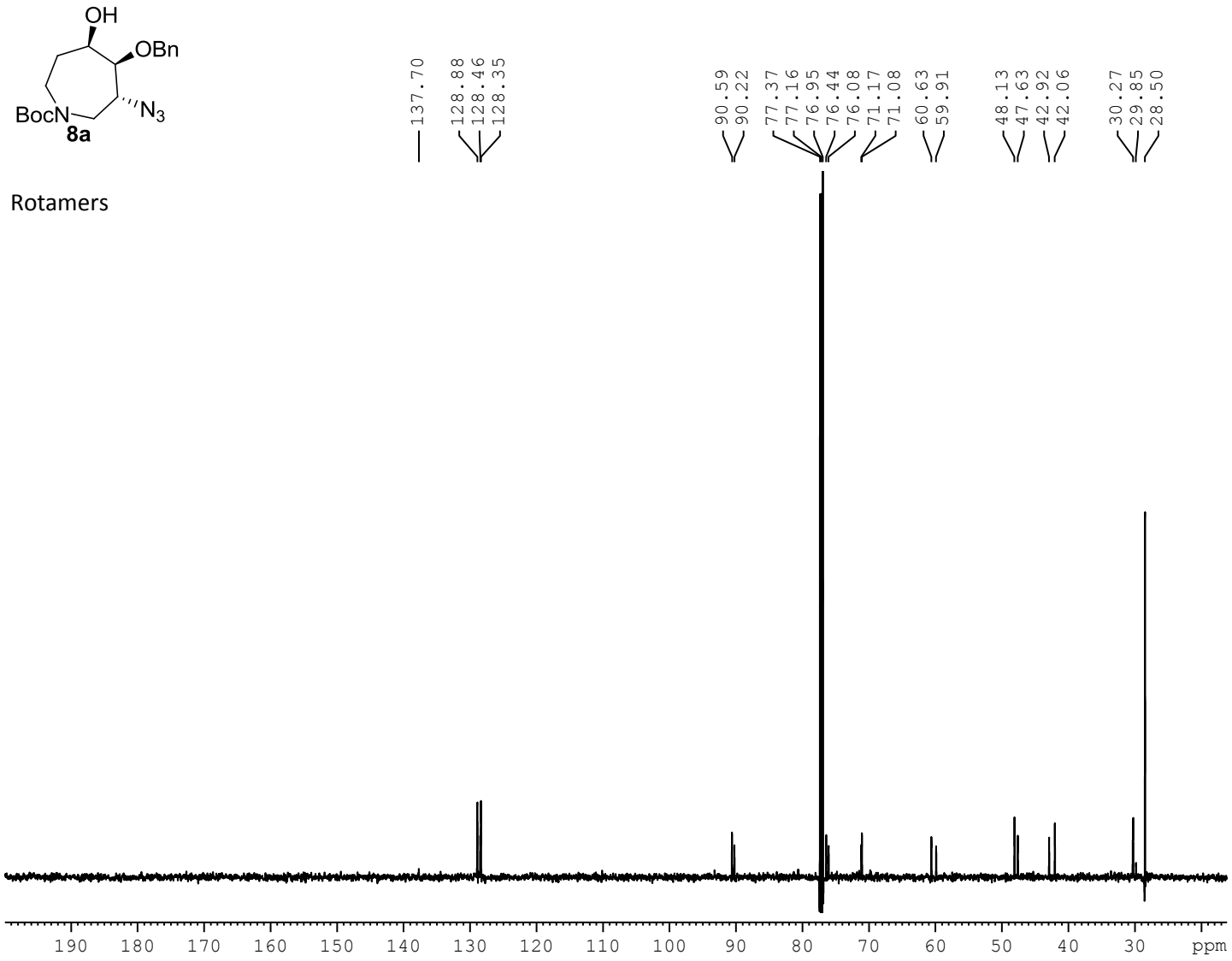
Table of contents:

Full NMR spectra of compounds discussed in chapter 2……..…..……263

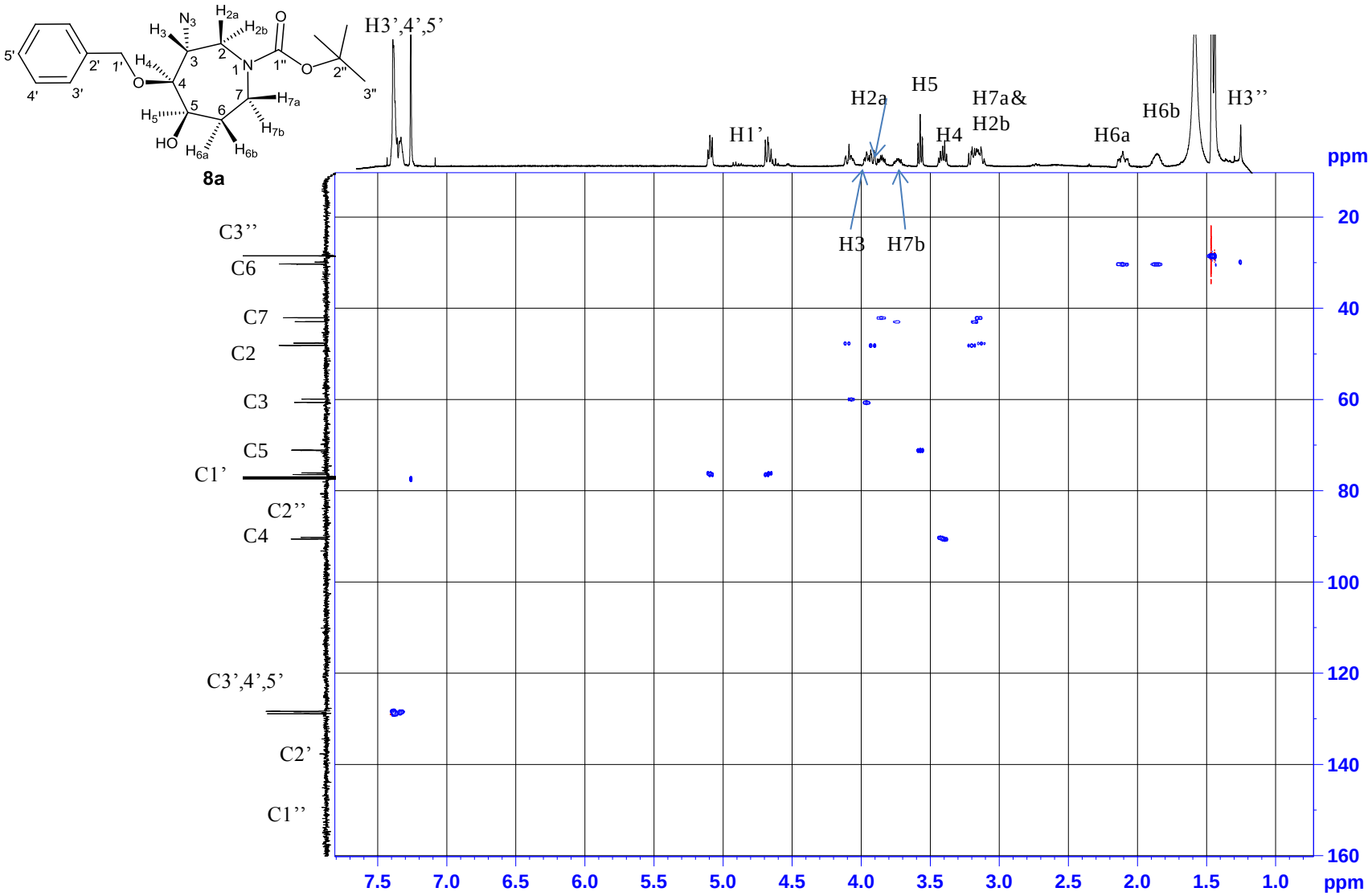
^{1}H-**8a**


OH
OBn
BocN
N3
8a
Rotamers
7.39 7.38 7.38 7.38 7.38 7.26
5.09 5.09 5.08 4.69 4.69 4.68 4.67 4.67 4.67 4.67 4.09 4.09 3.93 3.93 3.93 3.91 3.90 3.73 3.73 3.73 3.57 3.39 3.20 3.20 3.13 3.13 3.13 3.13
2.11 2.11 2.11 2.10 1.86 1.86 1.86 1.86 1.86 1.85 1.85 1.46
7.5 7.0 6.5 6.0 5.5 5.0 4.5 4.0 3.5 3.0 2.5 2.0 1.5 ppm
5.85 1.00 1.18 0.95 1.20 0.99 1.01 0.96 2.03 1.11 1.21 11.82

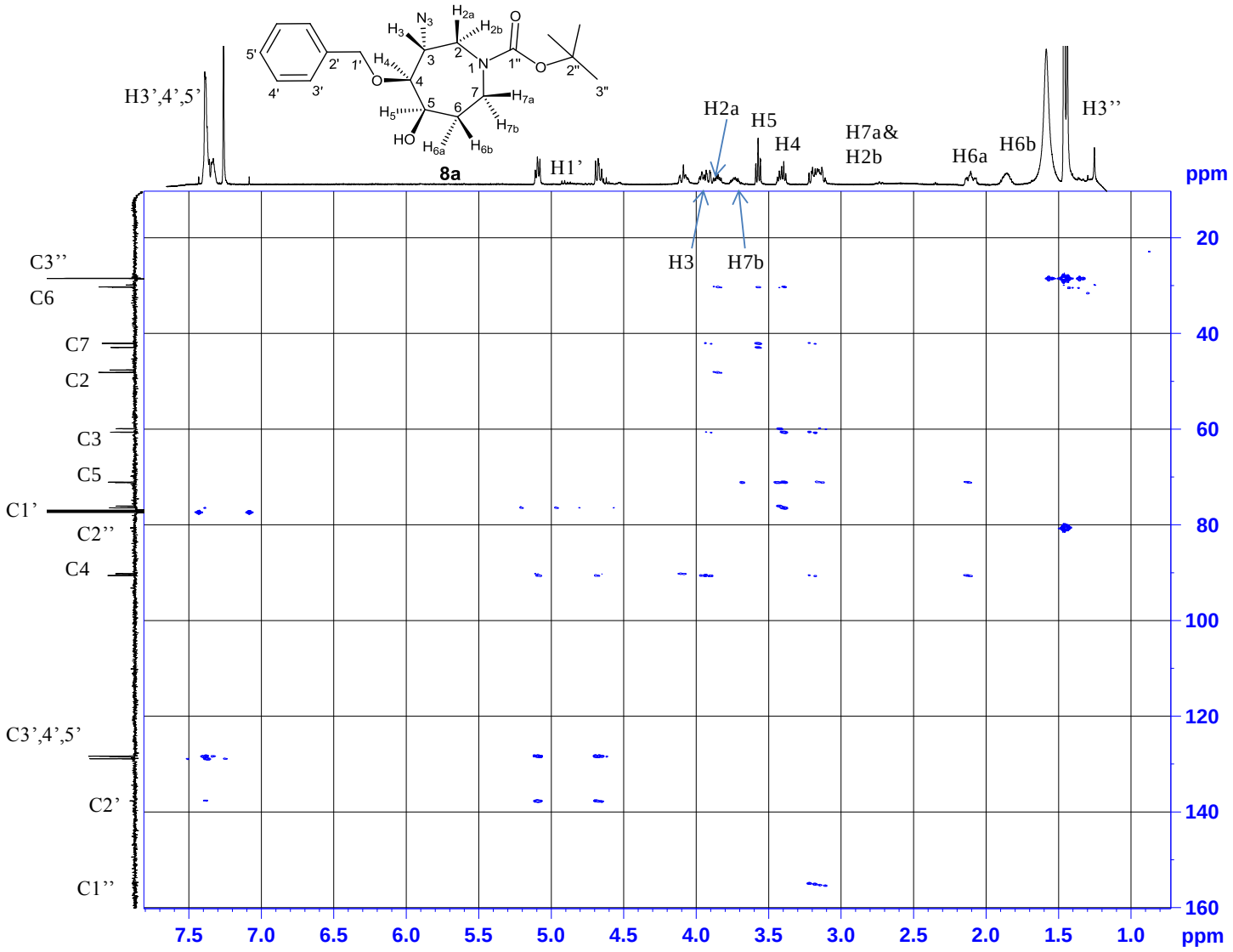
^{13}C-**8a**


OH
OBn
BocN
N3
8a
Rotamers
137.70
128.88
128.46
128.35
90.59
90.22
77.37
77.16
76.95
76.44
76.08
71.17
71.08
60.63
59.91
48.13
47.63
42.92
42.06
30.27
29.85
28.50
190
180
170
160
150
140
130
120
110
100
90
80
70
60
50
40
30
ppm

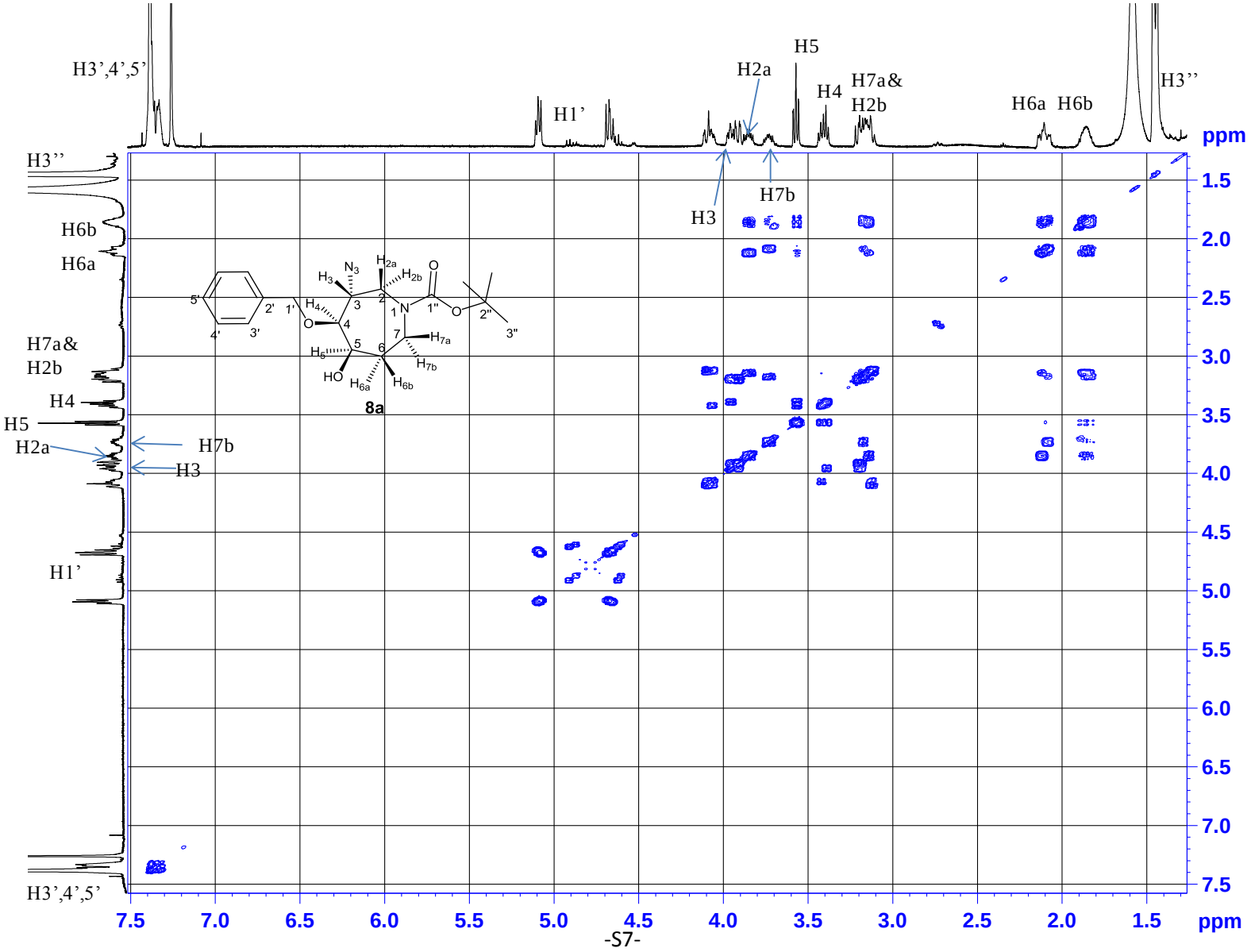
HSQC-**8a**


8a
H3',4',5'
H1'
H2a
H5
H7a&
H2b
H4
H6a
H6b
H3''
H3
H7b
C3''
C6
C7
C2
C3
C5
C1'
C2''
C4
C3',4',5'
C2'
C1''
ppm
20
40
60
80
100
120
140
160
7.5
7.0
6.5
6.0
5.5
5.0
4.5
4.0
3.5
3.0
2.5
2.0
1.5
1.0
ppm

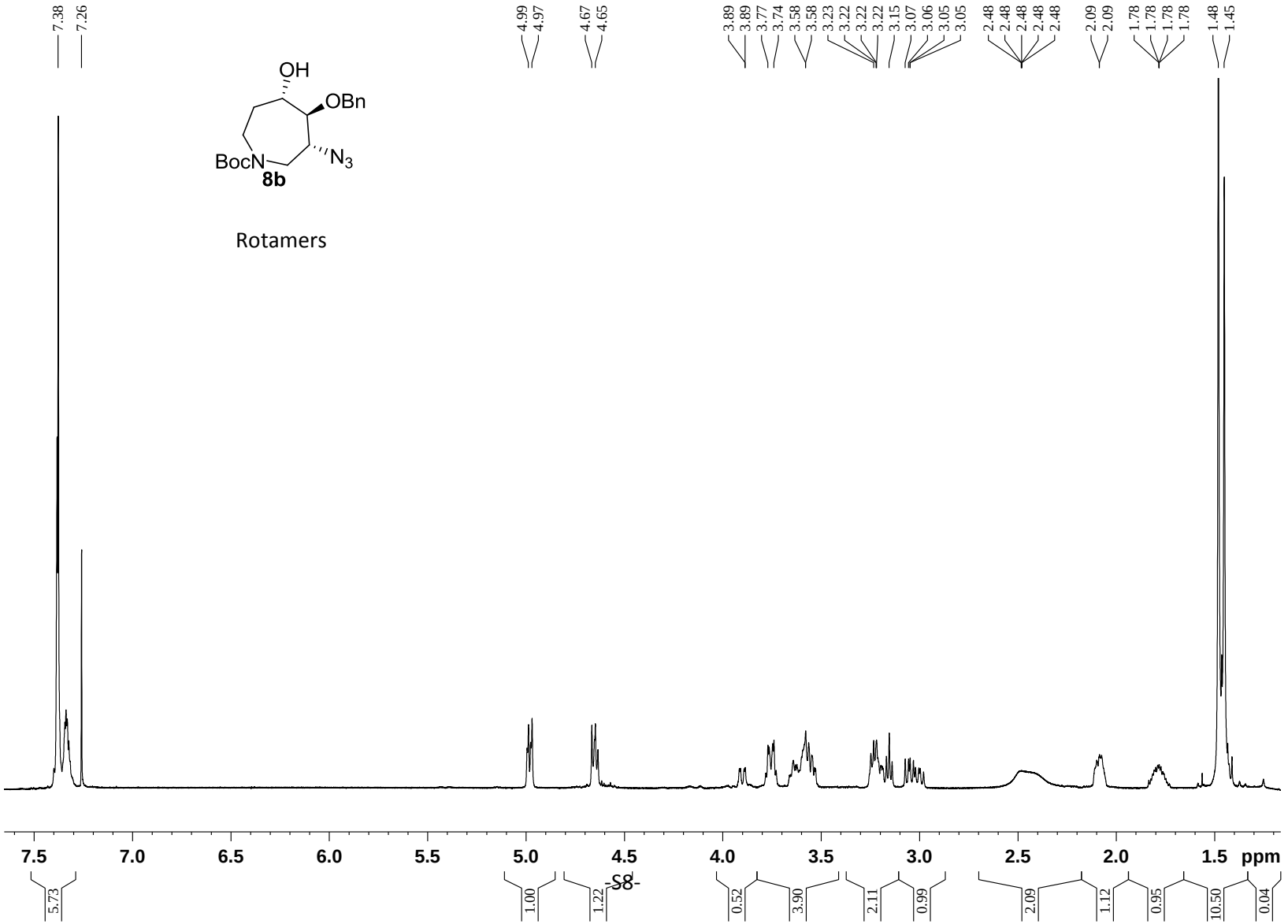
HMBC-**8a**


8a
H3',4',5'
H1'
H2a
H5
H4
H7a&
H2b
H6a
H6b
H3''
H3
H7b
C3''
C6
C7
C2
C3
C5
C1'
C2''
C4
C3',4',5'
C2'
C1''
ppm
20
40
60
80
100
120
140
160
7.5
7.0
6.5
6.0
5.5
5.0
4.5
4.0
3.5
3.0
2.5
2.0
1.5
1.0
ppm

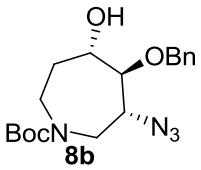
COSY-**8a**


H3',4',5'
H1'
H2a
H5
H4
H7a&
H2b
H6a
H6b
H3''
ppm
H3''
H6b
H6a
H7a&
H2b
H4
H5
H2a
H7b
H3
H1'
H3',4',5'
H3
H7b
8a
7.5
7.0
6.5
6.0
5.5
5.0
4.5
4.0
3.5
3.0
2.5
2.0
1.5
ppm

^{1}H-**8b**


7.38
7.26
4.99
4.97
4.67
4.65
3.89
3.89
3.77
3.74
3.58
3.58
3.23
3.22
3.22
3.22
3.15
3.07
3.06
3.05
3.05
2.48
2.48
2.48
2.48
2.48
2.09
2.09
1.78
1.78
1.78
1.78
1.48
1.45
OH
OBn
N3
BocN
8b
Rotamers
7.5
7.0
6.5
6.0
5.5
5.0
4.5
4.0
3.5
3.0
2.5
2.0
1.5
ppm
5.73
1.00
1.22
0.52
3.90
2.11
0.99
2.09
1.12
0.95
10.50
0.04

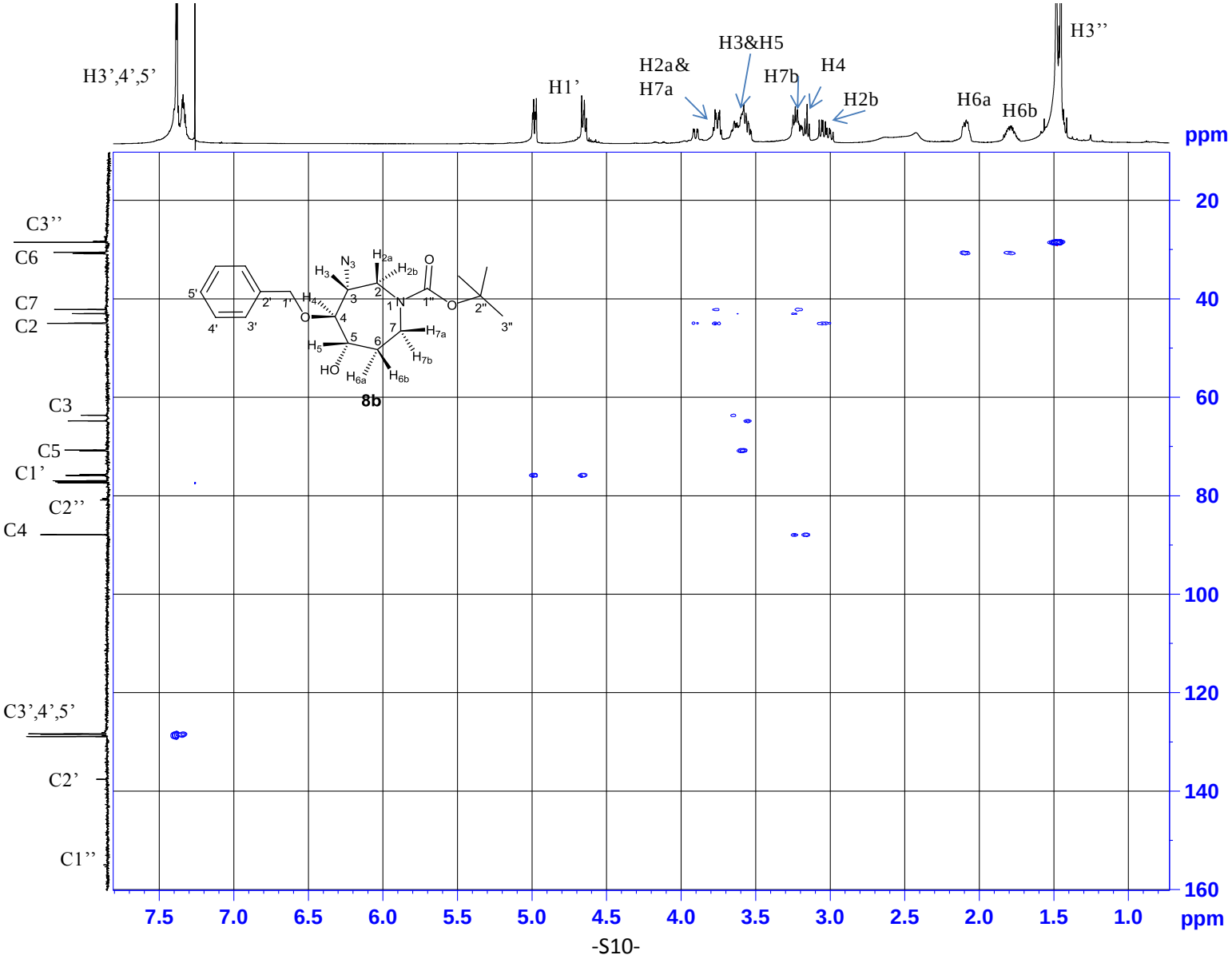
^{13}C-**8b**



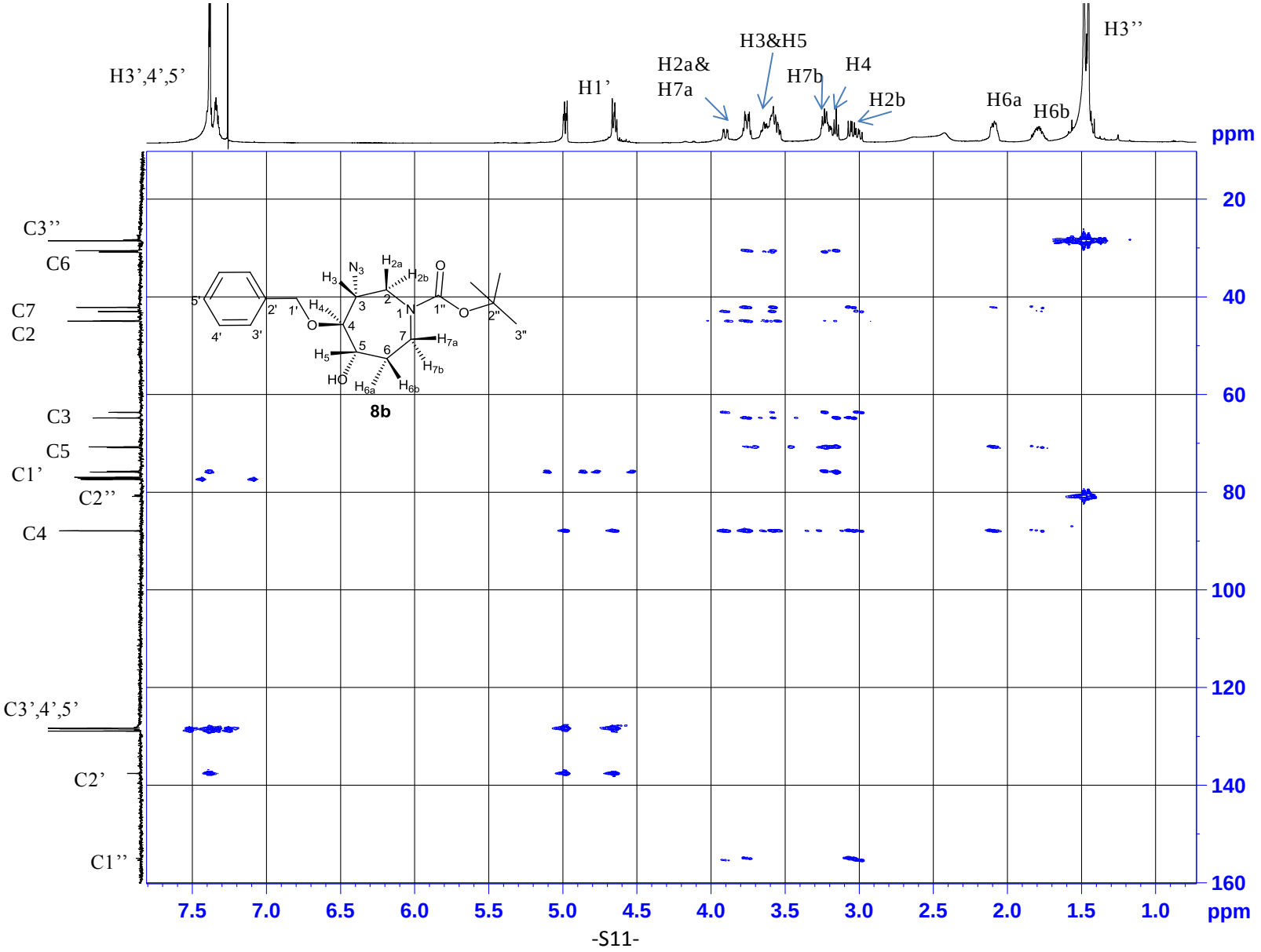
8b

Rotamers

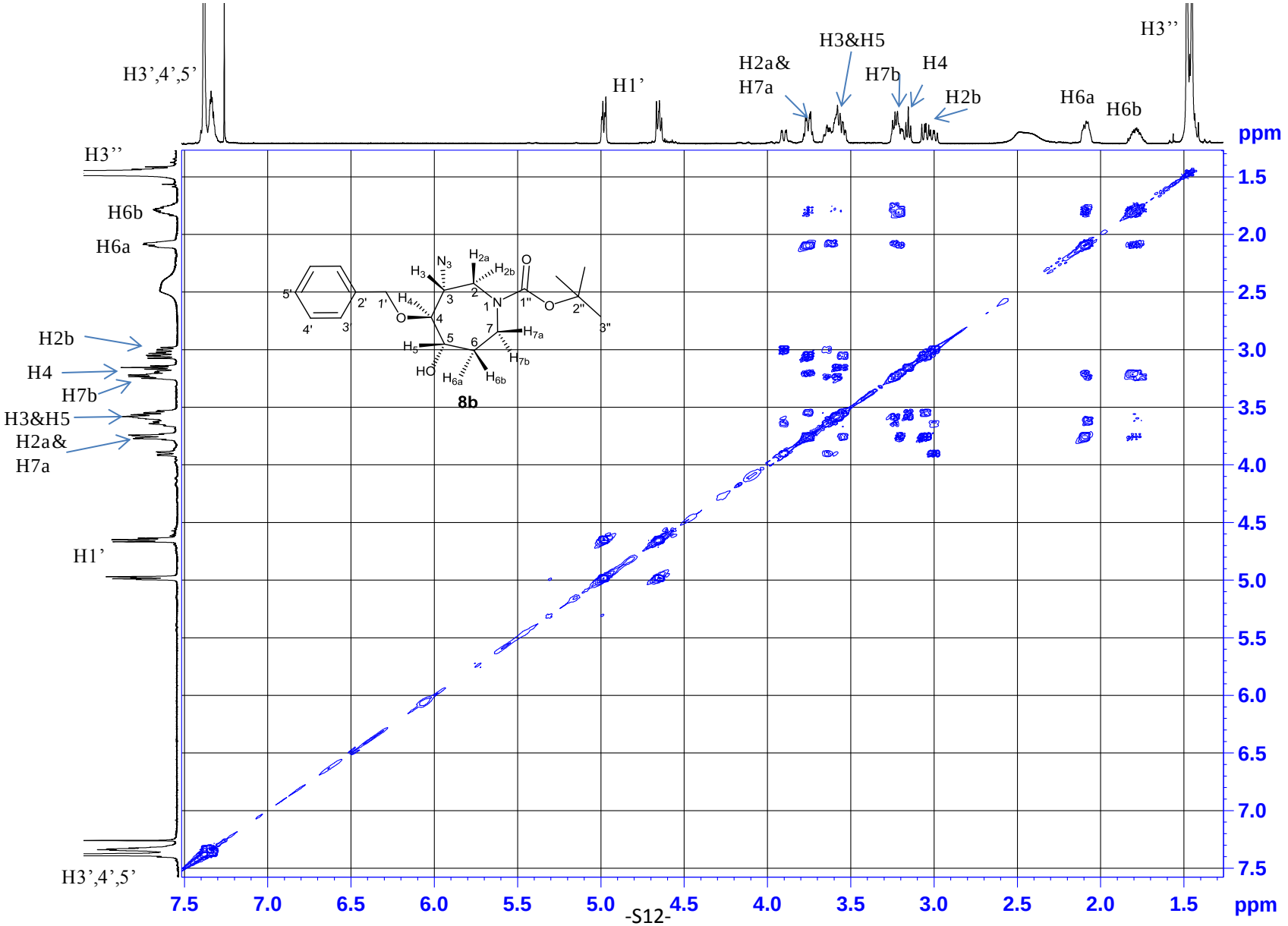
HSQC-**8b**


H3',4',5'
H1'
H2a&
H7a
H3&H5
H7b
H4
H2b
H6a
H6b
H3''
ppm
C3''
C6
C7
C2
C3
C5
C1'
C2''
C4
C3',4',5'
C2'
C1''
8b
7.5
7.0
6.5
6.0
5.5
5.0
4.5
4.0
3.5
3.0
2.5
2.0
1.5
1.0
ppm
20
40
60
80
100
120
140
160

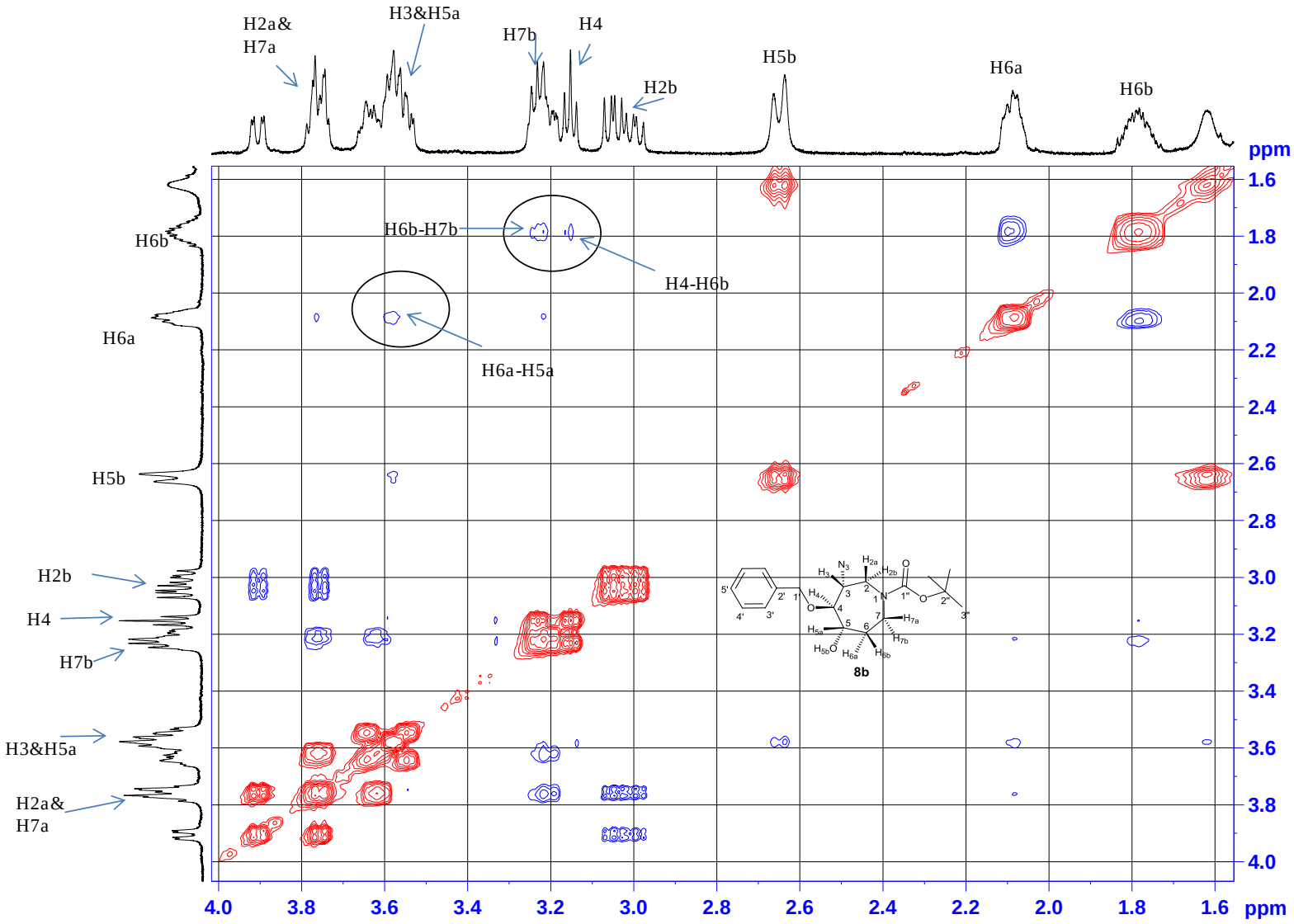
HMBC-**8b**


H3',4',5'
H1'
H2a&
H7a
H3&H5
H7b
H4
H2b
H6a
H6b
H3''
ppm
C3''
C6
C7
C2
C3
C5
C1'
C2''
C4
C3',4',5'
C2'
C1''
8b
7.5
7.0
6.5
6.0
5.5
5.0
4.5
4.0
3.5
3.0
2.5
2.0
1.5
1.0
ppm
20
40
60
80
100
120
140
160

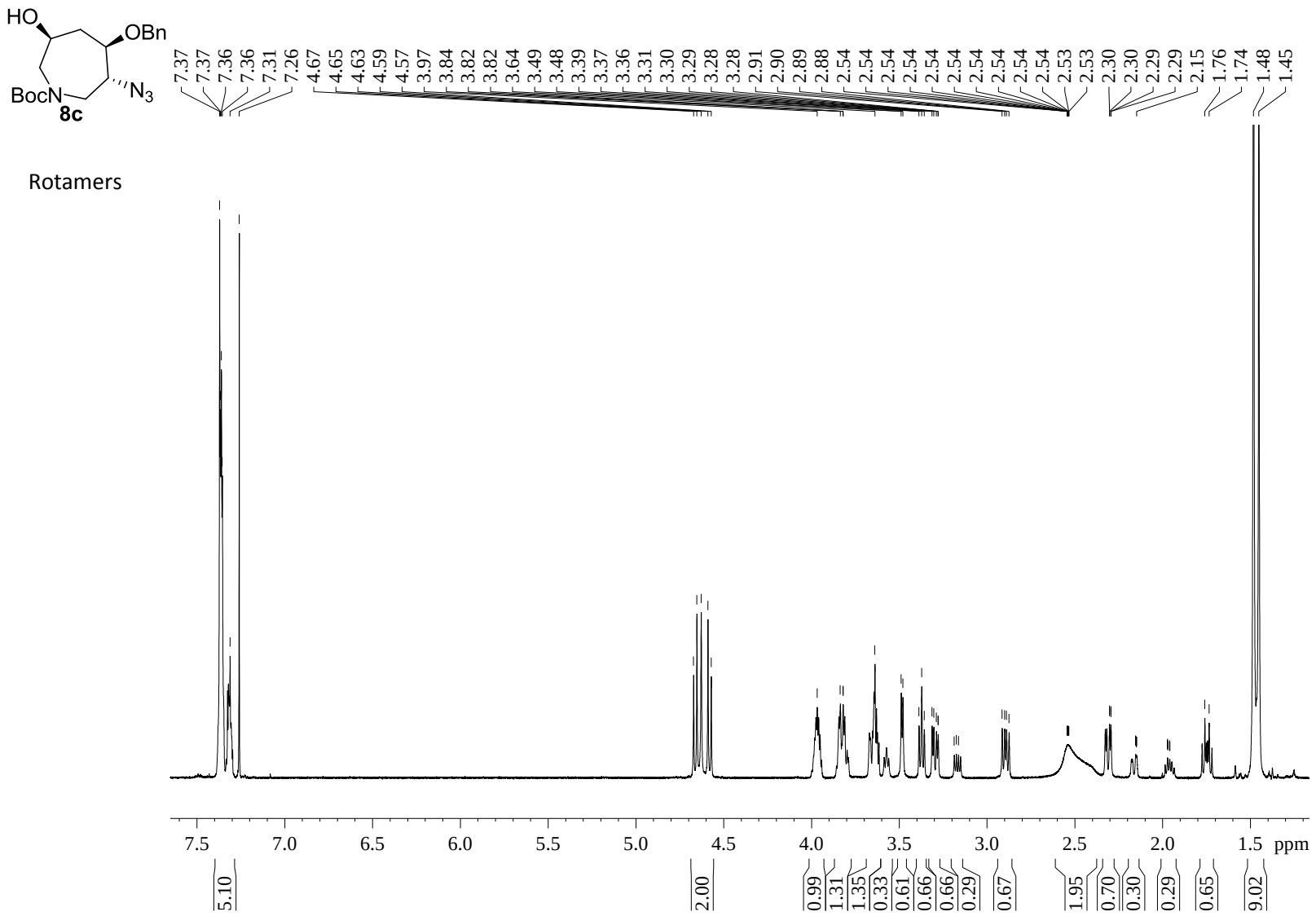
COSY-**8b**


H3',4',5'
H1'
H2a&
H7a
H3&H5
H7b
H4
H2b
H6a
H6b
H3''
ppm
1.5
2.0
2.5
3.0
3.5
4.0
4.5
5.0
5.5
6.0
6.5
7.0
7.5
8b

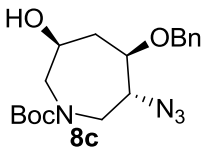
NOESY-**8b**


H2a&
H7a
H3&H5a
H7b
H4
H2b
H5b
H6a
H6b
ppm
H6b-H7b
H4-H6b
H6a-H5a
H6b
H6a
H5b
H2b
H4
H7b
H3&H5a
H2a&
H7a
8b
4.0
3.8
3.6
3.4
3.2
3.0
2.8
2.6
2.4
2.2
2.0
1.8
1.6
ppm

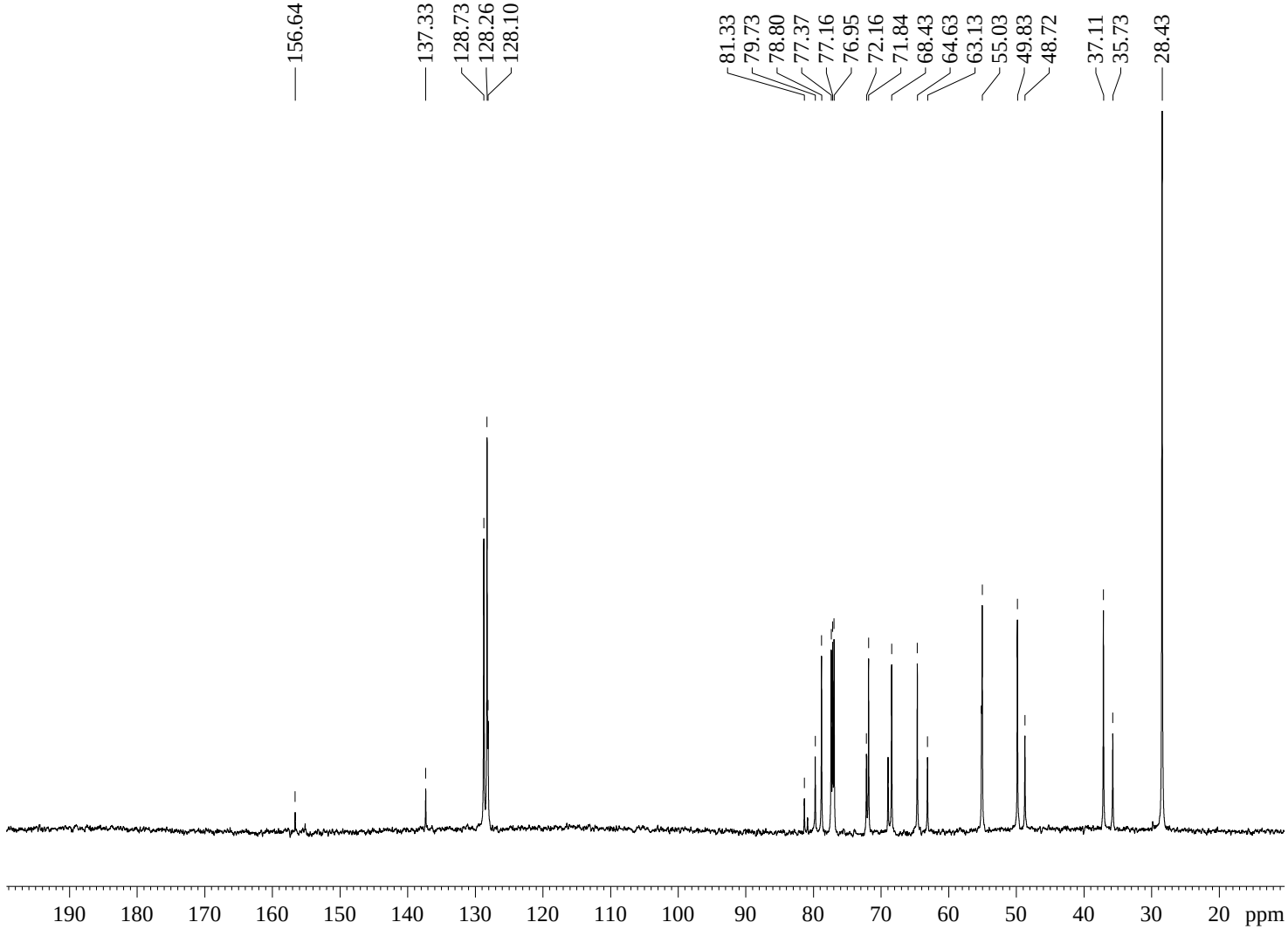
^{1}H-**8c**


HO
OBn
BocN
N3
8c
7.37 7.37 7.36 7.36 7.31 7.26 4.67 4.65 4.63 4.59 4.57 3.97 3.84 3.82 3.82 3.64 3.49 3.48 3.39 3.37 3.36 3.31 3.30 3.29 3.28 3.28 2.91 2.90 2.89 2.88 2.54 2.54 2.54 2.54 2.54 2.54 2.54 2.54 2.53 2.53 2.30 2.30 2.29 2.29 2.15 1.76 1.74 1.48 1.45
Rotamers
7.5 7.0 6.5 6.0 5.5 5.0 4.5 4.0 3.5 3.0 2.5 2.0 1.5 ppm
5.10 2.00 0.99 1.31 1.35 0.33 0.61 0.66 0.66 0.29 0.67 1.95 0.70 0.30 0.29 0.65 9.02

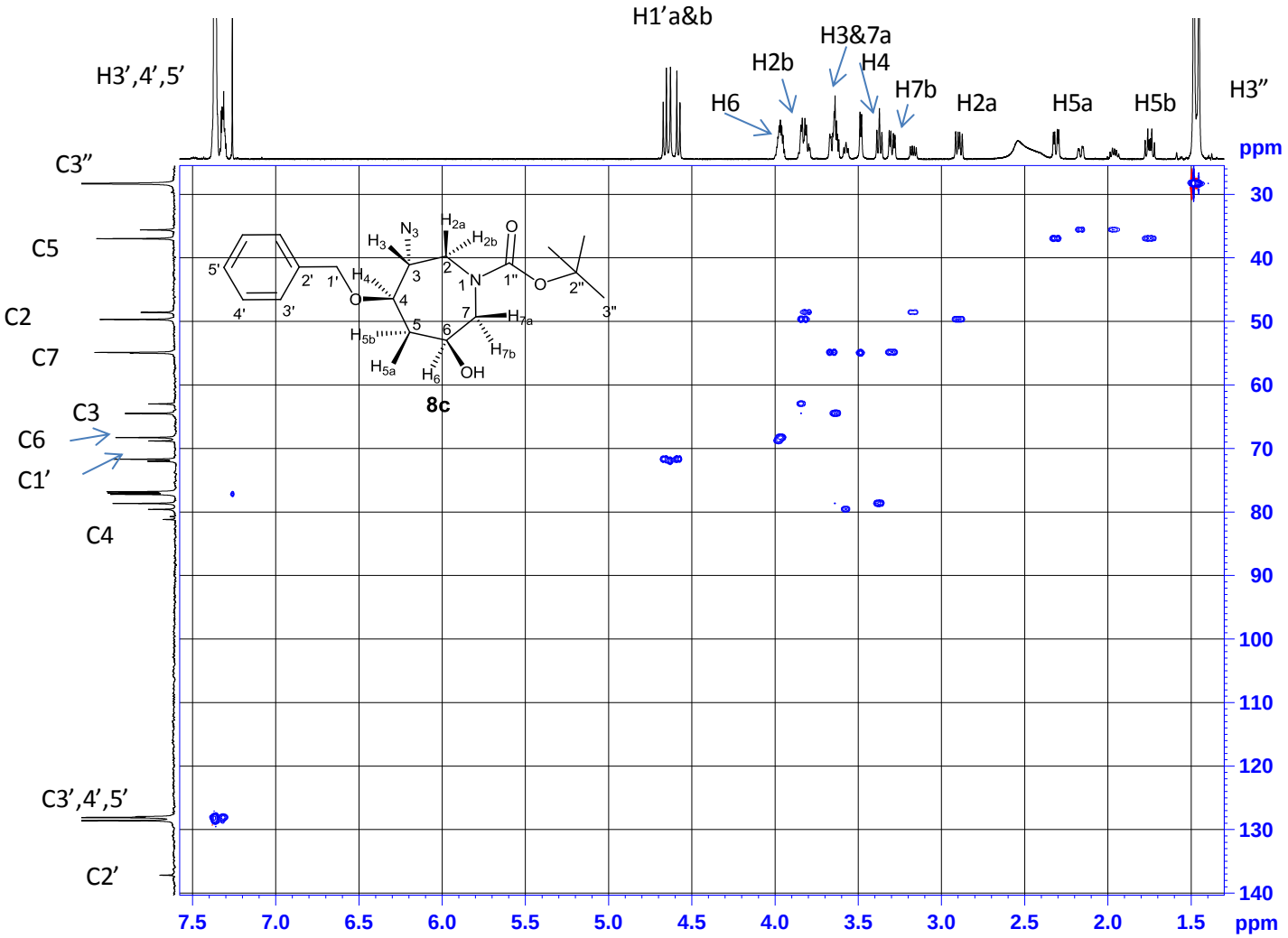
^{13}C-**8c**



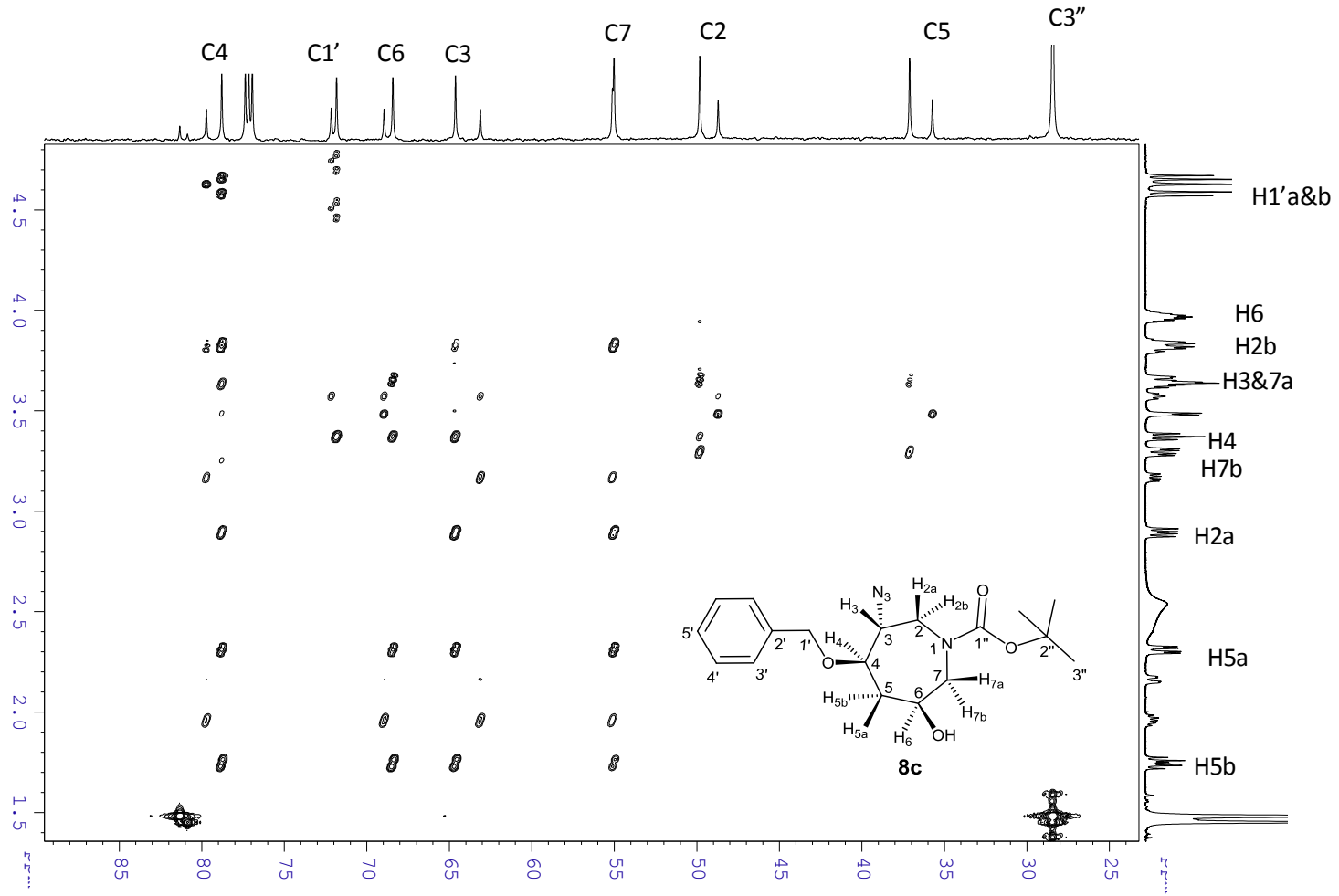
Rotamers



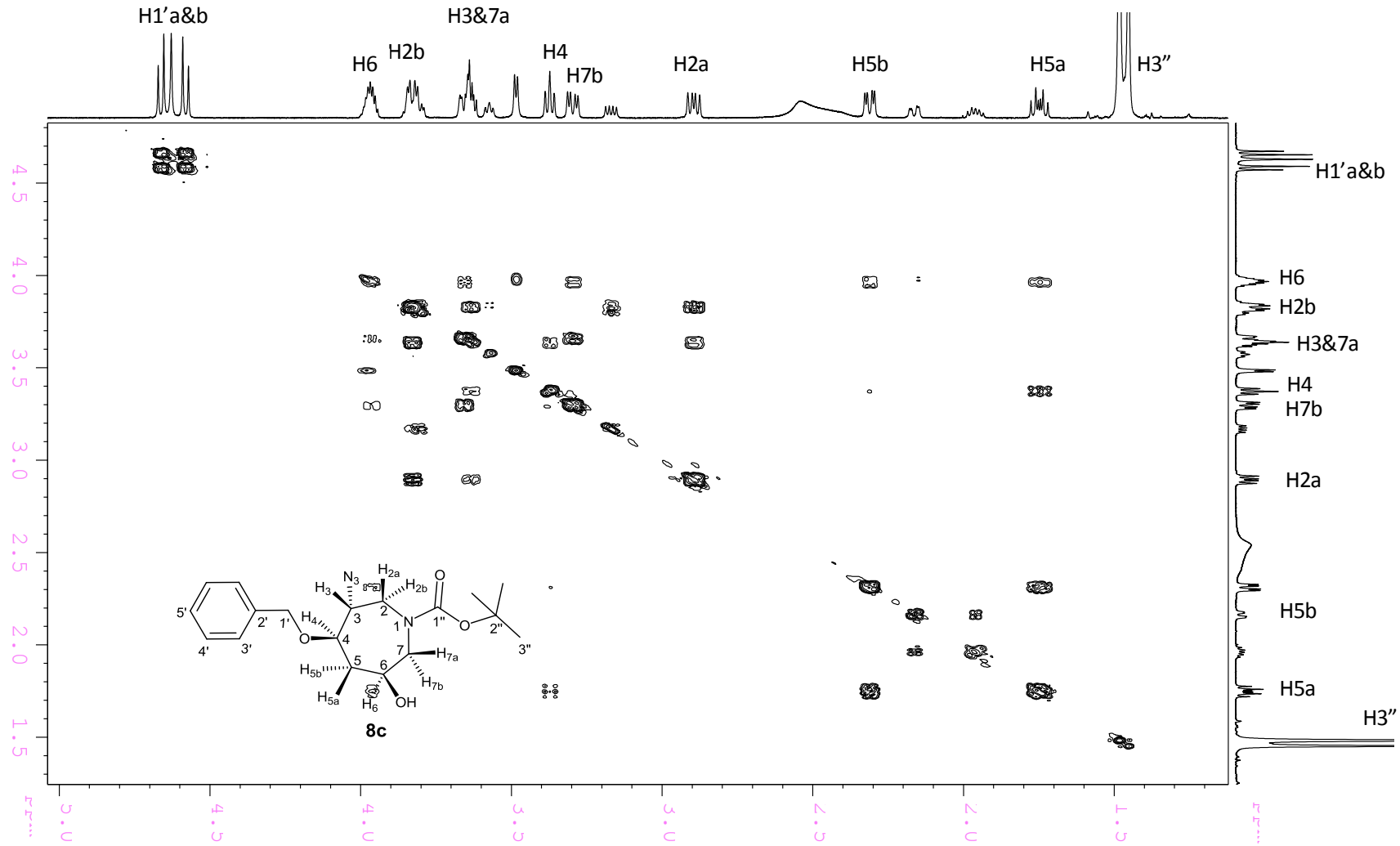
HSQC-**8c**


H1'a&b
H3&7a
H2b
H4
H6
H7b
H2a
H5a
H5b
H3"
H3',4',5'
ppm
C3"
C5
C2
C7
C3
C6
C1'
C4
C3',4',5'
C2'
8c
7.5
7.0
6.5
6.0
5.5
5.0
4.5
4.0
3.5
3.0
2.5
2.0
1.5
ppm

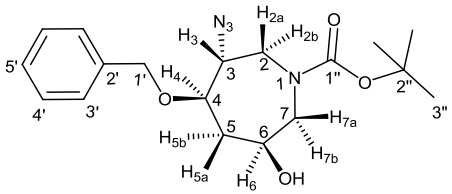
HMBC-**8c**



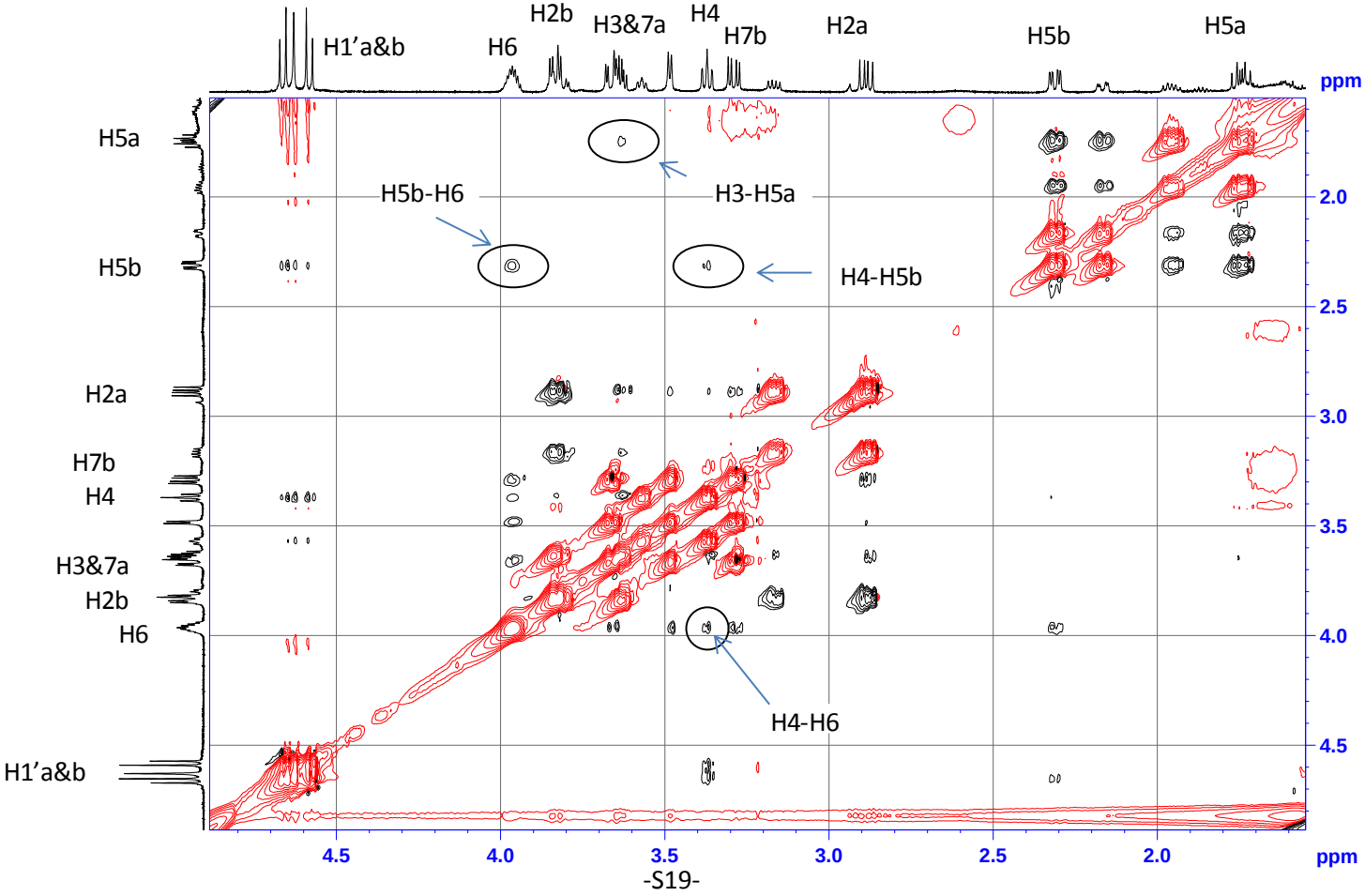
COSY-**8c**


H1'a&b
H6
H2b
H3&7a
H4
H7b
H2a
H5b
H5a
H3"
H1'a&b
H6
H2b
H3&7a
H4
H7b
H2a
H5b
H5a
H3"
8c

NOESY-**8c**

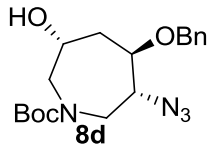


8c

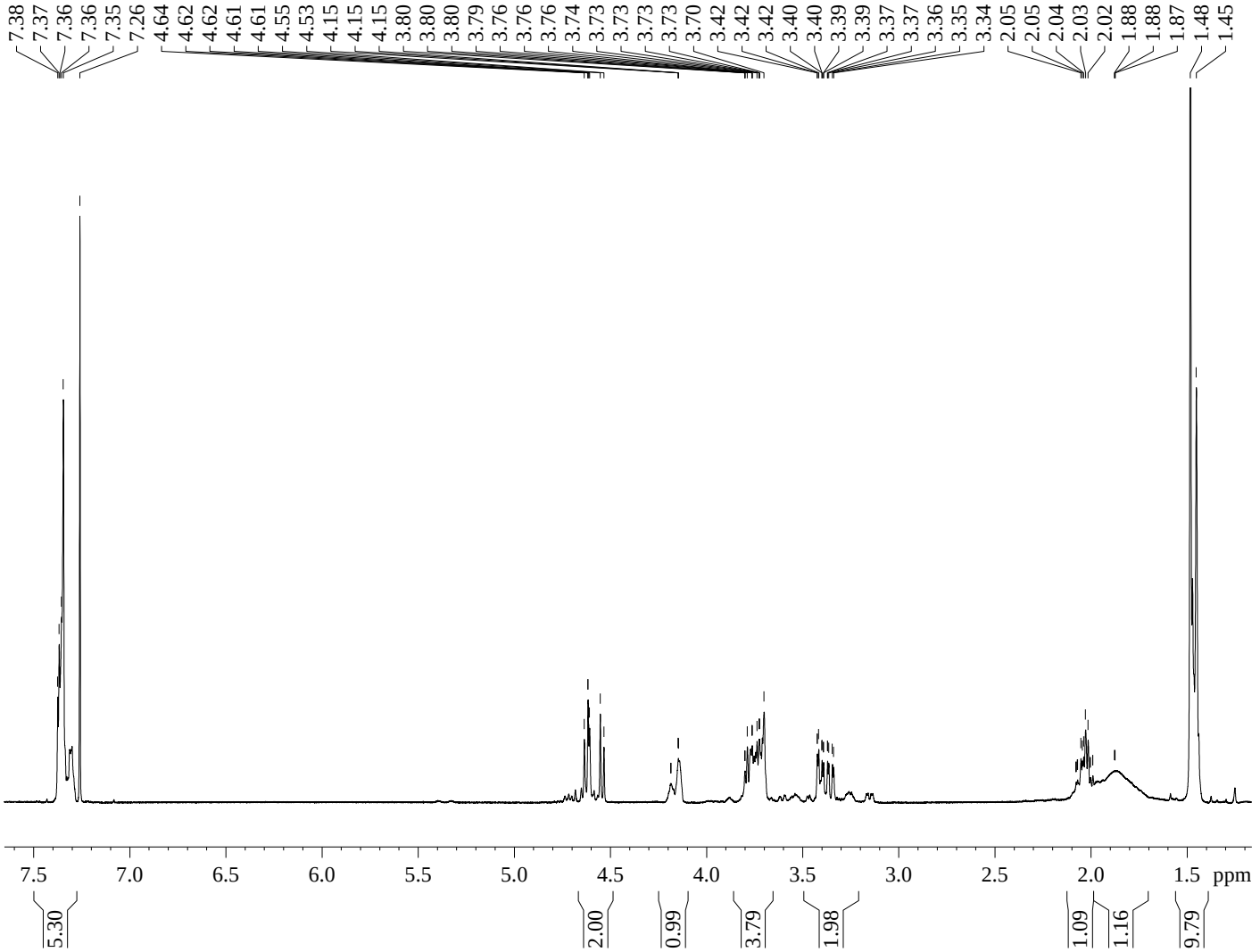


-S19-

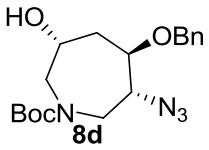
^{1}H-**8d**



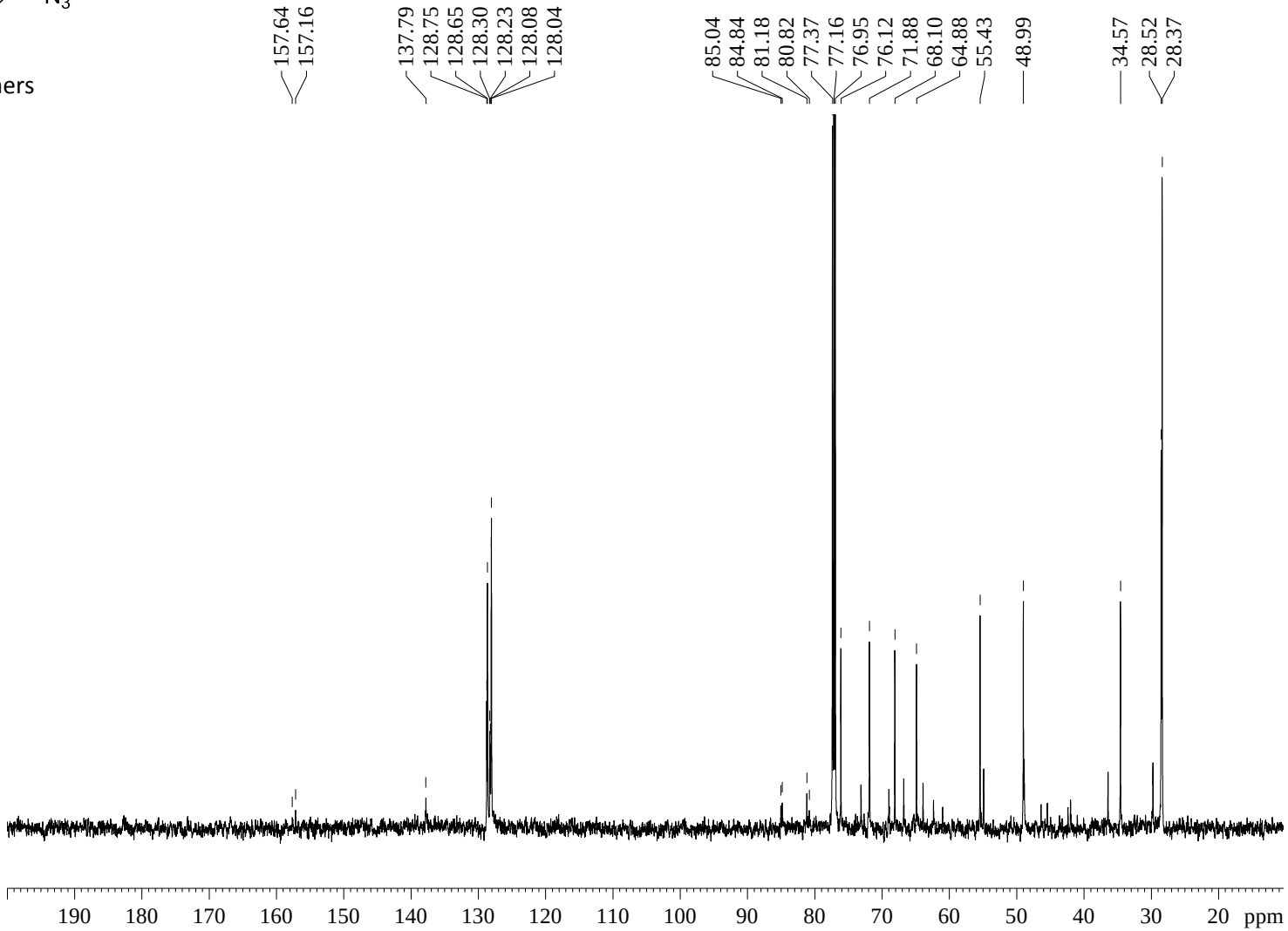
Rotamers



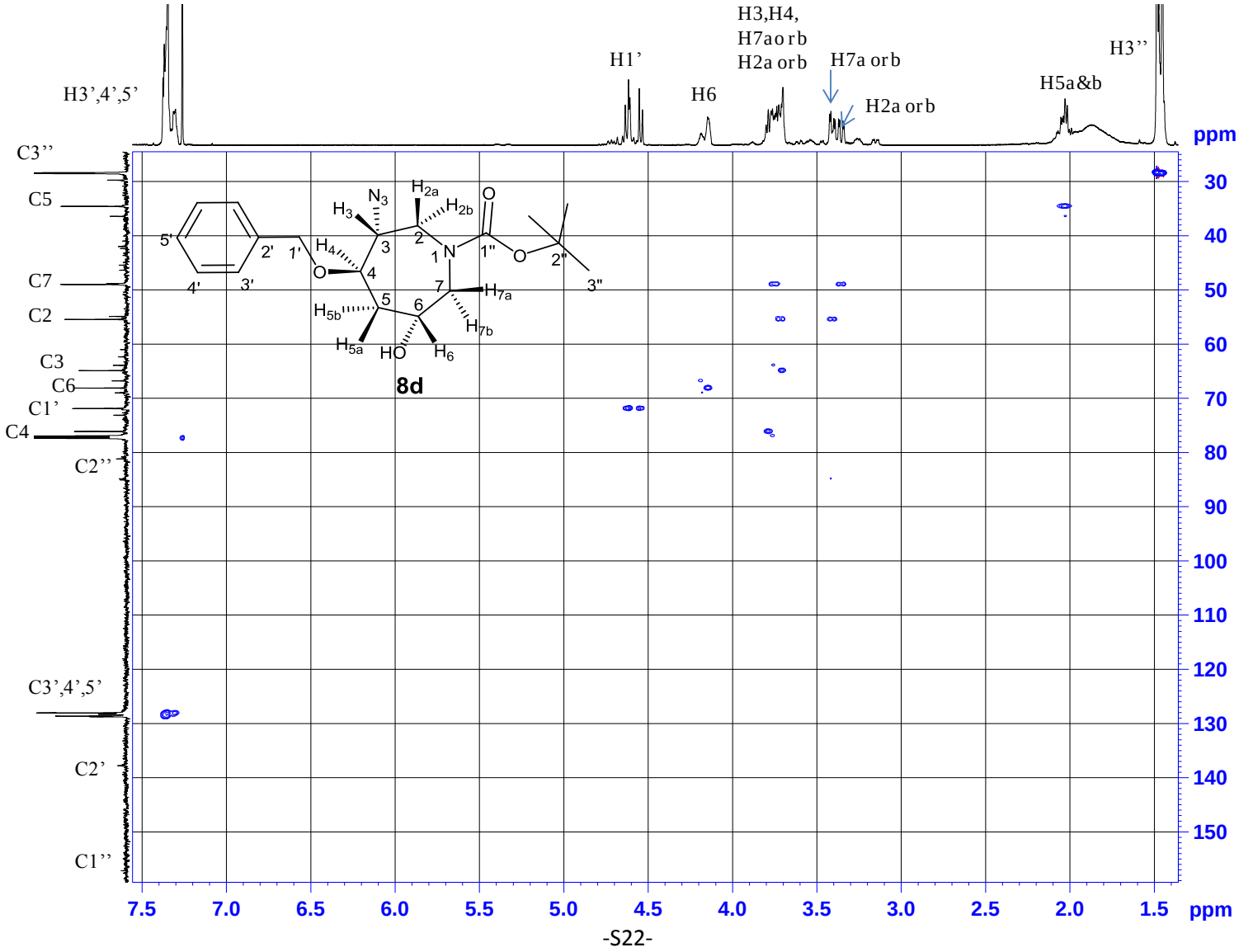
^{13}C-**8d**



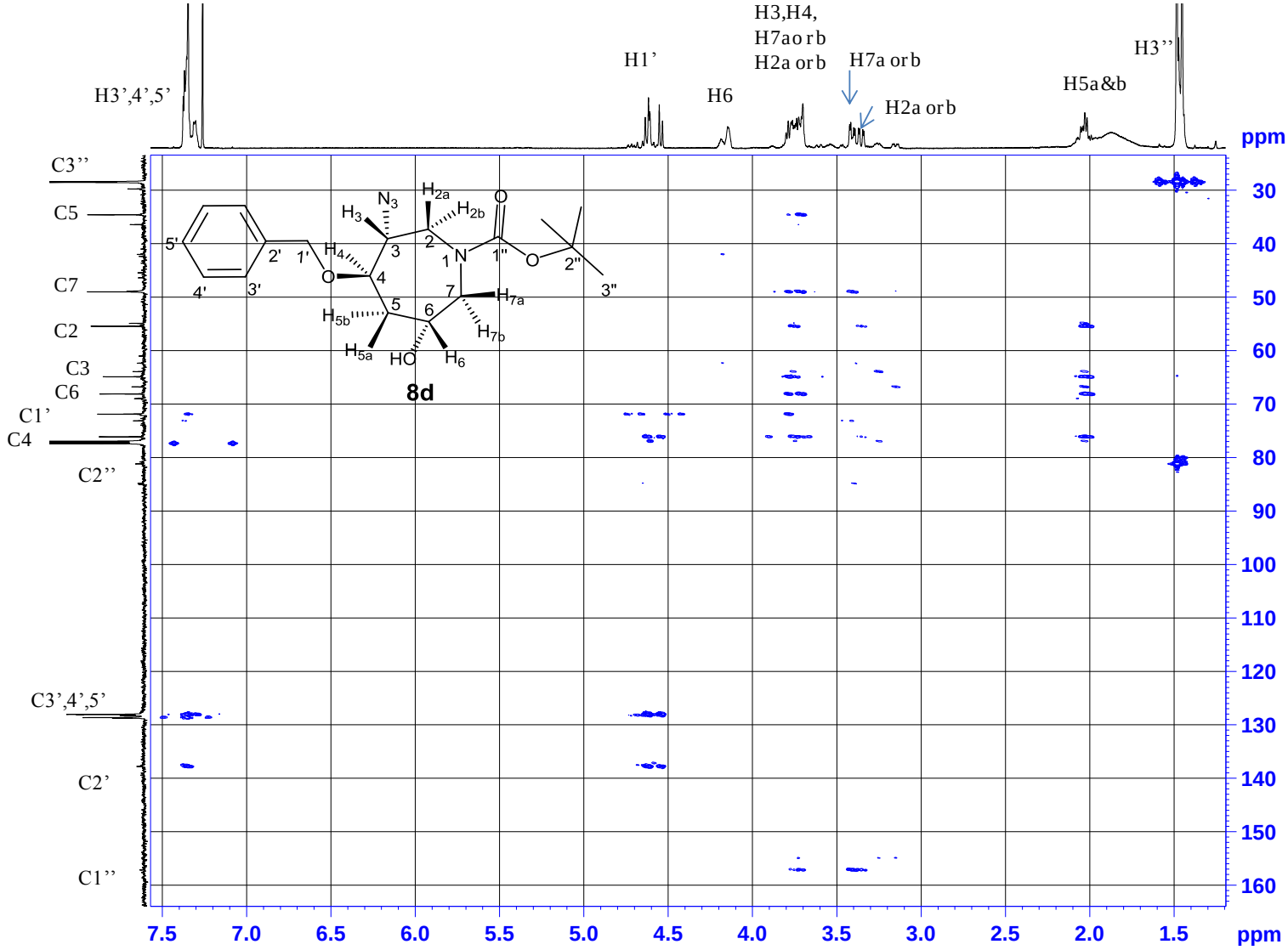
Rotamers



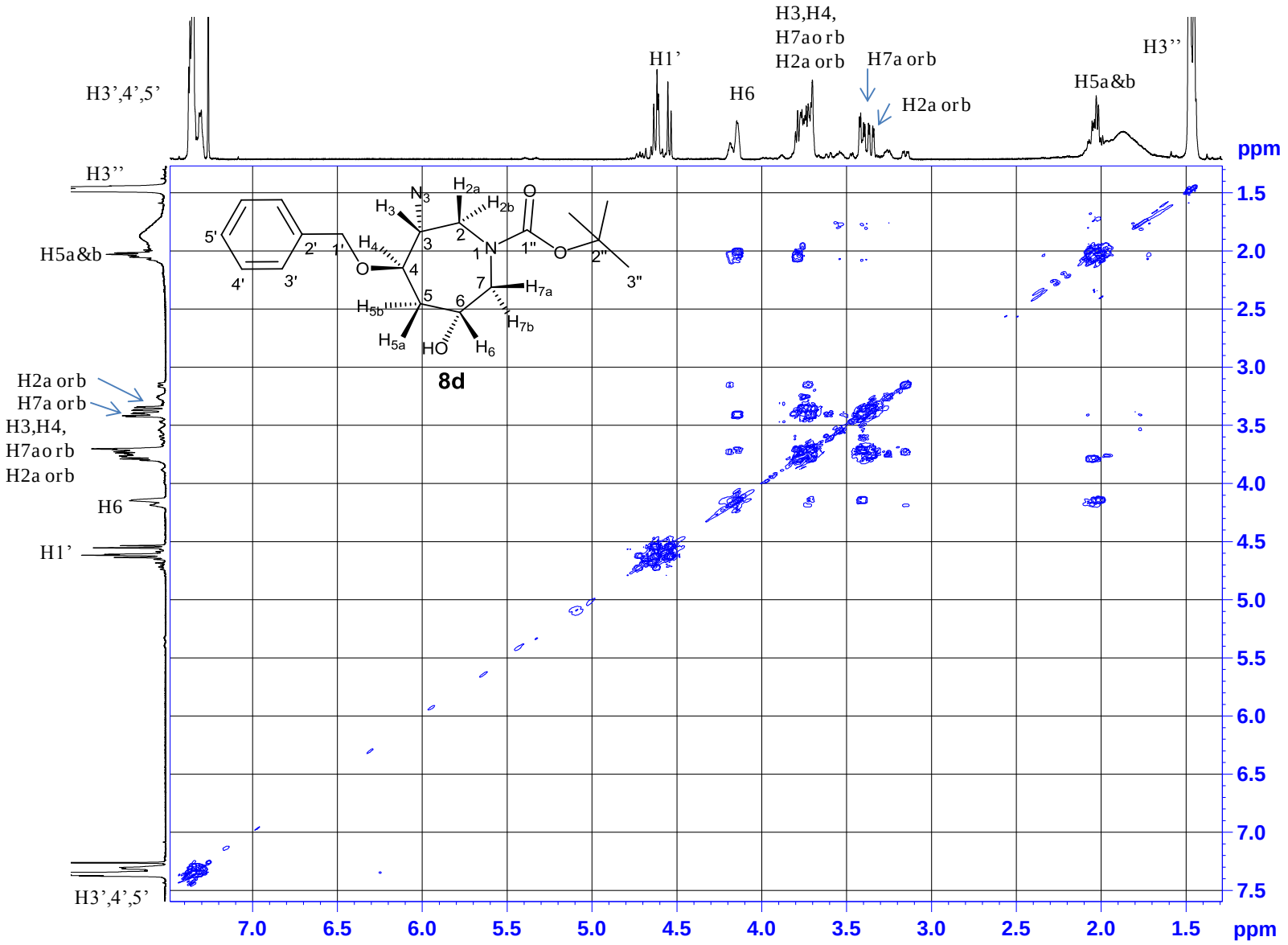
HSQC-**8d**


H3',4',5'
H1'
H6
H3,H4,
H7a o r b
H2a or b
H7a or b
H2a or b
H5a&b
H3''
ppm
C3''
C5
C7
C2
C3
C6
C1'
C4
C2''
C3',4',5'
C2'
C1''
8d
7.5
7.0
6.5
6.0
5.5
5.0
4.5
4.0
3.5
3.0
2.5
2.0
1.5
ppm

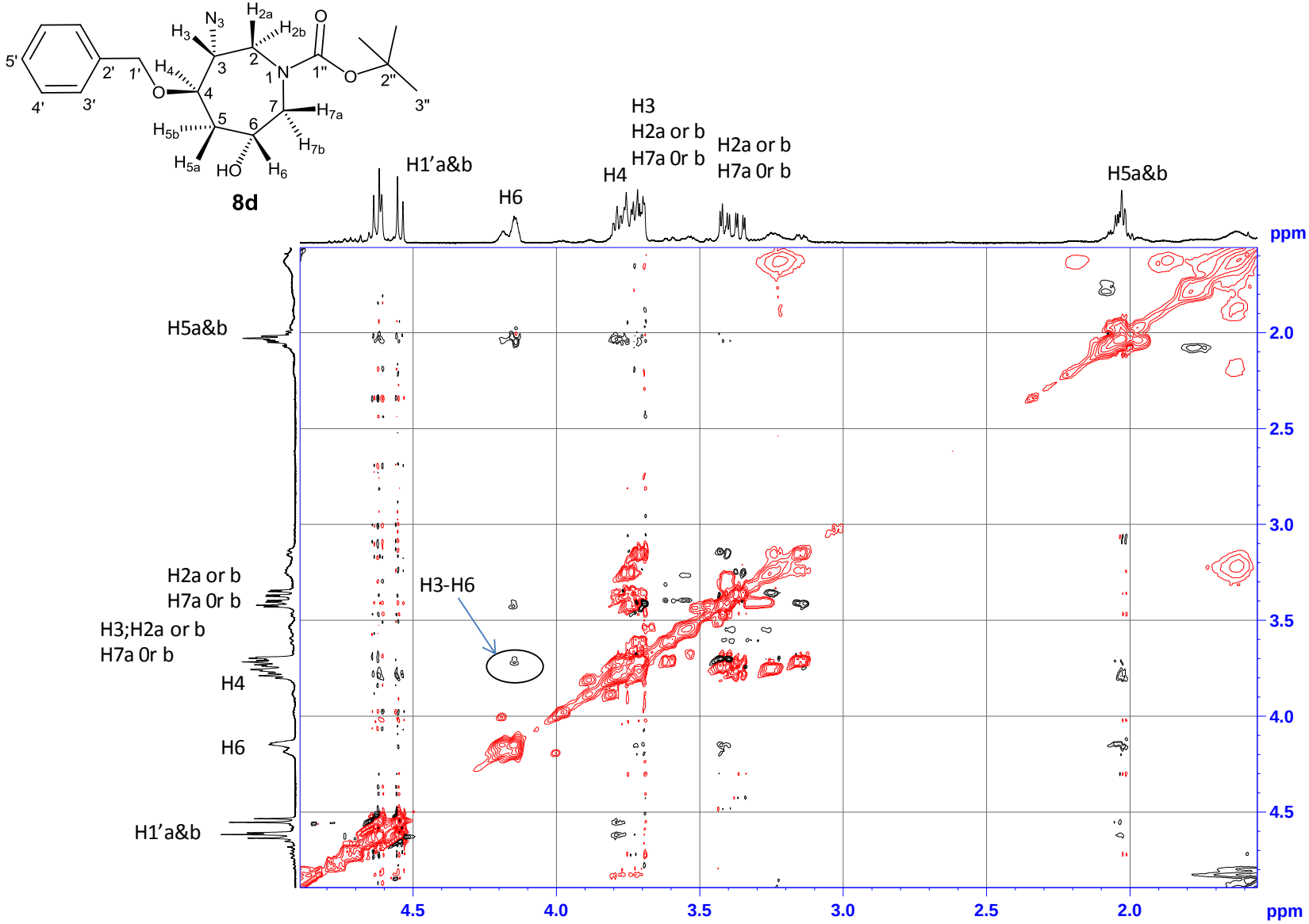
HMBC-**8d**


H3',4',5'
H1'
H6
H3,H4,
H7a or b
H2a or b
H7a or b
H2a or b
H5a&b
H3''
ppm
C3''
C5
C7
C2
C3
C6
C1'
C4
C2''
C3',4',5'
C2'
C1''
8d
7.5
7.0
6.5
6.0
5.5
5.0
4.5
4.0
3.5
3.0
2.5
2.0
1.5
ppm

COSY-**8d**

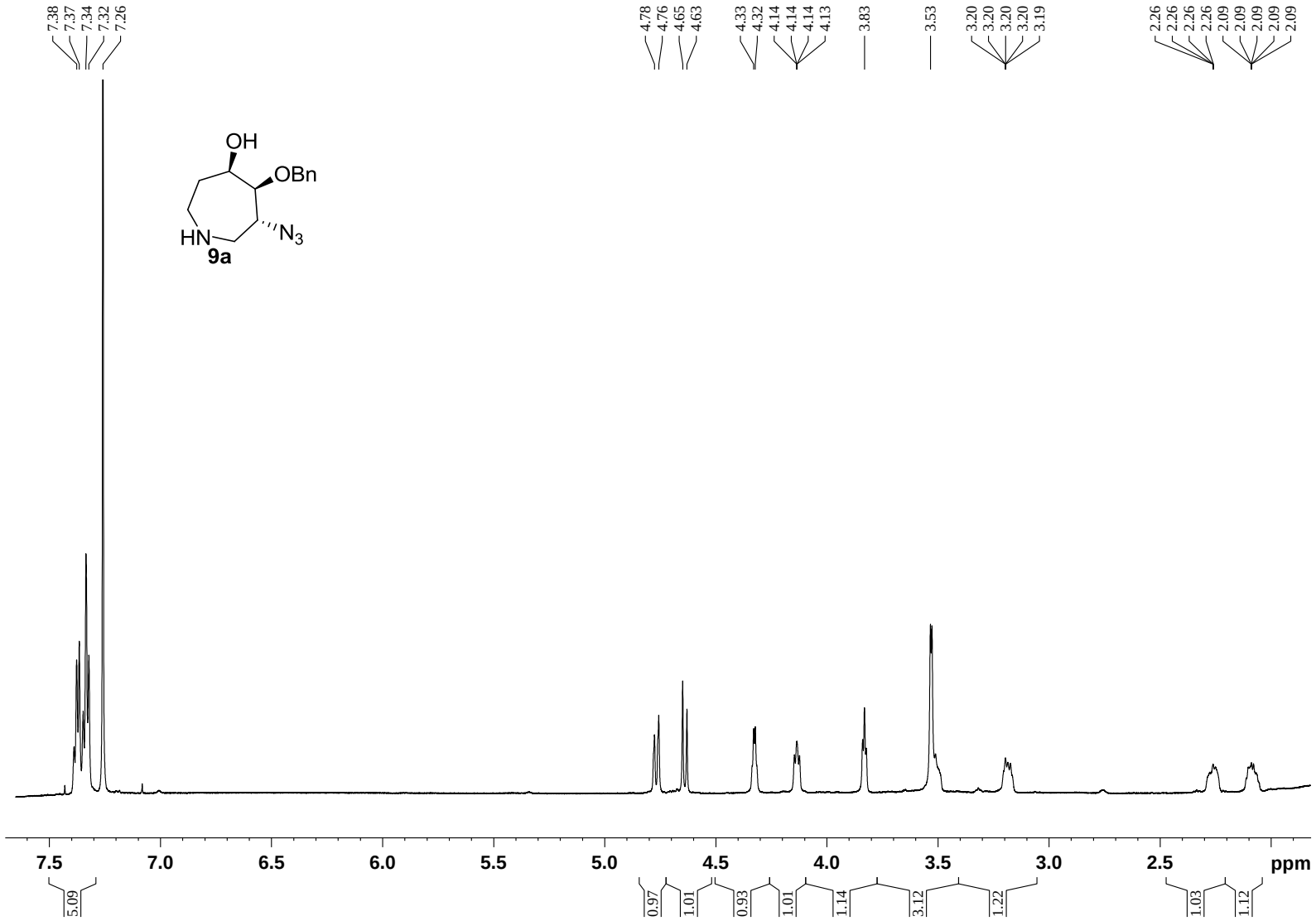

H3',4',5'
H1'
H6
H3,H4,
H7a o r b
H2a o r b
H7a o r b
H2a o r b
H5a&b
H3''
ppm
H3''
H5a&b
H2a o r b
H7a o r b
H3,H4,
H7a o r b
H2a o r b
H6
H1'
H3',4',5'
8d
7.0
6.5
6.0
5.5
5.0
4.5
4.0
3.5
3.0
2.5
2.0
1.5
ppm

NOESY-**8d**

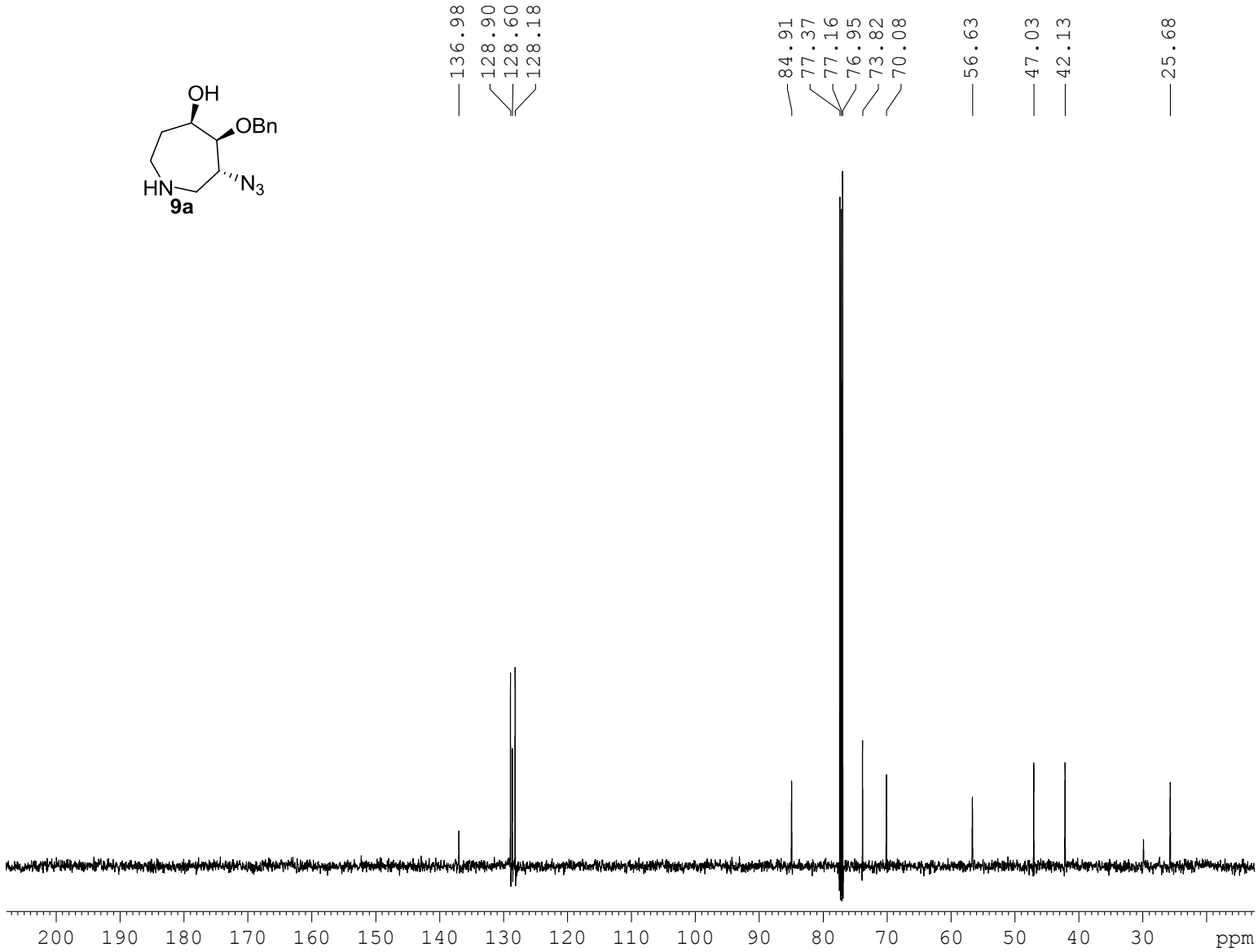

8d
H1'a&b
H6
H4
H3
H2a or b
H7a 0r b
H2a or b
H7a 0r b
H5a&b
ppm
H5a&b
H2a or b
H7a 0r b
H3;H2a or b
H7a 0r b
H4
H6
H1'a&b
H3-H6
2.0
2.5
3.0
3.5
4.0
4.5
4.5
4.0
3.5
3.0
2.5
2.0
ppm

-S25-

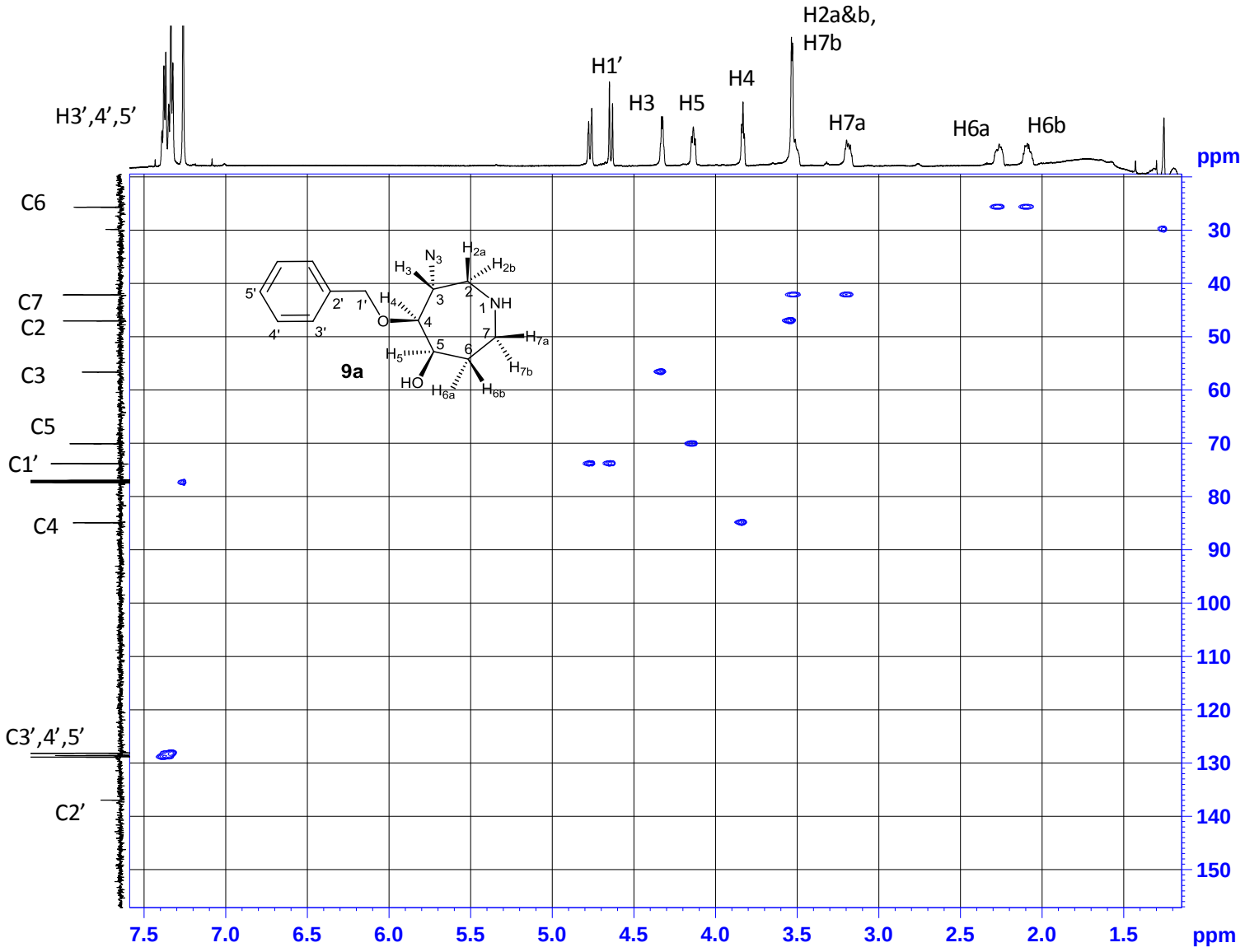
^{1}H-**9a**


7.38
7.37
7.34
7.32
7.26
4.78
4.76
4.65
4.63
4.33
4.32
4.14
4.14
4.14
4.13
3.83
3.53
3.20
3.20
3.20
3.20
3.19
2.26
2.26
2.26
2.26
2.09
2.09
2.09
2.09
OH
OBn
HN
N3
9a
7.5
7.0
6.5
6.0
5.5
5.0
4.5
4.0
3.5
3.0
2.5
ppm
5.09
0.97
1.01
0.93
1.01
1.14
3.12
1.22
1.03
1.12

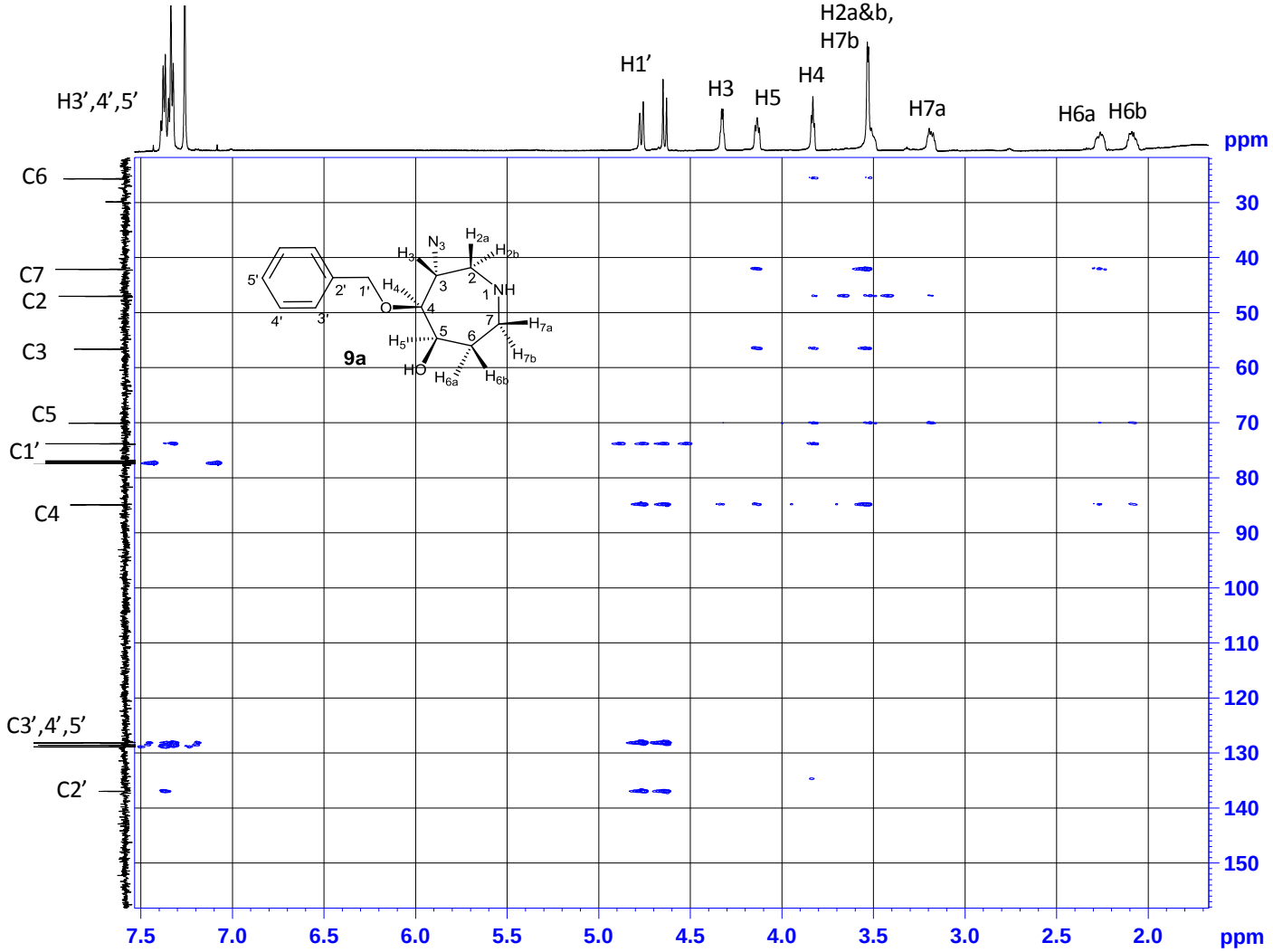
^{13}C-**9a**


OH
OBn
HN
N3
9a
136.98
128.90
128.60
128.18
84.91
77.37
77.16
76.95
73.82
70.08
56.63
47.03
42.13
25.68
200 190 180 170 160 150 140 130 120 110 100 90 80 70 60 50 40 30 ppm

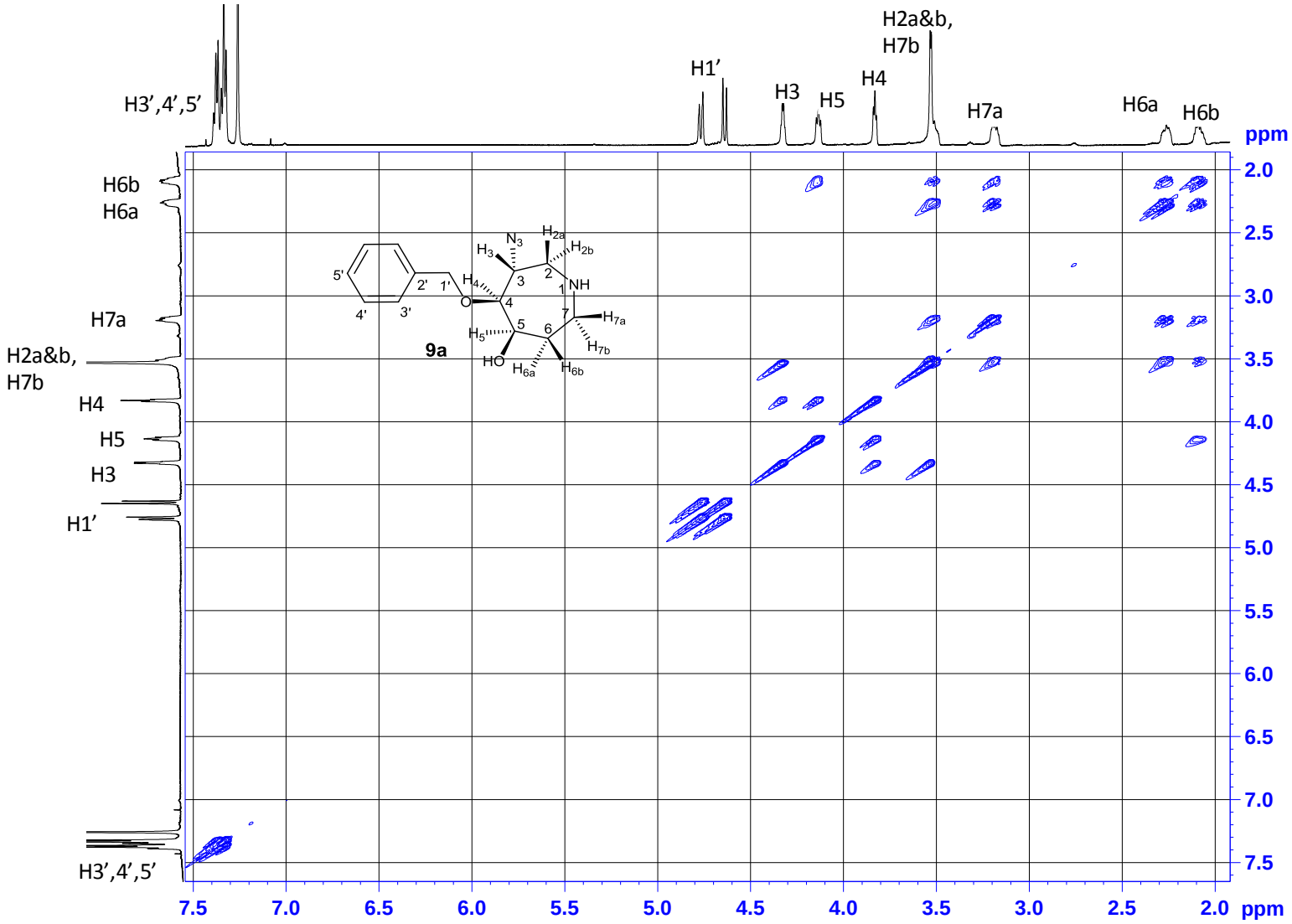
HSQC-**9a**


H3',4',5'
H1'
H3
H5
H4
H2a&b,
H7b
H7a
H6a
H6b
ppm
C6
C7
C2
C3
C5
C1'
C4
C3',4',5'
C2'
9a
7.5
7.0
6.5
6.0
5.5
5.0
4.5
4.0
3.5
3.0
2.5
2.0
1.5
ppm

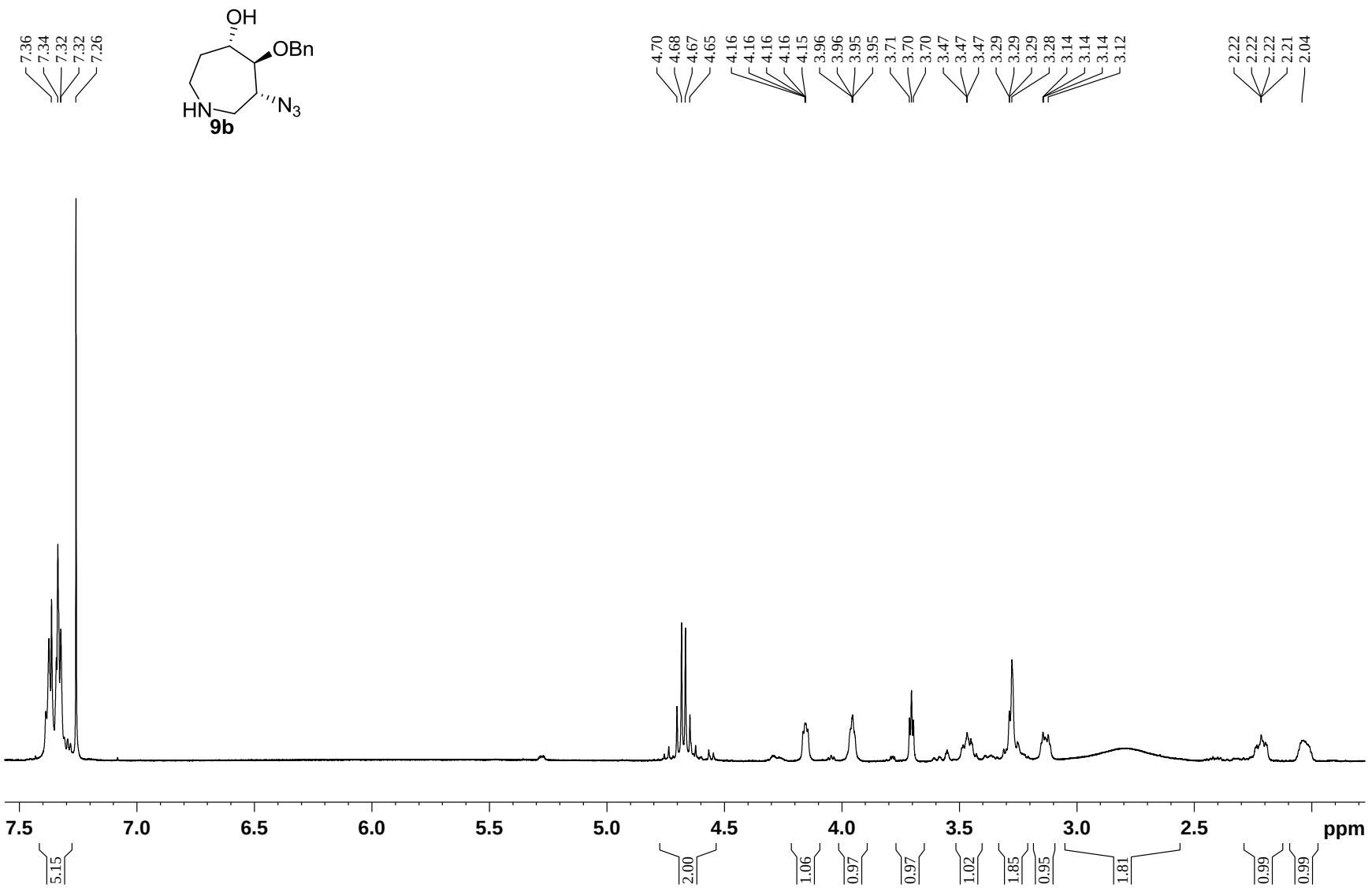
HMBC-**9a**


H3',4',5'
H1'
H3
H5
H4
H2a&b,
H7b
H7a
H6a
H6b
ppm
C6
C7
C2
C3
C5
C1'
C4
C3',4',5'
C2'
9a
7.5
7.0
6.5
6.0
5.5
5.0
4.5
4.0
3.5
3.0
2.5
2.0
ppm
30
40
50
60
70
80
90
100
110
120
130
140
150

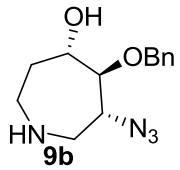
COSY-**9a**

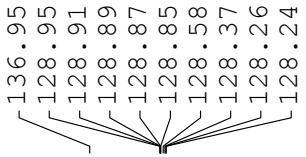

H3',4',5'
H1'
H3
H5
H4
H2a&b,
H7b
H7a
H6a
H6b
ppm
H6b
H6a
H7a
H2a&b,
H7b
H4
H5
H3
H1'
H3',4',5'
9a
7.5
7.0
6.5
6.0
5.5
5.0
4.5
4.0
3.5
3.0
2.5
2.0
ppm

^{1}H-**9b**

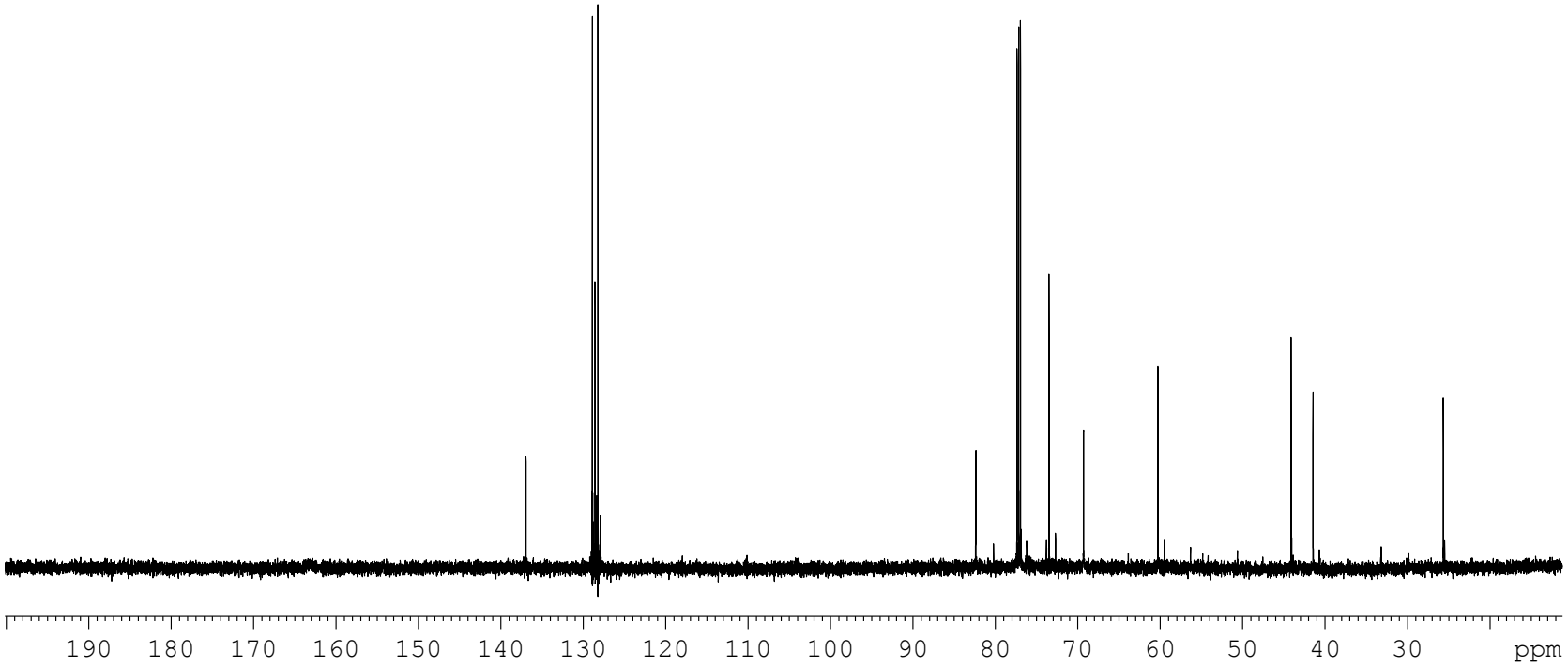

7.36
7.34
7.32
7.32
7.26
OH
OBn
HN
N3
9b
4.70
4.68
4.67
4.65
4.16
4.16
4.16
4.16
4.15
3.96
3.96
3.95
3.95
3.71
3.70
3.70
3.47
3.47
3.47
3.29
3.29
3.29
3.28
3.14
3.14
3.14
3.12
2.22
2.22
2.22
2.21
2.04
7.5
7.0
6.5
6.0
5.5
5.0
4.5
4.0
3.5
3.0
2.5
ppm
5.15
2.00
1.06
0.97
0.97
1.02
1.85
0.95
1.81
0.99
0.99

^{13}C-**9b**

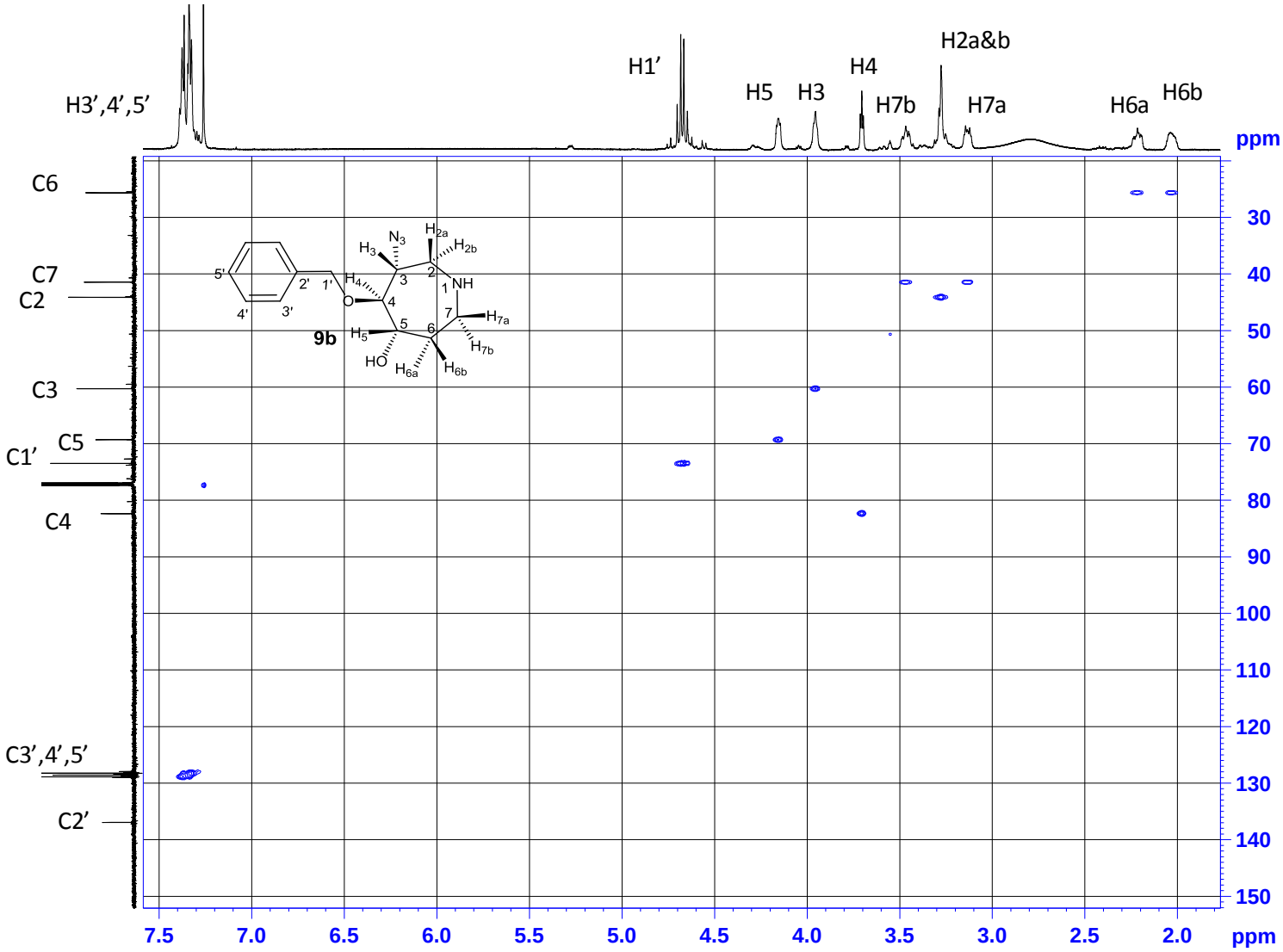

OH
OBn
HN
N_3
9b


136.95
128.95
128.91
128.89
128.87
128.85
128.58
128.37
128.26
128.24

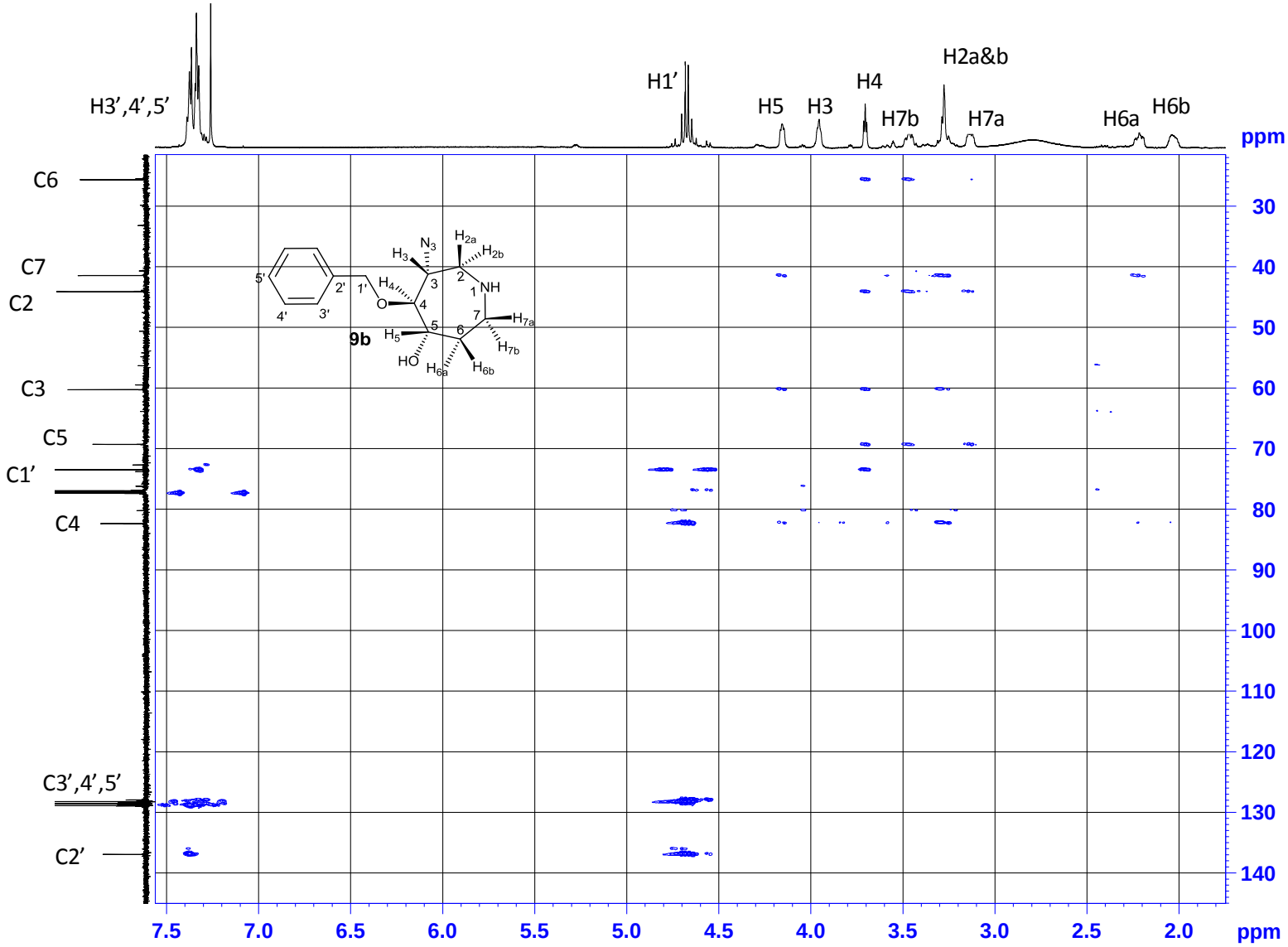

82.36
77.37
77.16
76.95
73.48
69.29
60.28
44.11
41.44
25.64


190
180
170
160
150
140
130
120
110
100
90
80
70
60
50
40
30
ppm

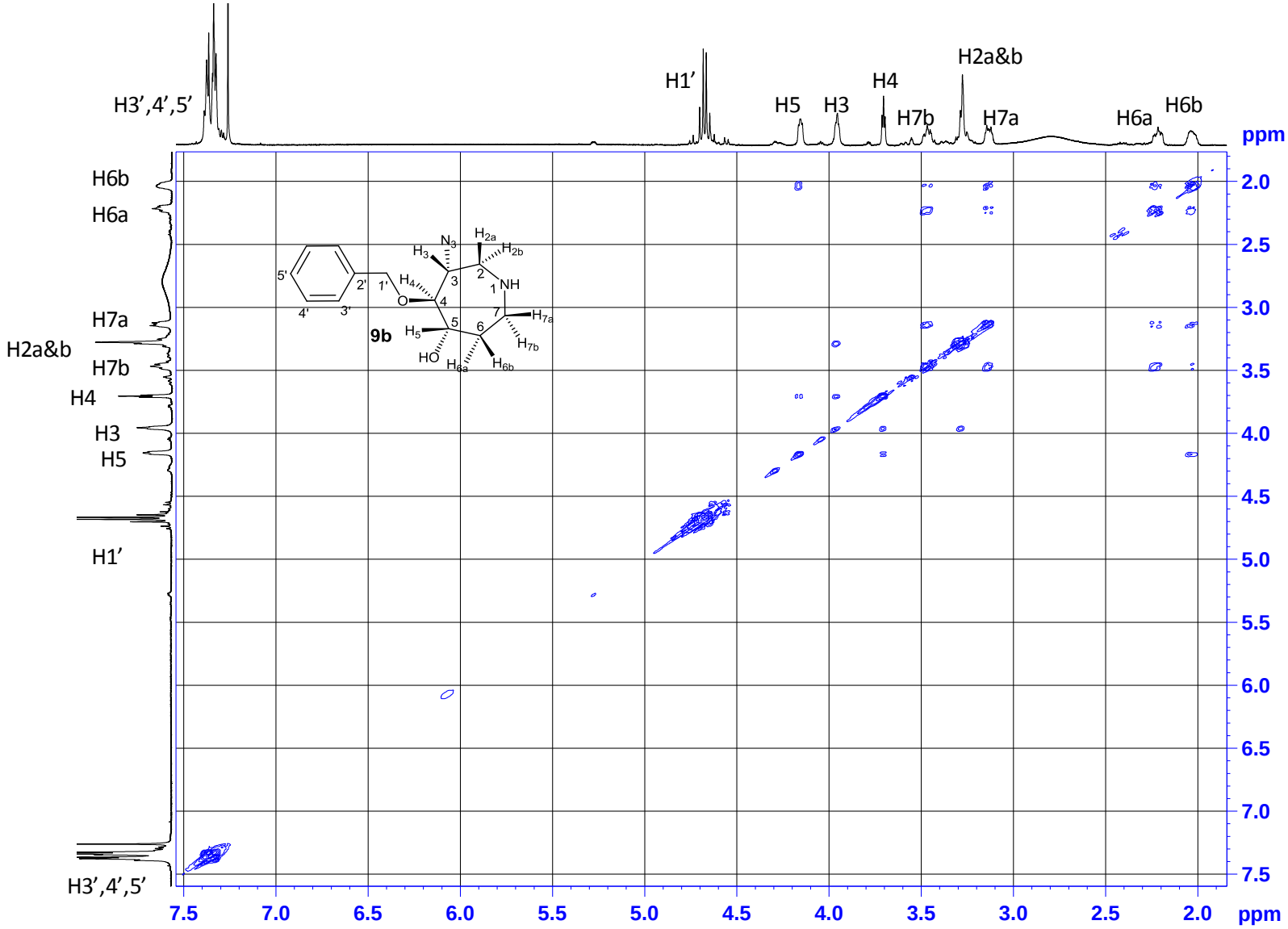
HSQC-**9b**


H3',4',5'
H1'
H5
H3
H4
H7b
H2a&b
H7a
H6a
H6b
ppm
C6
C7
C2
C3
C5
C1'
C4
C3',4',5'
C2'
9b
7.5
7.0
6.5
6.0
5.5
5.0
4.5
4.0
3.5
3.0
2.5
2.0
ppm

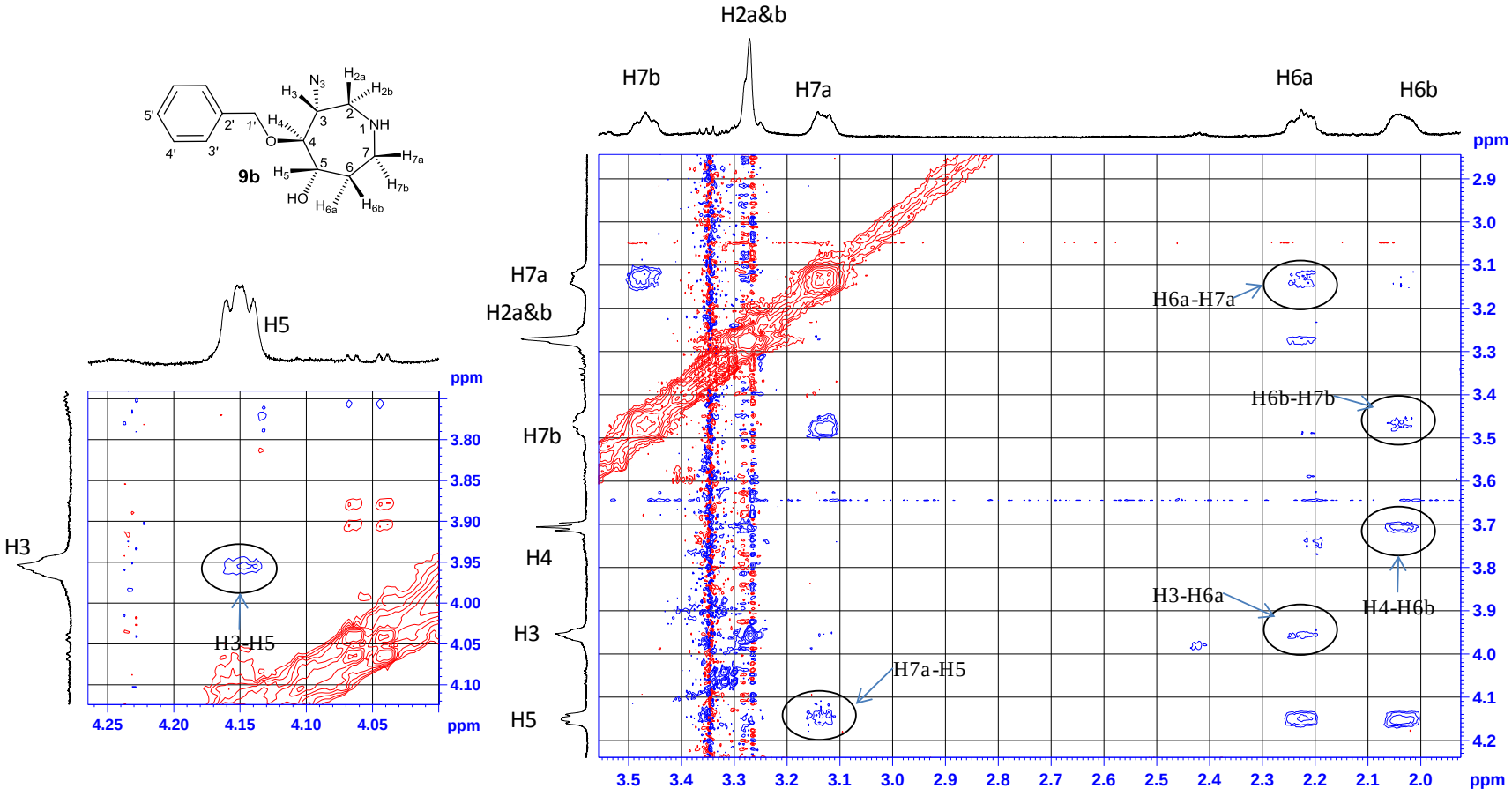
HMBC-**9b**


H3',4',5'
H1'
H5
H3
H4
H7b
H2a&b
H7a
H6a
H6b
ppm
C6
C7
C2
C3
C5
C1'
C4
C3',4',5'
C2'
9b
7.5
7.0
6.5
6.0
5.5
5.0
4.5
4.0
3.5
3.0
2.5
2.0
ppm

COSY-**9b**

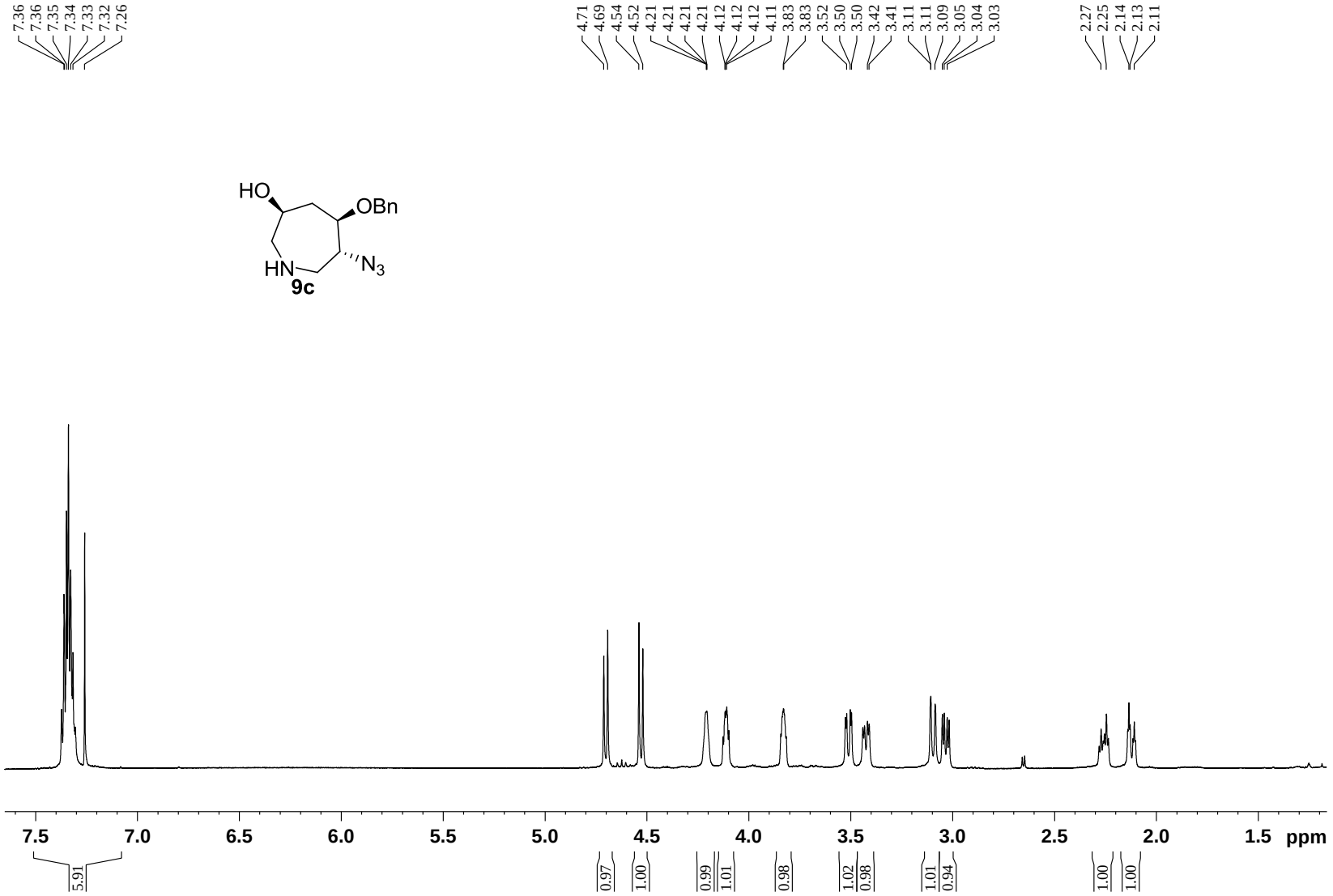

H3',4',5'
H1'
H5
H3
H4
H7b
H2a&b
H7a
H6a
H6b
ppm
H6b
H6a
H7a
H2a&b
H7b
H4
H3
H5
H1'
H3',4',5'
9b
7.5
7.0
6.5
6.0
5.5
5.0
4.5
4.0
3.5
3.0
2.5
2.0
ppm

NOESY-**9b**

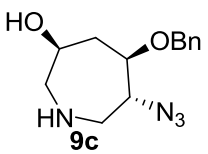

9b
H5
H3
H3-H5
H2a&b
H7b
H7a
H6a
H6b
H7a
H2a&b
H7b
H4
H3
H5
H6a-H7a
H6b-H7b
H3-H6a
H4-H6b
H7a-H5
ppm

-S36-

^{1}H-**9c**

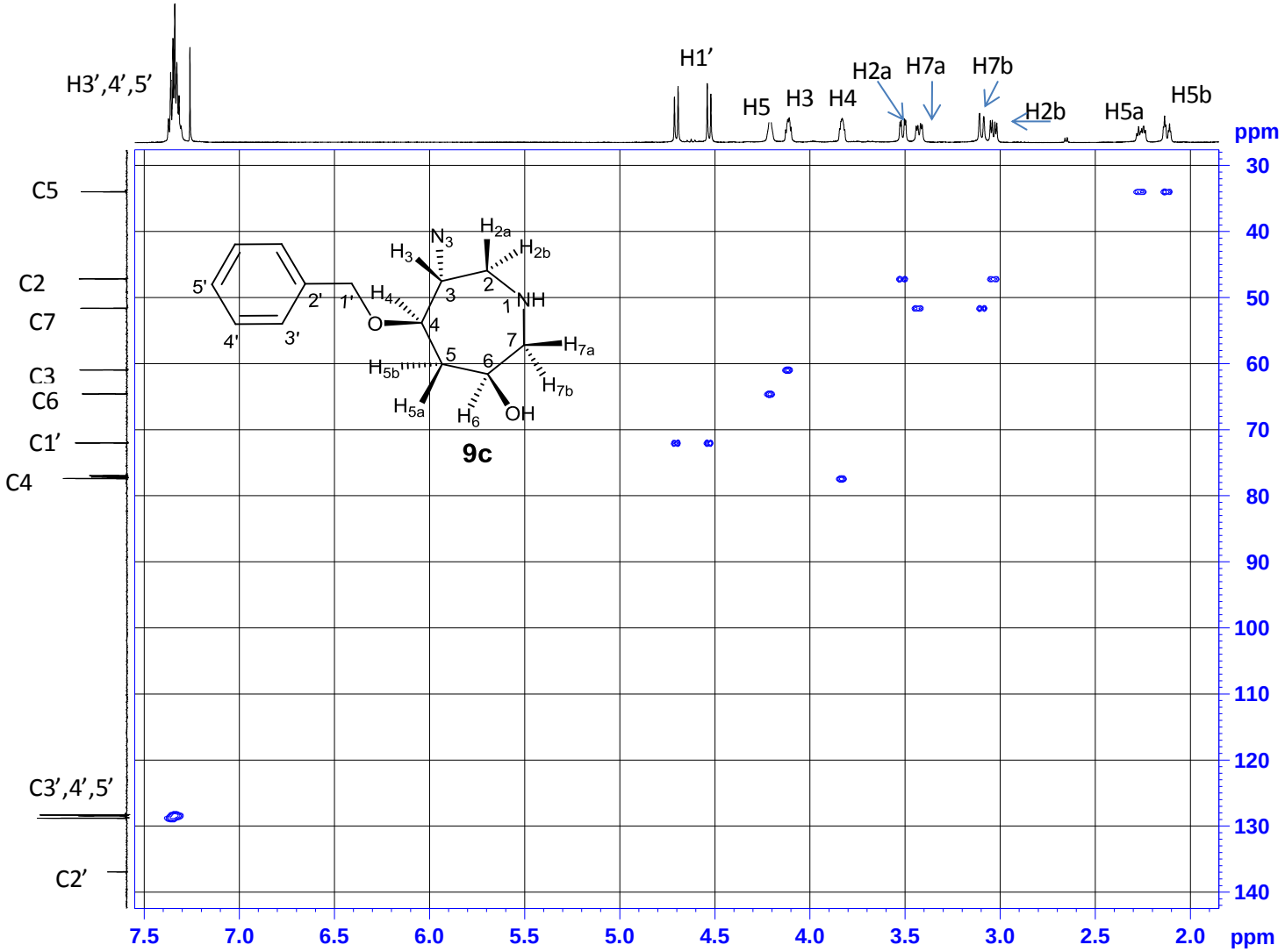

7.36
7.36
7.35
7.34
7.33
7.32
7.26
4.71
4.69
4.54
4.52
4.21
4.21
4.21
4.21
4.12
4.12
4.12
4.11
3.83
3.83
3.52
3.50
3.50
3.42
3.41
3.11
3.11
3.09
3.05
3.04
3.03
2.27
2.25
2.14
2.13
2.11
HO
OBn
HN
N3
9c
7.5
7.0
6.5
6.0
5.5
5.0
4.5
4.0
3.5
3.0
2.5
2.0
1.5
ppm
5.91
0.97
1.00
0.99
1.01
0.98
1.02
0.98
1.01
0.94
1.00
1.00

^{13}C-**9c**

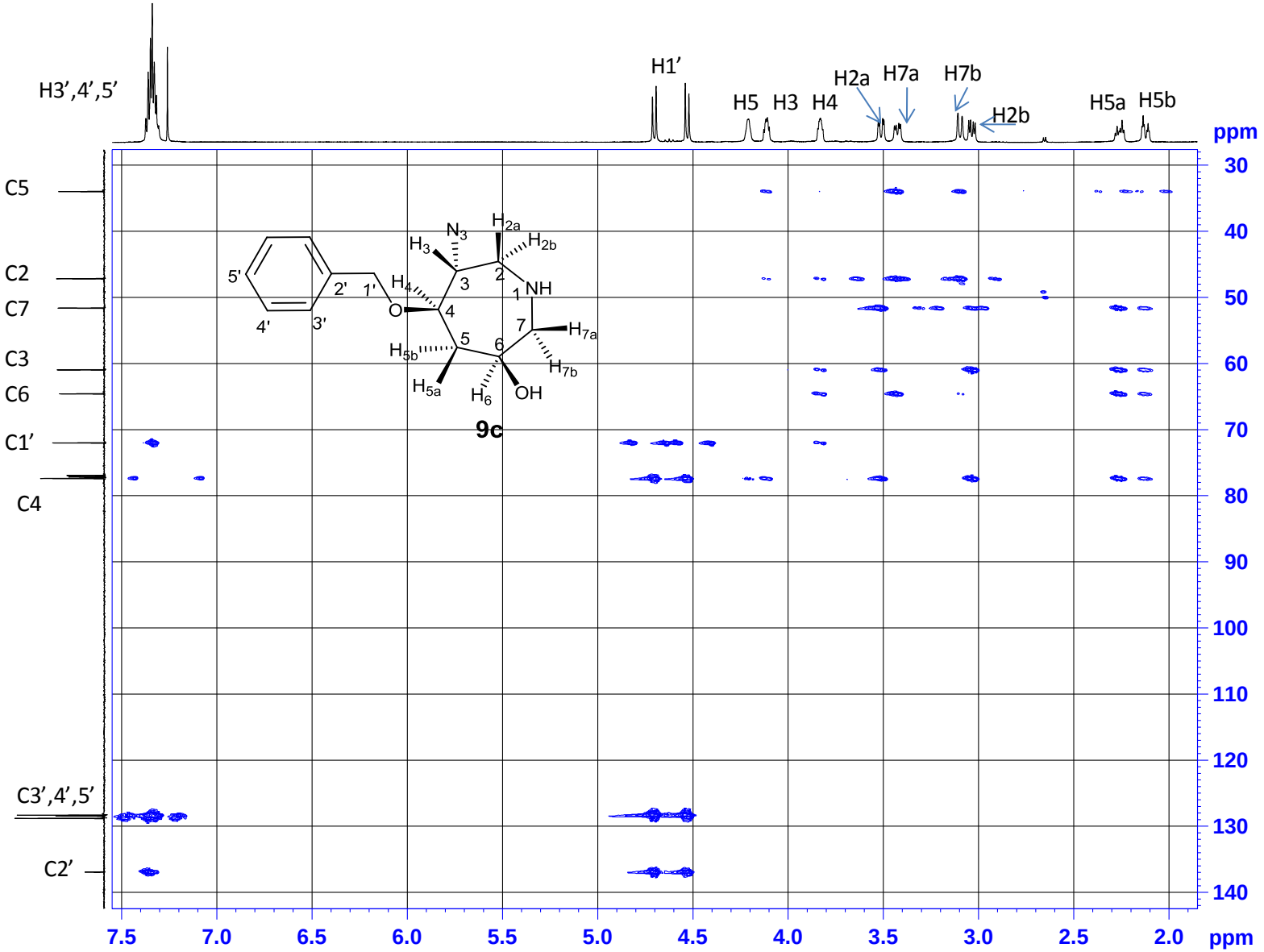

HO
OBn
HN
N3
9c

136.95
128.81
128.46
128.34
77.39
77.16
76.94
72.01
64.58
60.95
51.61
47.17
33.98
190 180 170 160 150 140 130 120 110 100 90 80 70 60 50 40 30 ppm

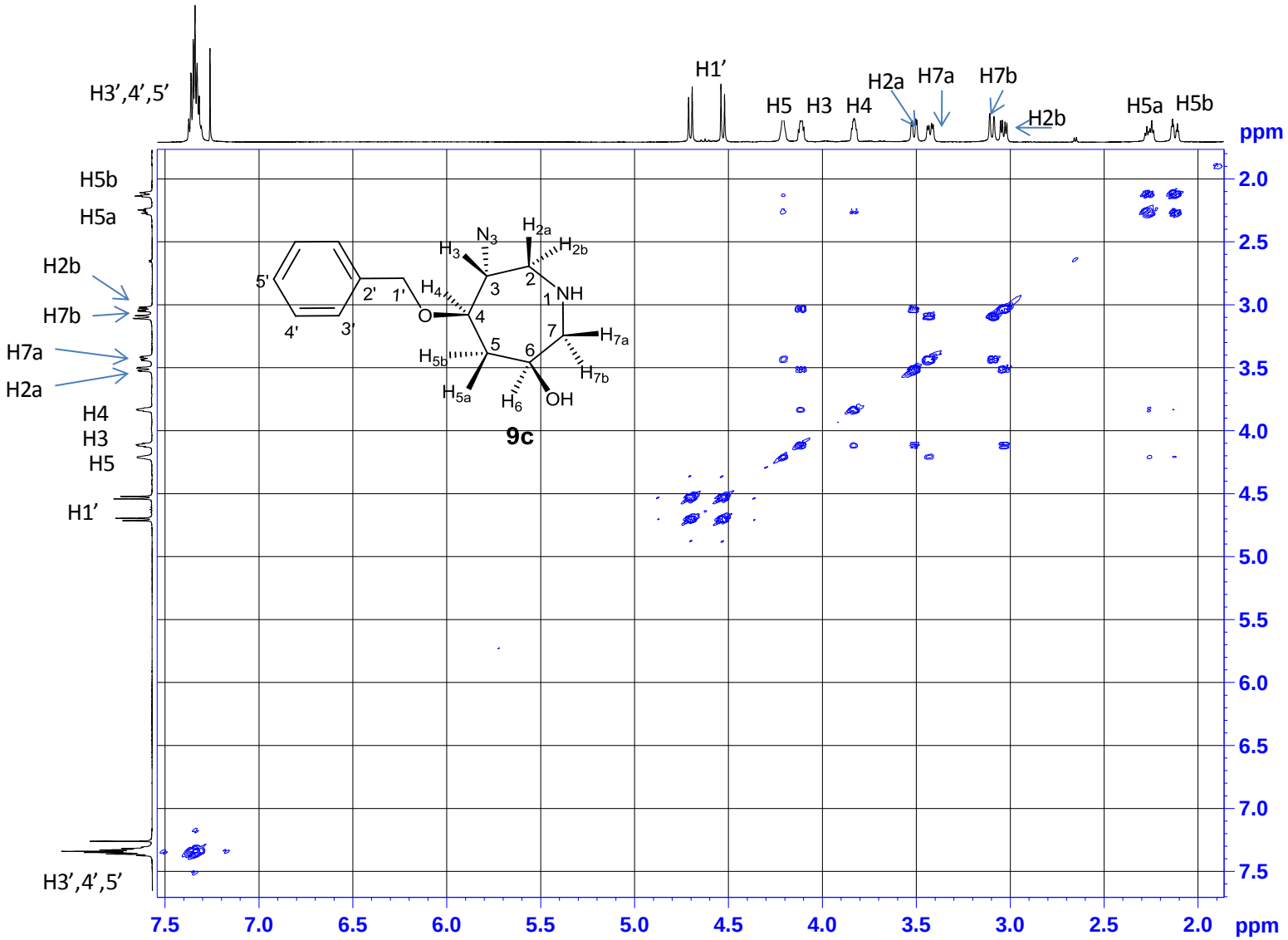
HSQC-**9c**


H3',4',5'
H1'
H5
H3
H4
H2a
H7a
H7b
H2b
H5a
H5b
ppm
C5
C2
C7
C3
C6
C1'
C4
C3',4',5'
C2'
9c
7.5
7.0
6.5
6.0
5.5
5.0
4.5
4.0
3.5
3.0
2.5
2.0
ppm

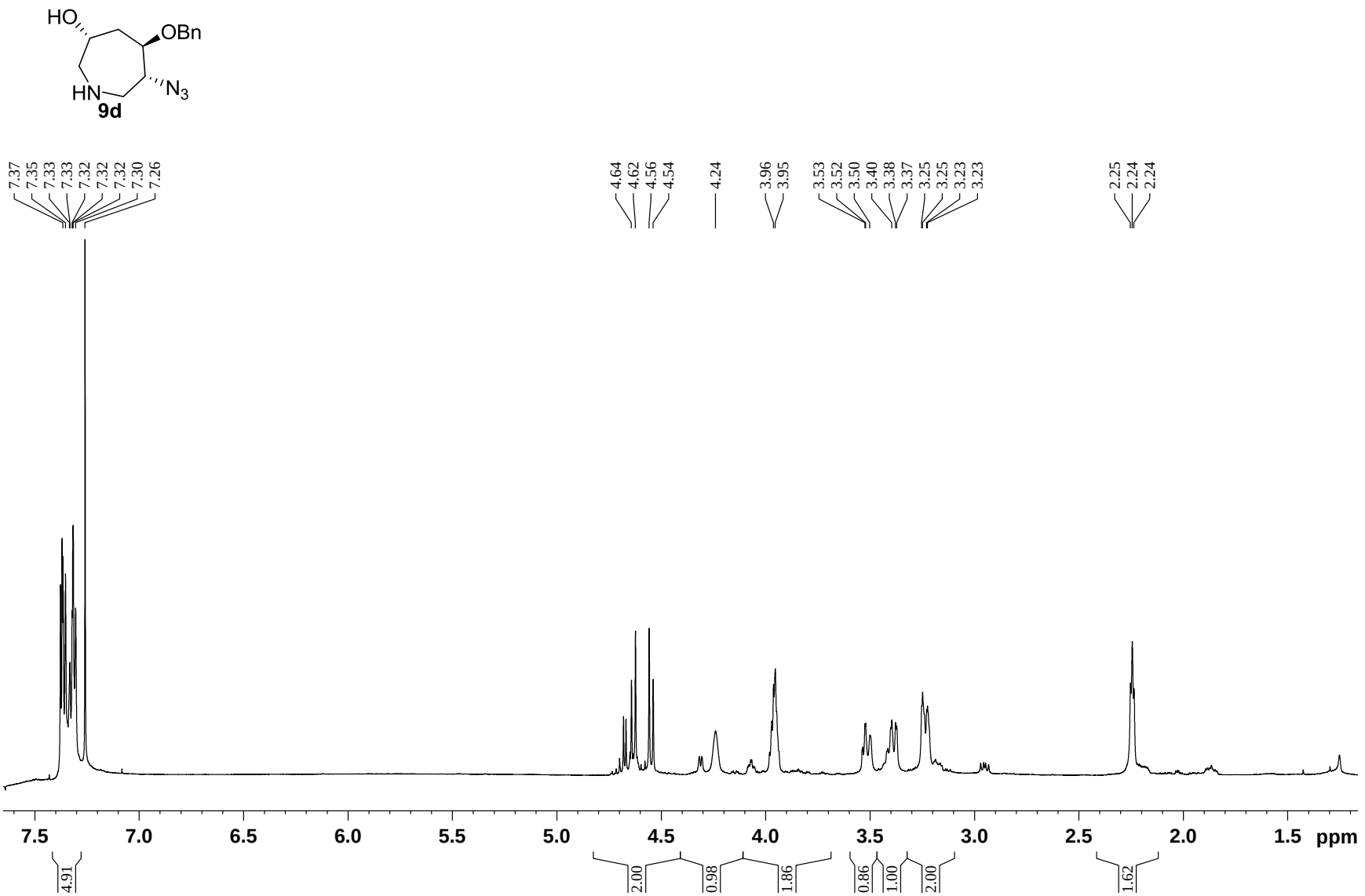
HMBC-**9c**


H3',4',5'
H1'
H5
H3
H4
H2a
H7a
H7b
H2b
H5a
H5b
ppm
C5
C2
C7
C3
C6
C1'
C4
C3',4',5'
C2'
9c
7.5
7.0
6.5
6.0
5.5
5.0
4.5
4.0
3.5
3.0
2.5
2.0
ppm

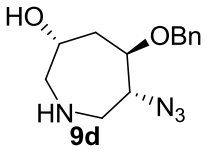
COSY-**9c**

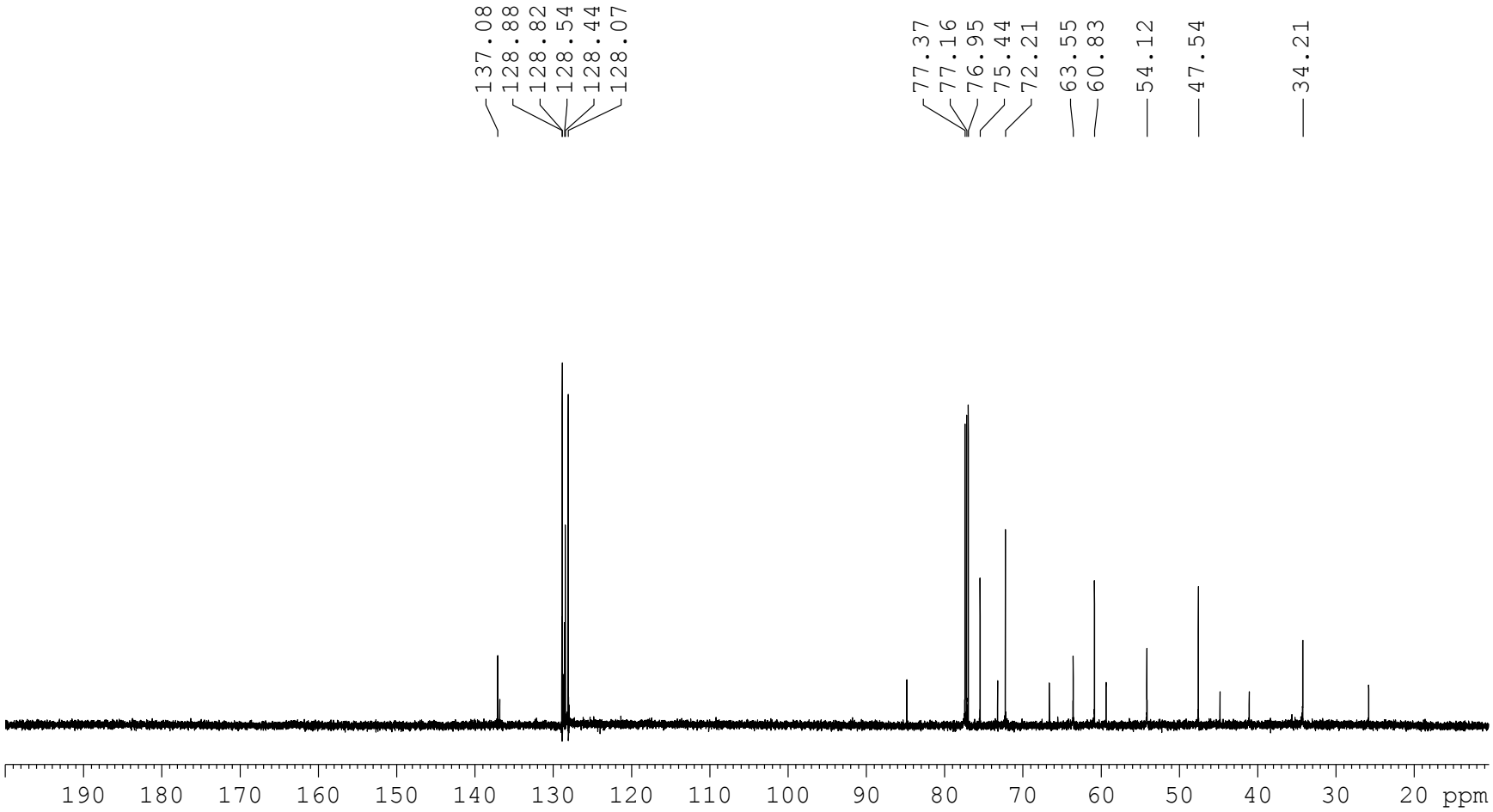

H3',4',5'
H1'
H5
H3
H4
H2a
H7a
H7b
H2b
H5a
H5b
ppm
2.0
2.5
3.0
3.5
4.0
4.5
5.0
5.5
6.0
6.5
7.0
7.5
N3
H2a
H2b
H3
H4
NH
OH
H5a
H5b
H6
H7a
H7b
9c

^{1}H-**9d**

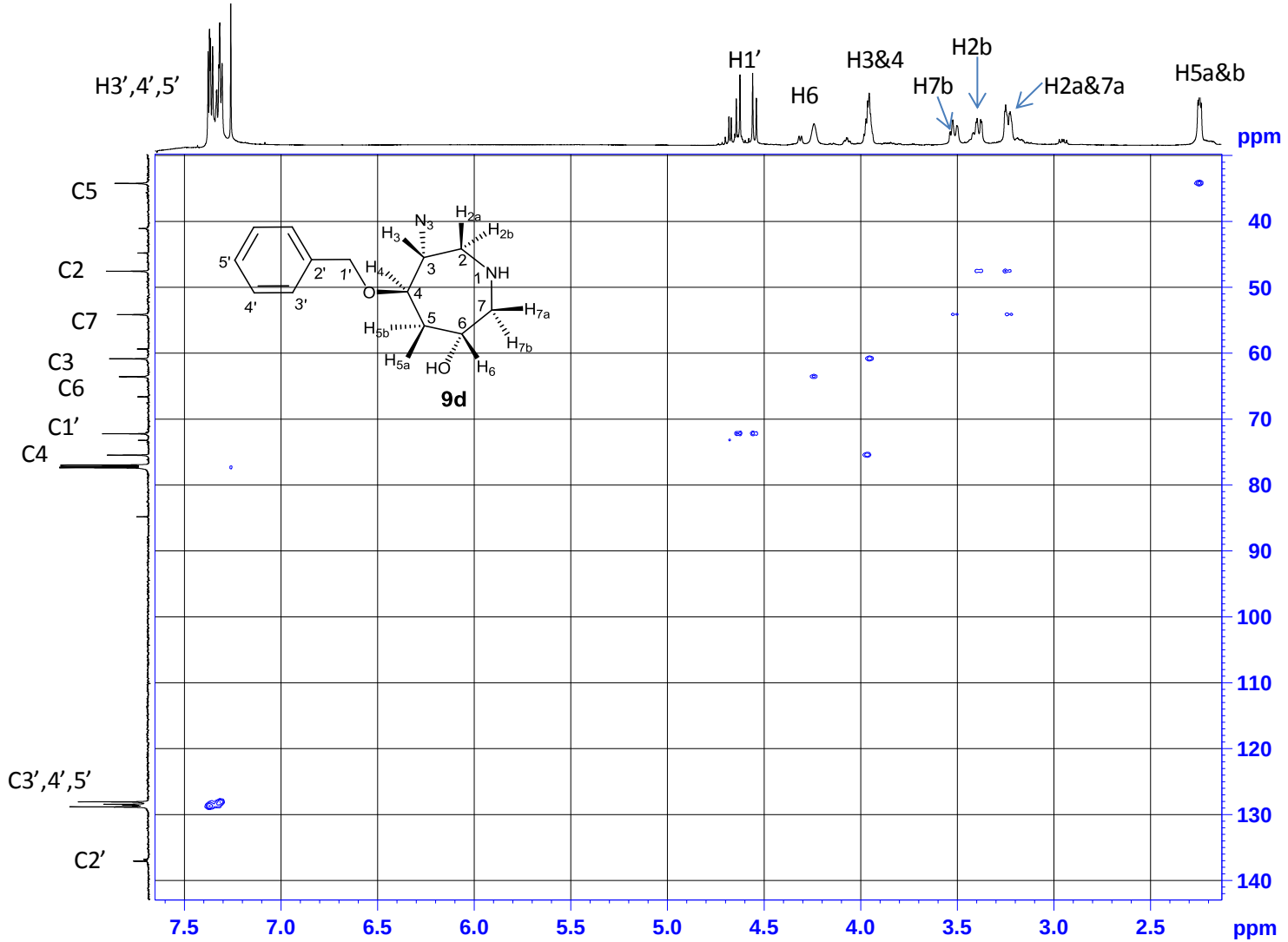

HO
OBn
HN
N3
9d
7.37
7.35
7.33
7.33
7.32
7.32
7.32
7.30
7.26
4.64
4.62
4.56
4.54
4.24
3.96
3.95
3.53
3.52
3.50
3.40
3.38
3.37
3.25
3.25
3.23
3.23
2.25
2.24
2.24
7.5
7.0
6.5
6.0
5.5
5.0
4.5
4.0
3.5
3.0
2.5
2.0
1.5
ppm
4.91
2.00
0.98
1.86
0.86
1.00
2.00
1.62

^{13}C-**9d**

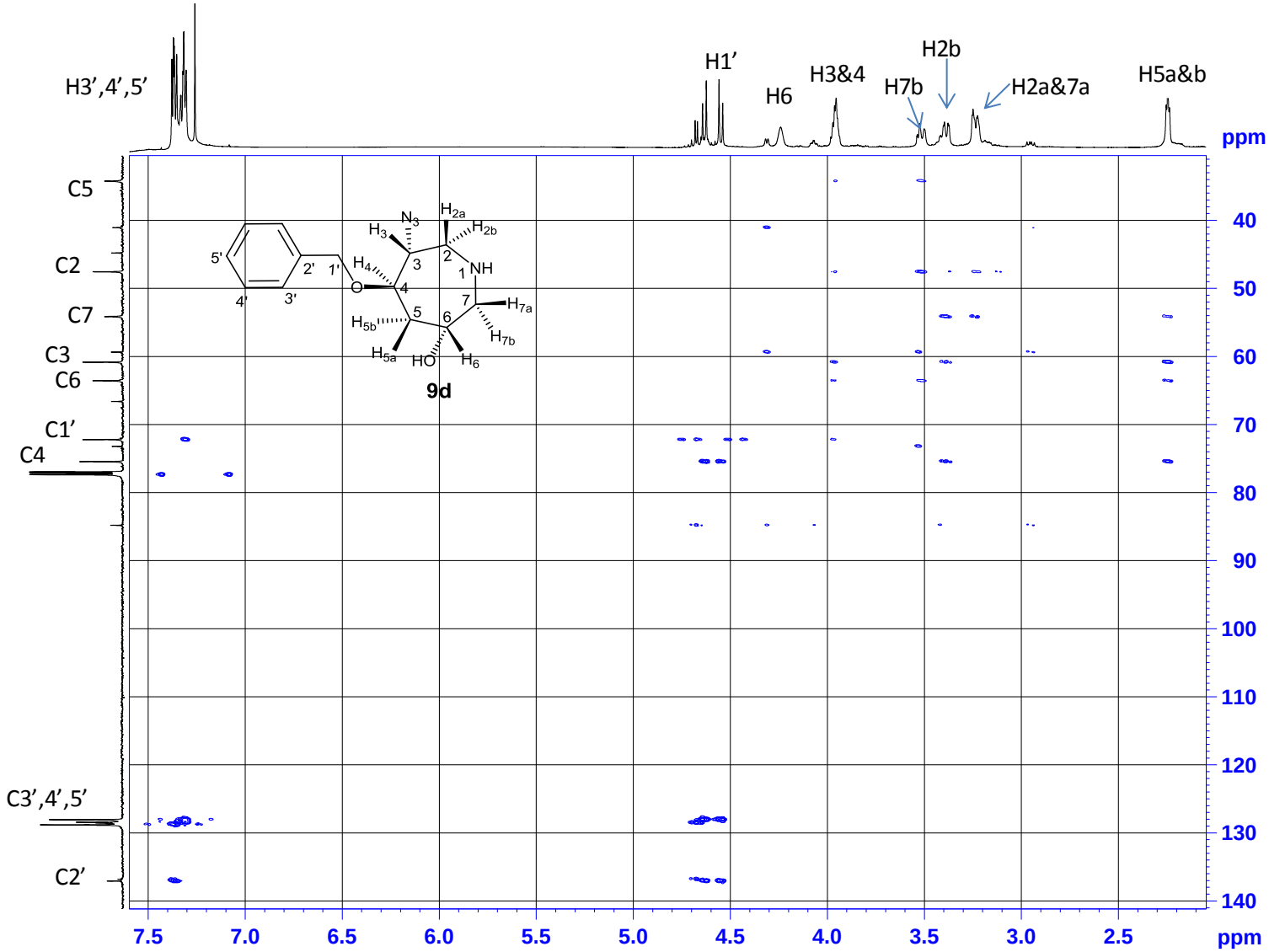

HO
OBn
HN
N3
9d


137.08
128.88
128.82
128.54
128.44
128.07
77.37
77.16
76.95
75.44
72.21
63.55
60.83
54.12
47.54
34.21
190 180 170 160 150 140 130 120 110 100 90 80 70 60 50 40 30 20 ppm

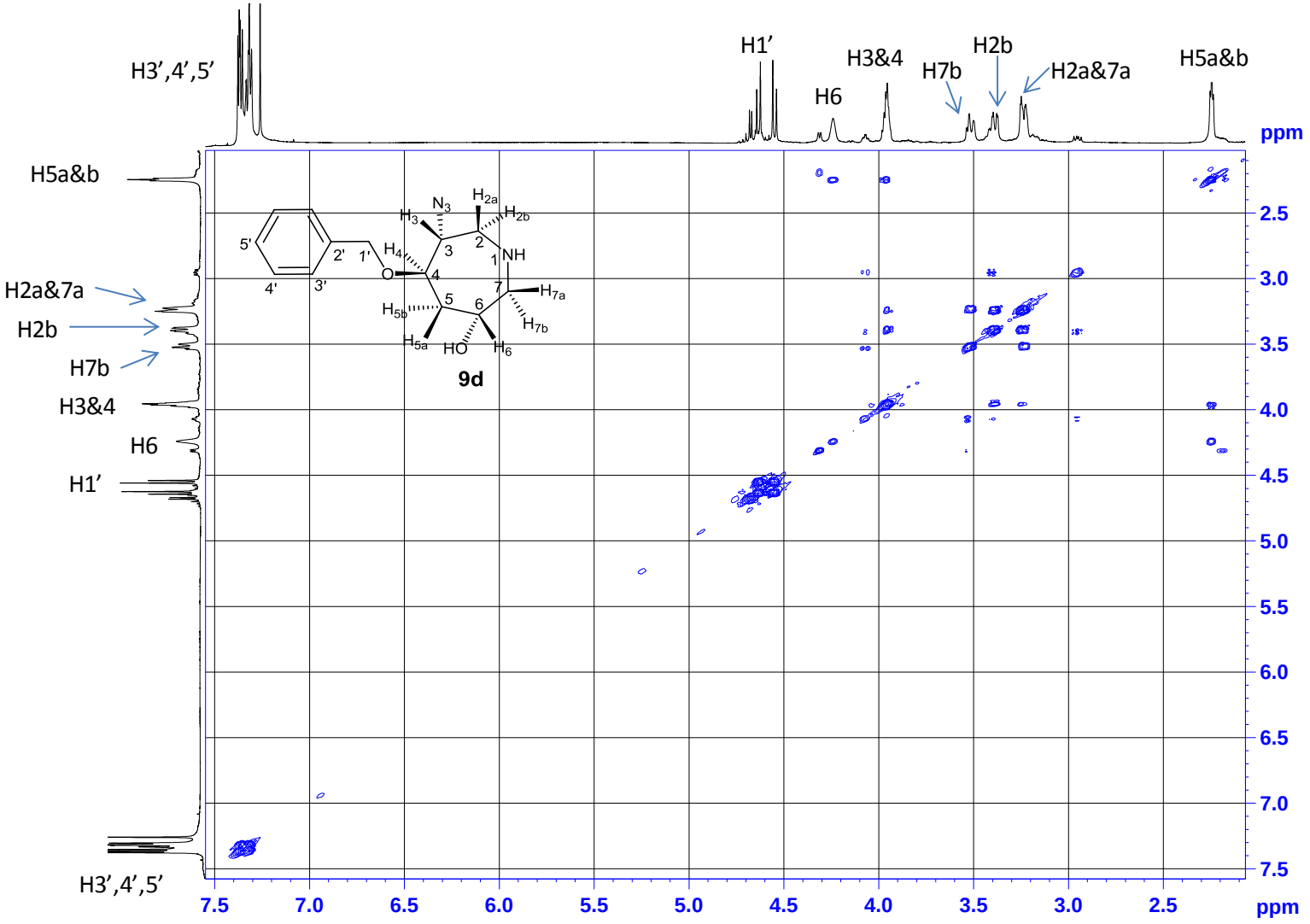
HSQC-9d


H3',4',5'
H1'
H6
H3&4
H7b
H2b
H2a&7a
H5a&b
ppm
C5
C2
C7
C3
C6
C1'
C4
C3',4',5'
C2'
9d
7.5
7.0
6.5
6.0
5.5
5.0
4.5
4.0
3.5
3.0
2.5
ppm

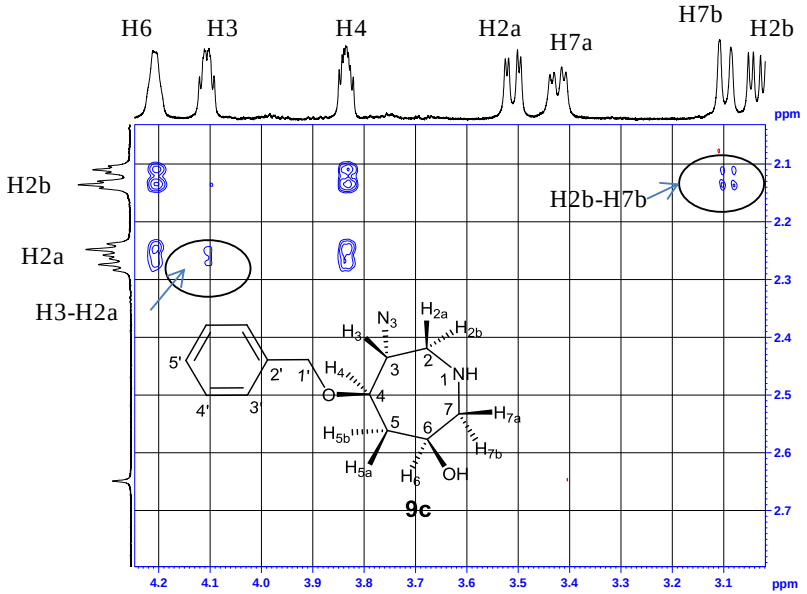
HMBC-9d

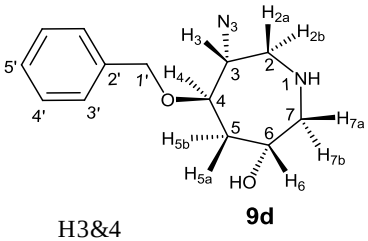

H3',4',5'
H1'
H6
H3&4
H7b
H2b
H2a&7a
H5a&b
ppm
C5
C2
C7
C3
C6
C1'
C4
C3',4',5'
C2'
9d
7.5
7.0
6.5
6.0
5.5
5.0
4.5
4.0
3.5
3.0
2.5
ppm

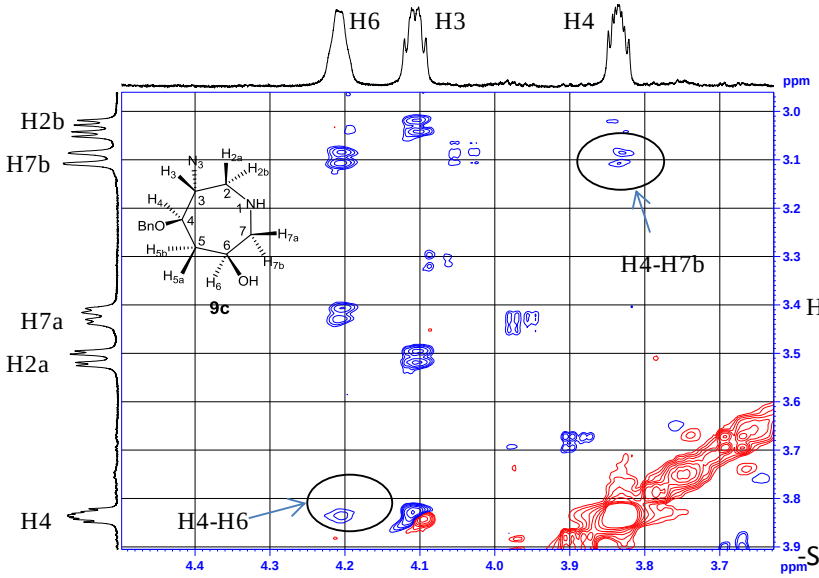
COSY-9d

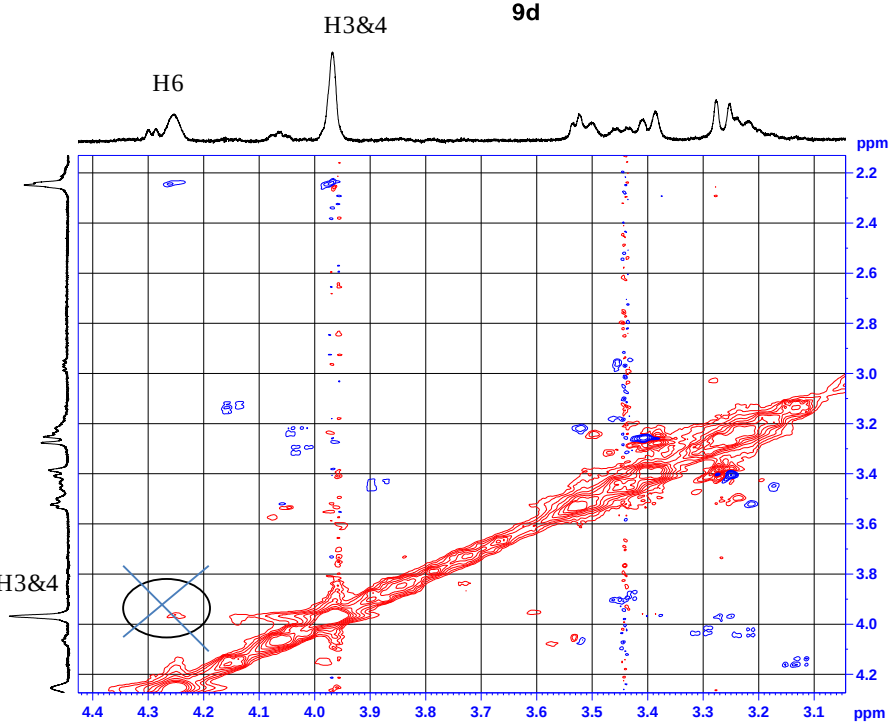

H3',4',5'
H1'
H6
H3&4
H7b
H2b
H2a&7a
H5a&b
ppm
H5a&b
H2a&7a
H2b
H7b
H3&4
H6
H1'
H3',4',5'
9d
7.5
7.0
6.5
6.0
5.5
5.0
4.5
4.0
3.5
3.0
2.5
ppm

NOESY Comparison – **9c** and **9d**

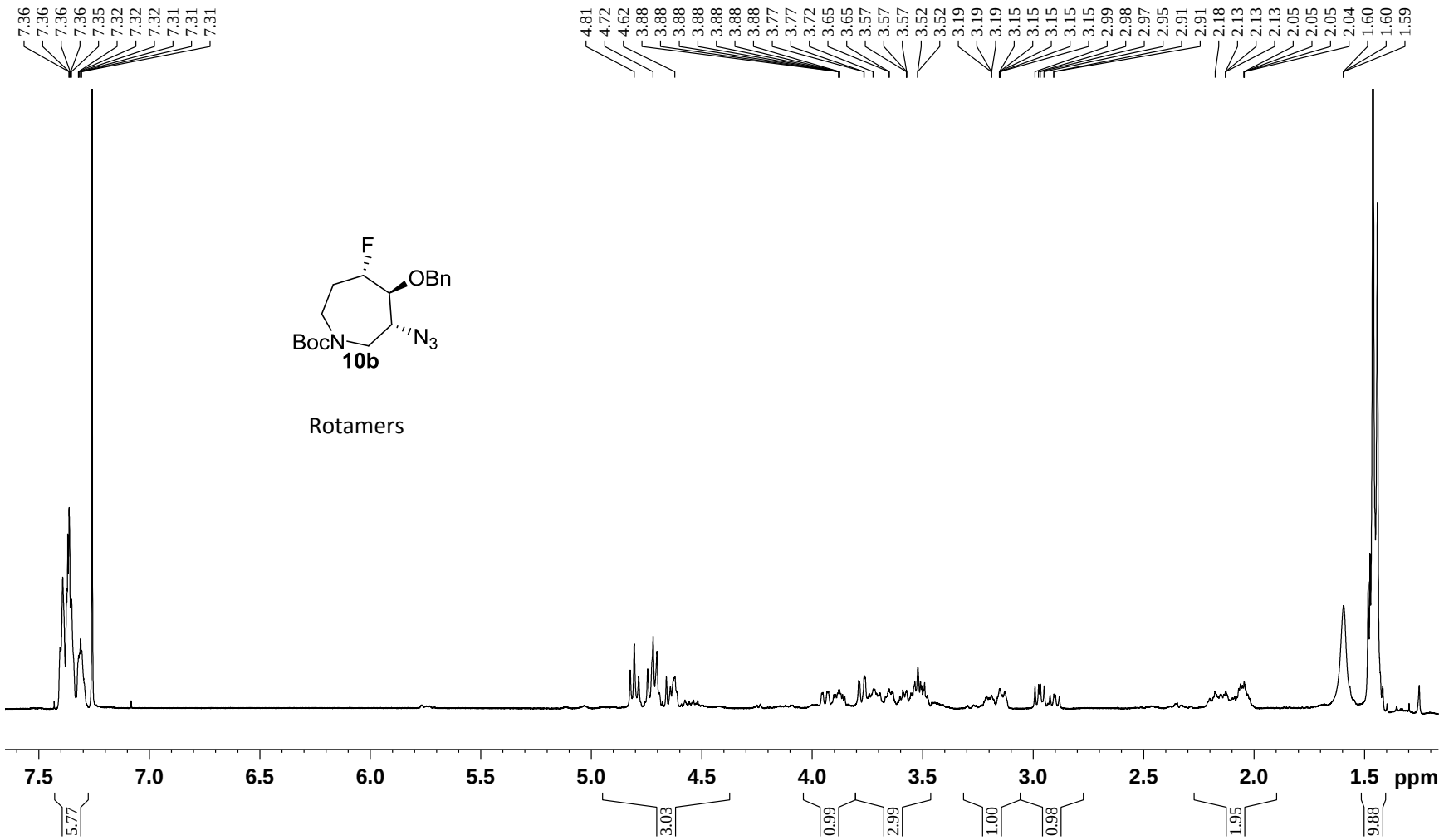




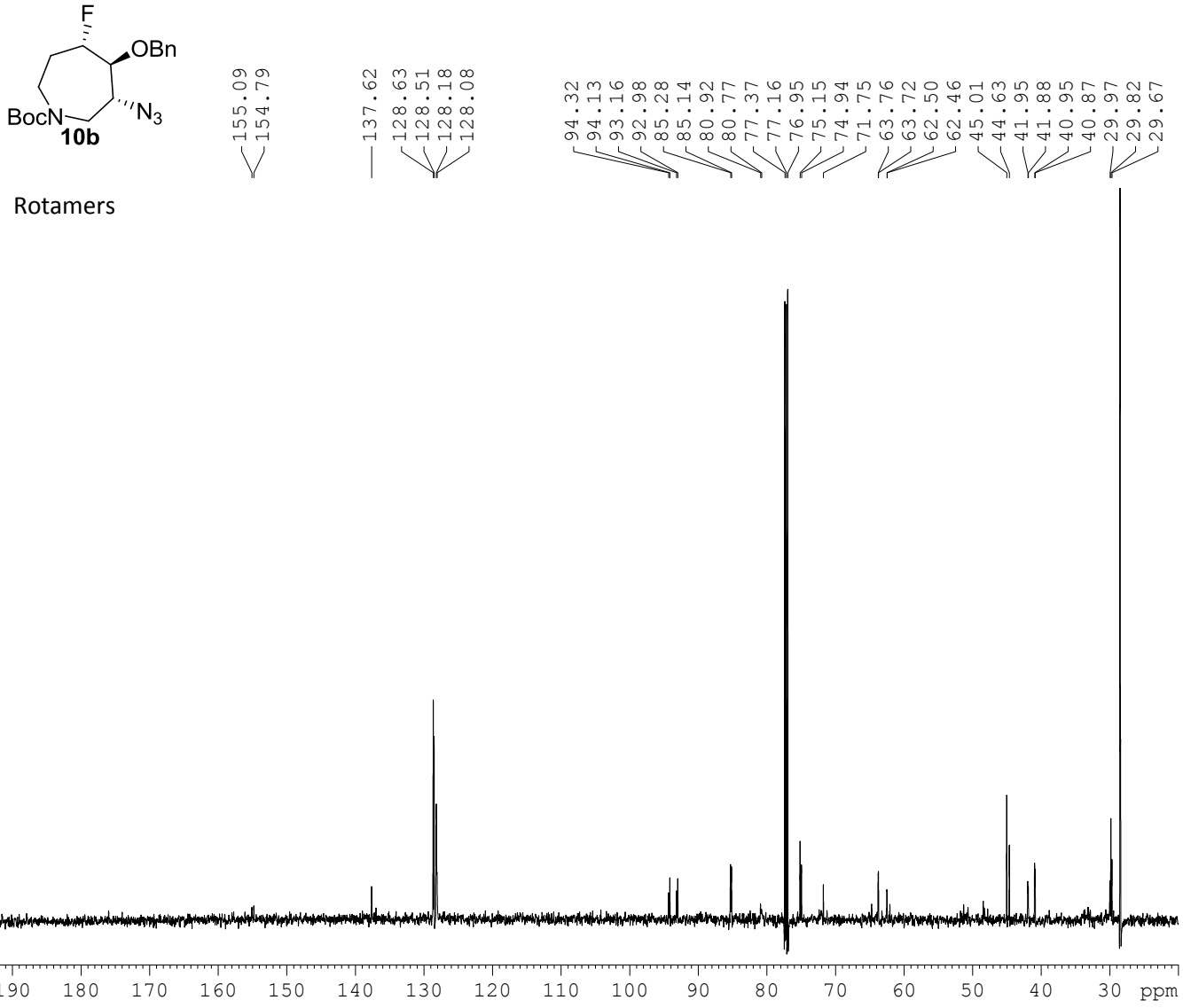




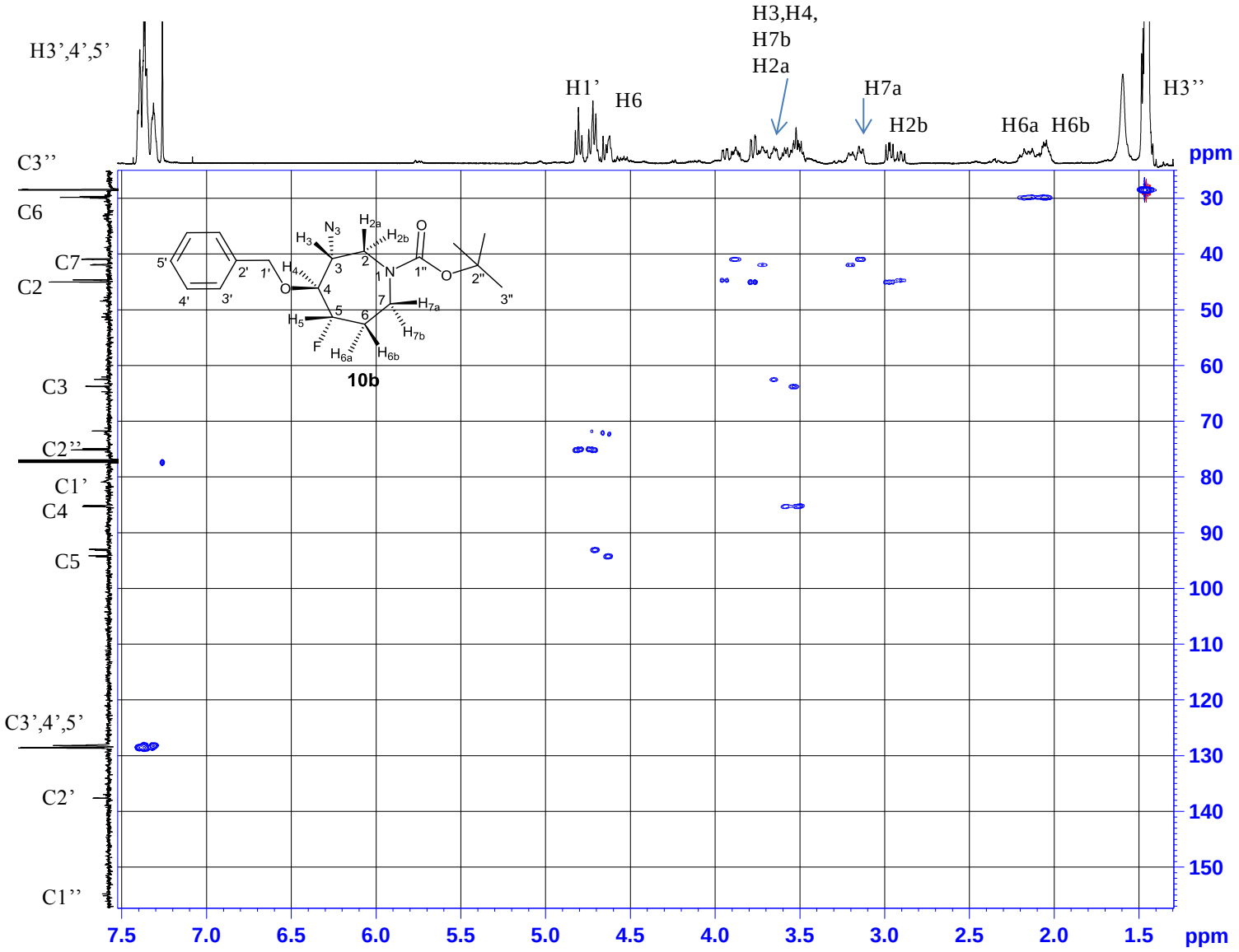
^{1}H-10b


7.36
7.36
7.36
7.36
7.35
7.32
7.32
7.32
7.31
7.31
7.31
4.81
4.72
4.62
3.88
3.88
3.88
3.88
3.88
3.88
3.77
3.77
3.72
3.65
3.57
3.57
3.57
3.52
3.52
3.19
3.19
3.19
3.15
3.15
3.15
3.15
2.99
2.98
2.97
2.95
2.91
2.91
2.18
2.13
2.13
2.13
2.05
2.05
2.05
2.04
1.60
1.60
1.59
F
OBn
BocN
N3
10b
Rotamers
7.5
7.0
6.5
6.0
5.5
5.0
4.5
4.0
3.5
3.0
2.5
2.0
1.5
ppm
5.77
3.03
0.99
2.99
1.00
0.98
1.95
9.88

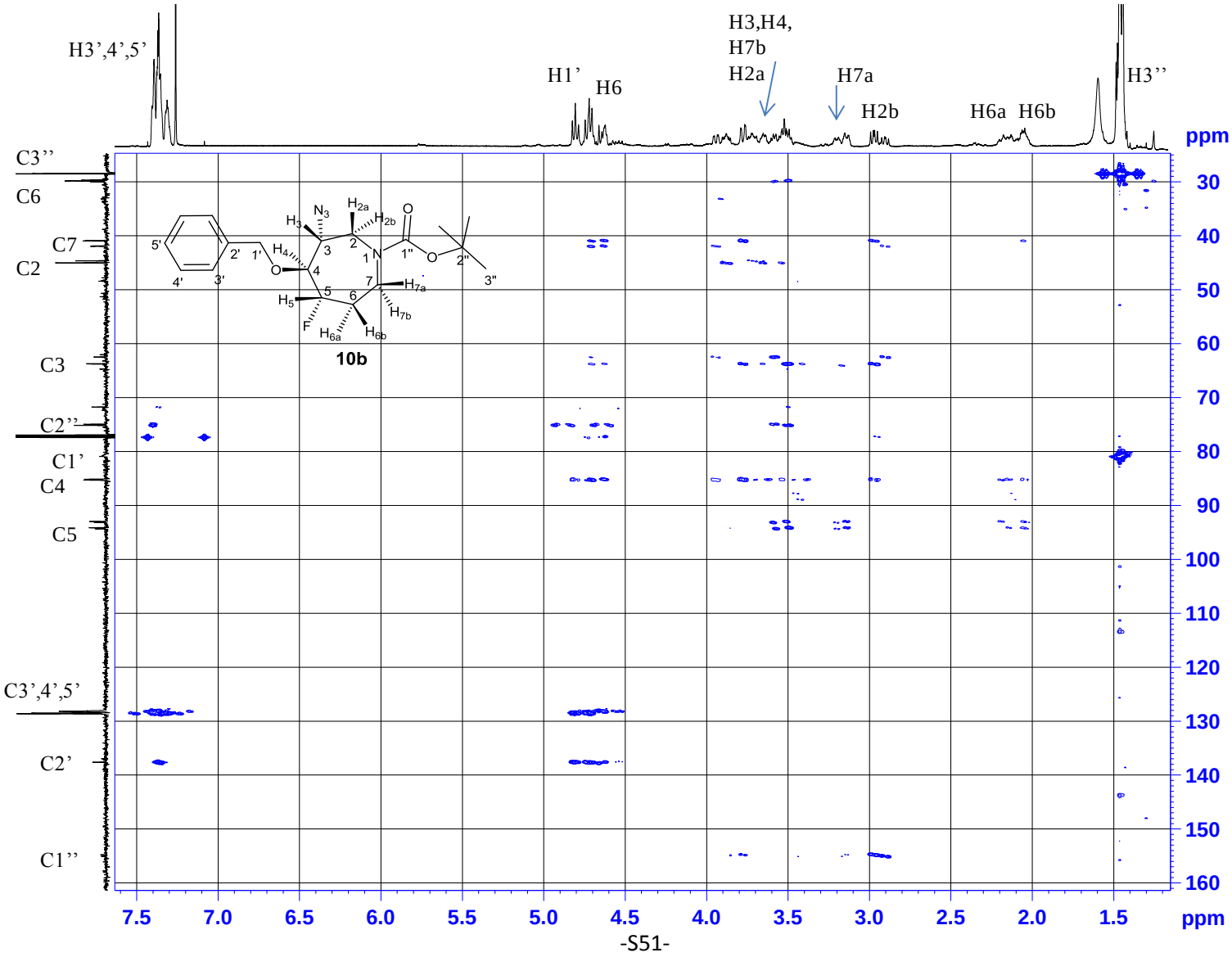
^{13}C-10b


F
OBn
BocN
N3
10b
Rotamers
155.09
154.79
137.62
128.63
128.51
128.18
128.08
94.32
94.13
93.16
92.98
85.28
85.14
80.92
80.77
77.37
77.16
76.95
75.15
74.94
71.75
63.76
63.72
62.50
62.46
45.01
44.63
41.95
41.88
40.95
40.87
29.97
29.82
29.67
190 180 170 160 150 140 130 120 110 100 90 80 70 60 50 40 30 ppm

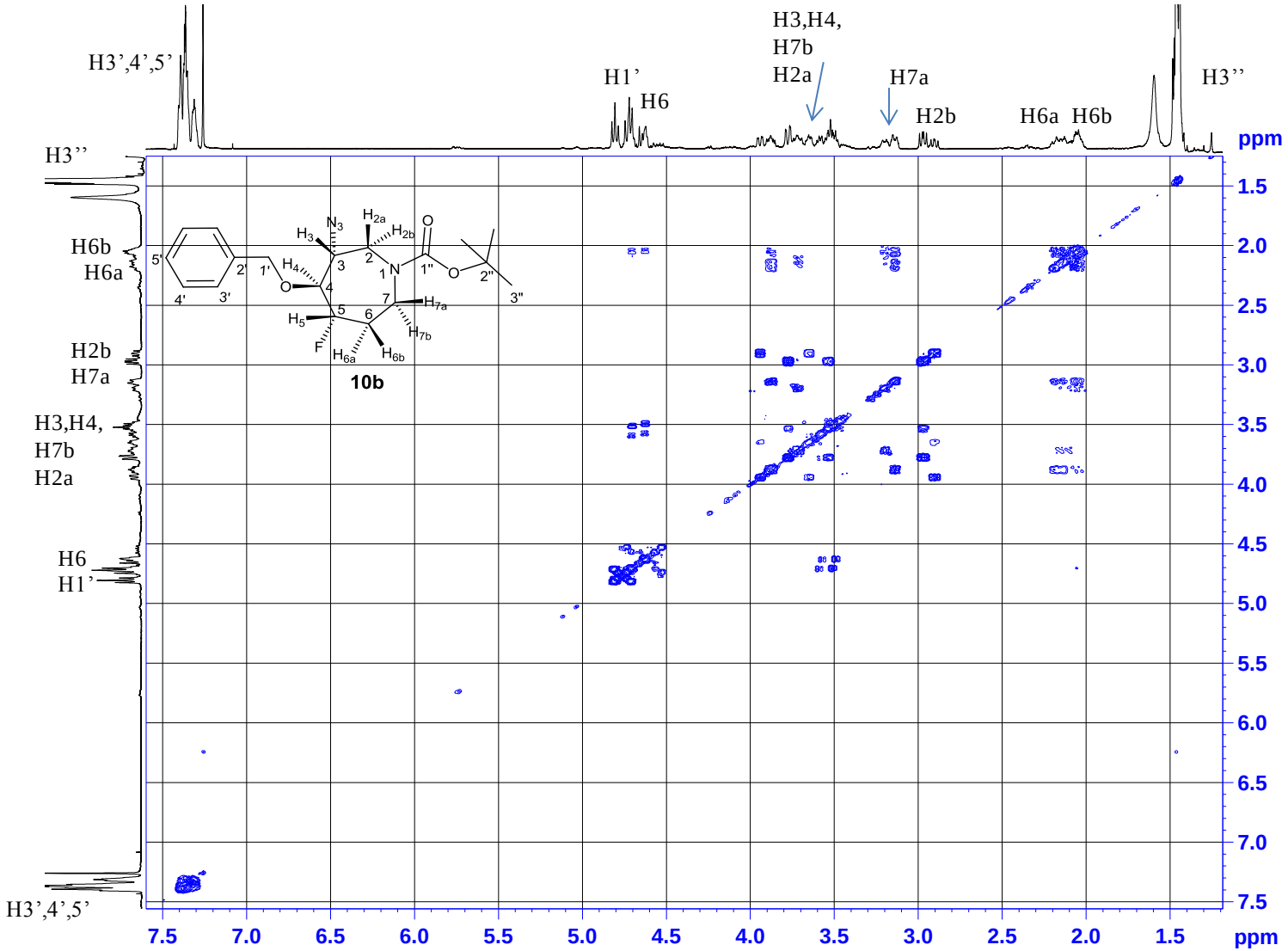
HSQC-10b


H3’,4’,5’
H1’
H6
H3,H4,
H7b
H2a
H7a
H2b
H6a
H6b
H3’’
ppm
C3’’
C6
C7
C2
C3
C2’’
C1’
C4
C5
C3’,4’,5’
C2’
C1’’
10b
7.5
7.0
6.5
6.0
5.5
5.0
4.5
4.0
3.5
3.0
2.5
2.0
1.5
ppm

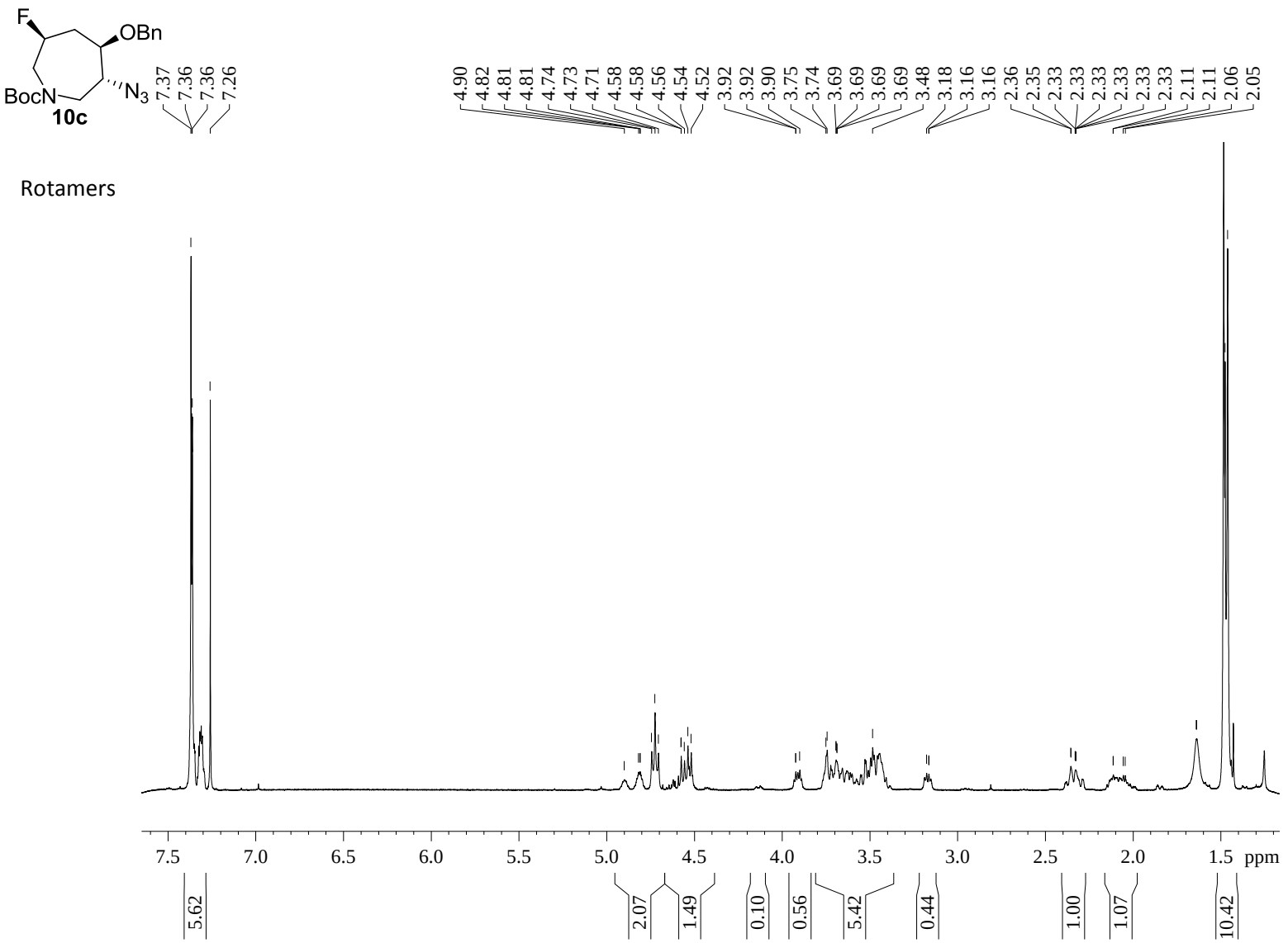
HMBC-10b


H3',4',5'
H1'
H6
H3,H4,
H7b
H2a
H7a
H2b
H6a H6b
H3''
ppm
C3''
C6
C7
C2
C3
C2''
C1'
C4
C5
C3',4',5'
C2'
C1''
10b
7.5 7.0 6.5 6.0 5.5 5.0 4.5 4.0 3.5 3.0 2.5 2.0 1.5 ppm
30 40 50 60 70 80 90 100 110 120 130 140 150 160

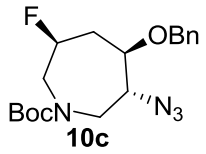
COSY-10b


H3’,4’,5’
H1’
H6
H3,H4,
H7b
H2a
H7a
H2b
H6a H6b
H3’’
ppm
H3’’
H6b
H6a
H2b
H7a
H3,H4,
H7b
H2a
H6
H1’
H3’,4’,5’
10b
7.5 7.0 6.5 6.0 5.5 5.0 4.5 4.0 3.5 3.0 2.5 2.0 1.5 ppm

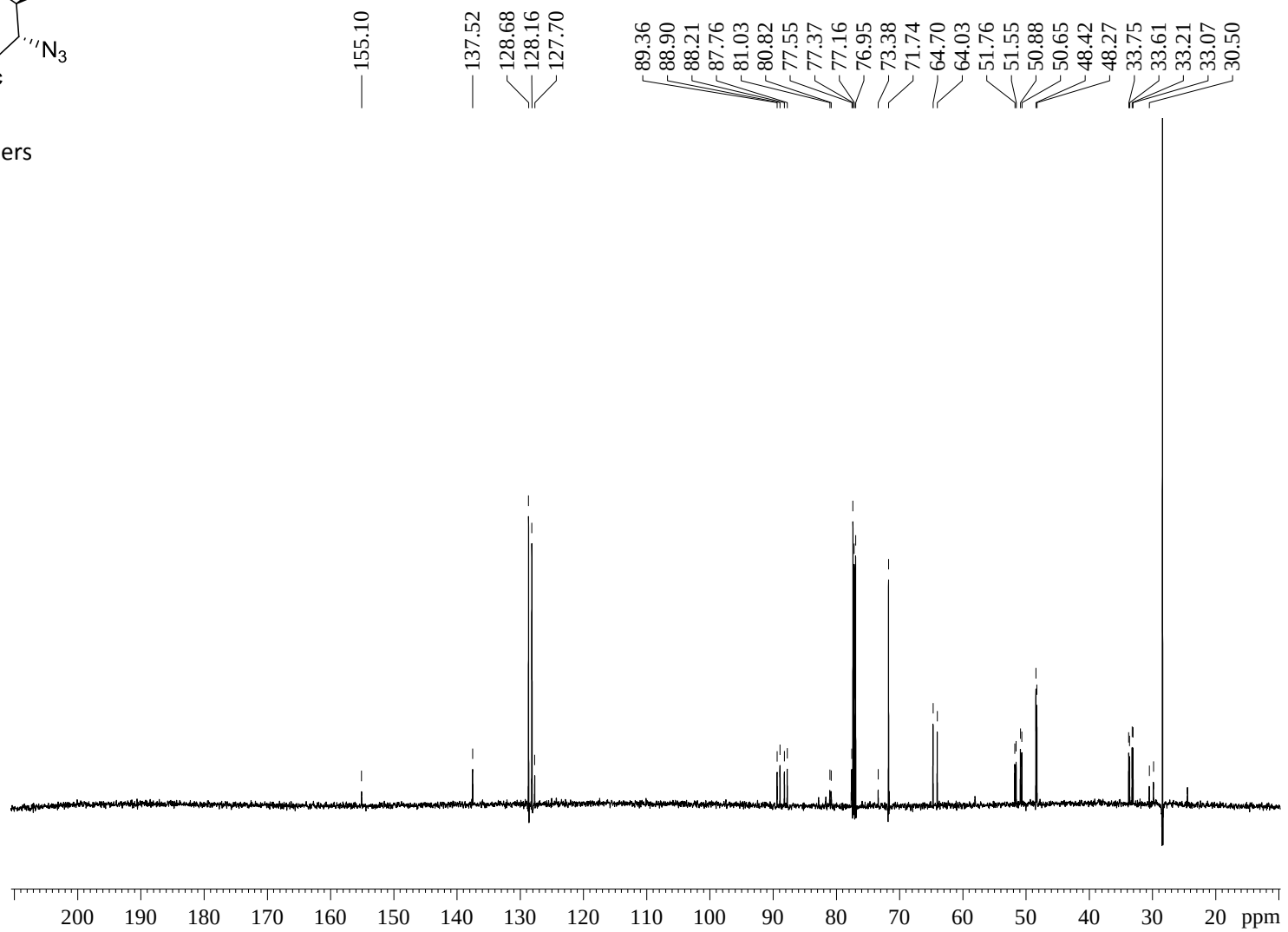
^{1}H-10c


F
OBn
BocN
N3
10c
7.37
7.36
7.36
7.26
4.90
4.82
4.81
4.81
4.74
4.73
4.71
4.58
4.58
4.56
4.54
4.52
3.92
3.92
3.90
3.75
3.74
3.69
3.69
3.69
3.69
3.48
3.18
3.16
3.16
2.36
2.35
2.33
2.33
2.33
2.33
2.33
2.11
2.11
2.06
2.05
Rotamers
7.5
7.0
6.5
6.0
5.5
5.0
4.5
4.0
3.5
3.0
2.5
2.0
1.5
ppm
5.62
2.07
1.49
0.10
0.56
5.42
0.44
1.00
1.07
10.42

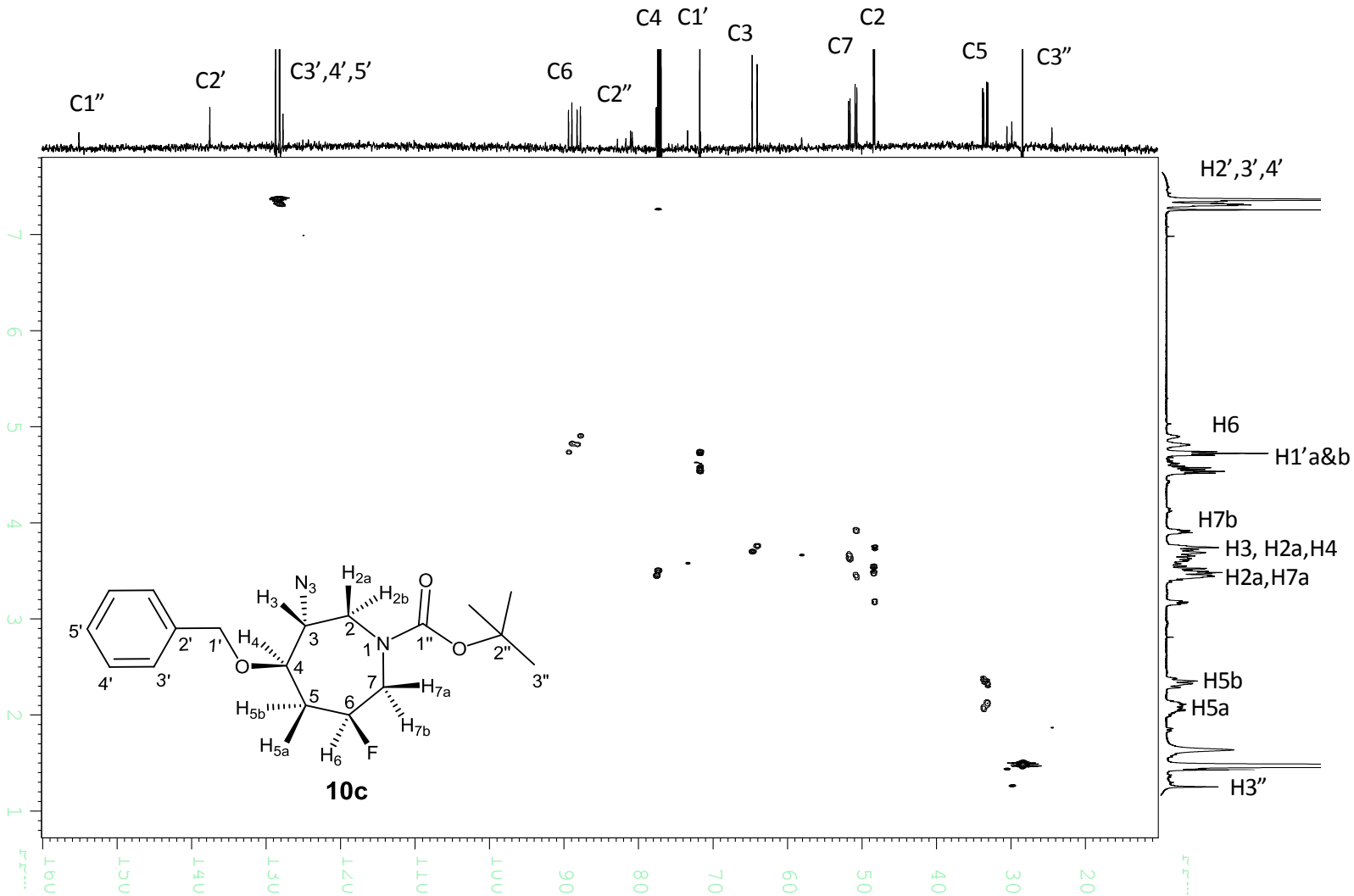
^{13}C-10c



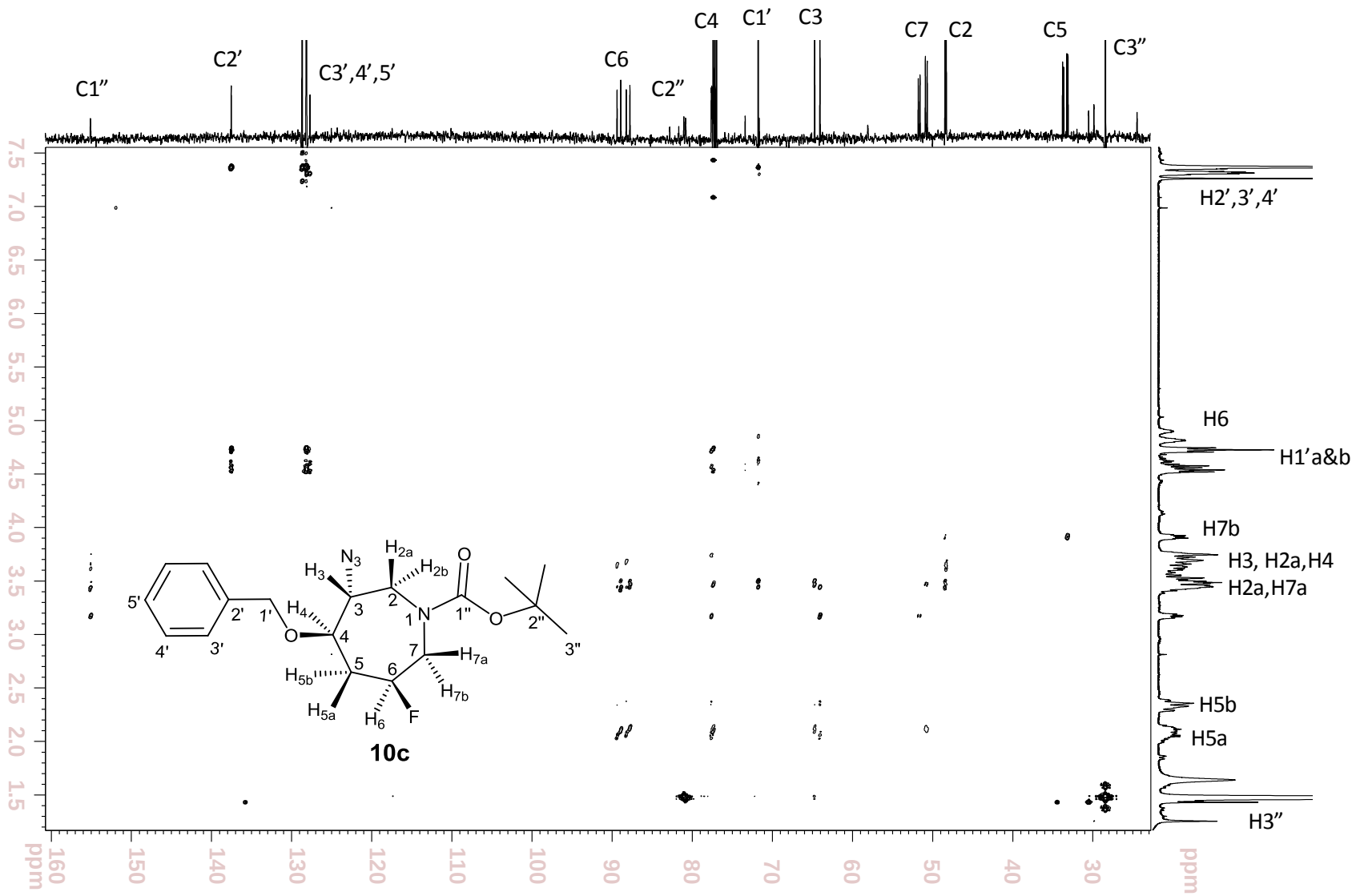
Rotamers



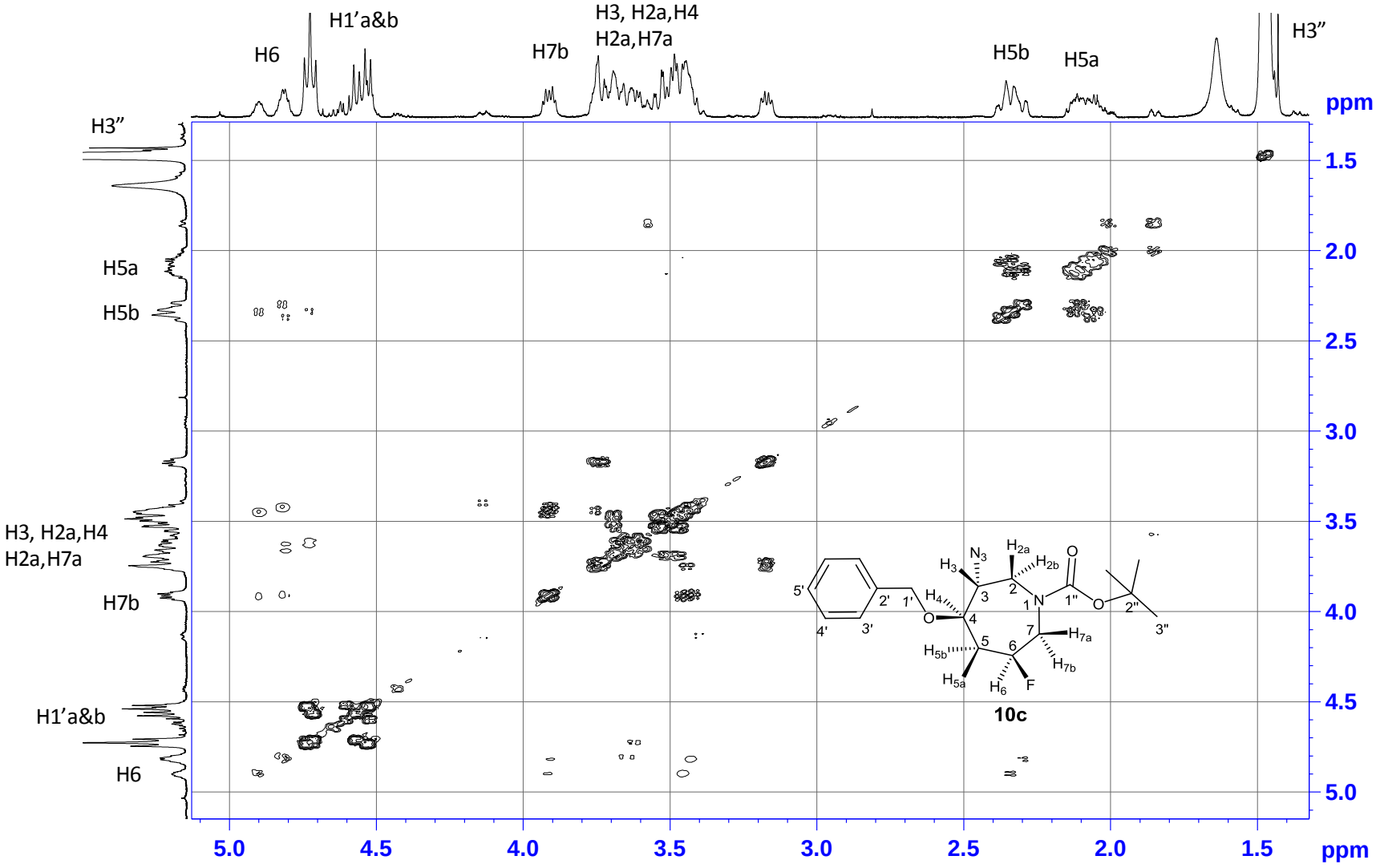
HSQC-10c


C1”
C2’
C3’,4’,5’
C6
C2”
C4
C1’
C3
C7
C2
C5
C3”
H2’,3’,4’
H6
H1’a&b
H7b
H3, H2a,H4
H2a,H7a
H5b
H5a
H3”
10c

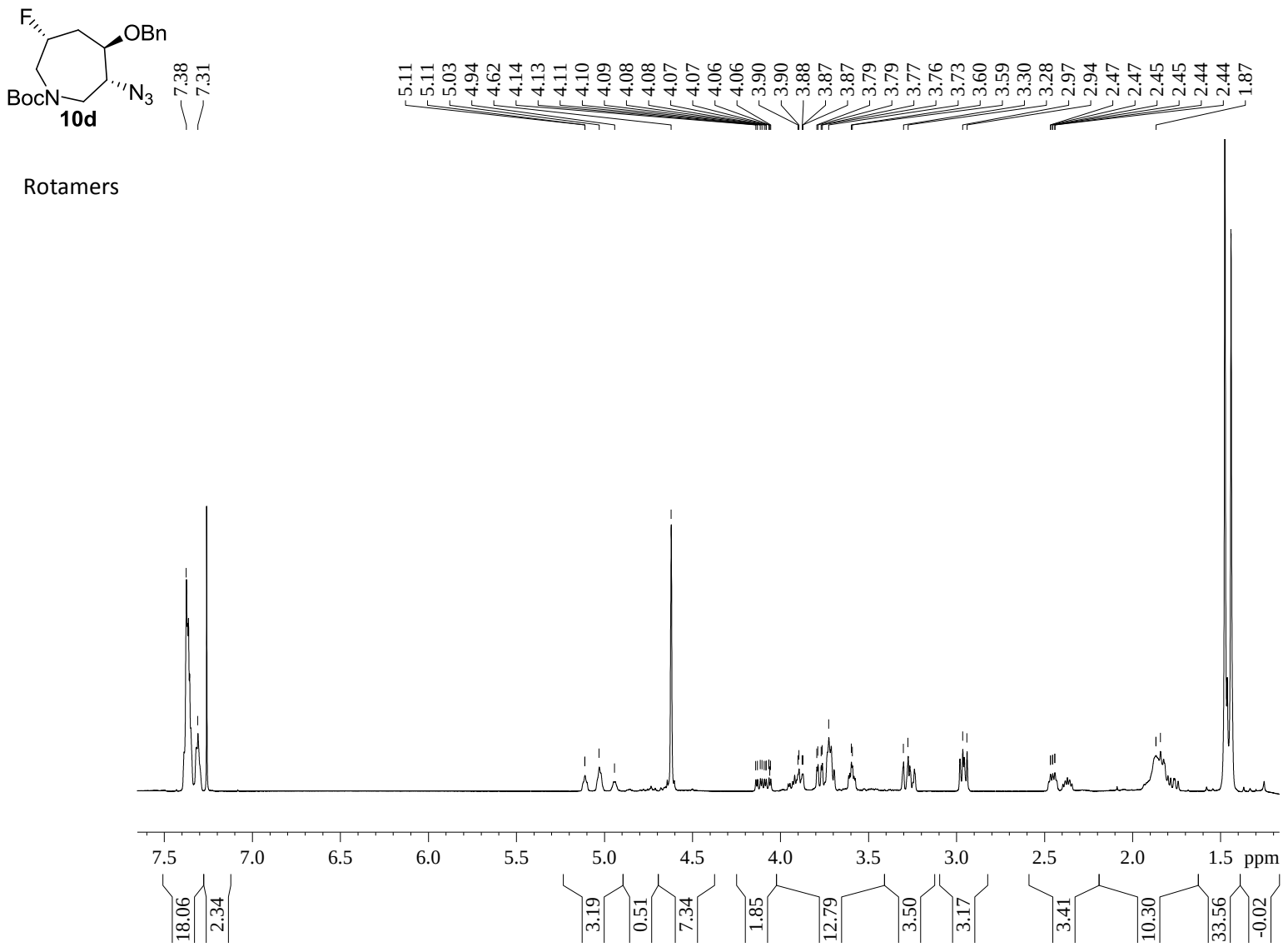
HMBC-10c


C1”
C2’
C3’,4’,5’
C6
C2”
C4
C1’
C3
C7
C2
C5
C3”
H2’,3’,4’
H6
H1’a&b
H7b
H3, H2a,H4
H2a,H7a
H5b
H5a
H3”
ppm
ppm
10c

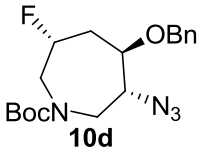
COSY-10c


H6
H1'a&b
H7b
H3, H2a,H4
H2a,H7a
H5b
H5a
H3"
ppm
1.5
2.0
2.5
3.0
3.5
4.0
4.5
5.0
10c

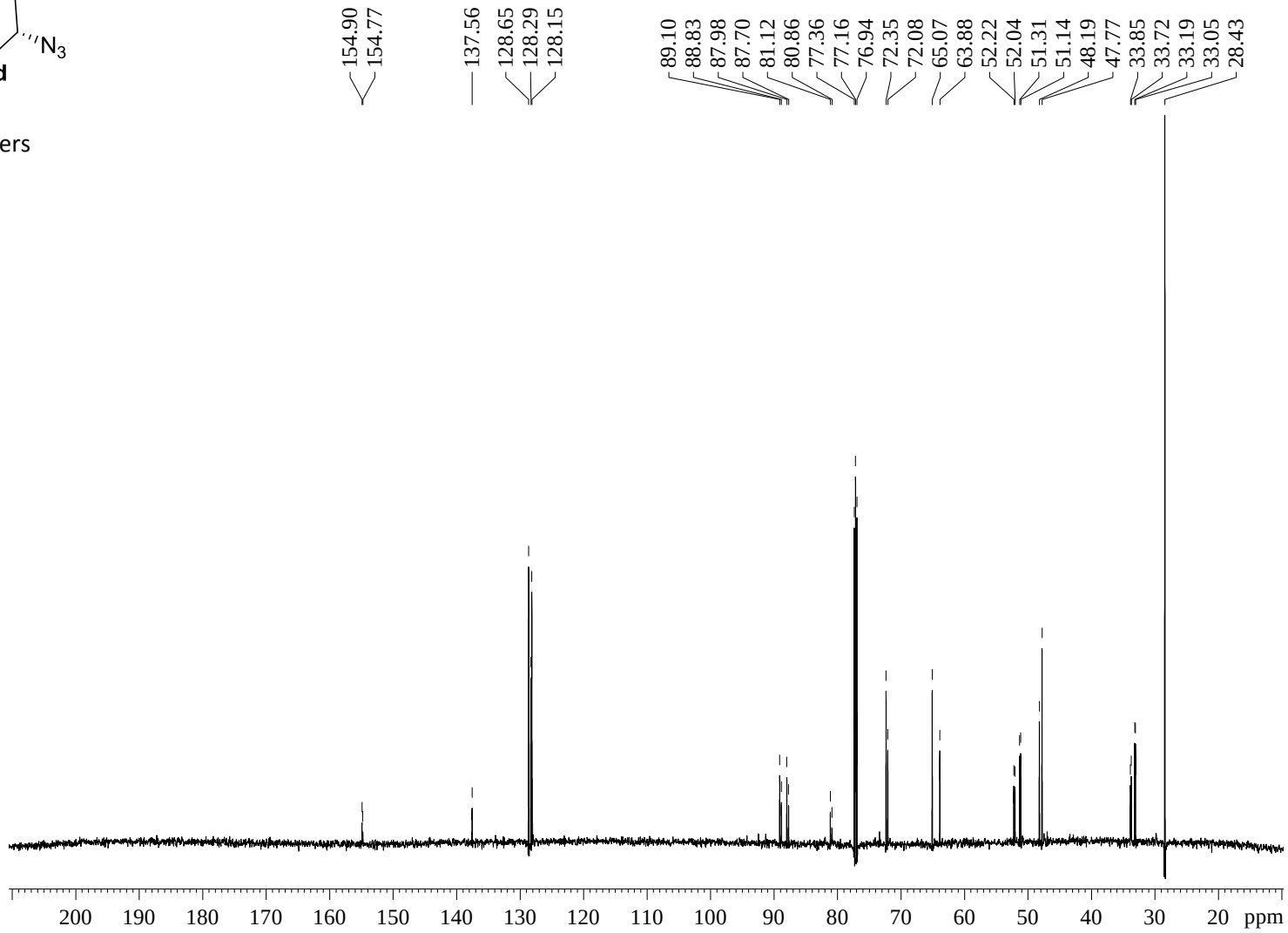
^{1}H-10d


F
OBn
BocN
N3
10d
7.38
7.31
5.11
5.11
5.03
4.94
4.62
4.14
4.13
4.11
4.10
4.09
4.08
4.08
4.07
4.07
4.06
4.06
3.90
3.90
3.88
3.87
3.87
3.79
3.79
3.77
3.76
3.73
3.60
3.59
3.30
3.28
2.97
2.94
2.47
2.47
2.45
2.45
2.44
2.44
1.87
Rotamers
7.5
7.0
6.5
6.0
5.5
5.0
4.5
4.0
3.5
3.0
2.5
2.0
1.5
ppm
18.06
2.34
3.19
0.51
7.34
1.85
12.79
3.50
3.17
3.41
10.30
33.56
-0.02

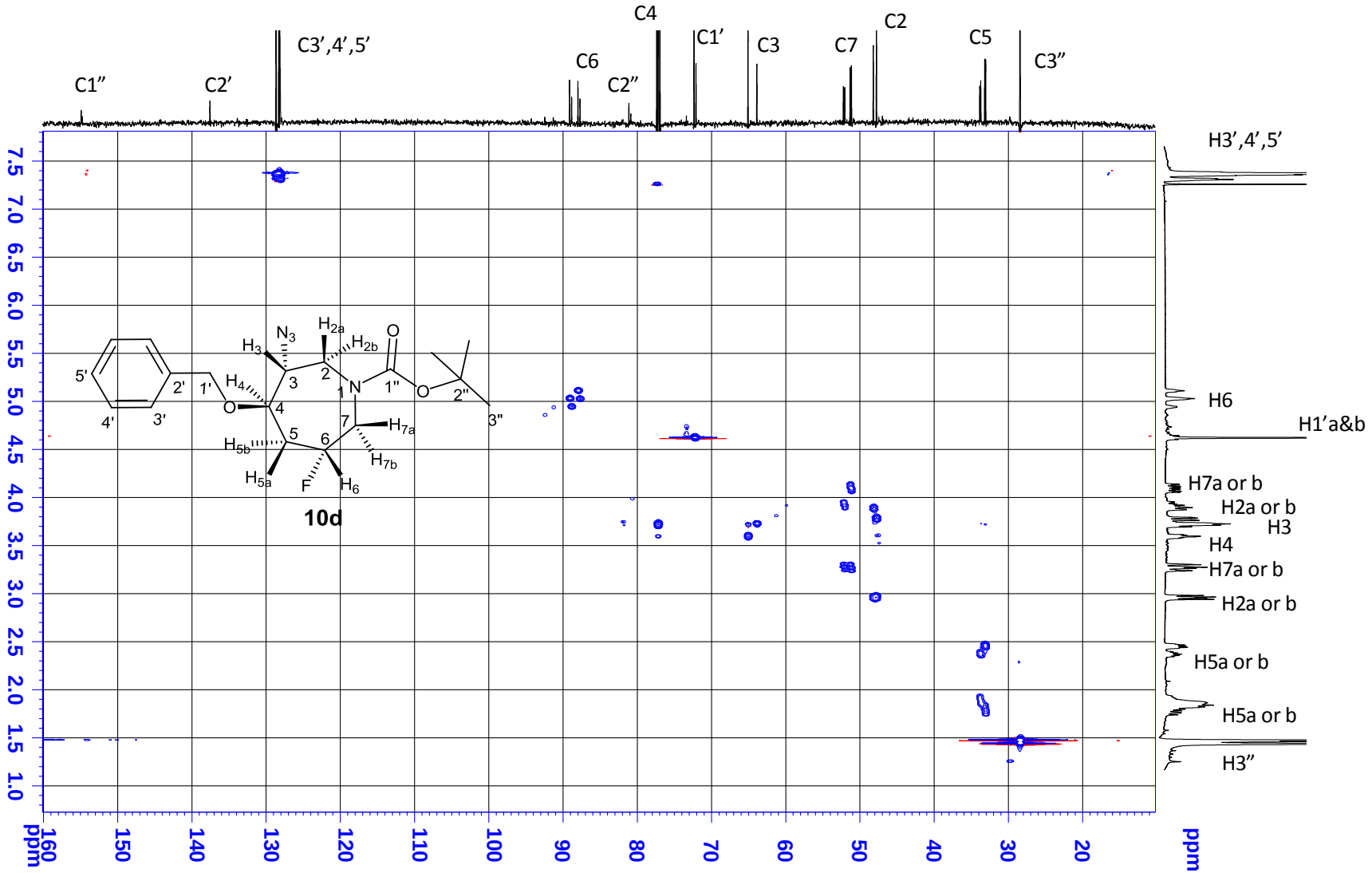
^{13}C-10d



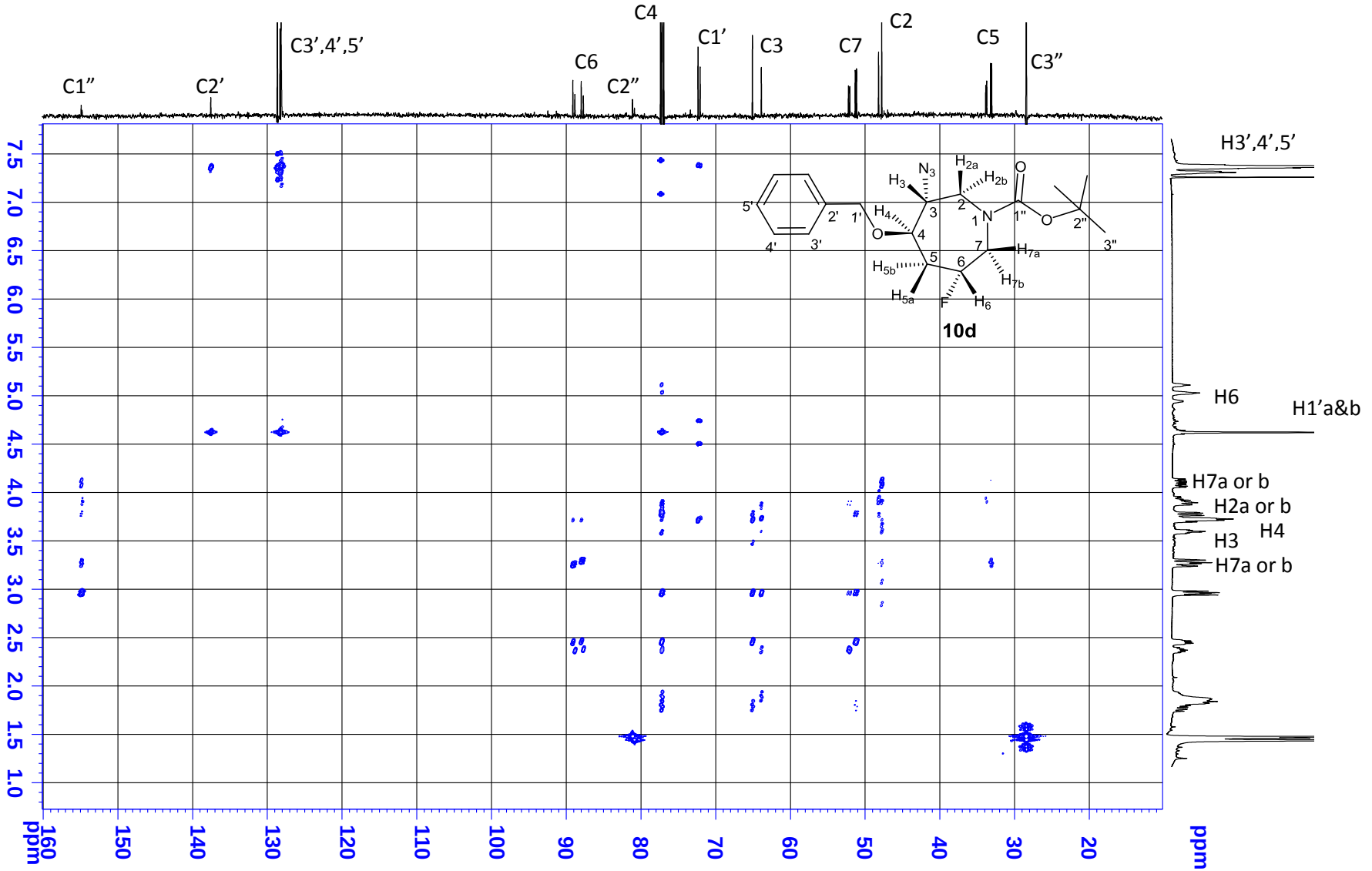
Rotamers



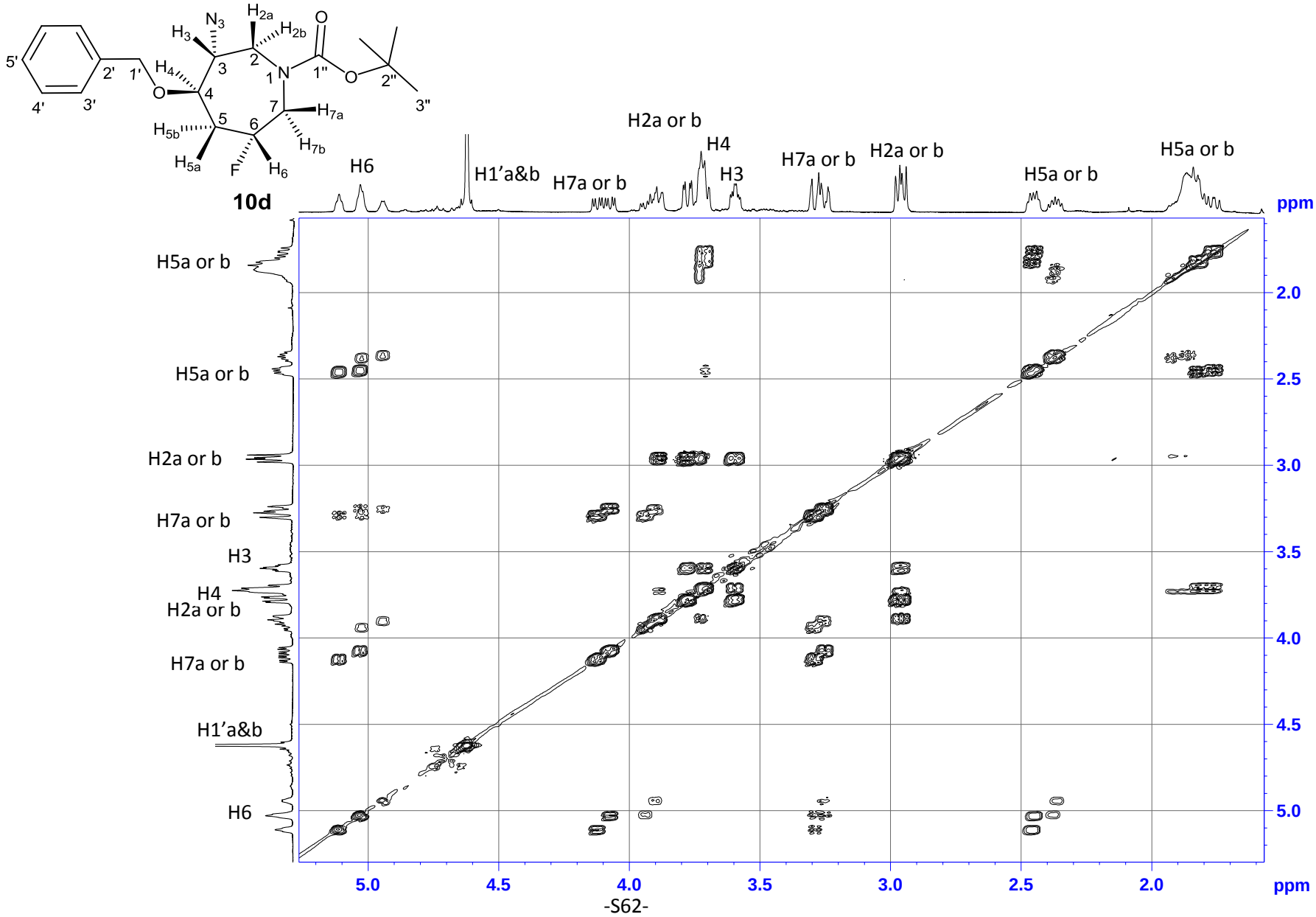
HSQC-10d


C1”
C2’
C3’,4’,5’
C6
C2”
C4
C1’
C3
C7
C2
C5
C3”
H3’,4’,5’
H6
H1’a&b
H7a or b
H2a or b
H3
H4
H7a or b
H2a or b
H5a or b
H5a or b
H3”
10d
ppm
ppm

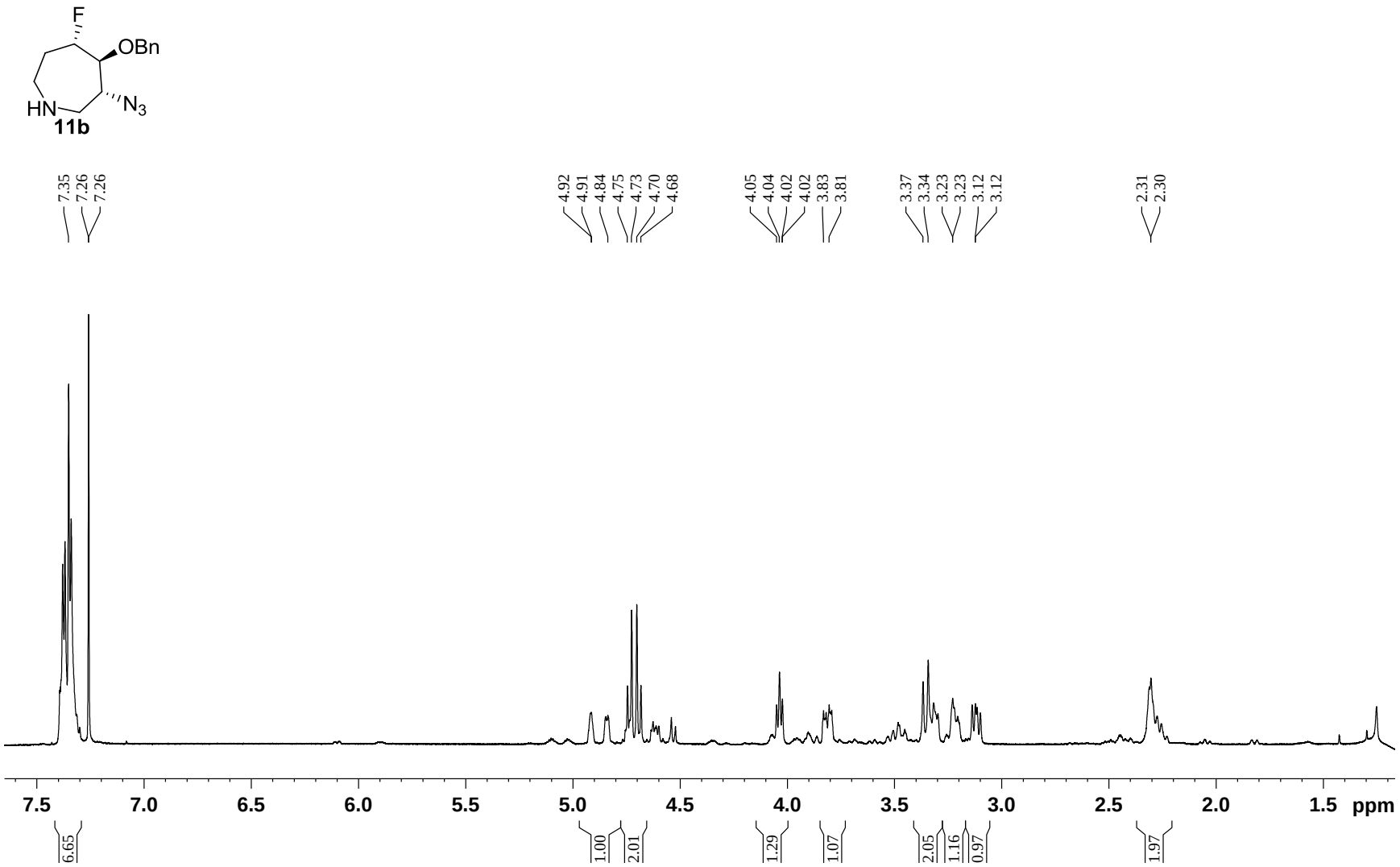
HMBC-10d


C1”
C2’
C3’,4’,5’
C6
C2”
C4
C1’
C3
C7
C2
C5
C3”
H3’,4’,5’
H6
H1’a&b
H7a or b
H2a or b
H3
H4
H7a or b
10d
ppm
ppm

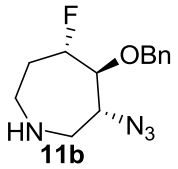
COSY-10d

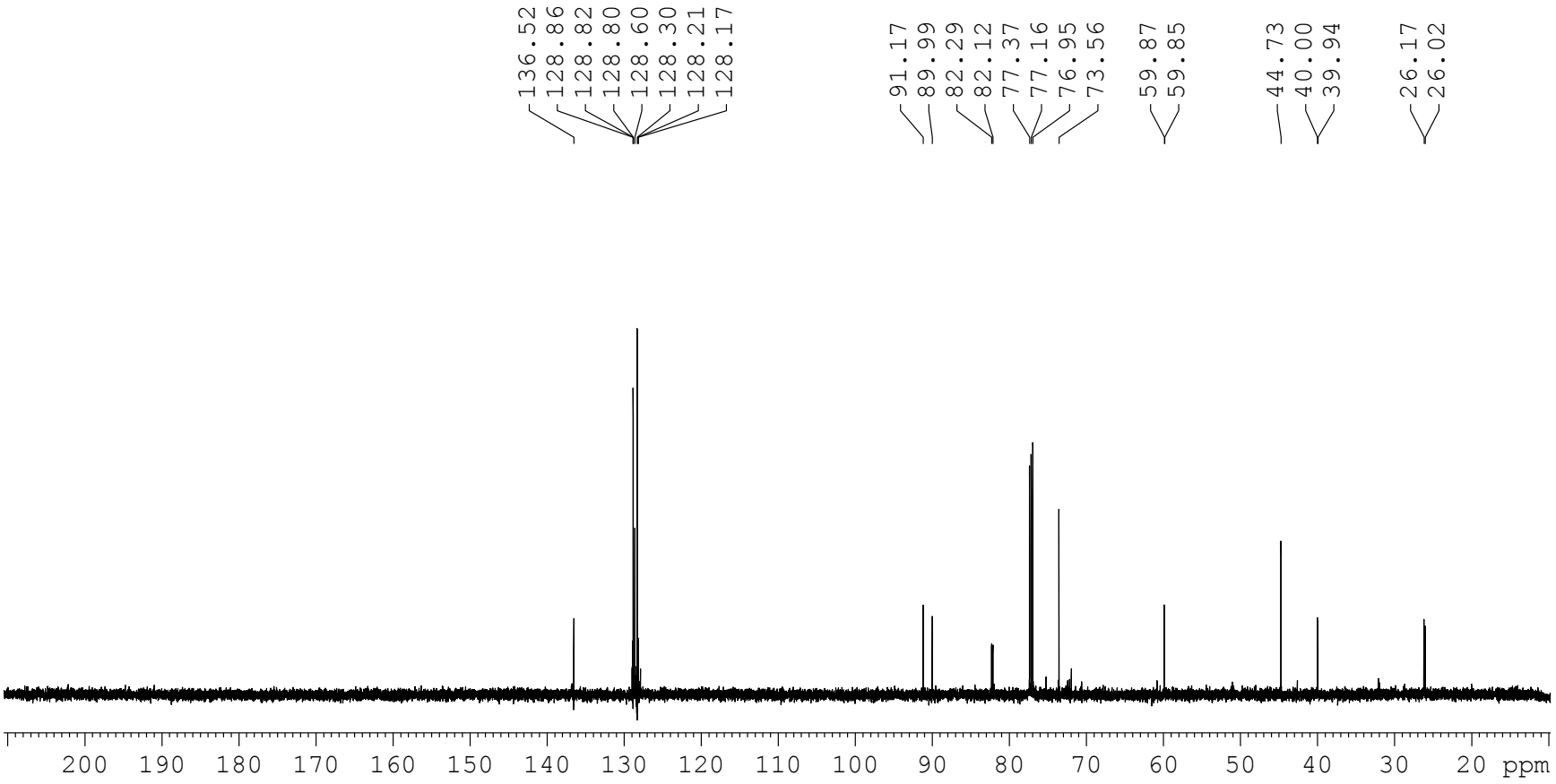

10d
H6
H1'a&b
H7a or b
H2a or b
H4
H3
H7a or b
H2a or b
H5a or b
H5a or b
ppm
H5a or b
H5a or b
H2a or b
H7a or b
H3
H4
H2a or b
H7a or b
H1'a&b
H6
2.0
2.5
3.0
3.5
4.0
4.5
5.0
5.0
4.5
4.0
3.5
3.0
2.5
2.0
ppm

^{1}H-11b

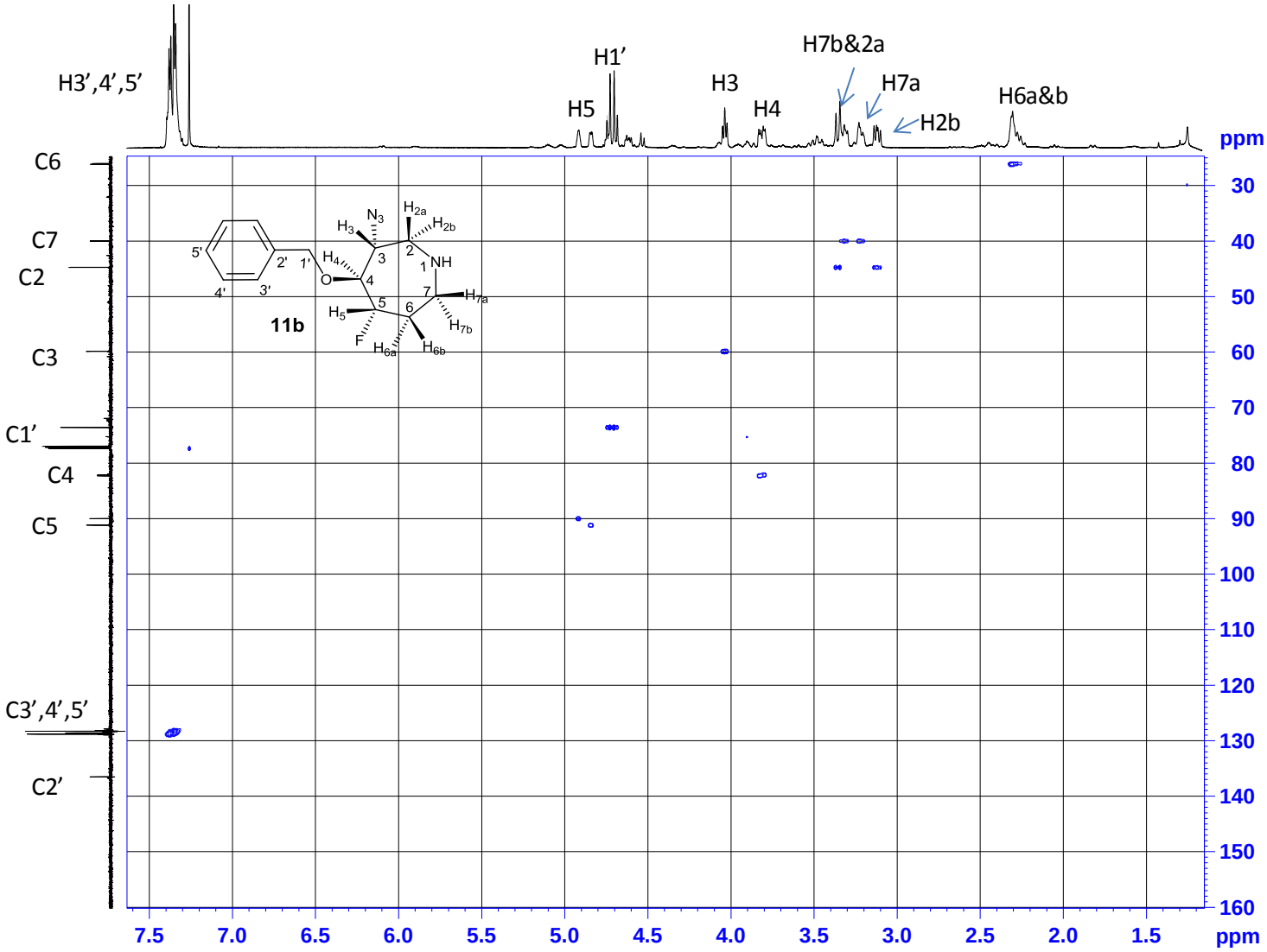

F
OBn
HN
N3
11b
7.35
7.26
7.26
4.92
4.91
4.84
4.75
4.73
4.70
4.68
4.05
4.04
4.02
4.02
3.83
3.81
3.37
3.34
3.23
3.23
3.12
3.12
2.31
2.30
7.5
7.0
6.5
6.0
5.5
5.0
4.5
4.0
3.5
3.0
2.5
2.0
1.5
ppm
6.65
1.00
2.01
1.29
1.07
2.05
1.16
0.97
1.97

^{13}C-11b

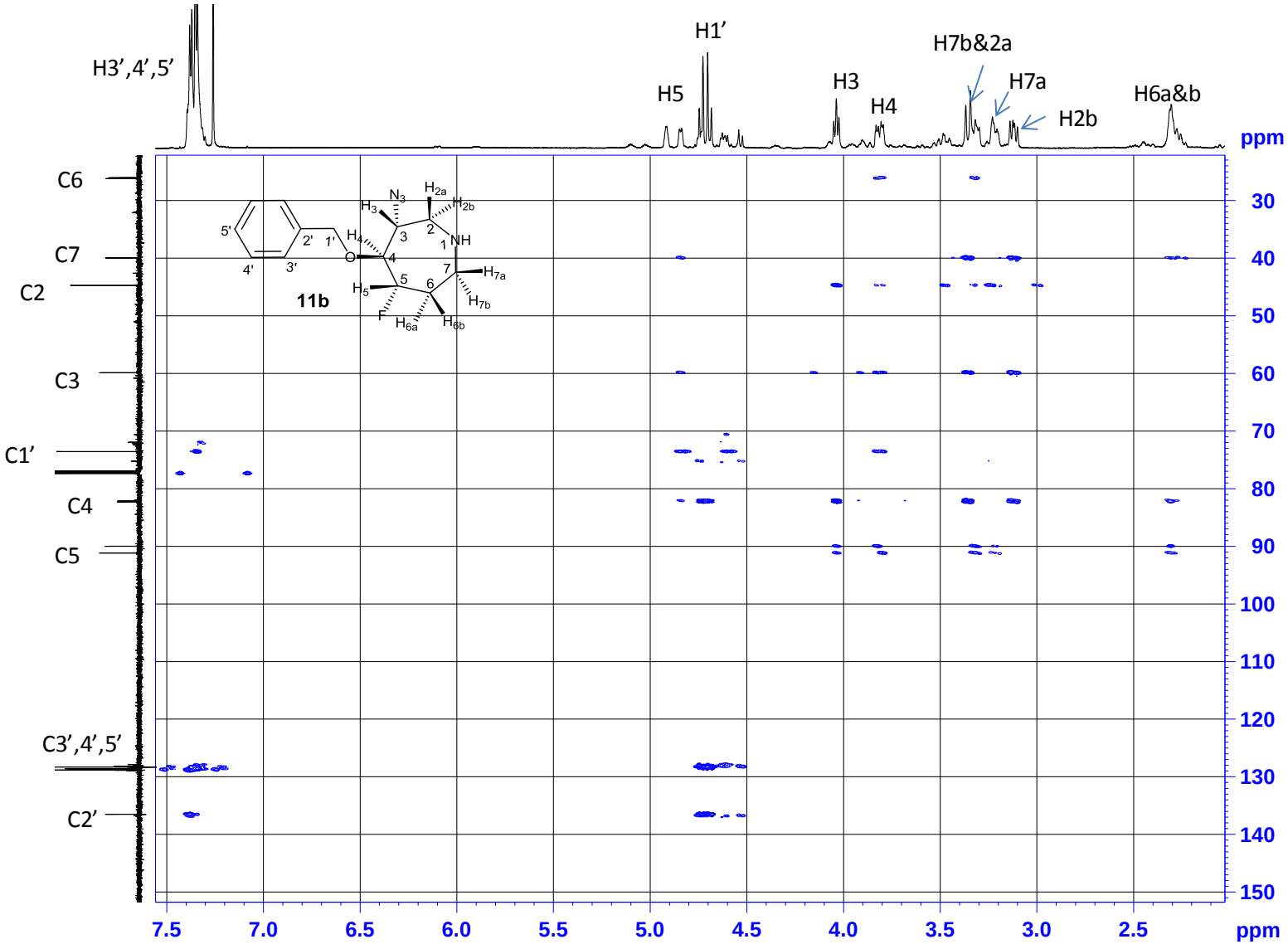

F
OBn
HN
N3
11b


136.52
128.86
128.82
128.80
128.60
128.30
128.21
128.17
91.17
89.99
82.29
82.12
77.37
77.16
76.95
73.56
59.87
59.85
44.73
40.00
39.94
26.17
26.02
200 190 180 170 160 150 140 130 120 110 100 90 80 70 60 50 40 30 20 ppm

HSQC-11b

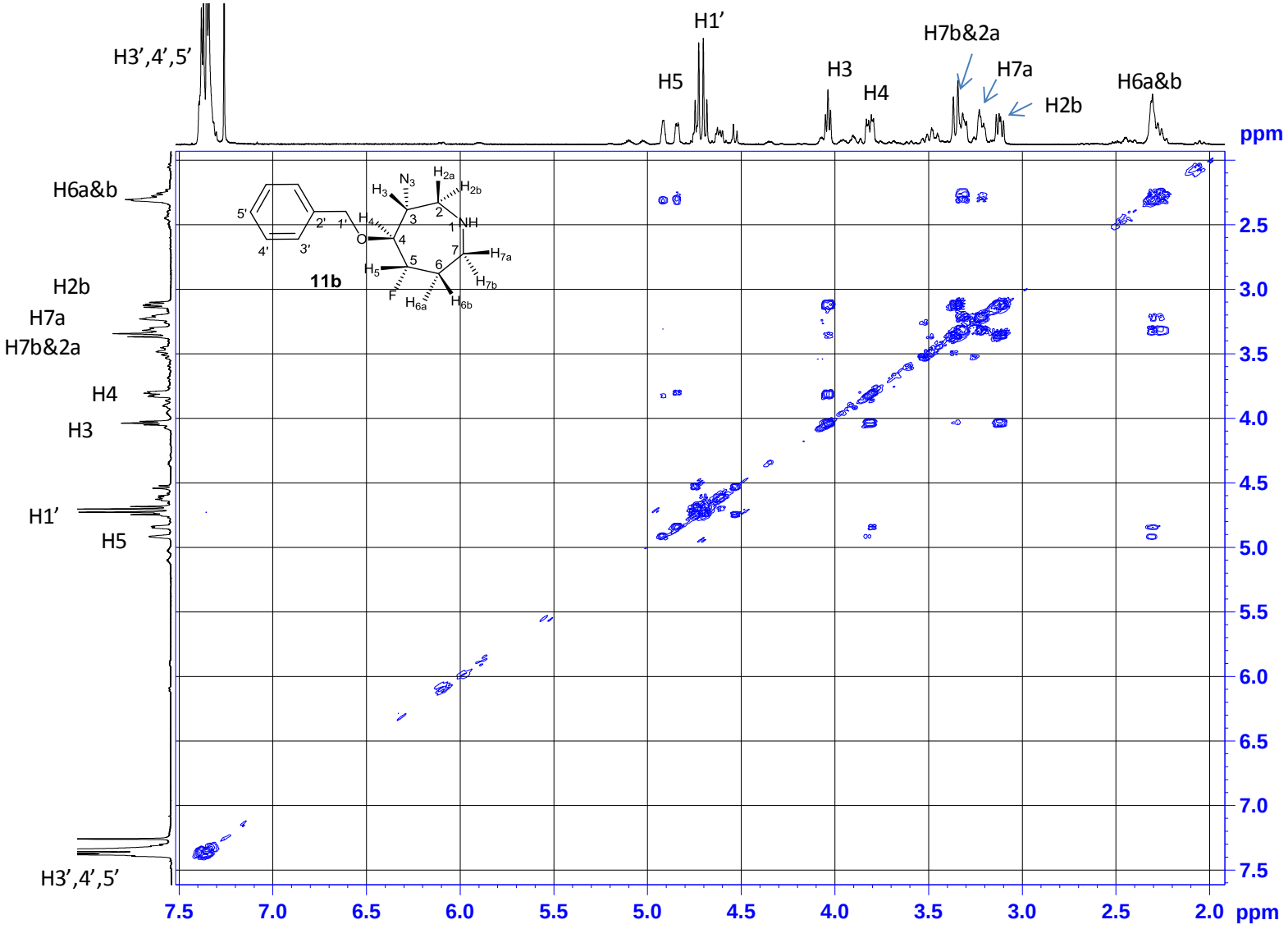

H3',4',5'
H5
H1'
H3
H4
H7b&2a
H7a
H2b
H6a&b
ppm
C6
C7
C2
C3
C1'
C4
C5
C3',4',5'
C2'
11b
7.5
7.0
6.5
6.0
5.5
5.0
4.5
4.0
3.5
3.0
2.5
2.0
1.5
ppm

HMBC-11b

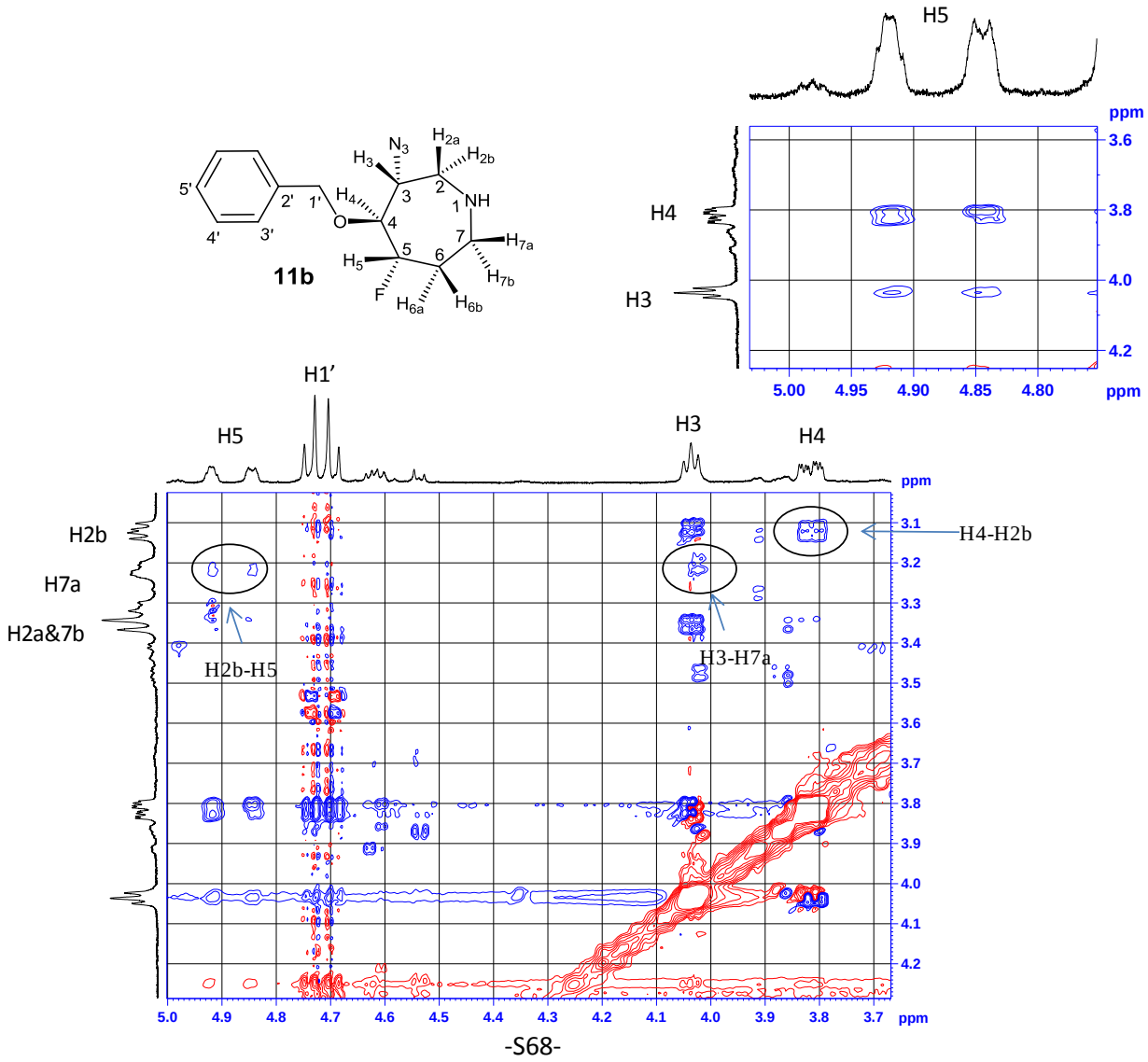

H3',4',5'
H1'
H5
H3
H4
H7b&2a
H7a
H2b
H6a&b
ppm
C6
C7
C2
C3
C1'
C4
C5
C3',4',5'
C2'
11b
7.5
7.0
6.5
6.0
5.5
5.0
4.5
4.0
3.5
3.0
2.5
ppm

-S66-

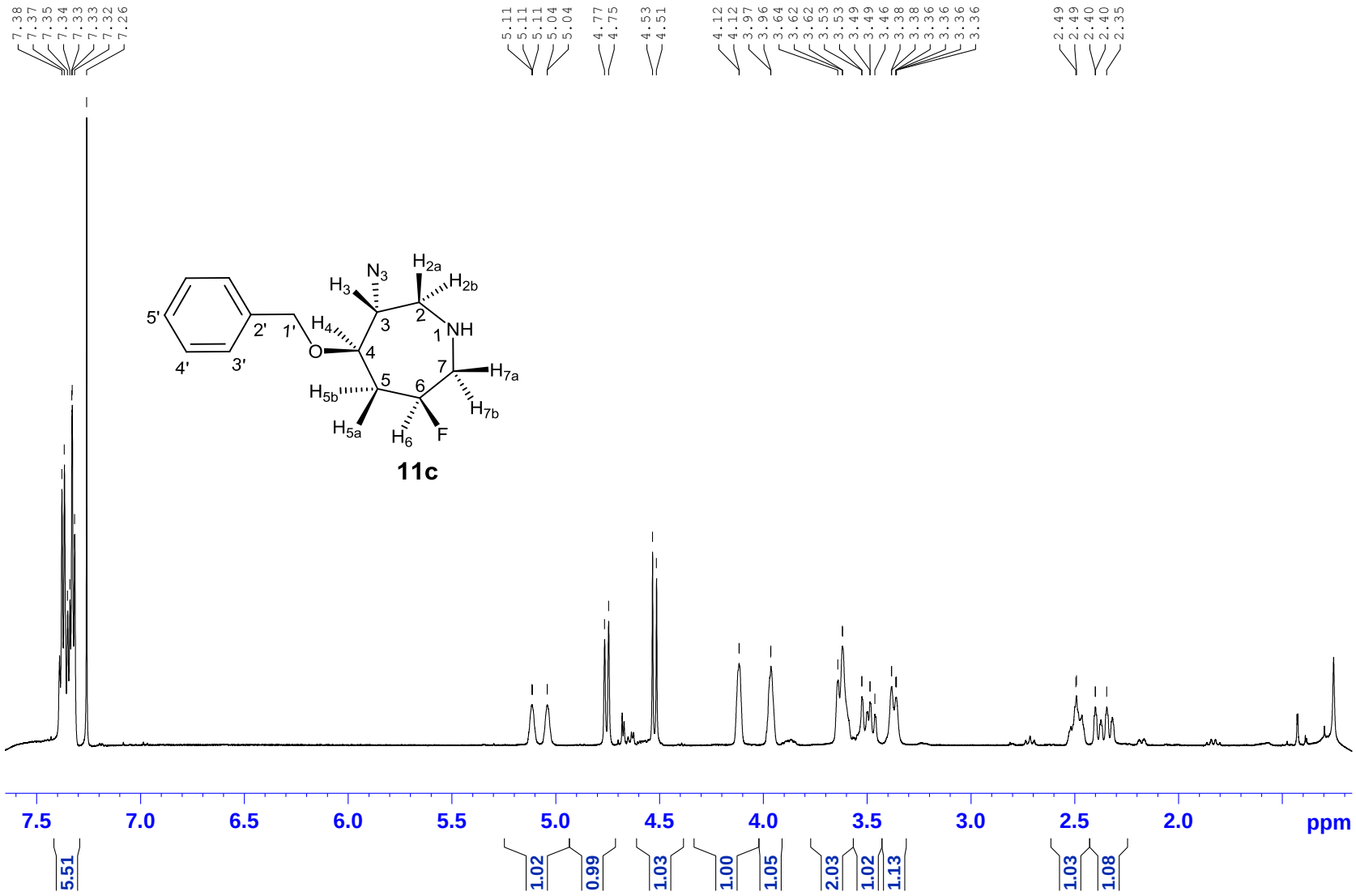
COSY-11b


H3',4',5'
H1'
H5
H3
H4
H7b&2a
H7a
H2b
H6a&b
ppm
11b
7.5
7.0
6.5
6.0
5.5
5.0
4.5
4.0
3.5
3.0
2.5
2.0
ppm

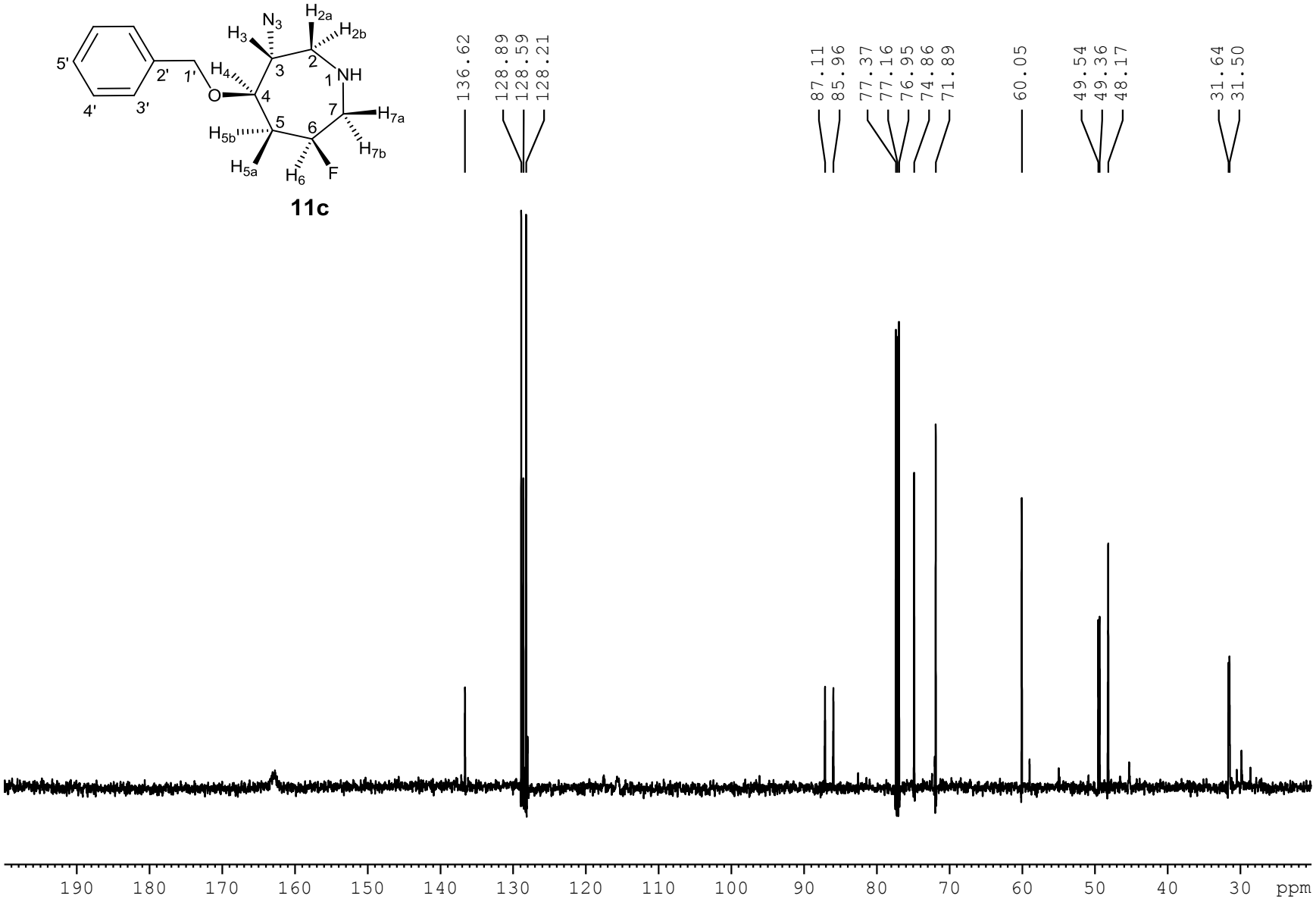
NOESY-11b



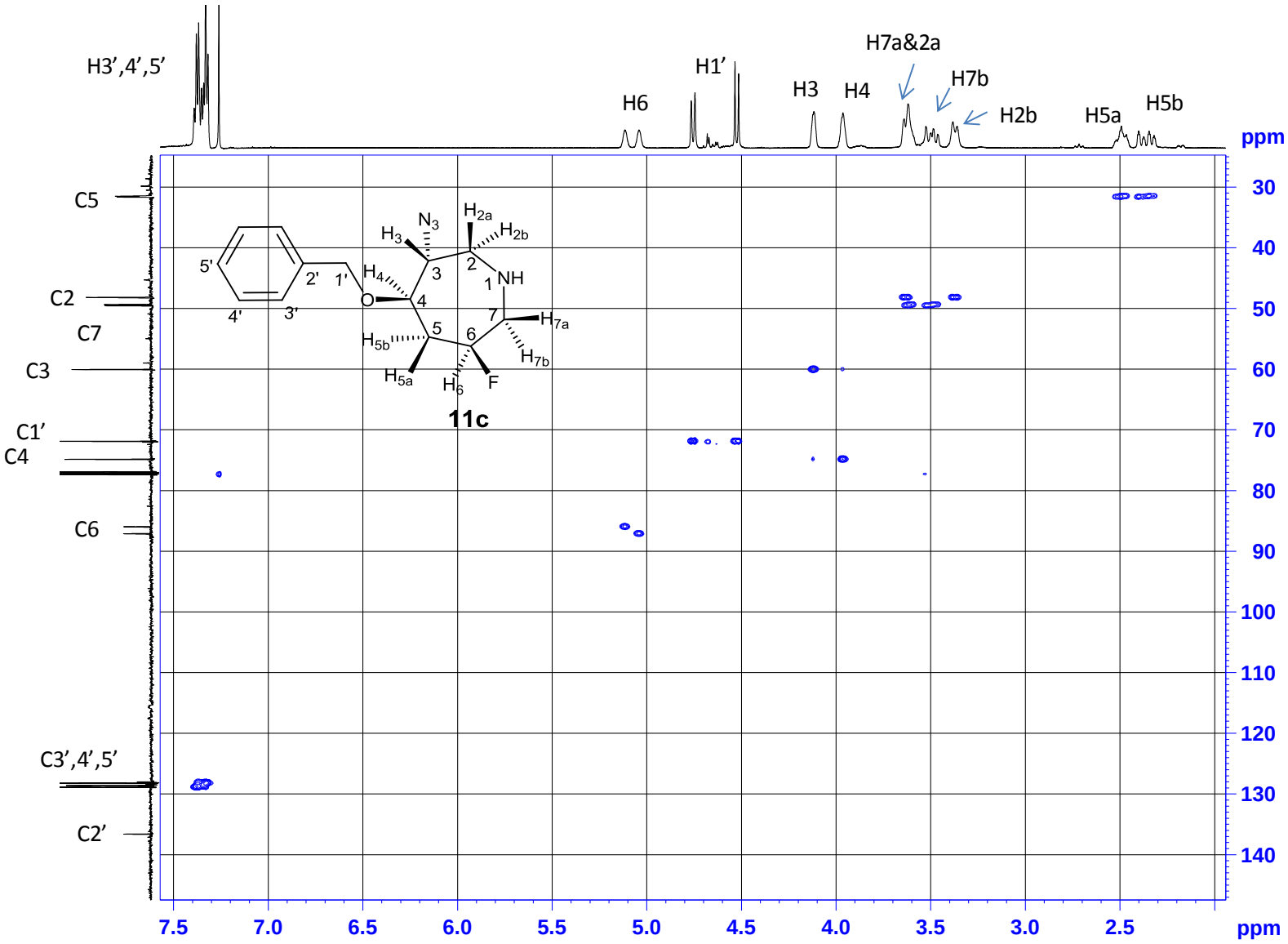
^{1}H-11c


7.38
7.37
7.35
7.34
7.33
7.33
7.32
7.26
5.11
5.11
5.11
5.04
5.04
4.77
4.75
4.53
4.51
4.12
4.12
3.97
3.96
3.64
3.62
3.62
3.53
3.53
3.49
3.49
3.46
3.38
3.38
3.36
3.36
3.36
3.36
2.49
2.49
2.40
2.40
2.35
N3
H2a
H3
H2b
2
3
1
NH
H4
O
4
7
H7a
5'
2'
1'
4'
3'
5
6
H5b
H7b
H5a
H6
F
11c
7.5
7.0
6.5
6.0
5.5
5.0
4.5
4.0
3.5
3.0
2.5
2.0
ppm
5.51
1.02
0.99
1.03
1.00
1.05
2.03
1.02
1.13
1.03
1.08

^{13}C-11c

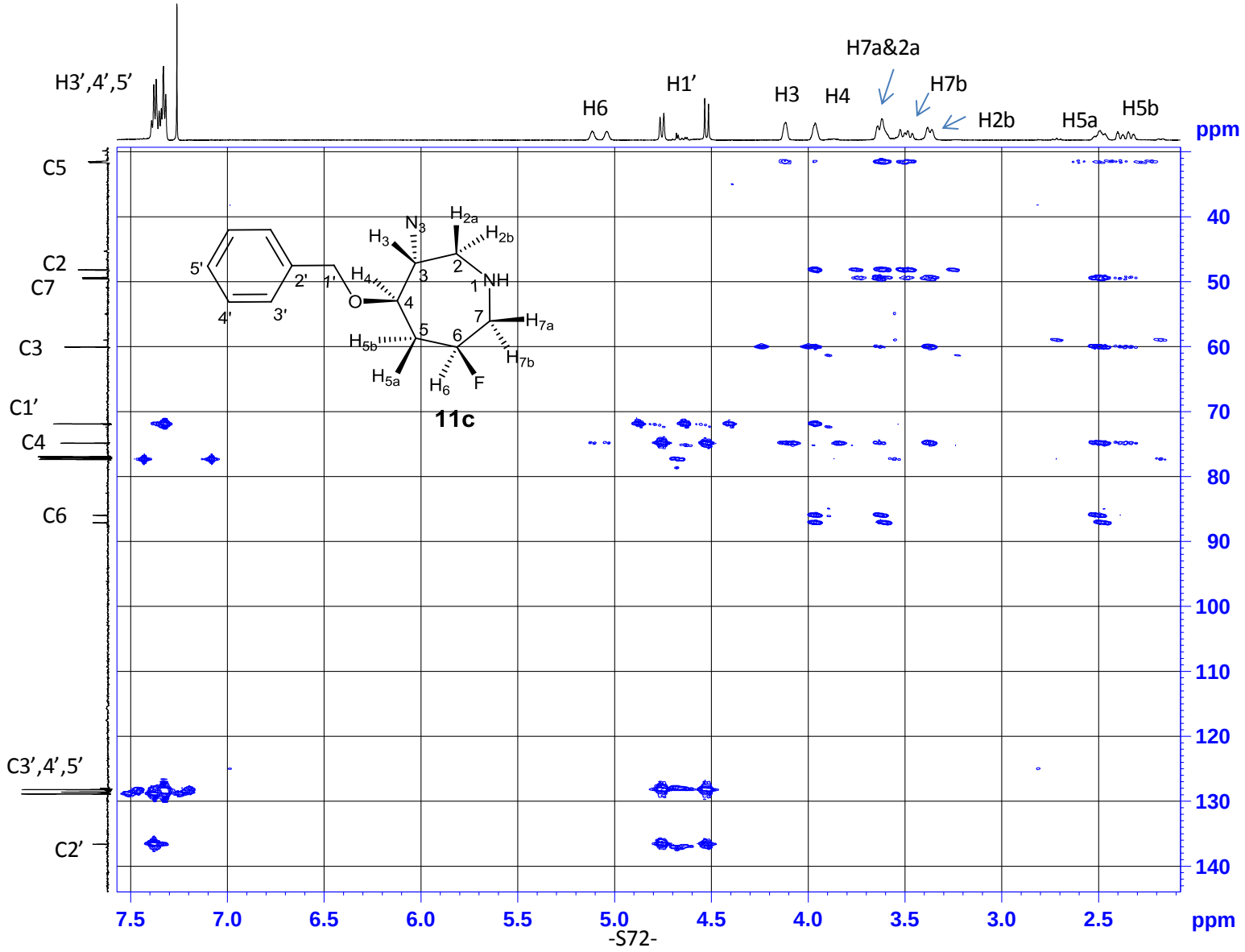

N3
H2a
H2b
H3
2
3
1
NH
H4
O
4
5
6
7
H7a
H7b
H5b
H5a
H6
F
5'
2'
1'
4'
3'
11c
136.62
128.89
128.59
128.21
87.11
85.96
77.37
77.16
76.95
74.86
71.89
60.05
49.54
49.36
48.17
31.64
31.50
190
180
170
160
150
140
130
120
110
100
90
80
70
60
50
40
30
ppm

HSQC-11c

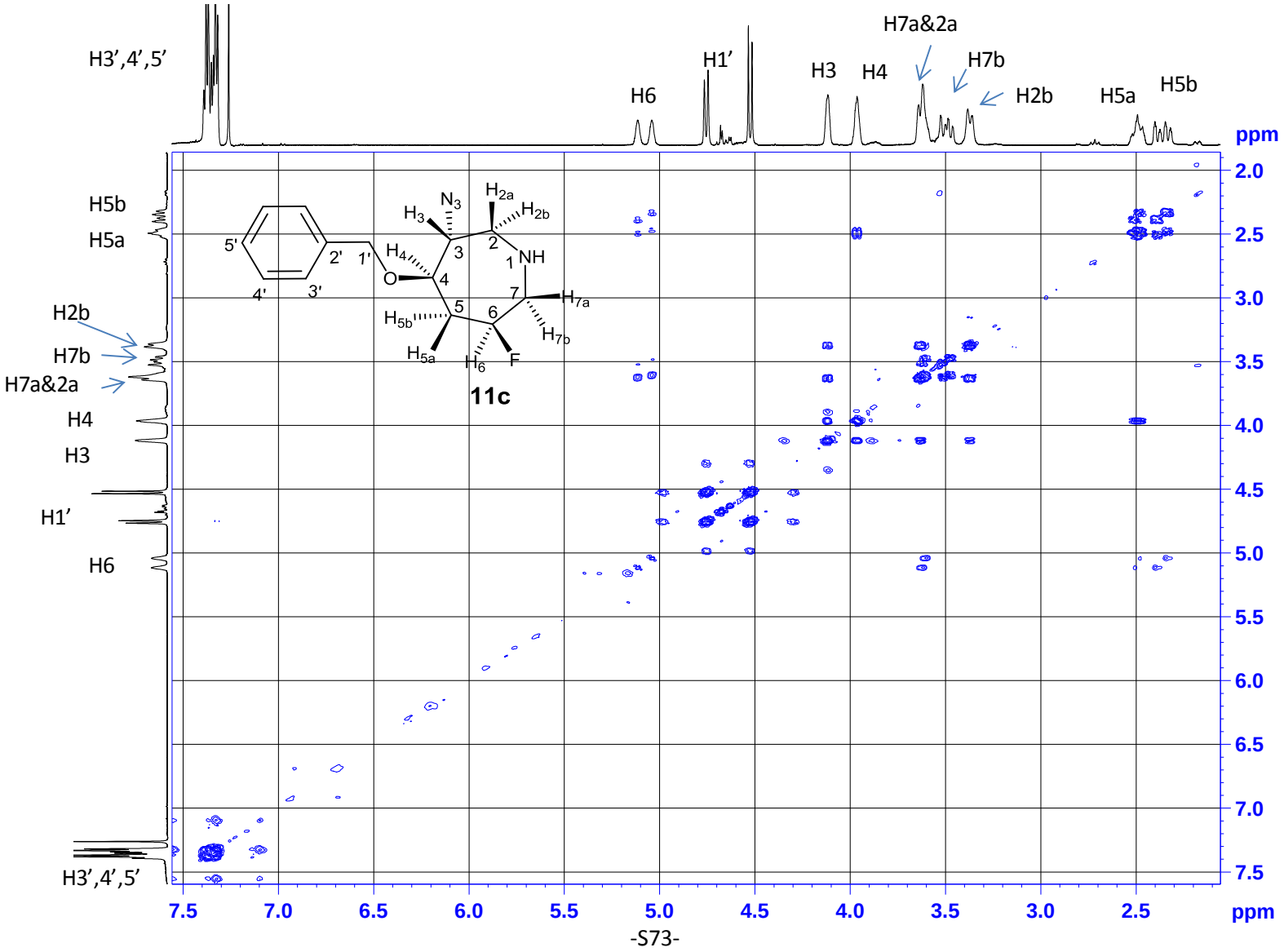

H3',4',5'
H6
H1'
H3
H4
H7a&2a
H7b
H2b
H5a
H5b
ppm
C5
C2
C7
C3
C1'
C4
C6
C3',4',5'
C2'
11c
7.5
7.0
6.5
6.0
5.5
5.0
4.5
4.0
3.5
3.0
2.5
ppm

-S71-

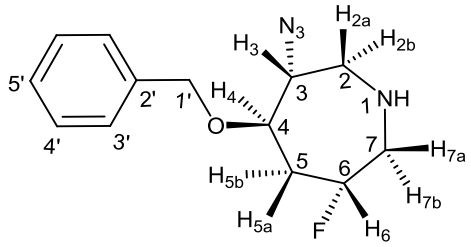
HMBC-11c


H3',4',5'
H6
H1'
H3
H4
H7a&2a
H7b
H2b
H5a
H5b
ppm
C5
C2
C7
C3
C1'
C4
C6
C3',4',5'
C2'
11c
7.5
7.0
6.5
6.0
5.5
5.0
4.5
4.0
3.5
3.0
2.5
ppm
40
50
60
70
80
90
100
110
120
130
140

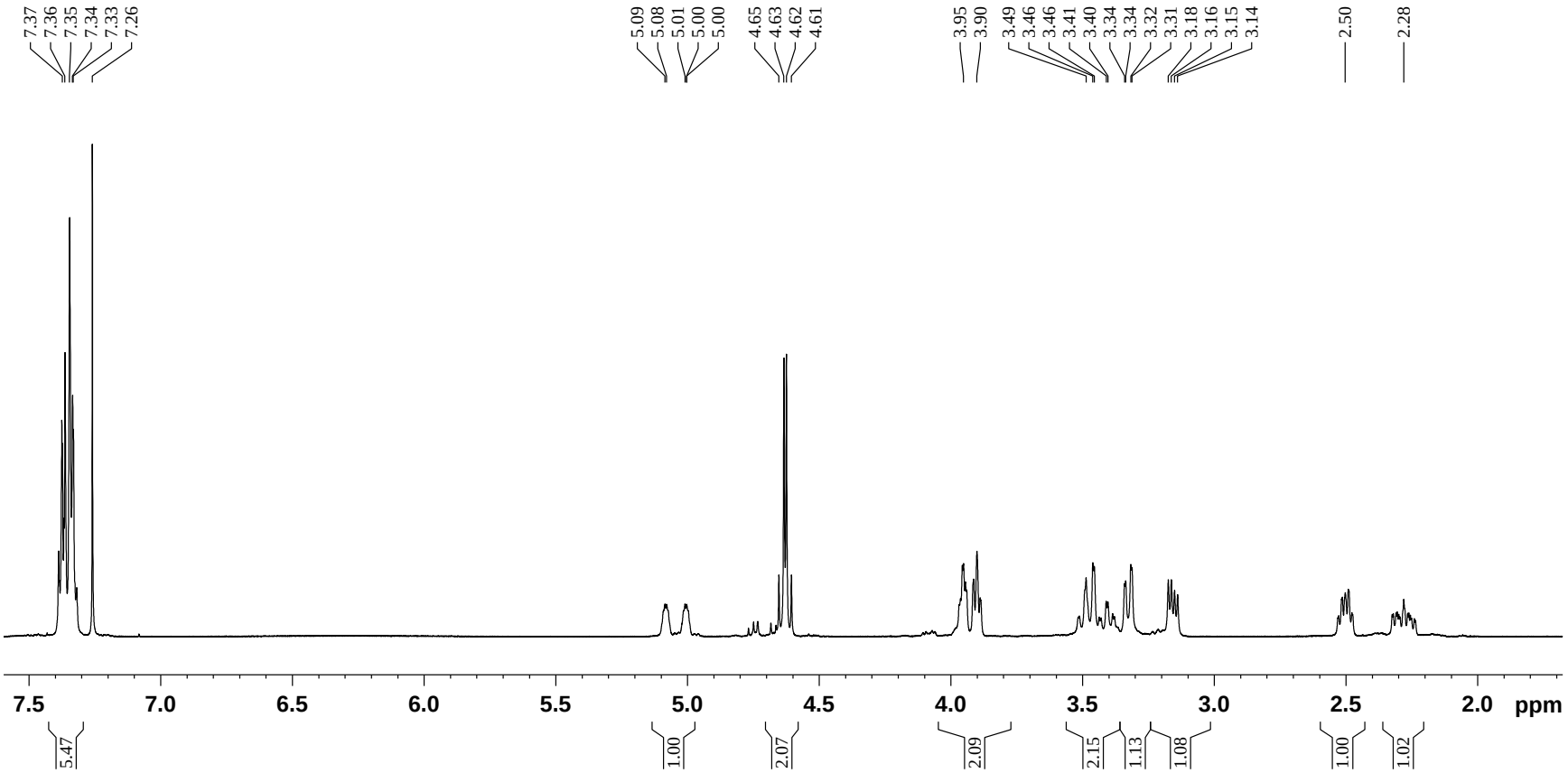
COSY-11c


H3',4',5'
H6
H1'
H3
H4
H7a&2a
H7b
H2b
H5a
H5b
ppm
2.0
2.5
3.0
3.5
4.0
4.5
5.0
5.5
6.0
6.5
7.0
7.5
11c
7.5
7.0
6.5
6.0
5.5
5.0
4.5
4.0
3.5
3.0
2.5
ppm

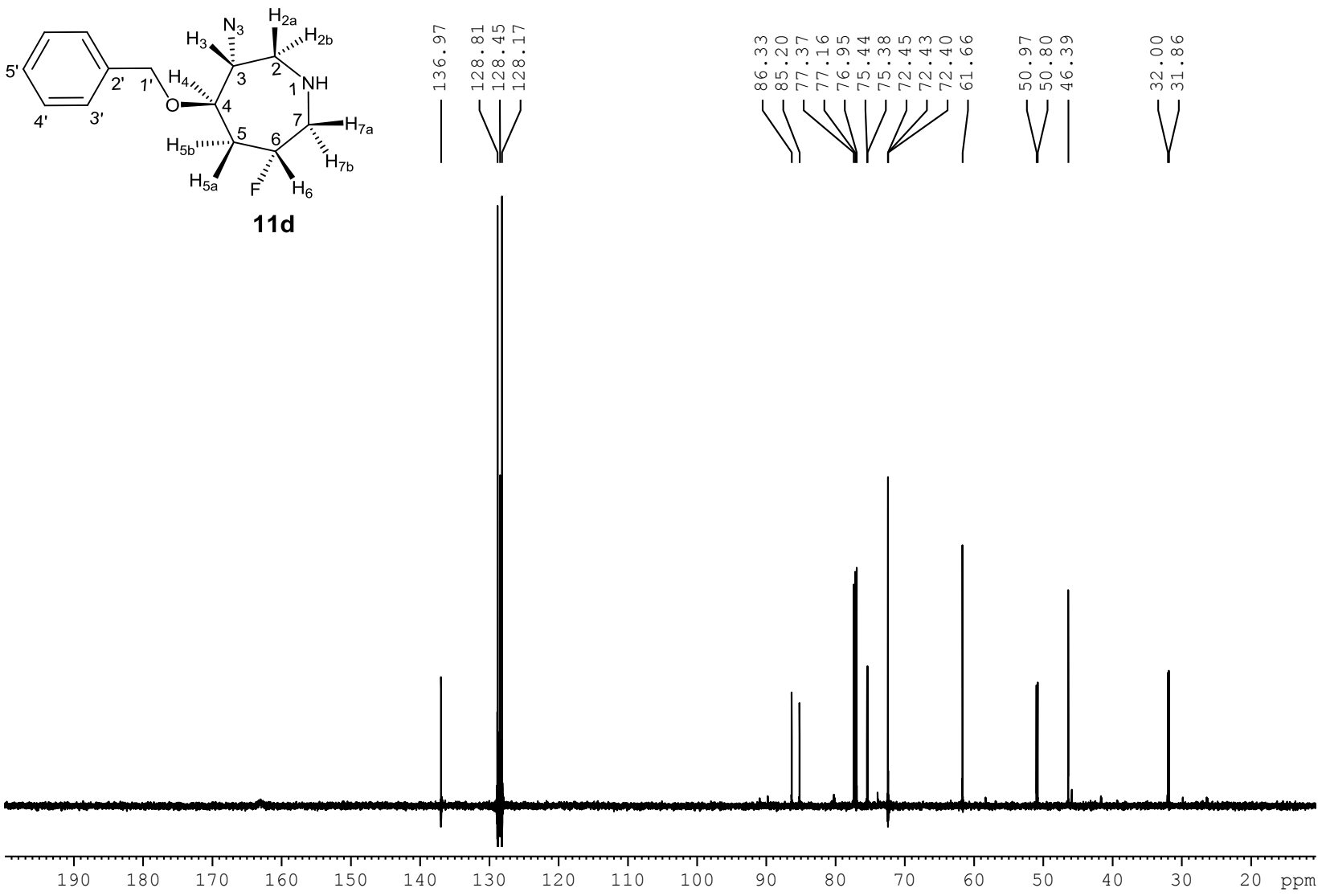
^{1}H-11d


N3
H2a
H2b
H3
2
3
1
NH
5'
2'
1'
H4
O
4
4'
3'
7
H7a
5
6
H5b
H7b
H5a
F
H6

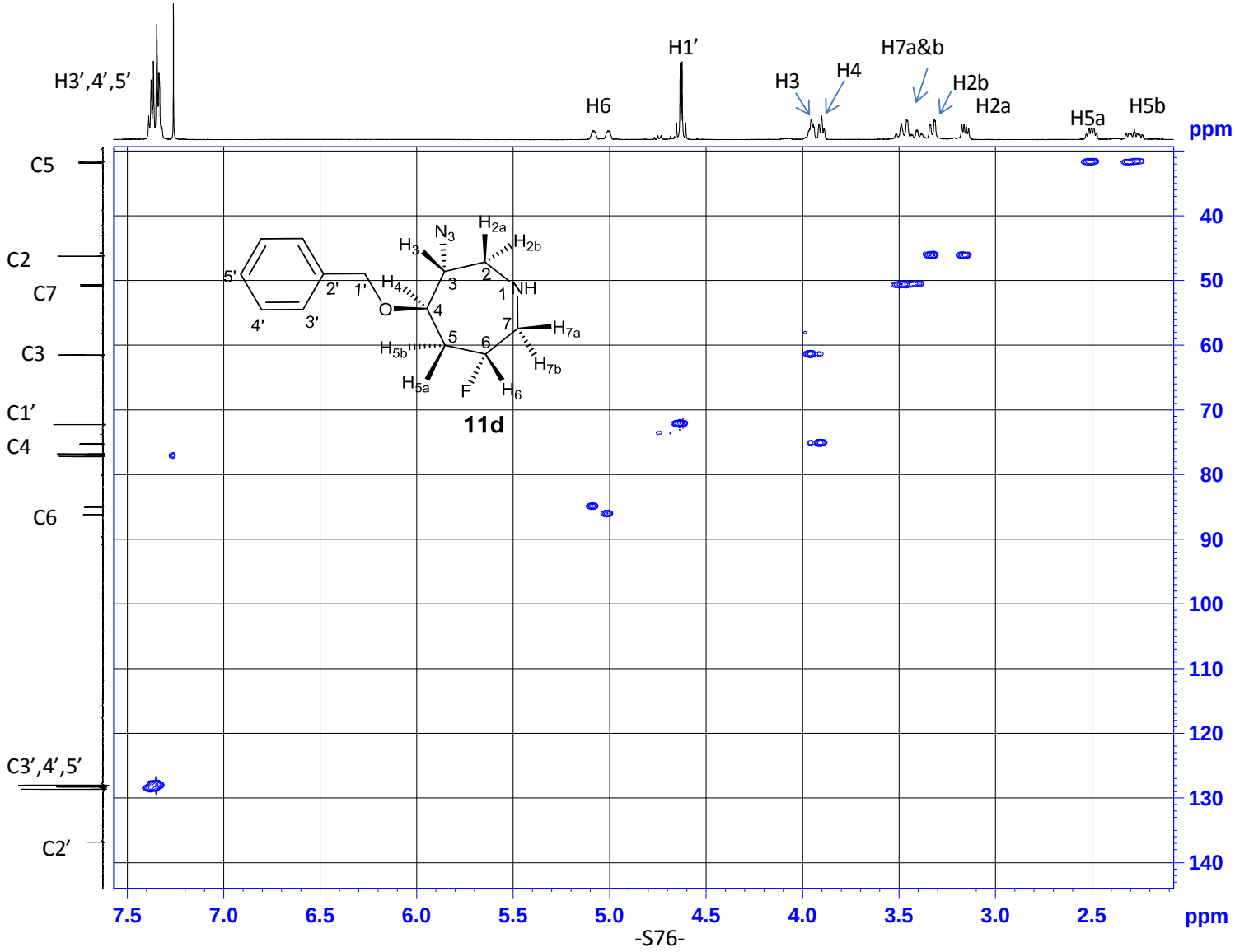
11d


7.37
7.36
7.35
7.34
7.33
7.26
5.09
5.08
5.01
5.00
5.00
4.65
4.63
4.62
4.61
3.95
3.90
3.49
3.46
3.46
3.41
3.40
3.34
3.34
3.32
3.31
3.18
3.16
3.15
3.14
2.50
2.28
7.5
7.0
6.5
6.0
5.5
5.0
4.5
4.0
3.5
3.0
2.5
2.0
ppm
5.47
1.00
2.07
2.09
2.15
1.13
1.08
1.00
1.02

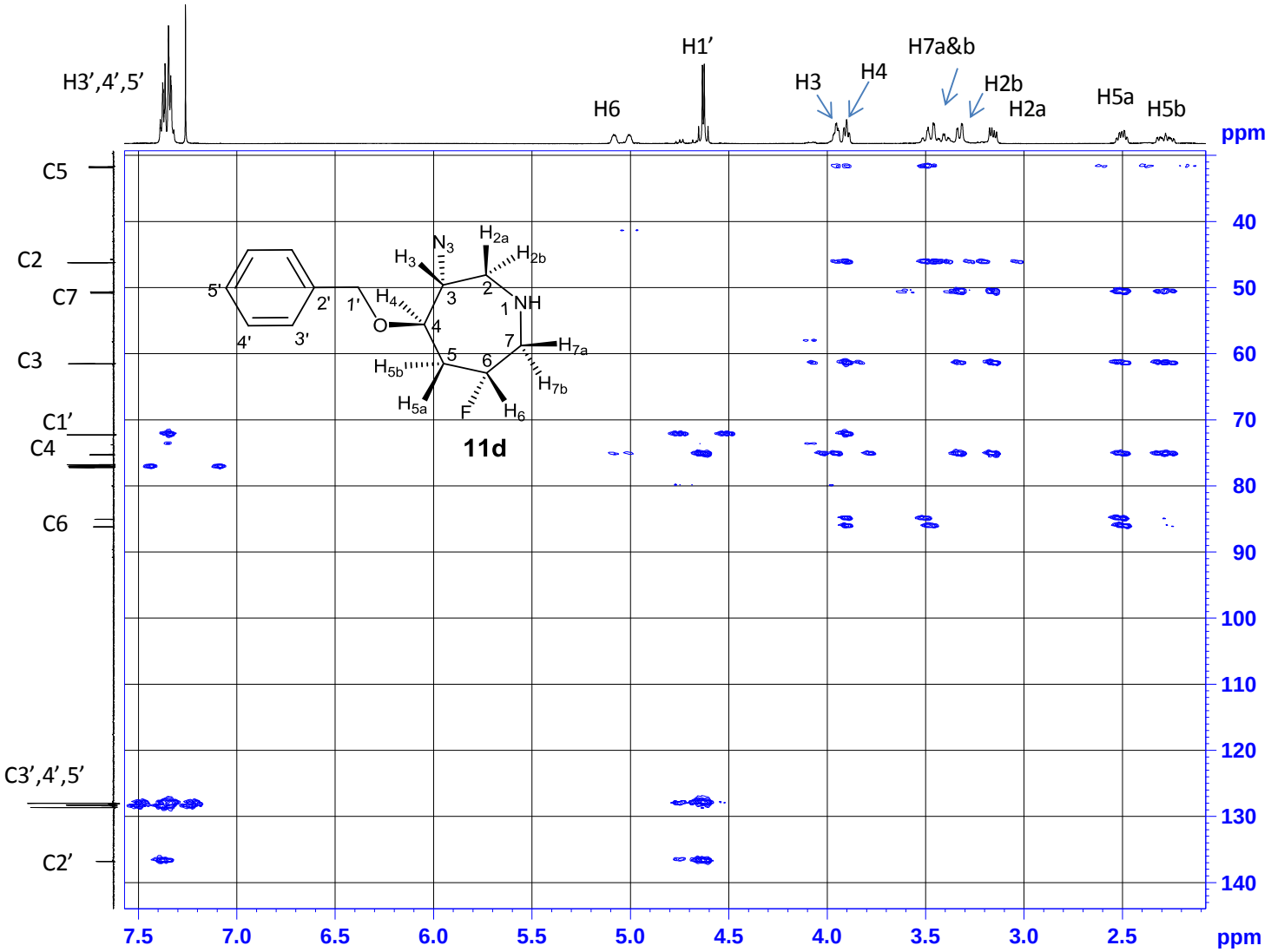
^{13}C-11d


N3
H2a
H3
H2b
5'
2'
1'
H4
3
2
1
NH
4'
3'
O
4
7
H7a
5
6
H5b
H7b
H5a
F
H6
11d
136.97
128.81
128.45
128.17
86.33
85.20
77.37
77.16
76.95
75.44
75.38
72.45
72.43
72.40
61.66
50.97
50.80
46.39
32.00
31.86
190
180
170
160
150
140
130
120
110
100
90
80
70
60
50
40
30
20
ppm

HSQC-11d

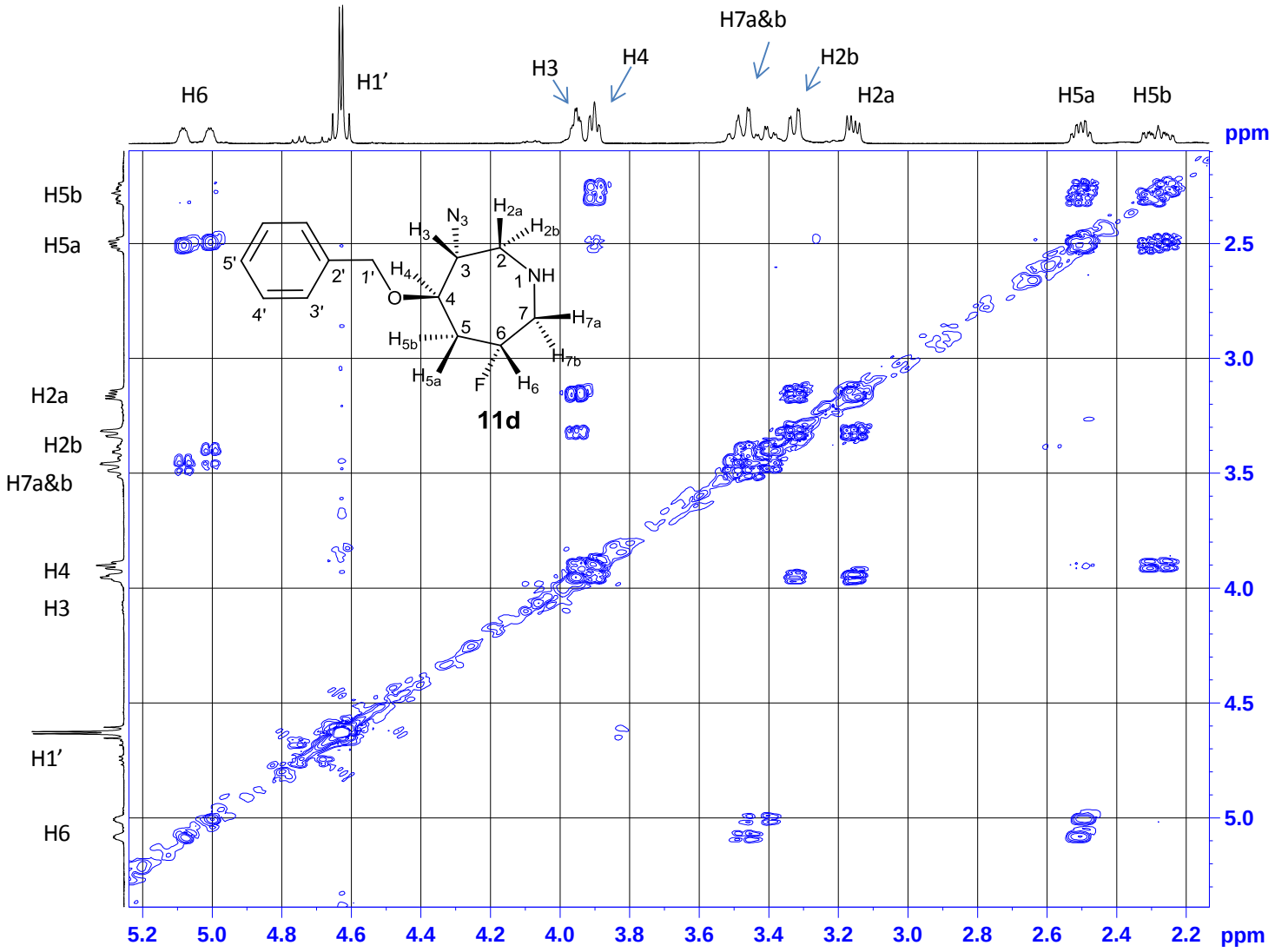

H3',4',5'
H6
H1'
H3
H4
H7a&b
H2b
H2a
H5a
H5b
ppm
C5
C2
C7
C3
C1'
C4
C6
C3',4',5'
C2'
11d
7.5
7.0
6.5
6.0
5.5
5.0
4.5
4.0
3.5
3.0
2.5
ppm

HMBC-11d

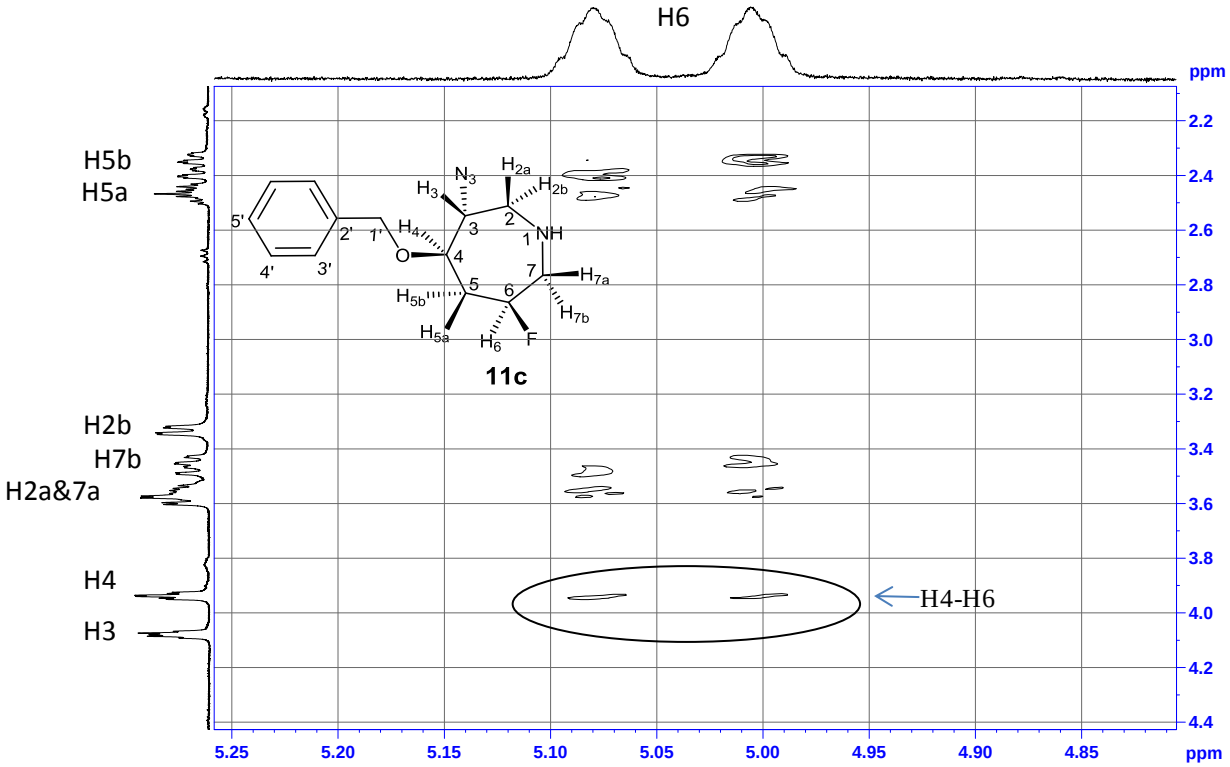

H3',4',5'
H6
H1'
H3
H4
H7a&b
H2b
H2a
H5a
H5b
ppm
C5
C2
C7
C3
C1'
C4
C6
C3',4',5'
C2'
11d
7.5
7.0
6.5
6.0
5.5
5.0
4.5
4.0
3.5
3.0
2.5
ppm

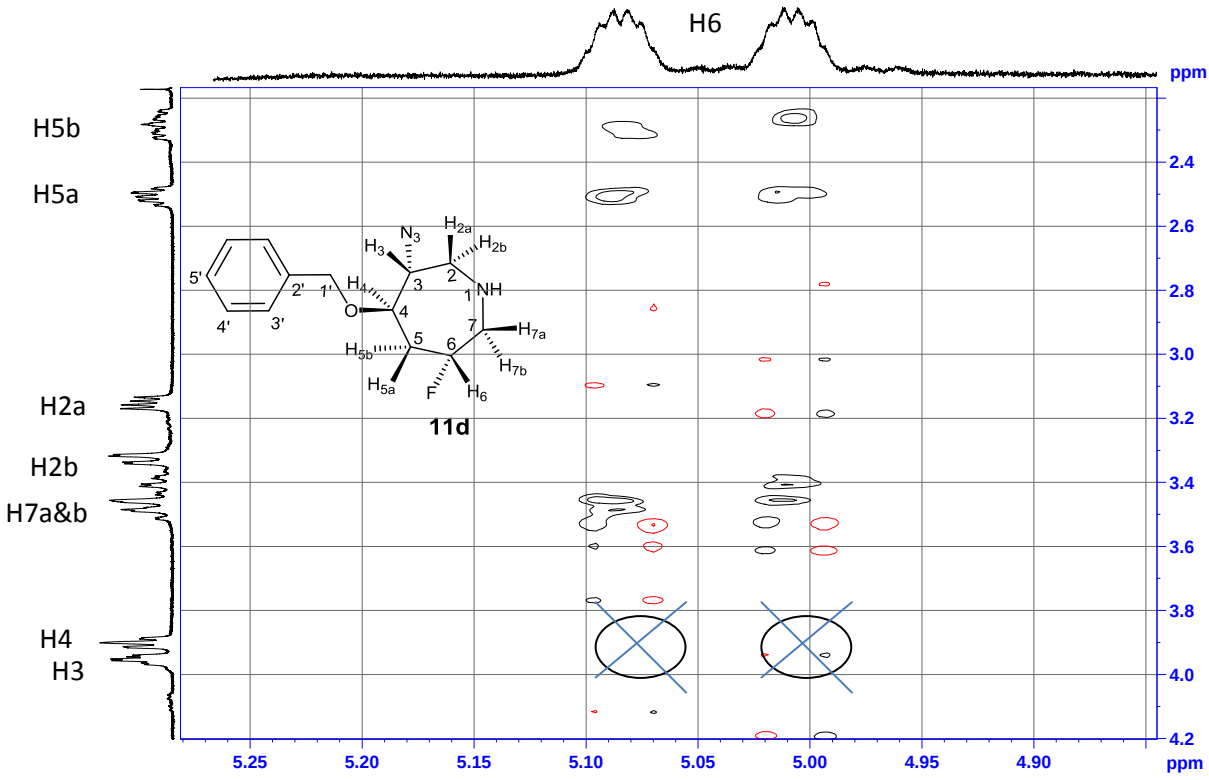
-S77-

COSY-11d

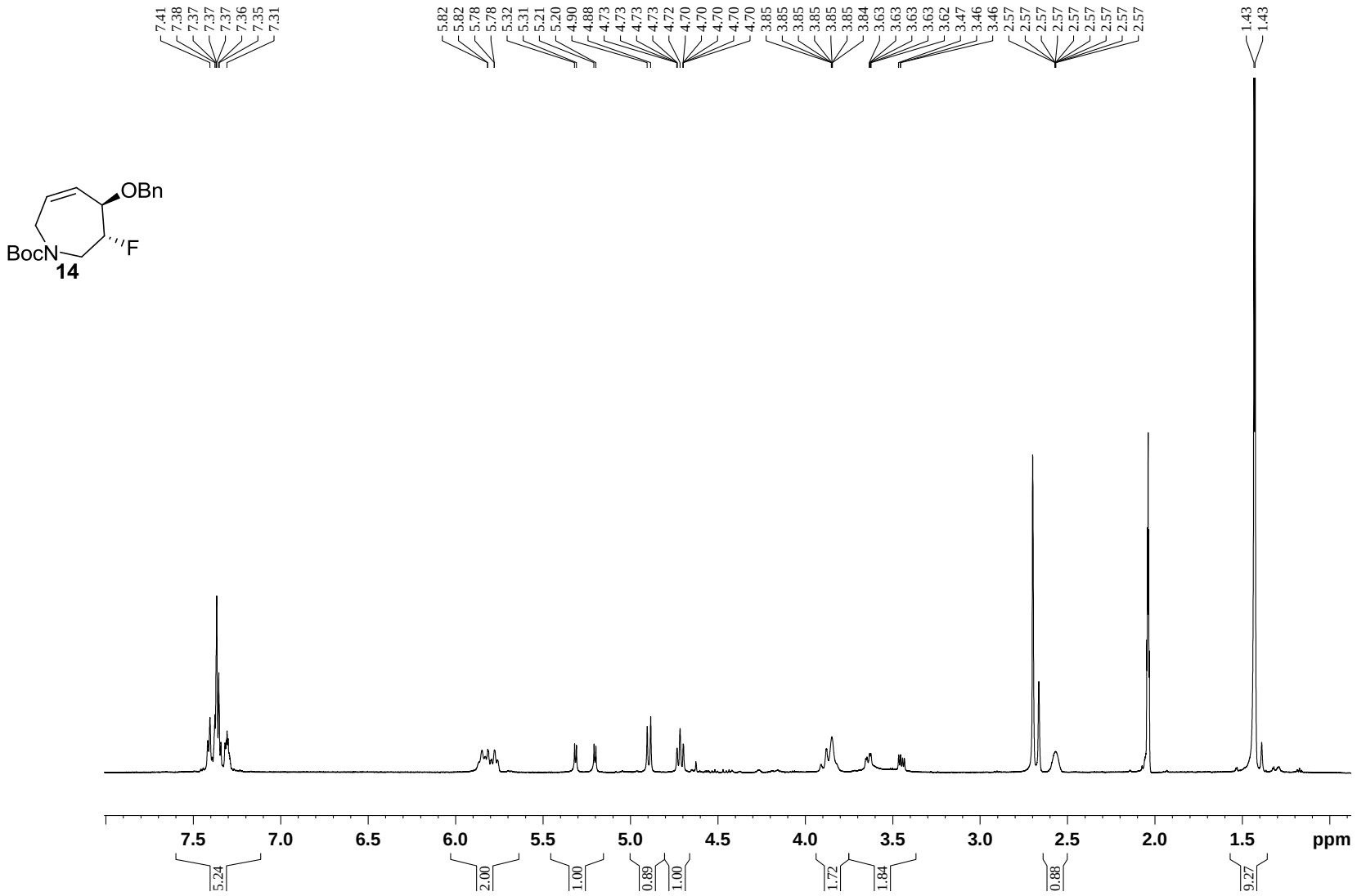

H7a&b
H4
H2b
H3
H1'
H6
H2a
H5a
H5b
ppm
H5b
H5a
H2a
H2b
H7a&b
H4
H3
H1'
H6
11d
5.2
5.0
4.8
4.6
4.4
4.2
4.0
3.8
3.6
3.4
3.2
3.0
2.8
2.6
2.4
2.2
ppm
2.5
3.0
3.5
4.0
4.5
5.0

NOESY Comparison 11c and **11d**

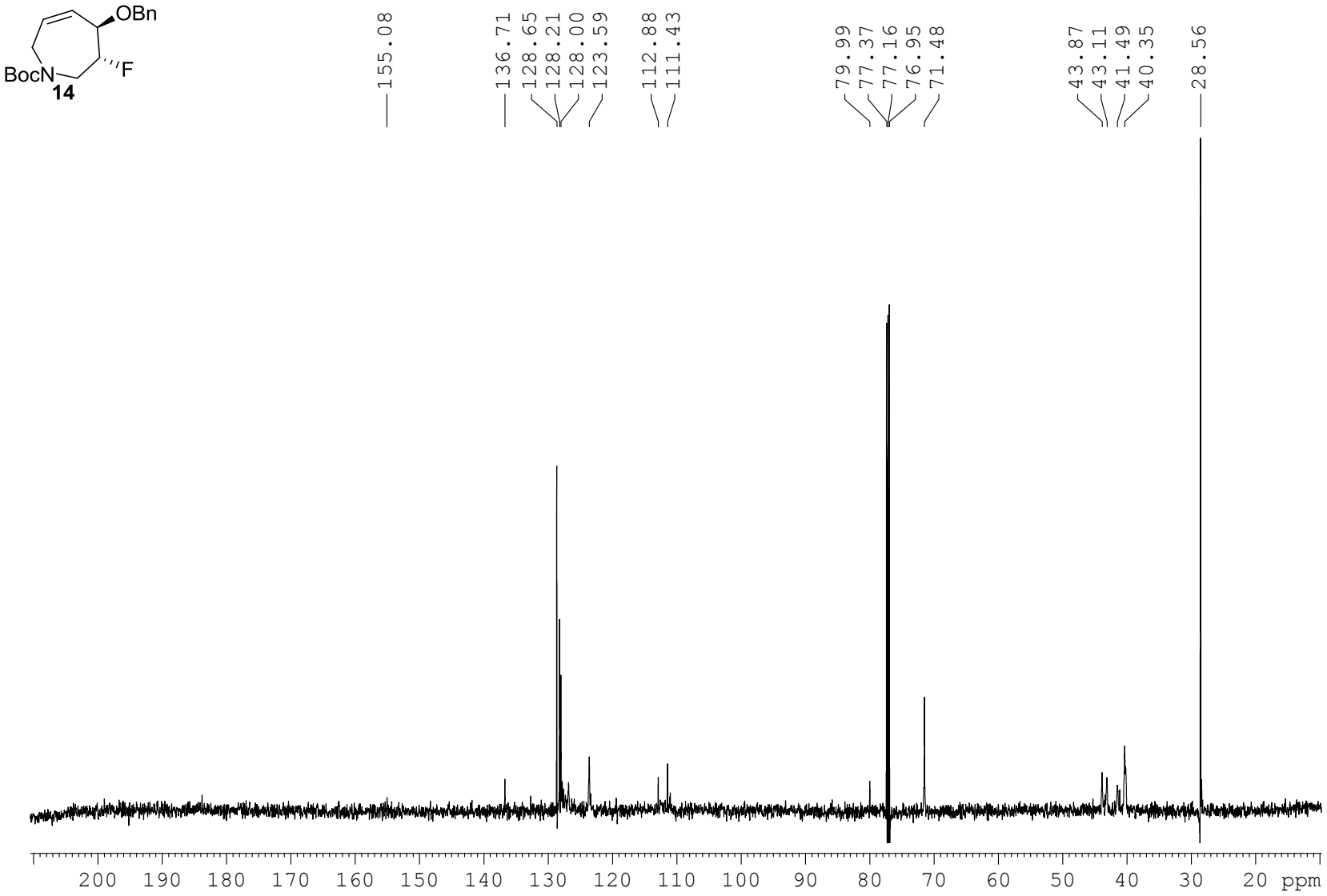




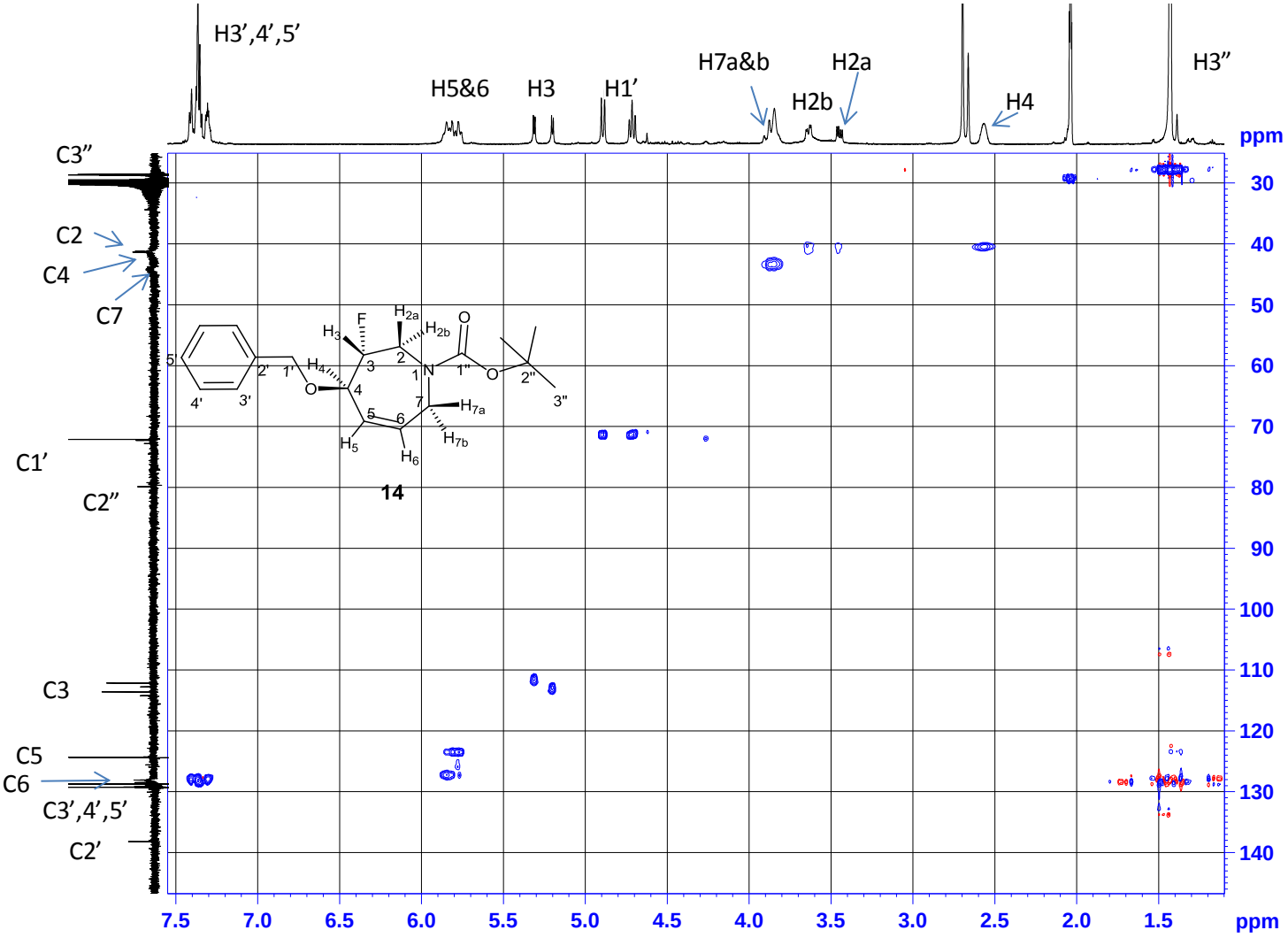
^{1}H-14


7.41 7.38 7.37 7.37 7.37 7.36 7.35 7.31
5.82 5.82 5.78 5.78 5.32 5.31 5.21 5.20 4.90 4.88 4.73 4.73 4.73 4.73 4.72 4.70 4.70 4.70 4.70
3.85 3.85 3.85 3.85 3.85 3.84 3.63 3.63 3.63 3.62 3.47 3.46 3.46
2.57 2.57 2.57 2.57 2.57 2.57 2.57 2.57
1.43 1.43
OBn
BocN
F
14
7.5 7.0 6.5 6.0 5.5 5.0 4.5 4.0 3.5 3.0 2.5 2.0 1.5 ppm
5.24 2.00 1.00 0.89 1.00 1.72 1.84 0.88 9.27

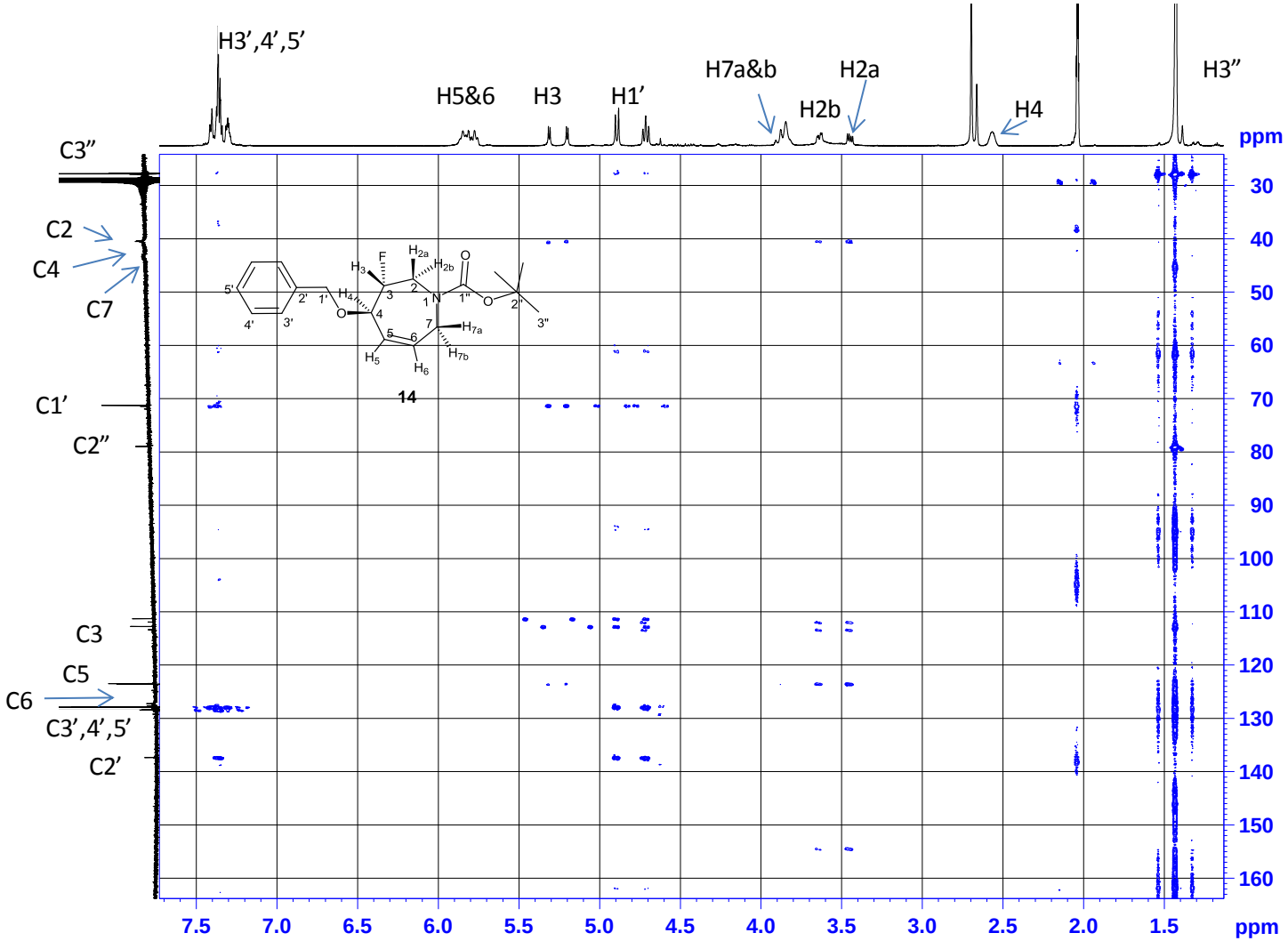
^{13}C-14


OBn
BocN
F
14
155.08
136.71
128.65
128.21
128.00
123.59
112.88
111.43
79.99
77.37
77.16
76.95
71.48
43.87
43.11
41.49
40.35
28.56
200 190 180 170 160 150 140 130 120 110 100 90 80 70 60 50 40 30 20 ppm

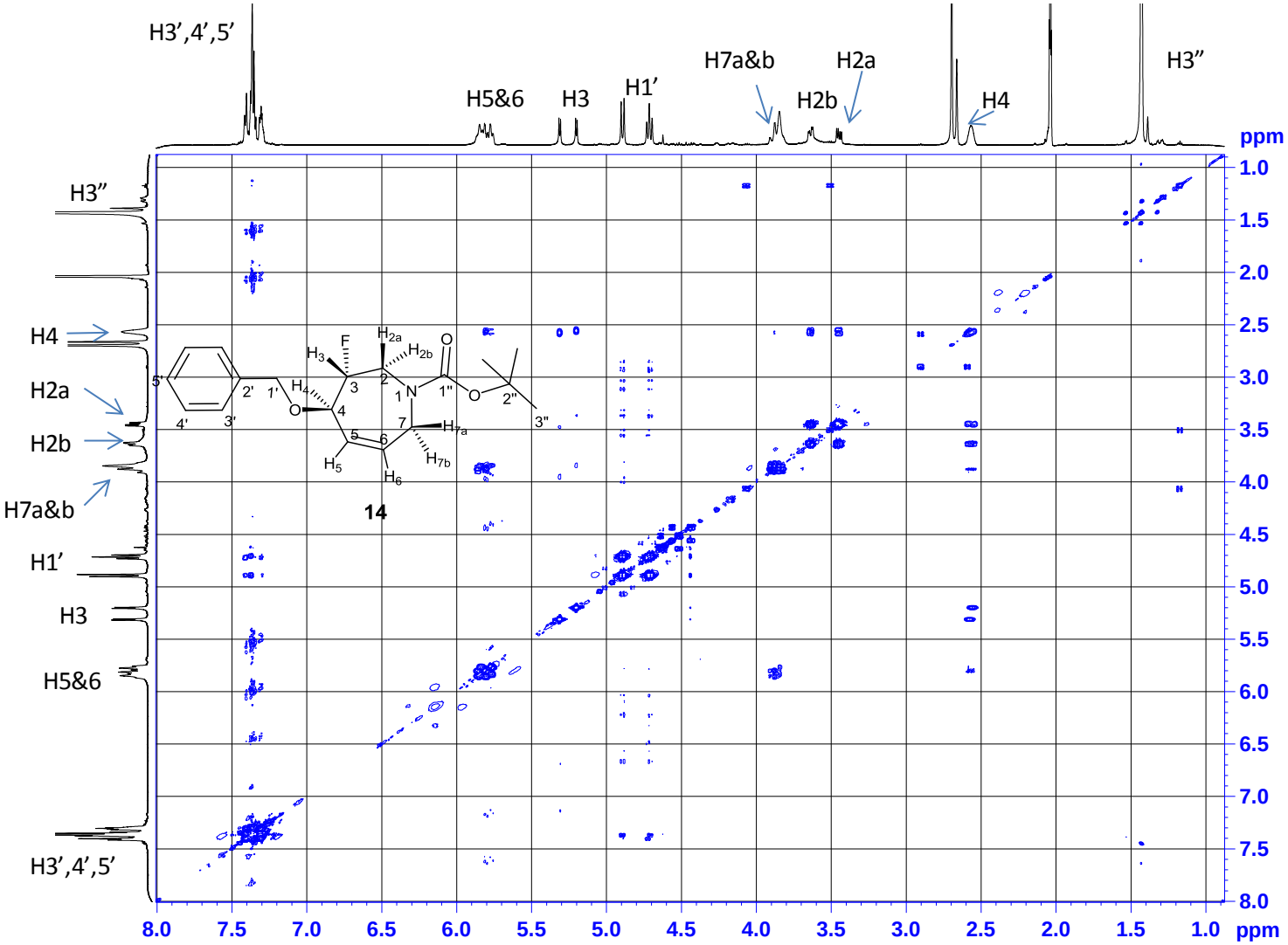
HSQC-14


H3',4',5'
H5&6
H3
H1'
H7a&b
H2b
H2a
H4
H3"
ppm
C3"
C2
C4
C7
C1'
C2"
C3
C5
C6
C3',4',5'
C2'
14
7.5
7.0
6.5
6.0
5.5
5.0
4.5
4.0
3.5
3.0
2.5
2.0
1.5
ppm

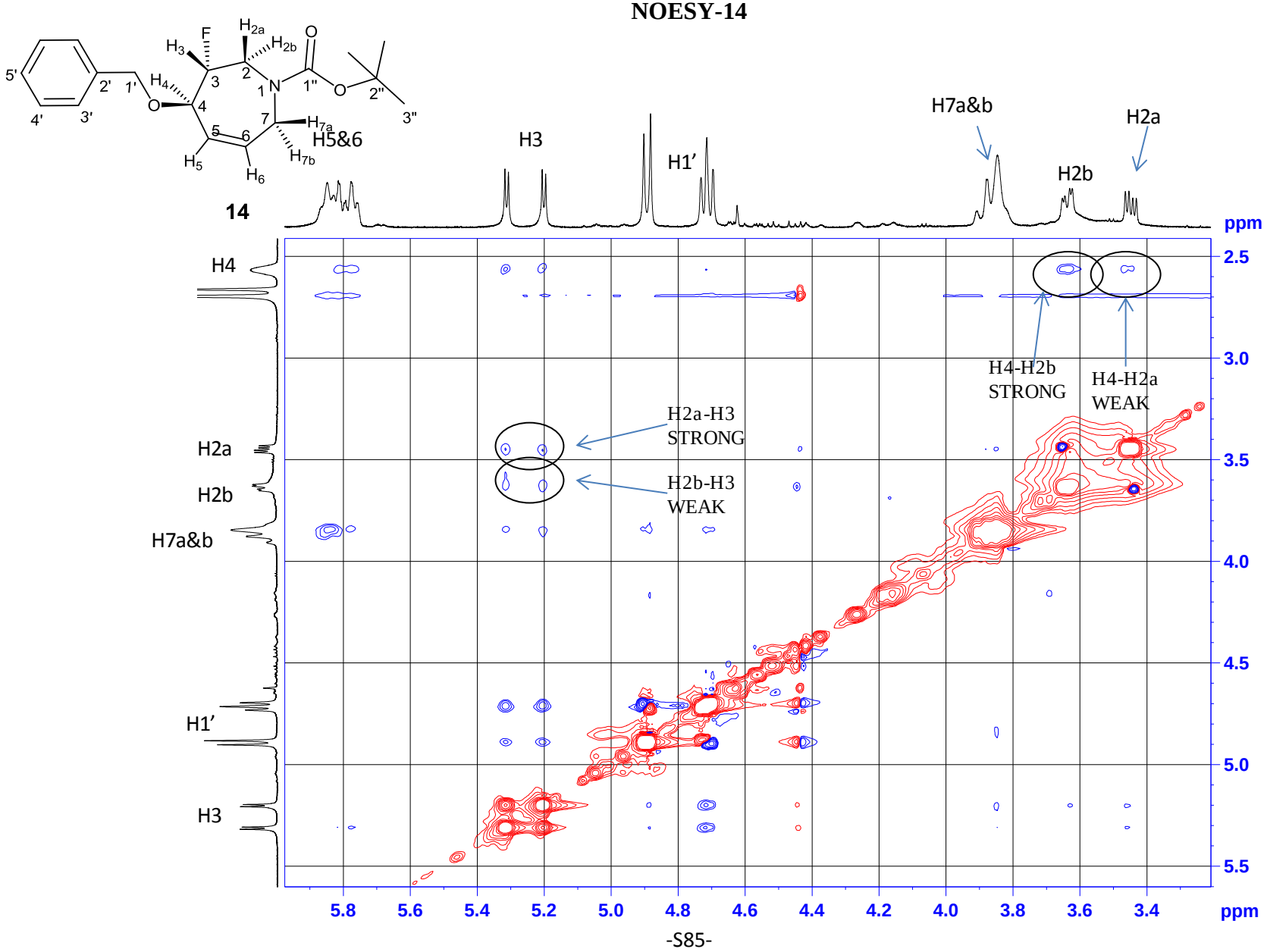
HMBC-14


H3',4',5'
H5&6
H3
H1'
H7a&b
H2a
H2b
H4
H3"
ppm
C3"
C2
C4
C7
C1'
C2"
C3
C5
C6
C3',4',5'
C2'
14
7.5
7.0
6.5
6.0
5.5
5.0
4.5
4.0
3.5
3.0
2.5
2.0
1.5
ppm

COSY-14


H3',4',5'
H5&6
H3
H1'
H7a&b
H2a
H2b
H4
H3"
ppm
H3"
H4
H2a
H2b
H7a&b
H1'
H3
H5&6
H3',4',5'
14
8.0
7.5
7.0
6.5
6.0
5.5
5.0
4.5
4.0
3.5
3.0
2.5
2.0
1.5
1.0
ppm

NOESY-14


14
H5&6
H3
H1'
H7a&b
H2b
H2a
ppm
H4
H2a
H2b
H7a&b
H1'
H3
H2a-H3
STRONG
H2b-H3
WEAK
H4-H2b
STRONG
H4-H2a
WEAK
2.5
3.0
3.5
4.0
4.5
5.0
5.5
5.8
5.6
5.4
5.2
5.0
4.8
4.6
4.4
4.2
4.0
3.8
3.6
3.4
ppm

-S85-

Appendix B

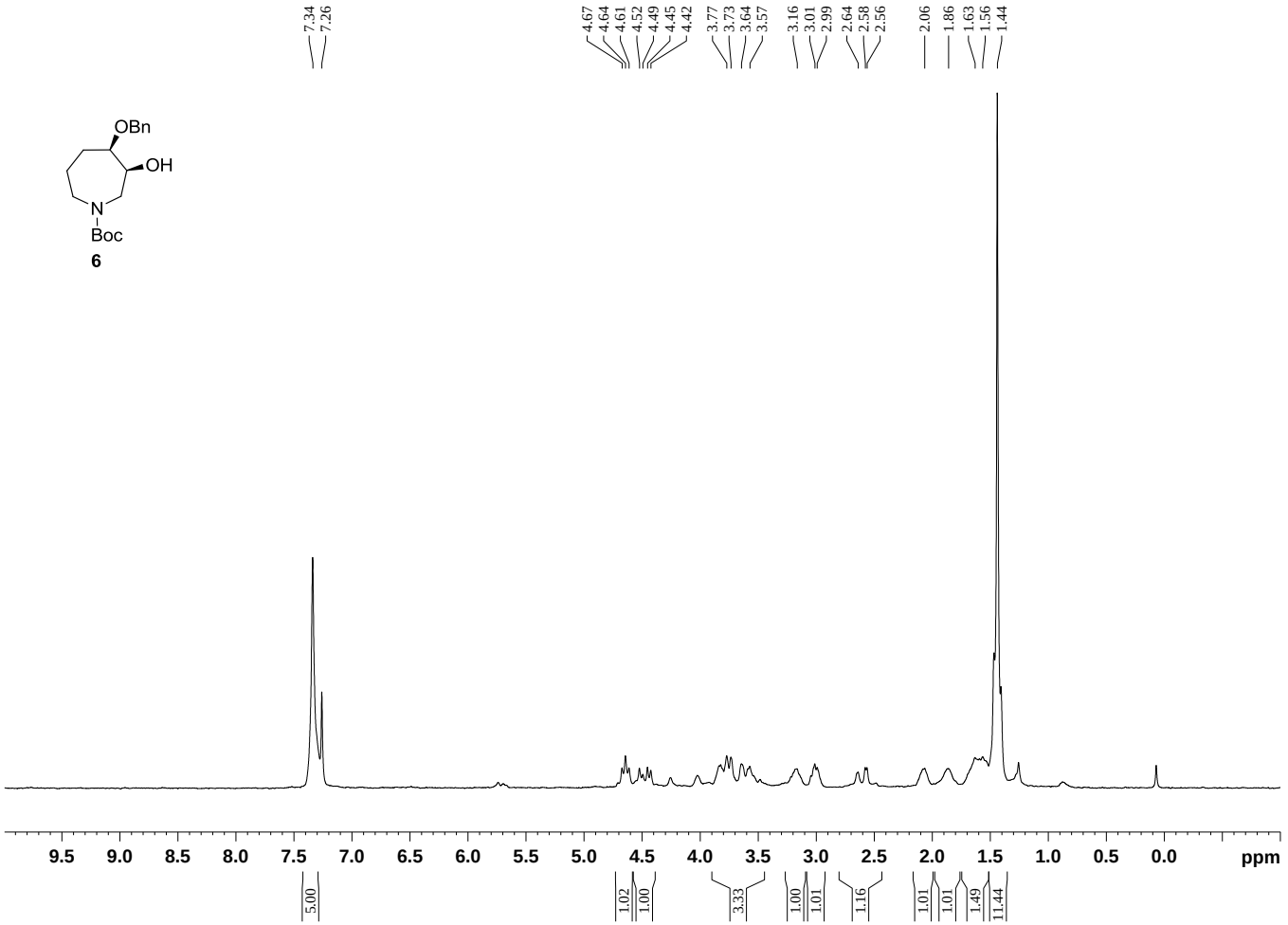
Table of contents:

Full NMR spectra of compounds discussed in chapter 3……..…..……347

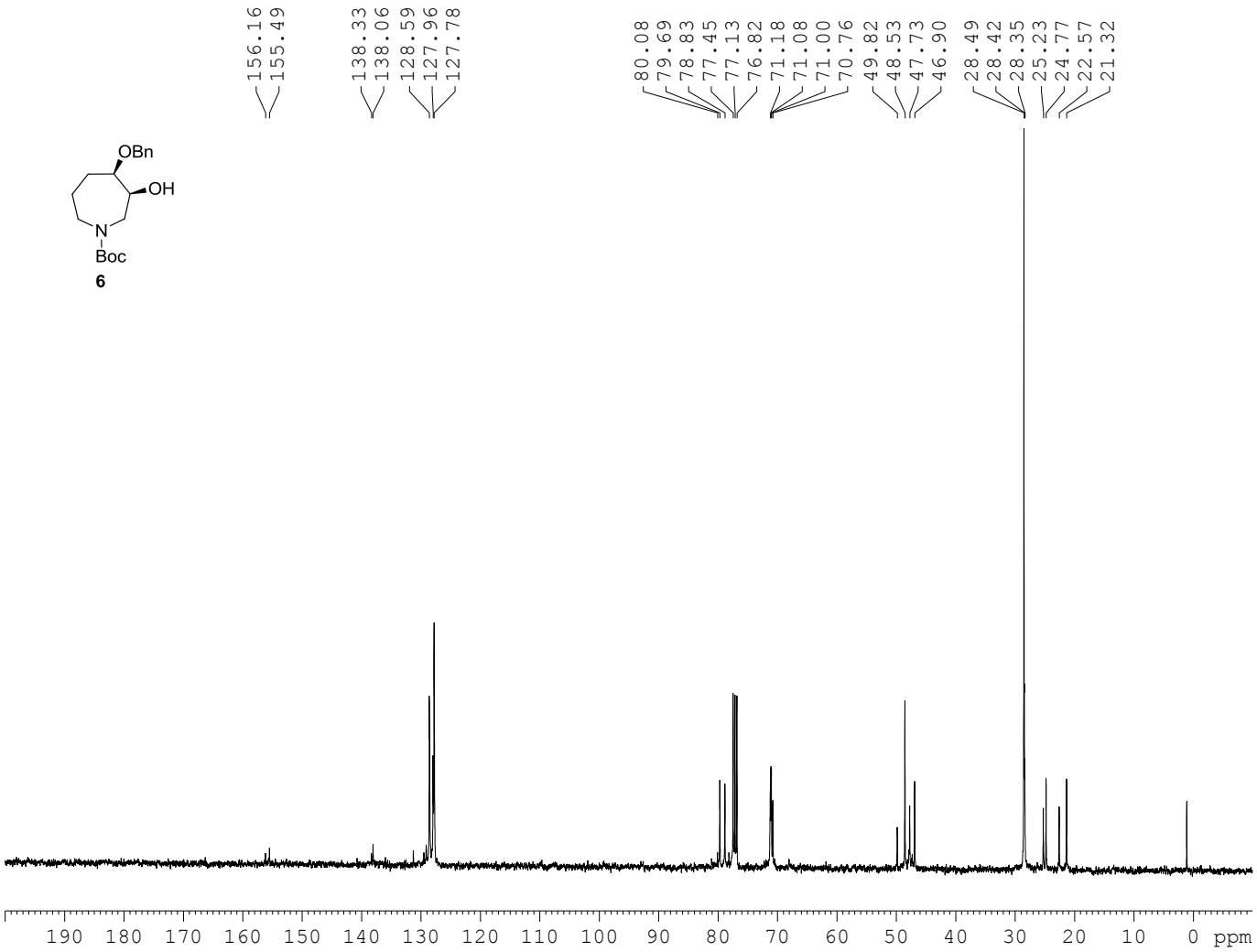
Simulated NMR spectra of compounds **3.1**, **2.11c**–**d**.....366

Conformational analysis details for compounds **3.1**, **2.11c**–**d**……369

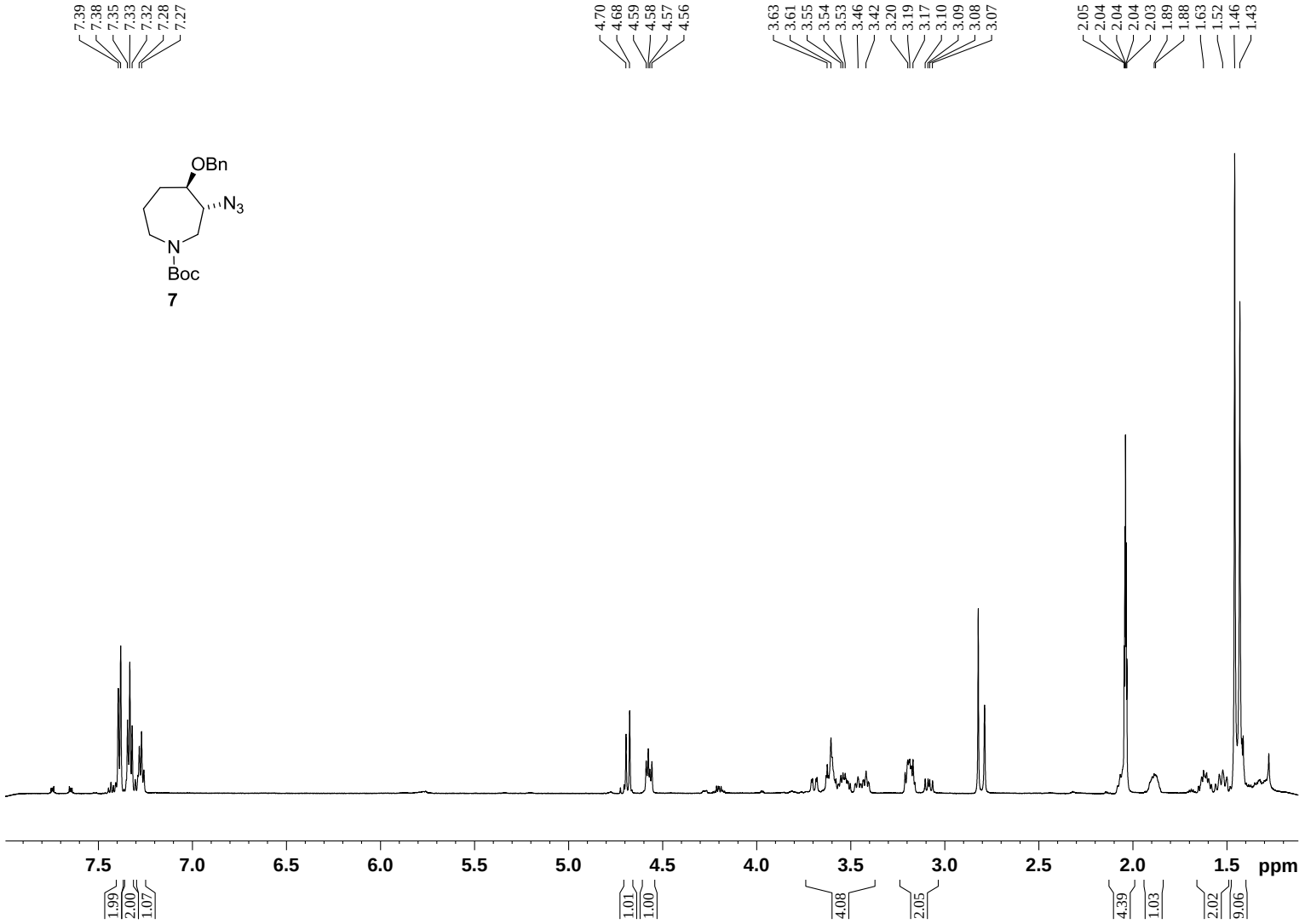
^{1}H NMR-**6**


7.34
7.26
4.67
4.64
4.61
4.52
4.49
4.45
4.42
3.77
3.73
3.64
3.57
3.16
3.01
2.99
2.64
2.58
2.56
2.06
1.86
1.63
1.56
1.44
OBn
OH
N
Boc
6
9.5
9.0
8.5
8.0
7.5
7.0
6.5
6.0
5.5
5.0
4.5
4.0
3.5
3.0
2.5
2.0
1.5
1.0
0.5
0.0
ppm
5.00
1.02
1.00
3.33
1.00
1.01
1.16
1.01
1.01
1.49
11.44

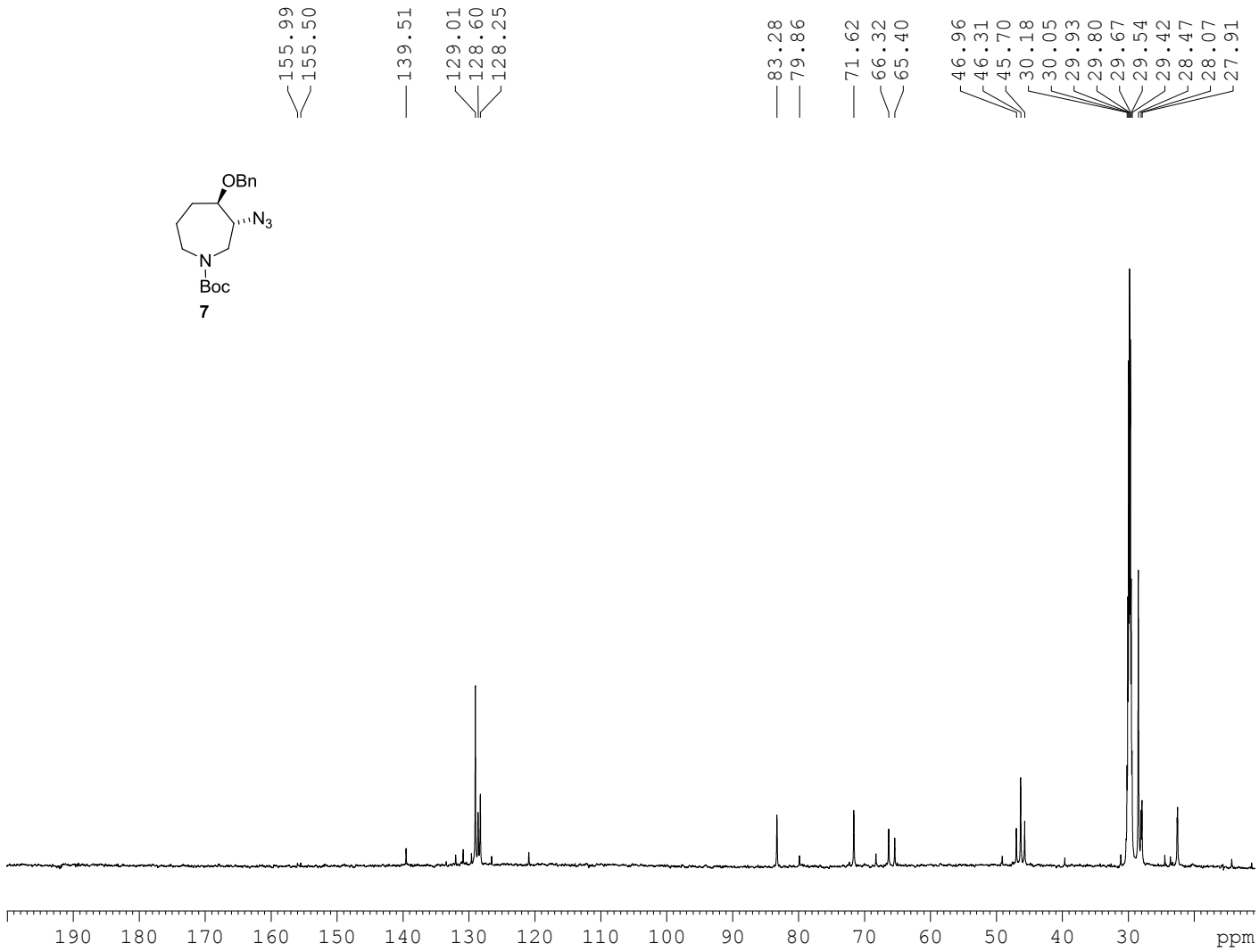
^{13}C NMR-**6**


156.16
155.49
138.33
138.06
128.59
127.96
127.78
80.08
79.69
78.83
77.45
77.13
76.82
71.18
71.08
71.00
70.76
49.82
48.53
47.73
46.90
28.49
28.42
28.35
25.23
24.77
22.57
21.32
OBn
OH
N
Boc
6
190 180 170 160 150 140 130 120 110 100 90 80 70 60 50 40 30 20 10 0 ppm

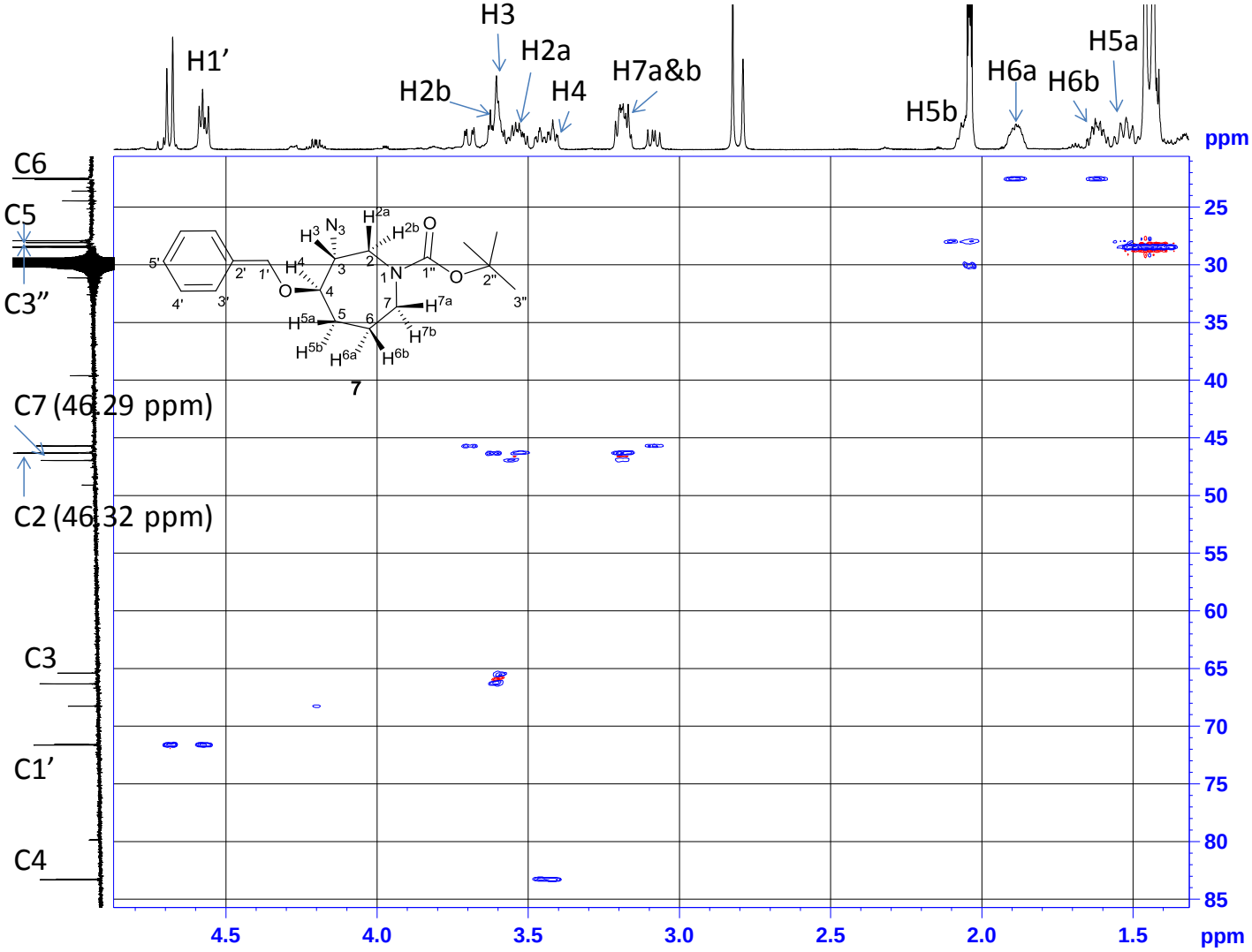
^{1}H NMR-**7**


7.39
7.38
7.35
7.33
7.32
7.28
7.27
4.70
4.68
4.59
4.58
4.57
4.56
3.63
3.61
3.55
3.54
3.53
3.46
3.42
3.20
3.19
3.17
3.10
3.09
3.08
3.07
2.05
2.04
2.04
2.04
2.03
1.89
1.88
1.63
1.52
1.46
1.43
OBn
N3
N
Boc
7
7.5
7.0
6.5
6.0
5.5
5.0
4.5
4.0
3.5
3.0
2.5
2.0
1.5
ppm
1.99
2.00
1.07
1.01
1.00
4.08
2.05
4.39
1.03
2.02
9.06

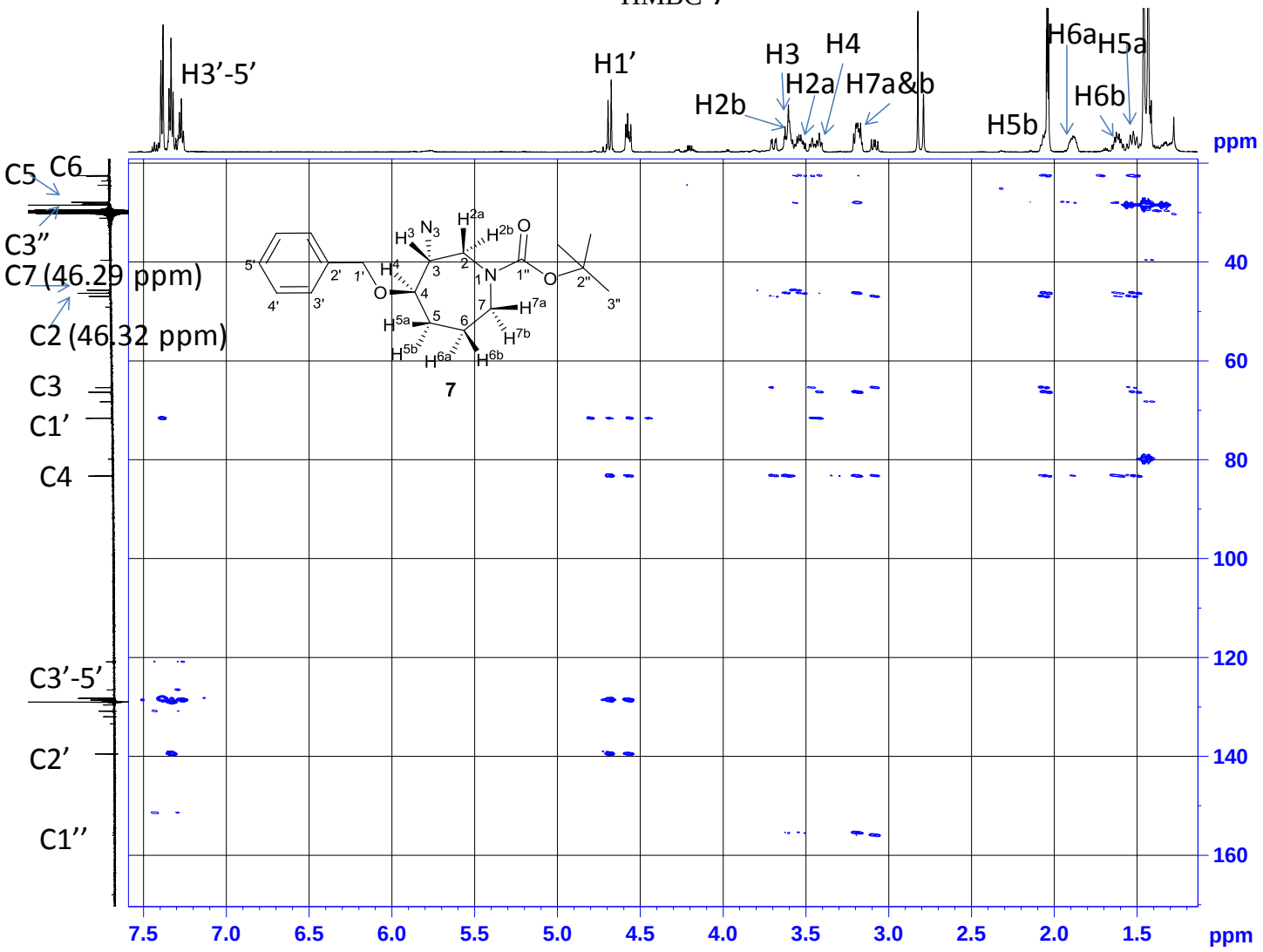
^{13}C NMR-**7**


155.99
155.50
139.51
129.01
128.60
128.25
83.28
79.86
71.62
66.32
65.40
46.96
46.31
45.70
30.18
30.05
29.93
29.80
29.67
29.54
29.42
28.47
28.07
27.91
OBn
N3
N
Boc
7
190 180 170 160 150 140 130 120 110 100 90 80 70 60 50 40 30 ppm

HSQC-7

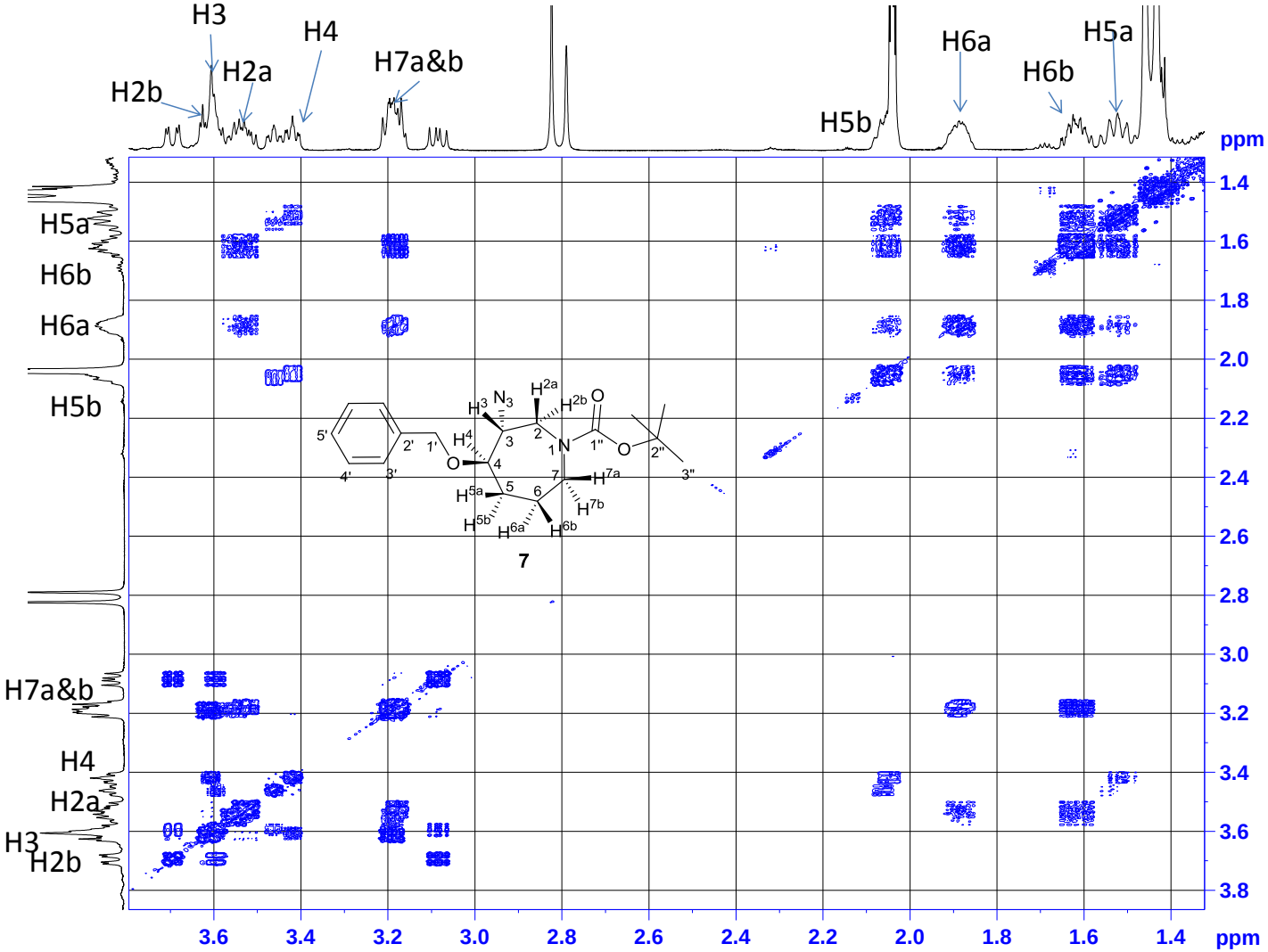

H1’
H3
H2a
H2b
H4
H7a&b
H5b
H6a
H6b
H5a
ppm
C6
C5
C3”
C7 (46.29 ppm)
C2 (46.32 ppm)
C3
C1’
C4
7
4.5
4.0
3.5
3.0
2.5
2.0
1.5
ppm

HMBC-7


H3’-5’
H1’
H2b
H3
H2a
H4
H7a&b
H5b
H6a
H6b
H5a
ppm
C5
C6
C3”
C7 (46.29 ppm)
C2 (46.32 ppm)
C3
C1’
C4
C3’-5’
C2’
C1’’
40
60
80
100
120
140
160
7.5
7.0
6.5
6.0
5.5
5.0
4.5
4.0
3.5
3.0
2.5
2.0
1.5
ppm

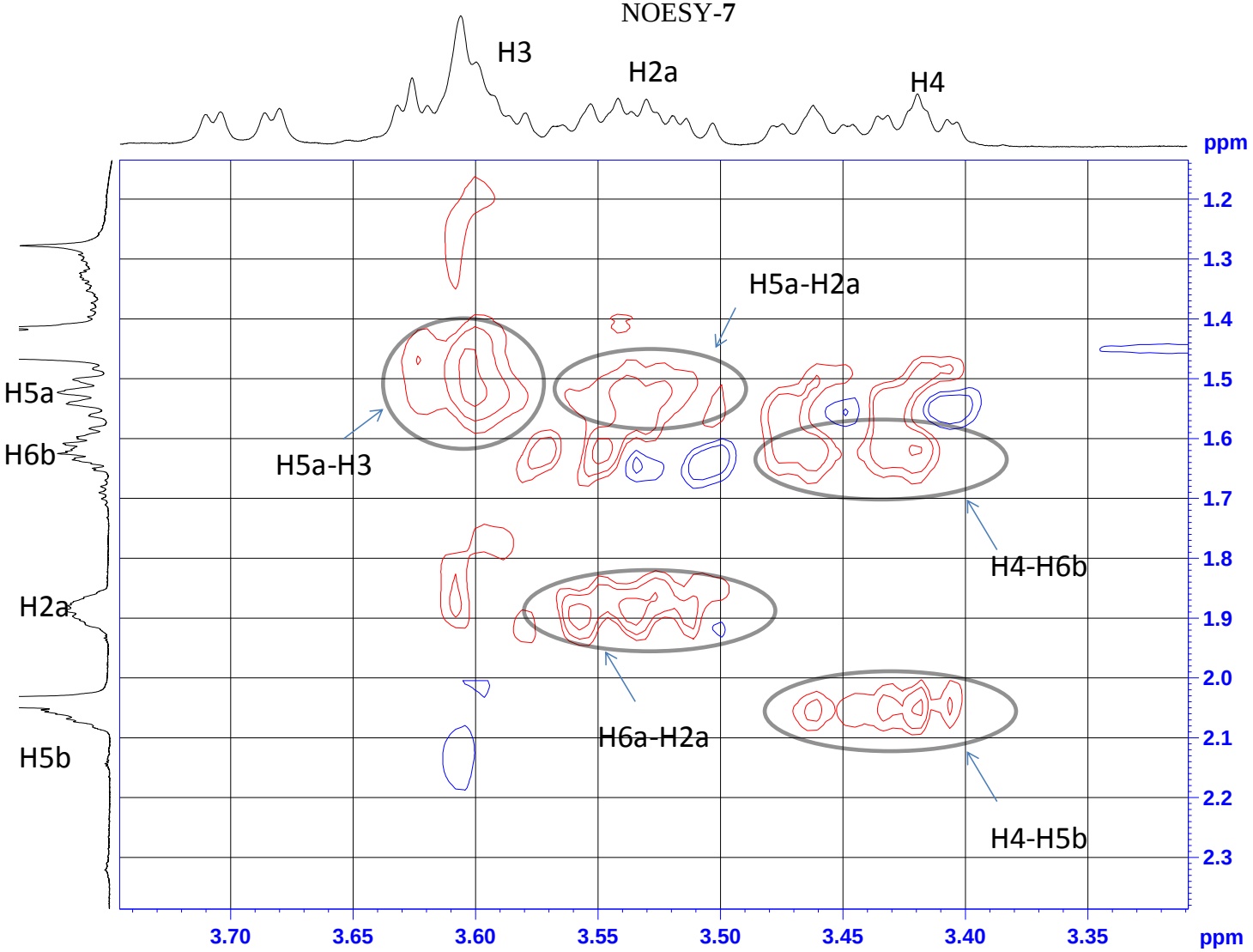
7

COSY-**7**

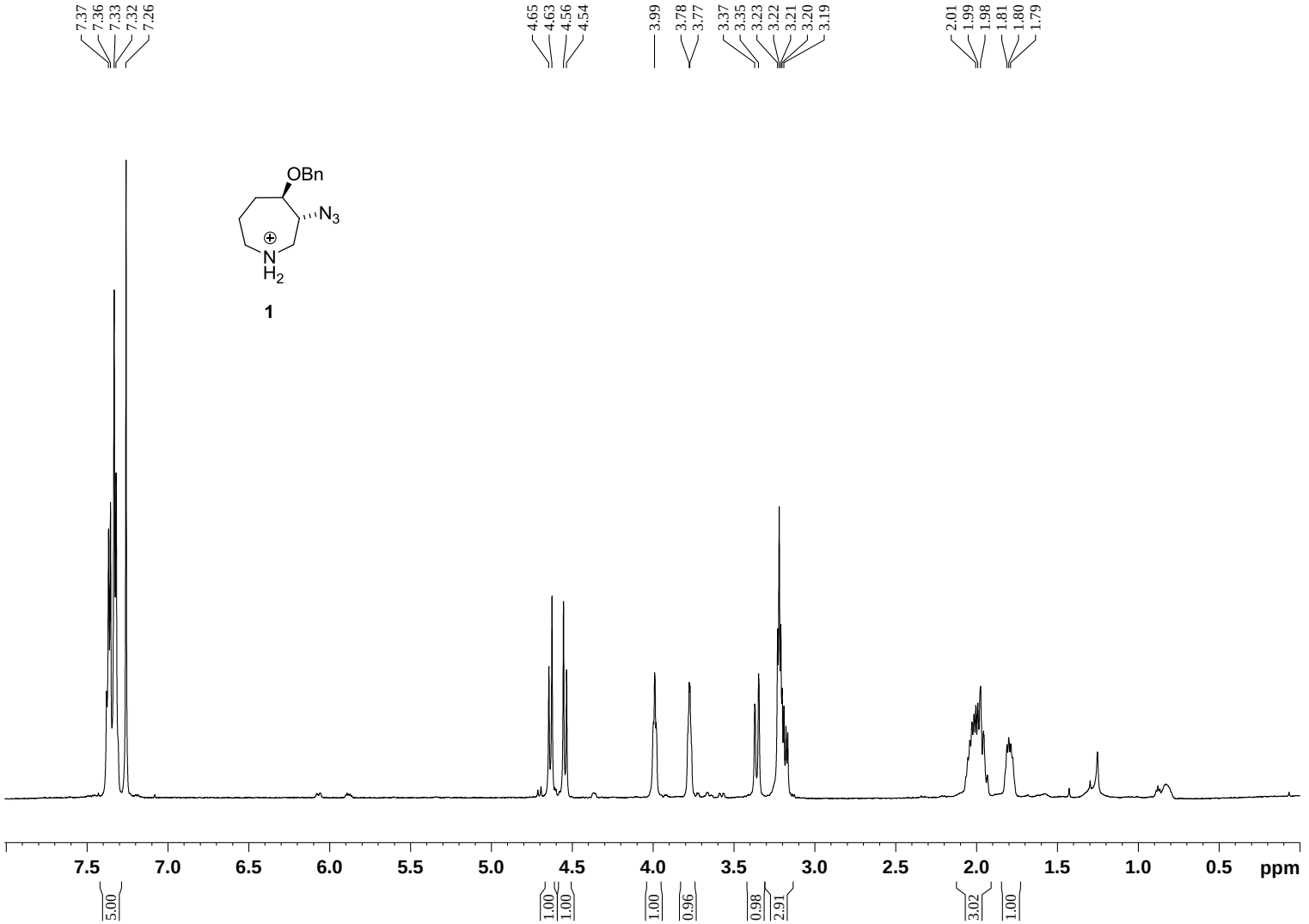

H3
H4
H7a&b
H2b
H2a
H5b
H6a
H6b
H5a
ppm
1.4
1.6
1.8
2.0
2.2
2.4
2.6
2.8
3.0
3.2
3.4
3.6
3.8
3.6
3.4
3.2
3.0
2.8
2.6
2.4
2.2
2.0
1.8
1.6
1.4
ppm

7

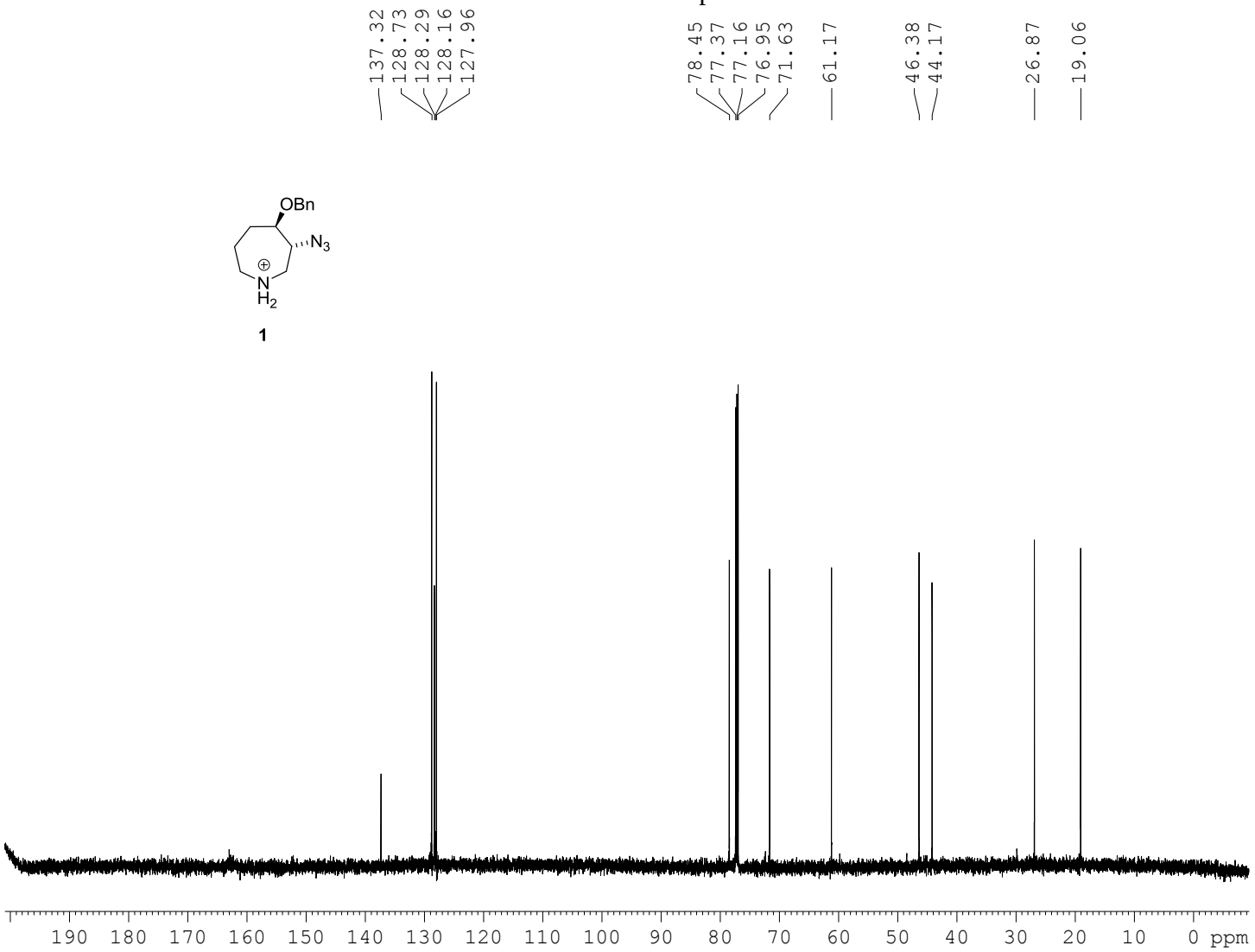
NOESY-7


H3
H2a
H4
ppm
1.2
1.3
1.4
1.5
1.6
1.7
1.8
1.9
2.0
2.1
2.2
2.3
H5a
H6b
H2a
H5b
H5a-H2a
H5a-H3
H4-H6b
H6a-H2a
H4-H5b
3.70
3.65
3.60
3.55
3.50
3.45
3.40
3.35
ppm

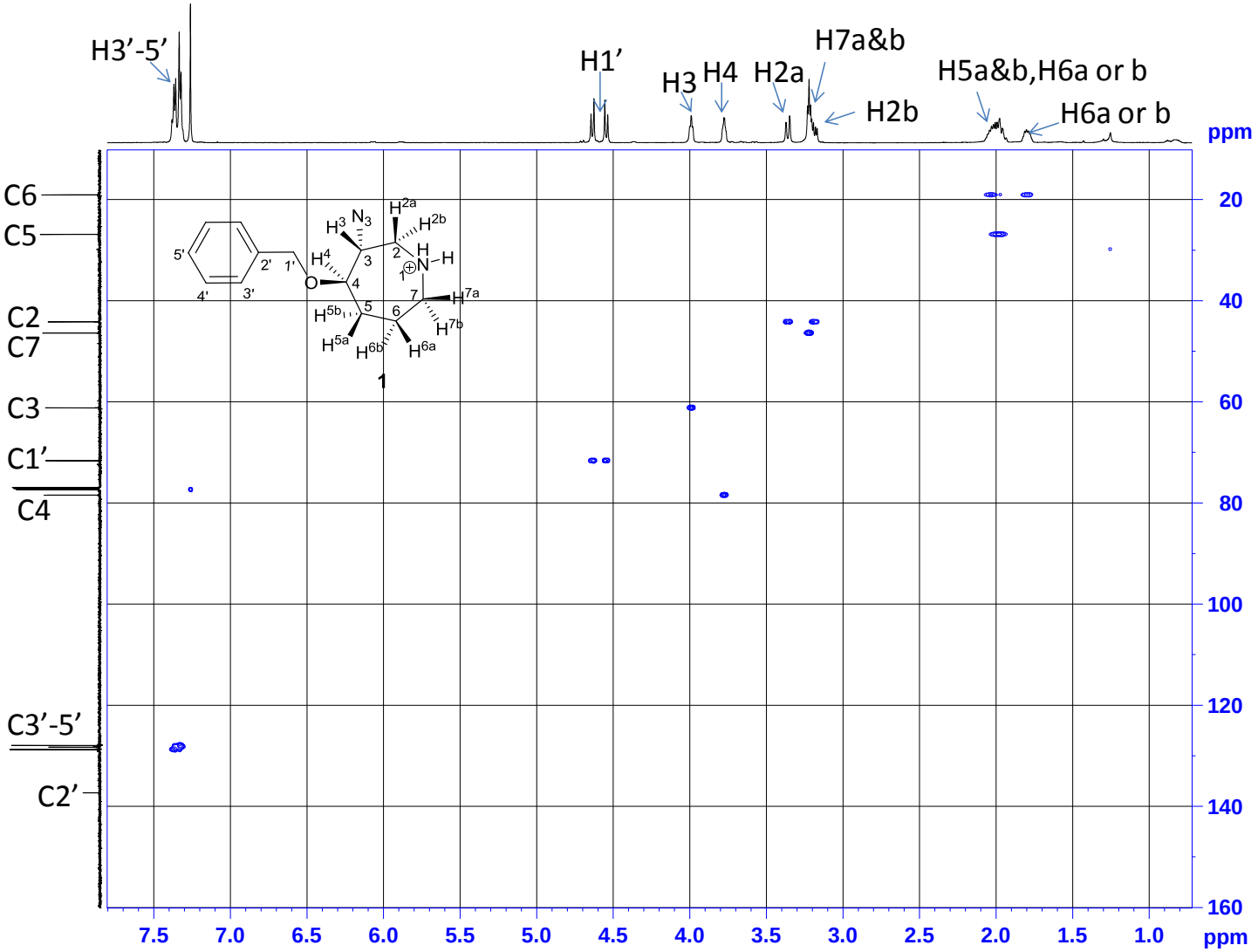
^{1}H NMR-azepane **1**



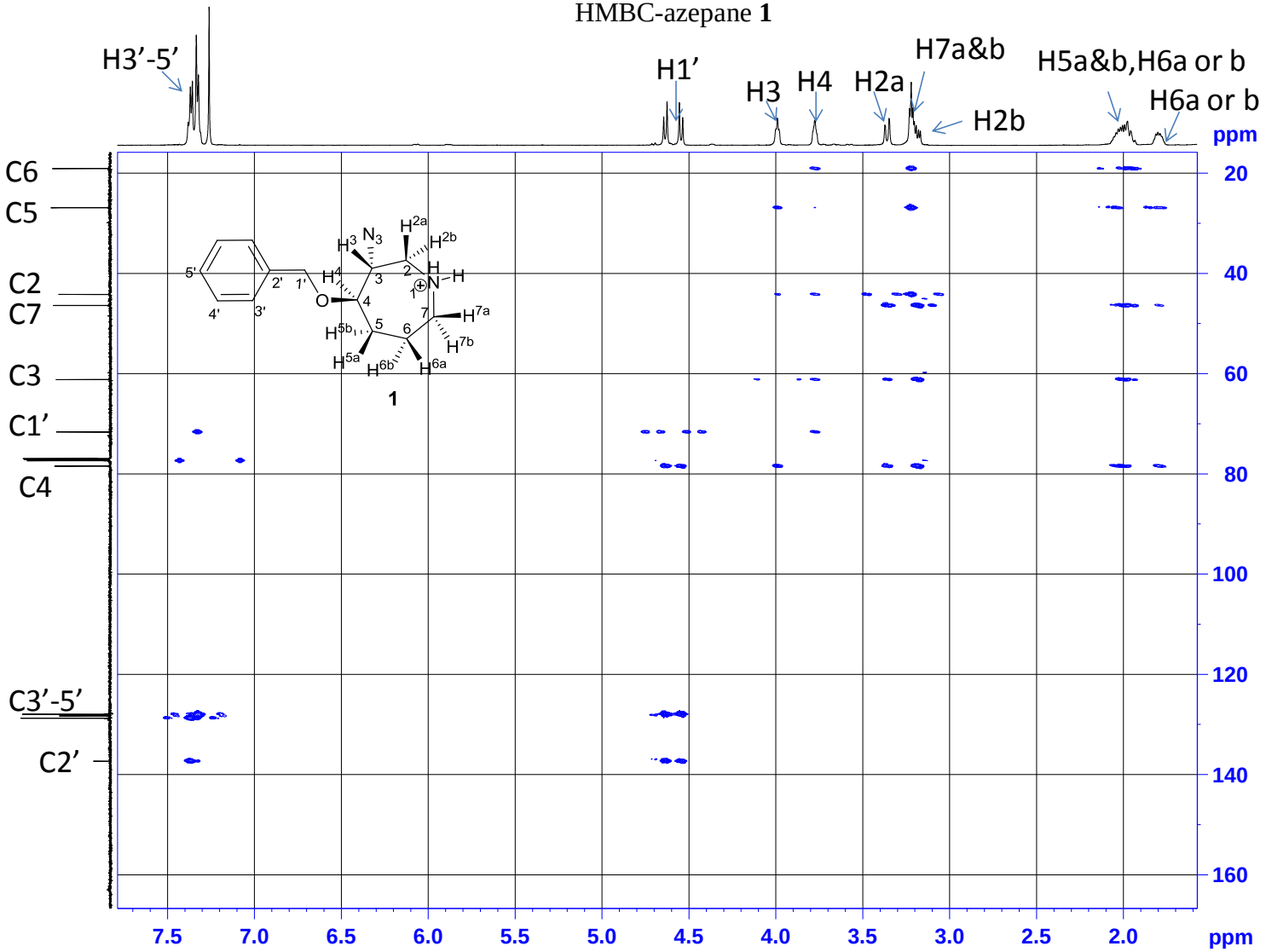
^{13}C NMR-azepane **1**



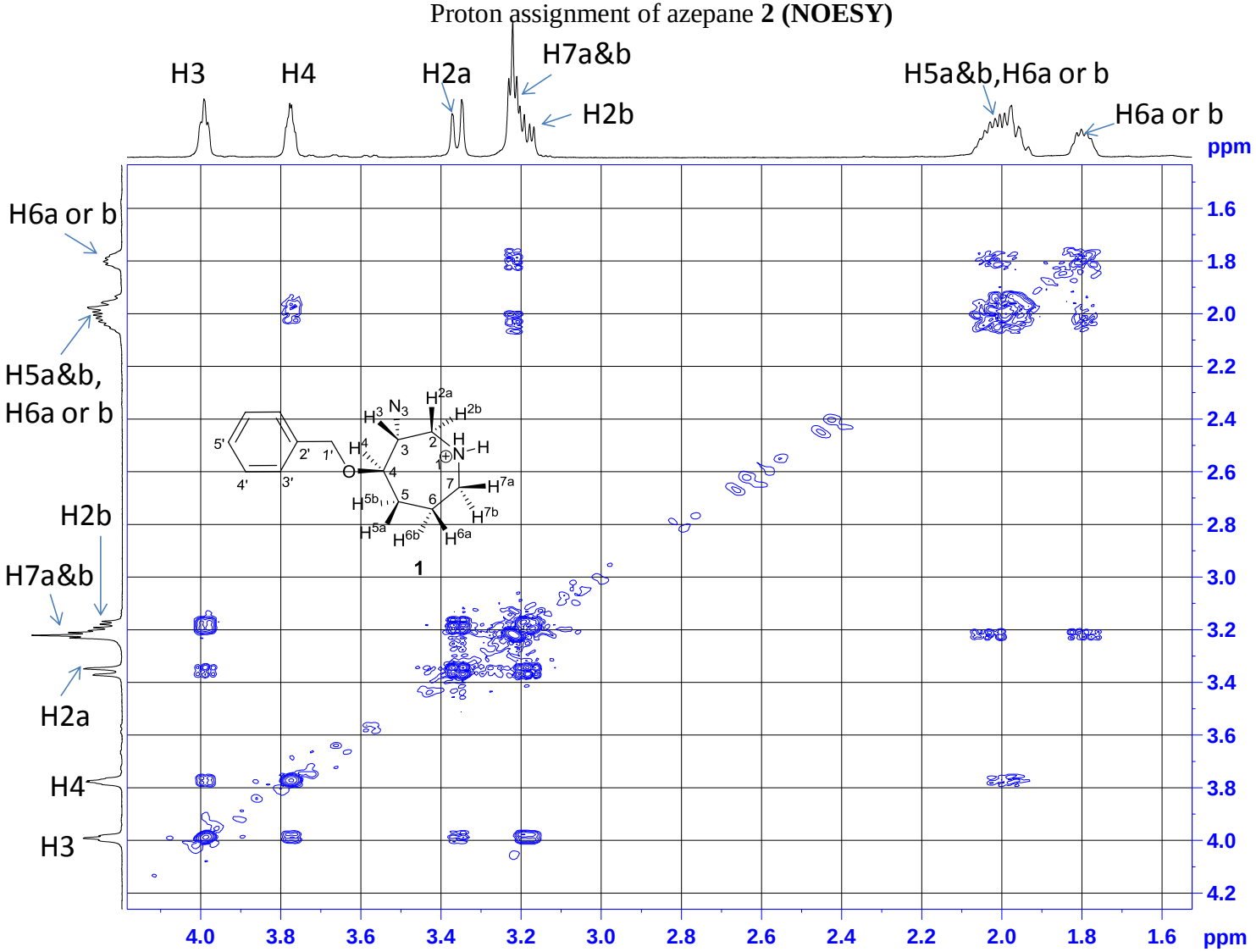
HSQC-azepane **1**



HMBC-azepane **1**

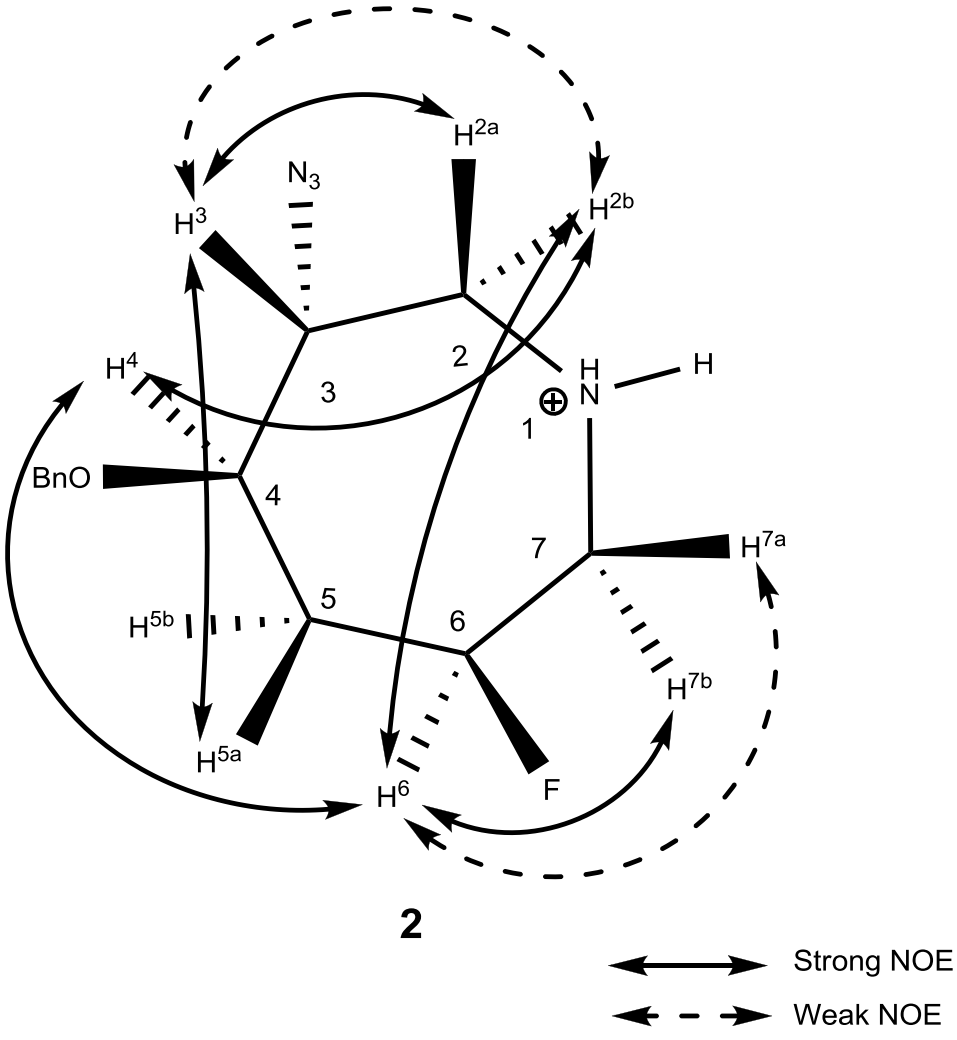


Proton assignment of azepane **2 (NOESY)**



1

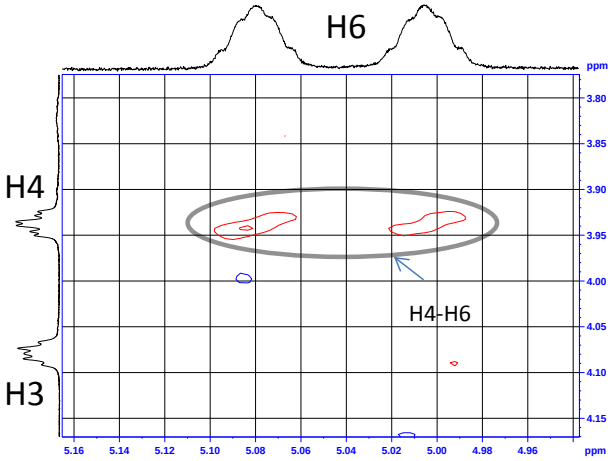
Proton assignment of azepane **2 (NOESY)**

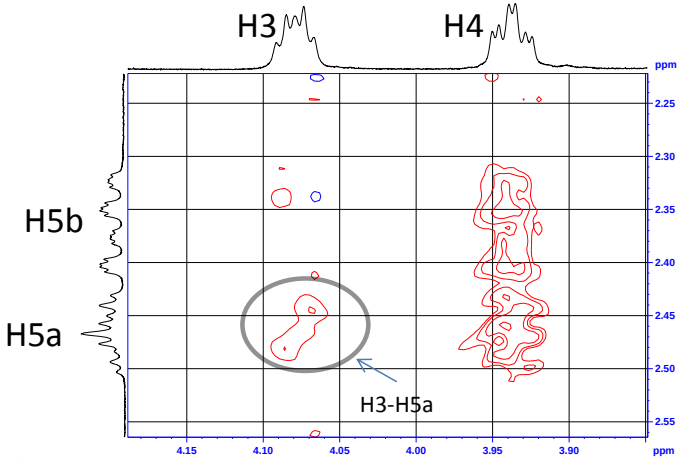


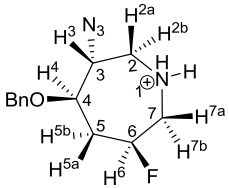
2

NOEs

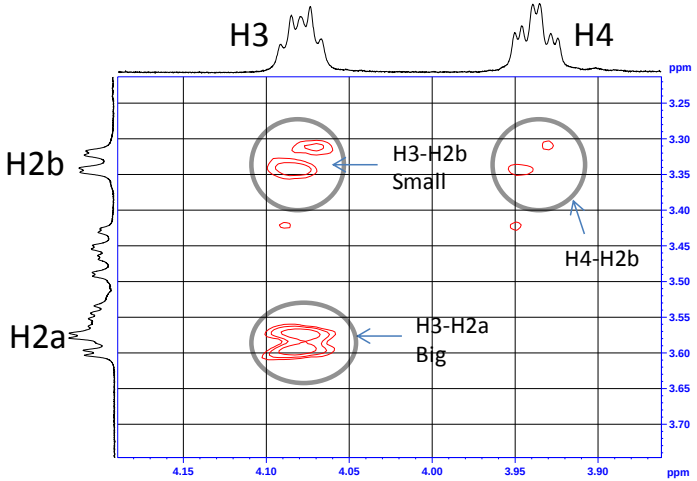
Proton assignment of azepane **3 (NOESY and experimental J values)**

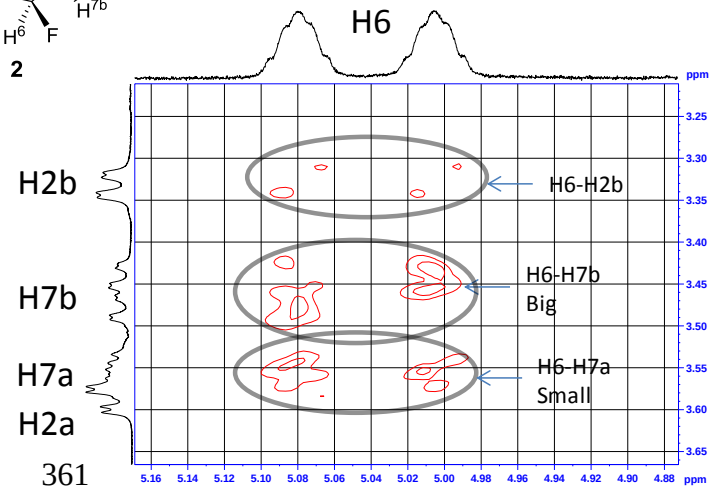




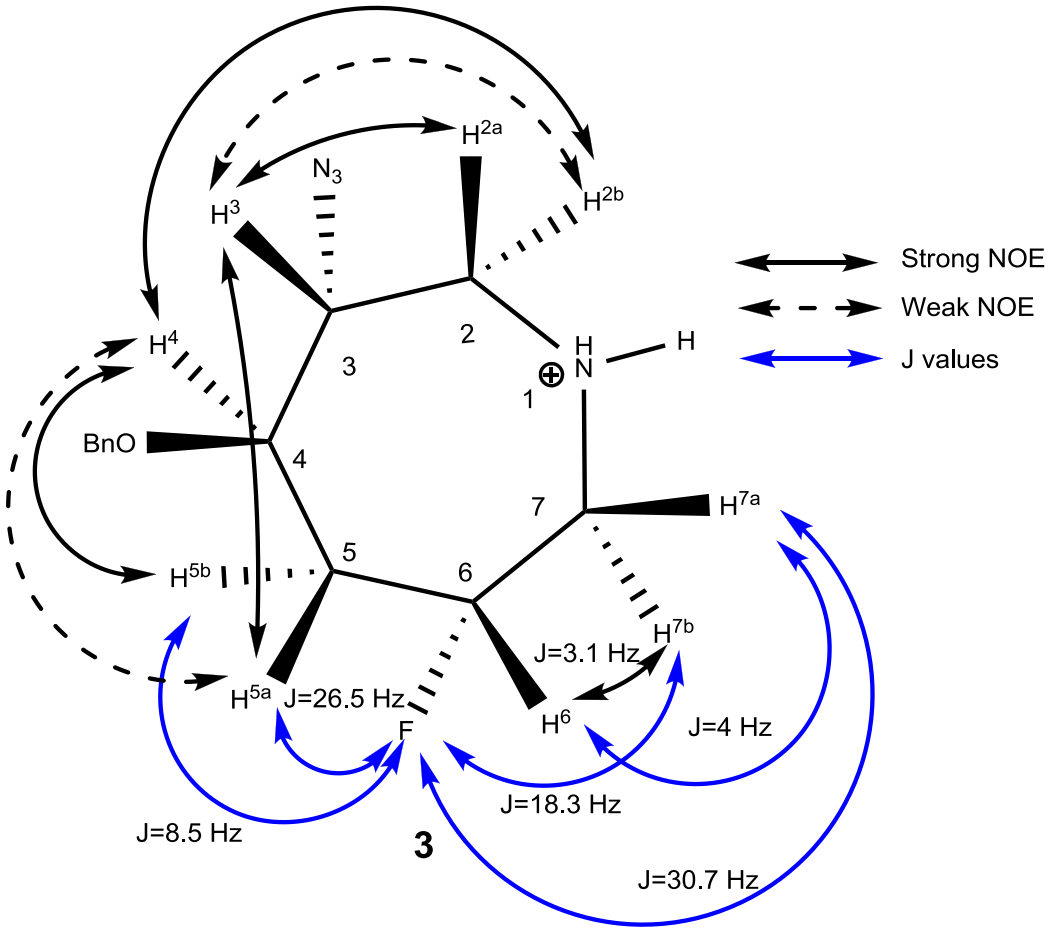


2

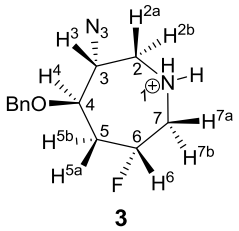




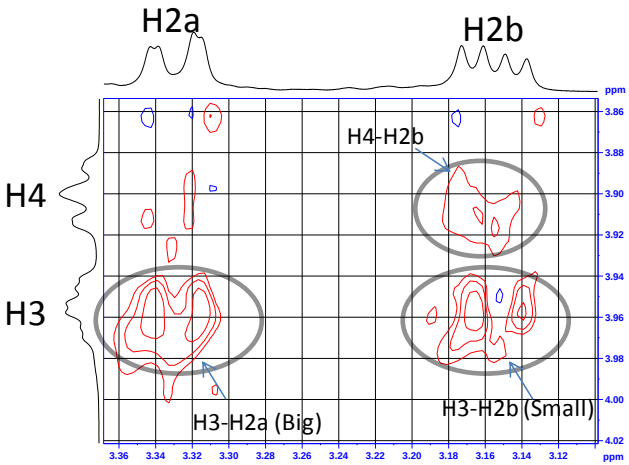
Proton assignment of azepane **3 (NOESY and experimental J values)**

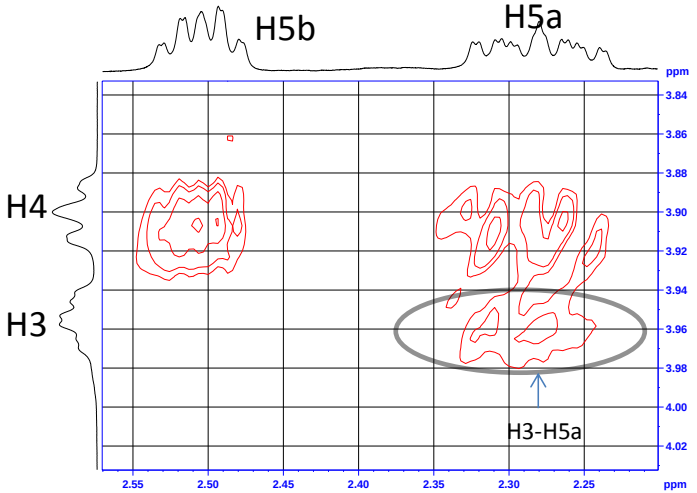


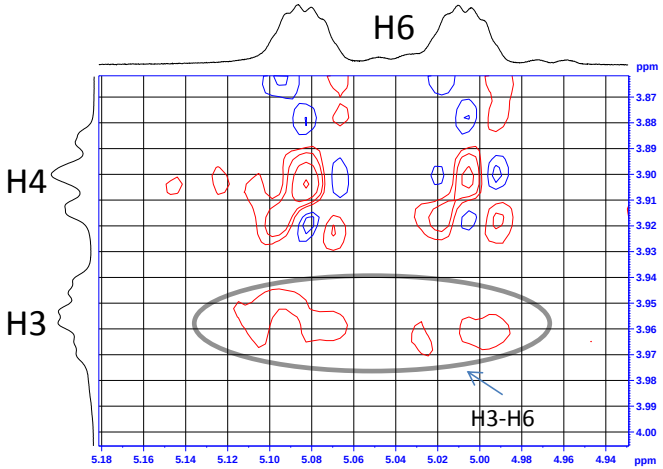
NOESY-**3**


H3
N3
H2a
H2b
H4
2
H
N–H
3
1
BnO
4
7
H7a
H5b
5
6
H7b
H5a
F
H6

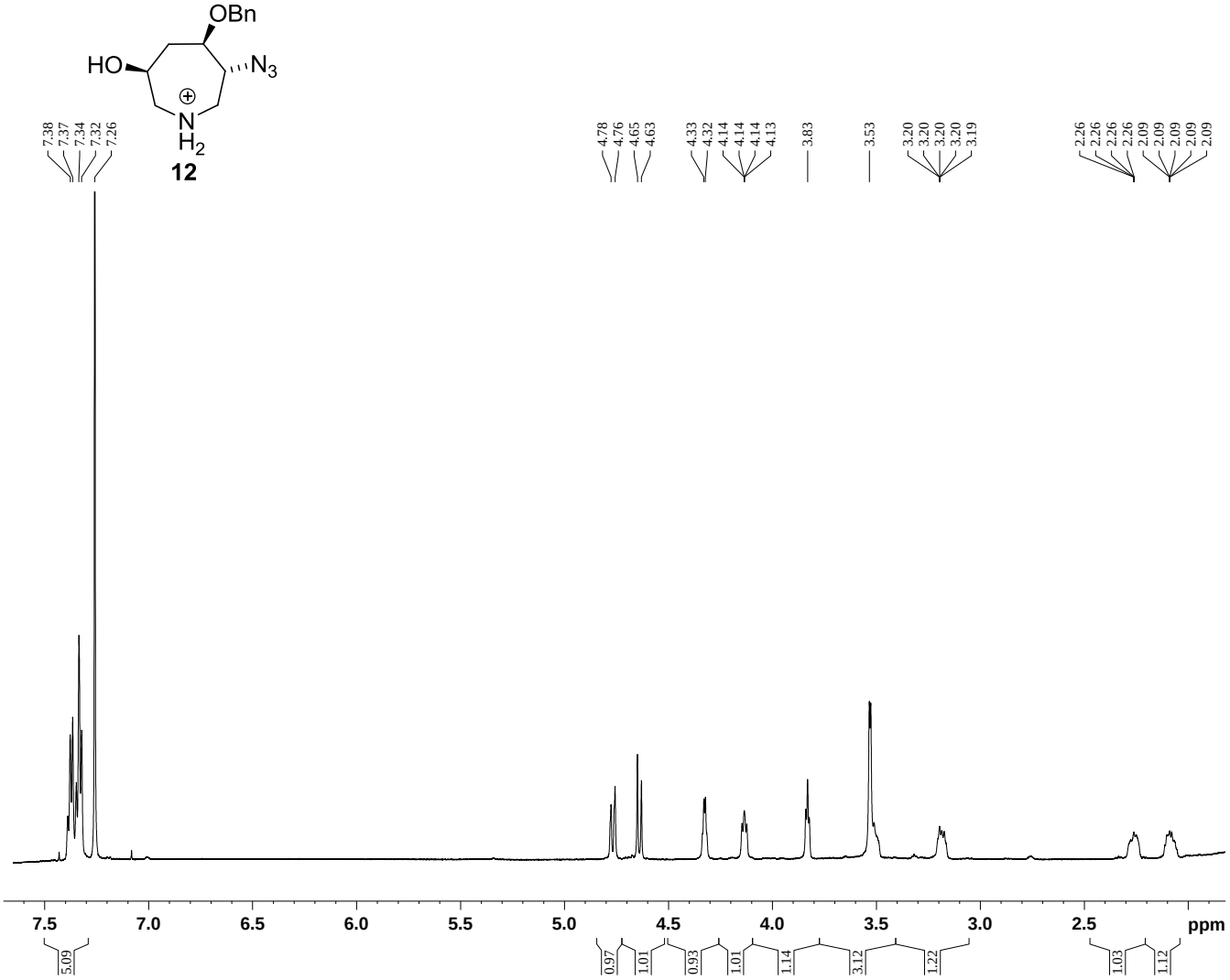
3


H2a
H2b
H4
H3
H4-H2b
H3-H2a (Big)
H3-H2b (Small)
ppm

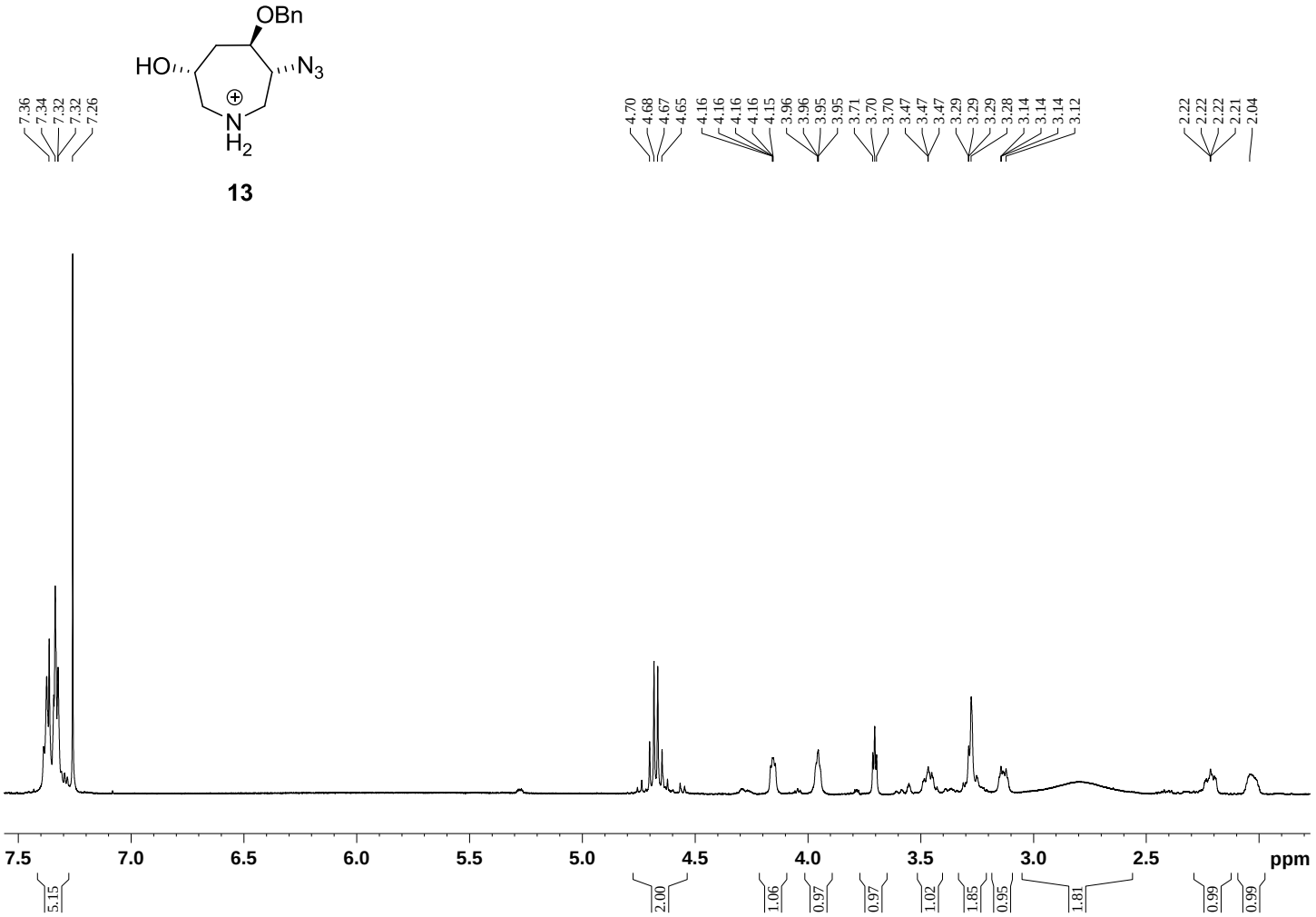

H5b
H5a
H4
H3
H3-H5a
ppm


H6
H4
H3
H3-H6
ppm

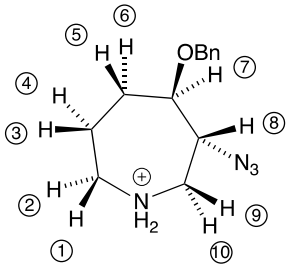
^{1}H NMR-**12**

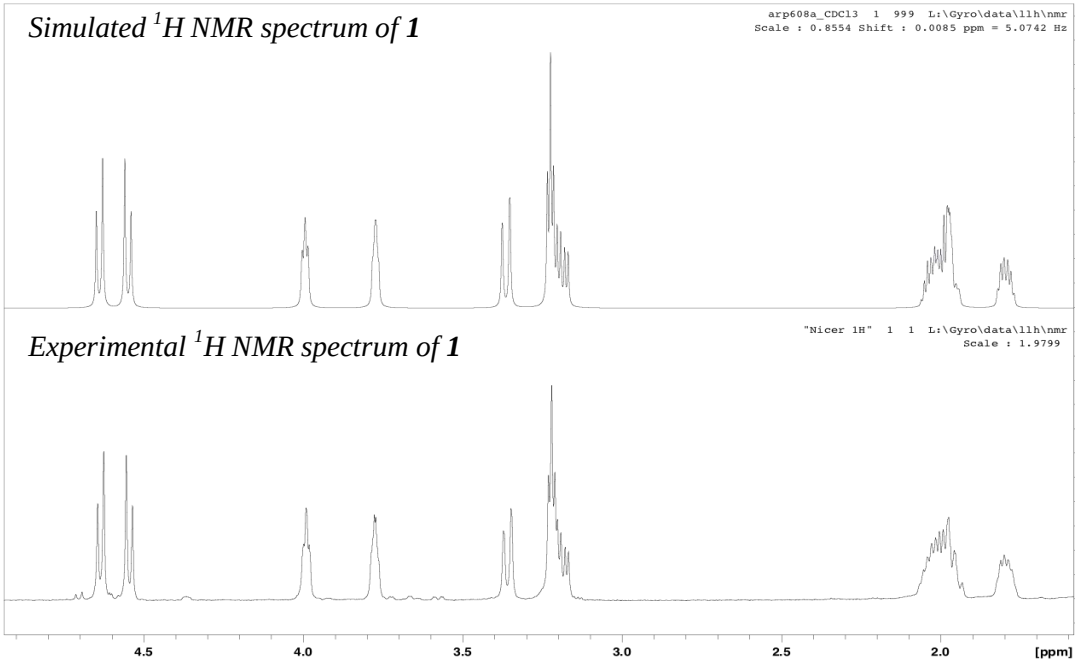

OBn
HO
N3
N
H2
12
7.38
7.37
7.34
7.32
7.26
4.78
4.76
4.65
4.63
4.33
4.32
4.14
4.14
4.14
4.13
3.83
3.53
3.20
3.20
3.20
3.20
3.19
2.26
2.26
2.26
2.26
2.09
2.09
2.09
2.09
7.5
7.0
6.5
6.0
5.5
5.0
4.5
4.0
3.5
3.0
2.5
ppm
5.09
0.97
1.01
0.93
1.01
1.14
3.12
1.22
1.03
1.12

^{1}H NMR-**13**


OBn
HO
N3
N
H2
13
7.36
7.34
7.32
7.32
7.26
4.70
4.68
4.67
4.65
4.16
4.16
4.16
4.16
4.15
3.96
3.96
3.95
3.95
3.71
3.70
3.70
3.47
3.47
3.47
3.29
3.29
3.29
3.28
3.14
3.14
3.14
3.12
2.22
2.22
2.22
2.21
2.04
7.5
7.0
6.5
6.0
5.5
5.0
4.5
4.0
3.5
3.0
2.5
ppm
5.15
2.00
1.06
0.97
0.97
1.02
1.85
0.95
1.81
0.99
0.99

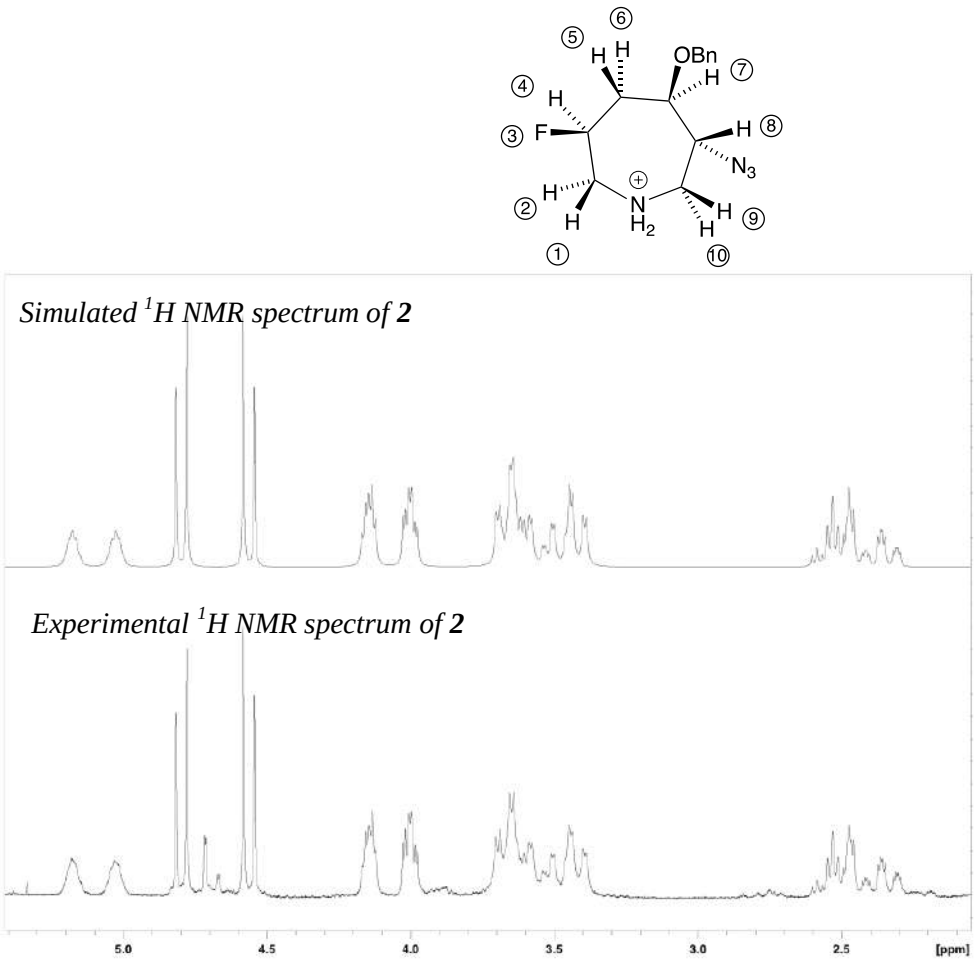
Simulated NMR spectra





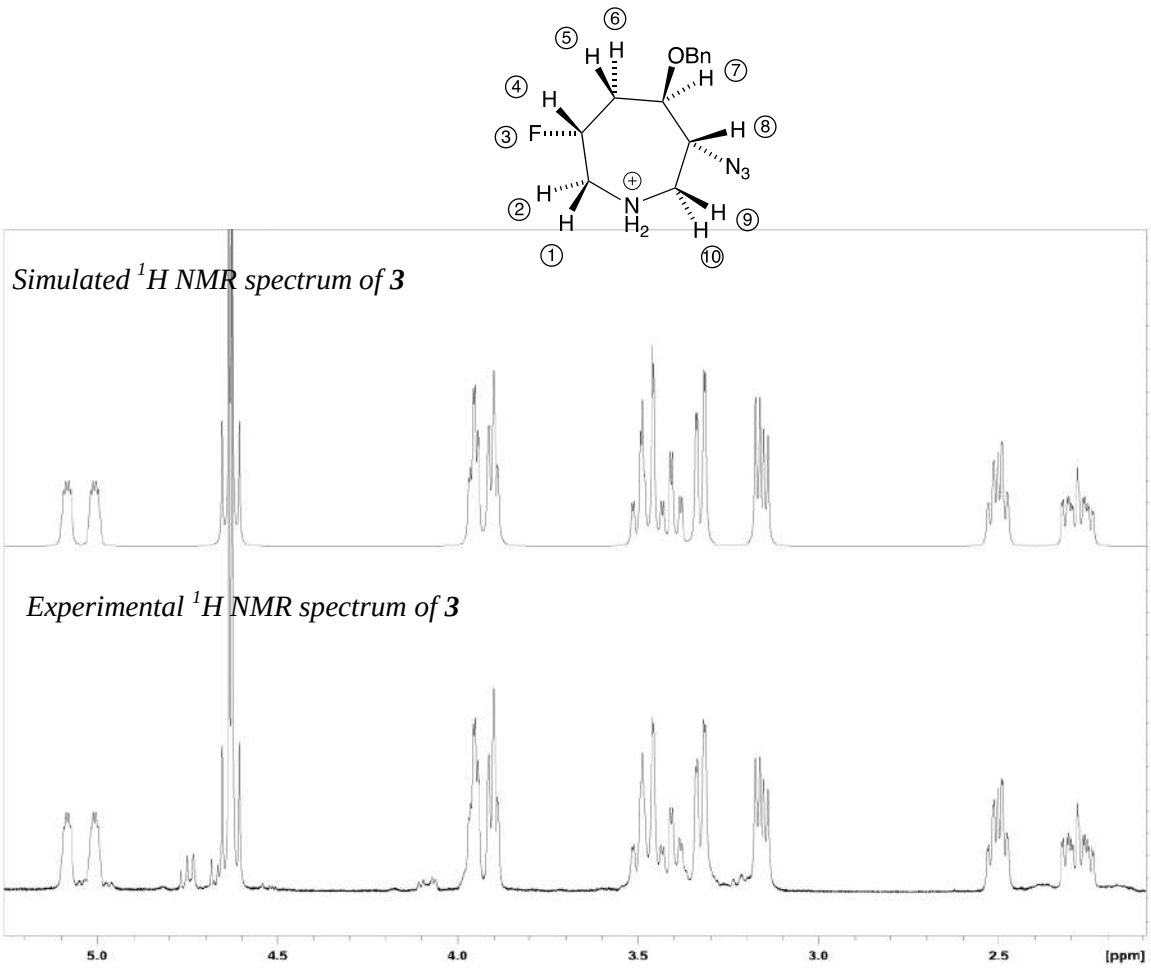
Nuclei	②	③	④	⑤	⑥	⑦	⑧	⑨	⑩
①	13.0 Hz	5.9 Hz	5.9 Hz	0.0 Hz	0.0 Hz	0.0 Hz	0.0 Hz	0.0 Hz	0.0 Hz
②		5.9 Hz	5.9 Hz	0.0 Hz	0.0 Hz	0.0 Hz	0.0 Hz	0.0 Hz	0.0 Hz
③			14.0 Hz	6.0 Hz	6.0 Hz	0.0 Hz	0.0 Hz	0.0 Hz	0.0 Hz
④				5.9 Hz	1.0 Hz	0.0 Hz	0.0 Hz	0.0 Hz	0.0 Hz
⑤					13.0 Hz	5.4 Hz	0.0 Hz	0.0 Hz	0.0 Hz
⑥						1.5 Hz	0.0 Hz	0.0 Hz	0.0 Hz
⑦							5.4 Hz	0.0 Hz	0.0 Hz
⑧								1.5 Hz	5.4 Hz
⑨									14.2 Hz

Figure 1: Expansion from the ^{1}H NMR spectrum of azepane **1**. The good match between the simulated and experimental spectra confirms that the *J* value assignments (see grid) are accurate.



Nuclei	②	③	④	⑤	⑥	⑦	⑧	⑨	⑩
①	14.1 Hz	8.0 Hz	4.0 Hz	0.0 Hz	0.0 Hz	0.0 Hz	0.0 Hz	0.0 Hz	0.0 Hz
②		24.0 Hz	3.0 Hz	0.0 Hz	0.0 Hz	0.0 Hz	0.0 Hz	0.0 Hz	0.0 Hz
③			45.4 Hz	16.2 Hz	33.4 Hz	0.0 Hz	0.0 Hz	0.0 Hz	0.0 Hz
④				5.1 Hz	4.4 Hz	0.0 Hz	0.0 Hz	0.0 Hz	0.0 Hz
⑤					16.1 Hz	6.0 Hz	0.0 Hz	0.0 Hz	0.0 Hz
⑥						2.7 Hz	0.0 Hz	0.0 Hz	0.0 Hz
⑦							6.7 Hz	0.0 Hz	0.0 Hz
⑧								3.5 Hz	4.1 Hz
⑨									14.1 Hz

Figure 2: Expansion from the ^{1}H NMR spectrum of azepane **2**. The good match between the simulated and experimental spectra confirms that the *J* value assignments (see grid) are accurate.



Nuclei	②	③	④	⑤	⑥	⑦	⑧	⑨	⑩
①	14.9 Hz	30.7 Hz	4.0 Hz	0.0 Hz	0.0 Hz	0.0 Hz	0.0 Hz	0.0 Hz	0.0 Hz
②		18.3 Hz	3.1 Hz	0.0 Hz	0.0 Hz	0.0 Hz	0.0 Hz	0.0 Hz	0.0 Hz
③			45.7 Hz	26.5 Hz	8.5 Hz	0.0 Hz	0.0 Hz	0.0 Hz	0.0 Hz
④				2.8 Hz	8.5 Hz	0.0 Hz	0.0 Hz	0.0 Hz	0.0 Hz
⑤					15.1 Hz	9.0 Hz	0.0 Hz	0.0 Hz	0.0 Hz
⑥						2.0 Hz	0.0 Hz	0.0 Hz	0.0 Hz
⑦							7.3 Hz	0.0 Hz	0.0 Hz
⑧								2.8 Hz	7.0 Hz
⑨									14.3 Hz

Figure 3: Expansion from the ^{1}H NMR spectrum of azepane **3**. The good match between the simulated and experimental spectra confirms that the *J* value assignments (see grid) are accurate.

Computational details

General

A conformational analysis was performed for azepanes **1**–**3**. The conformational search was performed as implemented in the program MOE. Conformers were generated by the stochastic method and minimized in the MMFF94X forcefield with chloroform as the solvent. Conformers within 3 kcal/mol in energy were clustered to identify unique members with different azepane ring conformations. For azepanes **2** and **3**, the representative conformers were subjected to DFT calculations as implemented in the program Turbomole.[3] A DFT geometry optimization (with the SV(P) basis set at the B3LYP level in COSMO solvent $CHCl_3$) was performed for each conformer with zero–point vibrational energy correction.

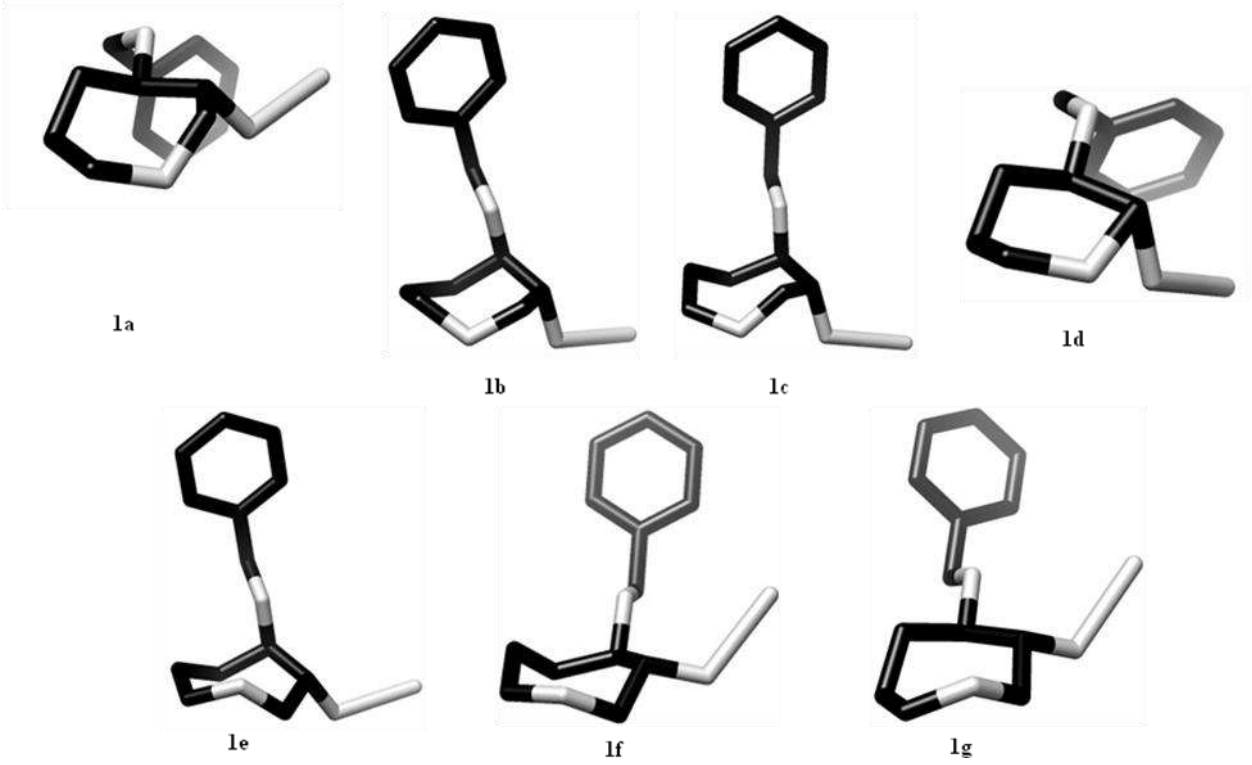
For each the geometries generated with the Turbomole program at the B3LYP/SV(P) level in solvent, single point energies were calculated using several DFT methods, specifically B3LYP[4a], B3LYP–D3, [4b] wB97X–D[4c] both in SMD chloroform solvent[4d] and in vacuum employing the 6–311++G(3df,2pd) basis set. In the case of the B3 series, single point MP2/ 6–311+G(2d,p) were also performed. The single point calculations were performed using the Gaussian 09, revision B (G09) package.[4e] The ultrafine grid was used for all DFT calculations. Final energies quoted include zero point vibrational energy corrections calculated at the B3LYP/SV(P)/COSMO chloroform level (Turbomole). DFT–D3 dispersion corrections[4b] were calculated using the DFTD3 program V2.0 Rev 1 without damping (e.g., using the command "dftd3 <geometry_xyz> –func b3lyp –zero). DFT–D3 dispersion corrections were added to the energies obtained from the B3LYP method.

NMR chemical shifts and couplings were calculated on each of the geometries using the G09 program. Coupling constants were calculated using the GIAO method at the B3LYP/6–311+G(d,p) level using the mixed method, wherein the Fermi contact contribution to the coupling is computed using the larger uG–w basis set.[4f] SMD chloroform solvent and an ultrafine grid were employed, as was the keyword CPHF=conver=10. It is possible to have average errors of 4 kcal/mol in SMD models for

some calculations.[4d] The calculated couplings were scaled by a factor of 0.91 to better fit the experimental data.

*Conformations of azepane **1** within 3 kcal/mol*

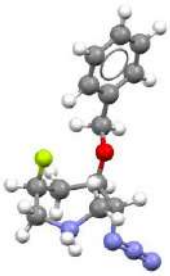
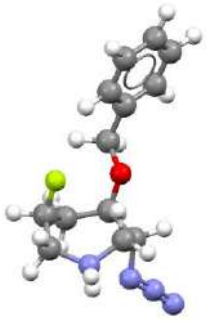
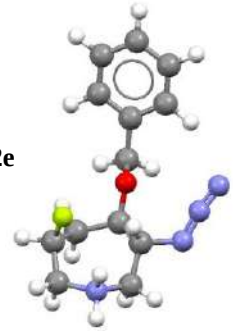
The seven conformers of azepane **1** within 3 kcal/mol are shown below (**1a**–**g**). The conformers are visualized using the program Chimera (UCSF Chimera, version 1.7). The carbon atoms are in black and the heteroatoms gray. In general, the conformers can be divided into two clusters of conformations, **1a**–**d** and **1e**–**g**, with different N-puckering. The cluster **1a**–**d** satisfies the azido *gauche* effect, while the cluster **1e**–**g** does not. The pseudo-equatorial vs. pseudo-axial preference is not pronounced as both clusters contained sidechain conformations in both positions.

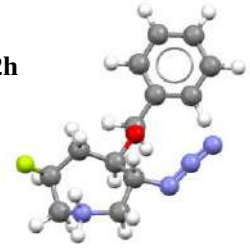


*Azepane **2***

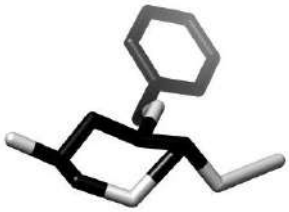
A representative member of each cluster (**2a**–**2i**) with distinct azepane ring conformation was geometry optimized, and the energy was calculated at several different levels of theory (Table 1).

Table 1: Low–energy conformers of azepane **2** with distinct ring conformations.

Geometry	Relative energy (kcal/mol)				
	B3LYP, vacuum	**B3LYP, $CHCl_3$**	**wB97X–D, $CHCl_3$**	**MP2, $CHCl_3$**	**B3LYP–D3, $CHCl_3$**
2a 	0.00	0.00	0.00	0.00	0.00
2b 	0.86	2.03	2.15	1.22	2.47
2c 	1.00	1.99	2.03	1.16	2.44
2d 	1.91	2.38	1.78	1.12	2.30
2e 	2.02	2.21	2.36	1.40	2.74

2f 	2.42	2.92	3.11	1.92	3.51
2g 	3.24	3.56	2.70	2.30	3.23
2h 	3.58	2.23	2.55	1.03	2.95
2i 	3.83	2.62	3.03	2.00	3.30

The energy difference in Table 1 includes contributions from side chain variations not related to ring conformational differences. In order to estimate the possible magnitude of such contribution, a side chain variation of conformer **2i** was investigated (B3LYP, vacuum) and found to contribute a variation of 2.32 kcal/mol. This suggests that energy differences in Table 1 alone are not sufficient in ranking these conformers.



2i

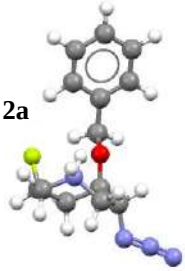
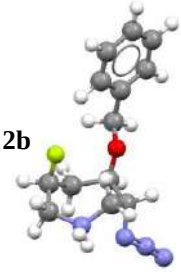


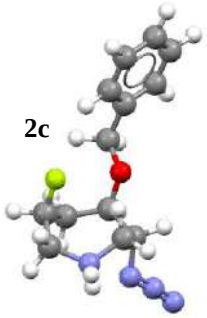
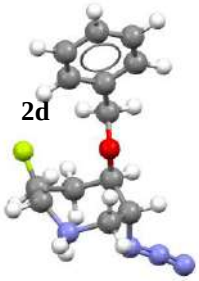
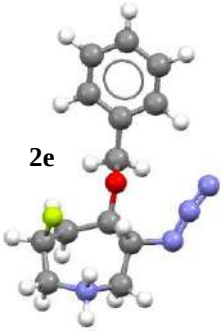
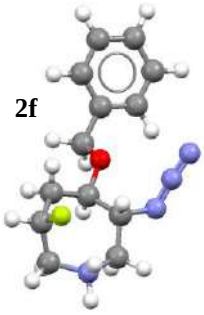
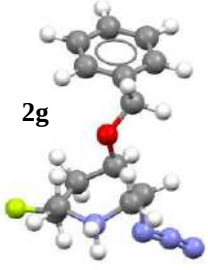
Overlay of **2i** with its congener

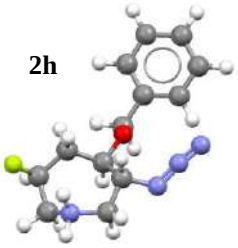
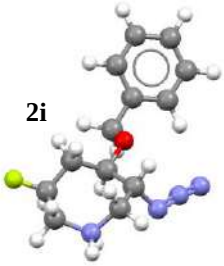
A complete set of NMR spin-spin coupling constants was calculated with a scaling factor of 0.91 (Fig. 4) for each conformer using the G09 method (see 4.1, third paragraph). When the calculated spin–spin coupling constants for each conformer were compared with the experimentally–determined values for **2**, no single conformer was found to match perfectly with all of the experimental values; this suggests that significant conformational averaging is occurring on the NMR timescale.

The following table (Table 2) depicts the ways that each low-energy geometry of **2** does or does not satisfy the conformational "preferences" described in the Manuscript Figure 1.

Table 2: Which individual geometries of **2** satisfy the conformational "preferences"?

Geometry	Conformational "preference" satisfied?		
	Diequatorial OBn/N_3 groups	**Azido *gauche* effect**	**Fluorine *gauche* effect**
2a 	No	No	Yes
2b 	No	Yes	Yes

2c 	No	Yes	Yes
2d 	No	Yes	No
2e 	Yes	No	Yes
2f 	Yes	No	Yes
2g 	No	Yes	No

2h 	Yes	No	Yes
2i 	Yes	Yes	No

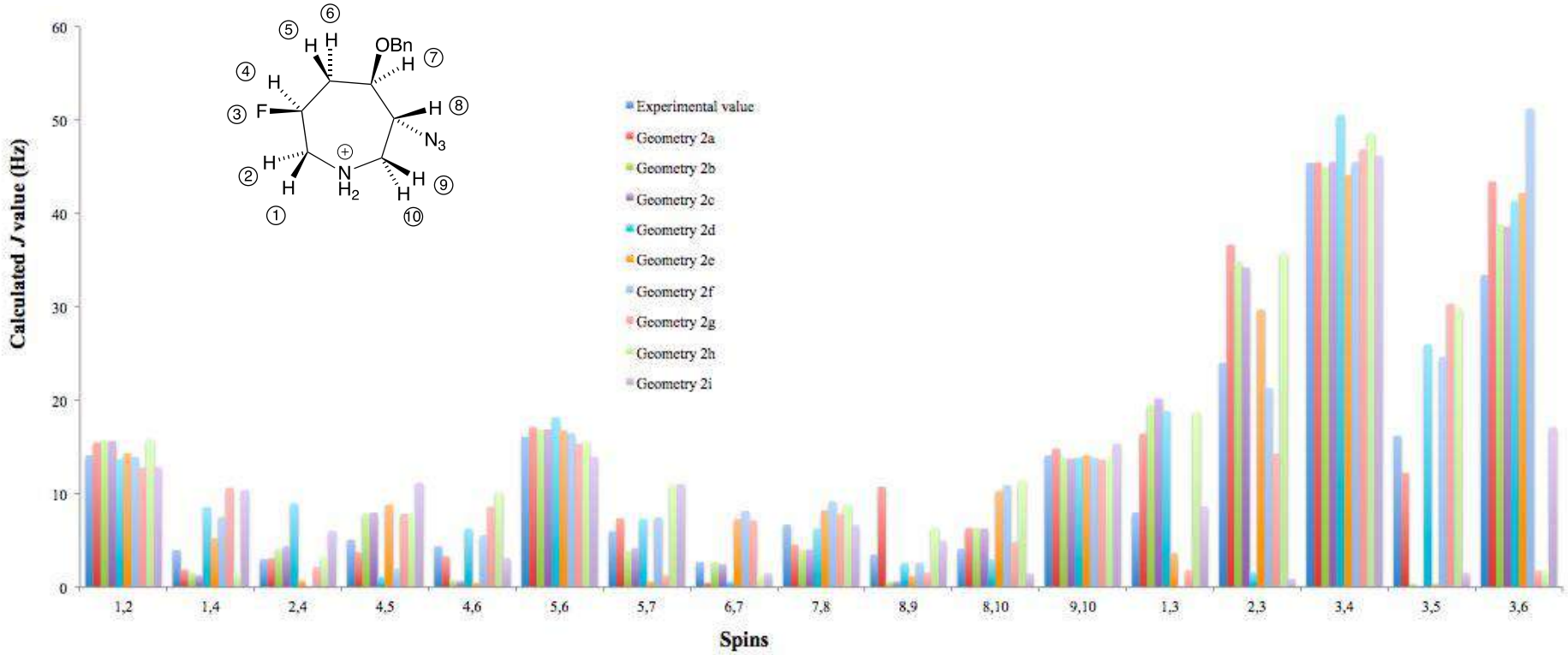


Figure 4: Calculated *J* values for each geometry of azepane **2**.

The following graph (Fig. 5a) illustrates that it was not possible to obtain a good match between experimental and calculated *J* values by using a combination of only **two** geometries (clear violation of J_{H3H5} coupling). Only by creating a weighted average of **three** geometries could a reasonably good match be obtained.

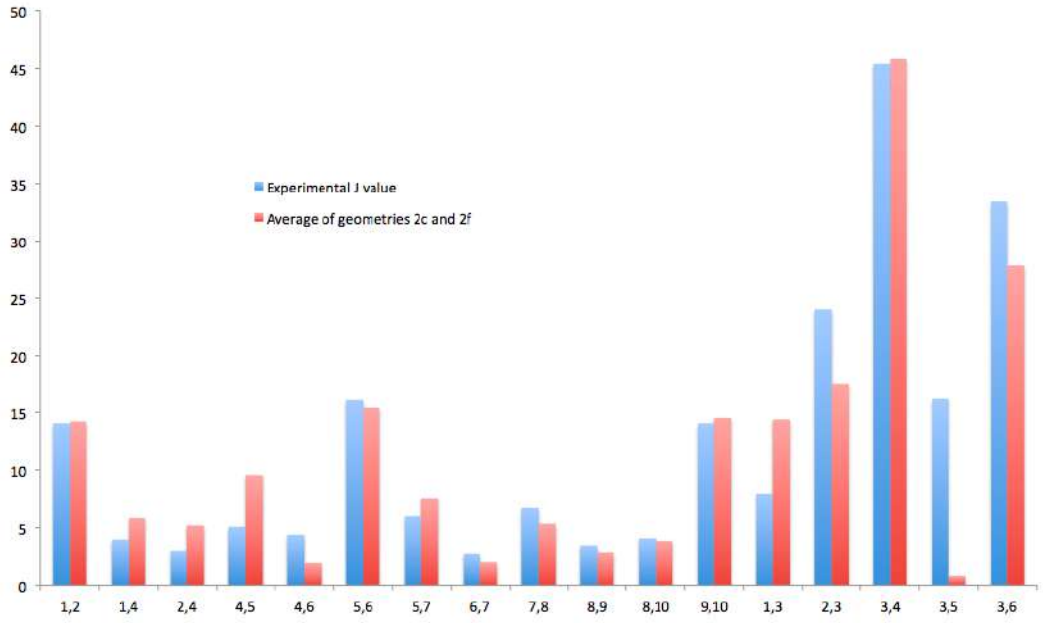


Fig. 5a: *J* values of azepane **2**, calculated for an average distribution of conformers **2e** and **2f**

A qualitative analysis suggested that **2c**, **2f** and **2i** could be significant contributors; each of these conformers satisfies two of the three conformational preferences described in Manuscript Fig. 1. A series of weighted averages of these three conformers were investigated, in order to determine the ratio of **2c** : **2f** : **2i** that gave the best match with the experimental *J* values. It was found that a ratio of 31:39:30 gave a weighted average set of *J* values that matched the experimental values reasonably well (Fig. 5b).

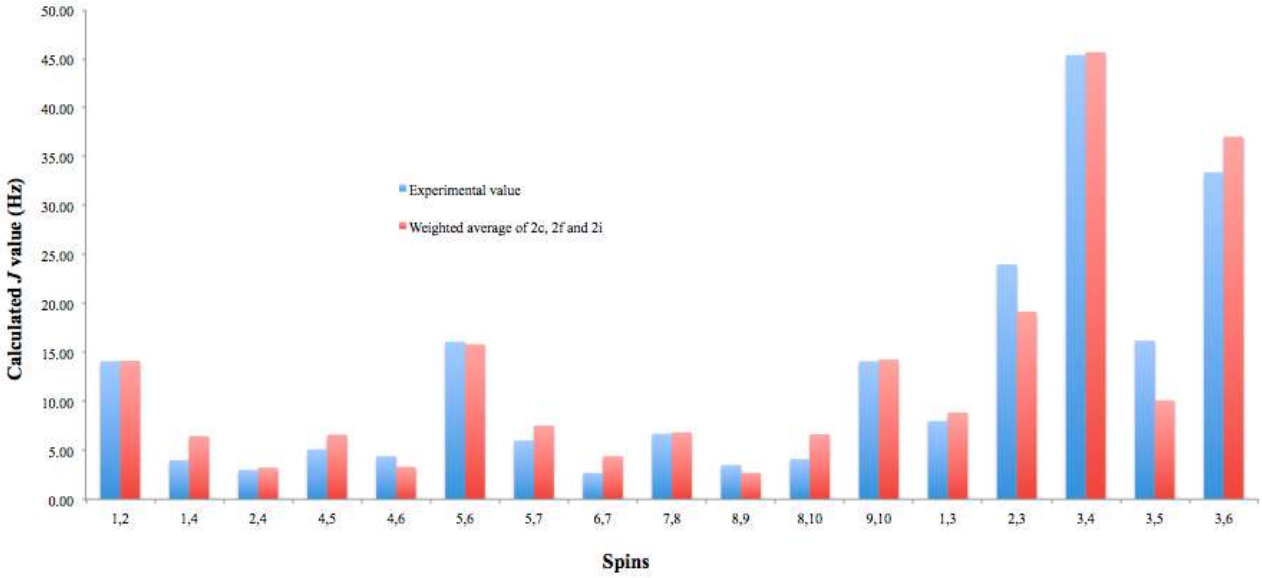
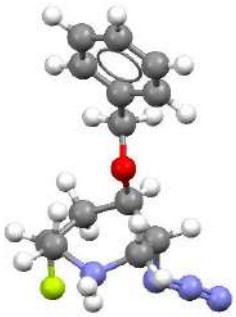


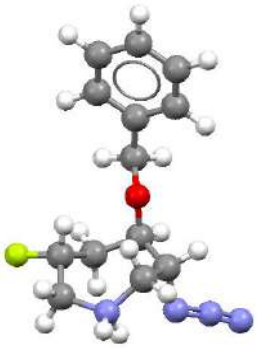
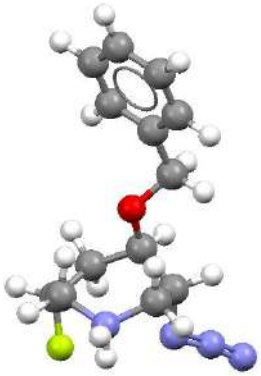
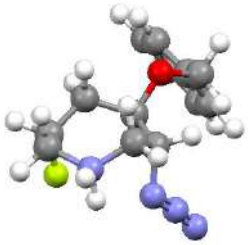
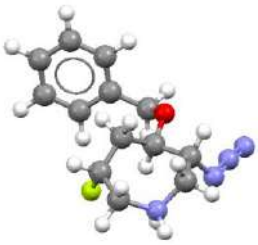
Figure 5b: *J* values of azepane **2**, calculated for a 31:39:30 distribution of conformers **2c**, **2f** and **2i**.

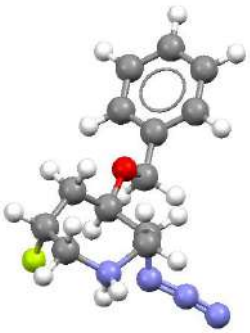
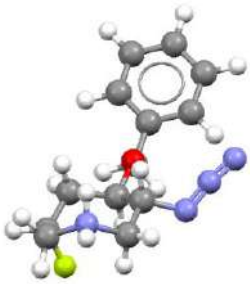
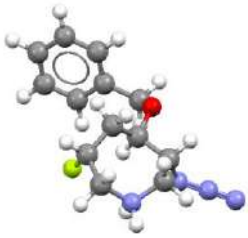
*4.4. Azepane **3***

A representative member of each cluster (**3a**–**3h**) with distinct azepane ring conformation was geometry optimised, and the energy was calculated at several different levels of theory (Table 3).

Table 3: Low–energy conformers of azepane **3** with distinct azepane ring conformations.

	Geometry	Relative energy (kcal/mol)		
		B3LYP, $CHCl_3$	**wB97X–D, $CHCl_3$**	**B3LYP–D3, $CHCl_3$**
3a		0.00	0.11	0.00

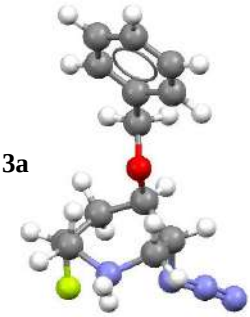
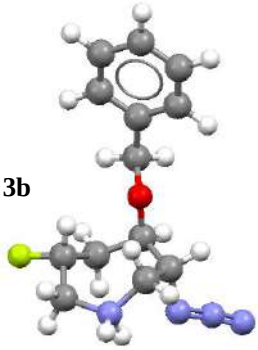
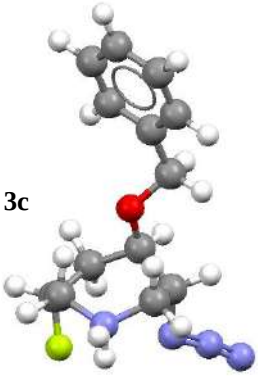
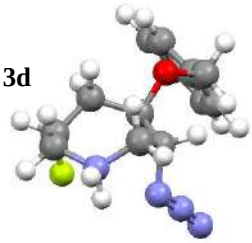
3b		0.78	1.05	1.02
3c		0.47	0.29	0.22
3d		1.36	0.08	0.16
3e		1.35	0.00	0.06

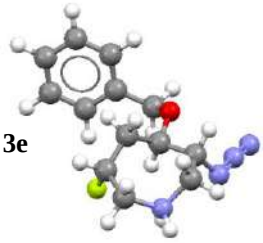
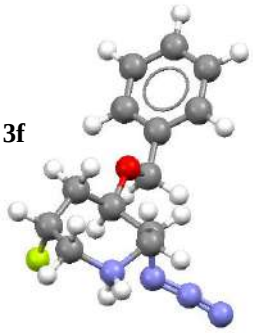
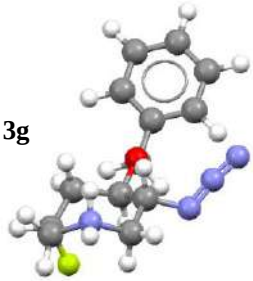
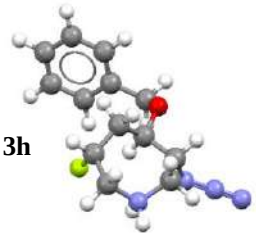
3f		1.28	2.03	1.93
3g		1.85	2.09	1.96
3h		2.43	1.65	1.82

A complete set of NMR spin-spin coupling constants was calculated with a scaling factor of 0.91 (Fig. 6) for each conformer using the G09 method (see 4.1, third paragraph). When the calculated spin–spin coupling constants for each conformer were compared with the experimentally–determined values for **3**, no single conformer was found to match perfectly with all of the experimental values, but conformer **3e** provided a fairly close match.

The following table (Table 4) depicts the ways that each low-energy geometry of **3** does or does not satisfy the conformational "preferences" described in the Manuscript Figure 1.

Table 4: Which individual geometries of **3** satisfy the conformational "preferences"?

Geometry	Conformational "preference" satisfied?		
	Diequatorial OBn/N_3 groups	**Azido *gauche* effect**	**Fluorine *gauche* effect**
3a 	No	Yes	Yes
3b 	No	Yes	No
3c 	No	Yes	Yes
3d 	No	Yes	Yes

3e 	Yes	Yes	Yes
3f 	No	Yes	Yes
3g 	Yes	No	Yes
3h 	Yes	Yes	Yes

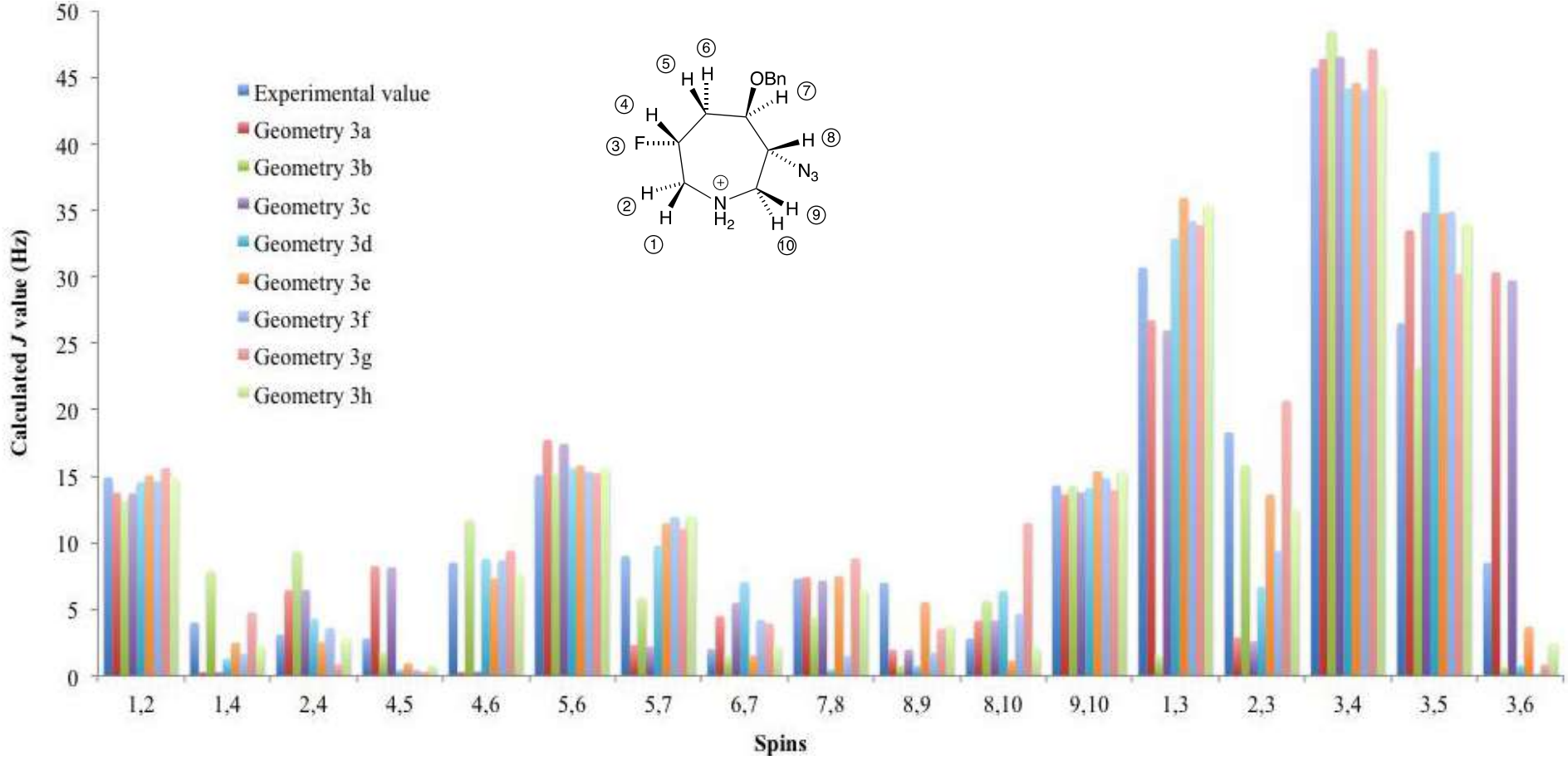


Figure 6: Calculated *J* values for each geometry of azepane **3**.

A qualitative analysis suggested that **3a** and **3e** were likely to be the most significant contributors. A series of weighted averages of these two conformers were investigated, in order to determine the ratio of **3a** : **3e** that gave the best match with the experimental *J* values. It was found that a ratio of 18 : 82 gave a weighted average set of *J* values that matched the experimental values reasonably well (Fig. 7).

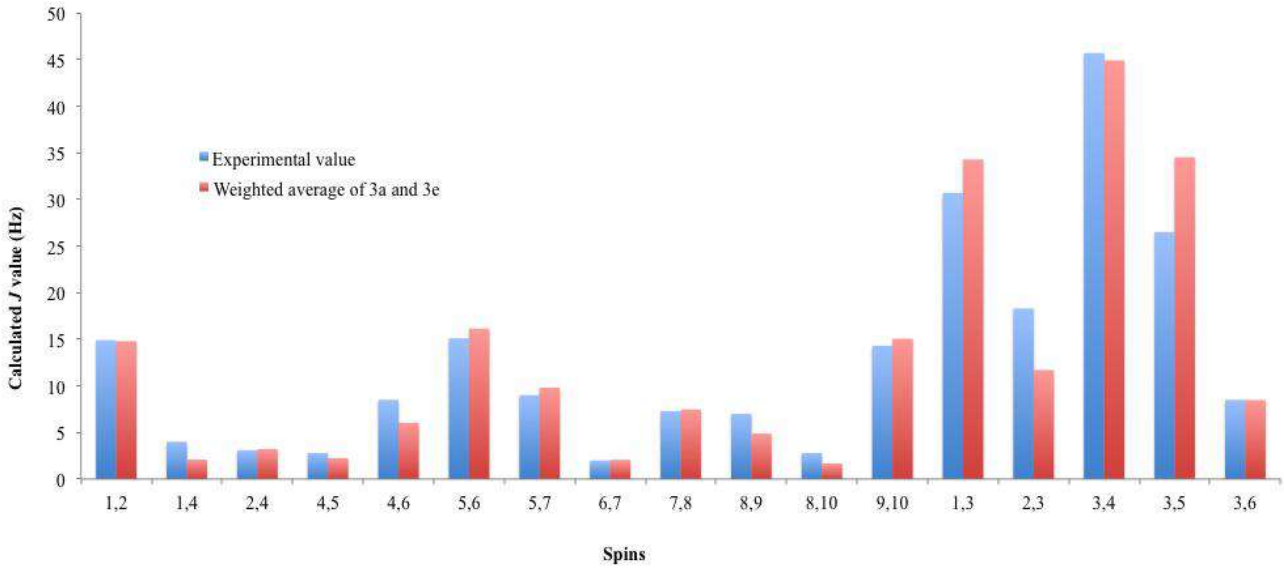


Figure 7: Coupling constants of azepane **3**, calculated for an 18 : 82 distribution of conformers **3a** and **3e**.

*4.5. Azepanes **2** and **3** compared to alcohols **12** and **13***

The proton coupling constants of azepanes **2** and **3** are compared to those from alcohols **12** and **13** in Table 5. From this comparison several dissimilarities are identified (bold) in addition to those that are similar. For azepane **2** and alcohol **12**, both seem to have many intermediate–sized *J* values, suggesting considerable averaging around the whole molecule. The overall pattern of large and small *J* values is (roughly) the same for both. For azepane **3** and alcohol **13**, both seem to have conformational biases. Some *J* values for **13** are, if anything, more extreme. However, the Karplus curve changes with OH vs F substituents and makes direct comparison of the two sets of *J* values difficult; and the *J* values are incomplete for the alcohol, due to signal overlap.

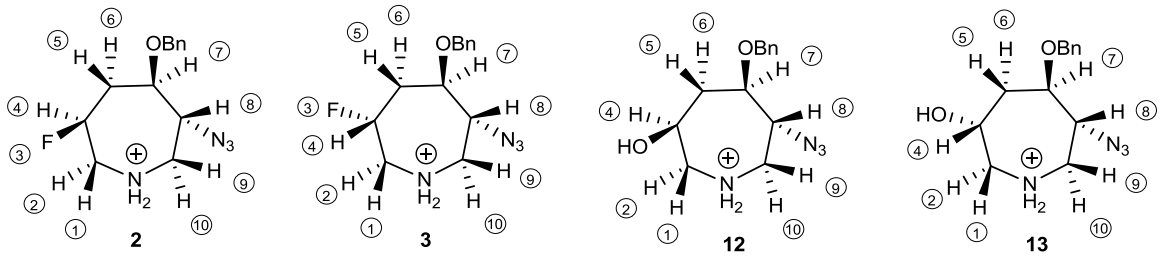


Table 5:. Proton coupling constants of **2**, **3**, **12**, and **13**.

Observed ^3J	**2**	**12**	**3**	**13**
H1 to H2	14.1	13.6	14.9	14.4
H1 to F3	8.0	–	30.7	–
H1 to H4	4.0	5.4	**4.0**	**2.7**
H2 to F3	24.0	–	18.3	–
H2 to H4	**3.0**	**1.2**	3.1	2.6
F3 to H4	45.4	–	45.7	–
F3 to H5	16.2	–	26.5	–
F3 to H6	33.4	–	8.5	–
H4 to H5	5.1	5.8	**2.8**	**NA[a]**
H4 to H6	4.4	3.6	**8.5**	**NA[a]**
H5 to H6	16.1	15.6	**15.1**	**NA[a]**
H5 to H7	6.0	6.1	**9.0**	**NA[a]**
H6 to H7	2.7	3.8	**2.0**	**NA[a]**
H7 to H8	6.7	6.6	7.3	6.5
H8 to H9	3.5	3.8	2.8	2.6
H8 to H10	**4.1**	**5.9**	**7.0**	**3.6**
H9 to H10	14.1	14.1	14.3	14.1

[a]H4 and H5 in **13** appears as one signal (triplet at 2.25 ppm). So, it was not possible to calculate ^3J involving H4 and H5.

In order to have a preliminary assessment if the conformational effects in azepane **3** are unique to fluorine substitution, the major conformer of azepane **3** was used to approximate the hypothetical major conformation of alcohol **13** assuming replacing the fluorine substitution with OH would result in no ring conformational change. By using Karplus equation[5], the observed ^3J constants of **13** (assuming from the same major ring conformer

as is the case with azepane **3**) were used to calculate the expected torsion angles of **13** for comparison to the simulated major conformer of azepane **3** (Table 6). However, the difficulty is that some of the calculated ^{3}J values of the simulated major conformer of **3** alone do not match to the observed ^{3}J of **3**, thus the differences in entries that are from inherently more disordered positions (see column 4 and Fig. 6) are not necessarily indicative of differential conformational outcomes between **13** and **3**. What is informative is that the torsion angles of H7 to H8 and H2 to H4 are fairly close in **13** and **3**, pointing to a likely similar ring conformation at least in the northwestern half of the ring. A full–scale analysis in due course will reveal whether the southwestern half the ring in **13** resembles that of **3** or not.

Table 6: Comparison of a hypothetical major conformation of **13** to that of **3**.

Observed ^{3}J of 13	**Calculated torsion angle of 13**	**Torsion angle of 3 (major conformer from simulation)**	**Match of the calculated ^{3}J of the major conformer of 3 to observed ^{3}J of 3 (Fig 6)**
H1 to H4: 2.71 Hz	−59 °	−53.7 °	No
H2 to H4: 2.58 Hz	69 °	67.6 °	Close
H7 to H8: 6.46 Hz	153 °	148 °	Yes
H9 to H8: 2.55 Hz	58 °	45.1°	No
H10 to H8: 3.58 Hz	58 °	−75.1°	No

3. References

[1] Füstner, A.; Thiel, O. R. *J. Org. Chem.* 2000, **65**, 1738.

[2] Reference 16a in the manuscript.

[3] a) Ahlrichs, R.; Bär, M.; Häser, M.; Horn, H.; Kölmel, C. *Chem. Phys. Lett. 1989*, **162**, 165. b) Schäfer, A.; Horn, H.; Ahlrichs, R. *J. Chem. Phys.* 1992, **97**, 2571. c) Treutler, O.; Ahlrichs, R. *J. Chem. Phys*. 1995, **102**, 346. d) A. Klamt, A.; Schüürmann, G. *J. Chem. Soc. Perkin Trans*. 2 1993, 799. e) Arnim, M. v. ; Ahlrichs, R. *J. Chem. Phys.* 1999, **111**, 9183.

[4] a) Becke, A. D. *J. Chem. Phys.*, 1993, **98**, 5648. b) Grimme, S.; Jens Antony, J.; Ehrlich, S.; Krieg, H. *J. Chem. Phys.* 2010, **132**, 154104. c) Chai, J.–D.; Head–Gordon, M. *Phys. Chem. Chem. Phys.*, 2008, **10**, 6615. d) Marenich, A. V.; Cramer, C. J.; Truhlar, D. G. *J. Phys. Chem. B*, 2009, **113**, 6378. e) Gaussian 09, Revision B.1, Frisch, M. J.; Trucks, G. W.; Schlegel, H. B.; Scuseria, G. E.; Robb, M. A.; Cheeseman, J. R.; Scalmani, G.; Barone, V.; Mennucci, B.; Petersson, G. A.; Nakatsuji, H.; Caricato, M.; Li, X.; Hratchian, H. P.; Izmaylov, A. F.; Bloino, J.; Zheng, G.; Sonnenberg, J. L.; Hada, M.; Ehara, M.; Toyota, K.; Fukuda, R.; Hasegawa, J.; Ishida, M.; Nakajima, T.; Honda, Y.; Kitao, O.; Nakai, H.; Vreven, T.; Montgomery, Jr., J. A.; Peralta, J. E.; Ogliaro, F.; Bearpark, M.; Heyd, J. J.; Brothers, E.; Kudin, K. N.; Staroverov, V. N.; Kobayashi, R.; Normand, J.; Raghavachari, K.; Rendell, A.; Burant, J. C.; Iyengar, S. S.; Tomasi, J.; Cossi, M.; Rega, N.; Millam, N. J.; Klene, M.; Knox, J. E.; Cross, J. B.; Bakken, V.; Adamo, C.; Jaramillo, J.; Gomperts, R.; Stratmann, R. E.; Yazyev, O.; Austin, A. J.; Cammi, R.; Pomelli, C.; Ochterski, J. W.; Martin, R. L.; Morokuma, K.; Zakrzewski, V. G.; Voth, G. A.; Salvador, P.; Dannenberg, J. J.; Dapprich, S.; Daniels, A. D.; Farkas, Ö.; Foresman, J. B.; Ortiz, J. V.; Cioslowski, J.; Fox, D. J. Gaussian, Inc., Wallingford CT, 2009. f) Deng, W.; Cheeseman, J.R.; Frisch, M.J. *J. Chem. Theory Comput.* 2006, **2**, 1028.

[5] Haasnoot, C.A.G.; DeLeeuw, F.A.A.M.; Altona, C. Tetrahedron, 1980, **36**, 2783.

Appendix C

Table of contents:

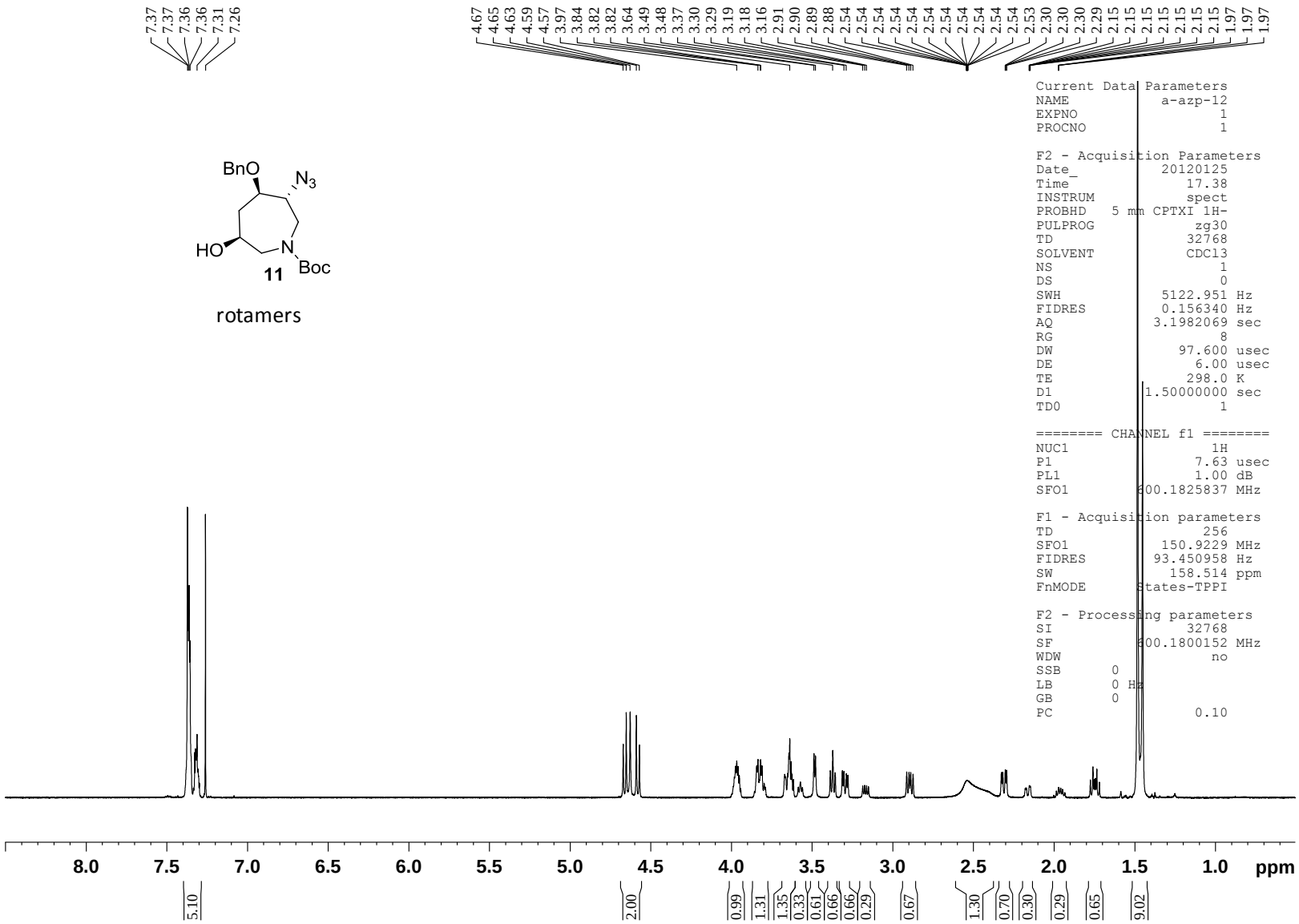
Full NMR spectra of compounds discussed in chapter 4……..…..……389

Varient temperature NMR spectra of compounds discussed in chapter 4……..……454

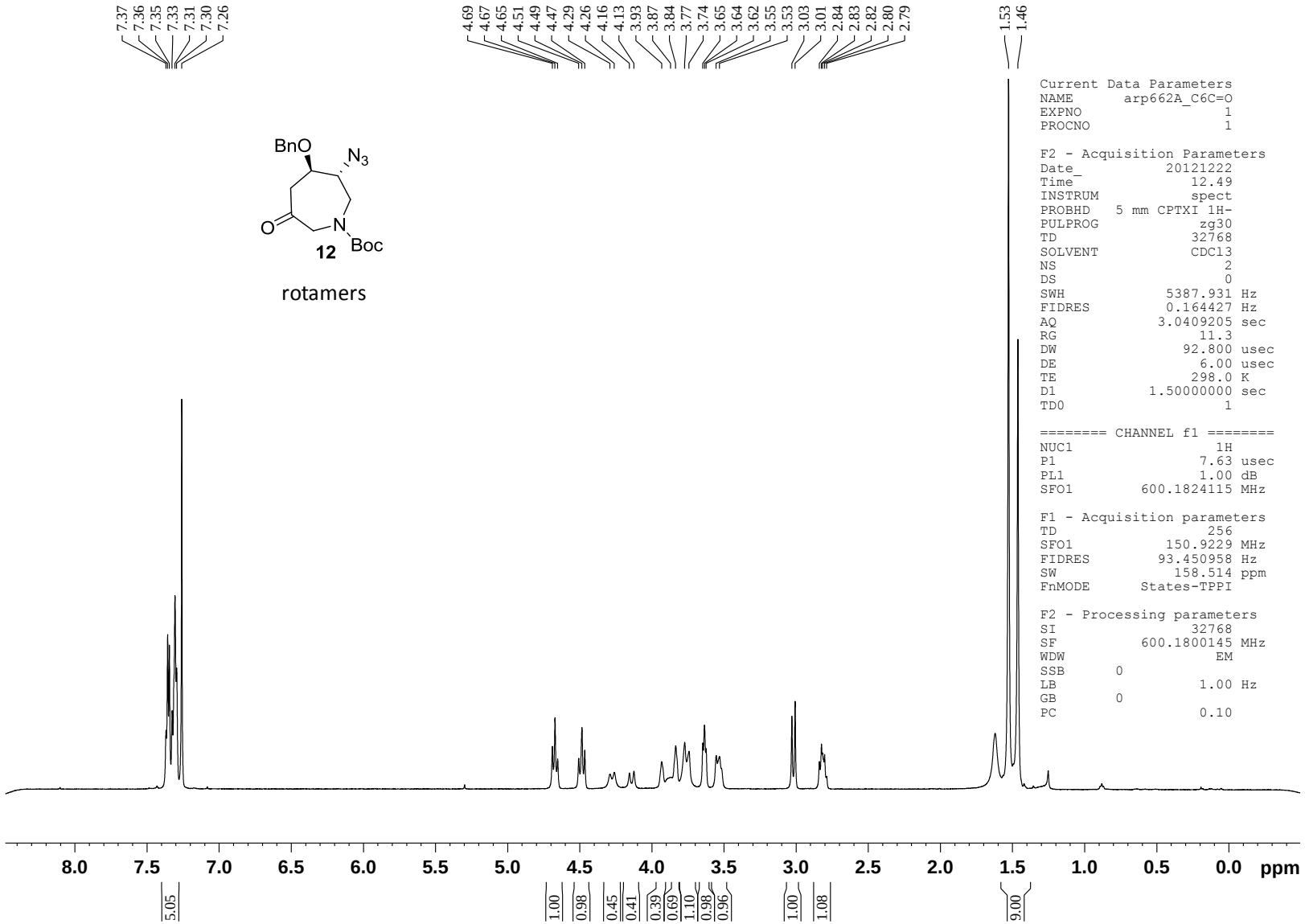
Simulated NMR spectra of compounds discussed in chapter 4.....464

Conformational analysis of compounds discussed in chapter 4…….…… 470

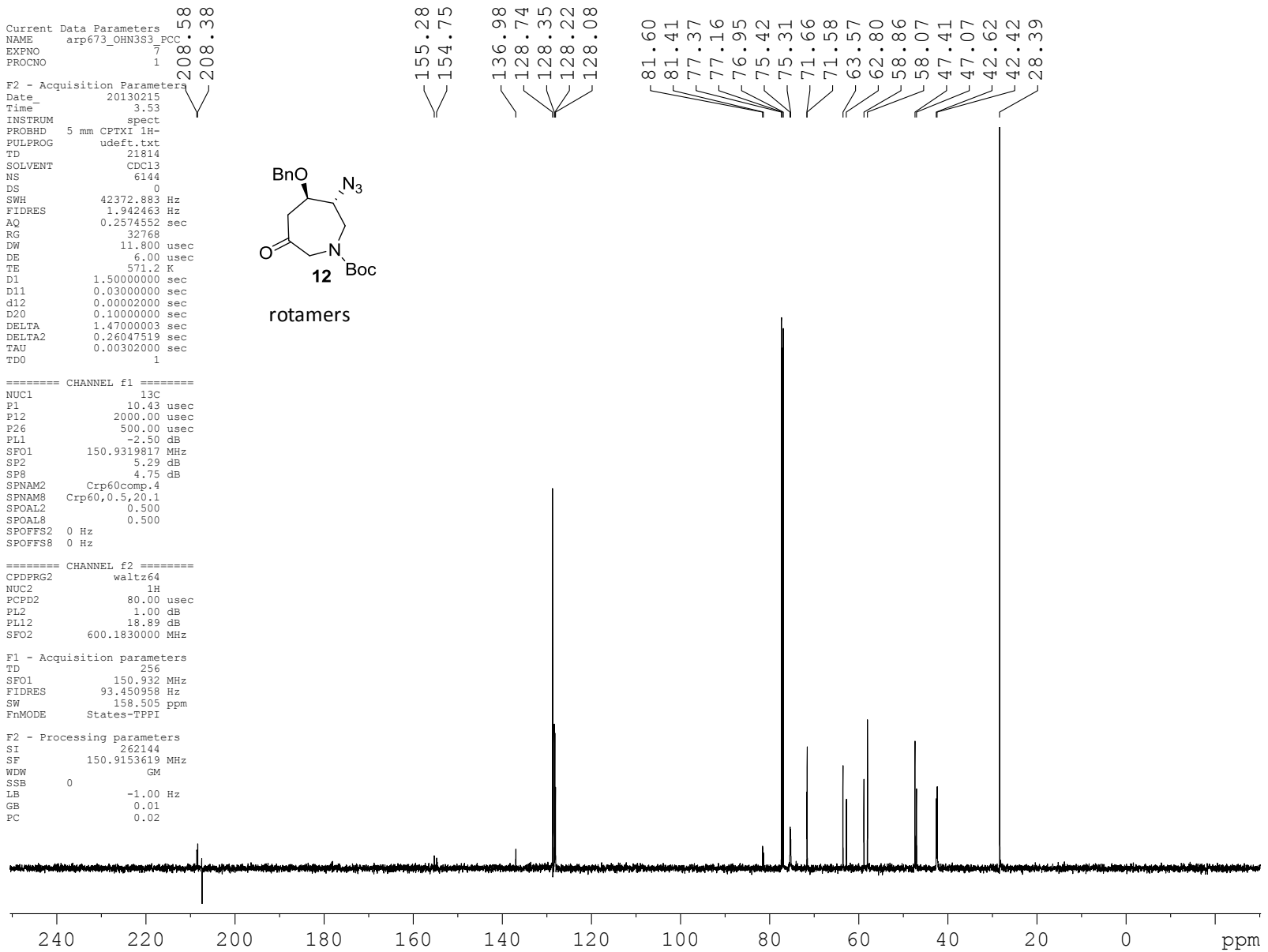
^{1}H NMR-**11**


7.37
7.37
7.36
7.36
7.31
7.26
4.67
4.65
4.63
4.59
4.57
3.97
3.84
3.82
3.82
3.64
3.49
3.48
3.37
3.30
3.29
3.19
3.18
3.16
2.91
2.90
2.89
2.88
2.54
2.54
2.54
2.54
2.54
2.54
2.54
2.54
2.54
2.54
2.54
2.53
2.30
2.30
2.30
2.29
2.15
2.15
2.15
2.15
2.15
2.15
1.97
1.97
1.97
BnO
N3
HO
N
Boc
11
rotamers
Current Data Parameters
NAME a-azp-12
EXPNO 1
PROCNO 1
F2 - Acquisition Parameters
Date_ 20120125
Time 17.38
INSTRUM spect
PROBHD 5 mm CPTXI 1H-
PULPROG zg30
TD 32768
SOLVENT CDCl3
NS 1
DS 0
SWH 5122.951 Hz
FIDRES 0.156340 Hz
AQ 3.1982069 sec
RG 8
DW 97.600 usec
DE 6.00 usec
TE 298.0 K
D1 1.50000000 sec
TD0 1
======== CHANNEL f1 ========
NUC1 1H
P1 7.63 usec
PL1 1.00 dB
SFO1 600.1825837 MHz
F1 - Acquisition parameters
TD 256
SFO1 150.9229 MHz
FIDRES 93.450958 Hz
SW 158.514 ppm
FnMODE States-TPPI
F2 - Processing parameters
SI 32768
SF 600.1800152 MHz
WDW no
SSB 0
LB 0 Hz
GB 0
PC 0.10
8.0
7.5
7.0
6.5
6.0
5.5
5.0
4.5
4.0
3.5
3.0
2.5
2.0
1.5
1.0
ppm
5.10
2.00
0.99
1.31
1.35
0.33
0.61
0.66
0.66
0.29
0.67
1.30
0.70
0.30
0.29
0.65
9.02

^{1}H NMR-**12**


7.37
7.36
7.35
7.33
7.31
7.30
7.26
4.69
4.67
4.65
4.51
4.49
4.47
4.29
4.26
4.16
4.13
3.93
3.87
3.84
3.77
3.74
3.65
3.64
3.62
3.55
3.53
3.03
3.01
2.84
2.83
2.82
2.80
2.79
1.53
1.46
BnO
N3
O
N
Boc
12
rotamers
Current Data Parameters
NAME arp662A_C6C=O
EXPNO 1
PROCNO 1
F2 - Acquisition Parameters
Date_ 20121222
Time 12.49
INSTRUM spect
PROBHD 5 mm CPTXI 1H-
PULPROG zg30
TD 32768
SOLVENT CDCl3
NS 2
DS 0
SWH 5387.931 Hz
FIDRES 0.164427 Hz
AQ 3.0409205 sec
RG 11.3
DW 92.800 usec
DE 6.00 usec
TE 298.0 K
D1 1.50000000 sec
TD0 1
======== CHANNEL f1 ========
NUC1 1H
P1 7.63 usec
PL1 1.00 dB
SFO1 600.1824115 MHz
F1 - Acquisition parameters
TD 256
SFO1 150.9229 MHz
FIDRES 93.450958 Hz
SW 158.514 ppm
FnMODE States-TPPI
F2 - Processing parameters
SI 32768
SF 600.1800145 MHz
WDW EM
SSB 0
LB 1.00 Hz
GB 0
PC 0.10
8.0
7.5
7.0
6.5
6.0
5.5
5.0
4.5
4.0
3.5
3.0
2.5
2.0
1.5
1.0
0.5
0.0
ppm
5.05
1.00
0.98
0.45
0.41
0.39
0.69
1.10
0.98
0.96
1.00
1.08
9.00

^{13}C NMR-**12**




```
Current Data Parameters
NAME      arp673_OHN3S3_PCC
EXPNO                     7
PROCNO                    1

F2 - Acquisition Parameters
Date_              20130215
Time                   3.53
INSTRUM               spect
PROBHD   5 mm CPTXI 1H-
PULPROG          udeft.txt
TD                    21814
SOLVENT               CDCl3
NS                     6144
DS                        0
SWH              42372.883 Hz
FIDRES            1.942463 Hz
AQ                0.2574552 sec
RG                    32768
DW                   11.800 usec
DE                    6.00 usec
TE                   571.2 K
D1             1.50000000 sec
D11            0.03000000 sec
d12            0.00002000 sec
D20            0.10000000 sec
DELTA          1.47000003 sec
DELTA2         0.26047519 sec
TAU            0.00302000 sec
TD0                       1

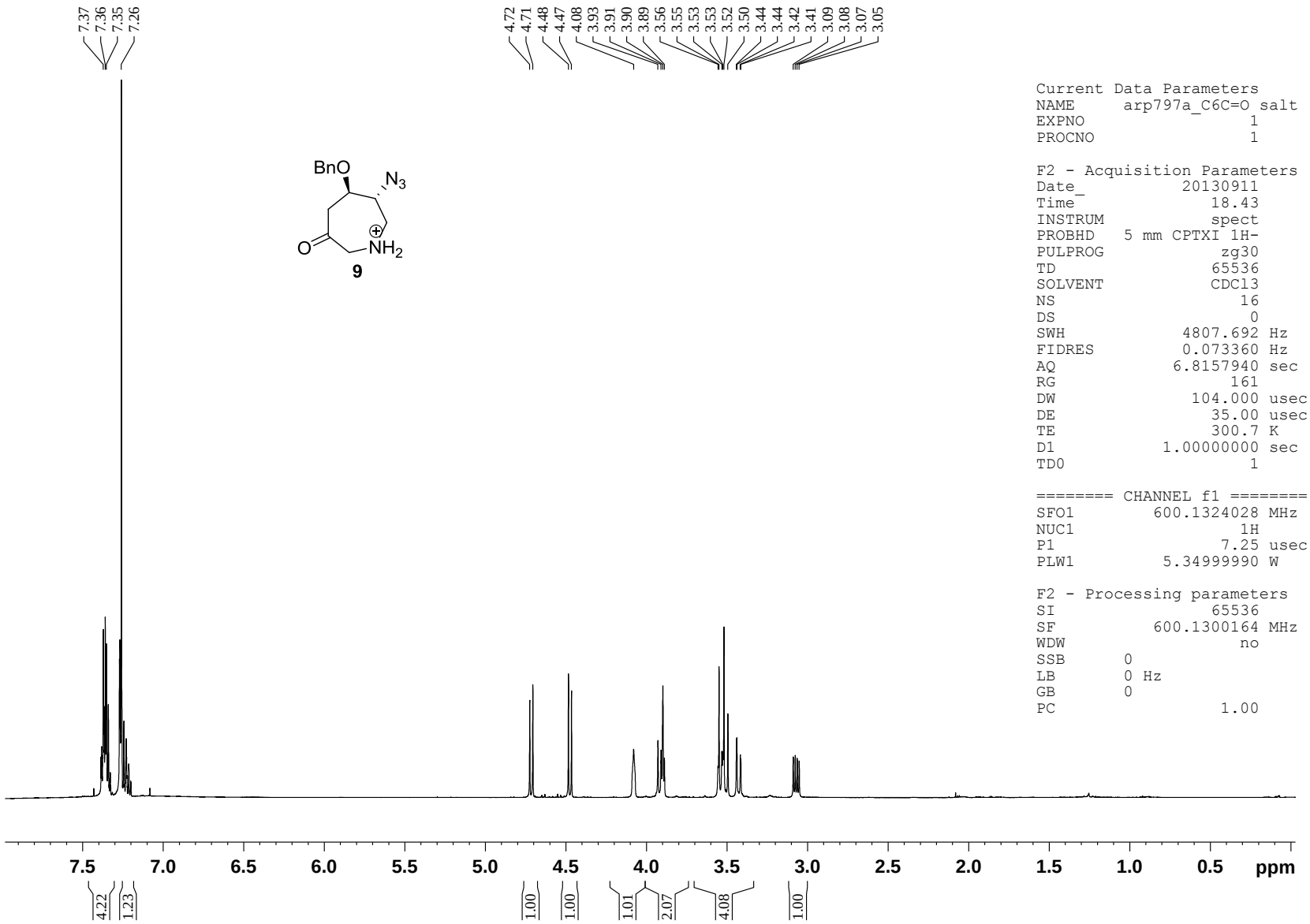
======== CHANNEL f1 ========
NUC1                   13C
P1                   10.43 usec
P12                2000.00 usec
P26                 500.00 usec
PL1                  -2.50 dB
SFO1          150.9319817 MHz
SP2                   5.29 dB
SP8                   4.75 dB
SPNAM2        Crp60comp.4
SPNAM8     Crp60,0.5,20.1
SPOAL2                0.500
SPOAL8                0.500
SPOFFS2   0 Hz
SPOFFS8   0 Hz

======== CHANNEL f2 ========
CPDPRG2            waltz64
NUC2                    1H
PCPD2                80.00 usec
PL2                   1.00 dB
PL12                 18.89 dB
SFO2          600.1830000 MHz

F1 - Acquisition parameters
TD                      256
SFO1               150.932 MHz
FIDRES          93.450958 Hz
SW                158.505 ppm
FnMODE        States-TPPI

F2 - Processing parameters
SI                   262144
SF            150.9153619 MHz
WDW                     GM
SSB       0
LB                   -1.00 Hz
GB                    0.01
PC                    0.02
```

^{1}H NMR-**9**



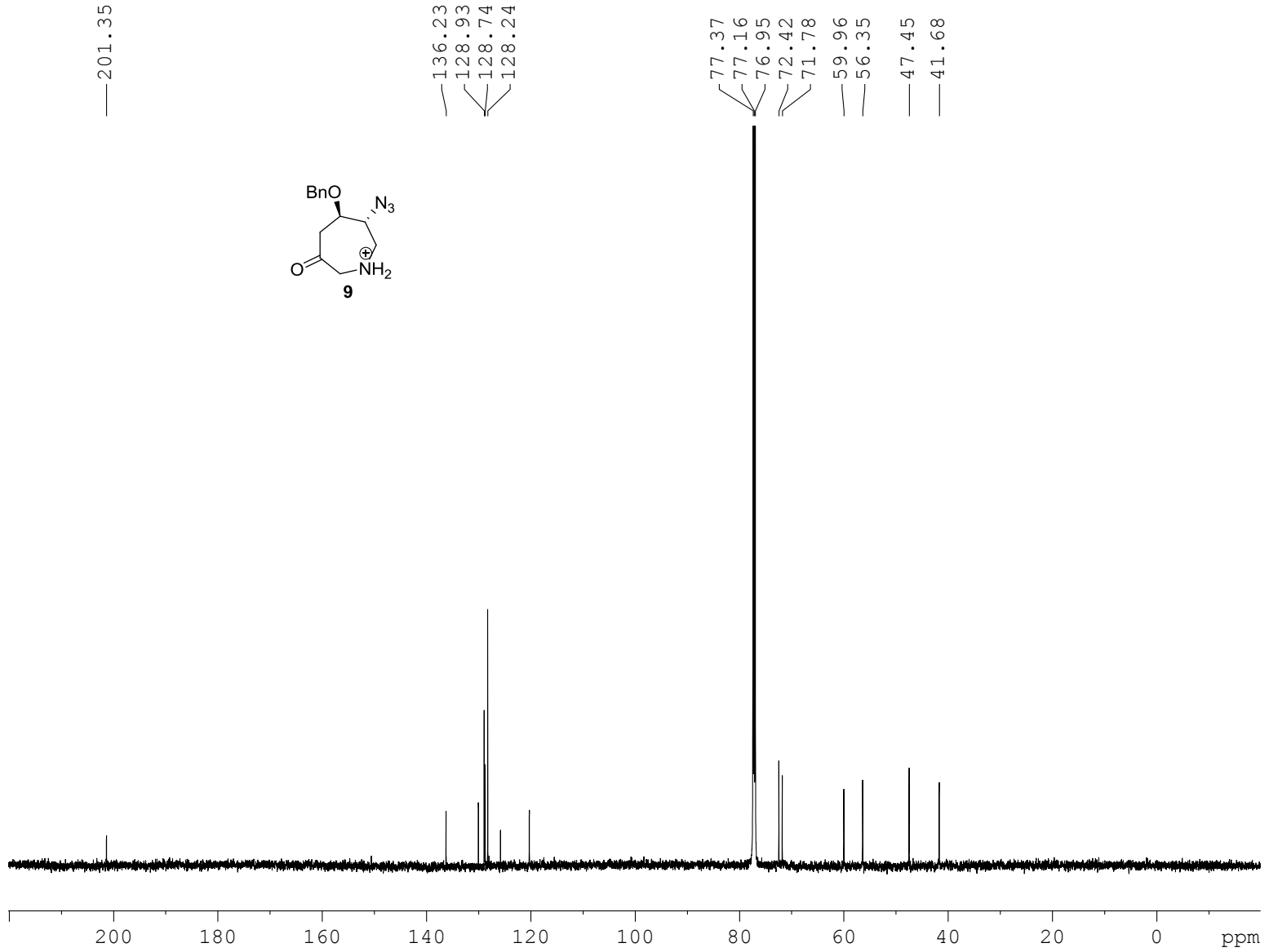

```
Current Data Parameters
NAME      arp797a_C6C=O salt
EXPNO                    1
PROCNO                   1

F2 - Acquisition Parameters
Date_           20130911
Time              18.43
INSTRUM           spect
PROBHD   5 mm CPTXI 1H-
PULPROG             zg30
TD                65536
SOLVENT           CDCl3
NS                   16
DS                    0
SWH            4807.692 Hz
FIDRES         0.073360 Hz
AQ             6.8157940 sec
RG                  161
DW               104.000 usec
DE                35.00 usec
TE                300.7 K
D1           1.00000000 sec
TD0                  1

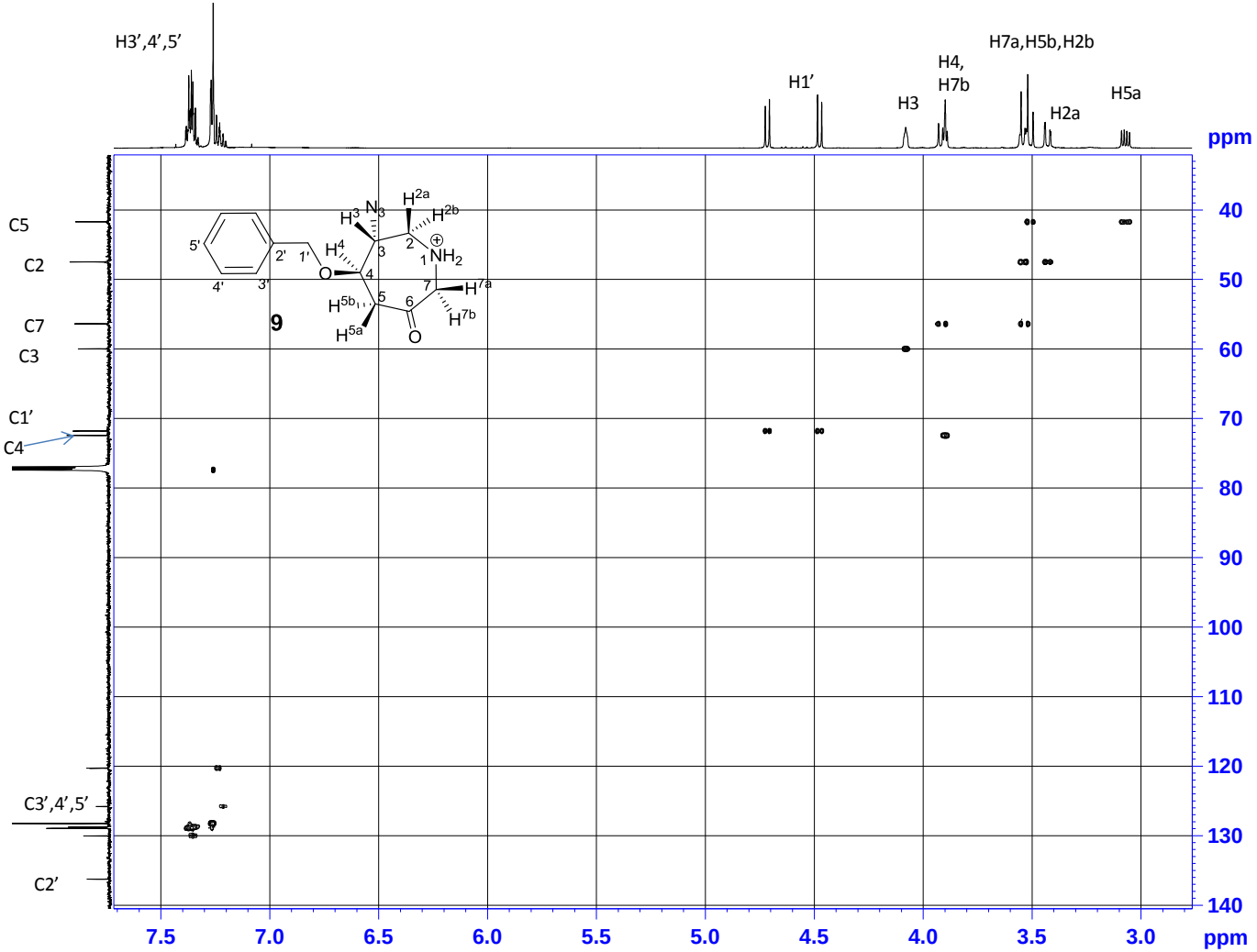
======== CHANNEL f1 ========
SFO1        600.1324028 MHz
NUC1                1H
P1                7.25 usec
PLW1         5.34999990 W

F2 - Processing parameters
SI                65536
SF          600.1300164 MHz
WDW                 no
SSB       0
LB        0 Hz
GB        0
PC                1.00
```

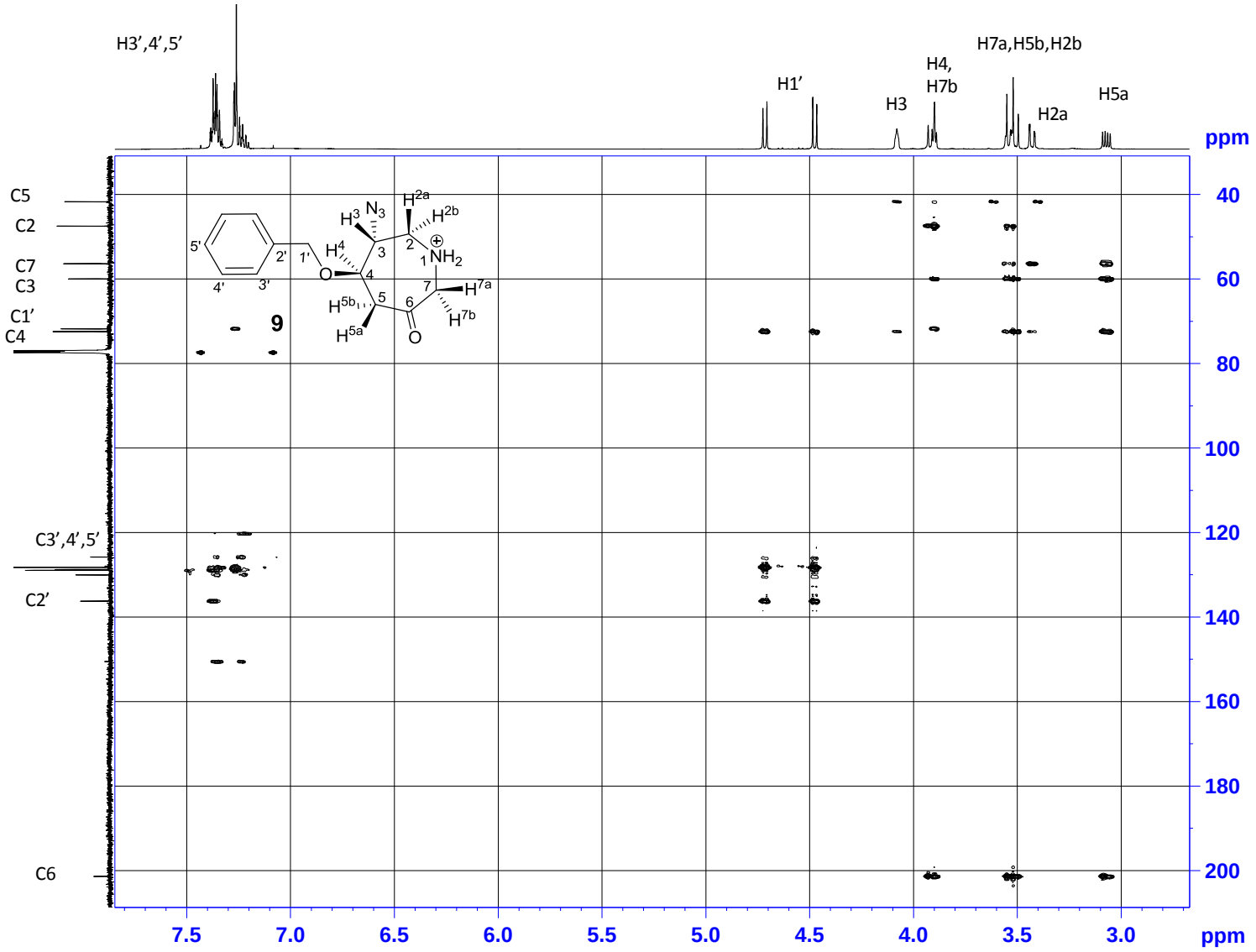
^{13}C NMR-**9**


201.35
136.23
128.93
128.74
128.24
77.37
77.16
76.95
72.42
71.78
59.96
56.35
47.45
41.68
BnO
N3
O
NH2
9
200
180
160
140
120
100
80
60
40
20
0
ppm

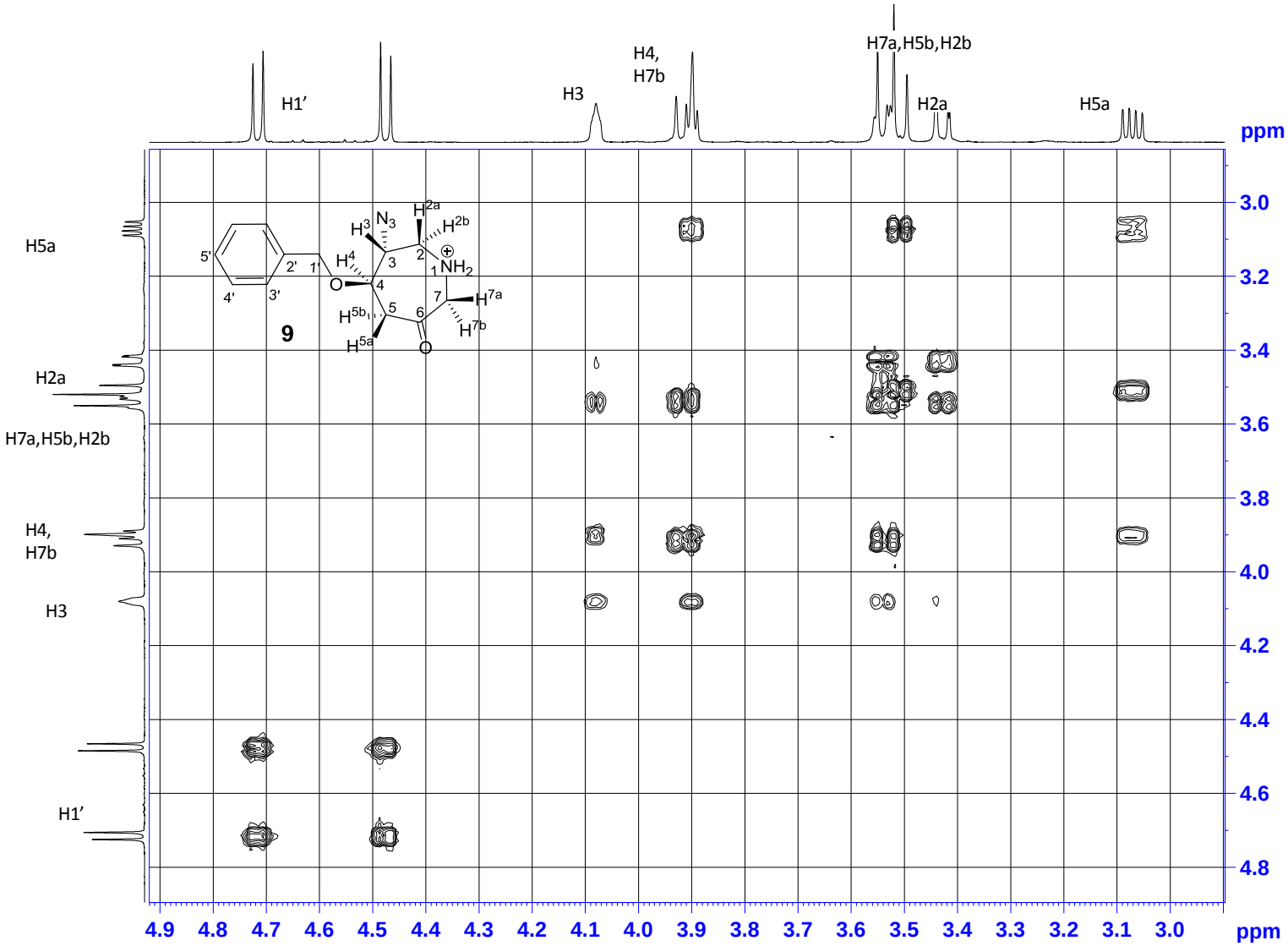
HSQC-**9**


H3',4',5'
H1'
H3
H4,
H7b
H7a,H5b,H2b
H2a
H5a
ppm
C5
C2
C7
C3
C1'
C4
C3',4',5'
C2'
9
7.5
7.0
6.5
6.0
5.5
5.0
4.5
4.0
3.5
3.0
ppm
40
50
60
70
80
90
100
110
120
130
140

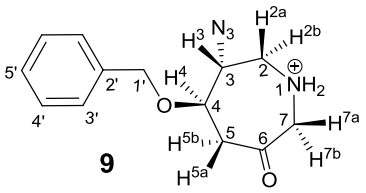
HMBC-**9**


H3',4',5'
H1'
H3
H4,
H7b
H7a,H5b,H2b
H2a
H5a
ppm
C5
C2
C7
C3
C1'
C4
C3',4',5'
C2'
C6
9
7.5
7.0
6.5
6.0
5.5
5.0
4.5
4.0
3.5
3.0
ppm

COSY-**9**

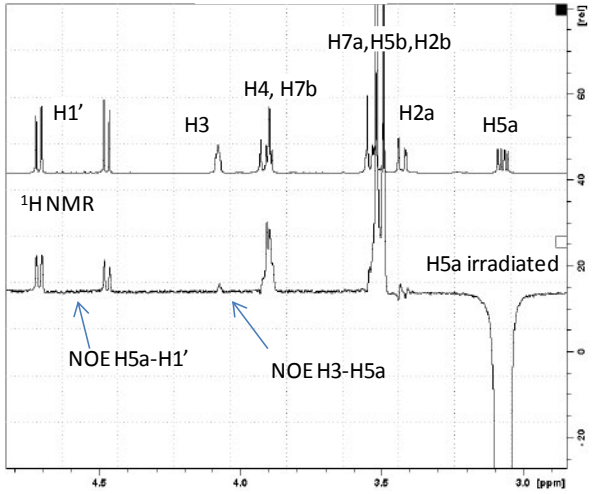

H1'
H3
H4,
H7b
H7a,H5b,H2b
H2a
H5a
ppm
3.0
3.2
3.4
3.6
3.8
4.0
4.2
4.4
4.6
4.8
4.9 4.8 4.7 4.6 4.5 4.4 4.3 4.2 4.1 4.0 3.9 3.8 3.7 3.6 3.5 3.4 3.3 3.2 3.1 3.0
ppm
9

NOESY-**9**

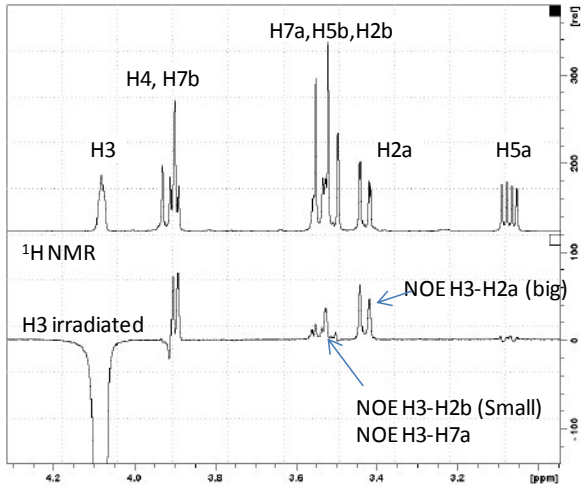


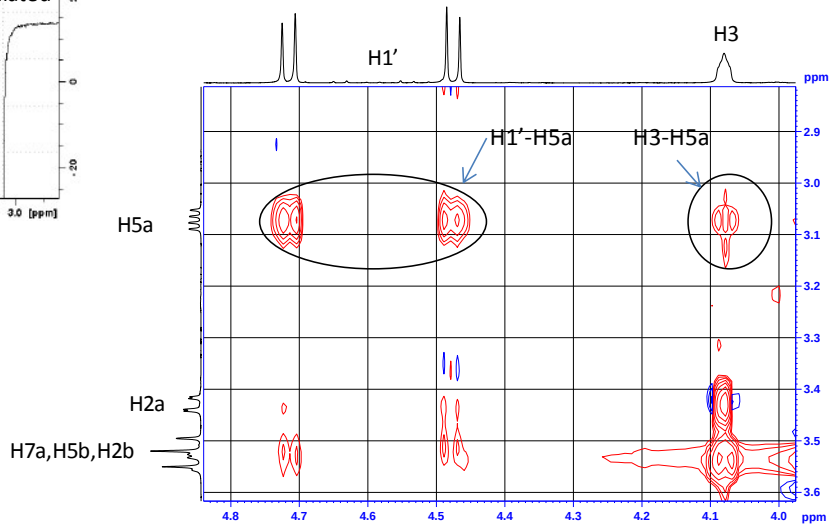
9

1D Selective NOESY

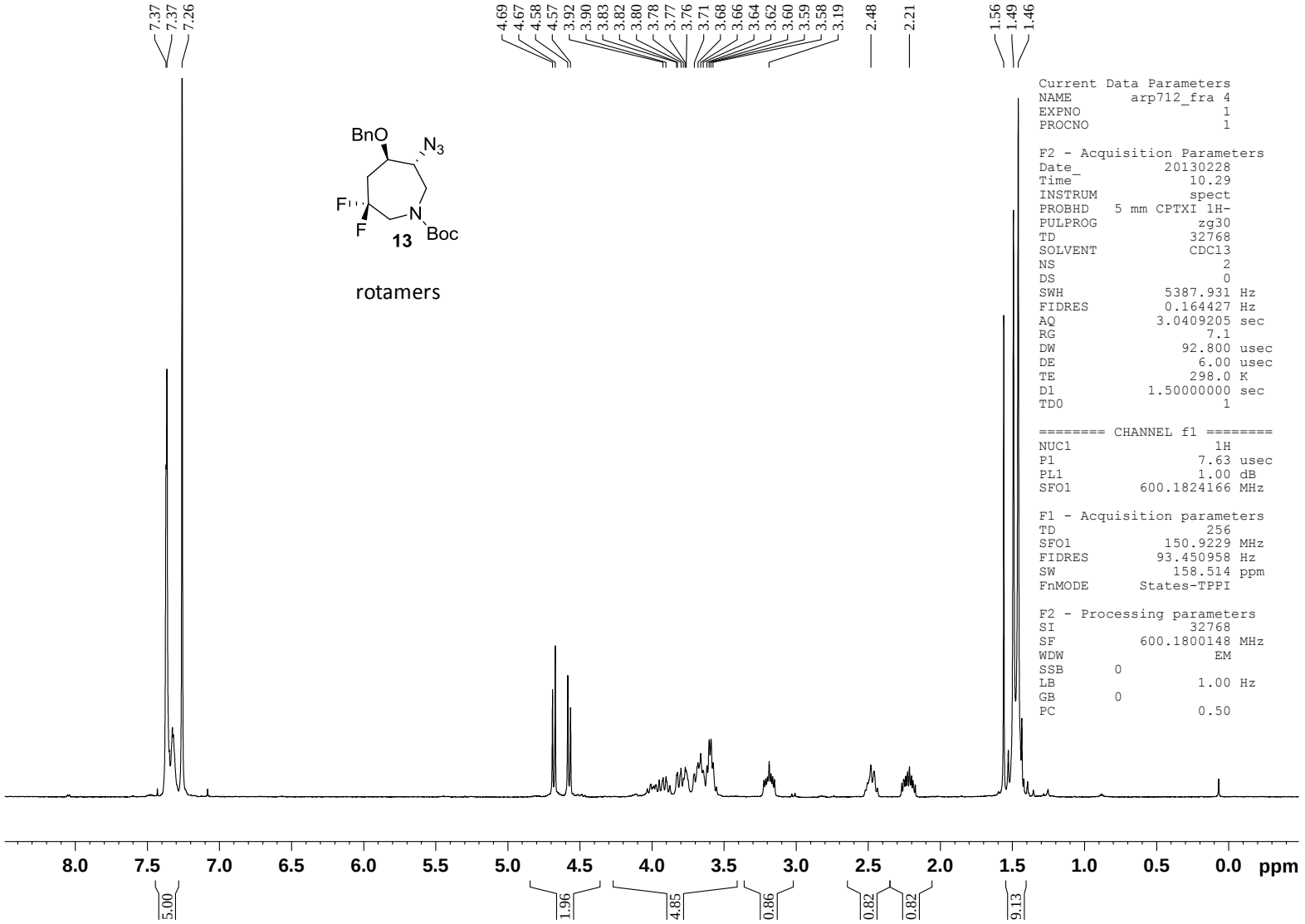


1D Selective NOESY

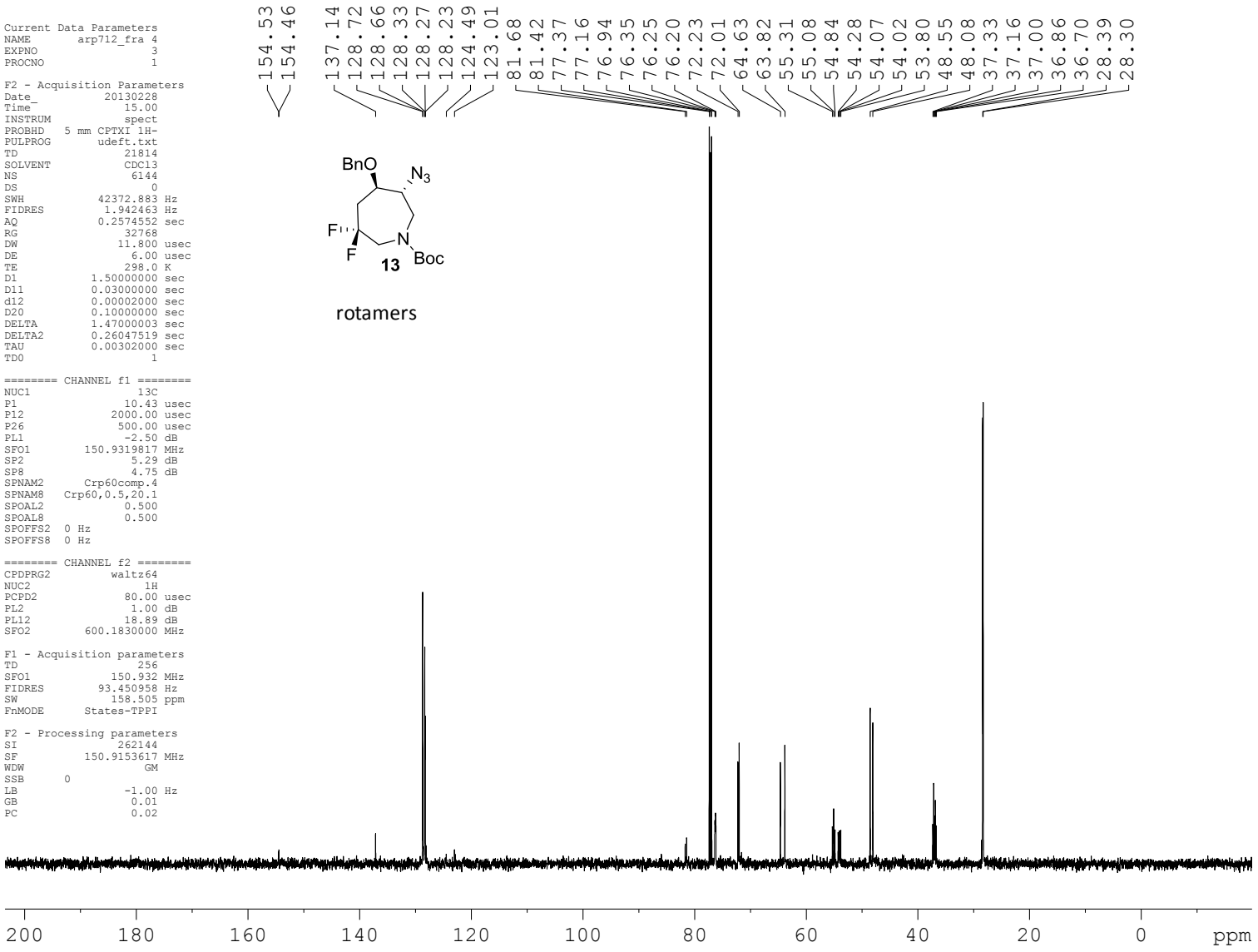




^{1}H NMR-**13**


7.37
7.37
7.26
4.69
4.67
4.58
4.57
3.92
3.90
3.83
3.82
3.80
3.78
3.77
3.76
3.71
3.68
3.66
3.64
3.62
3.60
3.59
3.58
3.19
2.48
2.21
1.56
1.49
1.46
BnO
N3
F
F
N
Boc
13
rotamers
Current Data Parameters
NAME arp712_fra 4
EXPNO 1
PROCNO 1
F2 - Acquisition Parameters
Date_ 20130228
Time 10.29
INSTRUM spect
PROBHD 5 mm CPTXI 1H-
PULPROG zg30
TD 32768
SOLVENT CDCl3
NS 2
DS 0
SWH 5387.931 Hz
FIDRES 0.164427 Hz
AQ 3.0409205 sec
RG 7.1
DW 92.800 usec
DE 6.00 usec
TE 298.0 K
D1 1.50000000 sec
TD0 1
======== CHANNEL f1 ========
NUC1 1H
P1 7.63 usec
PL1 1.00 dB
SFO1 600.1824166 MHz
F1 - Acquisition parameters
TD 256
SFO1 150.9229 MHz
FIDRES 93.450958 Hz
SW 158.514 ppm
FnMODE States-TPPI
F2 - Processing parameters
SI 32768
SF 600.1800148 MHz
WDW EM
SSB 0
LB 1.00 Hz
GB 0
PC 0.50
8.0
7.5
7.0
6.5
6.0
5.5
5.0
4.5
4.0
3.5
3.0
2.5
2.0
1.5
1.0
0.5
0.0
ppm
5.00
1.96
4.85
0.86
0.82
0.82
9.13

^{13}C NMR-**13**




```
Current Data Parameters
NAME       arp712_fra 4
EXPNO                3
PROCNO               1

F2 - Acquisition Parameters
Date_           20130228
Time               15.00
INSTRUM            spect
PROBHD   5 mm CPTXI 1H-
PULPROG       udeft.txt
TD                 21814
SOLVENT            CDC13
NS                  6144
DS                     0
SWH            42372.883 Hz
FIDRES          1.942463 Hz
AQ              0.2574552 sec
RG                  32768
DW                 11.800 usec
DE                  6.00 usec
TE                 298.0 K
D1            1.50000000 sec
D11           0.03000000 sec
d12           0.00002000 sec
D20           0.10000000 sec
DELTA         1.47000003 sec
DELTA2        0.26047519 sec
TAU           0.00302000 sec
TD0                    1

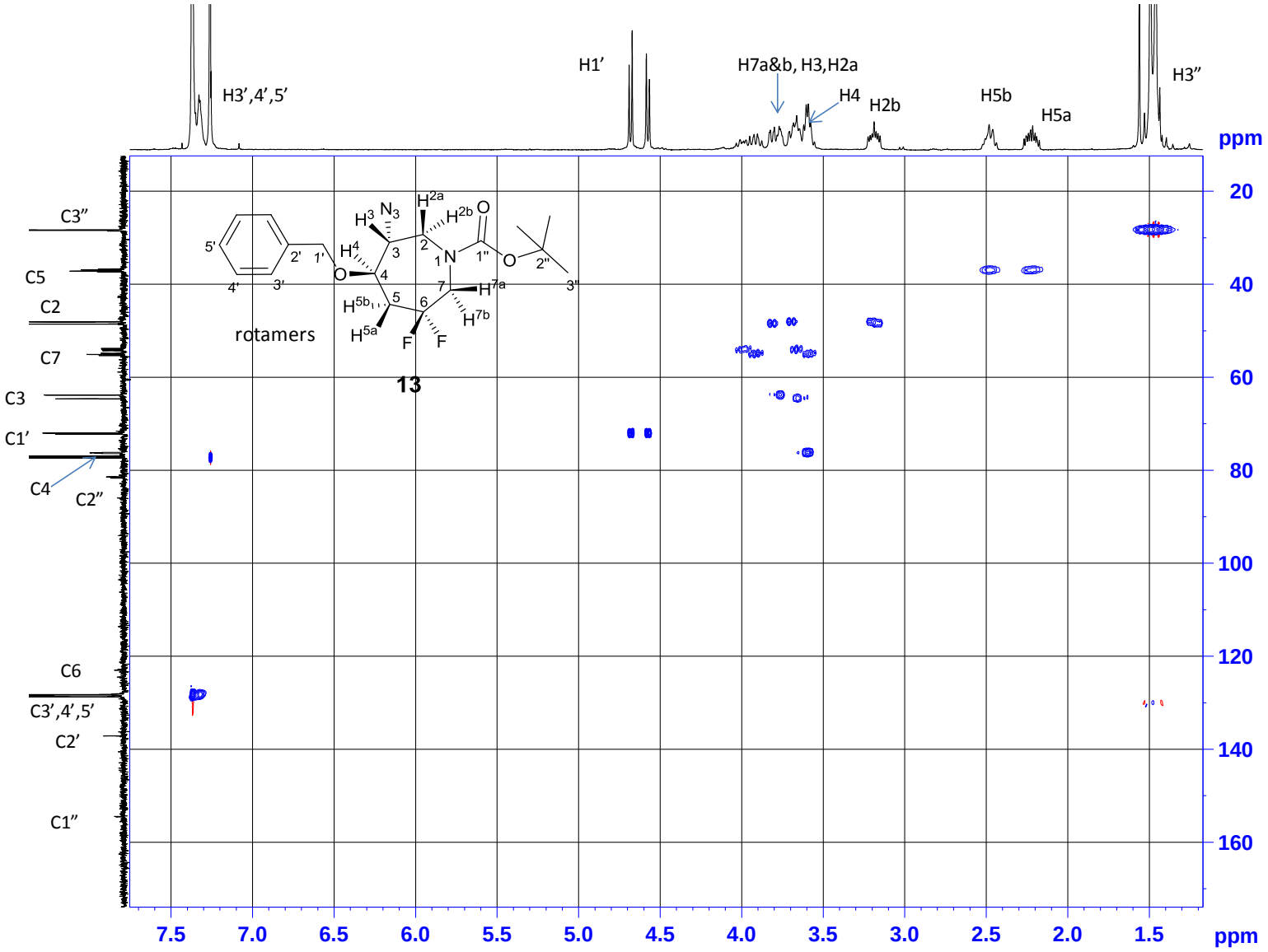
======== CHANNEL f1 ========
NUC1                13C
P1                10.43 usec
P12             2000.00 usec
P26              500.00 usec
PL1               -2.50 dB
SFO1         150.9319817 MHz
SP2                5.29 dB
SP8                4.75 dB
SPNAM2       Crp60comp.4
SPNAM8    Crp60,0.5,20.1
SPOAL2             0.500
SPOAL8             0.500
SPOFFS2  0 Hz
SPOFFS8  0 Hz

======== CHANNEL f2 ========
CPDPRG2          waltz64
NUC2                1H
PCPD2              80.00 usec
PL2                 1.00 dB
PL12               18.89 dB
SFO2         600.1830000 MHz

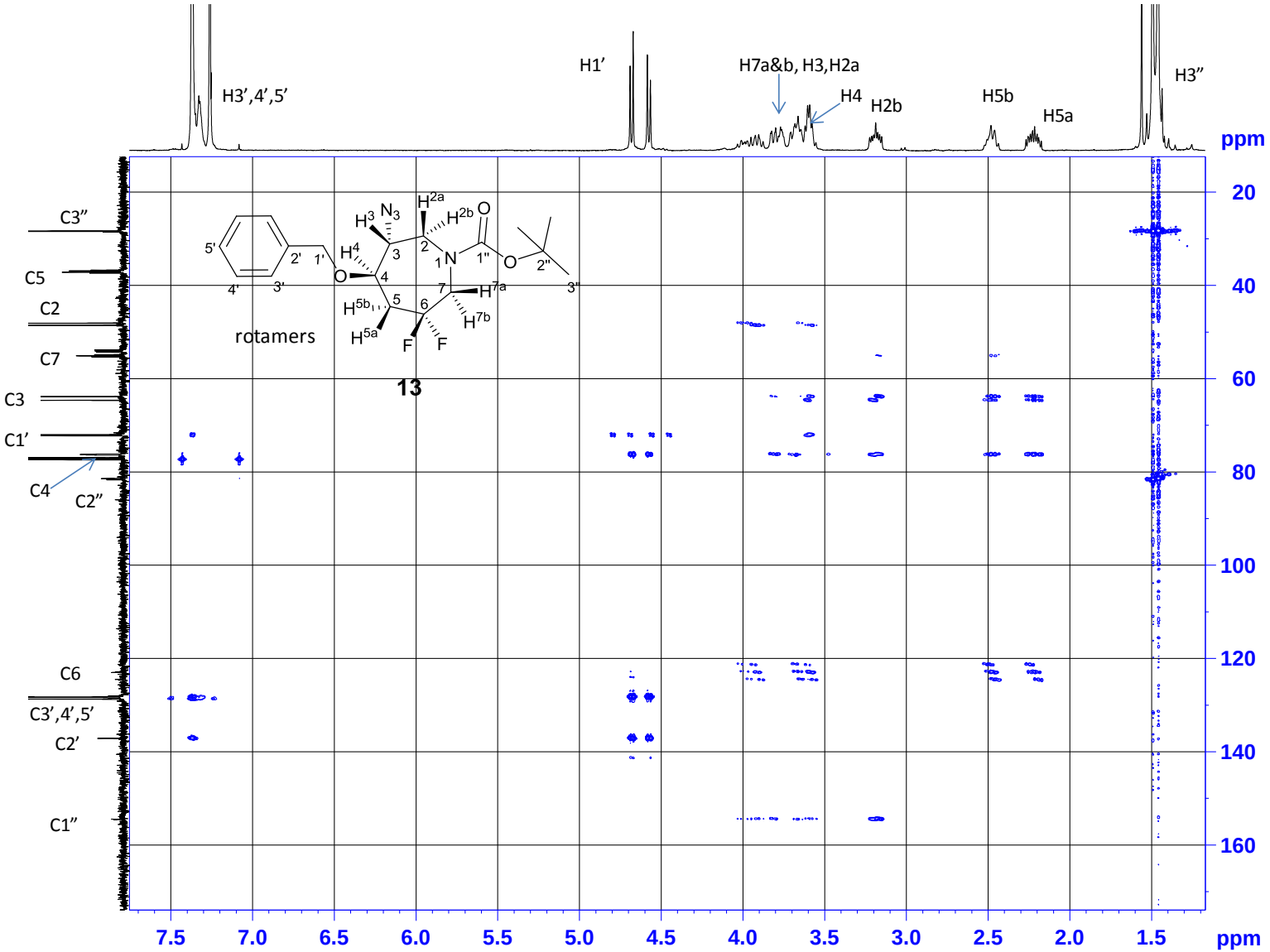
F1 - Acquisition parameters
TD                  256
SFO1            150.932 MHz
FIDRES         93.450958 Hz
SW                158.505 ppm
FnMODE       States-TPPI

F2 - Processing parameters
SI                  262144
SF             150.9153617 MHz
WDW                    GM
SSB      0
LB                 -1.00 Hz
GB                  0.01
PC                  0.02
```

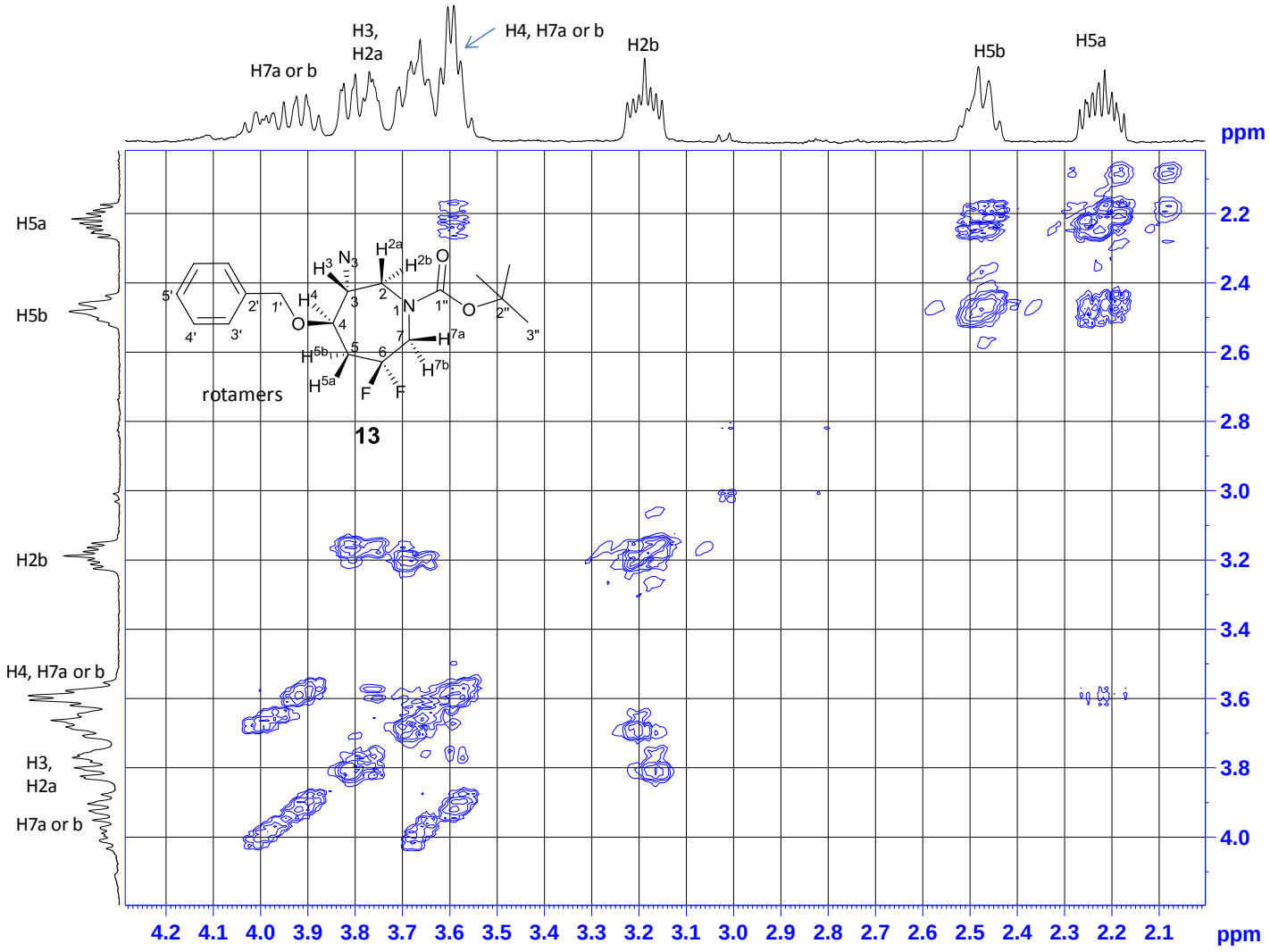
HSQC-**13**


H3',4',5'
H1'
H7a&b, H3,H2a
H4
H2b
H5b
H5a
H3"
ppm
20
40
60
80
100
120
140
160
C3"
C5
C2
C7
C3
C1'
C4
C2"
C6
C3',4',5'
C2'
C1"
rotamers
13
7.5
7.0
6.5
6.0
5.5
5.0
4.5
4.0
3.5
3.0
2.5
2.0
1.5
ppm

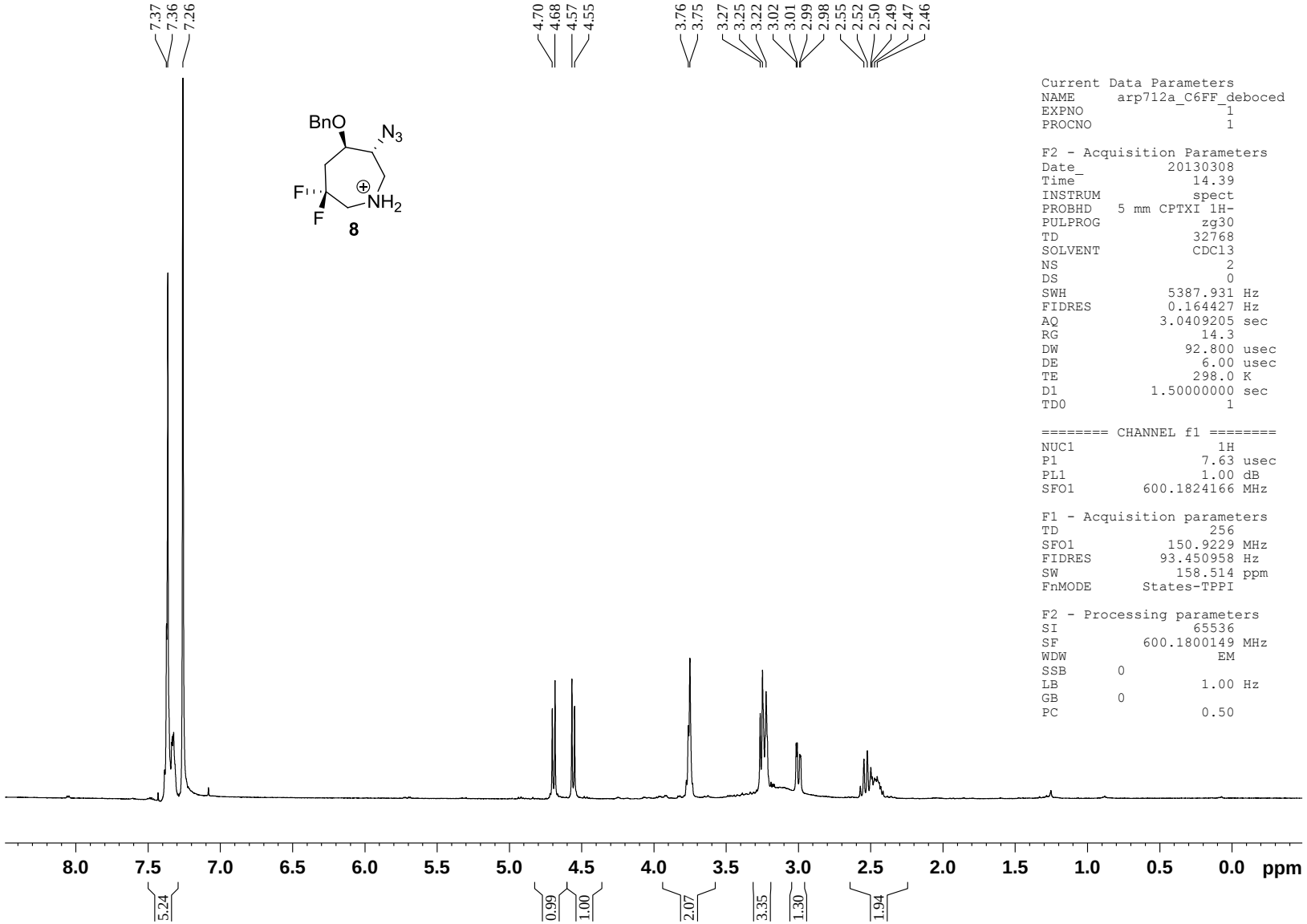
HMBC-**13**


H3',4',5'
H1'
H7a&b, H3,H2a
H4
H2b
H5b
H5a
H3"
ppm
C3"
C5
C2
C7
C3
C1'
C4
C2"
C6
C3',4',5'
C2'
C1"
rotamers
13
7.5
7.0
6.5
6.0
5.5
5.0
4.5
4.0
3.5
3.0
2.5
2.0
1.5
ppm

COSY-**13**


H7a or b
H3,
H2a
H4, H7a or b
H2b
H5b
H5a
ppm
rotamers
13
4.2 4.1 4.0 3.9 3.8 3.7 3.6 3.5 3.4 3.3 3.2 3.1 3.0 2.9 2.8 2.7 2.6 2.5 2.4 2.3 2.2 2.1
ppm
2.2
2.4
2.6
2.8
3.0
3.2
3.4
3.6
3.8
4.0

^{1}H NMR-**8**




```
Current Data Parameters
NAME      arp712a_C6FF_deboced
EXPNO                        1
PROCNO                       1

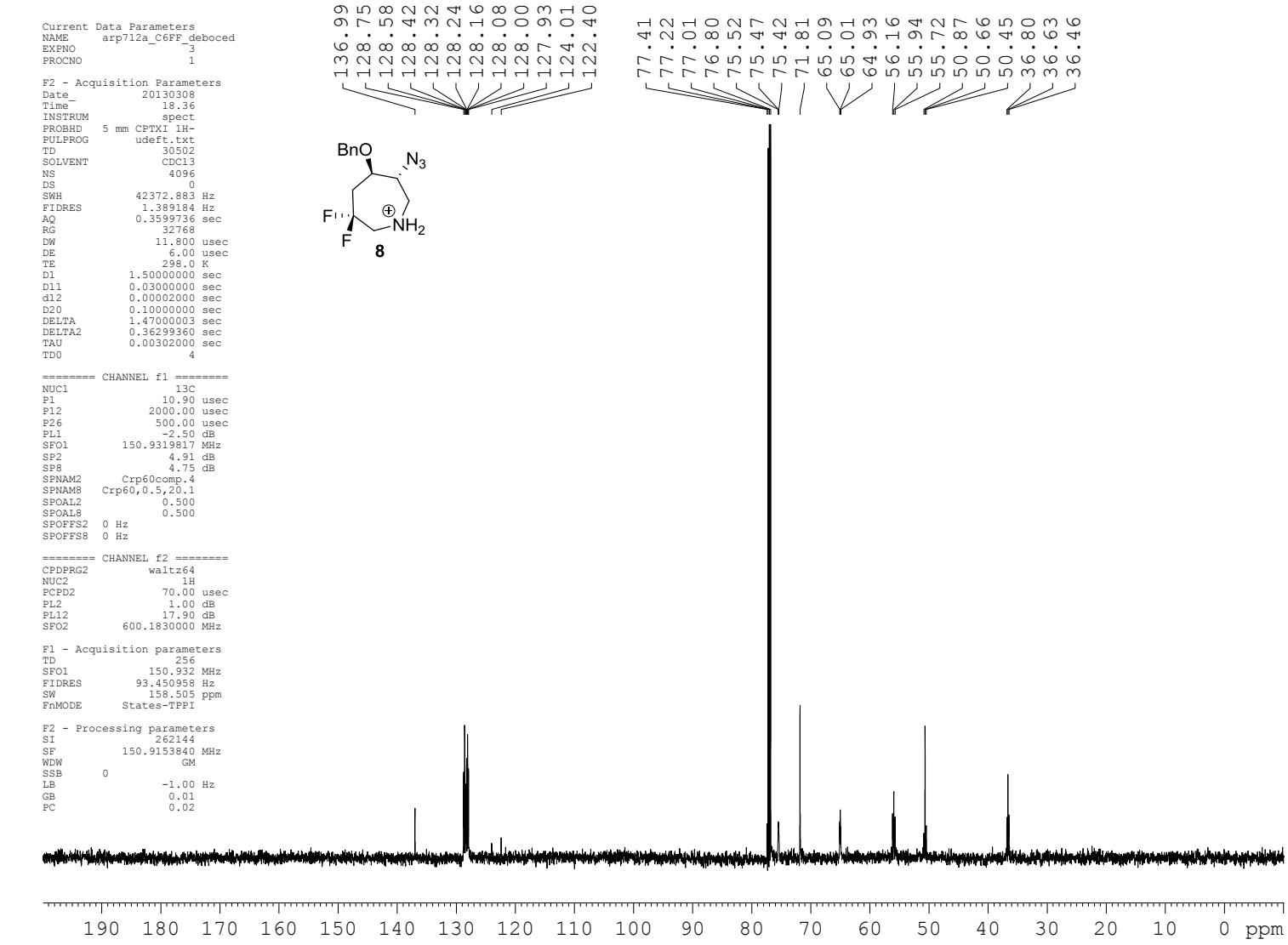
F2 - Acquisition Parameters
Date_              20130308
Time                  14.39
INSTRUM               spect
PROBHD   5 mm CPTXI 1H-
PULPROG                zg30
TD                    32768
SOLVENT               CDCl3
NS                        2
DS                        0
SWH                5387.931 Hz
FIDRES            0.164427 Hz
AQ                3.0409205 sec
RG                     14.3
DW                   92.800 usec
DE                    6.00 usec
TE                   298.0 K
D1              1.50000000 sec
TD0                       1

======== CHANNEL f1 ========
NUC1                     1H
P1                    7.63 usec
PL1                   1.00 dB
SFO1          600.1824166 MHz

F1 - Acquisition parameters
TD                      256
SFO1              150.9229 MHz
FIDRES           93.450958 Hz
SW                 158.514 ppm
FnMODE         States-TPPI

F2 - Processing parameters
SI                    65536
SF              600.1800149 MHz
WDW                      EM
SSB         0
LB                    1.00 Hz
GB          0
PC                    0.50
```

^{13}C NMR-**8**




```
Current Data Parameters
NAME     arp712a_C6FF_deboced
EXPNO                   3
PROCNO                  1

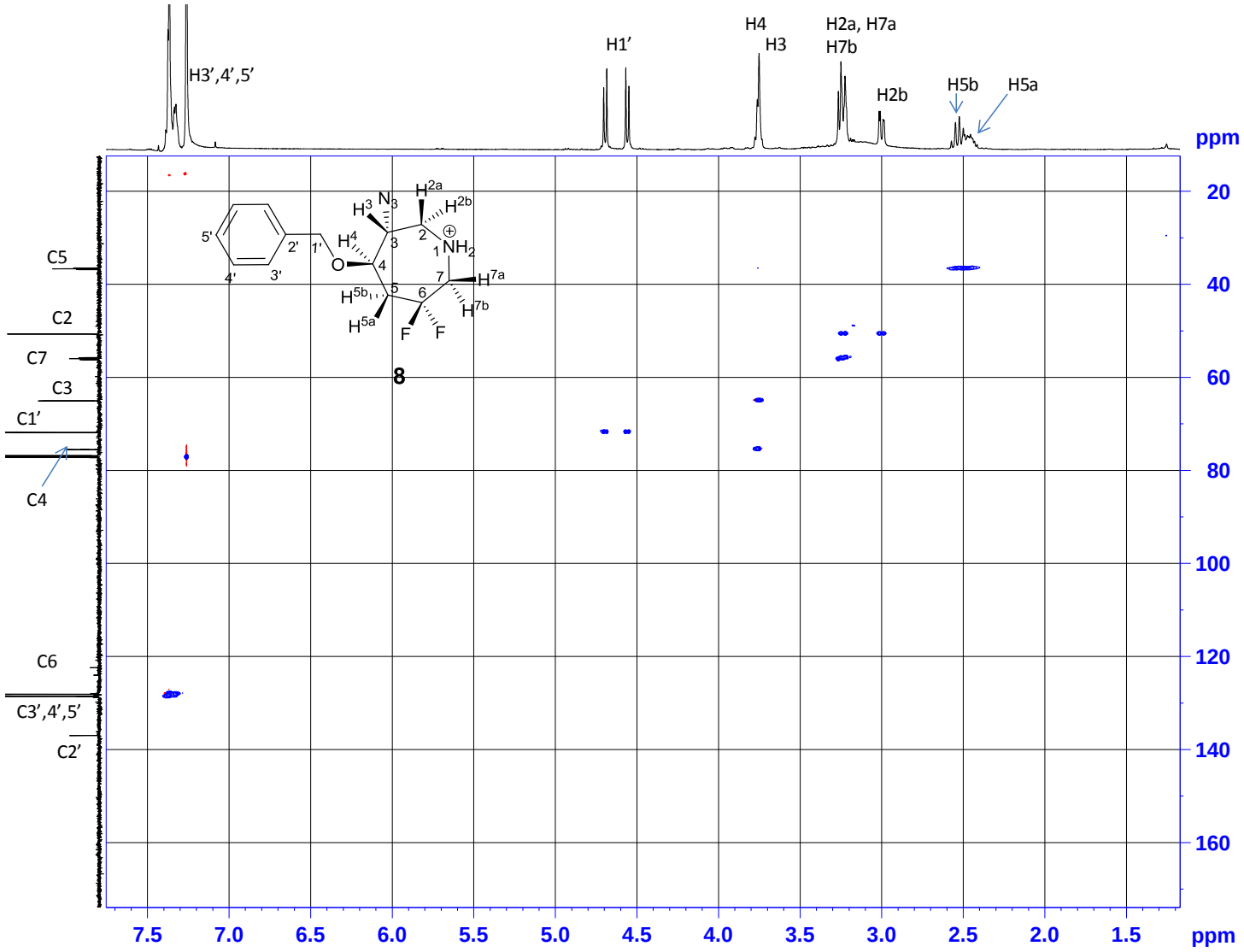
F2 - Acquisition Parameters
Date_           20130308
Time              18.36
INSTRUM           spect
PROBHD   5 mm CPTXI 1H-
PULPROG        udeft.txt
TD                30502
SOLVENT           CDCl3
NS                 4096
DS                    0
SWH           42372.883 Hz
FIDRES         1.389184 Hz
AQ            0.3599736 sec
RG                32768
DW               11.800 usec
DE                6.00 usec
TE                298.0 K
D1           1.50000000 sec
D11          0.03000000 sec
d12          0.00002000 sec
D20          0.10000000 sec
DELTA        1.47000003 sec
DELTA2       0.36299360 sec
TAU          0.00302000 sec
TD0                   4

======== CHANNEL f1 ========
NUC1                 13C
P1                10.90 usec
P12             2000.00 usec
P26              500.00 usec
PL1               -2.50 dB
SFO1        150.9319817 MHz
SP2               4.91 dB
SP8               4.75 dB
SPNAM2      Crp60comp.4
SPNAM8   Crp60,0.5,20.1
SPOAL2             0.500
SPOAL8             0.500
SPOFFS2  0 Hz
SPOFFS8  0 Hz

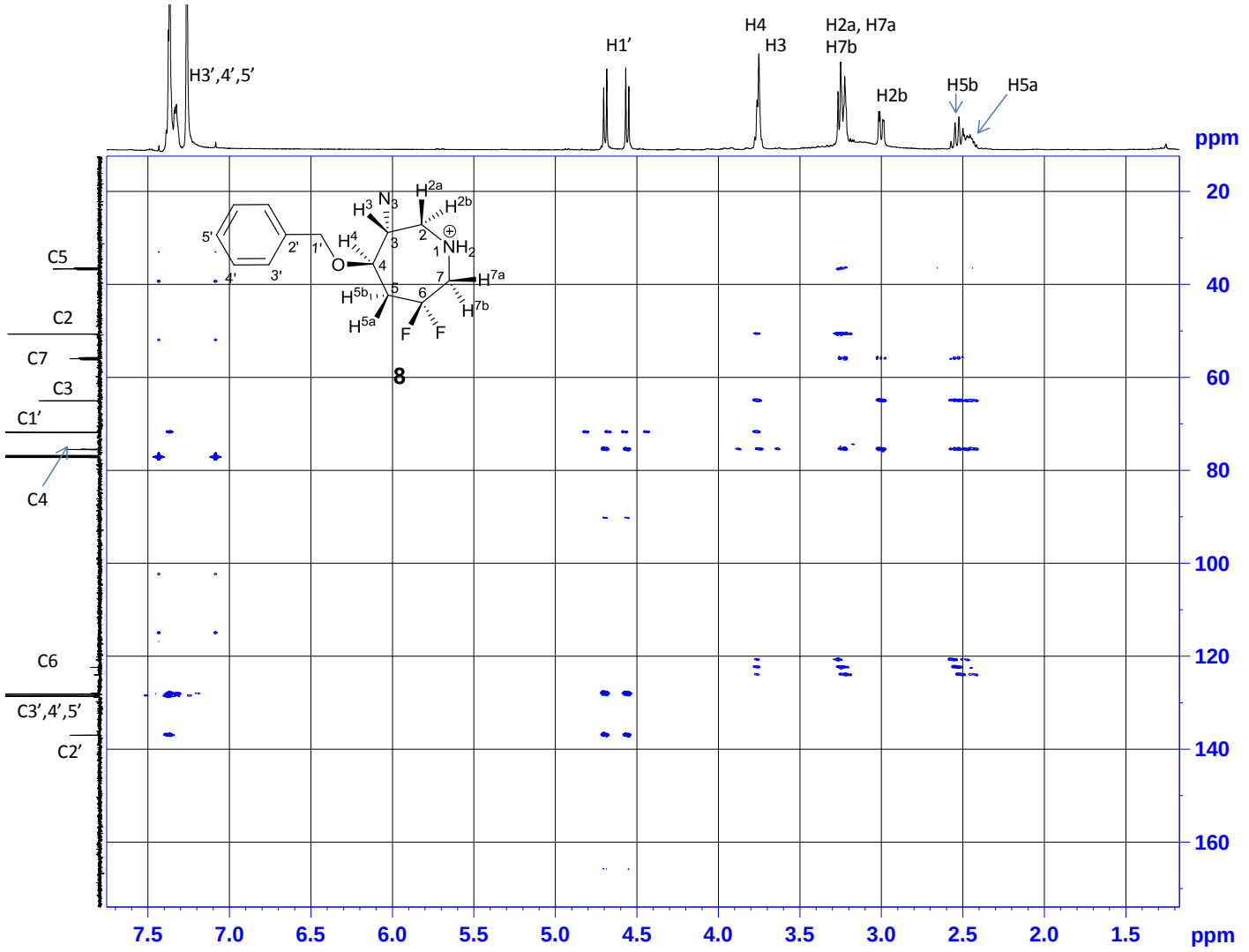
======== CHANNEL f2 ========
CPDPRG2          waltz64
NUC2                 1H
PCPD2             70.00 usec
PL2                1.00 dB
PL12              17.90 dB
SFO2        600.1830000 MHz

F1 - Acquisition parameters
TD                  256
SFO1            150.932 MHz
FIDRES        93.450958 Hz
SW              158.505 ppm
FnMODE      States-TPPI

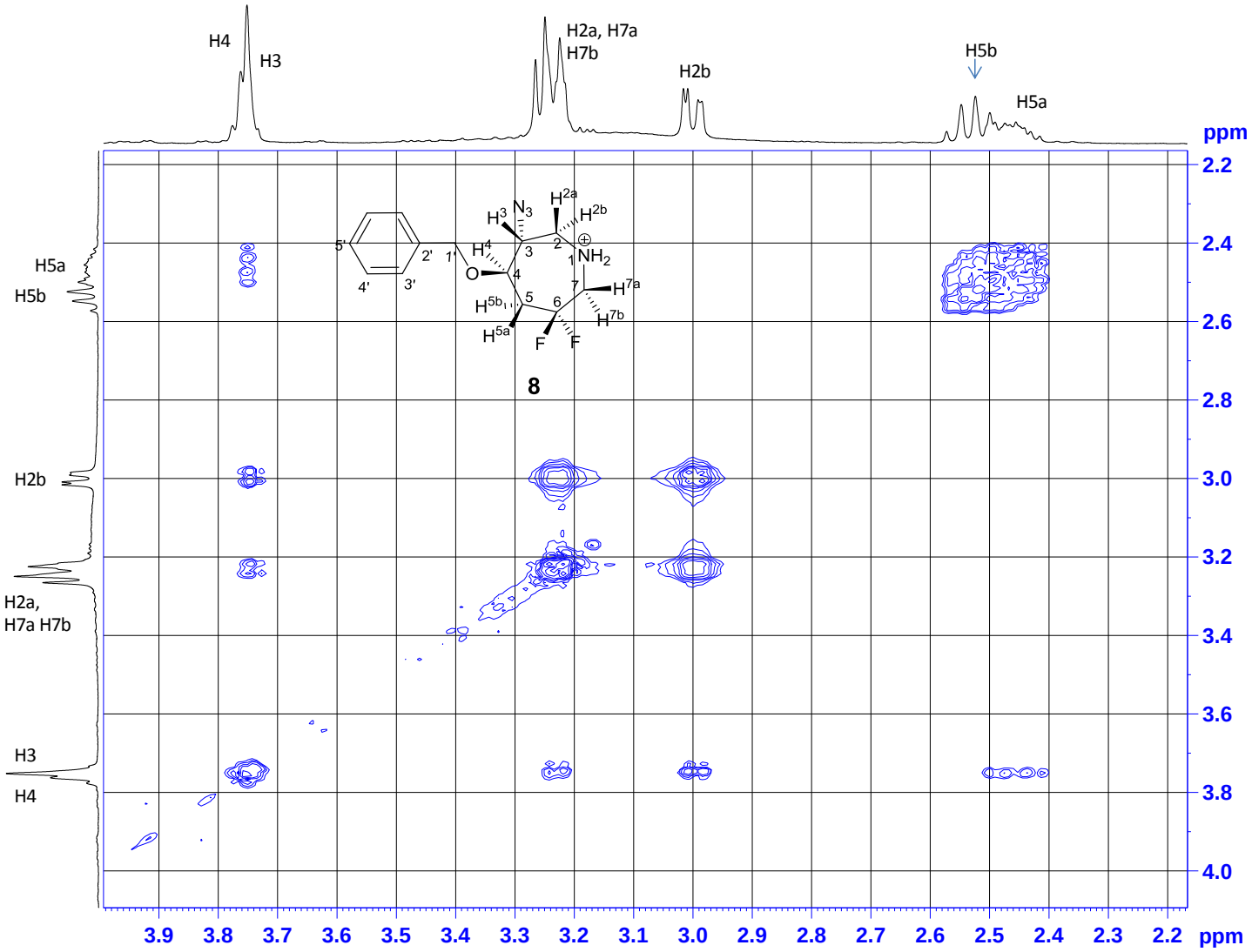
F2 - Processing parameters
SI                262144
SF          150.9153840 MHz
WDW                 GM
SSB      0
LB                -1.00 Hz
GB                 0.01
PC                 0.02
```

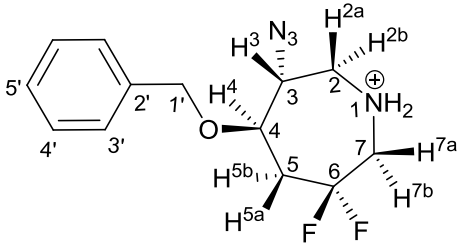

H3',4',5'
H1'
H4
H3
H2a, H7a
H7b
H2b
H5b
H5a
ppm
C5
C2
C7
C3
C1'
C4
C6
C3',4',5'
C2'
8
7.5
7.0
6.5
6.0
5.5
5.0
4.5
4.0
3.5
3.0
2.5
2.0
1.5
ppm

HMBC-**8**

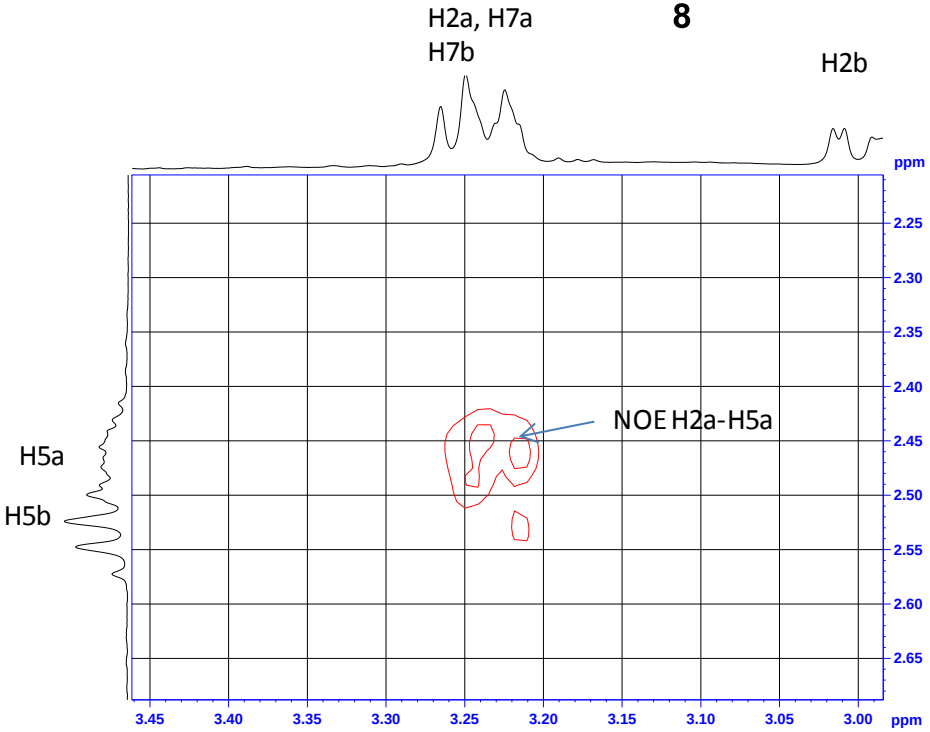

H3',4',5'
H1'
H4
H3
H2a, H7a
H7b
H2b
H5b
H5a
ppm
C5
C2
C7
C3
C1'
C4
C6
C3',4',5'
C2'
8
7.5
7.0
6.5
6.0
5.5
5.0
4.5
4.0
3.5
3.0
2.5
2.0
1.5
ppm
20
40
60
80
100
120
140
160

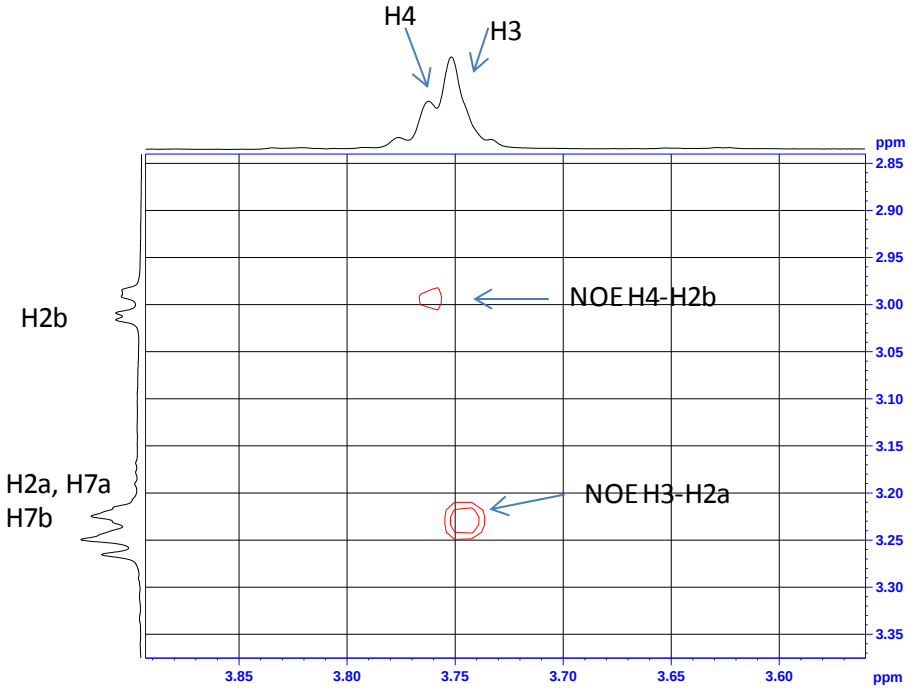
COSY-**8**


H4
H3
H2a, H7a
H7b
H2b
H5b
H5a
ppm
2.2
2.4
2.6
2.8
3.0
3.2
3.4
3.6
3.8
4.0
H5a
H5b
H2b
H2a,
H7a H7b
H3
H4
3.9 3.8 3.7 3.6 3.5 3.4 3.3 3.2 3.1 3.0 2.9 2.8 2.7 2.6 2.5 2.4 2.3 2.2 ppm
8

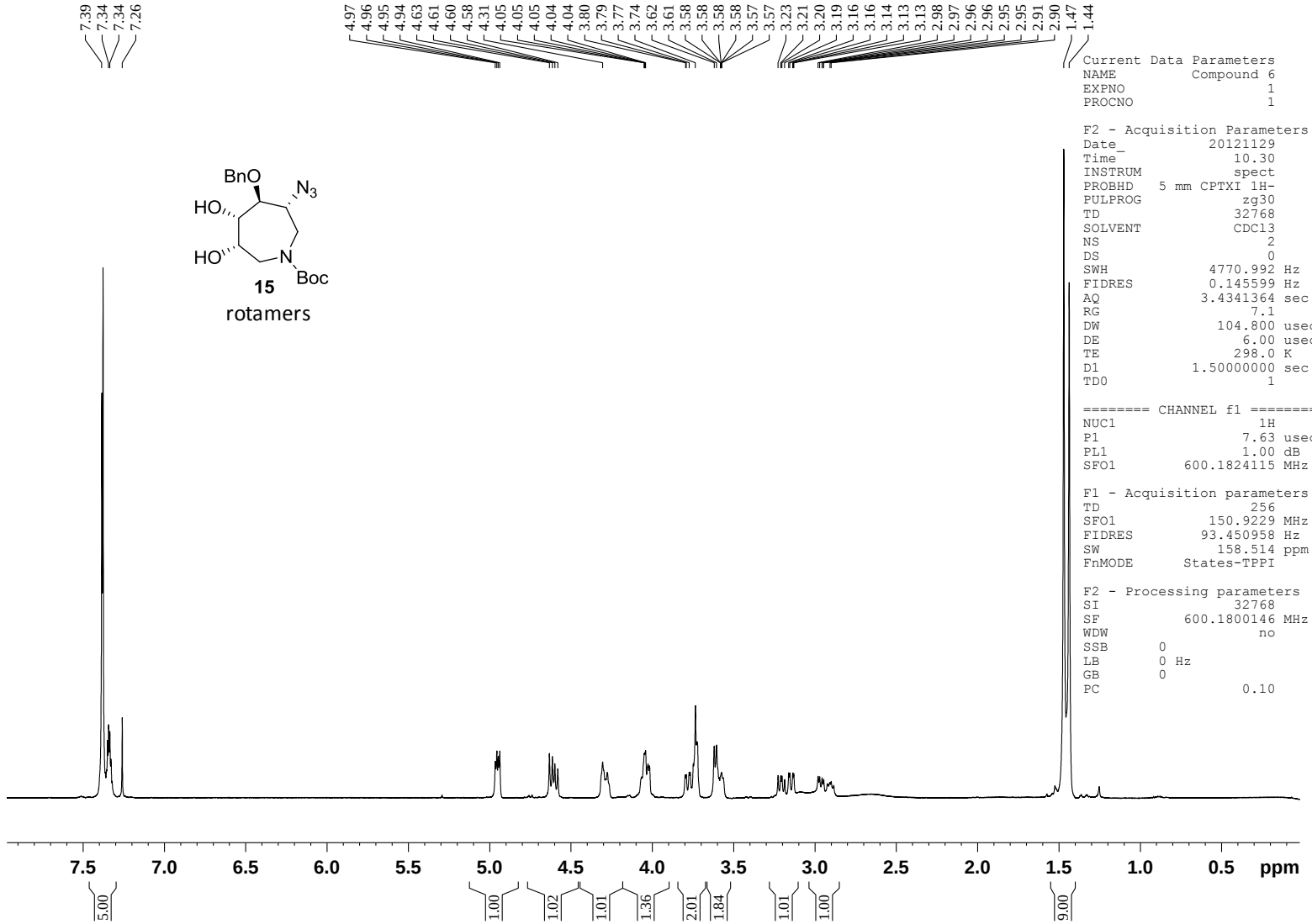

5'
2'
1'
4'
3'
O
4
3
2
1
NH2
5
6
7
F
F
N3
H3
H4
H2a
H2b
H5a
H5b
H7a
H7b

8

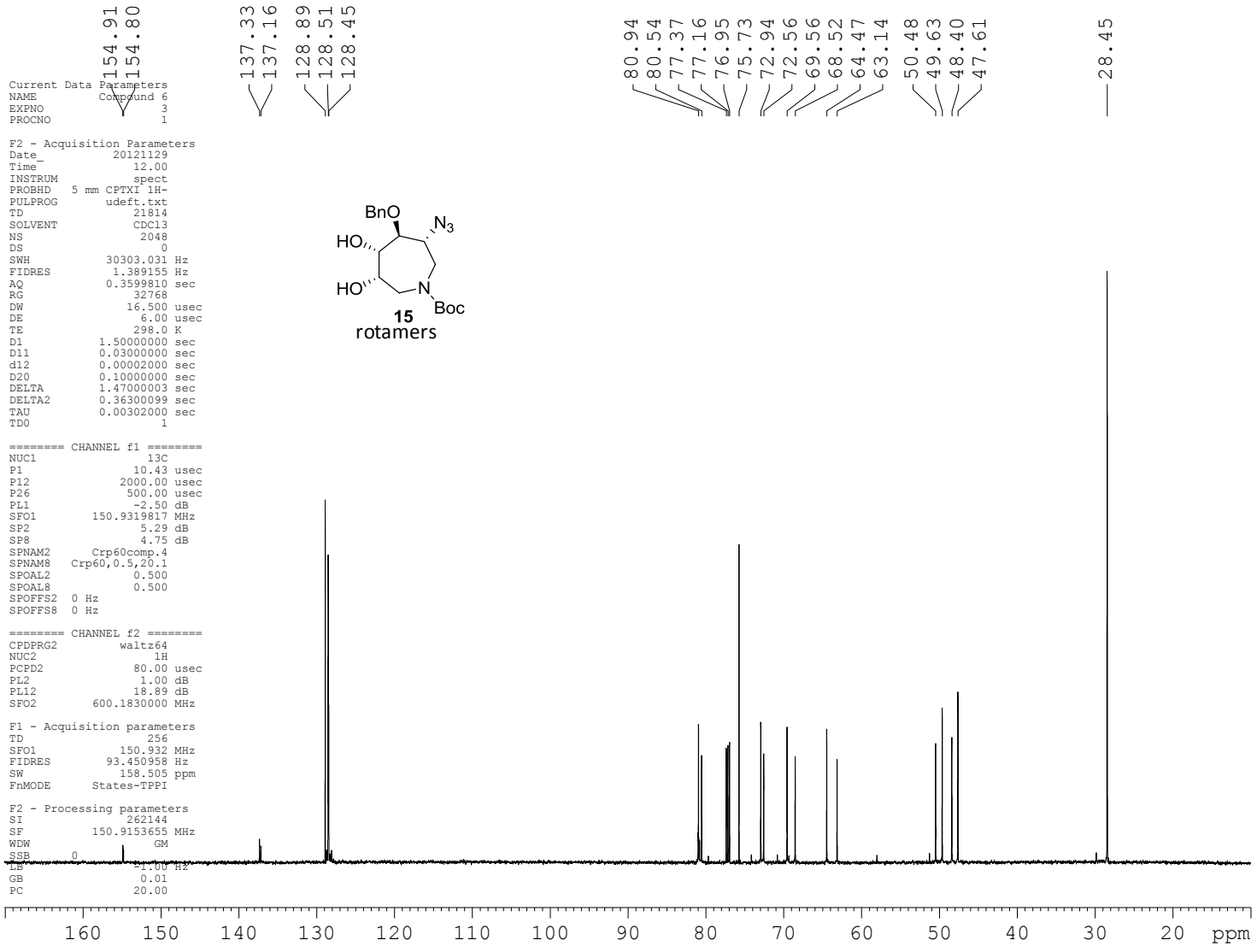

H2a, H7a
H7b
H2b
H5a
H5b
NOE H2a-H5a
ppm
2.25
2.30
2.35
2.40
2.45
2.50
2.55
2.60
2.65
3.45
3.40
3.35
3.30
3.25
3.20
3.15
3.10
3.05
3.00
ppm

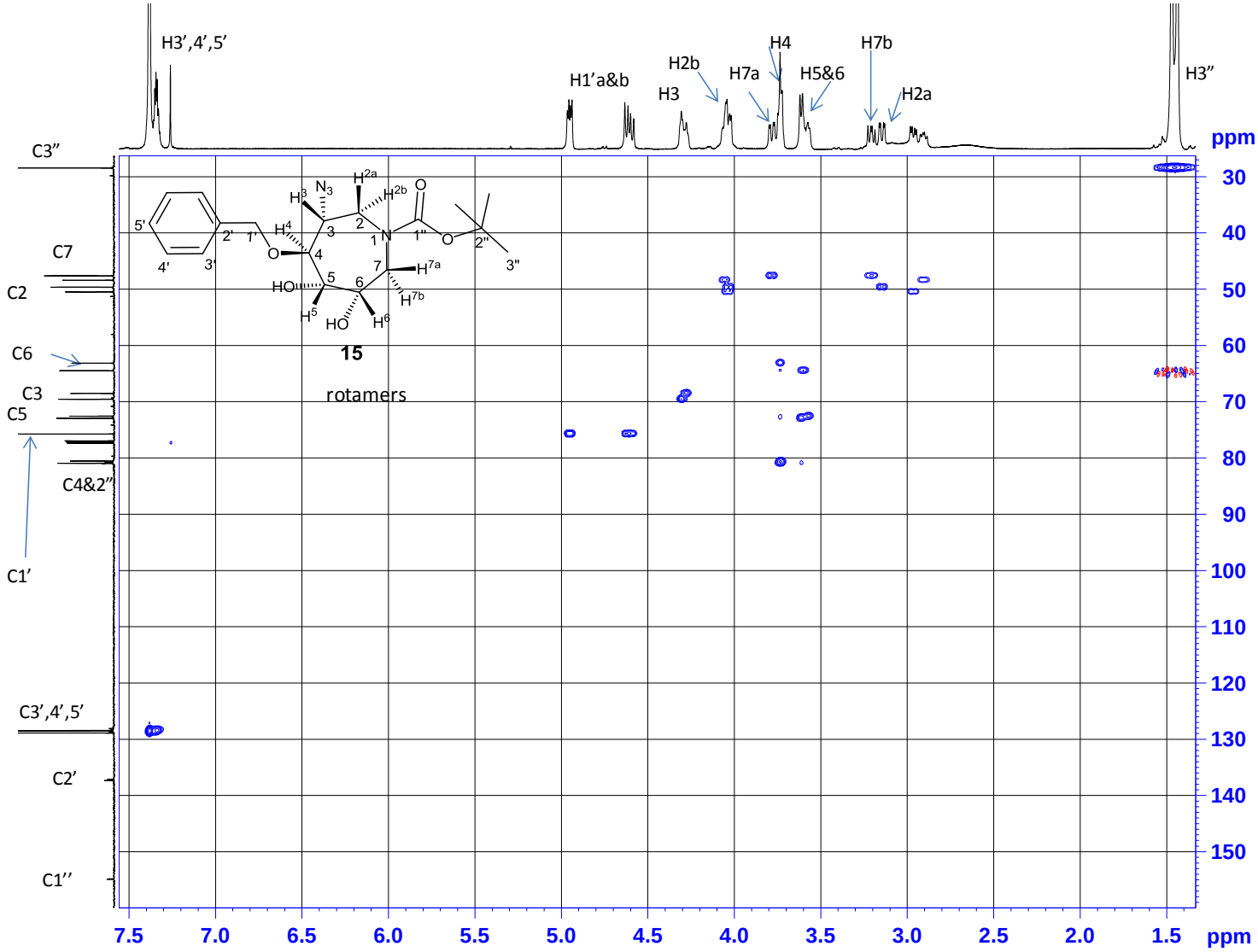

H4
H3
H2b
H2a, H7a
H7b
NOE H4-H2b
NOE H3-H2a
ppm
2.85
2.90
2.95
3.00
3.05
3.10
3.15
3.20
3.25
3.30
3.35
3.85
3.80
3.75
3.70
3.65
3.60
ppm

^{1}H NMR-**15**

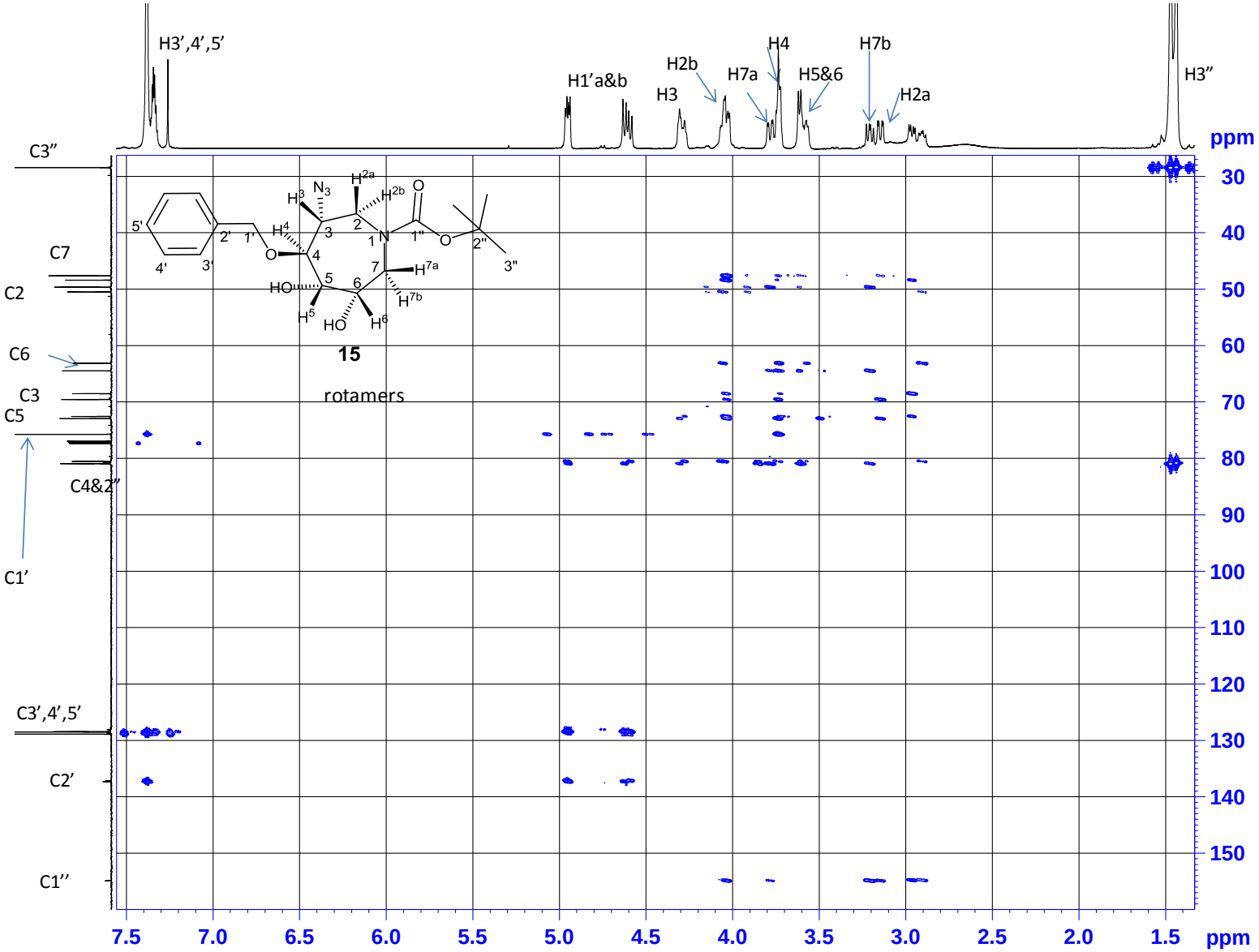

7.39
7.34
7.34
7.26
4.97
4.96
4.95
4.94
4.63
4.61
4.60
4.58
4.31
4.05
4.05
4.05
4.04
4.04
3.80
3.79
3.77
3.74
3.62
3.61
3.58
3.58
3.58
3.58
3.57
3.57
3.23
3.21
3.20
3.19
3.16
3.16
3.14
3.13
3.13
2.98
2.97
2.96
2.96
2.95
2.95
2.91
2.90
1.47
1.44
BnO
N3
HO
HO
N
Boc
15
rotamers
Current Data Parameters
NAME Compound 6
EXPNO 1
PROCNO 1
F2 - Acquisition Parameters
Date_ 20121129
Time 10.30
INSTRUM spect
PROBHD 5 mm CPTXI 1H-
PULPROG zg30
TD 32768
SOLVENT CDCl3
NS 2
DS 0
SWH 4770.992 Hz
FIDRES 0.145599 Hz
AQ 3.4341364 sec
RG 7.1
DW 104.800 usec
DE 6.00 usec
TE 298.0 K
D1 1.50000000 sec
TD0 1
======== CHANNEL f1 ========
NUC1 1H
P1 7.63 usec
PL1 1.00 dB
SFO1 600.1824115 MHz
F1 - Acquisition parameters
TD 256
SFO1 150.9229 MHz
FIDRES 93.450958 Hz
SW 158.514 ppm
FnMODE States-TPPI
F2 - Processing parameters
SI 32768
SF 600.1800146 MHz
WDW no
SSB 0
LB 0 Hz
GB 0
PC 0.10
7.5
7.0
6.5
6.0
5.5
5.0
4.5
4.0
3.5
3.0
2.5
2.0
1.5
1.0
0.5
ppm
5.00
1.00
1.02
1.01
1.36
2.01
1.84
1.01
1.00
9.00

^{13}C NMR-**15**

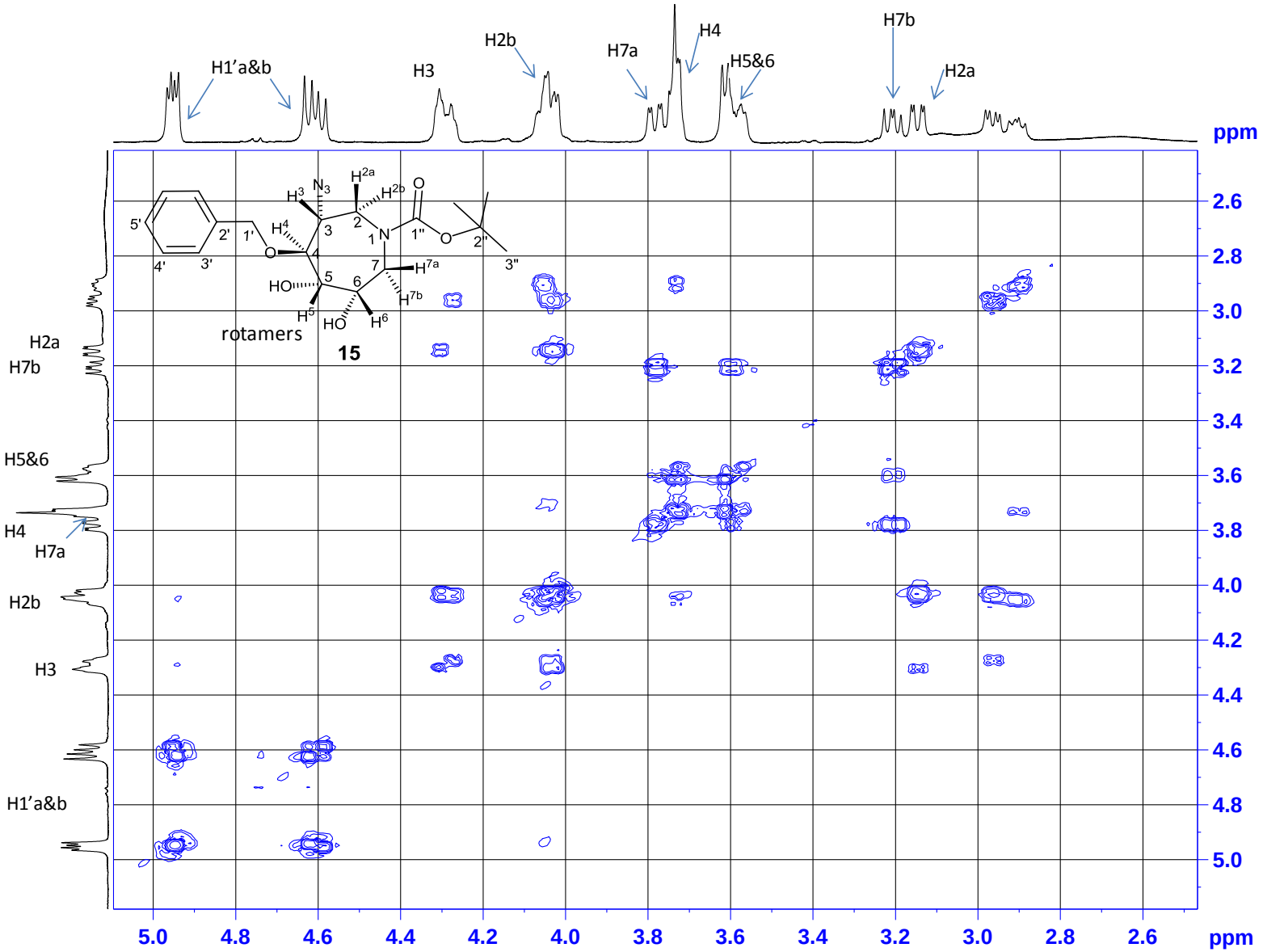

154.91
154.80
137.33
137.16
128.89
128.51
128.45
80.94
80.54
77.37
77.16
76.95
75.73
72.94
72.56
69.56
68.52
64.47
63.14
50.48
49.63
48.40
47.61
28.45
BnO
N3
HO
HO
N
Boc
15
rotamers
Current Data Parameters
NAME Compound 6
EXPNO 3
PROCNO 1
F2 - Acquisition Parameters
Date_ 20121129
Time 12.00
INSTRUM spect
PROBHD 5 mm CPTXI 1H-
PULPROG udeft.txt
TD 21814
SOLVENT CDC13
NS 2048
DS 0
SWH 30303.031 Hz
FIDRES 1.389155 Hz
AQ 0.3599810 sec
RG 32768
DW 16.500 usec
DE 6.00 usec
TE 298.0 K
D1 1.50000000 sec
D11 0.03000000 sec
d12 0.00002000 sec
D20 0.10000000 sec
DELTA 1.47000003 sec
DELTA2 0.36300099 sec
TAU 0.00302000 sec
TD0 1
======== CHANNEL f1 ========
NUC1 13C
P1 10.43 usec
P12 2000.00 usec
P26 500.00 usec
PL1 -2.50 dB
SFO1 150.9319817 MHz
SP2 5.29 dB
SP8 4.75 dB
SPNAM2 Crp60comp.4
SPNAM8 Crp60,0.5,20.1
SPOAL2 0.500
SPOAL8 0.500
SPOFFS2 0 Hz
SPOFFS8 0 Hz
======== CHANNEL f2 ========
CPDPRG2 waltz64
NUC2 1H
PCPD2 80.00 usec
PL2 1.00 dB
PL12 18.89 dB
SFO2 600.1830000 MHz
F1 - Acquisition parameters
TD 256
SFO1 150.932 MHz
FIDRES 93.450958 Hz
SW 158.505 ppm
FnMODE States-TPPI
F2 - Processing parameters
SI 262144
SF 150.9153655 MHz
WDW GM
SSB 0
LB 21.00 Hz
GB 0.01
PC 20.00
160
150
140
130
120
110
100
90
80
70
60
50
40
30
20
ppm


H3',4',5'
H1'a&b
H2b
H3
H7a
H4
H5&6
H7b
H2a
H3"
ppm
C3"
C7
C2
C6
C3
C5
C4&2"
C1'
C3',4',5'
C2'
C1''
15
rotamers
7.5
7.0
6.5
6.0
5.5
5.0
4.5
4.0
3.5
3.0
2.5
2.0
1.5
ppm

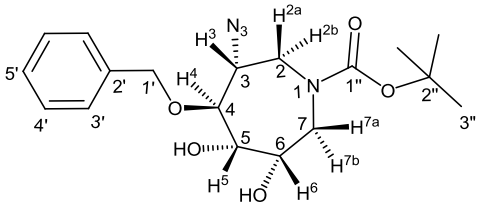
HMBC-**15**


H3',4',5'
H1'a&b
H2b
H3
H7a
H4
H5&6
H7b
H2a
H3"
ppm
C3"
C7
C2
C6
C3
C5
C4&2"
C1'
C3',4',5'
C2'
C1''
15
rotamers
7.5
7.0
6.5
6.0
5.5
5.0
4.5
4.0
3.5
3.0
2.5
2.0
1.5
ppm

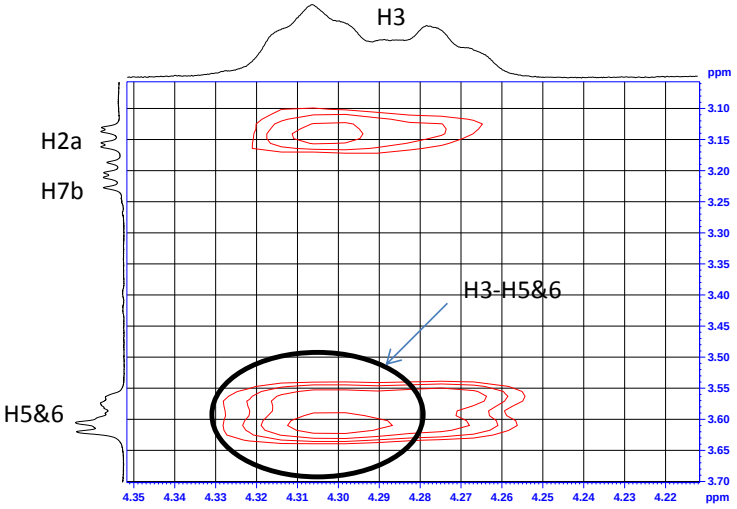
COSY-**15**


H1'a&b
H3
H2b
H7a
H4
H5&6
H7b
H2a
ppm
rotamers
15
H2a
H7b
H5&6
H4
H7a
H2b
H3
H1'a&b
5.0
4.8
4.6
4.4
4.2
4.0
3.8
3.6
3.4
3.2
3.0
2.8
2.6
ppm

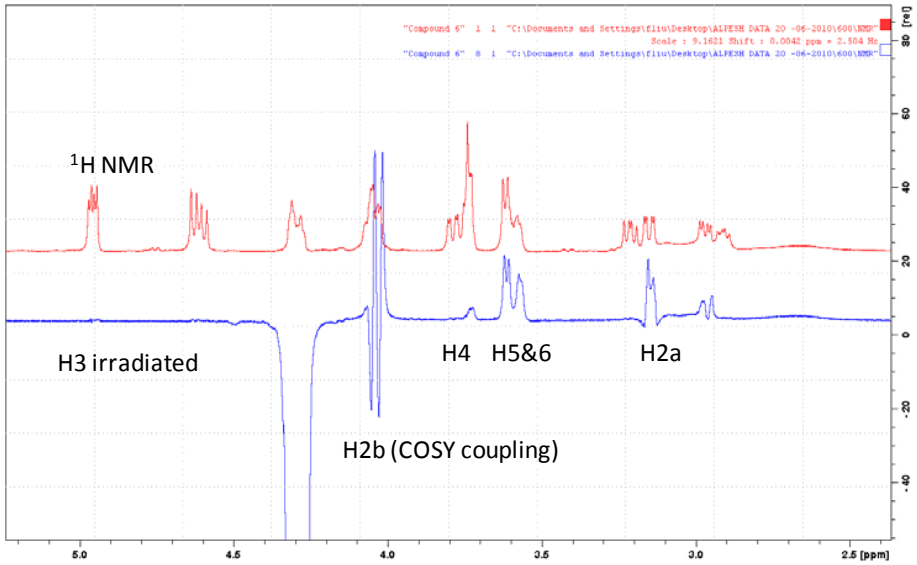
NOESY-**15**



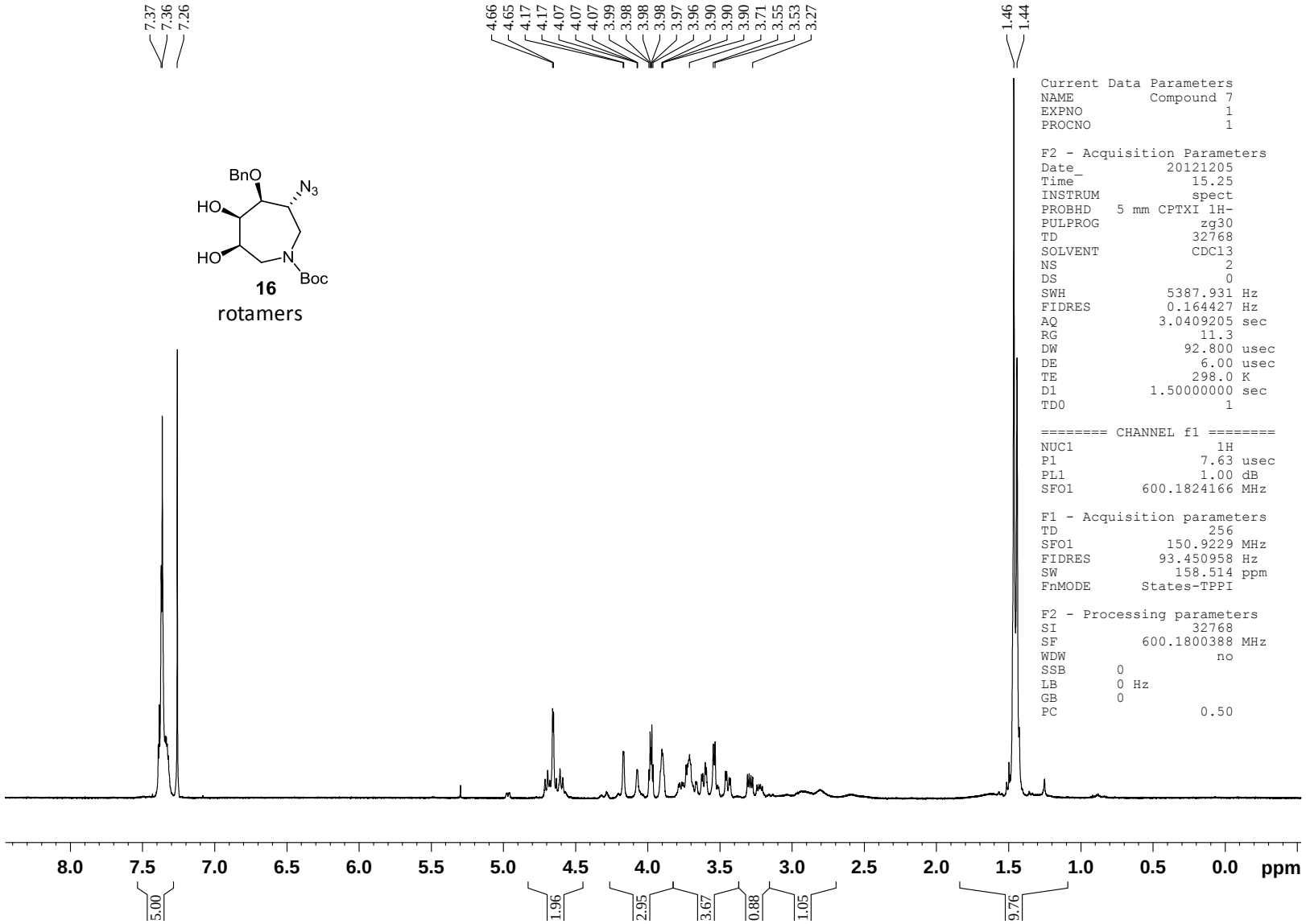
rotamers **15**



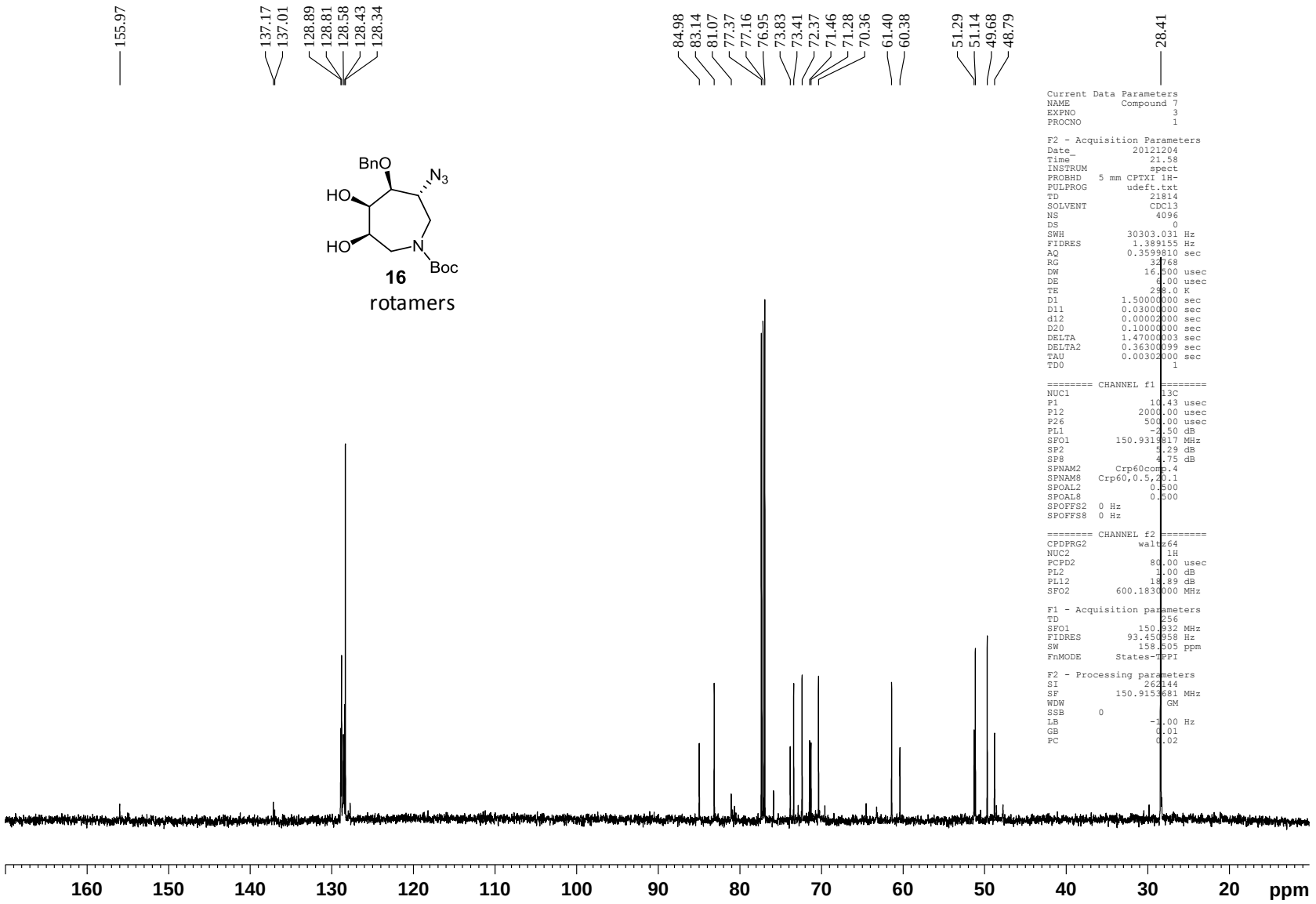
1D selective NOESY



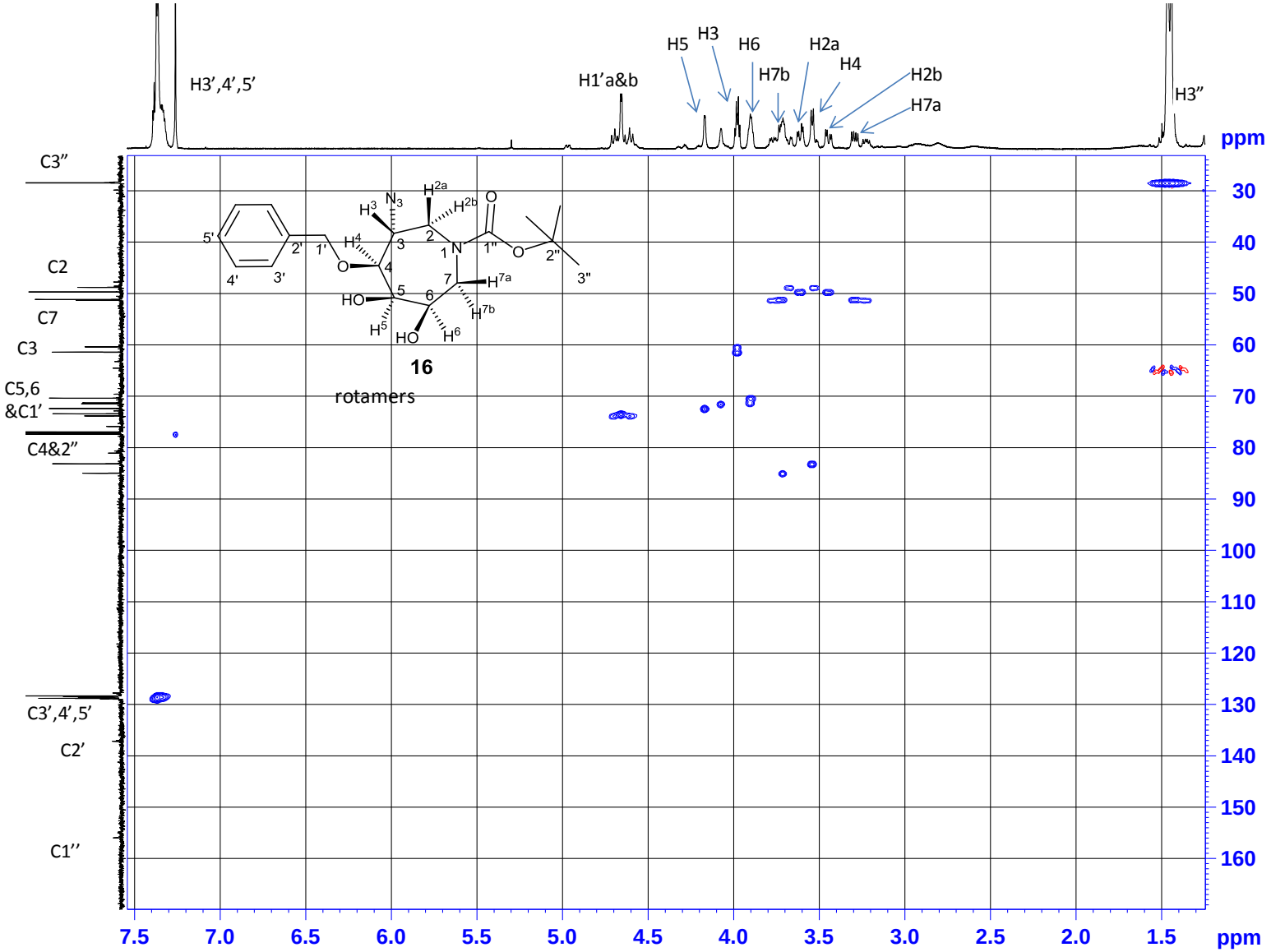
^{1}H NMR-**16**


7.37
7.36
7.26
4.66
4.65
4.17
4.17
4.07
4.07
4.07
3.99
3.98
3.98
3.97
3.96
3.90
3.90
3.90
3.71
3.55
3.53
3.27
1.46
1.44
BnO
N3
HO
HO
N
Boc
16
rotamers
Current Data Parameters
NAME Compound 7
EXPNO 1
PROCNO 1
F2 - Acquisition Parameters
Date_ 20121205
Time 15.25
INSTRUM spect
PROBHD 5 mm CPTXI 1H-
PULPROG zg30
TD 32768
SOLVENT CDCl3
NS 2
DS 0
SWH 5387.931 Hz
FIDRES 0.164427 Hz
AQ 3.0409205 sec
RG 11.3
DW 92.800 usec
DE 6.00 usec
TE 298.0 K
D1 1.50000000 sec
TD0 1
======== CHANNEL f1 ========
NUC1 1H
P1 7.63 usec
PL1 1.00 dB
SFO1 600.1824166 MHz
F1 - Acquisition parameters
TD 256
SFO1 150.9229 MHz
FIDRES 93.450958 Hz
SW 158.514 ppm
FnMODE States-TPPI
F2 - Processing parameters
SI 32768
SF 600.1800388 MHz
WDW no
SSB 0
LB 0 Hz
GB 0
PC 0.50
8.0
7.5
7.0
6.5
6.0
5.5
5.0
4.5
4.0
3.5
3.0
2.5
2.0
1.5
1.0
0.5
0.0
ppm
5.00
1.96
2.95
3.67
0.88
1.05
9.76

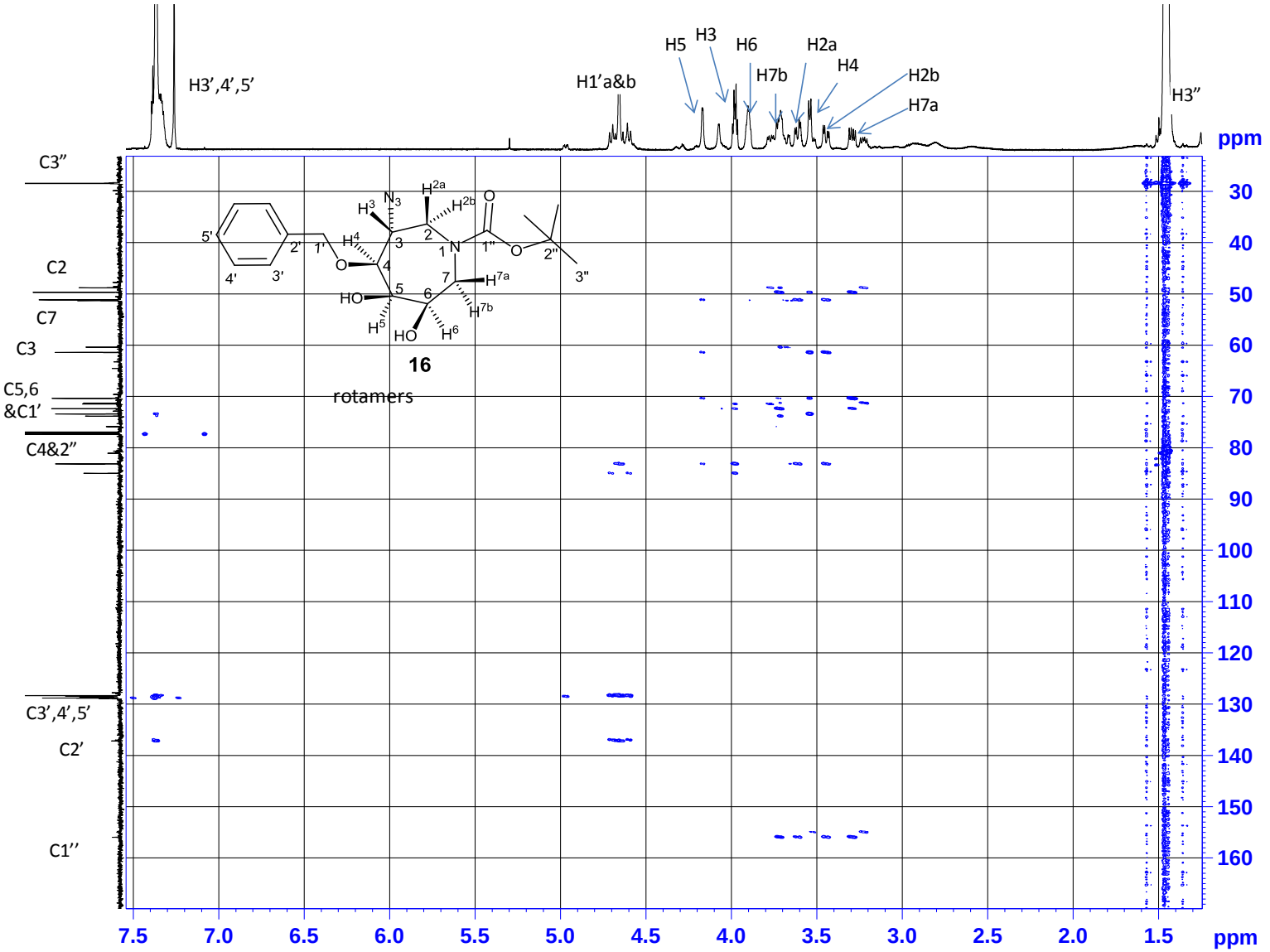
^{13}C NMR-**16**


155.97
137.17
137.01
128.89
128.81
128.58
128.43
128.34
84.98
83.14
81.07
77.37
77.16
76.95
73.83
73.41
72.37
71.46
71.28
70.36
61.40
60.38
51.29
51.14
49.68
48.79
28.41
BnO
N3
HO
HO
N
Boc
16
rotamers
Current Data Parameters
NAME Compound 7
EXPNO 3
PROCNO 1
F2 - Acquisition Parameters
Date_ 20121204
Time 21.58
INSTRUM spect
PROBHD 5 mm CPTXI 1H-
PULPROG udeft.txt
TD 21814
SOLVENT CDCl3
NS 4096
DS 0
SWH 30303.031 Hz
FIDRES 1.389155 Hz
AQ 0.3599810 sec
RG 32768
DW 16.500 usec
DE 6.00 usec
TE 298.0 K
D1 1.50000000 sec
D11 0.03000000 sec
d12 0.00002000 sec
D20 0.10000000 sec
DELTA 1.47000003 sec
DELTA2 0.36300099 sec
TAU 0.00302000 sec
TD0 1
======== CHANNEL f1 ========
NUC1 13C
P1 10.43 usec
P12 2000.00 usec
P26 500.00 usec
PL1 -2.50 dB
SFO1 150.9319817 MHz
SP2 5.29 dB
SP8 4.75 dB
SPNAM2 Crp60comp.4
SPNAM8 Crp60,0.5,20.1
SPOAL2 0.500
SPOAL8 0.500
SPOFFS2 0 Hz
SPOFFS8 0 Hz
======== CHANNEL f2 ========
CPDPRG2 waltz64
NUC2 1H
PCPD2 80.00 usec
PL2 1.00 dB
PL12 18.89 dB
SFO2 600.1830000 MHz
F1 - Acquisition parameters
TD 256
SFO1 150.932 MHz
FIDRES 93.450958 Hz
SW 158.505 ppm
FnMODE States-TPPI
F2 - Processing parameters
SI 262144
SF 150.9153681 MHz
WDW GM
SSB 0
LB -1.00 Hz
GB 0.01
PC 0.02
160
150
140
130
120
110
100
90
80
70
60
50
40
30
20
ppm

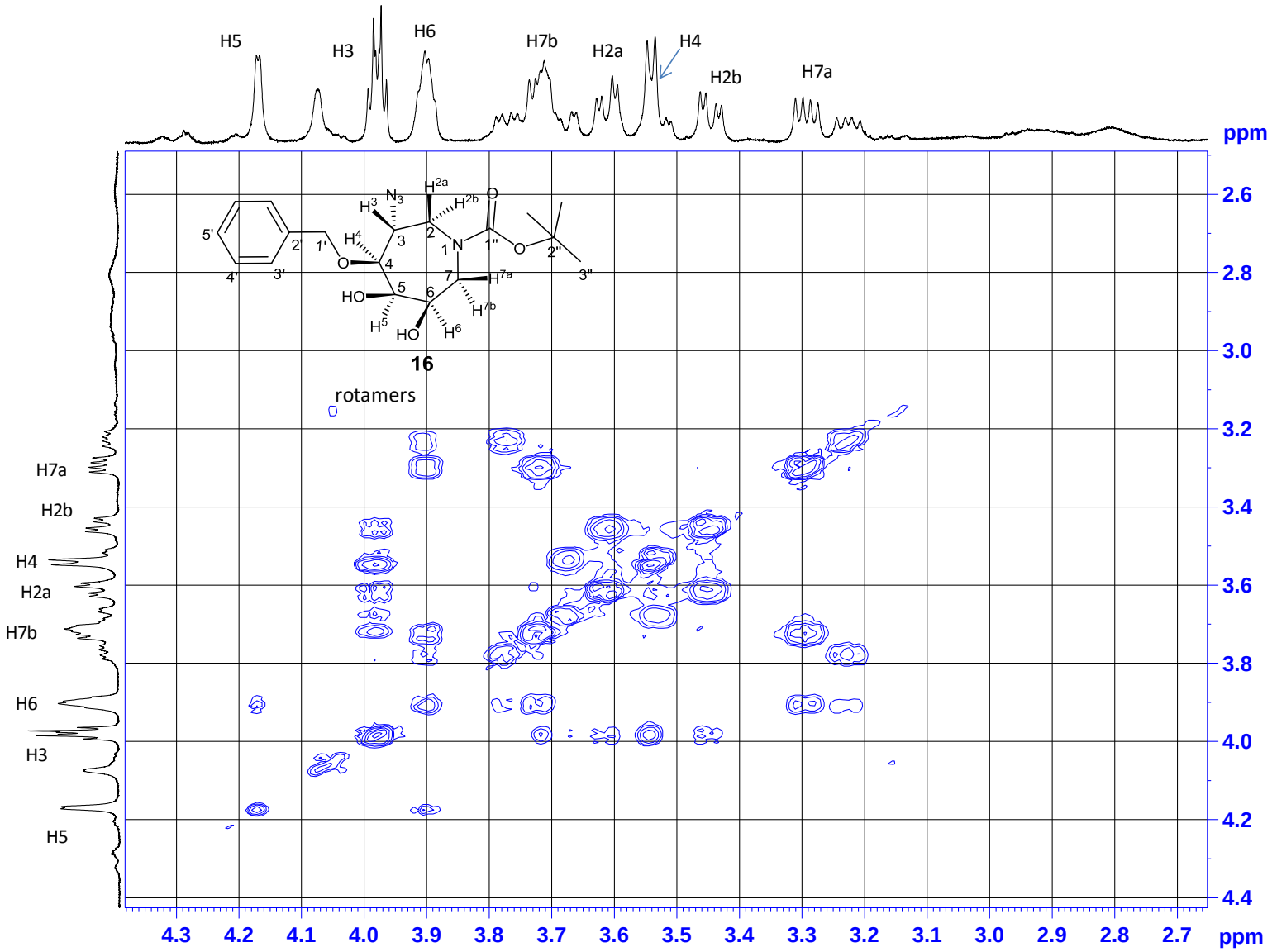
HSQC-**16**


H3',4',5'
H1'a&b
H5
H3
H6
H7b
H2a
H4
H2b
H7a
H3"
ppm
C3"
C2
C7
C3
C5,6
&C1'
C4&2"
C3',4',5'
C2'
C1''
16
rotamers
7.5
7.0
6.5
6.0
5.5
5.0
4.5
4.0
3.5
3.0
2.5
2.0
1.5
ppm

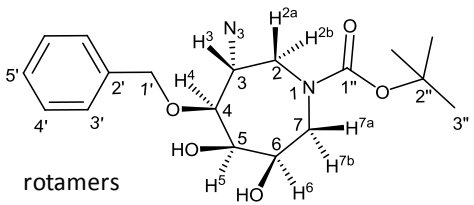
HMBC-**16**


H3',4',5'
H1'a&b
H5
H3
H6
H7b
H2a
H4
H2b
H7a
H3"
ppm
C3"
C2
C7
C3
C5,6
&C1'
C4&2"
C3',4',5'
C2'
C1''
16
rotamers
7.5
7.0
6.5
6.0
5.5
5.0
4.5
4.0
3.5
3.0
2.5
2.0
1.5
ppm

COSY-16

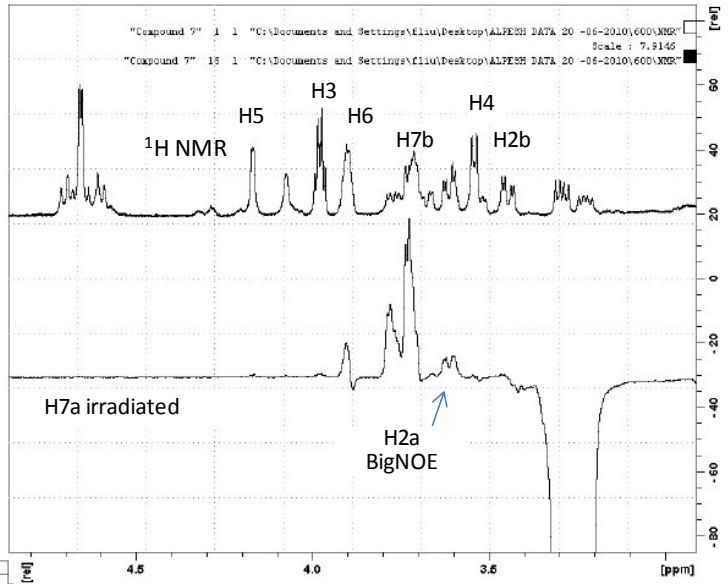

H5
H3
H6
H7b
H2a
H4
H2b
H7a
ppm
2.6
2.8
3.0
3.2
3.4
3.6
3.8
4.0
4.2
4.4
4.3
4.2
4.1
4.0
3.9
3.8
3.7
3.6
3.5
3.4
3.3
3.2
3.1
3.0
2.9
2.8
2.7
ppm
16
rotamers

NOESY-**16**

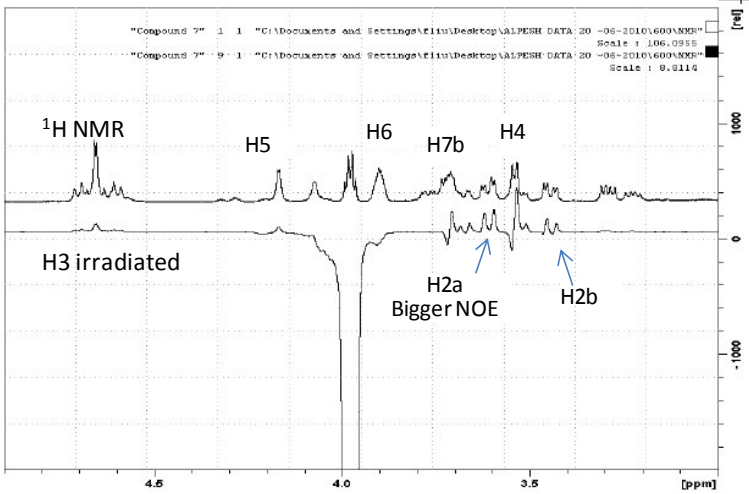


16

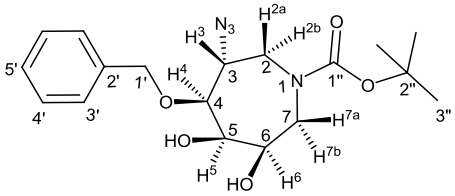
1D selective NOESY



1D selective NOESY



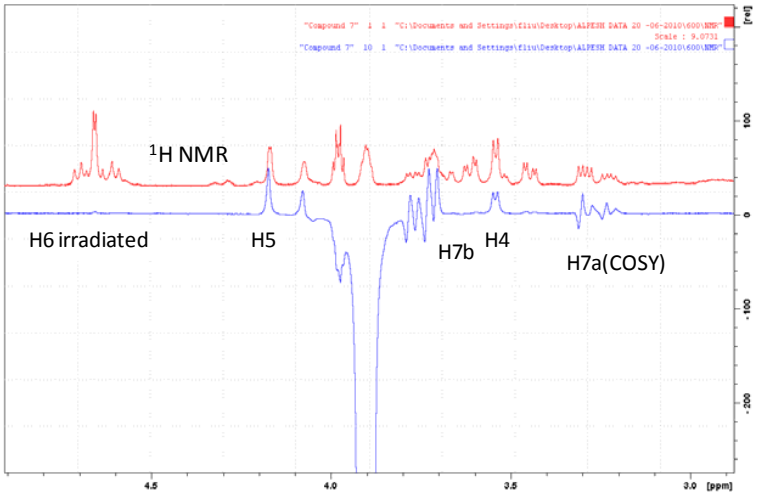
- H3 shows bigger NOE to H2a compared to H2b suggesting H2a is syn and H2b is anti.
- H7a shows bigger NOE to H2a compared to H2b meaning H7a is syn to H3 and anti to H4.
- H6 shows big NOE to H7b, H4 and H5 suggesting H6 and H5 both are syn to H4.
- Moreover, H5 also shows NOE to H4 and H7b confirming H5 is syn to H4.

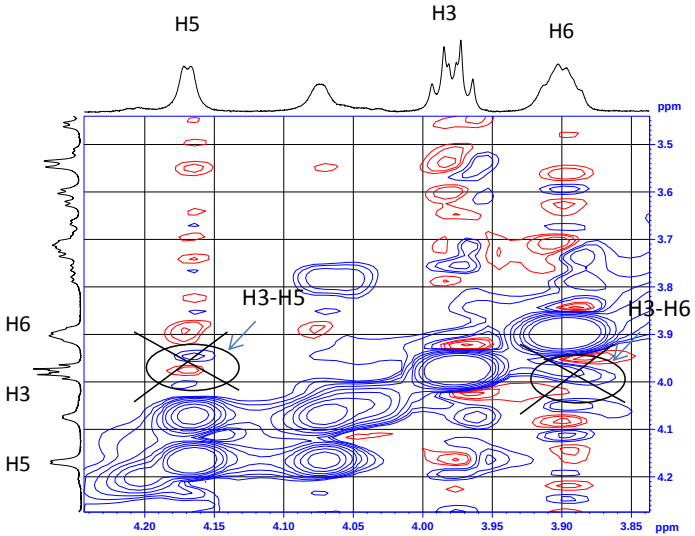


16

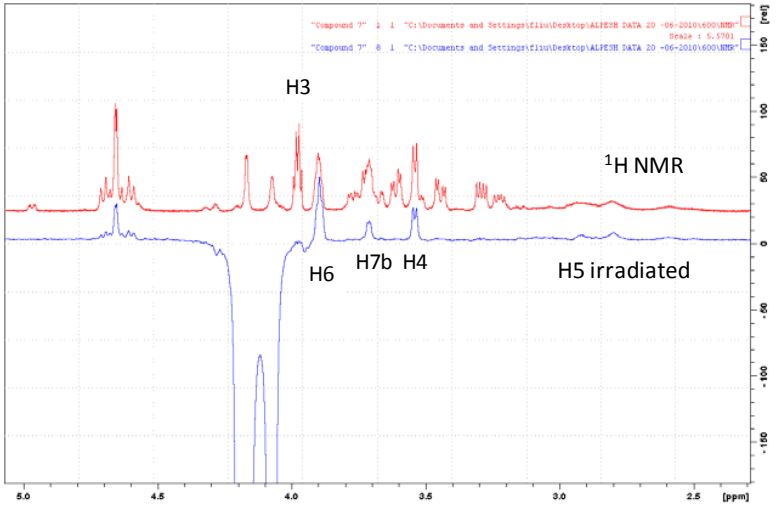
rotamers

1D selective NOESY

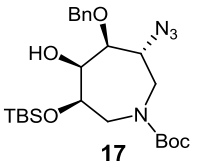




1D selective NOESY



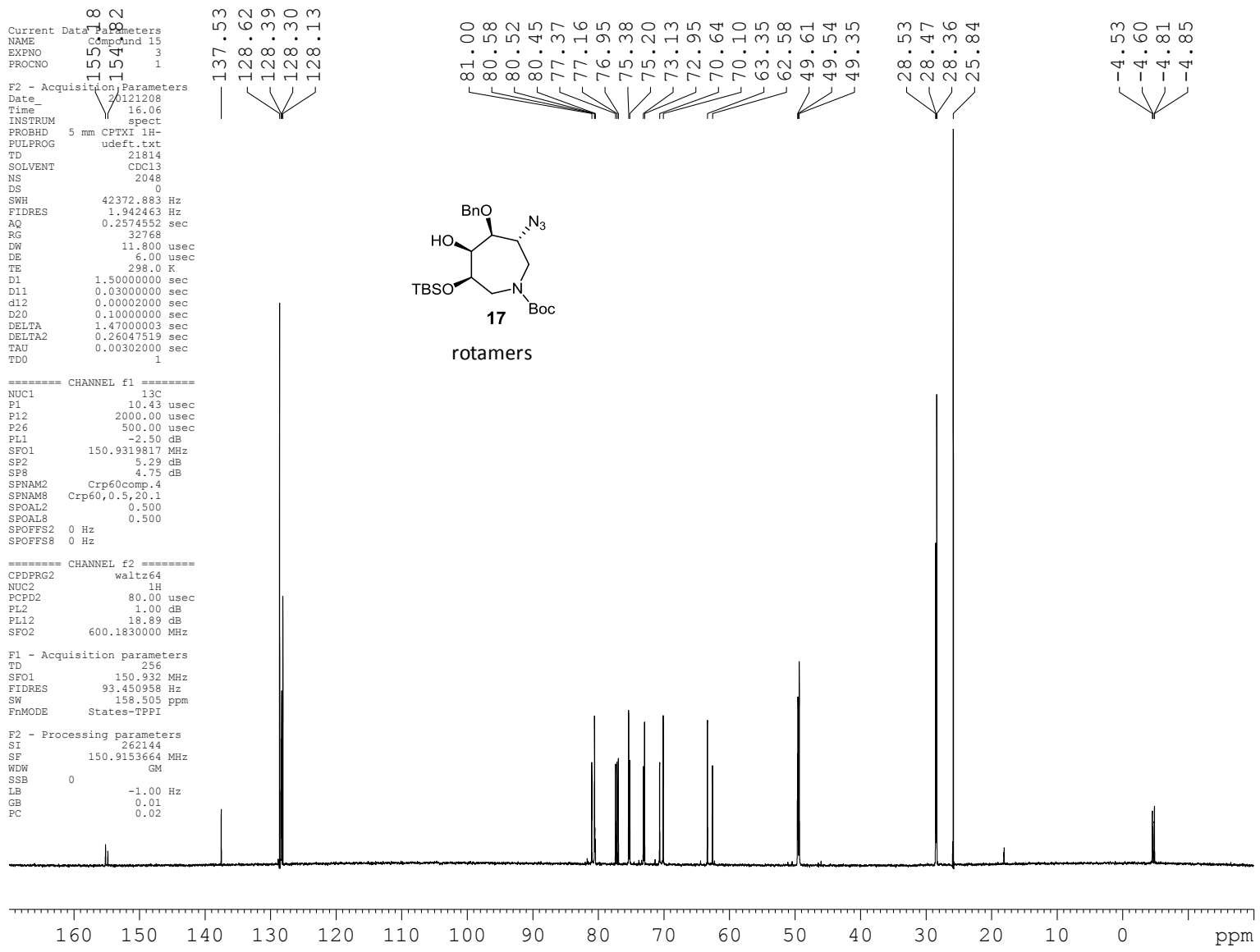
^{1}H NMR-**17**

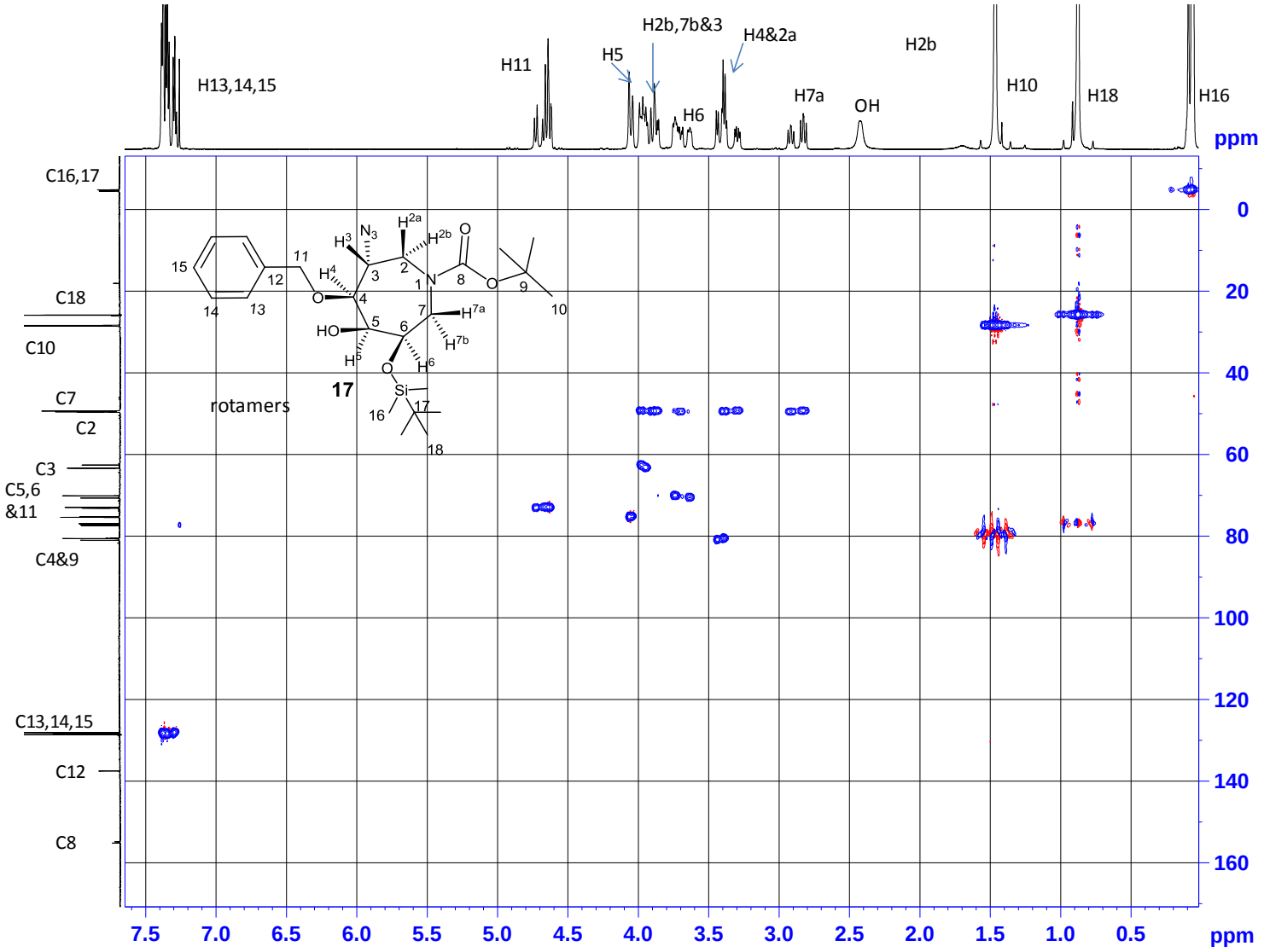


17

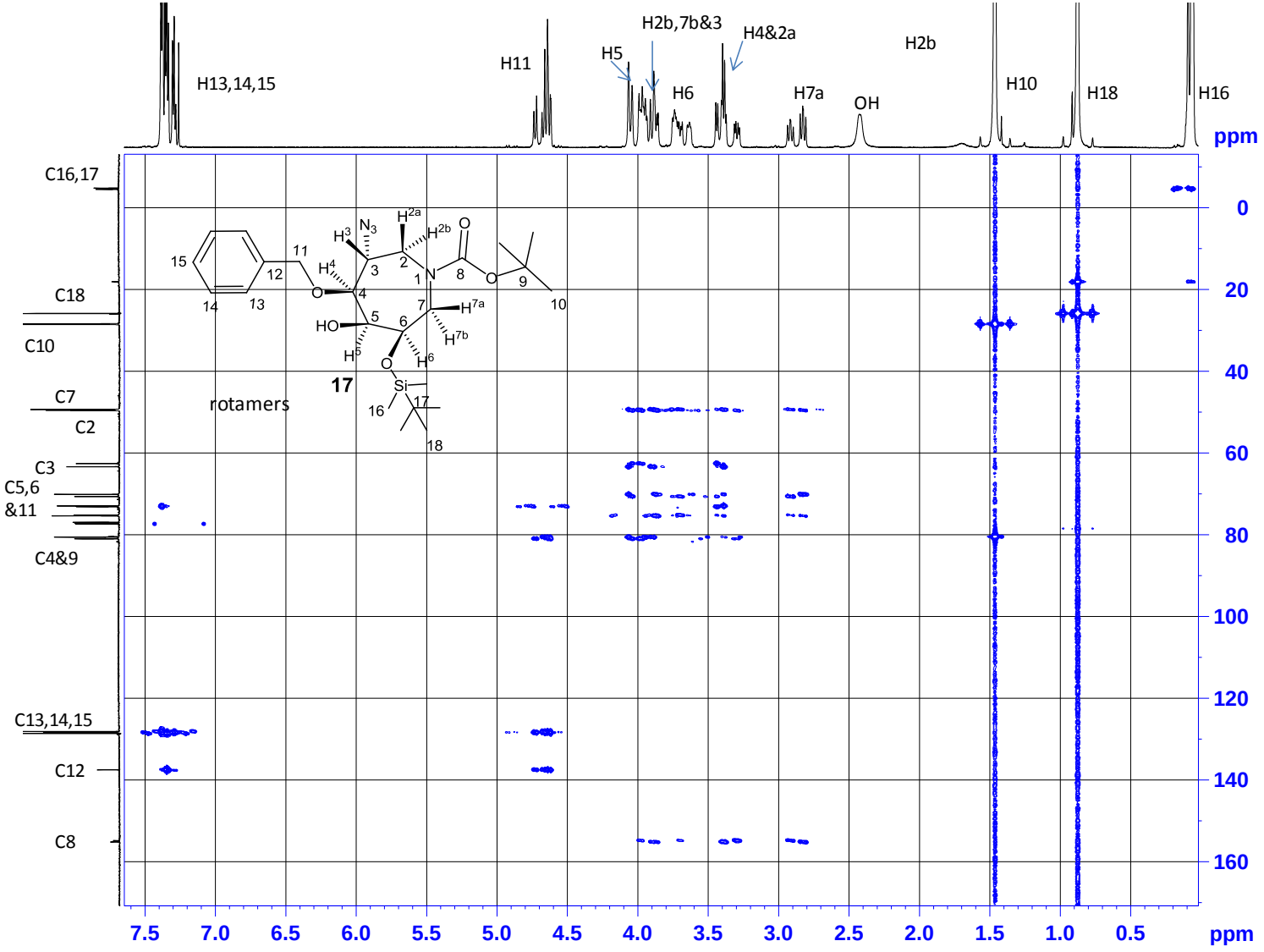
rotamers

^{13}C NMR-**17**

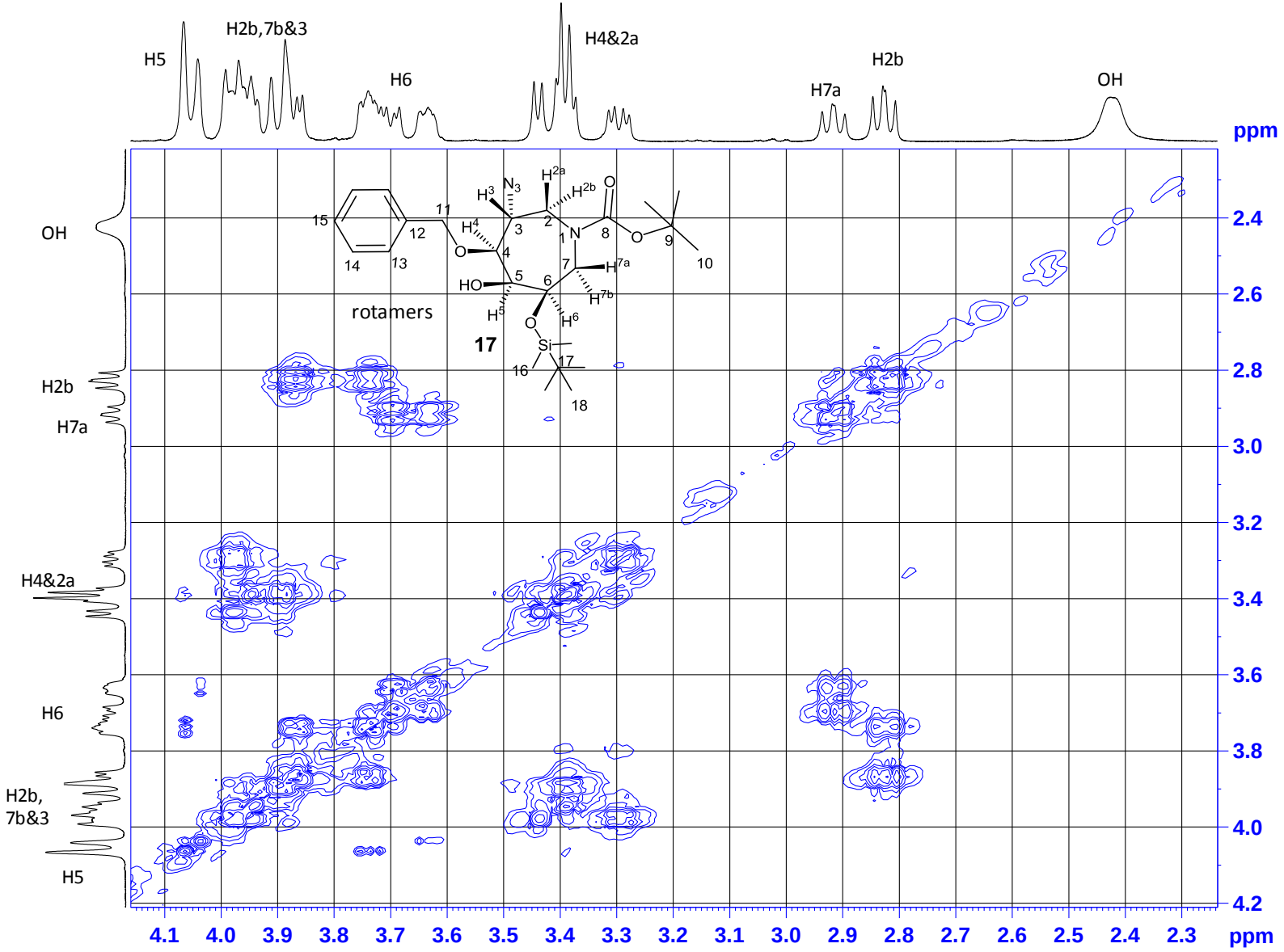

155.18
154.22
137.53
128.62
128.39
128.30
128.13
81.00
80.58
80.52
80.45
77.37
77.16
76.95
75.38
75.20
73.13
72.95
70.64
70.10
63.35
62.58
49.61
49.54
49.35
28.53
28.47
28.36
25.84
-4.53
-4.60
-4.81
-4.85
BnO
N3
HO
TBSO
N
Boc
17
rotamers
Current Data Parameters
NAME Compound 15
EXPNO 3
PROCNO 1
F2 - Acquisition Parameters
Date_ 20121208
Time 16.06
INSTRUM spect
PROBHD 5 mm CPTXI 1H-
PULPROG udeft.txt
TD 21814
SOLVENT CDCl3
NS 2048
DS 0
SWH 42372.883 Hz
FIDRES 1.942463 Hz
AQ 0.2574552 sec
RG 32768
DW 11.800 usec
DE 6.00 usec
TE 298.0 K
D1 1.50000000 sec
D11 0.03000000 sec
d12 0.00002000 sec
D20 0.10000000 sec
DELTA 1.47000003 sec
DELTA2 0.26047519 sec
TAU 0.00302000 sec
TD0 1
======== CHANNEL f1 ========
NUC1 13C
P1 10.43 usec
P12 2000.00 usec
P26 500.00 usec
PL1 -2.50 dB
SFO1 150.9319817 MHz
SP2 5.29 dB
SP8 4.75 dB
SPNAM2 Crp60comp.4
SPNAM8 Crp60,0.5,20.1
SPOAL2 0.500
SPOAL8 0.500
SPOFFS2 0 Hz
SPOFFS8 0 Hz
======== CHANNEL f2 ========
CPDPRG2 waltz64
NUC2 1H
PCPD2 80.00 usec
PL2 1.00 dB
PL12 18.89 dB
SFO2 600.1830000 MHz
F1 - Acquisition parameters
TD 256
SFO1 150.932 MHz
FIDRES 93.450958 Hz
SW 158.505 ppm
FnMODE States-TPPI
F2 - Processing parameters
SI 262144
SF 150.9153664 MHz
WDW GM
SSB 0
LB -1.00 Hz
GB 0.01
PC 0.02
160 150 140 130 120 110 100 90 80 70 60 50 40 30 20 10 0 ppm

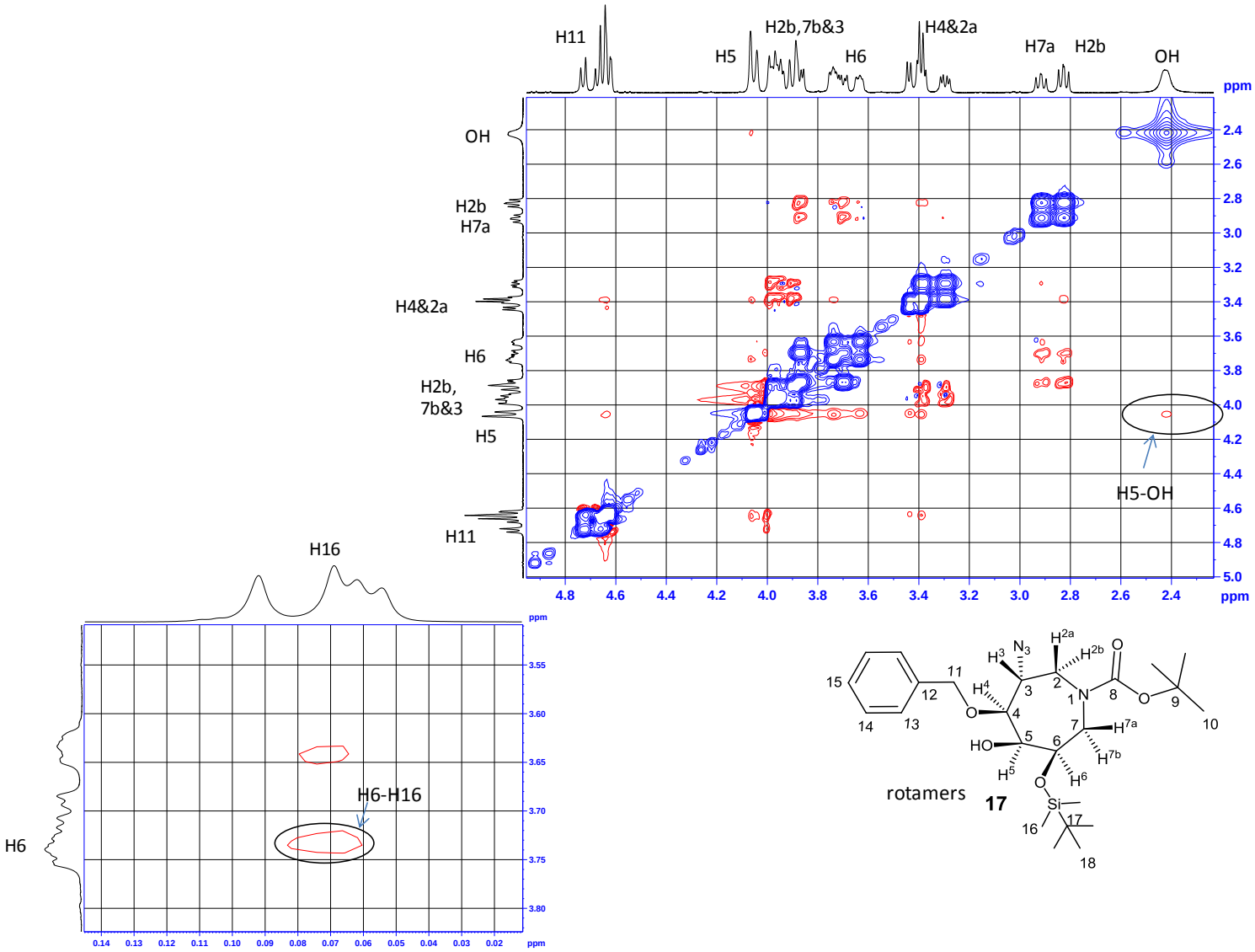

H13,14,15
H11
H5
H2b,7b&3
H4&2a
H6
H7a
OH
H2b
H10
H18
H16
ppm
C16,17
C18
C10
C7
C2
C3
C5,6
&11
C4&9
C13,14,15
C12
C8
rotamers
17
7.5
7.0
6.5
6.0
5.5
5.0
4.5
4.0
3.5
3.0
2.5
2.0
1.5
1.0
0.5
ppm

HMBC-**17**

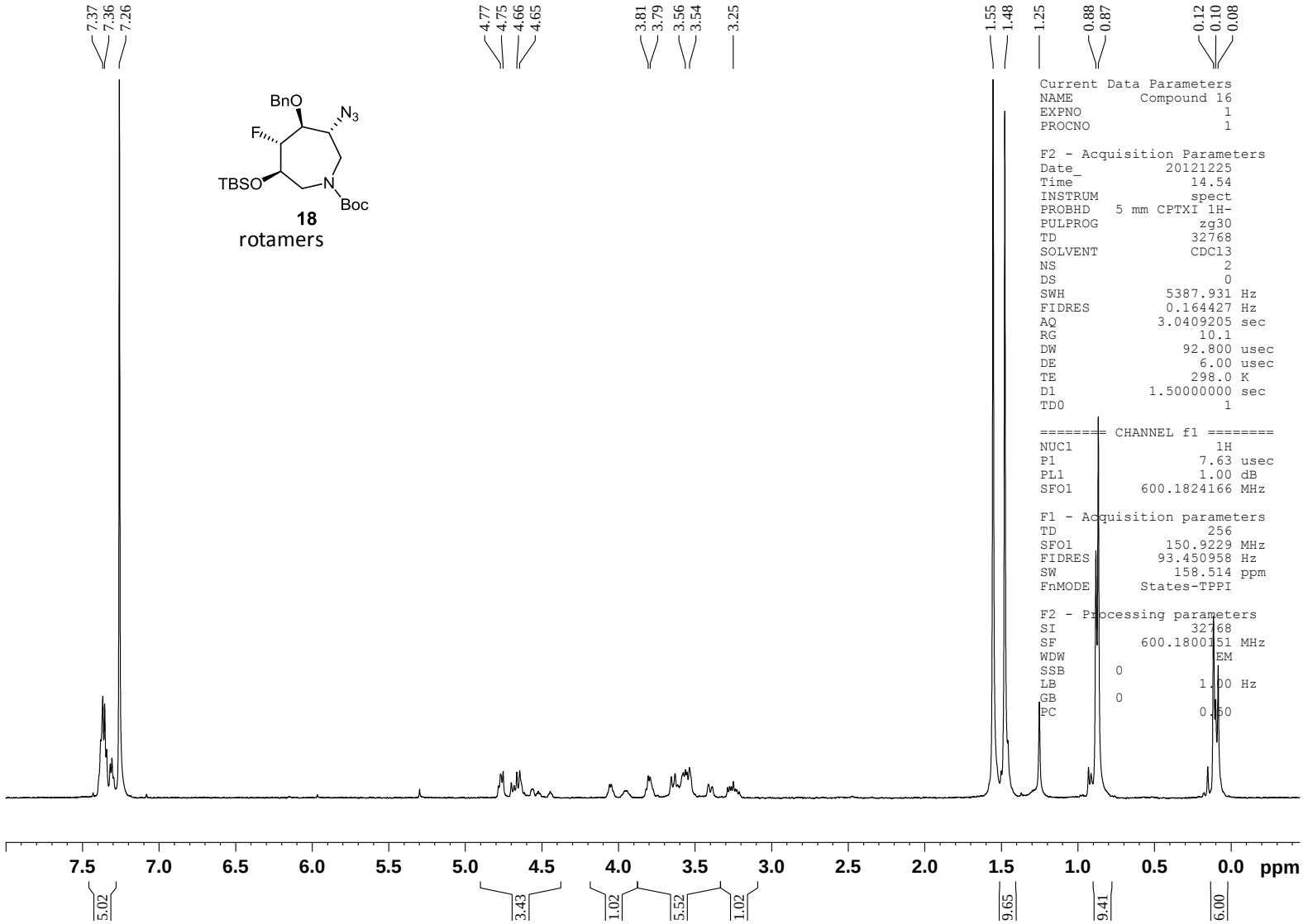

H13,14,15
H11
H5
H2b,7b&3
H4&2a
H6
H7a
OH
H2b
H10
H18
H16
ppm
C16,17
C18
C10
C7
C2
C3
C5,6
&11
C4&9
C13,14,15
C12
C8
rotamers
17
7.5
7.0
6.5
6.0
5.5
5.0
4.5
4.0
3.5
3.0
2.5
2.0
1.5
1.0
0.5
ppm
0
20
40
60
80
100
120
140
160

COSY-**17**

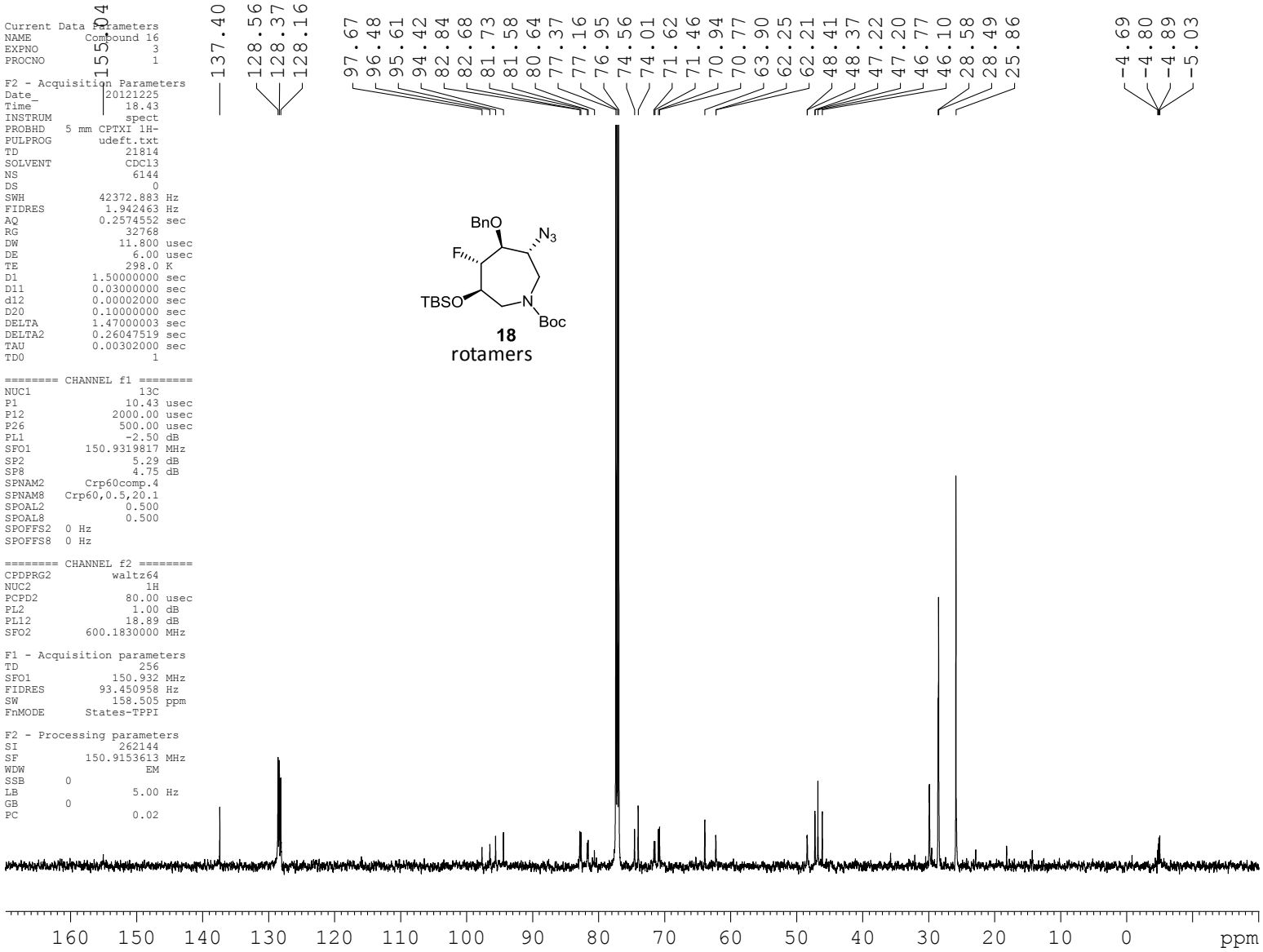

H5
H2b,7b&3
H6
H4&2a
H7a
H2b
OH
ppm
OH
H2b
H7a
H4&2a
H6
H2b,
7b&3
H5
rotamers
17
4.1
4.0
3.9
3.8
3.7
3.6
3.5
3.4
3.3
3.2
3.1
3.0
2.9
2.8
2.7
2.6
2.5
2.4
2.3
ppm
2.4
2.6
2.8
3.0
3.2
3.4
3.6
3.8
4.0
4.2


H11
H5
H2b,7b&3
H6
H4&2a
H7a
H2b
OH
ppm
OH
H2b
H7a
H4&2a
H6
H2b,
7b&3
H5
H11
H5-OH
4.8
4.6
4.4
4.2
4.0
3.8
3.6
3.4
3.2
3.0
2.8
2.6
2.4
ppm
H16
H6
H6-H16
0.14
0.13
0.12
0.11
0.10
0.09
0.08
0.07
0.06
0.05
0.04
0.03
0.02
ppm
rotamers
17

^{1}H NMR-**18**


7.37
7.36
7.26
4.77
4.75
4.66
4.65
3.81
3.79
3.56
3.54
3.25
1.55
1.48
1.25
0.88
0.87
0.12
0.10
0.08
BnO
N3
F
TBSO
N
Boc
18
rotamers
Current Data Parameters
NAME Compound 16
EXPNO 1
PROCNO 1
F2 - Acquisition Parameters
Date_ 20121225
Time 14.54
INSTRUM spect
PROBHD 5 mm CPTXI 1H-
PULPROG zg30
TD 32768
SOLVENT CDCl3
NS 2
DS 0
SWH 5387.931 Hz
FIDRES 0.164427 Hz
AQ 3.0409205 sec
RG 10.1
DW 92.800 usec
DE 6.00 usec
TE 298.0 K
D1 1.50000000 sec
TD0 1
======== CHANNEL f1 ========
NUC1 1H
P1 7.63 usec
PL1 1.00 dB
SFO1 600.1824166 MHz
F1 - Acquisition parameters
TD 256
SFO1 150.9229 MHz
FIDRES 93.450958 Hz
SW 158.514 ppm
FnMODE States-TPPI
F2 - Processing parameters
SI 32768
SF 600.1800151 MHz
WDW EM
SSB 0
LB 1.00 Hz
GB 0
PC 0.50
7.5
7.0
6.5
6.0
5.5
5.0
4.5
4.0
3.5
3.0
2.5
2.0
1.5
1.0
0.5
0.0
ppm
5.02
3.43
1.02
5.52
1.02
9.65
9.41
6.00

^{13}C NMR-**18**




```
Current Data Parameters
NAME        Compound 16
EXPNO             3
PROCNO            1

F2 - Acquisition Parameters
Date_          20121225
Time              18.43
INSTRUM           spect
PROBHD   5 mm CPTXI 1H-
PULPROG       udeft.txt
TD                21814
SOLVENT           CDCl3
NS                 6144
DS                    0
SWH           42372.883 Hz
FIDRES         1.942463 Hz
AQ            0.2574552 sec
RG                32768
DW               11.800 usec
DE                6.00 usec
TE                298.0 K
D1           1.50000000 sec
D11          0.03000000 sec
d12          0.00002000 sec
D20          0.10000000 sec
DELTA        1.47000003 sec
DELTA2       0.26047519 sec
TAU          0.00302000 sec
TD0                   1

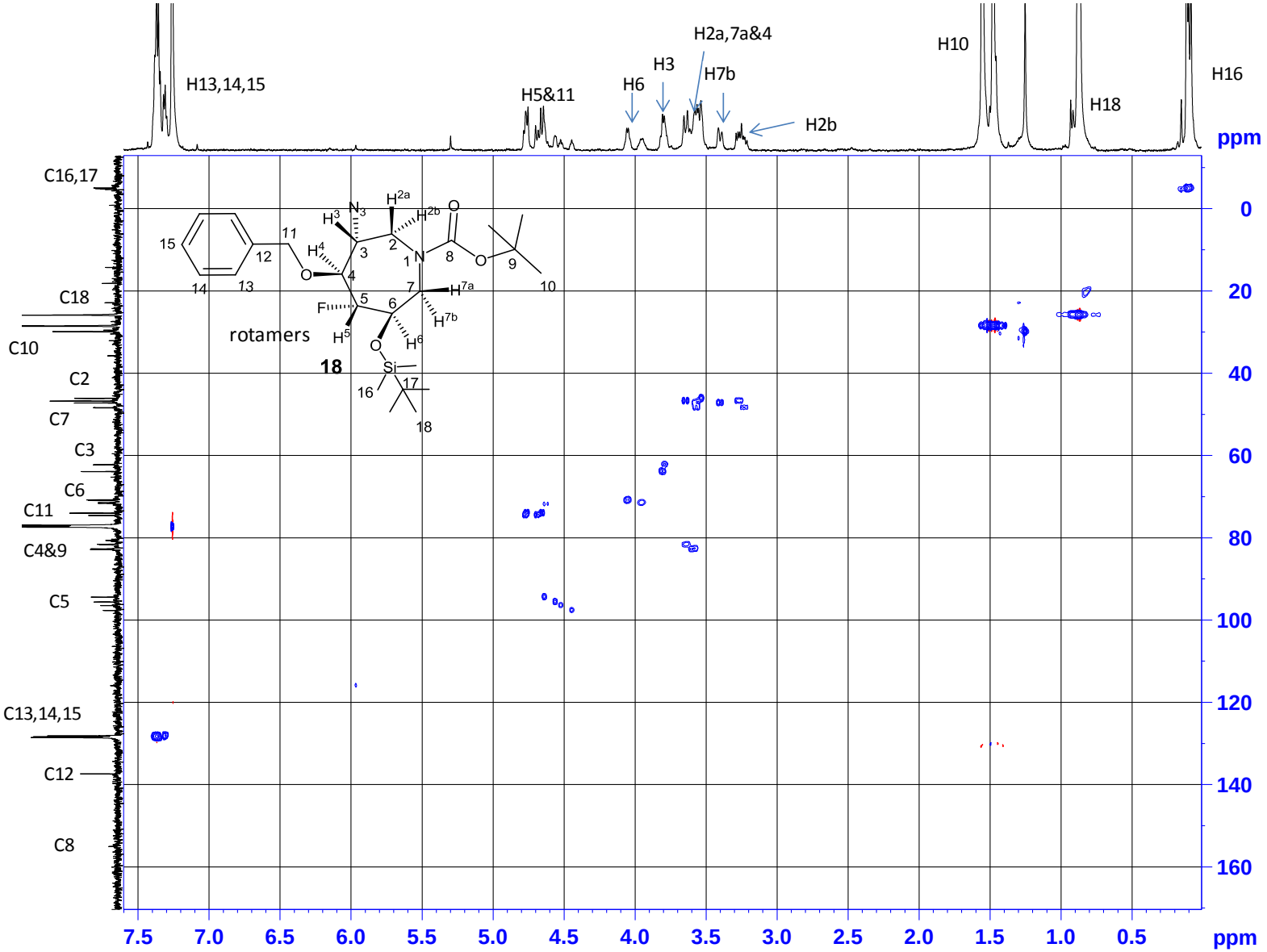
======== CHANNEL f1 ========
NUC1                13C
P1                10.43 usec
P12             2000.00 usec
P26              500.00 usec
PL1               -2.50 dB
SFO1        150.9319817 MHz
SP2                5.29 dB
SP8                4.75 dB
SPNAM2      Crp60comp.4
SPNAM8   Crp60,0.5,20.1
SPOAL2             0.500
SPOAL8             0.500
SPOFFS2  0 Hz
SPOFFS8  0 Hz

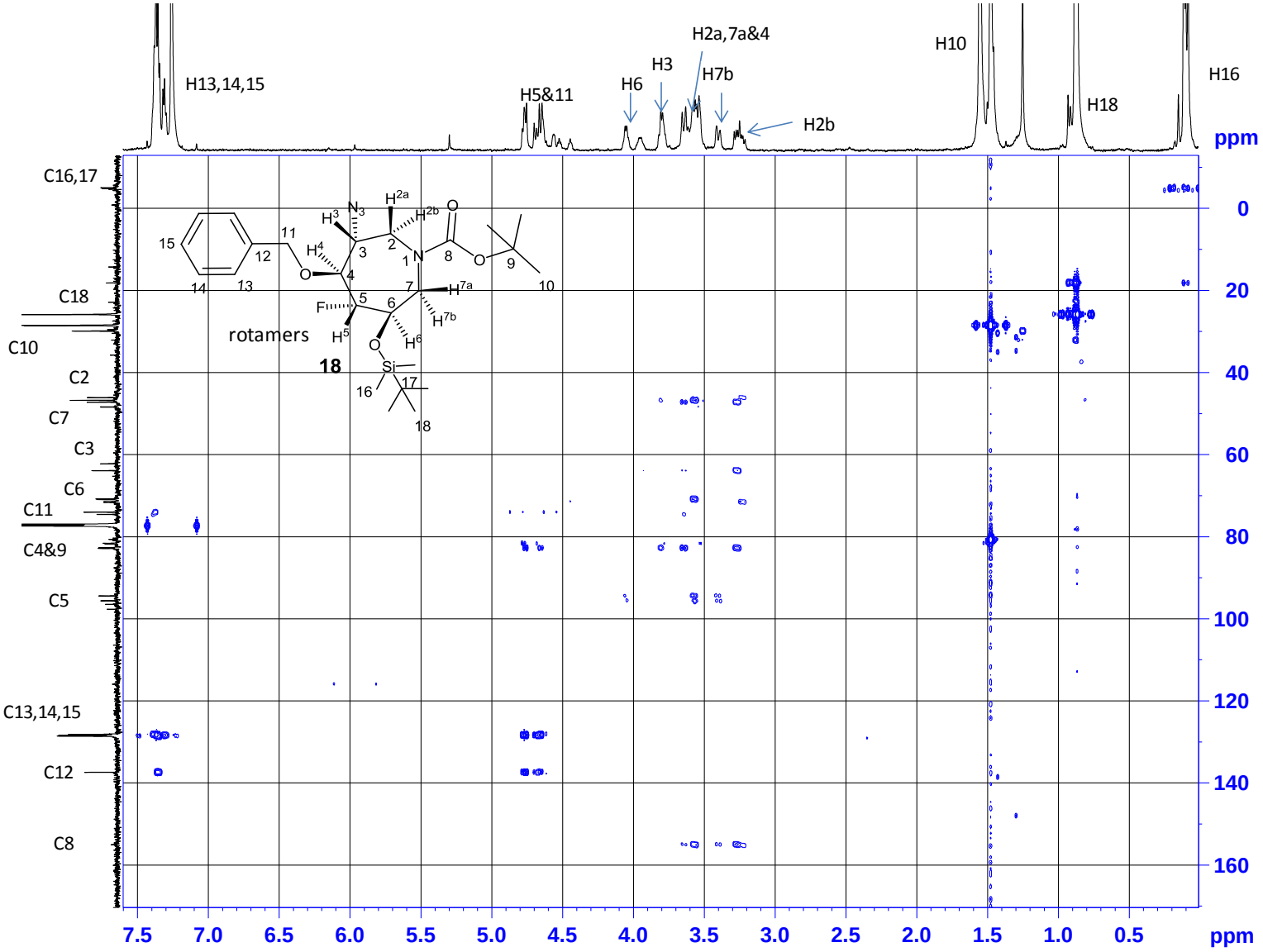
======== CHANNEL f2 ========
CPDPRG2          waltz64
NUC2                1H
PCPD2              80.00 usec
PL2                 1.00 dB
PL12               18.89 dB
SFO2        600.1830000 MHz

F1 - Acquisition parameters
TD                  256
SFO1            150.932 MHz
FIDRES         93.450958 Hz
SW              158.505 ppm
FnMODE       States-TPPI

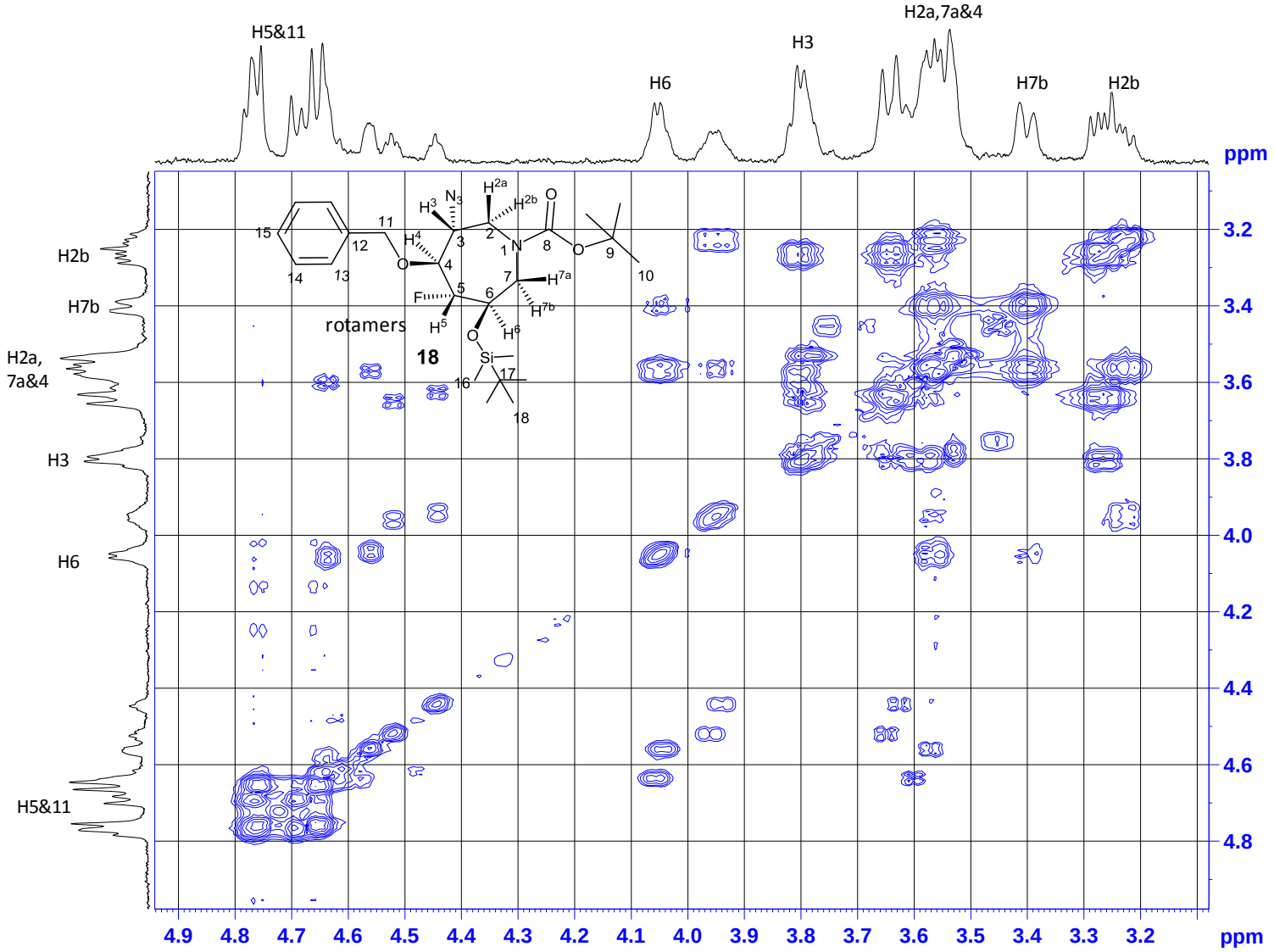
F2 - Processing parameters
SI                262144
SF          150.9153613 MHz
WDW                 EM
SSB      0
LB                5.00 Hz
GB       0
PC                0.02
```

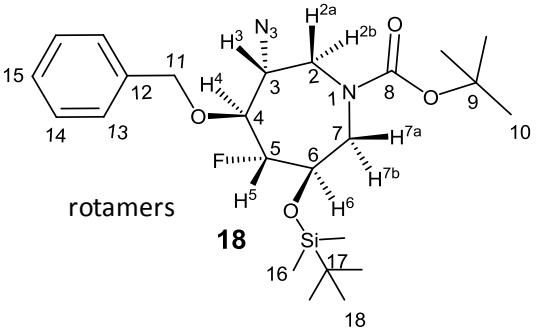
HSQC-**18**

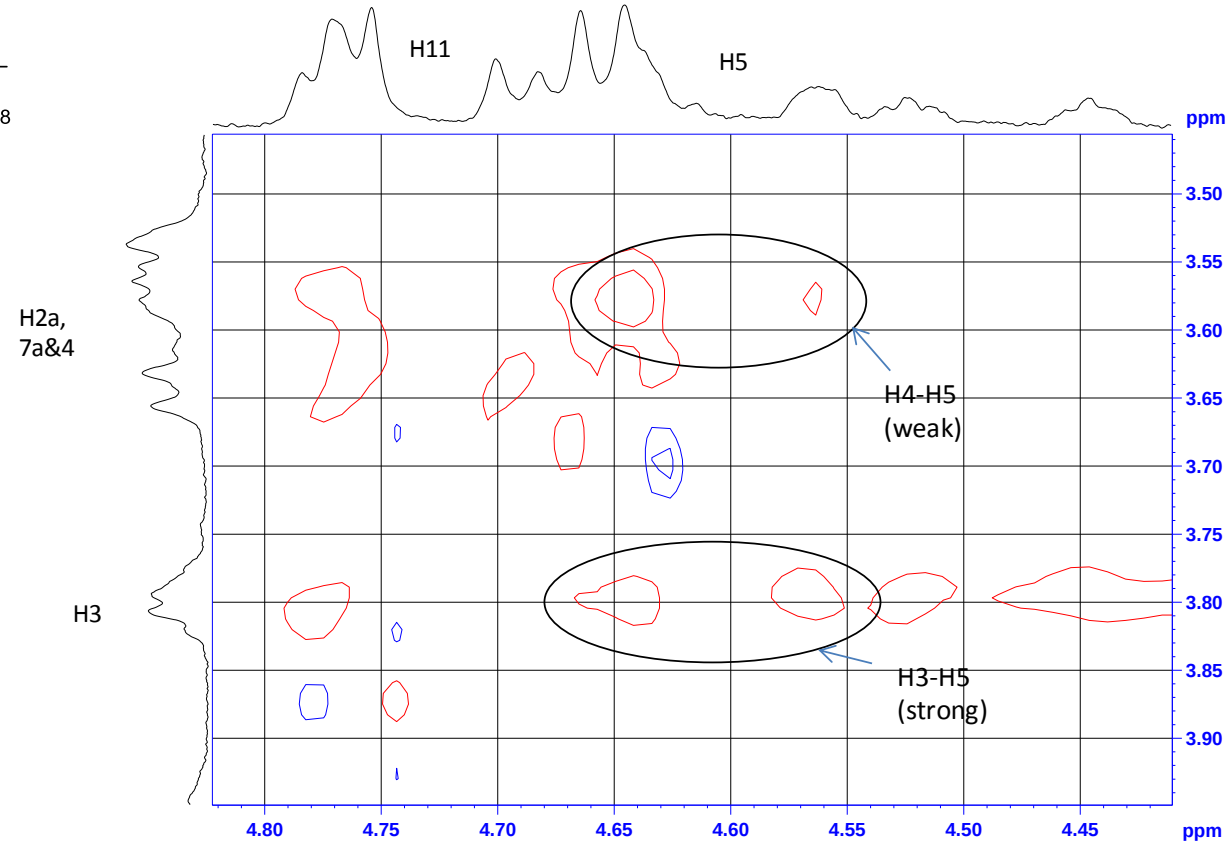

H13,14,15
H5&11
H6
H3
H2a,7a&4
H7b
H2b
H10
H18
H16
ppm
C16,17
C18
C10
C2
C7
C3
C6
C11
C4&9
C5
C13,14,15
C12
C8
rotamers
18
7.5
7.0
6.5
6.0
5.5
5.0
4.5
4.0
3.5
3.0
2.5
2.0
1.5
1.0
0.5
ppm


H13,14,15
H5&11
H6
H3
H2a,7a&4
H7b
H2b
H10
H18
H16
ppm
C16,17
C18
C10
C2
C7
C3
C6
C11
C4&9
C5
C13,14,15
C12
C8
rotamers
18
7.5
7.0
6.5
6.0
5.5
5.0
4.5
4.0
3.5
3.0
2.5
2.0
1.5
1.0
0.5
ppm

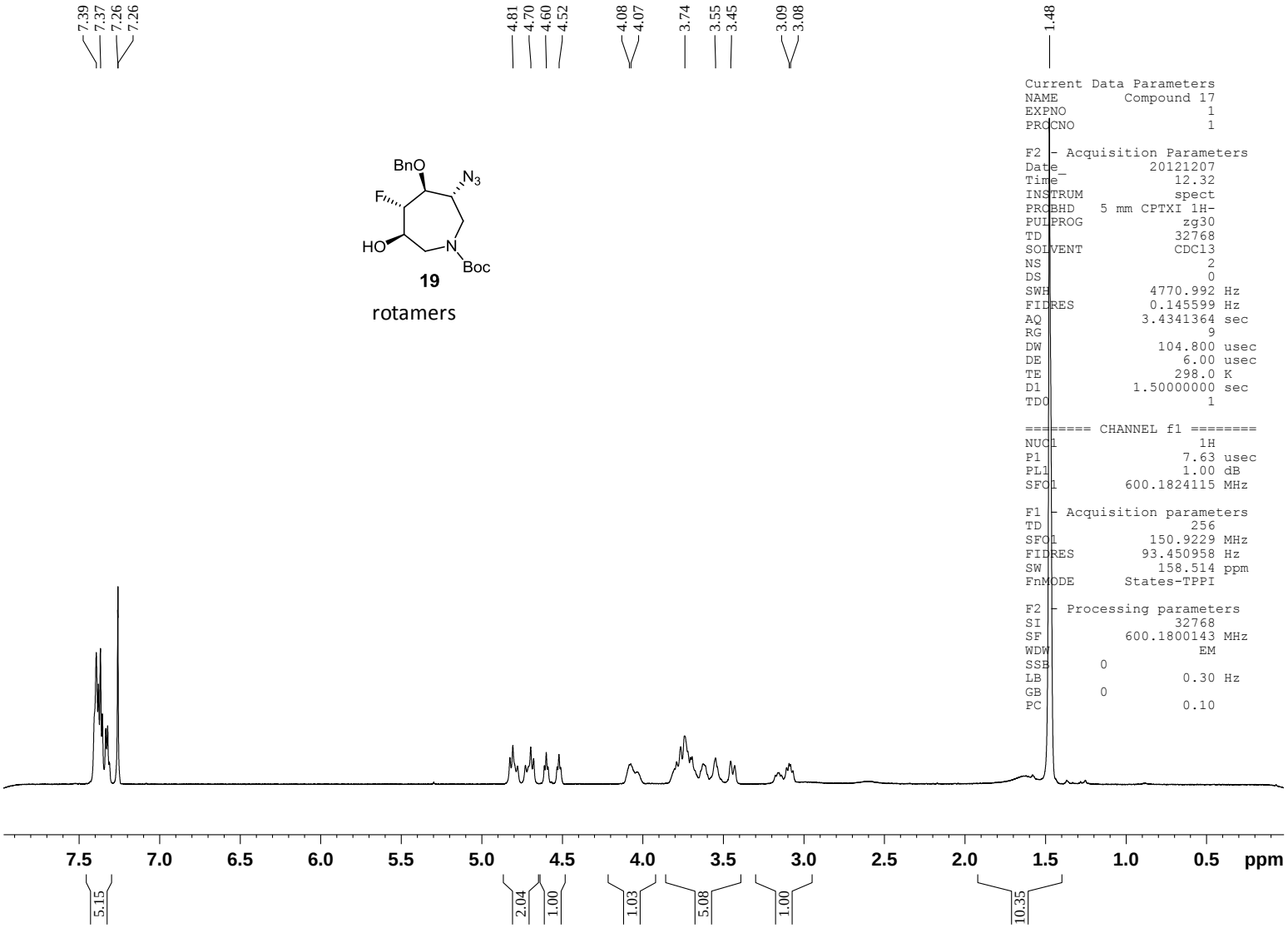
COSY-**18**


H5&11
H6
H3
H2a,7a&4
H7b
H2b
ppm
rotamers
18
4.9 4.8 4.7 4.6 4.5 4.4 4.3 4.2 4.1 4.0 3.9 3.8 3.7 3.6 3.5 3.4 3.3 3.2 ppm
3.2 3.4 3.6 3.8 4.0 4.2 4.4 4.6 4.8

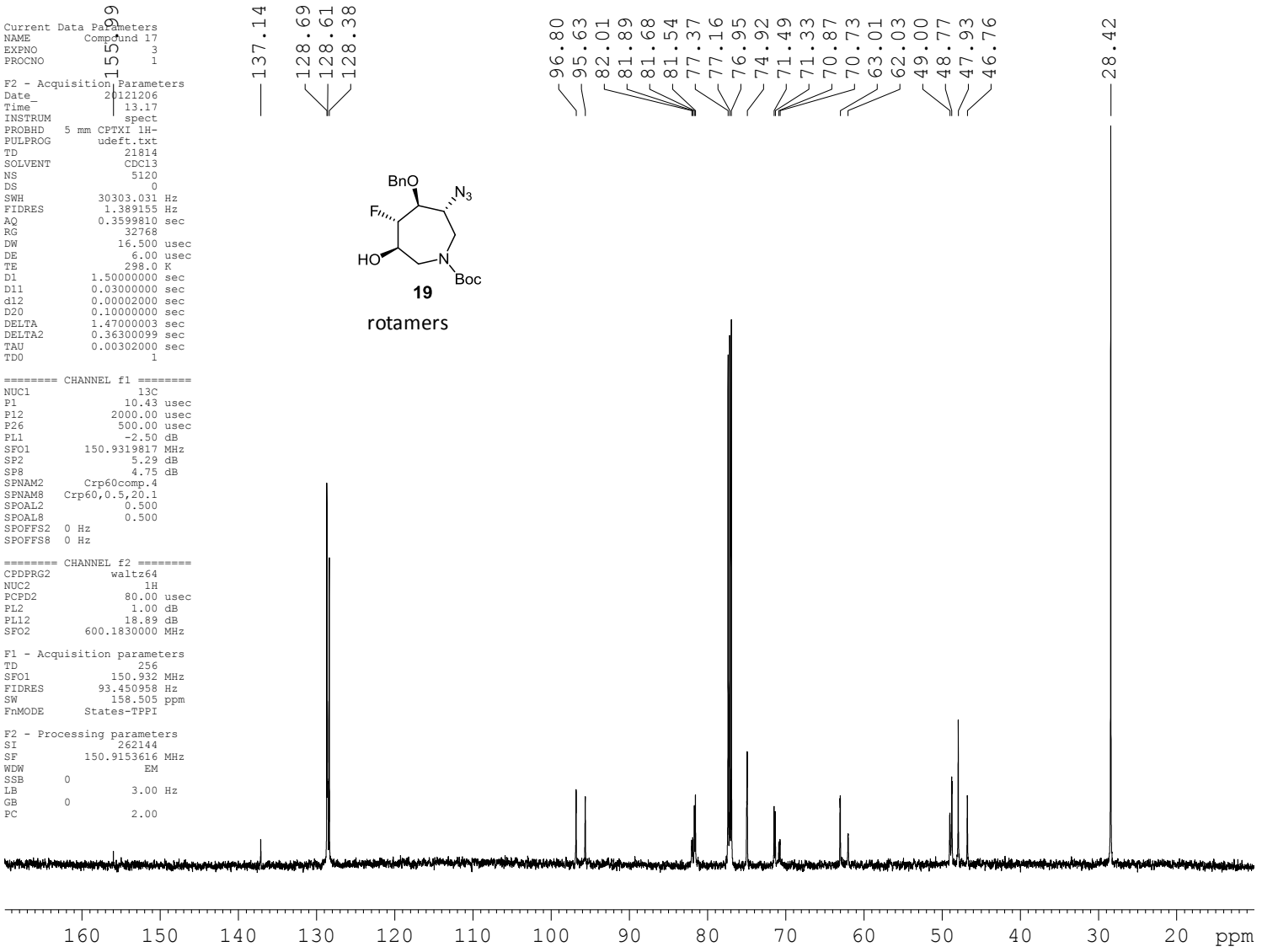

rotamers
18

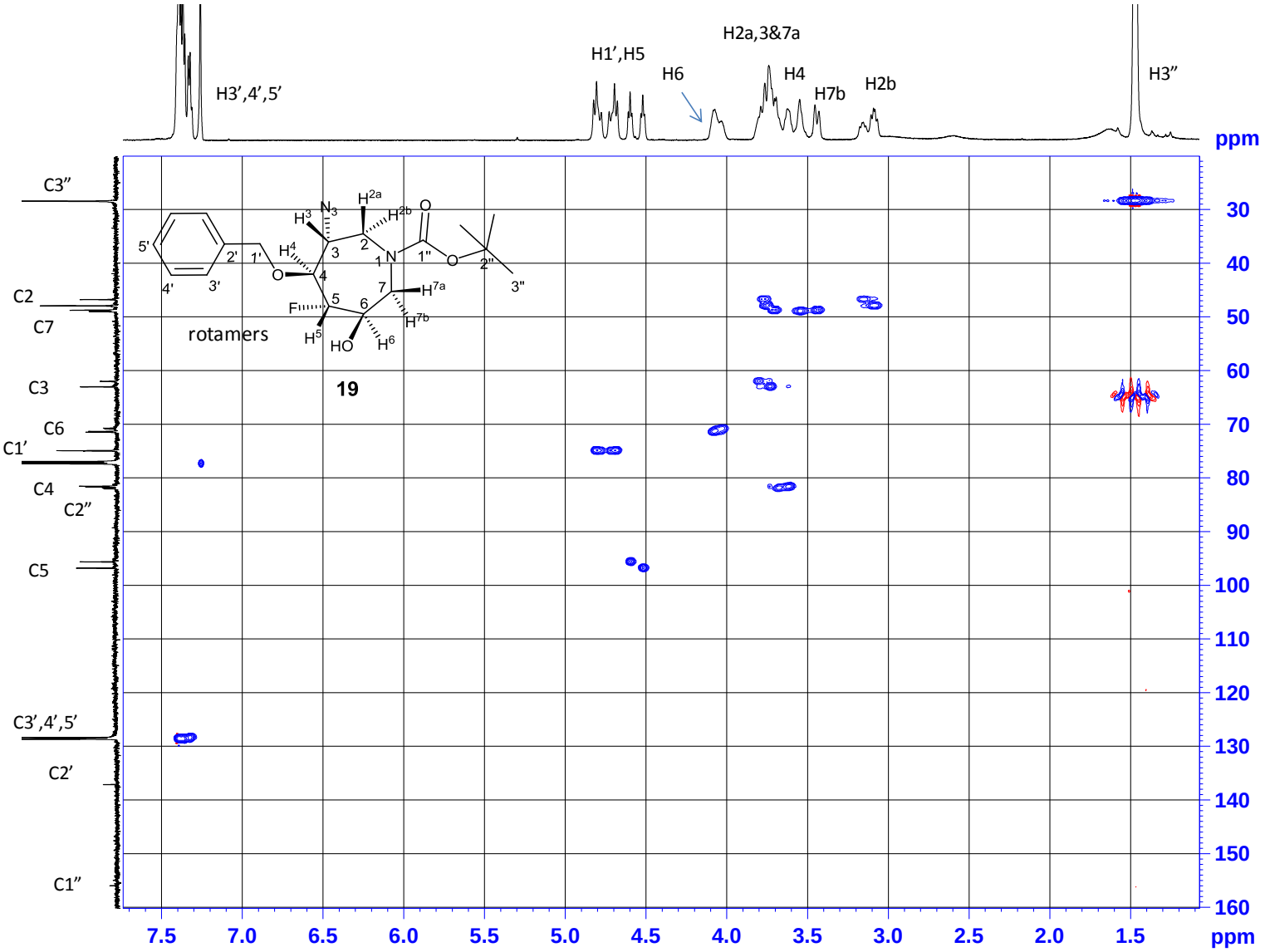

H11
H5
H2a,
7a&4
H3
H4-H5
(weak)
H3-H5
(strong)
ppm
3.50
3.55
3.60
3.65
3.70
3.75
3.80
3.85
3.90
4.80
4.75
4.70
4.65
4.60
4.55
4.50
4.45
ppm

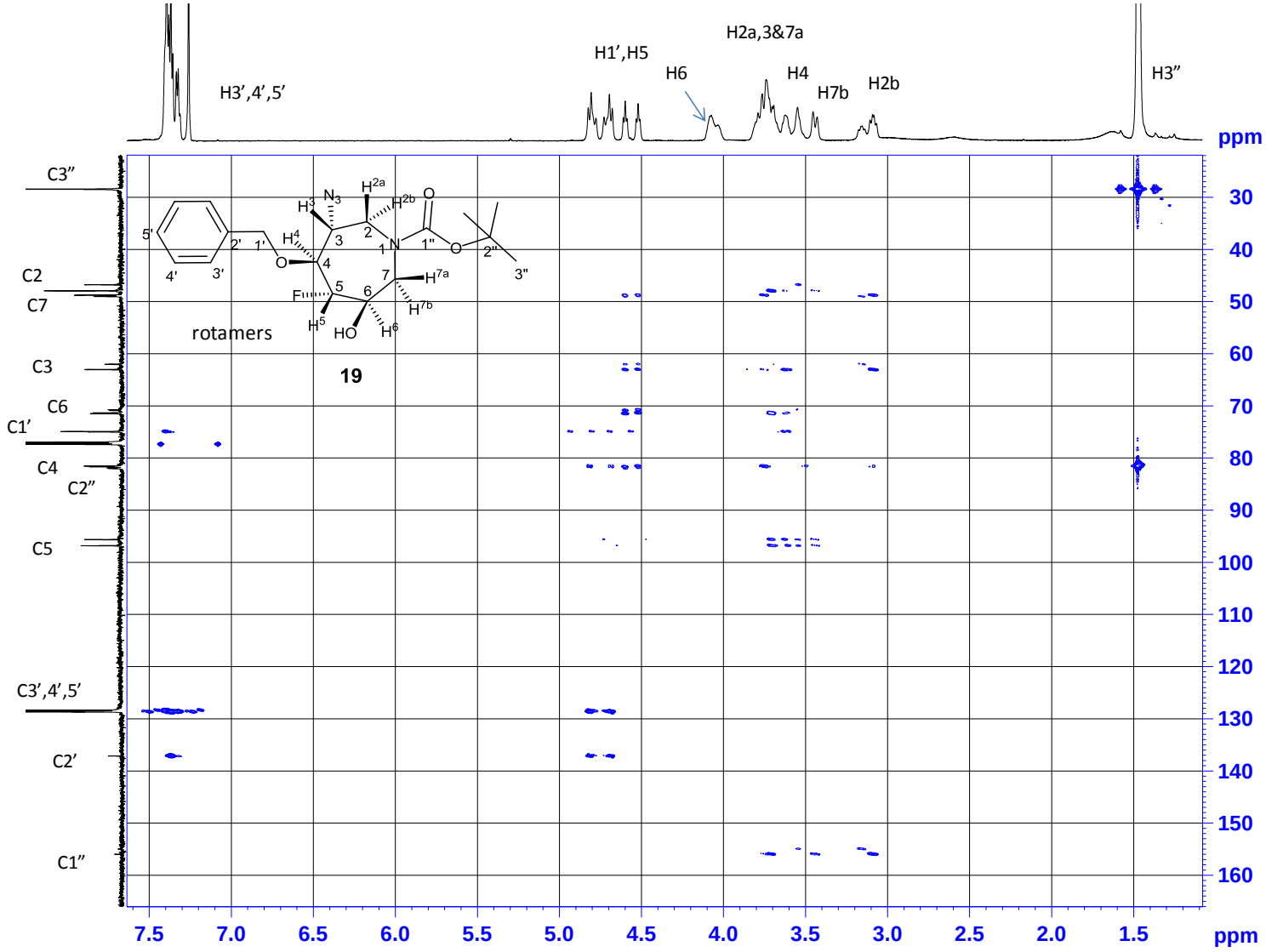
^{1}H NMR-**19**


7.39
7.37
7.26
7.26
4.81
4.70
4.60
4.52
4.08
4.07
3.74
3.55
3.45
3.09
3.08
1.48
BnO
N3
F
HO
N
Boc
19
rotamers
Current Data Parameters
NAME Compound 17
EXPNO 1
PROCNO 1
F2 - Acquisition Parameters
Date_ 20121207
Time 12.32
INSTRUM spect
PROBHD 5 mm CPTXI 1H-
PULPROG zg30
TD 32768
SOLVENT CDCl3
NS 2
DS 0
SWH 4770.992 Hz
FIDRES 0.145599 Hz
AQ 3.4341364 sec
RG 9
DW 104.800 usec
DE 6.00 usec
TE 298.0 K
D1 1.50000000 sec
TD0 1
======== CHANNEL f1 ========
NUC1 1H
P1 7.63 usec
PL1 1.00 dB
SFO1 600.1824115 MHz
F1 - Acquisition parameters
TD 256
SFO1 150.9229 MHz
FIDRES 93.450958 Hz
SW 158.514 ppm
FnMODE States-TPPI
F2 - Processing parameters
SI 32768
SF 600.1800143 MHz
WDW EM
SSB 0
LB 0.30 Hz
GB 0
PC 0.10
7.5
7.0
6.5
6.0
5.5
5.0
4.5
4.0
3.5
3.0
2.5
2.0
1.5
1.0
0.5
ppm
5.15
2.04
1.00
1.03
5.08
1.00
10.35

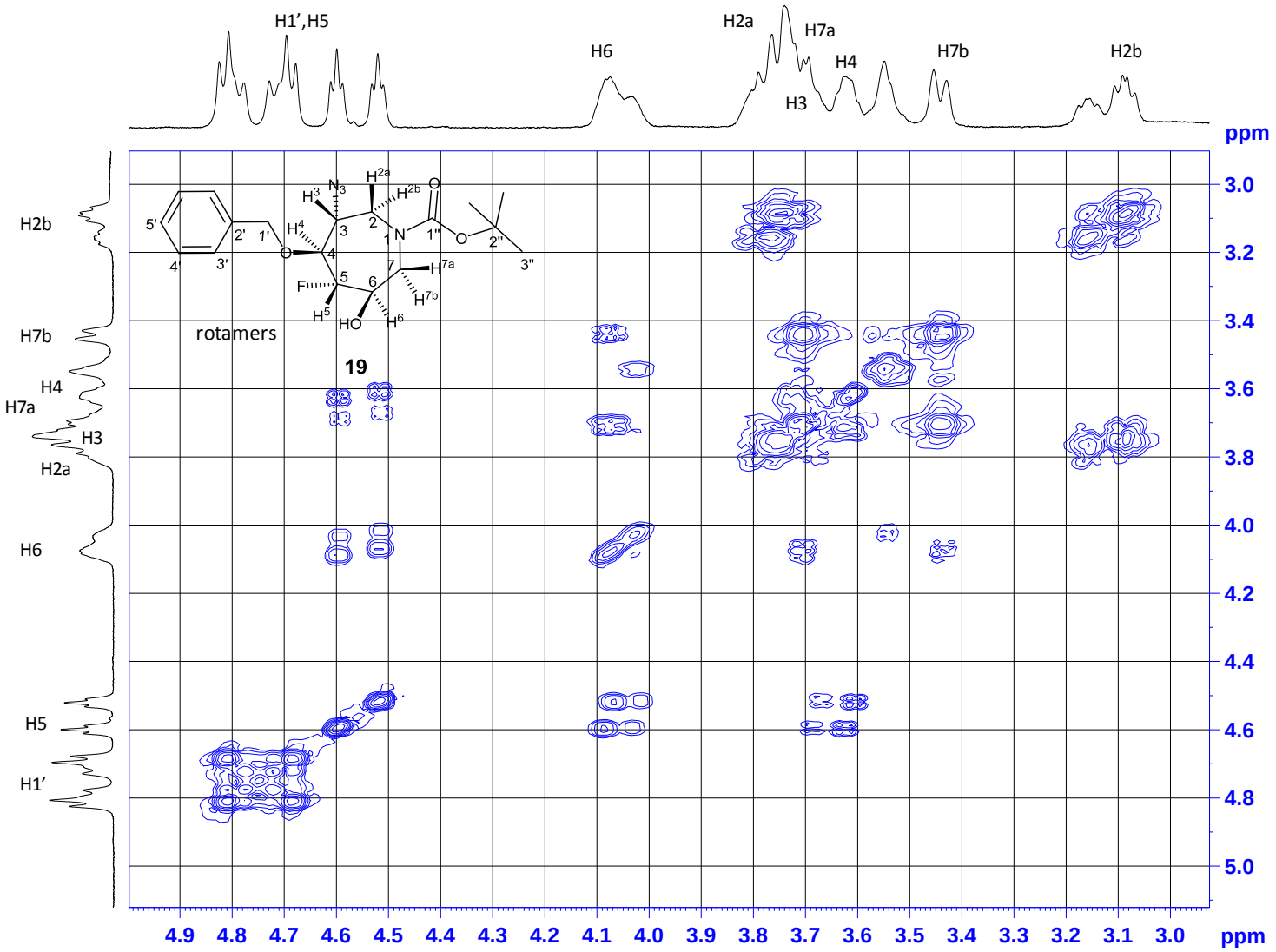
^{13}C NMR-**19**

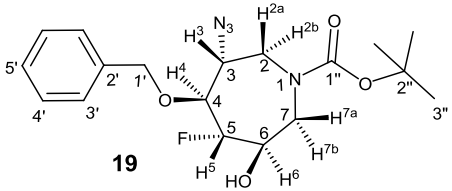

Current Data Parameters
NAME Compound 17
EXPNO 3
PROCNO 1
F2 - Acquisition Parameters
Date_ 20121206
Time 13.17
INSTRUM spect
PROBHD 5 mm CPTXI 1H-
PULPROG udeft.txt
TD 21814
SOLVENT CDCl3
NS 5120
DS 0
SWH 30303.031 Hz
FIDRES 1.389155 Hz
AQ 0.3599810 sec
RG 32768
DW 16.500 usec
DE 6.00 usec
TE 298.0 K
D1 1.50000000 sec
D11 0.03000000 sec
d12 0.00002000 sec
D20 0.10000000 sec
DELTA 1.47000003 sec
DELTA2 0.36300099 sec
TAU 0.00302000 sec
TD0 1
======== CHANNEL f1 ========
NUC1 13C
P1 10.43 usec
P12 2000.00 usec
P26 500.00 usec
PL1 -2.50 dB
SFO1 150.9319817 MHz
SP2 5.29 dB
SP8 4.75 dB
SPNAM2 Crp60comp.4
SPNAM8 Crp60,0.5,20.1
SPOAL2 0.500
SPOAL8 0.500
SPOFFS2 0 Hz
SPOFFS8 0 Hz
======== CHANNEL f2 ========
CPDPRG2 waltz64
NUC2 1H
PCPD2 80.00 usec
PL2 1.00 dB
PL12 18.89 dB
SFO2 600.1830000 MHz
F1 - Acquisition parameters
TD 256
SFO1 150.932 MHz
FIDRES 93.450958 Hz
SW 158.505 ppm
FnMODE States-TPPI
F2 - Processing parameters
SI 262144
SF 150.9153616 MHz
WDW EM
SSB 0
LB 3.00 Hz
GB 0
PC 2.00
15599
137.14
128.69
128.61
128.38
96.80
95.63
82.01
81.89
81.68
81.54
77.37
77.16
76.95
74.92
71.49
71.33
70.87
70.73
63.01
62.03
49.00
48.77
47.93
46.76
28.42
BnO
N3
F
HO
N
Boc
19
rotamers
160
150
140
130
120
110
100
90
80
70
60
50
40
30
20
ppm


H3',4',5'
H1',H5
H6
H2a,3&7a
H4
H7b
H2b
H3"
ppm
C3"
C2
C7
C3
C6
C1'
C4
C2"
C5
C3',4',5'
C2'
C1"
rotamers
19
7.5
7.0
6.5
6.0
5.5
5.0
4.5
4.0
3.5
3.0
2.5
2.0
1.5
ppm


H3',4',5'
H1',H5
H6
H2a,3&7a
H4
H7b
H2b
H3"
ppm
C3"
C2
C7
C3
C6
C1'
C4
C2"
C5
C3',4',5'
C2'
C1"
rotamers
19
7.5
7.0
6.5
6.0
5.5
5.0
4.5
4.0
3.5
3.0
2.5
2.0
1.5
ppm

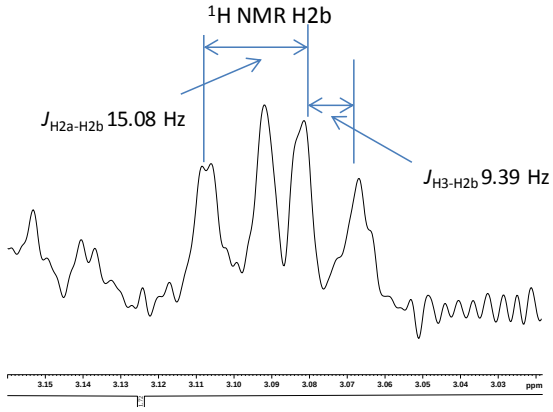
COSY-**19**


H1',H5
H6
H2a
H7a
H4
H3
H7b
H2b
ppm
rotamers
19
3.0
3.2
3.4
3.6
3.8
4.0
4.2
4.4
4.6
4.8
5.0
4.9 4.8 4.7 4.6 4.5 4.4 4.3 4.2 4.1 4.0 3.9 3.8 3.7 3.6 3.5 3.4 3.3 3.2 3.1 3.0
ppm

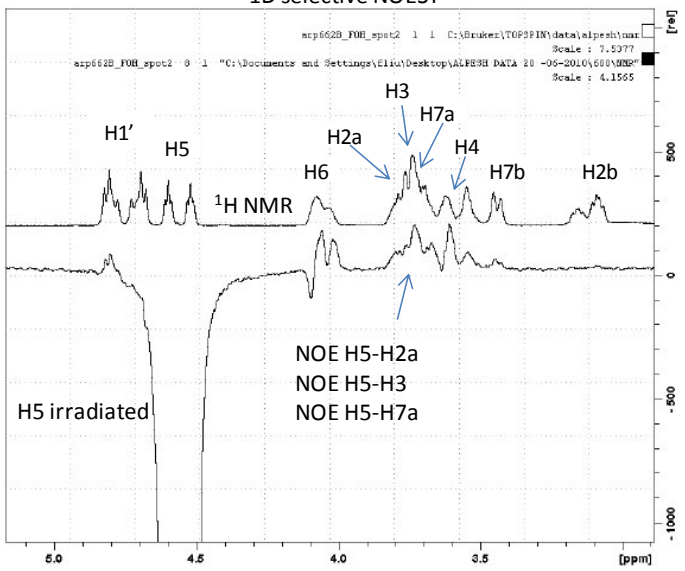


19

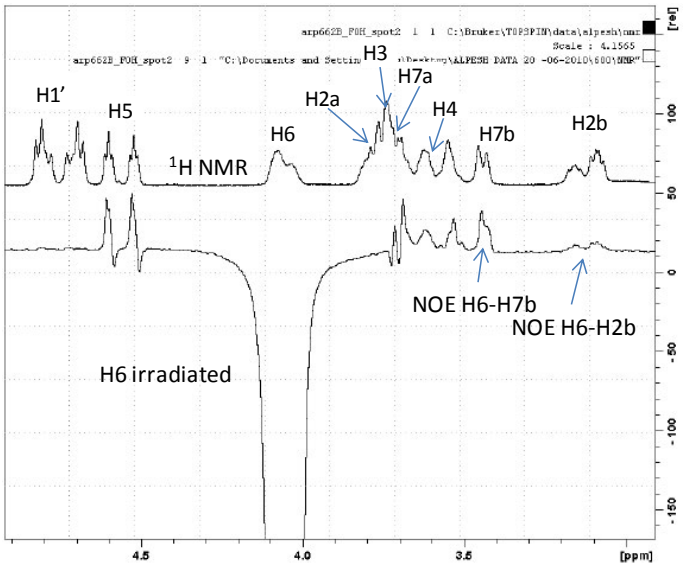
- Compound **18** has C3, C4 and C6 as known absolute chemistry stereocentres.
- **H2a and H2b** : $J_{H3\text{-}H2b}$ = 9.39 Hz suggests a clear *anti* torsion angles 155° or 208°). It is also supported by NOE H2b-H6.
- **H5** : H5 shows NOE to H3, H7a (bigger than H7b) and H2a (no measurable NOE to H2b). $J_{H5\text{-}H6}$ and $J_{H4\text{-}H5}$ both are 7 Hz supporting *trans* geometry in both the cases. H5 shows big NOE to H3 as well; further confirming H5 is *syn* to H3 and *trans* to H4 and H6.



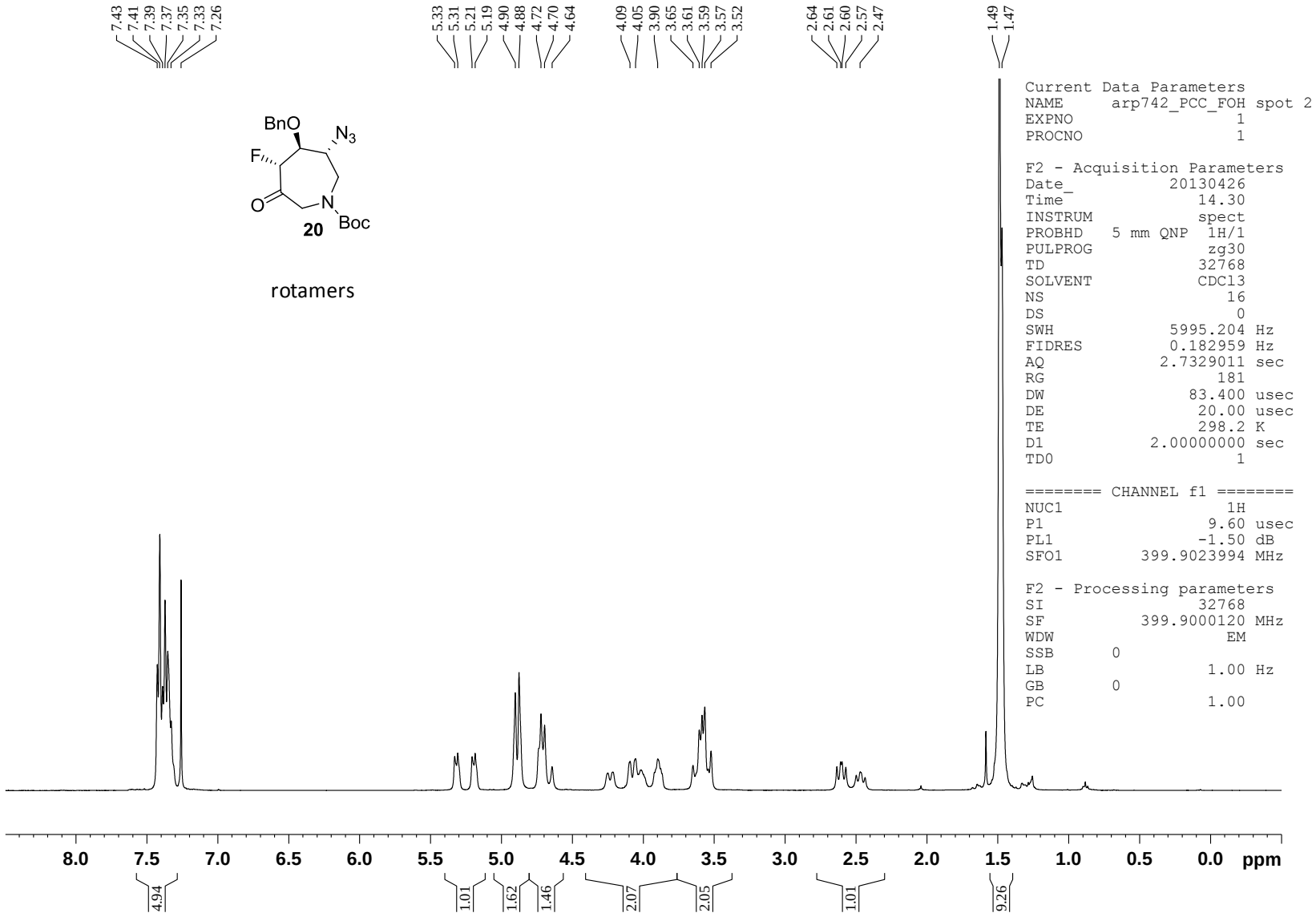
1D selective NOESY



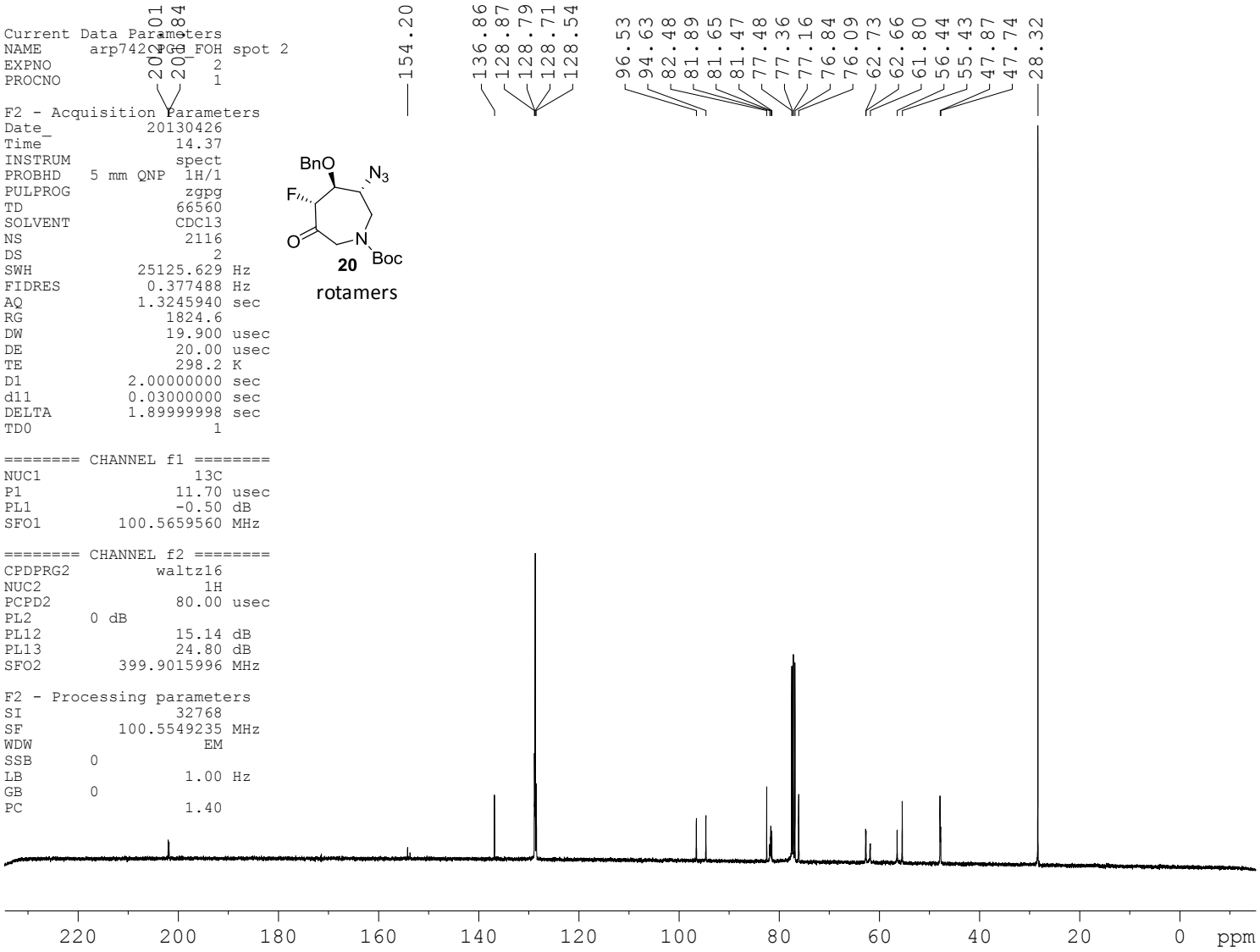
1D selective NOESY



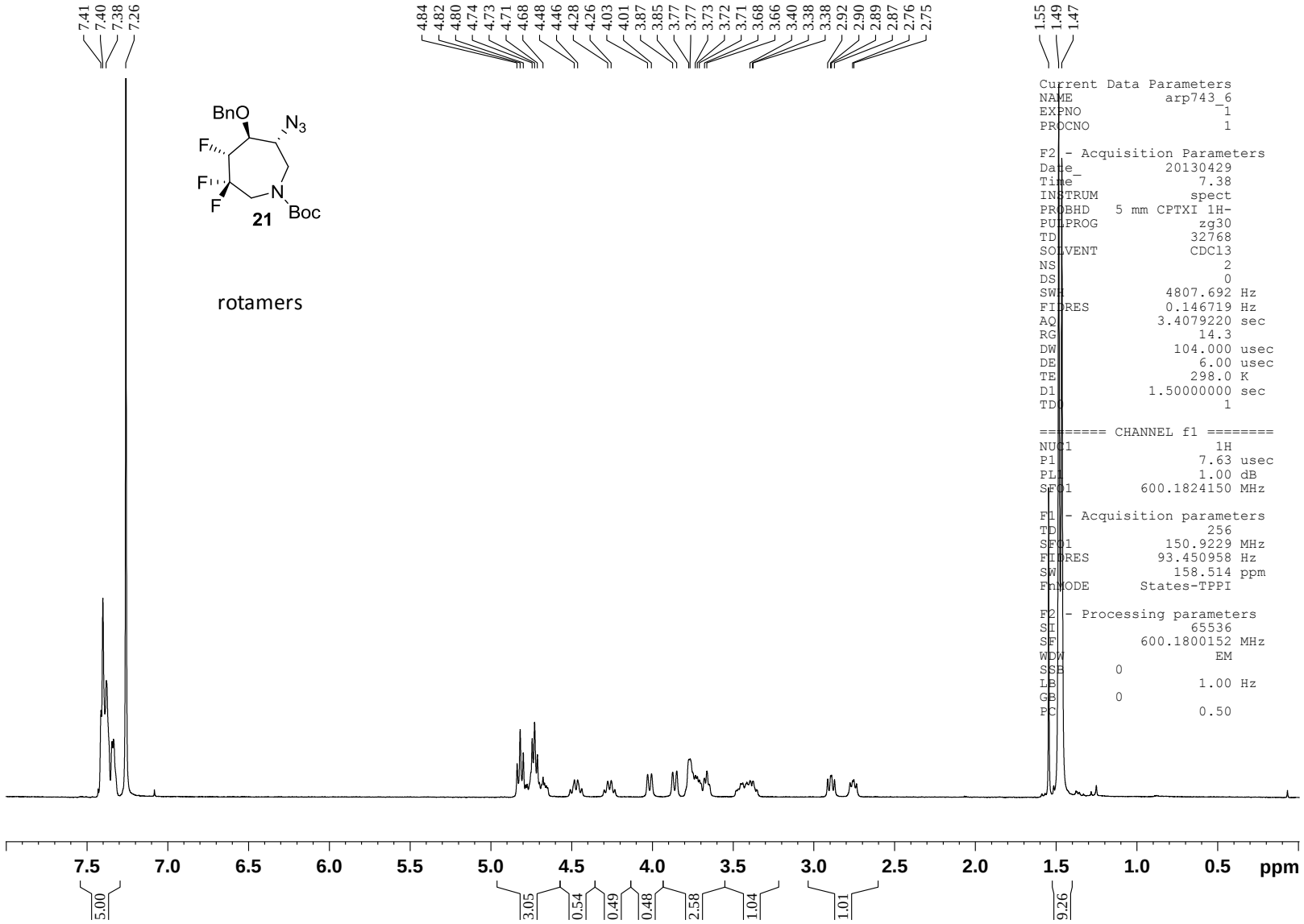
^{1}H NMR-**20**


7.43
7.41
7.39
7.37
7.35
7.33
7.26
5.33
5.31
5.21
5.19
4.90
4.88
4.72
4.70
4.64
4.09
4.05
3.90
3.65
3.61
3.59
3.57
3.52
2.64
2.61
2.60
2.57
2.47
1.49
1.47
BnO
N3
F
O
N
Boc
20
rotamers
Current Data Parameters
NAME arp742_PCC_FOH spot 2
EXPNO 1
PROCNO 1
F2 - Acquisition Parameters
Date_ 20130426
Time 14.30
INSTRUM spect
PROBHD 5 mm QNP 1H/1
PULPROG zg30
TD 32768
SOLVENT CDCl3
NS 16
DS 0
SWH 5995.204 Hz
FIDRES 0.182959 Hz
AQ 2.7329011 sec
RG 181
DW 83.400 usec
DE 20.00 usec
TE 298.2 K
D1 2.00000000 sec
TD0 1
======== CHANNEL f1 ========
NUC1 1H
P1 9.60 usec
PL1 -1.50 dB
SFO1 399.9023994 MHz
F2 - Processing parameters
SI 32768
SF 399.9000120 MHz
WDW EM
SSB 0
LB 1.00 Hz
GB 0
PC 1.00
8.0
7.5
7.0
6.5
6.0
5.5
5.0
4.5
4.0
3.5
3.0
2.5
2.0
1.5
1.0
0.5
0.0
ppm
4.94
1.01
1.62
1.46
2.07
2.05
1.01
9.26

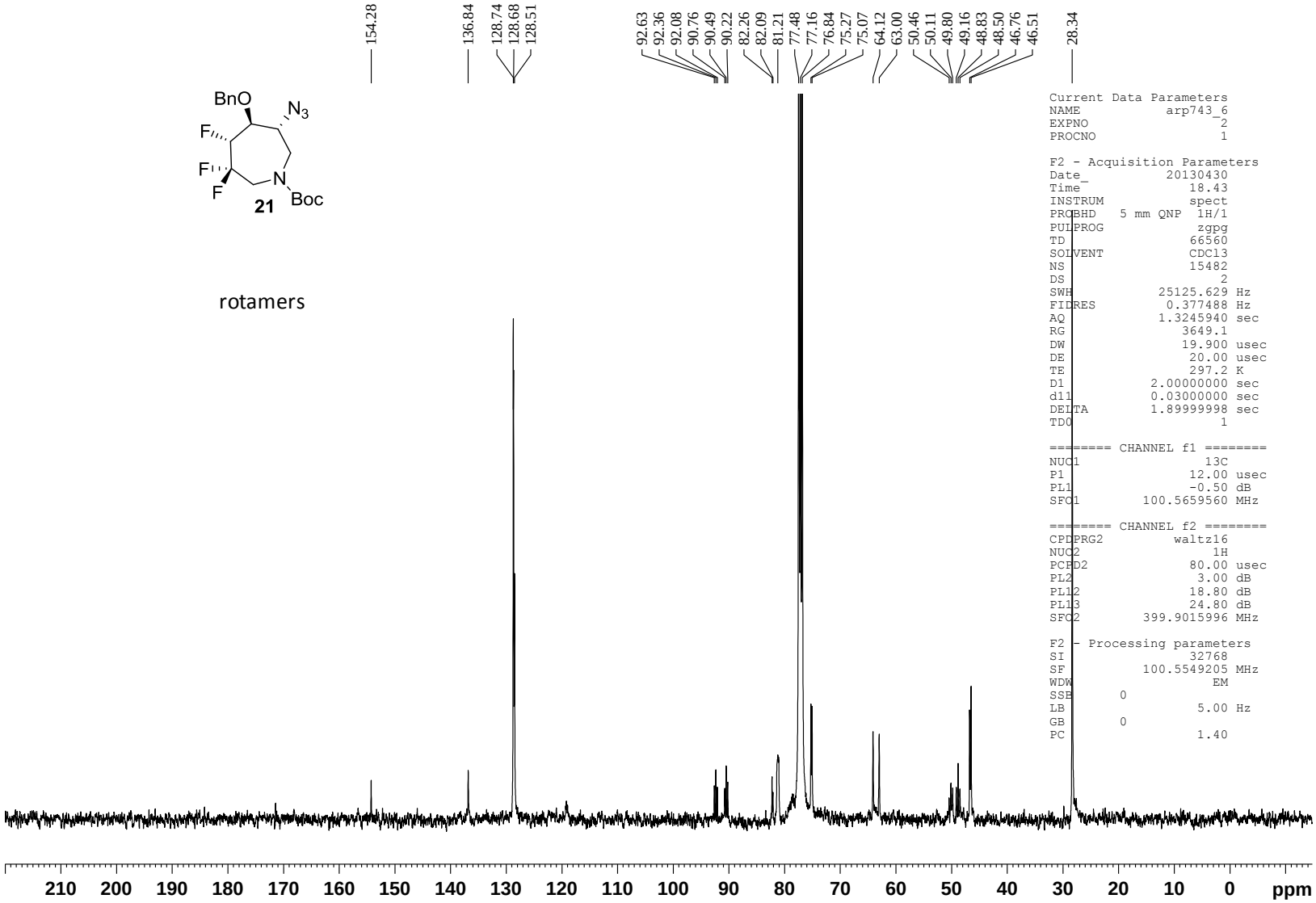
^{13}C NMR-**20**


201.01
200.84
154.20
136.86
128.87
128.79
128.71
128.54
96.53
94.63
82.48
81.89
81.65
81.47
77.48
77.36
77.16
76.84
76.09
62.73
62.66
61.80
56.44
55.43
47.87
47.74
28.32
BnO
N3
F
O
N
Boc
20
rotamers
Current Data Parameters
NAME arp7422_PGG_FOH spot 2
EXPNO 2
PROCNO 1
F2 - Acquisition Parameters
Date_ 20130426
Time 14.37
INSTRUM spect
PROBHD 5 mm QNP 1H/1
PULPROG zgpg
TD 66560
SOLVENT CDCl3
NS 2116
DS 2
SWH 25125.629 Hz
FIDRES 0.377488 Hz
AQ 1.3245940 sec
RG 1824.6
DW 19.900 usec
DE 20.00 usec
TE 298.2 K
D1 2.00000000 sec
d11 0.03000000 sec
DELTA 1.89999998 sec
TD0 1
======== CHANNEL f1 ========
NUC1 13C
P1 11.70 usec
PL1 -0.50 dB
SFO1 100.5659560 MHz
======== CHANNEL f2 ========
CPDPRG2 waltz16
NUC2 1H
PCPD2 80.00 usec
PL2 0 dB
PL12 15.14 dB
PL13 24.80 dB
SFO2 399.9015996 MHz
F2 - Processing parameters
SI 32768
SF 100.5549235 MHz
WDW EM
SSB 0
LB 1.00 Hz
GB 0
PC 1.40
220
200
180
160
140
120
100
80
60
40
20
0
ppm

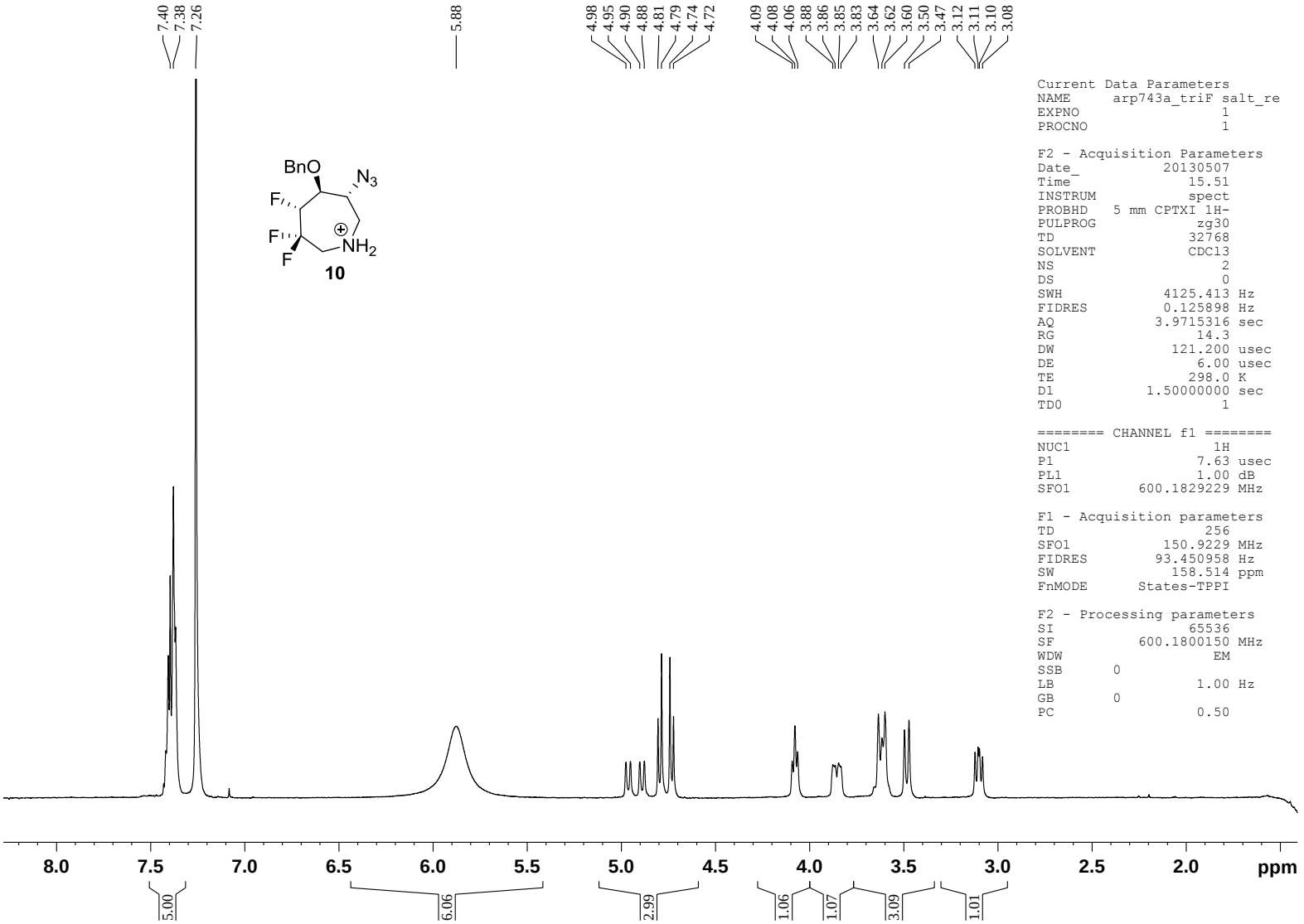
^{1}H NMR-**21**


7.41
7.40
7.38
7.26
4.84
4.82
4.80
4.74
4.73
4.71
4.68
4.48
4.46
4.28
4.26
4.03
4.01
3.87
3.85
3.77
3.77
3.73
3.72
3.71
3.68
3.66
3.40
3.38
3.38
2.92
2.90
2.89
2.87
2.76
2.75
1.55
1.49
1.47
BnO
N3
F
F
F
N
Boc
21
rotamers
Current Data Parameters
NAME arp743_6
EXPNO 1
PROCNO 1
F2 - Acquisition Parameters
Date_ 20130429
Time 7.38
INSTRUM spect
PROBHD 5 mm CPTXI 1H-
PULPROG zg30
TD 32768
SOLVENT CDCl3
NS 2
DS 0
SWH 4807.692 Hz
FIDRES 0.146719 Hz
AQ 3.4079220 sec
RG 14.3
DW 104.000 usec
DE 6.00 usec
TE 298.0 K
D1 1.50000000 sec
TD0 1
======== CHANNEL f1 ========
NUC1 1H
P1 7.63 usec
PL1 1.00 dB
SFO1 600.1824150 MHz
F1 - Acquisition parameters
TD 256
SFO1 150.9229 MHz
FIDRES 93.450958 Hz
SW 158.514 ppm
FnMODE States-TPPI
F2 - Processing parameters
SI 65536
SF 600.1800152 MHz
WDW EM
SSB 0
LB 1.00 Hz
GB 0
PC 0.50
7.5
7.0
6.5
6.0
5.5
5.0
4.5
4.0
3.5
3.0
2.5
2.0
1.5
1.0
0.5
ppm
5.00
3.05
0.54
0.49
0.48
2.58
1.04
1.01
9.26

^{13}C NMR-**21**


154.28
136.84
128.74
128.68
128.51
92.63
92.36
92.08
90.76
90.49
90.22
82.26
82.09
81.21
77.48
77.16
76.84
75.27
75.07
64.12
63.00
50.46
50.11
49.80
49.16
48.83
48.50
46.76
46.51
28.34
BnO
N3
F
F
F
N
Boc
21
rotamers
Current Data Parameters
NAME arp743_6
EXPNO 2
PROCNO 1
F2 - Acquisition Parameters
Date_ 20130430
Time 18.43
INSTRUM spect
PROBHD 5 mm QNP 1H/1
PULPROG zgpg
TD 66560
SOLVENT CDCl3
NS 15482
DS 2
SWH 25125.629 Hz
FIDRES 0.377488 Hz
AQ 1.3245940 sec
RG 3649.1
DW 19.900 usec
DE 20.00 usec
TE 297.2 K
D1 2.00000000 sec
d11 0.03000000 sec
DELTA 1.89999998 sec
TD0 1
======== CHANNEL f1 ========
NUC1 13C
P1 12.00 usec
PL1 -0.50 dB
SFO1 100.5659560 MHz
======== CHANNEL f2 ========
CPDPRG2 waltz16
NUC2 1H
PCPD2 80.00 usec
PL2 3.00 dB
PL12 18.80 dB
PL13 24.80 dB
SFO2 399.9015996 MHz
F2 - Processing parameters
SI 32768
SF 100.5549205 MHz
WDW EM
SSB 0
LB 5.00 Hz
GB 0
PC 1.40
210 200 190 180 170 160 150 140 130 120 110 100 90 80 70 60 50 40 30 20 10 0 ppm

^{1}H NMR-**10**




```
Current Data Parameters
NAME      arp743a_triF salt_re
EXPNO                  1
PROCNO                 1

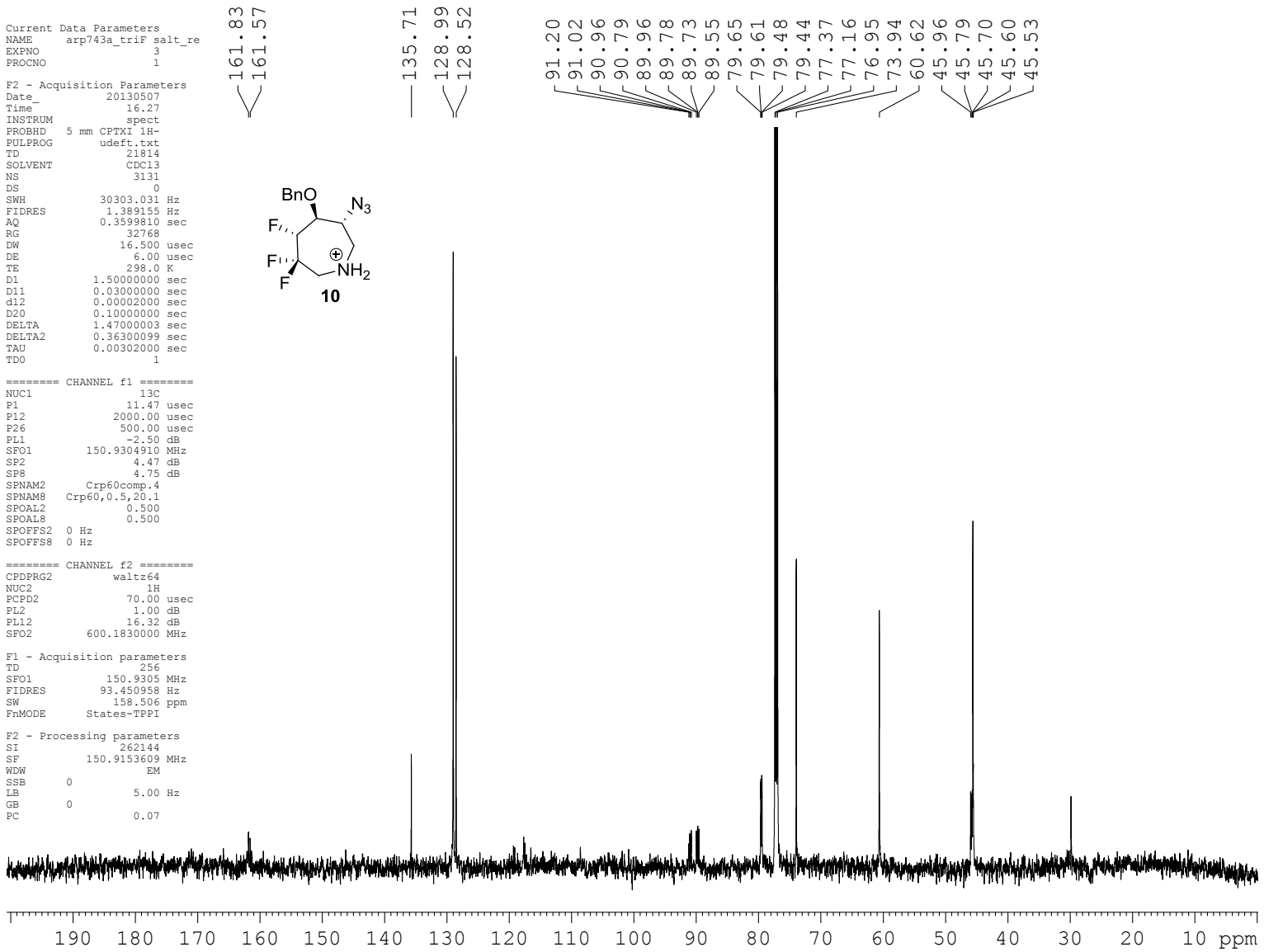
F2 - Acquisition Parameters
Date_           20130507
Time              15.51
INSTRUM           spect
PROBHD   5 mm CPTXI 1H-
PULPROG            zg30
TD                32768
SOLVENT           CDCl3
NS                    2
DS                    0
SWH            4125.413 Hz
FIDRES         0.125898 Hz
AQ            3.9715316 sec
RG                 14.3
DW              121.200 usec
DE                6.00 usec
TE               298.0 K
D1           1.50000000 sec
TD0                   1

======== CHANNEL f1 ========
NUC1                  1H
P1                 7.63 usec
PL1                1.00 dB
SFO1        600.1829229 MHz

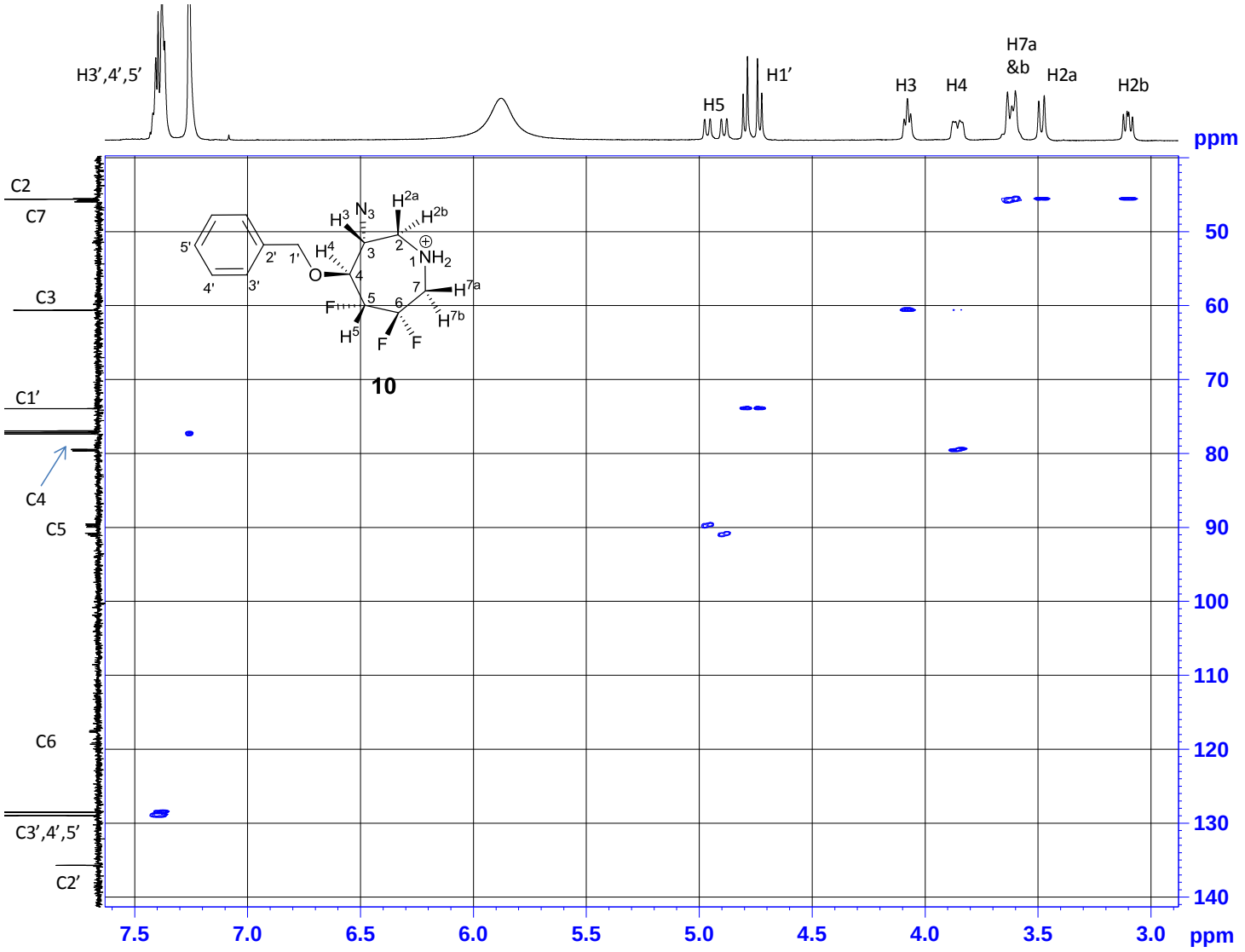
F1 - Acquisition parameters
TD                  256
SFO1           150.9229 MHz
FIDRES         93.450958 Hz
SW              158.514 ppm
FnMODE       States-TPPI

F2 - Processing parameters
SI                65536
SF           600.1800150 MHz
WDW                  EM
SSB       0
LB                 1.00 Hz
GB        0
PC                 0.50
```

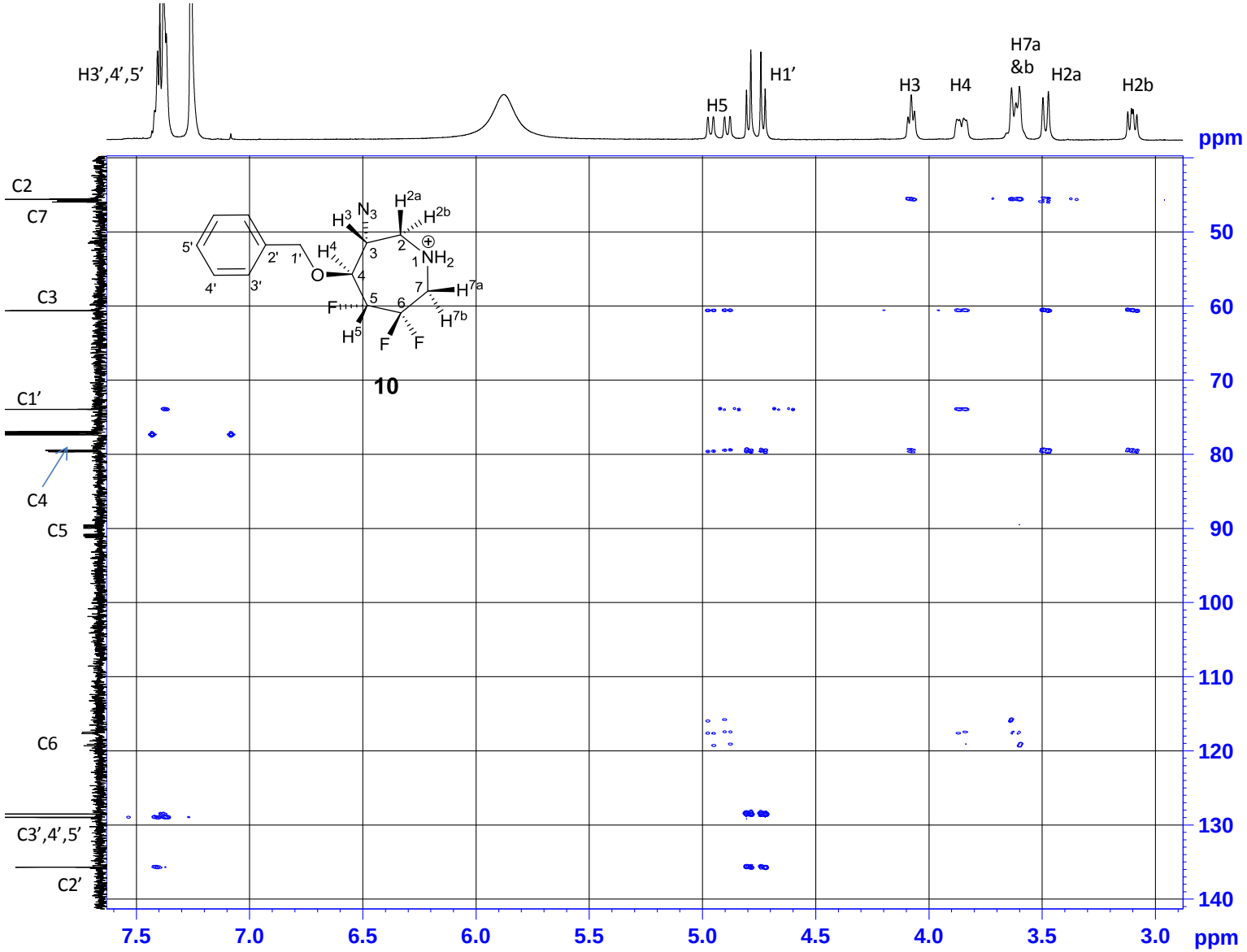
^{13}C NMR-**10**


161.83
161.57
135.71
128.99
128.52
91.20
91.02
90.96
90.79
89.96
89.78
89.73
89.55
79.65
79.61
79.48
79.44
77.37
77.16
76.95
73.94
60.62
45.96
45.79
45.70
45.60
45.53
BnO
N3
F
F
F
NH2
10
Current Data Parameters
NAME arp743a_triF salt_re
EXPNO 3
PROCNO 1
F2 - Acquisition Parameters
Date_ 20130507
Time 16.27
INSTRUM spect
PROBHD 5 mm CPTXI 1H-
PULPROG udeft.txt
TD 21814
SOLVENT CDCl3
NS 3131
DS 0
SWH 30303.031 Hz
FIDRES 1.389155 Hz
AQ 0.3599810 sec
RG 32768
DW 16.500 usec
DE 6.00 usec
TE 298.0 K
D1 1.50000000 sec
D11 0.03000000 sec
d12 0.00002000 sec
D20 0.10000000 sec
DELTA 1.47000003 sec
DELTA2 0.36300099 sec
TAU 0.00302000 sec
TD0 1
======== CHANNEL f1 ========
NUC1 13C
P1 11.47 usec
P12 2000.00 usec
P26 500.00 usec
PL1 -2.50 dB
SFO1 150.9304910 MHz
SP2 4.47 dB
SP8 4.75 dB
SPNAM2 Crp60comp.4
SPNAM8 Crp60,0.5,20.1
SPOAL2 0.500
SPOAL8 0.500
SPOFFS2 0 Hz
SPOFFS8 0 Hz
======== CHANNEL f2 ========
CPDPRG2 waltz64
NUC2 1H
PCPD2 70.00 usec
PL2 1.00 dB
PL12 16.32 dB
SFO2 600.1830000 MHz
F1 - Acquisition parameters
TD 256
SFO1 150.9305 MHz
FIDRES 93.450958 Hz
SW 158.506 ppm
FnMODE States-TPPI
F2 - Processing parameters
SI 262144
SF 150.9153609 MHz
WDW EM
SSB 0
LB 5.00 Hz
GB 0
PC 0.07
190 180 170 160 150 140 130 120 110 100 90 80 70 60 50 40 30 20 10 ppm

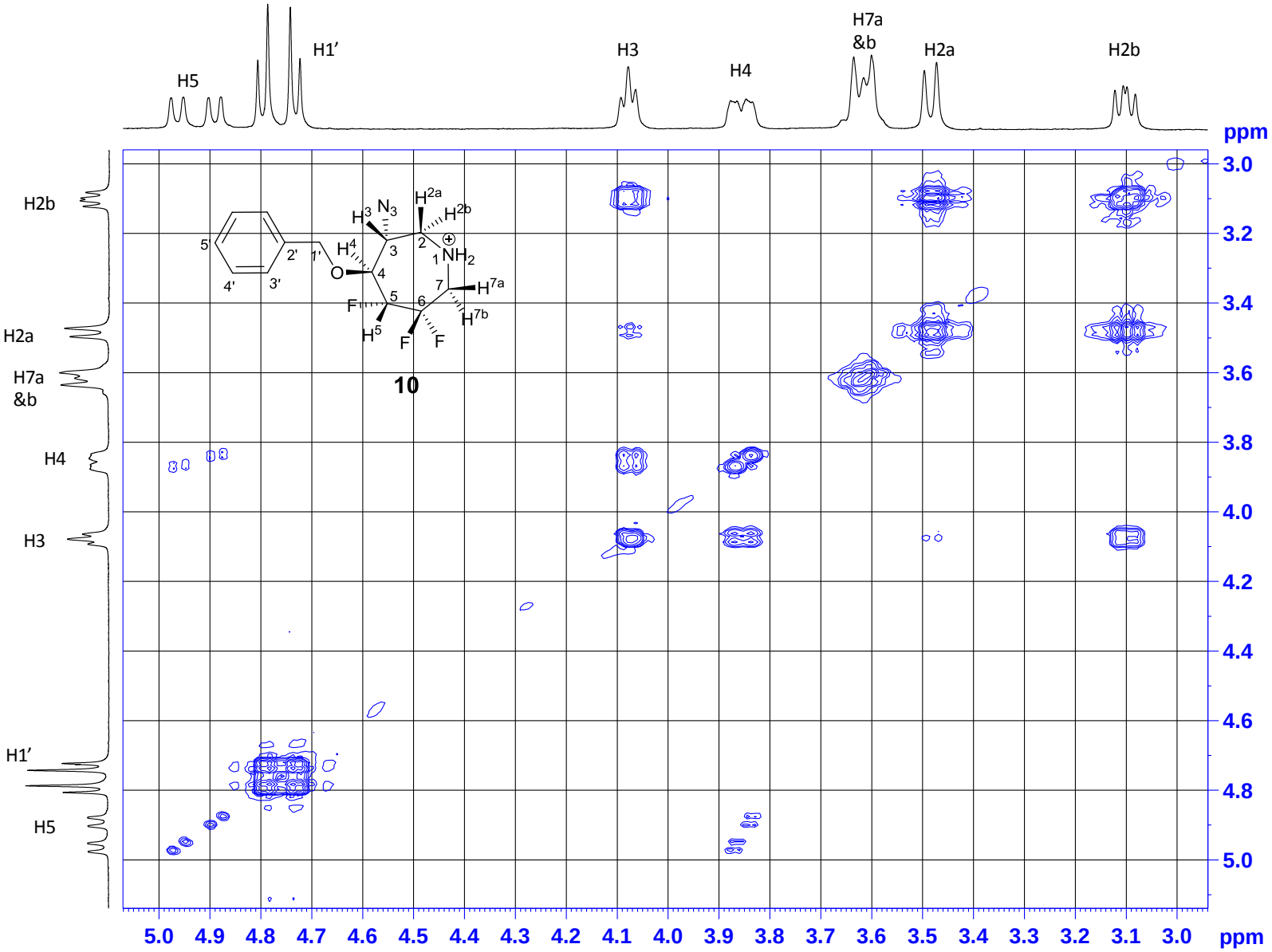
HSQC-**10**


H3',4',5'
H5
H1'
H3
H4
H7a
&b
H2a
H2b
ppm
C2
C7
C3
C1'
C4
C5
C6
C3',4',5'
C2'
10
7.5
7.0
6.5
6.0
5.5
5.0
4.5
4.0
3.5
3.0
ppm

HMBC-**10**

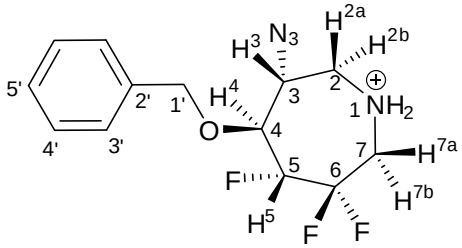

H3',4',5'
H5
H1'
H3
H4
H7a
&b
H2a
H2b
ppm
C2
C7
C3
C1'
C4
C5
C6
C3',4',5'
C2'
10
7.5
7.0
6.5
6.0
5.5
5.0
4.5
4.0
3.5
3.0
ppm

COSY-**10**


H5
H1'
H3
H4
H7a &b
H2a
H2b
ppm
3.0
3.2
3.4
3.6
3.8
4.0
4.2
4.4
4.6
4.8
5.0
5.0 4.9 4.8 4.7 4.6 4.5 4.4 4.3 4.2 4.1 4.0 3.9 3.8 3.7 3.6 3.5 3.4 3.3 3.2 3.1 3.0 ppm
10

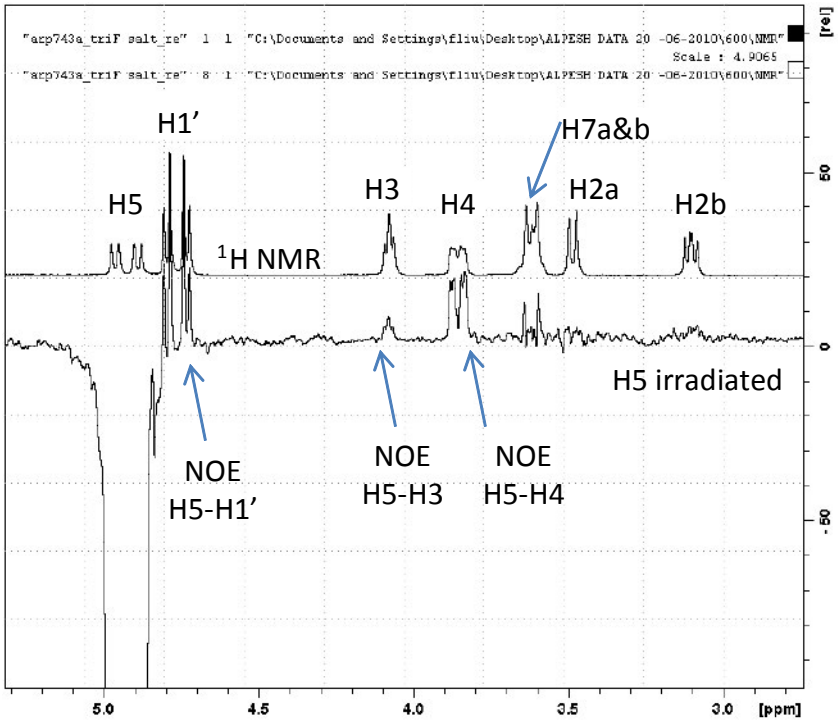
NOESY-**10**

- ❑ H2b shows NOE to H4 meaning H2b is syn to H4 and H2a is syn to H3.
- ❑ H5 shows NOE to H3 and H1'; meaning H5 is *syn* to H3 and *anti* to

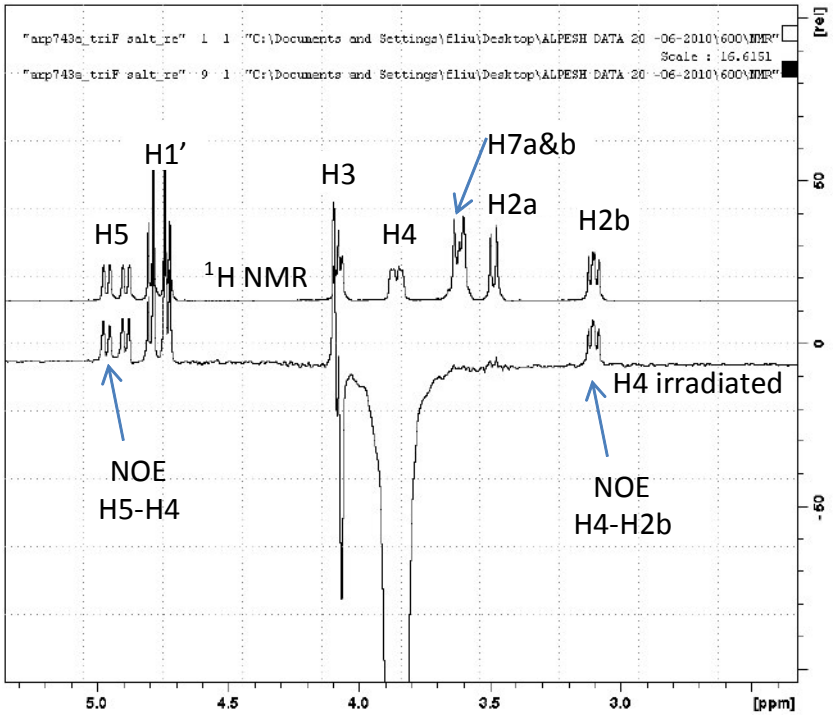


10

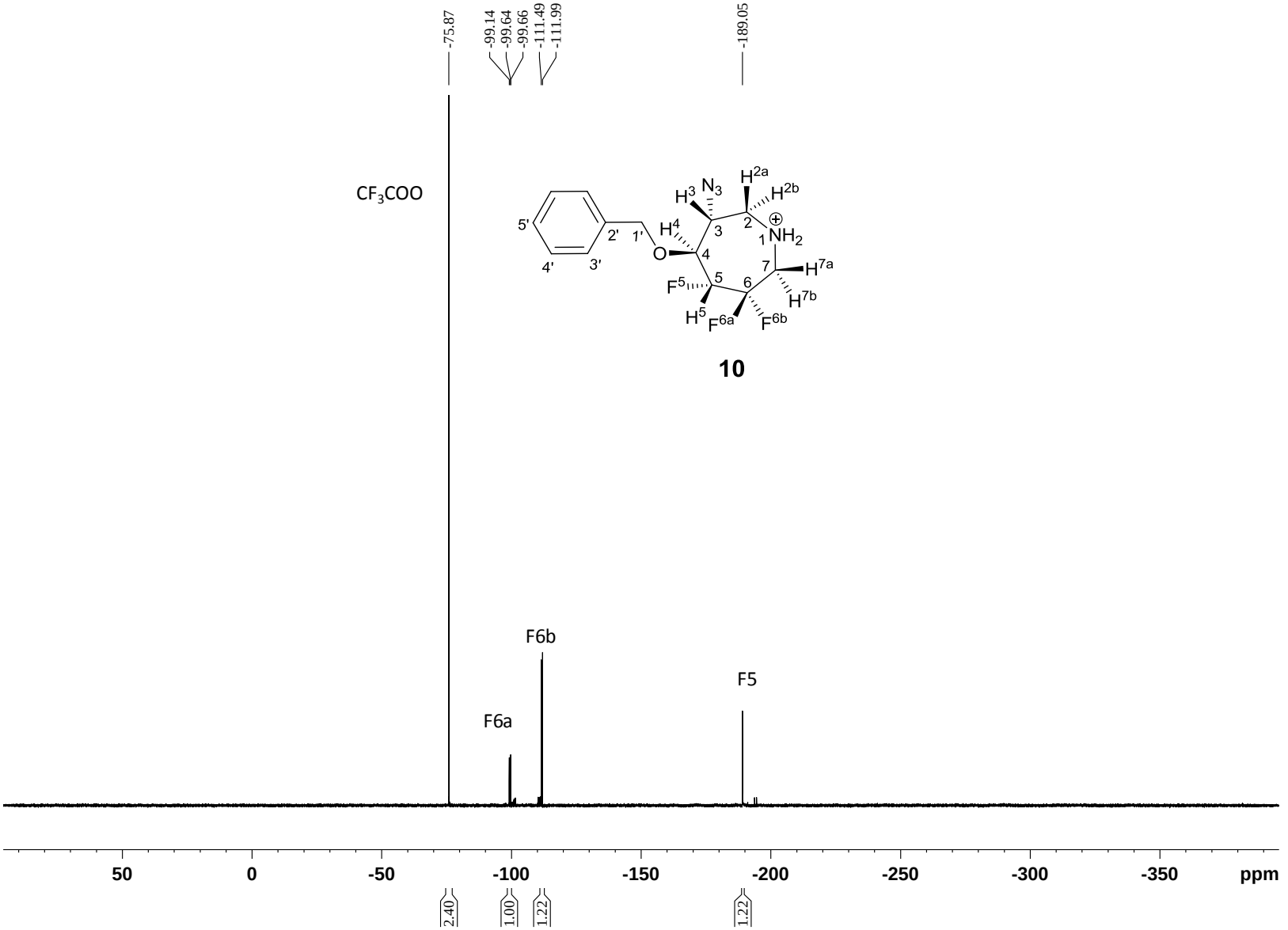
1D selective NOESY



1D selective NOESY

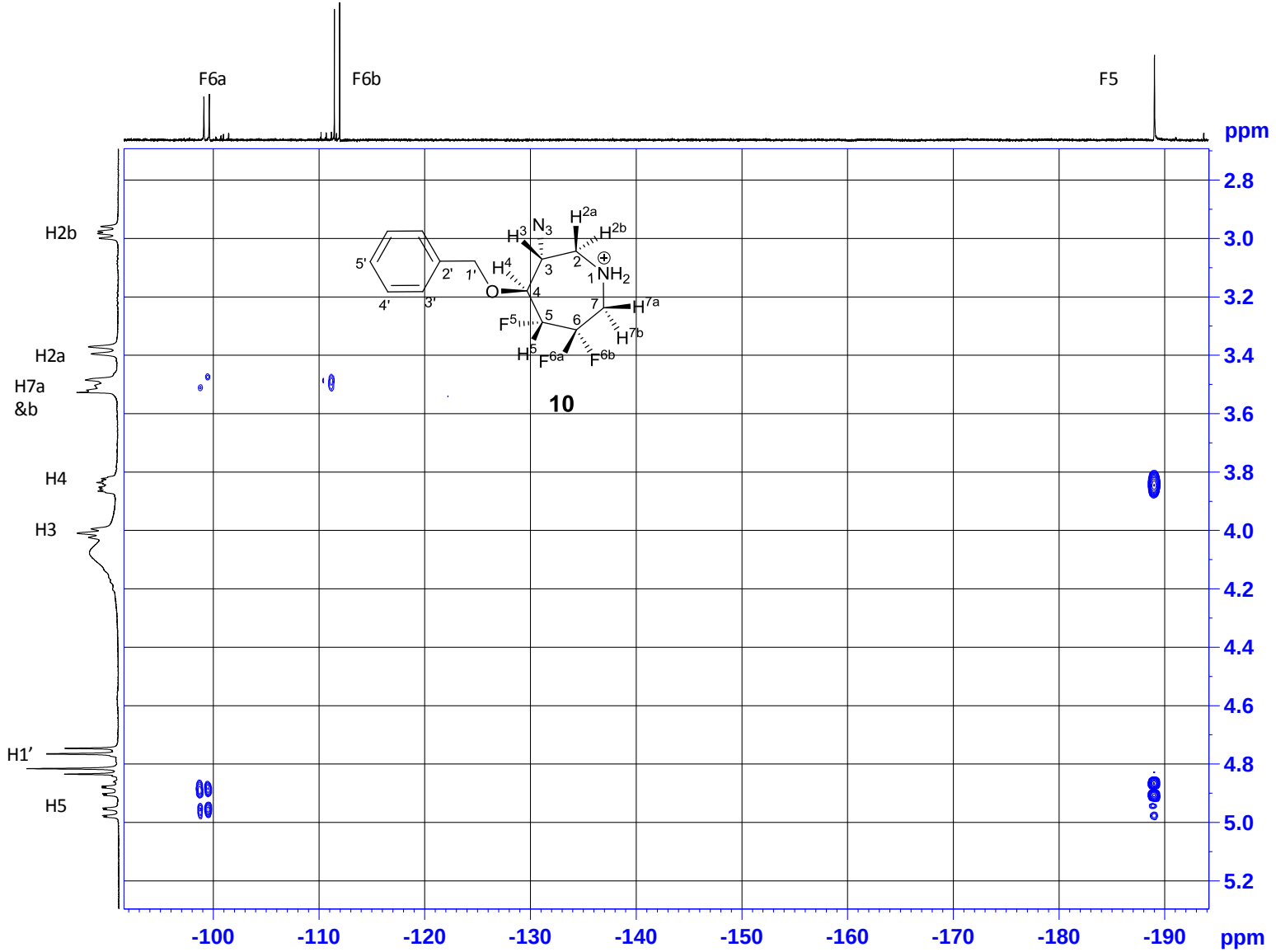


^{19}F NMR-**10**

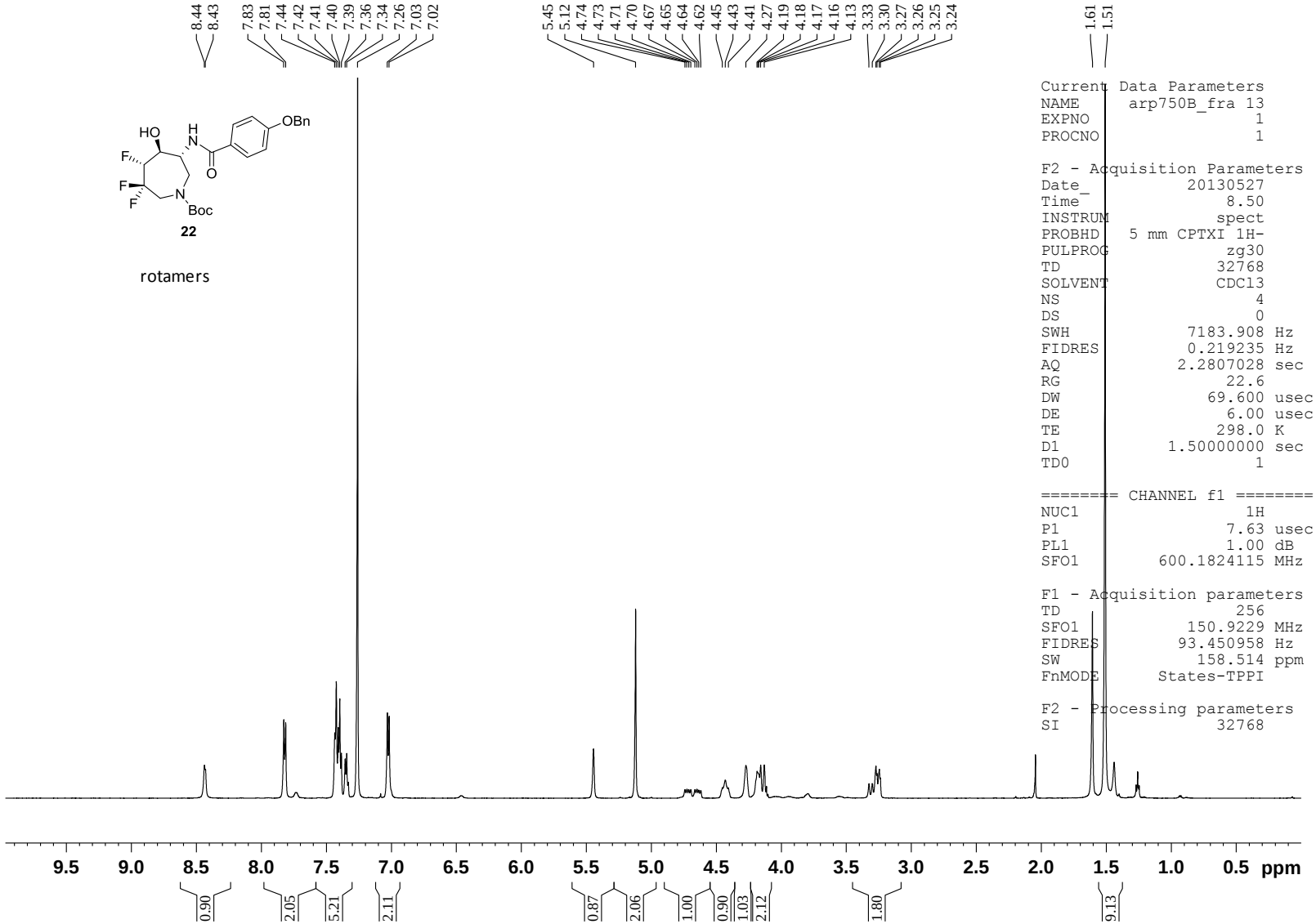

-75.87
-99.14
-99.64
-99.66
-111.49
-111.99
-189.05
CF3COO
F6b
F6a
F5
50
0
-50
-100
-150
-200
-250
-300
-350
ppm
2.40
1.00
1.22
1.22

10

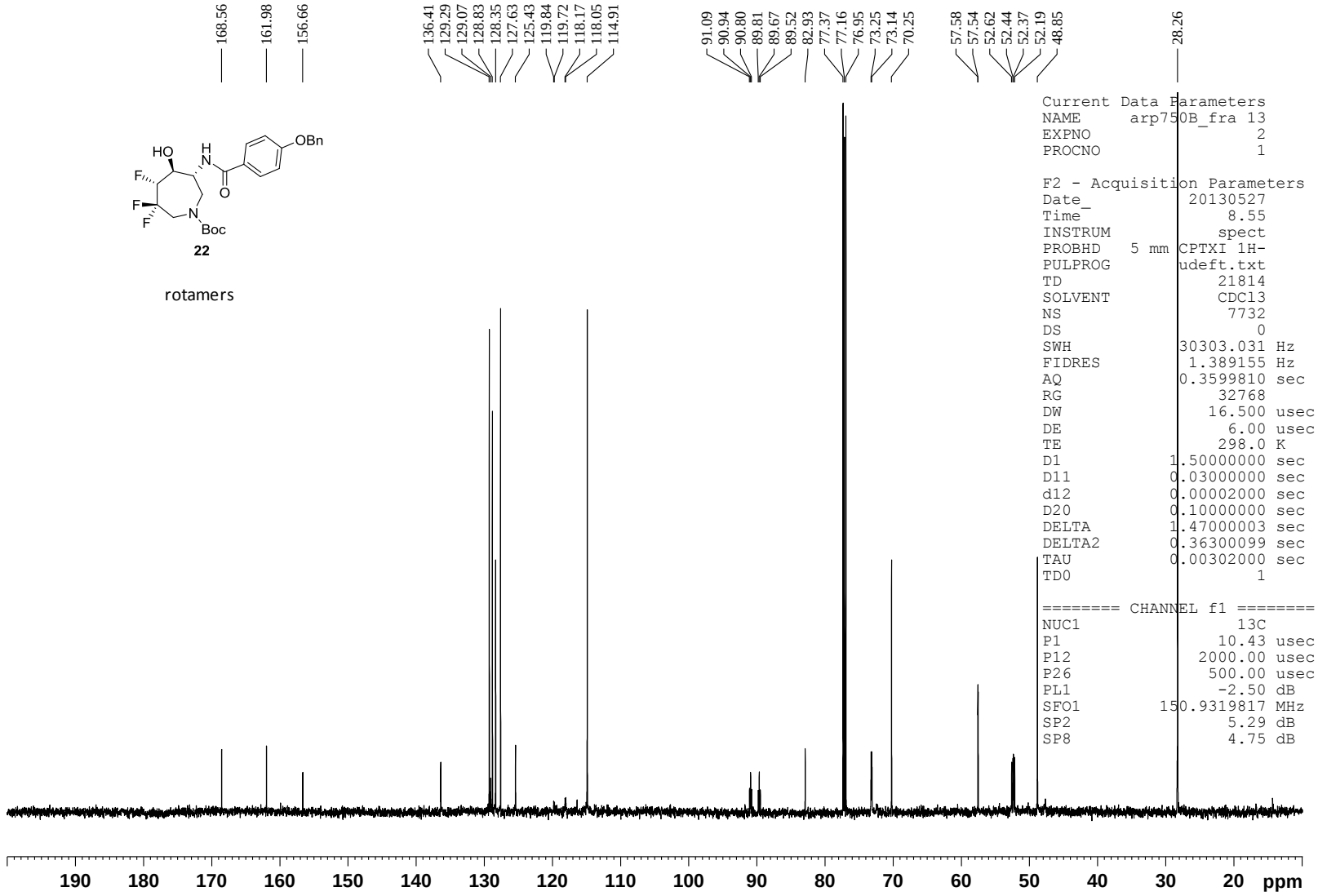
^{1}H-^{19}F HOESY-**10**



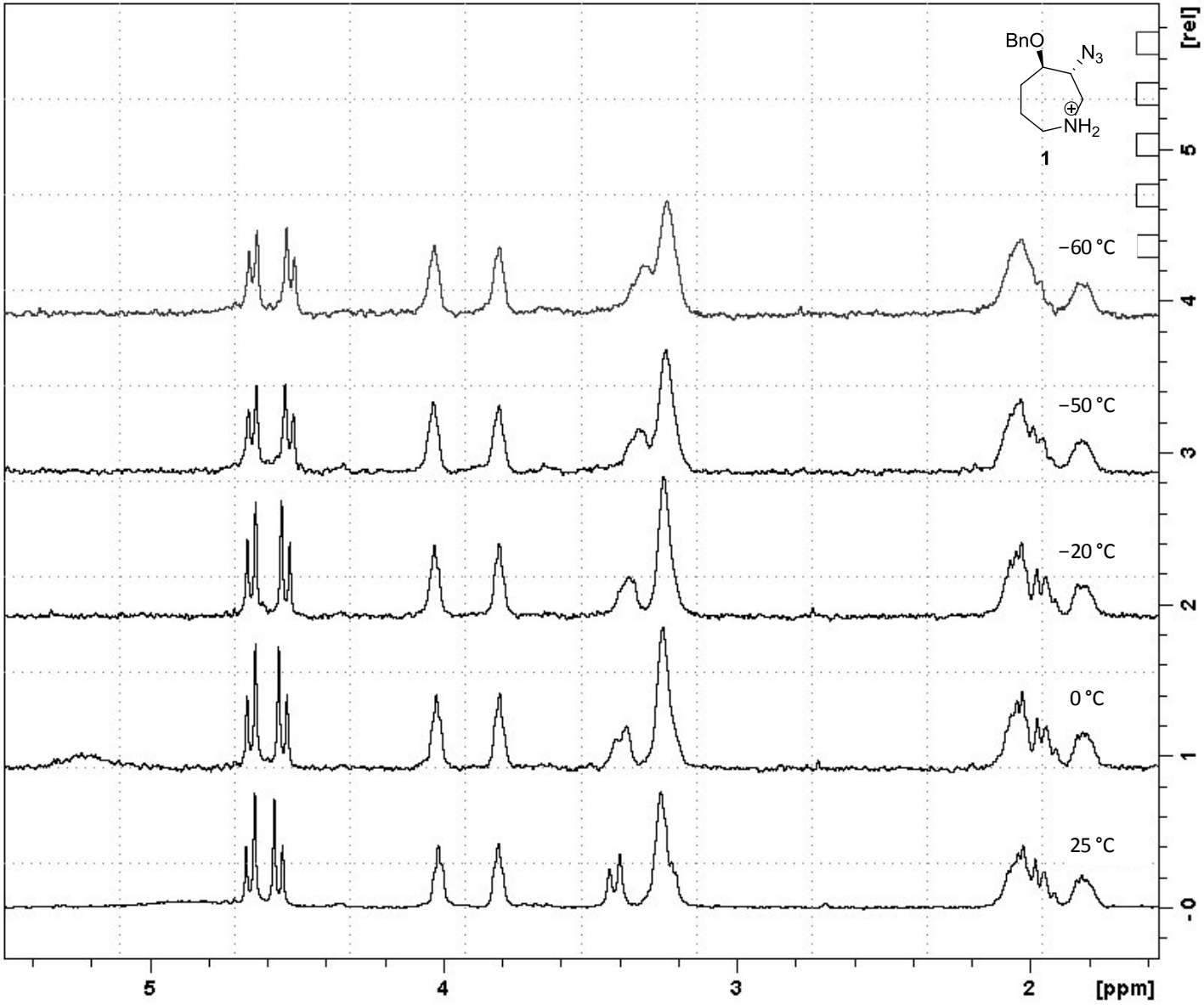
^{1}H NMR-**22**


8.44
8.43
7.83
7.81
7.44
7.42
7.41
7.40
7.39
7.36
7.34
7.26
7.03
7.02
5.45
5.12
4.74
4.73
4.71
4.70
4.67
4.65
4.64
4.62
4.45
4.43
4.41
4.27
4.19
4.18
4.17
4.16
4.13
3.33
3.30
3.27
3.26
3.25
3.24
1.61
1.51
HO
H
N
OBn
O
F
F
F
N
Boc
22
rotamers
Current Data Parameters
NAME arp750B_fra 13
EXPNO 1
PROCNO 1
F2 - Acquisition Parameters
Date_ 20130527
Time 8.50
INSTRUM spect
PROBHD 5 mm CPTXI 1H-
PULPROG zg30
TD 32768
SOLVENT CDCl3
NS 4
DS 0
SWH 7183.908 Hz
FIDRES 0.219235 Hz
AQ 2.2807028 sec
RG 22.6
DW 69.600 usec
DE 6.00 usec
TE 298.0 K
D1 1.50000000 sec
TD0 1
======== CHANNEL f1 ========
NUC1 1H
P1 7.63 usec
PL1 1.00 dB
SFO1 600.1824115 MHz
F1 - Acquisition parameters
TD 256
SFO1 150.9229 MHz
FIDRES 93.450958 Hz
SW 158.514 ppm
FnMODE States-TPPI
F2 - Processing parameters
SI 32768
9.5
9.0
8.5
8.0
7.5
7.0
6.5
6.0
5.5
5.0
4.5
4.0
3.5
3.0
2.5
2.0
1.5
1.0
0.5
ppm
0.90
2.05
5.21
2.11
0.87
2.06
1.00
0.90
1.03
2.12
1.80
9.13

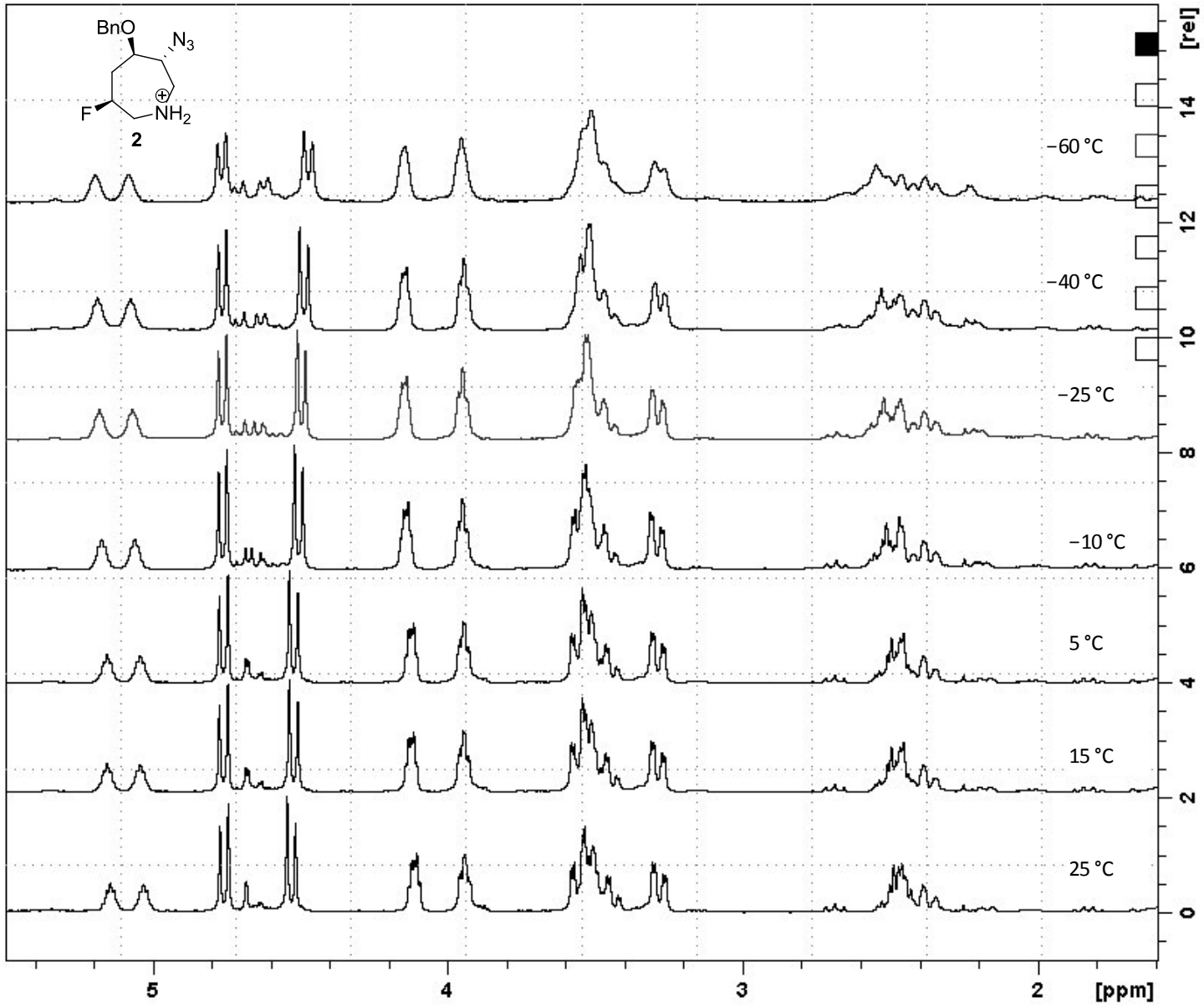
^{13}C NMR-**22**


168.56
161.98
156.66
136.41
129.29
129.07
128.83
128.35
127.63
125.43
119.84
119.72
118.17
118.05
114.91
91.09
90.94
90.80
89.81
89.67
89.52
82.93
77.37
77.16
76.95
73.25
73.14
70.25
57.58
57.54
52.62
52.44
52.37
52.19
48.85
28.26
HO
H
N
OBn
F
F
F
N
O
Boc
22
rotamers
Current Data Parameters
NAME arp750B_fra 13
EXPNO 2
PROCNO 1
F2 - Acquisition Parameters
Date_ 20130527
Time_ 8.55
INSTRUM spect
PROBHD 5 mm CPTXI 1H-
PULPROG udeft.txt
TD 21814
SOLVENT CDCl3
NS 7732
DS 0
SWH 30303.031 Hz
FIDRES 1.389155 Hz
AQ 0.3599810 sec
RG 32768
DW 16.500 usec
DE 6.00 usec
TE 298.0 K
D1 1.50000000 sec
D11 0.03000000 sec
d12 0.00002000 sec
D20 0.10000000 sec
DELTA 1.47000003 sec
DELTA2 0.36300099 sec
TAU 0.00302000 sec
TD0 1
======== CHANNEL f1 ========
NUC1 13C
P1 10.43 usec
P12 2000.00 usec
P26 500.00 usec
PL1 -2.50 dB
SFO1 150.9319817 MHz
SP2 5.29 dB
SP8 4.75 dB
190
180
170
160
150
140
130
120
110
100
90
80
70
60
50
40
30
20
ppm

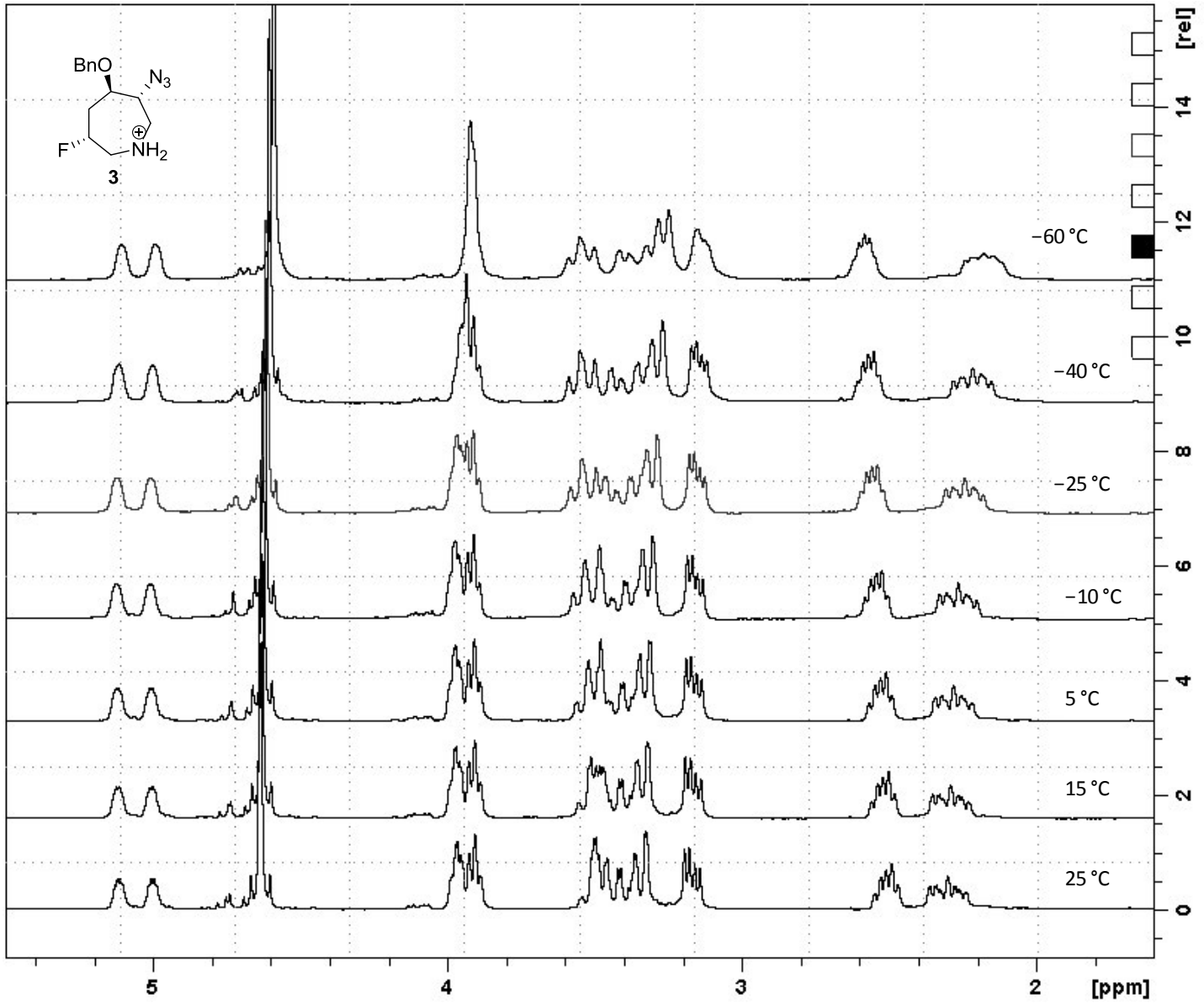
2. Variant temperature NMR studies:



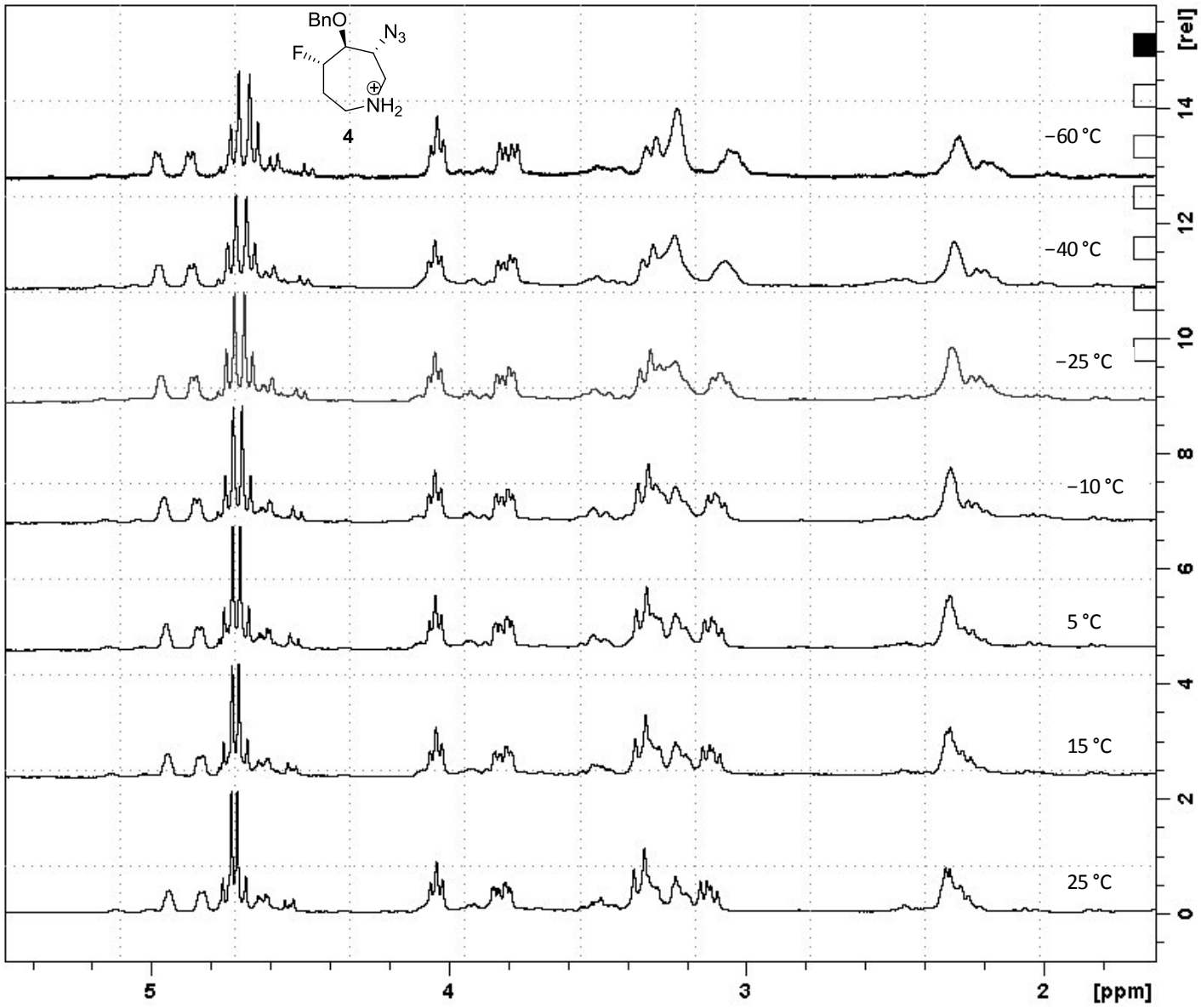
Variant temperature NMR studies



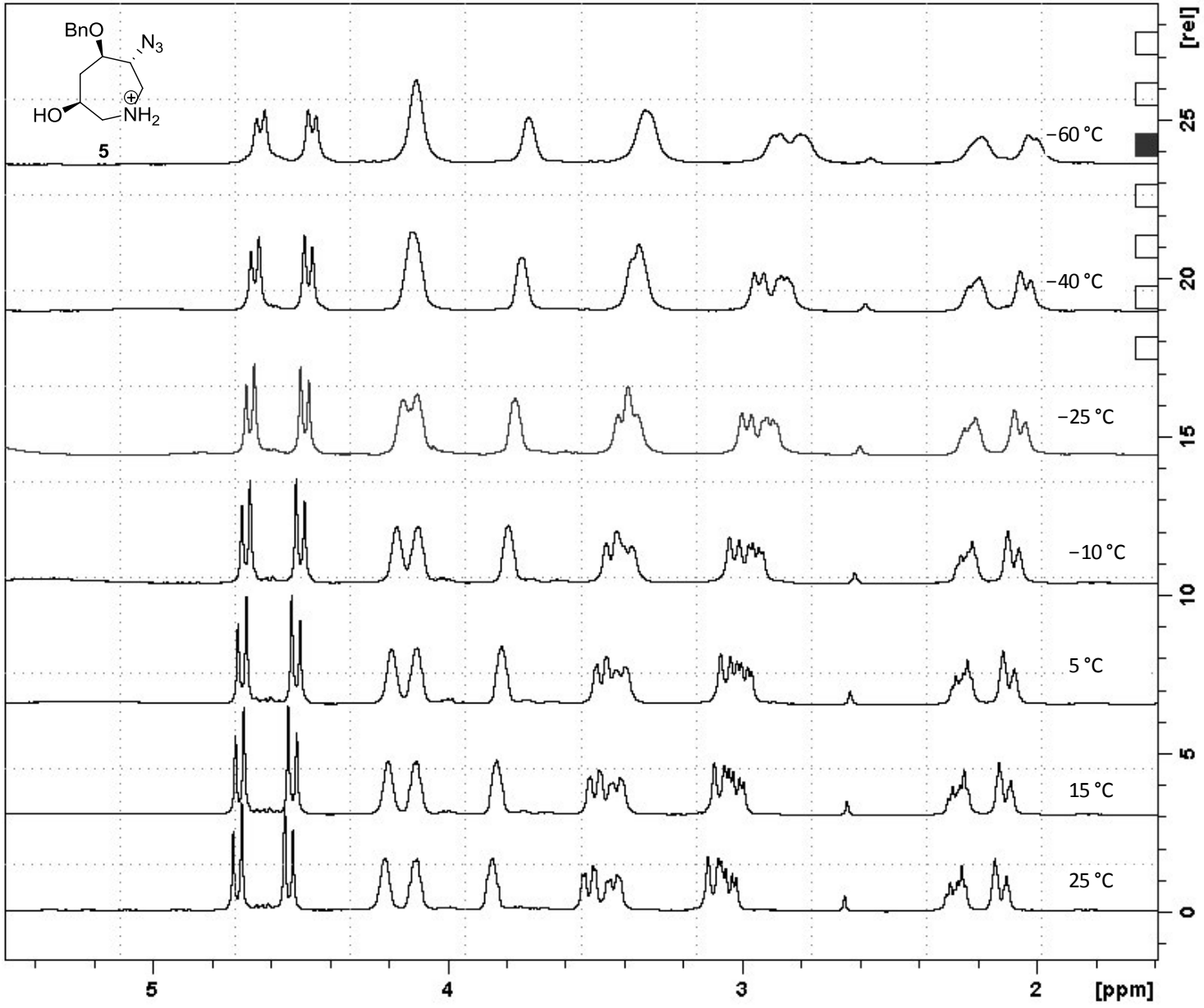
Variant temperature NMR studies



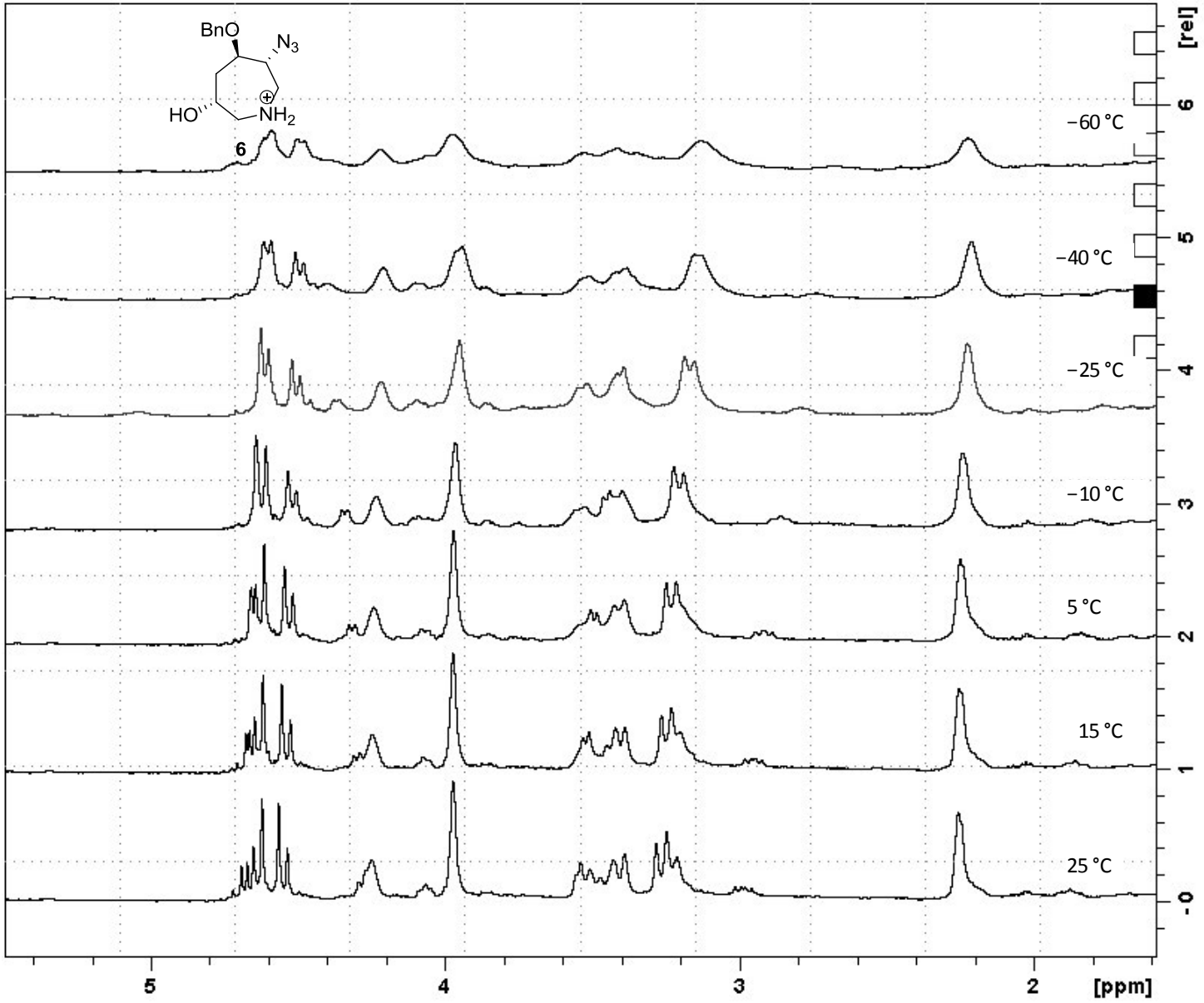
Variant temperature NMR studies



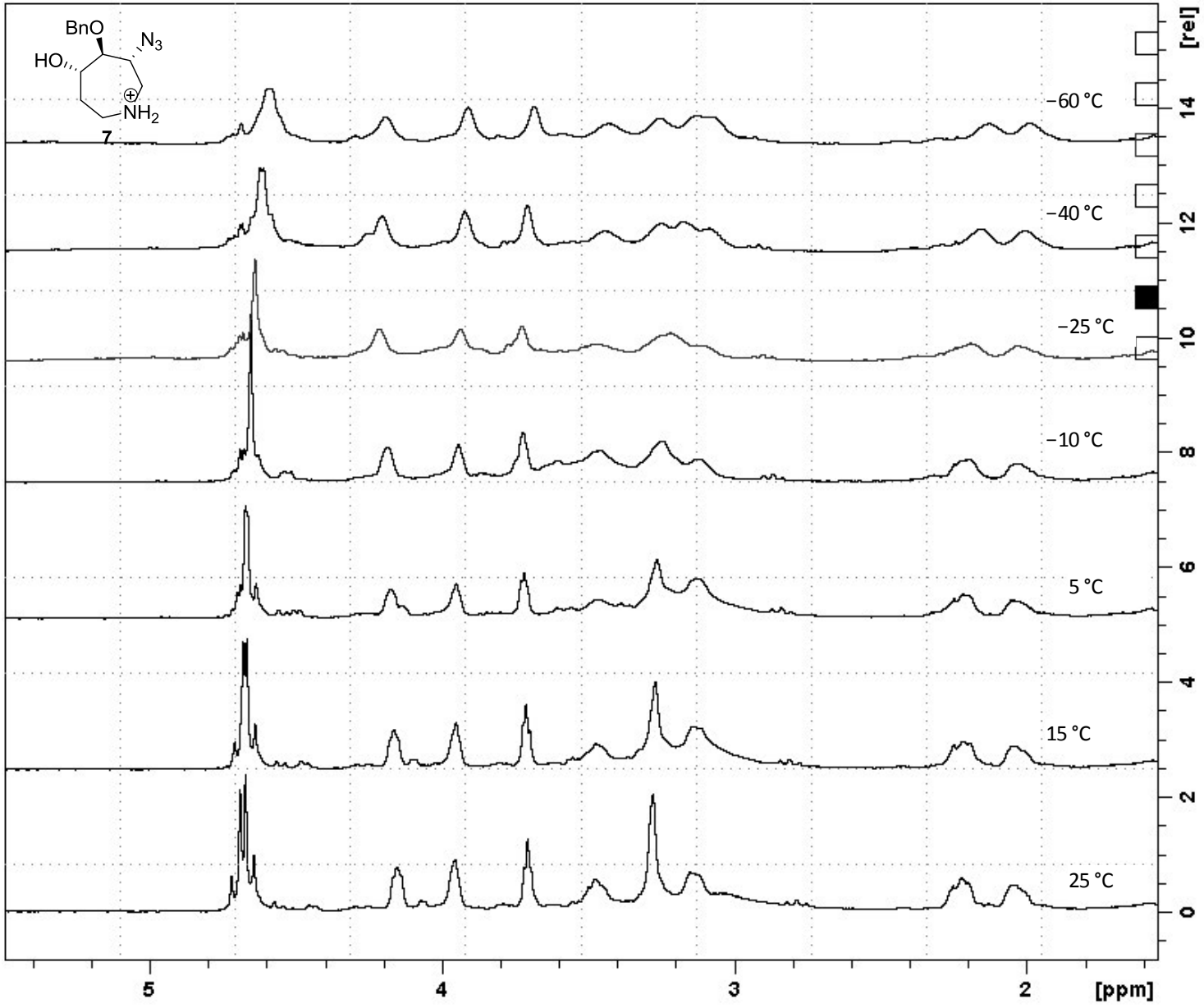
Variant temperature NMR studies



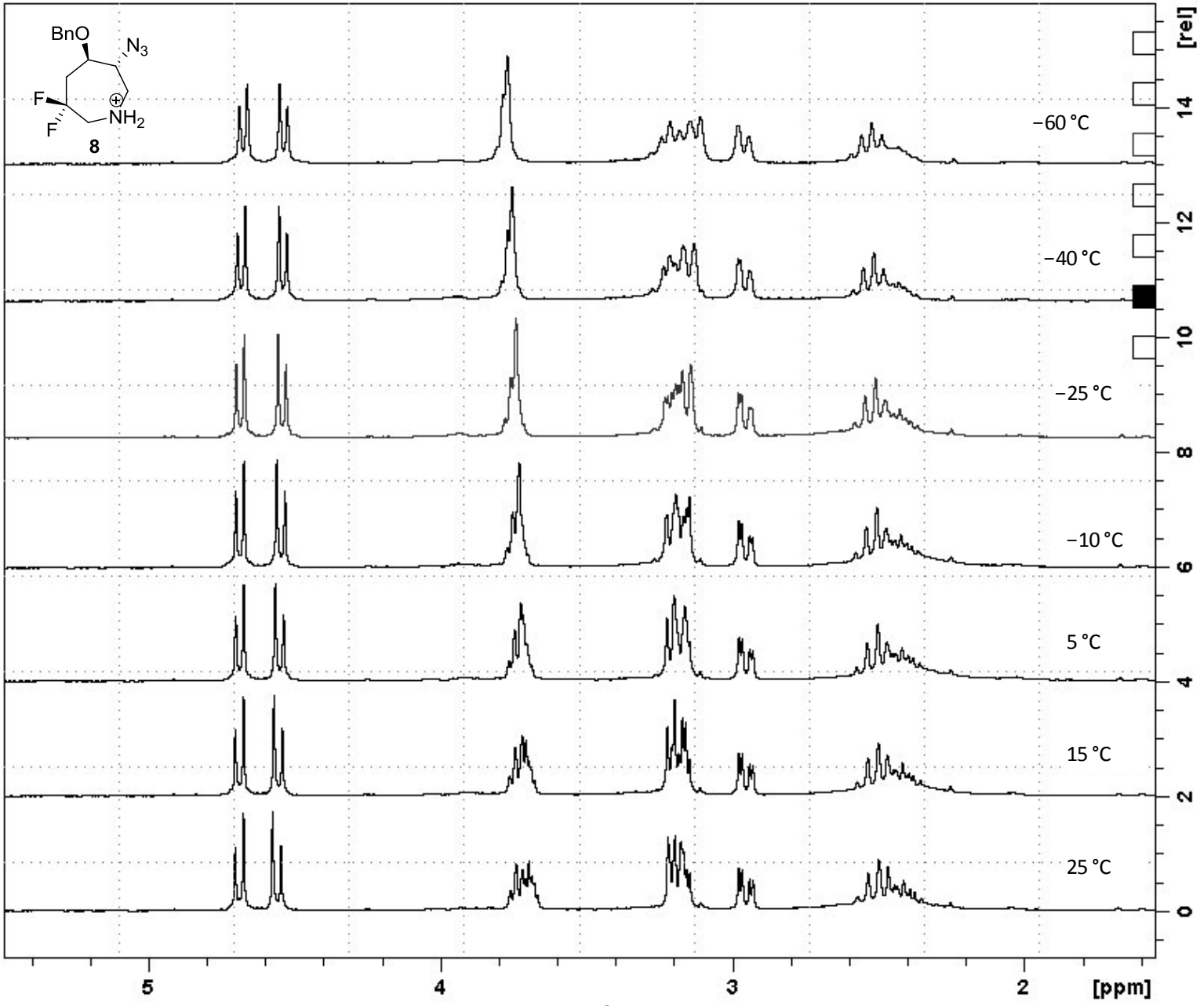
Variant temperature NMR studies



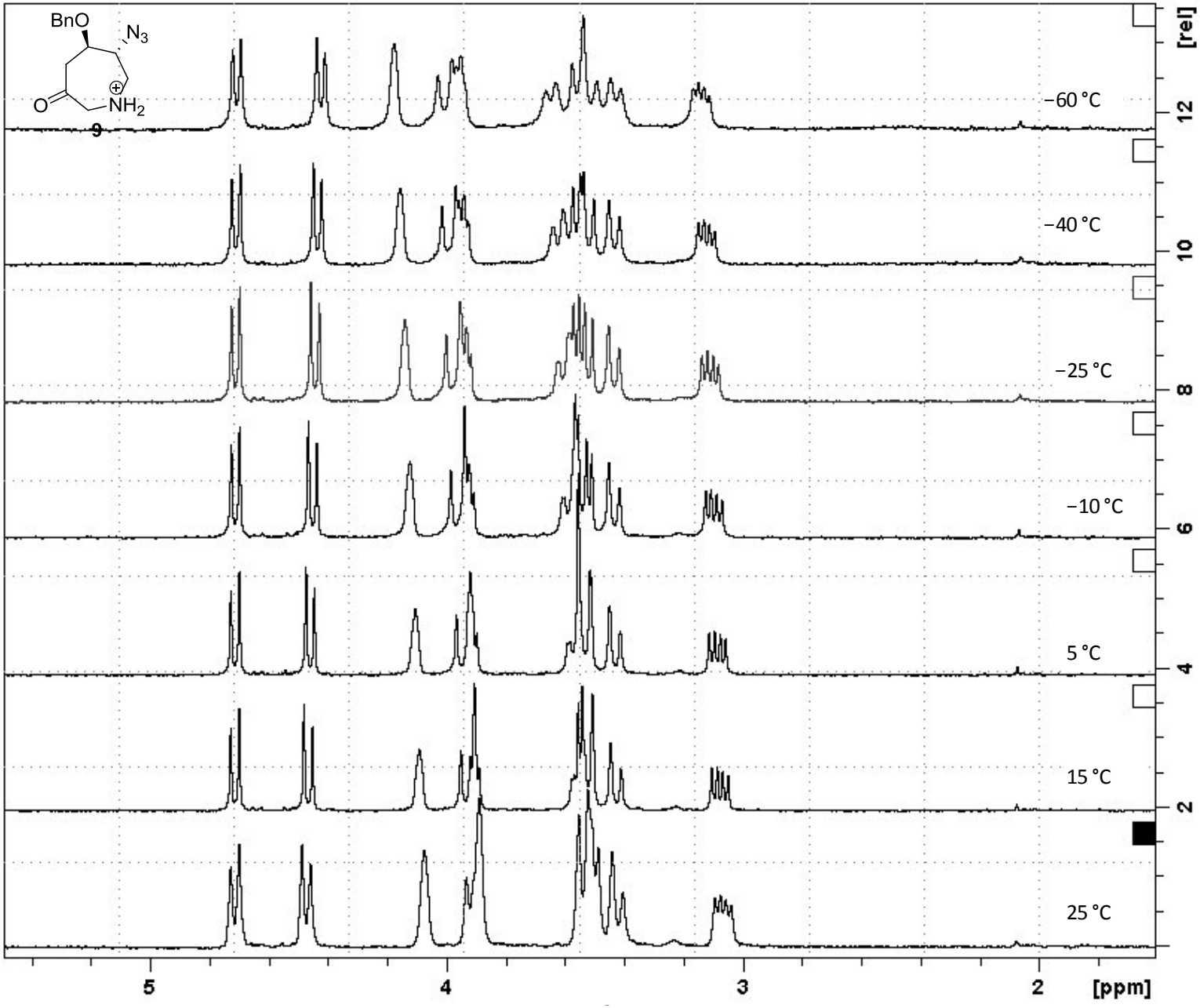
Variant temperature NMR studies



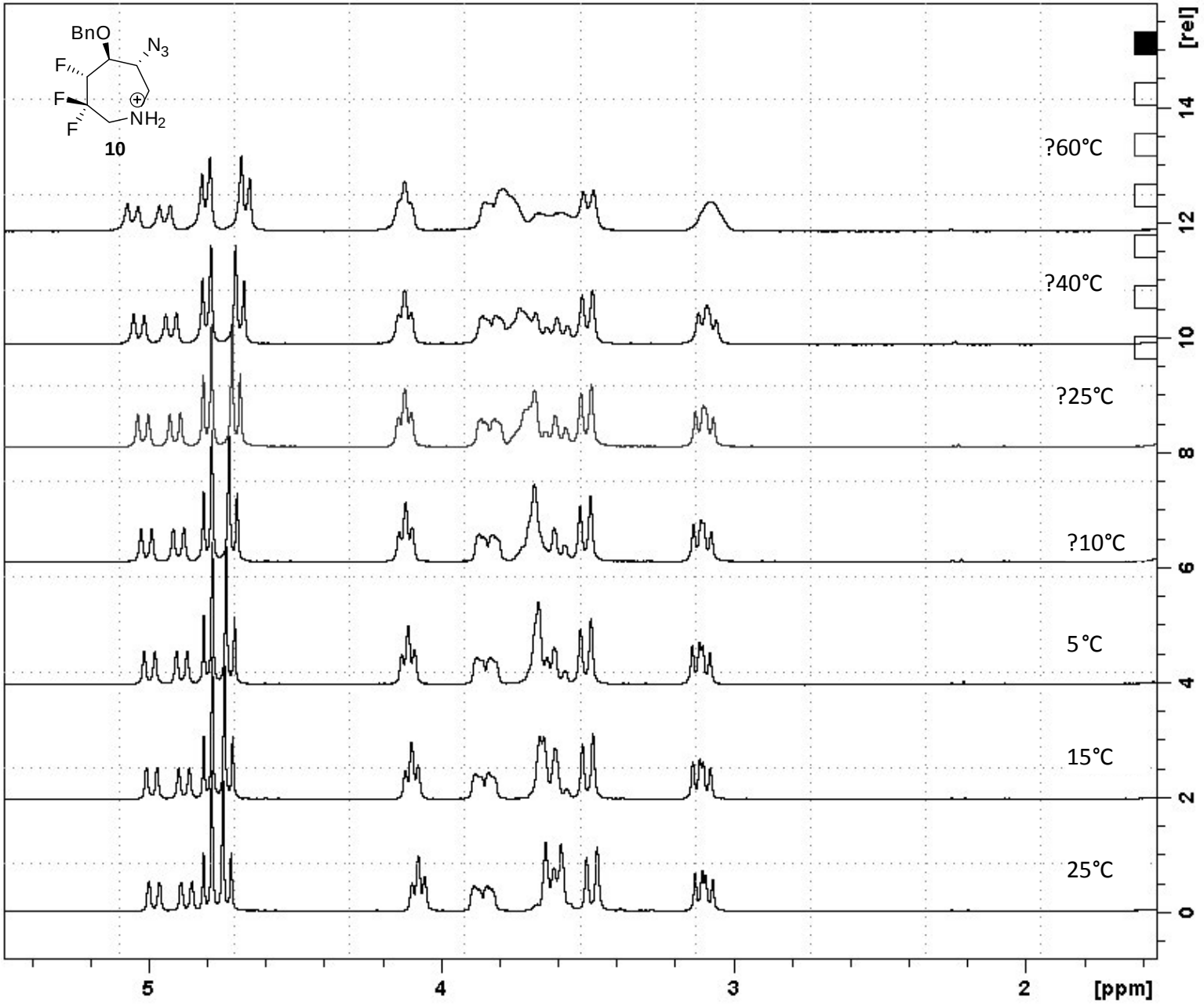
Variant temperature NMR studies



Variant temperature NMR studies

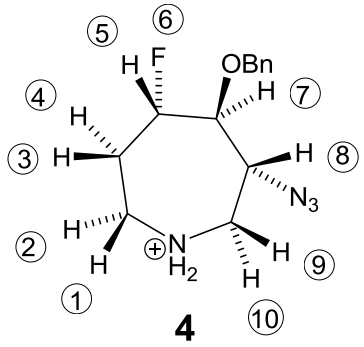


Variant temperature NMR studies

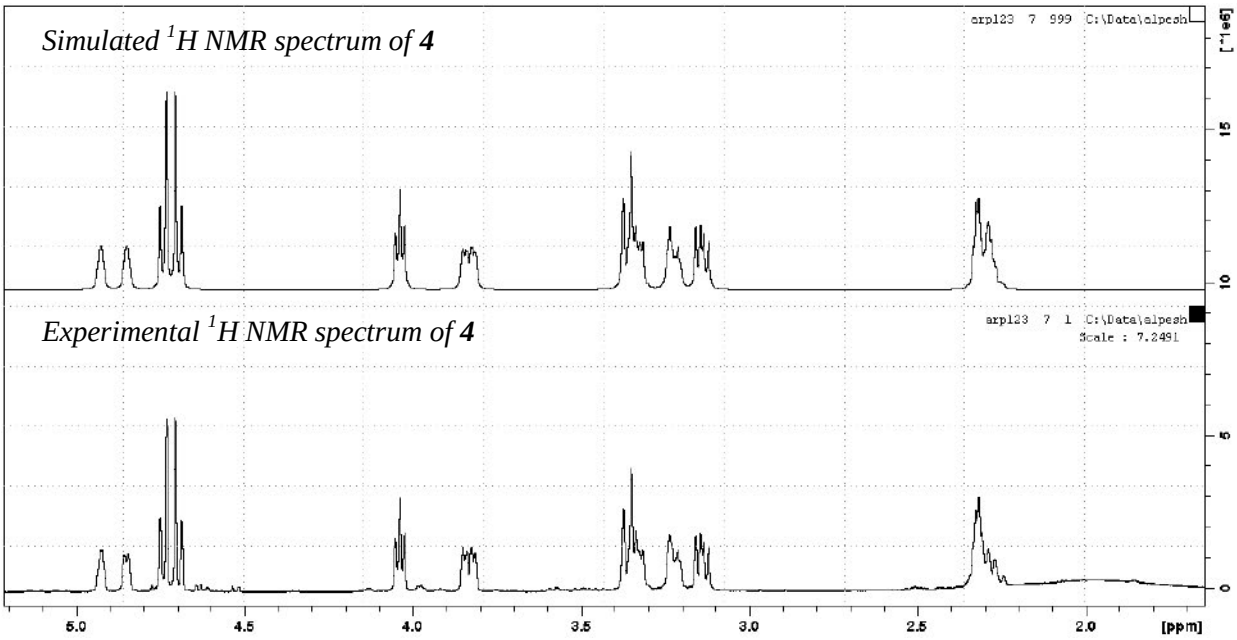


3. Simulated NMR spectra

The simulated spectra of azepanes **1**–**3** have been reported in communication. (Manuscript reference 17b). Following are the simulated spectra of azepanes **4**–**9**.

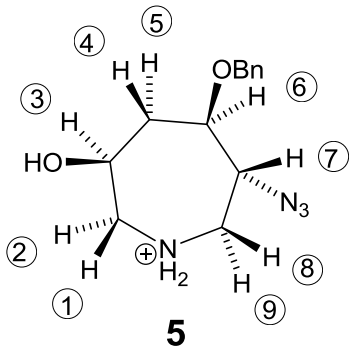


4

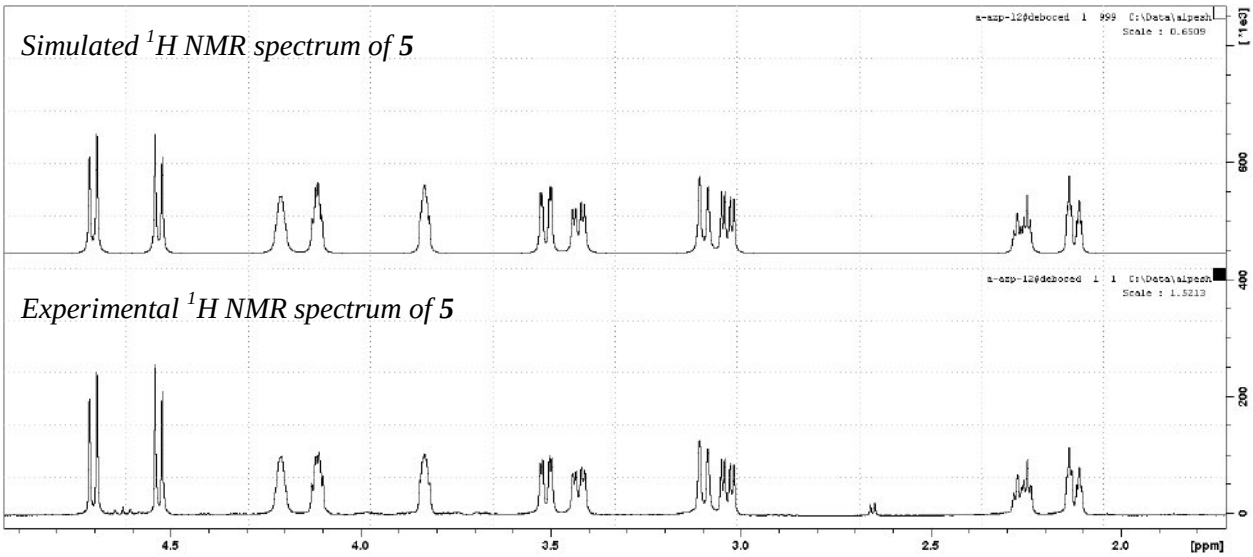


Nuclei	②	③	④	⑤	⑥	⑦	⑧	⑨	⑩
①	14.4 Hz	5.0 Hz	4.5 Hz	0.0 Hz	0.0 Hz	0.0 Hz	0.0 Hz	0.0 Hz	0.0 Hz
②		11.0 Hz	1.5 Hz	0.0 Hz	0.0 Hz	0.0 Hz	0.0 Hz	0.0 Hz	0.0 Hz
③			14.8 Hz	2.5 Hz	29.0 Hz	0.0 Hz	0.0 Hz	0.0 Hz	0.0 Hz
④				6.0 Hz	14.0 Hz	0.0 Hz	0.0 Hz	0.0 Hz	0.0 Hz
⑤					46.1 Hz	3.0 Hz	0.0 Hz	0.0 Hz	0.0 Hz
⑥						16.0 Hz	0.0 Hz	0.0 Hz	0.0 Hz
⑦							7.2 Hz	0.0 Hz	0.0 Hz
⑧								1.0 Hz	8.8 Hz
⑨									14.3 Hz

Figure 1: Expansion from the ^{1}H NMR spectrum of azepane **4**. The good match between the simulated and experimental spectra confirms that the *J* value assignments (see grid) are accurate.

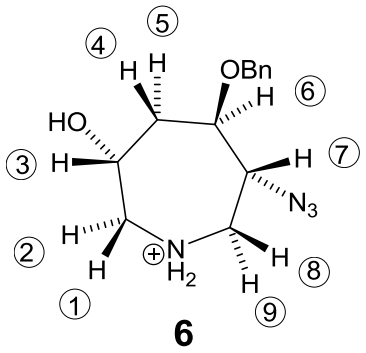


5

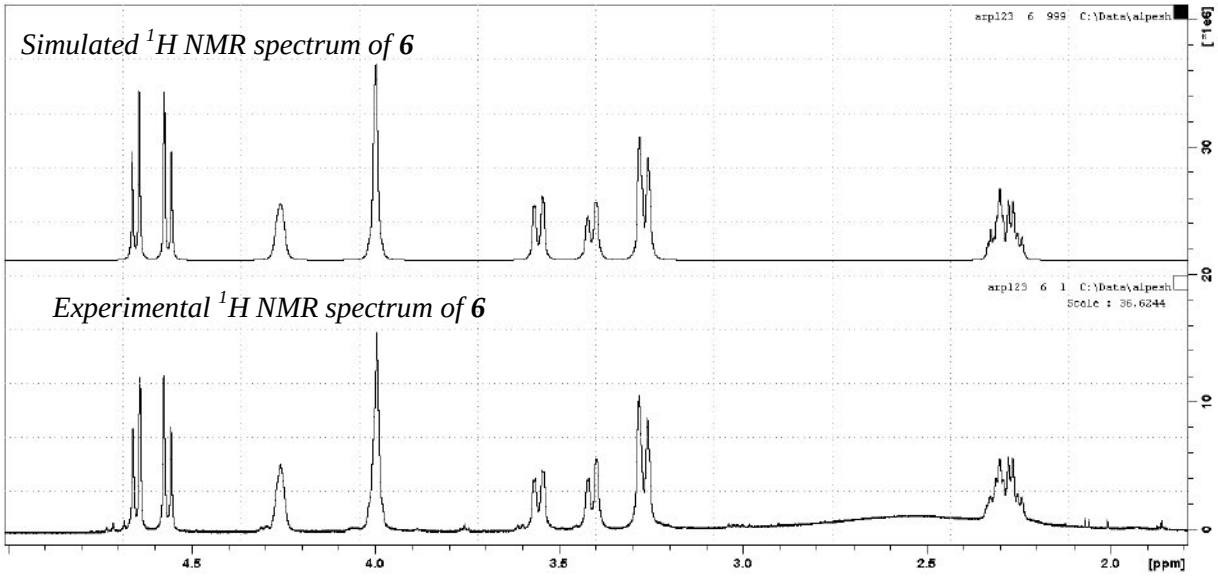


Nuclei	②	③	④	⑤	⑥	⑦	⑧	⑨
①	13.6 Hz	5.4 Hz	0.0 Hz	0.0 Hz	0.0 Hz	0.0 Hz	0.0 Hz	0.0 Hz
②		1.5 Hz	0.0 Hz	0.0 Hz	0.0 Hz	0.0 Hz	0.0 Hz	0.0 Hz
③			5.8 Hz	3.6 Hz	0.0 Hz	0.0 Hz	0.0 Hz	0.0 Hz
④				15.7 Hz	5.1 Hz	0.0 Hz	0.0 Hz	0.0 Hz
⑤					3.0 Hz	0.0 Hz	0.0 Hz	0.0 Hz
⑥						6.6 Hz	0.0 Hz	0.0 Hz
⑦							3.3 Hz	5.9 Hz
⑧								14.1 Hz

Figure 2: Expansion from the ^{1}H NMR spectrum of azepane **5**. The good match between the simulated and experimental spectra confirms that the *J* value assignments (see grid) are accurate.

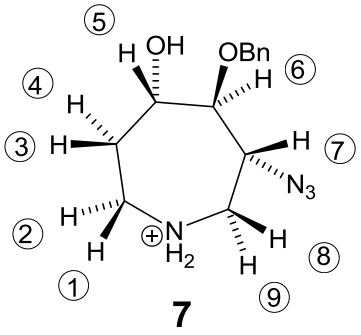


6

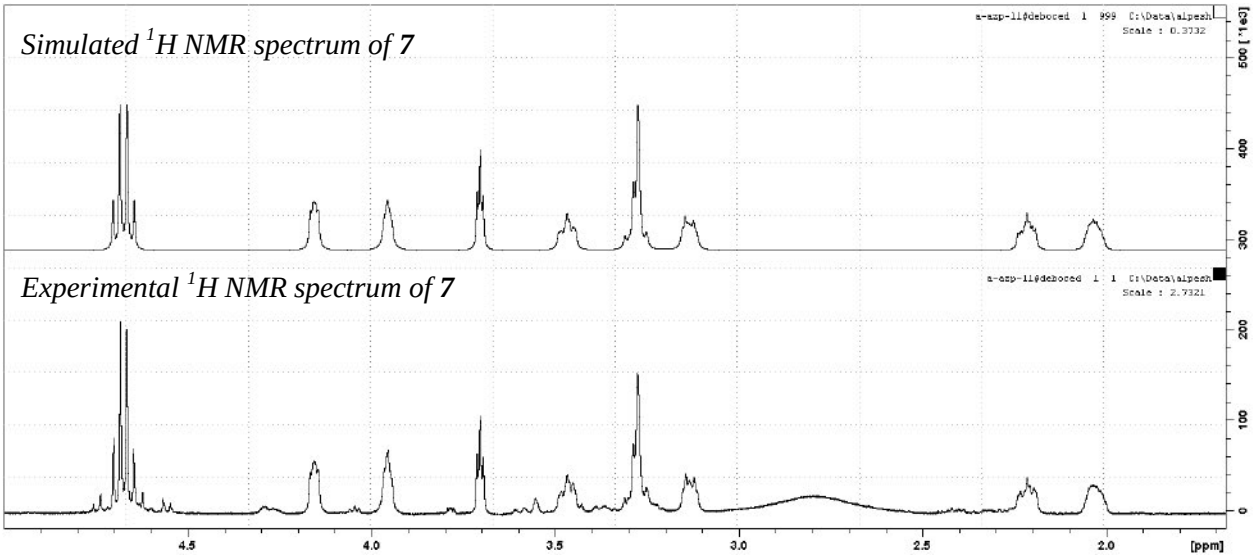


Nuclei	②	③	④	⑤	⑥	⑦	⑧	⑨
①	13.6 Hz	2.7 Hz	0.0 Hz	0.0 Hz	0.0 Hz	0.0 Hz	0.0 Hz	0.0 Hz
②		3.0 Hz	0.0 Hz	0.0 Hz	0.0 Hz	0.0 Hz	0.0 Hz	0.0 Hz
③			5.0 Hz	7.5 Hz	0.0 Hz	0.0 Hz	0.0 Hz	0.0 Hz
④				15.0 Hz	6.5 Hz	0.0 Hz	0.0 Hz	0.0 Hz
⑤					2.0 Hz	0.0 Hz	0.0 Hz	0.0 Hz
⑥						7.2 Hz	0.0 Hz	0.0 Hz
⑦							3.0 Hz	4.5 Hz
⑧								13.9 Hz

Figure 3: Expansion from the ^{1}H NMR spectrum of azepane **6**. The good match between the simulated and experimental spectra confirms that the *J* value assignments (see grid) are accurate.

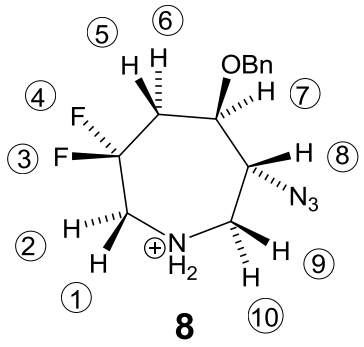


7

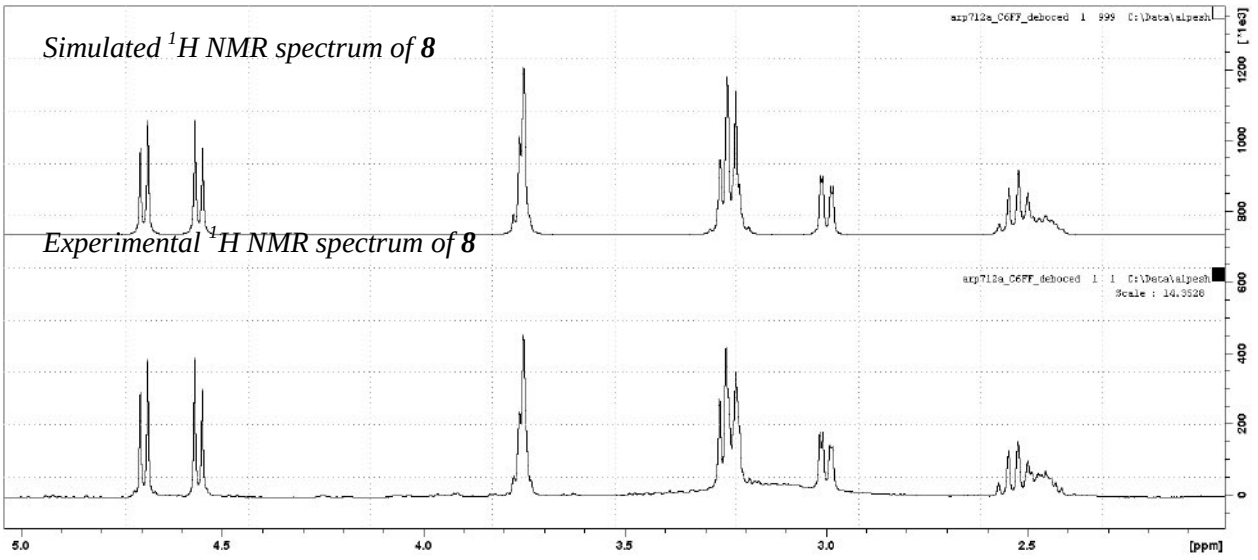


Nuclei	②	③	④	⑤	⑥	⑦	⑧	⑨
①	13.7 Hz	5.0 Hz	5.2 Hz	0.0 Hz	0.0 Hz	0.0 Hz	0.0 Hz	0.0 Hz
②		10.0 Hz	4.0 Hz	0.0 Hz	0.0 Hz	0.0 Hz	0.0 Hz	0.0 Hz
③			14.0 Hz	1.0 Hz	0.0 Hz	0.0 Hz	0.0 Hz	0.0 Hz
④				8.0 Hz	0.0 Hz	0.0 Hz	0.0 Hz	0.0 Hz
⑤					4.5 Hz	0.0 Hz	0.0 Hz	0.0 Hz
⑥						5.0 Hz	0.0 Hz	0.0 Hz
⑦							1.0 Hz	8.0 Hz
⑧								14.0 Hz

Figure 4: Expansion from the ^{1}H NMR spectrum of azepane **7**. The good match between the simulated and experimental spectra confirms that the *J* value assignments (see grid) are accurate.

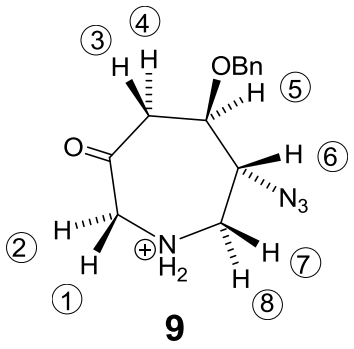


8

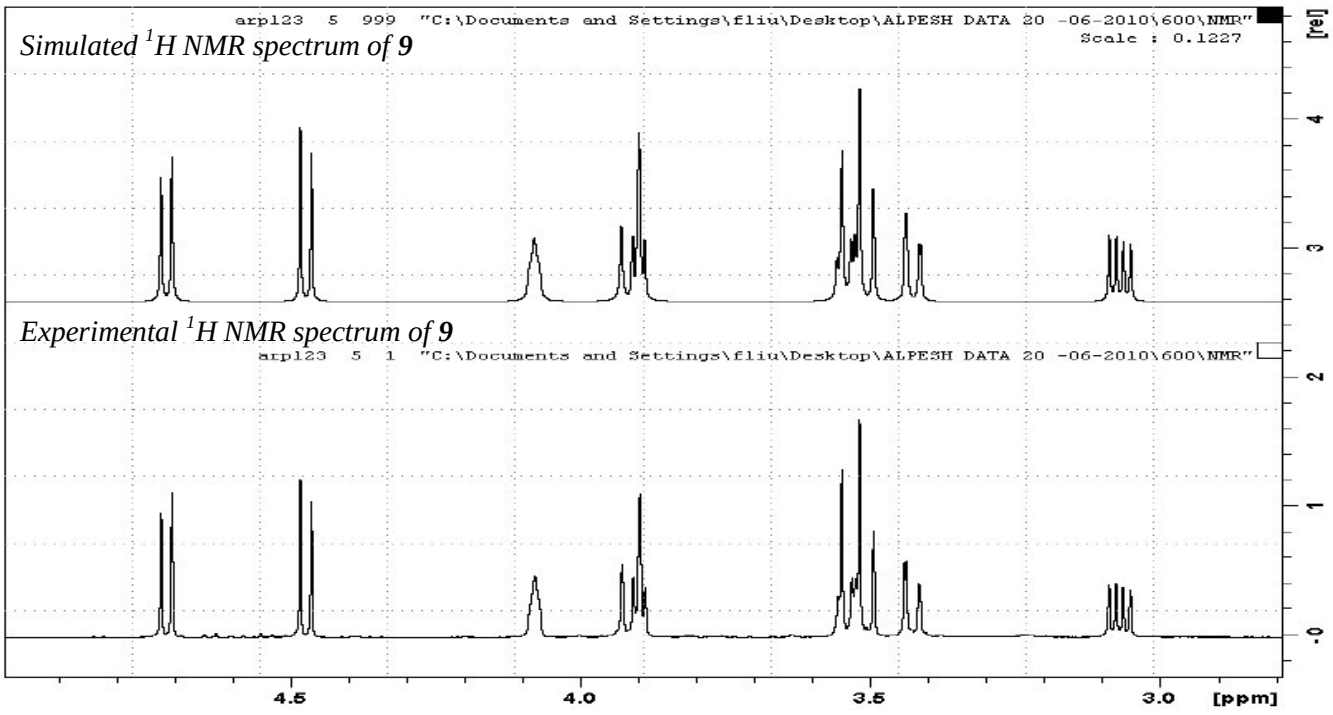


Nuclei	②	③	④	⑤	⑥	⑦	⑧	⑨	⑩
①	13.9 Hz	9.0 Hz	20.0 Hz	0.0 Hz	0.0 Hz	0.0 Hz	0.0 Hz	0.0 Hz	0.0 Hz
②		14.0 Hz	9.0 Hz	0.0 Hz	0.0 Hz	0.0 Hz	0.0 Hz	0.0 Hz	0.0 Hz
③			260 Hz	11.0 Hz	14.0 Hz	0.0 Hz	0.0 Hz	0.0 Hz	0.0 Hz
④				29.0 Hz	14.0 Hz	0.0 Hz	0.0 Hz	0.0 Hz	0.0 Hz
⑤					15.0 Hz	10.0 Hz	0.0 Hz	0.0 Hz	0.0 Hz
⑥						1.0 Hz	0.0 Hz	0.0 Hz	0.0 Hz
⑦							8.5 Hz	0.0 Hz	0.0 Hz
⑧								2.0 Hz	4.8 Hz
⑨									14.9 Hz

Figure 5: Expansion from the ^{1}H NMR spectrum of azepane **8**. The good match between the simulated and experimental spectra confirms that the *J* value assignments (see grid) are accurate.



9



Nuclei	②	③	④	⑤	⑥	⑦	⑧
①	18.3 Hz	0.0 Hz	0.0 Hz	0.0 Hz	0.0 Hz	0.0 Hz	0.0 Hz
②		0.0 Hz	0.0 Hz	0.0 Hz	0.0 Hz	0.0 Hz	0.0 Hz
③			14.8 Hz	7.4 Hz	0.0 Hz	0.0 Hz	0.0 Hz
④				1.2 Hz	0.0 Hz	0.0 Hz	0.0 Hz
⑤					5.4 Hz	0.0 Hz	0.0 Hz
⑥						2.0 Hz	4.1 Hz
⑦							14.5 Hz

Figure 6: Expansion from the ^{1}H NMR spectrum of azepane **9**. The good match between the simulated and experimental spectra confirms that the *J* value assignments (see grid) are accurate.

4. Conformational analysis details

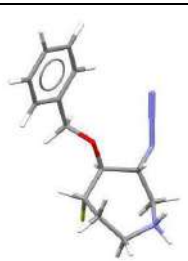
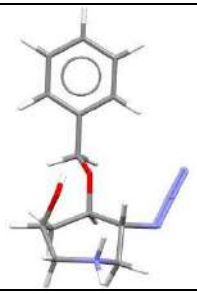
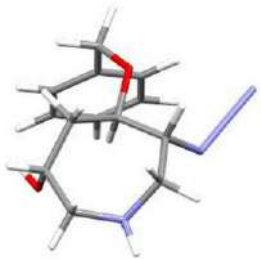
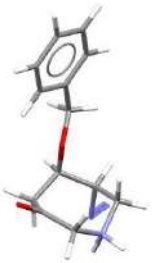
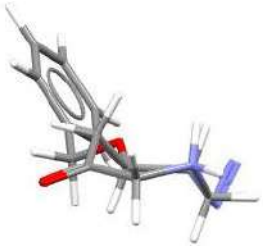
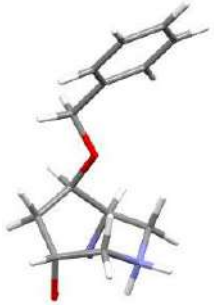
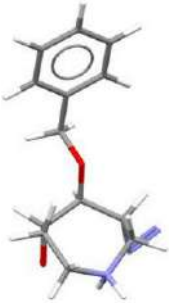
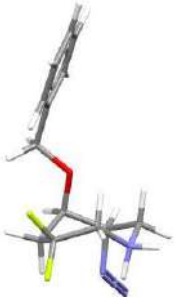
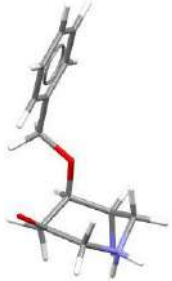
4.1. General

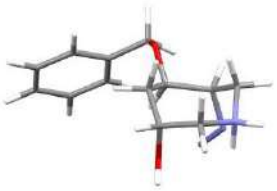
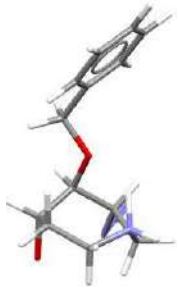
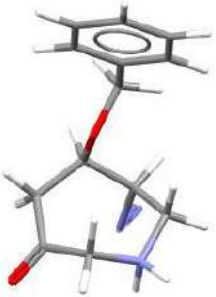
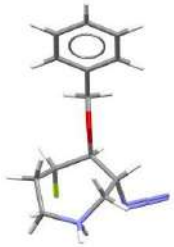
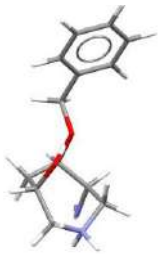
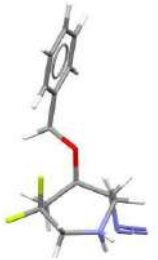
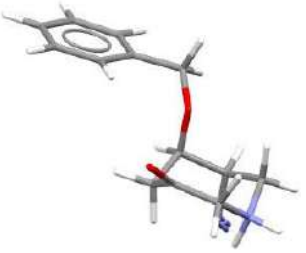
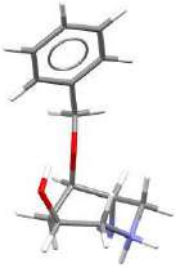
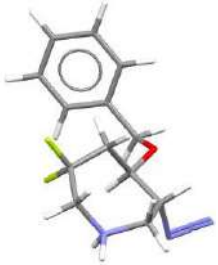
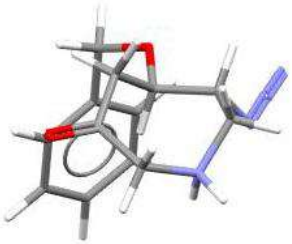
The conformational analysis of azepanes **1**–**3** was described earlier (ref 17b, ESI). Likewise, a conformational analysis was performed for each of the azepanes **4**–**10**. The conformational search was performed as implemented in the program MOE. Conformers were generated by the stochastic method and minimized in the MMFF94X forcefield with chloroform as the solvent. Conformers within 3–5 kcal/mol in energy were clustered to identify unique members with different azepane ring conformations. Each unique ring conformer was subjected to DFT geometry optimisation as implemented in the program Turbomole (with the SV(P) basis set at the B3LYP level in COSMO solvent $CHCl_3$). As observed earlier (ref 17b, ESI), the side chain OBn and azido substituents contribute 2 to 3 kcal/mol in energy variation. Thus the calculated energies of the conformers cannot be reliably used to rank conformational preferences and the conformations were extrapolated by *J*-based analysis as described (ref 25, manuscript).

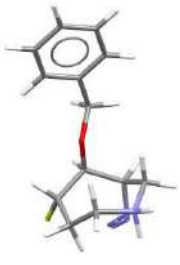
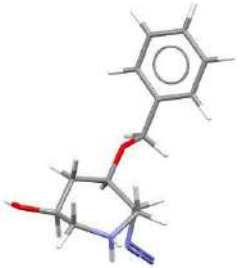
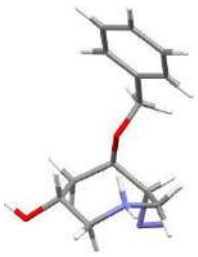
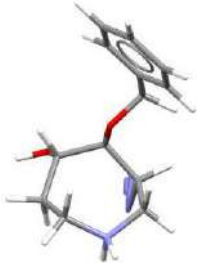
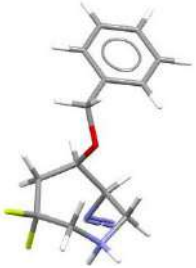
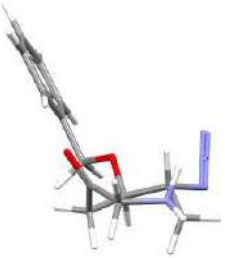
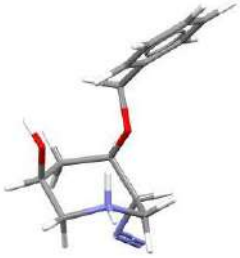
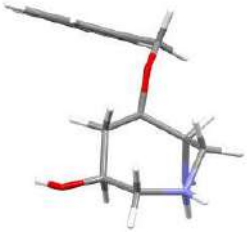
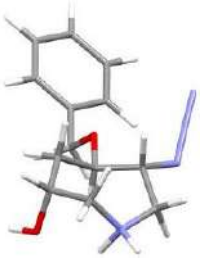
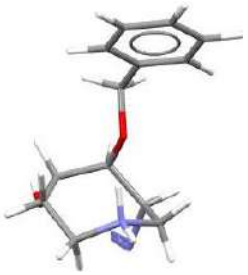
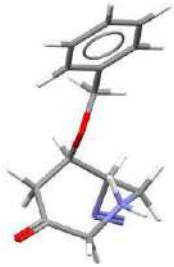
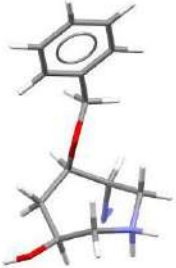
4.2. Conformations of azepanes 4–9 within 3–5 kcal/mol.

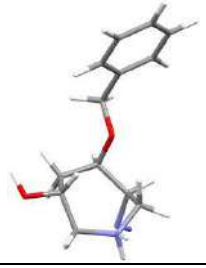
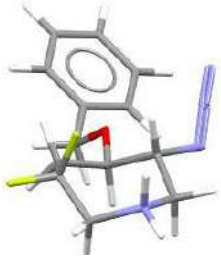
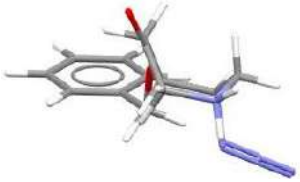
For azepanes **4–9**, a representative member of each cluster with distinct azepane ring conformation was geometry optimized. The conformers of azepanes **4–9** within 3–5 kcal/mol are shown in the following table (Table 1). The conformers are visualized using the program Chimera (UCSF Chimera, version 1.7).

Table 1: Geometries of azepanes **4–9**.

No	Azepane Geometries and relative energies (kcal/mol)					
	4	**5**	**6**	**7**	**8**	**9**
1						
	4a: 0.14	**5a**:0.32	**6a**: 3.18	**7a**: 0	**8a**: 2.62	**9a**: 0.41
2						
	4b: 1.74	**5b**: 0.32	**6b**: 6.39	**7b**: 2.18	**8b**: 2.67	**9b**: 2.59
3						
	4c: 0.00	**5c**: 3.35	**6c**: 0	**7c**: 0.34	**8c**: 1.20	**9c**: 20.21

4						
	4d: 1.63	**5d**: 3.30	**5d**: 2.65	**7d**: 1.57	**8d**: 0	**9d**: 3.52
5						
	4e: 0.98	**5e**: 0	**6e**: 3.51	**7e**: 1.48	**8e**: 1.72	**9e**: 0
6						
	4f: 3.87	**5f**: 1.63	**6f**: 2.69	**7f**: 0.45	**8f**: 3.76	**9f**: 5.70

7						
	4g: 1.46	**5g**: 3.27	**6g**: 3.96	**7g**: 2.17	**8g**: 0.97	**9g**: 0
8						
	4h: 1.56	**5h**: 0.34	**6h**: 4.52	**7h**: 1.89	**8h**: 1.11	**9h**: 2.51
9						
	4i: 2.27	**5i**: 2.89	**6i**: 2.04	**7i**: 22.15	**8i**: 3.18	**9i**: 3.93
10						

	4j: 4.49	**5j**: 3.46	**6j**: 4.40		**8j**: 2.51	**9j**: 4.93
11						
			6k: 4.49		**8k**: 3.63	**9k**: 5.22
12						
			6l: 3.40			**9l**: 8.19

4.3. Weighted contribution calculations for azepanes 4–9

Azepane **4**:

In azepane **4**, out of ten ring conformations found from a conformational search only two (**4a** and **4b**) could match all four characteristic $^{3}J_{HH}$ values extracted from its ^{1}H NMR spectrum. The following graph (Fig. 7) illustrates that it was possible to obtain a good match between experimental and calculated $^{3}J_{HH}$ values by creating a weighted average of these **two** geometries. Both **4a** and **4b** satisfied C3/C4 pseudo-diequatorial preference, however, the azido *gauche* effect was maintained in neither. The C5-F/C4-OBn *gauche* effect was satisfied in **4b** and not in **4a**.

A series of weighted averages of these conformers were investigated, in order to determine the best ratio of **4a** : **4b** for matching the experimental *J* values. It was found that a ratio of 60 : 40 gave a weighted average set of $^{3}J_{HH}$ values that matched the experimental values reasonably well (Fig. 7).

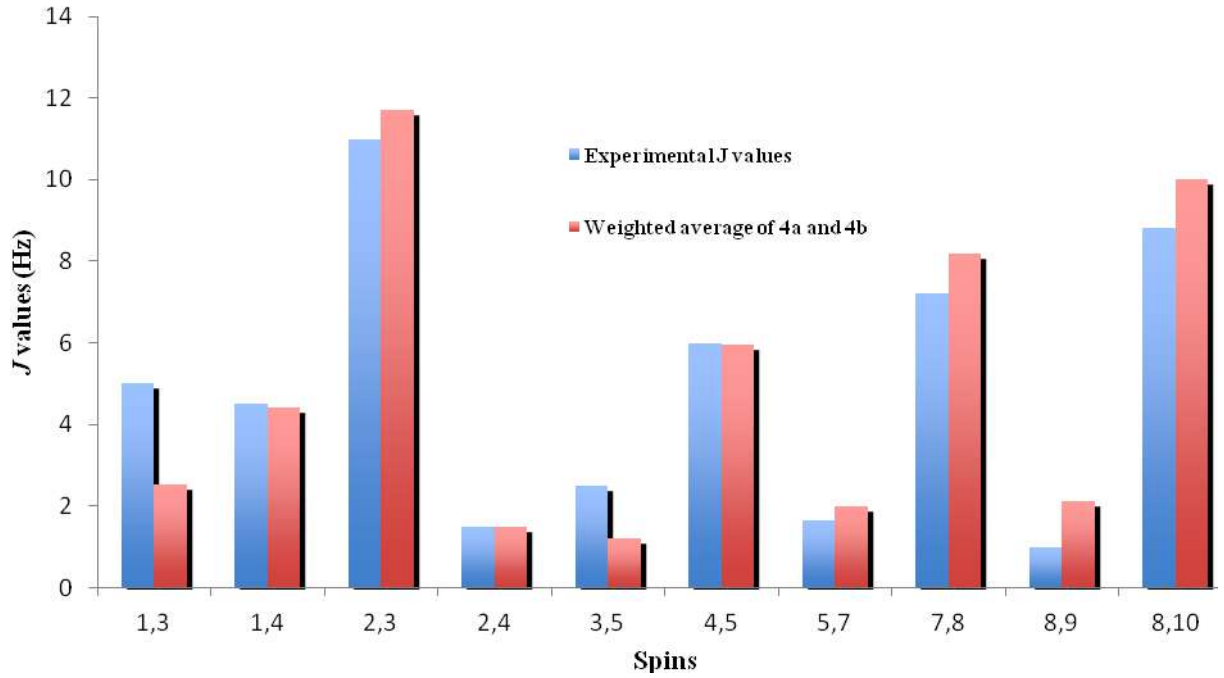


Figure 7: *J* values of azepane **4**, calculated for a 60:40 distribution of conformers **4a** and **4b**.

Azepane **6**:

In azepane **6**, out of twelve ring conformations found from a conformational search only two (**6a** and **6b**) could match the $^{3}J_{HH}$ values extracted from its ^{1}H NMR spectrum closely. The following graph (Fig. 8) illustrates that it was possible to obtain a good match between experimental and calculated $^{3}J_{HH}$ values by creating a weighted average of these **two** geometries. A series of weighted

averages of these conformers were investigated, in order to determine the ratio of **6a** : **6b** that gave the best match with the experimental $^{3}J_{HH}$ values. It was found that a ratio of 60 : 40 gave a weighted average set of *J* values that matched the experimental values reasonably well (Fig. 8).

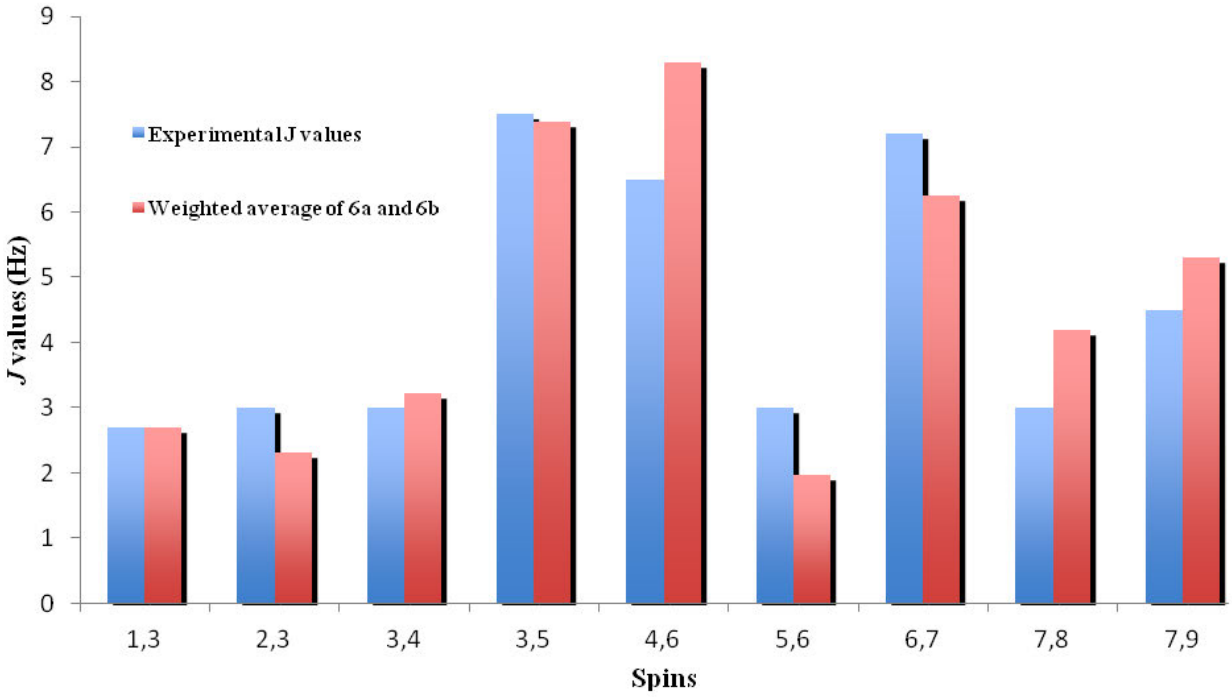


Figure 8: *J* values of azepane **6**, calculated for a 60:40 distribution of conformers **6a** and **6b**.

Azepane **7**:

In azepane **7**, out of nine ring conformations found from a conformational search none could match all three characteristic $^{3}J_{HH}$ values extracted from its ^{1}H NMR spectrum. The conformers **7a** and **7b** were found to have better match to experimental *J* values than others. The following graph (Fig. 9) illustrates that it was not possible to obtain a good match between experimental and calculated *J* values by creating a weighted average of these **two** geometries. This means there is at least three geometries contributed to the azepane **7**'s observed *J* values.

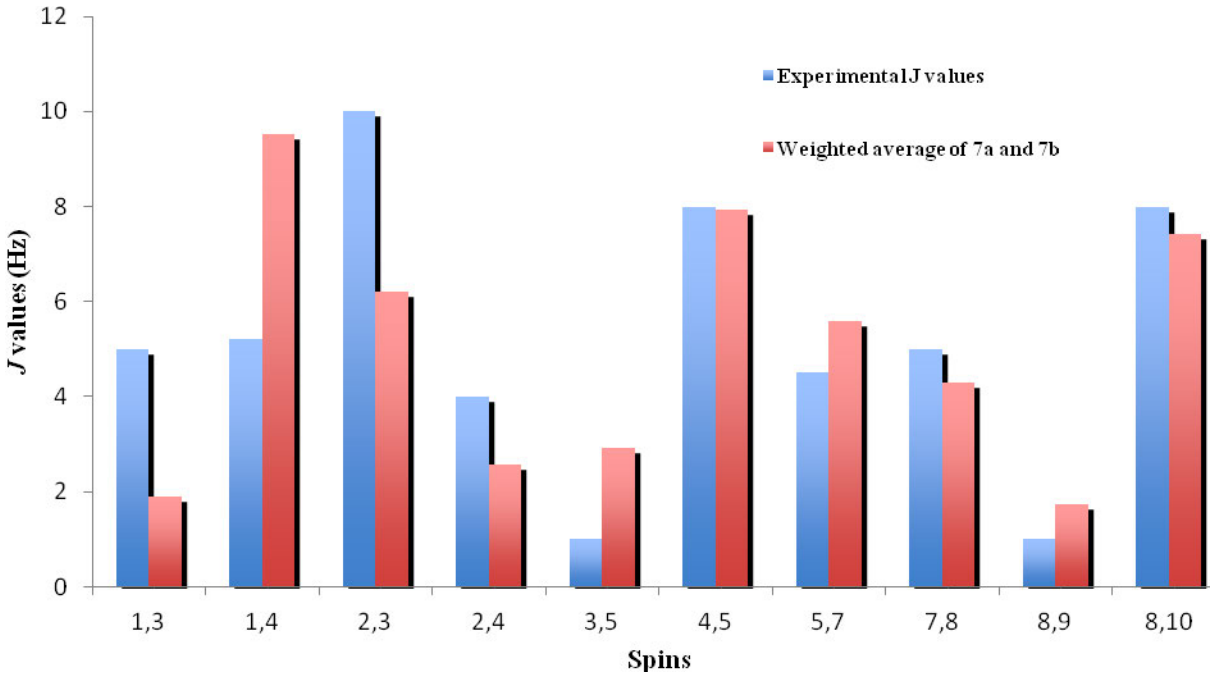


Figure 9: *J* values of azepane **7**, calculated for a 60:40 distribution of conformers **7a** and **7b** is the closest yet still unsatisfactory match.

Azepane **8**:

In azepane **8**, out of ten ring conformations found from a conformational search only two (**8a** and **8b**) could closely match $^{3}J_{HH}$ values extracted from its ^{1}H NMR spectrum. The following graph (Fig. 10) illustrates that it was possible to obtain a good match between experimental and calculated *J* values by creating a weighted average of these **two** geometries. A series of weighted averages of these conformers were investigated, in order to determine the ratio of **8a** : **8b** that gave the best match with the experimental *J* values. It was found that a ratio of 50 : 50 gave a weighted average set of *J* values that matched the experimental values reasonably well (Fig. 10).

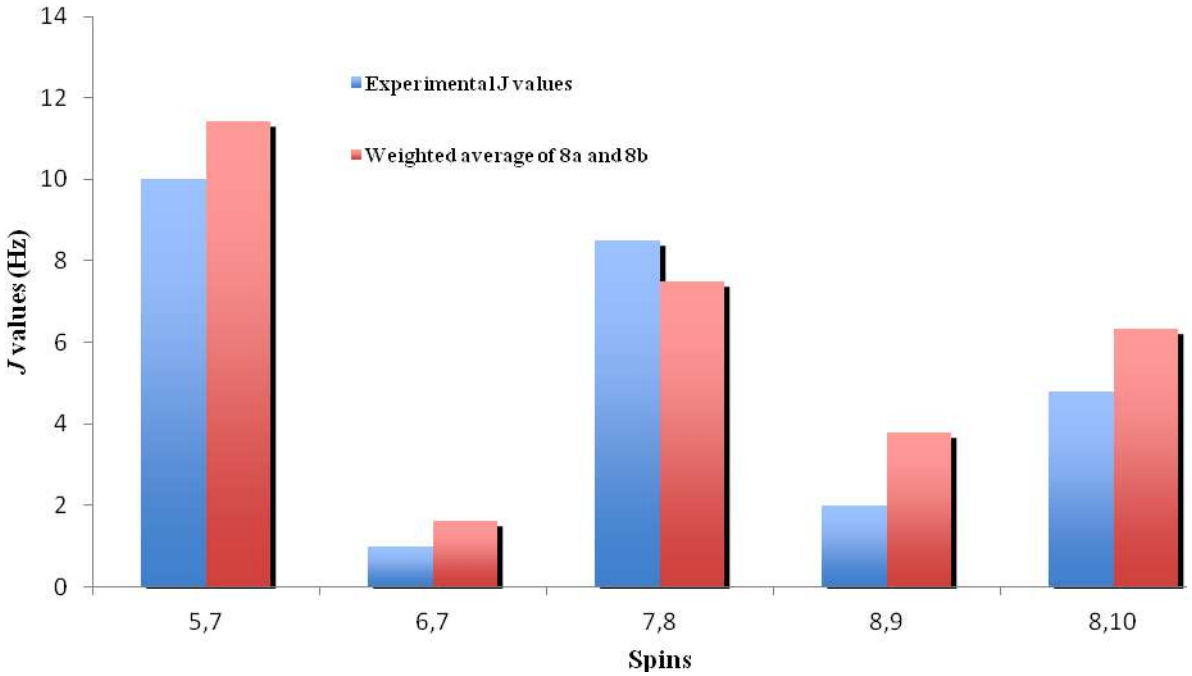


Figure 10: *J* values of azepane **8**, calculated for a 50:50 distribution of conformers **8a** and **8b**.

Azepane **9**:

In azepane **9**, from conformations found from a conformational search **9a** (with small contribution from **9b**) was found to match all four characteristic $^{3}J_{HH}$ values extracted from its ^{1}H NMR spectrum. The following graph (Fig. 11) illustrates that it was possible to obtain a good match between experimental and calculated *J* values by creating a weighted average of these **two** geometries. A series of weighted averages of these conformers were investigated, in order to determine the ratio of **9a** : **9b** that gave the best match with the experimental *J* values. It was found that a ratio of 80 : 20 gave a weighted average set of *J* values that matched the experimental values reasonably well (Fig. 11).

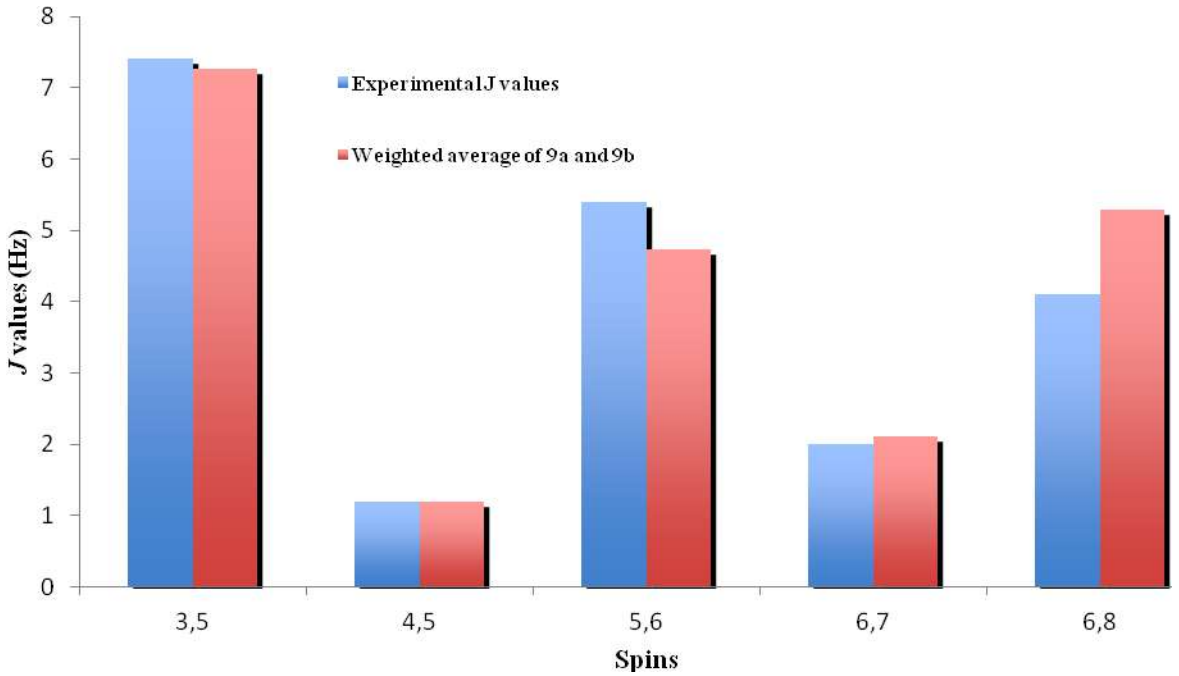
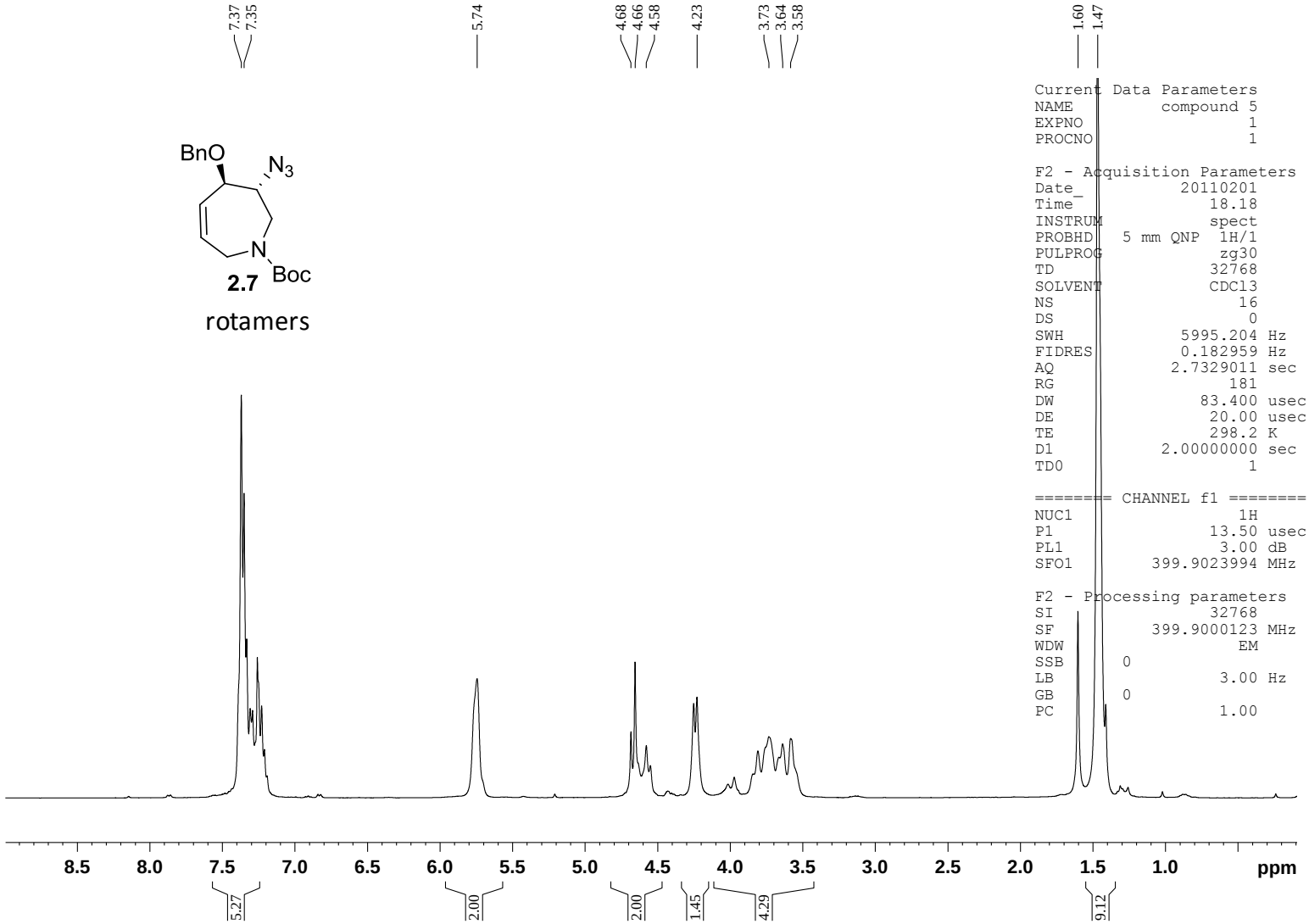


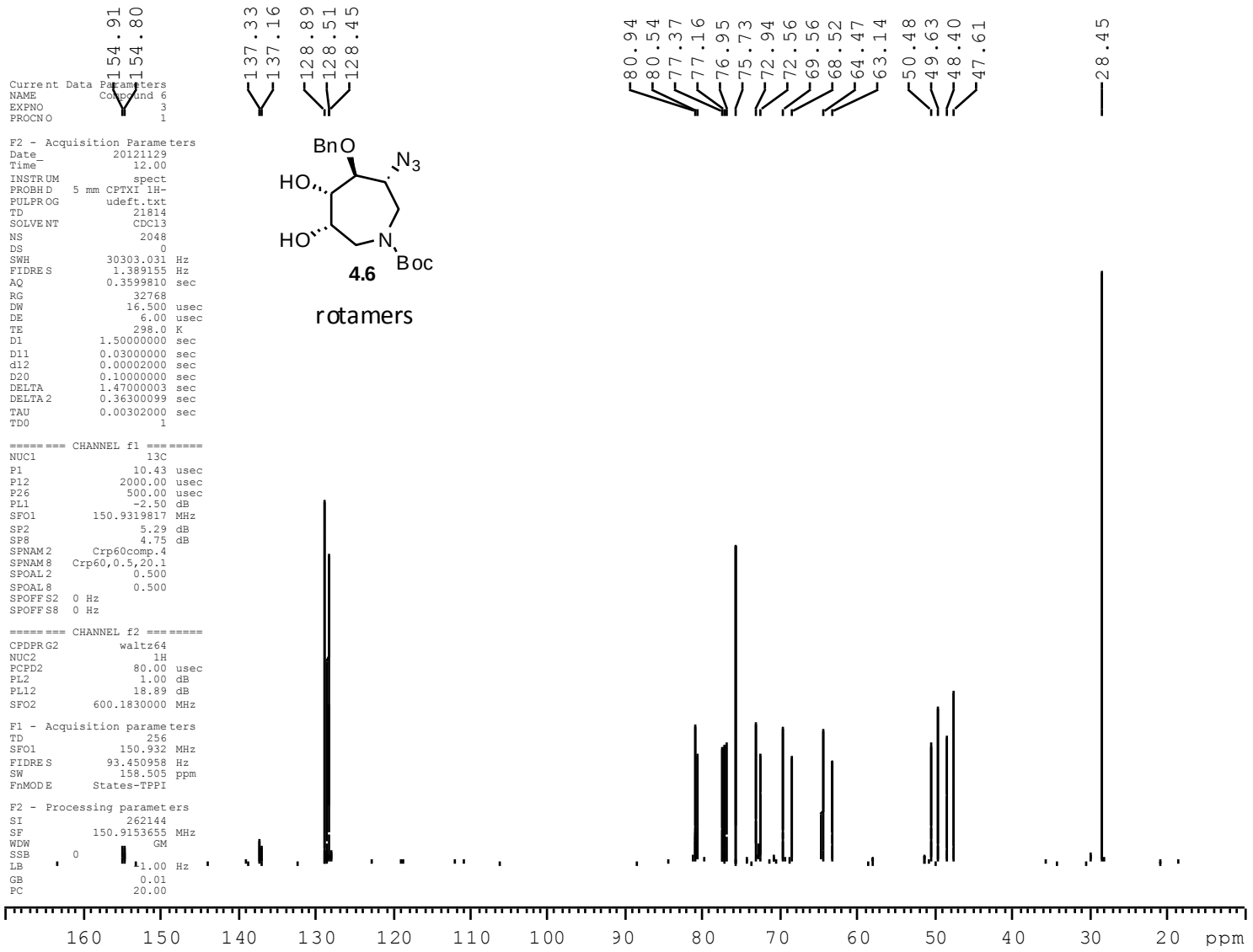
Figure 11: *J* values of azepane **9**, calculated for a 80:20 distribution of conformers **9a** and **9b**.

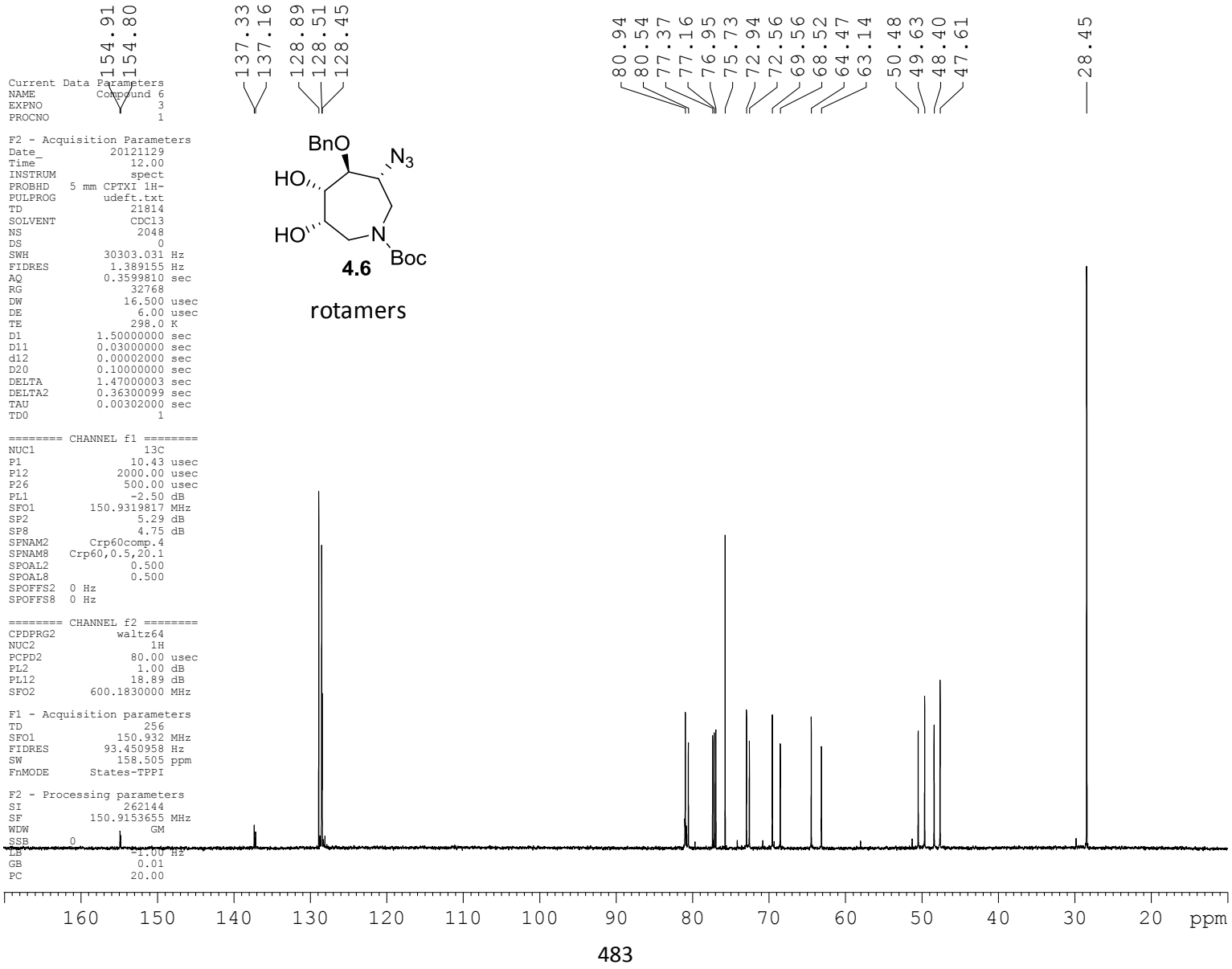
Appendix D

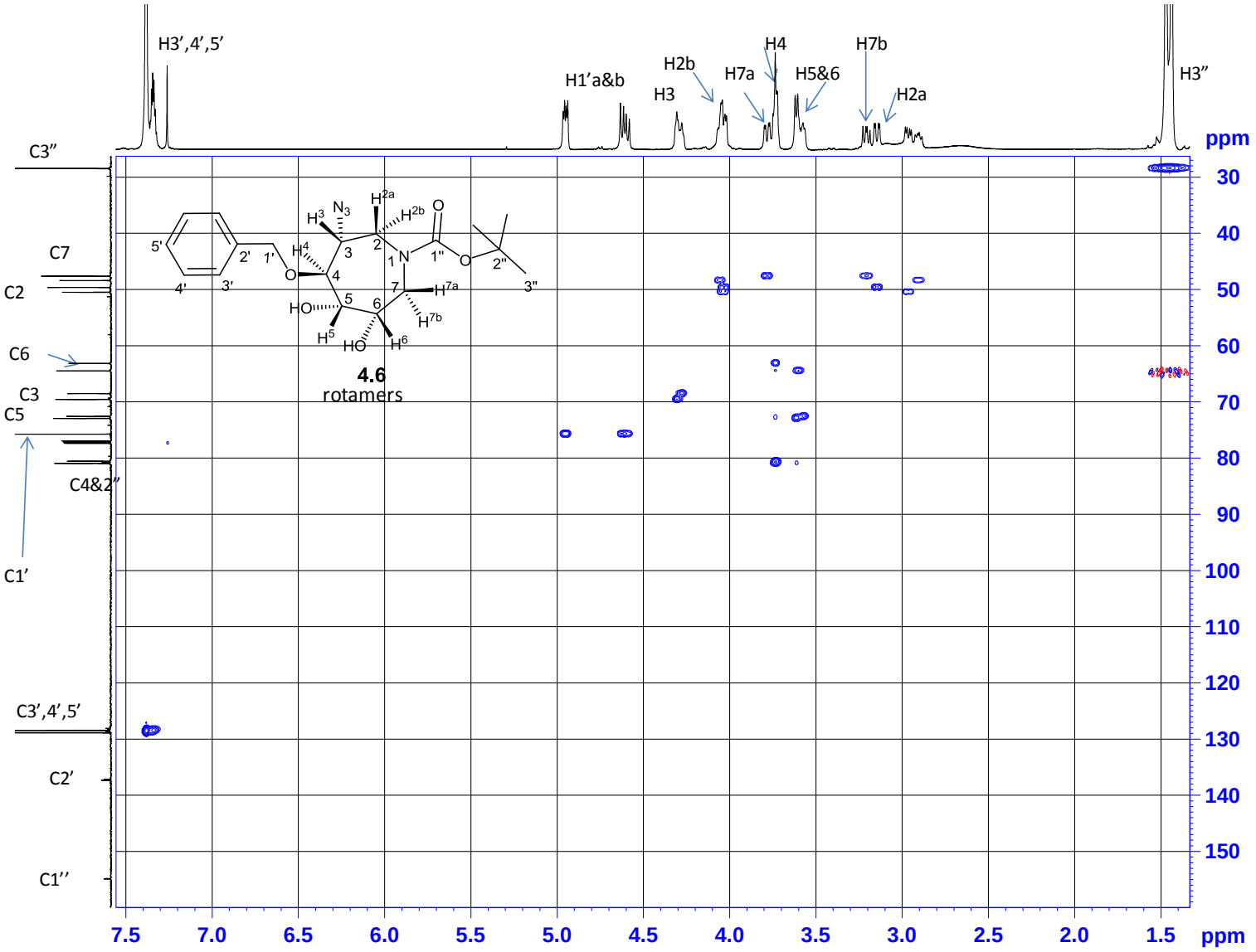
Table of contents:

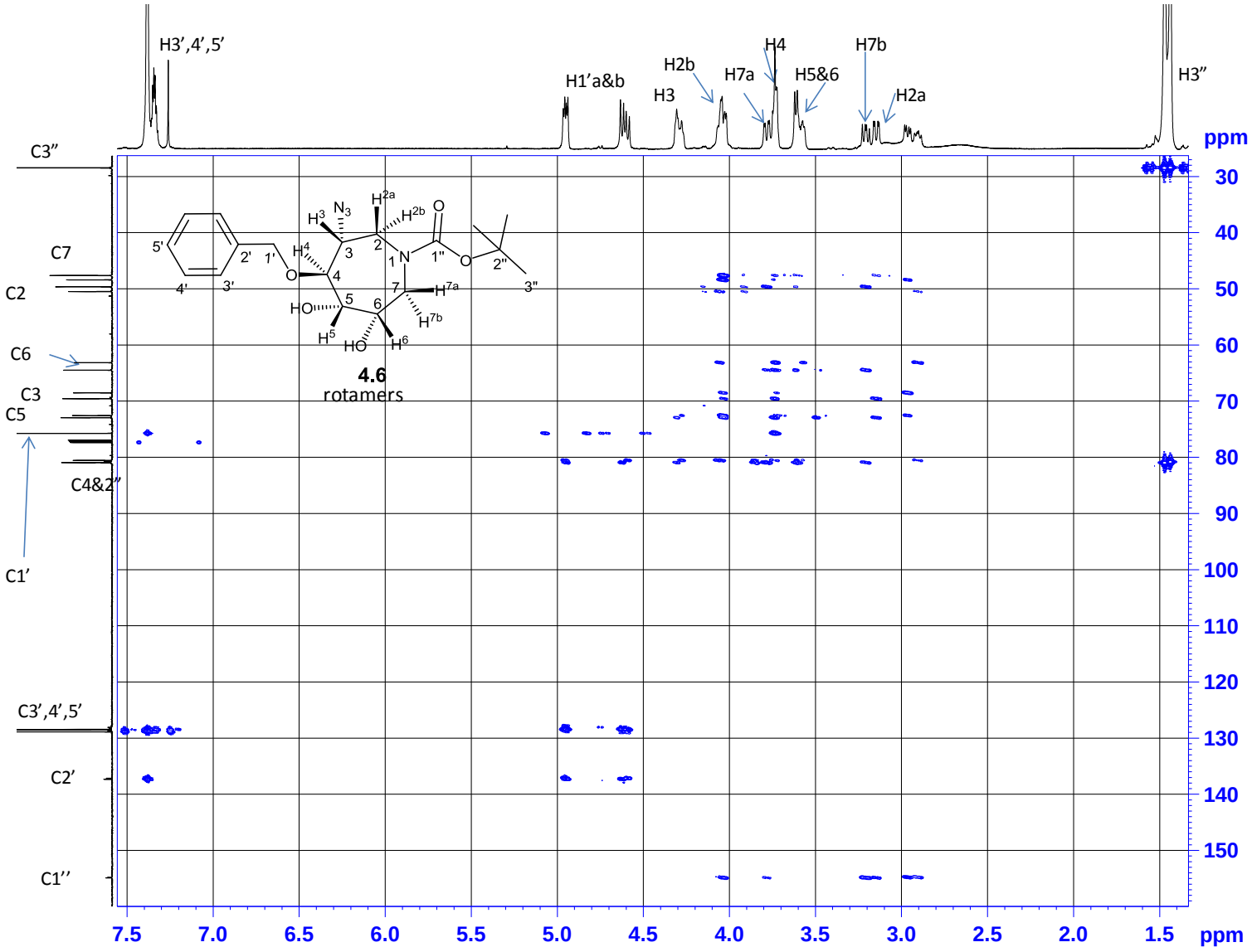
Full NMR spectra of compounds discussed in chapter 5……..…..……481

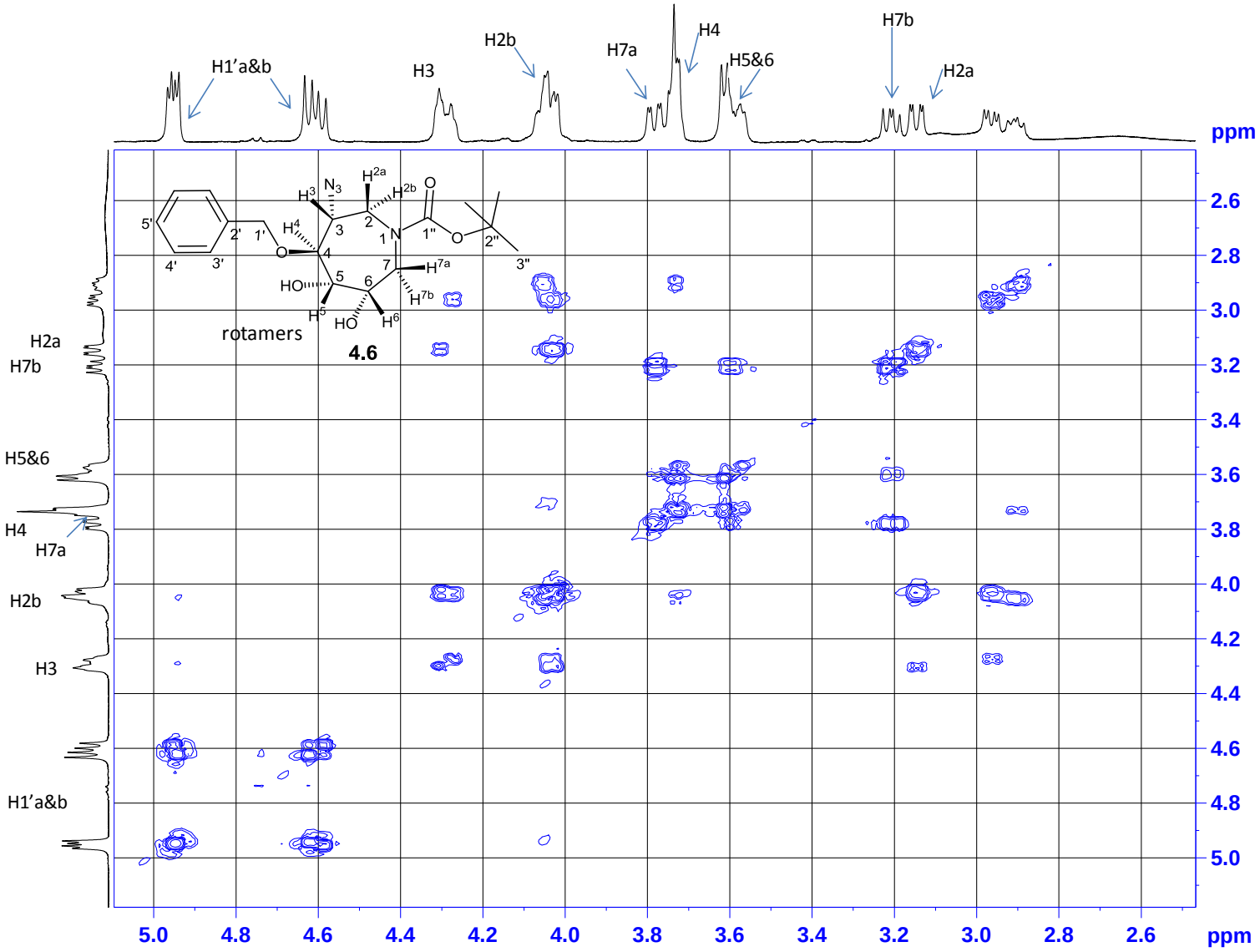

7.37
7.35
5.74
4.68
4.66
4.58
4.23
3.73
3.64
3.58
1.60
1.47
BnO
N3
N
Boc
2.7
rotamers
Current Data Parameters
NAME compound 5
EXPNO 1
PROCNO 1
F2 - Acquisition Parameters
Date_ 20110201
Time 18.18
INSTRUM spect
PROBHD 5 mm QNP 1H/1
PULPROG zg30
TD 32768
SOLVENT CDCl3
NS 16
DS 0
SWH 5995.204 Hz
FIDRES 0.182959 Hz
AQ 2.7329011 sec
RG 181
DW 83.400 usec
DE 20.00 usec
TE 298.2 K
D1 2.00000000 sec
TD0 1
======== CHANNEL f1 ========
NUC1 1H
P1 13.50 usec
PL1 3.00 dB
SFO1 399.9023994 MHz
F2 - Processing parameters
SI 32768
SF 399.9000123 MHz
WDW EM
SSB 0
LB 3.00 Hz
GB 0
PC 1.00
8.5
8.0
7.5
7.0
6.5
6.0
5.5
5.0
4.5
4.0
3.5
3.0
2.5
2.0
1.5
1.0
ppm
5.27
2.00
2.00
1.45
4.29
9.12

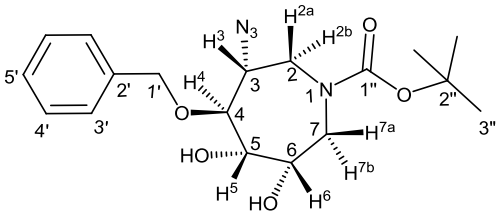

154.91
154.80
137.33
137.16
128.89
128.51
128.45
80.94
80.54
77.37
77.16
76.95
75.73
72.94
72.56
69.56
68.52
64.47
63.14
50.48
49.63
48.40
47.61
28.45
Current Data Parameters
NAME Compound 6
EXPNO 3
PROCNO 1
F2 - Acquisition Parameters
Date_ 20121129
Time 12.00
INSTRUM spect
PROBHD 5 mm CPTXI 1H-
PULPROG udeft.txt
TD 21814
SOLVENT CDC13
NS 2048
DS 0
SWH 30303.031 Hz
FIDRES 1.389155 Hz
AQ 0.3599810 sec
RG 32768
DW 16.500 usec
DE 6.00 usec
TE 298.0 K
D1 1.50000000 sec
D11 0.03000000 sec
d12 0.00002000 sec
D20 0.10000000 sec
DELTA 1.47000003 sec
DELTA2 0.36300099 sec
TAU 0.00302000 sec
TD0 1
======== CHANNEL f1 ========
NUC1 13C
P1 10.43 usec
P12 2000.00 usec
P26 500.00 usec
PL1 -2.50 dB
SFO1 150.9319817 MHz
SP2 5.29 dB
SP8 4.75 dB
SPNAM2 Crp60comp.4
SPNAM8 Crp60,0.5,20.1
SPOAL2 0.500
SPOAL8 0.500
SPOFFS2 0 Hz
SPOFFS8 0 Hz
======== CHANNEL f2 ========
CPDPRG2 waltz64
NUC2 1H
PCPD2 80.00 usec
PL2 1.00 dB
PL12 18.89 dB
SFO2 600.1830000 MHz
F1 - Acquisition parameters
TD 256
SFO1 150.932 MHz
FIDRES 93.450958 Hz
SW 158.505 ppm
FnMODE States-TPPI
F2 - Processing parameters
SI 262144
SF 150.9153655 MHz
WDW GM
SSB 0
LB 1.00 Hz
GB 0.01
PC 20.00
BnO
N3
HO
HO
N
Boc
4.6
rotamers
160
150
140
130
120
110
100
90
80
70
60
50
40
30
20
ppm


154.91
154.80
137.33
137.16
128.89
128.51
128.45
80.94
80.54
77.37
77.16
76.95
75.73
72.94
72.56
69.56
68.52
64.47
63.14
50.48
49.63
48.40
47.61
28.45
Current Data Parameters
NAME Compound 6
EXPNO 3
PROCNO 1
F2 - Acquisition Parameters
Date_ 20121129
Time 12.00
INSTRUM spect
PROBHD 5 mm CPTXI 1H-
PULPROG udeft.txt
TD 21814
SOLVENT CDCl3
NS 2048
DS 0
SWH 30303.031 Hz
FIDRES 1.389155 Hz
AQ 0.3599810 sec
RG 32768
DW 16.500 usec
DE 6.00 usec
TE 298.0 K
D1 1.50000000 sec
D11 0.03000000 sec
d12 0.00002000 sec
D20 0.10000000 sec
DELTA 1.47000003 sec
DELTA2 0.36300099 sec
TAU 0.00302000 sec
TD0 1
======== CHANNEL f1 ========
NUC1 13C
P1 10.43 usec
P12 2000.00 usec
P26 500.00 usec
PL1 -2.50 dB
SFO1 150.9319817 MHz
SP2 5.29 dB
SP8 4.75 dB
SPNAM2 Crp60comp.4
SPNAM8 Crp60,0.5,20.1
SPOAL2 0.500
SPOAL8 0.500
SPOFFS2 0 Hz
SPOFFS8 0 Hz
======== CHANNEL f2 ========
CPDPRG2 waltz64
NUC2 1H
PCPD2 80.00 usec
PL2 1.00 dB
PL12 18.89 dB
SFO2 600.1830000 MHz
F1 - Acquisition parameters
TD 256
SFO1 150.932 MHz
FIDRES 93.450958 Hz
SW 158.505 ppm
FnMODE States-TPPI
F2 - Processing parameters
SI 262144
SF 150.9153655 MHz
WDW GM
SSB 0
LB -1.00 Hz
GB 0.01
PC 20.00
BnO
N3
HO
HO
N
Boc
4.6
rotamers
160
150
140
130
120
110
100
90
80
70
60
50
40
30
20
ppm


H3',4',5'
H1'a&b
H3
H2b
H7a
H4
H5&6
H7b
H2a
H3"
ppm
C3"
C7
C2
C6
C3
C5
C4&2"
C1'
C3',4',5'
C2'
C1''
4.6
rotamers
7.5
7.0
6.5
6.0
5.5
5.0
4.5
4.0
3.5
3.0
2.5
2.0
1.5
ppm

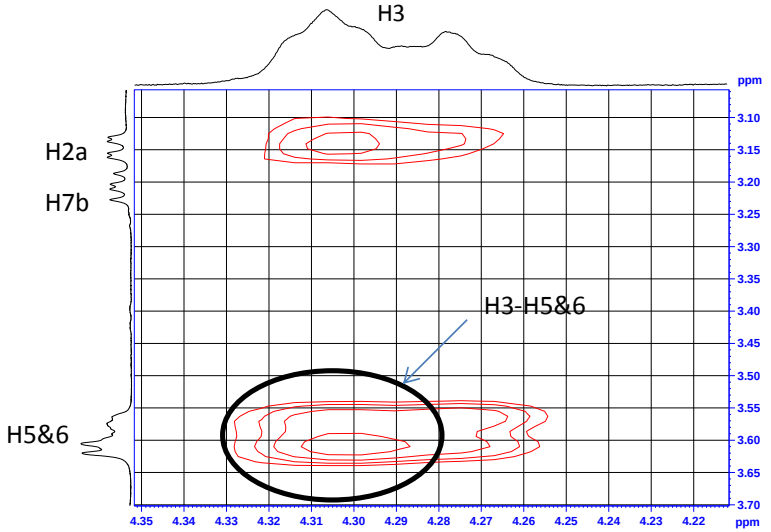

H3',4',5'
H1'a&b
H2b
H3
H7a
H4
H5&6
H7b
H2a
H3"
ppm
C3"
C7
C2
C6
C3
C5
C4&2"
C1'
C3',4',5'
C2'
C1''
4.6
rotamers
7.5
7.0
6.5
6.0
5.5
5.0
4.5
4.0
3.5
3.0
2.5
2.0
1.5
ppm


H1'a&b
H3
H2b
H7a
H4
H5&6
H7b
H2a
ppm
rotamers
4.6
H2a
H7b
H5&6
H4
H7a
H2b
H3
H1'a&b
5.0
4.8
4.6
4.4
4.2
4.0
3.8
3.6
3.4
3.2
3.0
2.8
2.6
ppm

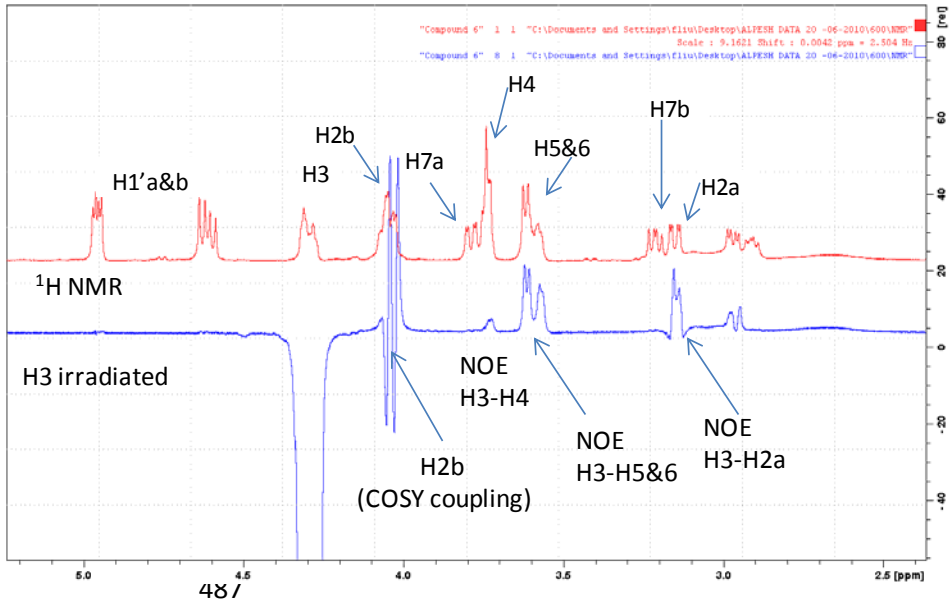


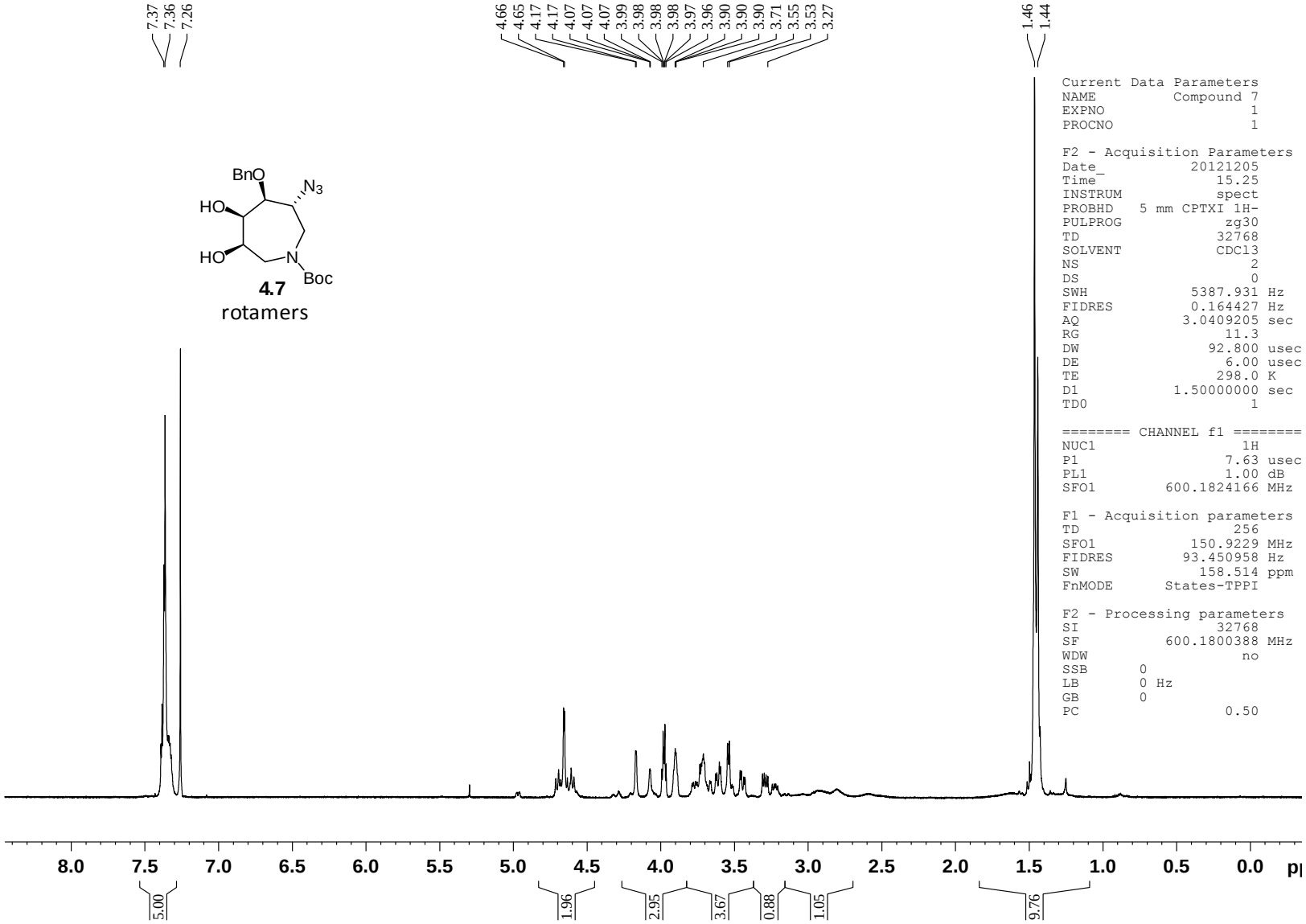
4.6

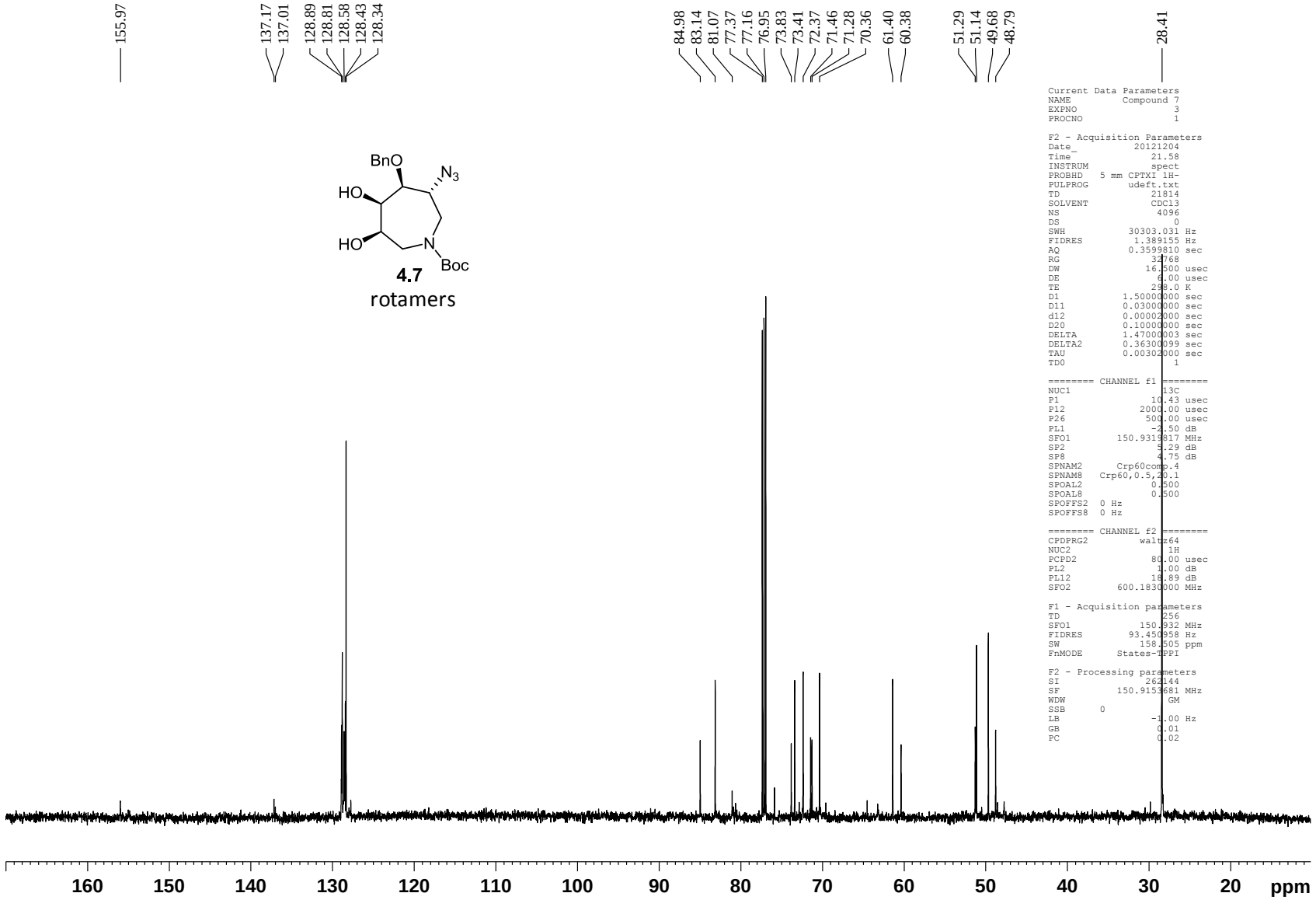
rotamers

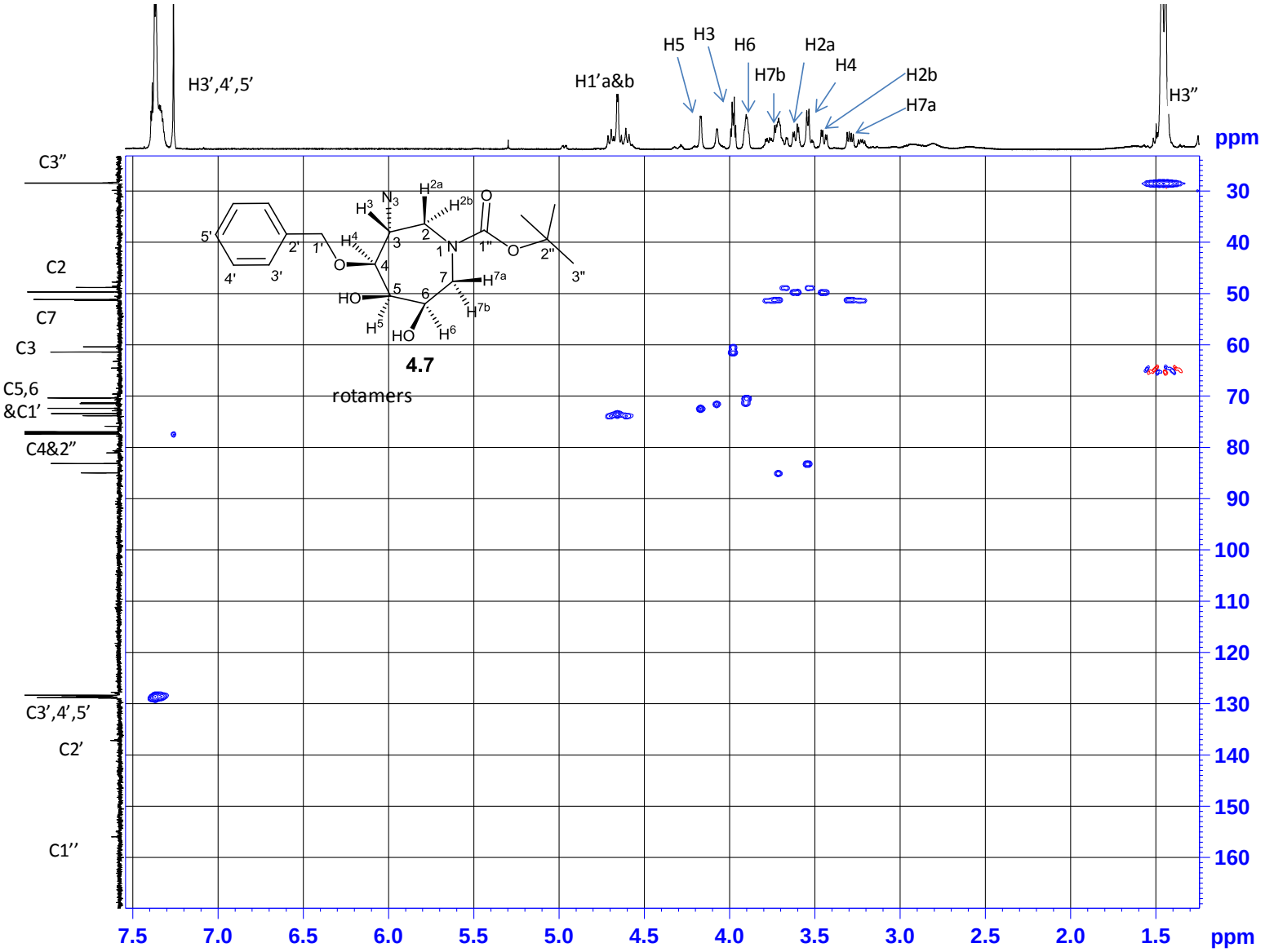


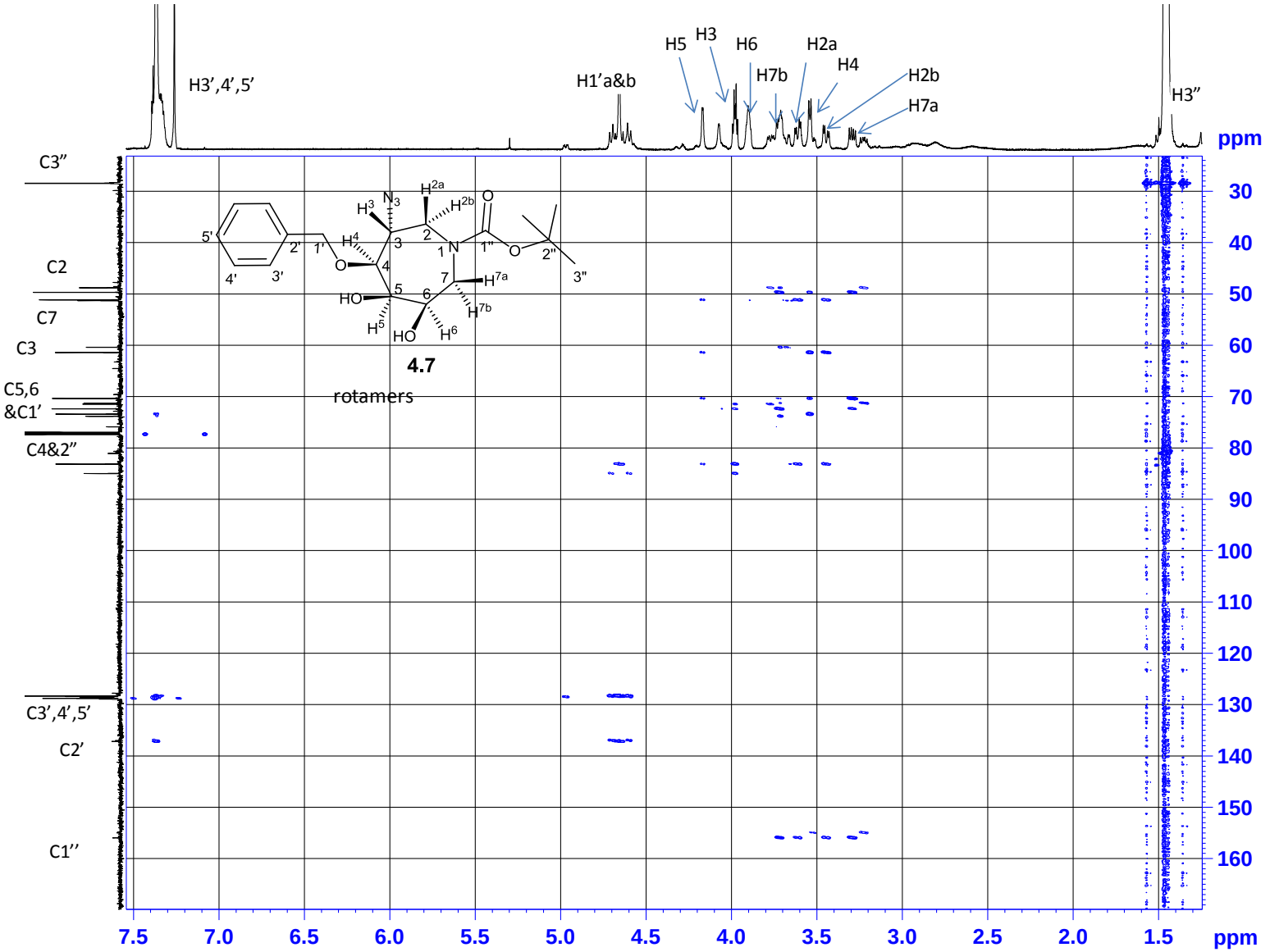
1D selective NOESY

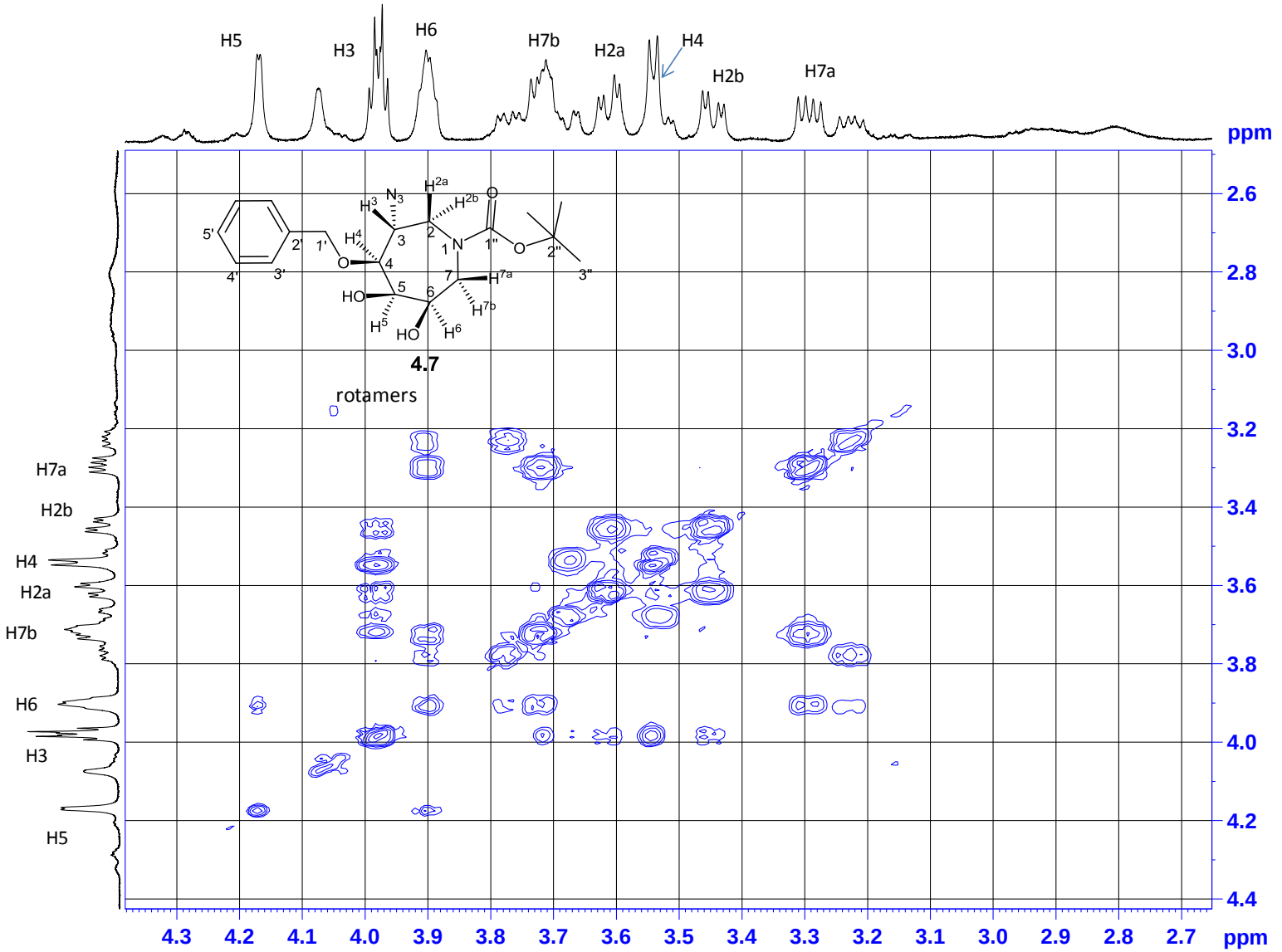


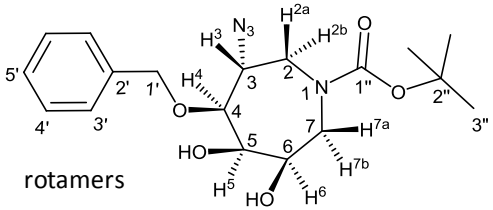

7.37
7.36
7.26
4.66
4.65
4.17
4.17
4.07
4.07
4.07
3.99
3.98
3.98
3.98
3.97
3.96
3.90
3.90
3.90
3.71
3.55
3.53
3.27
1.46
1.44
BnO
N3
HO
HO
N
Boc
4.7
rotamers
Current Data Parameters
NAME Compound 7
EXPNO 1
PROCNO 1
F2 - Acquisition Parameters
Date_ 20121205
Time 15.25
INSTRUM spect
PROBHD 5 mm CPTXI 1H-
PULPROG zg30
TD 32768
SOLVENT CDCl3
NS 2
DS 0
SWH 5387.931 Hz
FIDRES 0.164427 Hz
AQ 3.0409205 sec
RG 11.3
DW 92.800 usec
DE 6.00 usec
TE 298.0 K
D1 1.50000000 sec
TD0 1
======== CHANNEL f1 ========
NUC1 1H
P1 7.63 usec
PL1 1.00 dB
SFO1 600.1824166 MHz
F1 - Acquisition parameters
TD 256
SFO1 150.9229 MHz
FIDRES 93.450958 Hz
SW 158.514 ppm
FnMODE States-TPPI
F2 - Processing parameters
SI 32768
SF 600.1800388 MHz
WDW no
SSB 0
LB 0 Hz
GB 0
PC 0.50
8.0
7.5
7.0
6.5
6.0
5.5
5.0
4.5
4.0
3.5
3.0
2.5
2.0
1.5
1.0
0.5
0.0
5.00
1.96
2.95
3.67
0.88
1.05
9.76


155.97
137.17
137.01
128.89
128.81
128.58
128.43
128.34
84.98
83.14
81.07
77.37
77.16
76.95
73.83
73.41
72.37
71.46
71.28
70.36
61.40
60.38
51.29
51.14
49.68
48.79
28.41
BnO
N3
HO
HO
N
Boc
4.7
rotamers
Current Data Parameters
NAME Compound 7
EXPNO 3
PROCNO 1
F2 - Acquisition Parameters
Date_ 20121204
Time 21.58
INSTRUM spect
PROBHD 5 mm CPTXI 1H-
PULPROG udeft.txt
TD 21814
SOLVENT CDC13
NS 4096
DS 0
SWH 30303.031 Hz
FIDRES 1.389155 Hz
AQ 0.3599810 sec
RG 32768
DW 16.500 usec
DE 6.00 usec
TE 298.0 K
D1 1.50000000 sec
D11 0.03000000 sec
d12 0.00002000 sec
D20 0.10000000 sec
DELTA 1.47000003 sec
DELTA2 0.36300099 sec
TAU 0.00302000 sec
TD0 1
======== CHANNEL f1 ========
NUC1 13C
P1 10.43 usec
P12 2000.00 usec
P26 500.00 usec
PL1 -2.50 dB
SFO1 150.9319817 MHz
SP2 5.29 dB
SP8 4.75 dB
SPNAM2 Crp60comp.4
SPNAM8 Crp60,0.5,20.1
SPOAL2 0.500
SPOAL8 0.500
SPOFFS2 0 Hz
SPOFFS8 0 Hz
======== CHANNEL f2 ========
CPDPRG2 waltz64
NUC2 1H
PCPD2 80.00 usec
PL2 1.00 dB
PL12 18.89 dB
SFO2 600.1830000 MHz
F1 - Acquisition parameters
TD 256
SFO1 150.932 MHz
FIDRES 93.459958 Hz
SW 158.505 ppm
FnMODE States-TPPI
F2 - Processing parameters
SI 262144
SF 150.9153681 MHz
WDW GM
SSB 0
LB -1.00 Hz
GB 0.01
PC 0.02
160
150
140
130
120
110
100
90
80
70
60
50
40
30
20
ppm


H3',4',5'
H1'a&b
H5
H3
H6
H7b
H2a
H4
H2b
H7a
H3"
ppm
C3"
C2
C7
C3
C5,6
&C1'
C4&2"
C3',4',5'
C2'
C1''
4.7
rotamers
7.5
7.0
6.5
6.0
5.5
5.0
4.5
4.0
3.5
3.0
2.5
2.0
1.5
ppm


H3',4',5'
H1'a&b
H5
H3
H6
H7b
H2a
H4
H2b
H7a
H3"
ppm
C3"
C2
C7
C3
C5,6
&C1'
C4&2"
C3',4',5'
C2'
C1''
4.7
rotamers
7.5
7.0
6.5
6.0
5.5
5.0
4.5
4.0
3.5
3.0
2.5
2.0
1.5
ppm

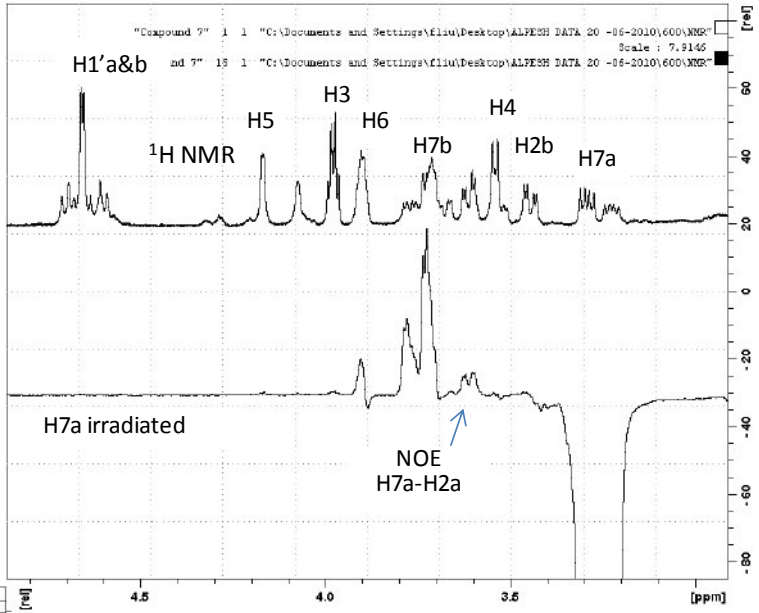

H5
H3
H6
H7b
H2a
H4
H2b
H7a
ppm
2.6
2.8
3.0
3.2
3.4
3.6
3.8
4.0
4.2
4.4
4.3
4.2
4.1
4.0
3.9
3.8
3.7
3.6
3.5
3.4
3.3
3.2
3.1
3.0
2.9
2.8
2.7
ppm
4.7
rotamers



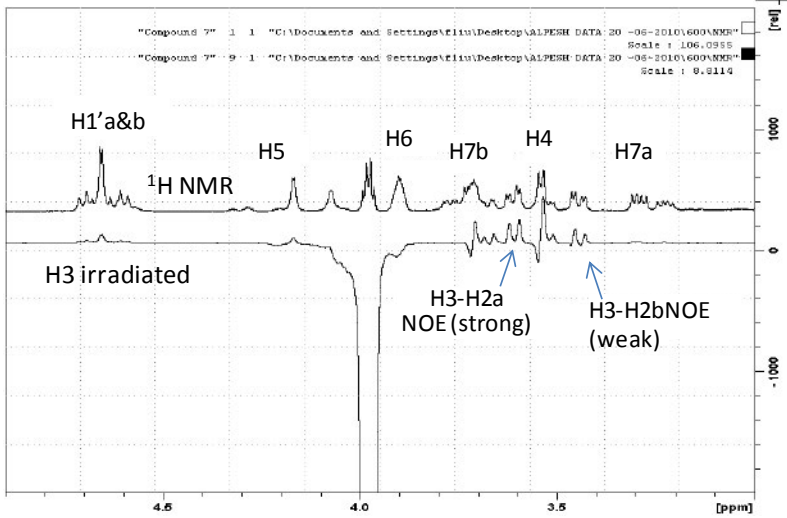
rotamers

4.7

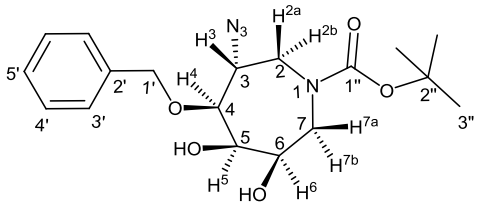
1D selective NOESY



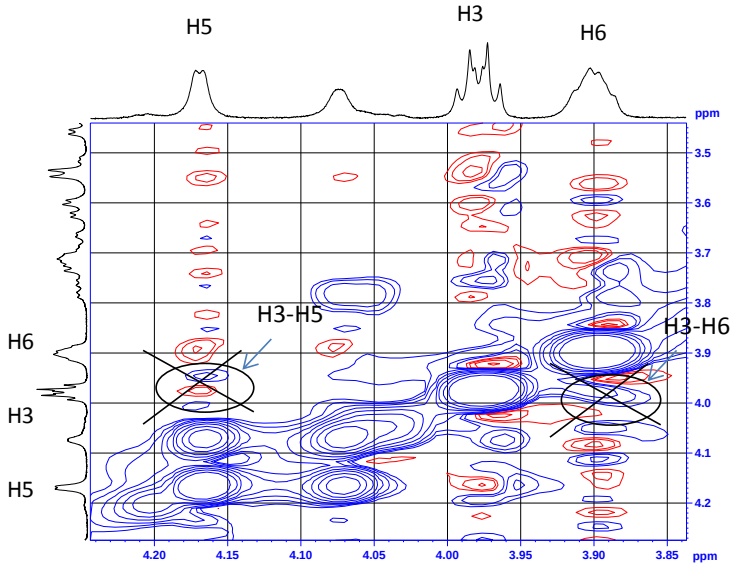
1D selective NOESY



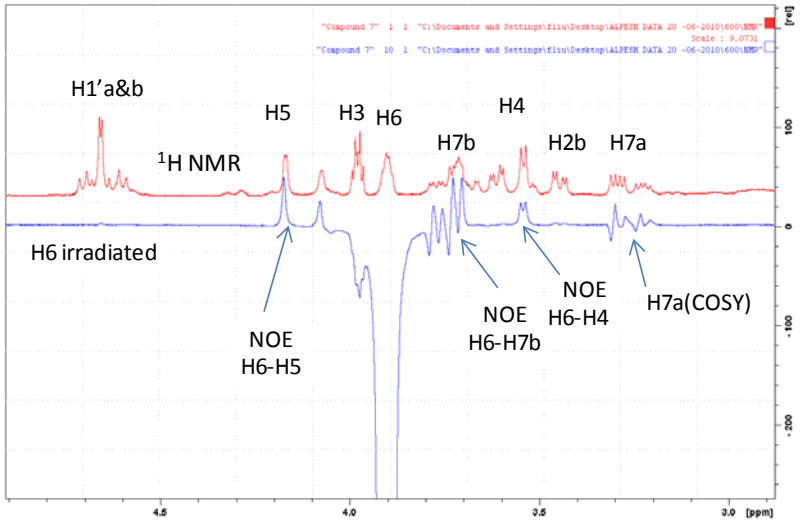
- H3 shows bigger NOE to H2a compared to H2b suggesting H2a is *cis* to H3 and H2b is *trans* to H3.
- H7a shows bigger NOE to H2a compared to H2b meaning H7a is *cis* to H3 and H2a.
- H6 shows big NOE to H7b, H4 and H5 suggesting H6 and H5 both are *cis* to H4.
- Moreover, H5 also shows NOE to H4 and H7b confirming H5 is *cis* to H4.



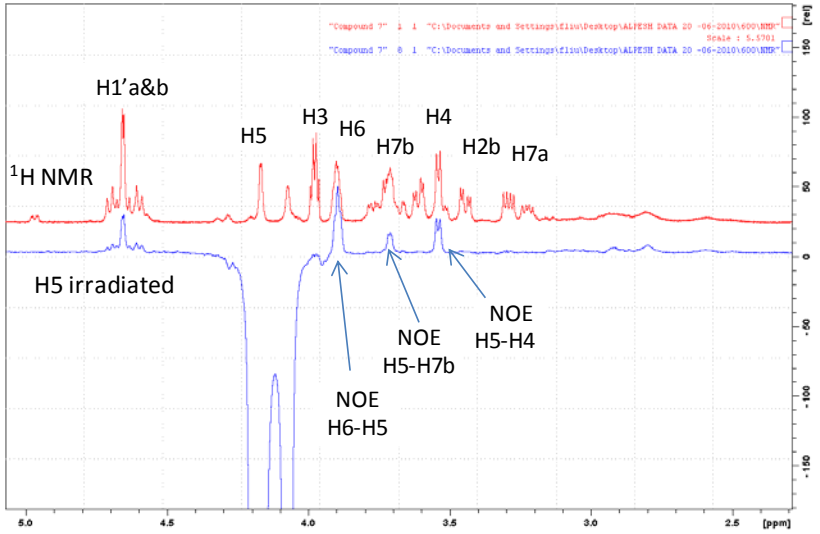
rotamers **4.7**

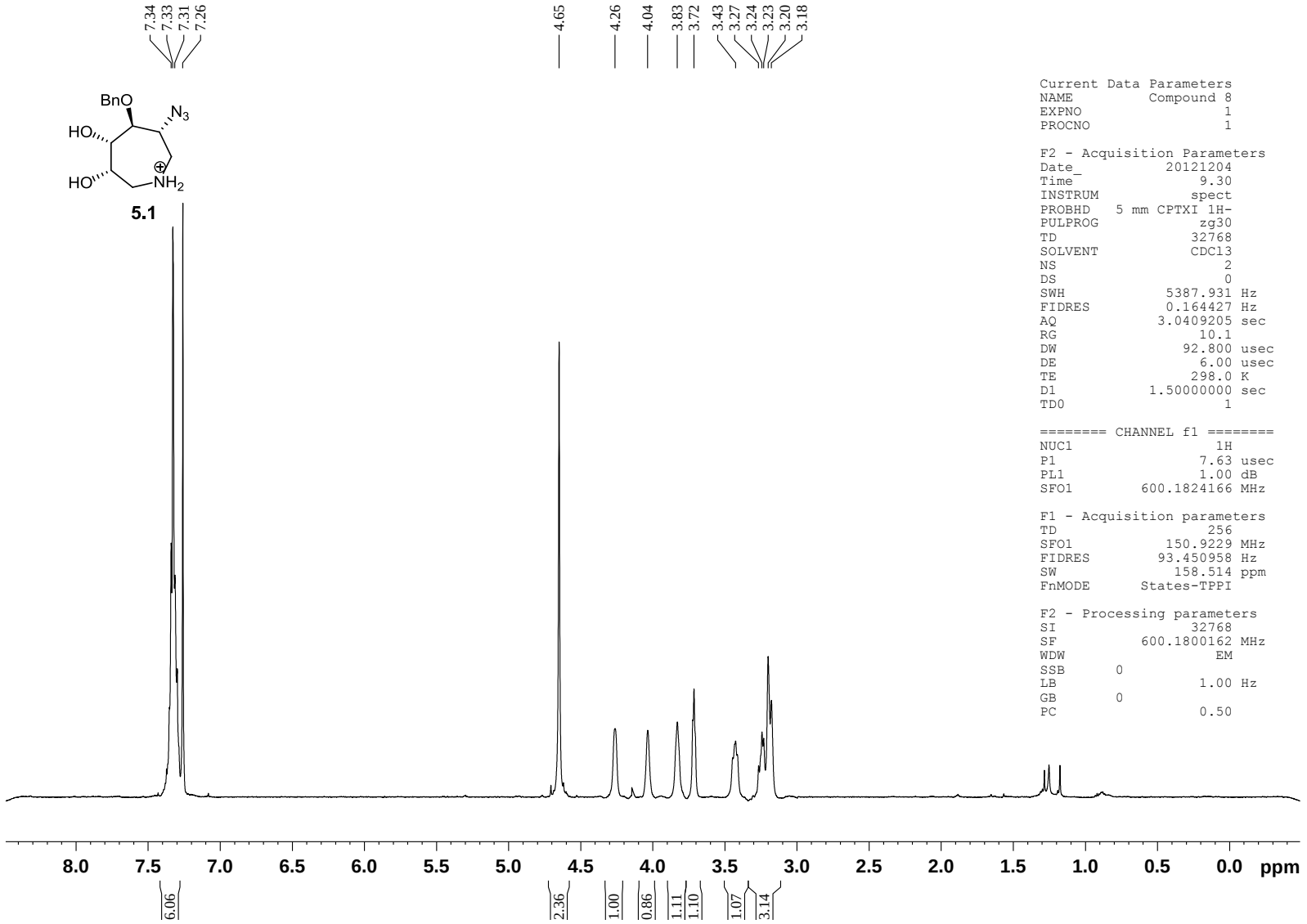


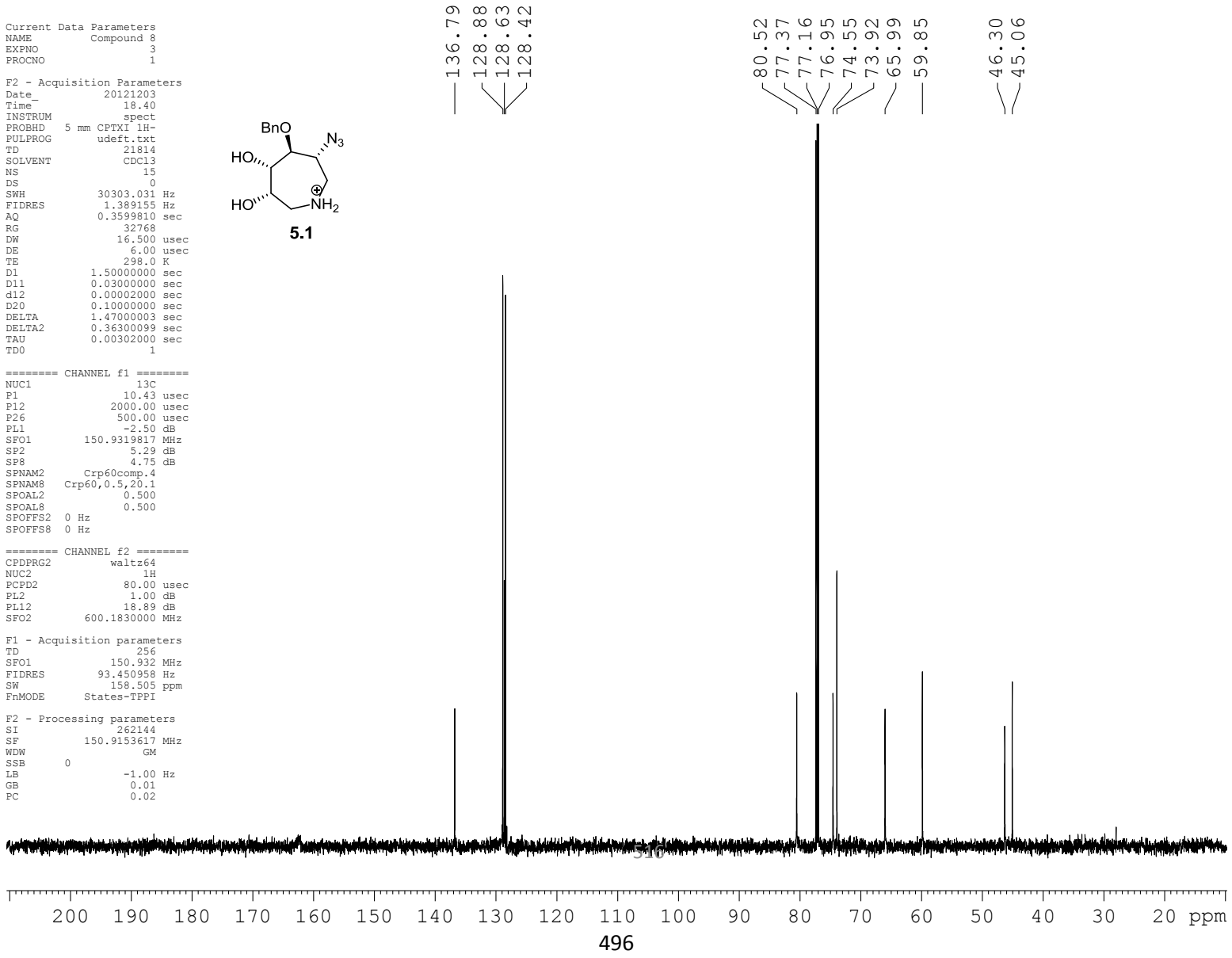
1D selective NOESY

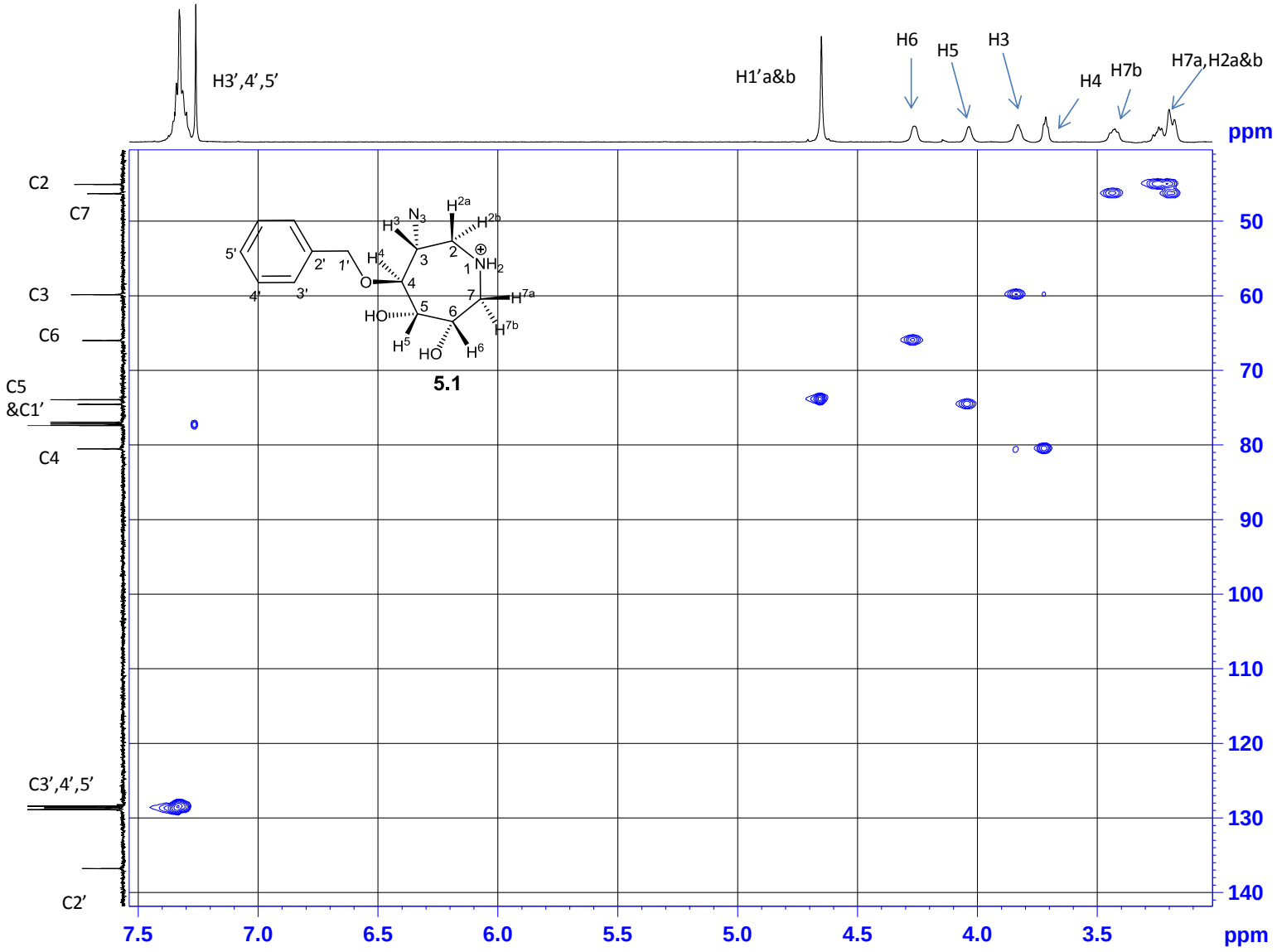


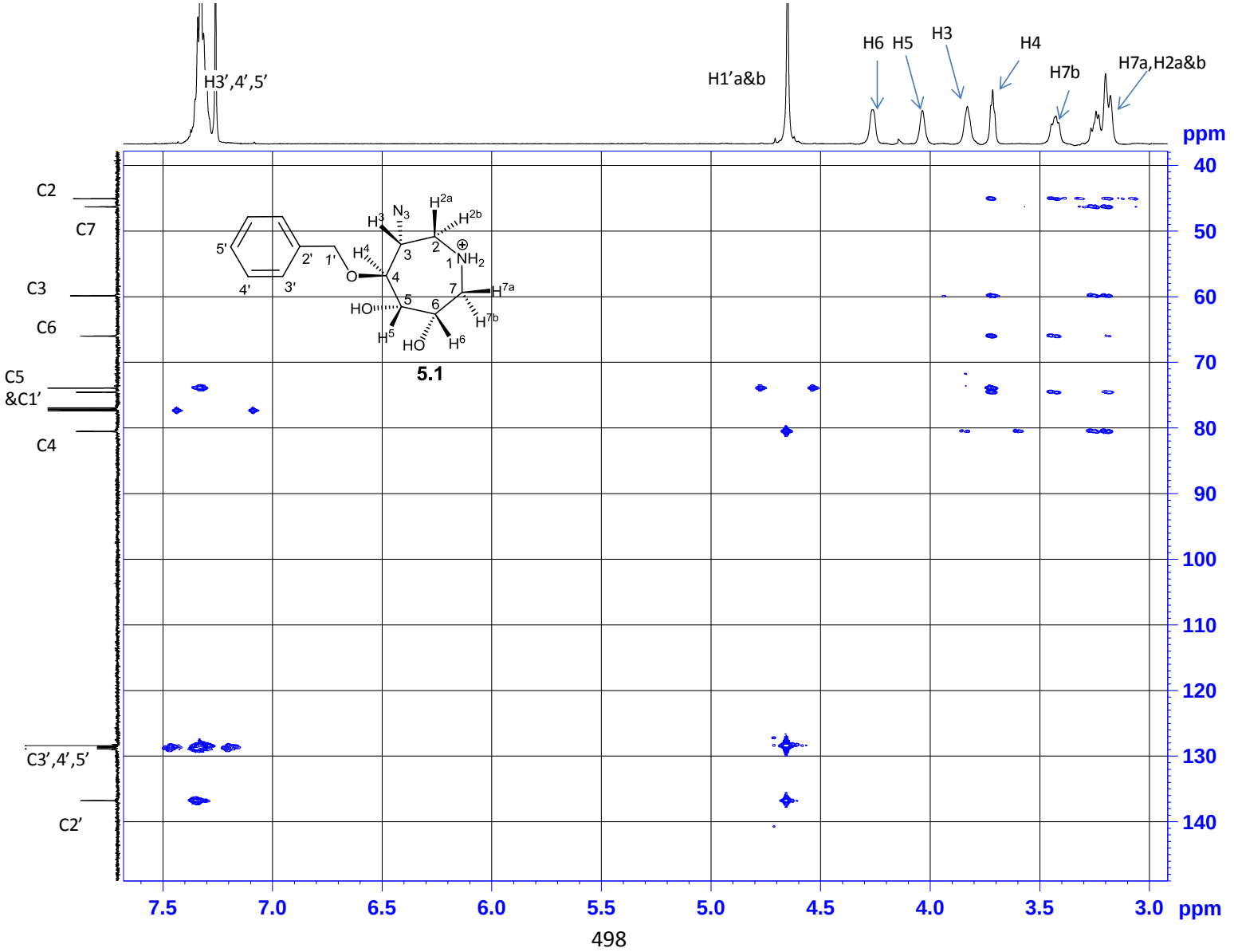
1D selective NOESY

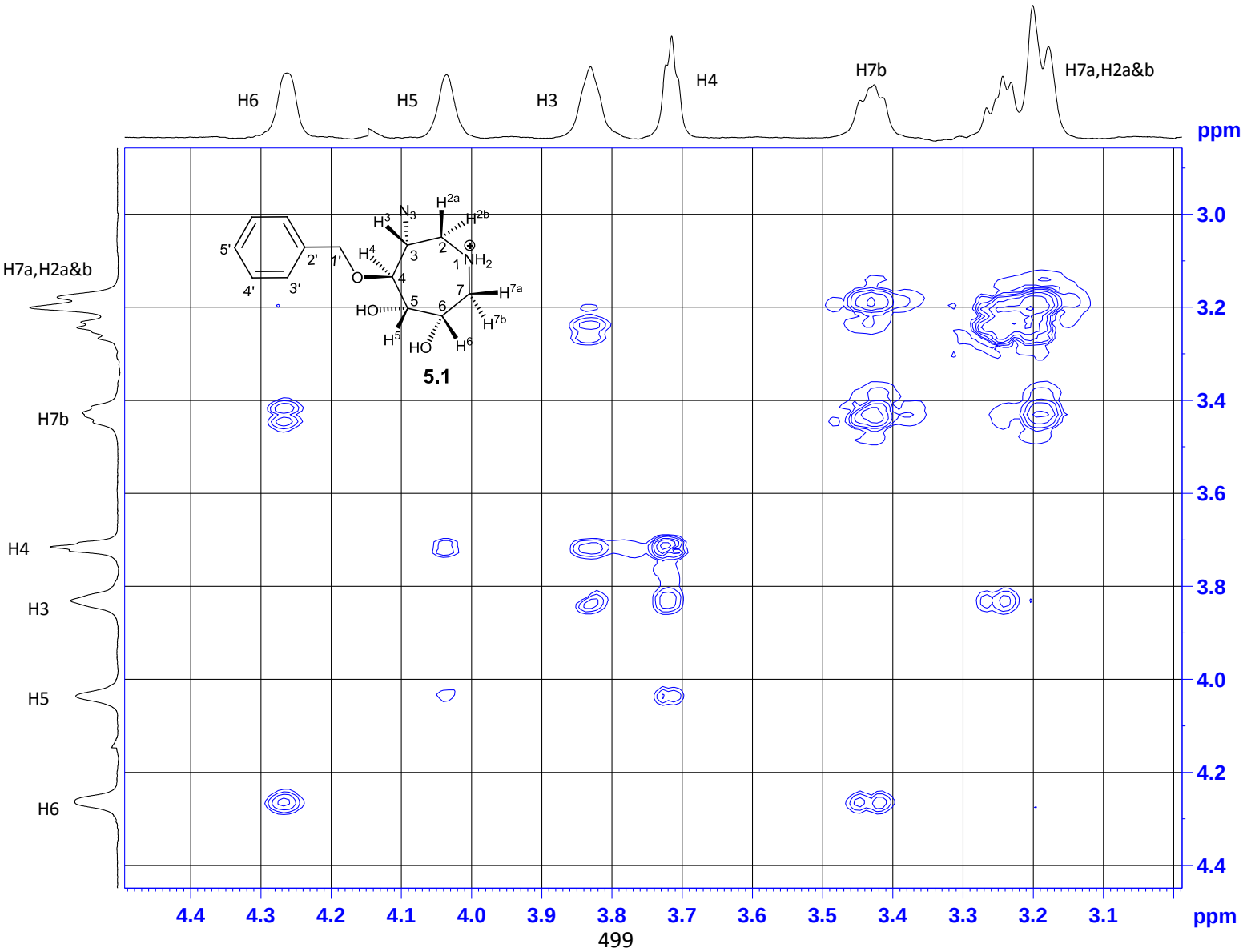


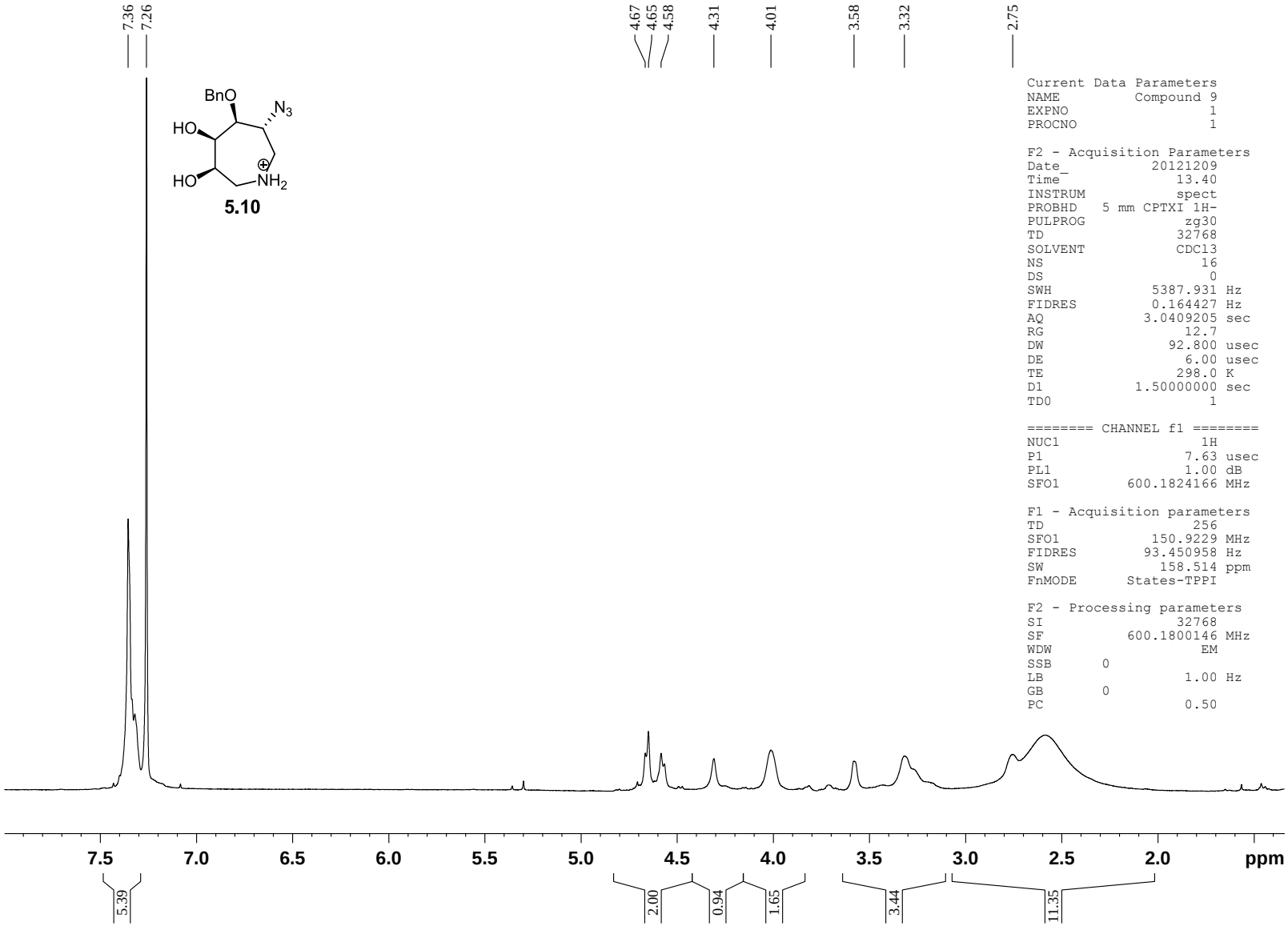

7.34
7.33
7.31
7.26
4.65
4.26
4.04
3.83
3.72
3.43
3.27
3.24
3.23
3.20
3.18
BnO
N3
HO
HO
NH2
5.1
Current Data Parameters
NAME Compound 8
EXPNO 1
PROCNO 1
F2 - Acquisition Parameters
Date_ 20121204
Time 9.30
INSTRUM spect
PROBHD 5 mm CPTXI 1H-
PULPROG zg30
TD 32768
SOLVENT CDCl3
NS 2
DS 0
SWH 5387.931 Hz
FIDRES 0.164427 Hz
AQ 3.0409205 sec
RG 10.1
DW 92.800 usec
DE 6.00 usec
TE 298.0 K
D1 1.50000000 sec
TD0 1
======== CHANNEL f1 ========
NUC1 1H
P1 7.63 usec
PL1 1.00 dB
SFO1 600.1824166 MHz
F1 - Acquisition parameters
TD 256
SFO1 150.9229 MHz
FIDRES 93.450958 Hz
SW 158.514 ppm
FnMODE States-TPPI
F2 - Processing parameters
SI 32768
SF 600.1800162 MHz
WDW EM
SSB 0
LB 1.00 Hz
GB 0
PC 0.50
8.0
7.5
7.0
6.5
6.0
5.5
5.0
4.5
4.0
3.5
3.0
2.5
2.0
1.5
1.0
0.5
0.0
ppm
6.06
2.36
1.00
0.86
1.11
1.10
1.07
3.14

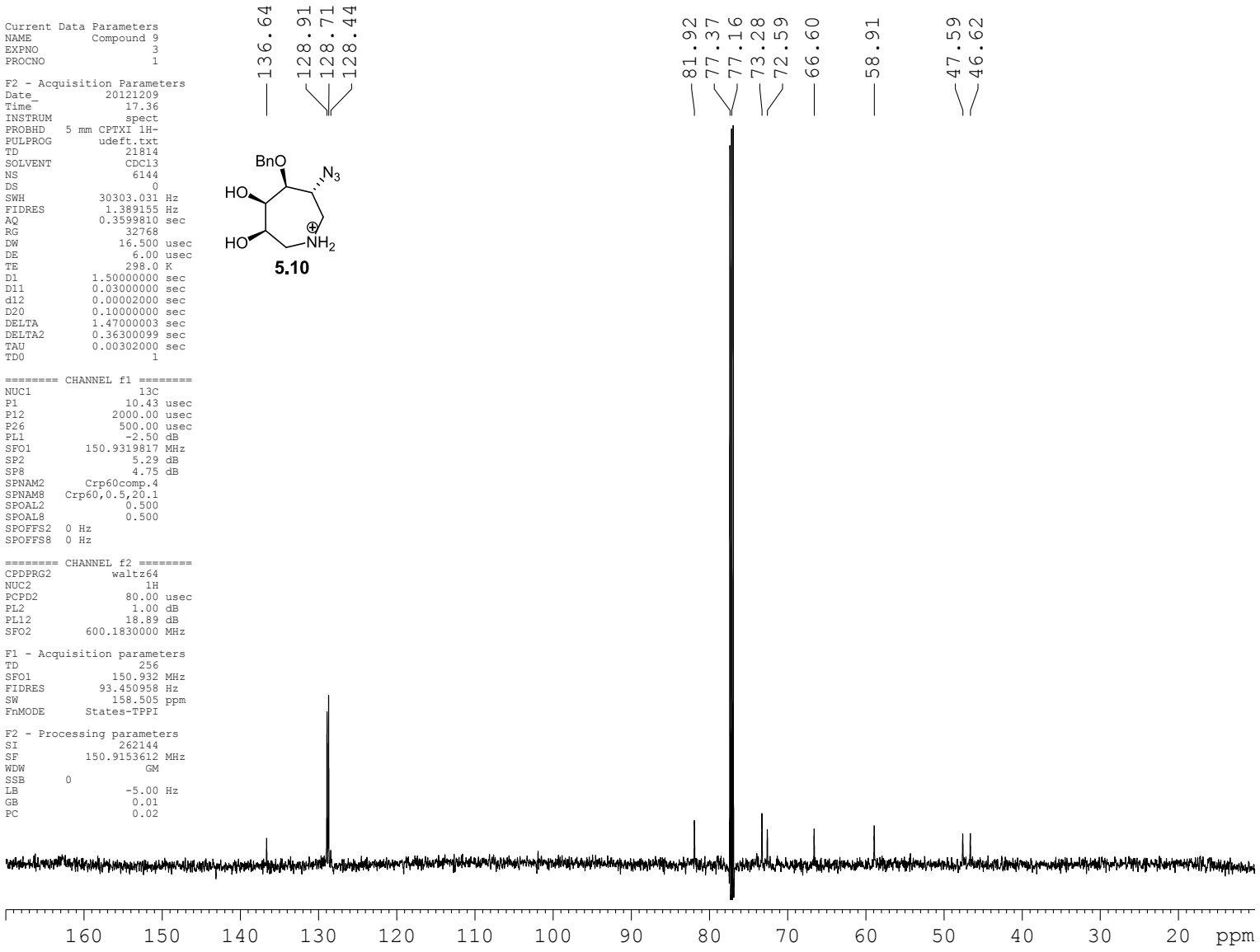

Current Data Parameters
NAME Compound 8
EXPNO 3
PROCNO 1
F2 - Acquisition Parameters
Date_ 20121203
Time 18.40
INSTRUM spect
PROBHD 5 mm CPTXI 1H-
PULPROG udeft.txt
TD 21814
SOLVENT CDCl3
NS 15
DS 0
SWH 30303.031 Hz
FIDRES 1.389155 Hz
AQ 0.3599810 sec
RG 32768
DW 16.500 usec
DE 6.00 usec
TE 298.0 K
D1 1.50000000 sec
D11 0.03000000 sec
d12 0.00002000 sec
D20 0.10000000 sec
DELTA 1.47000003 sec
DELTA2 0.36300099 sec
TAU 0.00302000 sec
TD0 1
======== CHANNEL f1 ========
NUC1 13C
P1 10.43 usec
P12 2000.00 usec
P26 500.00 usec
PL1 -2.50 dB
SFO1 150.9319817 MHz
SP2 5.29 dB
SP8 4.75 dB
SPNAM2 Crp60comp.4
SPNAM8 Crp60,0.5,20.1
SPOAL2 0.500
SPOAL8 0.500
SPOFFS2 0 Hz
SPOFFS8 0 Hz
======== CHANNEL f2 ========
CPDPRG2 waltz64
NUC2 1H
PCPD2 80.00 usec
PL2 1.00 dB
PL12 18.89 dB
SFO2 600.1830000 MHz
F1 - Acquisition parameters
TD 256
SFO1 150.932 MHz
FIDRES 93.450958 Hz
SW 158.505 ppm
FnMODE States-TPPI
F2 - Processing parameters
SI 262144
SF 150.9153617 MHz
WDW GM
SSB 0
LB -1.00 Hz
GB 0.01
PC 0.02
BnO
N3
HO
HO
NH2
5.1
136.79
128.88
128.63
128.42
80.52
77.37
77.16
76.95
74.55
73.92
65.99
59.85
46.30
45.06
200 190 180 170 160 150 140 130 120 110 100 90 80 70 60 50 40 30 20 ppm

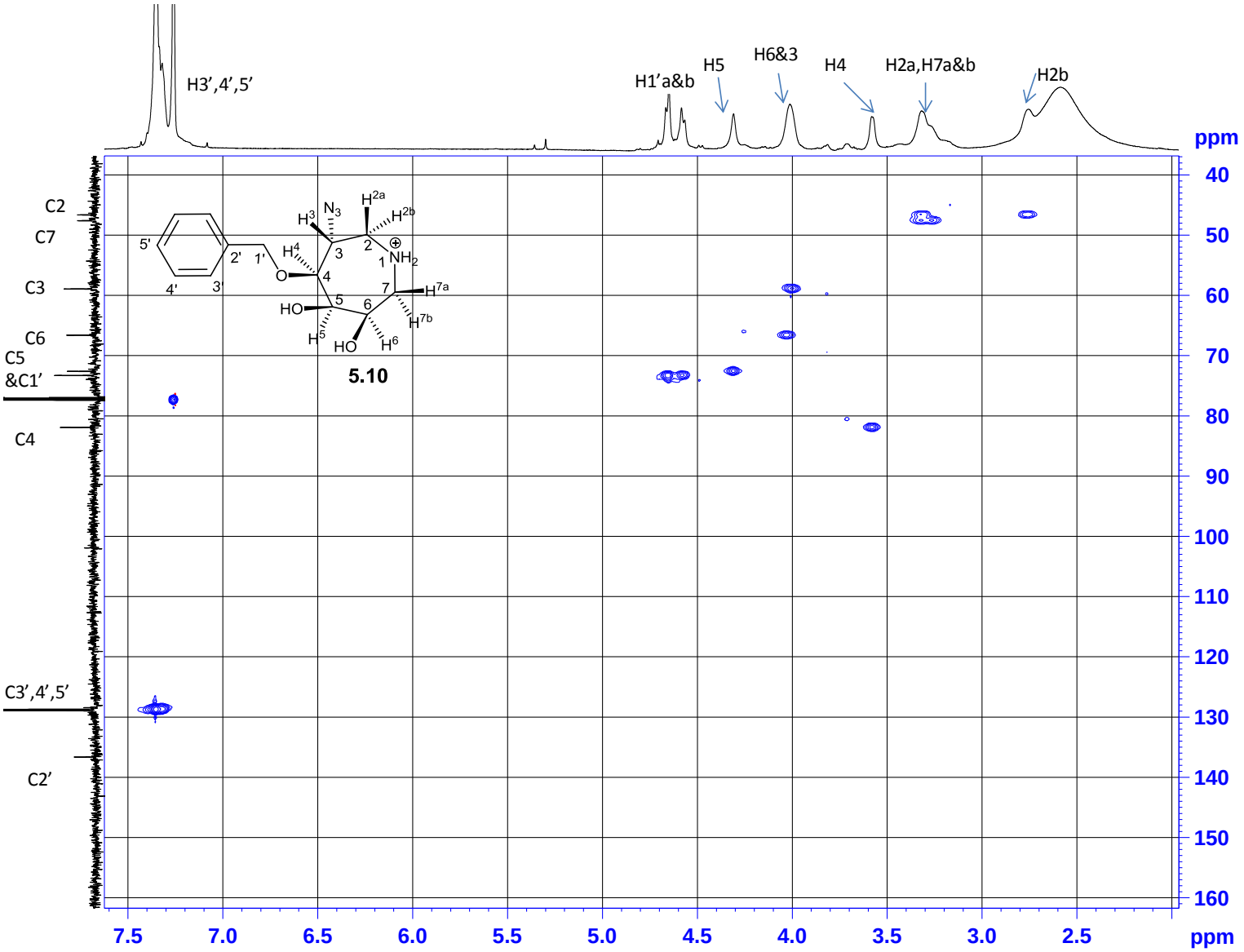

H3',4',5'
H1'a&b
H6
H5
H3
H4
H7b
H7a,H2a&b
ppm
C2
C7
C3
C6
C5
&C1'
C4
C3',4',5'
C2'
5.1
7.5
7.0
6.5
6.0
5.5
5.0
4.5
4.0
3.5
ppm
50
60
70
80
90
100
110
120
130
140

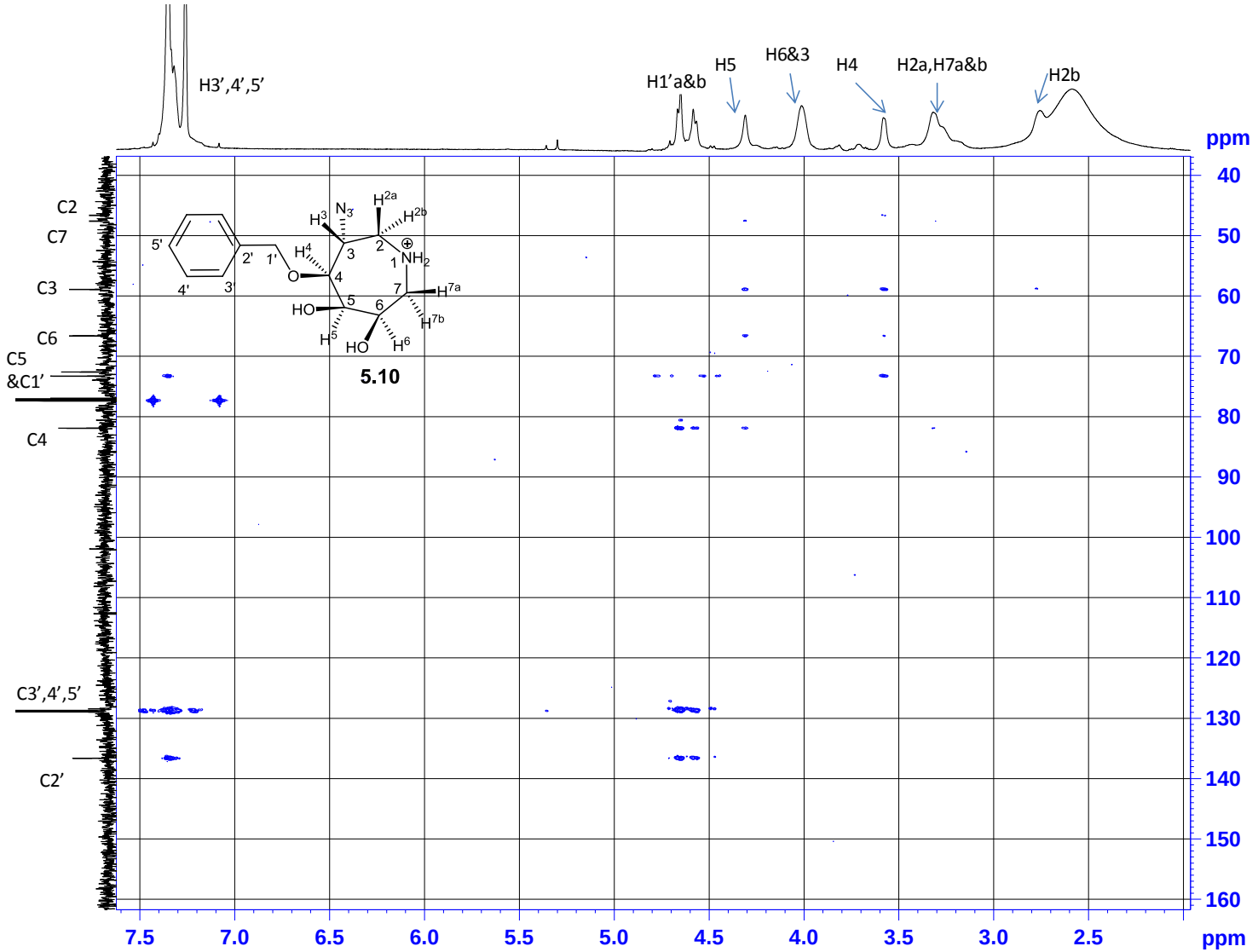

H3',4',5'
H1'a&b
H6
H5
H3
H4
H7b
H7a,H2a&b
ppm
C2
C7
C3
C6
C5
&C1'
C4
C3',4',5'
C2'
5.1
7.5
7.0
6.5
6.0
5.5
5.0
4.5
4.0
3.5
3.0
ppm

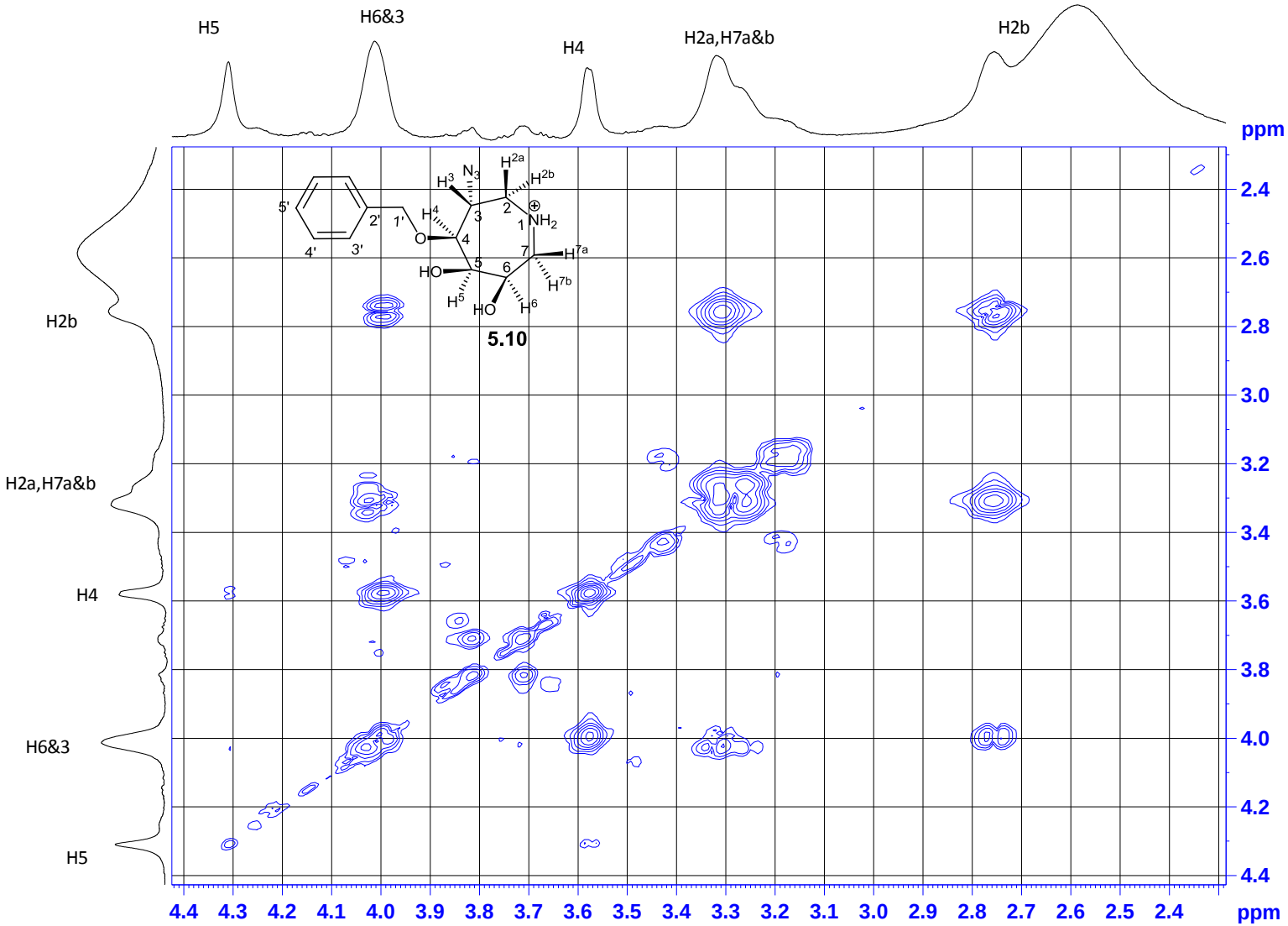

H6
H5
H3
H4
H7b
H7a,H2a&b
ppm
H7a,H2a&b
H7b
H4
H3
H5
H6
3.0
3.2
3.4
3.6
3.8
4.0
4.2
4.4
4.4
4.3
4.2
4.1
4.0
3.9
3.8
3.7
3.6
3.5
3.4
3.3
3.2
3.1
ppm
5.1

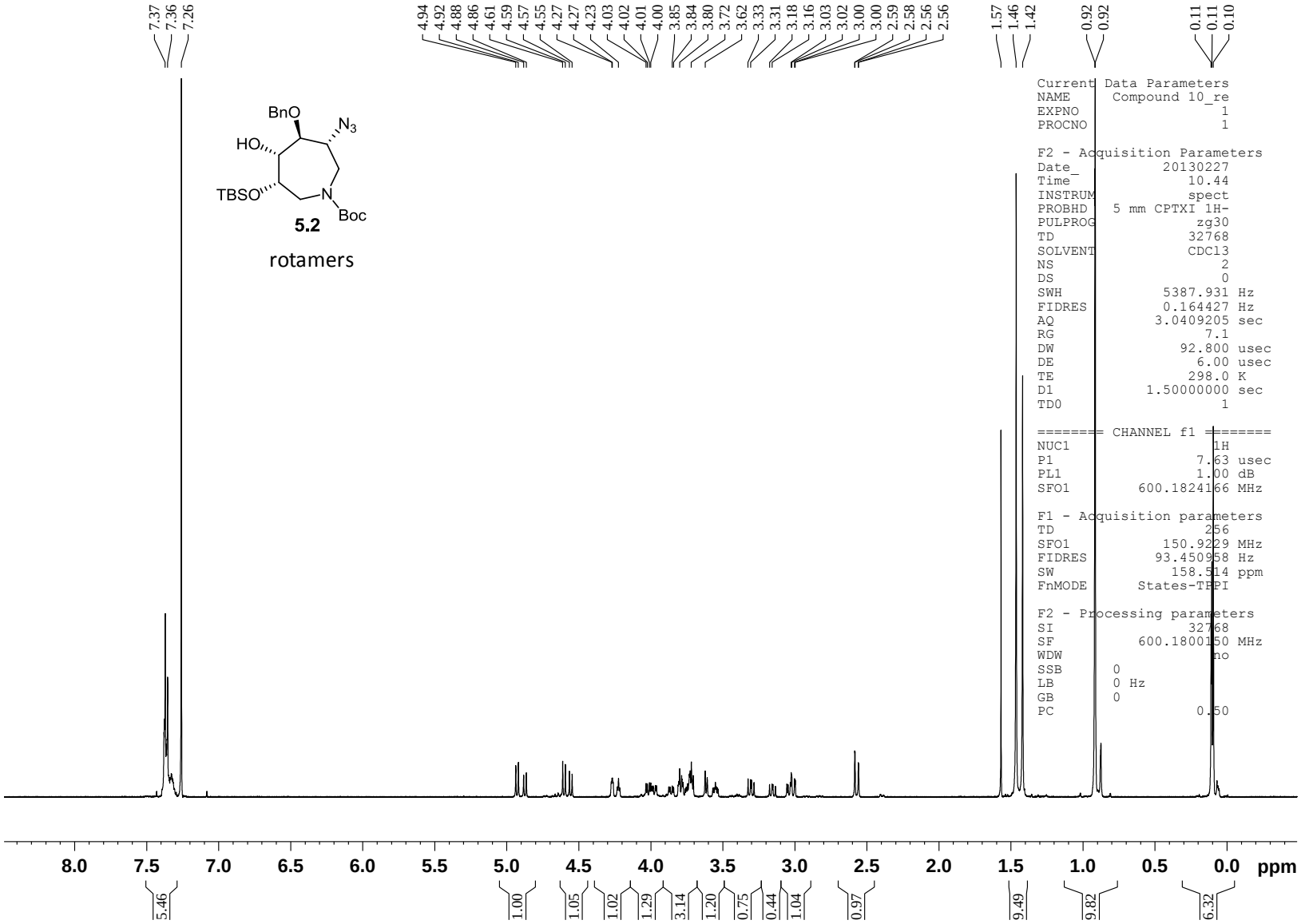

7.36
7.26
4.67
4.65
4.58
4.31
4.01
3.58
3.32
2.75
BnO
N3
HO
HO
NH2
5.10
Current Data Parameters
NAME Compound 9
EXPNO 1
PROCNO 1
F2 - Acquisition Parameters
Date_ 20121209
Time 13.40
INSTRUM spect
PROBHD 5 mm CPTXI 1H-
PULPROG zg30
TD 32768
SOLVENT CDCl3
NS 16
DS 0
SWH 5387.931 Hz
FIDRES 0.164427 Hz
AQ 3.0409205 sec
RG 12.7
DW 92.800 usec
DE 6.00 usec
TE 298.0 K
D1 1.50000000 sec
TD0 1
======== CHANNEL f1 ========
NUC1 1H
P1 7.63 usec
PL1 1.00 dB
SFO1 600.1824166 MHz
F1 - Acquisition parameters
TD 256
SFO1 150.9229 MHz
FIDRES 93.450958 Hz
SW 158.514 ppm
FnMODE States-TPPI
F2 - Processing parameters
SI 32768
SF 600.1800146 MHz
WDW EM
SSB 0
LB 1.00 Hz
GB 0
PC 0.50
7.5
7.0
6.5
6.0
5.5
5.0
4.5
4.0
3.5
3.0
2.5
2.0
ppm
5.39
2.00
0.94
1.65
3.44
11.35

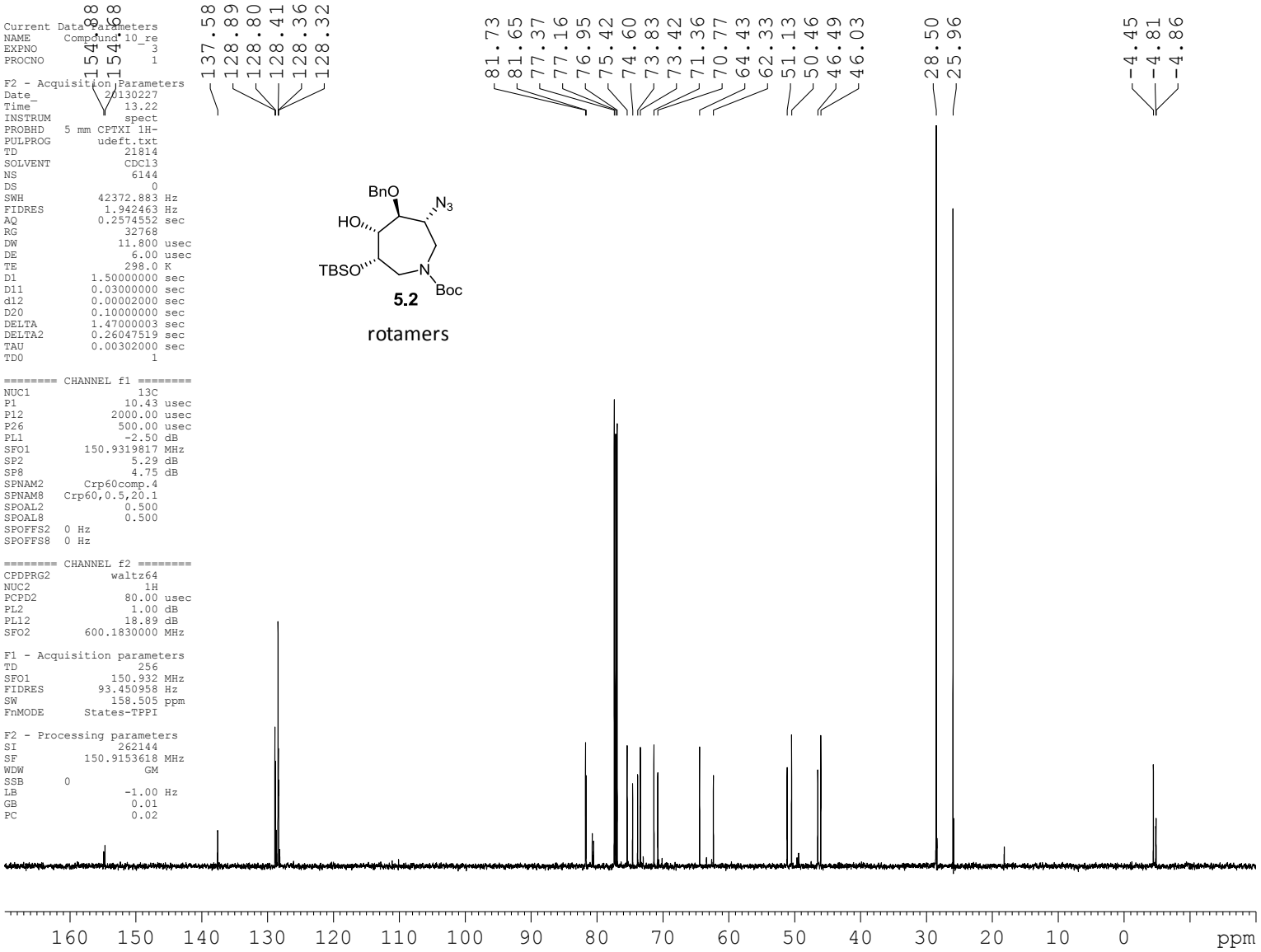

Current Data Parameters
NAME Compound 9
EXPNO 3
PROCNO 1
F2 - Acquisition Parameters
Date_ 20121209
Time 17.36
INSTRUM spect
PROBHD 5 mm CPTXI 1H-
PULPROG udeft.txt
TD 21814
SOLVENT CDCl3
NS 6144
DS 0
SWH 30303.031 Hz
FIDRES 1.389155 Hz
AQ 0.3599810 sec
RG 32768
DW 16.500 usec
DE 6.00 usec
TE 298.0 K
D1 1.50000000 sec
D11 0.03000000 sec
d12 0.00002000 sec
D20 0.10000000 sec
DELTA 1.47000003 sec
DELTA2 0.36300099 sec
TAU 0.00302000 sec
TD0 1
======== CHANNEL f1 ========
NUC1 13C
P1 10.43 usec
P12 2000.00 usec
P26 500.00 usec
PL1 -2.50 dB
SFO1 150.9319817 MHz
SP2 5.29 dB
SP8 4.75 dB
SPNAM2 Crp60comp.4
SPNAM8 Crp60,0.5,20.1
SPOAL2 0.500
SPOAL8 0.500
SPOFFS2 0 Hz
SPOFFS8 0 Hz
======== CHANNEL f2 ========
CPDPRG2 waltz64
NUC2 1H
PCPD2 80.00 usec
PL2 1.00 dB
PL12 18.89 dB
SFO2 600.1830000 MHz
F1 - Acquisition parameters
TD 256
SFO1 150.932 MHz
FIDRES 93.450958 Hz
SW 158.505 ppm
FnMODE States-TPPI
F2 - Processing parameters
SI 262144
SF 150.9153612 MHz
WDW GM
SSB 0
LB -5.00 Hz
GB 0.01
PC 0.02
136.64
128.91
128.71
128.44
81.92
77.37
77.16
73.28
72.59
66.60
58.91
47.59
46.62
BnO
N3
HO
HO
NH2
5.10
160
150
140
130
120
110
100
90
80
70
60
50
40
30
20
ppm

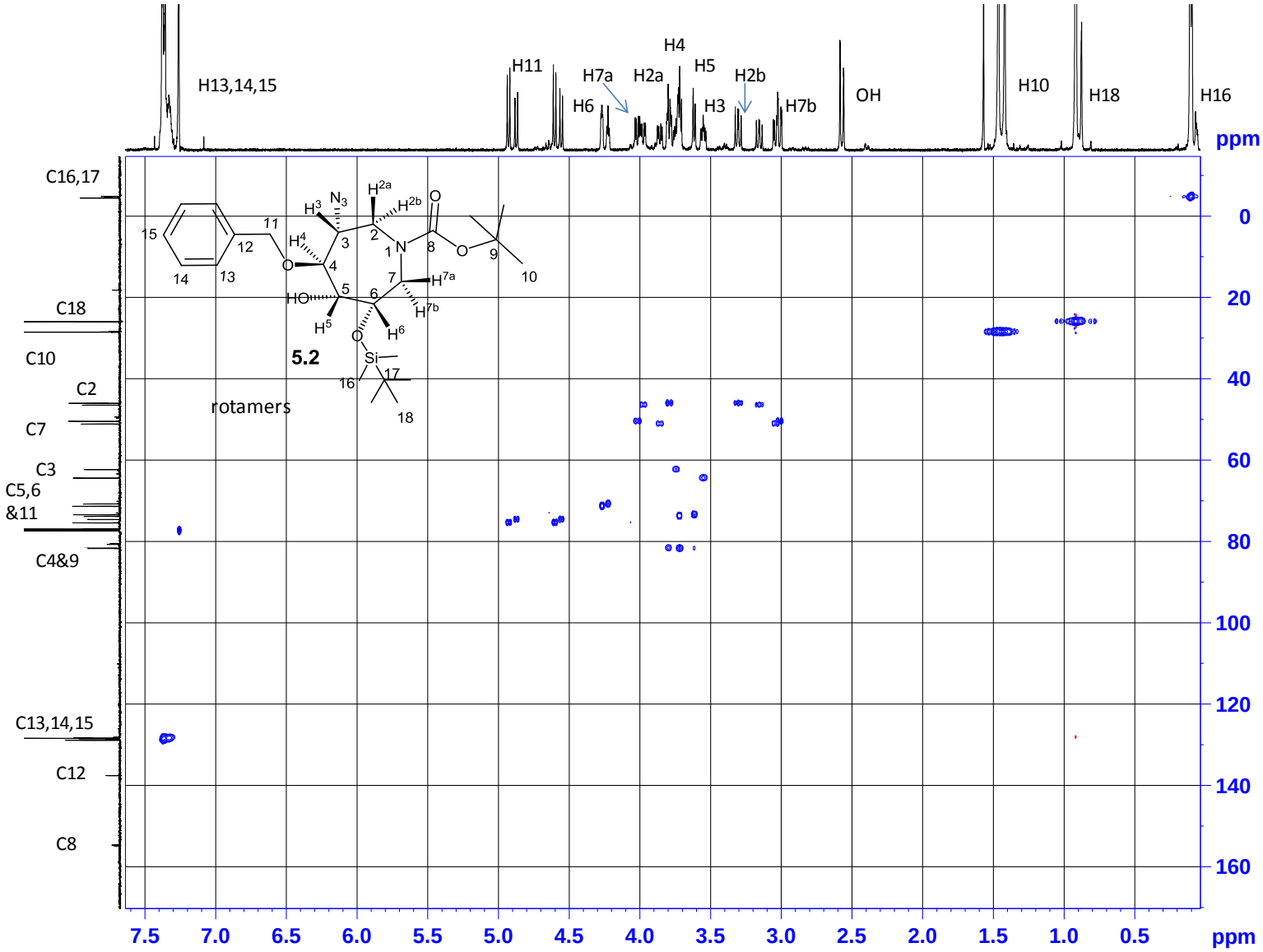

H3',4',5'
H1'a&b
H5
H6&3
H4
H2a,H7a&b
H2b
ppm
C2
C7
C3
C6
C5
&C1'
C4
C3',4',5'
C2'
5.10
7.5
7.0
6.5
6.0
5.5
5.0
4.5
4.0
3.5
3.0
2.5
ppm

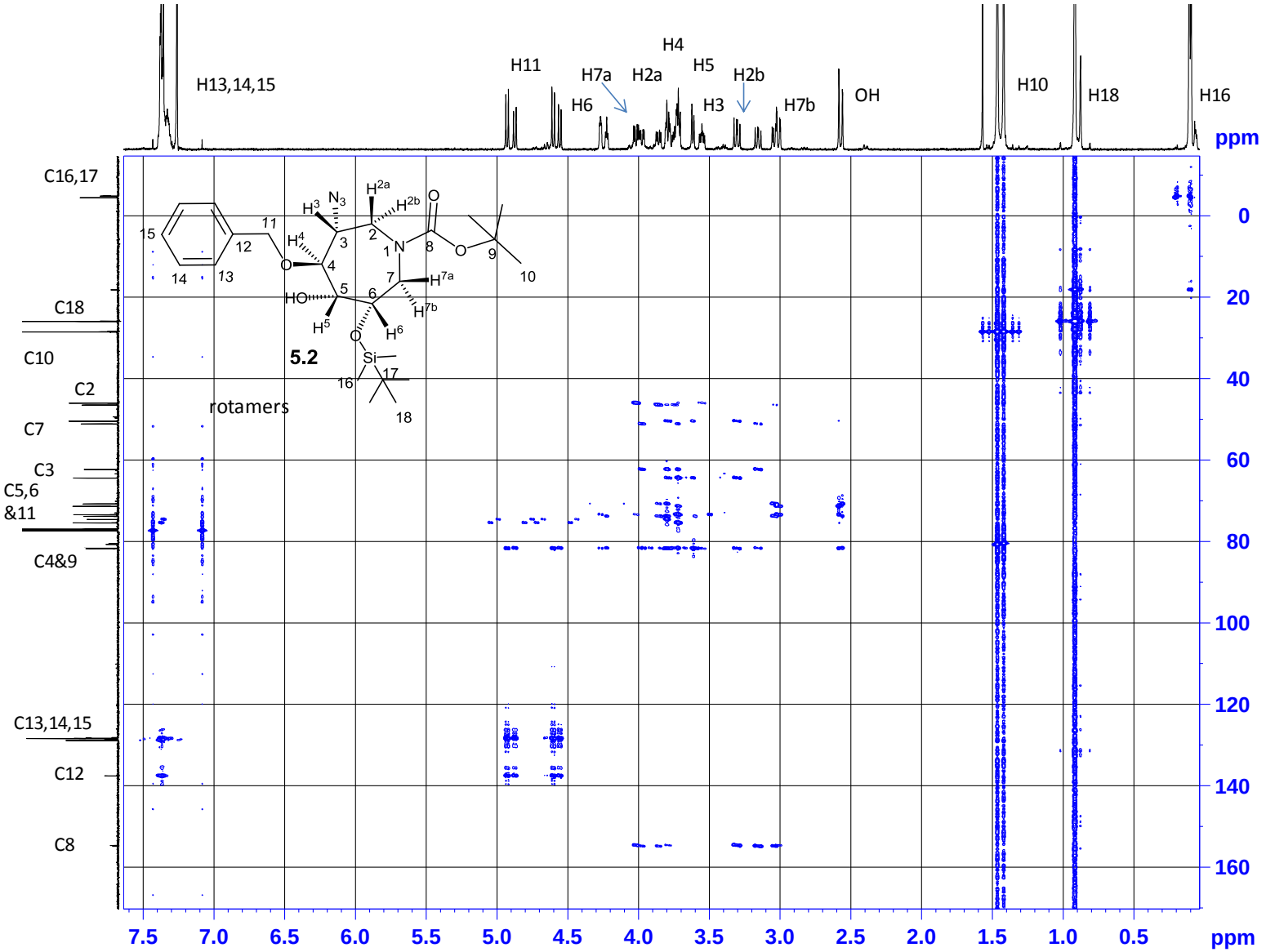

H3',4',5'
H1'a&b
H5
H6&3
H4
H2a,H7a&b
H2b
ppm
C2
C7
C3
C6
C5
&C1'
C4
C3',4',5'
C2'
5.10
7.5
7.0
6.5
6.0
5.5
5.0
4.5
4.0
3.5
3.0
2.5
ppm

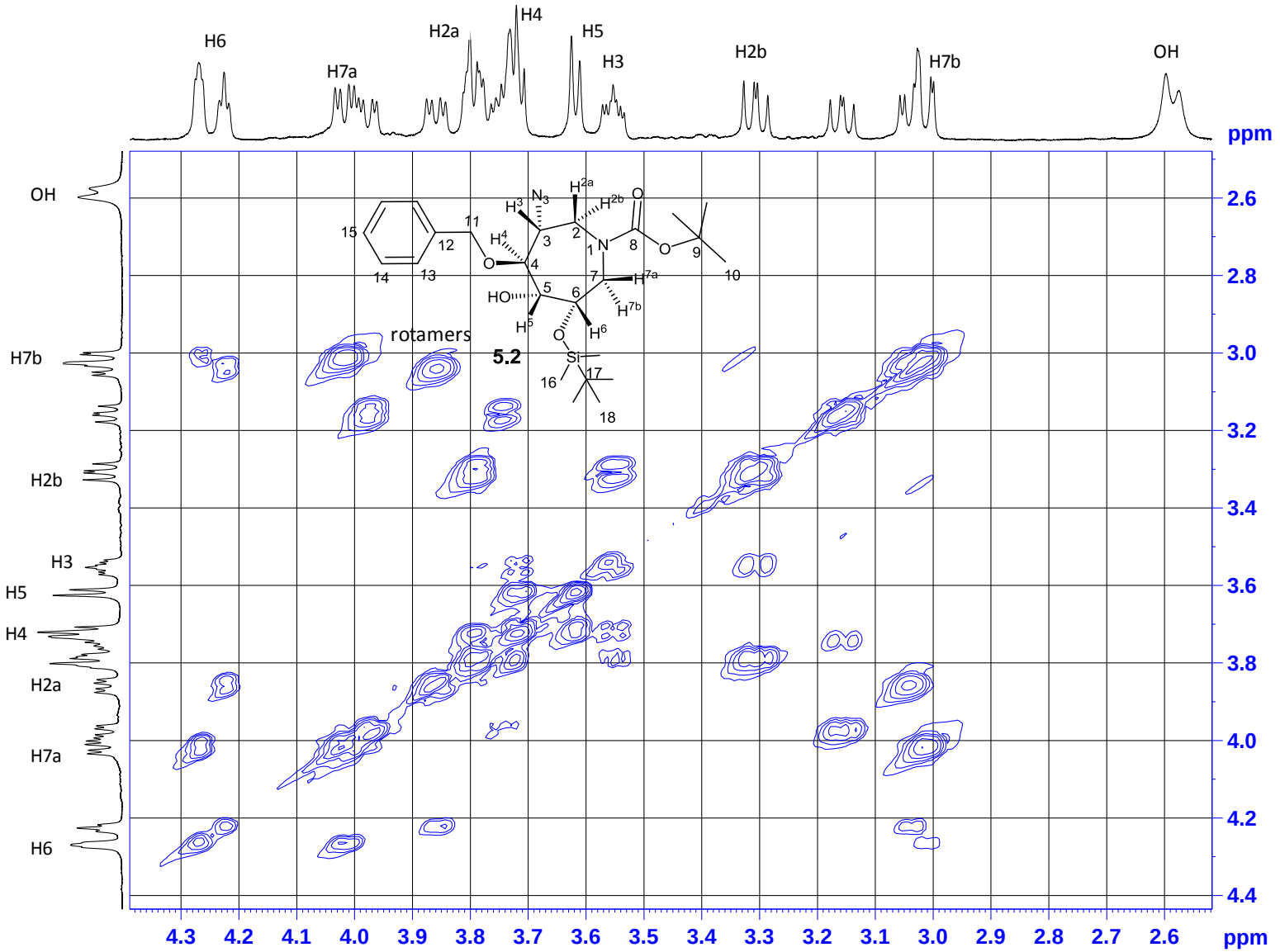

H5
H6&3
H4
H2a,H7a&b
H2b
ppm
2.4
2.6
2.8
3.0
3.2
3.4
3.6
3.8
4.0
4.2
4.4
5.10
4.4 4.3 4.2 4.1 4.0 3.9 3.8 3.7 3.6 3.5 3.4 3.3 3.2 3.1 3.0 2.9 2.8 2.7 2.6 2.5 2.4 ppm


7.37
7.36
7.26
4.94
4.92
4.88
4.86
4.61
4.59
4.57
4.55
4.27
4.27
4.23
4.03
4.02
4.01
4.00
3.85
3.84
3.80
3.72
3.62
3.33
3.31
3.18
3.16
3.03
3.02
3.00
3.00
2.59
2.58
2.56
2.56
1.57
1.46
1.42
0.92
0.92
0.11
0.11
0.10
BnO
N3
HO
TBSO
N
Boc
5.2
rotamers
Current Data Parameters
NAME Compound 10_re
EXPNO 1
PROCNO 1
F2 - Acquisition Parameters
Date_ 20130227
Time 10.44
INSTRUM spect
PROBHD 5 mm CPTXI 1H-
PULPROG zg30
TD 32768
SOLVENT CDCl3
NS 2
DS 0
SWH 5387.931 Hz
FIDRES 0.164427 Hz
AQ 3.0409205 sec
RG 7.1
DW 92.800 usec
DE 6.00 usec
TE 298.0 K
D1 1.50000000 sec
TD0 1
======== CHANNEL f1 ========
NUC1 1H
P1 7.63 usec
PL1 1.00 dB
SFO1 600.1824166 MHz
F1 - Acquisition parameters
TD 256
SFO1 150.9229 MHz
FIDRES 93.450958 Hz
SW 158.514 ppm
FnMODE States-TPPI
F2 - Processing parameters
SI 32768
SF 600.1800150 MHz
WDW no
SSB 0
LB 0 Hz
GB 0
PC 0.50
8.0
7.5
7.0
6.5
6.0
5.5
5.0
4.5
4.0
3.5
3.0
2.5
2.0
1.5
1.0
0.5
0.0
ppm
5.46
1.00
1.05
1.02
1.29
3.14
1.20
0.75
0.44
1.04
0.97
9.49
9.82
6.32

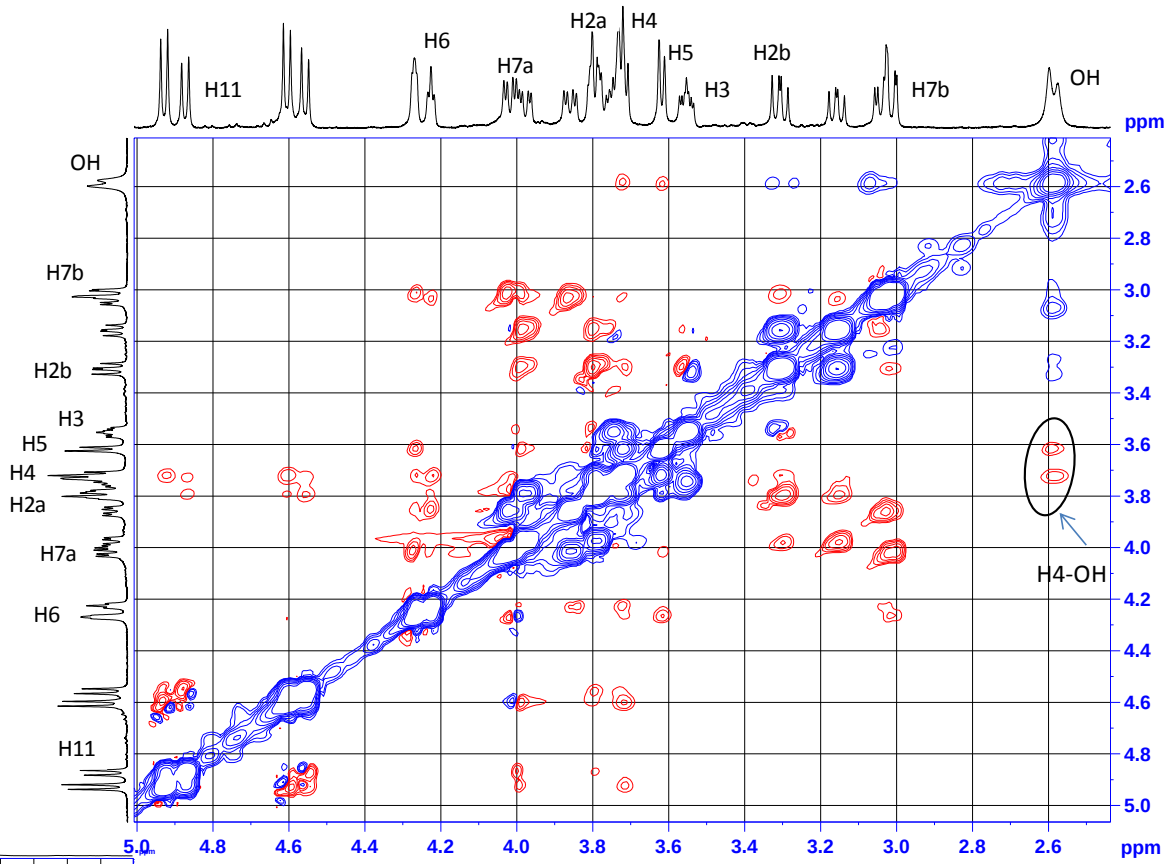

154.98
154.68
137.58
128.89
128.80
128.41
128.36
128.32
81.73
81.65
77.37
77.16
76.95
75.42
74.60
73.83
73.42
71.36
70.77
64.43
62.33
51.13
50.46
46.49
46.03
28.50
25.96
-4.45
-4.81
-4.86
Current Data Parameters
NAME Compound 10_re
EXPNO 3
PROCNO 1
F2 - Acquisition Parameters
Date_ 20130227
Time 13.22
INSTRUM spect
PROBHD 5 mm CPTXI 1H-
PULPROG udeft.txt
TD 21814
SOLVENT CDCl3
NS 6144
DS 0
SWH 42372.883 Hz
FIDRES 1.942463 Hz
AQ 0.2574552 sec
RG 32768
DW 11.800 usec
DE 6.00 usec
TE 298.0 K
D1 1.50000000 sec
D11 0.03000000 sec
d12 0.00002000 sec
D20 0.10000000 sec
DELTA 1.47000003 sec
DELTA2 0.26047519 sec
TAU 0.00302000 sec
TD0 1
======== CHANNEL f1 ========
NUC1 13C
P1 10.43 usec
P12 2000.00 usec
P26 500.00 usec
PL1 -2.50 dB
SFO1 150.9319817 MHz
SP2 5.29 dB
SP8 4.75 dB
SPNAM2 Crp60comp.4
SPNAM8 Crp60,0.5,20.1
SPOAL2 0.500
SPOAL8 0.500
SPOFFS2 0 Hz
SPOFFS8 0 Hz
======== CHANNEL f2 ========
CPDPRG2 waltz64
NUC2 1H
PCPD2 80.00 usec
PL2 1.00 dB
PL12 18.89 dB
SFO2 600.1830000 MHz
F1 - Acquisition parameters
TD 256
SFO1 150.932 MHz
FIDRES 93.450958 Hz
SW 158.505 ppm
FnMODE States-TPPI
F2 - Processing parameters
SI 262144
SF 150.9153618 MHz
WDW GM
SSB 0
LB -1.00 Hz
GB 0.01
PC 0.02
BnO
N3
HO
TBSO
N
Boc
5.2
rotamers
160 150 140 130 120 110 100 90 80 70 60 50 40 30 20 10 0 ppm

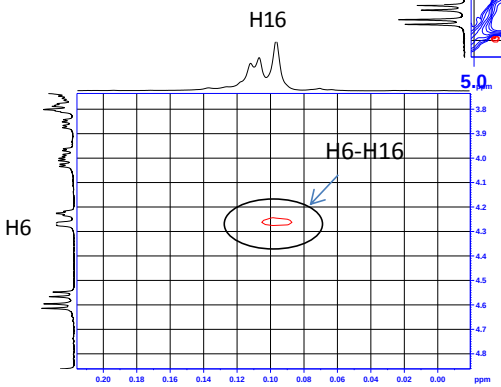

H13,14,15
H11
H7a
H2a
H4
H5
H2b
H6
H3
H7b
OH
H10
H18
H16
ppm
C16,17
C18
C10
C2
C7
C3
C5,6
&11
C4&9
C13,14,15
C12
C8
5.2
rotamers
0
20
40
60
80
100
120
140
160
7.5
7.0
6.5
6.0
5.5
5.0
4.5
4.0
3.5
3.0
2.5
2.0
1.5
1.0
0.5
ppm

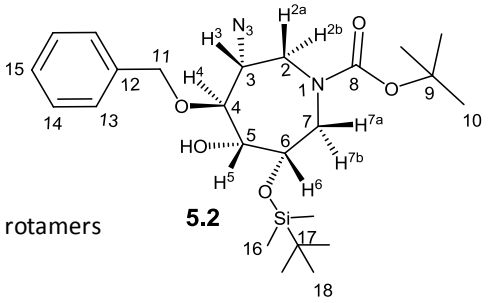

H13,14,15
H11
H6
H7a
H2a
H4
H5
H3
H2b
H7b
OH
H10
H18
H16
ppm
C16,17
C18
C10
C2
C7
C3
C5,6
&11
C4&9
C13,14,15
C12
C8
5.2
rotamers
0
20
40
60
80
100
120
140
160
7.5
7.0
6.5
6.0
5.5
5.0
4.5
4.0
3.5
3.0
2.5
2.0
1.5
1.0
0.5
ppm


H6
H7a
H2a
H4
H5
H3
H2b
H7b
OH
ppm
rotamers
5.2
4.3 4.2 4.1 4.0 3.9 3.8 3.7 3.6 3.5 3.4 3.3 3.2 3.1 3.0 2.9 2.8 2.7 2.6 ppm
2.6 2.8 3.0 3.2 3.4 3.6 3.8 4.0 4.2 4.4

C6 regiochemistry of OTBS
Is evidenced by NOE
of H4 to OH and
H6 to H16.

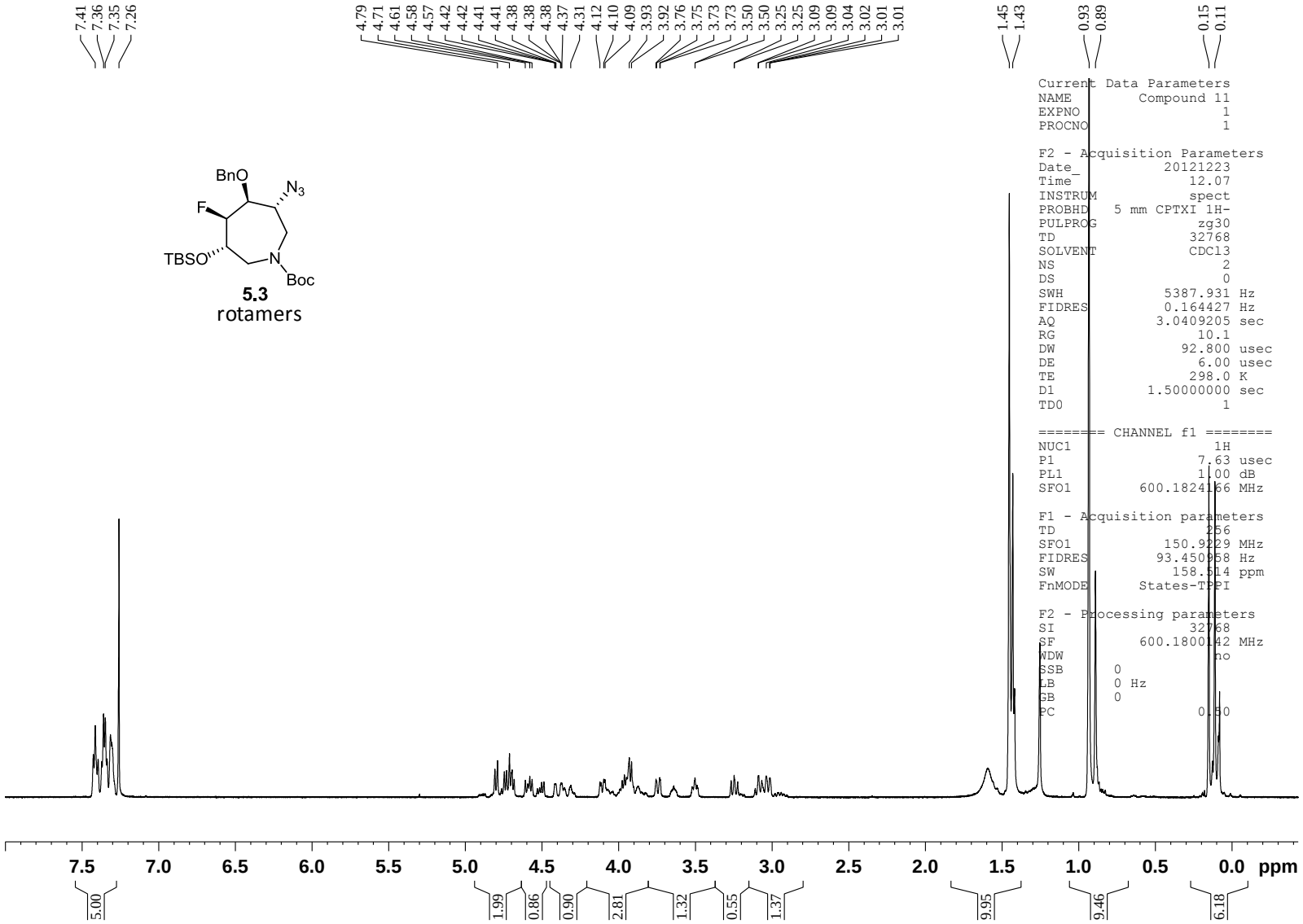


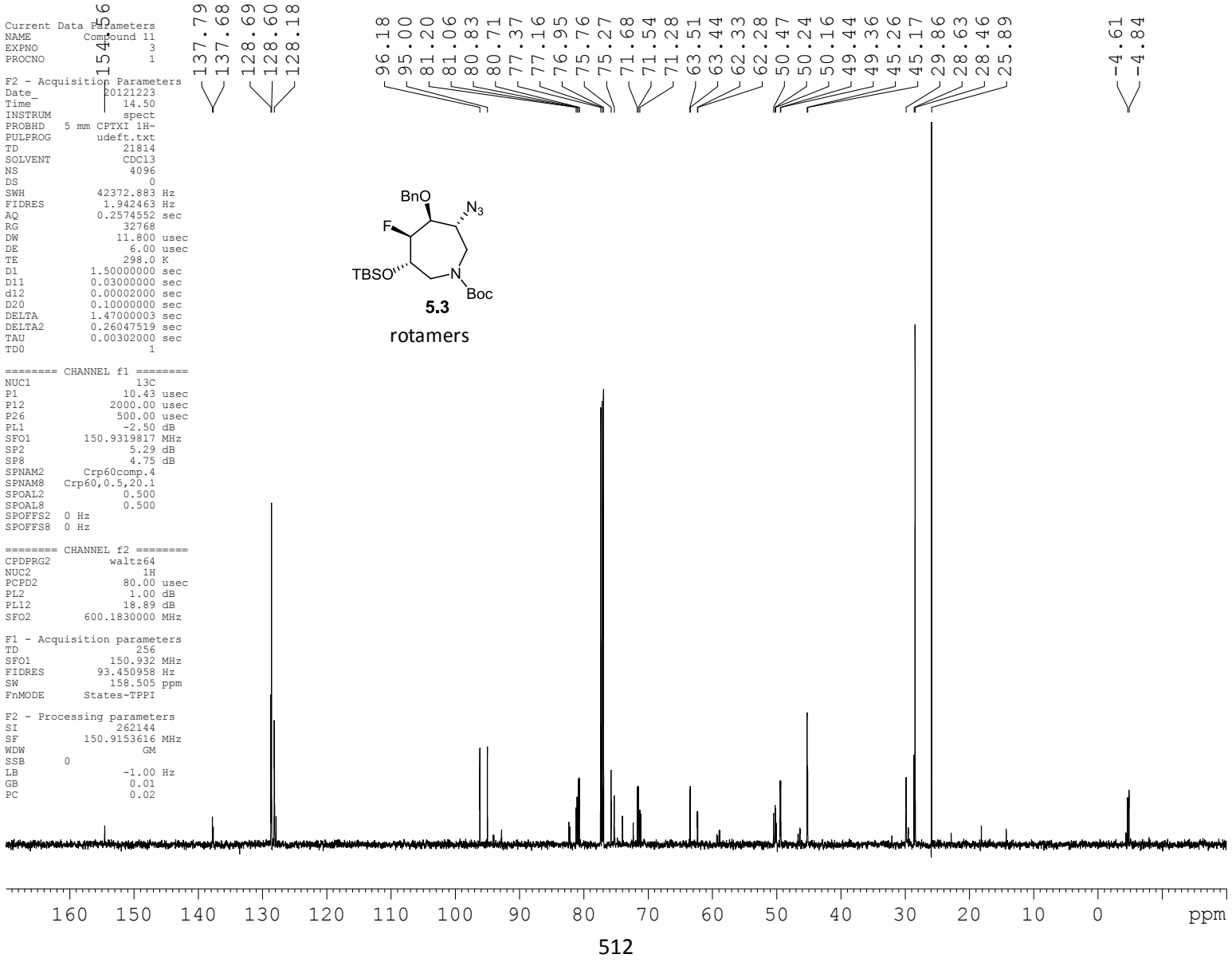


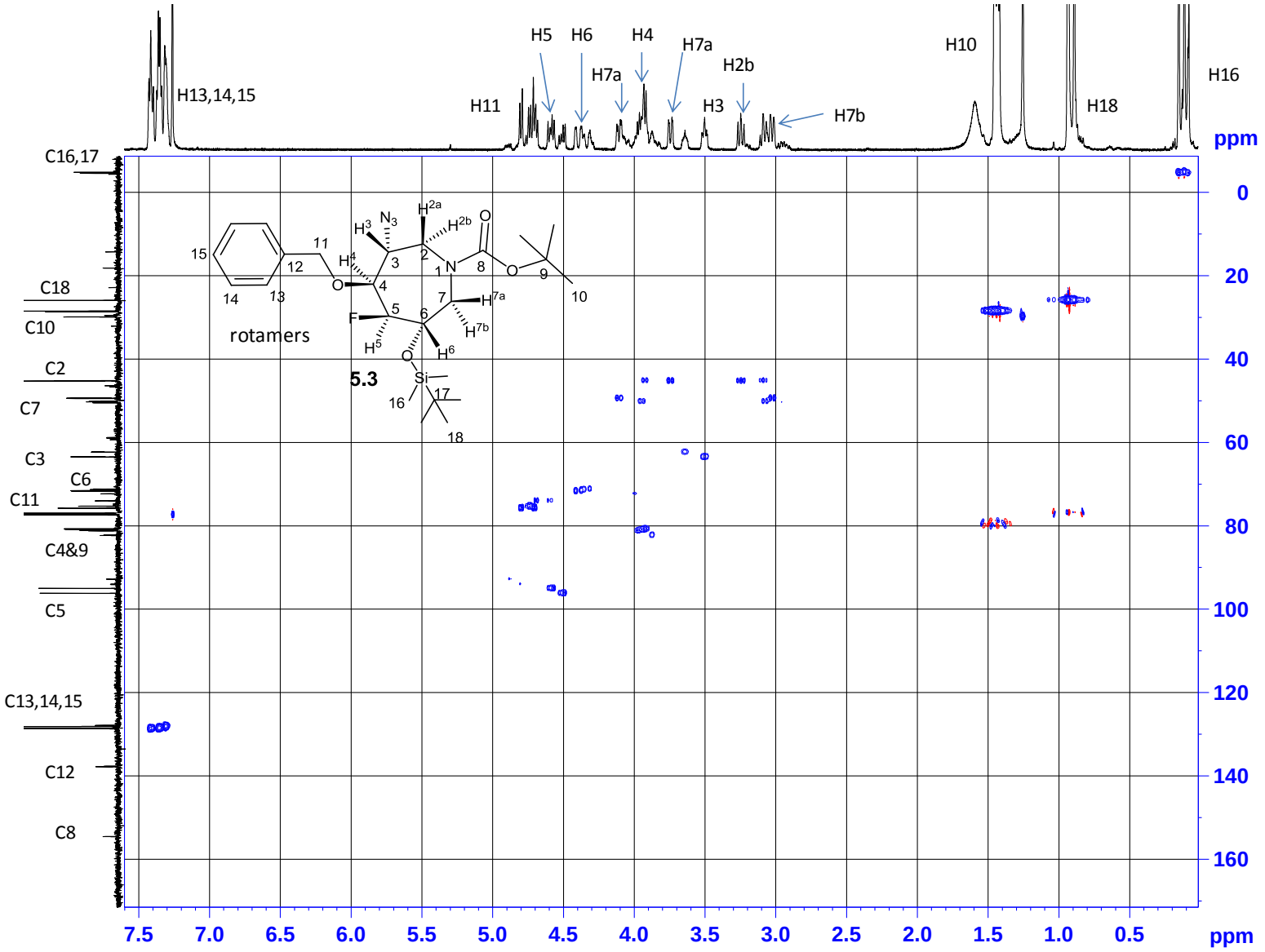


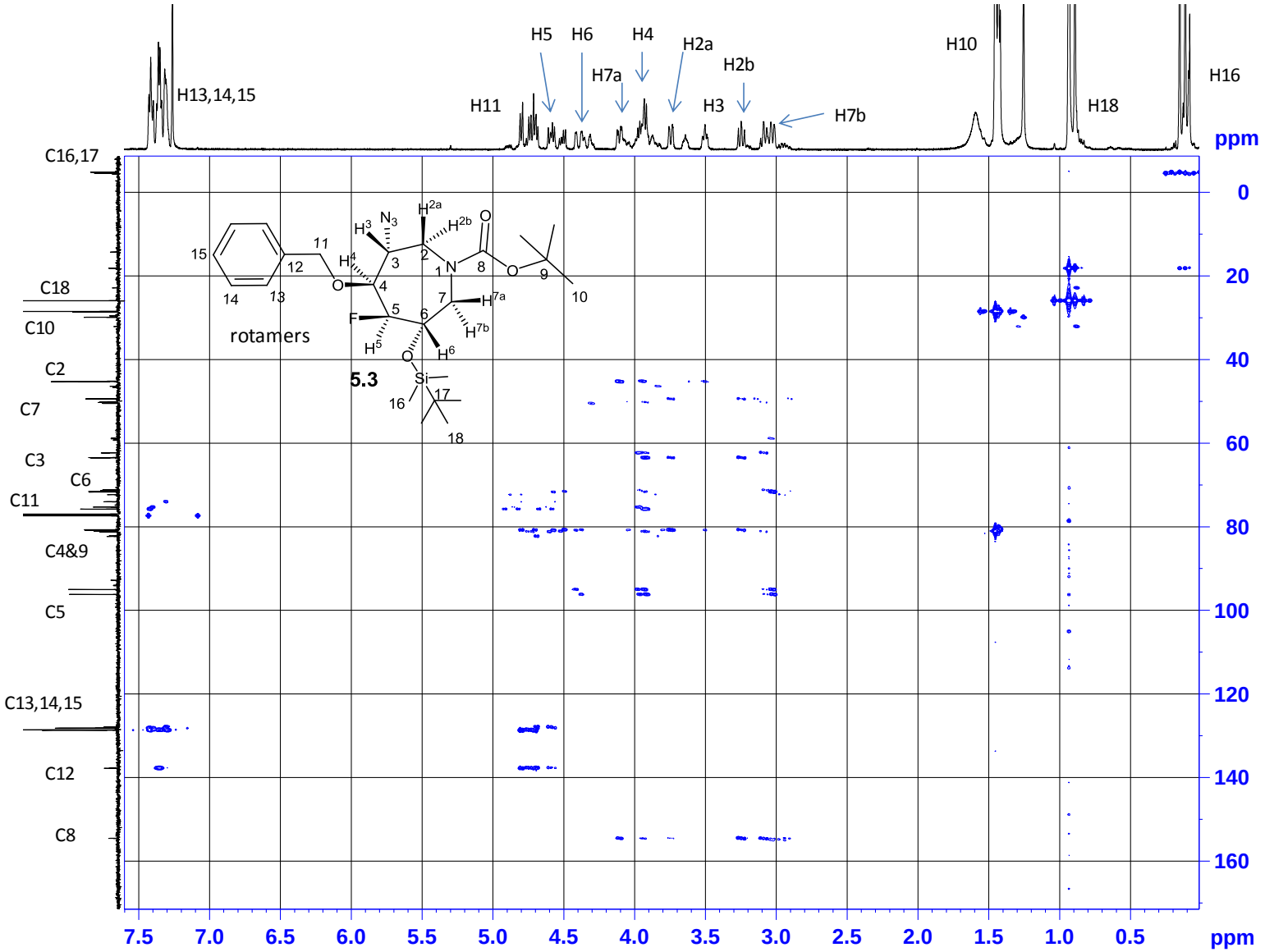
rotamers

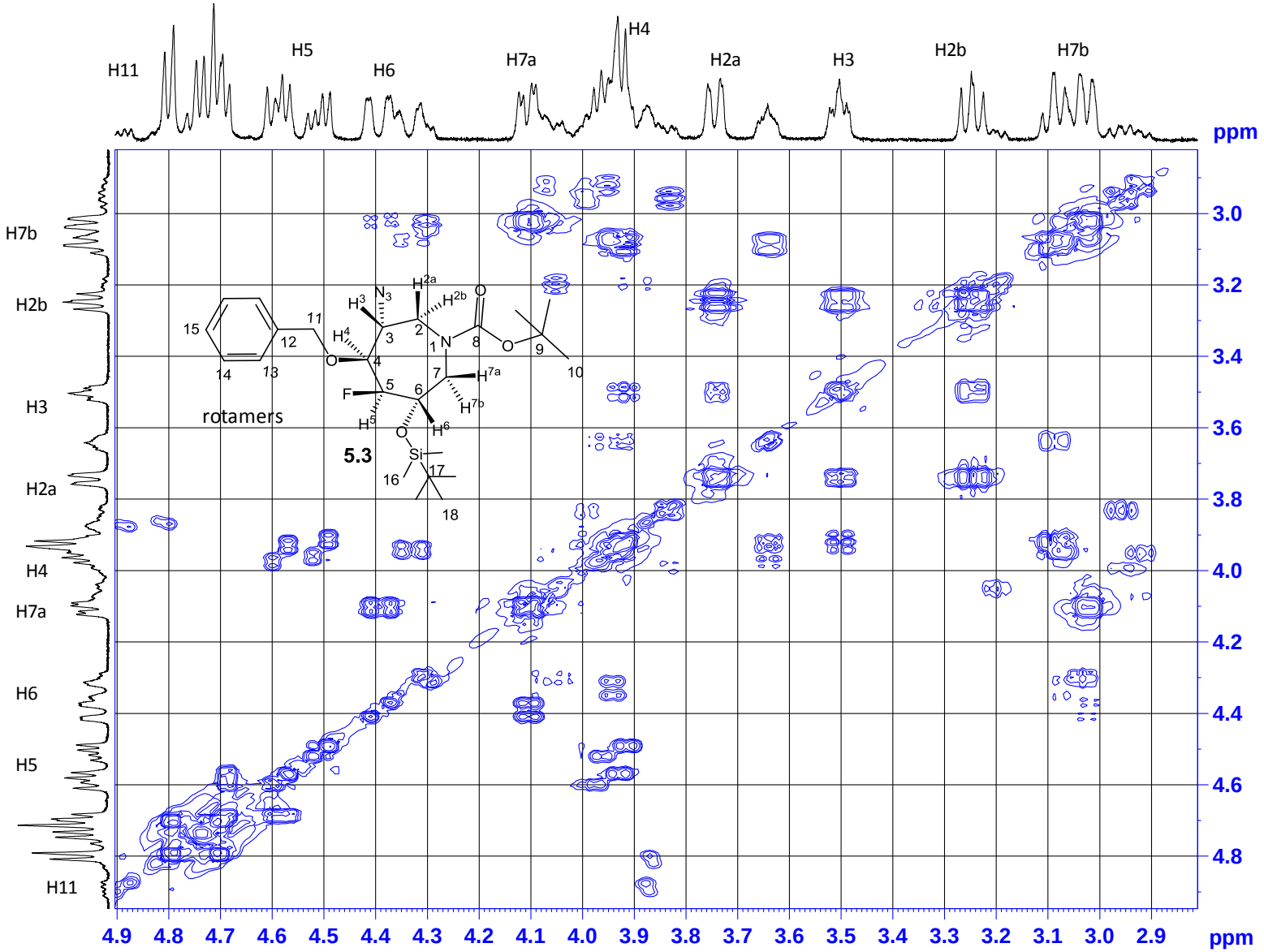
5.2

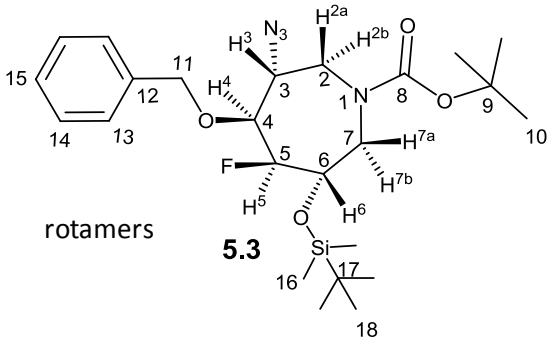

7.41
7.36
7.35
7.26
4.79
4.71
4.61
4.58
4.57
4.42
4.42
4.41
4.41
4.38
4.38
4.38
4.37
4.31
4.12
4.10
4.09
3.93
3.92
3.76
3.75
3.73
3.73
3.50
3.50
3.25
3.25
3.09
3.09
3.04
3.02
3.01
3.01
1.45
1.43
0.93
0.89
0.15
0.11
BnO
N3
F
TBSO
N
Boc
5.3
rotamers
Current Data Parameters
NAME Compound 11
EXPNO 1
PROCNO 1
F2 - Acquisition Parameters
Date_ 20121223
Time 12.07
INSTRUM spect
PROBHD 5 mm CPTXI 1H-
PULPROG zg30
TD 32768
SOLVENT CDCl3
NS 2
DS 0
SWH 5387.931 Hz
FIDRES 0.164427 Hz
AQ 3.0409205 sec
RG 10.1
DW 92.800 usec
DE 6.00 usec
TE 298.0 K
D1 1.50000000 sec
TD0 1
======== CHANNEL f1 ========
NUC1 1H
P1 7.63 usec
PL1 1.00 dB
SFO1 600.1824166 MHz
F1 - Acquisition parameters
TD 256
SFO1 150.9229 MHz
FIDRES 93.450958 Hz
SW 158.514 ppm
FnMODE States-TPPI
F2 - Processing parameters
SI 32768
SF 600.1800142 MHz
WDW no
SSB 0
LB 0 Hz
GB 0
PC 0.50
7.5
7.0
6.5
6.0
5.5
5.0
4.5
4.0
3.5
3.0
2.5
2.0
1.5
1.0
0.5
0.0
ppm
5.00
1.99
0.86
0.90
2.81
1.32
0.55
1.37
9.95
9.46
6.18

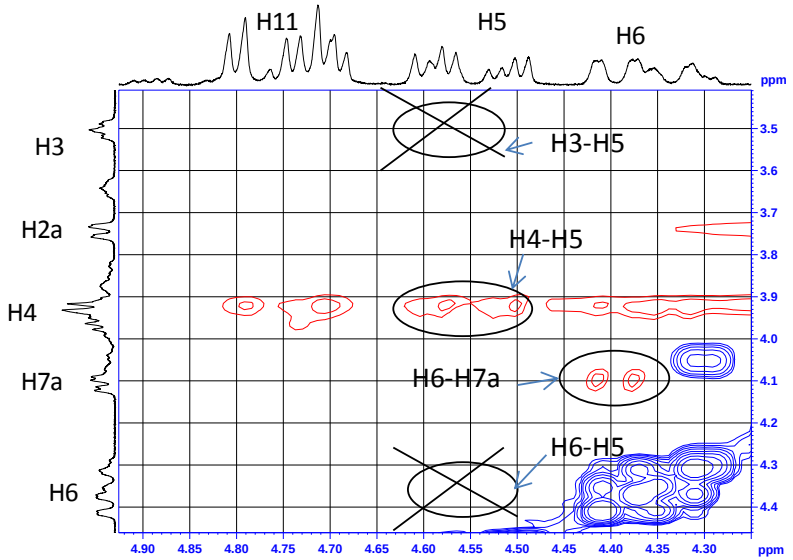

154.46
137.79
137.68
128.69
128.60
128.18
96.18
95.00
81.20
81.06
80.83
80.71
77.37
77.16
76.95
75.76
75.27
71.68
71.54
71.28
63.51
63.44
62.33
62.28
50.47
50.24
50.16
49.44
49.36
45.26
45.17
29.86
28.63
28.46
25.89
-4.61
-4.84
Current Data Parameters
NAME Compound 11
EXPNO 3
PROCNO 1
F2 - Acquisition Parameters
Date_ 20121223
Time_ 14.50
INSTRUM spect
PROBHD 5 mm CPTXI 1H-
PULPROG udeft.txt
TD 21814
SOLVENT CDCl3
NS 4096
DS 0
SWH 42372.883 Hz
FIDRES 1.942463 Hz
AQ 0.2574552 sec
RG 32768
DW 11.800 usec
DE 6.00 usec
TE 298.0 K
D1 1.50000000 sec
D11 0.03000000 sec
d12 0.00002000 sec
D20 0.10000000 sec
DELTA 1.47000003 sec
DELTA2 0.26047519 sec
TAU 0.00302000 sec
TD0 1
======== CHANNEL f1 ========
NUC1 13C
P1 10.43 usec
P12 2000.00 usec
P26 500.00 usec
PL1 -2.50 dB
SFO1 150.9319817 MHz
SP2 5.29 dB
SP8 4.75 dB
SPNAM2 Crp60comp.4
SPNAM8 Crp60,0.5,20.1
SPOAL2 0.500
SPOAL8 0.500
SPOFFS2 0 Hz
SPOFFS8 0 Hz
======== CHANNEL f2 ========
CPDPRG2 waltz64
NUC2 1H
PCPD2 80.00 usec
PL2 1.00 dB
PL12 18.89 dB
SFO2 600.1830000 MHz
F1 - Acquisition parameters
TD 256
SFO1 150.932 MHz
FIDRES 93.450958 Hz
SW 158.505 ppm
FnMODE States-TPPI
F2 - Processing parameters
SI 262144
SF 150.9153616 MHz
WDW GM
SSB 0
LB -1.00 Hz
GB 0.01
PC 0.02
BnO
N3
F
TBSO
N
Boc
5.3
rotamers
160
150
140
130
120
110
100
90
80
70
60
50
40
30
20
10
0
ppm


H13,14,15
H11
H5
H6
H7a
H4
H7a
H3
H2b
H7b
H10
H18
H16
ppm
C16,17
C18
C10
C2
C7
C3
C6
C11
C4&9
C5
C13,14,15
C12
C8
rotamers
5.3
0
20
40
60
80
100
120
140
160
7.5
7.0
6.5
6.0
5.5
5.0
4.5
4.0
3.5
3.0
2.5
2.0
1.5
1.0
0.5
ppm

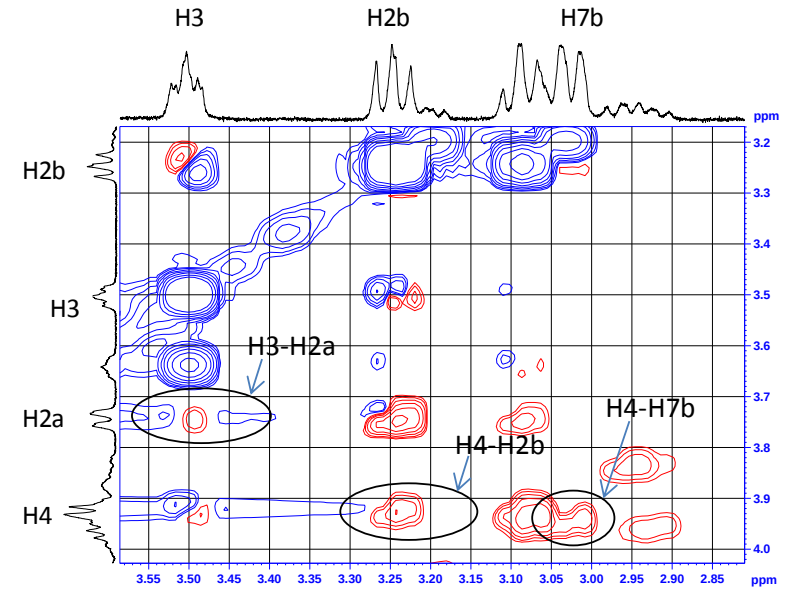

H13,14,15
H11
H5
H6
H7a
H4
H2a
H3
H2b
H7b
H10
H18
H16
ppm
C16,17
C18
C10
C2
C7
C3
C6
C11
C4&9
C5
C13,14,15
C12
C8
rotamers
5.3
7.5
7.0
6.5
6.0
5.5
5.0
4.5
4.0
3.5
3.0
2.5
2.0
1.5
1.0
0.5
ppm

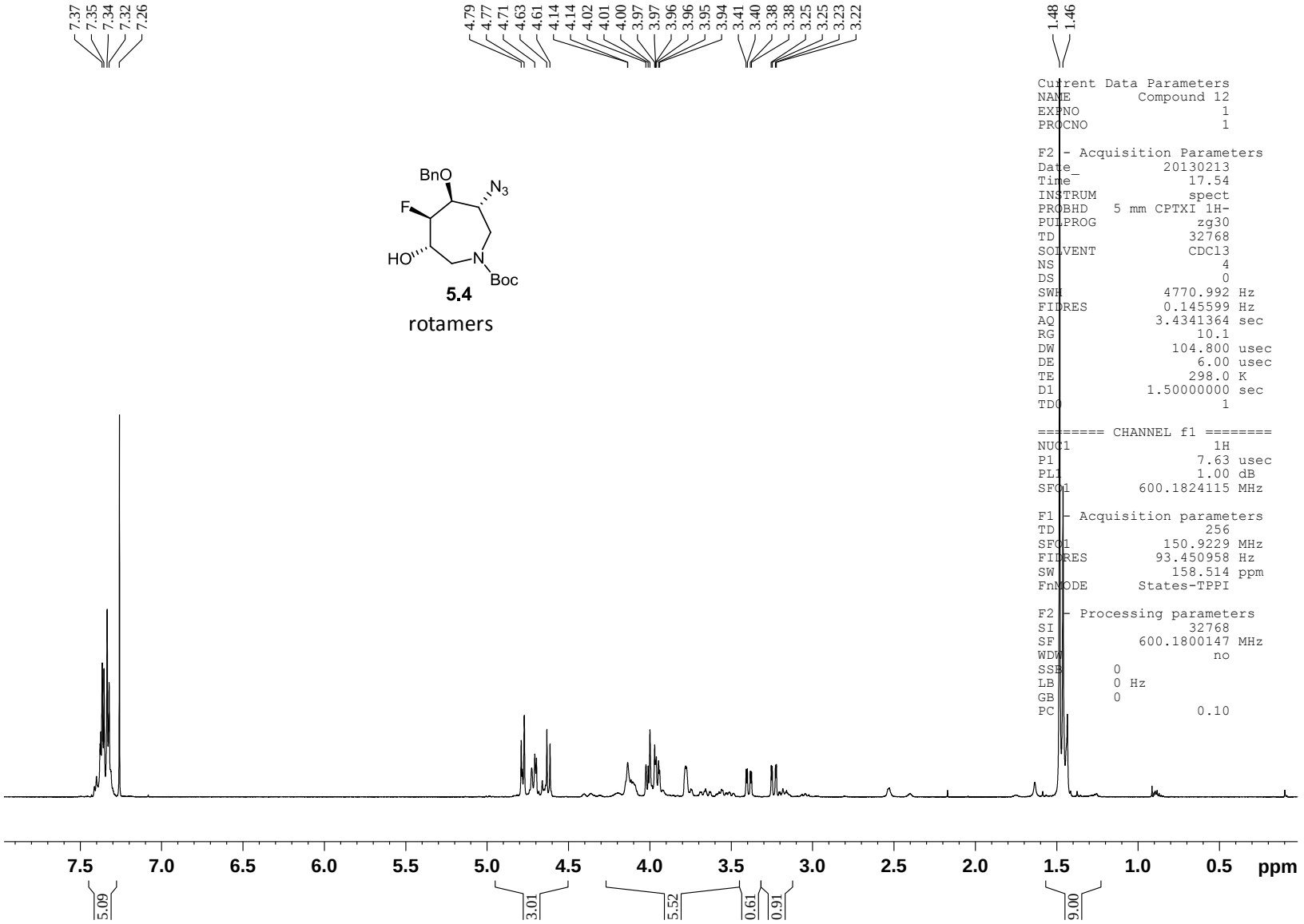

H11
H5
H6
H7a
H4
H2a
H3
H2b
H7b
ppm
rotamers
5.3
4.9 4.8 4.7 4.6 4.5 4.4 4.3 4.2 4.1 4.0 3.9 3.8 3.7 3.6 3.5 3.4 3.3 3.2 3.1 3.0 2.9
3.0 3.2 3.4 3.6 3.8 4.0 4.2 4.4 4.6 4.8

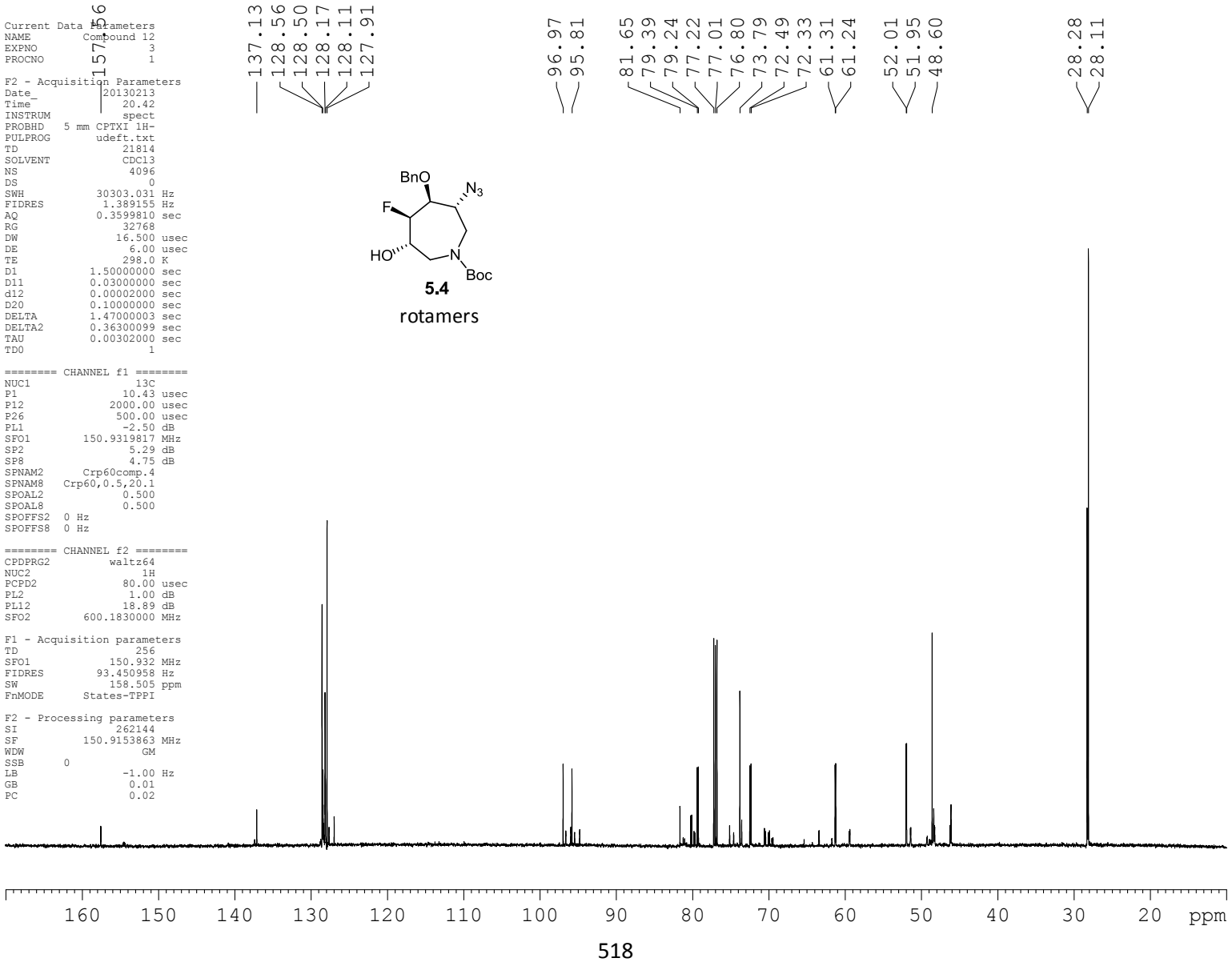


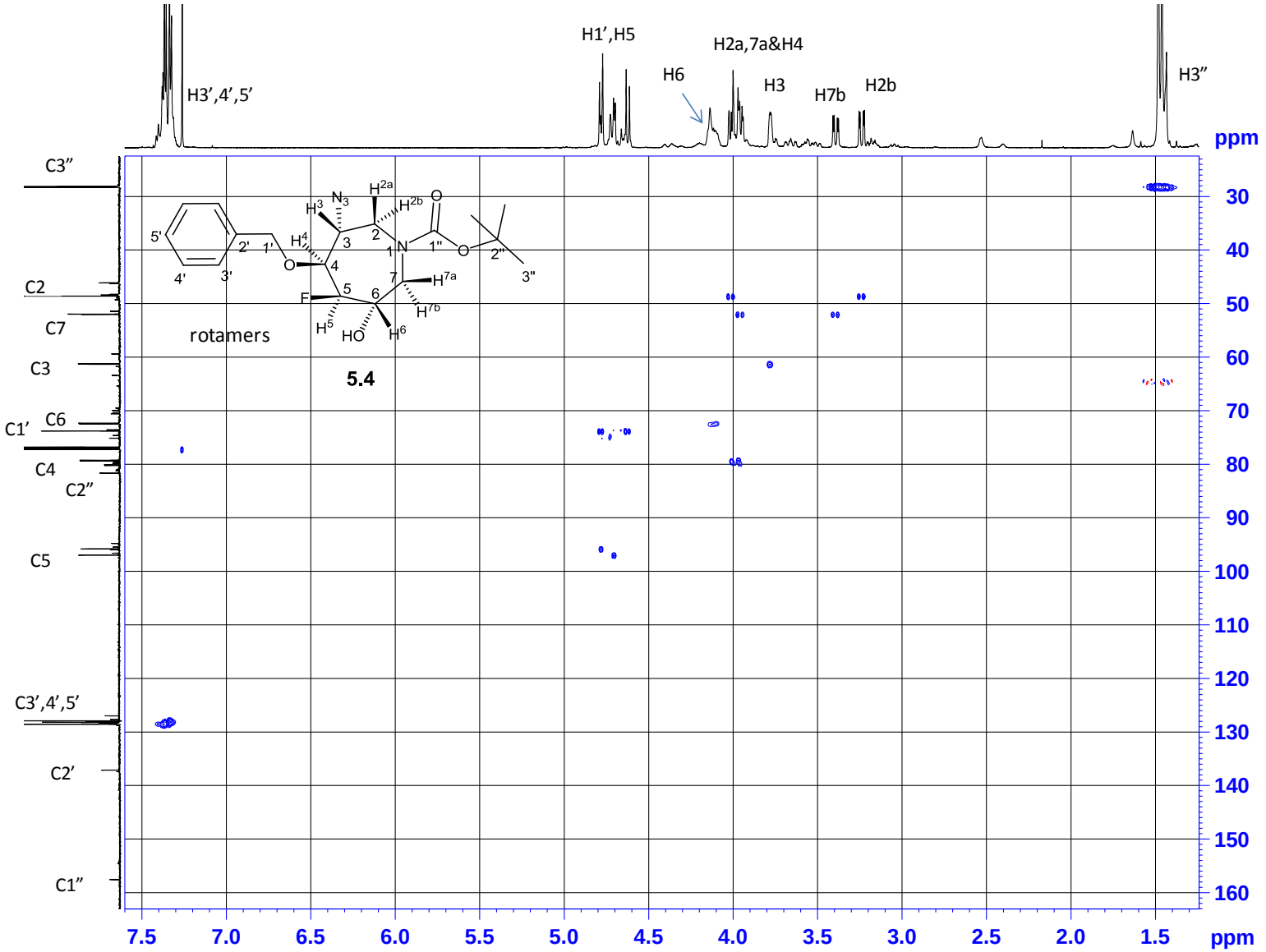


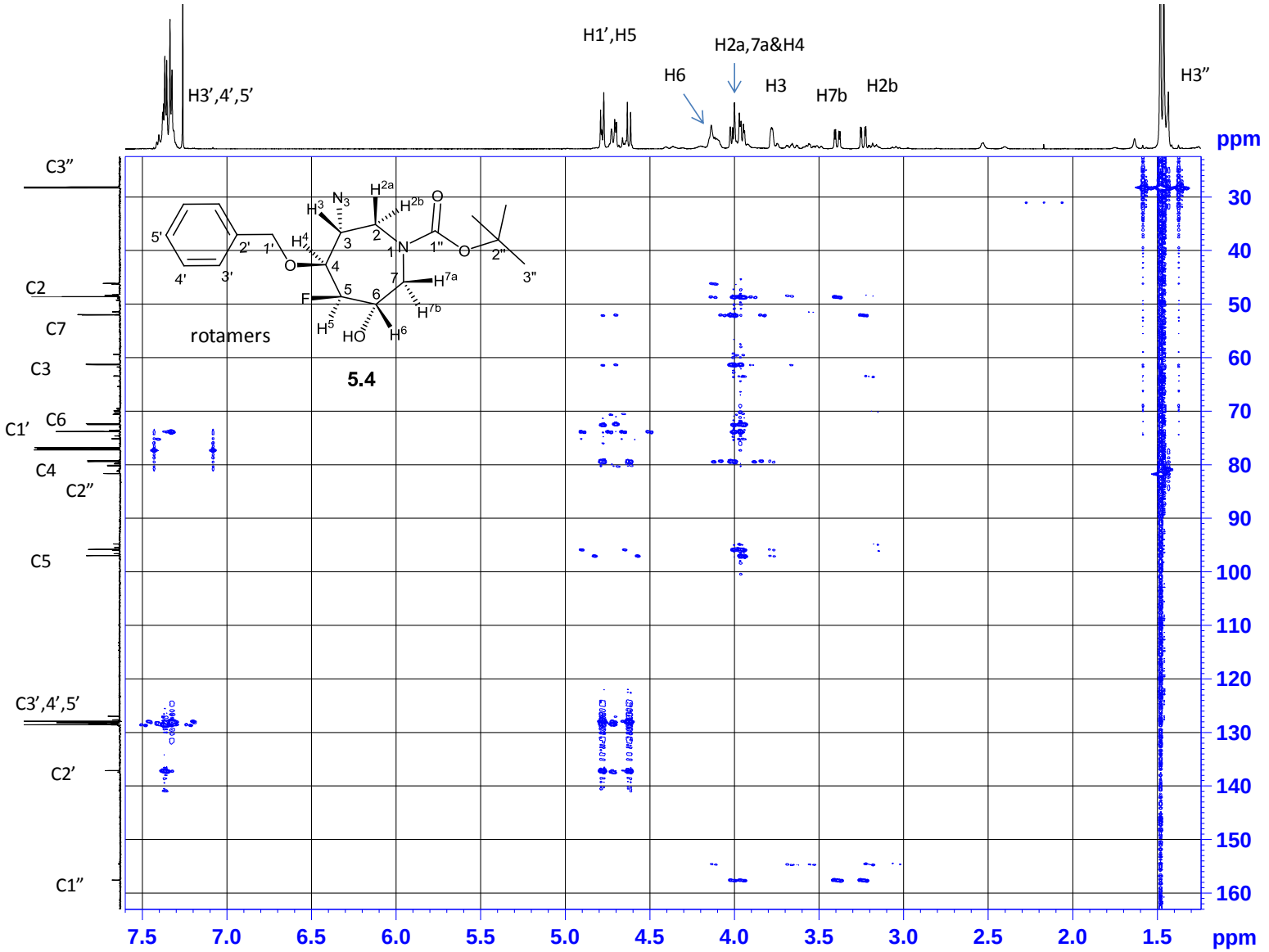
- C3, C4 and C6 are stereocentres with known stereochemistry and stereochemistry at C5 is of interest.
- H5 shows big NOE to H4 while no measureable NOE to H6 and H3 suggests H5 is *cis* to H4.
- H7a shows NOE to H6 while H7b shows NOE to H4 meaning H7a is *trans* and H7b is *cis* to H4.
- Moreover, H2b shows NOE to H4 and H3 shows NOE to H2a suggesting H2a is *trans* and H2b is *cis* to H4.
- Based on NOE data the absolute C5 stereochemistry is *S* (*cis* to C4 OBn).

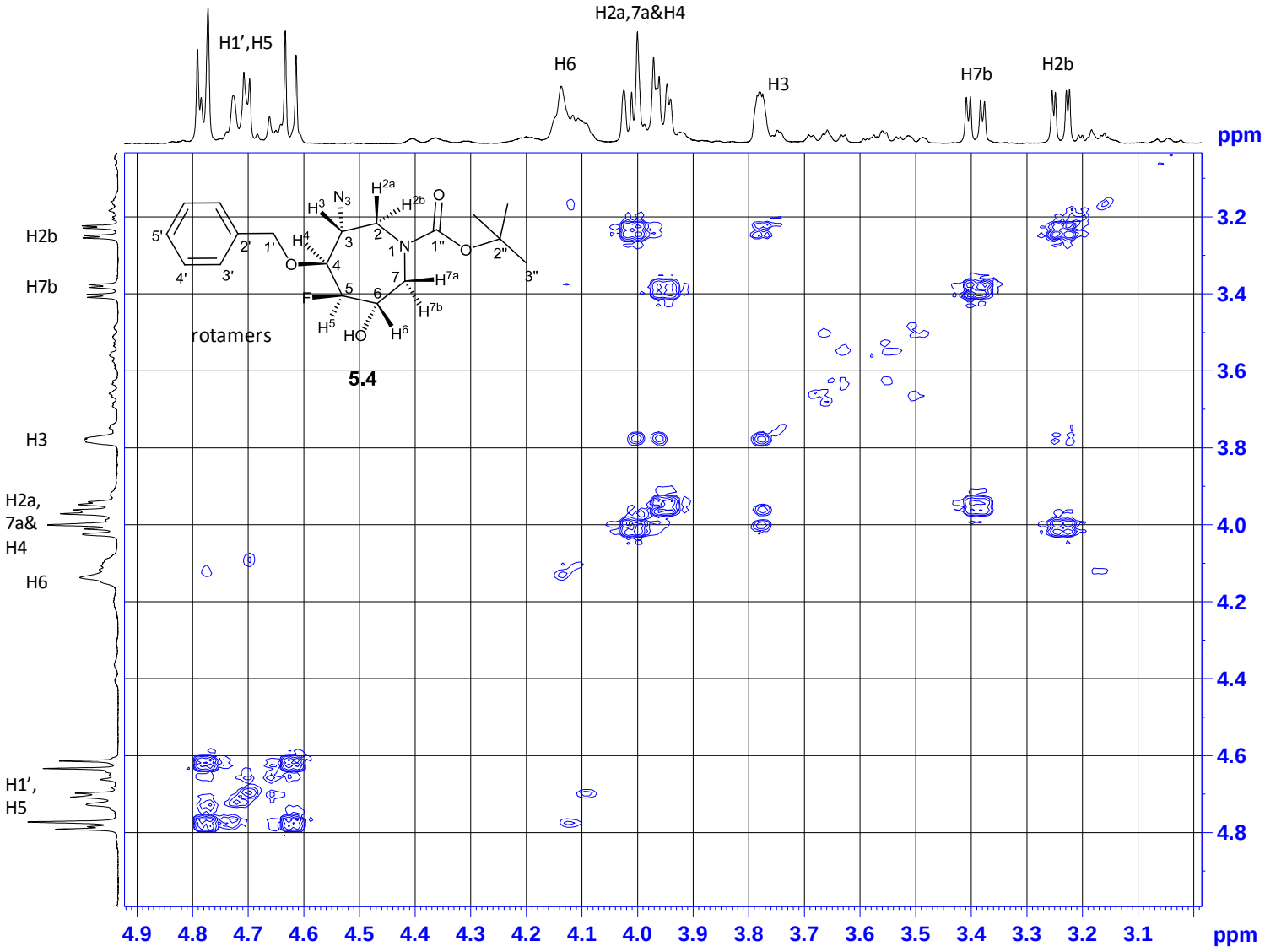


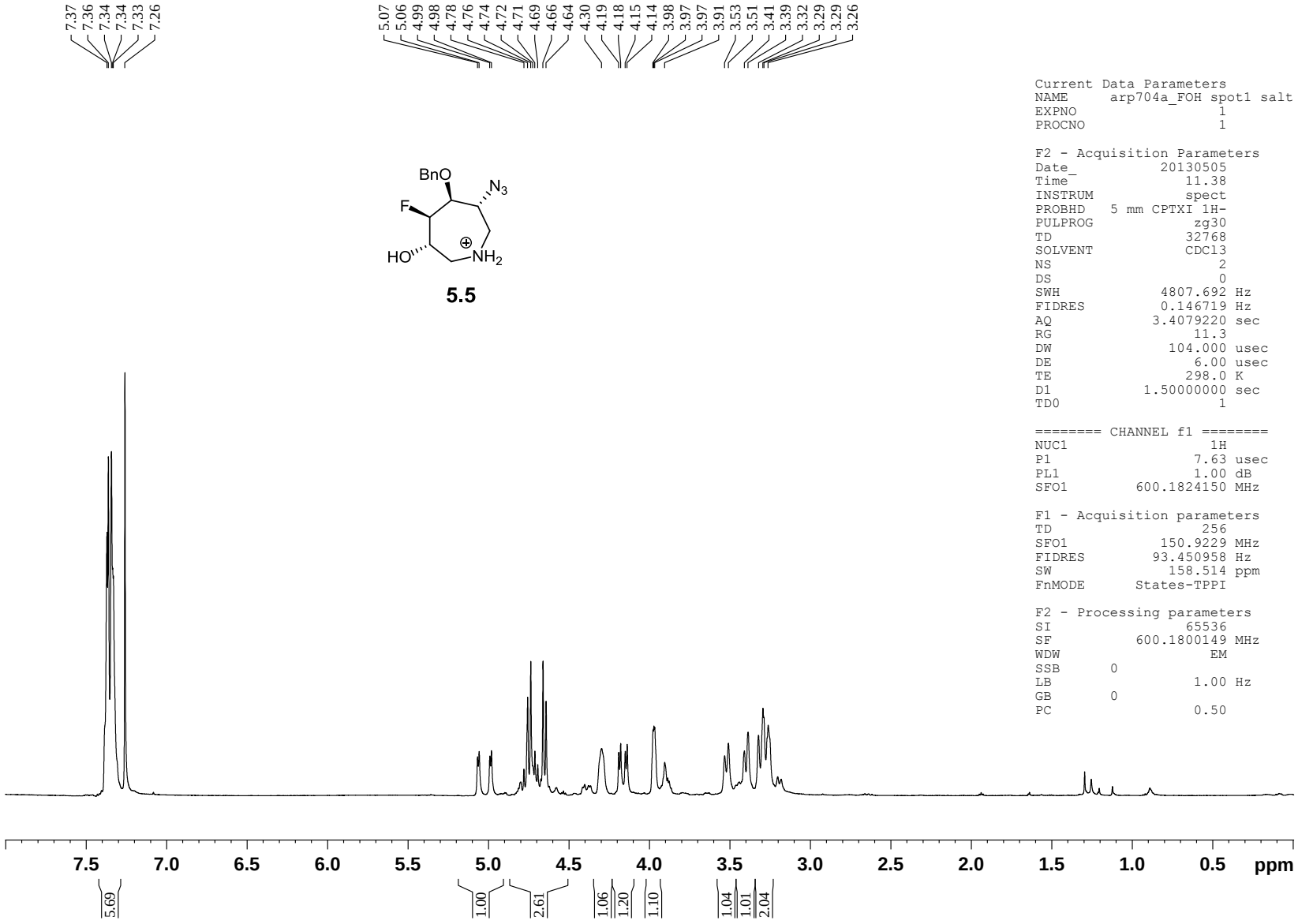

7.37
7.35
7.34
7.32
7.26
4.79
4.77
4.71
4.63
4.61
4.14
4.14
4.02
4.01
4.00
3.97
3.97
3.96
3.96
3.95
3.94
3.41
3.40
3.38
3.38
3.25
3.25
3.23
3.22
1.48
1.46
BnO
N3
F
HO
N
Boc
5.4
rotamers
Current Data Parameters
NAME Compound 12
EXPNO 1
PROCNO 1
F2 - Acquisition Parameters
Date_ 20130213
Time 17.54
INSTRUM spect
PROBHD 5 mm CPTXI 1H-
PULPROG zg30
TD 32768
SOLVENT CDCl3
NS 4
DS 0
SWH 4770.992 Hz
FIDRES 0.145599 Hz
AQ 3.4341364 sec
RG 10.1
DW 104.800 usec
DE 6.00 usec
TE 298.0 K
D1 1.50000000 sec
TD0 1
======== CHANNEL f1 ========
NUC1 1H
P1 7.63 usec
PL1 1.00 dB
SFO1 600.1824115 MHz
F1 - Acquisition parameters
TD 256
SFO1 150.9229 MHz
FIDRES 93.450958 Hz
SW 158.514 ppm
FnMODE States-TPPI
F2 - Processing parameters
SI 32768
SF 600.1800147 MHz
WDW no
SSB 0
LB 0 Hz
GB 0
PC 0.10
7.5
7.0
6.5
6.0
5.5
5.0
4.5
4.0
3.5
3.0
2.5
2.0
1.5
1.0
0.5
ppm
5.09
3.01
5.52
0.61
0.91
9.00

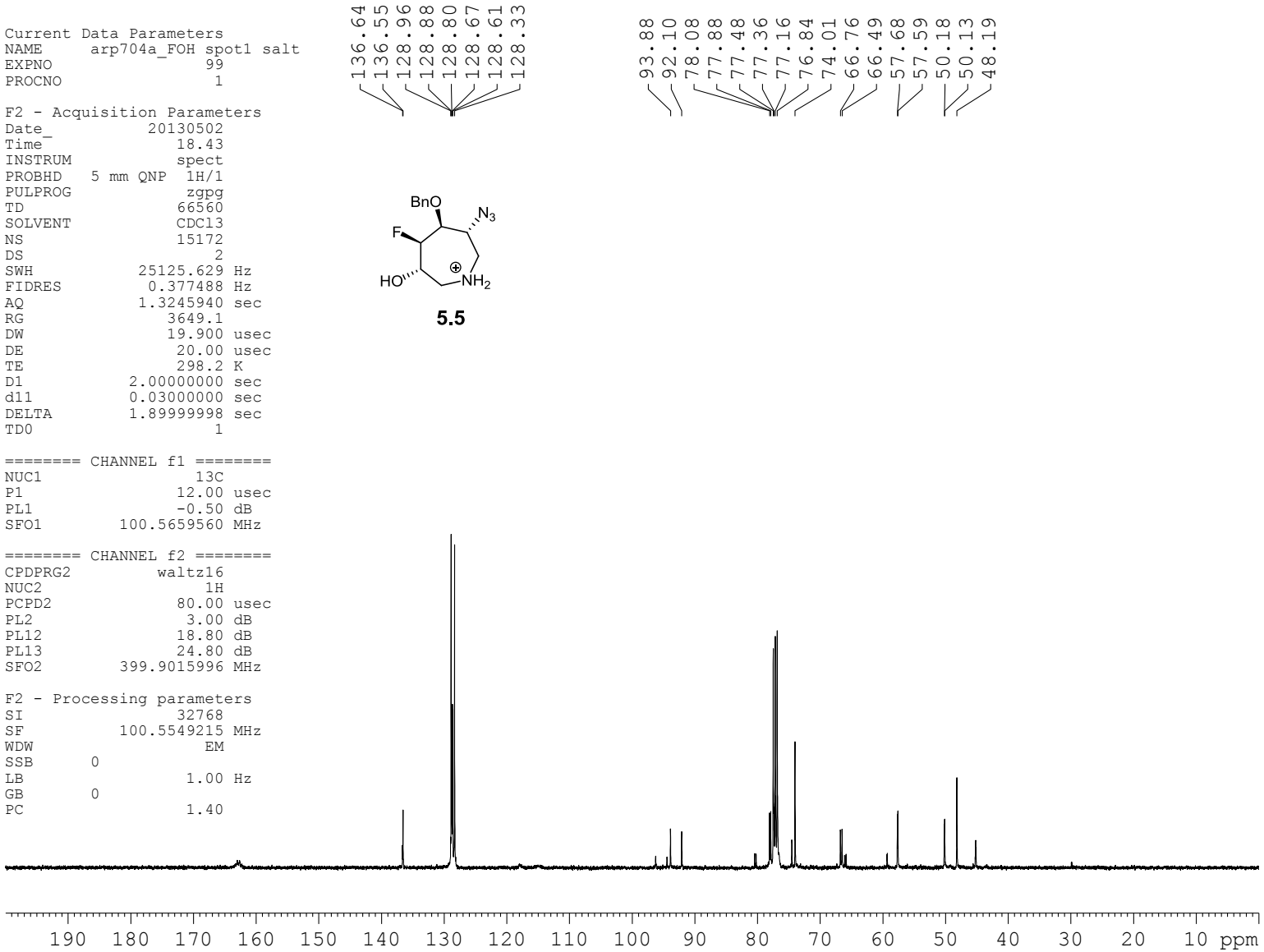

157.16
137.13
128.56
128.50
128.17
128.11
127.91
96.97
95.81
81.65
79.39
79.24
77.22
77.01
76.80
73.79
72.49
72.33
61.31
61.24
52.01
51.95
48.60
28.28
28.11
Current Data Parameters
NAME Compound 12
EXPNO 3
PROCNO 1
F2 - Acquisition Parameters
Date_ 20130213
Time_ 20.42
INSTRUM spect
PROBHD 5 mm CPTXI 1H-
PULPROG udeft.txt
TD 21814
SOLVENT CDCl3
NS 4096
DS 0
SWH 30303.031 Hz
FIDRES 1.389155 Hz
AQ 0.3599810 sec
RG 32768
DW 16.500 usec
DE 6.00 usec
TE 298.0 K
D1 1.50000000 sec
D11 0.03000000 sec
d12 0.00002000 sec
D20 0.10000000 sec
DELTA 1.47000003 sec
DELTA2 0.36300099 sec
TAU 0.00302000 sec
TD0 1
======== CHANNEL f1 ========
NUC1 13C
P1 10.43 usec
P12 2000.00 usec
P26 500.00 usec
PL1 -2.50 dB
SFO1 150.9319817 MHz
SP2 5.29 dB
SP8 4.75 dB
SPNAM2 Crp60comp.4
SPNAM8 Crp60,0.5,20.1
SPOAL2 0.500
SPOAL8 0.500
SPOFFS2 0 Hz
SPOFFS8 0 Hz
======== CHANNEL f2 ========
CPDPRG2 waltz64
NUC2 1H
PCPD2 80.00 usec
PL2 1.00 dB
PL12 18.89 dB
SFO2 600.1830000 MHz
F1 - Acquisition parameters
TD 256
SFO1 150.932 MHz
FIDRES 93.450958 Hz
SW 158.505 ppm
FnMODE States-TPPI
F2 - Processing parameters
SI 262144
SF 150.9153863 MHz
WDW GM
SSB 0
LB -1.00 Hz
GB 0.01
PC 0.02
BnO
N3
F
HO
N
Boc
5.4
rotamers
160
150
140
130
120
110
100
90
80
70
60
50
40
30
20
ppm

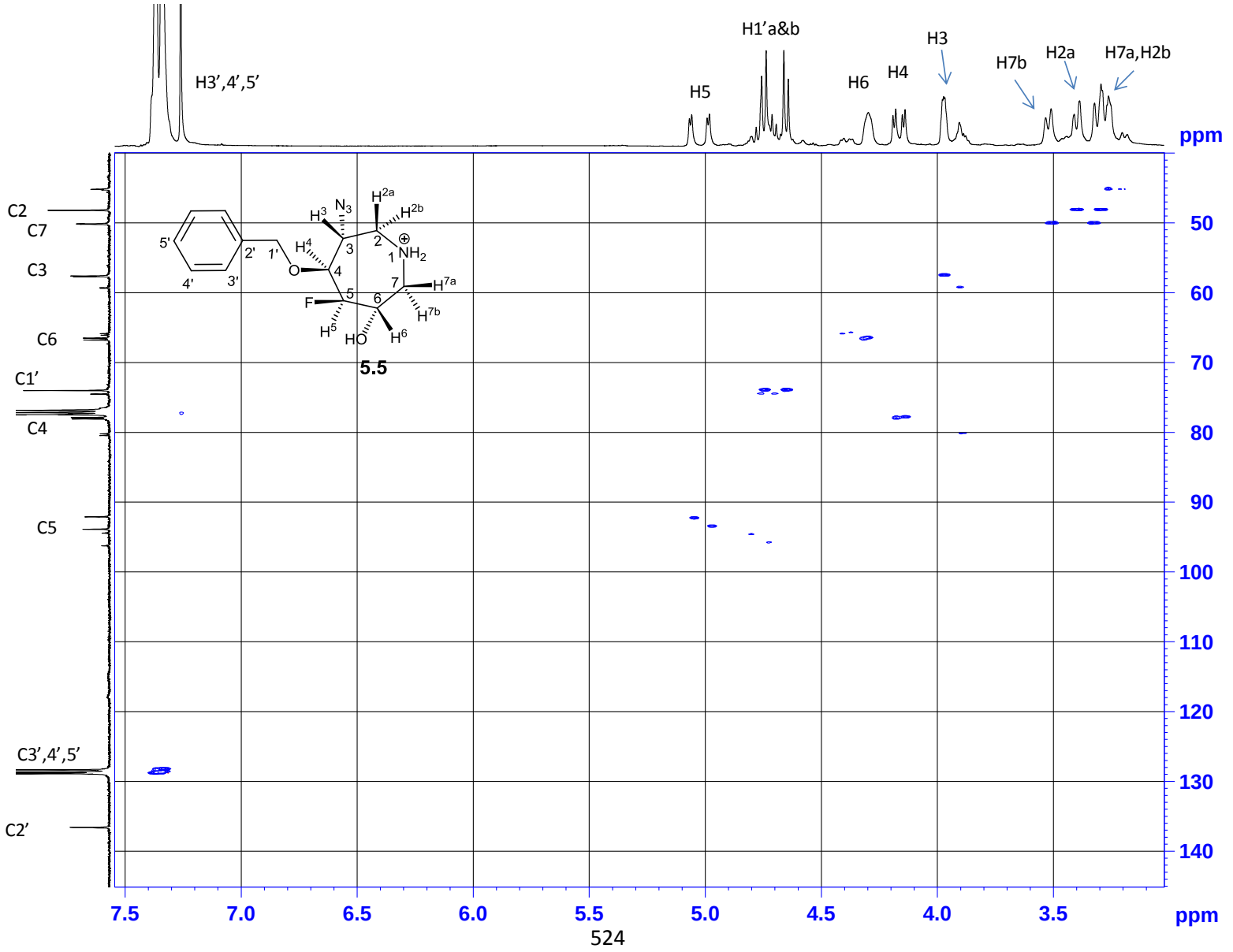

H3',4',5'
H1',H5
H6
H2a,7a&H4
H3
H7b
H2b
H3"
ppm
C3"
C2
C7
C3
C1'
C6
C4
C2"
C5
C3',4',5'
C2'
C1"
rotamers
5.4
30
40
50
60
70
80
90
100
110
120
130
140
150
160
7.5
7.0
6.5
6.0
5.5
5.0
4.5
4.0
3.5
3.0
2.5
2.0
1.5
ppm

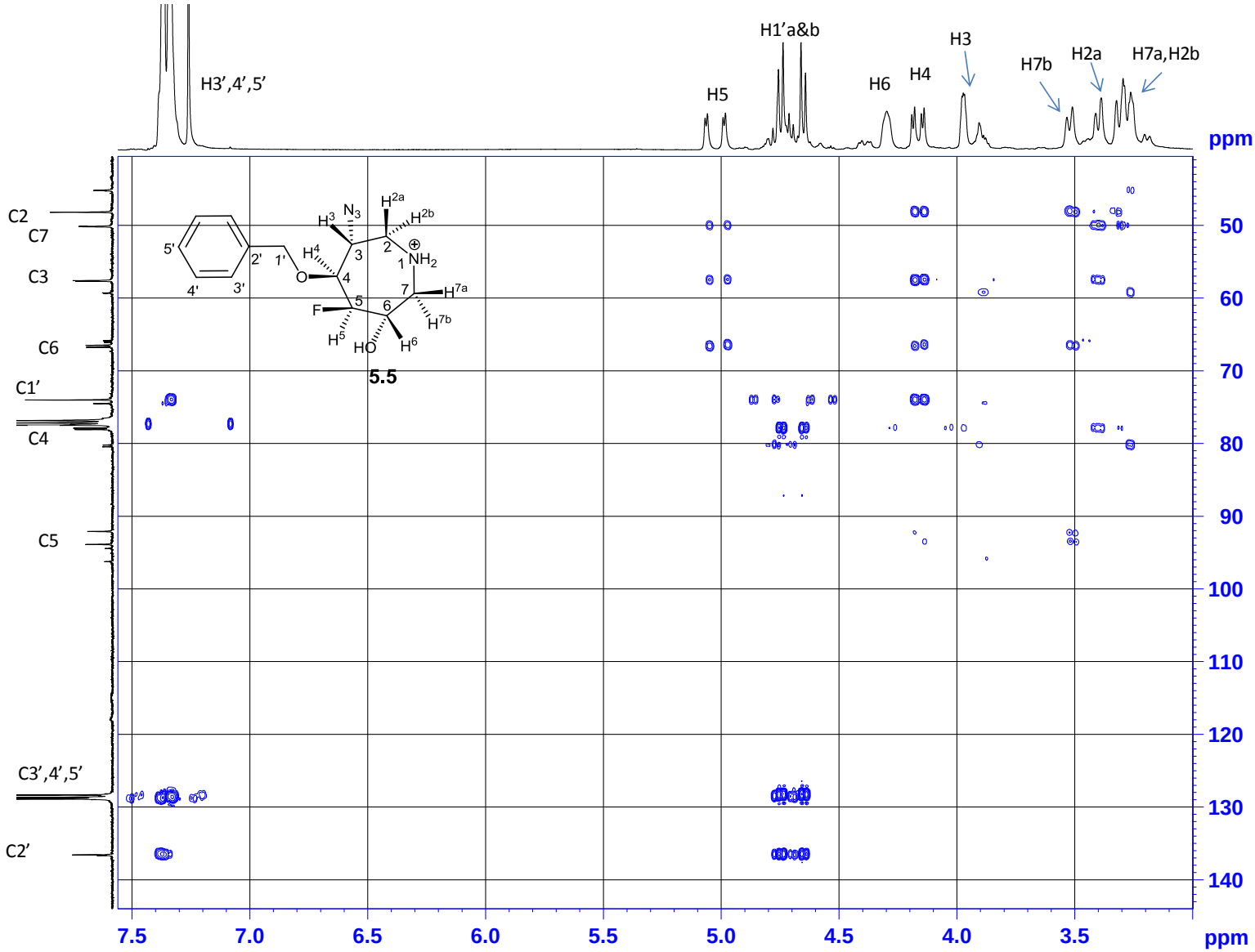

H3',4',5'
H1',H5
H6
H2a,7a&H4
H3
H7b
H2b
H3"
ppm
C3"
C2
C7
C3
C1'
C6
C4
C2"
C5
C3',4',5'
C2'
C1"
rotamers
5.4
7.5
7.0
6.5
6.0
5.5
5.0
4.5
4.0
3.5
3.0
2.5
2.0
1.5
ppm

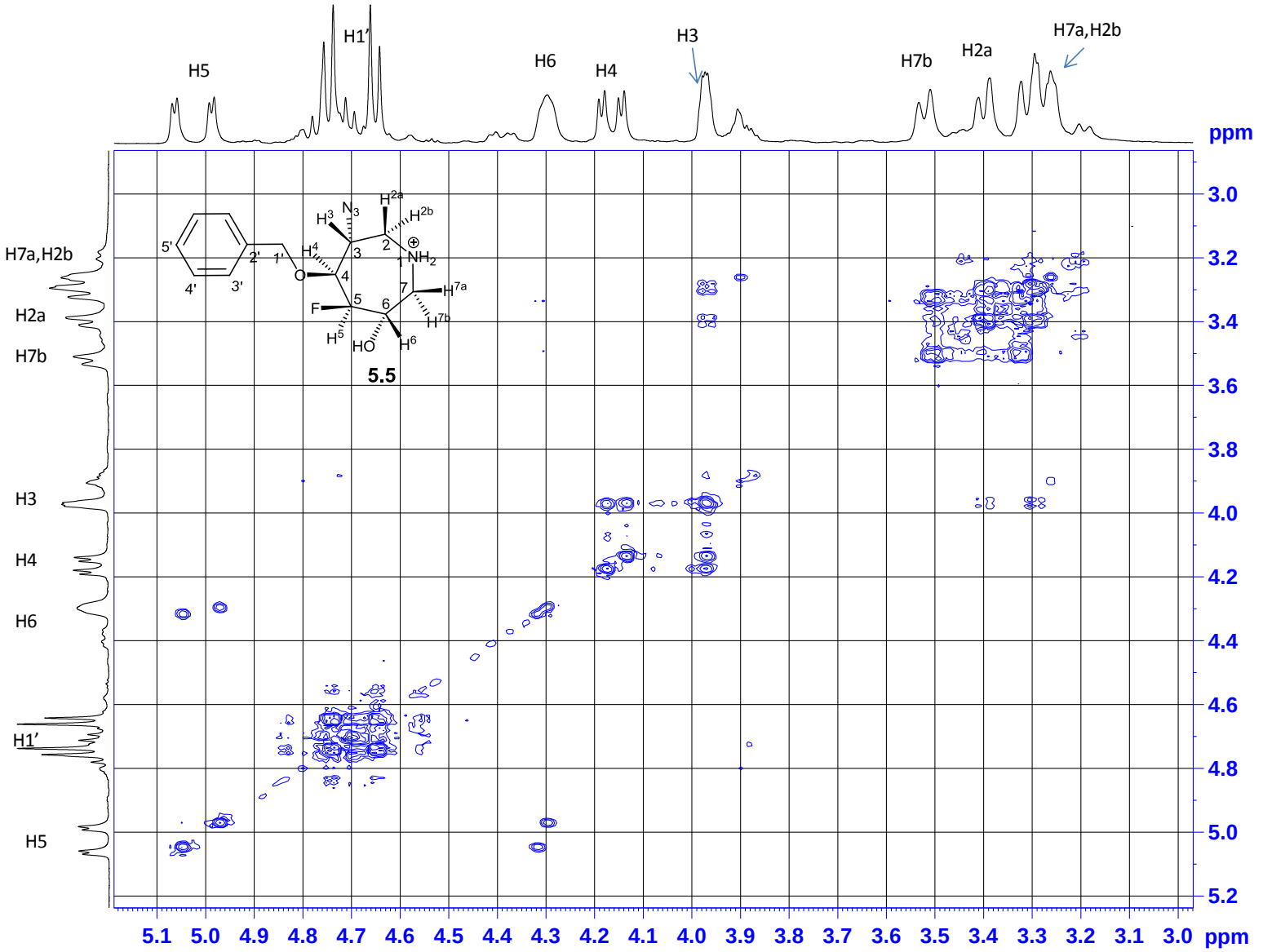

H1',H5
H6
H2a,7a&H4
H3
H7b
H2b
ppm
H2b
H7b
H3
H2a,
7a&
H4
H6
H1',
H5
rotamers
5.4
3.2
3.4
3.6
3.8
4.0
4.2
4.4
4.6
4.8
4.9 4.8 4.7 4.6 4.5 4.4 4.3 4.2 4.1 4.0 3.9 3.8 3.7 3.6 3.5 3.4 3.3 3.2 3.1
ppm

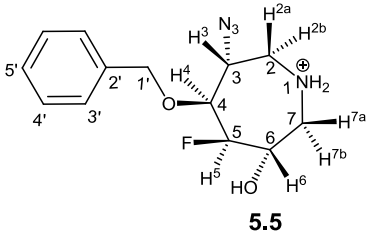

7.37
7.36
7.34
7.34
7.33
7.26
5.07
5.06
4.99
4.98
4.78
4.76
4.74
4.72
4.71
4.69
4.66
4.64
4.30
4.19
4.18
4.15
4.14
3.98
3.97
3.97
3.91
3.53
3.51
3.41
3.39
3.32
3.29
3.29
3.26
BnO
N3
F
HO
NH2
5.5
Current Data Parameters
NAME arp704a_FOH spot1 salt
EXPNO 1
PROCNO 1
F2 - Acquisition Parameters
Date_ 20130505
Time 11.38
INSTRUM spect
PROBHD 5 mm CPTXI 1H-
PULPROG zg30
TD 32768
SOLVENT CDCl3
NS 2
DS 0
SWH 4807.692 Hz
FIDRES 0.146719 Hz
AQ 3.4079220 sec
RG 11.3
DW 104.000 usec
DE 6.00 usec
TE 298.0 K
D1 1.50000000 sec
TD0 1
======== CHANNEL f1 ========
NUC1 1H
P1 7.63 usec
PL1 1.00 dB
SFO1 600.1824150 MHz
F1 - Acquisition parameters
TD 256
SFO1 150.9229 MHz
FIDRES 93.450958 Hz
SW 158.514 ppm
FnMODE States-TPPI
F2 - Processing parameters
SI 65536
SF 600.1800149 MHz
WDW EM
SSB 0
LB 1.00 Hz
GB 0
PC 0.50
7.5
7.0
6.5
6.0
5.5
5.0
4.5
4.0
3.5
3.0
2.5
2.0
1.5
1.0
0.5
ppm
5.69
1.00
2.61
1.06
1.20
1.10
1.04
1.01
2.04


Current Data Parameters
NAME arp704a_FOH spot1 salt
EXPNO 99
PROCNO 1
F2 - Acquisition Parameters
Date_ 20130502
Time 18.43
INSTRUM spect
PROBHD 5 mm QNP 1H/1
PULPROG zgpg
TD 66560
SOLVENT CDCl3
NS 15172
DS 2
SWH 25125.629 Hz
FIDRES 0.377488 Hz
AQ 1.3245940 sec
RG 3649.1
DW 19.900 usec
DE 20.00 usec
TE 298.2 K
D1 2.00000000 sec
d11 0.03000000 sec
DELTA 1.89999998 sec
TD0 1
======== CHANNEL f1 ========
NUC1 13C
P1 12.00 usec
PL1 -0.50 dB
SFO1 100.5659560 MHz
======== CHANNEL f2 ========
CPDPRG2 waltz16
NUC2 1H
PCPD2 80.00 usec
PL2 3.00 dB
PL12 18.80 dB
PL13 24.80 dB
SFO2 399.9015996 MHz
F2 - Processing parameters
SI 32768
SF 100.5549215 MHz
WDW EM
SSB 0
LB 1.00 Hz
GB 0
PC 1.40
136.64
136.55
128.96
128.88
128.80
128.67
128.61
128.33
93.88
92.10
78.08
77.88
77.48
77.36
77.16
76.84
74.01
66.76
66.49
57.68
57.59
50.18
50.13
48.19
BnO
N3
F
HO
NH2
5.5
190 180 170 160 150 140 130 120 110 100 90 80 70 60 50 40 30 20 10 ppm


H3',4',5'
H5
H1'a&b
H6
H4
H3
H7b
H2a
H7a,H2b
ppm
C2
C7
C3
C6
C1'
C4
C5
C3',4',5'
C2'
5.5
7.5
7.0
6.5
6.0
5.5
5.0
4.5
4.0
3.5
ppm

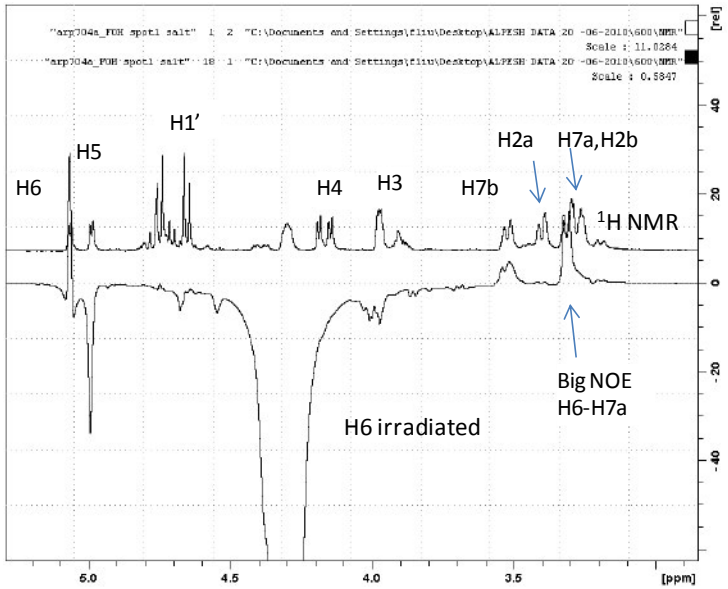

H3',4',5'
H5
H1'a&b
H6
H4
H3
H7b
H2a
H7a,H2b
ppm
C2
C7
C3
C6
C1'
C4
C5
C3',4',5'
C2'
5.5
7.5
7.0
6.5
6.0
5.5
5.0
4.5
4.0
3.5
ppm
50
60
70
80
90
100
110
120
130
140


H5
H1'
H6
H4
H3
H7b
H2a
H7a,H2b
ppm
H7a,H2b
H2a
H7b
H3
H4
H6
H1'
H5
5.5
3.0
3.2
3.4
3.6
3.8
4.0
4.2
4.4
4.6
4.8
5.0
5.2
5.1 5.0 4.9 4.8 4.7 4.6 4.5 4.4 4.3 4.2 4.1 4.0 3.9 3.8 3.7 3.6 3.5 3.4 3.3 3.2 3.1 3.0 ppm

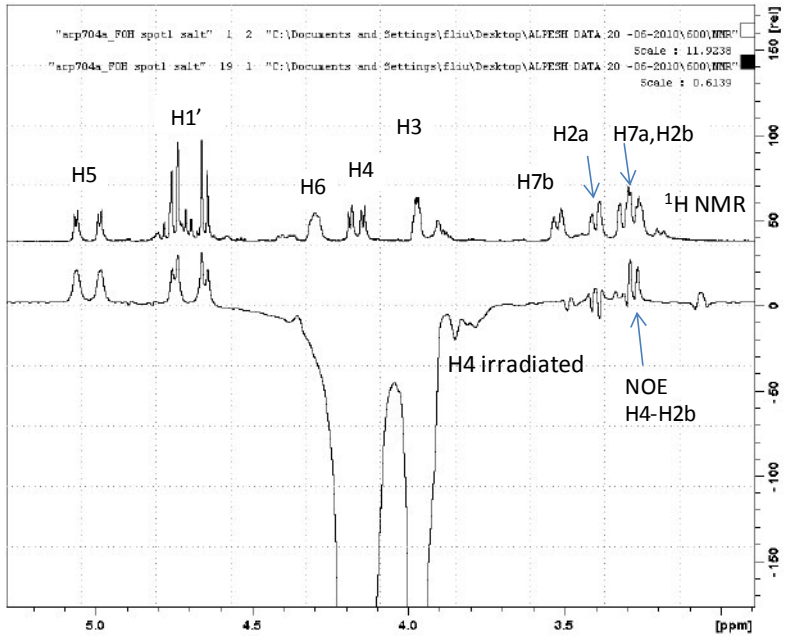


5.5

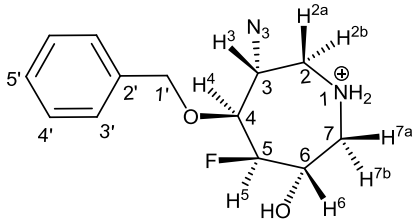
1D selective NOESY



1D selective NOESY

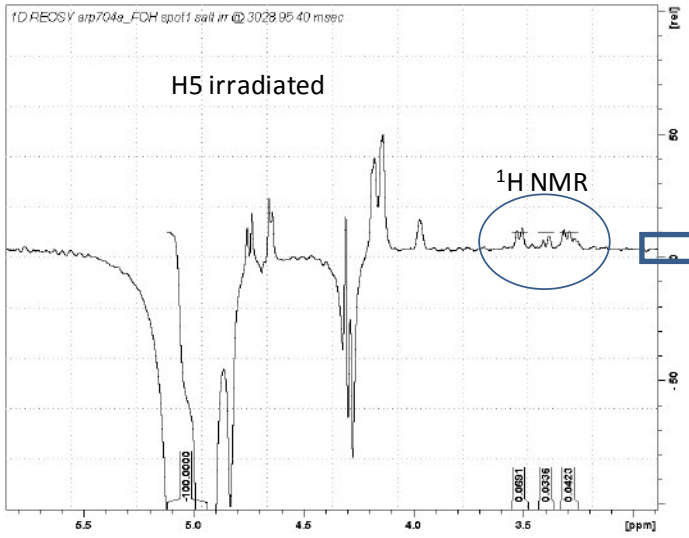


- Compound **5.5** has three stereocentres (C3, C4 and C6) having known absolute stereochemistry
- H4 shows NOE with H2b while no measurable NOE with H2a meaning H2b is *cis* and H2a is *trans* to H4.
- H6 shows significantly large NOE with H7a compared to H7b suggesting H7a is *cis* and H7b is *trans* to H6.
- H5 shows big NOE to H4 and small to H3 which leads to no where. However, quantitative 1D NOE of H5-H7b (7%) is almost double of H5-H7a NOE. Which clearly suggests H5 is *trans* to H4.
- J_{H5-H4} (1.4 Hz) and J_{H5-H6} (6.22 Hz) also support that H5 and H4 are *cis* while H5 and H6 are *trans*.

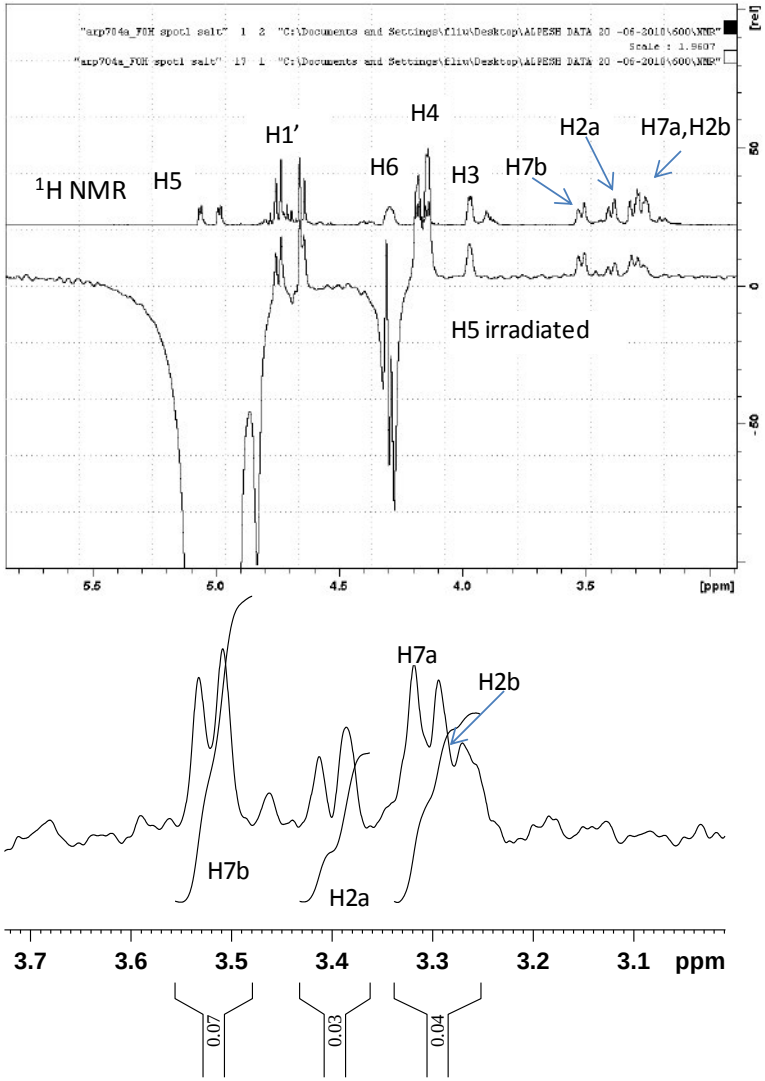


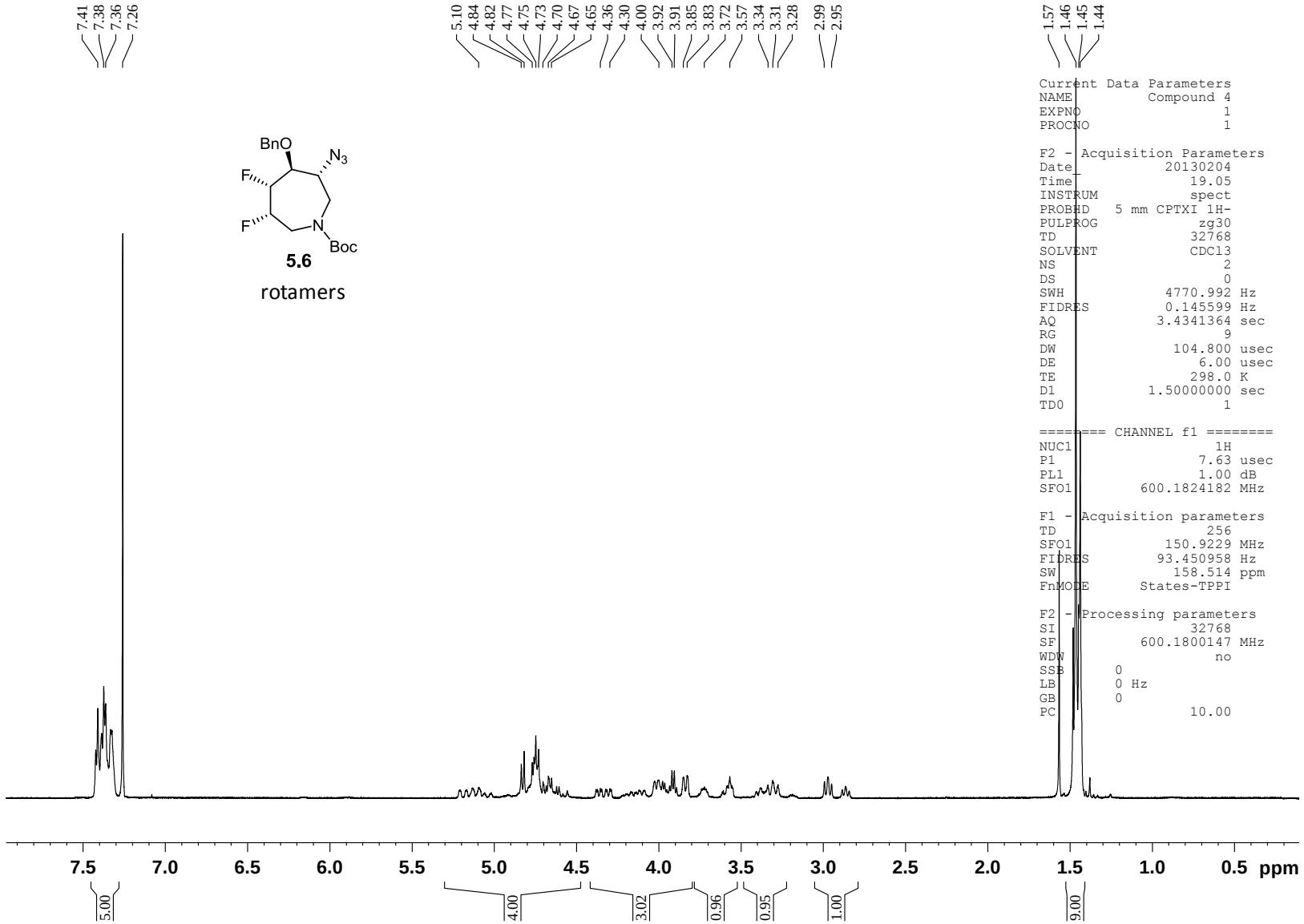
5.5

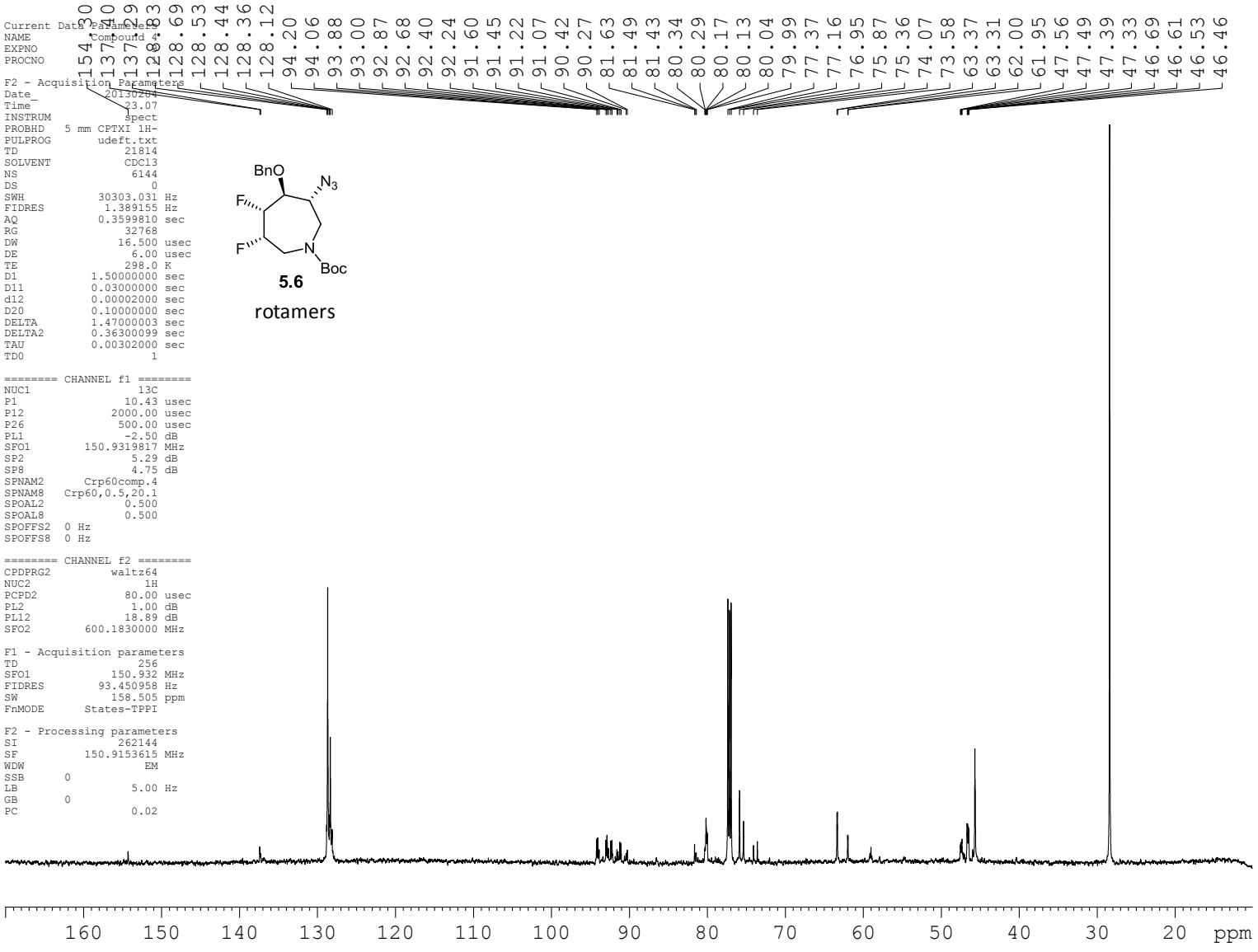
1D selective NOESY

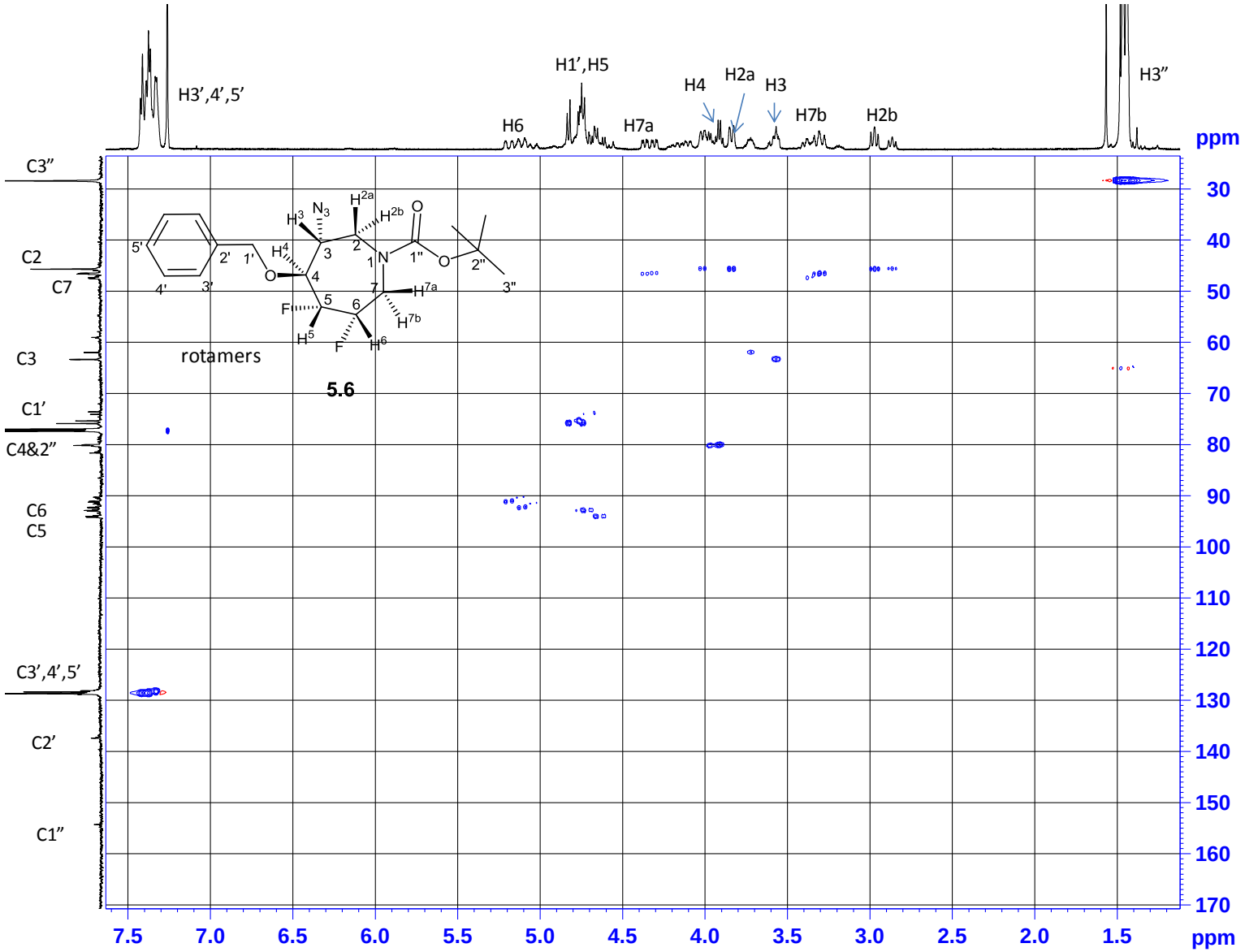


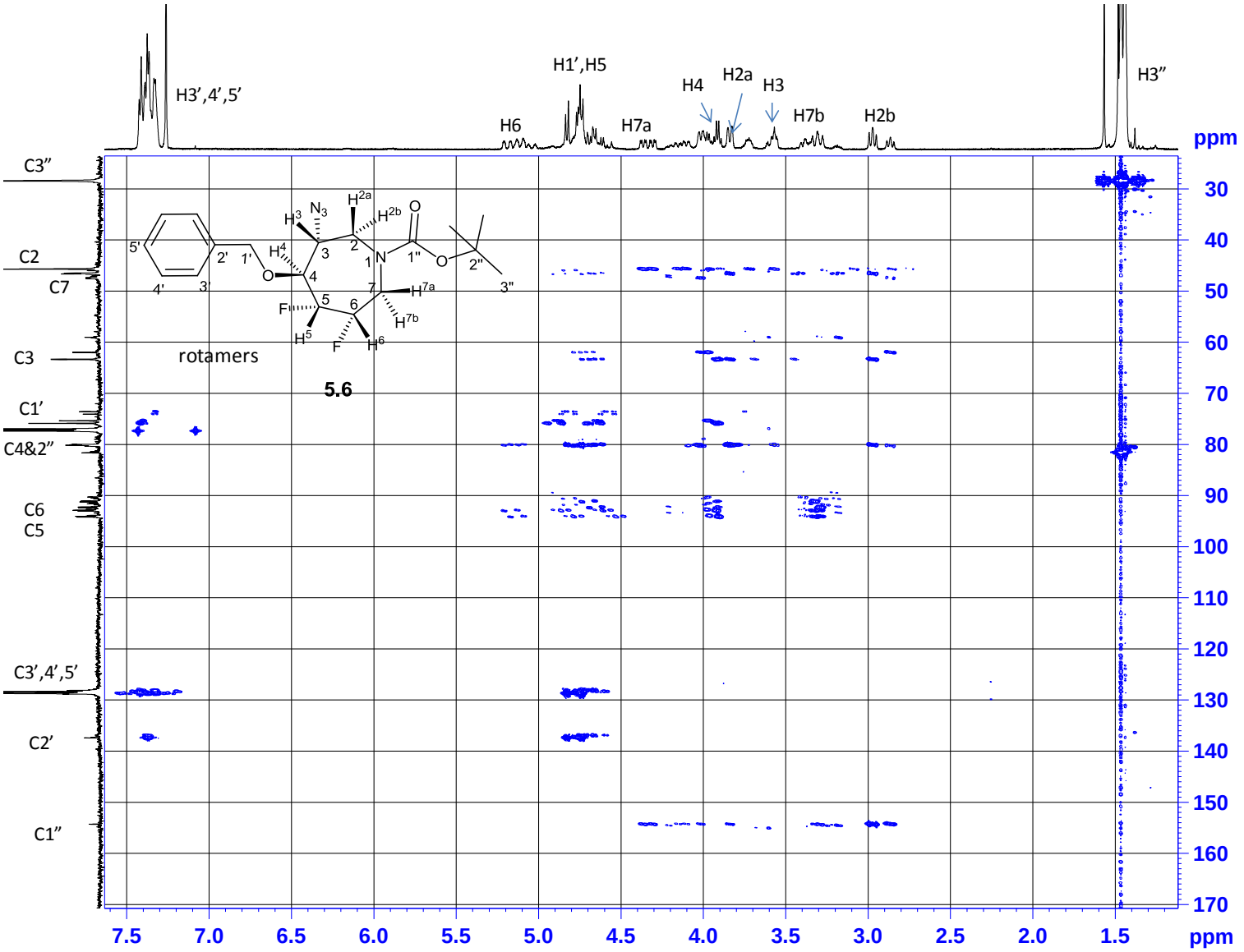
1D selective NOESY

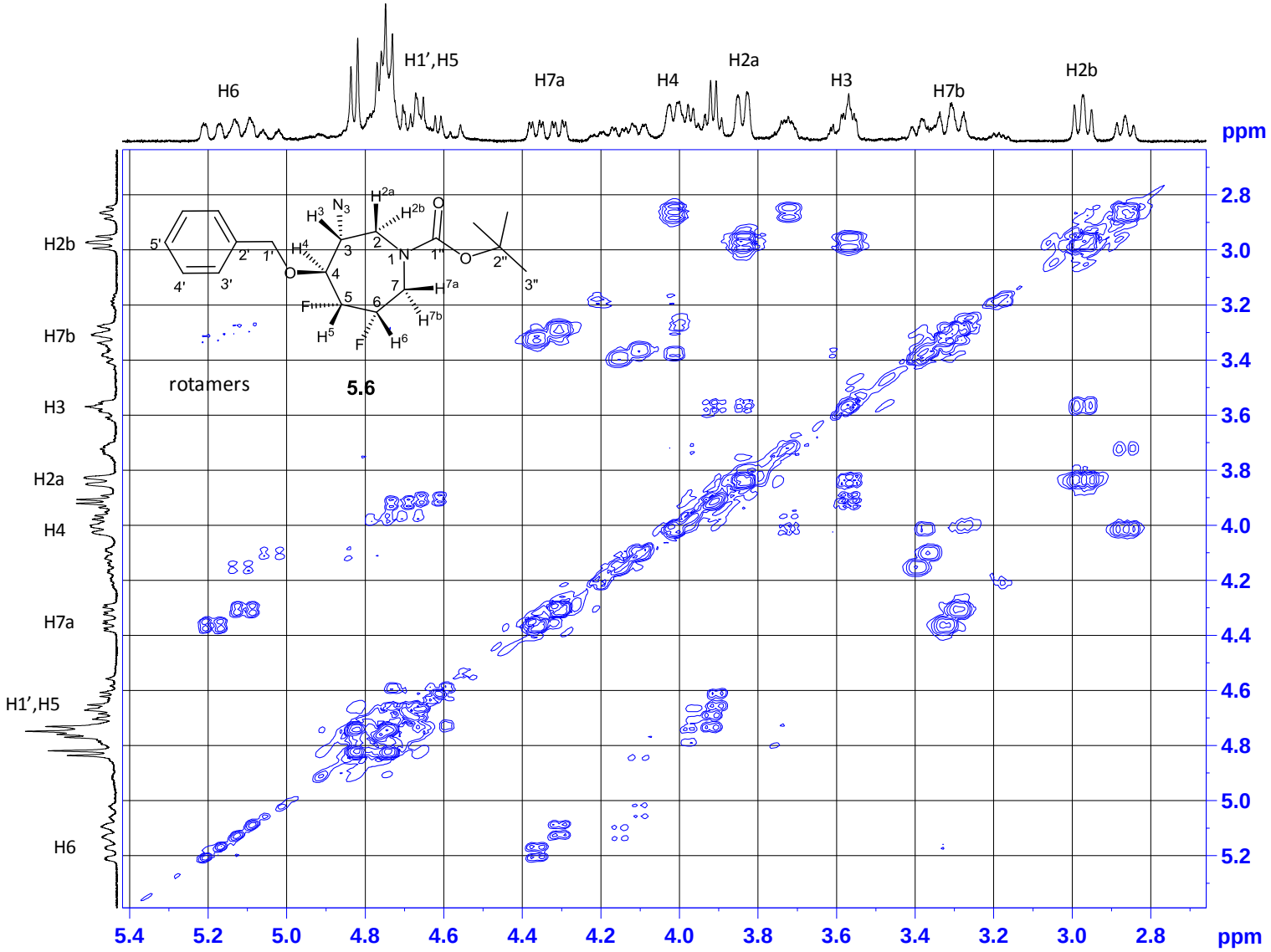


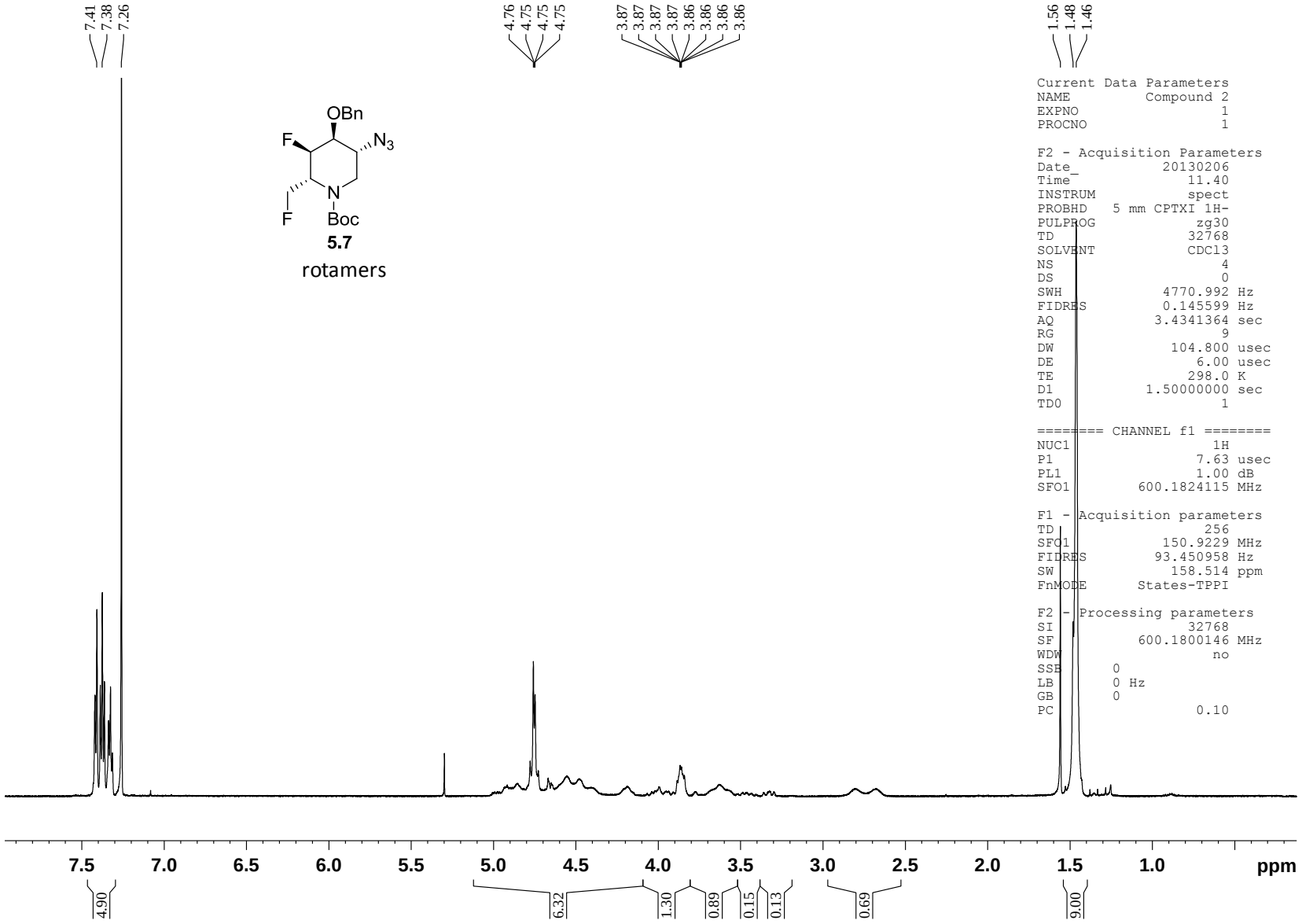

7.41
7.38
7.36
7.26
5.10
4.84
4.82
4.77
4.75
4.73
4.70
4.67
4.65
4.36
4.30
4.00
3.92
3.91
3.85
3.83
3.72
3.57
3.34
3.31
3.28
2.99
2.95
1.57
1.46
1.45
1.44
BnO
N3
F
F
N
Boc
5.6
rotamers
Current Data Parameters
NAME Compound 4
EXPNO 1
PROCNO 1
F2 - Acquisition Parameters
Date_ 20130204
Time 19.05
INSTRUM spect
PROBHD 5 mm CPTXI 1H-
PULPROG zg30
TD 32768
SOLVENT CDCl3
NS 2
DS 0
SWH 4770.992 Hz
FIDRES 0.145599 Hz
AQ 3.4341364 sec
RG 9
DW 104.800 usec
DE 6.00 usec
TE 298.0 K
D1 1.50000000 sec
TD0 1
======== CHANNEL f1 ========
NUC1 1H
P1 7.63 usec
PL1 1.00 dB
SFO1 600.1824182 MHz
F1 - Acquisition parameters
TD 256
SFO1 150.9229 MHz
FIDRES 93.450958 Hz
SW 158.514 ppm
FnMODE States-TPPI
F2 - Processing parameters
SI 32768
SF 600.1800147 MHz
WDW no
SSB 0
LB 0 Hz
GB 0
PC 10.00
7.5
7.0
6.5
6.0
5.5
5.0
4.5
4.0
3.5
3.0
2.5
2.0
1.5
1.0
0.5
ppm
5.00
4.00
3.02
0.96
0.95
1.00
9.00

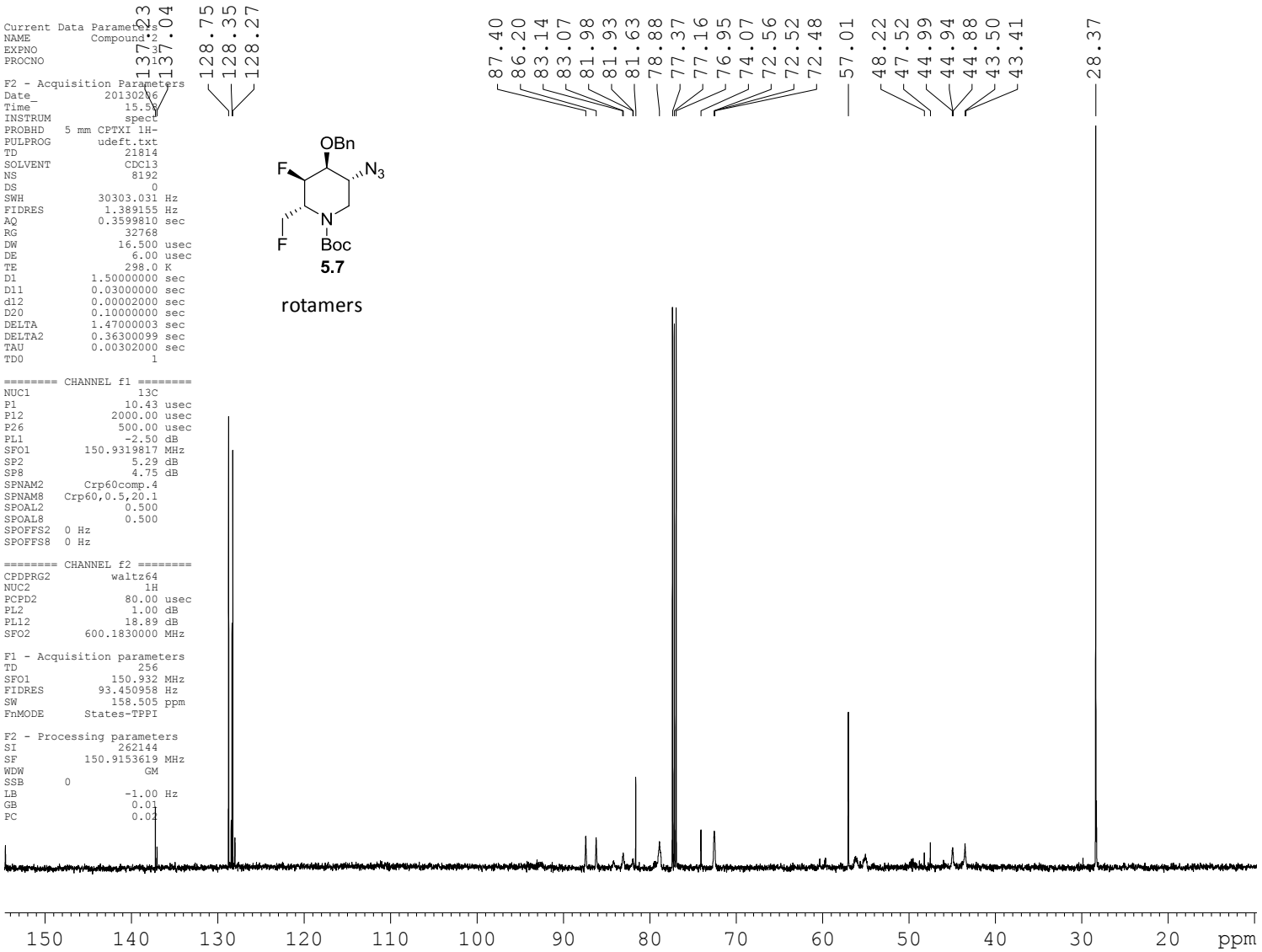

154.30
137.00
136.79
128.83
128.69
128.53
128.44
128.36
128.12
94.20
94.06
93.88
93.00
92.87
92.68
92.40
92.24
91.60
91.45
91.22
91.07
90.42
90.27
81.63
81.49
81.43
80.34
80.29
80.17
80.13
80.04
79.99
77.37
77.16
76.95
75.87
75.36
74.07
73.58
63.37
63.31
62.00
61.95
47.56
47.49
47.39
47.33
46.69
46.61
46.53
46.46
Current Data Parameters
NAME Compound 4
EXPNO 1
PROCNO 1
F2 - Acquisition Parameters
Date_ 20130204
Time 23.07
INSTRUM spect
PROBHD 5 mm CPTXI 1H-
PULPROG udeft.txt
TD 21814
SOLVENT CDCl3
NS 6144
DS 0
SWH 30303.031 Hz
FIDRES 1.389155 Hz
AQ 0.3599810 sec
RG 32768
DW 16.500 usec
DE 6.00 usec
TE 298.0 K
D1 1.50000000 sec
D11 0.03000000 sec
d12 0.00002000 sec
D20 0.10000000 sec
DELTA 1.47000003 sec
DELTA2 0.36300099 sec
TAU 0.00302000 sec
TD0 1
======== CHANNEL f1 ========
NUC1 13C
P1 10.43 usec
P12 2000.00 usec
P26 500.00 usec
PL1 -2.50 dB
SFO1 150.9319817 MHz
SP2 5.29 dB
SP8 4.75 dB
SPNAM2 Crp60comp.4
SPNAM8 Crp60,0.5,20.1
SPOAL2 0.500
SPOAL8 0.500
SPOFFS2 0 Hz
SPOFFS8 0 Hz
======== CHANNEL f2 ========
CPDPRG2 waltz64
NUC2 1H
PCPD2 80.00 usec
PL2 1.00 dB
PL12 18.89 dB
SFO2 600.1830000 MHz
F1 - Acquisition parameters
TD 256
SFO1 150.932 MHz
FIDRES 93.450958 Hz
SW 158.505 ppm
FnMODE States-TPPI
F2 - Processing parameters
SI 262144
SF 150.9153615 MHz
WDW EM
SSB 0
LB 5.00 Hz
GB 0
PC 0.02
BnO
N3
F
F
N
Boc
5.6
rotamers
160
150
140
130
120
110
100
90
80
70
60
50
40
30
20
ppm

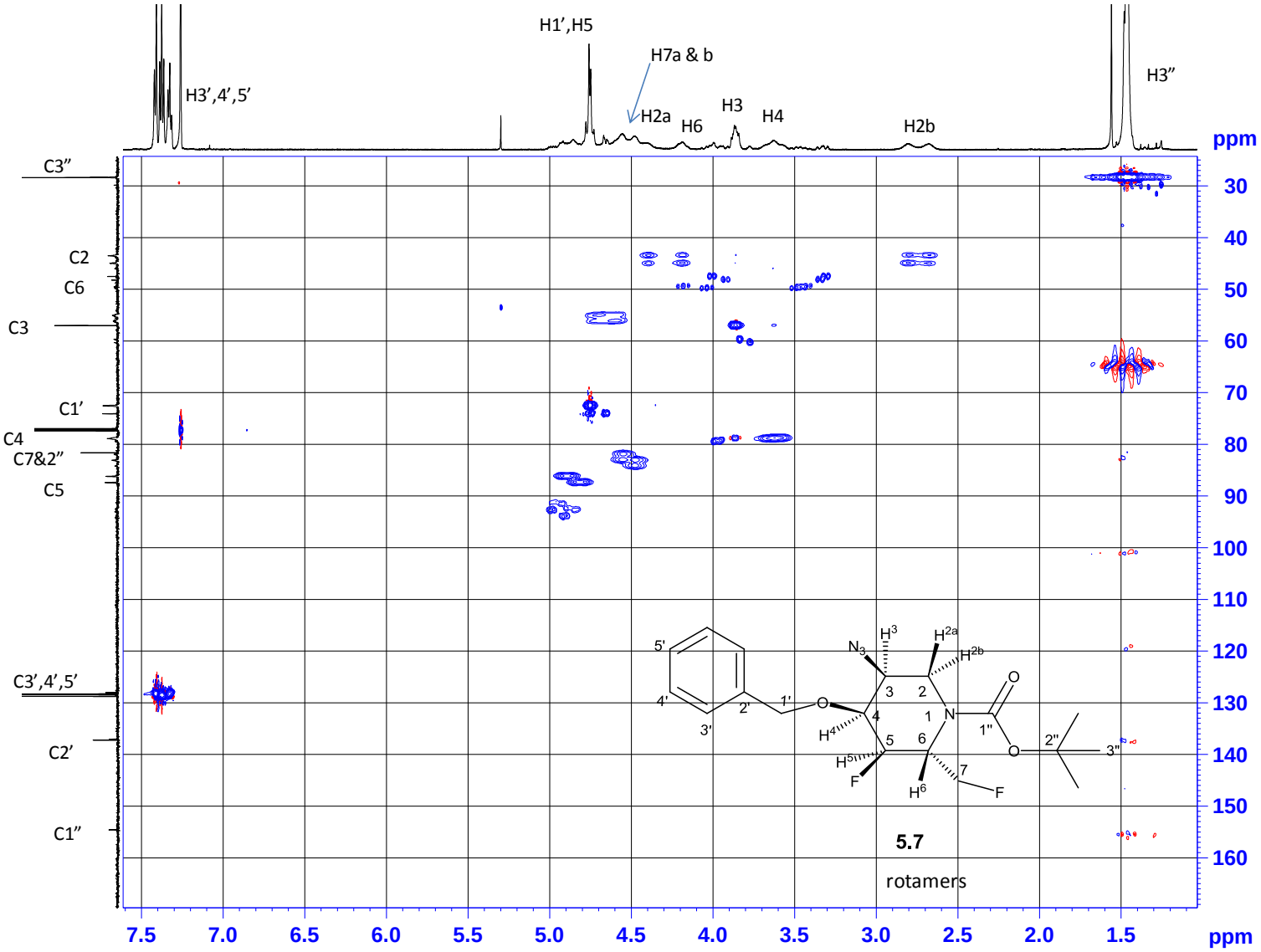

H3',4',5'
H6
H1',H5
H7a
H4
H2a
H3
H7b
H2b
H3"
ppm
C3"
C2
C7
C3
C1'
C4&2"
C6
C5
C3',4',5'
C2'
C1"
rotamers
5.6
7.5
7.0
6.5
6.0
5.5
5.0
4.5
4.0
3.5
3.0
2.5
2.0
1.5
ppm

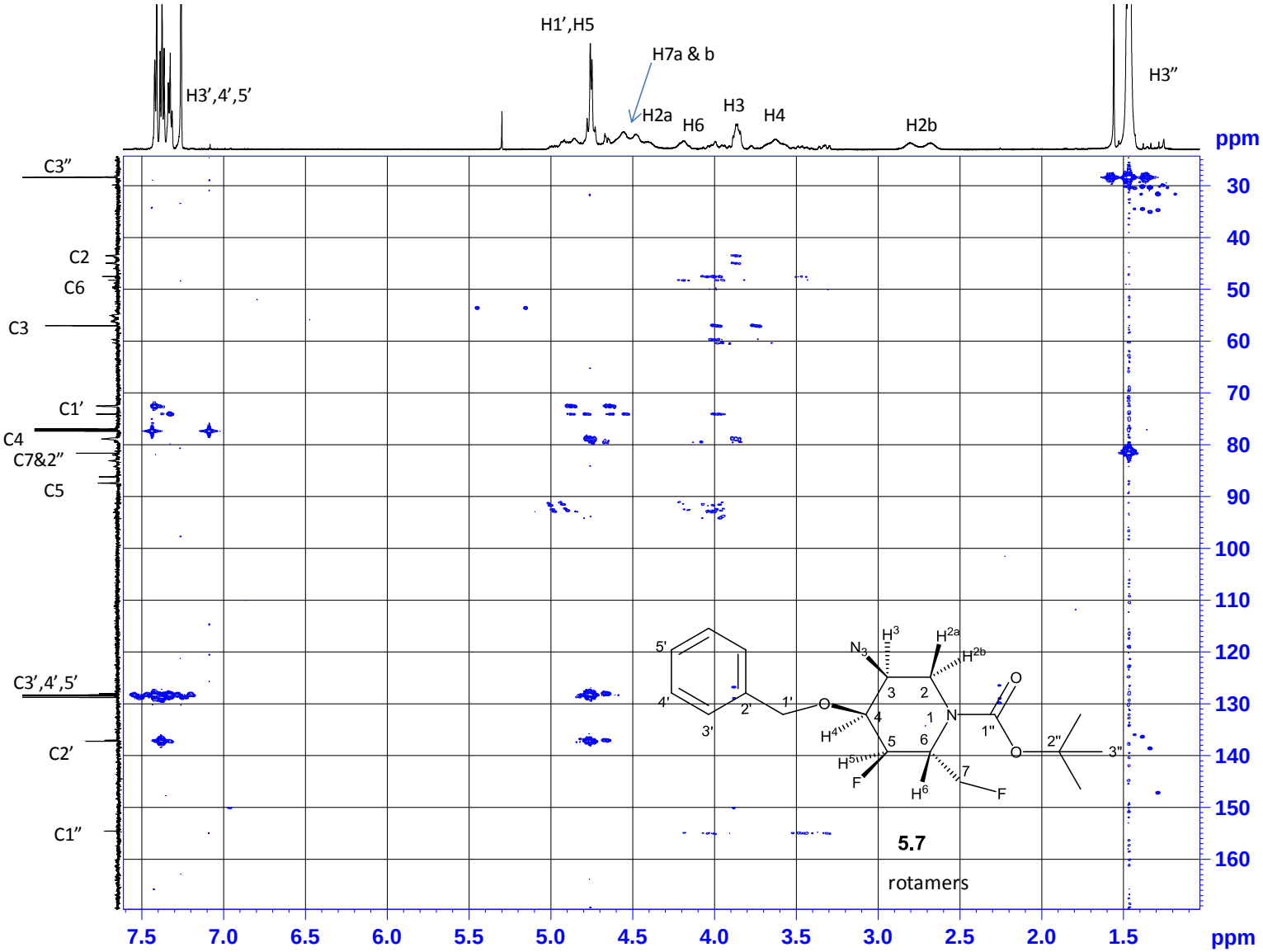

H3',4',5'
H6
H1',H5
H7a
H4
H2a
H3
H7b
H2b
H3"
ppm
C3"
C2
C7
C3
C1'
C4&2"
C6
C5
C3',4',5'
C2'
C1"
rotamers
5.6
7.5
7.0
6.5
6.0
5.5
5.0
4.5
4.0
3.5
3.0
2.5
2.0
1.5
ppm

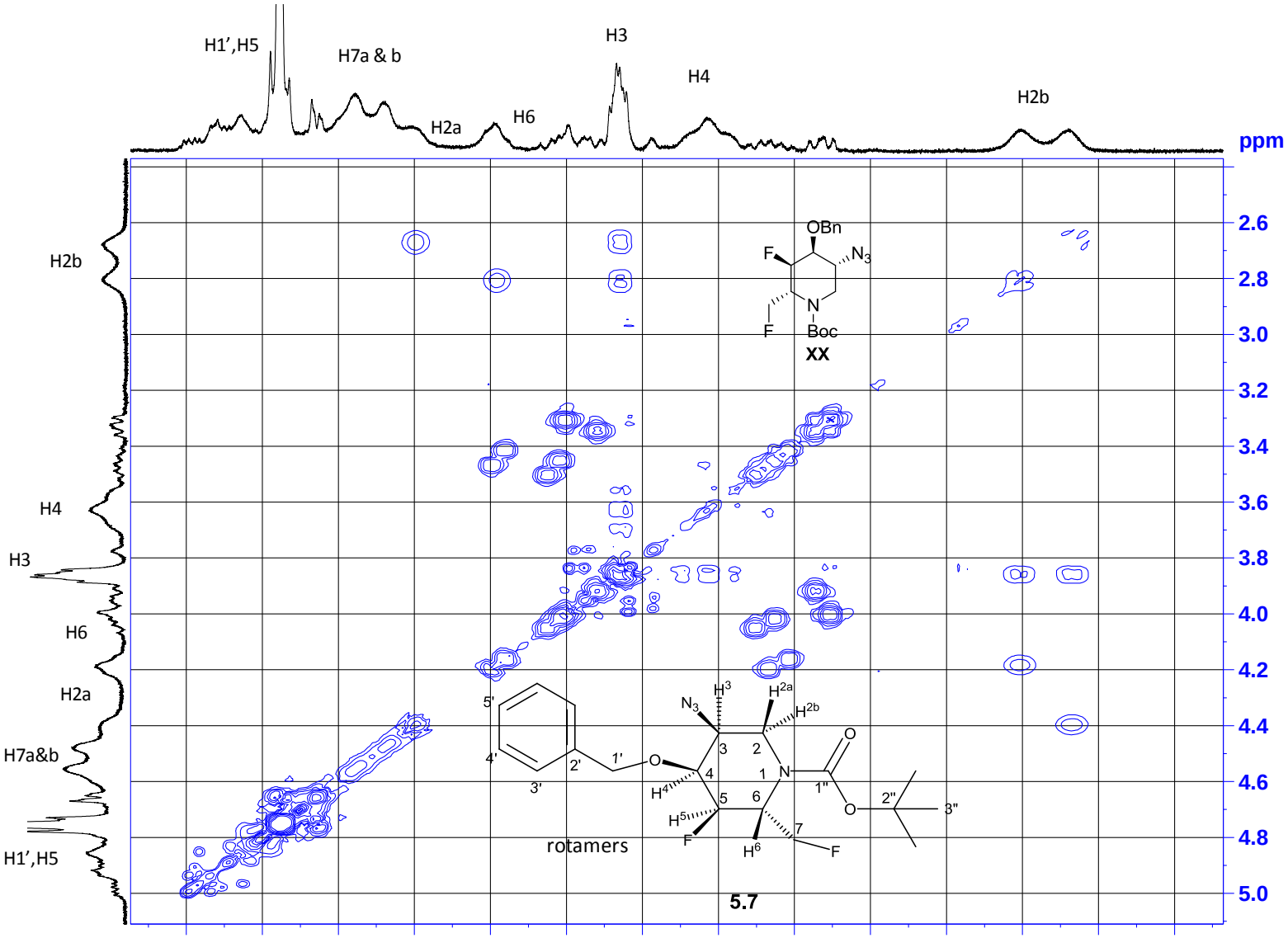

H6
H1',H5
H7a
H4
H2a
H3
H7b
H2b
ppm
rotamers
5.6
5.4
5.2
5.0
4.8
4.6
4.4
4.2
4.0
3.8
3.6
3.4
3.2
3.0
2.8
ppm

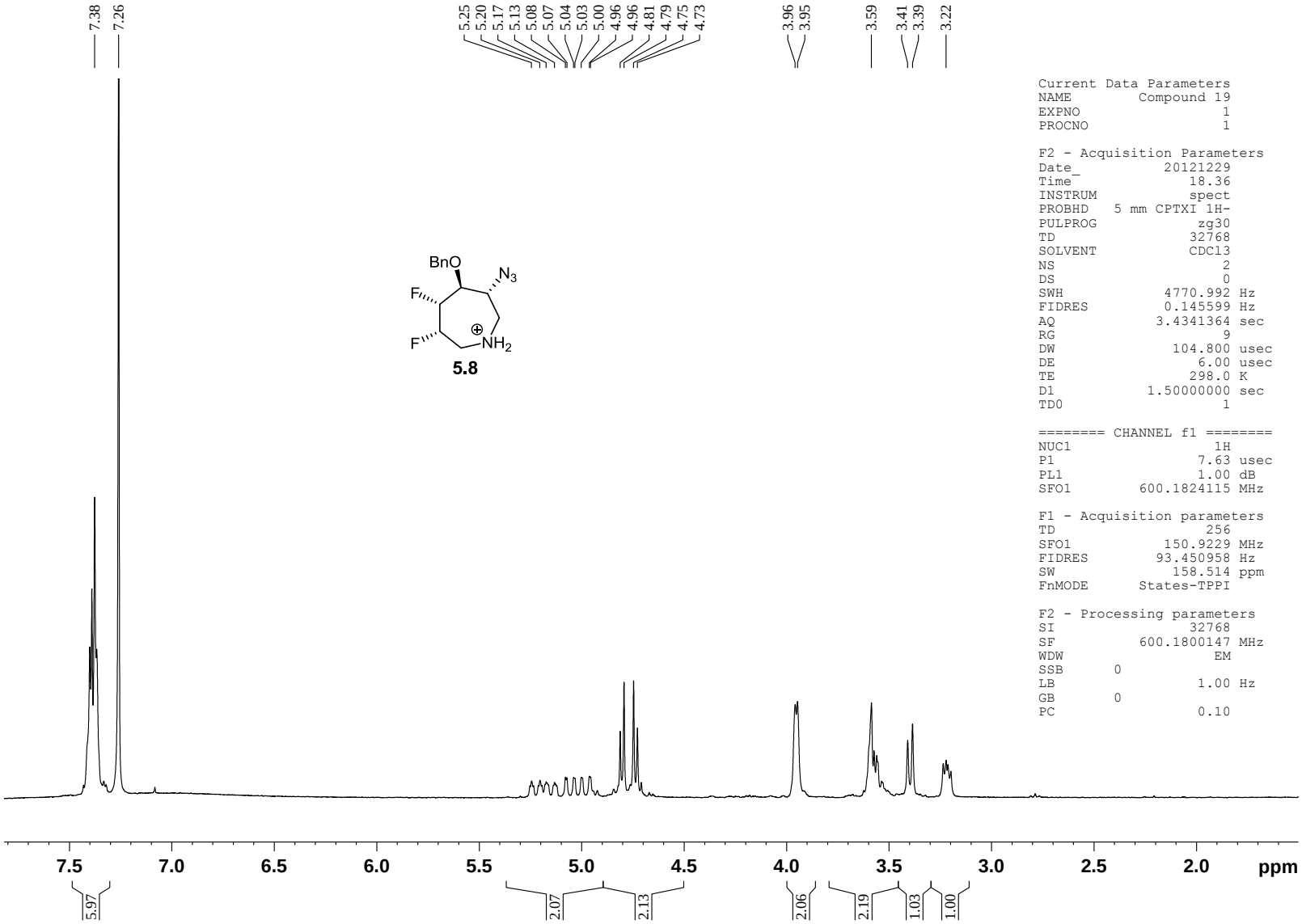

7.41
7.38
7.26
4.76
4.75
4.75
4.75
3.87
3.87
3.87
3.87
3.86
3.86
3.86
3.86
1.56
1.48
1.46
OBn
F
N3
N
F
Boc
5.7
rotamers
Current Data Parameters
NAME Compound 2
EXPNO 1
PROCNO 1
F2 - Acquisition Parameters
Date_ 20130206
Time 11.40
INSTRUM spect
PROBHD 5 mm CPTXI 1H-
PULPROG zg30
TD 32768
SOLVENT CDCl3
NS 4
DS 0
SWH 4770.992 Hz
FIDRES 0.145599 Hz
AQ 3.4341364 sec
RG 9
DW 104.800 usec
DE 6.00 usec
TE 298.0 K
D1 1.50000000 sec
TD0 1
======== CHANNEL f1 ========
NUC1 1H
P1 7.63 usec
PL1 1.00 dB
SFO1 600.1824115 MHz
F1 - Acquisition parameters
TD 256
SFO1 150.9229 MHz
FIDRES 93.450958 Hz
SW 158.514 ppm
FnMODE States-TPPI
F2 - Processing parameters
SI 32768
SF 600.1800146 MHz
WDW no
SSB 0
LB 0 Hz
GB 0
PC 0.10
7.5
7.0
6.5
6.0
5.5
5.0
4.5
4.0
3.5
3.0
2.5
2.0
1.5
1.0
ppm
4.90
6.32
1.30
0.89
0.15
0.13
0.69
9.00

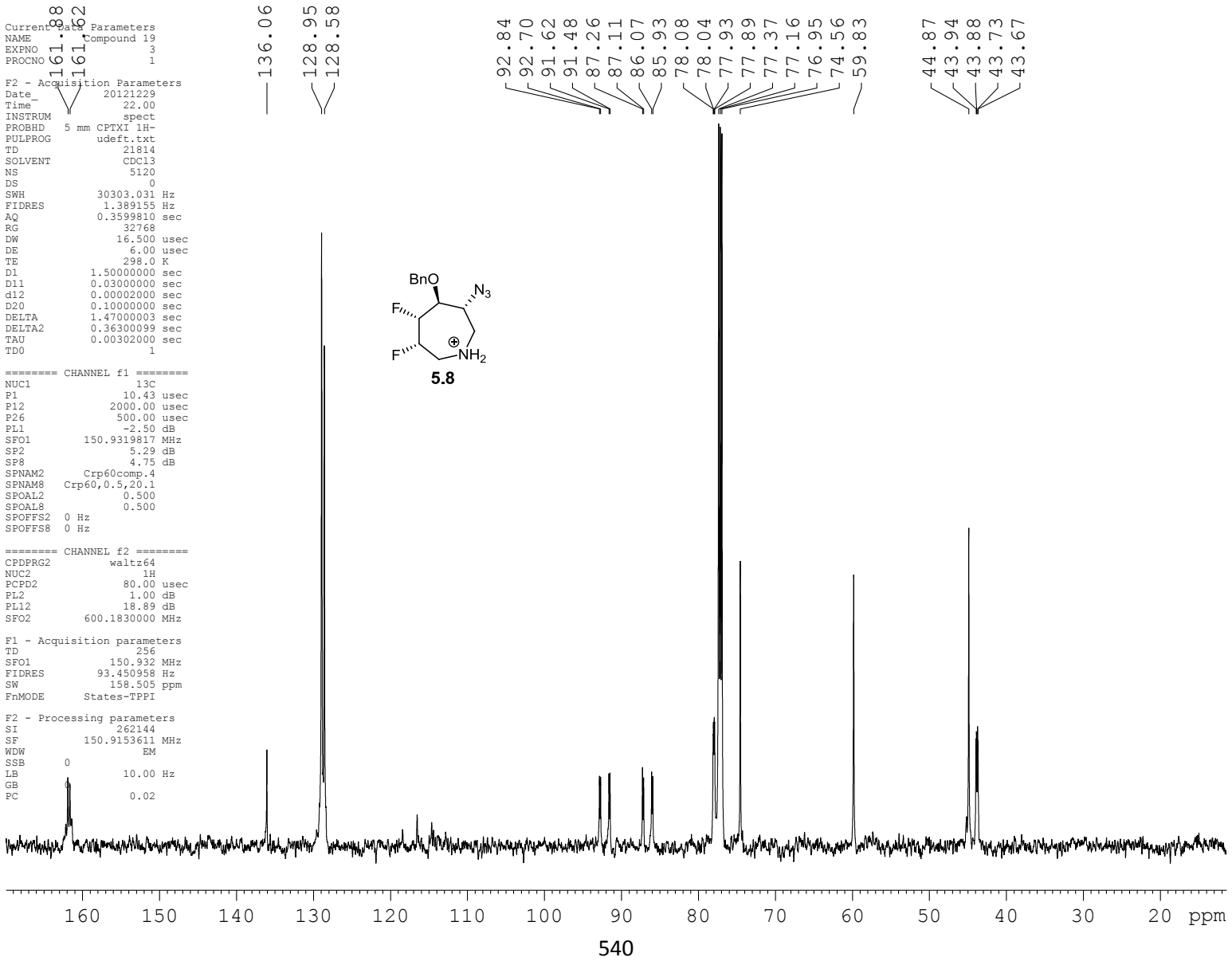

137.33
137.04
128.75
128.35
128.27
87.40
86.20
83.14
83.07
81.98
81.93
81.63
78.88
77.37
77.16
76.95
74.07
72.56
72.52
72.48
57.01
48.22
47.52
44.99
44.94
44.88
43.50
43.41
28.37
OBn
F
N3
F
N
Boc
5.7
rotamers
Current Data Parameters
NAME Compound•2
EXPNO 3
PROCNO 1
F2 - Acquisition Parameters
Date_ 20130206
Time 15.59
INSTRUM spect
PROBHD 5 mm CPTXI 1H-
PULPROG udeft.txt
TD 21814
SOLVENT CDCl3
NS 8192
DS 0
SWH 30303.031 Hz
FIDRES 1.389155 Hz
AQ 0.3599810 sec
RG 32768
DW 16.500 usec
DE 6.00 usec
TE 298.0 K
D1 1.50000000 sec
D11 0.03000000 sec
d12 0.00002000 sec
D20 0.10000000 sec
DELTA 1.47000003 sec
DELTA2 0.36300099 sec
TAU 0.00302000 sec
TD0 1
======== CHANNEL f1 ========
NUC1 13C
P1 10.43 usec
P12 2000.00 usec
P26 500.00 usec
PL1 -2.50 dB
SFO1 150.9319817 MHz
SP2 5.29 dB
SP8 4.75 dB
SPNAM2 Crp60comp.4
SPNAM8 Crp60,0.5,20.1
SPOAL2 0.500
SPOAL8 0.500
SPOFFS2 0 Hz
SPOFFS8 0 Hz
======== CHANNEL f2 ========
CPDPRG2 waltz64
NUC2 1H
PCPD2 80.00 usec
PL2 1.00 dB
PL12 18.89 dB
SFO2 600.1830000 MHz
F1 - Acquisition parameters
TD 256
SFO1 150.932 MHz
FIDRES 93.450958 Hz
SW 158.505 ppm
FnMODE States-TPPI
F2 - Processing parameters
SI 262144
SF 150.9153619 MHz
WDW GM
SSB 0
LB -1.00 Hz
GB 0.01
PC 0.02
150
140
130
120
110
100
90
80
70
60
50
40
30
20
ppm

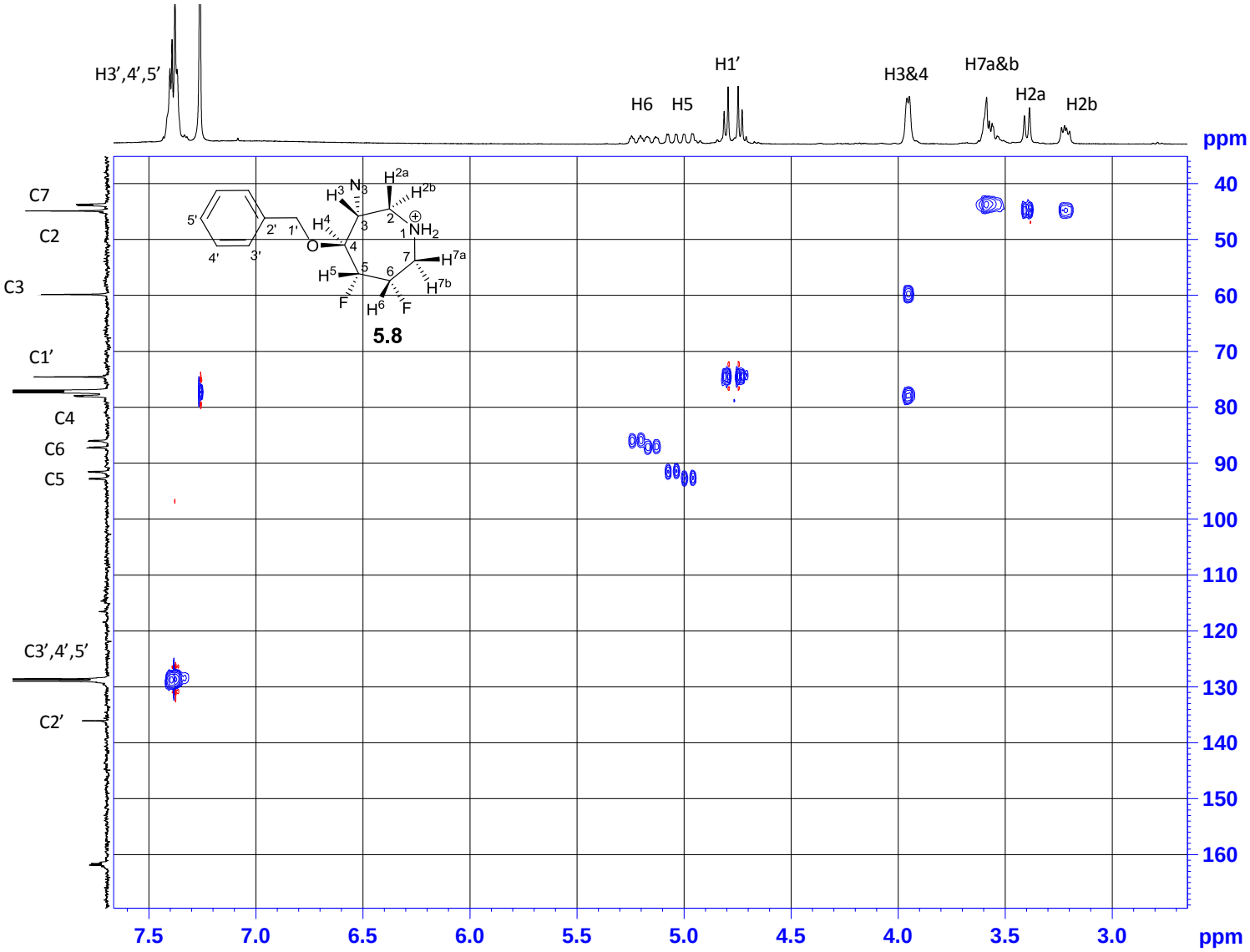

H1',H5
H7a & b
H3',4',5'
H2a
H6
H3
H4
H2b
H3"
ppm
C3"
C2
C6
C3
C1'
C4
C7&2"
C5
C3',4',5'
C2'
C1"
5'
4'
3'
2'
1'
O
N3
H3
H2a
H2b
3
2
1
N
4
5
6
7
H4
H5
F
H6
F
O
1"
O
2"
3"
5.7
rotamers
30
40
50
60
70
80
90
100
110
120
130
140
150
160
7.5
7.0
6.5
6.0
5.5
5.0
4.5
4.0
3.5
3.0
2.5
2.0
1.5
ppm

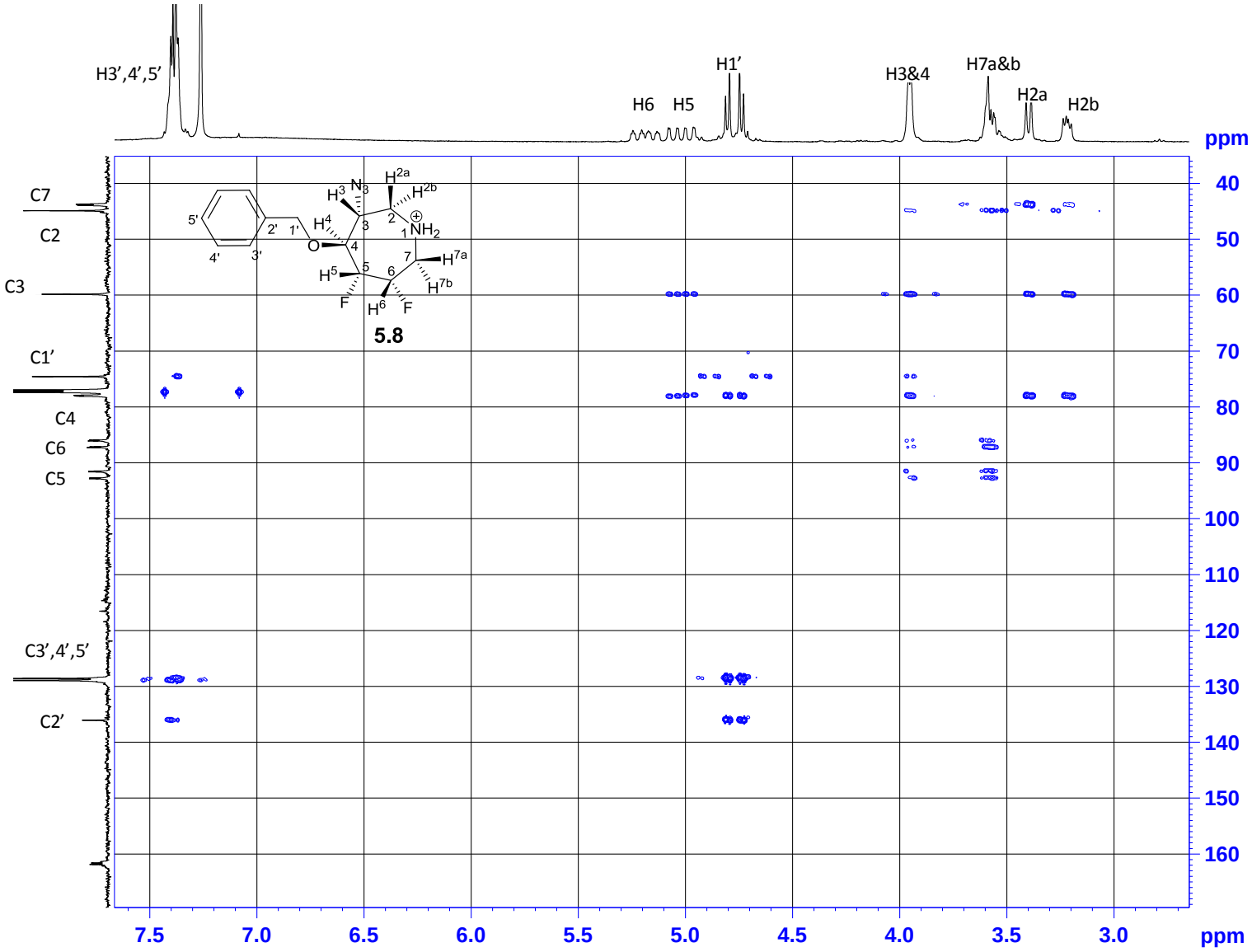

H1',H5
H7a & b
H3''
H3',4',5'
H2a
H6
H3
H4
H2b
ppm
C3''
C2
C6
C3
C1'
C4
C7&2''
C5
C3',4',5'
C2'
C1''
30
40
50
60
70
80
90
100
110
120
130
140
150
160
7.5
7.0
6.5
6.0
5.5
5.0
4.5
4.0
3.5
3.0
2.5
2.0
1.5
ppm
5.7
rotamers

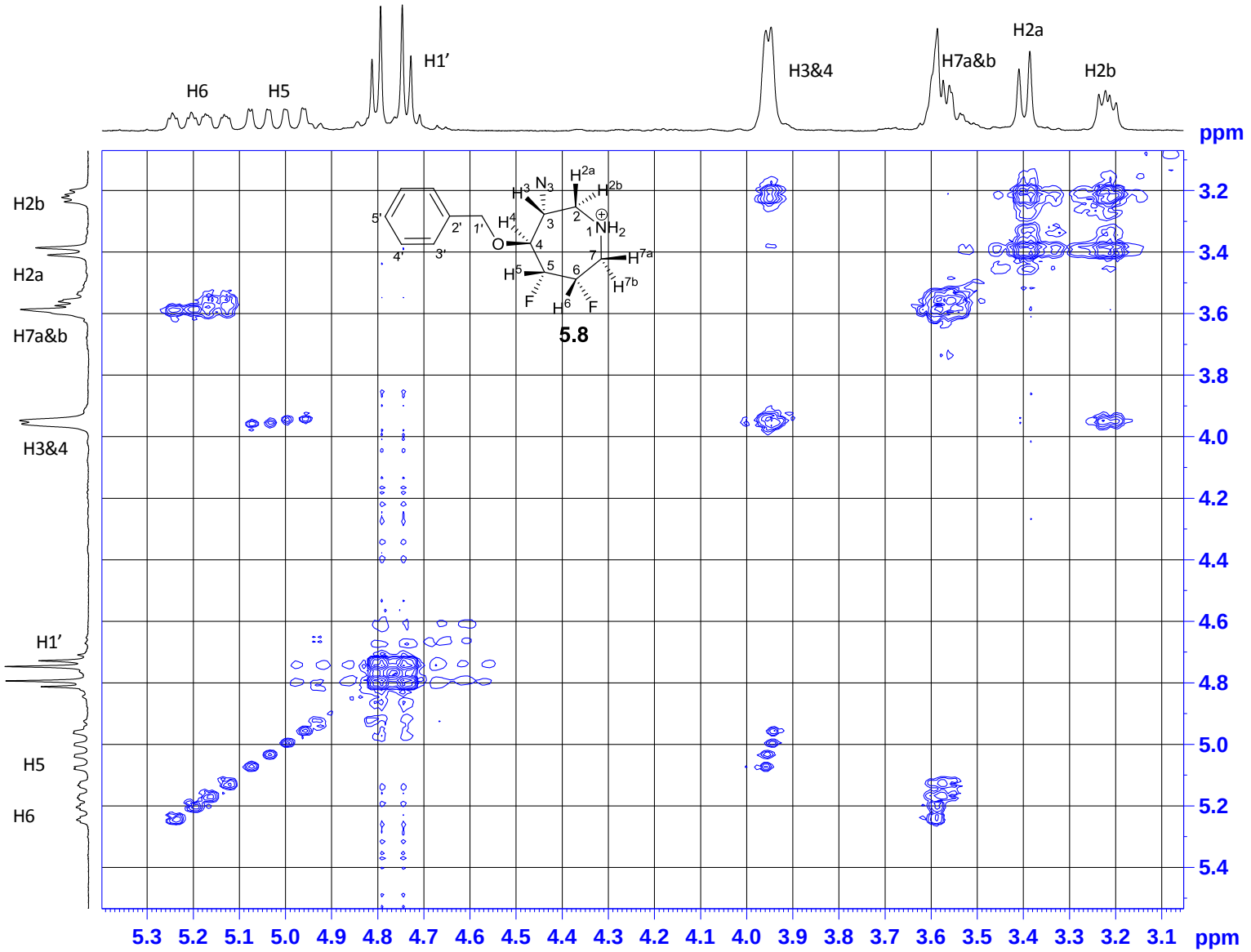

H1',H5
H7a & b
H2a
H6
H3
H4
H2b
ppm
OBn
F
N3
N
F
Boc
XX
rotamers
5.7
5.0
4.8
4.6
4.4
4.2
4.0
3.8
3.6
3.4
3.2
3.0
2.8
2.6
2.4

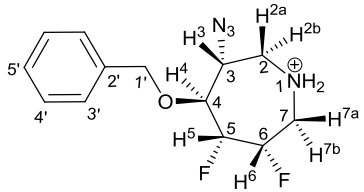

7.38
7.26
5.25
5.20
5.17
5.13
5.08
5.07
5.04
5.03
5.00
4.96
4.96
4.81
4.79
4.75
4.73
3.96
3.95
3.59
3.41
3.39
3.22
BnO
N3
F
F
NH2
5.8
Current Data Parameters
NAME Compound 19
EXPNO 1
PROCNO 1
F2 - Acquisition Parameters
Date_ 20121229
Time 18.36
INSTRUM spect
PROBHD 5 mm CPTXI 1H-
PULPROG zg30
TD 32768
SOLVENT CDCl3
NS 2
DS 0
SWH 4770.992 Hz
FIDRES 0.145599 Hz
AQ 3.4341364 sec
RG 9
DW 104.800 usec
DE 6.00 usec
TE 298.0 K
D1 1.50000000 sec
TD0 1
======== CHANNEL f1 ========
NUC1 1H
P1 7.63 usec
PL1 1.00 dB
SFO1 600.1824115 MHz
F1 - Acquisition parameters
TD 256
SFO1 150.9229 MHz
FIDRES 93.450958 Hz
SW 158.514 ppm
FnMODE States-TPPI
F2 - Processing parameters
SI 32768
SF 600.1800147 MHz
WDW EM
SSB 0
LB 1.00 Hz
GB 0
PC 0.10
7.5
7.0
6.5
6.0
5.5
5.0
4.5
4.0
3.5
3.0
2.5
2.0
ppm
5.97
2.07
2.13
2.06
2.19
1.03
1.00


161.88
161.62
136.06
128.95
128.58
92.84
92.70
91.62
91.48
87.26
87.11
86.07
85.93
78.08
78.04
77.93
77.89
77.37
77.16
76.95
74.56
59.83
44.87
43.94
43.88
43.73
43.67
Current Data Parameters
NAME Compound 19
EXPNO 3
PROCNO 1
F2 - Acquisition Parameters
Date_ 20121229
Time_ 22.00
INSTRUM spect
PROBHD 5 mm CPTXI 1H-
PULPROG udeft.txt
TD 21814
SOLVENT CDCl3
NS 5120
DS 0
SWH 30303.031 Hz
FIDRES 1.389155 Hz
AQ 0.3599810 sec
RG 32768
DW 16.500 usec
DE 6.00 usec
TE 298.0 K
D1 1.50000000 sec
D11 0.03000000 sec
d12 0.00002000 sec
D20 0.10000000 sec
DELTA 1.47000003 sec
DELTA2 0.36300099 sec
TAU 0.00302000 sec
TD0 1
======== CHANNEL f1 ========
NUC1 13C
P1 10.43 usec
P12 2000.00 usec
P26 500.00 usec
PL1 -2.50 dB
SFO1 150.9319817 MHz
SP2 5.29 dB
SP8 4.75 dB
SPNAM2 Crp60comp.4
SPNAM8 Crp60,0.5,20.1
SPOAL2 0.500
SPOAL8 0.500
SPOFFS2 0 Hz
SPOFFS8 0 Hz
======== CHANNEL f2 ========
CPDPRG2 waltz64
NUC2 1H
PCPD2 80.00 usec
PL2 1.00 dB
PL12 18.89 dB
SFO2 600.1830000 MHz
F1 - Acquisition parameters
TD 256
SFO1 150.932 MHz
FIDRES 93.450958 Hz
SW 158.505 ppm
FnMODE States-TPPI
F2 - Processing parameters
SI 262144
SF 150.9153611 MHz
WDW EM
SSB 0
LB 10.00 Hz
GB 0
PC 0.02
BnO
N3
F
F
NH2
5.8
160
150
140
130
120
110
100
90
80
70
60
50
40
30
20
ppm


H3',4',5'
H6
H5
H1'
H3&4
H7a&b
H2a
H2b
ppm
C7
C2
C3
C1'
C4
C6
C5
C3',4',5'
C2'
5.8
7.5
7.0
6.5
6.0
5.5
5.0
4.5
4.0
3.5
3.0
ppm


H3',4',5'
H6
H5
H1'
H3&4
H7a&b
H2a
H2b
ppm
C7
C2
C3
C1'
C4
C6
C5
C3',4',5'
C2'
5.8
7.5
7.0
6.5
6.0
5.5
5.0
4.5
4.0
3.5
3.0
ppm

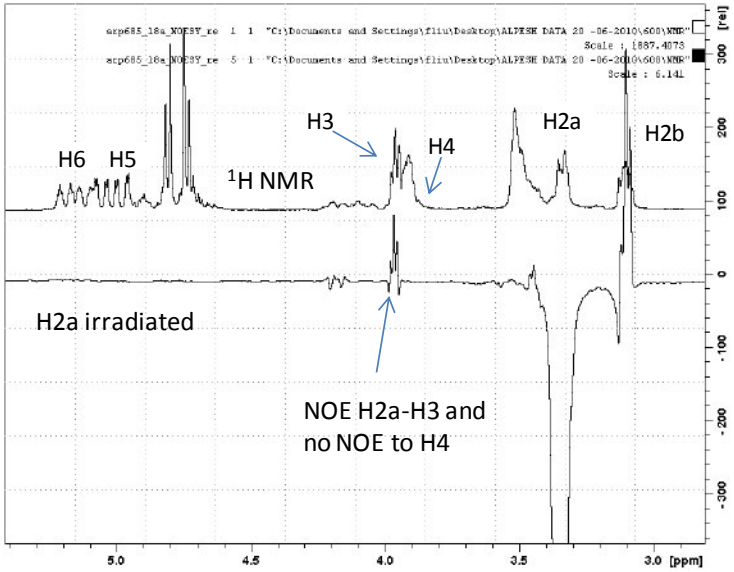

H6
H5
H1′
H3&4
H7a&b
H2a
H2b
ppm
5.8
5.3 5.2 5.1 5.0 4.9 4.8 4.7 4.6 4.5 4.4 4.3 4.2 4.1 4.0 3.9 3.8 3.7 3.6 3.5 3.4 3.3 3.2 3.1 ppm



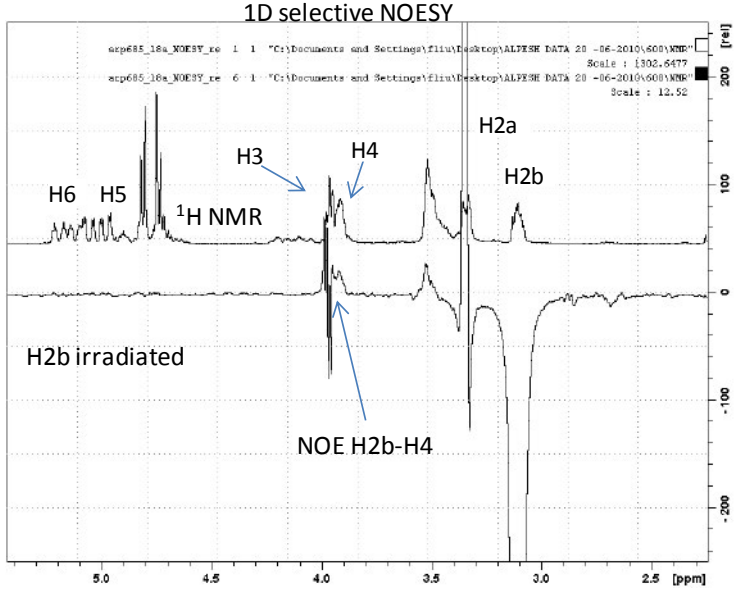
5.8

NB: The observed shifts in the 1H NMR signals is because of addition of a drop of TFA (intentionally!!) to separate H3 and H4.

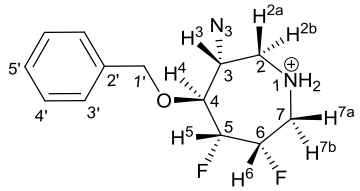
1D selective NOESY



1D selective NOESY



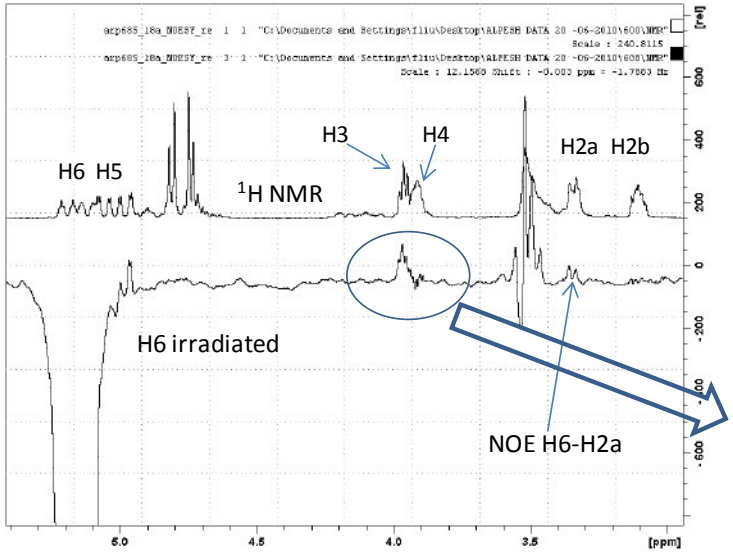
- Compound **5.8** has two stereocentres (C3, C4) having known absolute stereochemistry
- H2b shows NOE to H4 while H2a shows NOE to H3 suggesting H2a is *trans* and H2b is *cis* to H4.
- H5 and H6 show big NOE with H3 and H2a while no measurable NOE to H2b meaning H5 and H6 are both *cis* to H3. $J_{H5\text{-}H6}$ (1 Hz) also supports that H5 and H6 are *cis*.



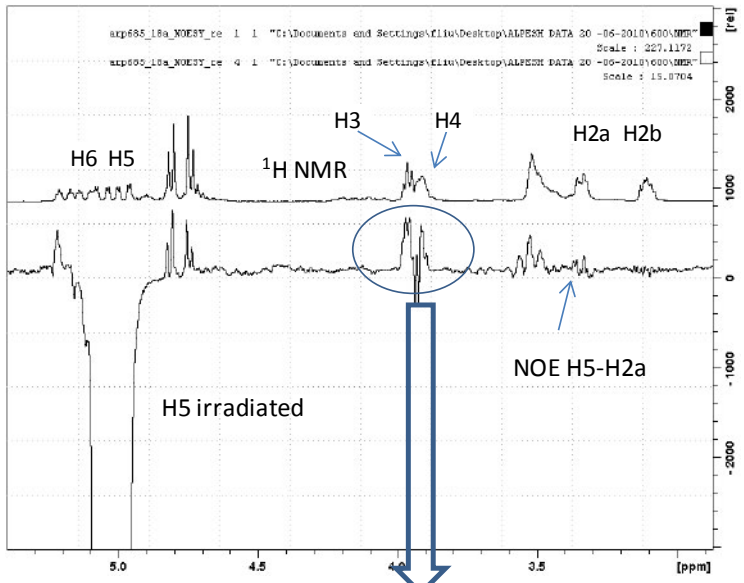
5.8

NB: The observed shifts in the 1H NMR signals is because of addition of a drop of TFA (intentionally!!) to separate H3 and H4.

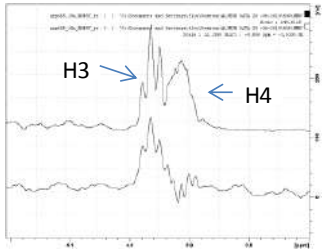
1D selective NOESY



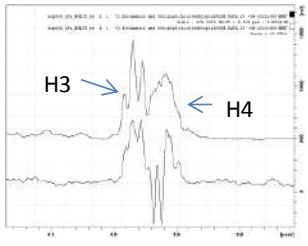
1D selective NOESY

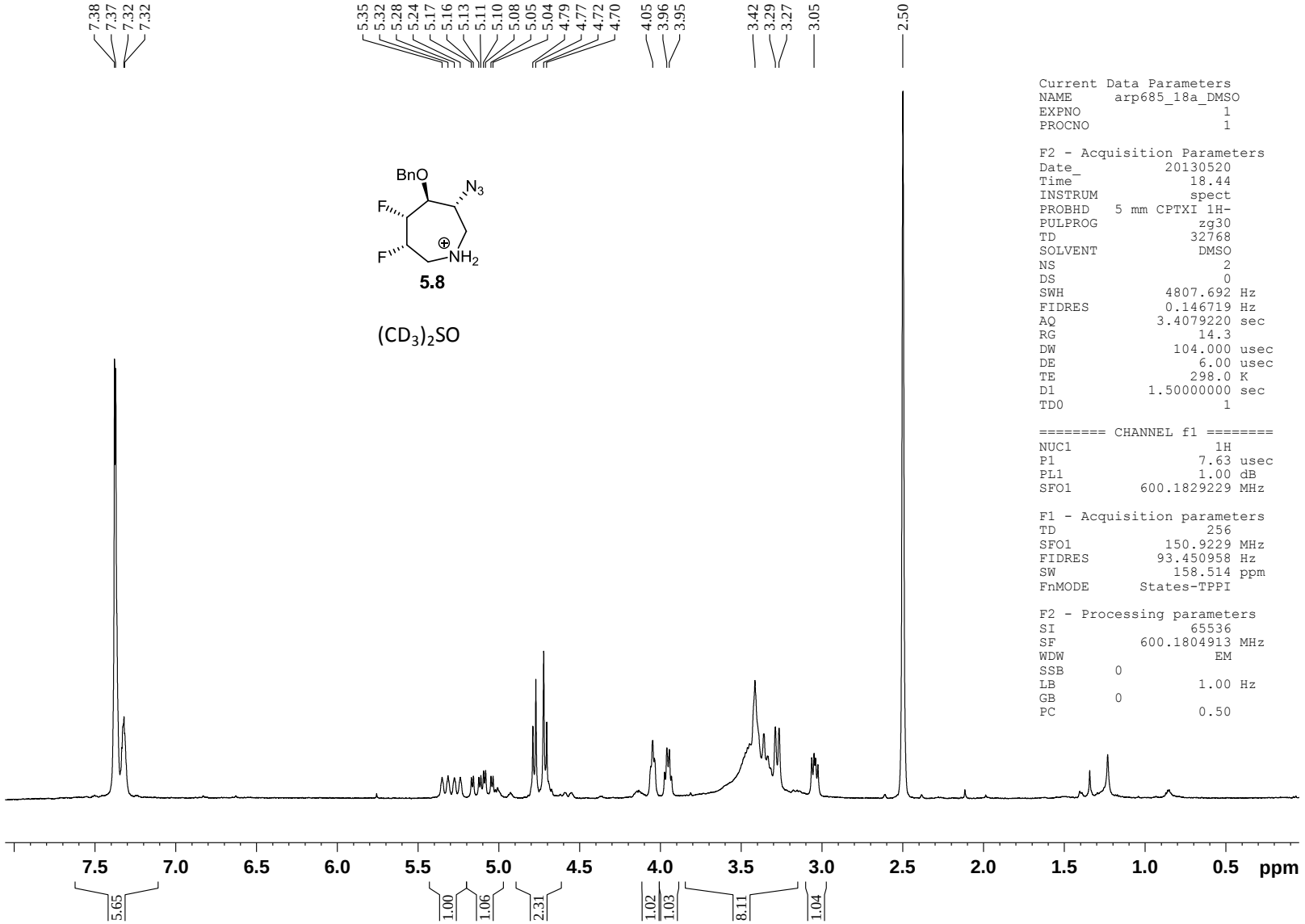


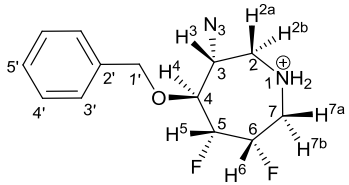
NOE H6-H3



NOE H5-H3



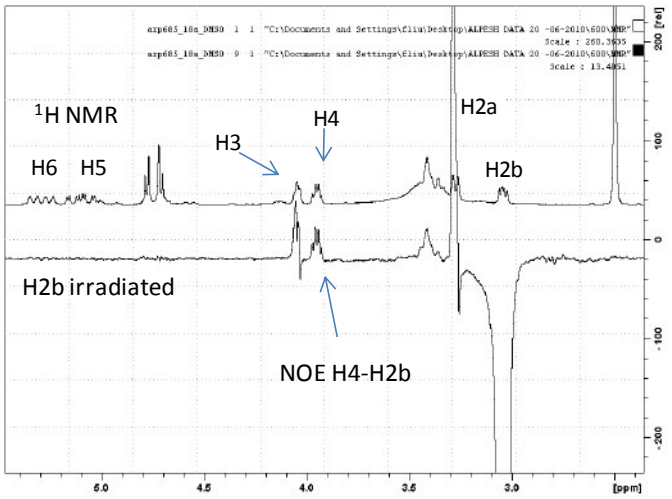

7.38
7.37
7.32
7.32
5.35
5.32
5.28
5.24
5.17
5.16
5.13
5.11
5.10
5.08
5.05
5.04
4.79
4.77
4.72
4.70
4.05
3.96
3.95
3.42
3.29
3.27
3.05
2.50
BnO
N3
F
F
NH2
5.8
(CD3)2SO
Current Data Parameters
NAME arp685_18a_DMSO
EXPNO 1
PROCNO 1
F2 - Acquisition Parameters
Date_ 20130520
Time 18.44
INSTRUM spect
PROBHD 5 mm CPTXI 1H-
PULPROG zg30
TD 32768
SOLVENT DMSO
NS 2
DS 0
SWH 4807.692 Hz
FIDRES 0.146719 Hz
AQ 3.4079220 sec
RG 14.3
DW 104.000 usec
DE 6.00 usec
TE 298.0 K
D1 1.50000000 sec
TD0 1
======== CHANNEL f1 ========
NUC1 1H
P1 7.63 usec
PL1 1.00 dB
SFO1 600.1829229 MHz
F1 - Acquisition parameters
TD 256
SFO1 150.9229 MHz
FIDRES 93.450958 Hz
SW 158.514 ppm
FnMODE States-TPPI
F2 - Processing parameters
SI 65536
SF 600.1804913 MHz
WDW EM
SSB 0
LB 1.00 Hz
GB 0
PC 0.50
7.5
7.0
6.5
6.0
5.5
5.0
4.5
4.0
3.5
3.0
2.5
2.0
1.5
1.0
0.5
ppm
5.65
1.00
1.06
2.31
1.02
1.03
8.11
1.04



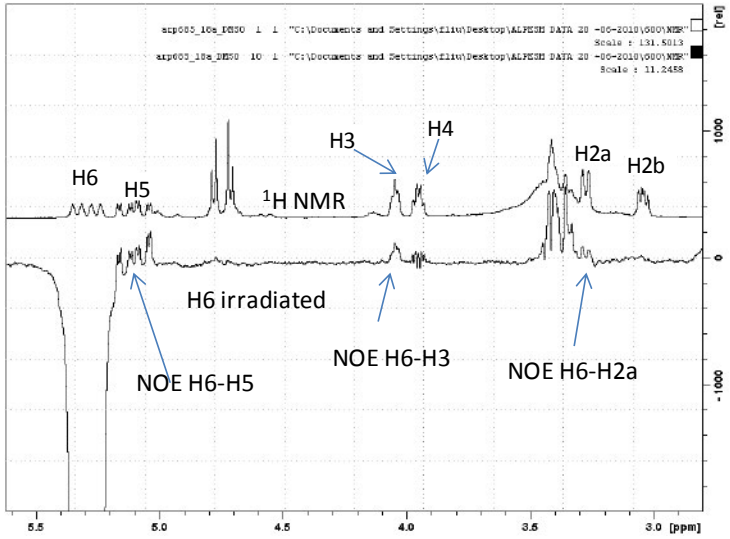
5.8

NB: The experiments were done in DMSO-*D*6.

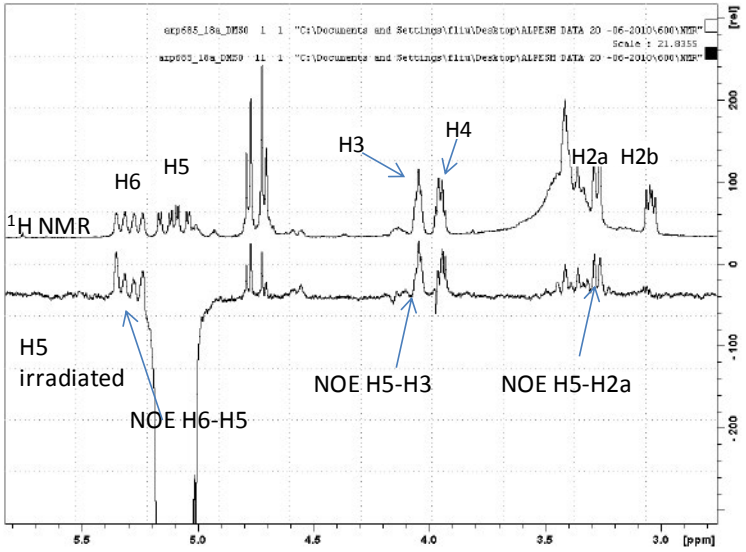
1D selective NOESY

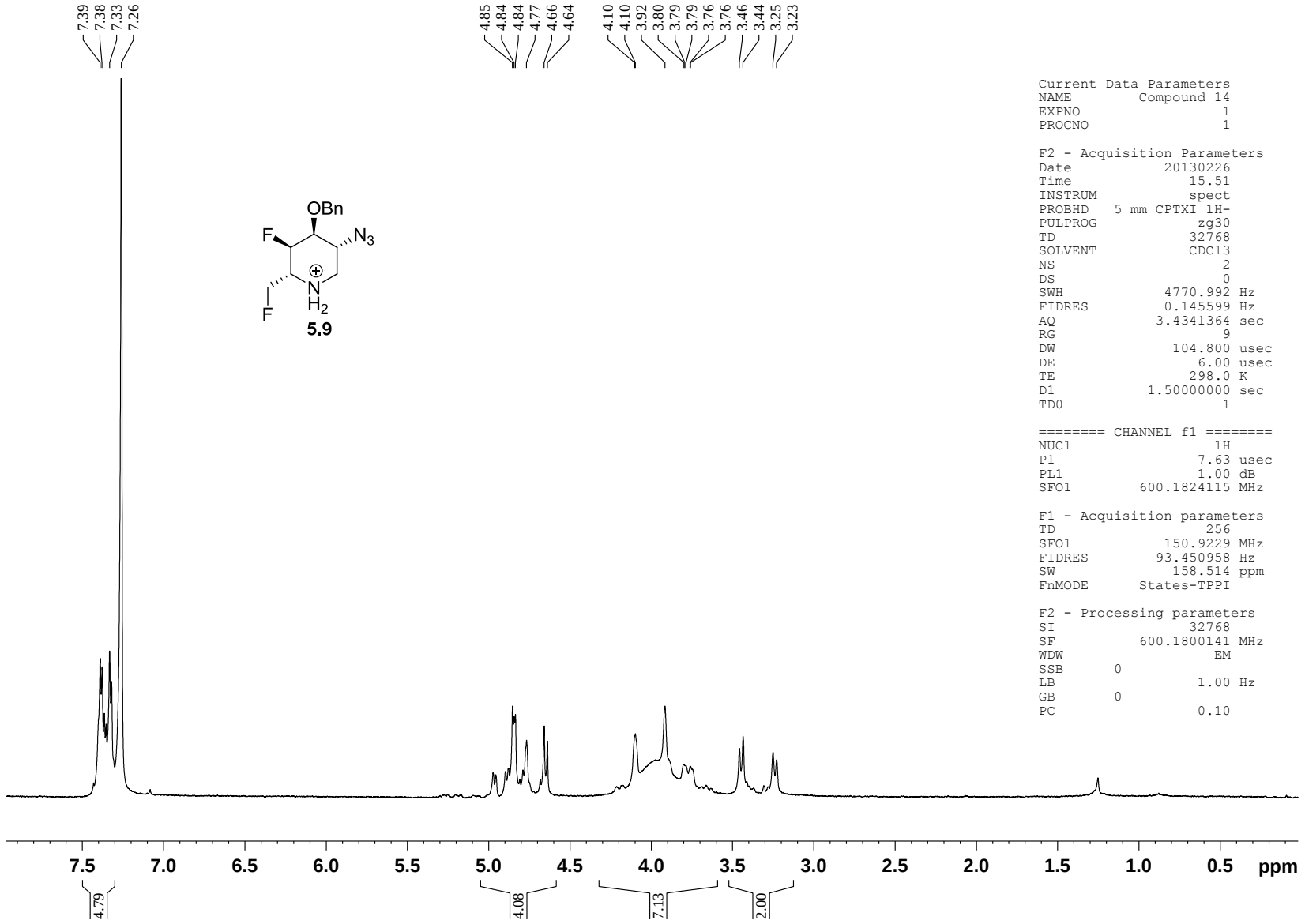


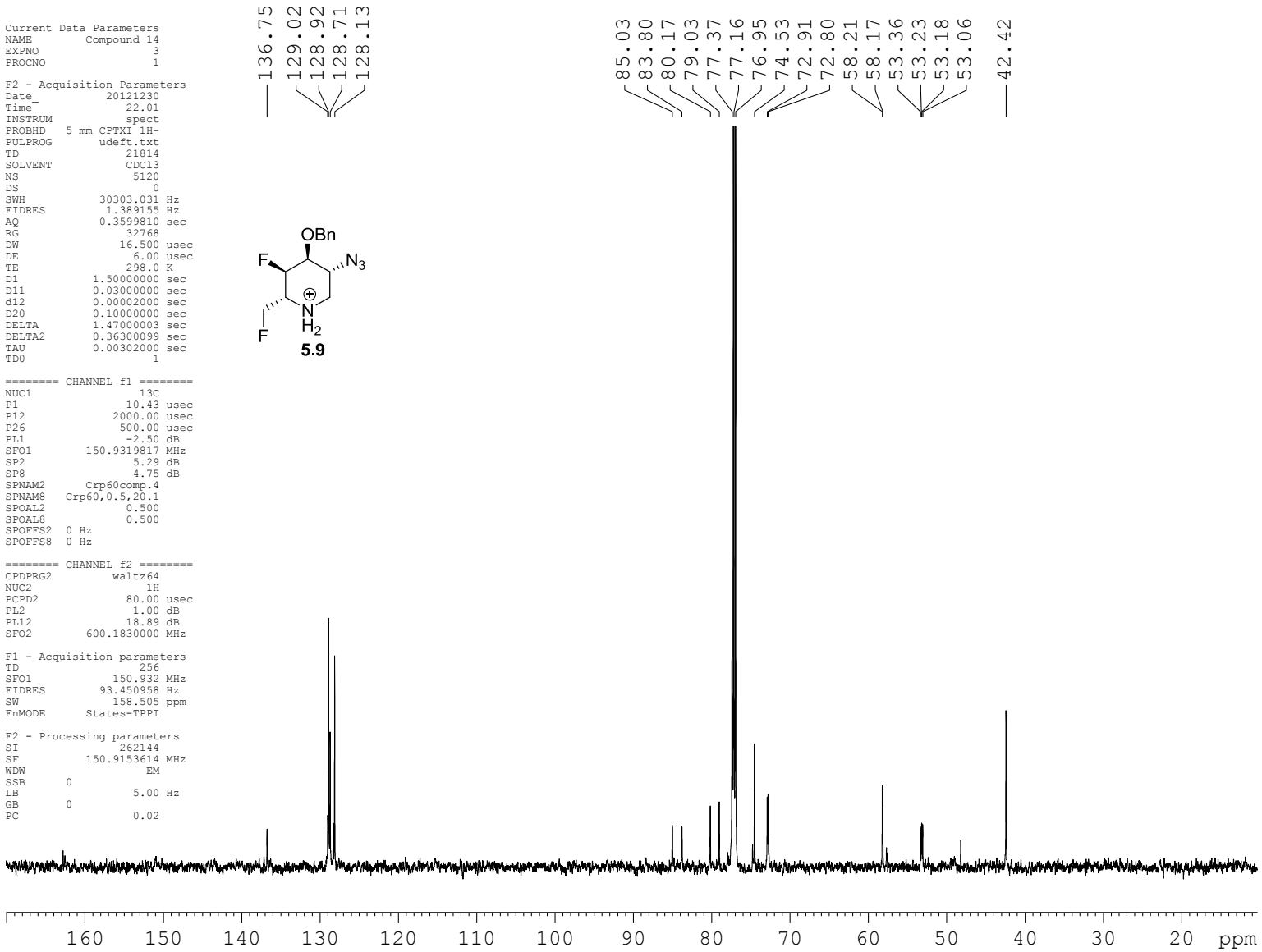
1D selective NOESY

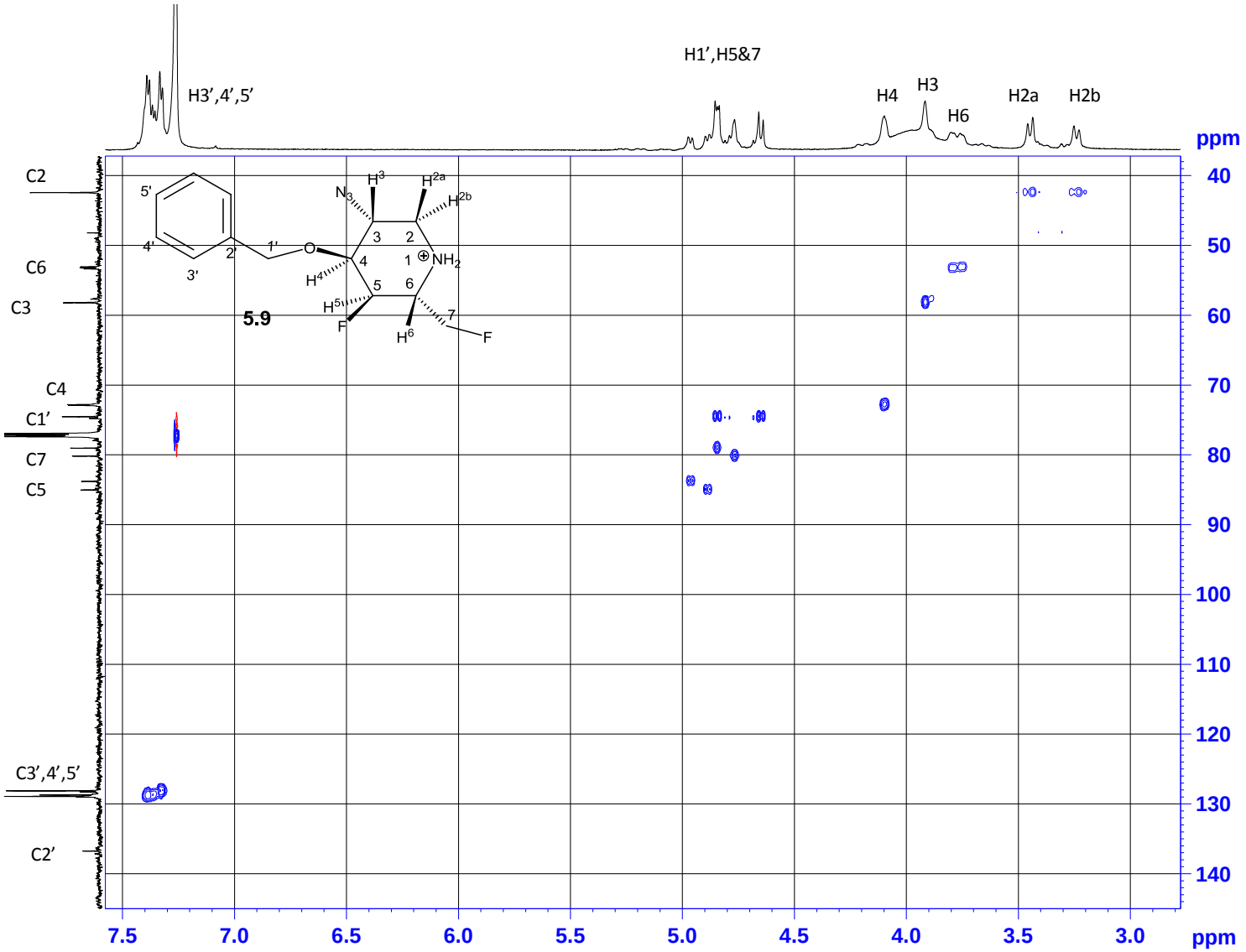


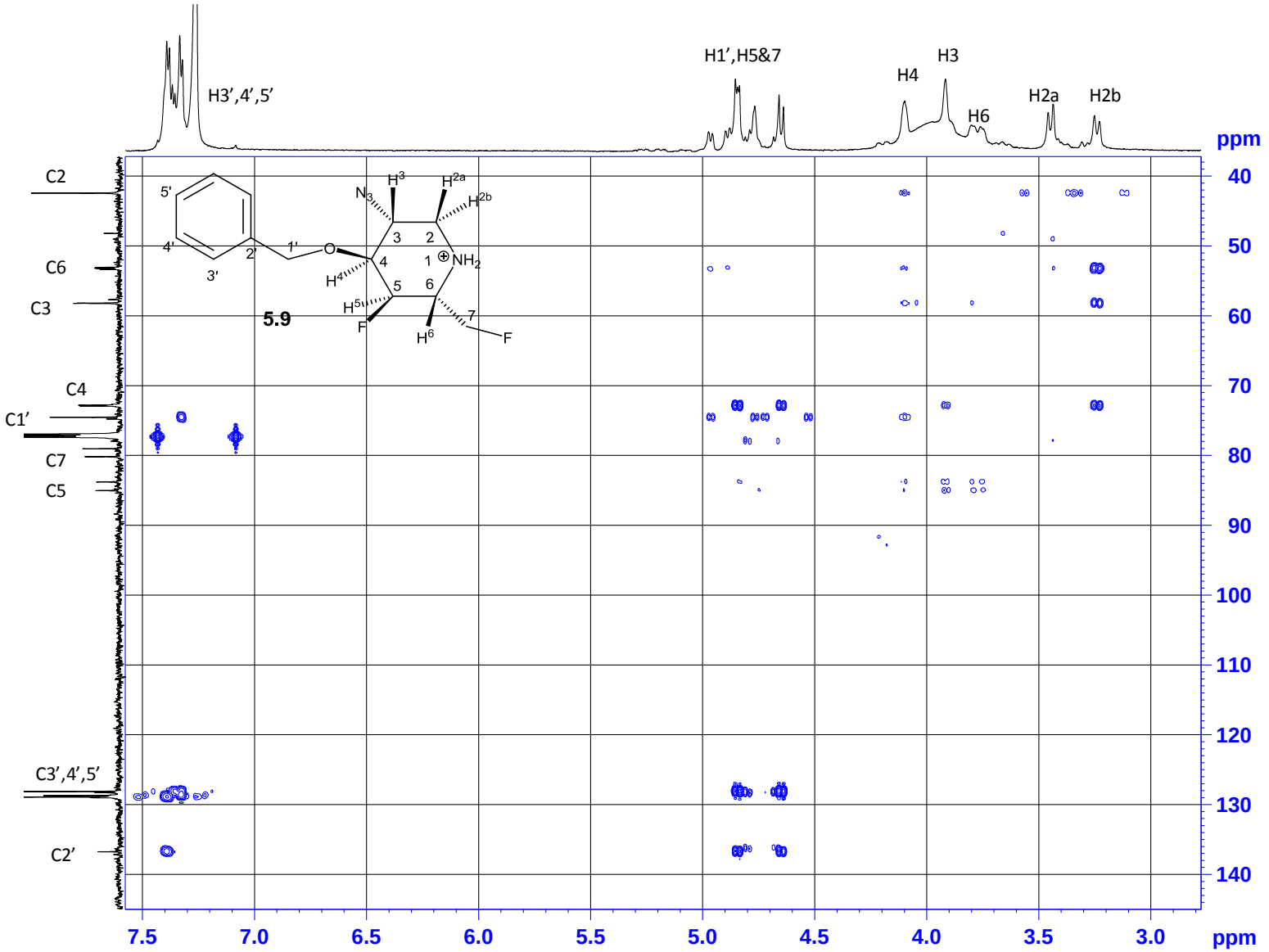
1D selective NOESY

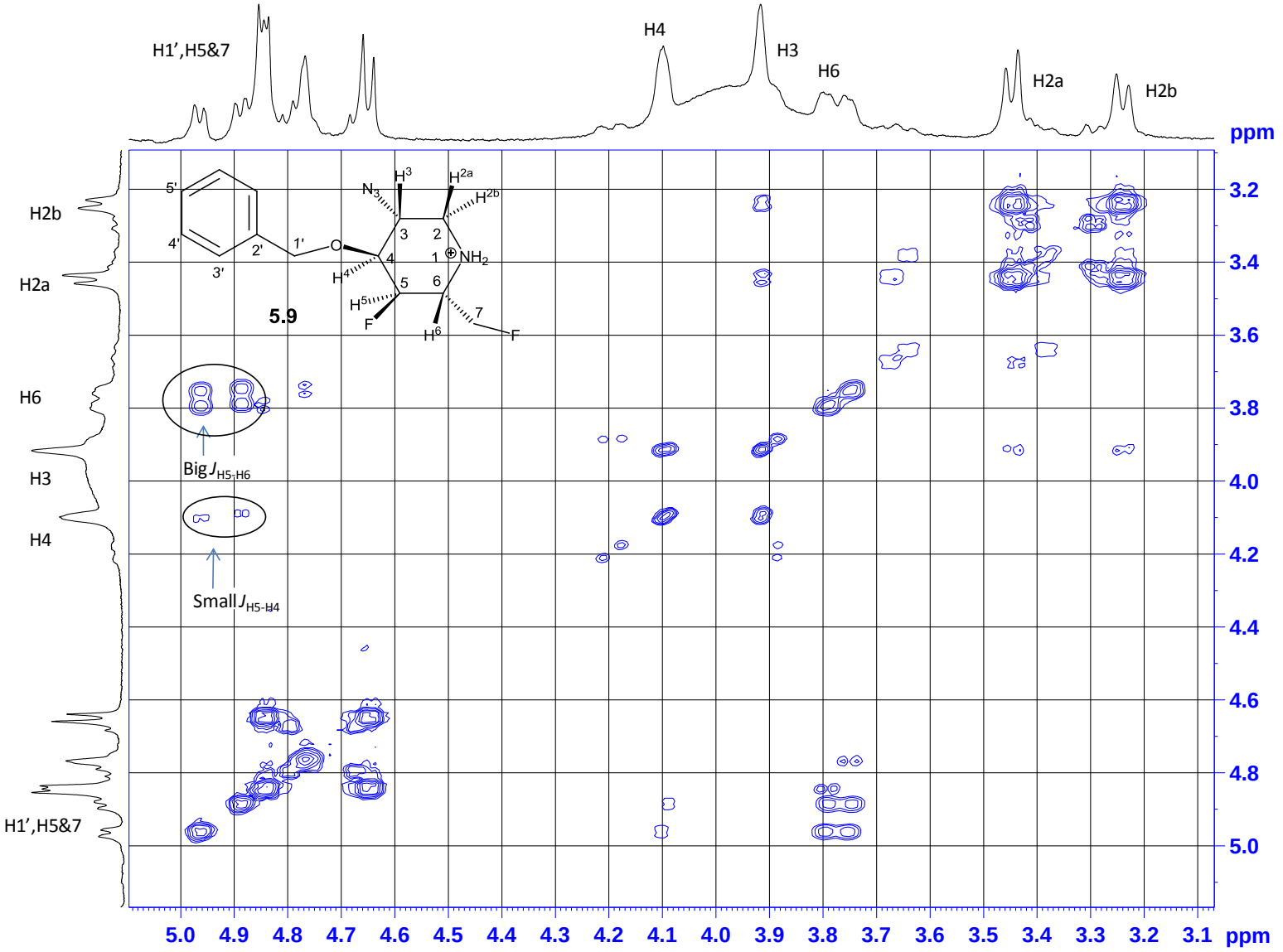


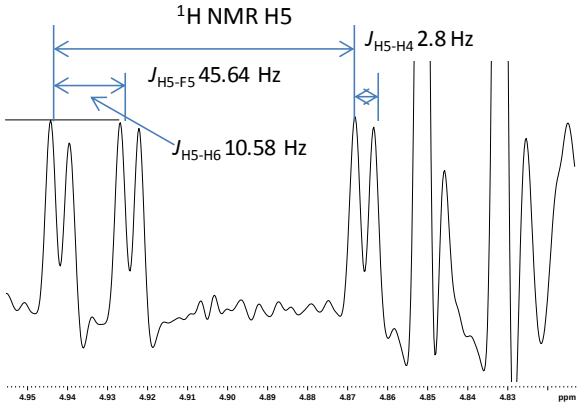

7.39
7.38
7.33
7.26
4.85
4.84
4.84
4.77
4.66
4.64
4.10
4.10
3.92
3.80
3.79
3.79
3.76
3.76
3.46
3.44
3.25
3.23
OBn
F
N3
N
H2
F
5.9
Current Data Parameters
NAME Compound 14
EXPNO 1
PROCNO 1
F2 - Acquisition Parameters
Date_ 20130226
Time 15.51
INSTRUM spect
PROBHD 5 mm CPTXI 1H-
PULPROG zg30
TD 32768
SOLVENT CDCl3
NS 2
DS 0
SWH 4770.992 Hz
FIDRES 0.145599 Hz
AQ 3.4341364 sec
RG 9
DW 104.800 usec
DE 6.00 usec
TE 298.0 K
D1 1.50000000 sec
TD0 1
======== CHANNEL f1 ========
NUC1 1H
P1 7.63 usec
PL1 1.00 dB
SFO1 600.1824115 MHz
F1 - Acquisition parameters
TD 256
SFO1 150.9229 MHz
FIDRES 93.450958 Hz
SW 158.514 ppm
FnMODE States-TPPI
F2 - Processing parameters
SI 32768
SF 600.1800141 MHz
WDW EM
SSB 0
LB 1.00 Hz
GB 0
PC 0.10
7.5
7.0
6.5
6.0
5.5
5.0
4.5
4.0
3.5
3.0
2.5
2.0
1.5
1.0
0.5
ppm
4.79
4.08
7.13
2.00

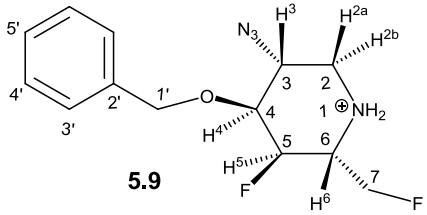

Current Data Parameters
NAME Compound 14
EXPNO 3
PROCNO 1
F2 - Acquisition Parameters
Date_ 20121230
Time 22.01
INSTRUM spect
PROBHD 5 mm CPTXI 1H-
PULPROG udeft.txt
TD 21814
SOLVENT CDC13
NS 5120
DS 0
SWH 30303.031 Hz
FIDRES 1.389155 Hz
AQ 0.3599810 sec
RG 32768
DW 16.500 usec
DE 6.00 usec
TE 298.0 K
D1 1.50000000 sec
D11 0.03000000 sec
d12 0.00002000 sec
D20 0.10000000 sec
DELTA 1.47000003 sec
DELTA2 0.36300099 sec
TAU 0.00302000 sec
TD0 1
======== CHANNEL f1 ========
NUC1 13C
P1 10.43 usec
P12 2000.00 usec
P26 500.00 usec
PL1 -2.50 dB
SFO1 150.9319817 MHz
SP2 5.29 dB
SP8 4.75 dB
SPNAM2 Crp60comp.4
SPNAM8 Crp60,0.5,20.1
SPOAL2 0.500
SPOAL8 0.500
SPOFFS2 0 Hz
SPOFFS8 0 Hz
======== CHANNEL f2 ========
CPDPRG2 waltz64
NUC2 1H
PCPD2 80.00 usec
PL2 1.00 dB
PL12 18.89 dB
SFO2 600.1830000 MHz
F1 - Acquisition parameters
TD 256
SFO1 150.932 MHz
FIDRES 93.450958 Hz
SW 158.505 ppm
FnMODE States-TPPI
F2 - Processing parameters
SI 262144
SF 150.9153614 MHz
WDW EM
SSB 0
LB 5.00 Hz
GB 0
PC 0.02
136.75
129.02
128.92
128.71
128.13
85.03
83.80
80.17
79.03
77.37
77.16
76.95
74.53
72.91
72.80
58.21
58.17
53.36
53.23
53.18
53.06
42.42
OBn
F
N3
N
H2
F
5.9
160
150
140
130
120
110
100
90
80
70
60
50
40
30
20
ppm


H3',4',5'
H1',H5&7
H4
H3
H6
H2a
H2b
ppm
C2
C6
C3
C4
C1'
C7
C5
C3',4',5'
C2'
5.9
7.5
7.0
6.5
6.0
5.5
5.0
4.5
4.0
3.5
3.0
ppm


H3',4',5'
H1',H5&7
H4
H3
H6
H2a
H2b
ppm
C2
C6
C3
C4
C1'
C7
C5
C3',4',5'
C2'
5.9
7.5
7.0
6.5
6.0
5.5
5.0
4.5
4.0
3.5
3.0
ppm

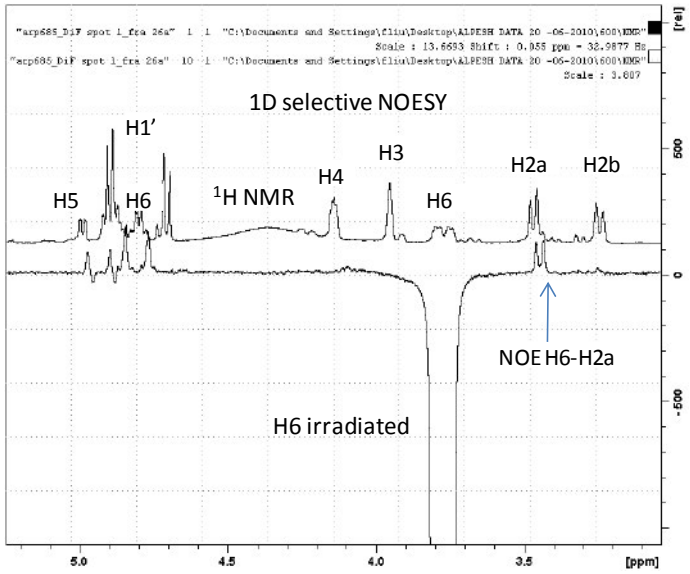

H1',H5&7
H4
H3
H6
H2a
H2b
ppm
5.9
Big J_{H5-H6}
Small J_{H5-H4}
5.0 4.9 4.8 4.7 4.6 4.5 4.4 4.3 4.2 4.1 4.0 3.9 3.8 3.7 3.6 3.5 3.4 3.3 3.2 3.1 ppm

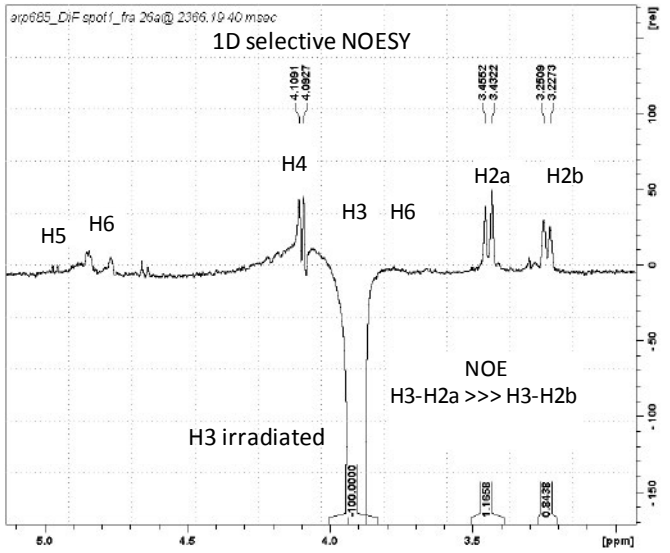


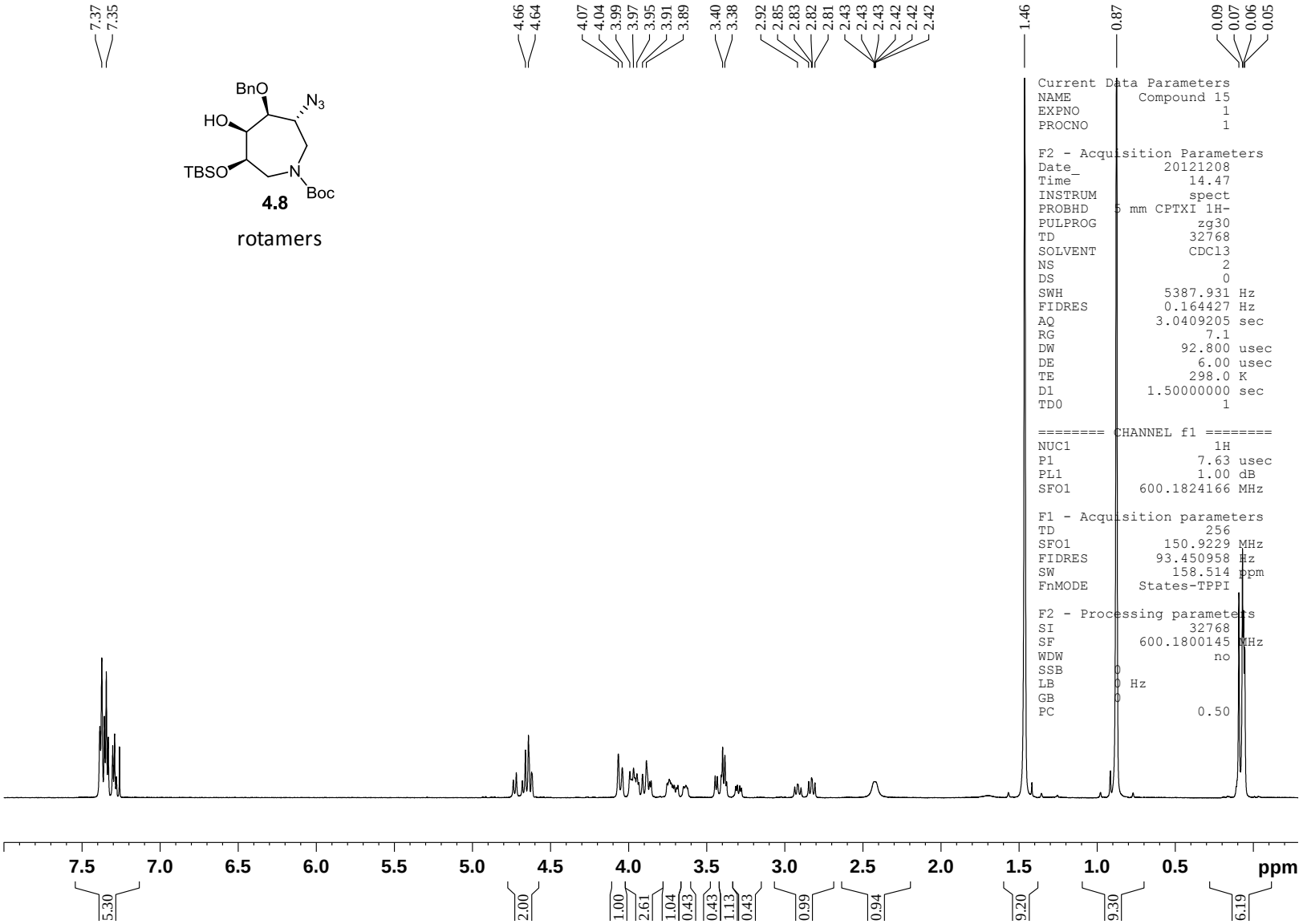


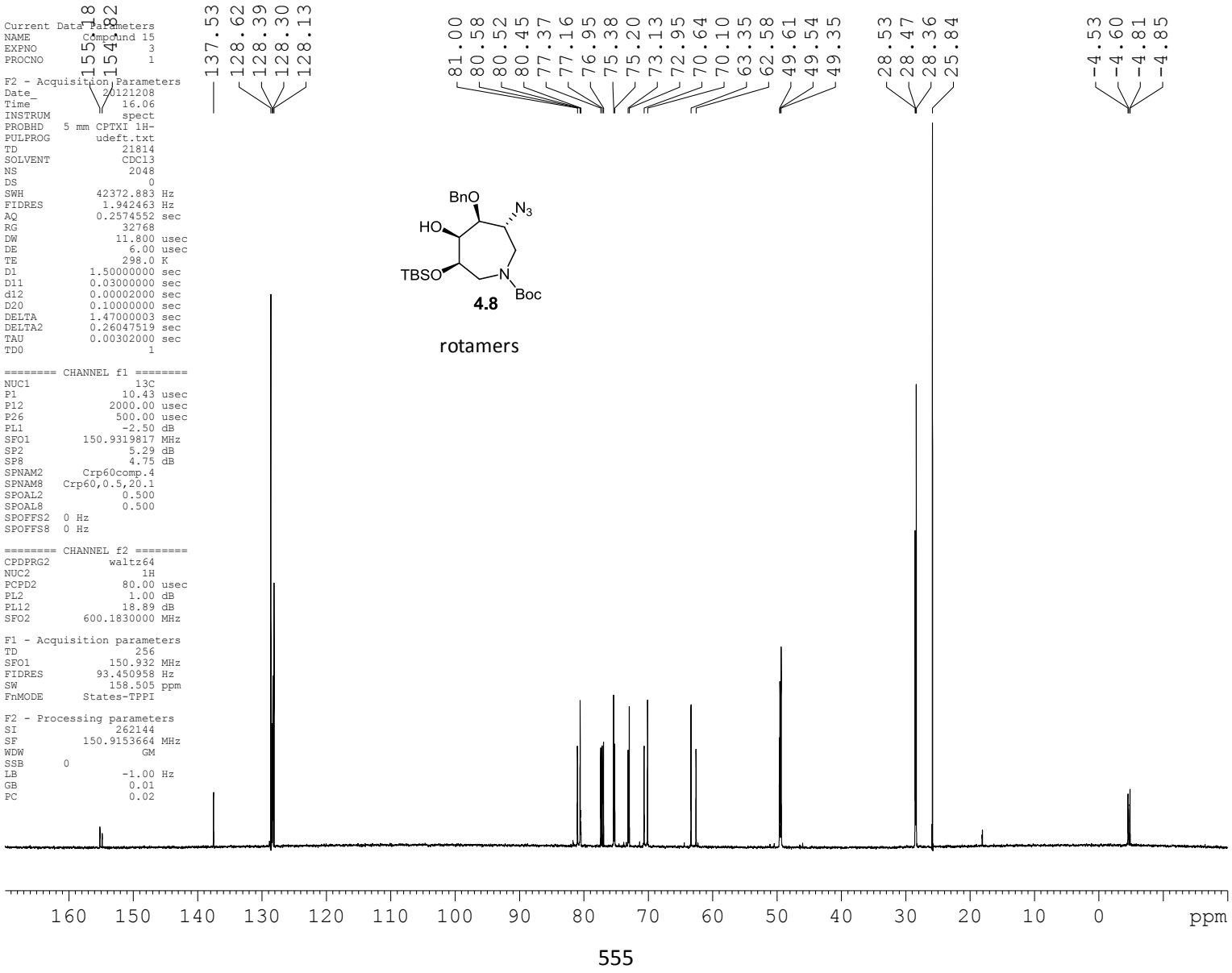
5.9

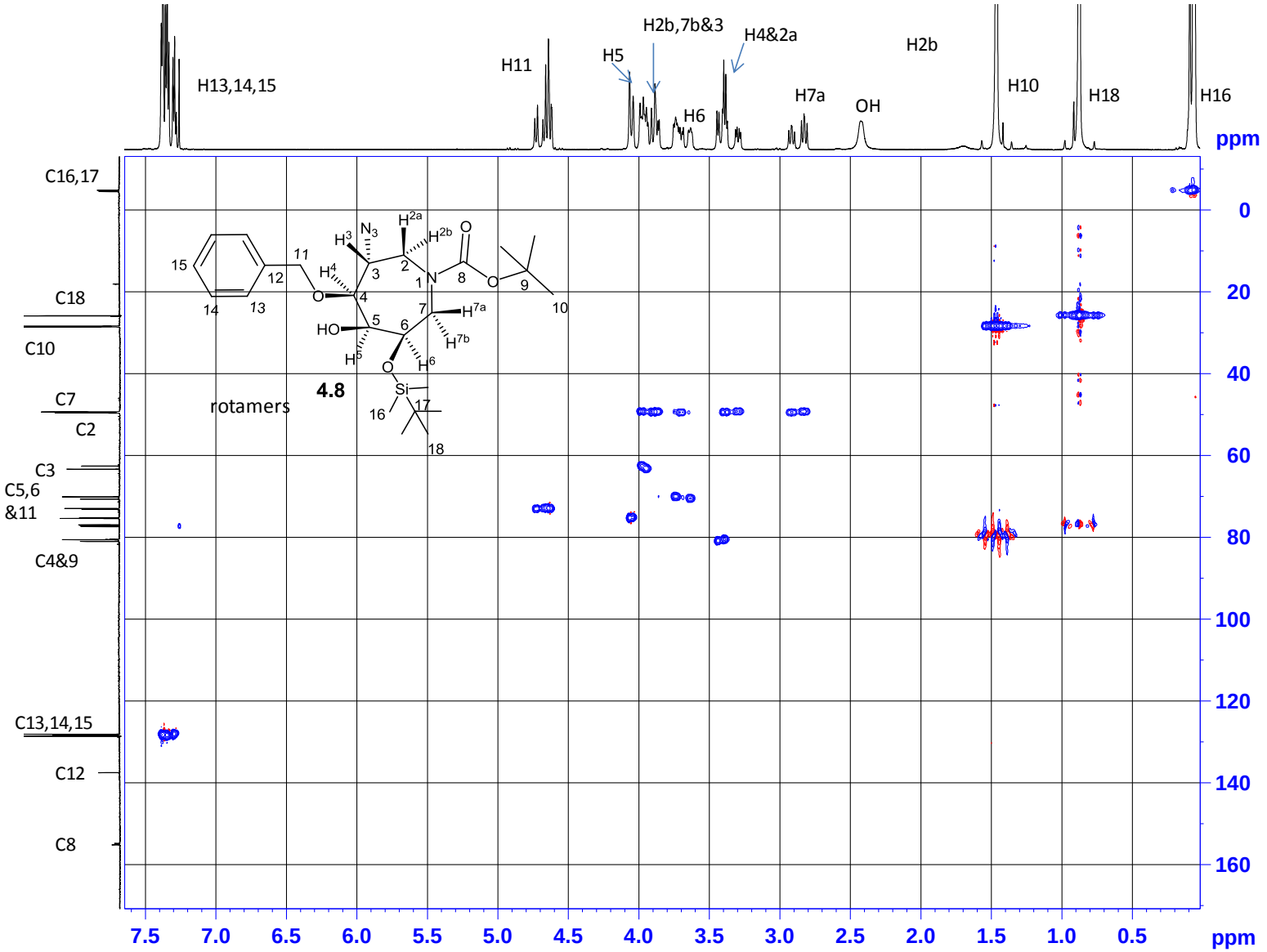
- Compound **5.9** has two stereocentres (C3, C4) having known absolute stereochemistry
- H3-H2a NOE is bigger than H3-H2b NOE suggesting H2a is *cis* and H2b is *trans* to H3.
- H6 shows NOE to H2a and no measurable NOE to H2b meaning H6 is *cis* to H3.
- J_{H5-H6} 10.58 Hz clearly suggests diaxial configuration of H5 and H6 meaning H5 is *trans* to H3. Moreover, J_{H4-H5} 2.8 Hz clearly suggests H4 and H5 are *cis*.

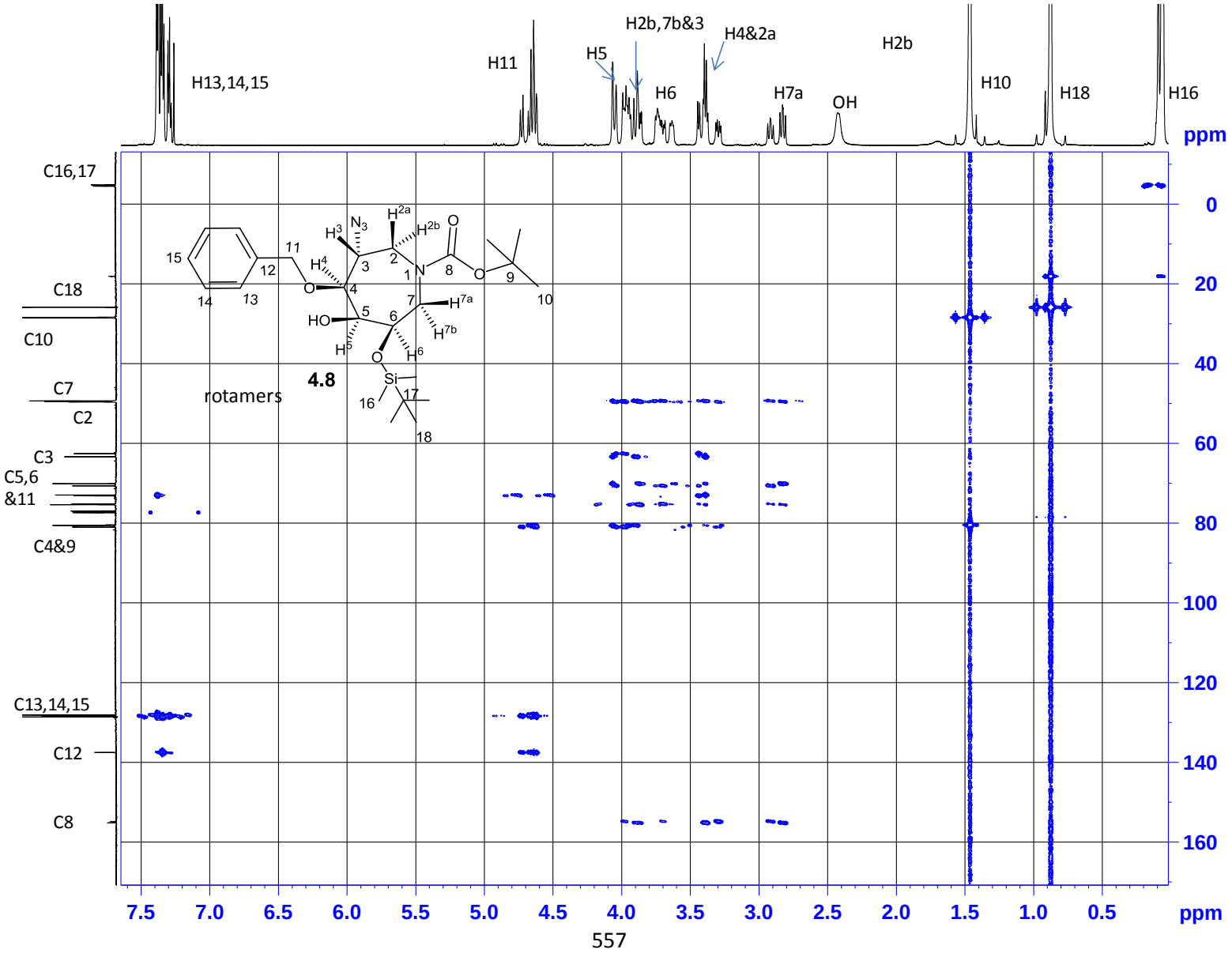


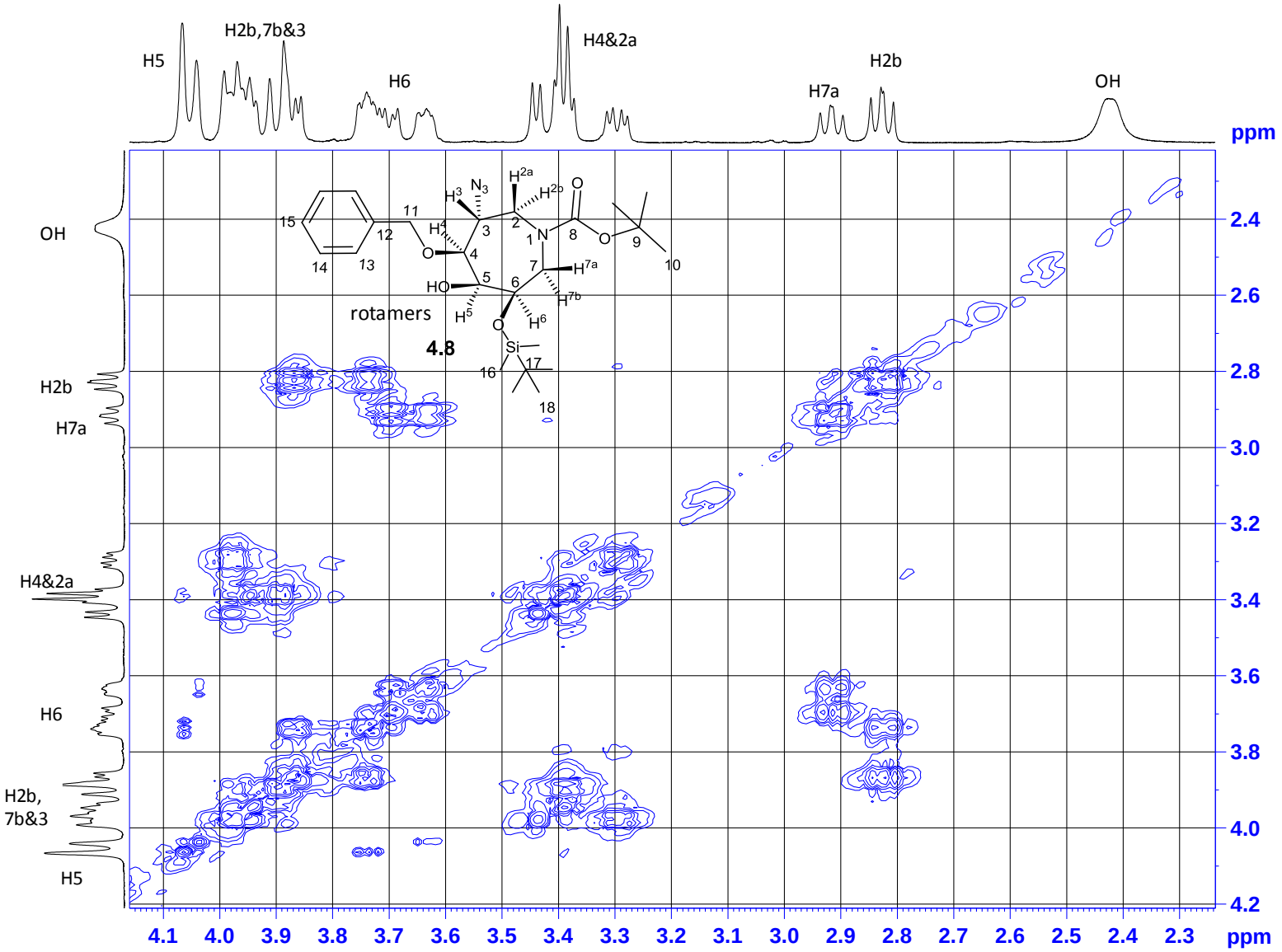


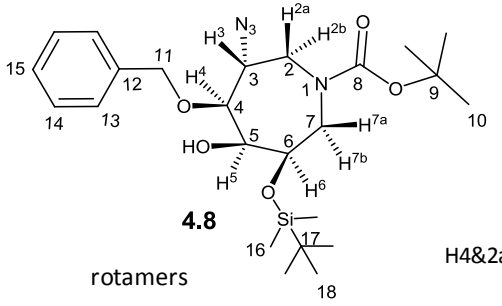

7.37
7.35
4.66
4.64
4.07
4.04
3.99
3.97
3.95
3.91
3.89
3.40
3.38
2.92
2.85
2.83
2.82
2.81
2.43
2.43
2.43
2.42
2.42
2.42
1.46
0.87
0.09
0.07
0.06
0.05
BnO
N3
HO
TBSO
N
Boc
4.8
rotamers
Current Data Parameters
NAME Compound 15
EXPNO 1
PROCNO 1
F2 - Acquisition Parameters
Date_ 20121208
Time 14.47
INSTRUM spect
PROBHD 5 mm CPTXI 1H-
PULPROG zg30
TD 32768
SOLVENT CDCl3
NS 2
DS 0
SWH 5387.931 Hz
FIDRES 0.164427 Hz
AQ 3.0409205 sec
RG 7.1
DW 92.800 usec
DE 6.00 usec
TE 298.0 K
D1 1.50000000 sec
TD0 1
======== CHANNEL f1 ========
NUC1 1H
P1 7.63 usec
PL1 1.00 dB
SFO1 600.1824166 MHz
F1 - Acquisition parameters
TD 256
SFO1 150.9229 MHz
FIDRES 93.450958 Hz
SW 158.514 ppm
FnMODE States-TPPI
F2 - Processing parameters
SI 32768
SF 600.1800145 MHz
WDW no
SSB 0
LB 0 Hz
GB 0
PC 0.50
7.5
7.0
6.5
6.0
5.5
5.0
4.5
4.0
3.5
3.0
2.5
2.0
1.5
1.0
0.5
ppm
5.30
2.00
1.00
2.61
1.04
0.43
0.43
1.13
0.43
0.99
0.94
9.20
9.30
6.19

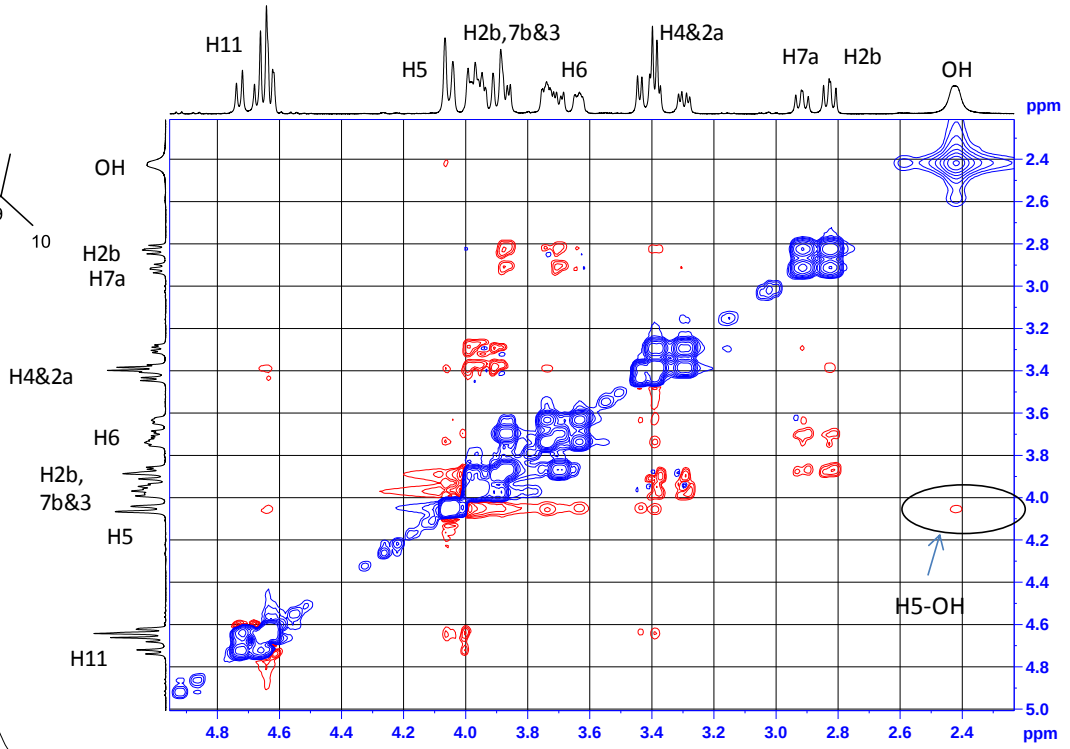

155.18
154.82
137.53
128.62
128.39
128.30
128.13
81.00
80.58
80.52
80.45
77.37
77.16
76.95
75.38
75.20
73.13
72.95
70.64
70.10
63.35
62.58
49.61
49.54
49.35
28.53
28.47
28.36
25.84
-4.53
-4.60
-4.81
-4.85
Current Data Parameters
NAME Compound 15
EXPNO 3
PROCNO 1
F2 - Acquisition Parameters
Date_ 20121208
Time 16.06
INSTRUM spect
PROBHD 5 mm CPTXI 1H-
PULPROG udeft.txt
TD 21814
SOLVENT CDCl3
NS 2048
DS 0
SWH 42372.883 Hz
FIDRES 1.942463 Hz
AQ 0.2574552 sec
RG 32768
DW 11.800 usec
DE 6.00 usec
TE 298.0 K
D1 1.50000000 sec
D11 0.03000000 sec
d12 0.00002000 sec
D20 0.10000000 sec
DELTA 1.47000003 sec
DELTA2 0.26047519 sec
TAU 0.00302000 sec
TD0 1
======== CHANNEL f1 ========
NUC1 13C
P1 10.43 usec
P12 2000.00 usec
P26 500.00 usec
PL1 -2.50 dB
SFO1 150.9319817 MHz
SP2 5.29 dB
SP8 4.75 dB
SPNAM2 Crp60comp.4
SPNAM8 Crp60,0.5,20.1
SPOAL2 0.500
SPOAL8 0.500
SPOFFS2 0 Hz
SPOFFS8 0 Hz
======== CHANNEL f2 ========
CPDPRG2 waltz64
NUC2 1H
PCPD2 80.00 usec
PL2 1.00 dB
PL12 18.89 dB
SFO2 600.1830000 MHz
F1 - Acquisition parameters
TD 256
SFO1 150.932 MHz
FIDRES 93.450958 Hz
SW 158.505 ppm
FnMODE States-TPPI
F2 - Processing parameters
SI 262144
SF 150.9153664 MHz
WDW GM
SSB 0
LB -1.00 Hz
GB 0.01
PC 0.02
BnO
N3
HO
TBSO
N
Boc
4.8
rotamers
160
150
140
130
120
110
100
90
80
70
60
50
40
30
20
10
0
ppm

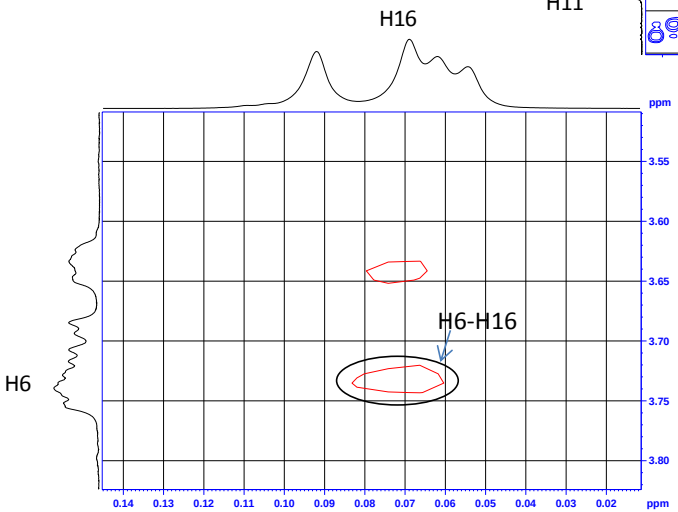

H13,14,15
H11
H5
H2b,7b&3
H4&2a
H6
H7a
OH
H2b
H10
H18
H16
ppm
C16,17
C18
C10
C7
C2
C3
C5,6
&11
C4&9
C13,14,15
C12
C8
rotamers
4.8
0
20
40
60
80
100
120
140
160
7.5
7.0
6.5
6.0
5.5
5.0
4.5
4.0
3.5
3.0
2.5
2.0
1.5
1.0
0.5
ppm

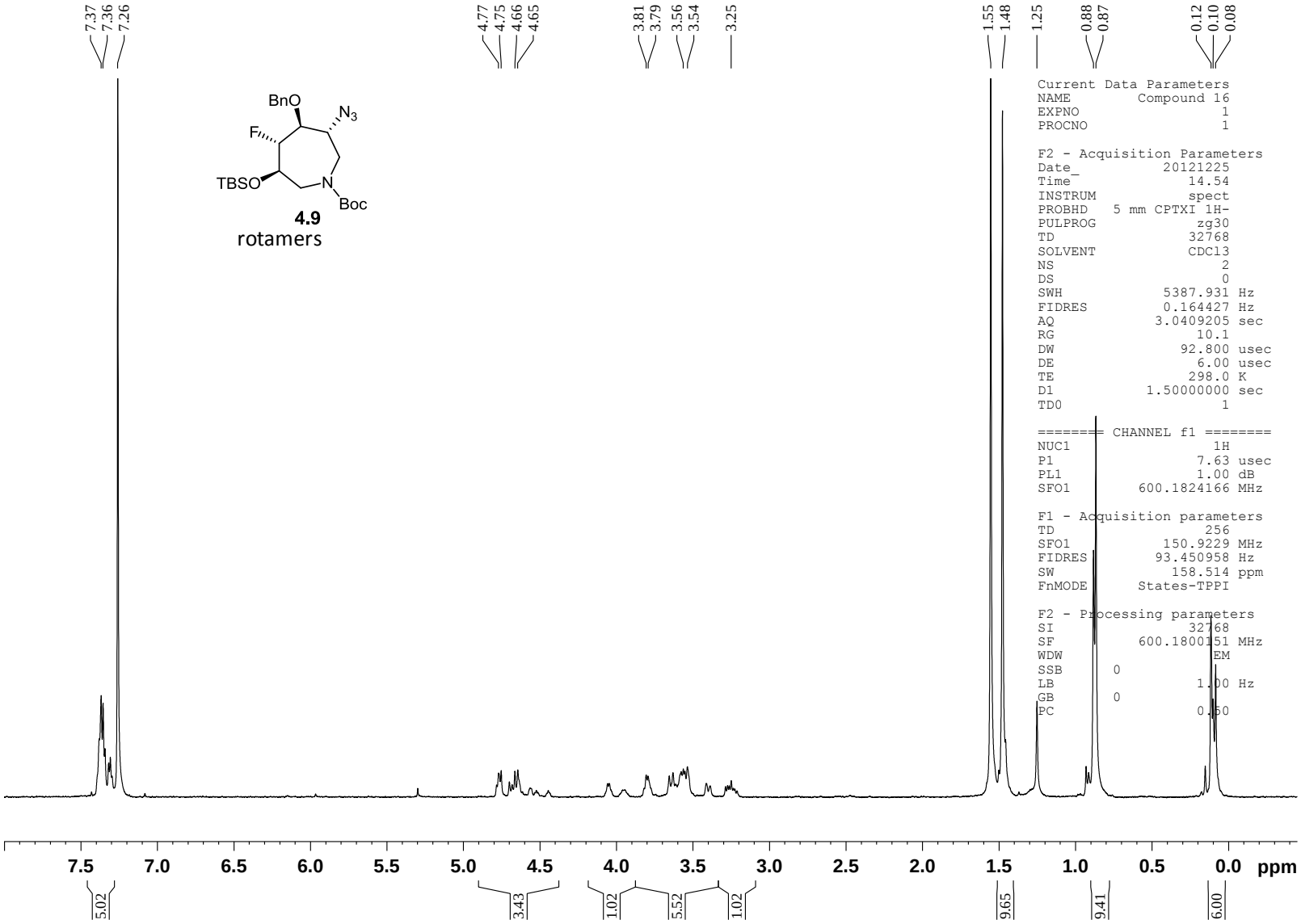

H13,14,15
H11
H5
H2b,7b&3
H4&2a
H6
H7a
OH
H2b
H10
H18
H16
ppm
C16,17
C18
C10
C7
C2
C3
C5,6
&11
C4&9
C13,14,15
C12
C8
rotamers
4.8
0
20
40
60
80
100
120
140
160
7.5
7.0
6.5
6.0
5.5
5.0
4.5
4.0
3.5
3.0
2.5
2.0
1.5
1.0
0.5
ppm

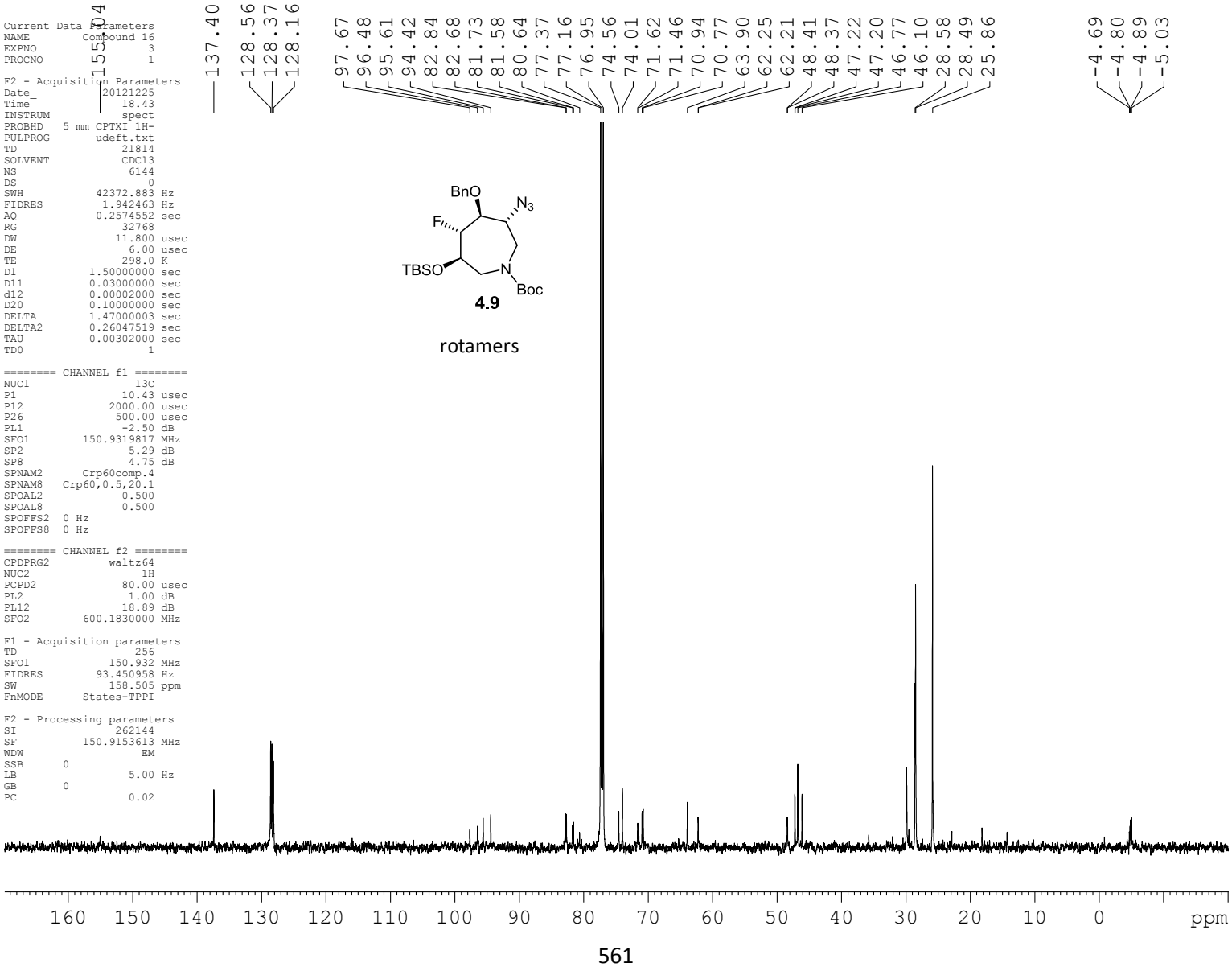

H5
H2b,7b&3
H6
H4&2a
H7a
H2b
OH
ppm
OH
H2b
H7a
H4&2a
H6
H2b,
7b&3
H5
rotamers
4.8
4.1 4.0 3.9 3.8 3.7 3.6 3.5 3.4 3.3 3.2 3.1 3.0 2.9 2.8 2.7 2.6 2.5 2.4 2.3 ppm
2.4 2.6 2.8 3.0 3.2 3.4 3.6 3.8 4.0 4.2

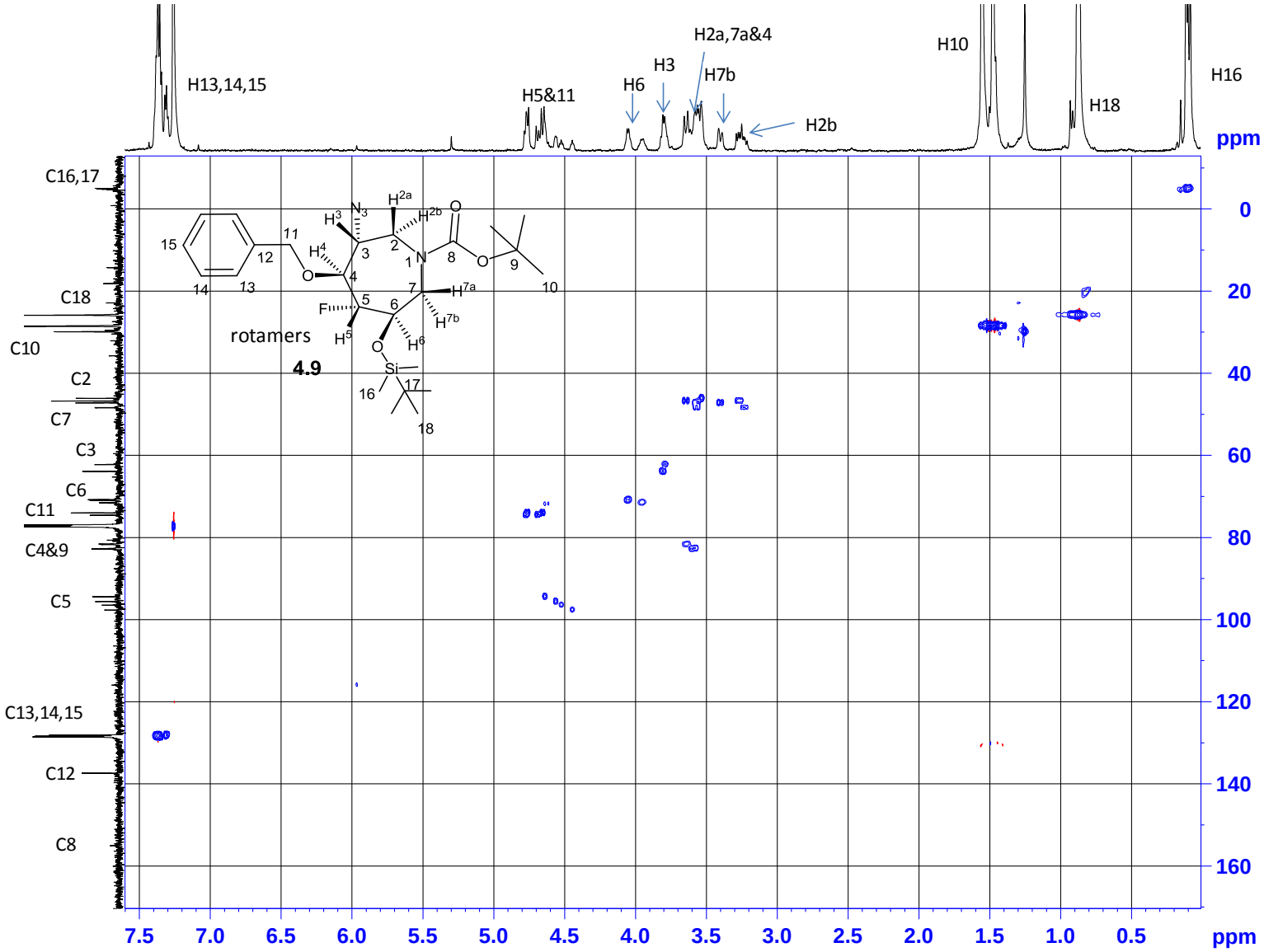

4.8
rotamers

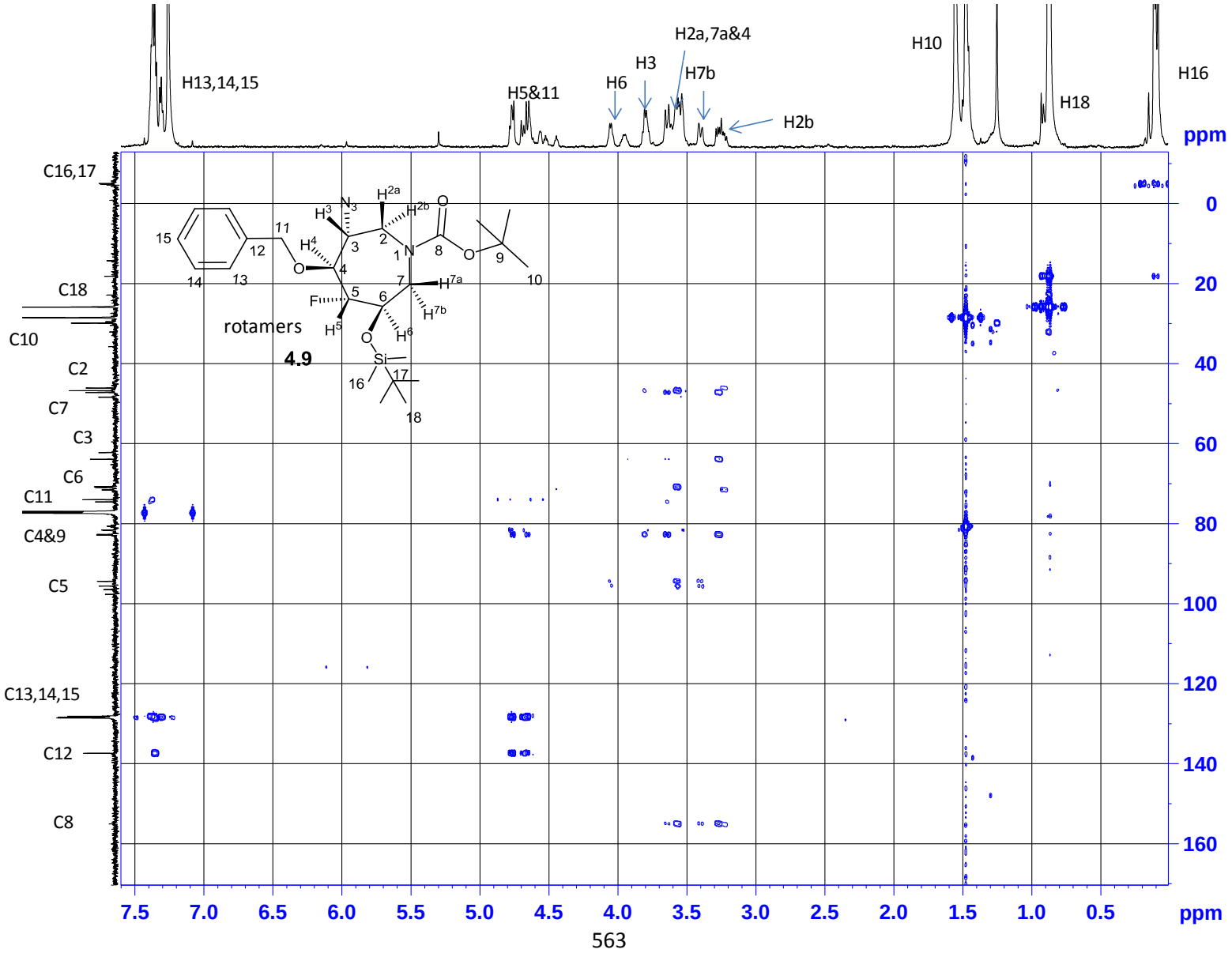

H11
H5
H2b,7b&3
H6
H4&2a
H7a
H2b
OH
OH
H2b
H7a
H4&2a
H6
H2b,
7b&3
H5
H11
H5-OH
ppm

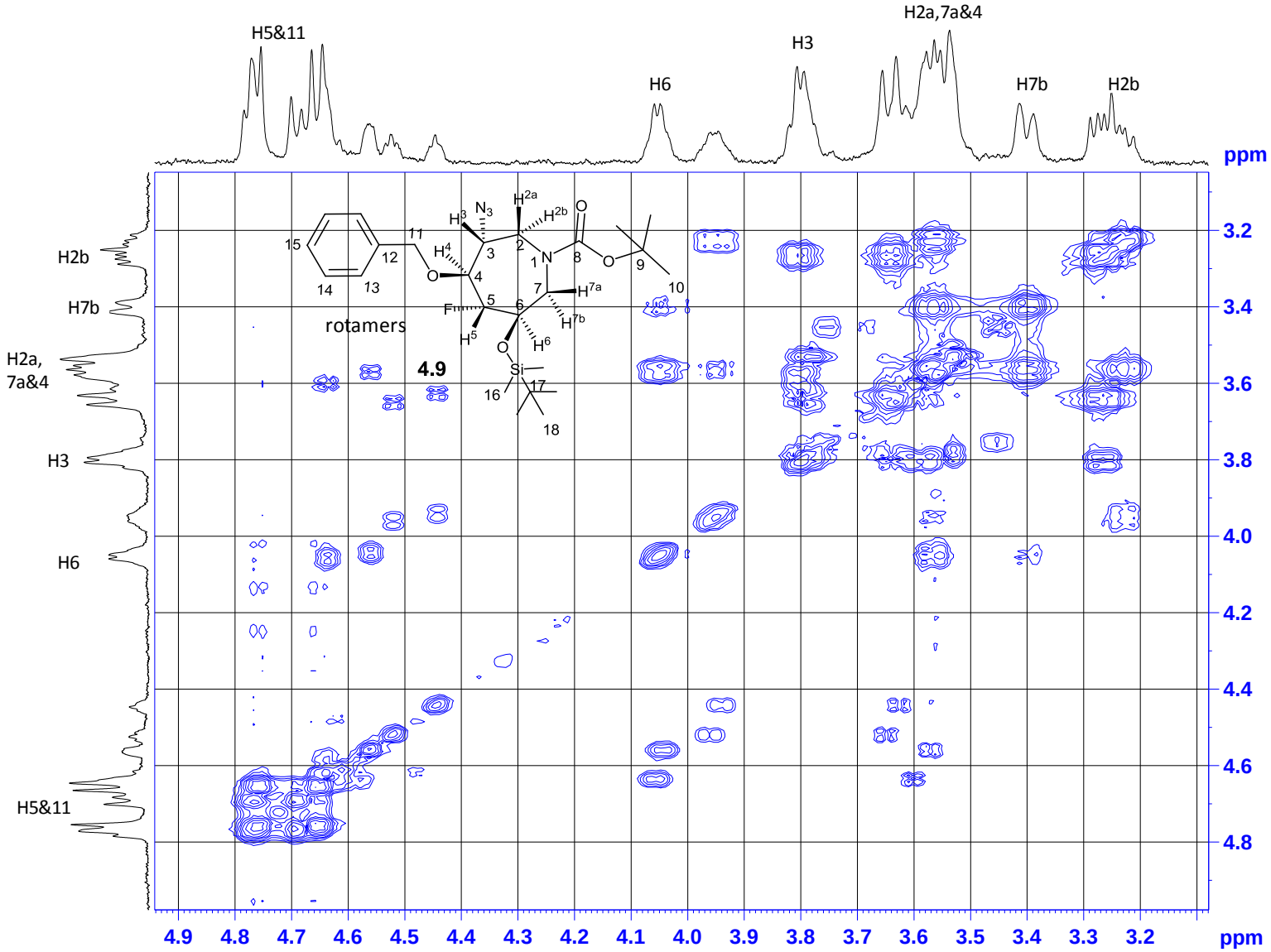

H16
H6
H6-H16
ppm

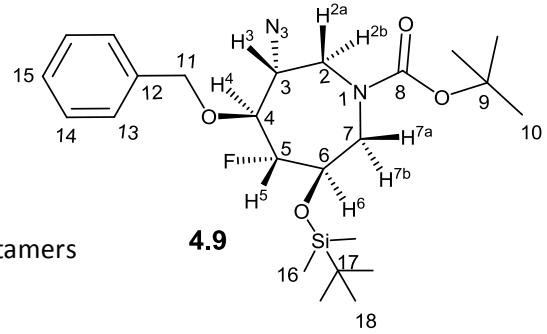

7.37
7.36
7.26
4.77
4.75
4.66
4.65
3.81
3.79
3.56
3.54
3.25
1.55
1.48
1.25
0.88
0.87
0.12
0.10
0.08
BnO
N3
F
TBSO
N
Boc
4.9
rotamers
Current Data Parameters
NAME Compound 16
EXPNO 1
PROCNO 1
F2 - Acquisition Parameters
Date_ 20121225
Time 14.54
INSTRUM spect
PROBHD 5 mm CPTXI 1H-
PULPROG zg30
TD 32768
SOLVENT CDCl3
NS 2
DS 0
SWH 5387.931 Hz
FIDRES 0.164427 Hz
AQ 3.0409205 sec
RG 10.1
DW 92.800 usec
DE 6.00 usec
TE 298.0 K
D1 1.50000000 sec
TD0 1
======== CHANNEL f1 ========
NUC1 1H
P1 7.63 usec
PL1 1.00 dB
SFO1 600.1824166 MHz
F1 - Acquisition parameters
TD 256
SFO1 150.9229 MHz
FIDRES 93.450958 Hz
SW 158.514 ppm
FnMODE States-TPPI
F2 - Processing parameters
SI 32768
SF 600.1800151 MHz
WDW EM
SSB 0
LB 1.00 Hz
GB 0
PC 0.50
7.5
7.0
6.5
6.0
5.5
5.0
4.5
4.0
3.5
3.0
2.5
2.0
1.5
1.0
0.5
0.0
ppm
5.02
3.43
1.02
5.52
1.02
9.65
9.41
6.00


155.04
137.40
128.56
128.37
128.16
97.67
96.48
95.61
94.42
82.84
82.68
81.73
81.58
80.64
77.37
77.16
76.95
74.56
74.01
71.62
71.46
70.94
70.77
63.90
62.25
62.21
48.41
48.37
47.22
47.20
46.77
46.10
28.58
28.49
25.86
-4.69
-4.80
-4.89
-5.03
BnO
N3
F
TBSO
N
Boc
4.9
rotamers
Current Data Parameters
NAME Compound 16
EXPNO 3
PROCNO 1
F2 - Acquisition Parameters
Date_ 20121225
Time 18.43
INSTRUM spect
PROBHD 5 mm CPTXI 1H-
PULPROG udeft.txt
TD 21814
SOLVENT CDC13
NS 6144
DS 0
SWH 42372.883 Hz
FIDRES 1.942463 Hz
AQ 0.2574552 sec
RG 32768
DW 11.800 usec
DE 6.00 usec
TE 298.0 K
D1 1.50000000 sec
D11 0.03000000 sec
d12 0.00002000 sec
D20 0.10000000 sec
DELTA 1.47000003 sec
DELTA2 0.26047519 sec
TAU 0.00302000 sec
TD0 1
======== CHANNEL f1 ========
NUC1 13C
P1 10.43 usec
P12 2000.00 usec
P26 500.00 usec
PL1 -2.50 dB
SFO1 150.9319817 MHz
SP2 5.29 dB
SP8 4.75 dB
SPNAM2 Crp60comp.4
SPNAM8 Crp60,0.5,20.1
SPOAL2 0.500
SPOAL8 0.500
SPOFFS2 0 Hz
SPOFFS8 0 Hz
======== CHANNEL f2 ========
CPDPRG2 waltz64
NUC2 1H
PCPD2 80.00 usec
PL2 1.00 dB
PL12 18.89 dB
SFO2 600.1830000 MHz
F1 - Acquisition parameters
TD 256
SFO1 150.932 MHz
FIDRES 93.450958 Hz
SW 158.505 ppm
FnMODE States-TPPI
F2 - Processing parameters
SI 262144
SF 150.9153613 MHz
WDW EM
SSB 0
LB 5.00 Hz
GB 0
PC 0.02
160 150 140 130 120 110 100 90 80 70 60 50 40 30 20 10 0 ppm

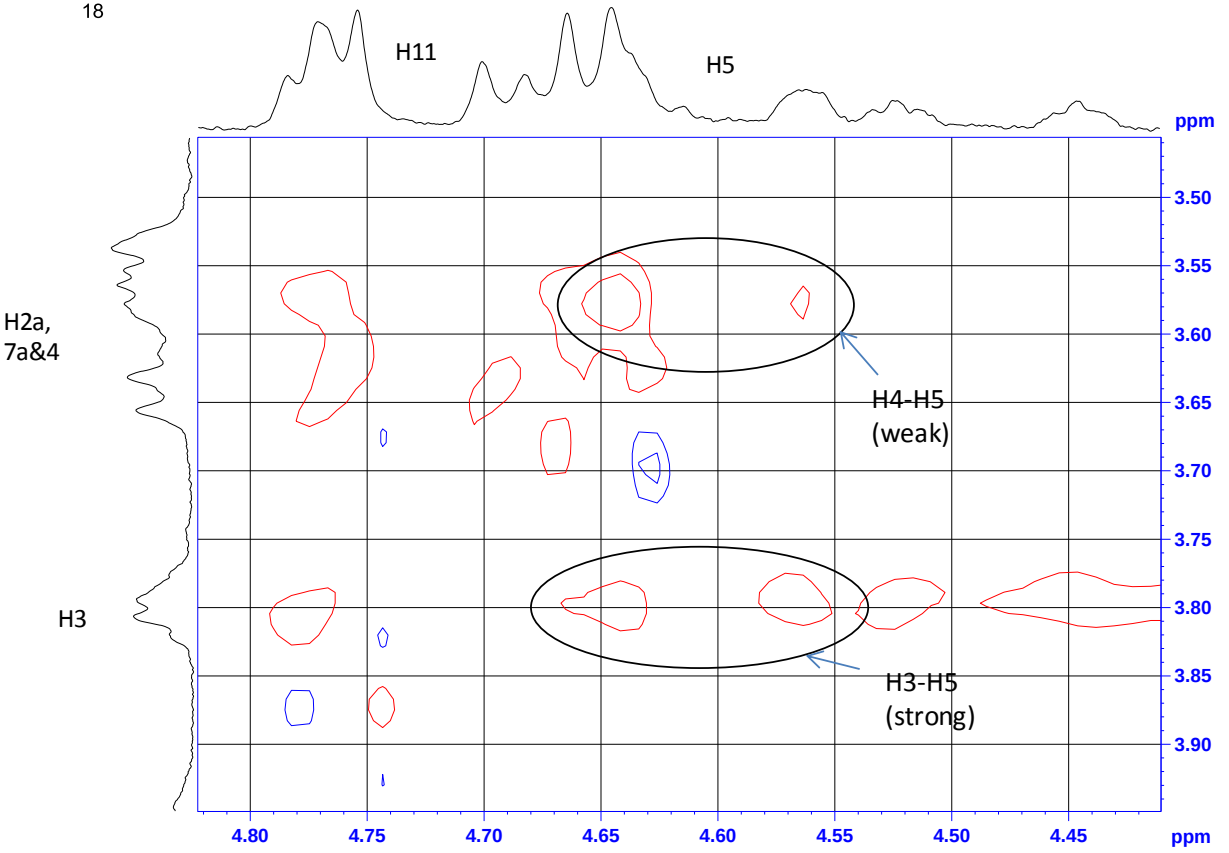

H13,14,15
H5&11
H6
H3
H2a,7a&4
H7b
H2b
H10
H18
H16
ppm
C16,17
C18
C10
C2
C7
C3
C6
C11
C4&9
C5
C13,14,15
C12
C8
rotamers
4.9
0
20
40
60
80
100
120
140
160
7.5
7.0
6.5
6.0
5.5
5.0
4.5
4.0
3.5
3.0
2.5
2.0
1.5
1.0
0.5
ppm

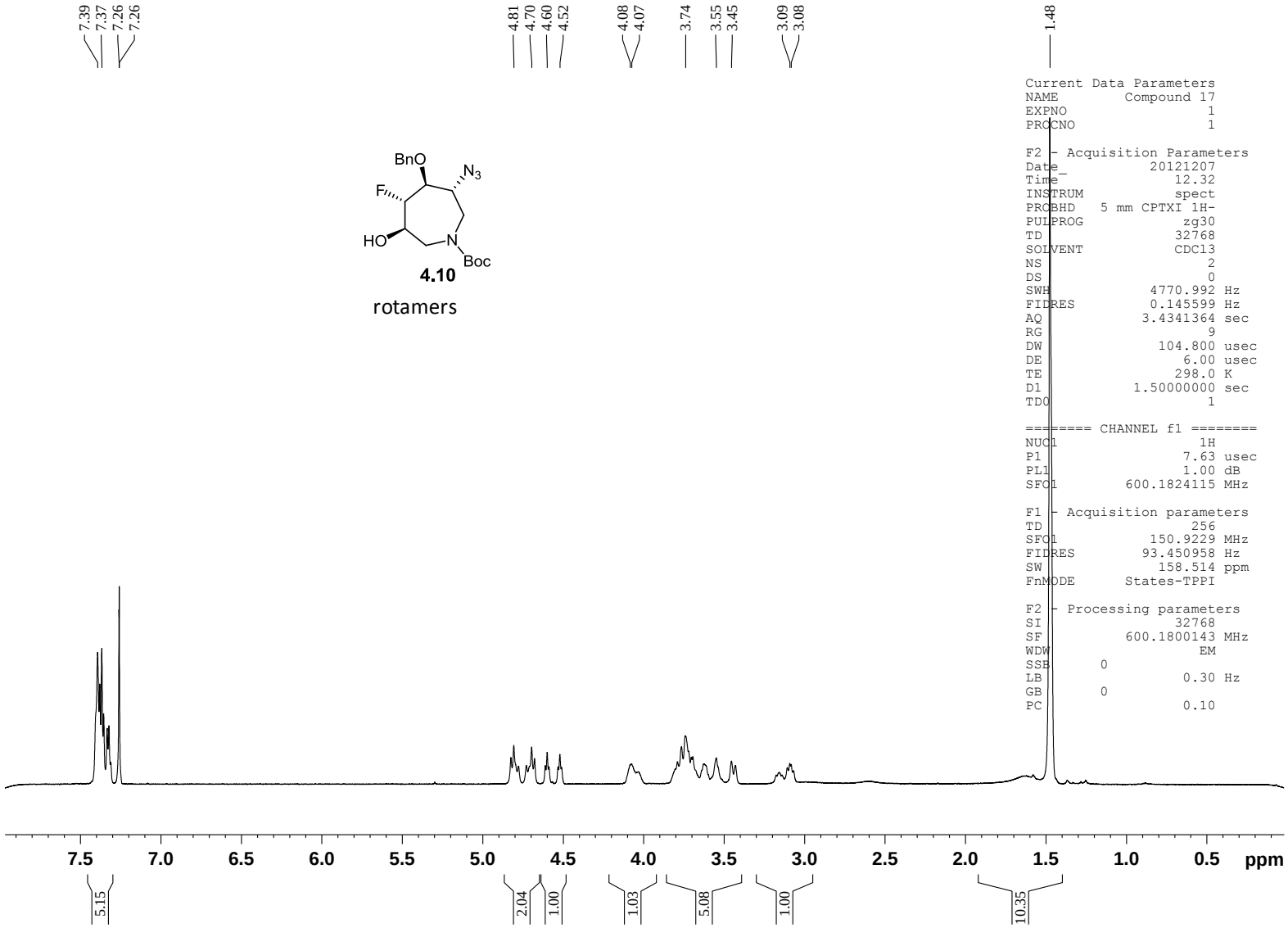

H13,14,15
H5&11
H6
H3
H2a,7a&4
H7b
H2b
H10
H18
H16
ppm
C16,17
C18
C10
C2
C7
C3
C6
C11
C4&9
C5
C13,14,15
C12
C8
rotamers
4.9
0
20
40
60
80
100
120
140
160
7.5
7.0
6.5
6.0
5.5
5.0
4.5
4.0
3.5
3.0
2.5
2.0
1.5
1.0
0.5
ppm

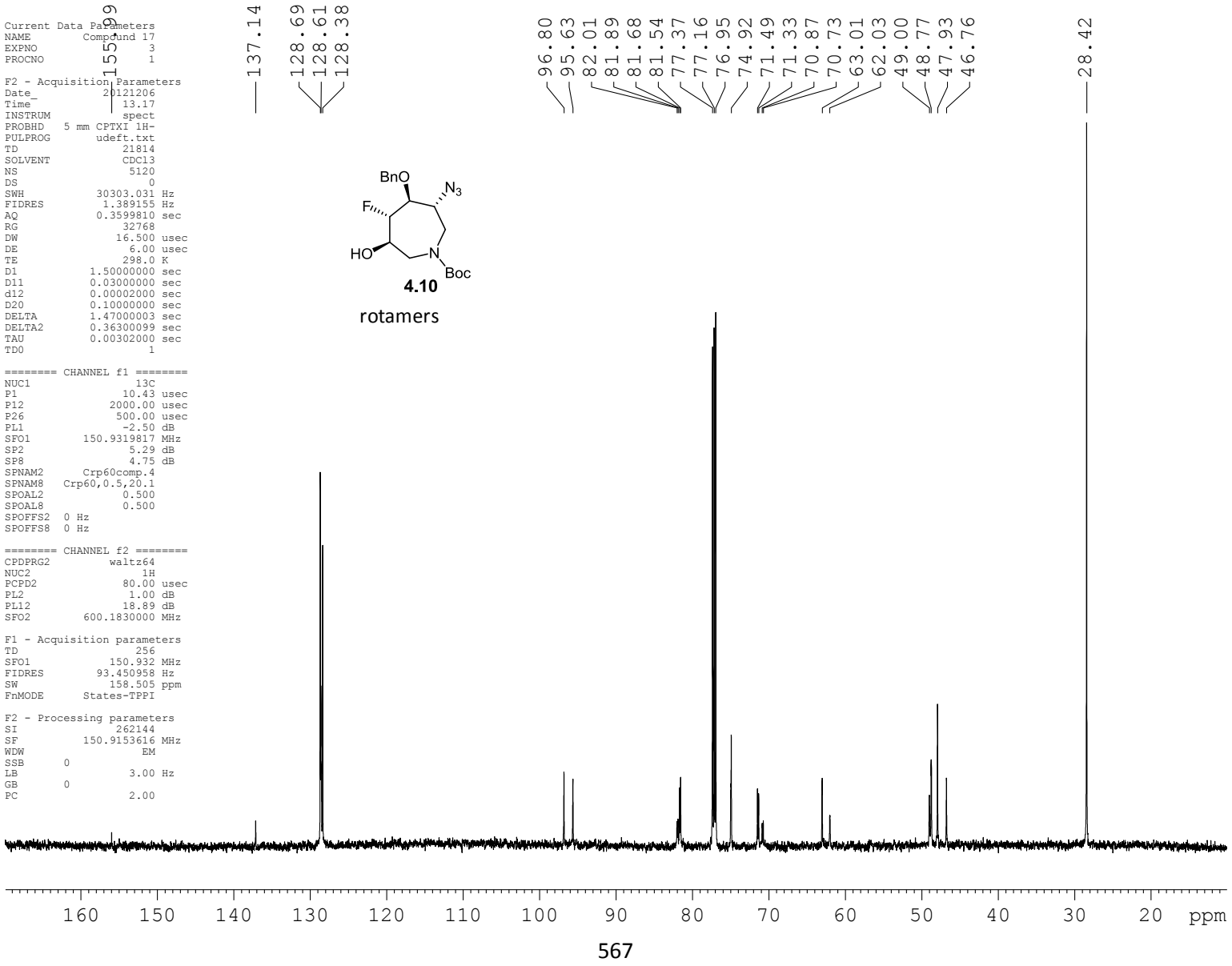

H5&11
H6
H3
H2a,7a&4
H7b
H2b
ppm
H2b
H7b
H2a,
7a&4
H3
H6
H5&11
rotamers
4.9
3.2
3.4
3.6
3.8
4.0
4.2
4.4
4.6
4.8
4.9 4.8 4.7 4.6 4.5 4.4 4.3 4.2 4.1 4.0 3.9 3.8 3.7 3.6 3.5 3.4 3.3 3.2
ppm

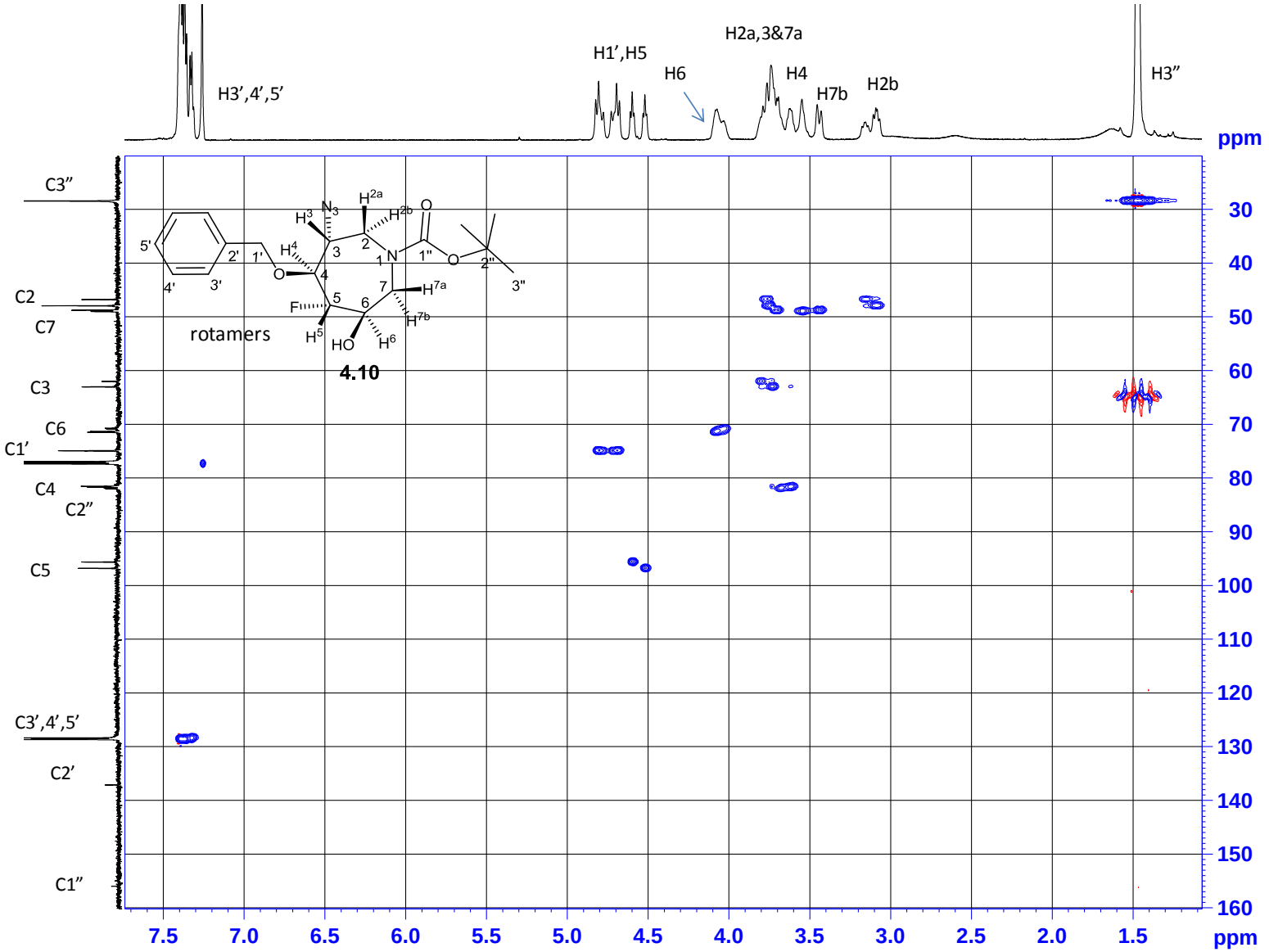

H2a
N3
H3
H2b
O
15
11
12
H4
3
2
1
N
8
O
9
10
14
13
O
4
7
H7a
F
5
6
H7b
H5
H6
O
Si
16
17
18

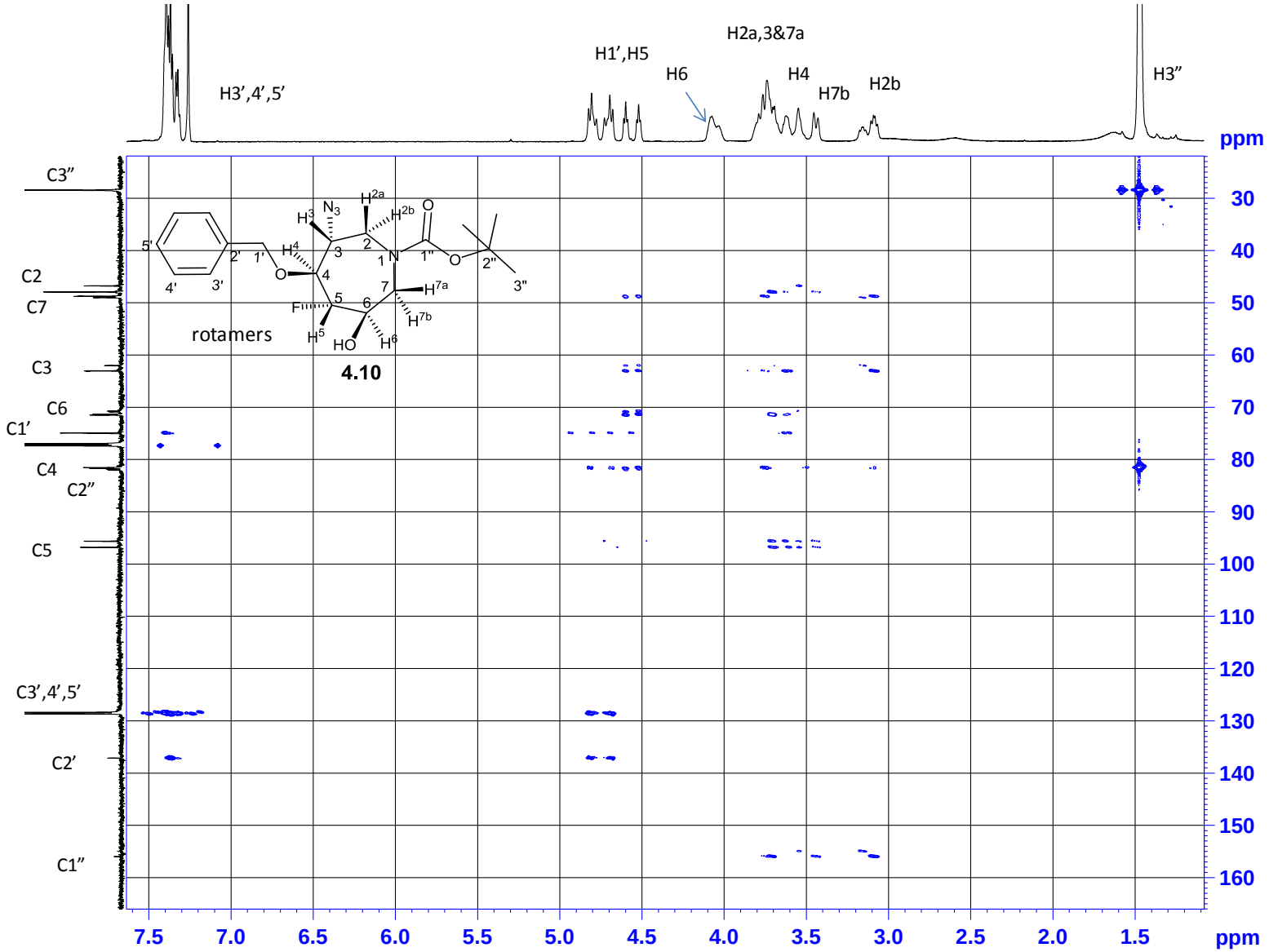
rotamers **4.9**

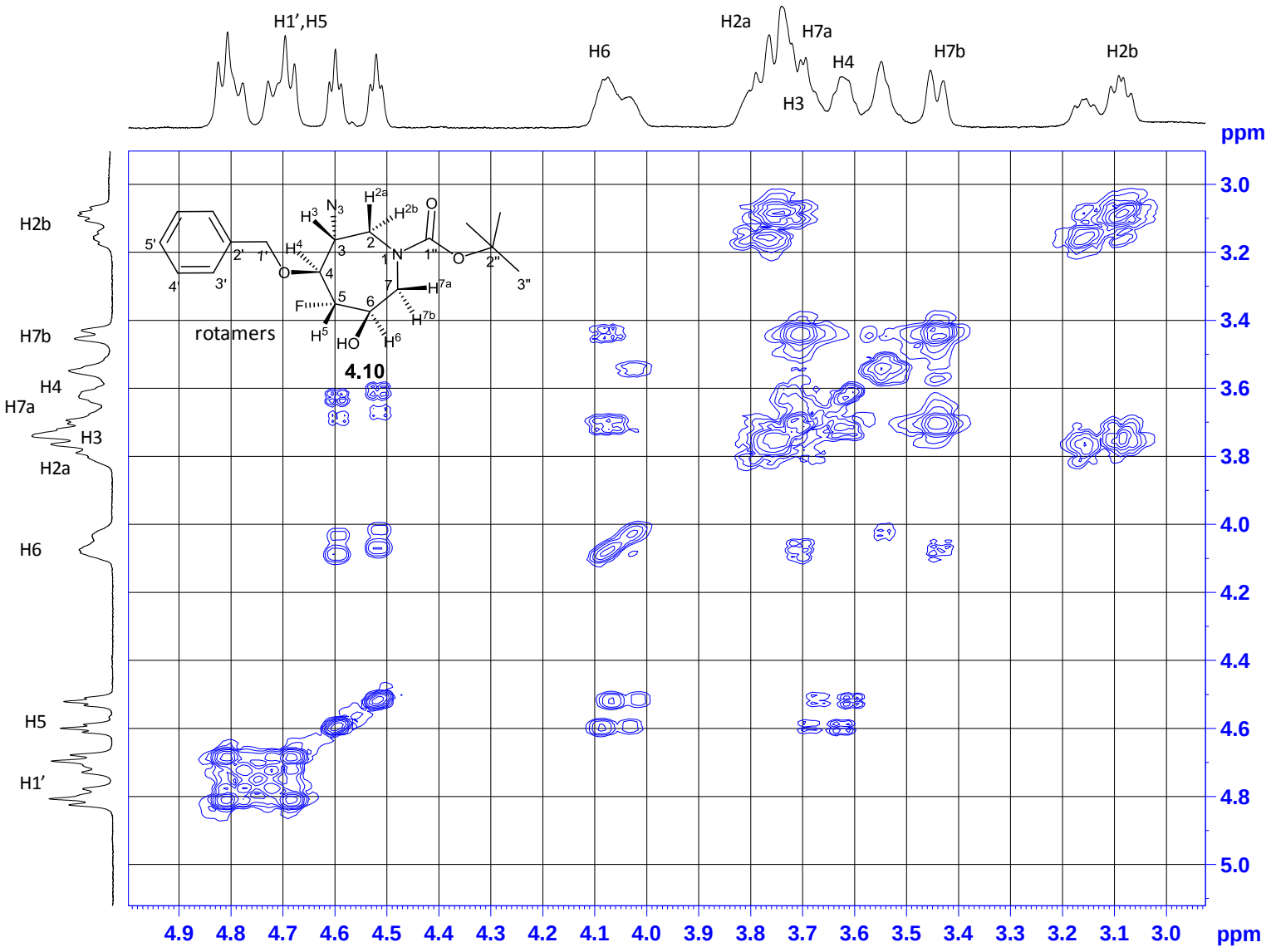

H11
H5
ppm
3.50
3.55
3.60
3.65
3.70
3.75
3.80
3.85
3.90
H2a,
7a&4
H3
H4-H5
(weak)
H3-H5
(strong)
4.80
4.75
4.70
4.65
4.60
4.55
4.50
4.45
ppm

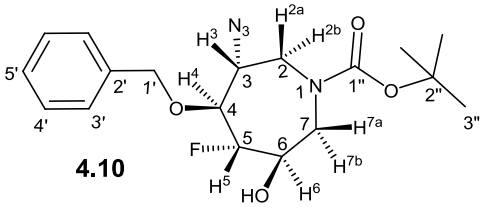

7.39
7.37
7.26
7.26
4.81
4.70
4.60
4.52
4.08
4.07
3.74
3.55
3.45
3.09
3.08
1.48
BnO
N3
F
HO
N
Boc
4.10
rotamers
Current Data Parameters
NAME Compound 17
EXPNO 1
PROCNO 1
F2 - Acquisition Parameters
Date_ 20121207
Time 12.32
INSTRUM spect
PROBHD 5 mm CPTXI 1H-
PULPROG zg30
TD 32768
SOLVENT CDCl3
NS 2
DS 0
SWH 4770.992 Hz
FIDRES 0.145599 Hz
AQ 3.4341364 sec
RG 9
DW 104.800 usec
DE 6.00 usec
TE 298.0 K
D1 1.50000000 sec
TD0 1
======== CHANNEL f1 ========
NUC1 1H
P1 7.63 usec
PL1 1.00 dB
SFO1 600.1824115 MHz
F1 - Acquisition parameters
TD 256
SFO1 150.9229 MHz
FIDRES 93.450958 Hz
SW 158.514 ppm
FnMODE States-TPPI
F2 - Processing parameters
SI 32768
SF 600.1800143 MHz
WDW EM
SSB 0
LB 0.30 Hz
GB 0
PC 0.10
7.5
7.0
6.5
6.0
5.5
5.0
4.5
4.0
3.5
3.0
2.5
2.0
1.5
1.0
0.5
ppm
5.15
2.04
1.00
1.03
5.08
1.00
10.35


Current Data Parameters
NAME Compound 17
EXPNO 3
PROCNO 1
F2 - Acquisition Parameters
Date_ 20121206
Time 13.17
INSTRUM spect
PROBHD 5 mm CPTXI 1H-
PULPROG udeft.txt
TD 21814
SOLVENT CDCl3
NS 5120
DS 0
SWH 30303.031 Hz
FIDRES 1.389155 Hz
AQ 0.3599810 sec
RG 32768
DW 16.500 usec
DE 6.00 usec
TE 298.0 K
D1 1.50000000 sec
D11 0.03000000 sec
d12 0.00002000 sec
D20 0.10000000 sec
DELTA 1.47000003 sec
DELTA2 0.36300099 sec
TAU 0.00302000 sec
TD0 1
======== CHANNEL f1 ========
NUC1 13C
P1 10.43 usec
P12 2000.00 usec
P26 500.00 usec
PL1 -2.50 dB
SFO1 150.9319817 MHz
SP2 5.29 dB
SP8 4.75 dB
SPNAM2 Crp60comp.4
SPNAM8 Crp60,0.5,20.1
SPOAL2 0.500
SPOAL8 0.500
SPOFFS2 0 Hz
SPOFFS8 0 Hz
======== CHANNEL f2 ========
CPDPRG2 waltz64
NUC2 1H
PCPD2 80.00 usec
PL2 1.00 dB
PL12 18.89 dB
SFO2 600.1830000 MHz
F1 - Acquisition parameters
TD 256
SFO1 150.932 MHz
FIDRES 93.450958 Hz
SW 158.505 ppm
FnMODE States-TPPI
F2 - Processing parameters
SI 262144
SF 150.9153616 MHz
WDW EM
SSB 0
LB 3.00 Hz
GB 0
PC 2.00
155.99
137.14
128.69
128.61
128.38
96.80
95.63
82.01
81.89
81.68
81.54
77.37
77.16
76.95
74.92
71.49
71.33
70.87
70.73
63.01
62.03
49.00
48.77
47.93
46.76
28.42
BnO
N3
F
HO
N
Boc
4.10
rotamers
160
150
140
130
120
110
100
90
80
70
60
50
40
30
20
ppm


H3',4',5'
H1',H5
H6
H2a,3&7a
H4
H7b
H2b
H3"
ppm
C3"
C2
C7
C3
C6
C1'
C4
C2"
C5
C3',4',5'
C2'
C1"
rotamers
4.10
7.5
7.0
6.5
6.0
5.5
5.0
4.5
4.0
3.5
3.0
2.5
2.0
1.5
ppm
30
40
50
60
70
80
90
100
110
120
130
140
150
160

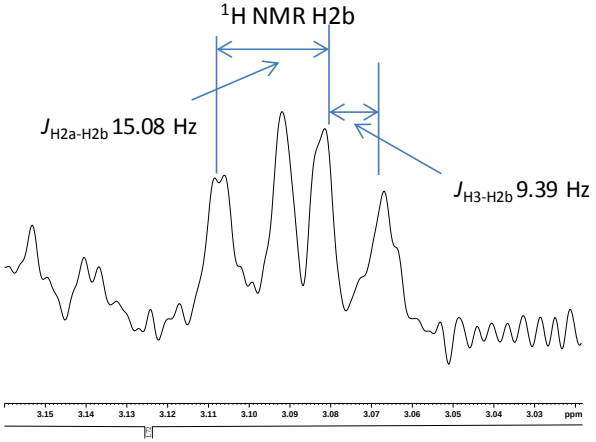

H3',4',5'
H1',H5
H6
H2a,3&7a
H4
H7b
H2b
H3"
ppm
C3"
C2
C7
C3
C6
C1'
C4
C2"
C5
C3',4',5'
C2'
C1"
rotamers
4.10
7.5
7.0
6.5
6.0
5.5
5.0
4.5
4.0
3.5
3.0
2.5
2.0
1.5
ppm


H1',H5
H6
H2a
H7a
H4
H3
H7b
H2b
ppm
H2b
H7b
H4
H7a
H3
H2a
H6
H5
H1'
rotamers
4.10
3.0
3.2
3.4
3.6
3.8
4.0
4.2
4.4
4.6
4.8
5.0
4.9 4.8 4.7 4.6 4.5 4.4 4.3 4.2 4.1 4.0 3.9 3.8 3.7 3.6 3.5 3.4 3.3 3.2 3.1 3.0
ppm

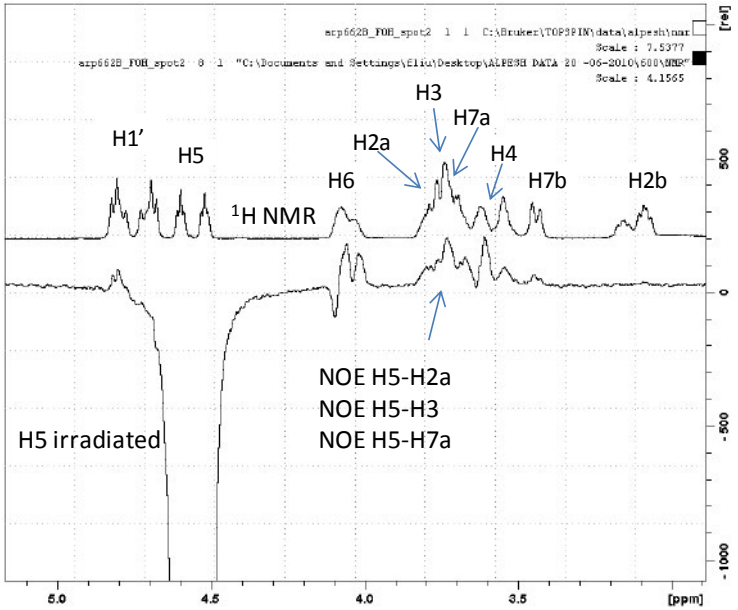


4.10

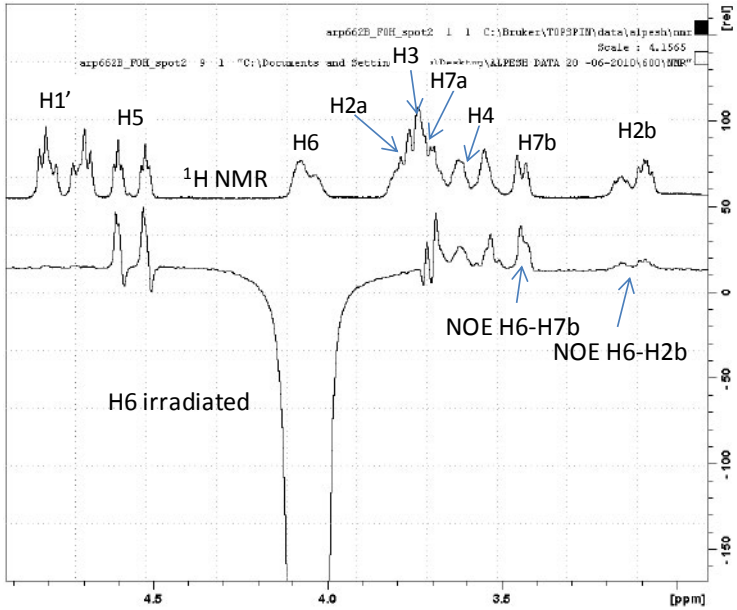
- Compound **4.10** has C3, C4 and C6 as known absolute chemistry stereocentres.
- **H2a and H2b** : $J_{H3\text{-}H2b}$ = 9.39 Hz suggests a clear *anti* meaning H2b is *trans* to H3 (torsion angles 155° or 208°). It is also supported by NOE H2b-H6.
- **H5** : H5 shows NOE to H3, H7a (bigger than H7b) and H2a (no measurable NOE to H2b). $J_{H5\text{-}H6}$ and $J_{H4\text{-}H5}$ both are 7 Hz supporting *trans* geometry in both the cases. H5 shows big NOE to H3 as well; further confirming H5 is *cis* to H3.

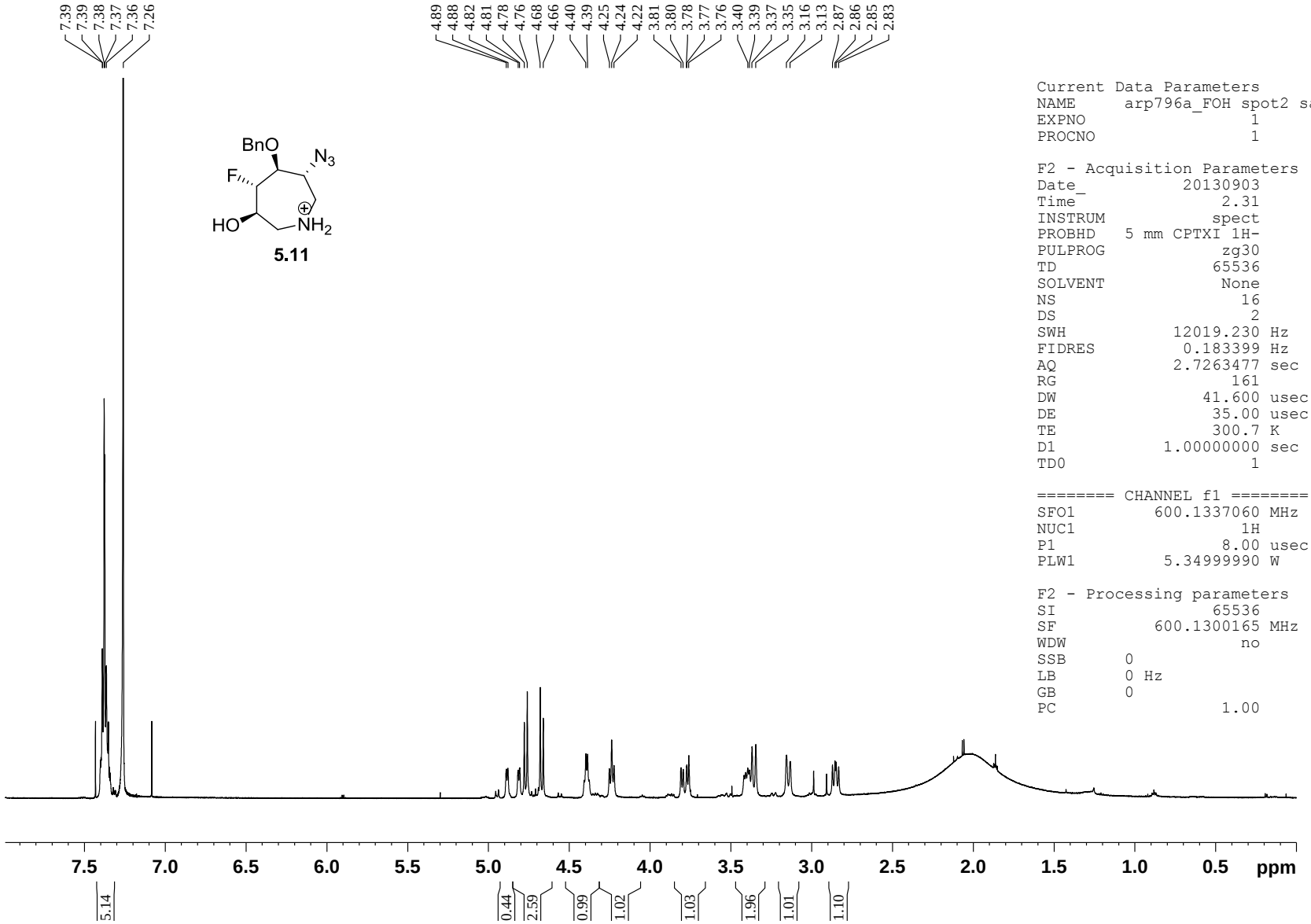


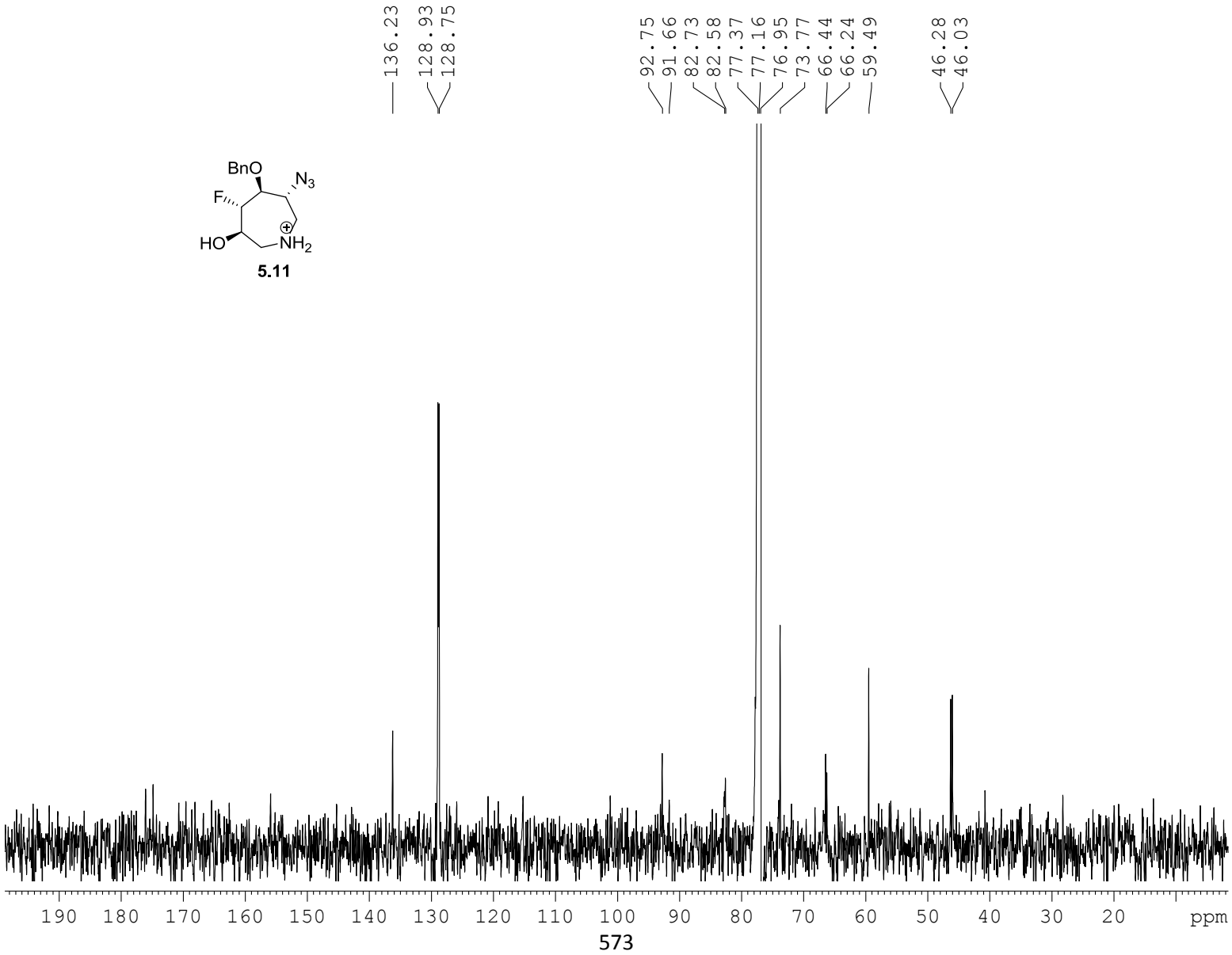
1D selective NOESY

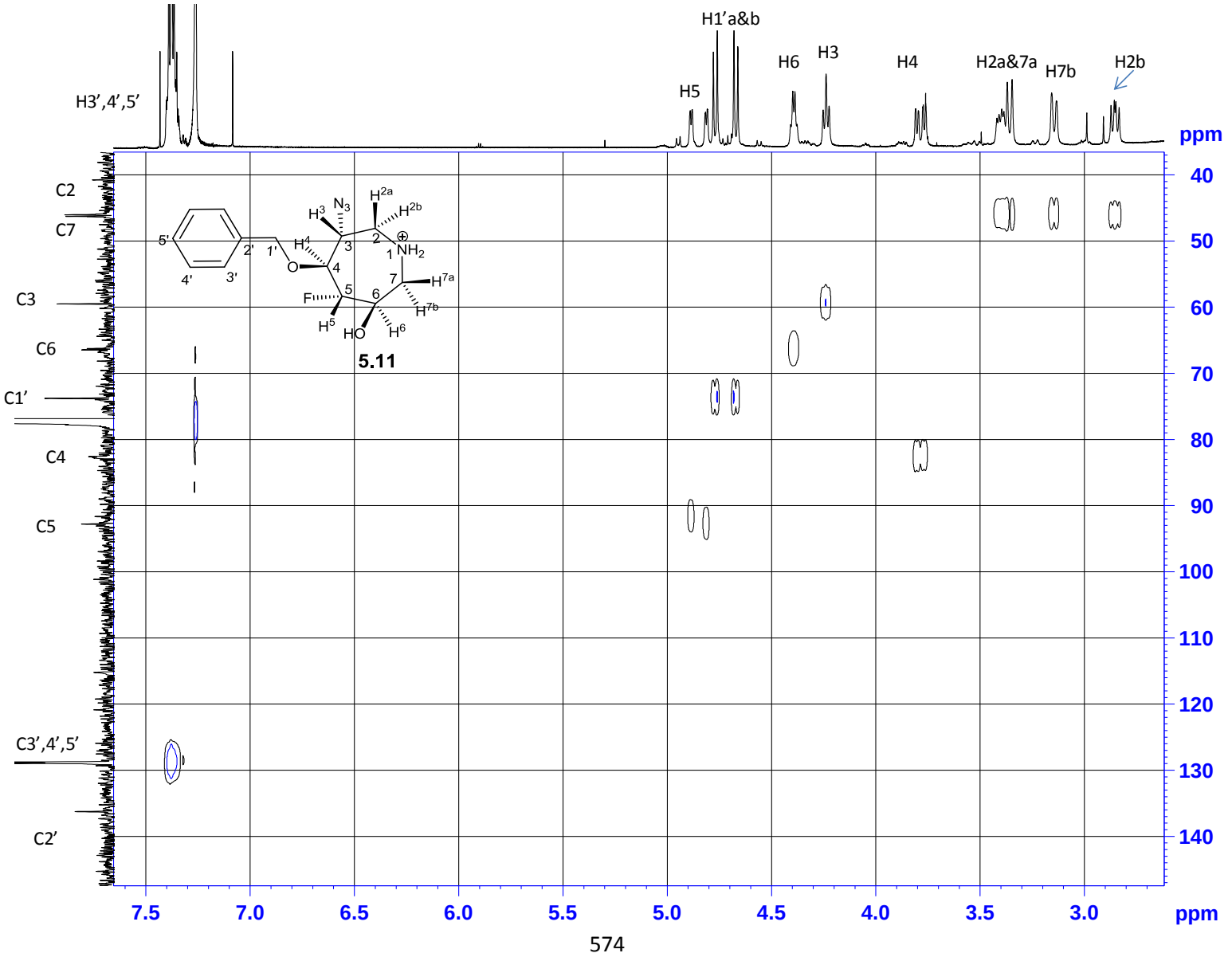


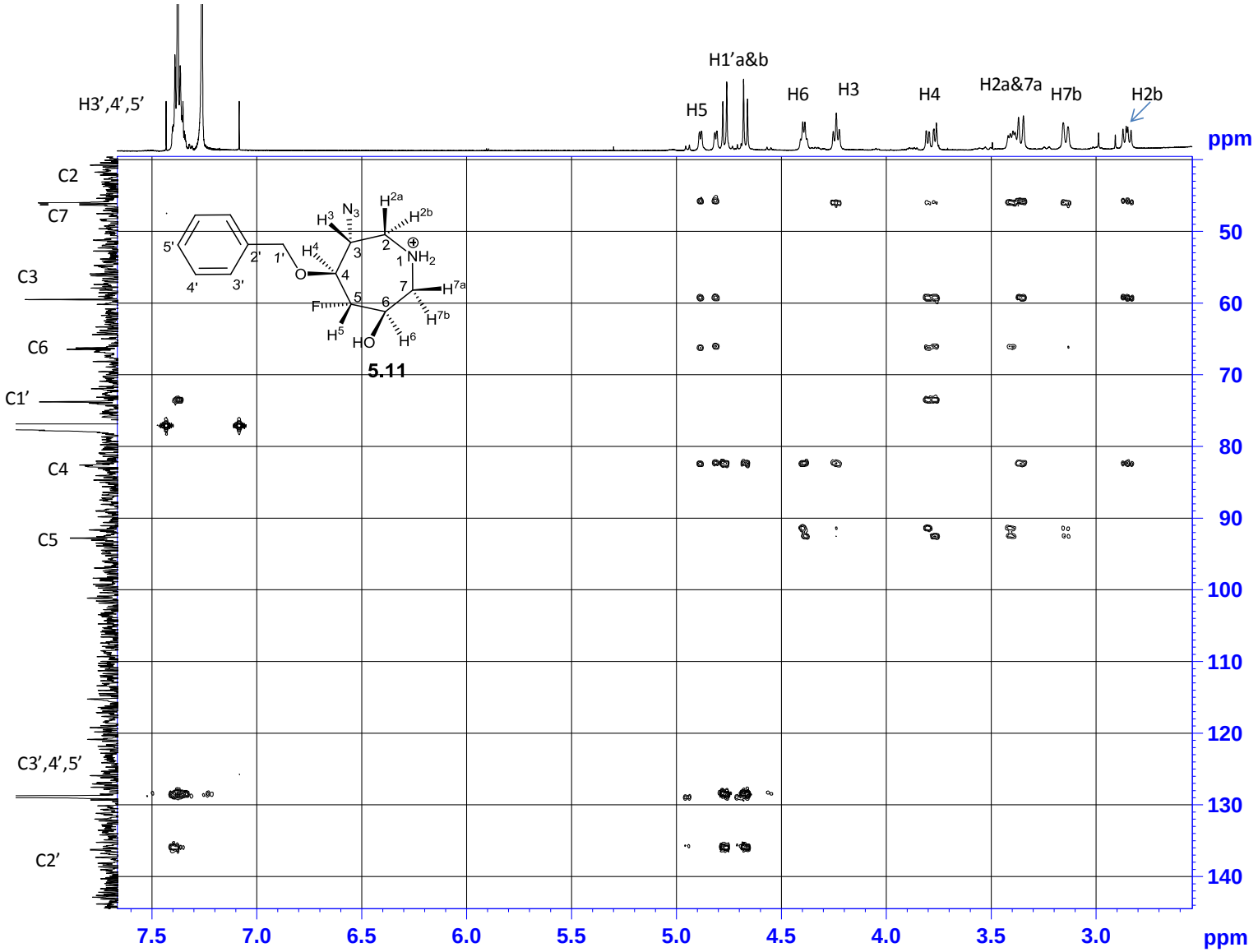
1D selective NOESY

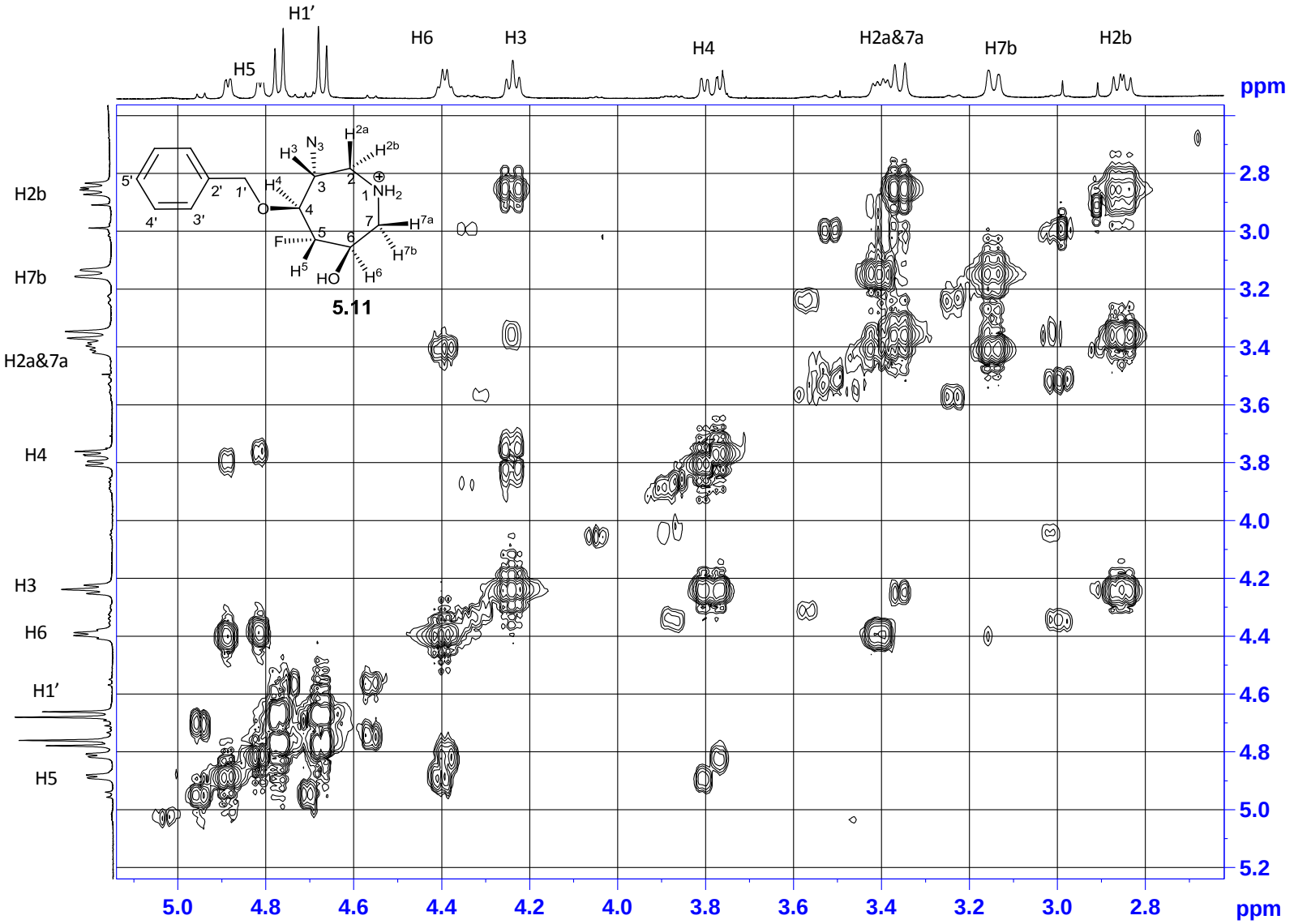


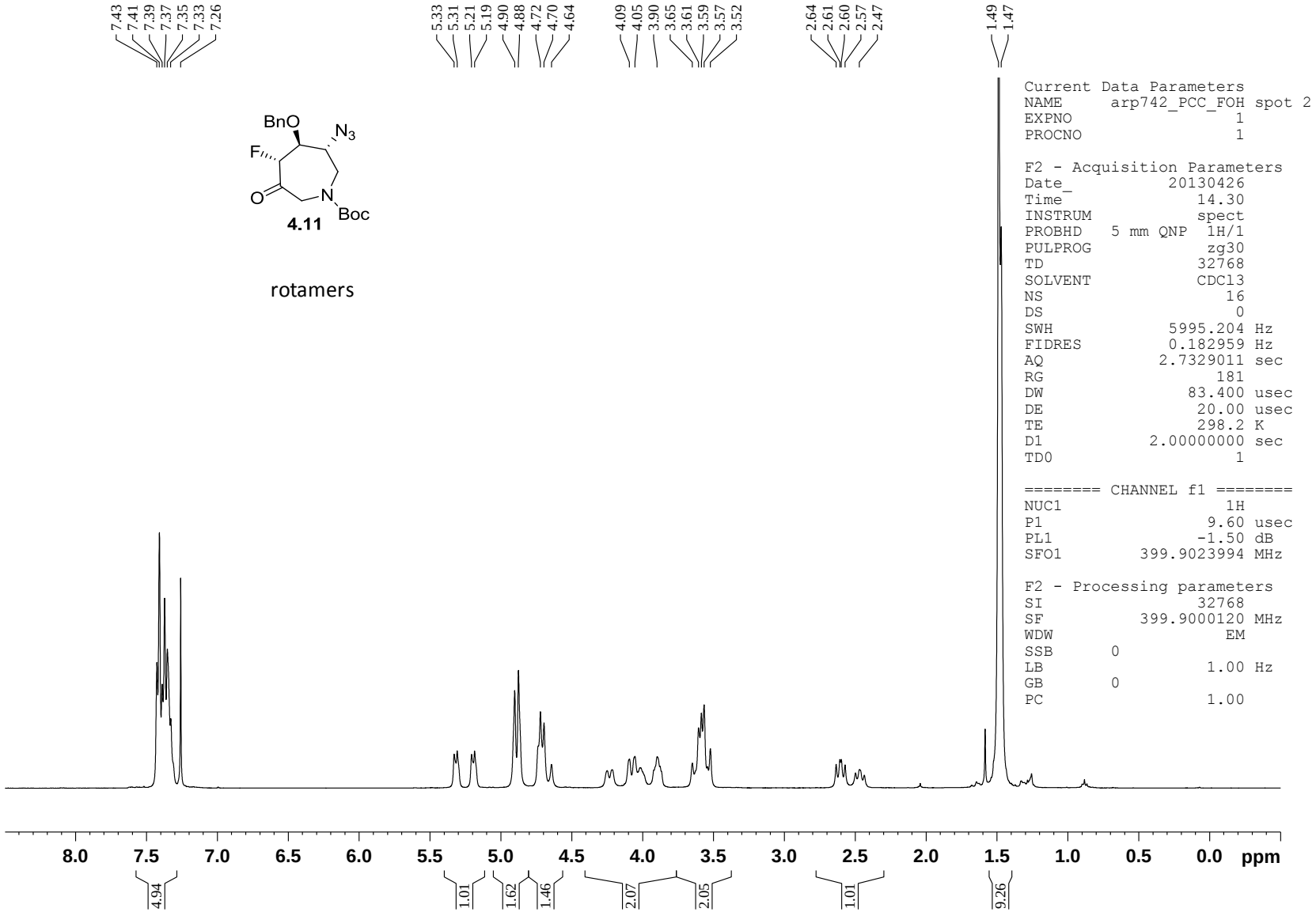

7.39
7.39
7.38
7.37
7.36
7.26
4.89
4.88
4.82
4.81
4.78
4.76
4.68
4.66
4.40
4.39
4.25
4.24
4.22
3.81
3.80
3.78
3.77
3.76
3.40
3.39
3.37
3.35
3.16
3.13
2.87
2.86
2.85
2.83
BnO
N3
F
HO
NH2
5.11
Current Data Parameters
NAME arp796a_FOH spot2 s
EXPNO 1
PROCNO 1
F2 - Acquisition Parameters
Date_ 20130903
Time 2.31
INSTRUM spect
PROBHD 5 mm CPTXI 1H-
PULPROG zg30
TD 65536
SOLVENT None
NS 16
DS 2
SWH 12019.230 Hz
FIDRES 0.183399 Hz
AQ 2.7263477 sec
RG 161
DW 41.600 usec
DE 35.00 usec
TE 300.7 K
D1 1.00000000 sec
TD0 1
======== CHANNEL f1 ========
SFO1 600.1337060 MHz
NUC1 1H
P1 8.00 usec
PLW1 5.34999990 W
F2 - Processing parameters
SI 65536
SF 600.1300165 MHz
WDW no
SSB 0
LB 0 Hz
GB 0
PC 1.00
7.5
7.0
6.5
6.0
5.5
5.0
4.5
4.0
3.5
3.0
2.5
2.0
1.5
1.0
0.5
ppm
5.14
0.44
2.59
0.99
1.02
1.03
1.96
1.01
1.10

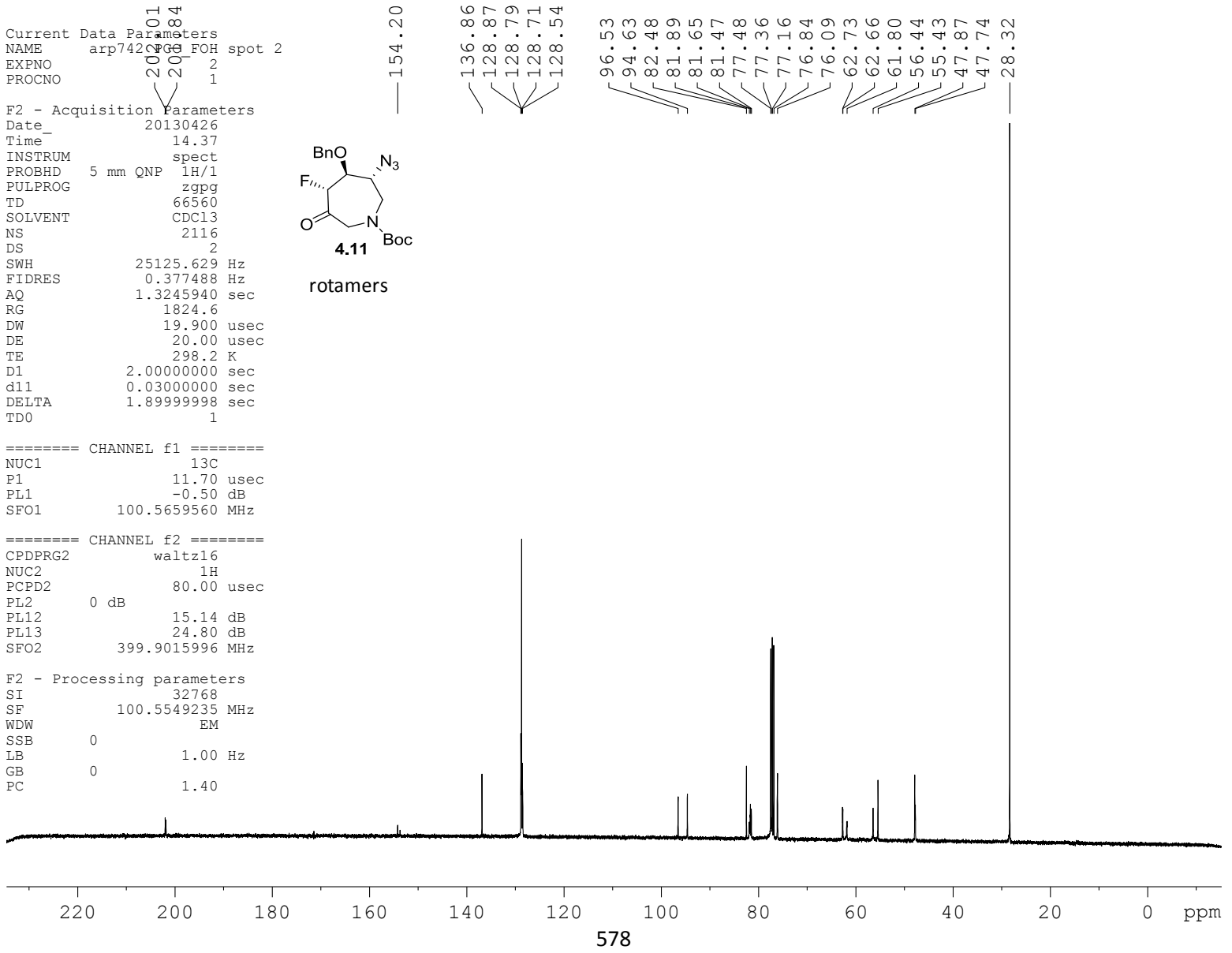

136.23
128.93
128.75
92.75
91.66
82.73
82.58
77.37
77.16
76.95
73.77
66.44
66.24
59.49
46.28
46.03
BnO
N3
F
HO
NH2
5.11
190 180 170 160 150 140 130 120 110 100 90 80 70 60 50 40 30 20 ppm

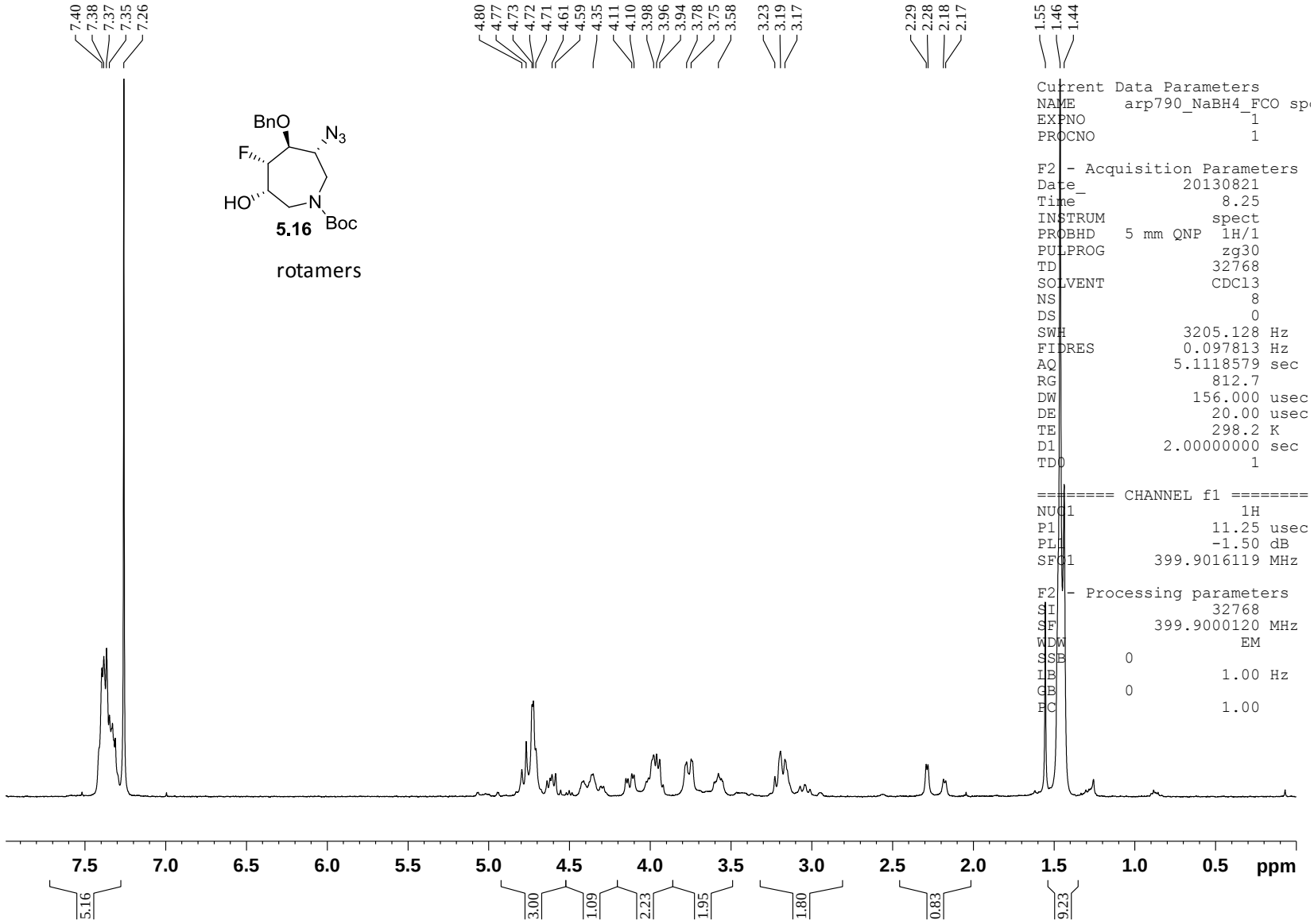

H3',4',5'
H1'a&b
H5
H6
H3
H4
H2a&7a
H7b
H2b
ppm
C2
C7
C3
C6
C1'
C4
C5
C3',4',5'
C2'
5.11
7.5
7.0
6.5
6.0
5.5
5.0
4.5
4.0
3.5
3.0
ppm

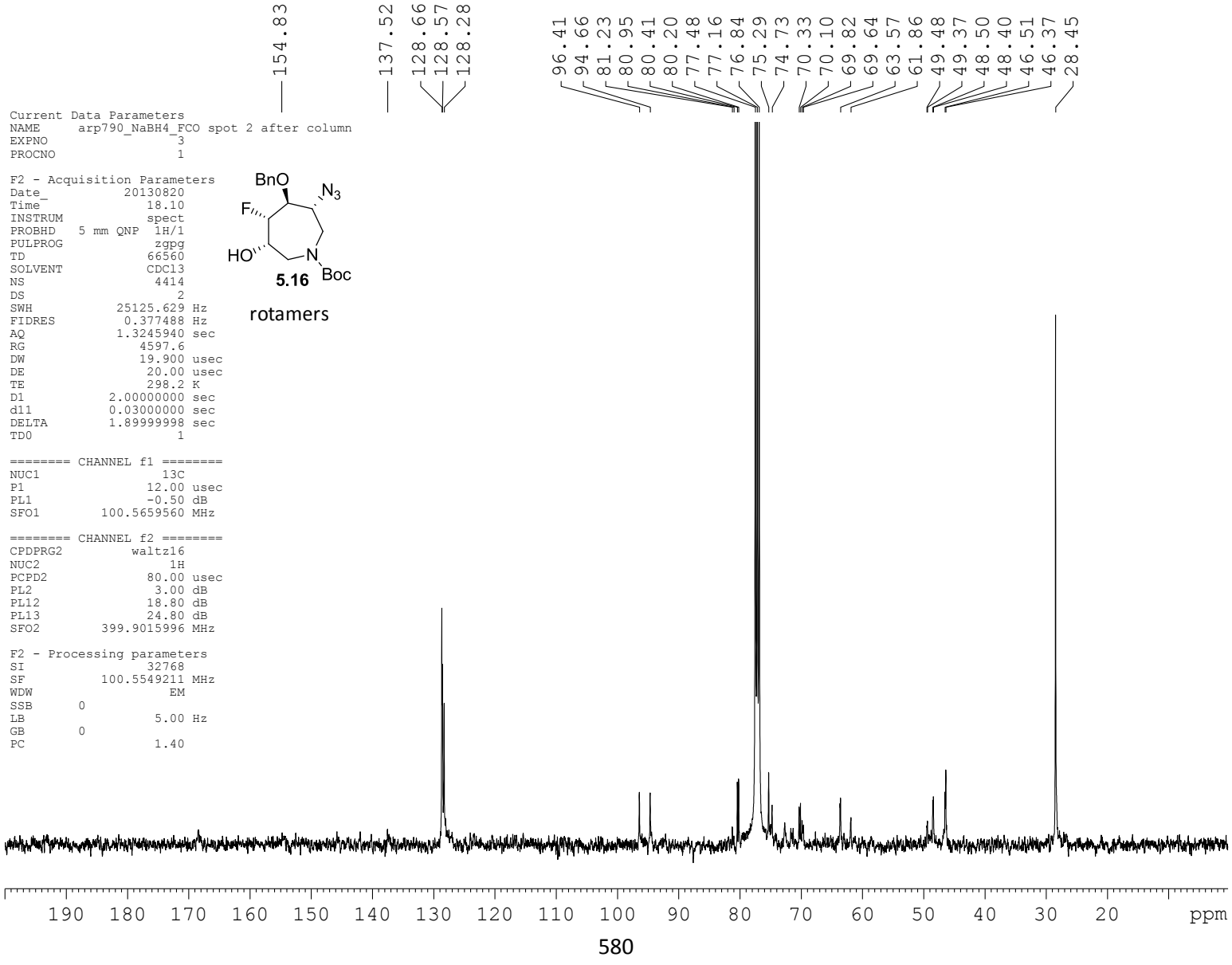

H3',4',5'
H1'a&b
H5
H6
H3
H4
H2a&7a
H7b
H2b
ppm
C2
C7
C3
C6
C1'
C4
C5
C3',4',5'
C2'
5.11
7.5
7.0
6.5
6.0
5.5
5.0
4.5
4.0
3.5
3.0
ppm

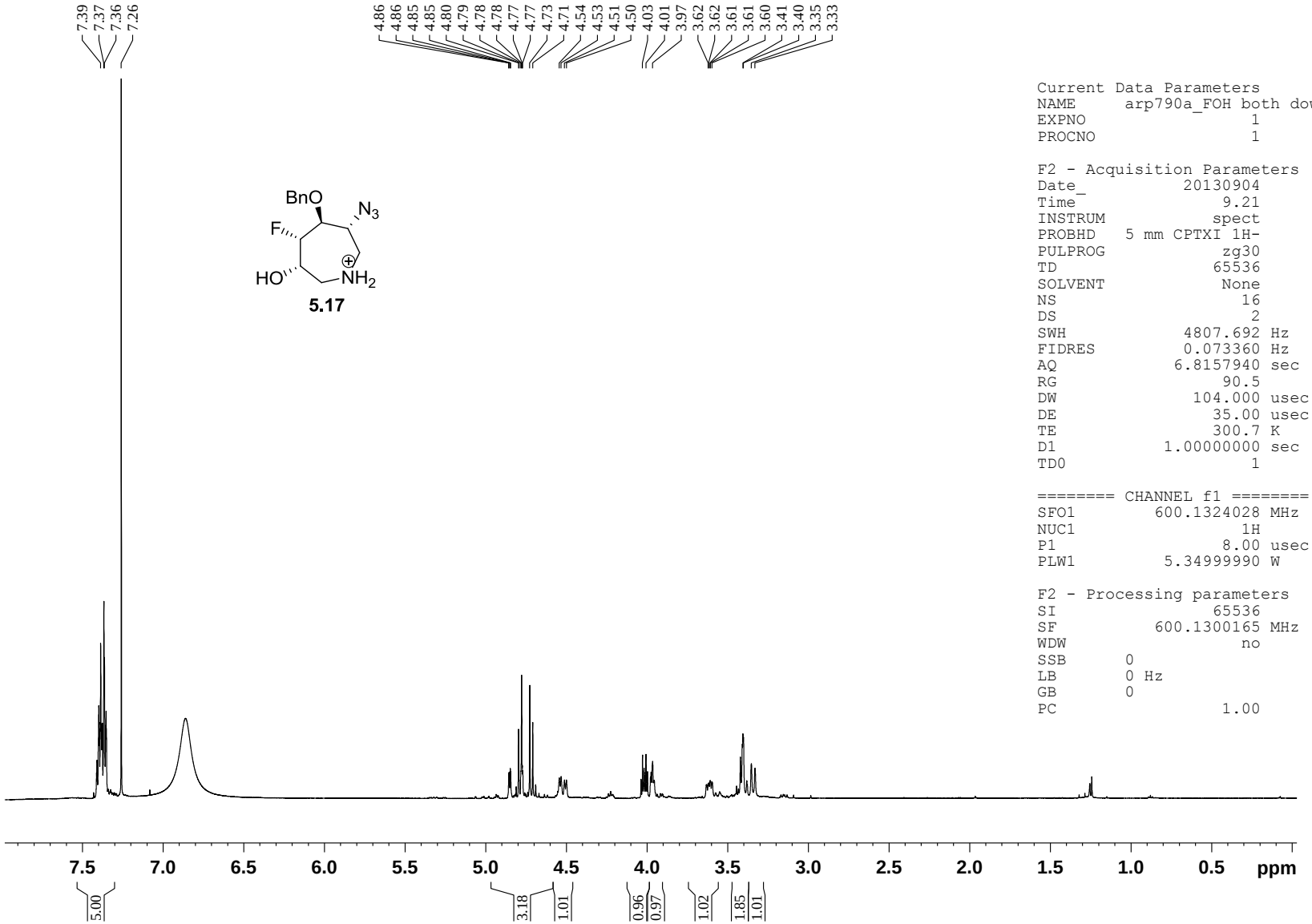

H1'
H5
H6
H3
H4
H2a&7a
H7b
H2b
ppm
H2b
H7b
H2a&7a
H4
H3
H6
H1'
H5
5.11
5.0
4.8
4.6
4.4
4.2
4.0
3.8
3.6
3.4
3.2
3.0
2.8
ppm

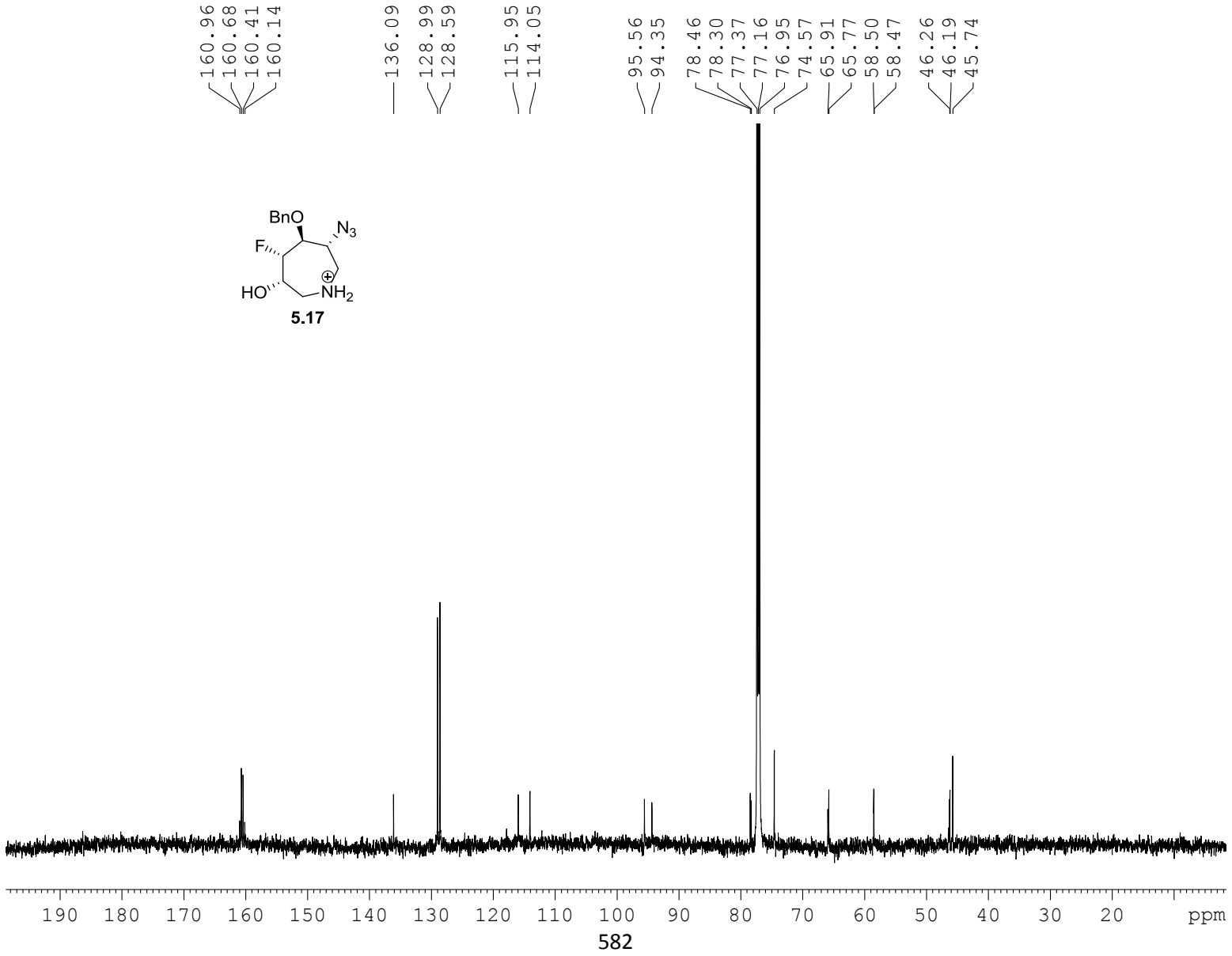

7.43
7.41
7.39
7.37
7.35
7.33
7.26
5.33
5.31
5.21
5.19
4.90
4.88
4.72
4.70
4.64
4.09
4.05
3.90
3.65
3.61
3.59
3.57
3.52
2.64
2.61
2.60
2.57
2.47
1.49
1.47
BnO
N3
F
O
N
Boc
4.11
rotamers
Current Data Parameters
NAME arp742_PCC_FOH spot 2
EXPNO 1
PROCNO 1
F2 - Acquisition Parameters
Date_ 20130426
Time 14.30
INSTRUM spect
PROBHD 5 mm QNP 1H/1
PULPROG zg30
TD 32768
SOLVENT CDCl3
NS 16
DS 0
SWH 5995.204 Hz
FIDRES 0.182959 Hz
AQ 2.7329011 sec
RG 181
DW 83.400 usec
DE 20.00 usec
TE 298.2 K
D1 2.00000000 sec
TD0 1
======== CHANNEL f1 ========
NUC1 1H
P1 9.60 usec
PL1 -1.50 dB
SFO1 399.9023994 MHz
F2 - Processing parameters
SI 32768
SF 399.9000120 MHz
WDW EM
SSB 0
LB 1.00 Hz
GB 0
PC 1.00
8.0
7.5
7.0
6.5
6.0
5.5
5.0
4.5
4.0
3.5
3.0
2.5
2.0
1.5
1.0
0.5
0.0
ppm
4.94
1.01
1.62
1.46
2.07
2.05
1.01
9.26

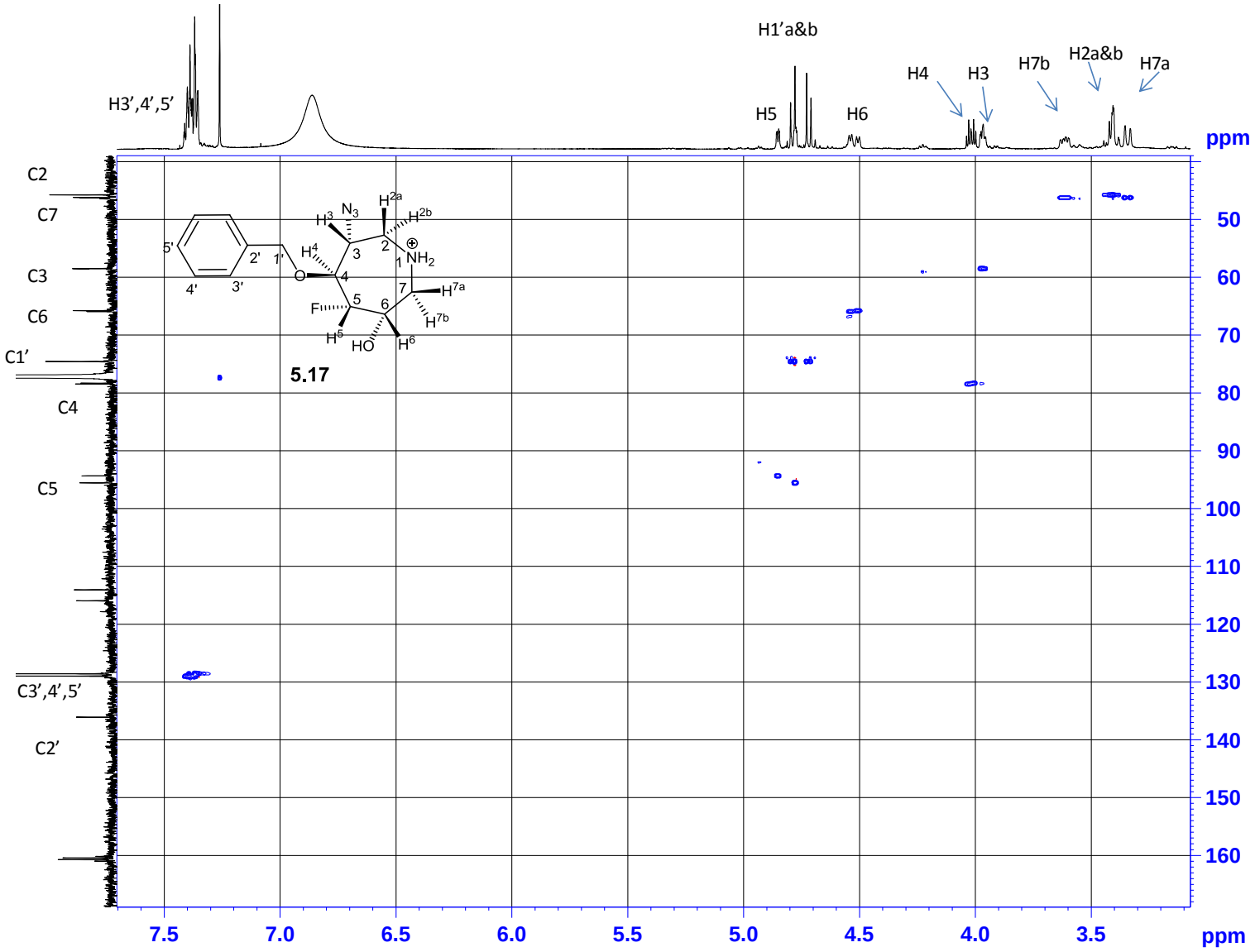

Current Data Parameters
NAME arp7422_PGG_FOH spot 2
EXPNO 2
PROCNO 1
F2 - Acquisition Parameters
Date_ 20130426
Time 14.37
INSTRUM spect
PROBHD 5 mm QNP 1H/1
PULPROG zgpg
TD 66560
SOLVENT CDCl3
NS 2116
DS 2
SWH 25125.629 Hz
FIDRES 0.377488 Hz
AQ 1.3245940 sec
RG 1824.6
DW 19.900 usec
DE 20.00 usec
TE 298.2 K
D1 2.00000000 sec
d11 0.03000000 sec
DELTA 1.89999998 sec
TD0 1
======== CHANNEL f1 ========
NUC1 13C
P1 11.70 usec
PL1 -0.50 dB
SFO1 100.5659560 MHz
======== CHANNEL f2 ========
CPDPRG2 waltz16
NUC2 1H
PCPD2 80.00 usec
PL2 0 dB
PL12 15.14 dB
PL13 24.80 dB
SFO2 399.9015996 MHz
F2 - Processing parameters
SI 32768
SF 100.5549235 MHz
WDW EM
SSB 0
LB 1.00 Hz
GB 0
PC 1.40
20.01
20.84
154.20
136.86
128.87
128.79
128.71
128.54
96.53
94.63
82.48
81.89
81.65
81.47
77.48
77.36
77.16
76.84
76.09
62.73
62.66
61.80
56.44
55.43
47.87
47.74
28.32
BnO
N3
F
O
N
Boc
4.11
rotamers
220
200
180
160
140
120
100
80
60
40
20
0
ppm

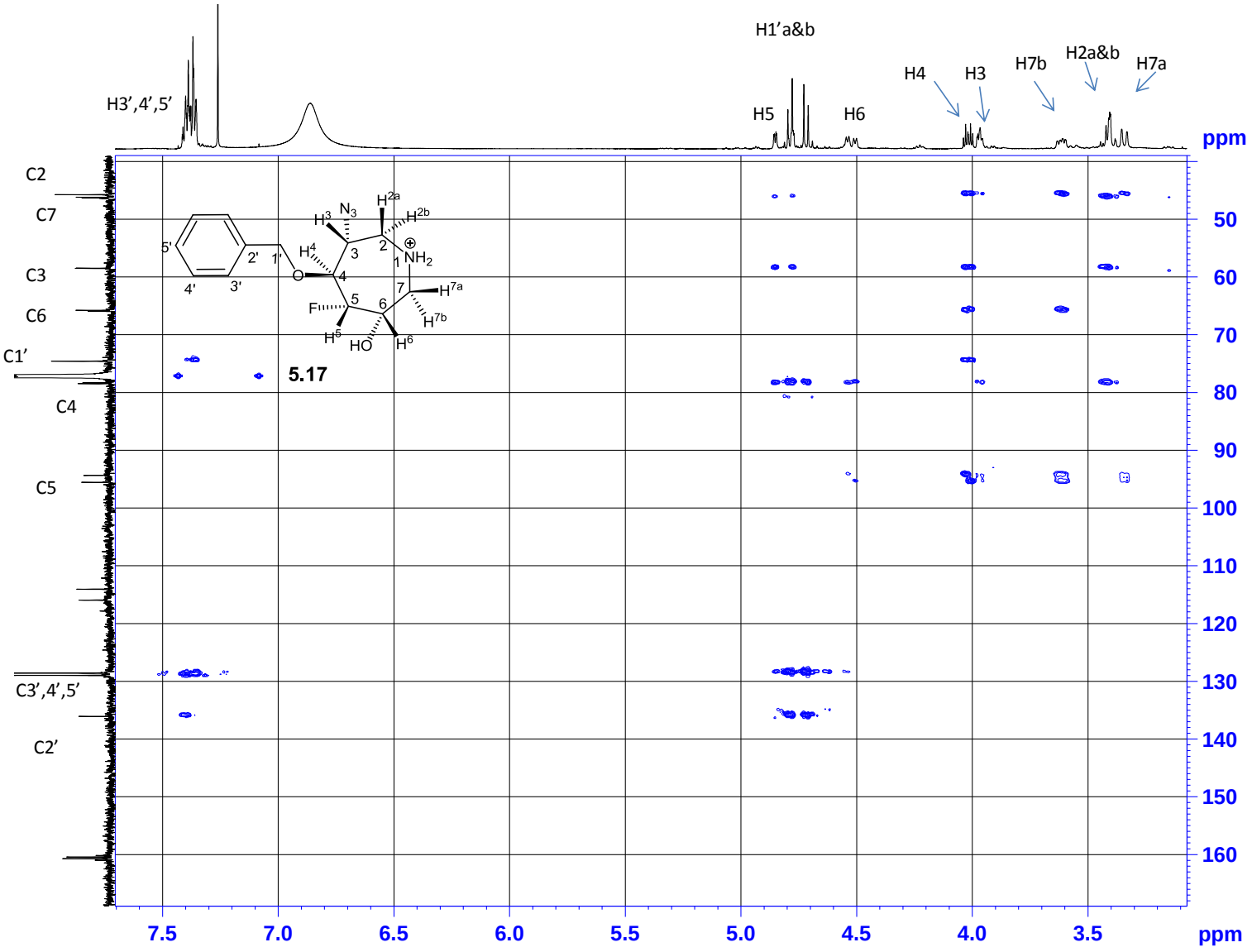

7.40
7.38
7.37
7.35
7.26
4.80
4.77
4.73
4.72
4.71
4.61
4.59
4.35
4.11
4.10
3.98
3.96
3.94
3.78
3.75
3.58
3.23
3.19
3.17
2.29
2.28
2.18
2.17
1.55
1.46
1.44
BnO
N3
F
HO
N
Boc
5.16
rotamers
Current Data Parameters
NAME arp790_NaBH4_FCO sp
EXPNO 1
PROCNO 1
F2 - Acquisition Parameters
Date_ 20130821
Time 8.25
INSTRUM spect
PROBHD 5 mm QNP 1H/1
PULPROG zg30
TD 32768
SOLVENT CDCl3
NS 8
DS 0
SWH 3205.128 Hz
FIDRES 0.097813 Hz
AQ 5.1118579 sec
RG 812.7
DW 156.000 usec
DE 20.00 usec
TE 298.2 K
D1 2.00000000 sec
TD0 1
======== CHANNEL f1 ========
NUC1 1H
P1 11.25 usec
PL1 -1.50 dB
SFO1 399.9016119 MHz
F2 - Processing parameters
SI 32768
SF 399.9000120 MHz
WDW EM
SSB 0
LB 1.00 Hz
GB 0
PC 1.00
7.5
7.0
6.5
6.0
5.5
5.0
4.5
4.0
3.5
3.0
2.5
2.0
1.5
1.0
0.5
ppm
5.16
3.00
1.09
2.23
1.95
1.80
0.83
9.23

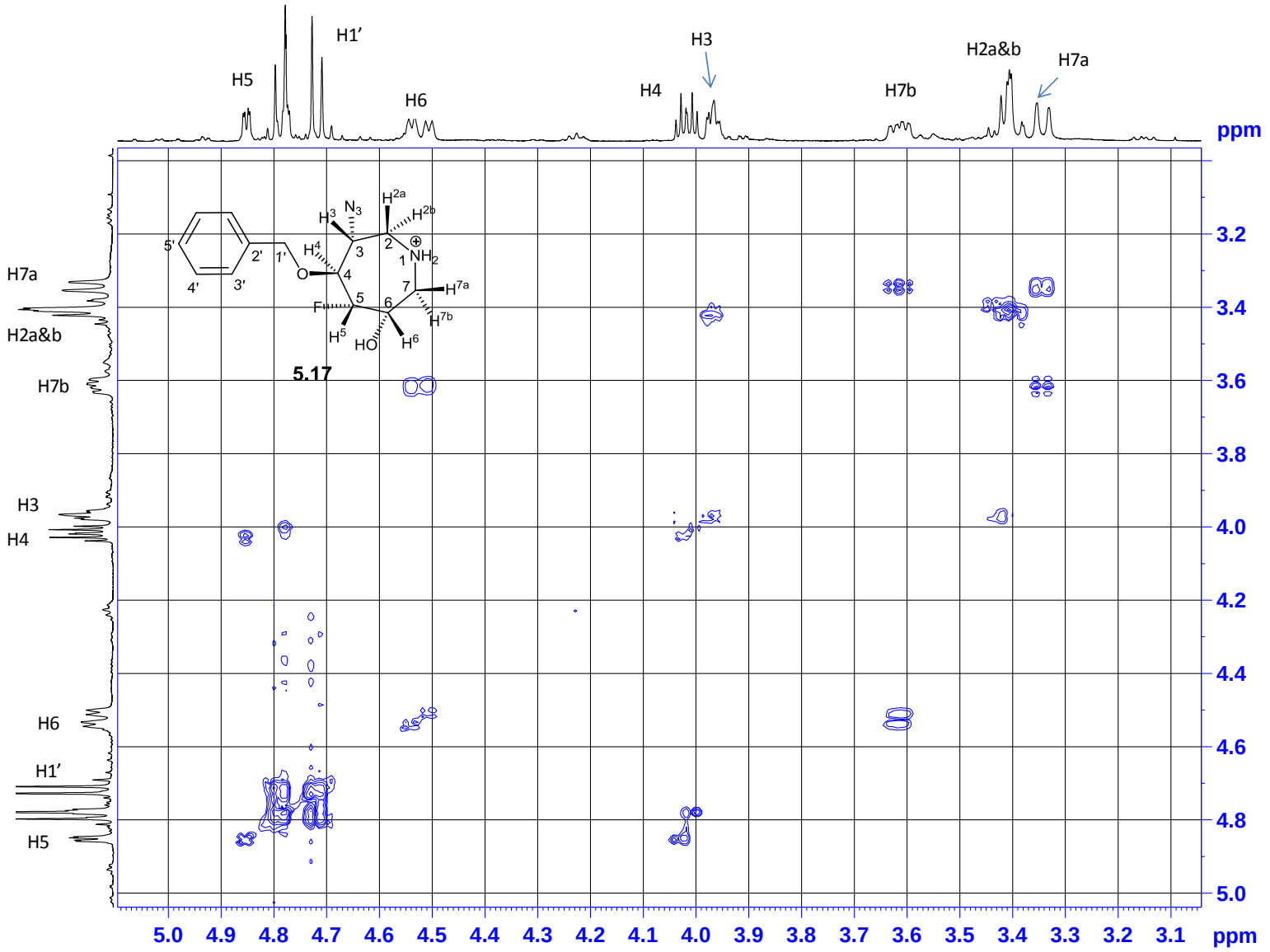

154.83
137.52
128.66
128.57
128.28
96.41
94.66
81.23
80.95
80.41
80.20
77.48
77.16
76.84
75.29
74.73
70.33
70.10
69.82
69.64
63.57
61.86
49.48
49.37
48.50
48.40
46.51
46.37
28.45
Current Data Parameters
NAME arp790_NaBH4_FCO spot 2 after column
EXPNO 3
PROCNO 1
F2 - Acquisition Parameters
Date_ 20130820
Time 18.10
INSTRUM spect
PROBHD 5 mm QNP 1H/1
PULPROG zgpg
TD 66560
SOLVENT CDCl3
NS 4414
DS 2
SWH 25125.629 Hz
FIDRES 0.377488 Hz
AQ 1.3245940 sec
RG 4597.6
DW 19.900 usec
DE 20.00 usec
TE 298.2 K
D1 2.00000000 sec
d11 0.03000000 sec
DELTA 1.89999998 sec
TD0 1
======== CHANNEL f1 ========
NUC1 13C
P1 12.00 usec
PL1 -0.50 dB
SFO1 100.5659560 MHz
======== CHANNEL f2 ========
CPDPRG2 waltz16
NUC2 1H
PCPD2 80.00 usec
PL2 3.00 dB
PL12 18.80 dB
PL13 24.80 dB
SFO2 399.9015996 MHz
F2 - Processing parameters
SI 32768
SF 100.5549211 MHz
WDW EM
SSB 0
LB 5.00 Hz
GB 0
PC 1.40
BnO
N3
F
HO
N
Boc
5.16
rotamers
190 180 170 160 150 140 130 120 110 100 90 80 70 60 50 40 30 20 ppm

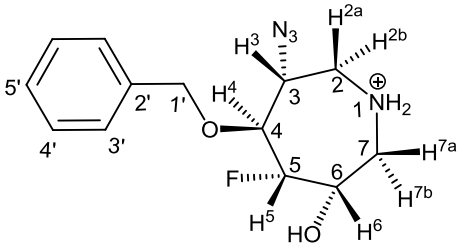

7.39
7.37
7.36
7.26
4.86
4.86
4.85
4.85
4.80
4.79
4.78
4.78
4.77
4.77
4.73
4.71
4.54
4.53
4.51
4.50
4.03
4.01
3.97
3.62
3.62
3.61
3.61
3.60
3.41
3.40
3.35
3.33
BnO
N3
F
HO
NH2
5.17
Current Data Parameters
NAME arp790a_FOH both do
EXPNO 1
PROCNO 1
F2 - Acquisition Parameters
Date_ 20130904
Time 9.21
INSTRUM spect
PROBHD 5 mm CPTXI 1H-
PULPROG zg30
TD 65536
SOLVENT None
NS 16
DS 2
SWH 4807.692 Hz
FIDRES 0.073360 Hz
AQ 6.8157940 sec
RG 90.5
DW 104.000 usec
DE 35.00 usec
TE 300.7 K
D1 1.00000000 sec
TD0 1
======== CHANNEL f1 ========
SFO1 600.1324028 MHz
NUC1 1H
P1 8.00 usec
PLW1 5.34999990 W
F2 - Processing parameters
SI 65536
SF 600.1300165 MHz
WDW no
SSB 0
LB 0 Hz
GB 0
PC 1.00
7.5
7.0
6.5
6.0
5.5
5.0
4.5
4.0
3.5
3.0
2.5
2.0
1.5
1.0
0.5
ppm
5.00
3.18
1.01
0.96
0.97
1.02
1.85
1.01


160.96
160.68
160.41
160.14
136.09
128.99
128.59
115.95
114.05
95.56
94.35
78.46
78.30
77.37
77.16
76.95
74.57
65.91
65.77
58.50
58.47
46.26
46.19
45.74
BnO
N3
F
HO
NH2
5.17
190
180
170
160
150
140
130
120
110
100
90
80
70
60
50
40
30
20
ppm

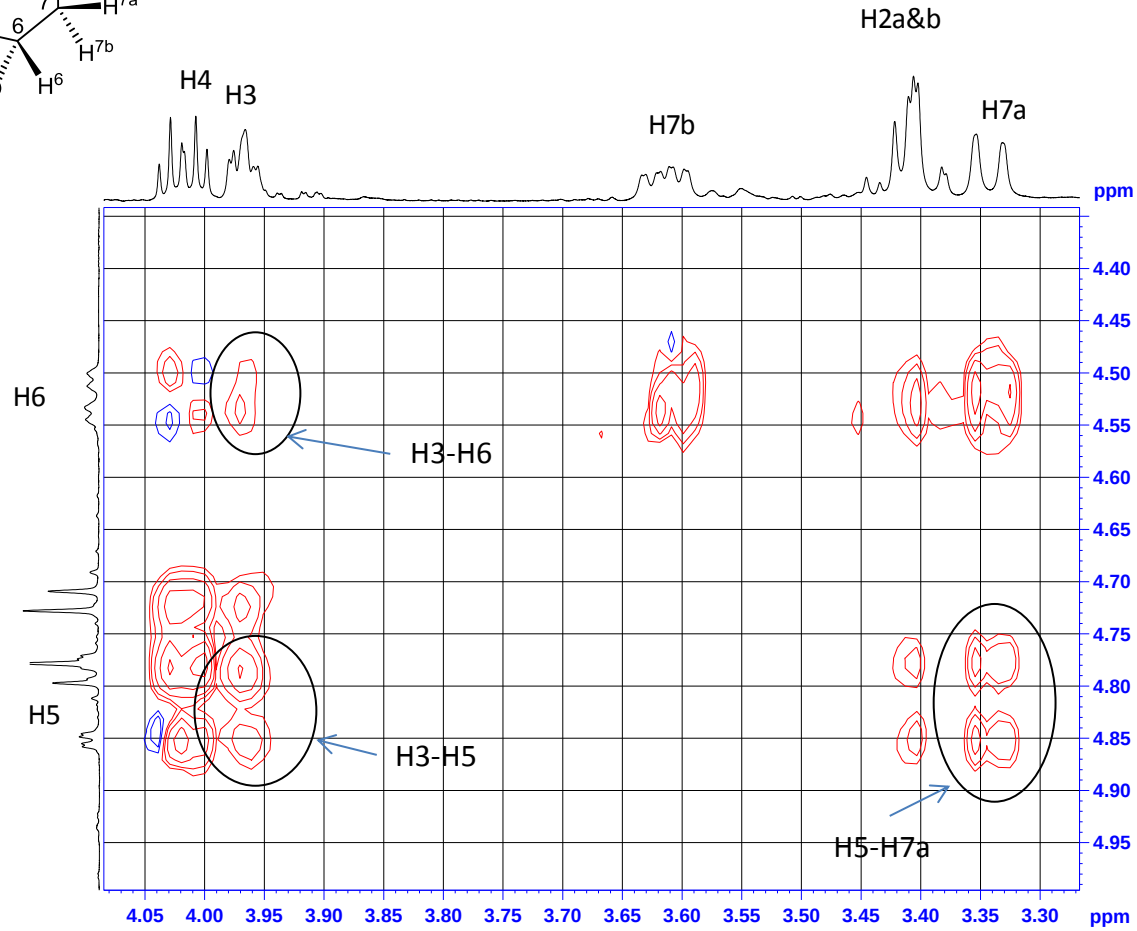

H3',4',5'
H1'a&b
H5
H6
H4
H3
H7b
H2a&b
H7a
ppm
C2
C7
C3
C6
C1'
C4
C5
C3',4',5'
C2'
5.17
7.5
7.0
6.5
6.0
5.5
5.0
4.5
4.0
3.5
ppm

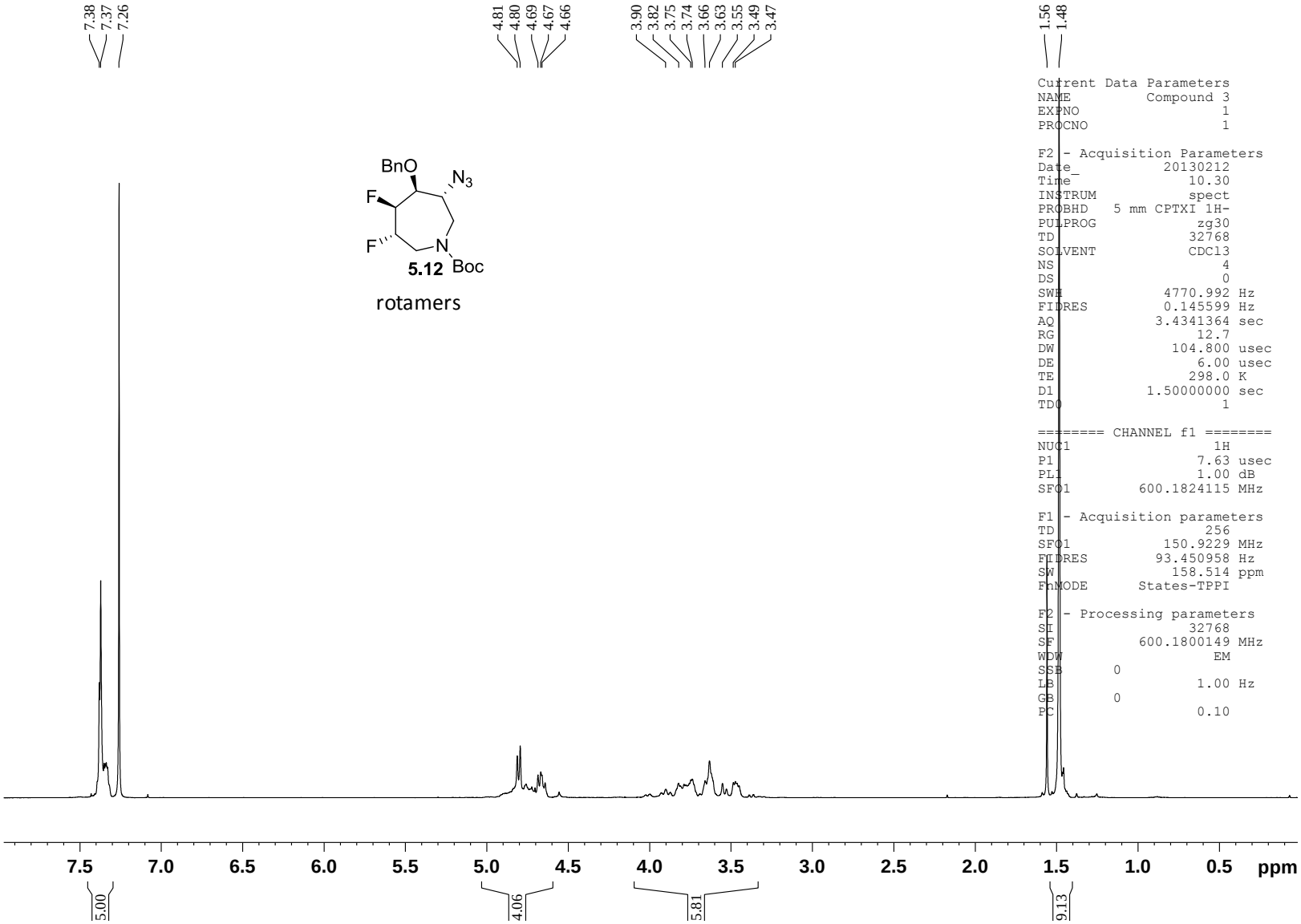

H3',4',5'
H1'a&b
H5
H6
H4
H3
H7b
H2a&b
H7a
ppm
C2
C7
C3
C6
C1'
C4
C5
C3',4',5'
C2'
5.17
7.5
7.0
6.5
6.0
5.5
5.0
4.5
4.0
3.5
ppm

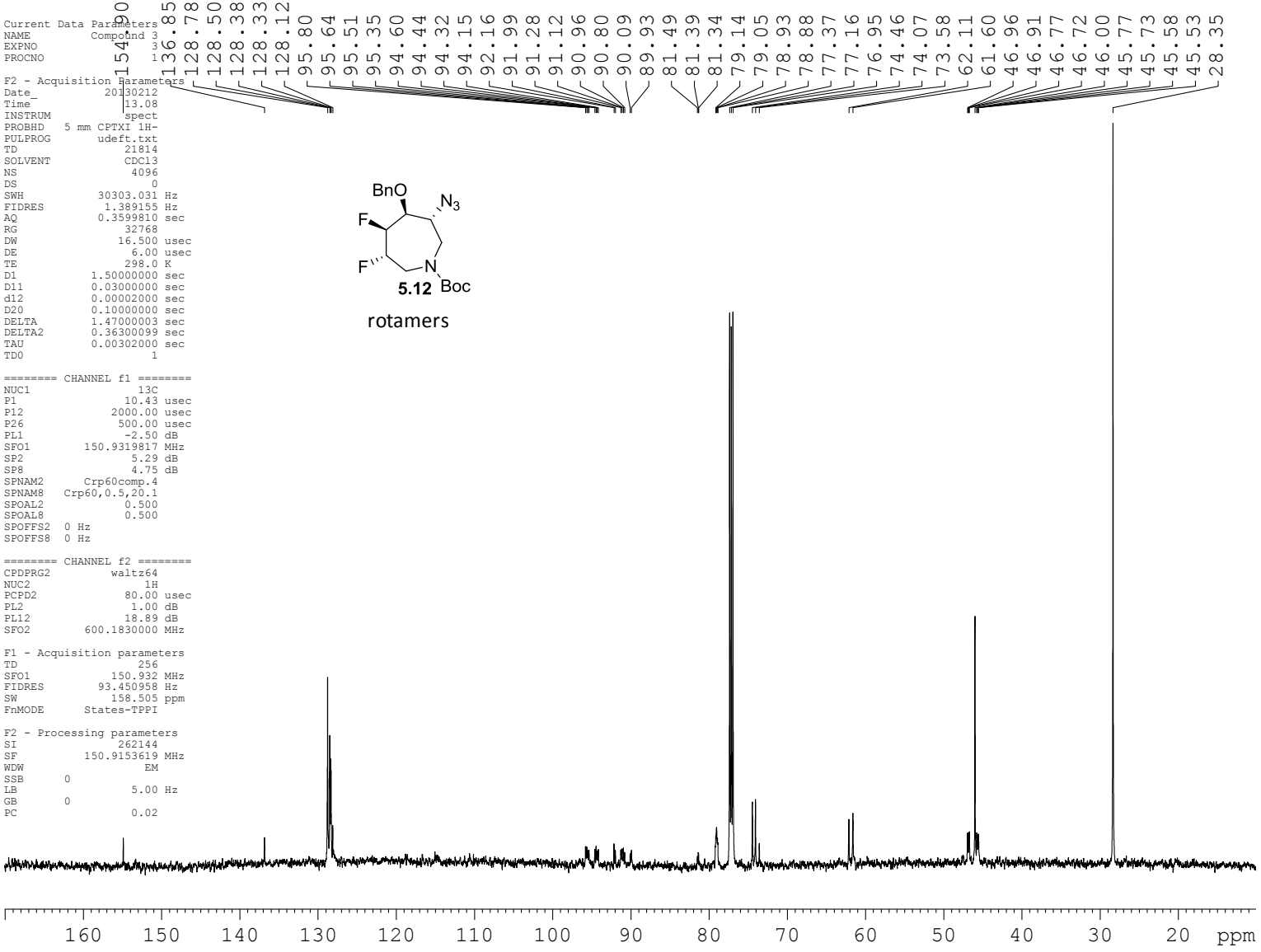

H5
H1'
H6
H4
H3
H7b
H2a&b
H7a
ppm
5.17
5.0 4.9 4.8 4.7 4.6 4.5 4.4 4.3 4.2 4.1 4.0 3.9 3.8 3.7 3.6 3.5 3.4 3.3 3.2 3.1 ppm

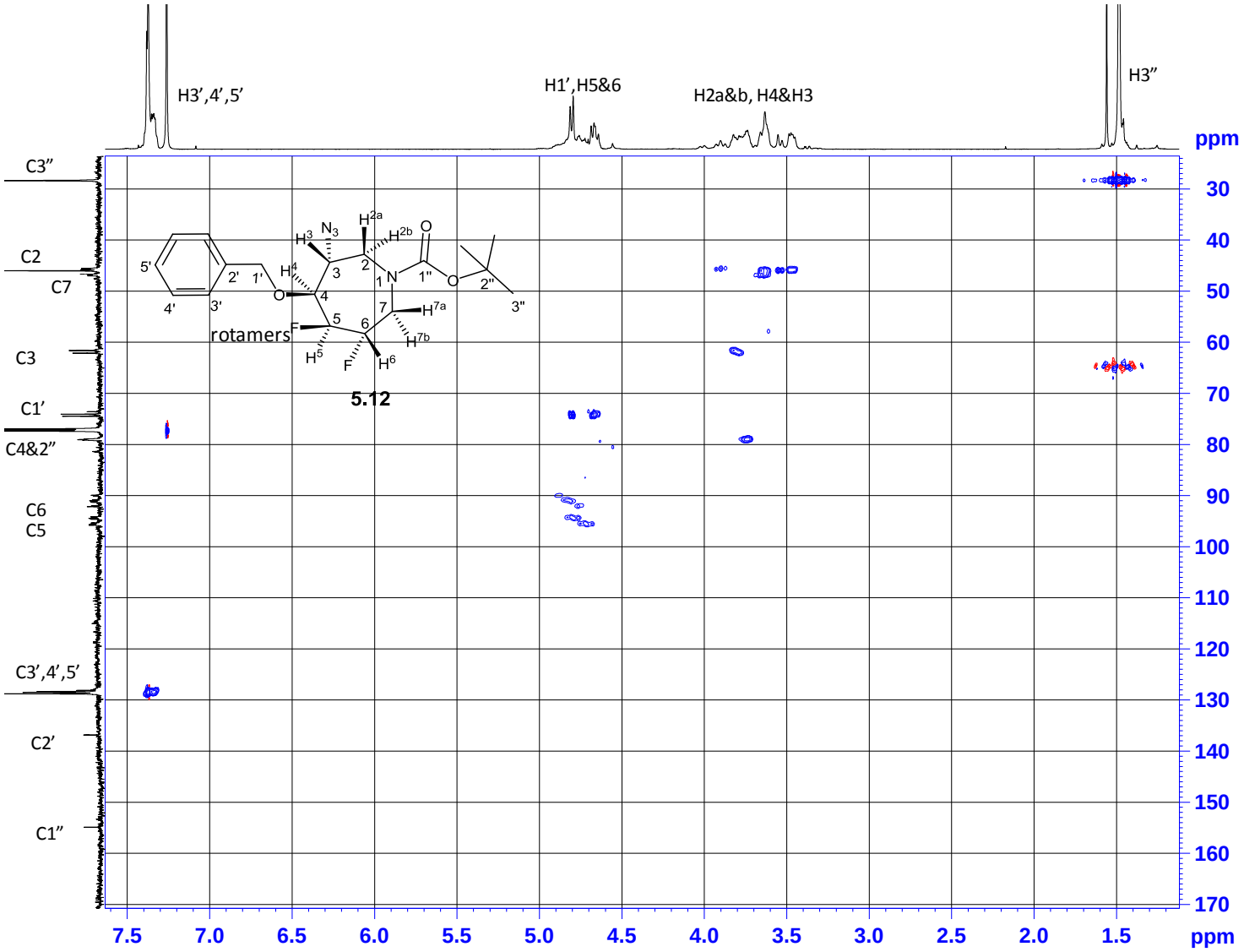

5'
2'
1'
O
4'
3'
4
3
2
1
5
6
7
F
HO
H^3
N_3
H^{2a}
H^{2b}
H^4
NH_2
H^{7a}
H^{7b}
H^5
H^6

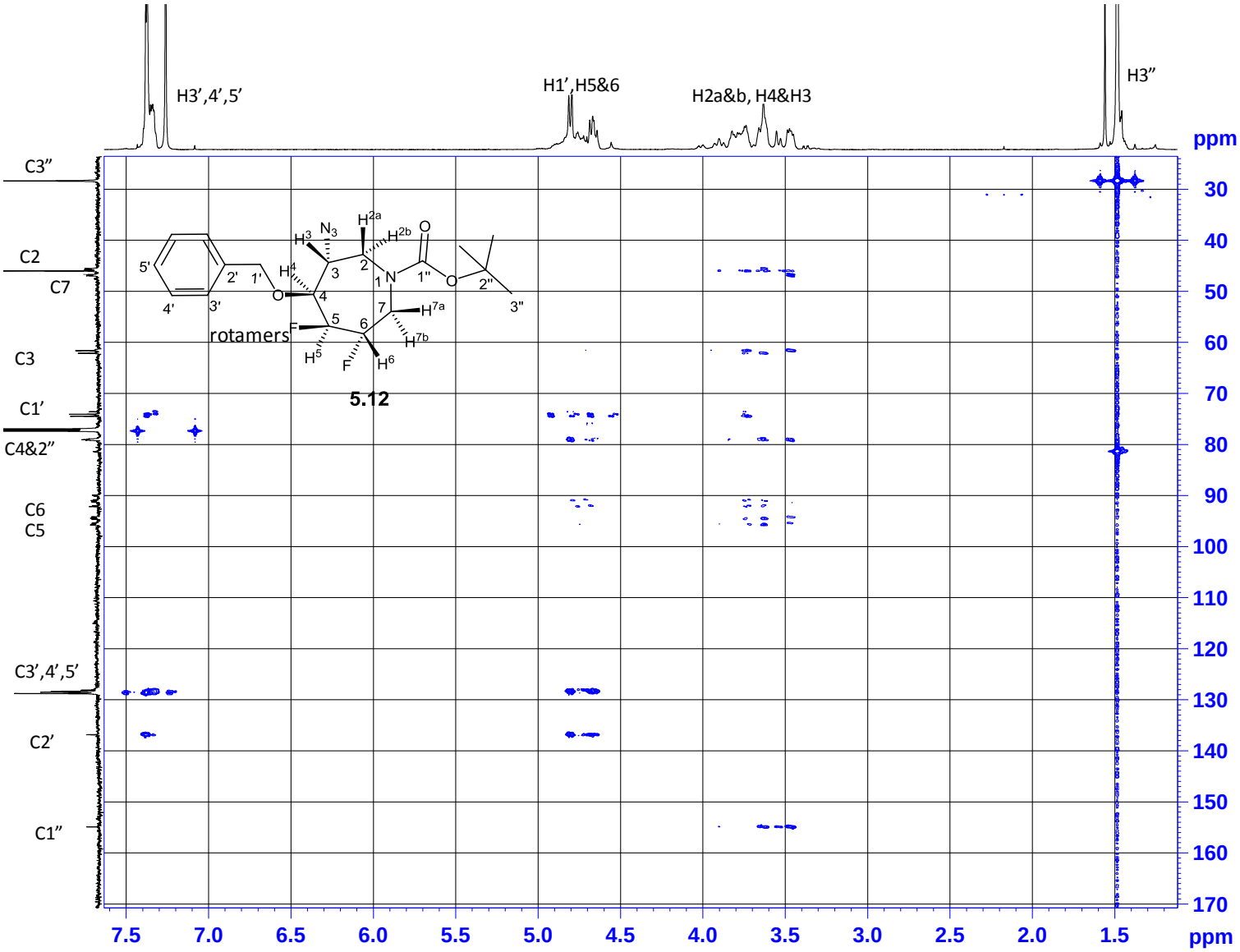
5.17

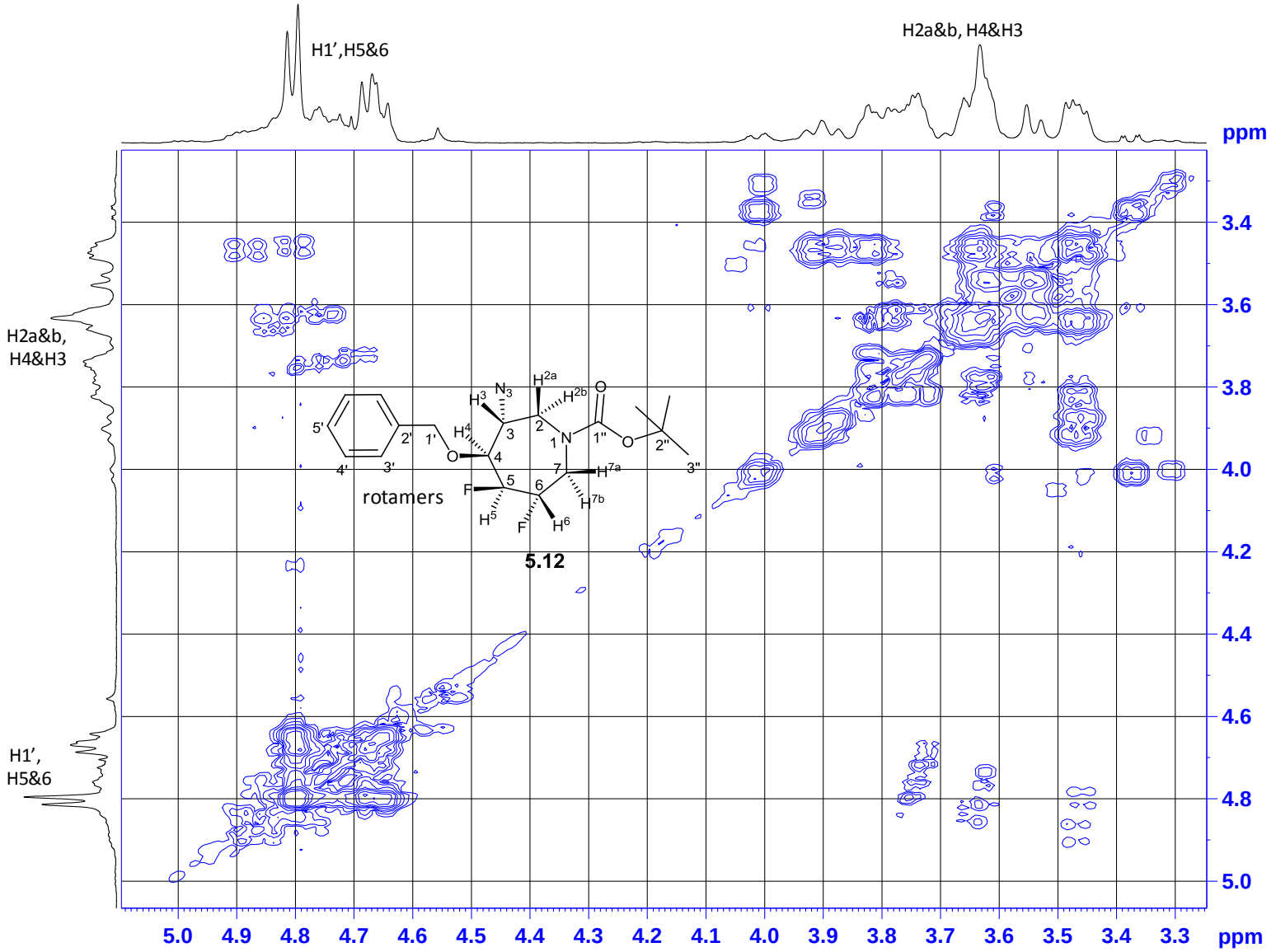

H4
H3
H7b
H2a&b
H7a
ppm
H6
H3-H6
H1'
H5
H3-H5
H5-H7a
4.40
4.45
4.50
4.55
4.60
4.65
4.70
4.75
4.80
4.85
4.90
4.95
4.05
4.00
3.95
3.90
3.85
3.80
3.75
3.70
3.65
3.60
3.55
3.50
3.45
3.40
3.35
3.30
ppm

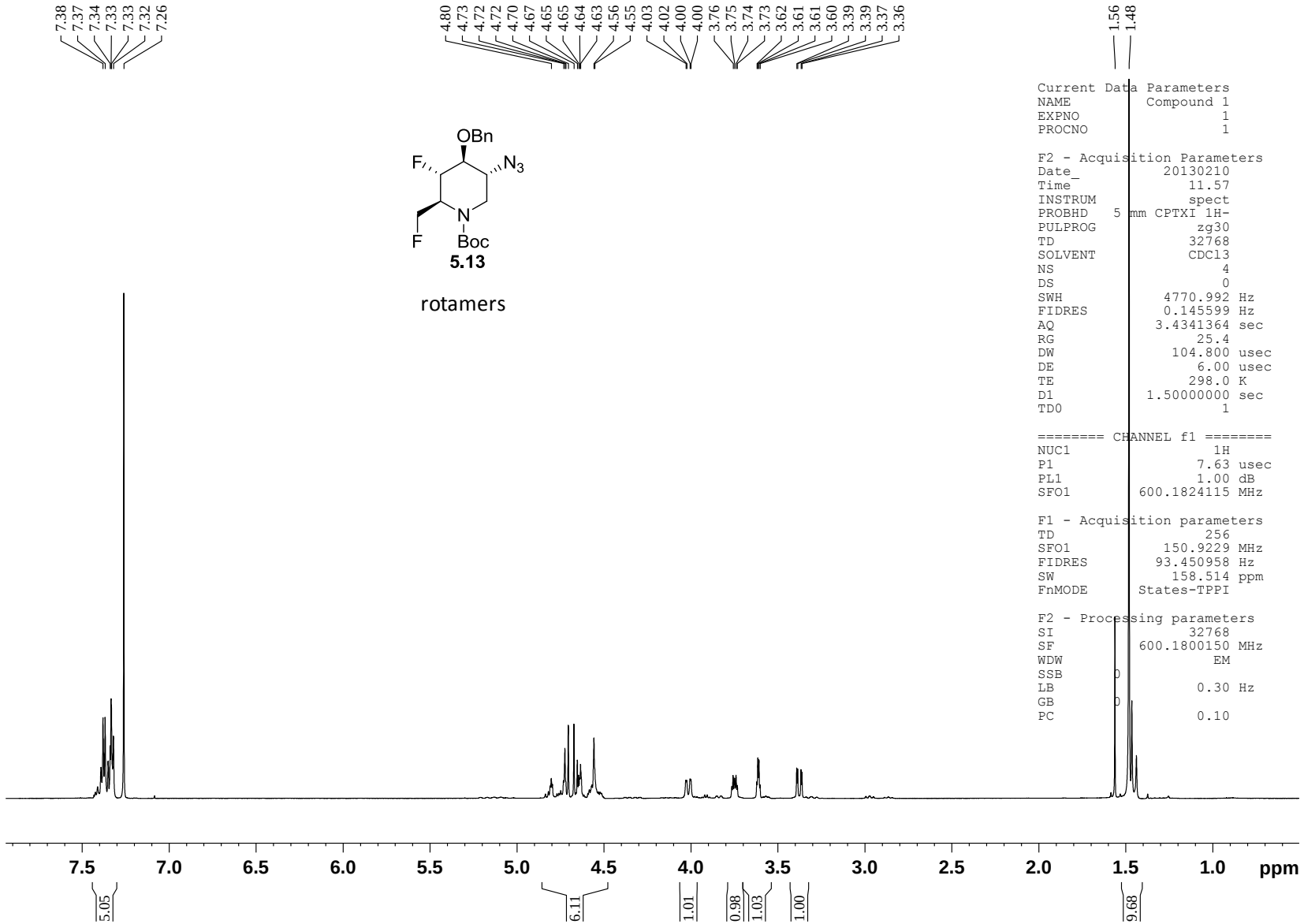

7.38
7.37
7.26
4.81
4.80
4.69
4.67
4.66
3.90
3.82
3.75
3.74
3.66
3.63
3.55
3.49
3.47
1.56
1.48
BnO
N3
F
F
N
Boc
5.12
rotamers
Current Data Parameters
NAME Compound 3
EXPNO 1
PROCNO 1
F2 - Acquisition Parameters
Date_ 20130212
Time 10.30
INSTRUM spect
PROBHD 5 mm CPTXI 1H-
PULPROG zg30
TD 32768
SOLVENT CDCl3
NS 4
DS 0
SWH 4770.992 Hz
FIDRES 0.145599 Hz
AQ 3.4341364 sec
RG 12.7
DW 104.800 usec
DE 6.00 usec
TE 298.0 K
D1 1.50000000 sec
TD0 1
======== CHANNEL f1 ========
NUC1 1H
P1 7.63 usec
PL1 1.00 dB
SFO1 600.1824115 MHz
F1 - Acquisition parameters
TD 256
SFO1 150.9229 MHz
FIDRES 93.450958 Hz
SW 158.514 ppm
FnMODE States-TPPI
F2 - Processing parameters
SI 32768
SF 600.1800149 MHz
WDW EM
SSB 0
LB 1.00 Hz
GB 0
PC 0.10
7.5
7.0
6.5
6.0
5.5
5.0
4.5
4.0
3.5
3.0
2.5
2.0
1.5
1.0
0.5
ppm
5.00
4.06
5.81
9.13

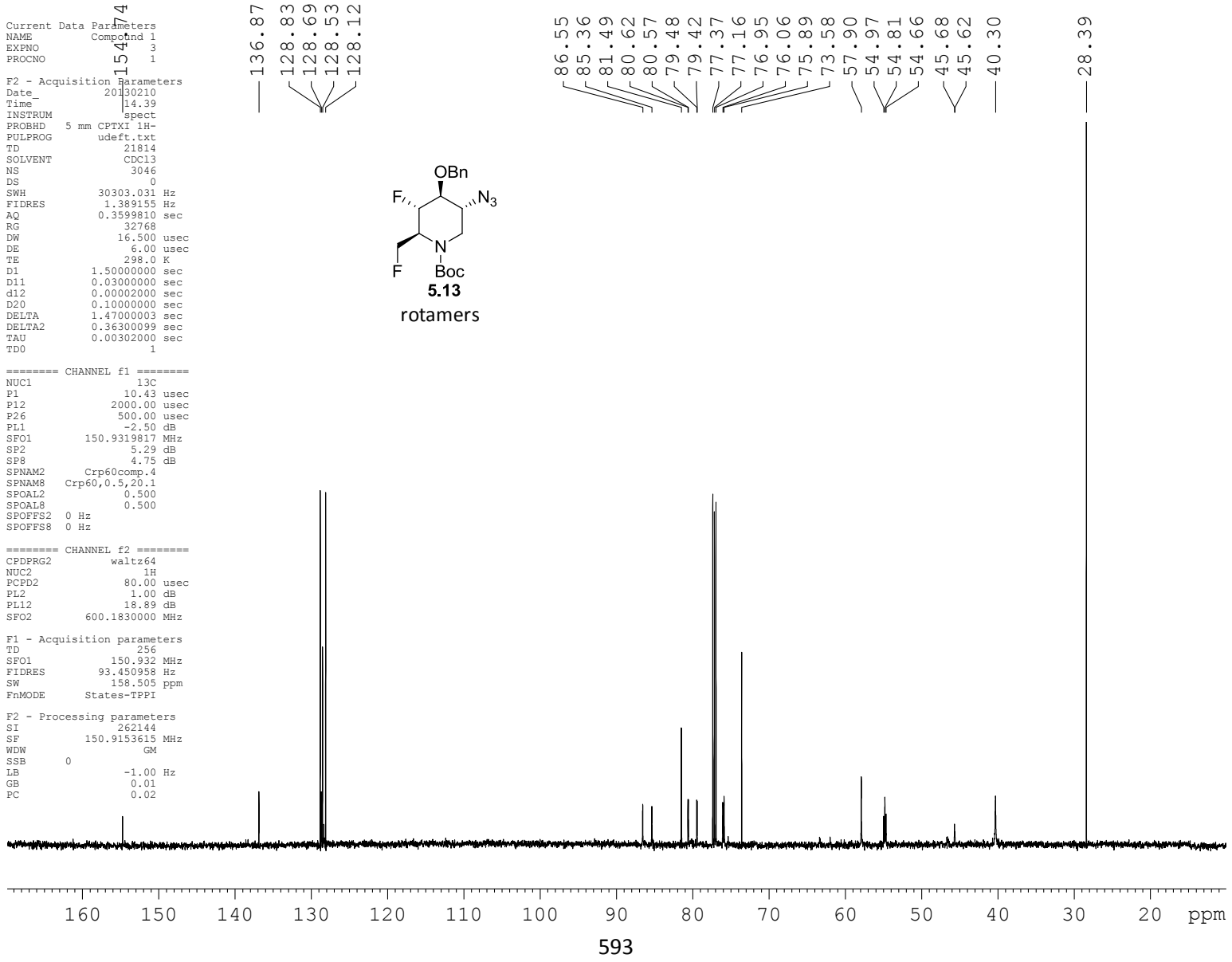

154.90
136.85
128.78
128.50
128.38
128.33
128.12
95.80
95.64
95.51
95.35
94.60
94.44
94.32
94.15
92.16
91.99
91.28
91.12
90.96
90.80
90.09
89.93
81.49
81.39
81.34
79.14
79.05
78.93
78.88
77.37
77.16
76.95
74.46
74.07
73.58
62.11
61.60
46.96
46.91
46.77
46.72
46.00
45.77
45.73
45.58
45.53
28.35
Current Data Parameters
NAME Compound 3
EXPNO 3
PROCNO 1
F2 - Acquisition parameters
Date_ 20130212
Time 13.08
INSTRUM spect
PROBHD 5 mm CPTXI 1H-
PULPROG udeft.txt
TD 21814
SOLVENT CDCl3
NS 4096
DS 0
SWH 30303.031 Hz
FIDRES 1.389155 Hz
AQ 0.3599810 sec
RG 32768
DW 16.500 usec
DE 6.00 usec
TE 298.0 K
D1 1.50000000 sec
D11 0.03000000 sec
d12 0.00002000 sec
D20 0.10000000 sec
DELTA 1.47000003 sec
DELTA2 0.36300099 sec
TAU 0.00302000 sec
TD0 1
======== CHANNEL f1 ========
NUC1 13C
P1 10.43 usec
P12 2000.00 usec
P26 500.00 usec
PL1 -2.50 dB
SFO1 150.9319817 MHz
SP2 5.29 dB
SP8 4.75 dB
SPNAM2 Crp60comp.4
SPNAM8 Crp60,0.5,20.1
SPOAL2 0.500
SPOAL8 0.500
SPOFFS2 0 Hz
SPOFFS8 0 Hz
======== CHANNEL f2 ========
CPDPRG2 waltz64
NUC2 1H
PCPD2 80.00 usec
PL2 1.00 dB
PL12 18.89 dB
SFO2 600.1830000 MHz
F1 - Acquisition parameters
TD 256
SFO1 150.932 MHz
FIDRES 93.450958 Hz
SW 158.505 ppm
FnMODE States-TPPI
F2 - Processing parameters
SI 262144
SF 150.9153619 MHz
WDW EM
SSB 0
LB 5.00 Hz
GB 0
PC 0.02
BnO
N3
F
F
N
Boc
5.12
rotamers
160
150
140
130
120
110
100
90
80
70
60
50
40
30
20
ppm

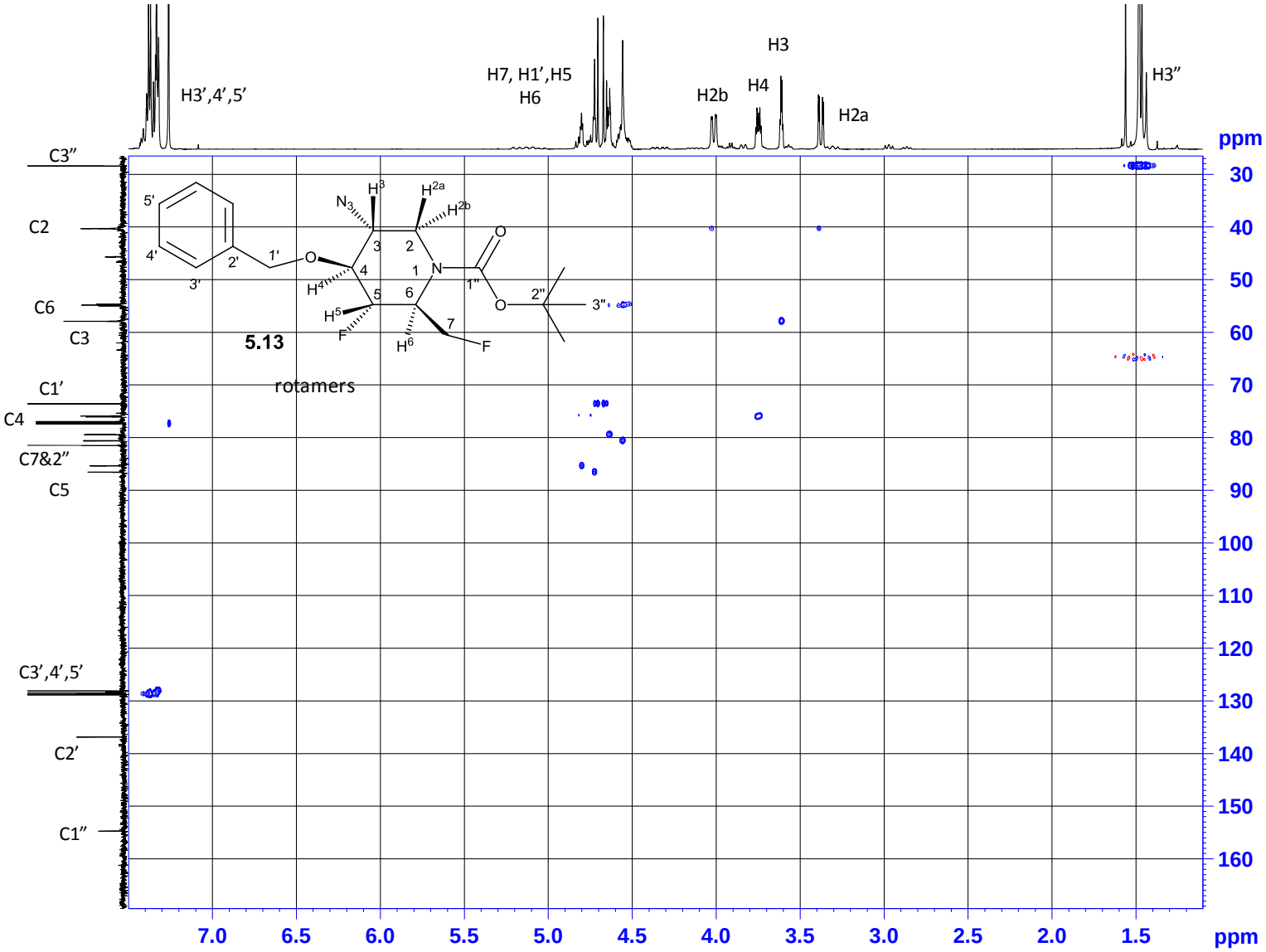

H3',4',5'
H1',H5&6
H2a&b, H4&H3
H3"
ppm
C3"
C2
C7
C3
C1'
C4&2"
C6
C5
C3',4',5'
C2'
C1"
rotamers
5.12
7.5
7.0
6.5
6.0
5.5
5.0
4.5
4.0
3.5
3.0
2.5
2.0
1.5
ppm

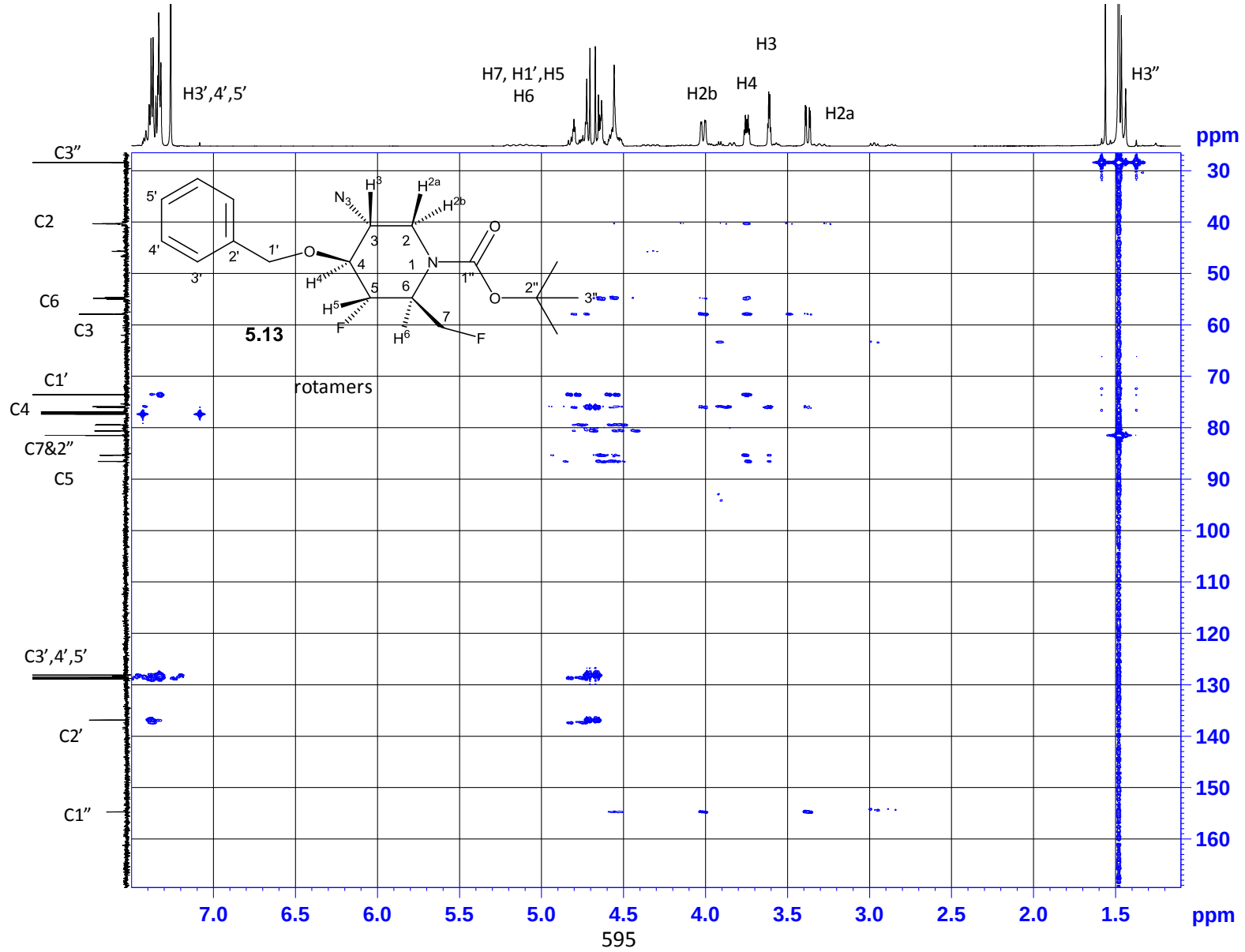

H3',4',5'
H1',H5&6
H2a&b, H4&H3
H3"
ppm
C3"
C2
C7
C3
C1'
C4&2"
C6
C5
C3',4',5'
C2'
C1"
rotamers
5.12
7.5
7.0
6.5
6.0
5.5
5.0
4.5
4.0
3.5
3.0
2.5
2.0
1.5
ppm

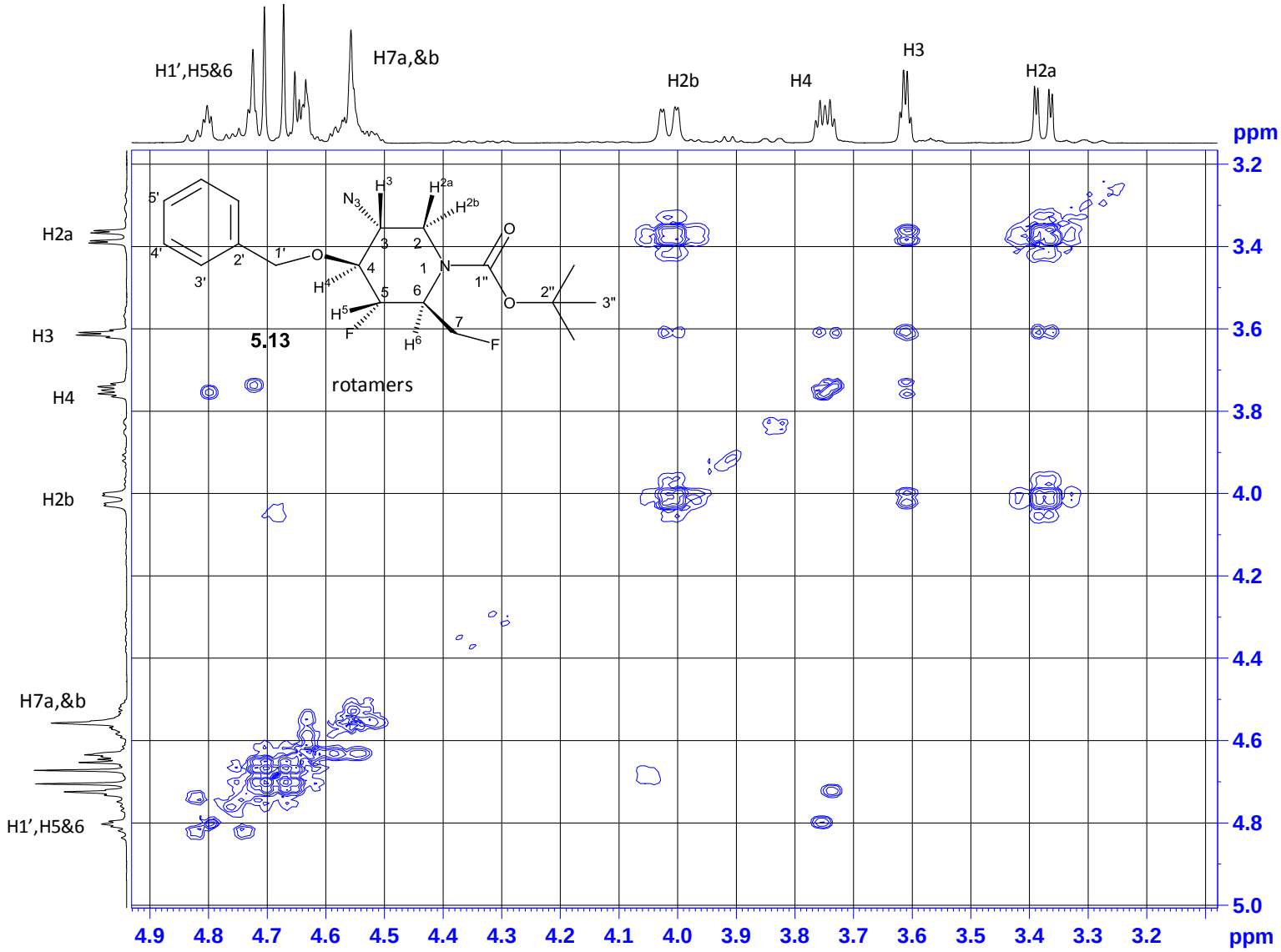

H1',H5&6
H2a&b, H4&H3
ppm
H2a&b,
H4&H3
H1',
H5&6
rotamers
5.12
3.4
3.6
3.8
4.0
4.2
4.4
4.6
4.8
5.0
5.0 4.9 4.8 4.7 4.6 4.5 4.4 4.3 4.2 4.1 4.0 3.9 3.8 3.7 3.6 3.5 3.4 3.3 ppm

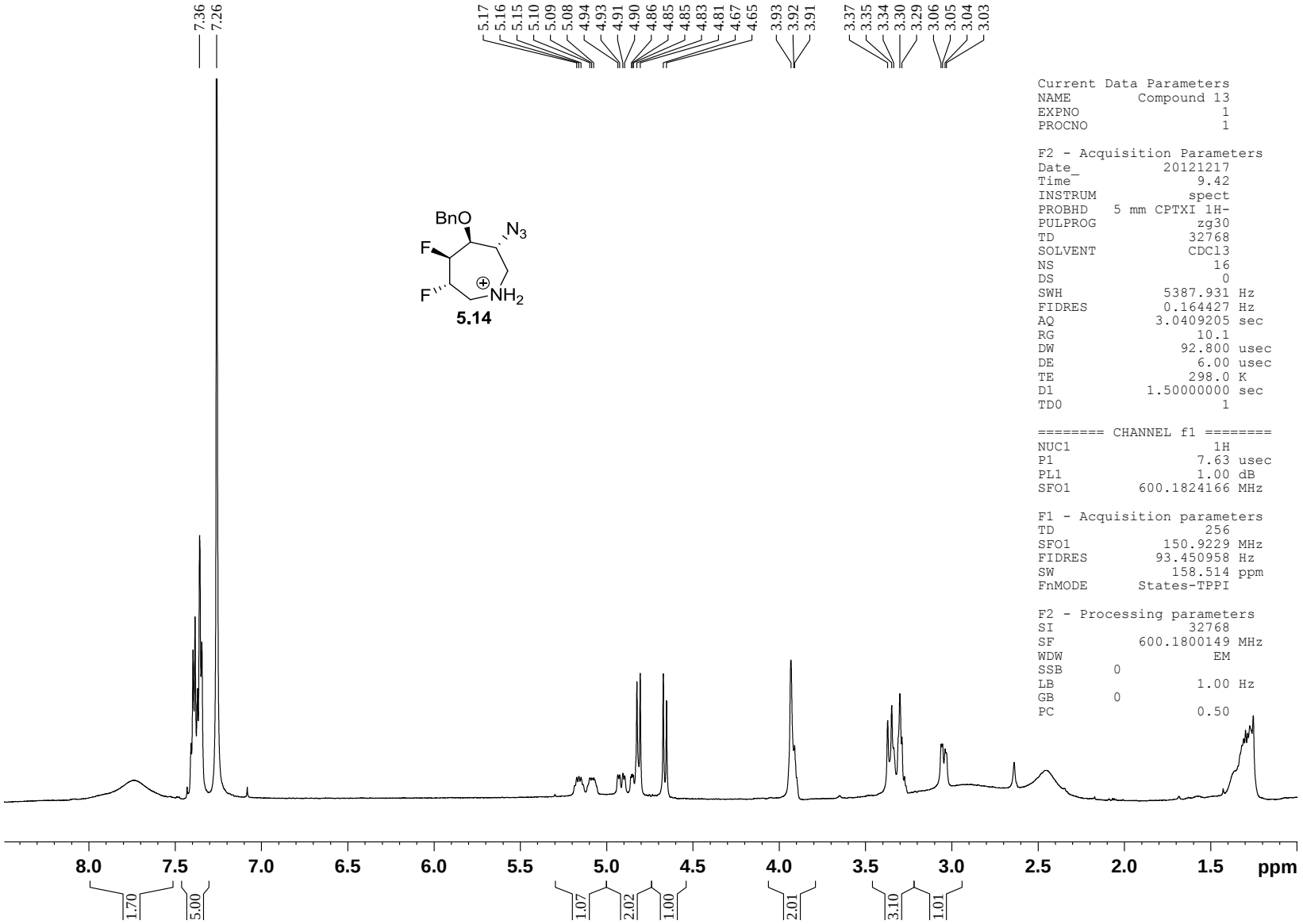

7.38
7.37
7.34
7.33
7.33
7.32
7.26
4.80
4.73
4.72
4.72
4.70
4.67
4.65
4.65
4.64
4.63
4.56
4.55
4.03
4.02
4.00
4.00
3.76
3.75
3.74
3.73
3.62
3.61
3.61
3.60
3.39
3.39
3.37
3.36
1.56
1.48
OBn
F
N3
N
F
Boc
5.13
rotamers
Current Data Parameters
NAME Compound 1
EXPNO 1
PROCNO 1
F2 - Acquisition Parameters
Date_ 20130210
Time 11.57
INSTRUM spect
PROBHD 5 mm CPTXI 1H-
PULPROG zg30
TD 32768
SOLVENT CDCl3
NS 4
DS 0
SWH 4770.992 Hz
FIDRES 0.145599 Hz
AQ 3.4341364 sec
RG 25.4
DW 104.800 usec
DE 6.00 usec
TE 298.0 K
D1 1.50000000 sec
TD0 1
======== CHANNEL f1 ========
NUC1 1H
P1 7.63 usec
PL1 1.00 dB
SFO1 600.1824115 MHz
F1 - Acquisition parameters
TD 256
SFO1 150.9229 MHz
FIDRES 93.450958 Hz
SW 158.514 ppm
FnMODE States-TPPI
F2 - Processing parameters
SI 32768
SF 600.1800150 MHz
WDW EM
SSB 0
LB 0.30 Hz
GB 0
PC 0.10
7.5
7.0
6.5
6.0
5.5
5.0
4.5
4.0
3.5
3.0
2.5
2.0
1.5
1.0
ppm
5.05
6.11
1.01
0.98
1.03
1.00
9.68

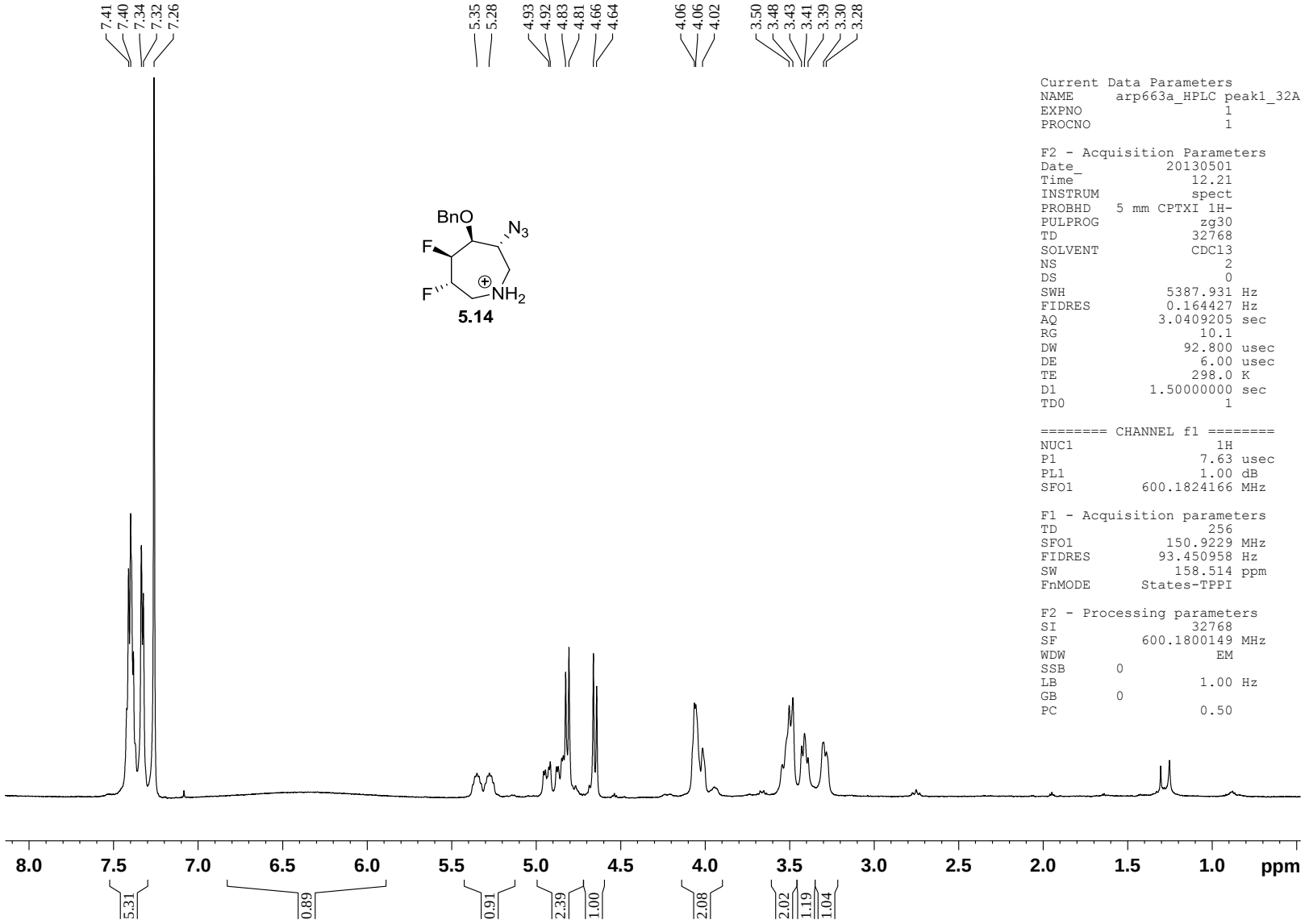

Current Data Parameters
NAME Compound 1
EXPNO 3
PROCNO 1
F2 - Acquisition Parameters
Date_ 20130210
Time_ 14.39
INSTRUM spect
PROBHD 5 mm CPTXI 1H-
PULPROG udeft.txt
TD 21814
SOLVENT CDCl3
NS 3046
DS 0
SWH 30303.031 Hz
FIDRES 1.389155 Hz
AQ 0.3599810 sec
RG 32768
DW 16.500 usec
DE 6.00 usec
TE 298.0 K
D1 1.50000000 sec
D11 0.03000000 sec
d12 0.00002000 sec
D20 0.10000000 sec
DELTA 1.47000003 sec
DELTA2 0.36300099 sec
TAU 0.00302000 sec
TD0 1
======== CHANNEL f1 ========
NUC1 13C
P1 10.43 usec
P12 2000.00 usec
P26 500.00 usec
PL1 -2.50 dB
SFO1 150.9319817 MHz
SP2 5.29 dB
SP8 4.75 dB
SPNAM2 Crp60comp.4
SPNAM8 Crp60,0.5,20.1
SPOAL2 0.500
SPOAL8 0.500
SPOFFS2 0 Hz
SPOFFS8 0 Hz
======== CHANNEL f2 ========
CPDPRG2 waltz64
NUC2 1H
PCPD2 80.00 usec
PL2 1.00 dB
PL12 18.89 dB
SFO2 600.1830000 MHz
F1 - Acquisition parameters
TD 256
SFO1 150.932 MHz
FIDRES 93.450958 Hz
SW 158.505 ppm
FnMODE States-TPPI
F2 - Processing parameters
SI 262144
SF 150.9153615 MHz
WDW GM
SSB 0
LB -1.00 Hz
GB 0.01
PC 0.02
154.74
136.87
128.83
128.69
128.53
128.12
86.55
85.36
81.49
80.62
80.57
79.48
79.42
77.37
77.16
76.95
76.06
75.89
73.58
57.90
54.97
54.81
54.66
45.68
45.62
40.30
28.39
OBn
F
N3
N
F
Boc
5.13
rotamers
160
150
140
130
120
110
100
90
80
70
60
50
40
30
20
ppm


H3’,4’,5’
H7, H1’,H5
H6
H2b
H4
H3
H2a
H3”
ppm
C3”
C2
C6
C3
C1’
C4
C7&2”
C5
C3’,4’,5’
C2’
C1”
5.13
rotamers
7.0
6.5
6.0
5.5
5.0
4.5
4.0
3.5
3.0
2.5
2.0
1.5
ppm

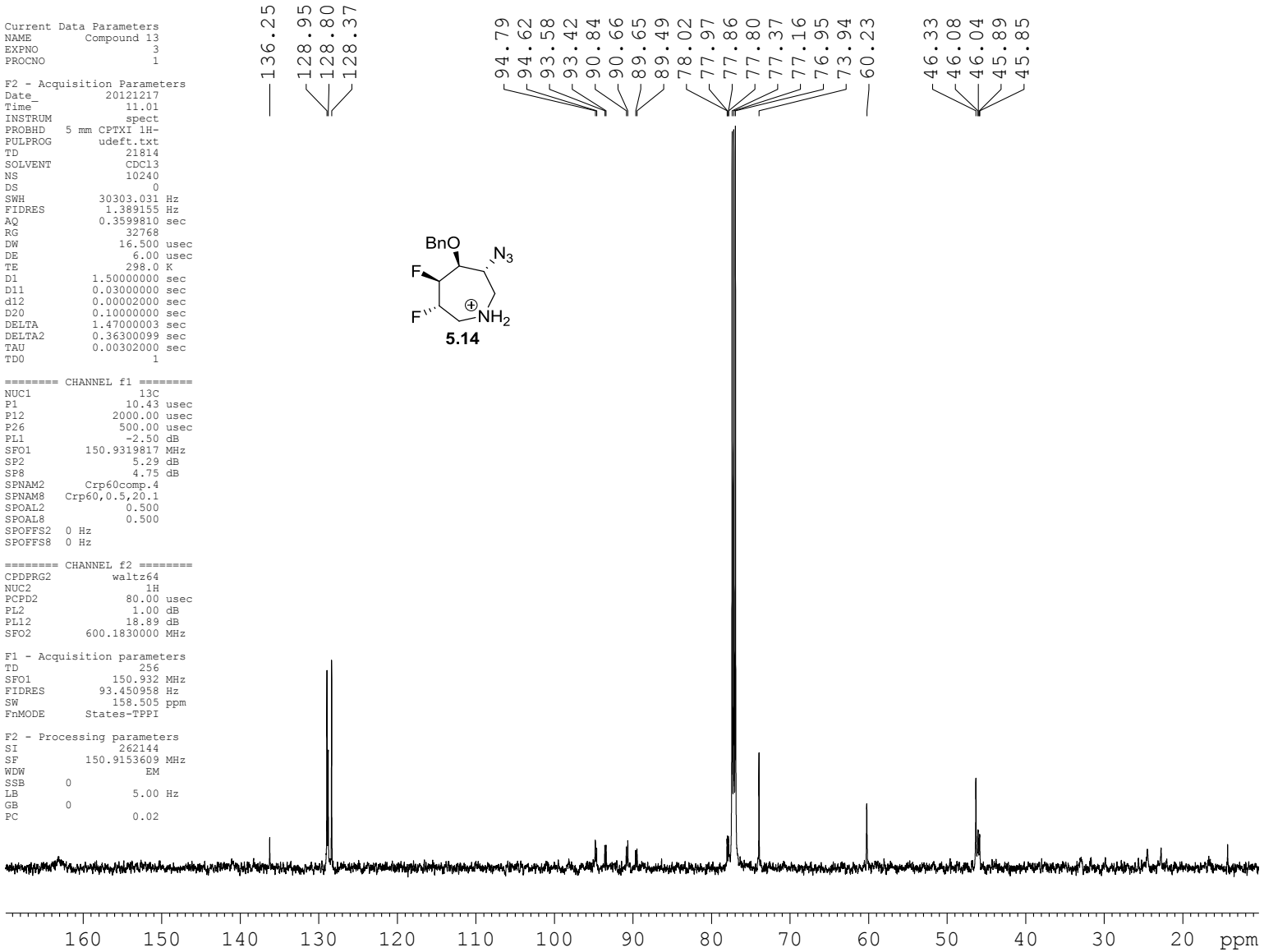

H3',4',5'
H7, H1',H5
H6
H2b
H3
H4
H2a
H3"
ppm
C3"
C2
C6
C3
C1'
C4
C7&2"
C5
C3',4',5'
C2'
C1"
5.13
rotamers
7.0
6.5
6.0
5.5
5.0
4.5
4.0
3.5
3.0
2.5
2.0
1.5
ppm

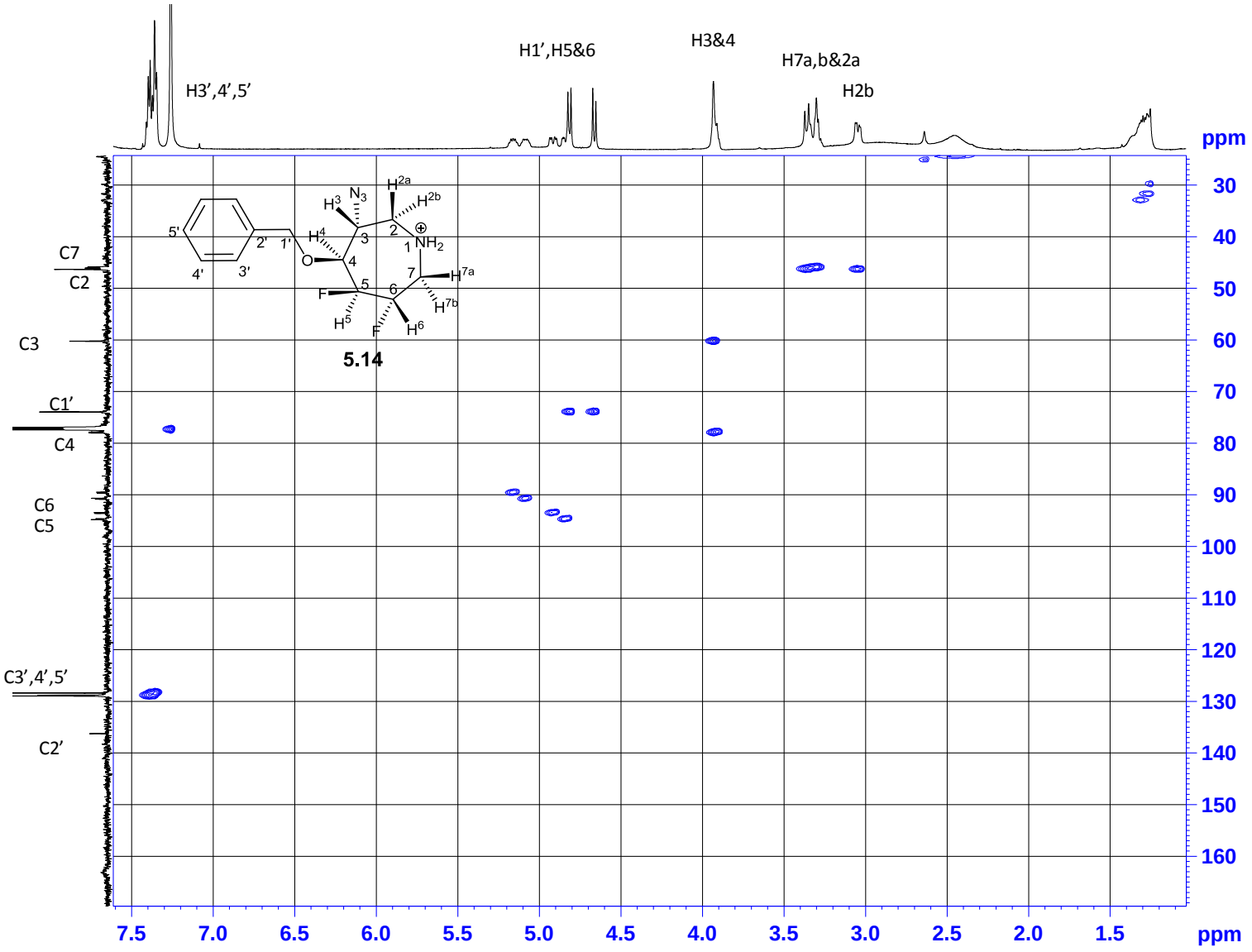

H1',H5&6
H7a,&b
H2b
H4
H3
H2a
ppm
3.2
3.4
3.6
3.8
4.0
4.2
4.4
4.6
4.8
5.0
5.13
rotamers
4.9
4.8
4.7
4.6
4.5
4.4
4.3
4.2
4.1
4.0
3.9
3.8
3.7
3.6
3.5
3.4
3.3
3.2
ppm

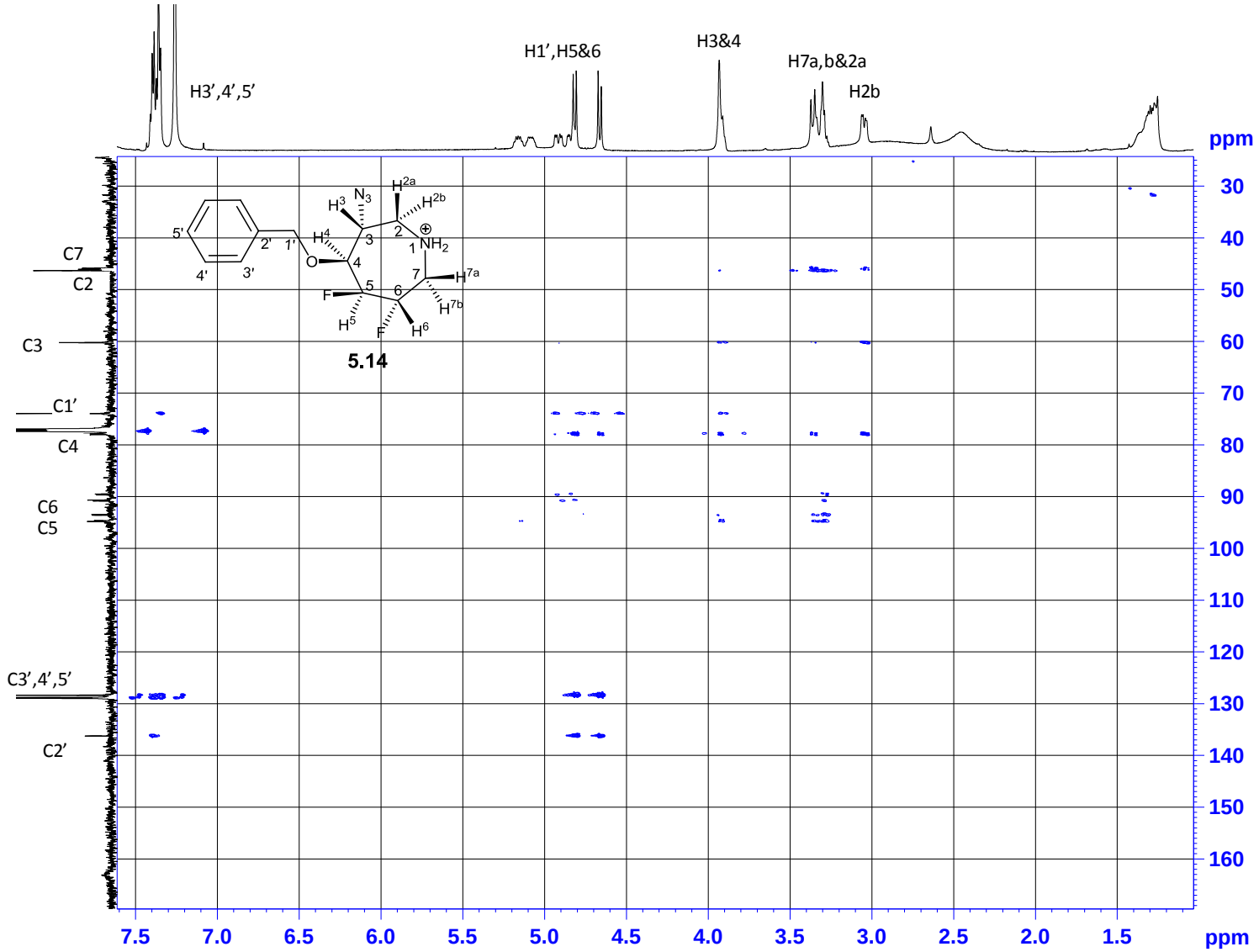

7.36
7.26
5.17
5.16
5.15
5.10
5.09
5.08
4.94
4.93
4.91
4.90
4.86
4.85
4.85
4.83
4.81
4.67
4.65
3.93
3.92
3.91
3.37
3.35
3.34
3.30
3.29
3.06
3.05
3.04
3.03
BnO
N3
F
F
NH2
5.14
Current Data Parameters
NAME Compound 13
EXPNO 1
PROCNO 1
F2 - Acquisition Parameters
Date_ 20121217
Time 9.42
INSTRUM spect
PROBHD 5 mm CPTXI 1H-
PULPROG zg30
TD 32768
SOLVENT CDCl3
NS 16
DS 0
SWH 5387.931 Hz
FIDRES 0.164427 Hz
AQ 3.0409205 sec
RG 10.1
DW 92.800 usec
DE 6.00 usec
TE 298.0 K
D1 1.50000000 sec
TD0 1
======== CHANNEL f1 ========
NUC1 1H
P1 7.63 usec
PL1 1.00 dB
SFO1 600.1824166 MHz
F1 - Acquisition parameters
TD 256
SFO1 150.9229 MHz
FIDRES 93.450958 Hz
SW 158.514 ppm
FnMODE States-TPPI
F2 - Processing parameters
SI 32768
SF 600.1800149 MHz
WDW EM
SSB 0
LB 1.00 Hz
GB 0
PC 0.50
8.0
7.5
7.0
6.5
6.0
5.5
5.0
4.5
4.0
3.5
3.0
2.5
2.0
1.5
ppm
1.70
5.00
1.07
2.02
1.00
2.01
3.10
1.01

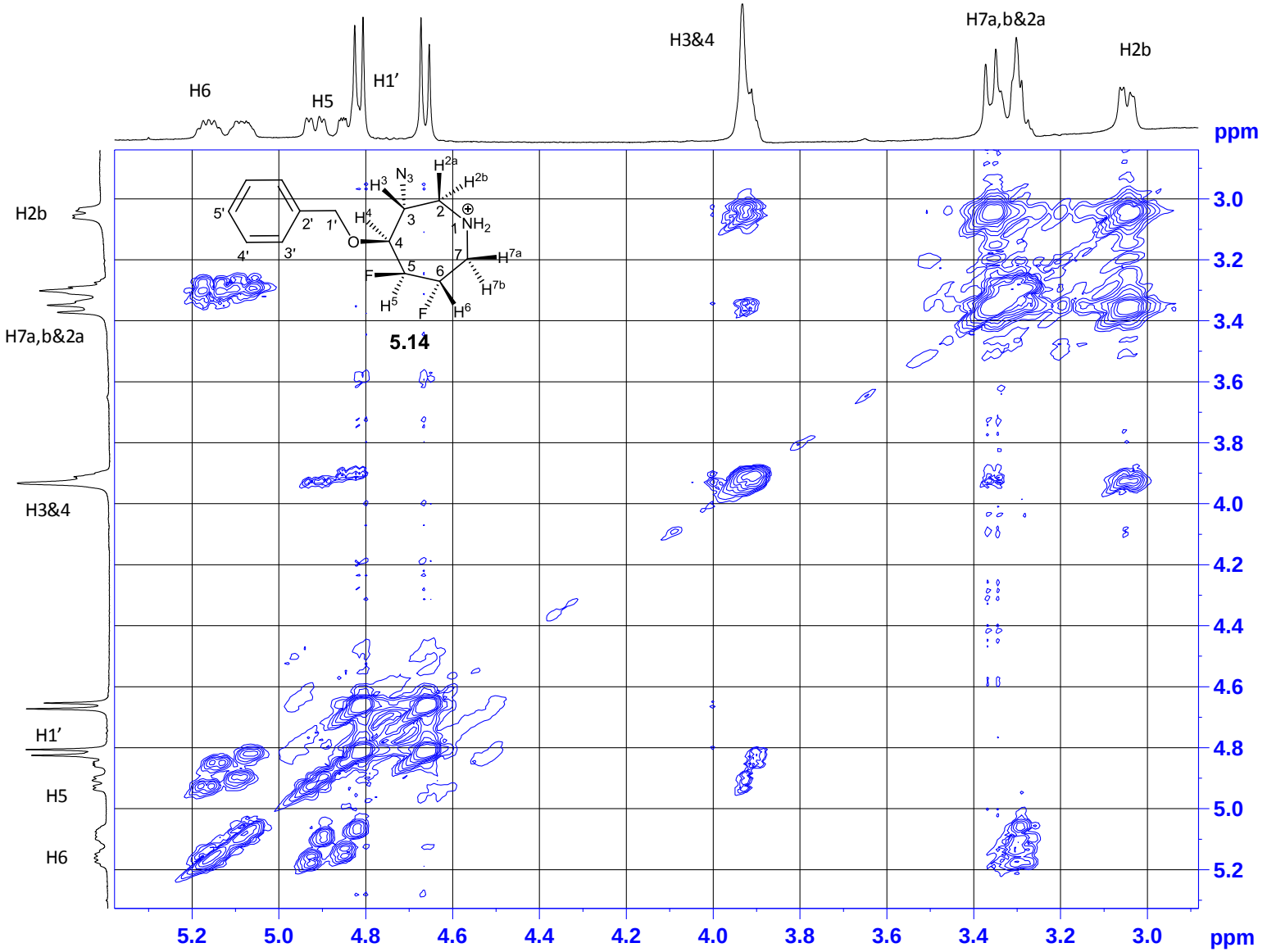


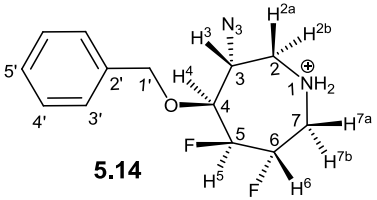
598 NB: ^{1}H NMR with a drop of TFA to shift the H3 and H4.


Current Data Parameters
NAME Compound 13
EXPNO 3
PROCNO 1
F2 - Acquisition Parameters
Date_ 20121217
Time 11.01
INSTRUM spect
PROBHD 5 mm CPTXI 1H-
PULPROG udeft.txt
TD 21814
SOLVENT CDCl3
NS 10240
DS 0
SWH 30303.031 Hz
FIDRES 1.389155 Hz
AQ 0.3599810 sec
RG 32768
DW 16.500 usec
DE 6.00 usec
TE 298.0 K
D1 1.50000000 sec
D11 0.03000000 sec
d12 0.00002000 sec
D20 0.10000000 sec
DELTA 1.47000003 sec
DELTA2 0.36300099 sec
TAU 0.00302000 sec
TD0 1
======== CHANNEL f1 ========
NUC1 13C
P1 10.43 usec
P12 2000.00 usec
P26 500.00 usec
PL1 -2.50 dB
SFO1 150.9319817 MHz
SP2 5.29 dB
SP8 4.75 dB
SPNAM2 Crp60comp.4
SPNAM8 Crp60,0.5,20.1
SPOAL2 0.500
SPOAL8 0.500
SPOFFS2 0 Hz
SPOFFS8 0 Hz
======== CHANNEL f2 ========
CPDPRG2 waltz64
NUC2 1H
PCPD2 80.00 usec
PL2 1.00 dB
PL12 18.89 dB
SFO2 600.1830000 MHz
F1 - Acquisition parameters
TD 256
SFO1 150.932 MHz
FIDRES 93.450958 Hz
SW 158.505 ppm
FnMODE States-TPPI
F2 - Processing parameters
SI 262144
SF 150.9153609 MHz
WDW EM
SSB 0
LB 5.00 Hz
GB 0
PC 0.02
136.25
128.95
128.80
128.37
94.79
94.62
93.58
93.42
90.84
90.66
89.65
89.49
78.02
77.97
77.86
77.80
77.37
77.16
76.95
73.94
60.23
46.33
46.08
46.04
45.89
45.85
BnO
N3
F
F
NH2
5.14
160
150
140
130
120
110
100
90
80
70
60
50
40
30
20
ppm


H3',4',5'
H1',H5&6
H3&4
H7a,b&2a
H2b
ppm
C7
C2
C3
C1'
C4
C6
C5
C3',4',5'
C2'
5.14
7.5
7.0
6.5
6.0
5.5
5.0
4.5
4.0
3.5
3.0
2.5
2.0
1.5
ppm


H3',4',5'
H1',H5&6
H3&4
H7a,b&2a
H2b
ppm
C7
C2
C3
C1'
C4
C6
C5
C3',4',5'
C2'
5.14
7.5
7.0
6.5
6.0
5.5
5.0
4.5
4.0
3.5
3.0
2.5
2.0
1.5
ppm

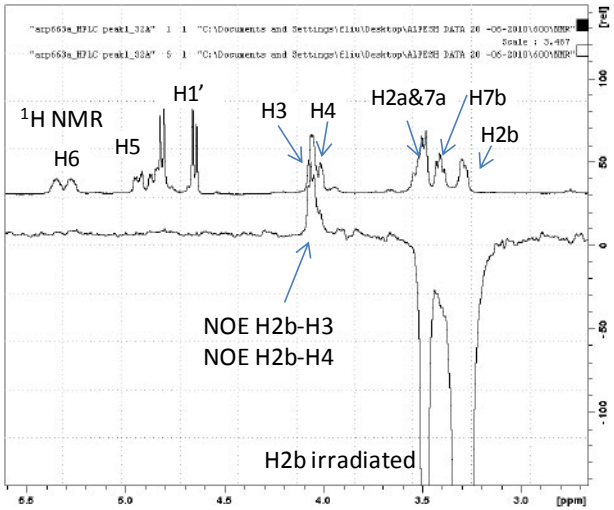

H6
H5
H1'
H3&4
H7a,b&2a
H2b
ppm
5.14
5.2
5.0
4.8
4.6
4.4
4.2
4.0
3.8
3.6
3.4
3.2
3.0



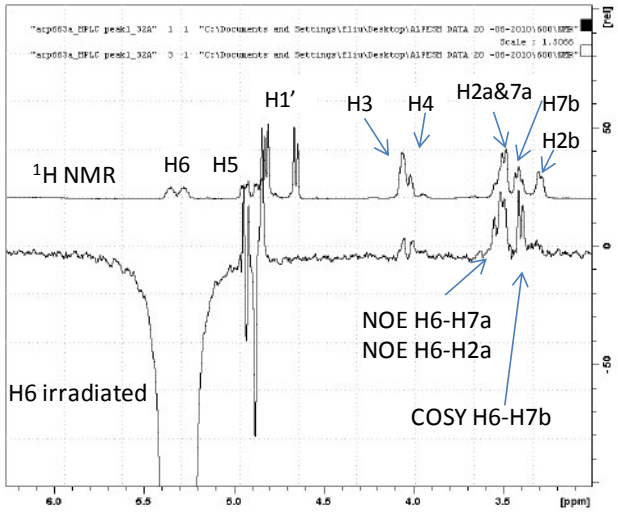
5.14

- **H2a and H2b** : H2b shows NOE to H4 suggesting H2b is *cis* to H4. Moreover, $J_{H3\text{-}H2a}$ = 1.4 Hz suggests a clear *gauche* meaning H3 and H2a are *cis*. while big $J_{H3\text{-}H2b}$ (7 Hz) means H2b is *trans* to H3. H3-H2a torsion angle can be either 72° or 89°. And H3-H2b torsion angle can be either **33°**, 139°, 224°, or 330°. Now if we presume 72° torsion for H3-H2a then H3-H2b can be either 33° or 180°. 180 is not on list for H3-H2b torsion angles. So, it can very well be 33°. While in case of 89° torsion between H3-H2a results in H3-H2b torsion possibilities of 33°, 201°; again 33° is on list. All this suggests H2a is *cis* and H2b is *trans* to H3.
- **H6** : H6 shows big NOE with H2a and no measurable NOE with H2b. This clearly indicates H6 and H2a are in same phase (both *cis* to H3) H6 also shows up NOE with H3 and H7a (bigger compared to H7b) which again supports that H6 is *cis* to H3.
- **H7a and H7b** : Now, $J_{H7b\text{-}H6}$ = 8.2 Hz and $J_{H7a\text{-}H6}$ = 2.3 Hz clearly suggests H7b-H6 *trans* and H7a-H6 *cis* configuration.
- **H5** : Big $J_{H5\text{-}H6}$ (7 Hz) hints that they are *trans*. H5 shows NOE to H7b while no measurable NOE with H7a; suggesting H5 and H7b are in same phase. (both *cis* to H4!!)

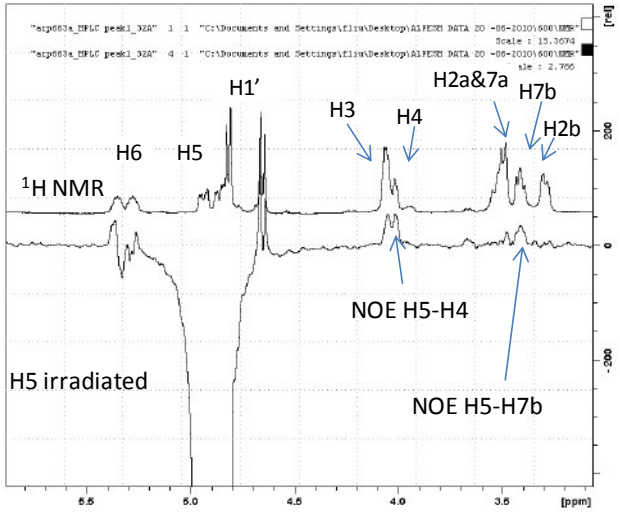
1D selective NOESY

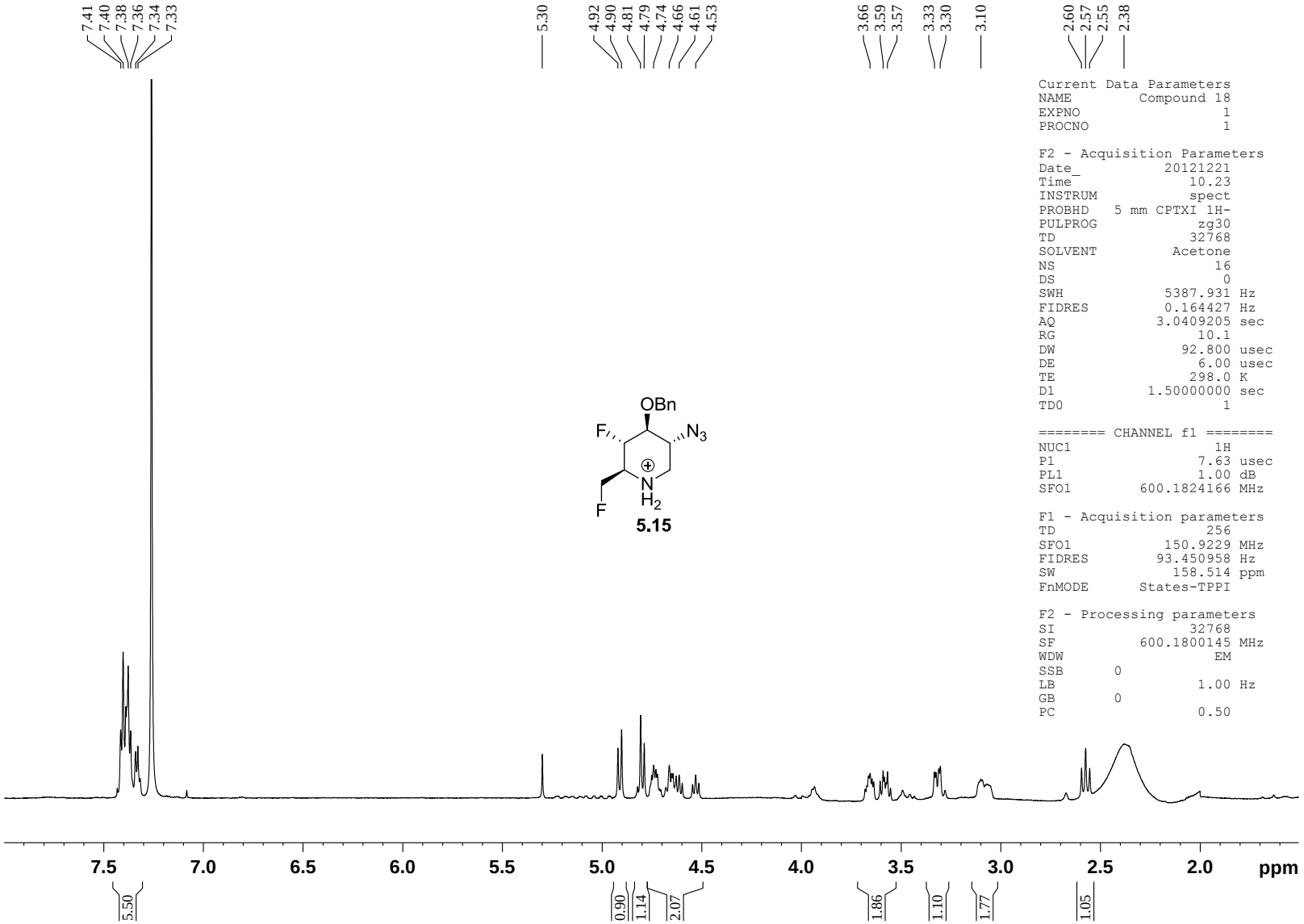


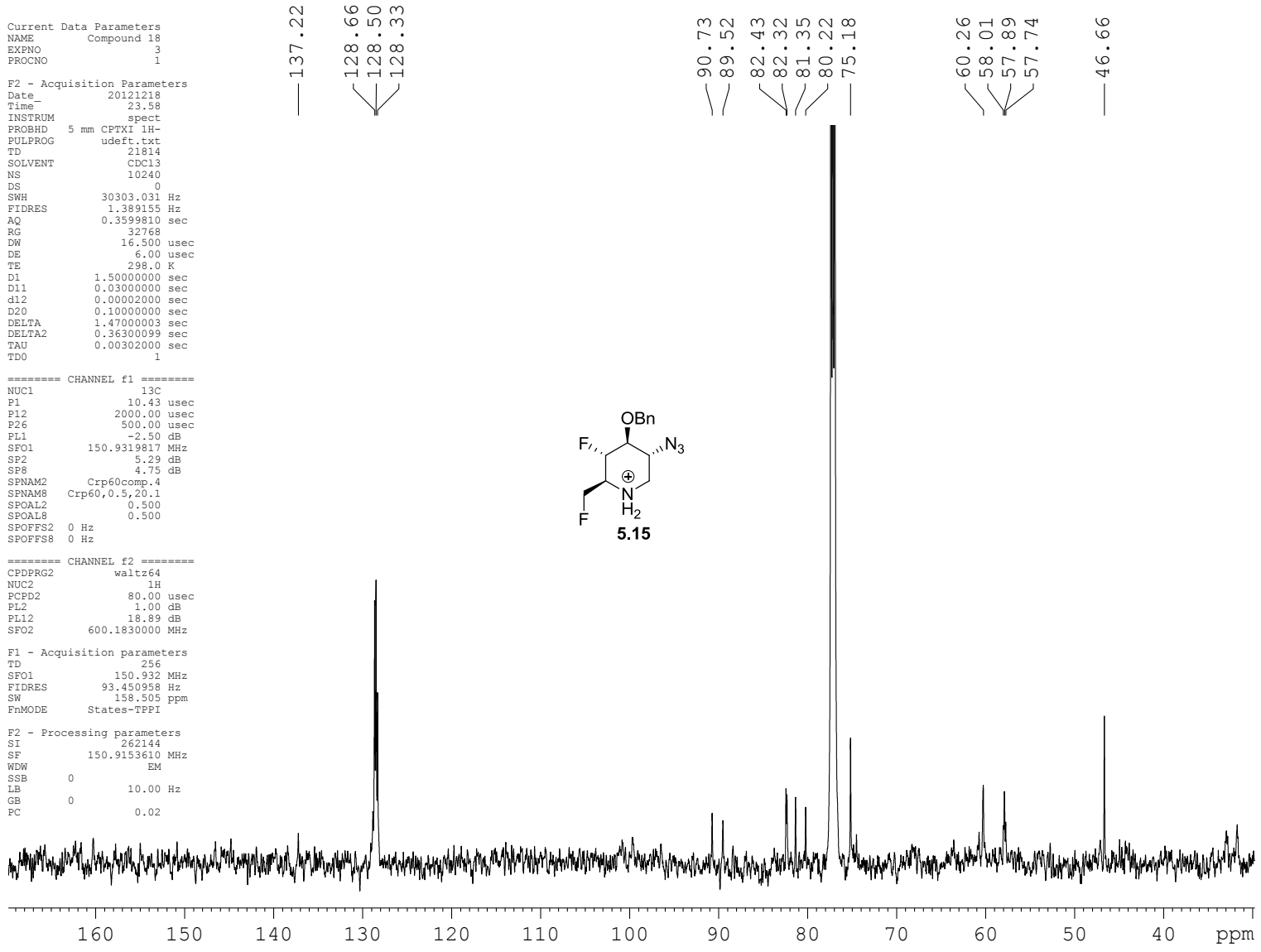
1D selective NOESY

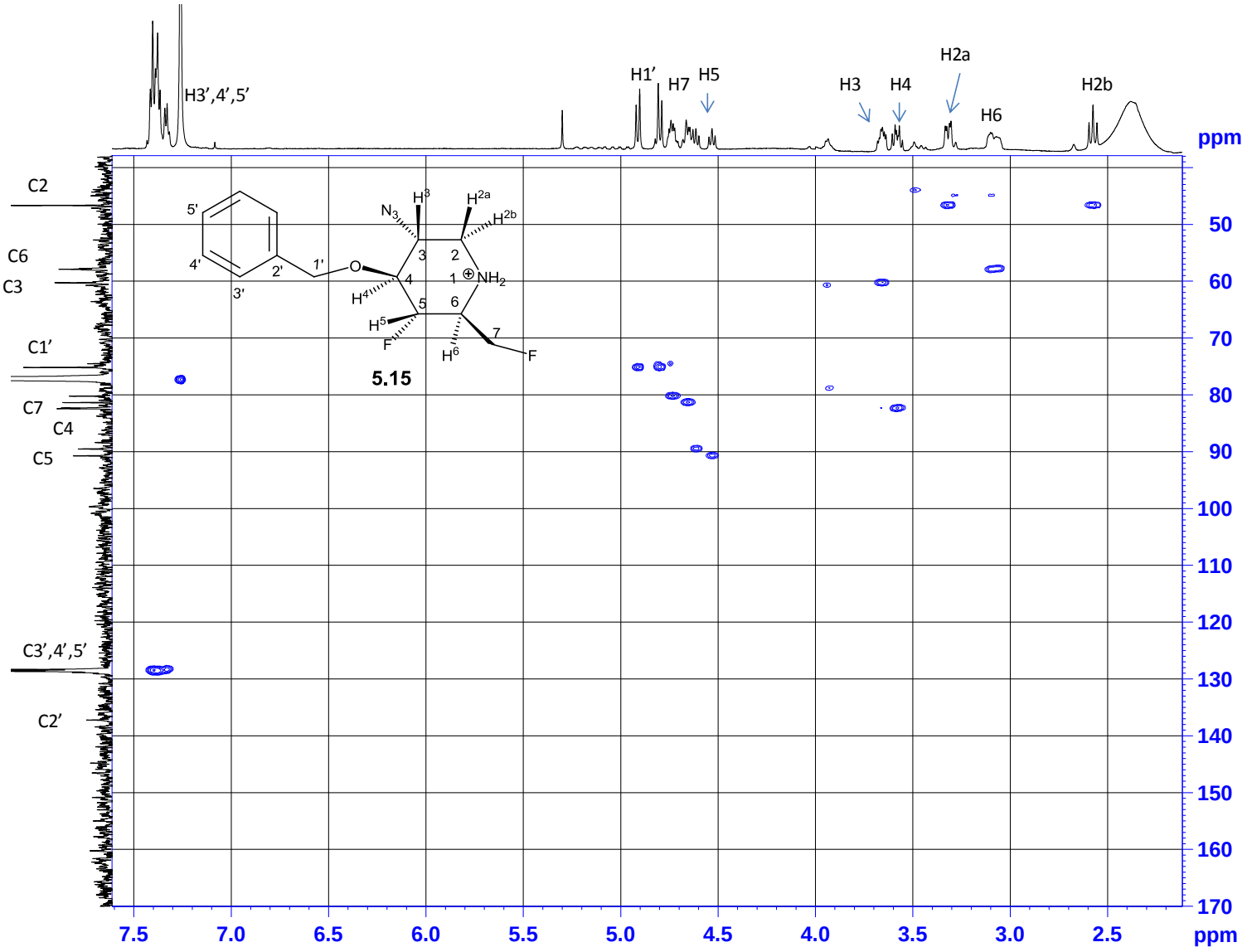


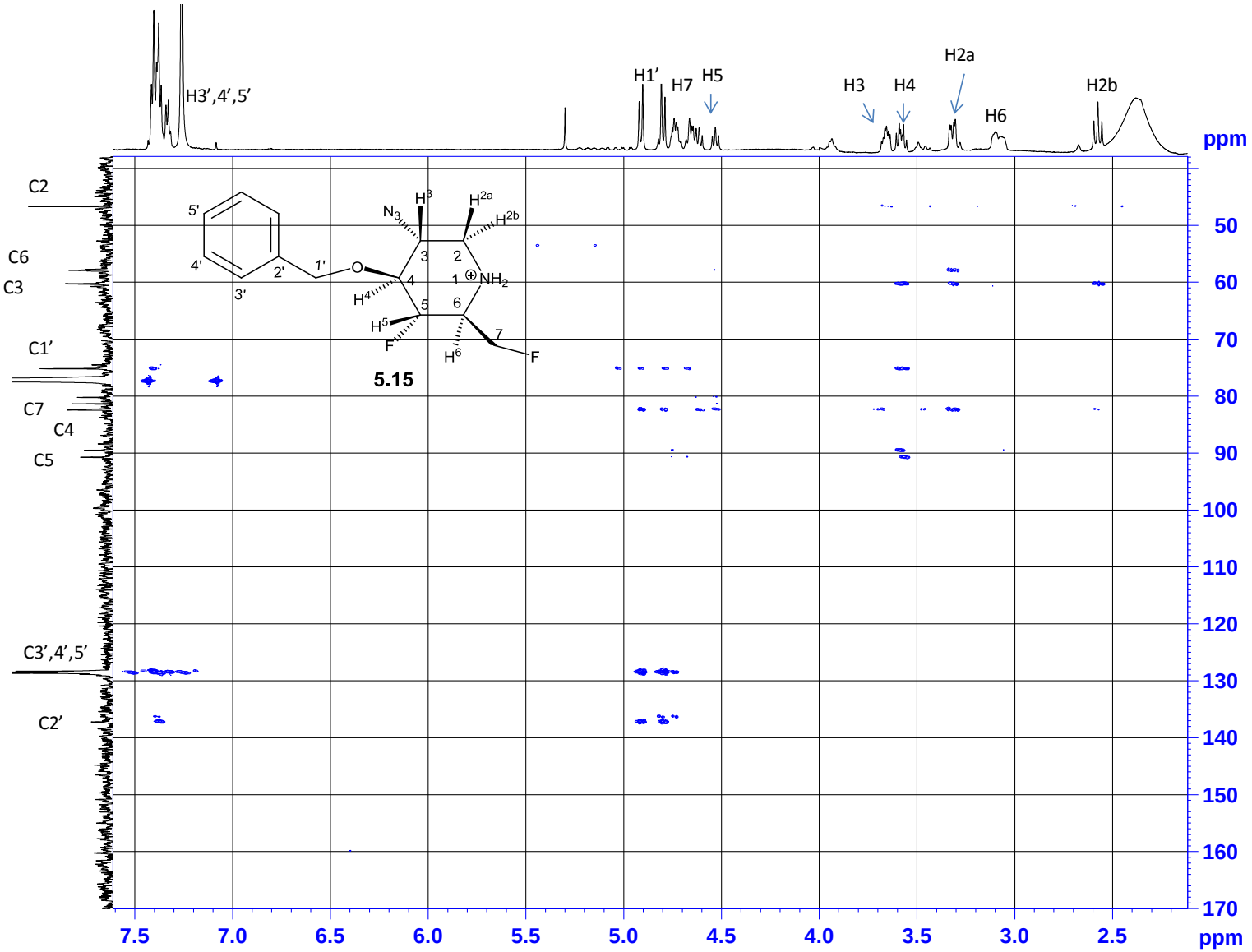
1D selective NOESY

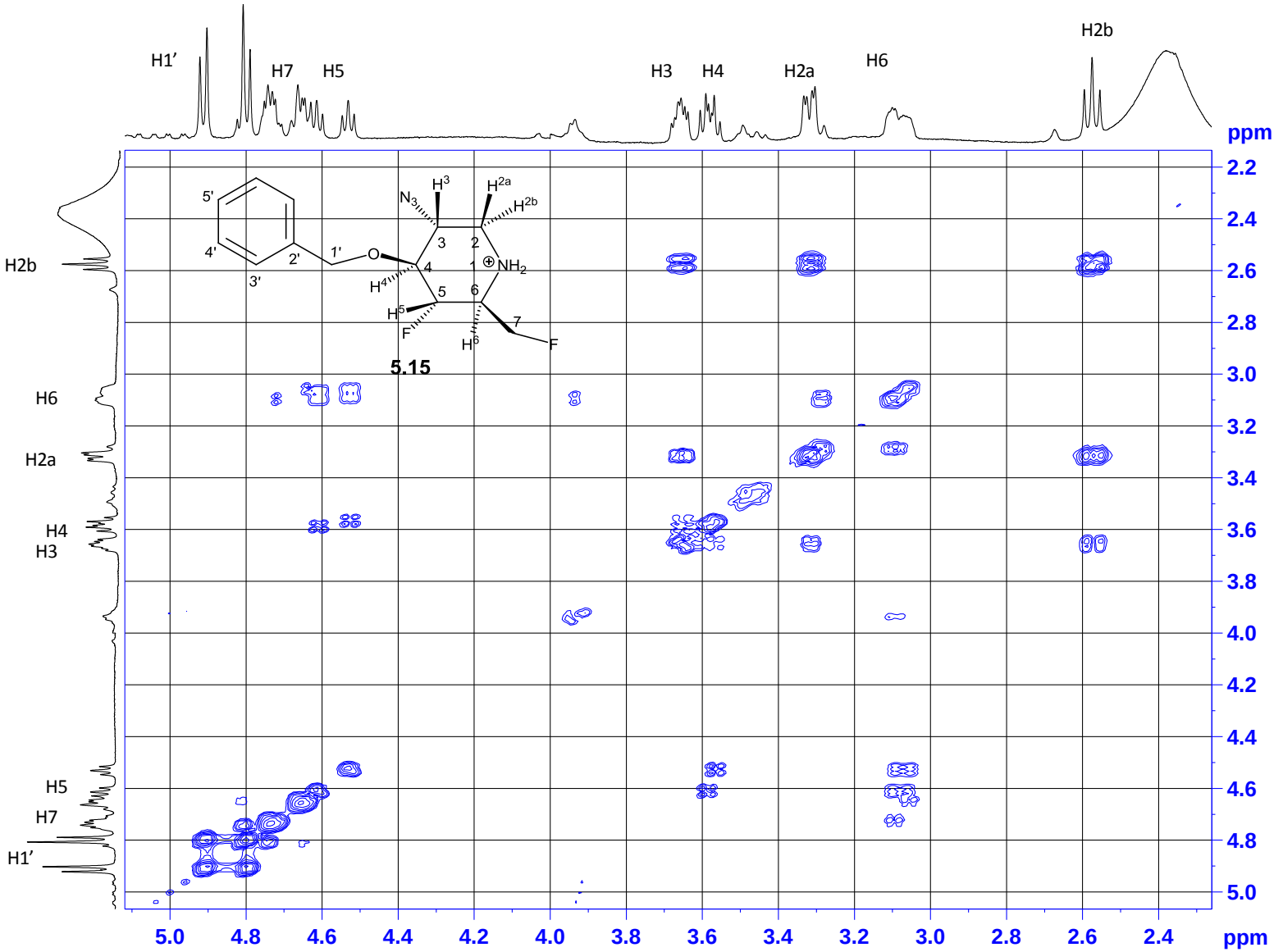


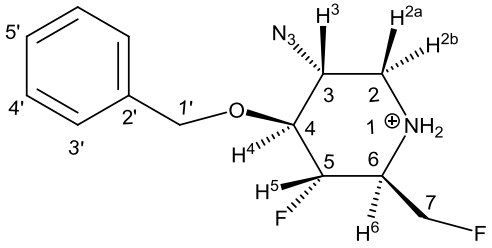

7.41
7.40
7.38
7.36
7.34
7.33
5.30
4.92
4.90
4.81
4.79
4.74
4.66
4.61
4.53
3.66
3.59
3.57
3.33
3.30
3.10
2.60
2.57
2.55
2.38
OBn
F
N3
N
H2
F
5.15
Current Data Parameters
NAME Compound 18
EXPNO 1
PROCNO 1
F2 - Acquisition Parameters
Date_ 20121221
Time 10.23
INSTRUM spect
PROBHD 5 mm CPTXI 1H-
PULPROG zg30
TD 32768
SOLVENT Acetone
NS 16
DS 0
SWH 5387.931 Hz
FIDRES 0.164427 Hz
AQ 3.0409205 sec
RG 10.1
DW 92.800 usec
DE 6.00 usec
TE 298.0 K
D1 1.50000000 sec
TD0 1
======== CHANNEL f1 ========
NUC1 1H
P1 7.63 usec
PL1 1.00 dB
SFO1 600.1824166 MHz
F1 - Acquisition parameters
TD 256
SFO1 150.9229 MHz
FIDRES 93.450958 Hz
SW 158.514 ppm
FnMODE States-TPPI
F2 - Processing parameters
SI 32768
SF 600.1800145 MHz
WDW EM
SSB 0
LB 1.00 Hz
GB 0
PC 0.50
7.5
7.0
6.5
6.0
5.5
5.0
4.5
4.0
3.5
3.0
2.5
2.0
ppm
5.50
0.90
1.14
2.07
1.86
1.10
1.77
1.05


Current Data Parameters
NAME Compound 18
EXPNO 3
PROCNO 1
F2 - Acquisition Parameters
Date_ 20121218
Time_ 23.58
INSTRUM spect
PROBHD 5 mm CPTXI 1H-
PULPROG udeft.txt
TD 21814
SOLVENT CDCl3
NS 10240
DS 0
SWH 30303.031 Hz
FIDRES 1.389155 Hz
AQ 0.3599810 sec
RG 32768
DW 16.500 usec
DE 6.00 usec
TE 298.0 K
D1 1.50000000 sec
D11 0.03000000 sec
d12 0.00002000 sec
D20 0.10000000 sec
DELTA 1.47000003 sec
DELTA2 0.36300099 sec
TAU 0.00302000 sec
TD0 1
======== CHANNEL f1 ========
NUC1 13C
P1 10.43 usec
P12 2000.00 usec
P26 500.00 usec
PL1 -2.50 dB
SFO1 150.9319817 MHz
SP2 5.29 dB
SP8 4.75 dB
SPNAM2 Crp60comp.4
SPNAM8 Crp60,0.5,20.1
SPOAL2 0.500
SPOAL8 0.500
SPOFFS2 0 Hz
SPOFFS8 0 Hz
======== CHANNEL f2 ========
CPDPRG2 waltz64
NUC2 1H
PCPD2 80.00 usec
PL2 1.00 dB
PL12 18.89 dB
SFO2 600.1830000 MHz
F1 - Acquisition parameters
TD 256
SFO1 150.932 MHz
FIDRES 93.450958 Hz
SW 158.505 ppm
FnMODE States-TPPI
F2 - Processing parameters
SI 262144
SF 150.9153610 MHz
WDW EM
SSB 0
LB 10.00 Hz
GB 0
PC 0.02
137.22
128.66
128.50
128.33
90.73
89.52
82.43
82.32
81.35
80.22
75.18
60.26
58.01
57.89
57.74
46.66
OBn
F
N3
N
H2
F
5.15
160
150
140
130
120
110
100
90
80
70
60
50
40
ppm


H3',4',5'
H1'
H7
H5
H3
H4
H2a
H6
H2b
ppm
C2
C6
C3
C1'
C7
C4
C5
C3',4',5'
C2'
5'
4'
3'
2'
1'
O
N3
H3
H2a
H2b
4
3
2
1
NH2
5
6
7
H4
H5
F
H6
F
5.15
50
60
70
80
90
100
110
120
130
140
150
160
170
7.5
7.0
6.5
6.0
5.5
5.0
4.5
4.0
3.5
3.0
2.5
ppm

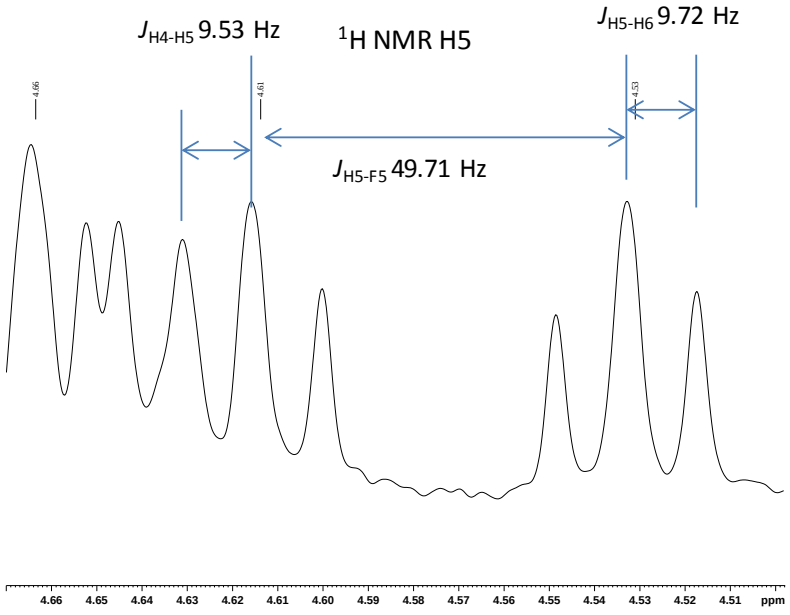

H3',4',5'
H1'
H7
H5
H3
H4
H2a
H6
H2b
ppm
C2
C6
C3
C1'
C7
C4
C5
C3',4',5'
C2'
5'
4'
3'
2'
1'
O
N3
H3
H2a
H2b
3
2
4
1
NH2
H4
5
6
H5
F
H6
7
F
5.15
50
60
70
80
90
100
110
120
130
140
150
160
170
7.5
7.0
6.5
6.0
5.5
5.0
4.5
4.0
3.5
3.0
2.5
ppm


H1'
H7
H5
H3
H4
H2a
H6
H2b
ppm
5.15
5'
4'
3'
2'
1'
O
N3
H3
H2a
H2b
NH2
H4
H5
F
H6
F
H2b
H6
H2a
H4
H3
H5
H7
H1'
5.0
4.8
4.6
4.4
4.2
4.0
3.8
3.6
3.4
3.2
3.0
2.8
2.6
2.4
ppm

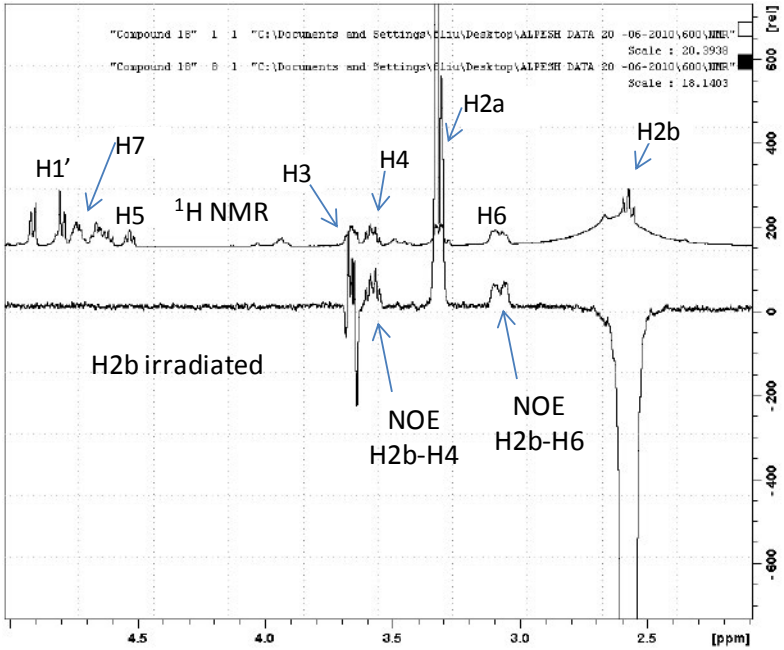


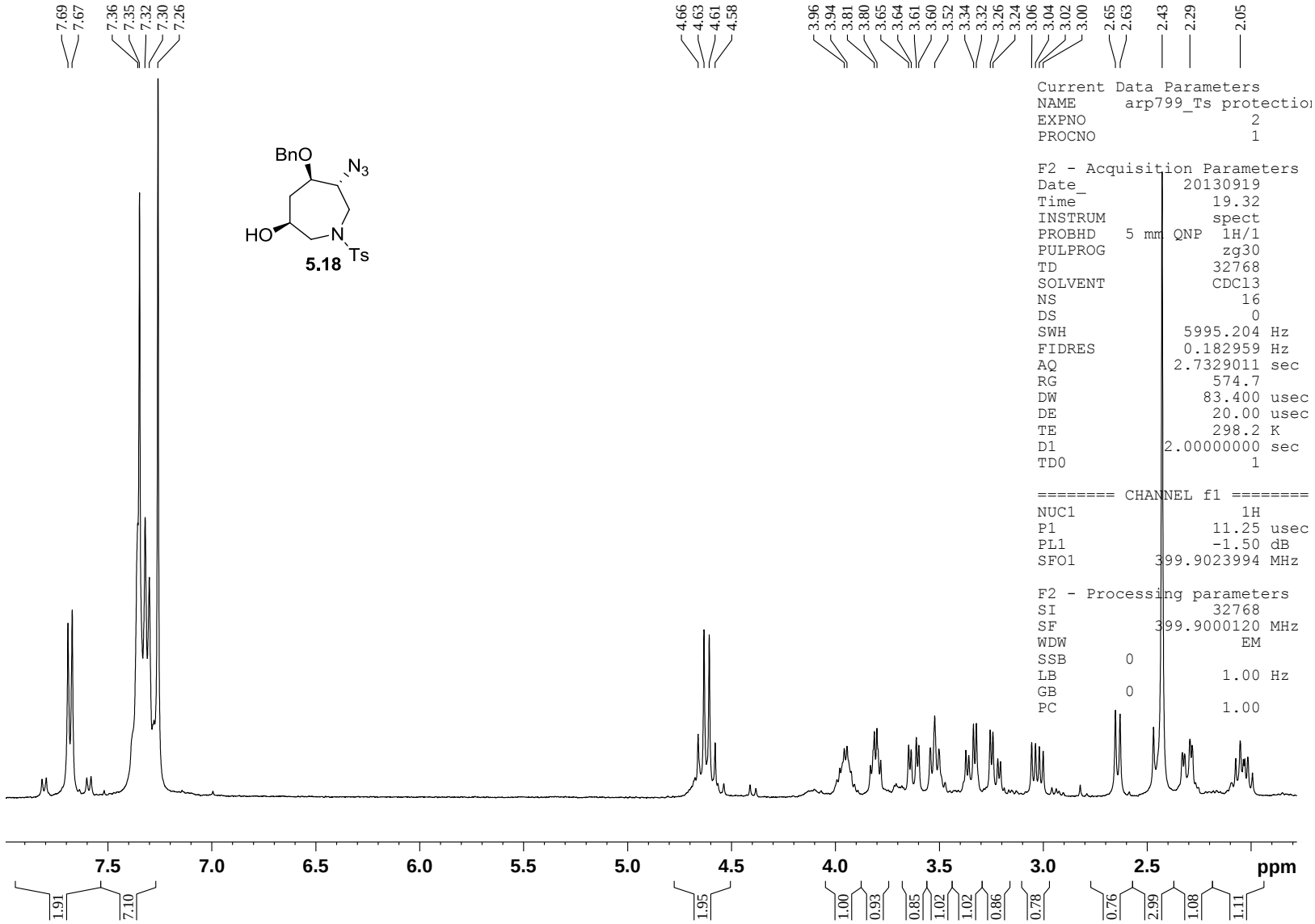
5.15

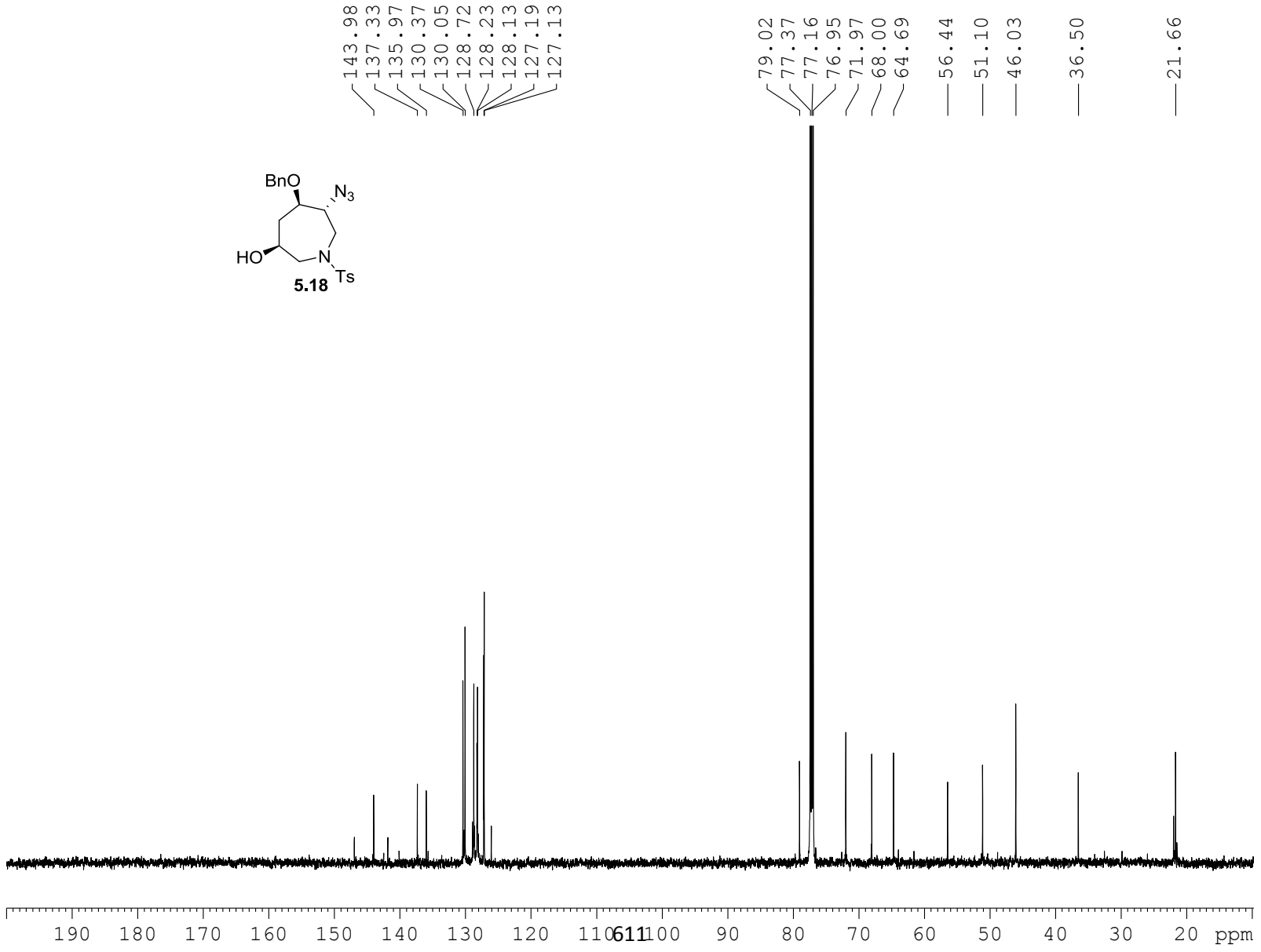
- $J_{H5\text{-}H4}$ (9.53 Hz) and $J_{H5\text{-}H6}$ (9.72 Hz) clearly suggests H4, H5 and H6 are axial; meaning H5 *trans* and H6 is *cis* to H4.
- $J_{H2b\text{-}H3}$ (12.53 Hz) clearly suggests H3, H2b are axial; meaning H2b is *trans* to H3 which is supported by NOE H2b-H4. Now, H2b shows NOE to H6 further confirming H6 and H2b are both *cis* to H4.

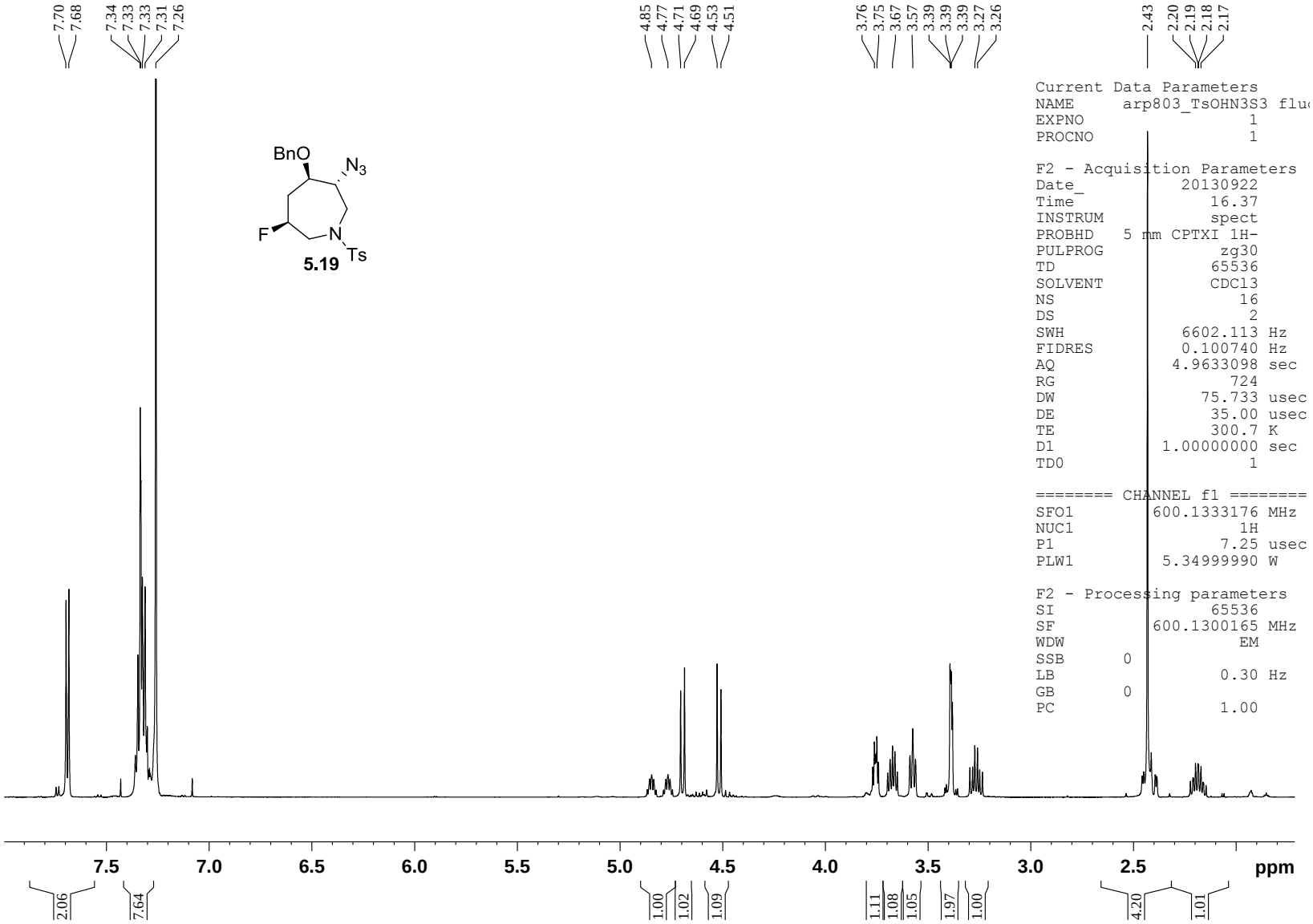


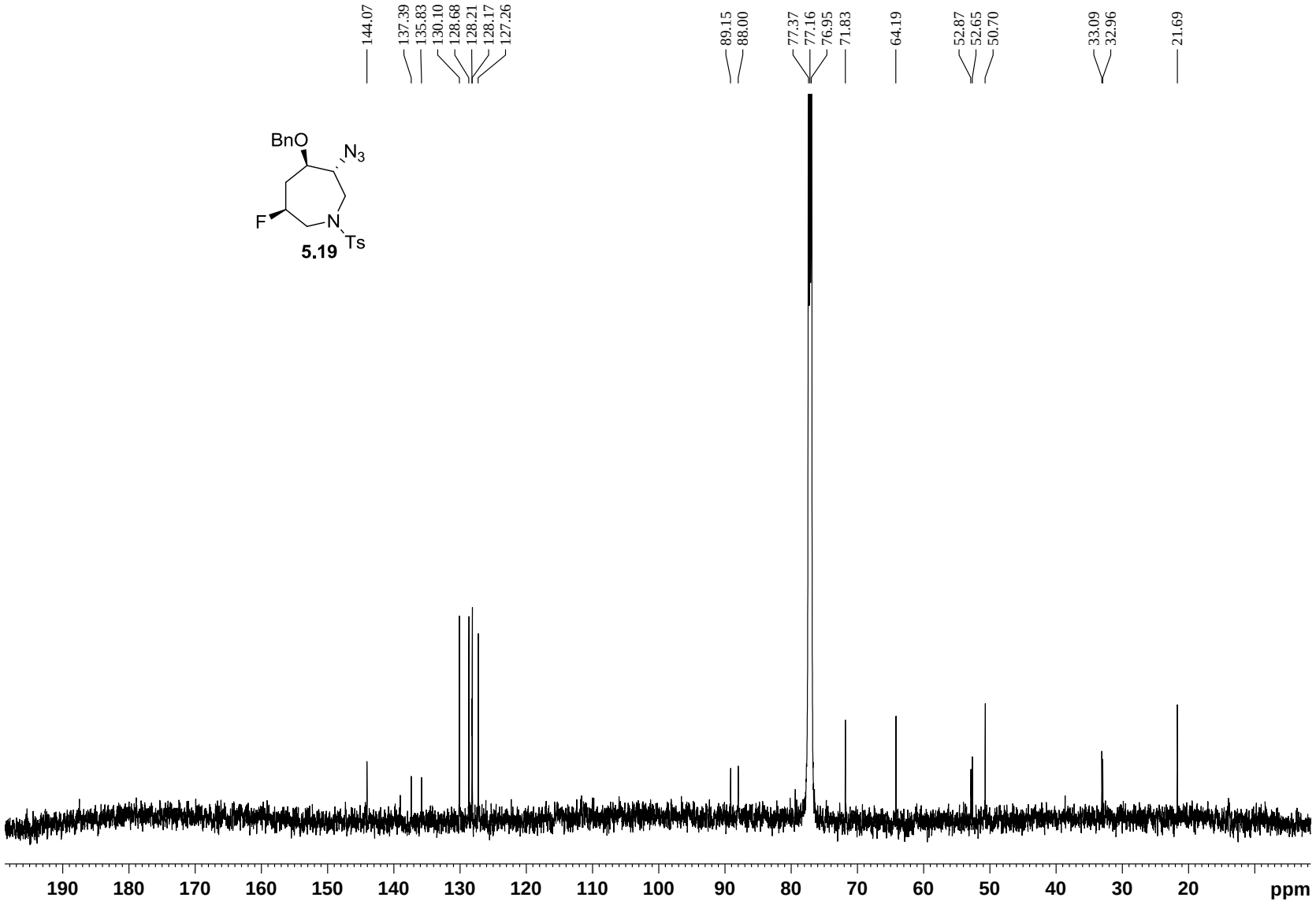
1D selective NOESY

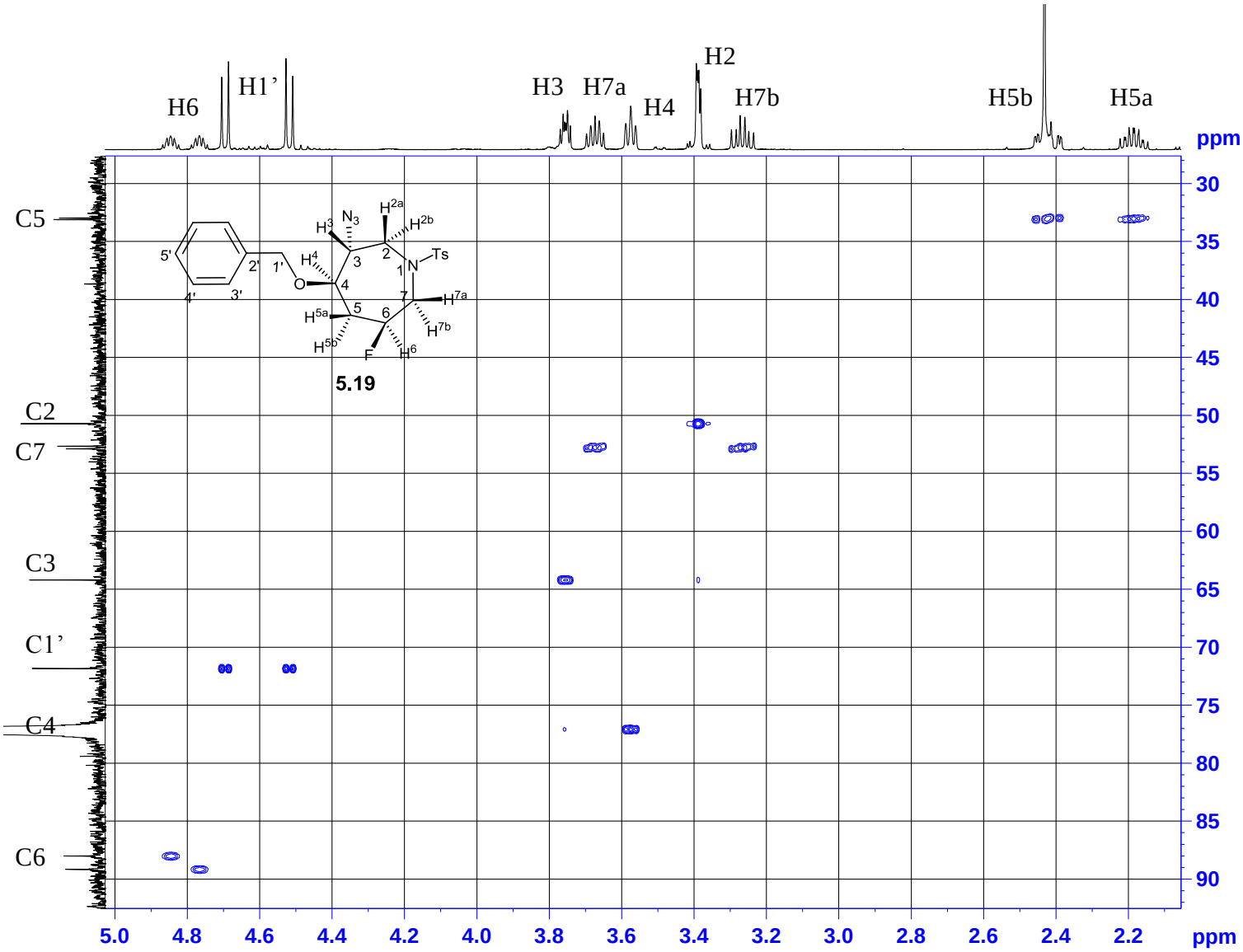


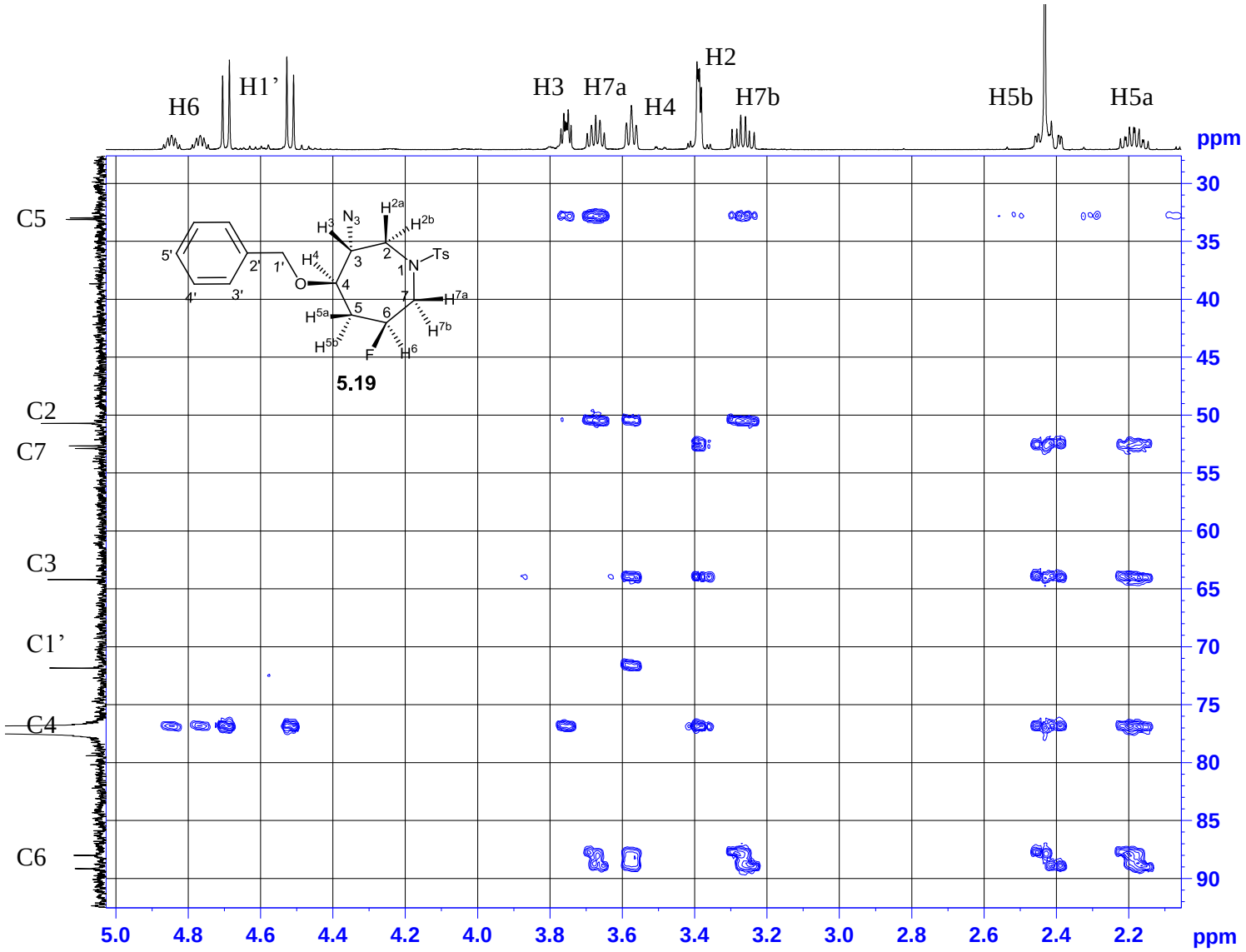

7.69
7.67
7.36
7.35
7.32
7.30
7.26
4.66
4.63
4.61
4.58
3.96
3.94
3.81
3.80
3.65
3.64
3.61
3.60
3.52
3.34
3.32
3.26
3.24
3.06
3.04
3.02
3.00
2.65
2.63
2.43
2.29
2.05
BnO
N3
HO
N
Ts
5.18
Current Data Parameters
NAME arp799_Ts protectio
EXPNO 2
PROCNO 1
F2 - Acquisition Parameters
Date_ 20130919
Time 19.32
INSTRUM spect
PROBHD 5 mm QNP 1H/1
PULPROG zg30
TD 32768
SOLVENT CDCl3
NS 16
DS 0
SWH 5995.204 Hz
FIDRES 0.182959 Hz
AQ 2.7329011 sec
RG 574.7
DW 83.400 usec
DE 20.00 usec
TE 298.2 K
D1 2.00000000 sec
TD0 1
======== CHANNEL f1 ========
NUC1 1H
P1 11.25 usec
PL1 -1.50 dB
SFO1 399.9023994 MHz
F2 - Processing parameters
SI 32768
SF 399.9000120 MHz
WDW EM
SSB 0
LB 1.00 Hz
GB 0
PC 1.00
7.5
7.0
6.5
6.0
5.5
5.0
4.5
4.0
3.5
3.0
2.5
ppm
1.91
7.10
1.95
1.00
0.93
0.85
1.02
1.02
0.86
0.78
0.76
2.99
1.08
1.11

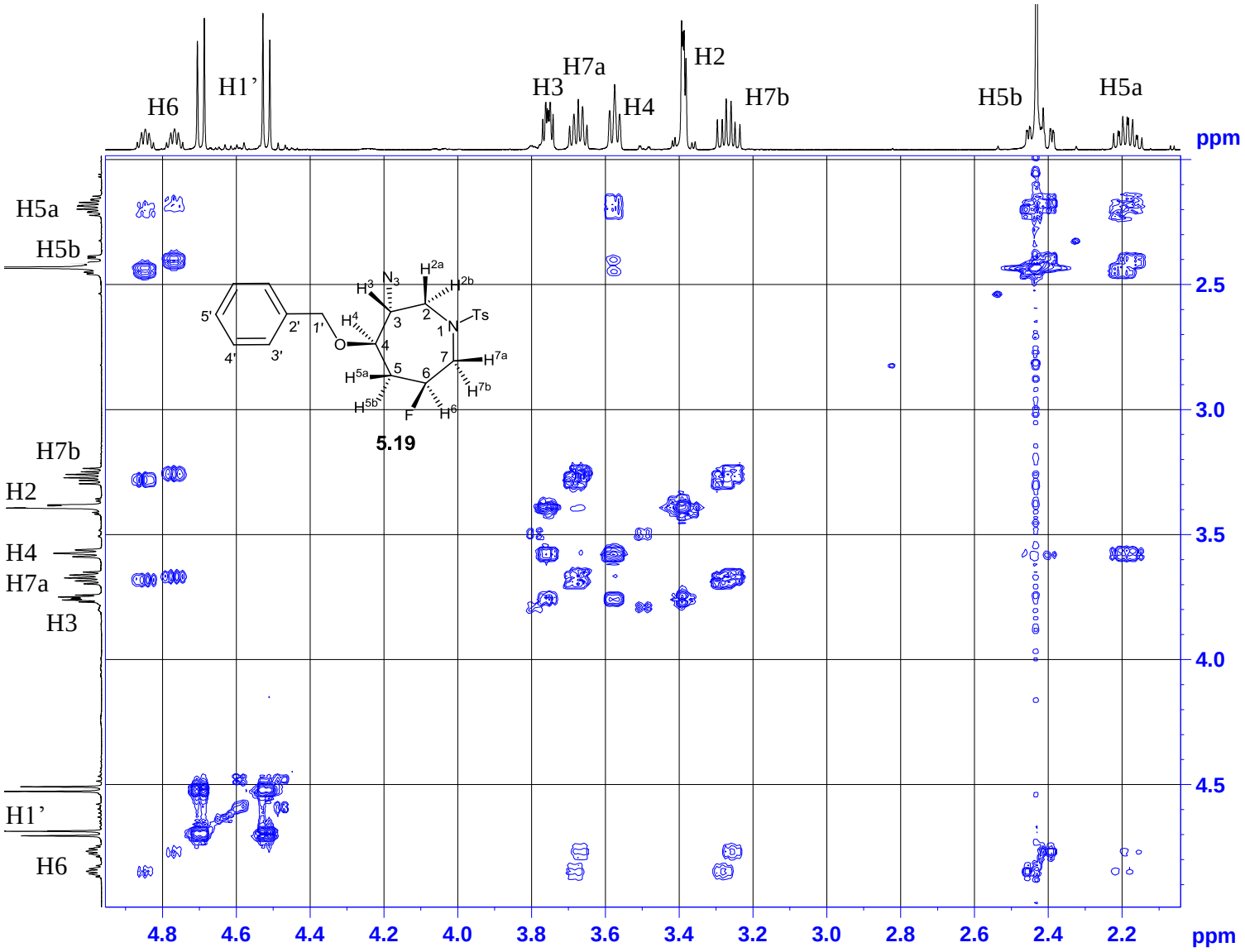

143.98
137.33
135.97
130.37
130.05
128.72
128.23
128.13
127.19
127.13
79.02
77.37
77.16
76.95
71.97
68.00
64.69
56.44
51.10
46.03
36.50
21.66
BnO
N3
HO
N
Ts
5.18
190 180 170 160 150 140 130 120 110 100 90 80 70 60 50 40 30 20 ppm

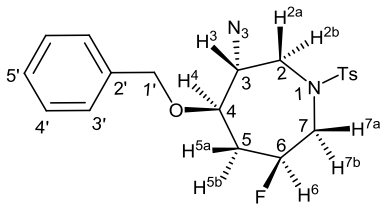

7.70
7.68
7.34
7.33
7.33
7.31
7.26
4.85
4.77
4.71
4.69
4.53
4.51
3.76
3.75
3.67
3.57
3.39
3.39
3.39
3.27
3.26
2.43
2.20
2.19
2.18
2.17
BnO
N3
F
N
Ts
5.19
Current Data Parameters
NAME arp803_TsOHN3S3 flu
EXPNO 1
PROCNO 1
F2 - Acquisition Parameters
Date_ 20130922
Time 16.37
INSTRUM spect
PROBHD 5 mm CPTXI 1H-
PULPROG zg30
TD 65536
SOLVENT CDCl3
NS 16
DS 2
SWH 6602.113 Hz
FIDRES 0.100740 Hz
AQ 4.9633098 sec
RG 724
DW 75.733 usec
DE 35.00 usec
TE 300.7 K
D1 1.00000000 sec
TD0 1
======== CHANNEL f1 ========
SFO1 600.1333176 MHz
NUC1 1H
P1 7.25 usec
PLW1 5.34999990 W
F2 - Processing parameters
SI 65536
SF 600.1300165 MHz
WDW EM
SSB 0
LB 0.30 Hz
GB 0
PC 1.00
7.5
7.0
6.5
6.0
5.5
5.0
4.5
4.0
3.5
3.0
2.5
ppm
2.06
7.64
1.00
1.02
1.09
1.11
1.08
1.05
1.97
1.00
4.20
1.01


144.07
137.39
135.83
130.10
128.68
128.21
128.17
127.26
89.15
88.00
77.37
77.16
76.95
71.83
64.19
52.87
52.65
50.70
33.09
32.96
21.69
BnO
N3
F
N
Ts
5.19
190
180
170
160
150
140
130
120
110
100
90
80
70
60
50
40
30
20
ppm

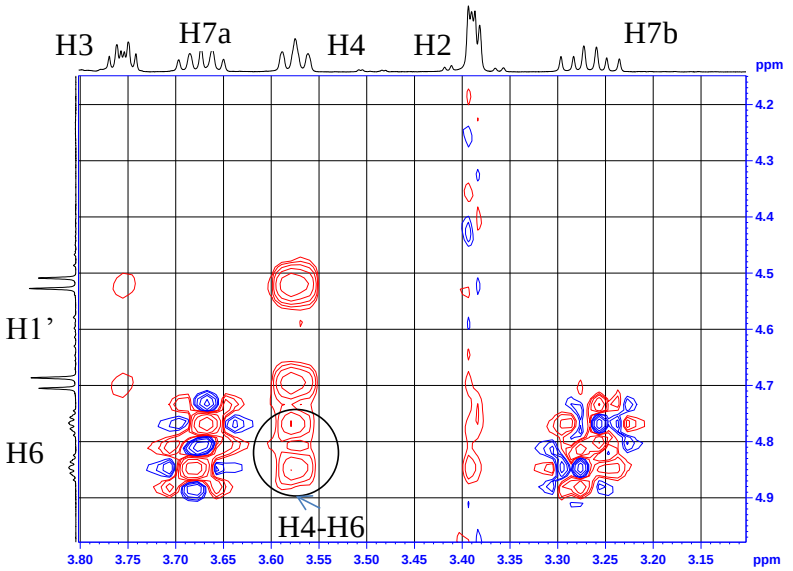

H6
H1’
H3
H7a
H4
H2
H7b
H5b
H5a
ppm
C5
C2
C7
C3
C1’
C4
C6
5.19
5.0
4.8
4.6
4.4
4.2
4.0
3.8
3.6
3.4
3.2
3.0
2.8
2.6
2.4
2.2
ppm
30
35
40
45
50
55
60
65
70
75
80
85
90

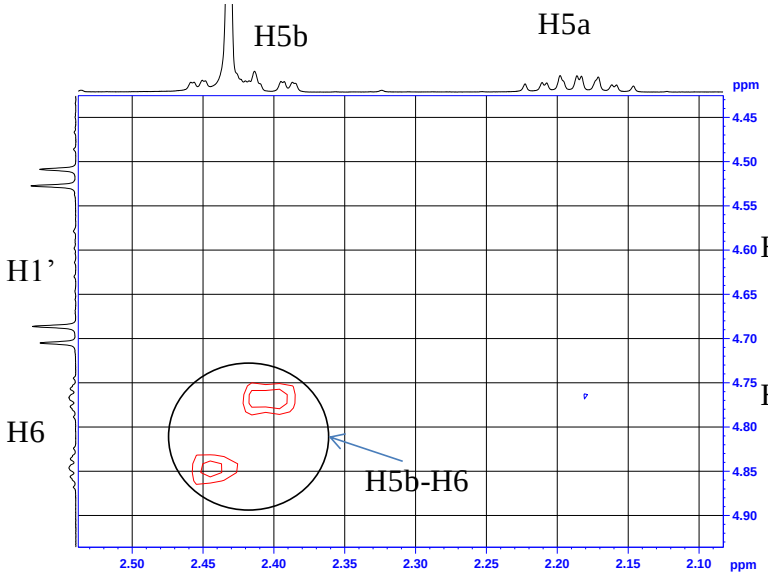

H6
H1'
H3
H7a
H4
H2
H7b
H5b
H5a
ppm
C5
C2
C7
C3
C1'
C4
C6
5.19
5.0
4.8
4.6
4.4
4.2
4.0
3.8
3.6
3.4
3.2
3.0
2.8
2.6
2.4
2.2
ppm
30
35
40
45
50
55
60
65
70
75
80
85
90

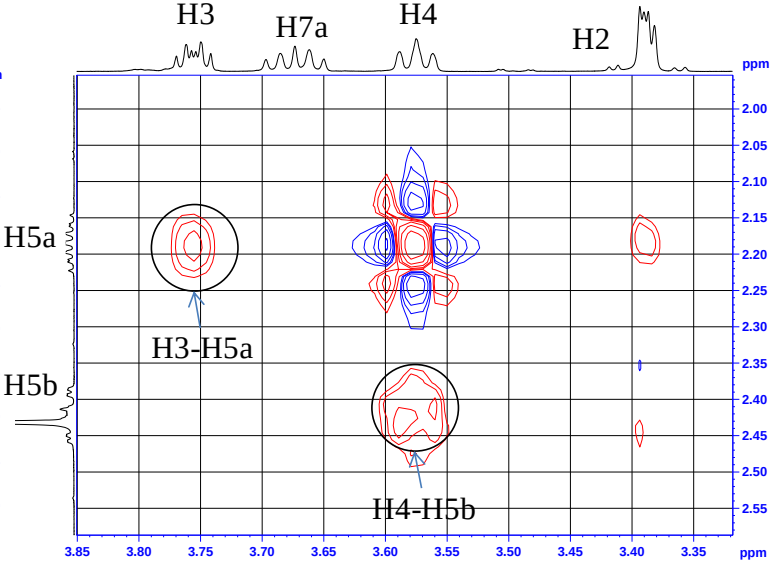

H6
H1’
H3
H7a
H4
H2
H7b
H5b
H5a
ppm
H5a
H5b
H7b
H2
H4
H7a
H3
H1’
H6
2.5
3.0
3.5
4.0
4.5
4.8
4.6
4.4
4.2
4.0
3.8
3.6
3.4
3.2
3.0
2.8
2.6
2.4
2.2
ppm
5.19

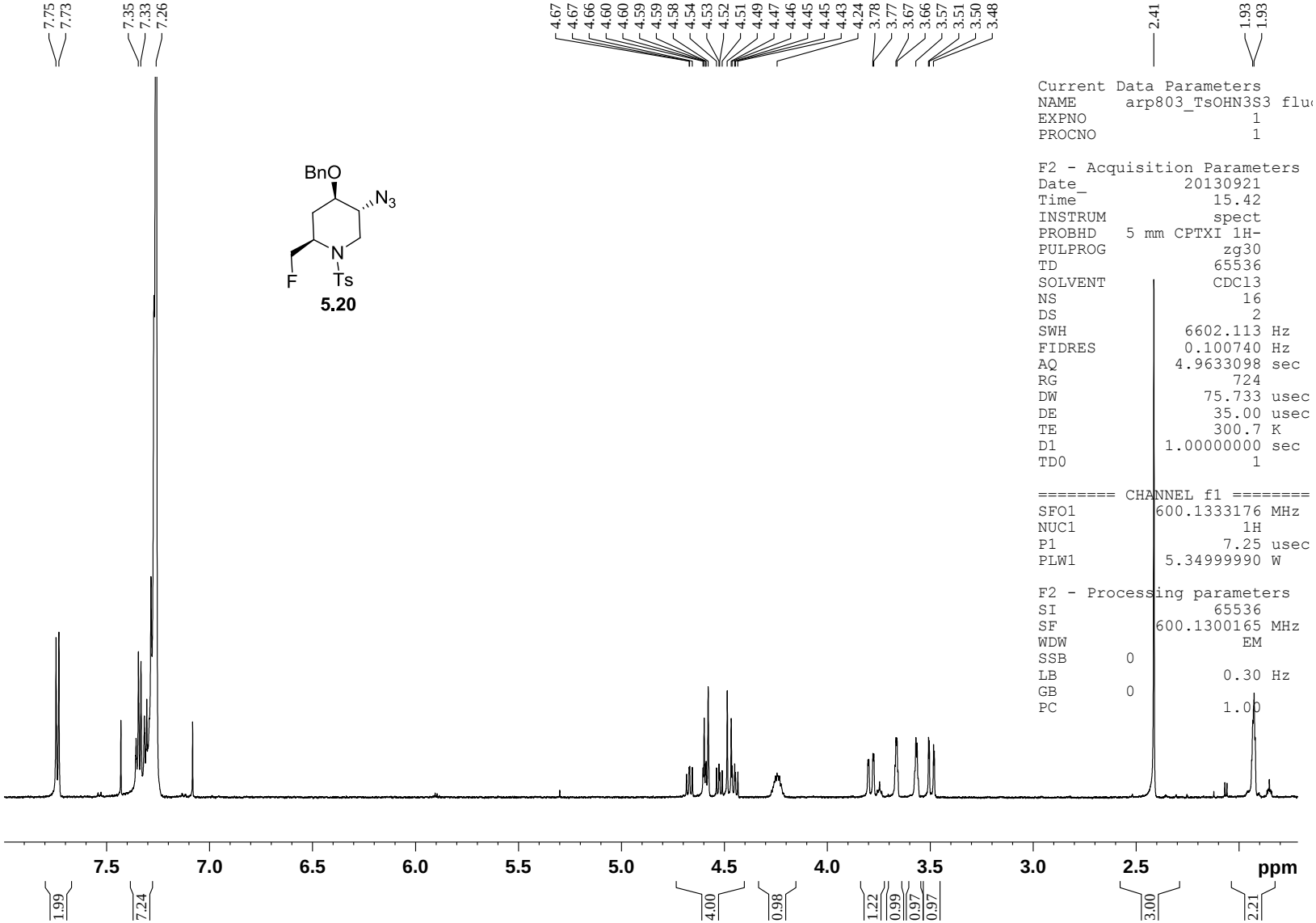

5'
4'
3'
2'
1'
O
4
3
2
1
N
Ts
5
6
7
F
H^3
N_3
H^{2a}
H^{2b}
H^4
H^{5a}
H^{5b}
H^6
H^{7a}
H^{7b}

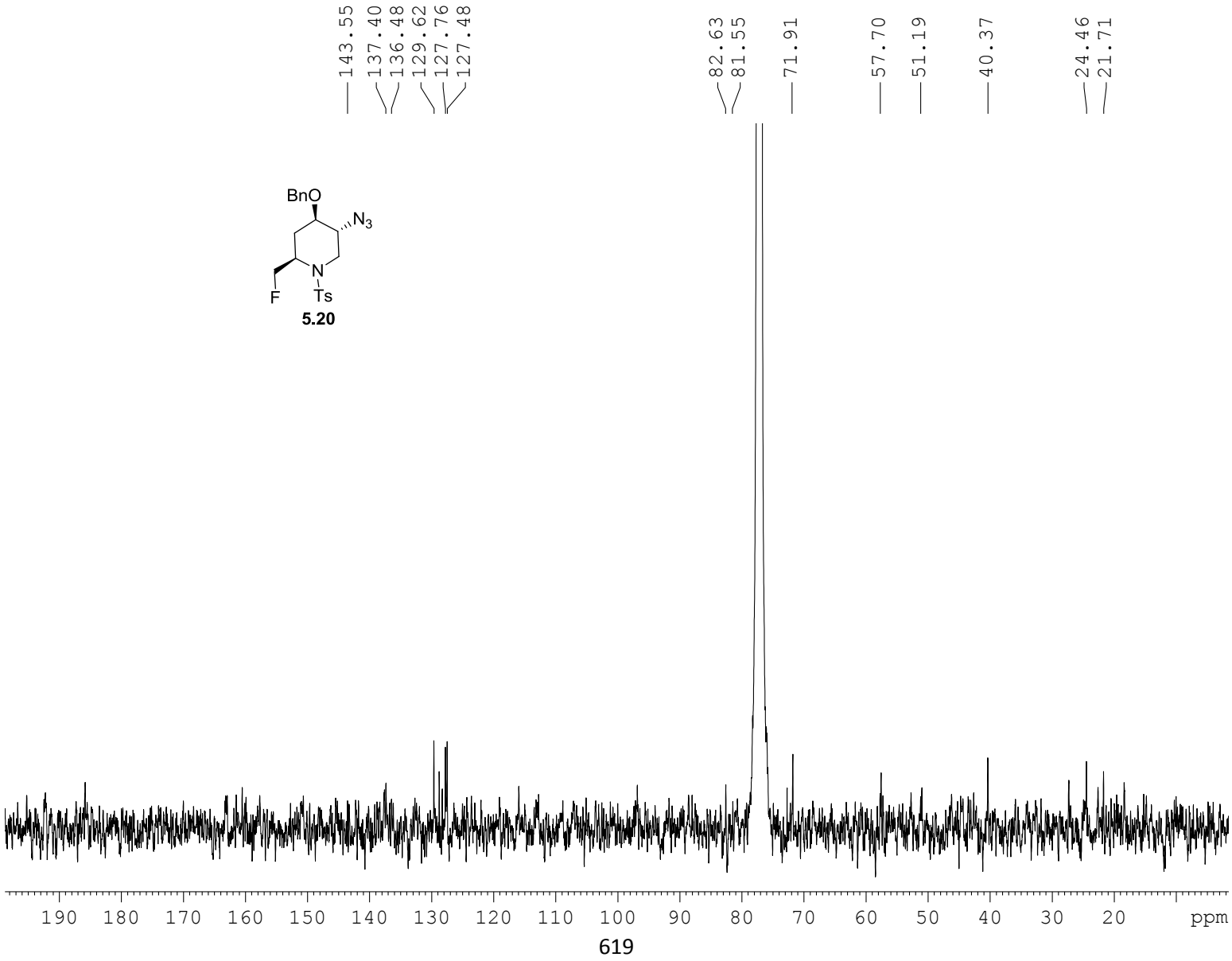
5.19

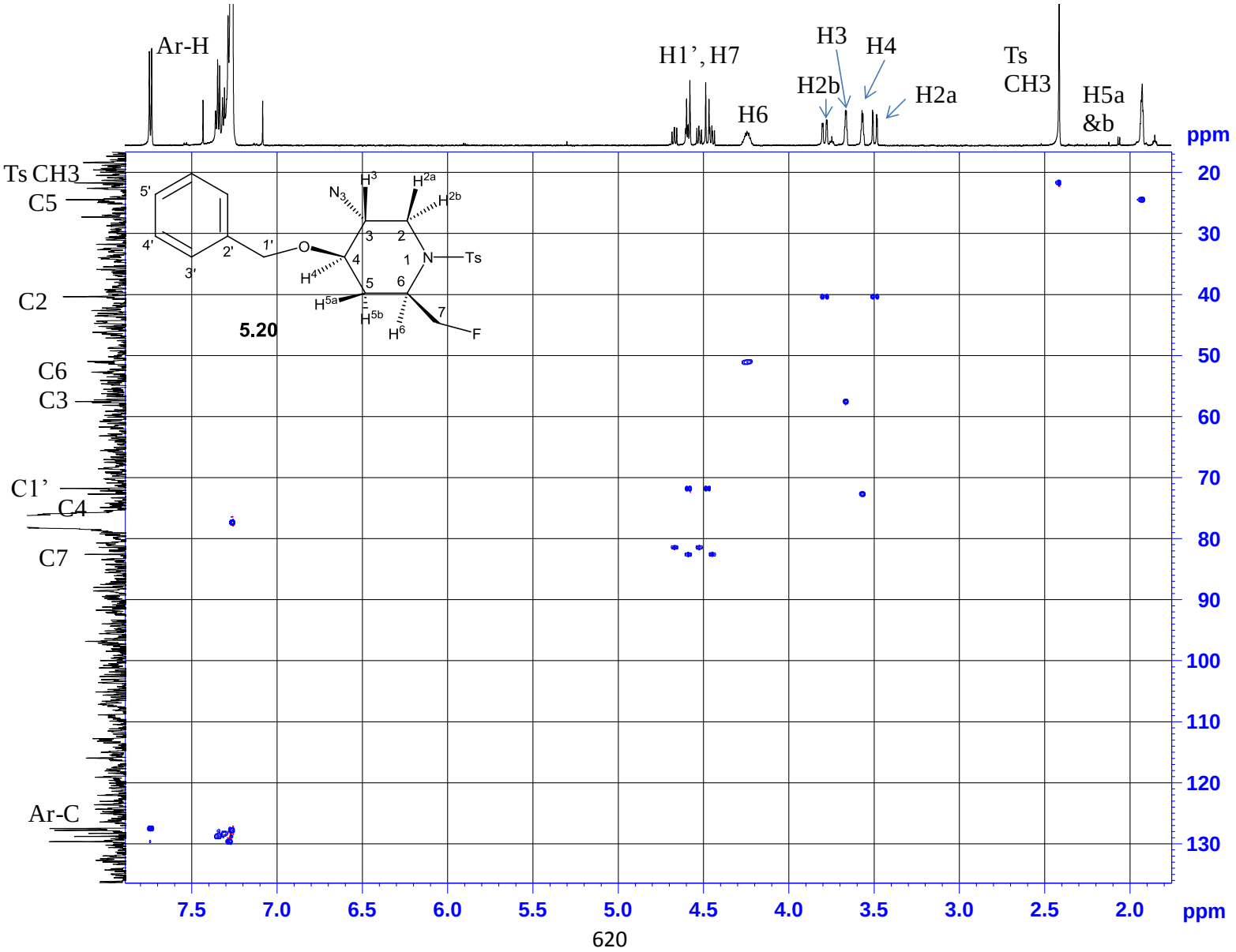

H3
H7a
H4
H2
H7b
H1'
H6
H4-H6
ppm

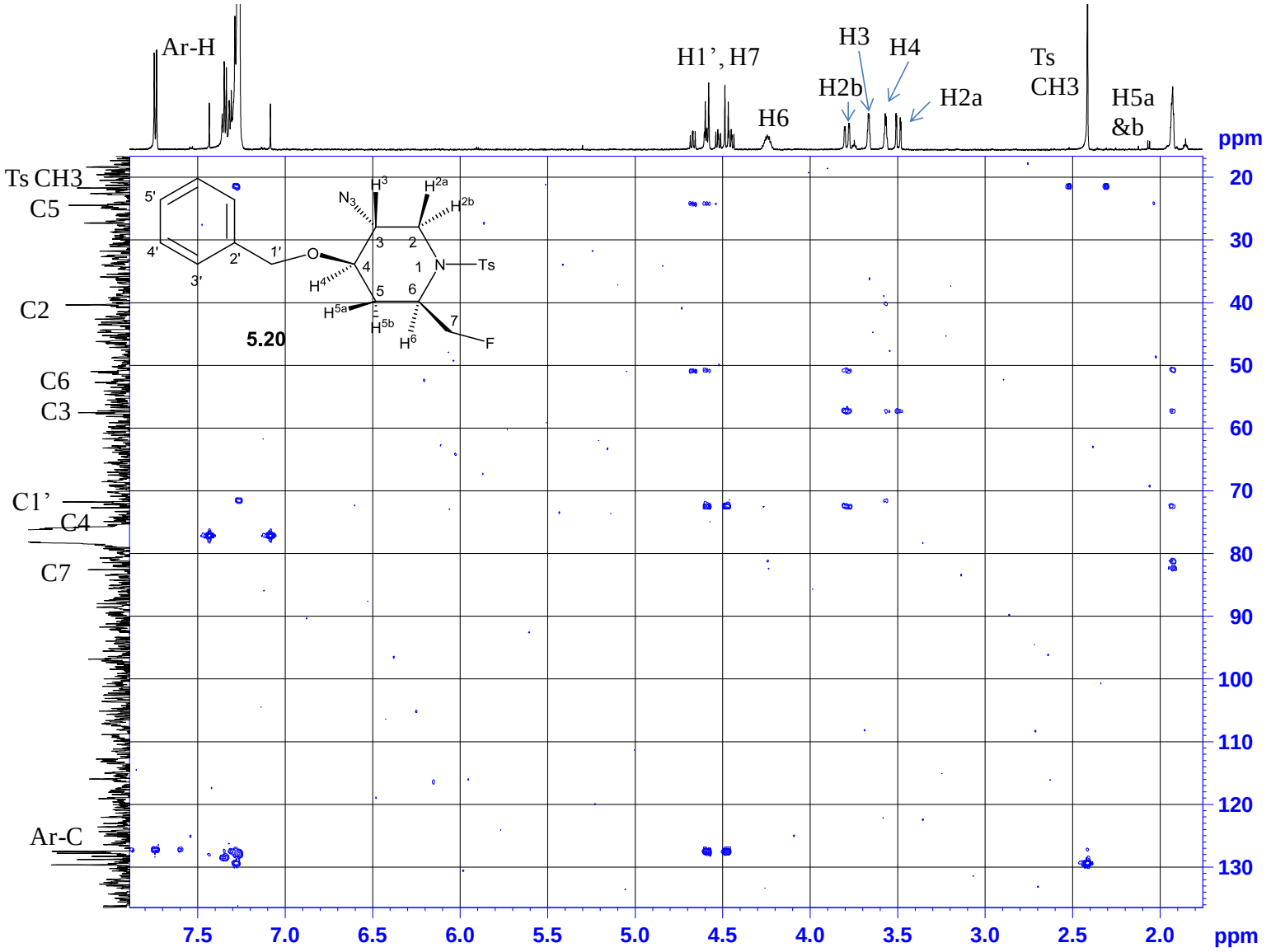

H5b
H5a
H1'
H6
H5b-H6
ppm

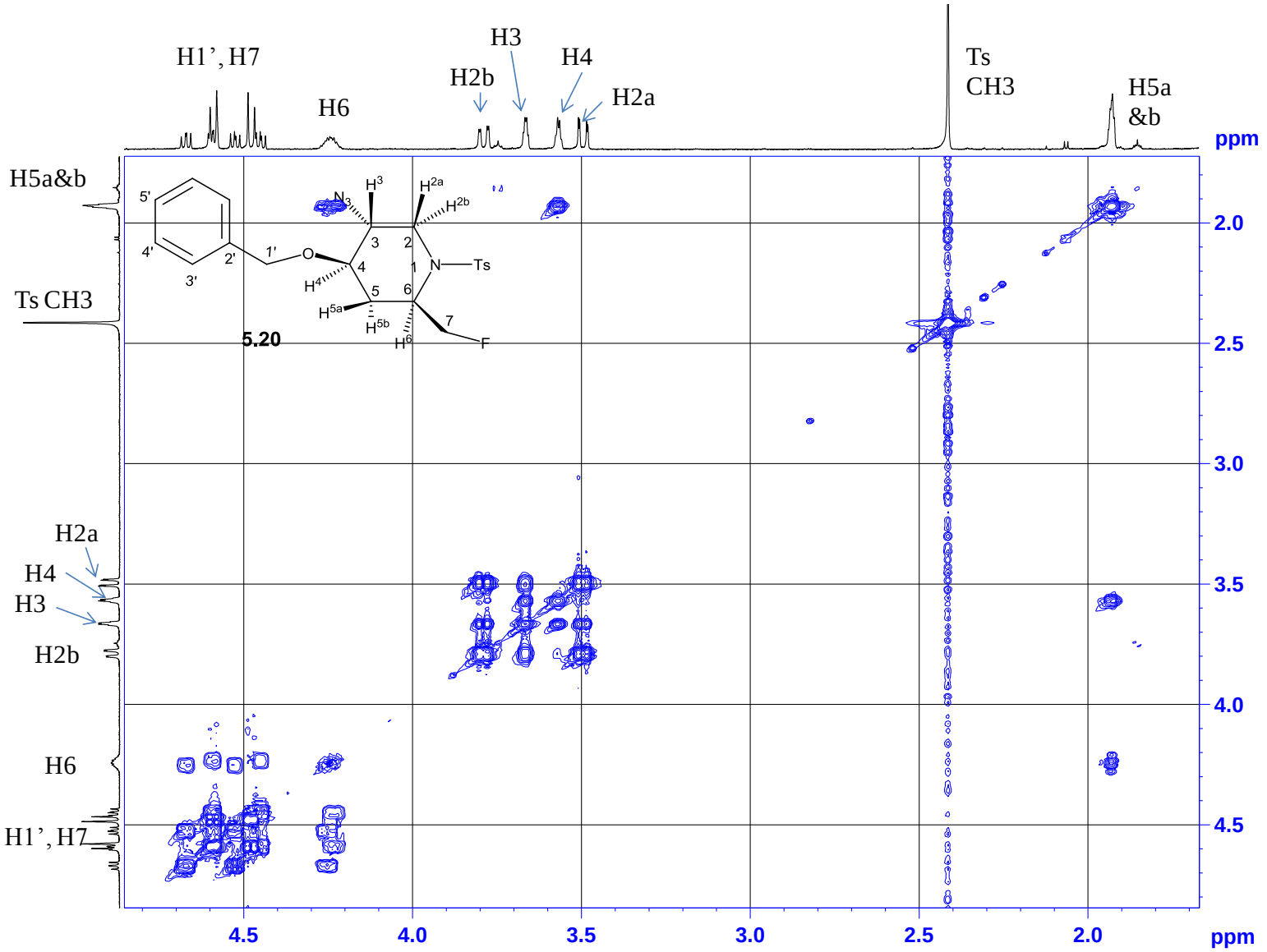

H3
H7a
H4
H2
H5a
H5b
H3-H5a
H4-H5b
ppm

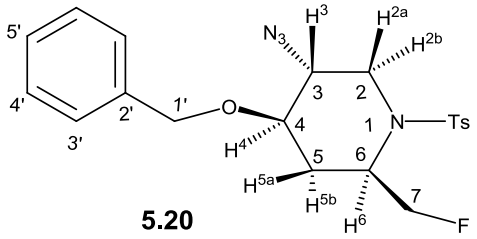

7.75
7.73
7.35
7.33
7.26
4.67
4.67
4.66
4.60
4.60
4.59
4.59
4.58
4.54
4.53
4.52
4.51
4.49
4.47
4.46
4.45
4.45
4.43
4.24
3.78
3.77
3.67
3.66
3.57
3.51
3.50
3.48
2.41
1.93
1.93
BnO
N3
N
F
Ts
5.20
Current Data Parameters
NAME arp803_TsOHN3S3 flu
EXPNO 1
PROCNO 1
F2 - Acquisition Parameters
Date_ 20130921
Time 15.42
INSTRUM spect
PROBHD 5 mm CPTXI 1H-
PULPROG zg30
TD 65536
SOLVENT CDCl3
NS 16
DS 2
SWH 6602.113 Hz
FIDRES 0.100740 Hz
AQ 4.9633098 sec
RG 724
DW 75.733 usec
DE 35.00 usec
TE 300.7 K
D1 1.00000000 sec
TD0 1
======== CHANNEL f1 ========
SFO1 600.1333176 MHz
NUC1 1H
P1 7.25 usec
PLW1 5.34999990 W
F2 - Processing parameters
SI 65536
SF 600.1300165 MHz
WDW EM
SSB 0
LB 0.30 Hz
GB 0
PC 1.00
7.5
7.0
6.5
6.0
5.5
5.0
4.5
4.0
3.5
3.0
2.5
ppm
1.99
7.24
4.00
0.98
1.22
0.99
0.97
0.97
3.00
2.21


143.55
137.40
136.48
129.62
127.76
127.48
82.63
81.55
71.91
57.70
51.19
40.37
24.46
21.71
BnO
N3
N
F
Ts
5.20
190 180 170 160 150 140 130 120 110 100 90 80 70 60 50 40 30 20 ppm

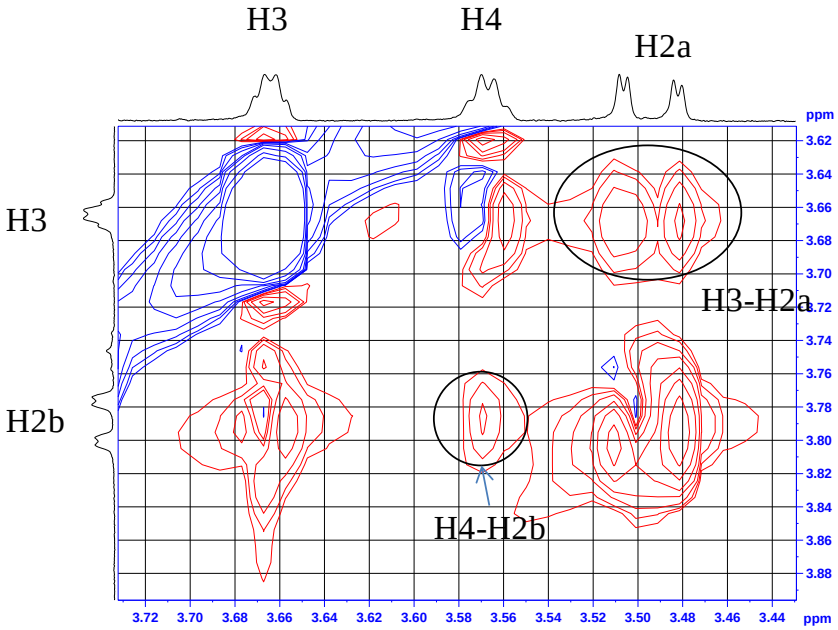

Ar-H
H1', H7
H6
H3
H4
H2b
H2a
Ts CH3
H5a &b
ppm
Ts CH3
C5
C2
C6
C3
C1'
C4
C7
Ar-C
5.20
7.5
7.0
6.5
6.0
5.5
5.0
4.5
4.0
3.5
3.0
2.5
2.0
ppm

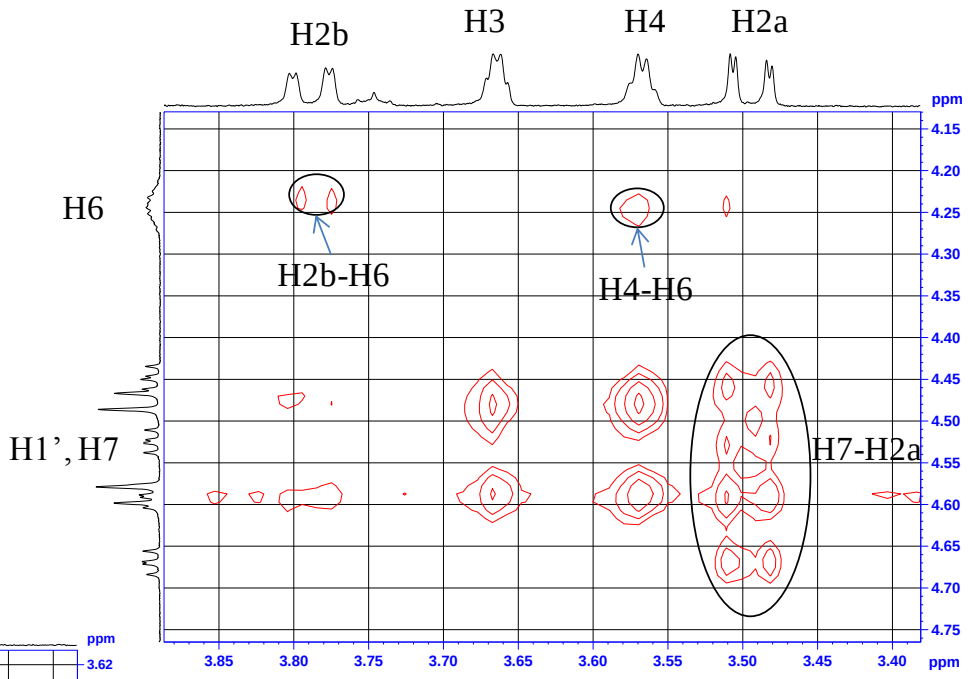

Ar-H
H1', H7
H6
H3
H4
H2b
H2a
Ts CH3
H5a &b
ppm
Ts CH3
C5
C2
C6
C3
C1'
C4
C7
Ar-C
5.20
7.5
7.0
6.5
6.0
5.5
5.0
4.5
4.0
3.5
3.0
2.5
2.0
ppm

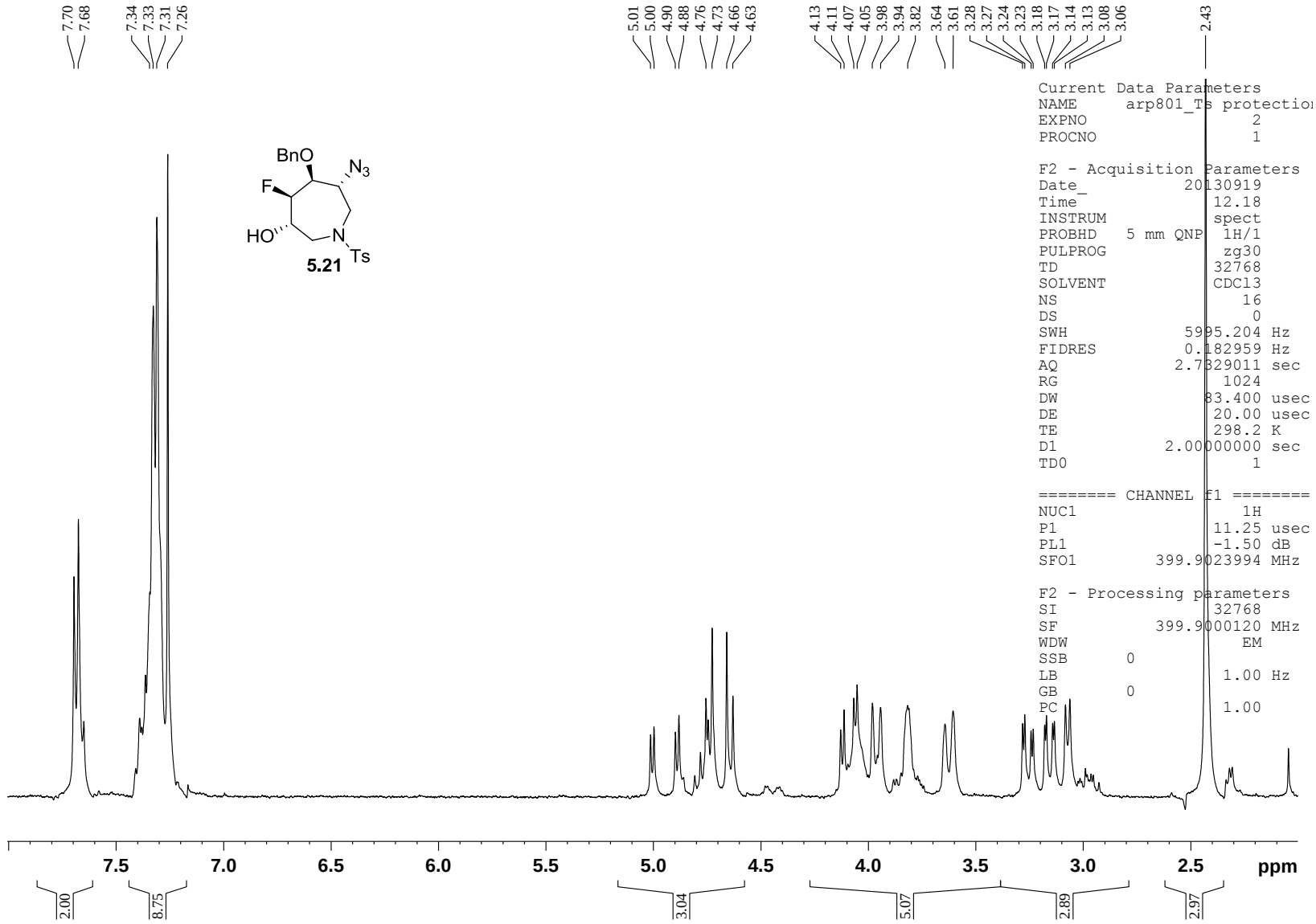

H1', H7
H6
H2b
H3
H4
H2a
Ts
CH3
H5a
&b
ppm
H5a&b
Ts CH3
H2a
H4
H3
H2b
H6
H1', H7
5.20
4.5
4.0
3.5
3.0
2.5
2.0
ppm

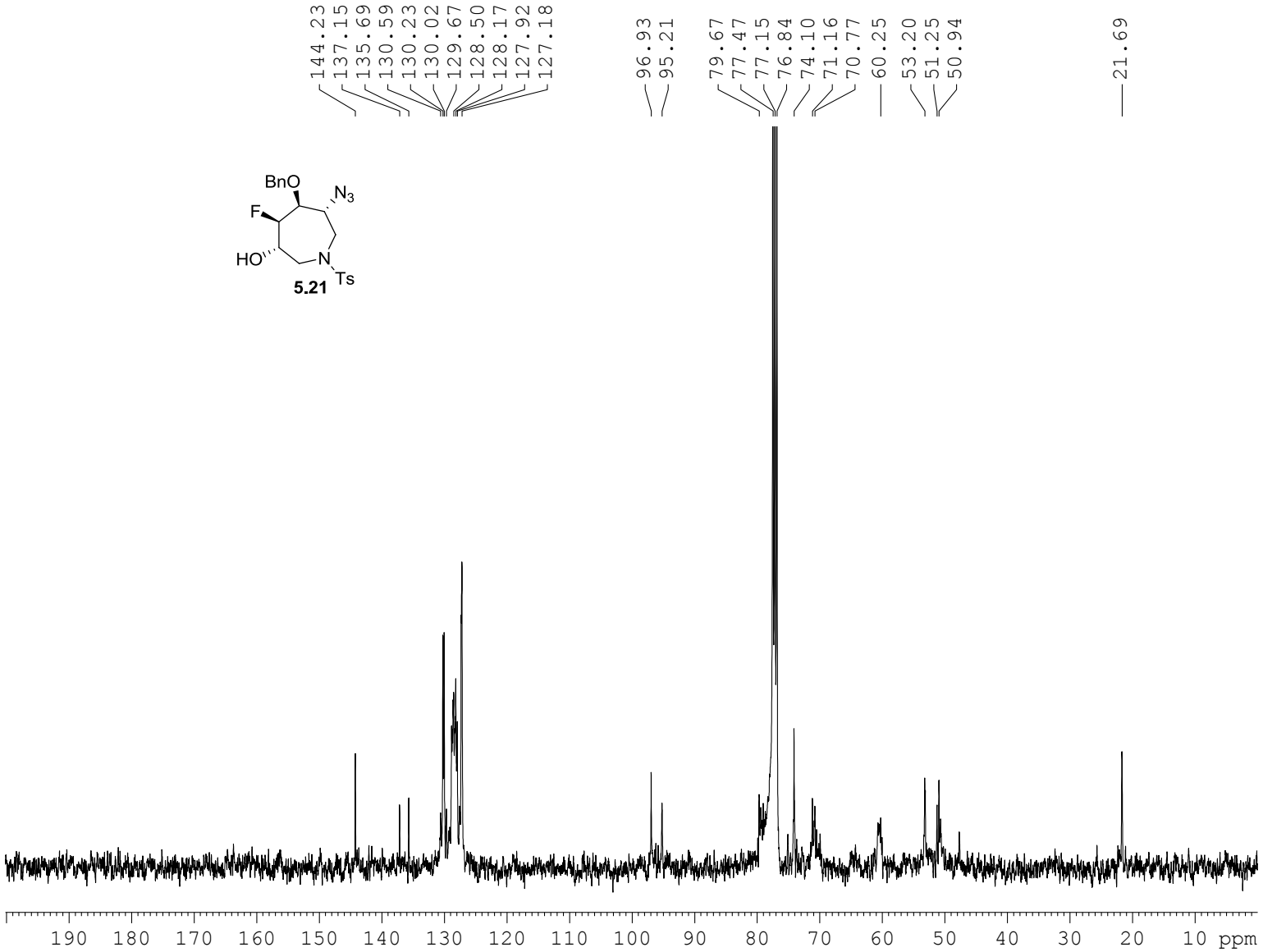

5'
4'
3'
2'
1'
O
4
3
2
1
N
Ts
5
6
7
F
N3
H3
H2a
H2b
H4
H5a
H5b
H6

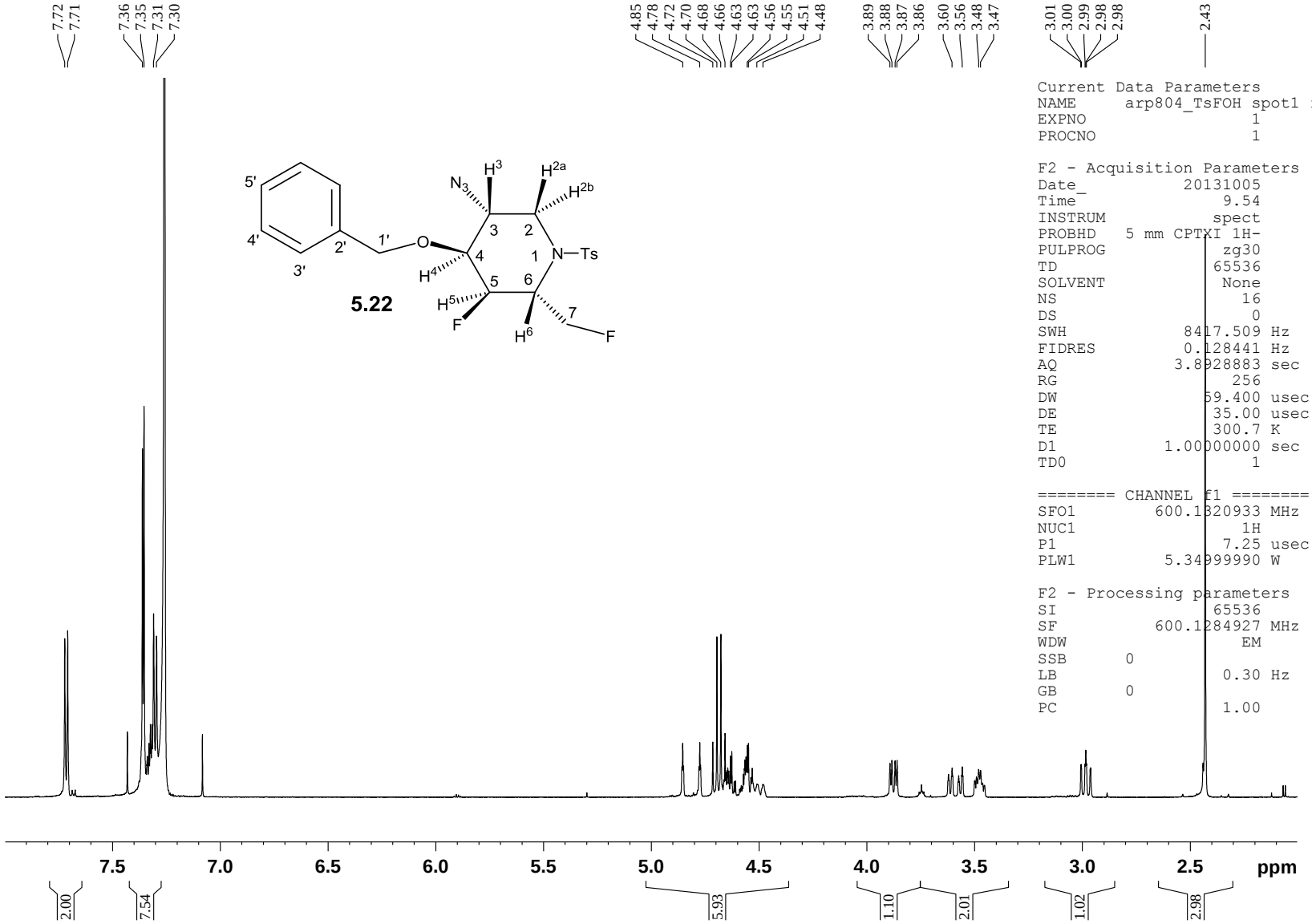
5.20

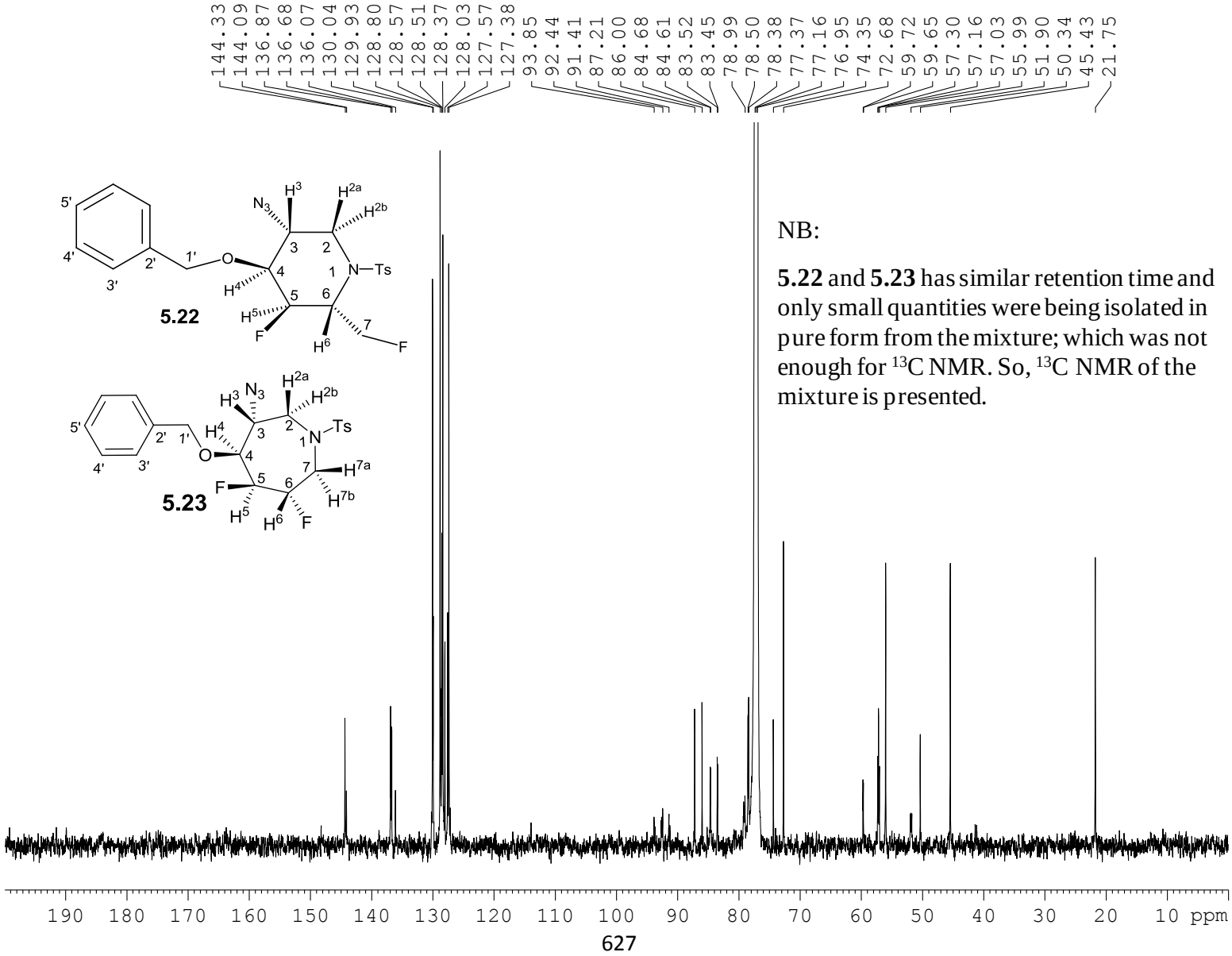

H3
H4
H2a
H3
H2b
H3-H2a
H4-H2b
ppm
3.72 3.70 3.68 3.66 3.64 3.62 3.60 3.58 3.56 3.54 3.52 3.50 3.48 3.46 3.44 ppm
3.62 3.64 3.66 3.68 3.70 3.72 3.74 3.76 3.78 3.80 3.82 3.84 3.86 3.88

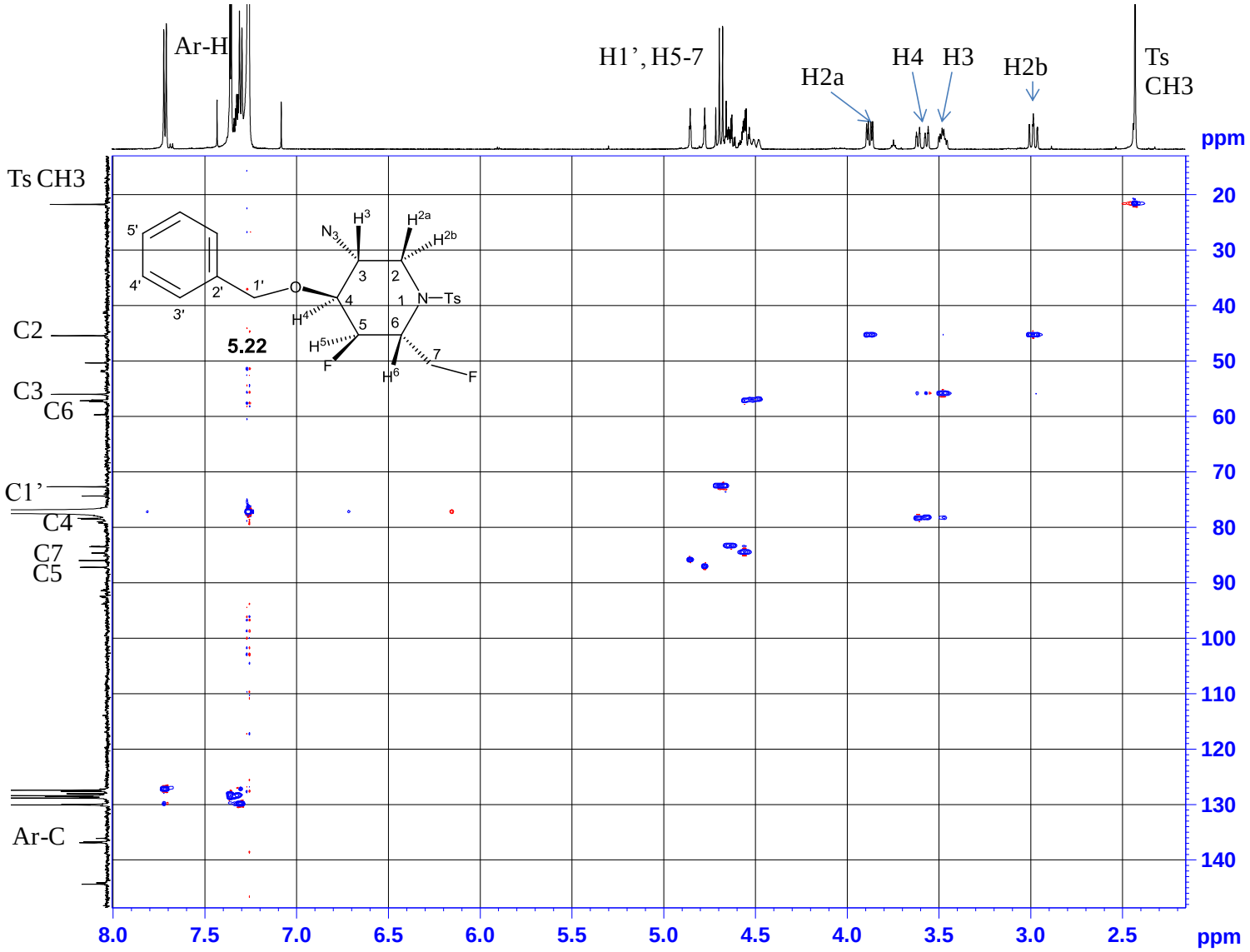

H2b
H3
H4
H2a
H6
H2b-H6
H4-H6
H1', H7
H7-H2a
ppm
3.85 3.80 3.75 3.70 3.65 3.60 3.55 3.50 3.45 3.40 ppm
4.15 4.20 4.25 4.30 4.35 4.40 4.45 4.50 4.55 4.60 4.65 4.70 4.75

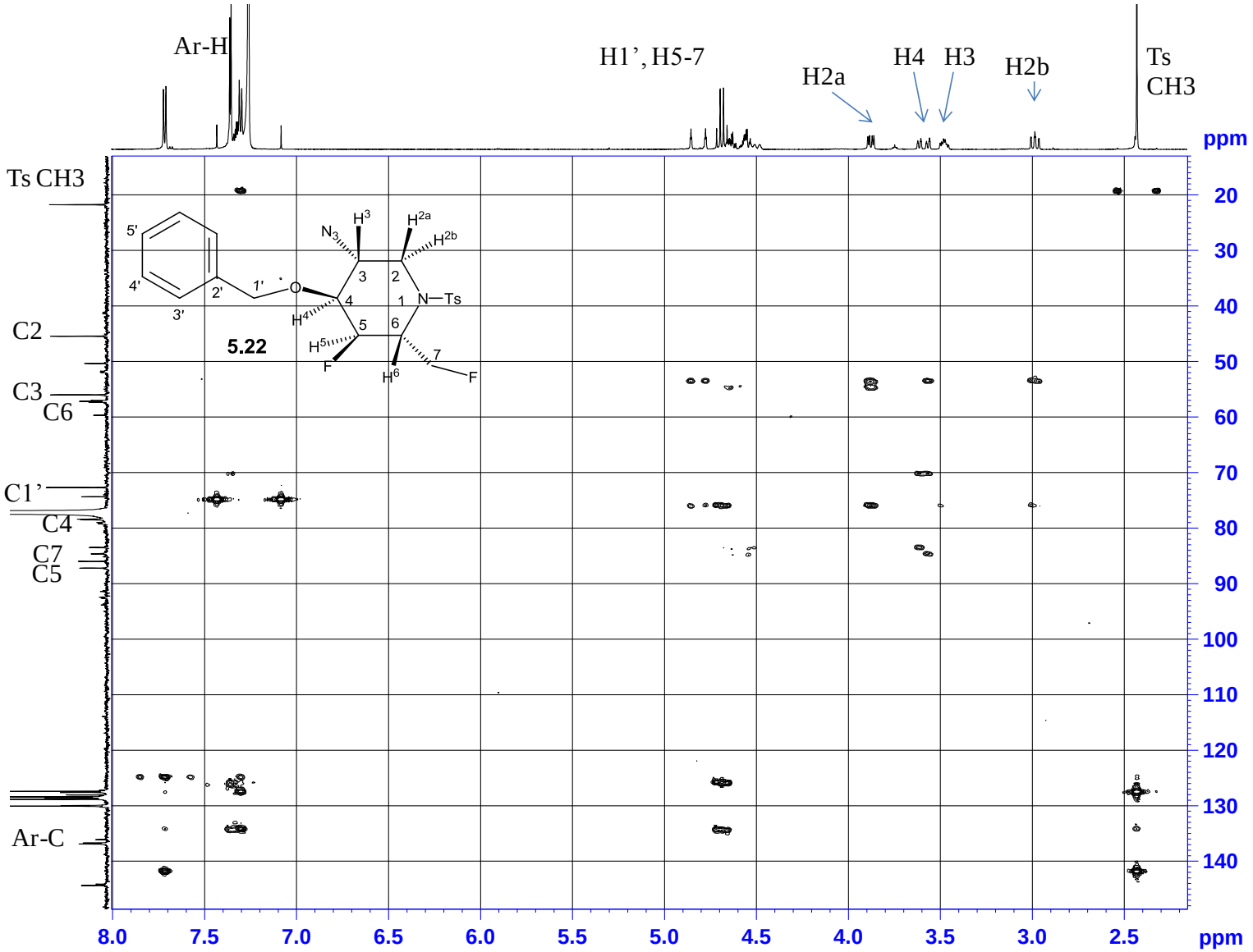

7.70
7.68
7.34
7.33
7.31
7.26
5.01
5.00
4.90
4.88
4.76
4.73
4.66
4.63
4.13
4.11
4.07
4.05
3.98
3.94
3.82
3.64
3.61
3.28
3.27
3.24
3.23
3.18
3.17
3.14
3.13
3.08
3.06
2.43
BnO
N3
F
HO
N
Ts
5.21
Current Data Parameters
NAME arp801_Ts protectio
EXPNO 2
PROCNO 1
F2 - Acquisition Parameters
Date_ 20130919
Time 12.18
INSTRUM spect
PROBHD 5 mm QNP 1H/1
PULPROG zg30
TD 32768
SOLVENT CDCl3
NS 16
DS 0
SWH 5995.204 Hz
FIDRES 0.182959 Hz
AQ 2.7329011 sec
RG 1024
DW 83.400 usec
DE 20.00 usec
TE 298.2 K
D1 2.00000000 sec
TD0 1
======== CHANNEL f1 ========
NUC1 1H
P1 11.25 usec
PL1 -1.50 dB
SFO1 399.9023994 MHz
F2 - Processing parameters
SI 32768
SF 399.9000120 MHz
WDW EM
SSB 0
LB 1.00 Hz
GB 0
PC 1.00
7.5
7.0
6.5
6.0
5.5
5.0
4.5
4.0
3.5
3.0
2.5
ppm
2.00
8.75
3.04
5.07
2.89
2.97

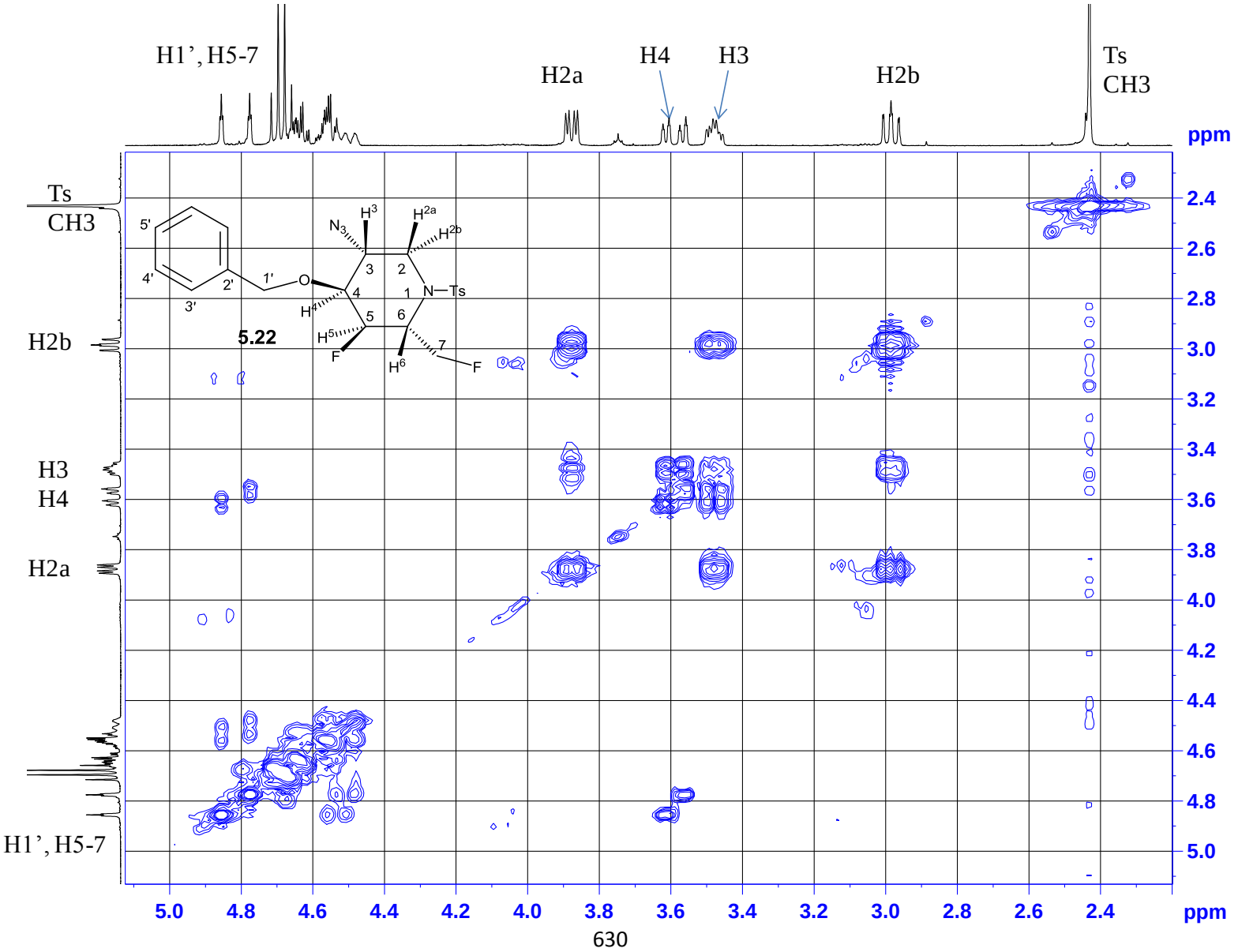

144.23
137.15
135.69
130.59
130.23
130.02
129.67
128.50
128.17
127.92
127.18
96.93
95.21
79.67
77.47
77.15
76.84
74.10
71.16
70.77
60.25
53.20
51.25
50.94
21.69
BnO
N3
F
HO
N
Ts
5.21
190 180 170 160 150 140 130 120 110 100 90 80 70 60 50 40 30 20 10 ppm

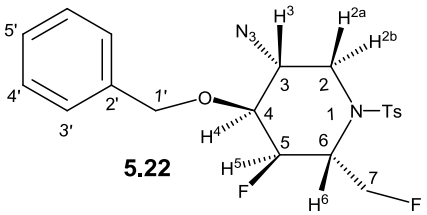

7.72
7.71
7.36
7.35
7.31
7.30
4.85
4.78
4.72
4.70
4.68
4.66
4.63
4.63
4.56
4.55
4.51
4.48
3.89
3.88
3.87
3.86
3.60
3.56
3.48
3.47
3.01
3.00
2.99
2.98
2.98
2.43
5.22
Current Data Parameters
NAME arp804_TsFOH spot1
EXPNO 1
PROCNO 1
F2 - Acquisition Parameters
Date_ 20131005
Time 9.54
INSTRUM spect
PROBHD 5 mm CPTXI 1H-
PULPROG zg30
TD 65536
SOLVENT None
NS 16
DS 0
SWH 8417.509 Hz
FIDRES 0.128441 Hz
AQ 3.8928883 sec
RG 256
DW 59.400 usec
DE 35.00 usec
TE 300.7 K
D1 1.00000000 sec
TD0 1
======== CHANNEL f1 ========
SFO1 600.1320933 MHz
NUC1 1H
P1 7.25 usec
PLW1 5.34999990 W
F2 - Processing parameters
SI 65536
SF 600.1284927 MHz
WDW EM
SSB 0
LB 0.30 Hz
GB 0
PC 1.00
7.5
7.0
6.5
6.0
5.5
5.0
4.5
4.0
3.5
3.0
2.5
ppm
2.00
7.54
5.93
1.10
2.01
1.02
2.98


144.33
144.09
136.87
136.68
136.07
130.04
129.93
128.80
128.57
128.51
128.37
128.03
127.57
127.38
93.85
92.44
91.41
87.21
86.00
84.68
84.61
83.52
83.45
78.99
78.50
78.38
77.37
77.16
76.95
74.35
72.68
59.72
59.65
57.30
57.16
57.03
55.99
51.90
50.34
45.43
21.75
5.22
5.23
NB:
5.22 and 5.23 has similar retention time and only small quantities were being isolated in pure form from the mixture; which was not enough for 13C NMR. So, 13C NMR of the mixture is presented.
190 180 170 160 150 140 130 120 110 100 90 80 70 60 50 40 30 20 10 ppm

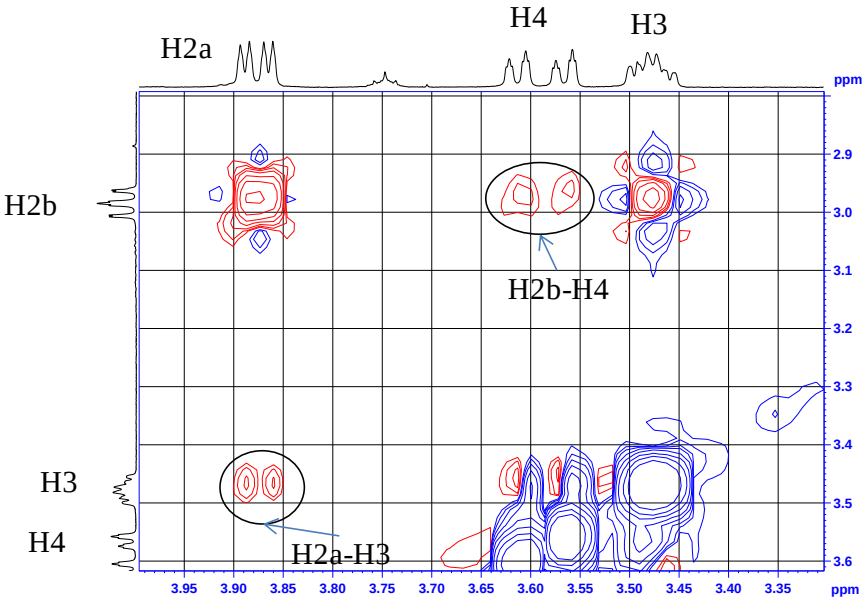

Ar-H
H1', H5-7
H2a
H4
H3
H2b
Ts CH3
ppm
Ts CH3
C2
C3
C6
C1'
C4
C7
C5
Ar-C
5.22
8.0
7.5
7.0
6.5
6.0
5.5
5.0
4.5
4.0
3.5
3.0
2.5
ppm

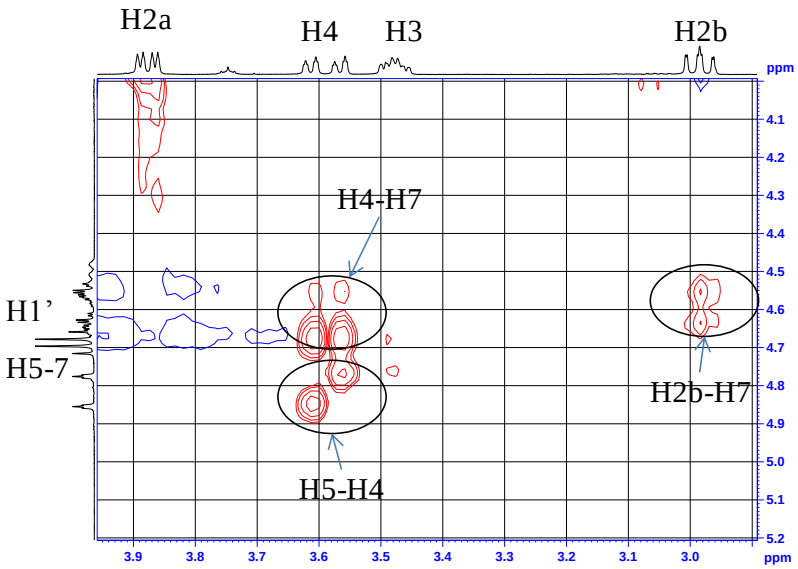

Ar-H
H1', H5-7
H2a
H4
H3
H2b
Ts CH3
ppm
Ts CH3
C2
C3
C6
C1'
C4
C7
C5
Ar-C
5.22
8.0
7.5
7.0
6.5
6.0
5.5
5.0
4.5
4.0
3.5
3.0
2.5
ppm

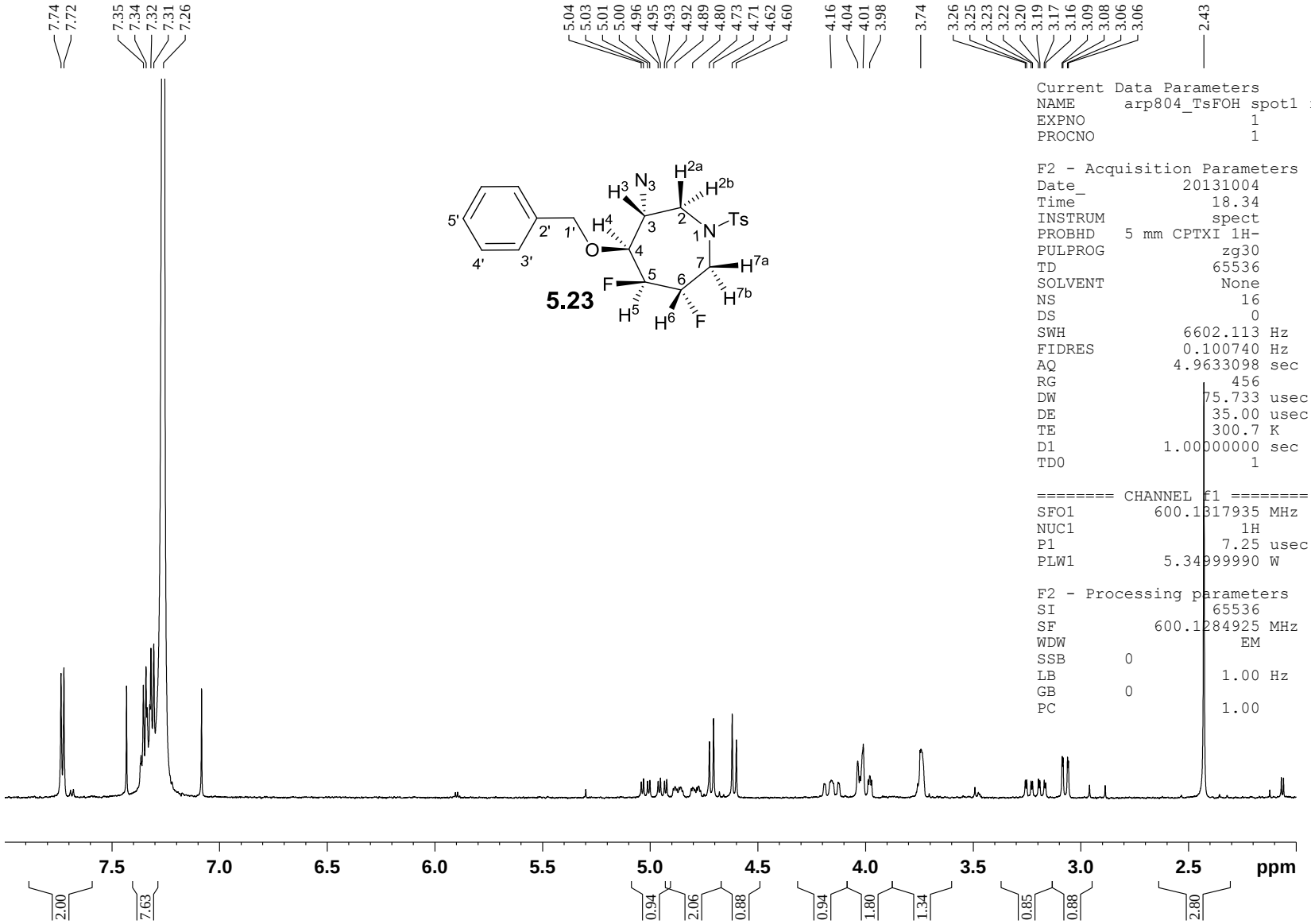

H1', H5-7
H2a
H4
H3
H2b
Ts
CH3
ppm
Ts
CH3
H2b
H3
H4
H2a
H1', H5-7
5.22
5.0
4.8
4.6
4.4
4.2
4.0
3.8
3.6
3.4
3.2
3.0
2.8
2.6
2.4
ppm

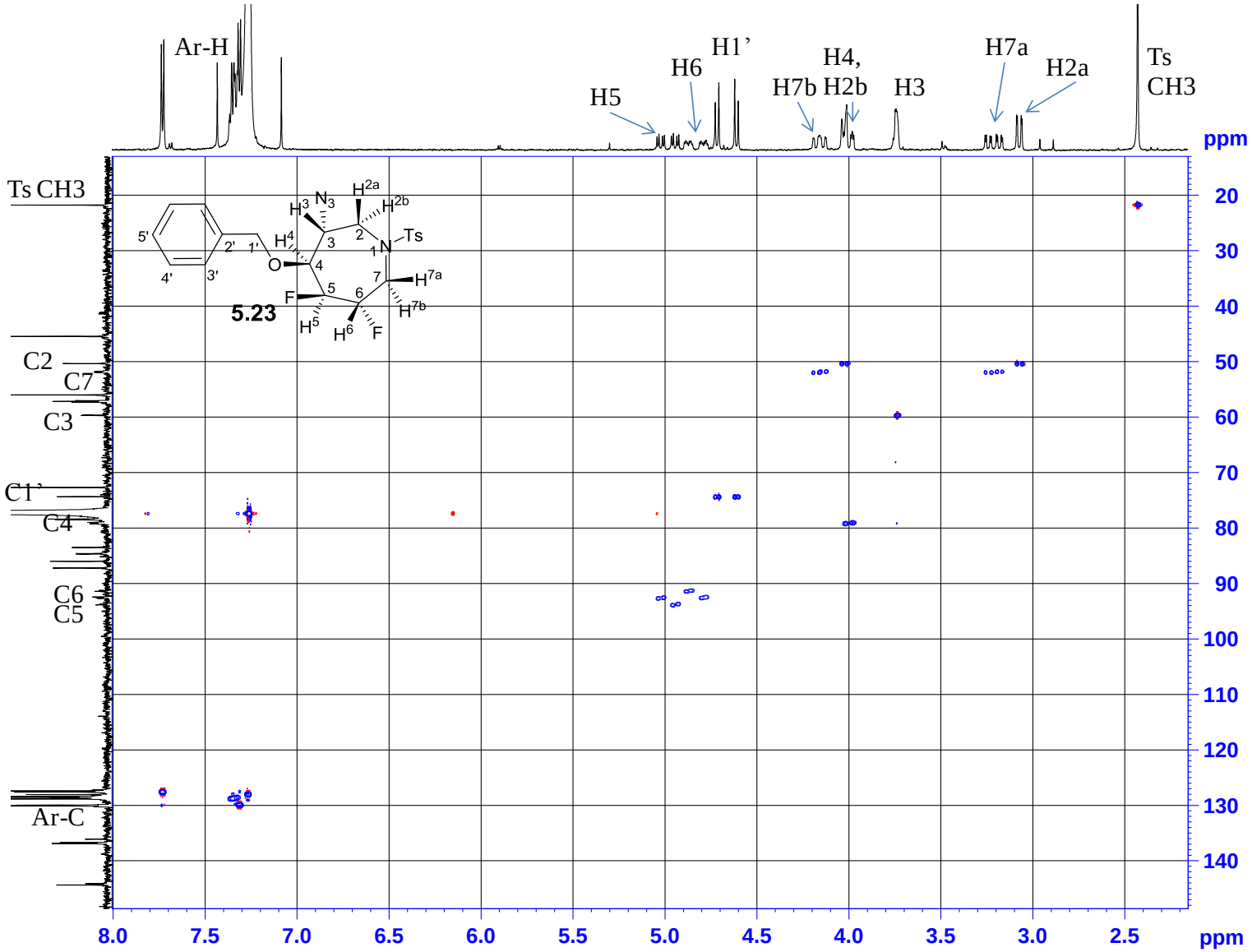

5'
4'
3'
2'
1'
O
3
2
4
1
N—Ts
5
6
7
F
F
N3
H3
H2a
H2b
H4
H5
H6

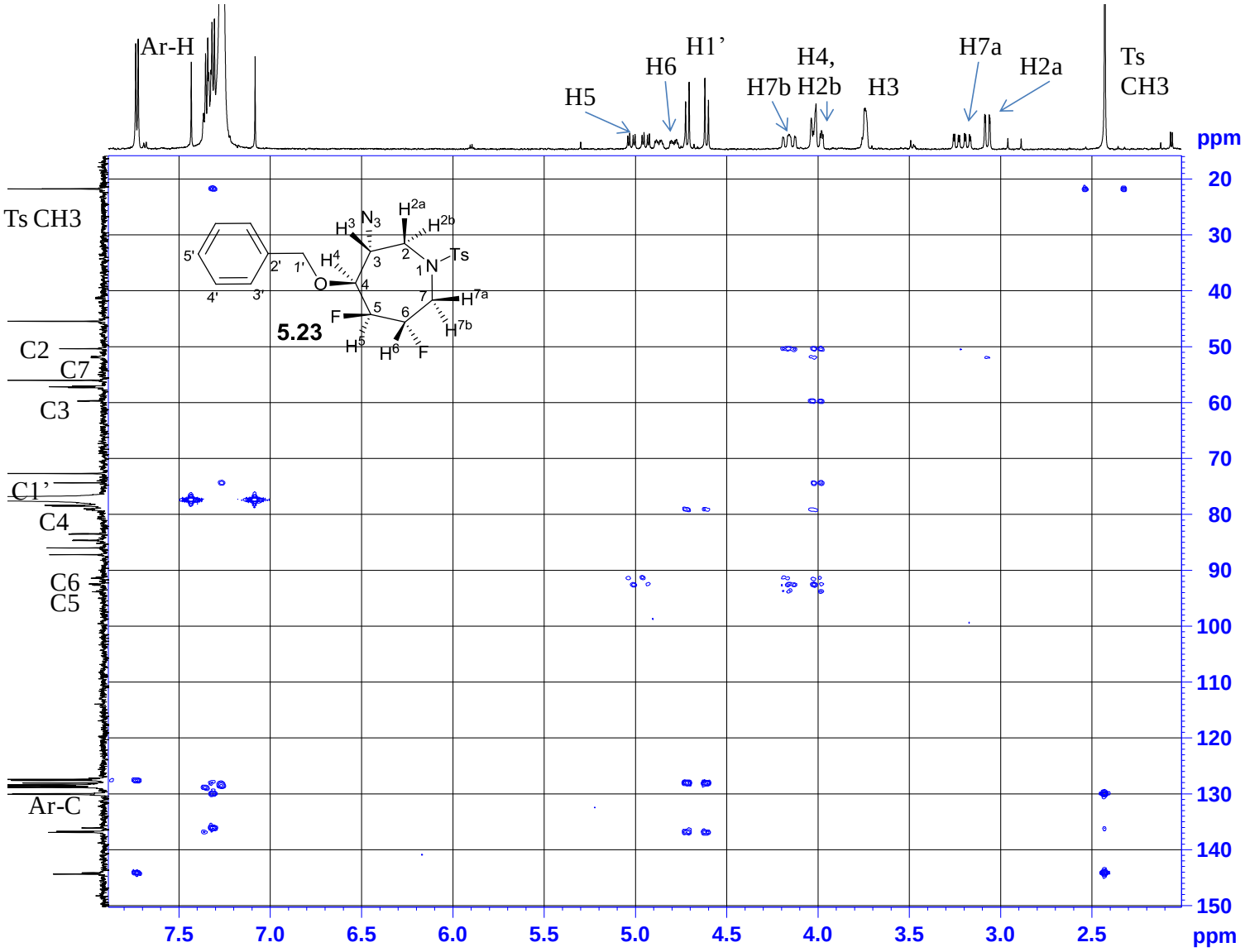
5.22

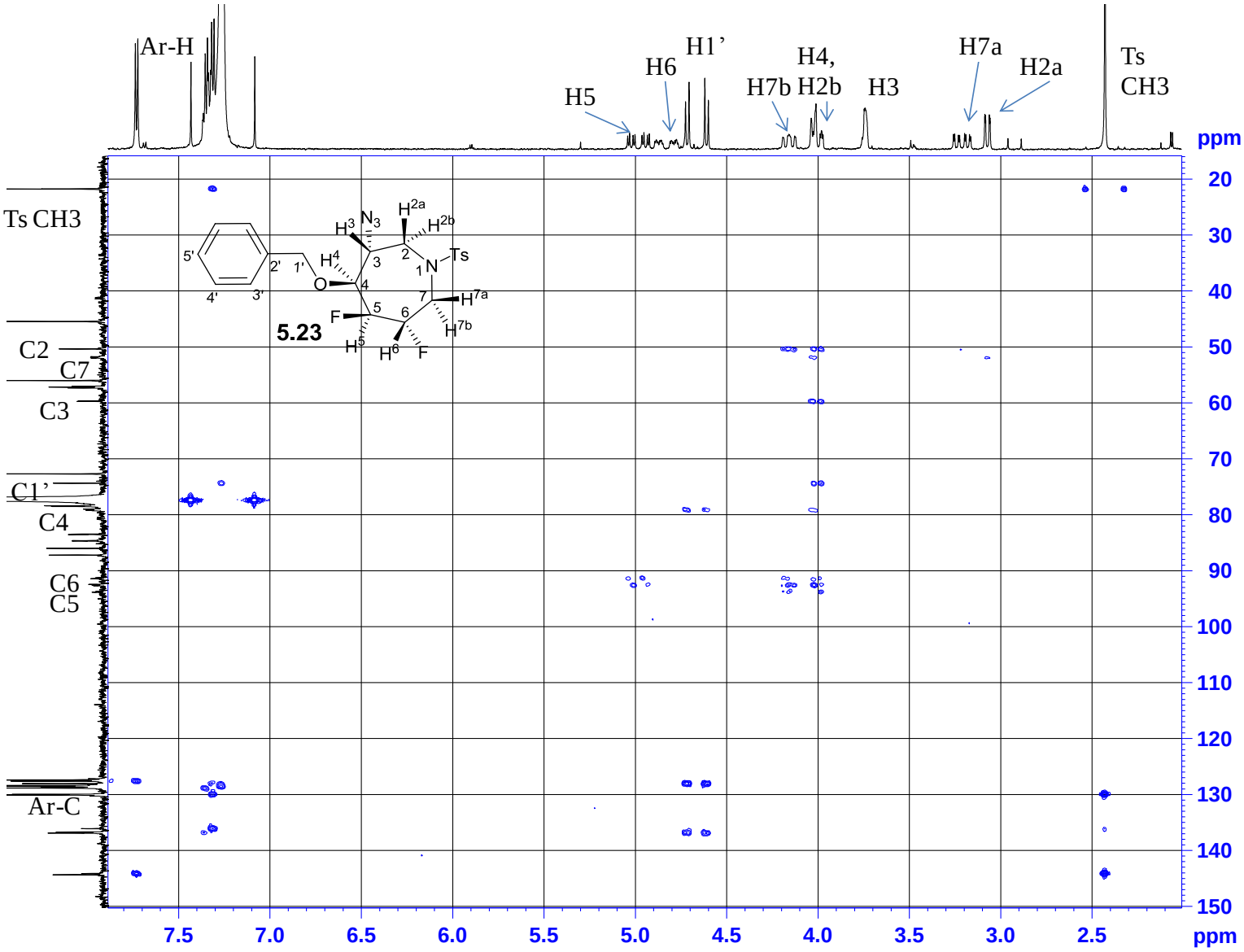

H2a
H4
H3
ppm
H2b
H2b-H4
H3
H4
H2a-H3
3.95
3.90
3.85
3.80
3.75
3.70
3.65
3.60
3.55
3.50
3.45
3.40
3.35
2.9
3.0
3.1
3.2
3.3
3.4
3.5
3.6

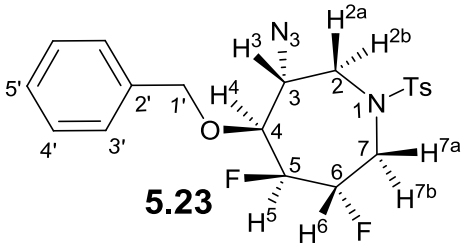

H2a
H4
H3
H2b
ppm
H4-H7
H1’
H5-7
H2b-H7
H5-H4
3.9
3.8
3.7
3.6
3.5
3.4
3.3
3.2
3.1
3.0
ppm
4.1
4.2
4.3
4.4
4.5
4.6
4.7
4.8
4.9
5.0
5.1
5.2


7.74
7.72
7.35
7.34
7.32
7.31
7.26
5.04
5.03
5.01
5.00
4.96
4.95
4.93
4.92
4.89
4.80
4.73
4.71
4.62
4.60
4.16
4.04
4.01
3.98
3.74
3.26
3.25
3.23
3.22
3.20
3.19
3.17
3.16
3.09
3.08
3.06
3.06
2.43
5.23
Current Data Parameters
NAME arp804_TsFOH spot1
EXPNO 1
PROCNO 1
F2 - Acquisition Parameters
Date_ 20131004
Time 18.34
INSTRUM spect
PROBHD 5 mm CPTXI 1H-
PULPROG zg30
TD 65536
SOLVENT None
NS 16
DS 0
SWH 6602.113 Hz
FIDRES 0.100740 Hz
AQ 4.9633098 sec
RG 456
DW 75.733 usec
DE 35.00 usec
TE 300.7 K
D1 1.00000000 sec
TD0 1
======== CHANNEL f1 ========
SFO1 600.1317935 MHz
NUC1 1H
P1 7.25 usec
PLW1 5.34999990 W
F2 - Processing parameters
SI 65536
SF 600.1284925 MHz
WDW EM
SSB 0
LB 1.00 Hz
GB 0
PC 1.00
7.5
7.0
6.5
6.0
5.5
5.0
4.5
4.0
3.5
3.0
2.5
ppm
2.00
7.63
0.94
2.06
0.88
0.94
1.80
1.34
0.85
0.88
2.80

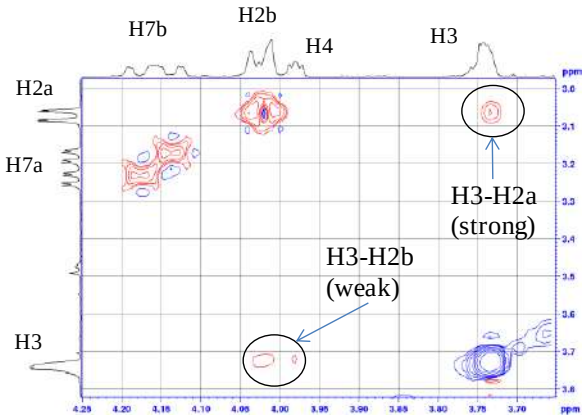

Ar-H
H5
H6
H1’
H7b
H4,
H2b
H3
H7a
H2a
Ts
CH3
ppm
Ts CH3
C2
C7
C3
C1’
C4
C6
C5
Ar-C
5.23
8.0
7.5
7.0
6.5
6.0
5.5
5.0
4.5
4.0
3.5
3.0
2.5
ppm

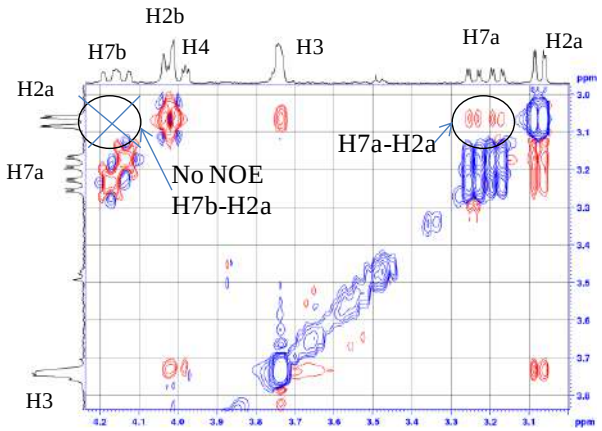

Ar-H
H5
H6
H1'
H4,
H7b H2b
H3
H7a
H2a
Ts
CH3
ppm
Ts CH3
C2
C7
C3
C1'
C4
C6
C5
Ar-C
5.23
20
30
40
50
60
70
80
90
100
110
120
130
140
150
7.5
7.0
6.5
6.0
5.5
5.0
4.5
4.0
3.5
3.0
2.5
ppm

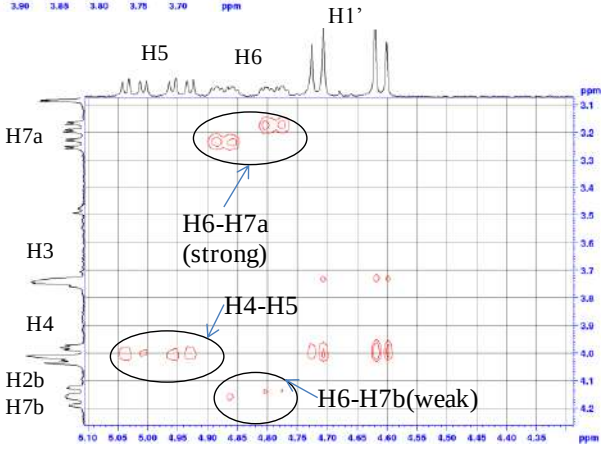

Ar-H
H5
H6
H1'
H4,
H7b H2b
H3
H7a
H2a
Ts
CH3
ppm
Ts CH3
C2
C7
C3
C1'
C4
C6
C5
Ar-C
5.23
20
30
40
50
60
70
80
90
100
110
120
130
140
150
7.5
7.0
6.5
6.0
5.5
5.0
4.5
4.0
3.5
3.0
2.5
ppm

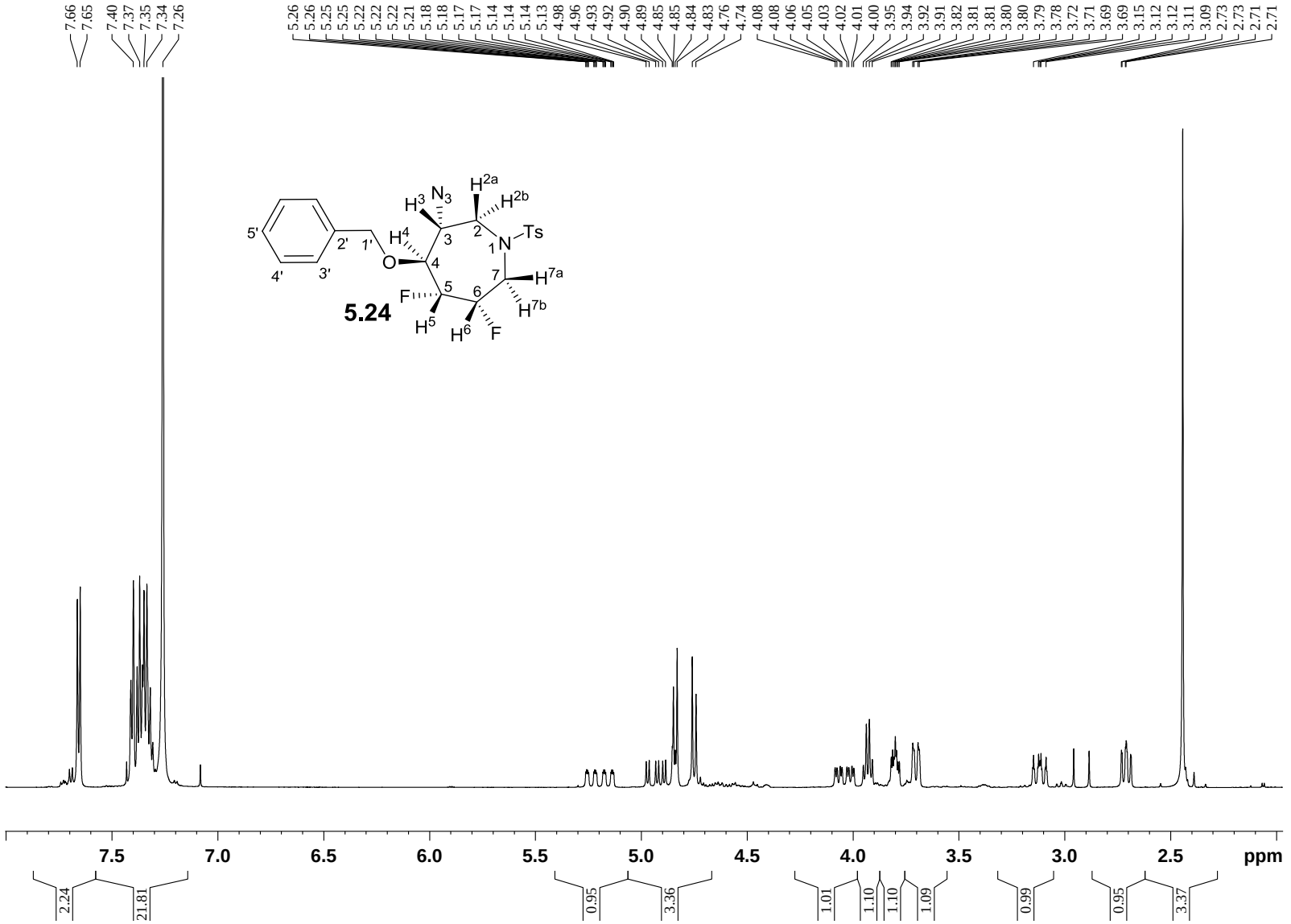

5'
4'
3'
2'
1'
O
4
3
2
1
N
Ts
5
6
7
F
F
H3
N3
H2a
H2b
H4
H7a
H7b
H5
H6

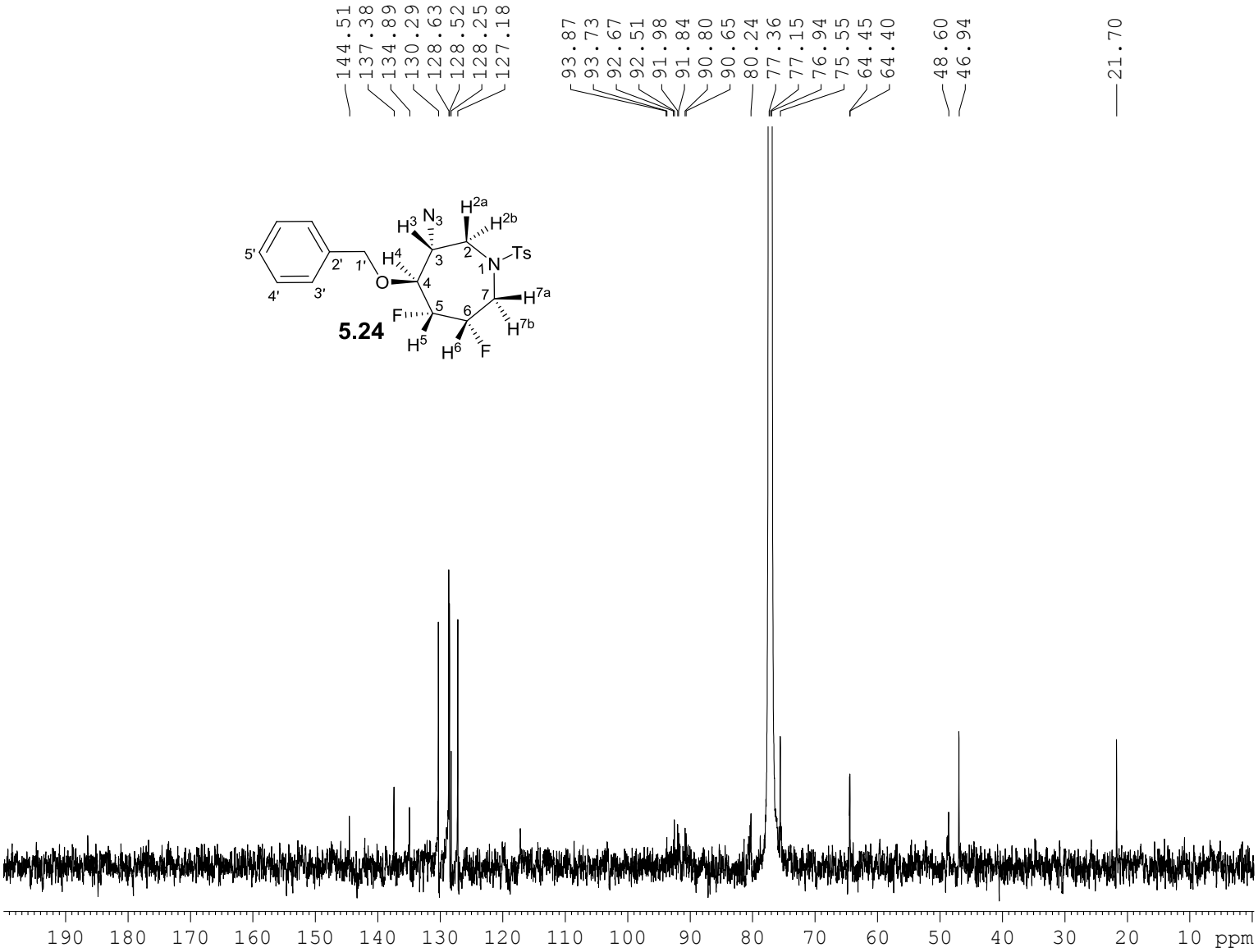
5.23

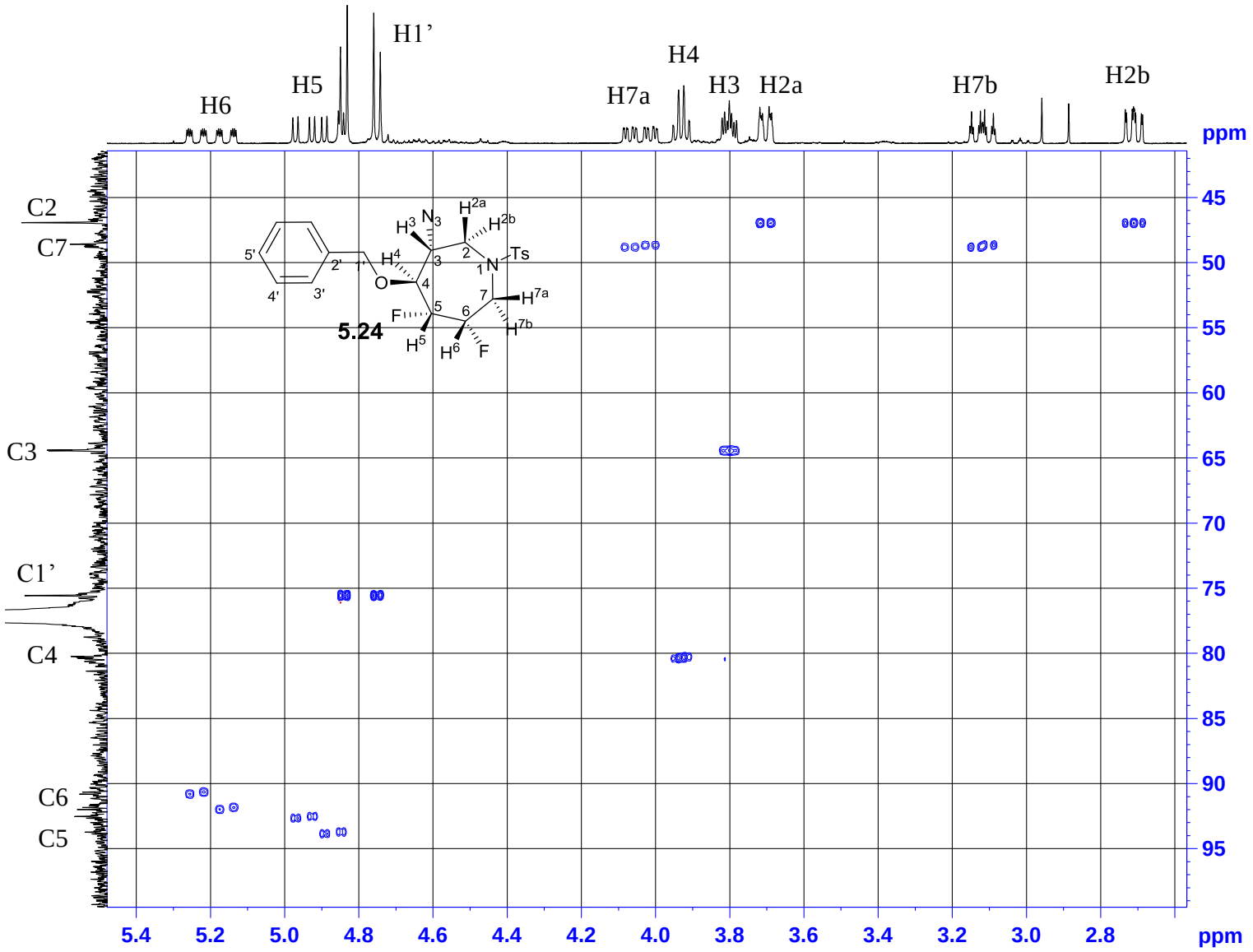

H7b
H2b
H4
H3
H2a
H7a
H3-H2a
(strong)
H3-H2b
(weak)
H3

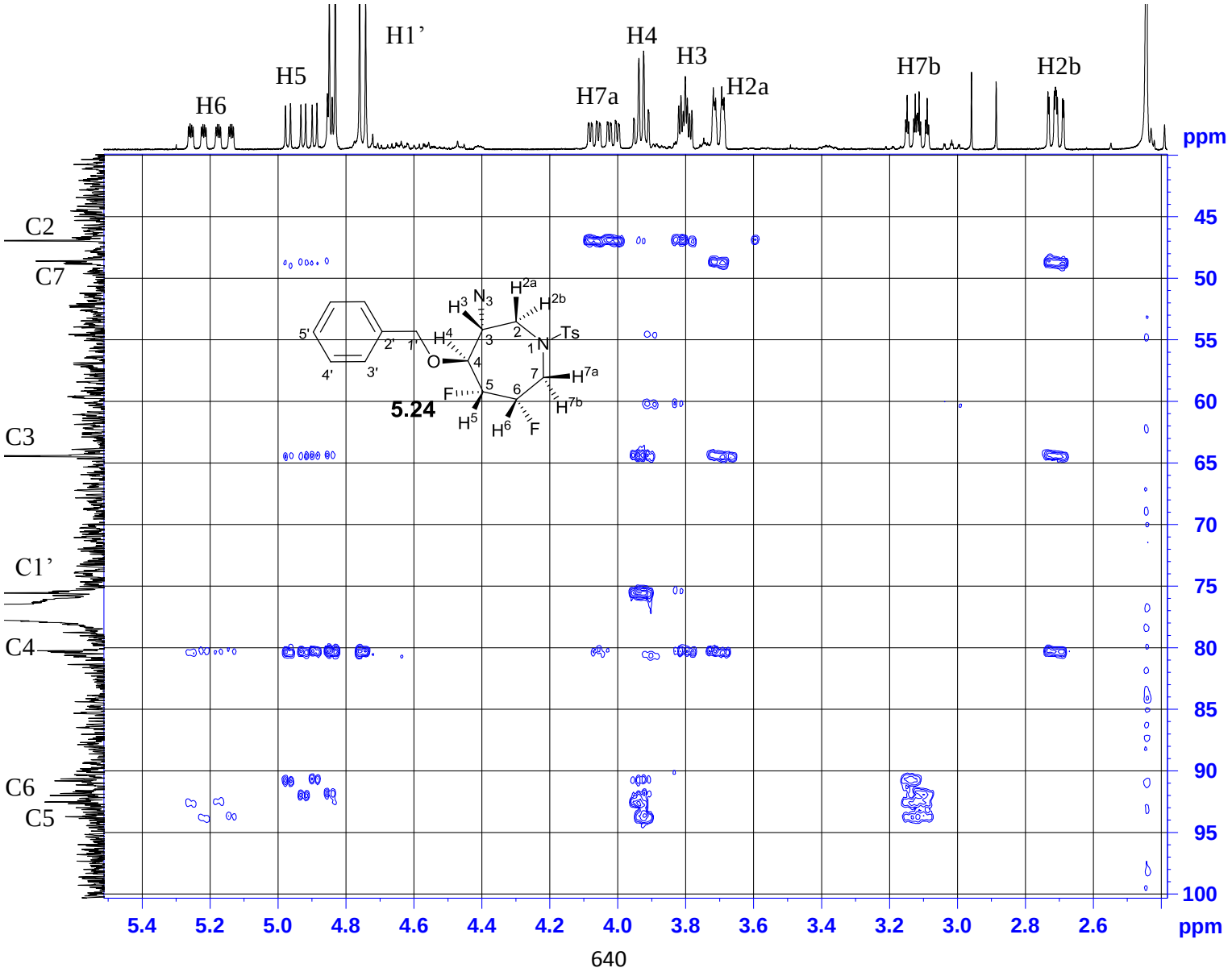

H2b
H7b
H4
H3
H7a
H2a
H2a
H7a
No NOE
H7b-H2a
H7a-H2a
H3

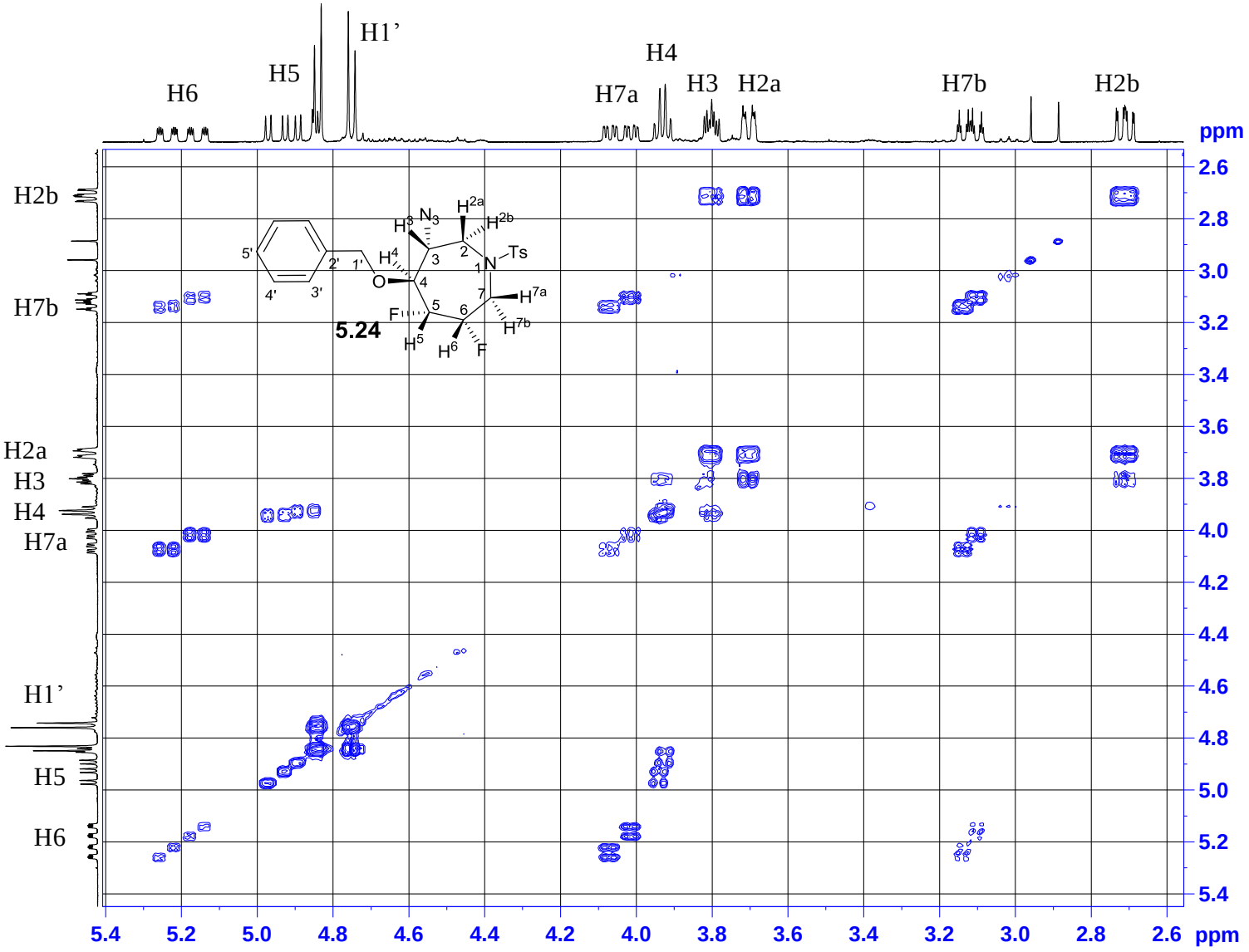

H1'
H5
H6
H7a
H6-H7a
(strong)
H3
H4-H5
H4
H2b
H7b
H6-H7b(weak)

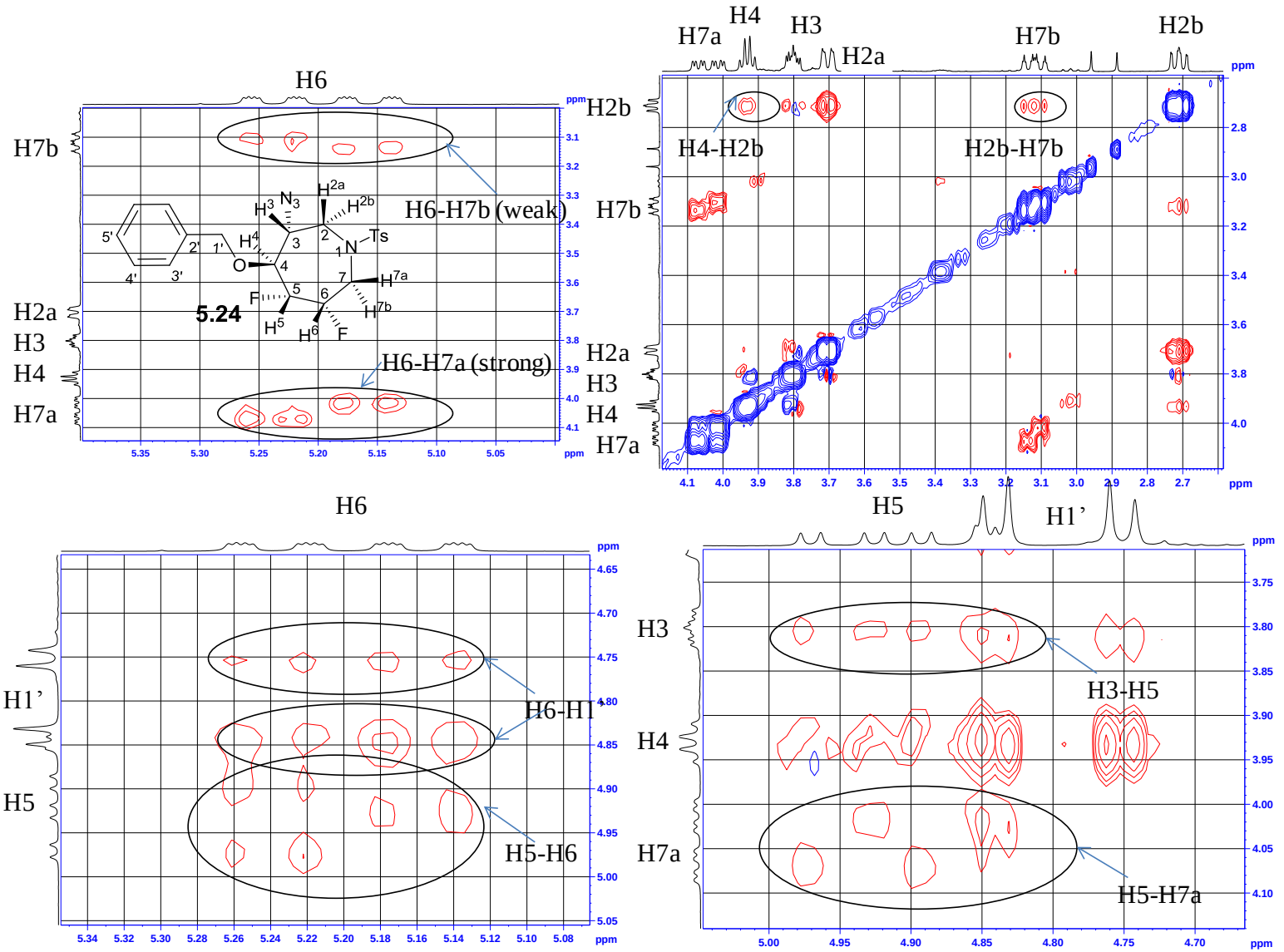

7.66
7.65
7.40
7.37
7.35
7.34
7.26
5.26
5.26
5.25
5.25
5.22
5.22
5.22
5.21
5.18
5.18
5.17
5.17
5.14
5.14
5.14
5.13
4.98
4.96
4.93
4.92
4.90
4.89
4.85
4.85
4.84
4.83
4.76
4.74
4.08
4.08
4.06
4.05
4.03
4.02
4.01
4.00
3.95
3.94
3.92
3.91
3.82
3.81
3.81
3.80
3.80
3.79
3.78
3.72
3.71
3.69
3.69
3.15
3.12
3.12
3.11
3.09
2.73
2.73
2.71
2.71
5.24
7.5
7.0
6.5
6.0
5.5
5.0
4.5
4.0
3.5
3.0
2.5
ppm
2.24
21.81
0.95
3.36
1.01
1.10
1.10
1.09
0.99
0.95
3.37


144.51
137.38
134.89
130.29
128.63
128.52
128.25
127.18
93.87
93.73
92.67
92.51
91.98
91.84
90.80
90.65
80.24
77.36
77.15
76.94
75.55
64.45
64.40
48.60
46.94
21.70
5.24
190 180 170 160 150 140 130 120 110 100 90 80 70 60 50 40 30 20 10 ppm


H6
H5
H1'
H7a
H4
H3
H2a
H7b
H2b
ppm
C2
C7
C3
C1'
C4
C6
C5
5.24
5.4
5.2
5.0
4.8
4.6
4.4
4.2
4.0
3.8
3.6
3.4
3.2
3.0
2.8
ppm


H6
H5
H1’
H7a
H4
H3
H2a
H7b
H2b
ppm
C2
C7
C3
C1’
C4
C6
C5
5.24
5.4
5.2
5.0
4.8
4.6
4.4
4.2
4.0
3.8
3.6
3.4
3.2
3.0
2.8
2.6
ppm
45
50
55
60
65
70
75
80
85
90
95
100


H6
H5
H1’
H7a
H4
H3
H2a
H7b
H2b
ppm
H2b
H7b
H2a
H3
H4
H7a
H1’
H5
H6
5.24
5.4
5.2
5.0
4.8
4.6
4.4
4.2
4.0
3.8
3.6
3.4
3.2
3.0
2.8
2.6
ppm

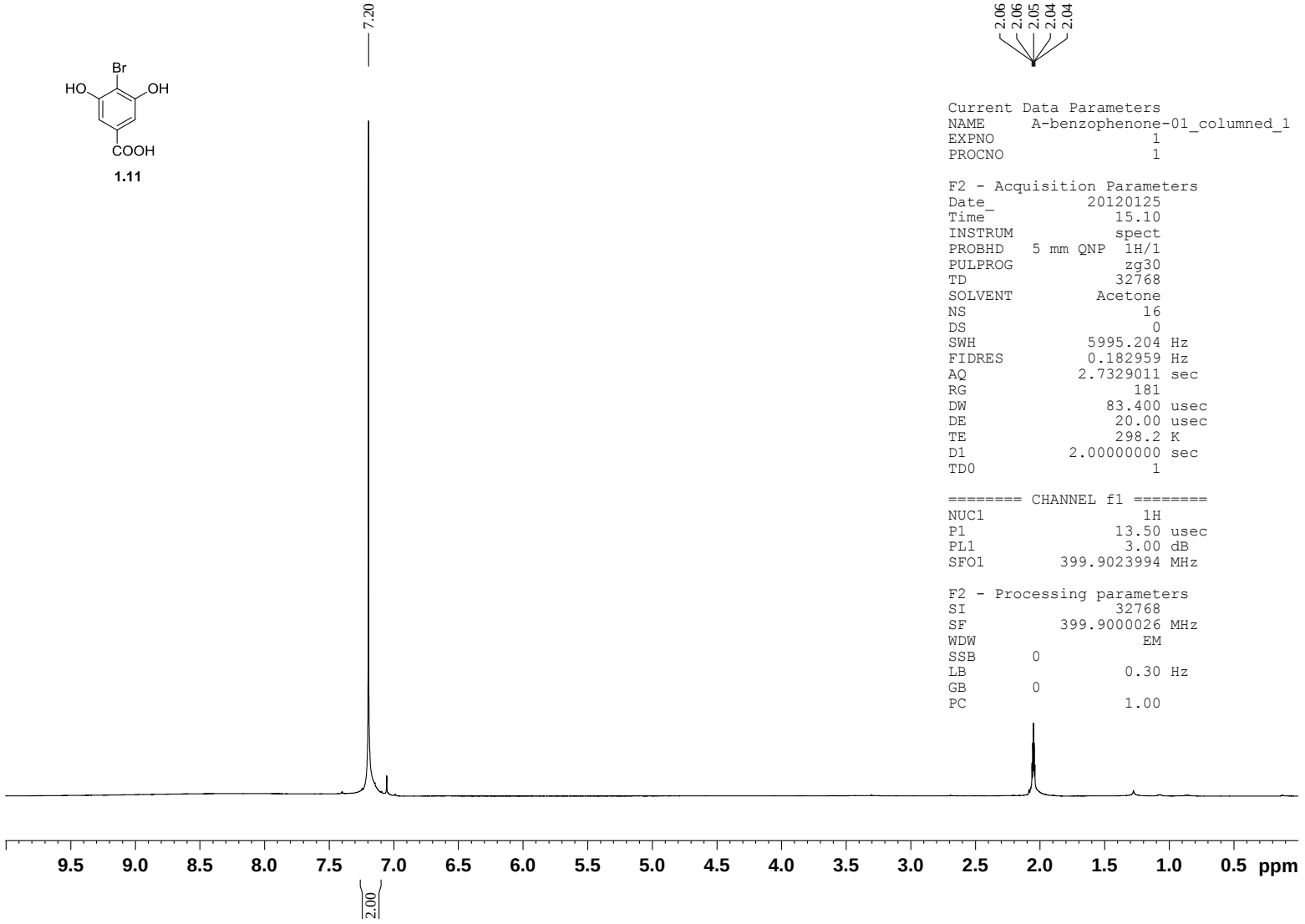

H6
H7b
H2a
H3
H4
H7a
H6-H7b (weak)
H6-H7a (strong)
5.24
H4
H3
H7a
H2a
H7b
H2b
H4-H2b
H2b-H7b
H6
H1’
H5
H6-H1’
H5-H6
H5
H1’
H3
H4
H7a
H3-H5
H5-H7a

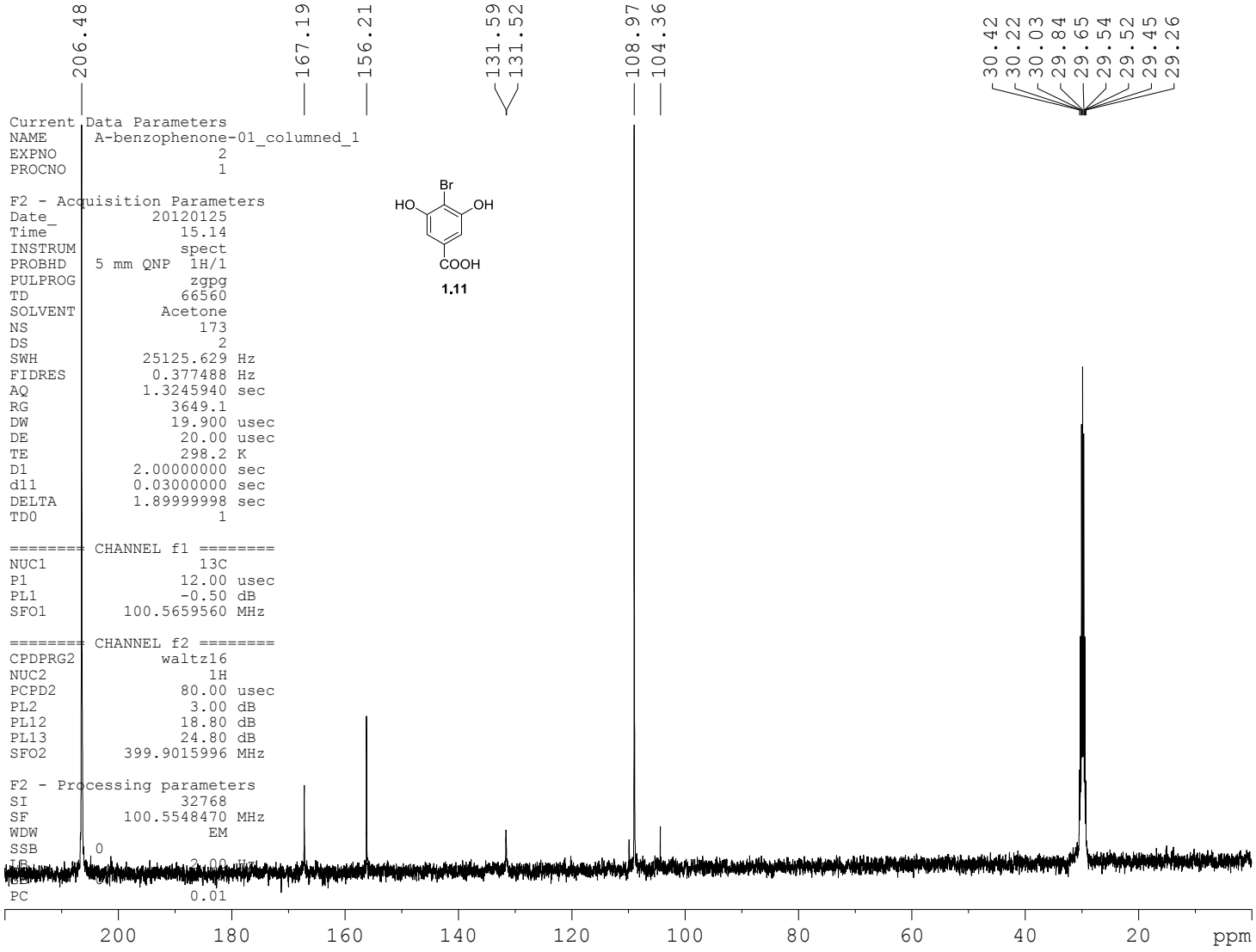
Appendix E

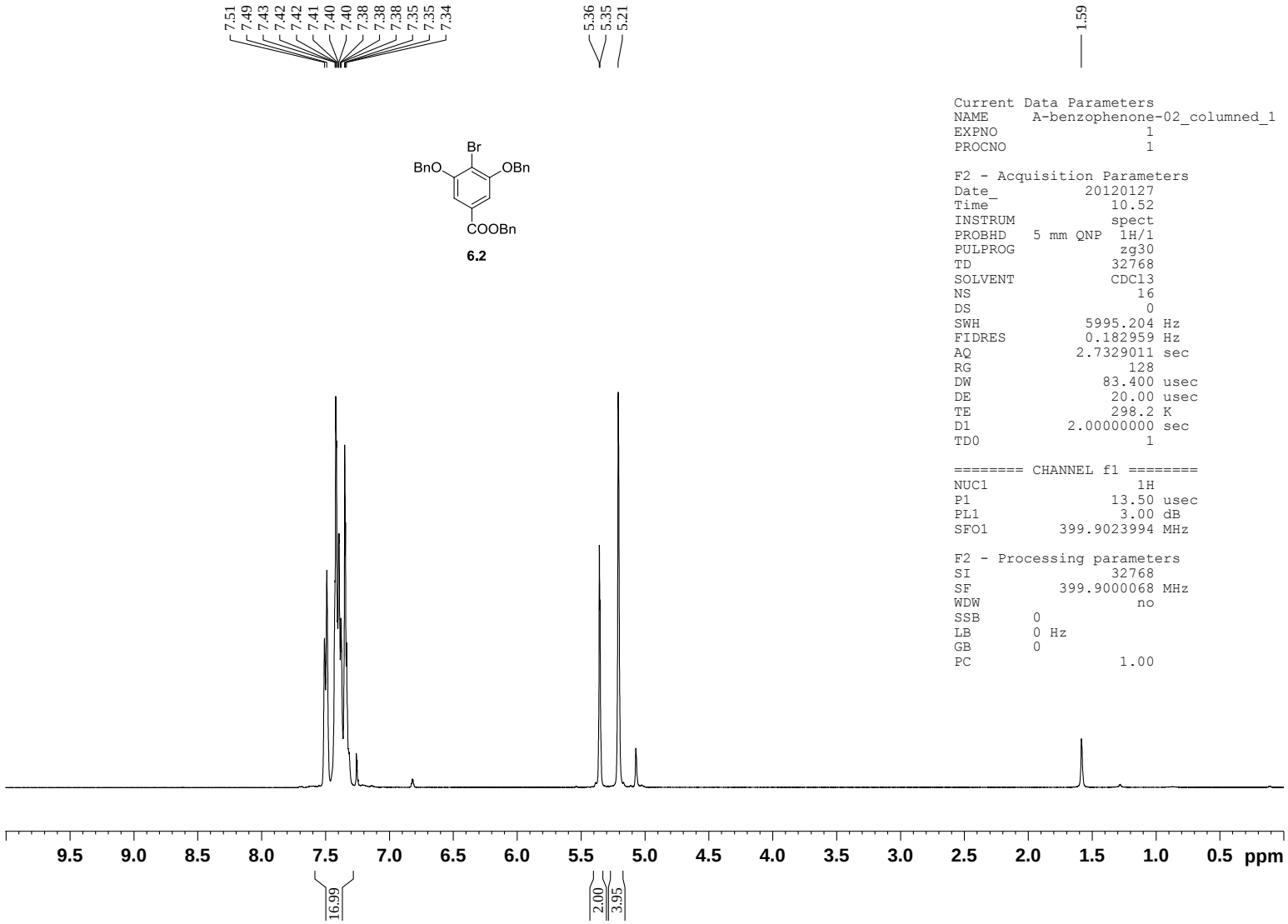
Table of contents:

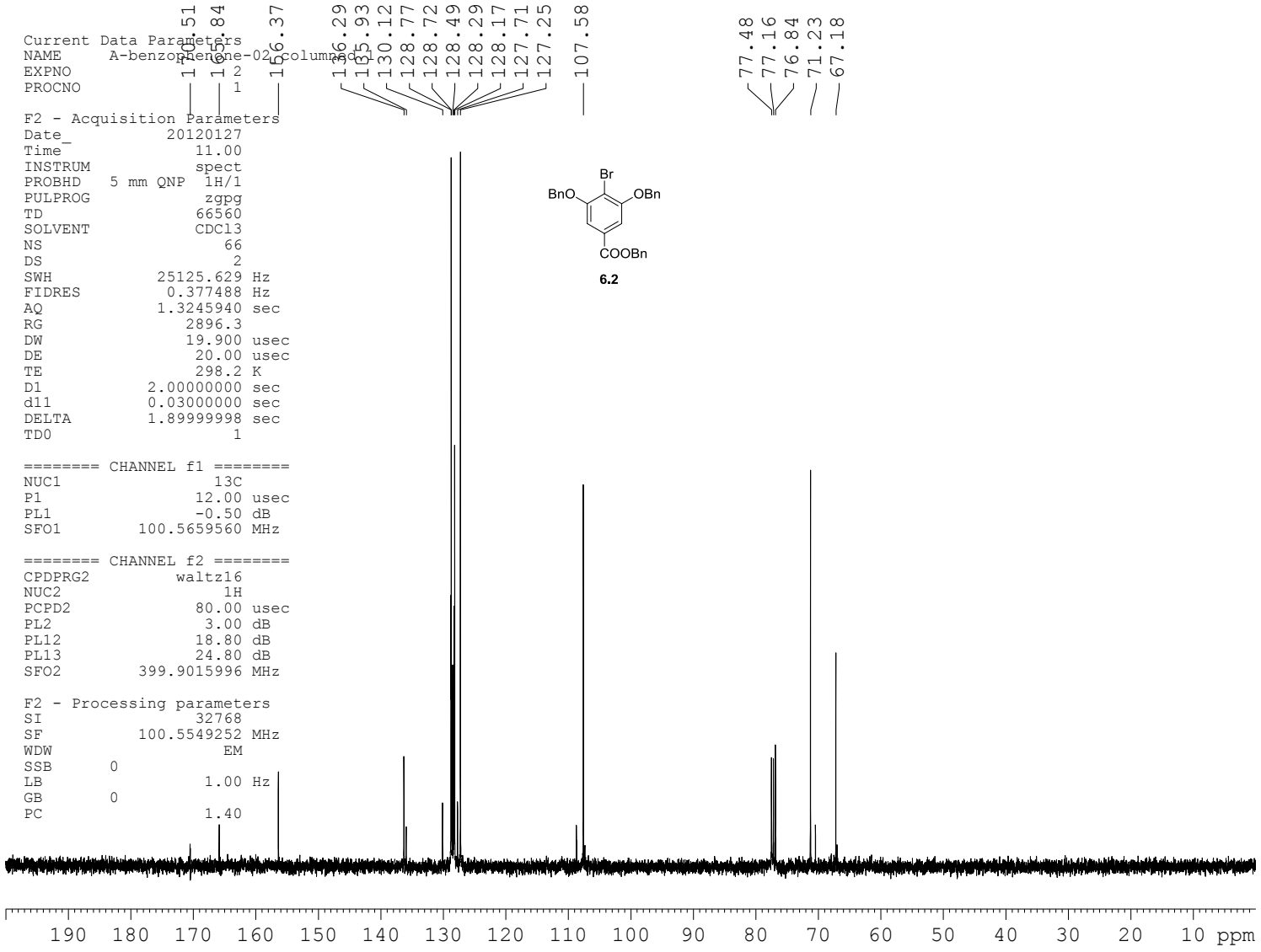
Full NMR spectra of compounds discussed in chapter 6……..…..……644

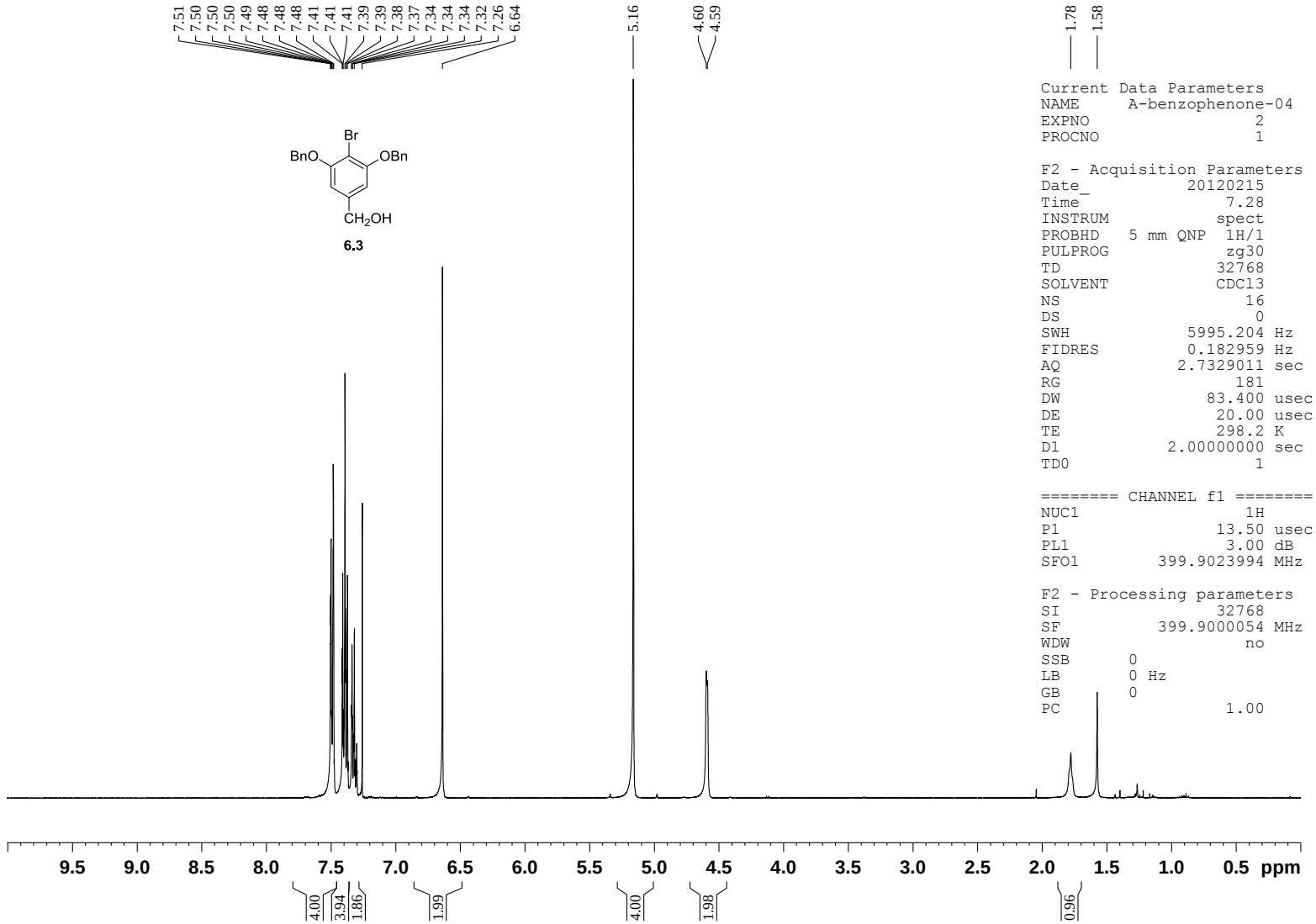
Binding curve images of fluorinated balanol analogues……..……729

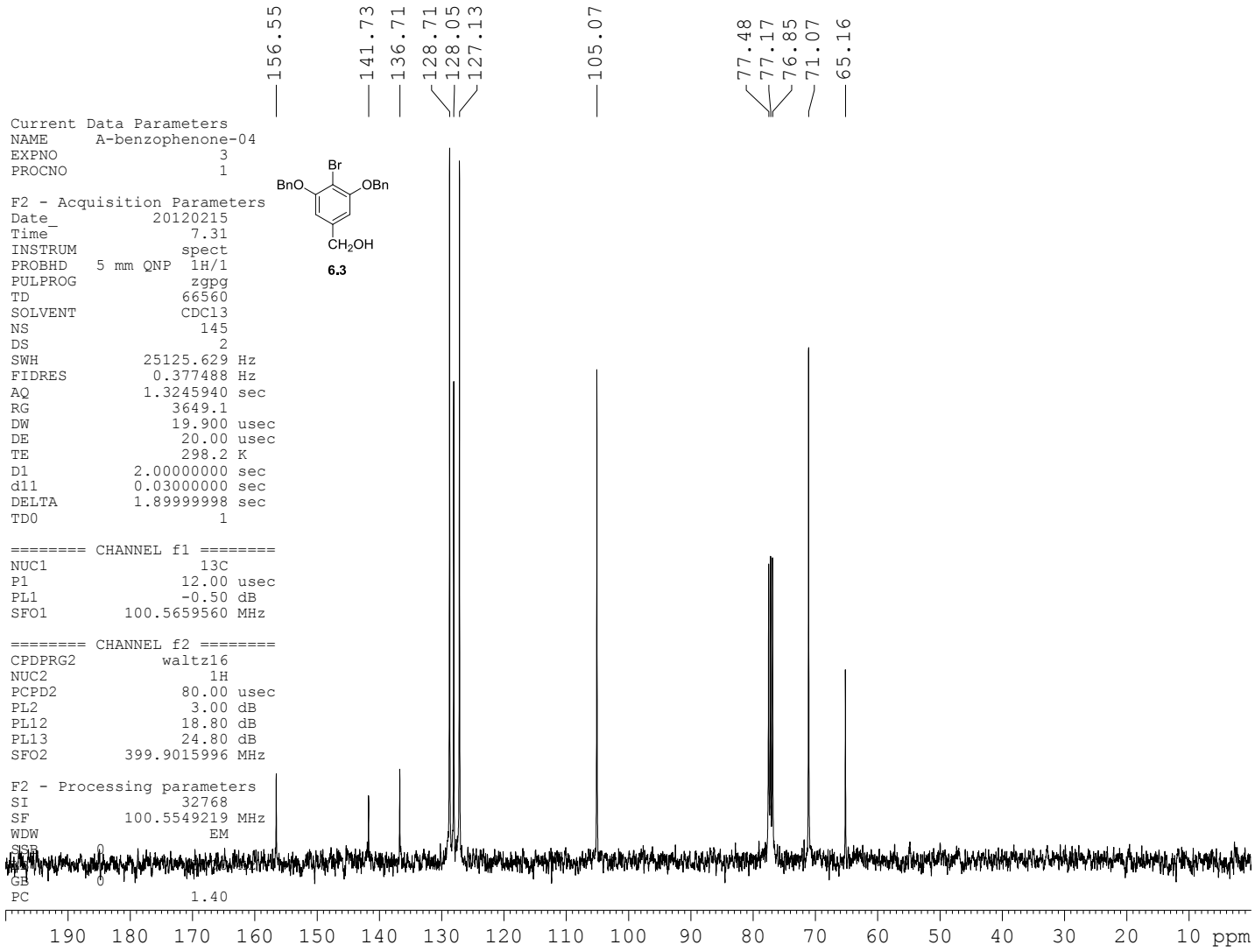

Br
HO
OH
COOH
1.11
7.20
2.06
2.06
2.05
2.04
2.04
Current Data Parameters
NAME A-benzophenone-01_columned_1
EXPNO 1
PROCNO 1
F2 - Acquisition Parameters
Date_ 20120125
Time 15.10
INSTRUM spect
PROBHD 5 mm QNP 1H/1
PULPROG zg30
TD 32768
SOLVENT Acetone
NS 16
DS 0
SWH 5995.204 Hz
FIDRES 0.182959 Hz
AQ 2.7329011 sec
RG 181
DW 83.400 usec
DE 20.00 usec
TE 298.2 K
D1 2.00000000 sec
TD0 1
======== CHANNEL f1 ========
NUC1 1H
P1 13.50 usec
PL1 3.00 dB
SFO1 399.9023994 MHz
F2 - Processing parameters
SI 32768
SF 399.9000026 MHz
WDW EM
SSB 0
LB 0.30 Hz
GB 0
PC 1.00
9.5 9.0 8.5 8.0 7.5 7.0 6.5 6.0 5.5 5.0 4.5 4.0 3.5 3.0 2.5 2.0 1.5 1.0 0.5 ppm
2.00

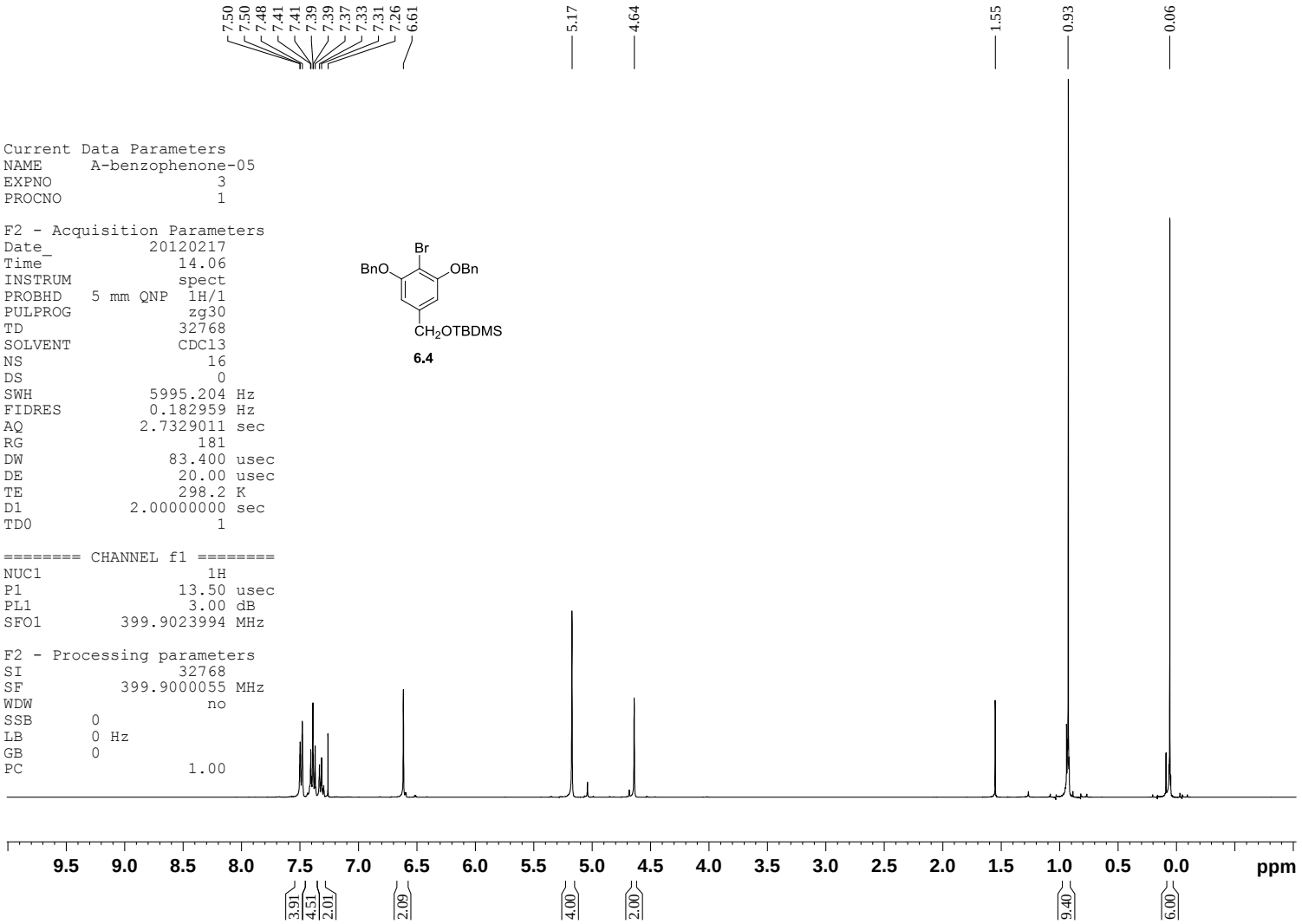

206.48
167.19
156.21
131.59
131.52
108.97
104.36
30.42
30.22
30.03
29.84
29.65
29.54
29.52
29.45
29.26
Br
HO
OH
COOH
1.11
Current Data Parameters
NAME A-benzophenone-01_columned_1
EXPNO 2
PROCNO 1
F2 - Acquisition Parameters
Date_ 20120125
Time 15.14
INSTRUM spect
PROBHD 5 mm QNP 1H/1
PULPROG zgpg
TD 66560
SOLVENT Acetone
NS 173
DS 2
SWH 25125.629 Hz
FIDRES 0.377488 Hz
AQ 1.3245940 sec
RG 3649.1
DW 19.900 usec
DE 20.00 usec
TE 298.2 K
D1 2.00000000 sec
d11 0.03000000 sec
DELTA 1.89999998 sec
TD0 1
======== CHANNEL f1 ========
NUC1 13C
P1 12.00 usec
PL1 -0.50 dB
SFO1 100.5659560 MHz
======== CHANNEL f2 ========
CPDPRG2 waltz16
NUC2 1H
PCPD2 80.00 usec
PL2 3.00 dB
PL12 18.80 dB
PL13 24.80 dB
SFO2 399.9015996 MHz
F2 - Processing parameters
SI 32768
SF 100.5548470 MHz
WDW EM
SSB 0
LB 2.00 Hz
GB 0
PC 0.01
200
180
160
140
120
100
80
60
40
20
ppm

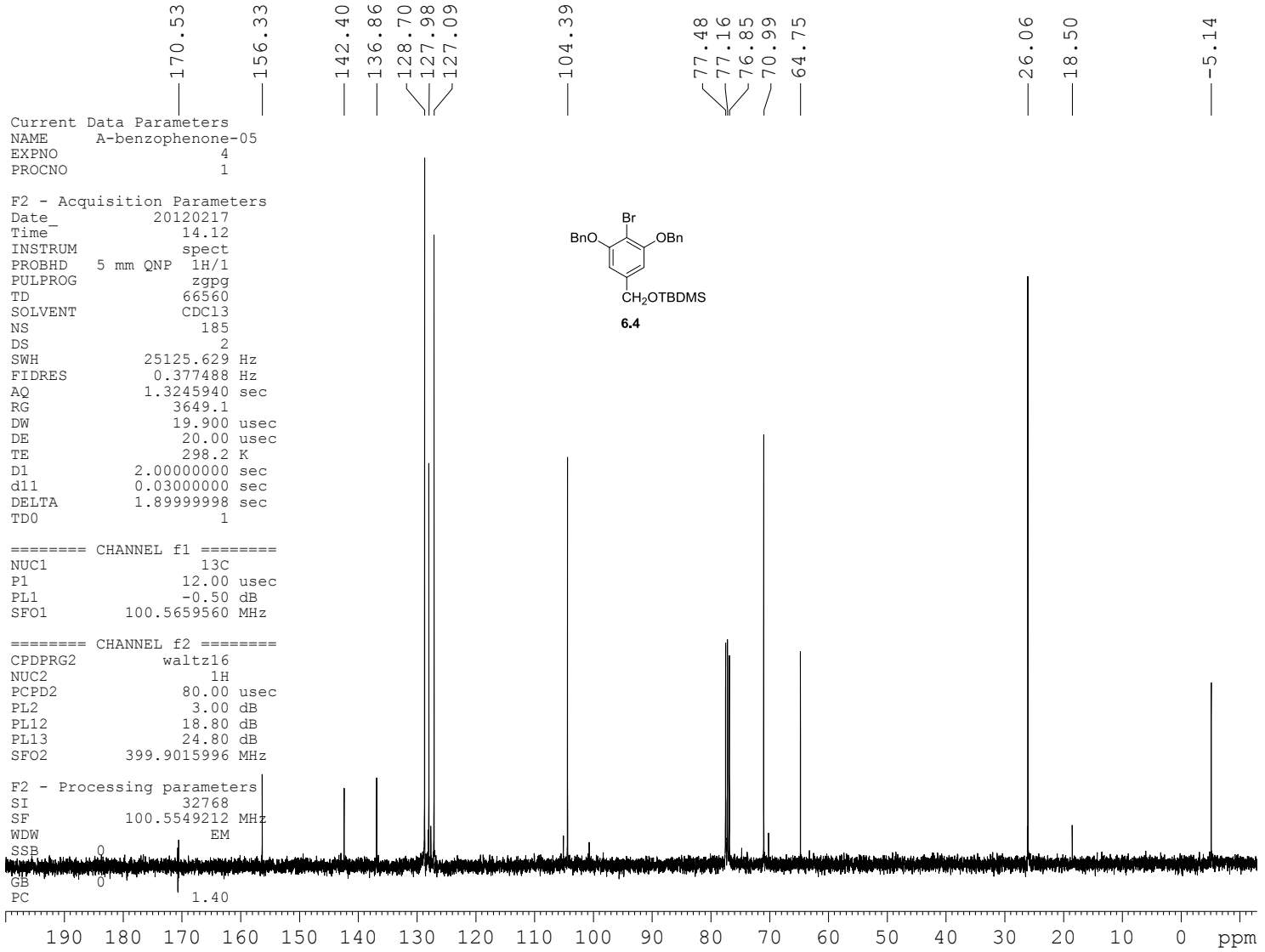

7.51
7.49
7.43
7.42
7.42
7.41
7.40
7.40
7.38
7.38
7.38
7.35
7.35
7.34
5.36
5.35
5.21
1.59
Br
BnO
OBn
COOBn
6.2
Current Data Parameters
NAME A-benzophenone-02_columned_1
EXPNO 1
PROCNO 1
F2 - Acquisition Parameters
Date_ 20120127
Time 10.52
INSTRUM spect
PROBHD 5 mm QNP 1H/1
PULPROG zg30
TD 32768
SOLVENT CDCl3
NS 16
DS 0
SWH 5995.204 Hz
FIDRES 0.182959 Hz
AQ 2.7329011 sec
RG 128
DW 83.400 usec
DE 20.00 usec
TE 298.2 K
D1 2.00000000 sec
TD0 1
======== CHANNEL f1 ========
NUC1 1H
P1 13.50 usec
PL1 3.00 dB
SFO1 399.9023994 MHz
F2 - Processing parameters
SI 32768
SF 399.9000068 MHz
WDW no
SSB 0
LB 0 Hz
GB 0
PC 1.00
9.5 9.0 8.5 8.0 7.5 7.0 6.5 6.0 5.5 5.0 4.5 4.0 3.5 3.0 2.5 2.0 1.5 1.0 0.5 ppm
16.99
2.00
3.95

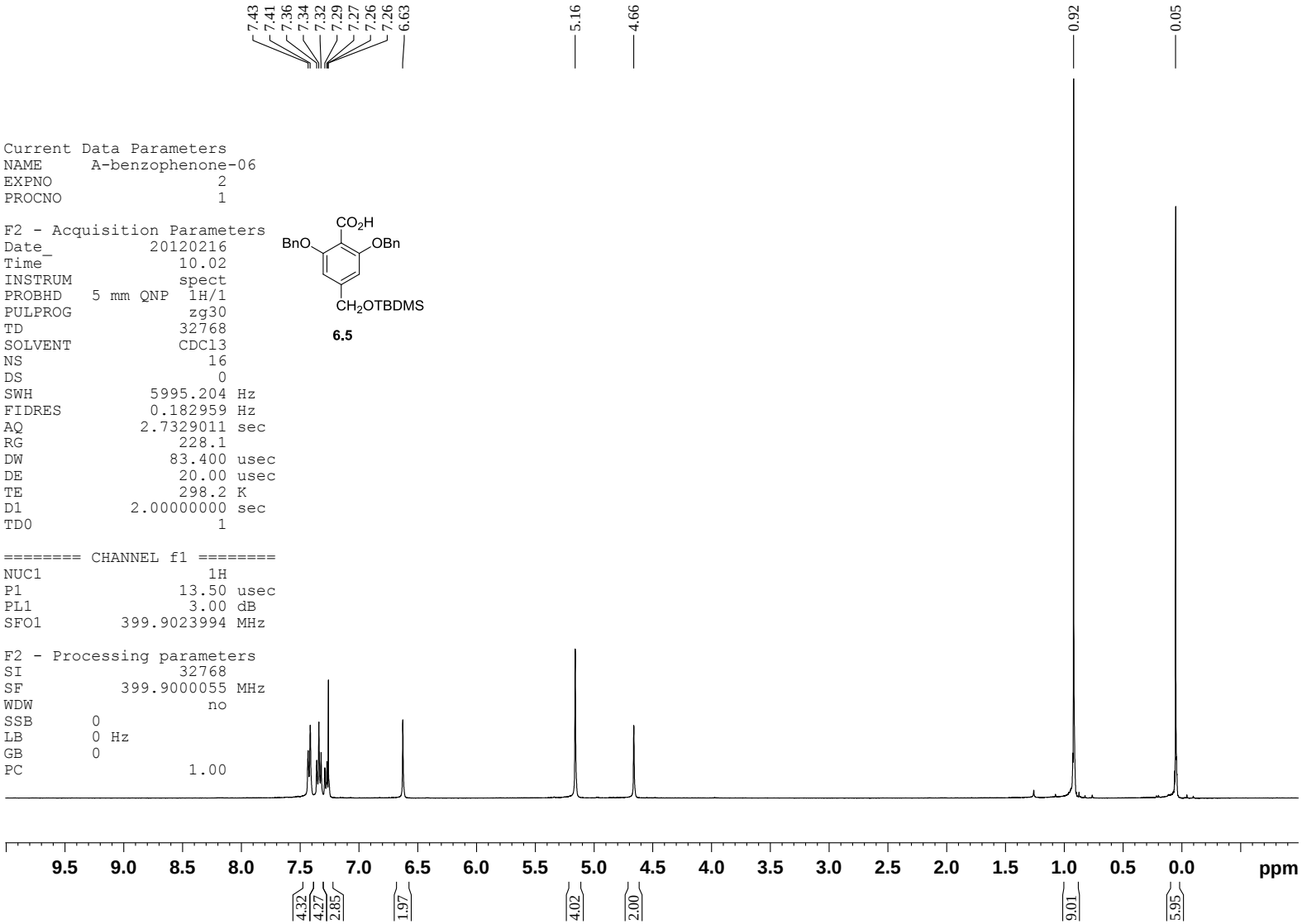

Current Data Parameters
NAME A-benzophenone-02_column_mod
EXPNO 2
PROCNO 1
F2 - Acquisition Parameters
Date_ 20120127
Time 11.00
INSTRUM spect
PROBHD 5 mm QNP 1H/1
PULPROG zgpg
TD 66560
SOLVENT CDCl3
NS 66
DS 2
SWH 25125.629 Hz
FIDRES 0.377488 Hz
AQ 1.3245940 sec
RG 2896.3
DW 19.900 usec
DE 20.00 usec
TE 298.2 K
D1 2.00000000 sec
d11 0.03000000 sec
DELTA 1.89999998 sec
TD0 1
======== CHANNEL f1 ========
NUC1 13C
P1 12.00 usec
PL1 -0.50 dB
SFO1 100.5659560 MHz
======== CHANNEL f2 ========
CPDPRG2 waltz16
NUC2 1H
PCPD2 80.00 usec
PL2 3.00 dB
PL12 18.80 dB
PL13 24.80 dB
SFO2 399.9015996 MHz
F2 - Processing parameters
SI 32768
SF 100.5549252 MHz
WDW EM
SSB 0
LB 1.00 Hz
GB 0
PC 1.40
165.51
155.84
156.37
136.29
135.93
130.12
128.77
128.72
128.49
128.29
128.17
127.71
127.25
107.58
77.48
77.16
76.84
71.23
67.18
Br
BnO
OBn
COOBn
6.2
190 180 170 160 150 140 130 120 110 100 90 80 70 60 50 40 30 20 10 ppm

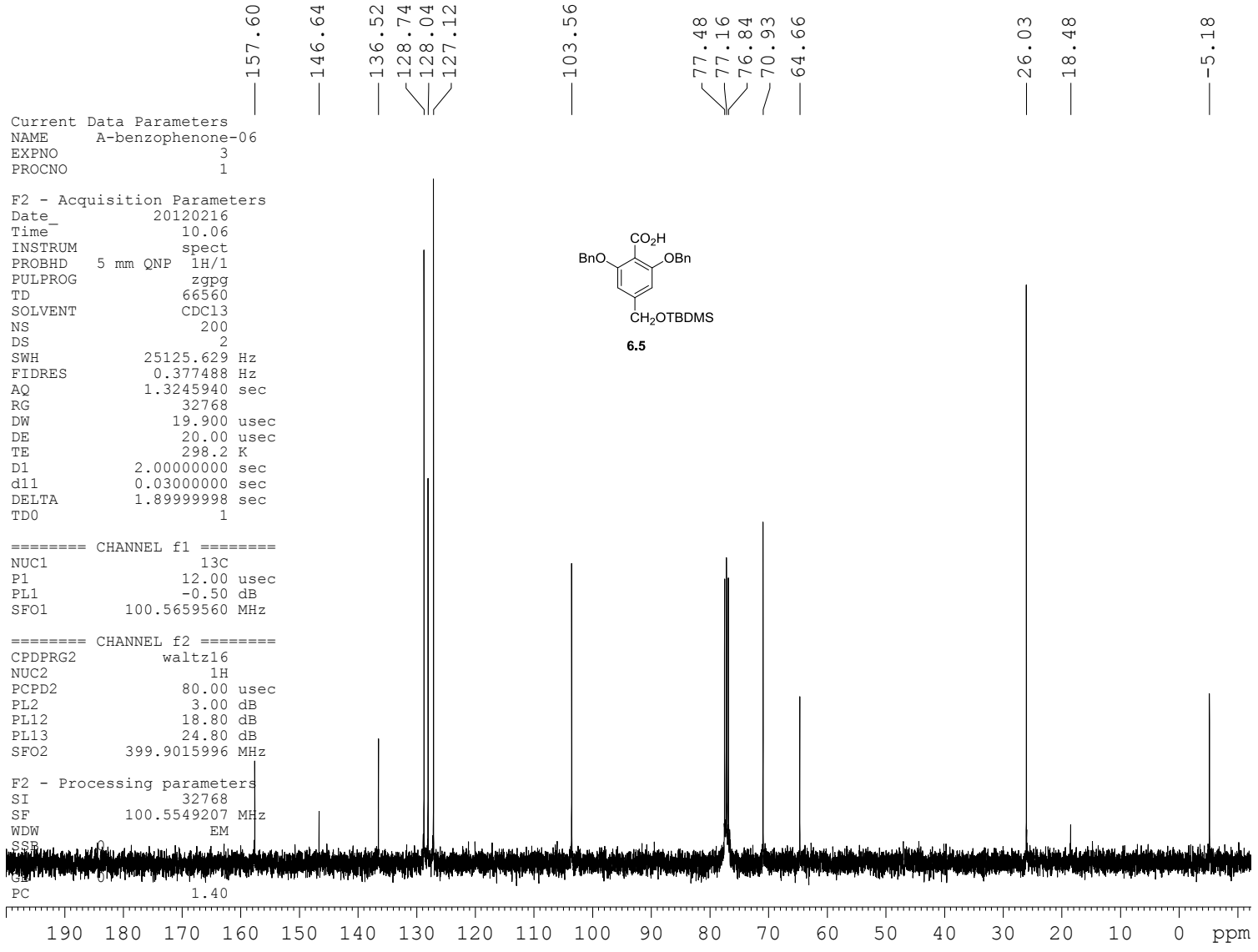

7.51
7.50
7.50
7.50
7.49
7.48
7.48
7.48
7.41
7.41
7.41
7.39
7.39
7.38
7.37
7.34
7.34
7.34
7.32
7.26
6.64
5.16
4.60
4.59
1.78
1.58
Br
BnO
OBn
CH2OH
6.3
Current Data Parameters
NAME A-benzophenone-04
EXPNO 2
PROCNO 1
F2 - Acquisition Parameters
Date_ 20120215
Time 7.28
INSTRUM spect
PROBHD 5 mm QNP 1H/1
PULPROG zg30
TD 32768
SOLVENT CDCl3
NS 16
DS 0
SWH 5995.204 Hz
FIDRES 0.182959 Hz
AQ 2.7329011 sec
RG 181
DW 83.400 usec
DE 20.00 usec
TE 298.2 K
D1 2.00000000 sec
TD0 1
======== CHANNEL f1 ========
NUC1 1H
P1 13.50 usec
PL1 3.00 dB
SFO1 399.9023994 MHz
F2 - Processing parameters
SI 32768
SF 399.9000054 MHz
WDW no
SSB 0
LB 0 Hz
GB 0
PC 1.00
9.5 9.0 8.5 8.0 7.5 7.0 6.5 6.0 5.5 5.0 4.5 4.0 3.5 3.0 2.5 2.0 1.5 1.0 0.5 ppm
4.00
3.94
1.86
1.99
4.00
1.98
0.96

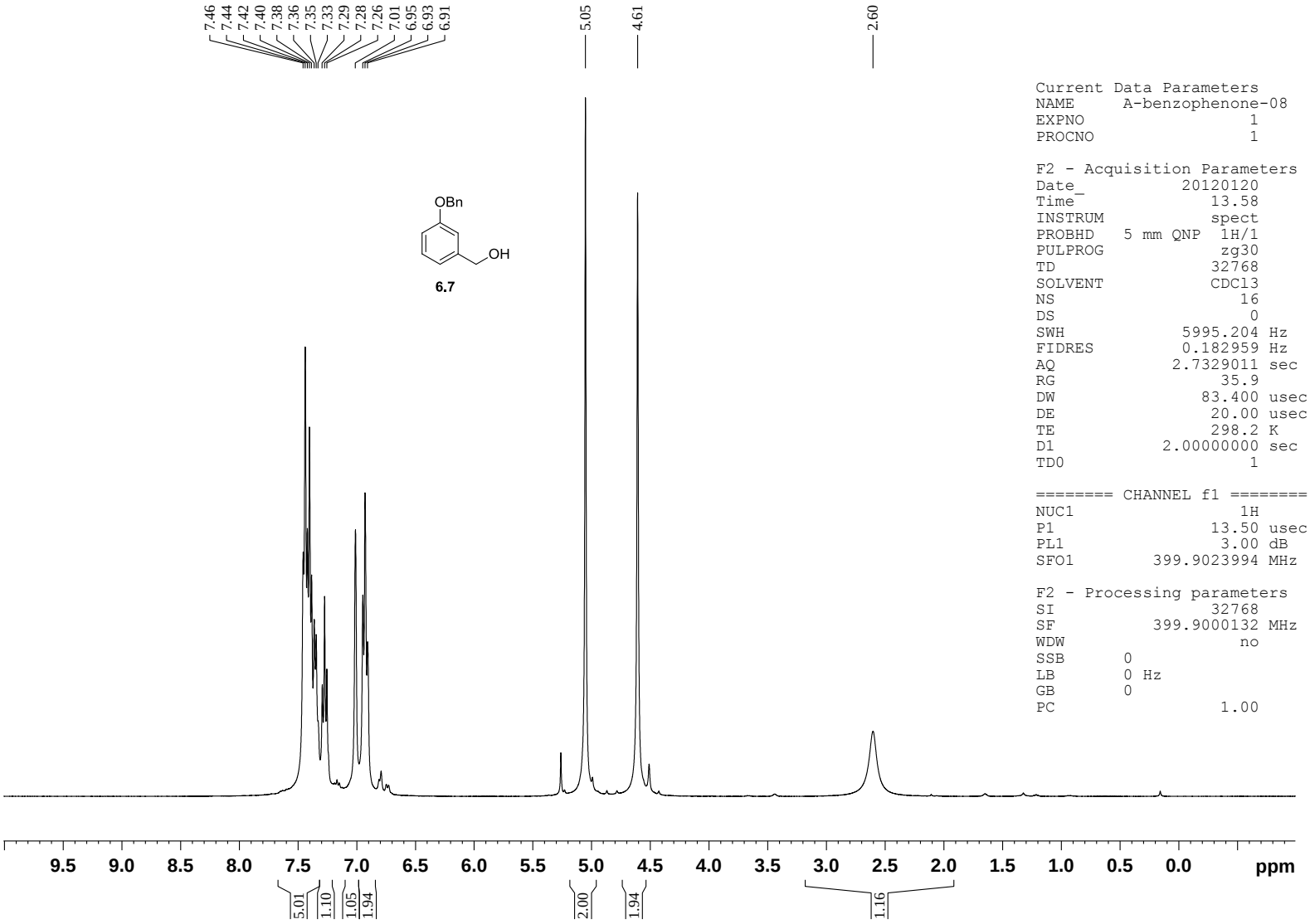

156.55
141.73
136.71
128.71
128.05
127.13
105.07
77.48
77.17
76.85
71.07
65.16
Current Data Parameters
NAME A-benzophenone-04
EXPNO 3
PROCNO 1
F2 - Acquisition Parameters
Date_ 20120215
Time 7.31
INSTRUM spect
PROBHD 5 mm QNP 1H/1
PULPROG zgpg
TD 66560
SOLVENT CDCl3
NS 145
DS 2
SWH 25125.629 Hz
FIDRES 0.377488 Hz
AQ 1.3245940 sec
RG 3649.1
DW 19.900 usec
DE 20.00 usec
TE 298.2 K
D1 2.00000000 sec
d11 0.03000000 sec
DELTA 1.89999998 sec
TD0 1
======== CHANNEL f1 ========
NUC1 13C
P1 12.00 usec
PL1 -0.50 dB
SFO1 100.5659560 MHz
======== CHANNEL f2 ========
CPDPRG2 waltz16
NUC2 1H
PCPD2 80.00 usec
PL2 3.00 dB
PL12 18.80 dB
PL13 24.80 dB
SFO2 399.9015996 MHz
F2 - Processing parameters
SI 32768
SF 100.5549219 MHz
WDW EM
SSB 0
GB 0
PC 1.40
Br
BnO
OBn
CH2OH
6.3
190 180 170 160 150 140 130 120 110 100 90 80 70 60 50 40 30 20 10 ppm

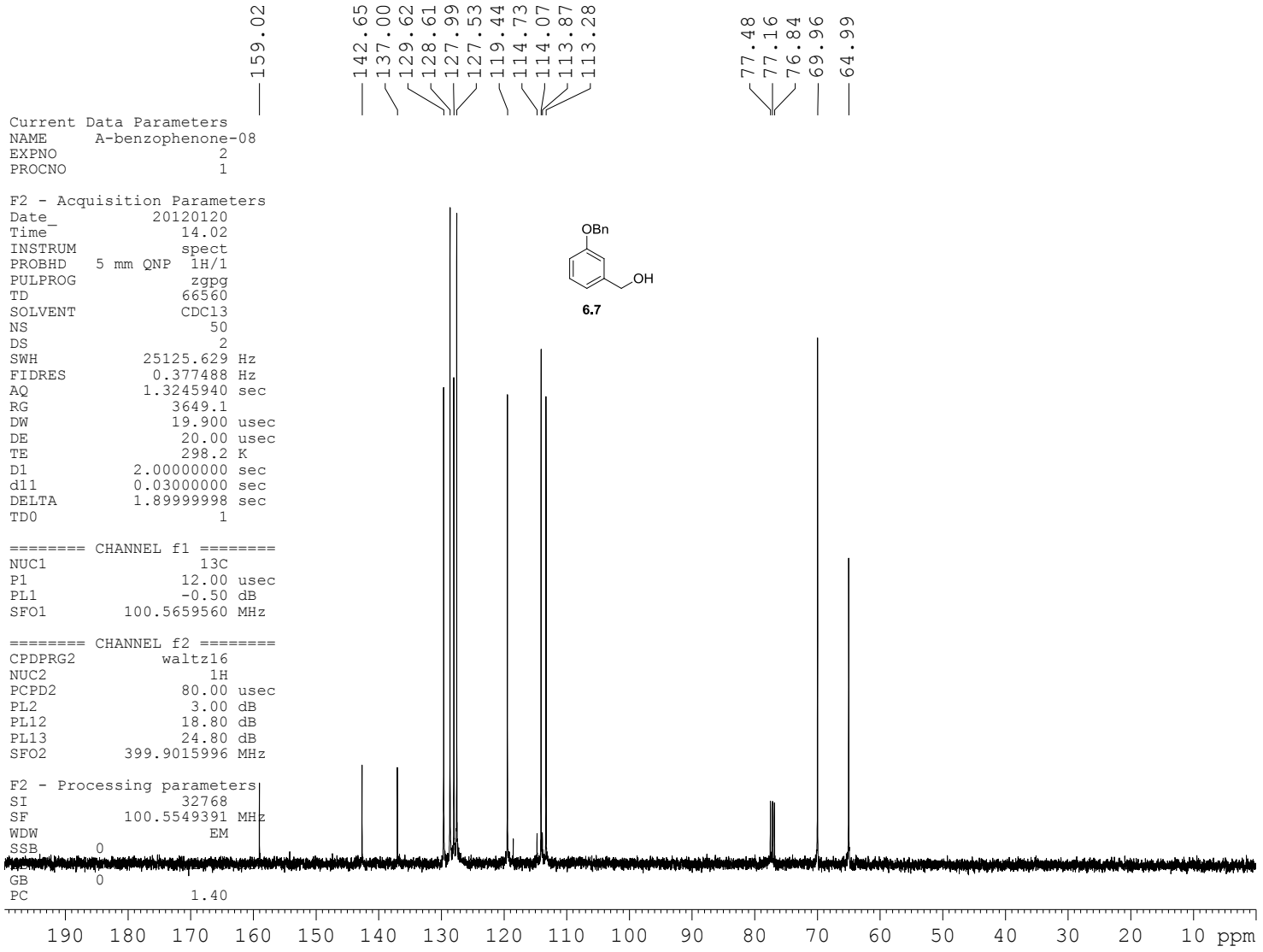

7.50
7.50
7.48
7.41
7.41
7.39
7.39
7.37
7.33
7.31
7.26
6.61
5.17
4.64
1.55
0.93
0.06
Current Data Parameters
NAME A-benzophenone-05
EXPNO 3
PROCNO 1
F2 - Acquisition Parameters
Date_ 20120217
Time 14.06
INSTRUM spect
PROBHD 5 mm QNP 1H/1
PULPROG zg30
TD 32768
SOLVENT CDC13
NS 16
DS 0
SWH 5995.204 Hz
FIDRES 0.182959 Hz
AQ 2.7329011 sec
RG 181
DW 83.400 usec
DE 20.00 usec
TE 298.2 K
D1 2.00000000 sec
TD0 1
======== CHANNEL f1 ========
NUC1 1H
P1 13.50 usec
PL1 3.00 dB
SFO1 399.9023994 MHz
F2 - Processing parameters
SI 32768
SF 399.9000055 MHz
WDW no
SSB 0
LB 0 Hz
GB 0
PC 1.00
Br
BnO
OBn
CH2OTBDMS
6.4
9.5 9.0 8.5 8.0 7.5 7.0 6.5 6.0 5.5 5.0 4.5 4.0 3.5 3.0 2.5 2.0 1.5 1.0 0.5 0.0 ppm
3.91
4.51
2.01
2.09
4.00
2.00
9.40
6.00

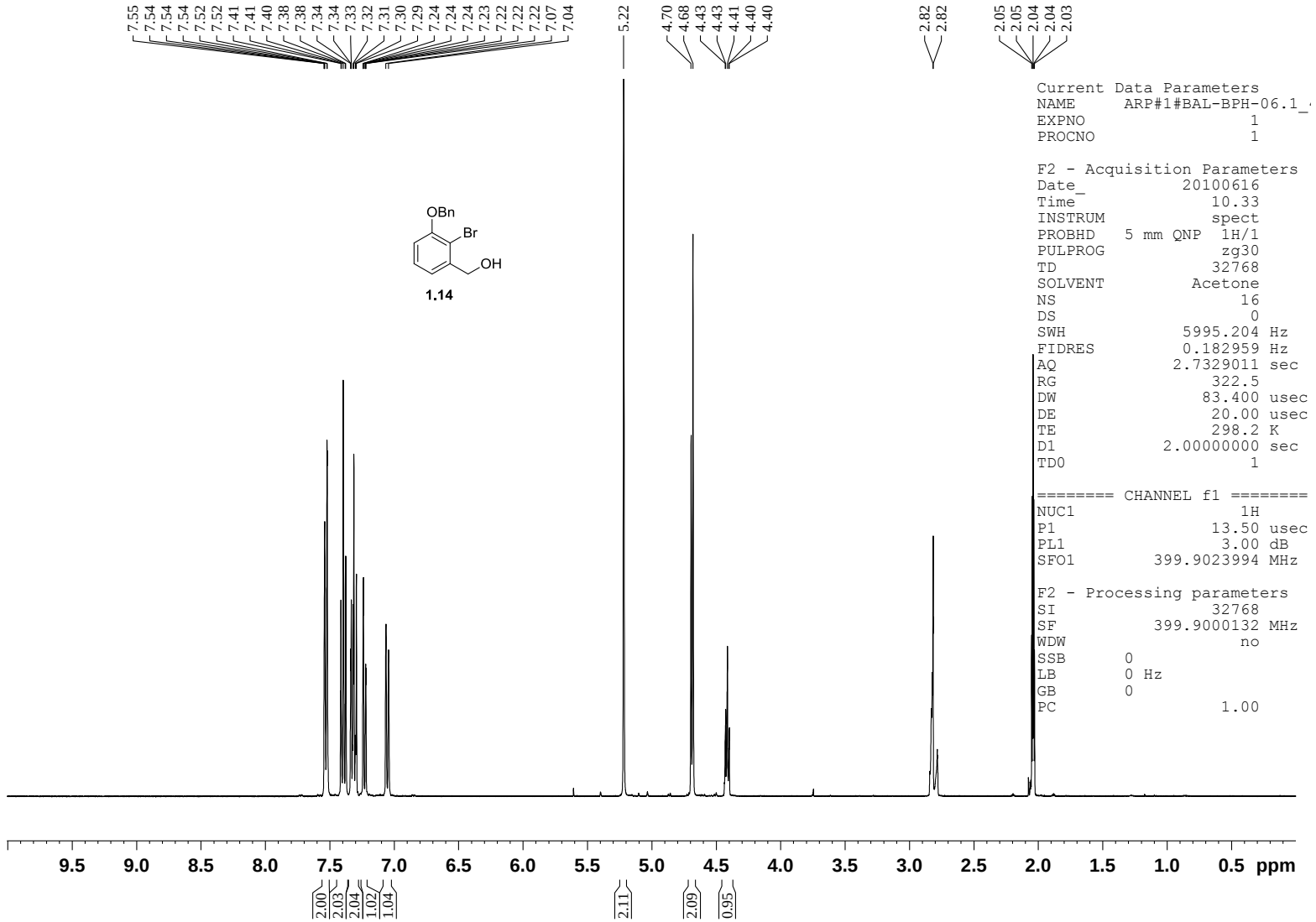

170.53
156.33
142.40
136.86
128.70
127.98
127.09
104.39
77.48
77.16
76.85
70.99
64.75
26.06
18.50
-5.14
Current Data Parameters
NAME A-benzophenone-05
EXPNO 4
PROCNO 1
F2 - Acquisition Parameters
Date_ 20120217
Time 14.12
INSTRUM spect
PROBHD 5 mm QNP 1H/1
PULPROG zgpg
TD 66560
SOLVENT CDCl3
NS 185
DS 2
SWH 25125.629 Hz
FIDRES 0.377488 Hz
AQ 1.3245940 sec
RG 3649.1
DW 19.900 usec
DE 20.00 usec
TE 298.2 K
D1 2.00000000 sec
d11 0.03000000 sec
DELTA 1.89999998 sec
TD0 1
======== CHANNEL f1 ========
NUC1 13C
P1 12.00 usec
PL1 -0.50 dB
SFO1 100.5659560 MHz
======== CHANNEL f2 ========
CPDPRG2 waltz16
NUC2 1H
PCPD2 80.00 usec
PL2 3.00 dB
PL12 18.80 dB
PL13 24.80 dB
SFO2 399.9015996 MHz
F2 - Processing parameters
SI 32768
SF 100.5549212 MHz
WDW EM
SSB 0
LB 0
GB 0
PC 1.40
Br
BnO
OBn
CH2OTBDMS
6.4
190 180 170 160 150 140 130 120 110 100 90 80 70 60 50 40 30 20 10 0 ppm

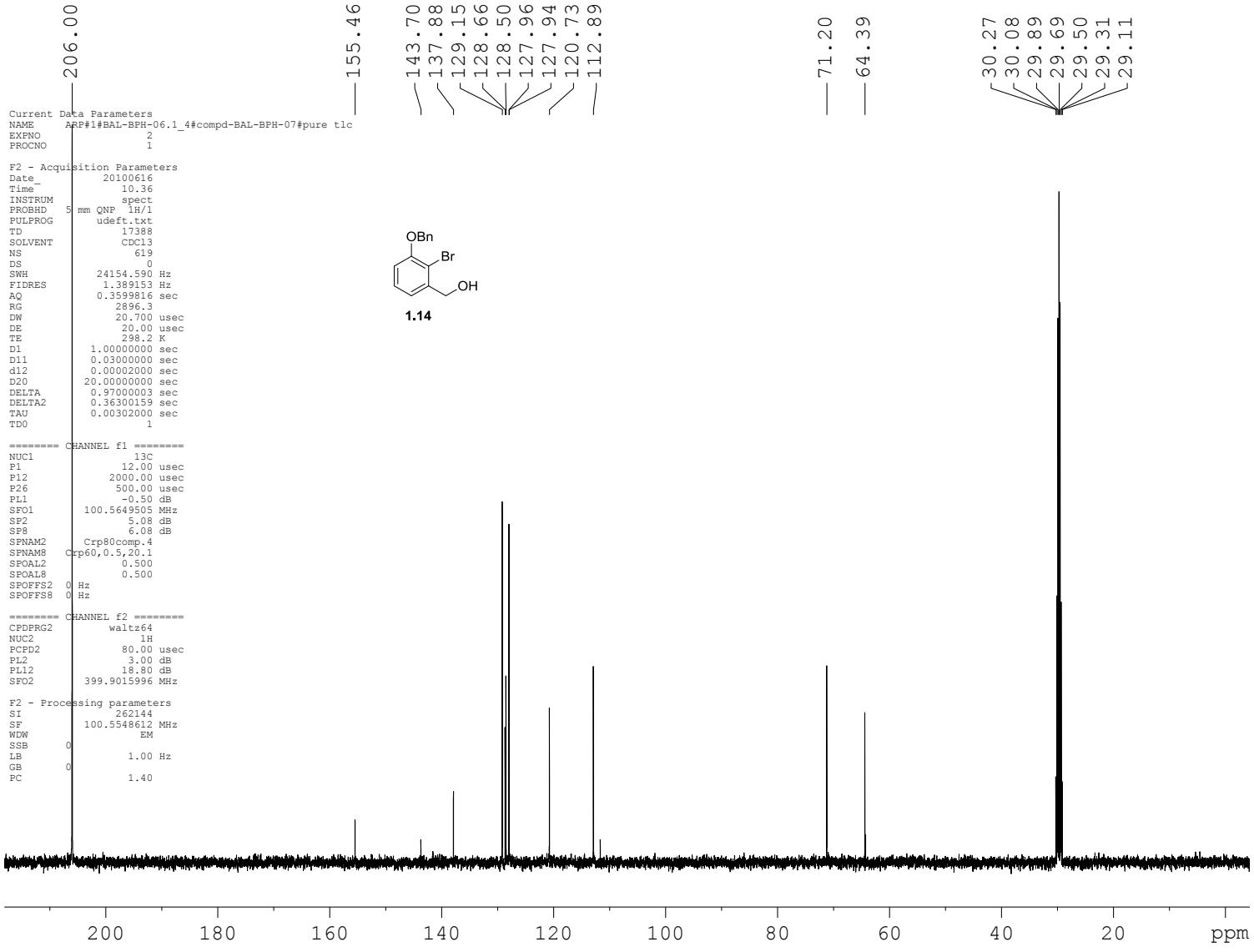

7.43
7.41
7.36
7.34
7.32
7.29
7.27
7.26
7.26
6.63
5.16
4.66
0.92
0.05
Current Data Parameters
NAME A-benzophenone-06
EXPNO 2
PROCNO 1
F2 - Acquisition Parameters
Date_ 20120216
Time 10.02
INSTRUM spect
PROBHD 5 mm QNP 1H/1
PULPROG zg30
TD 32768
SOLVENT CDCl3
NS 16
DS 0
SWH 5995.204 Hz
FIDRES 0.182959 Hz
AQ 2.7329011 sec
RG 228.1
DW 83.400 usec
DE 20.00 usec
TE 298.2 K
D1 2.00000000 sec
TD0 1
======== CHANNEL f1 ========
NUC1 1H
P1 13.50 usec
PL1 3.00 dB
SFO1 399.9023994 MHz
F2 - Processing parameters
SI 32768
SF 399.9000055 MHz
WDW no
SSB 0
LB 0 Hz
GB 0
PC 1.00
CO2H
BnO
OBn
CH2OTBDMS
6.5
9.5
9.0
8.5
8.0
7.5
7.0
6.5
6.0
5.5
5.0
4.5
4.0
3.5
3.0
2.5
2.0
1.5
1.0
0.5
0.0
ppm
4.32
4.27
2.85
1.97
4.02
2.00
9.01
5.95


157.60
146.64
136.52
128.74
128.04
127.12
103.56
77.48
77.16
76.84
70.93
64.66
26.03
18.48
-5.18
Current Data Parameters
NAME A-benzophenone-06
EXPNO 3
PROCNO 1
F2 - Acquisition Parameters
Date_ 20120216
Time 10.06
INSTRUM spect
PROBHD 5 mm QNP 1H/1
PULPROG zgpg
TD 66560
SOLVENT CDCl3
NS 200
DS 2
SWH 25125.629 Hz
FIDRES 0.377488 Hz
AQ 1.3245940 sec
RG 32768
DW 19.900 usec
DE 20.00 usec
TE 298.2 K
D1 2.00000000 sec
d11 0.03000000 sec
DELTA 1.89999998 sec
TD0 1
======== CHANNEL f1 ========
NUC1 13C
P1 12.00 usec
PL1 -0.50 dB
SFO1 100.5659560 MHz
======== CHANNEL f2 ========
CPDPRG2 waltz16
NUC2 1H
PCPD2 80.00 usec
PL2 3.00 dB
PL12 18.80 dB
PL13 24.80 dB
SFO2 399.9015996 MHz
F2 - Processing parameters
SI 32768
SF 100.5549207 MHz
WDW EM
SSB 0
GB 0
PC 1.40
CO2H
BnO
OBn
CH2OTBDMS
6.5
190 180 170 160 150 140 130 120 110 100 90 80 70 60 50 40 30 20 10 0 ppm


7.46
7.44
7.42
7.40
7.38
7.36
7.35
7.33
7.29
7.28
7.26
7.01
6.95
6.93
6.91
5.05
4.61
2.60
OBn
OH
6.7
Current Data Parameters
NAME A-benzophenone-08
EXPNO 1
PROCNO 1
F2 - Acquisition Parameters
Date_ 20120120
Time 13.58
INSTRUM spect
PROBHD 5 mm QNP 1H/1
PULPROG zg30
TD 32768
SOLVENT CDCl3
NS 16
DS 0
SWH 5995.204 Hz
FIDRES 0.182959 Hz
AQ 2.7329011 sec
RG 35.9
DW 83.400 usec
DE 20.00 usec
TE 298.2 K
D1 2.00000000 sec
TD0 1
======== CHANNEL f1 ========
NUC1 1H
P1 13.50 usec
PL1 3.00 dB
SFO1 399.9023994 MHz
F2 - Processing parameters
SI 32768
SF 399.9000132 MHz
WDW no
SSB 0
LB 0 Hz
GB 0
PC 1.00
9.5 9.0 8.5 8.0 7.5 7.0 6.5 6.0 5.5 5.0 4.5 4.0 3.5 3.0 2.5 2.0 1.5 1.0 0.5 0.0 ppm
5.01
1.10
1.05
1.94
2.00
1.94
1.16


159.02
142.65
137.00
129.62
128.61
127.99
127.53
119.44
114.73
114.07
113.87
113.28
77.48
77.16
76.84
69.96
64.99
OBn
OH
6.7
Current Data Parameters
NAME A-benzophenone-08
EXPNO 2
PROCNO 1
F2 - Acquisition Parameters
Date_ 20120120
Time 14.02
INSTRUM spect
PROBHD 5 mm QNP 1H/1
PULPROG zgpg
TD 66560
SOLVENT CDCl3
NS 50
DS 2
SWH 25125.629 Hz
FIDRES 0.377488 Hz
AQ 1.3245940 sec
RG 3649.1
DW 19.900 usec
DE 20.00 usec
TE 298.2 K
D1 2.00000000 sec
d11 0.03000000 sec
DELTA 1.89999998 sec
TD0 1
======== CHANNEL f1 ========
NUC1 13C
P1 12.00 usec
PL1 -0.50 dB
SFO1 100.5659560 MHz
======== CHANNEL f2 ========
CPDPRG2 waltz16
NUC2 1H
PCPD2 80.00 usec
PL2 3.00 dB
PL12 18.80 dB
PL13 24.80 dB
SFO2 399.9015996 MHz
F2 - Processing parameters
SI 32768
SF 100.5549391 MHz
WDW EM
SSB 0
GB 0
PC 1.40
190 180 170 160 150 140 130 120 110 100 90 80 70 60 50 40 30 20 10 ppm


7.55 7.54 7.54 7.54 7.52 7.52 7.41 7.41 7.40 7.38 7.38 7.34 7.34 7.33 7.32 7.31 7.30 7.29 7.24 7.24 7.24 7.23 7.22 7.22 7.22 7.07 7.04
5.22
4.70 4.68 4.43 4.43 4.41 4.40 4.40
2.82 2.82
2.05 2.05 2.04 2.04 2.03
OBn
Br
OH
1.14
Current Data Parameters
NAME ARP#1#BAL-BPH-06.1_
EXPNO 1
PROCNO 1
F2 - Acquisition Parameters
Date_ 20100616
Time 10.33
INSTRUM spect
PROBHD 5 mm QNP 1H/1
PULPROG zg30
TD 32768
SOLVENT Acetone
NS 16
DS 0
SWH 5995.204 Hz
FIDRES 0.182959 Hz
AQ 2.7329011 sec
RG 322.5
DW 83.400 usec
DE 20.00 usec
TE 298.2 K
D1 2.00000000 sec
TD0 1
======== CHANNEL f1 ========
NUC1 1H
P1 13.50 usec
PL1 3.00 dB
SFO1 399.9023994 MHz
F2 - Processing parameters
SI 32768
SF 399.9000132 MHz
WDW no
SSB 0
LB 0 Hz
GB 0
PC 1.00
9.5 9.0 8.5 8.0 7.5 7.0 6.5 6.0 5.5 5.0 4.5 4.0 3.5 3.0 2.5 2.0 1.5 1.0 0.5 ppm
2.00 2.03 2.04 1.02 1.04
2.11
2.09
0.95



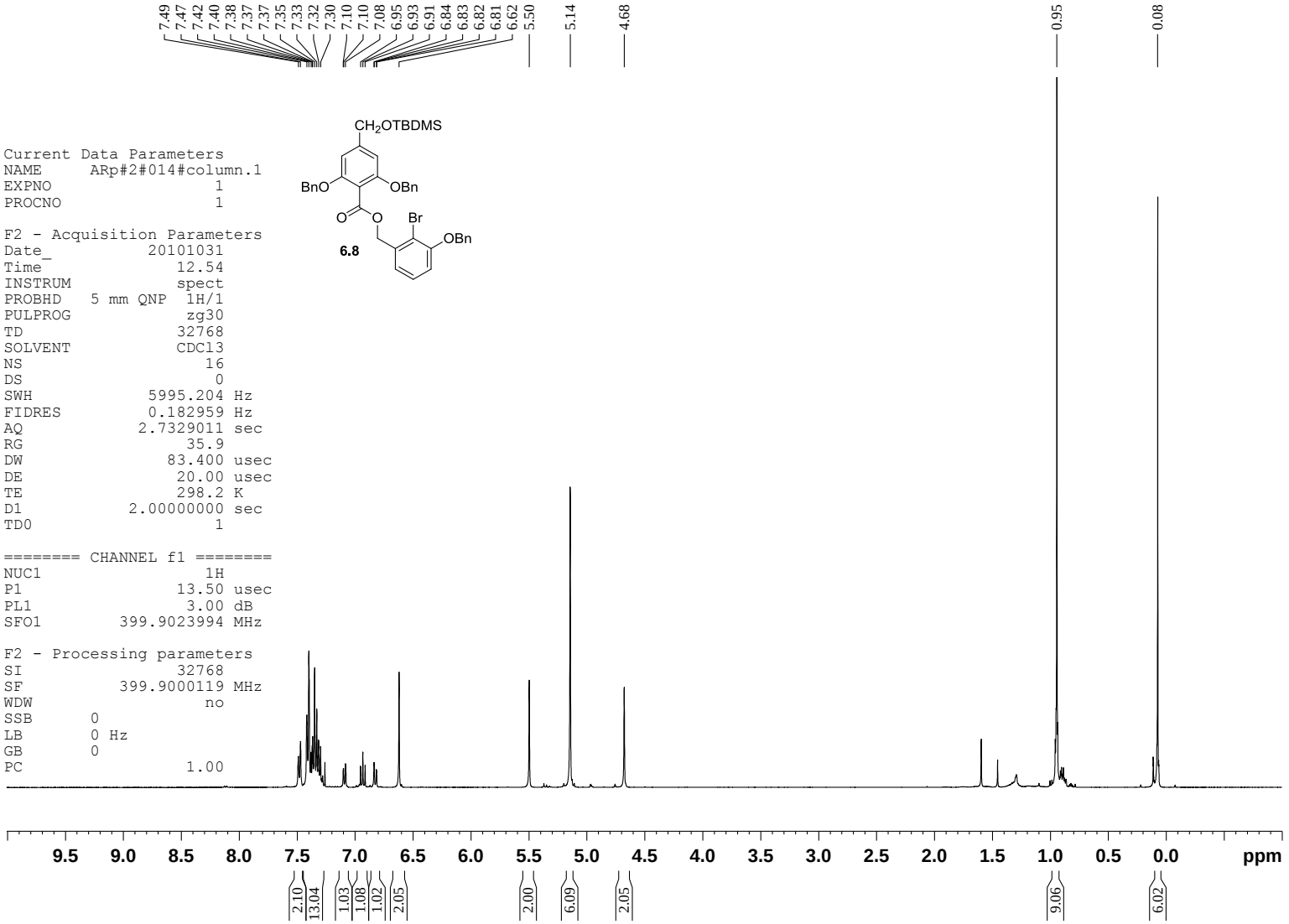

```
Current Data Parameters
NAME     AAP#1#BAL-BPH-06.1_4#compd-BAL-BPH-07#pure tlc
EXPNO                 2
PROCNO                1

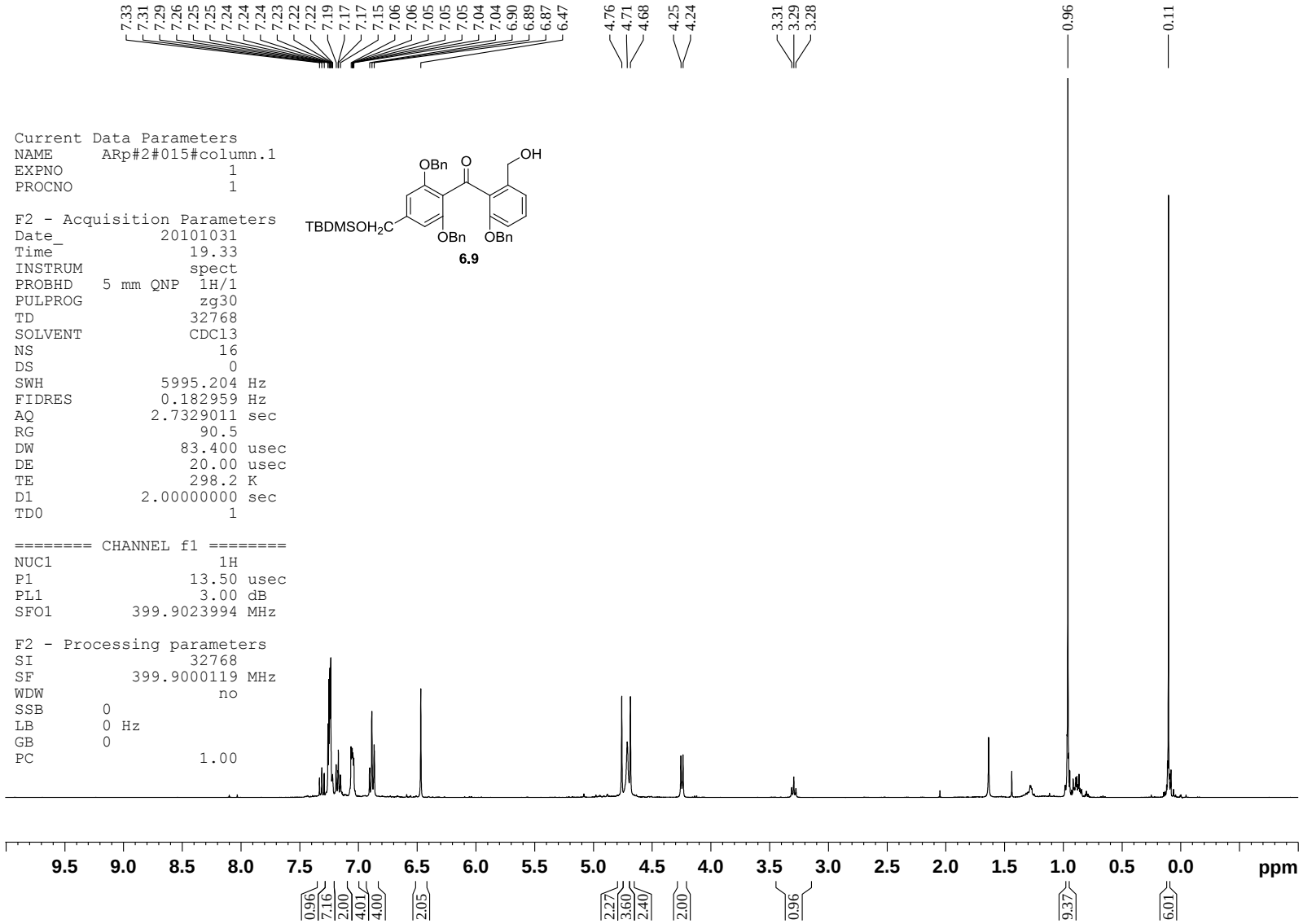
F2 - Acquisition Parameters
Date_              20100616
Time                 10.36
INSTRUM              spect
PROBHD   5 mm QNP  1H/1
PULPROG          udeft.txt
TD                   17388
SOLVENT              CDCl3
NS                     619
DS                       0
SWH              24154.590 Hz
FIDRES               1.389153 Hz
AQ               0.3599816 sec
RG                    2896.3
DW                   20.700 usec
DE                   20.00 usec
TE                   298.2 K
D1                1.00000000 sec
D11               0.03000000 sec
d12               0.00002000 sec
D20              20.00000000 sec
DELTA             0.97000003 sec
DELTA2            0.36300159 sec
TAU               0.00302000 sec
TD0                      1

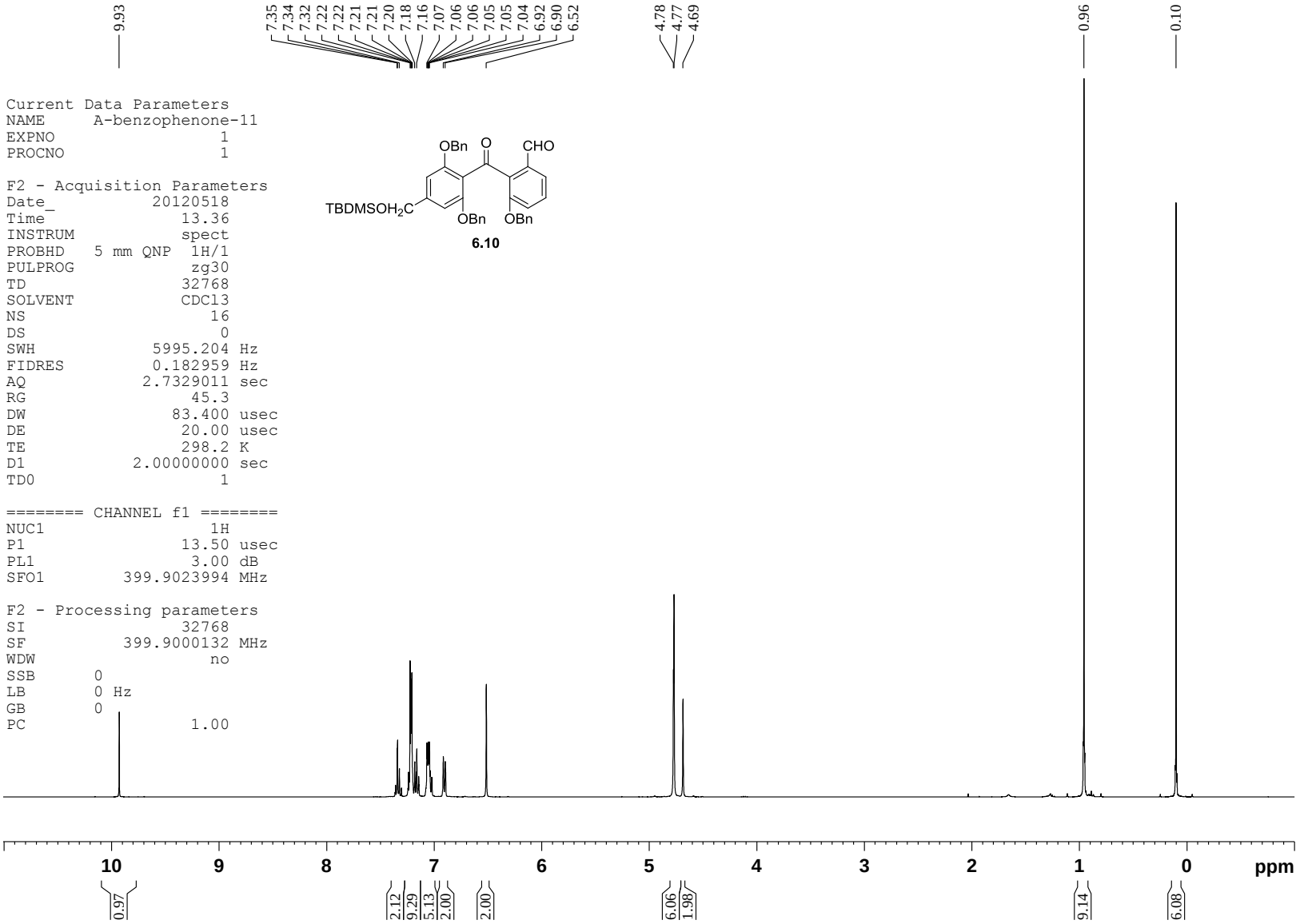
======== CHANNEL f1 ========
NUC1                   13C
P1                   12.00 usec
P12                2000.00 usec
P26                 500.00 usec
PL1                  -0.50 dB
SFO1            100.5649505 MHz
SP2                   5.08 dB
SP8                   6.08 dB
SPNAM2         Crp80comp.4
SPNAM8      Crp60,0.5,20.1
SPOAL2                0.500
SPOAL8                0.500
SPOFFS2  0 Hz
SPOFFS8  0 Hz

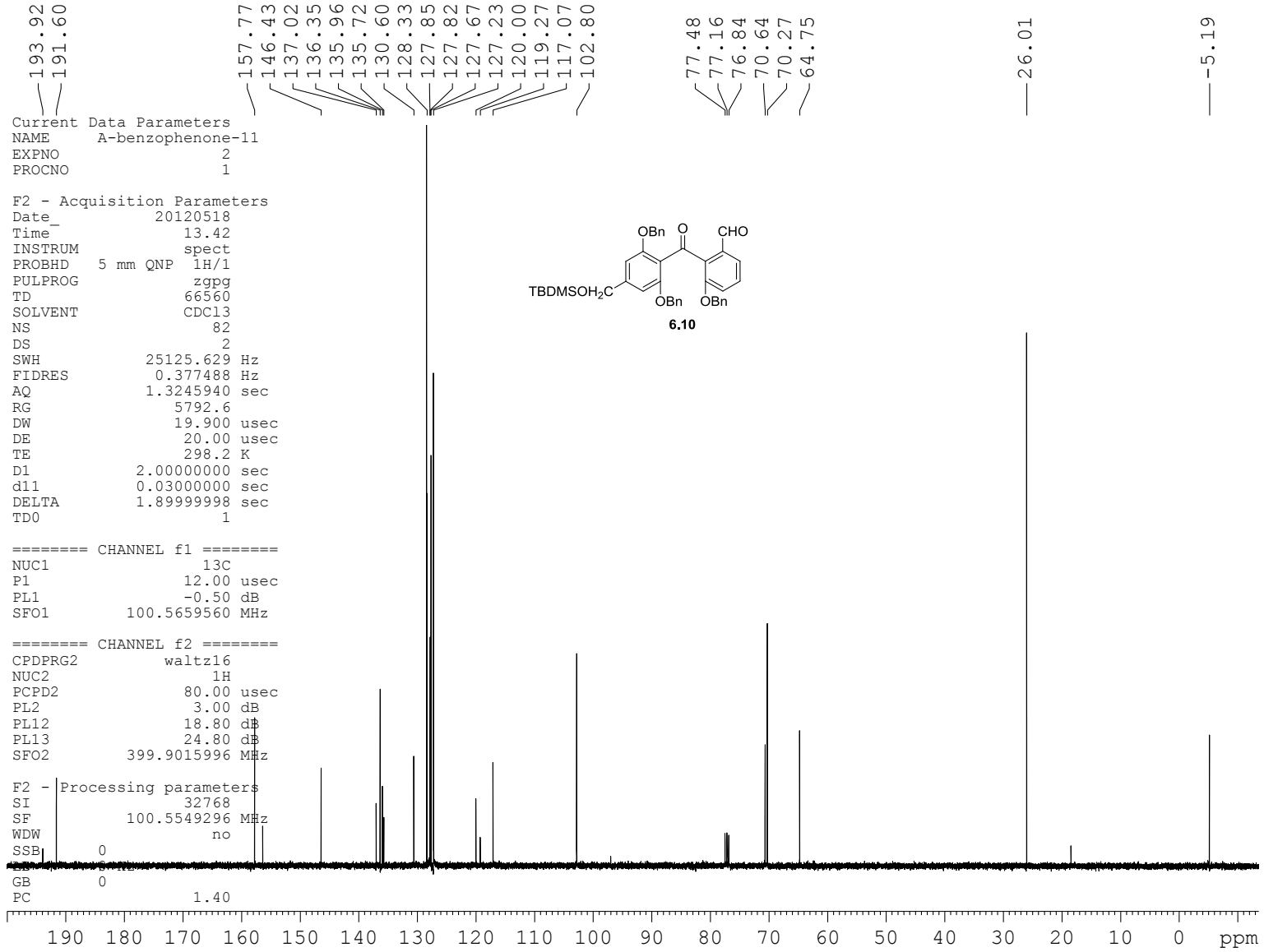
======== CHANNEL f2 ========
CPDPRG2             waltz64
NUC2                   1H
PCPD2                80.00 usec
PL2                   3.00 dB
PL12                 18.80 dB
SFO2            399.9015996 MHz

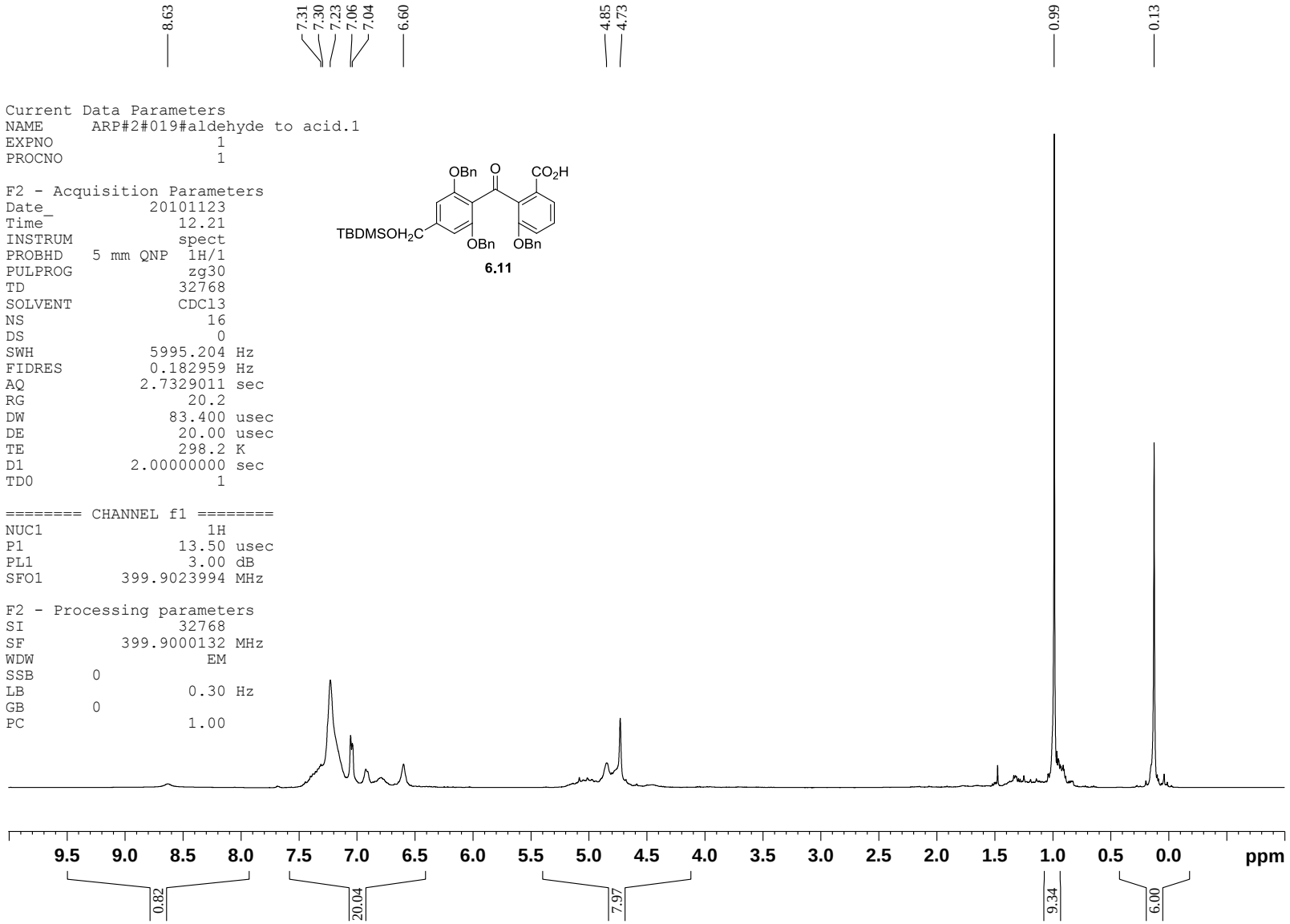
F2 - Processing parameters
SI                   262144
SF              100.5548612 MHz
WDW                    EM
SSB      0
LB                    1.00 Hz
GB       0
PC                    1.40
```

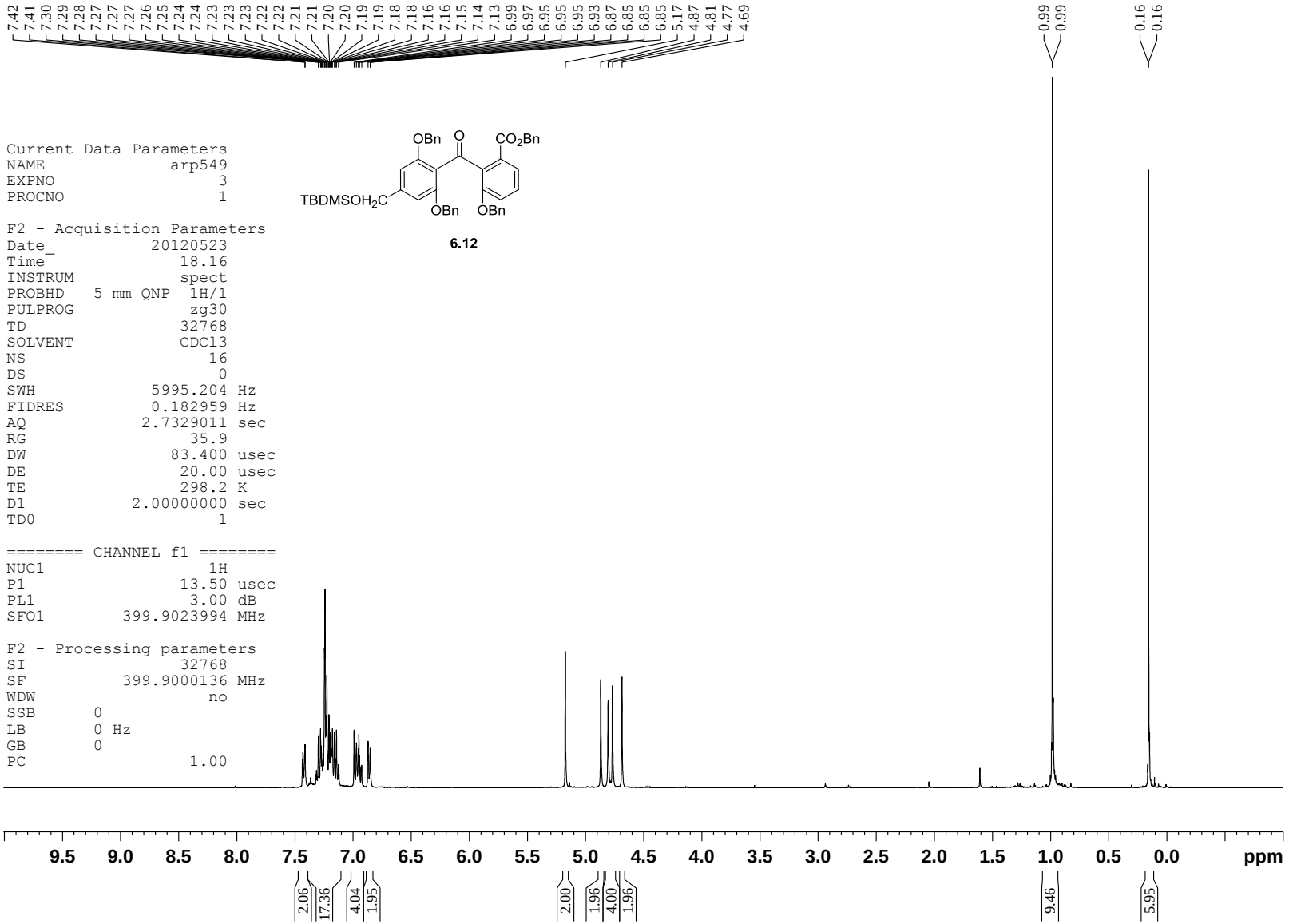

7.49
7.47
7.42
7.40
7.38
7.37
7.37
7.35
7.33
7.32
7.30
7.10
7.10
7.08
6.95
6.93
6.91
6.84
6.83
6.82
6.81
6.62
5.50
5.14
4.68
0.95
0.08
CH2OTBDMS
BnO
OBn
O
O
Br
OBn
6.8
Current Data Parameters
NAME ARp#2#014#column.1
EXPNO 1
PROCNO 1
F2 - Acquisition Parameters
Date_ 20101031
Time 12.54
INSTRUM spect
PROBHD 5 mm QNP 1H/1
PULPROG zg30
TD 32768
SOLVENT CDCl3
NS 16
DS 0
SWH 5995.204 Hz
FIDRES 0.182959 Hz
AQ 2.7329011 sec
RG 35.9
DW 83.400 usec
DE 20.00 usec
TE 298.2 K
D1 2.00000000 sec
TD0 1
======== CHANNEL f1 ========
NUC1 1H
P1 13.50 usec
PL1 3.00 dB
SFO1 399.9023994 MHz
F2 - Processing parameters
SI 32768
SF 399.9000119 MHz
WDW no
SSB 0
LB 0 Hz
GB 0
PC 1.00
9.5
9.0
8.5
8.0
7.5
7.0
6.5
6.0
5.5
5.0
4.5
4.0
3.5
3.0
2.5
2.0
1.5
1.0
0.5
0.0
ppm
2.10
13.04
1.03
1.08
1.02
2.05
2.00
6.09
2.05
9.06
6.02

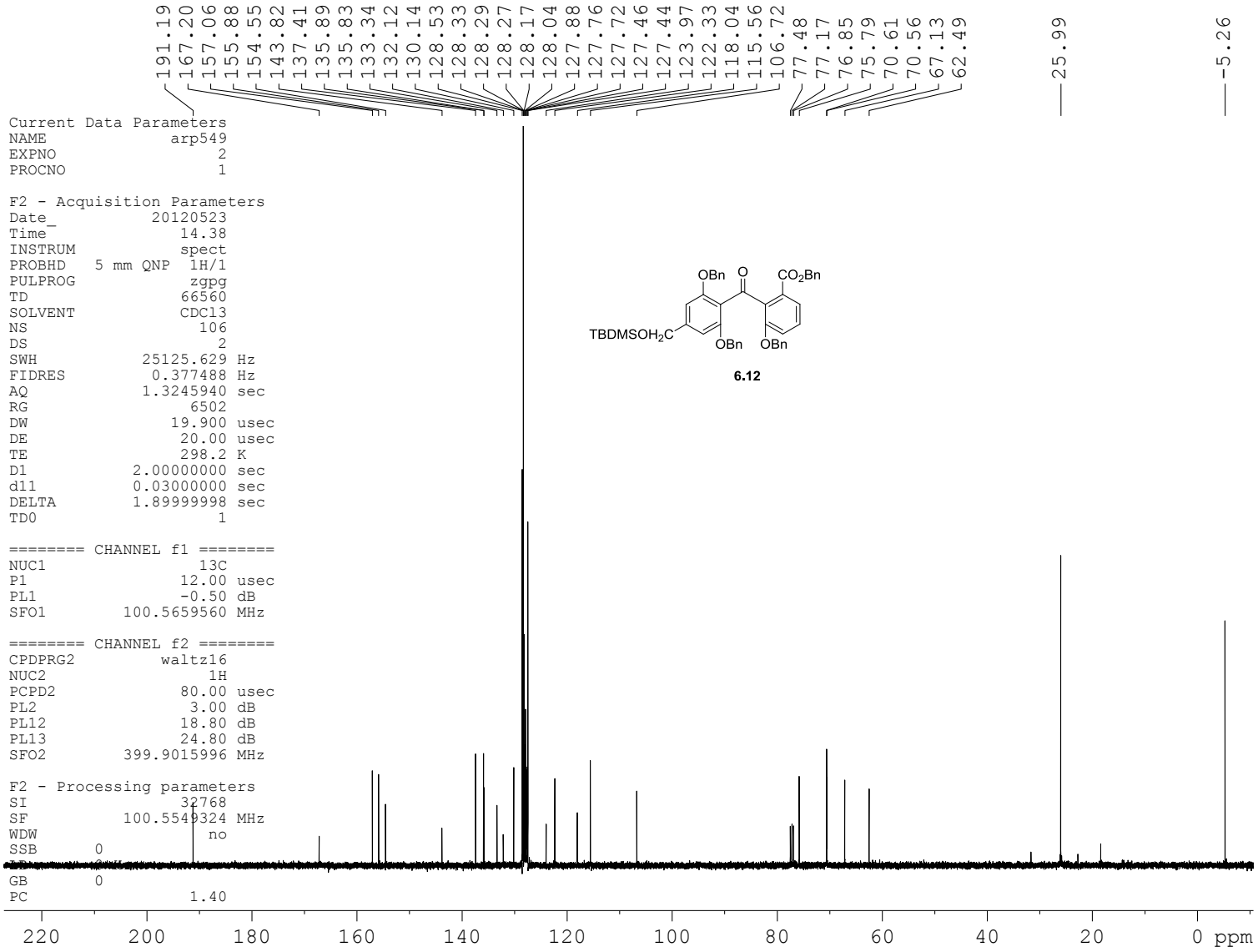

7.33
7.31
7.29
7.26
7.25
7.25
7.24
7.24
7.24
7.23
7.22
7.22
7.19
7.17
7.17
7.15
7.06
7.06
7.05
7.05
7.05
7.04
7.04
6.90
6.89
6.87
6.47
4.76
4.71
4.68
4.25
4.24
3.31
3.29
3.28
0.96
0.11
Current Data Parameters
NAME ARp#2#015#column.1
EXPNO 1
PROCNO 1
F2 - Acquisition Parameters
Date_ 20101031
Time 19.33
INSTRUM spect
PROBHD 5 mm QNP 1H/1
PULPROG zg30
TD 32768
SOLVENT CDCl3
NS 16
DS 0
SWH 5995.204 Hz
FIDRES 0.182959 Hz
AQ 2.7329011 sec
RG 90.5
DW 83.400 usec
DE 20.00 usec
TE 298.2 K
D1 2.00000000 sec
TD0 1
======== CHANNEL f1 ========
NUC1 1H
P1 13.50 usec
PL1 3.00 dB
SFO1 399.9023994 MHz
F2 - Processing parameters
SI 32768
SF 399.9000119 MHz
WDW no
SSB 0
LB 0 Hz
GB 0
PC 1.00
OBn
O
OH
TBDMSOH2C
OBn
OBn
6.9
9.5
9.0
8.5
8.0
7.5
7.0
6.5
6.0
5.5
5.0
4.5
4.0
3.5
3.0
2.5
2.0
1.5
1.0
0.5
0.0
ppm
0.96
7.16
2.00
4.01
4.00
2.05
2.27
3.60
2.40
2.00
0.96
9.37
6.01

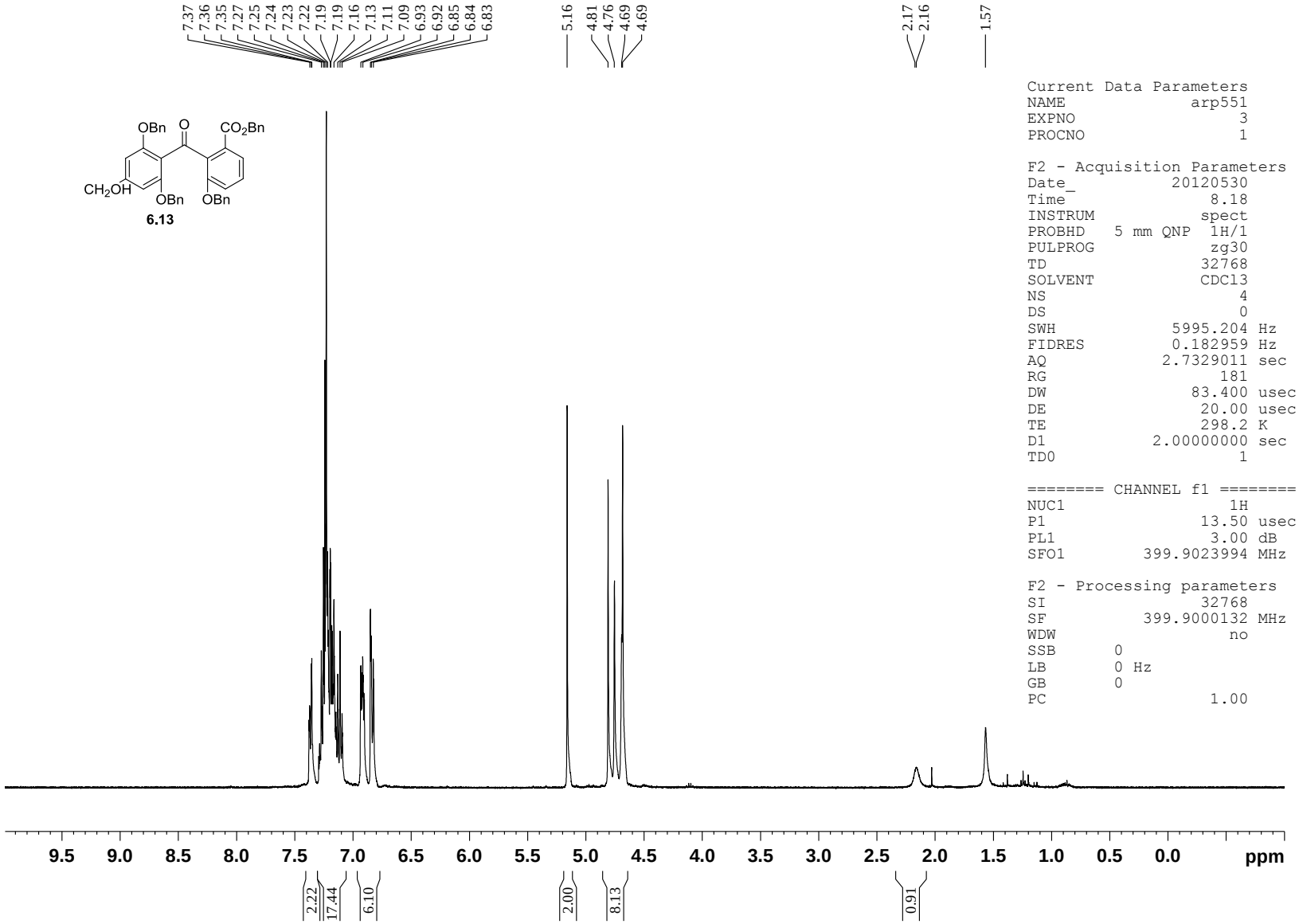

9.93
7.35
7.34
7.32
7.22
7.22
7.21
7.21
7.20
7.18
7.16
7.07
7.06
7.06
7.05
7.05
7.04
6.92
6.90
6.52
4.78
4.77
4.69
0.96
0.10
Current Data Parameters
NAME A-benzophenone-11
EXPNO 1
PROCNO 1
F2 - Acquisition Parameters
Date_ 20120518
Time 13.36
INSTRUM spect
PROBHD 5 mm QNP 1H/1
PULPROG zg30
TD 32768
SOLVENT CDCl3
NS 16
DS 0
SWH 5995.204 Hz
FIDRES 0.182959 Hz
AQ 2.7329011 sec
RG 45.3
DW 83.400 usec
DE 20.00 usec
TE 298.2 K
D1 2.00000000 sec
TD0 1
======== CHANNEL f1 ========
NUC1 1H
P1 13.50 usec
PL1 3.00 dB
SFO1 399.9023994 MHz
F2 - Processing parameters
SI 32768
SF 399.9000132 MHz
WDW no
SSB 0
LB 0 Hz
GB 0
PC 1.00
OBn
O
CHO
TBDMSOH2C
OBn
OBn
6.10
10
9
8
7
6
5
4
3
2
1
0
ppm
0.97
2.12
9.29
5.13
2.00
2.00
6.06
1.98
9.14
6.08

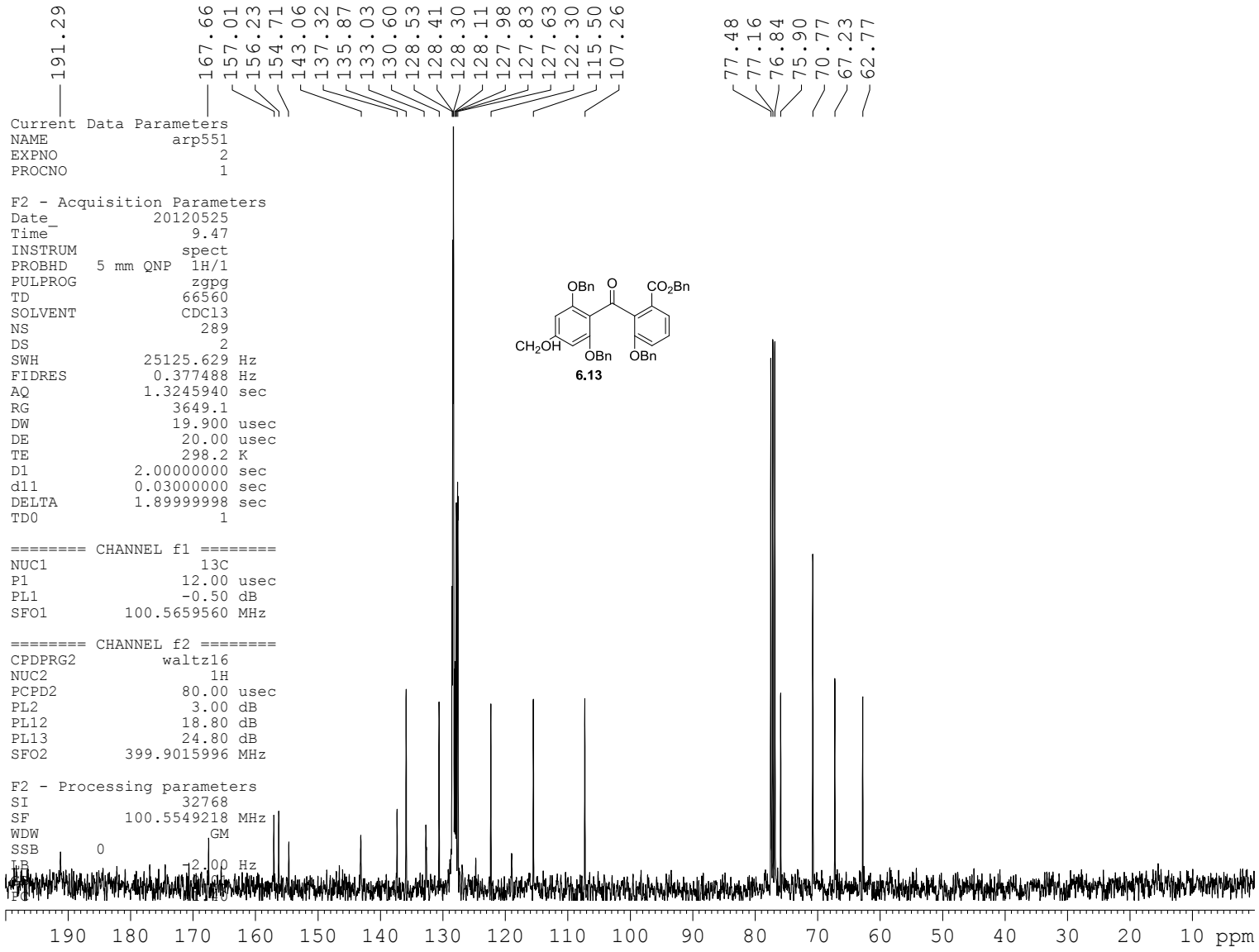

193.92
191.60
157.77
146.43
137.02
136.35
135.96
135.72
130.60
128.33
127.85
127.82
127.67
127.23
120.00
119.27
117.07
102.80
77.48
77.16
76.84
70.64
70.27
64.75
26.01
-5.19
Current Data Parameters
NAME A-benzophenone-11
EXPNO 2
PROCNO 1
F2 - Acquisition Parameters
Date_ 20120518
Time 13.42
INSTRUM spect
PROBHD 5 mm QNP 1H/1
PULPROG zgpg
TD 66560
SOLVENT CDCl3
NS 82
DS 2
SWH 25125.629 Hz
FIDRES 0.377488 Hz
AQ 1.3245940 sec
RG 5792.6
DW 19.900 usec
DE 20.00 usec
TE 298.2 K
D1 2.00000000 sec
d11 0.03000000 sec
DELTA 1.89999998 sec
TD0 1
======== CHANNEL f1 ========
NUC1 13C
P1 12.00 usec
PL1 -0.50 dB
SFO1 100.5659560 MHz
======== CHANNEL f2 ========
CPDPRG2 waltz16
NUC2 1H
PCPD2 80.00 usec
PL2 3.00 dB
PL12 18.80 dB
PL13 24.80 dB
SFO2 399.9015996 MHz
F2 - Processing parameters
SI 32768
SF 100.5549296 MHz
WDW no
SSB 0
LB 1.00 Hz
GB 0
PC 1.40
OBn
O
CHO
TBDMSOH2C
OBn
OBn
6.10
190 180 170 160 150 140 130 120 110 100 90 80 70 60 50 40 30 20 10 0 ppm

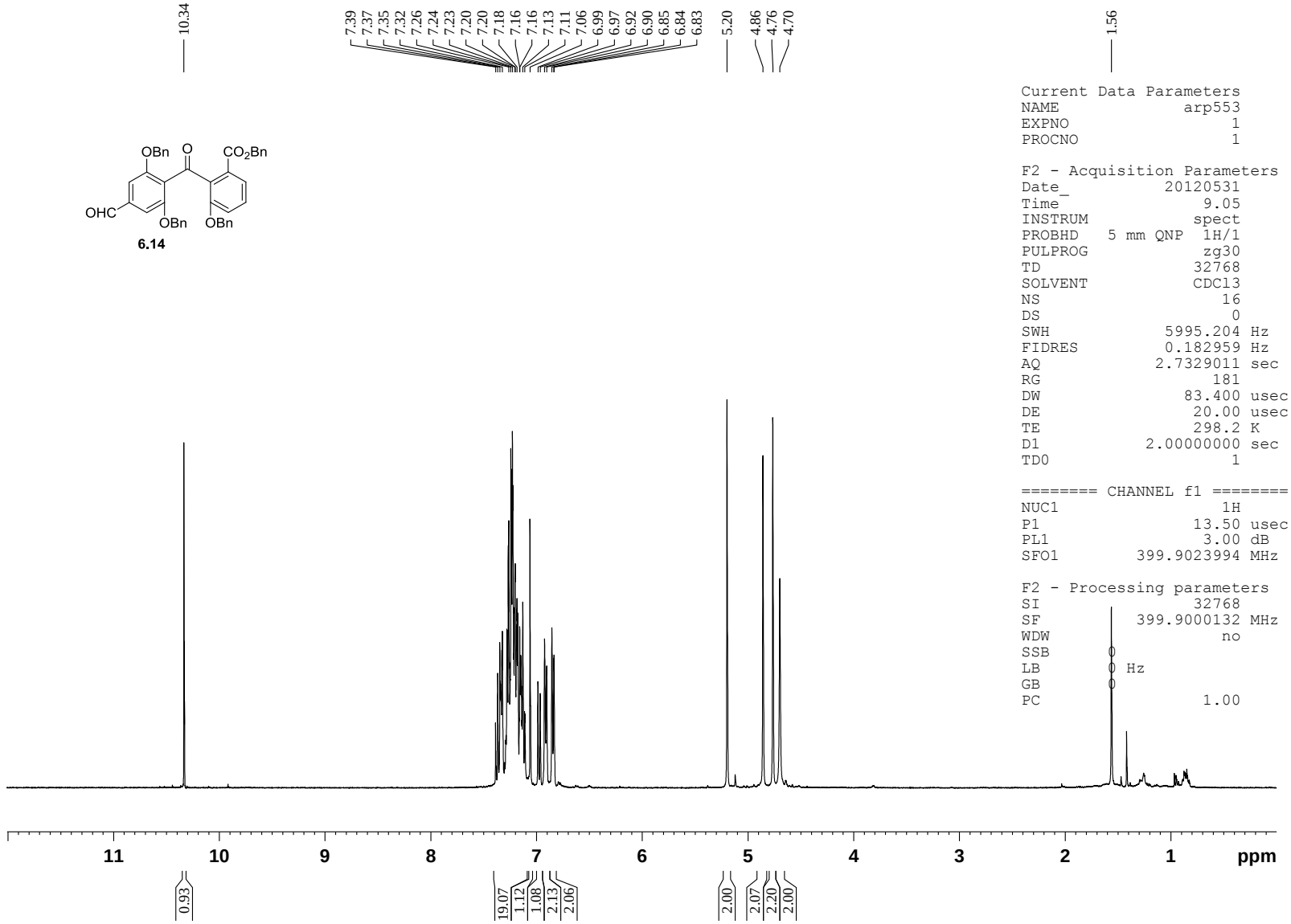

8.63
7.31
7.30
7.23
7.06
7.04
6.60
4.85
4.73
0.99
0.13
Current Data Parameters
NAME ARP#2#019#aldehyde to acid.1
EXPNO 1
PROCNO 1
F2 - Acquisition Parameters
Date_ 20101123
Time 12.21
INSTRUM spect
PROBHD 5 mm QNP 1H/1
PULPROG zg30
TD 32768
SOLVENT CDCl3
NS 16
DS 0
SWH 5995.204 Hz
FIDRES 0.182959 Hz
AQ 2.7329011 sec
RG 20.2
DW 83.400 usec
DE 20.00 usec
TE 298.2 K
D1 2.00000000 sec
TD0 1
======== CHANNEL f1 ========
NUC1 1H
P1 13.50 usec
PL1 3.00 dB
SFO1 399.9023994 MHz
F2 - Processing parameters
SI 32768
SF 399.9000132 MHz
WDW EM
SSB 0
LB 0.30 Hz
GB 0
PC 1.00
OBn
O
CO2H
TBDMSOH2C
OBn
OBn
6.11
9.5
9.0
8.5
8.0
7.5
7.0
6.5
6.0
5.5
5.0
4.5
4.0
3.5
3.0
2.5
2.0
1.5
1.0
0.5
0.0
ppm
0.82
20.04
7.97
9.34
6.00

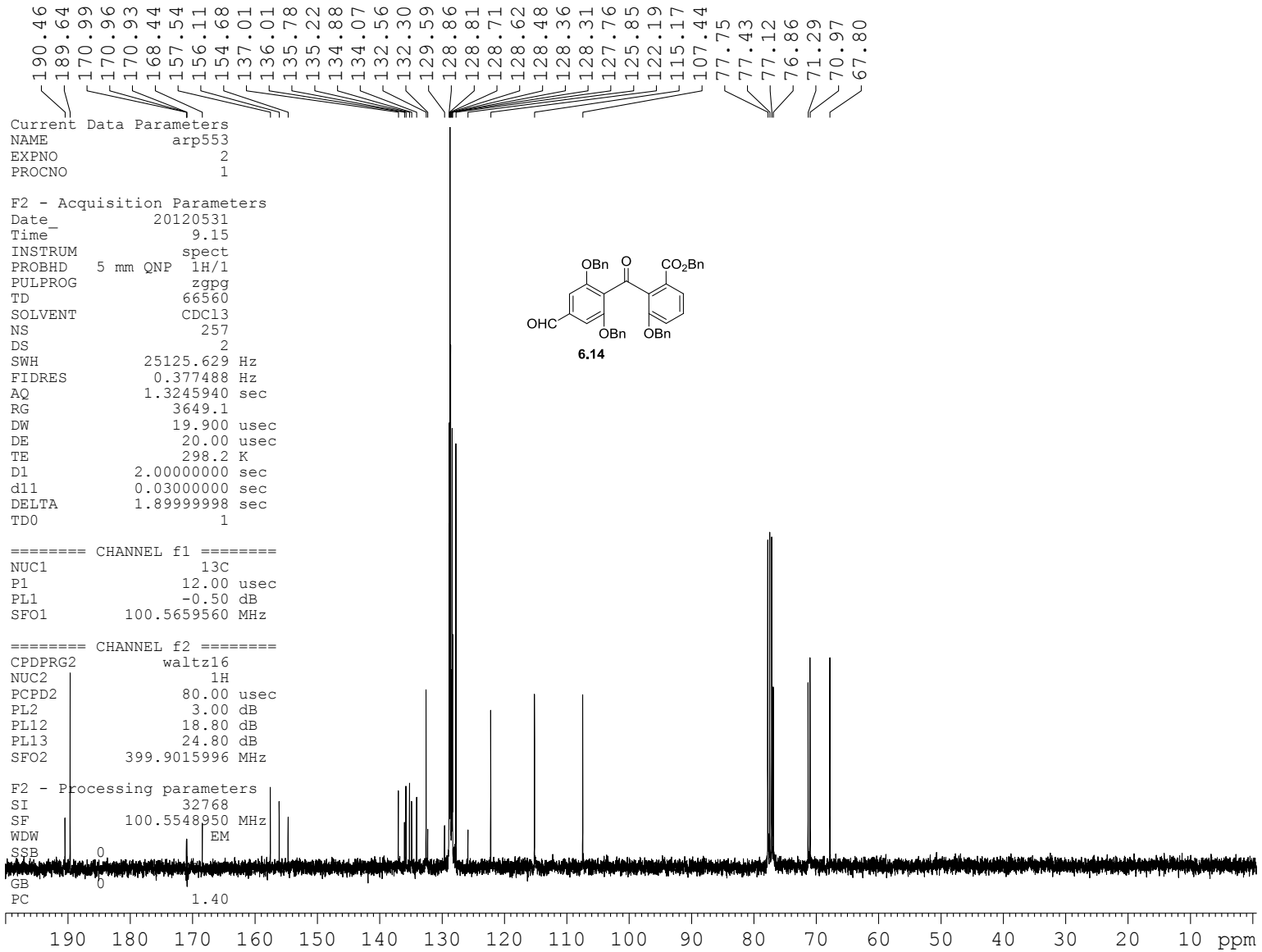

7.42 7.41 7.30 7.29 7.28 7.27 7.27 7.27 7.26 7.25 7.24 7.24 7.23 7.23 7.23 7.22 7.22 7.21 7.21 7.20 7.20 7.19 7.19 7.18 7.18 7.16 7.16 7.15 7.14 7.13 6.99 6.97 6.95 6.95 6.95 6.93 6.87 6.85 6.85 6.85 5.17 4.87 4.81 4.77 4.69
0.99 0.99 0.16 0.16
Current Data Parameters
NAME arp549
EXPNO 3
PROCNO 1
F2 - Acquisition Parameters
Date_ 20120523
Time 18.16
INSTRUM spect
PROBHD 5 mm QNP 1H/1
PULPROG zg30
TD 32768
SOLVENT CDCl3
NS 16
DS 0
SWH 5995.204 Hz
FIDRES 0.182959 Hz
AQ 2.7329011 sec
RG 35.9
DW 83.400 usec
DE 20.00 usec
TE 298.2 K
D1 2.00000000 sec
TD0 1
======== CHANNEL f1 ========
NUC1 1H
P1 13.50 usec
PL1 3.00 dB
SFO1 399.9023994 MHz
F2 - Processing parameters
SI 32768
SF 399.9000136 MHz
WDW no
SSB 0
LB 0 Hz
GB 0
PC 1.00
OBn
O
CO2Bn
TBDMSOH2C
OBn
OBn
6.12
9.5 9.0 8.5 8.0 7.5 7.0 6.5 6.0 5.5 5.0 4.5 4.0 3.5 3.0 2.5 2.0 1.5 1.0 0.5 0.0 ppm
2.06 17.36 4.04 1.95 2.00 1.96 4.00 1.96 9.46 5.95

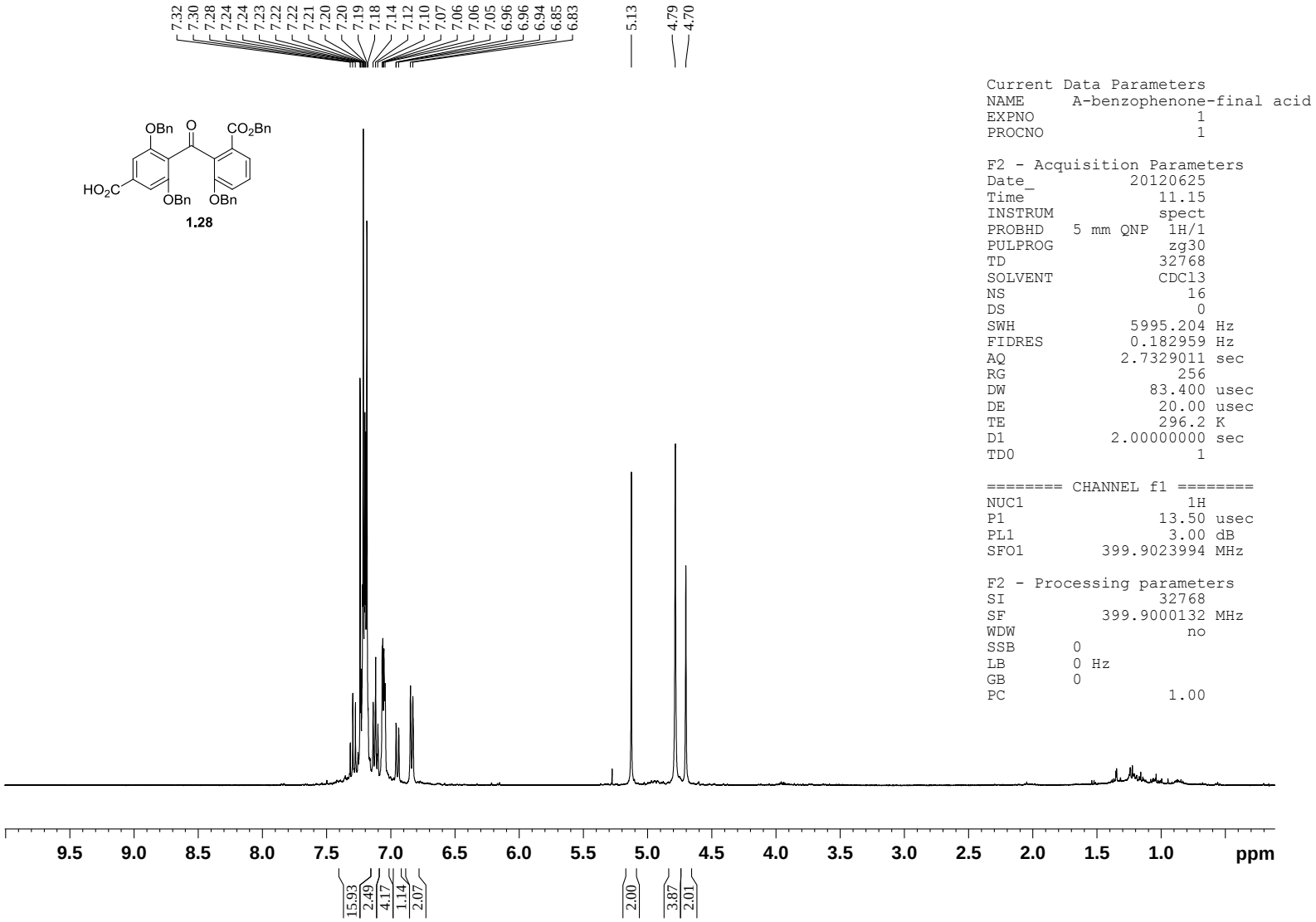

191.19
167.20
157.06
155.88
154.55
143.82
137.41
135.89
135.83
133.34
132.12
130.14
128.53
128.33
128.29
128.27
128.17
128.04
127.88
127.76
127.72
127.46
127.44
123.97
122.33
118.04
115.56
106.72
77.48
77.17
76.85
75.79
70.61
70.56
67.13
62.49
25.99
-5.26
Current Data Parameters
NAME arp549
EXPNO 2
PROCNO 1
F2 - Acquisition Parameters
Date_ 20120523
Time 14.38
INSTRUM spect
PROBHD 5 mm QNP 1H/1
PULPROG zgpg
TD 66560
SOLVENT CDCl3
NS 106
DS 2
SWH 25125.629 Hz
FIDRES 0.377488 Hz
AQ 1.3245940 sec
RG 6502
DW 19.900 usec
DE 20.00 usec
TE 298.2 K
D1 2.00000000 sec
d11 0.03000000 sec
DELTA 1.89999998 sec
TD0 1
======== CHANNEL f1 ========
NUC1 13C
P1 12.00 usec
PL1 -0.50 dB
SFO1 100.5659560 MHz
======== CHANNEL f2 ========
CPDPRG2 waltz16
NUC2 1H
PCPD2 80.00 usec
PL2 3.00 dB
PL12 18.80 dB
PL13 24.80 dB
SFO2 399.9015996 MHz
F2 - Processing parameters
SI 32768
SF 100.5540324 MHz
WDW no
SSB 0
LB
GB 0
PC 1.40
OBn
O
CO2Bn
TBDMSOH2C
OBn
OBn
6.12
220
200
180
160
140
120
100
80
60
40
20
0 ppm

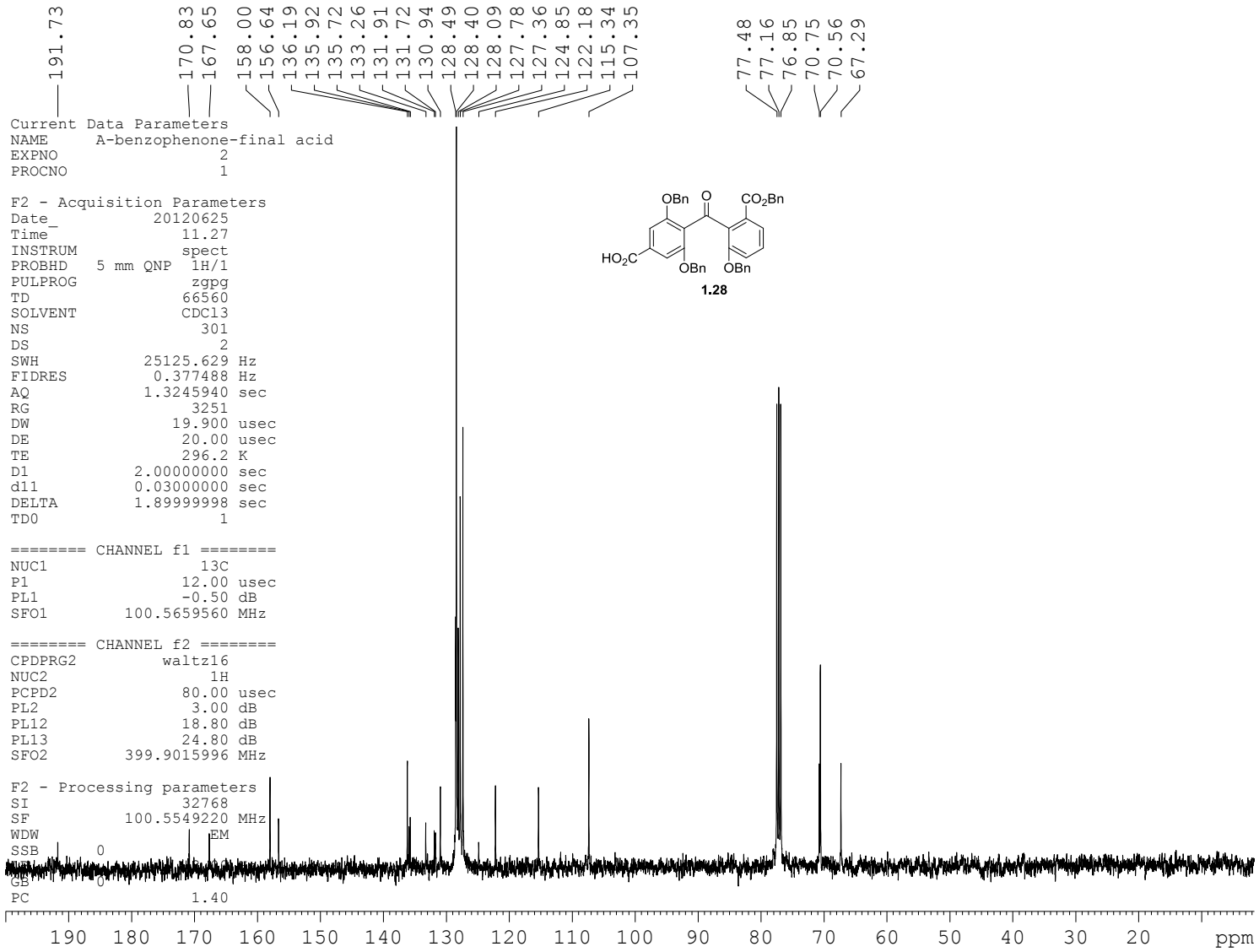

7.37
7.36
7.35
7.27
7.25
7.24
7.23
7.22
7.19
7.19
7.16
7.13
7.11
7.09
6.93
6.92
6.85
6.84
6.83
5.16
4.81
4.76
4.69
4.69
2.17
2.16
1.57
OBn
O
CO2Bn
CH2OH
OBn
OBn
6.13
Current Data Parameters
NAME arp551
EXPNO 3
PROCNO 1
F2 - Acquisition Parameters
Date_ 20120530
Time 8.18
INSTRUM spect
PROBHD 5 mm QNP 1H/1
PULPROG zg30
TD 32768
SOLVENT CDCl3
NS 4
DS 0
SWH 5995.204 Hz
FIDRES 0.182959 Hz
AQ 2.7329011 sec
RG 181
DW 83.400 usec
DE 20.00 usec
TE 298.2 K
D1 2.00000000 sec
TD0 1
======== CHANNEL f1 ========
NUC1 1H
P1 13.50 usec
PL1 3.00 dB
SFO1 399.9023994 MHz
F2 - Processing parameters
SI 32768
SF 399.9000132 MHz
WDW no
SSB 0
LB 0 Hz
GB 0
PC 1.00
9.5 9.0 8.5 8.0 7.5 7.0 6.5 6.0 5.5 5.0 4.5 4.0 3.5 3.0 2.5 2.0 1.5 1.0 0.5 0.0 ppm
2.22
17.44
6.10
2.00
8.13
0.91

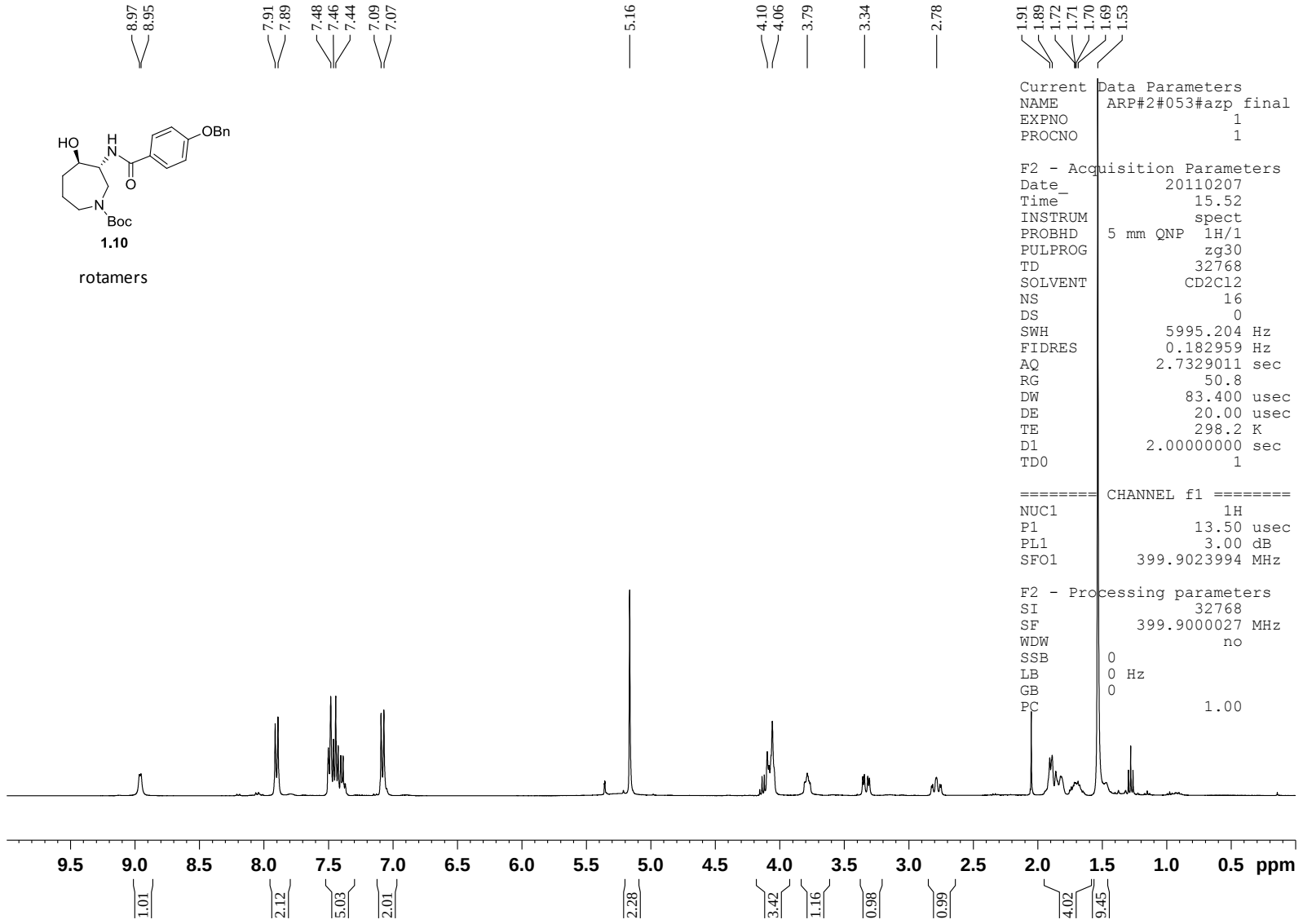

191.29
167.66
157.01
156.23
154.71
143.06
137.32
135.87
133.03
130.60
128.53
128.41
128.30
128.11
127.98
127.83
127.63
122.30
115.50
107.26
77.48
77.16
76.84
75.90
70.77
67.23
62.77
Current Data Parameters
NAME arp551
EXPNO 2
PROCNO 1
F2 - Acquisition Parameters
Date_ 20120525
Time 9.47
INSTRUM spect
PROBHD 5 mm QNP 1H/1
PULPROG zgpg
TD 66560
SOLVENT CDCl3
NS 289
DS 2
SWH 25125.629 Hz
FIDRES 0.377488 Hz
AQ 1.3245940 sec
RG 3649.1
DW 19.900 usec
DE 20.00 usec
TE 298.2 K
D1 2.00000000 sec
d11 0.03000000 sec
DELTA 1.89999998 sec
TD0 1
======== CHANNEL f1 ========
NUC1 13C
P1 12.00 usec
PL1 -0.50 dB
SFO1 100.5659560 MHz
======== CHANNEL f2 ========
CPDPRG2 waltz16
NUC2 1H
PCPD2 80.00 usec
PL2 3.00 dB
PL12 18.80 dB
PL13 24.80 dB
SFO2 399.9015996 MHz
F2 - Processing parameters
SI 32768
SF 100.5549218 MHz
WDW GM
SSB 0
LB -2.00 Hz
OBn
O
CO2Bn
CH2OH
OBn
OBn
6.13
190 180 170 160 150 140 130 120 110 100 90 80 70 60 50 40 30 20 10 ppm

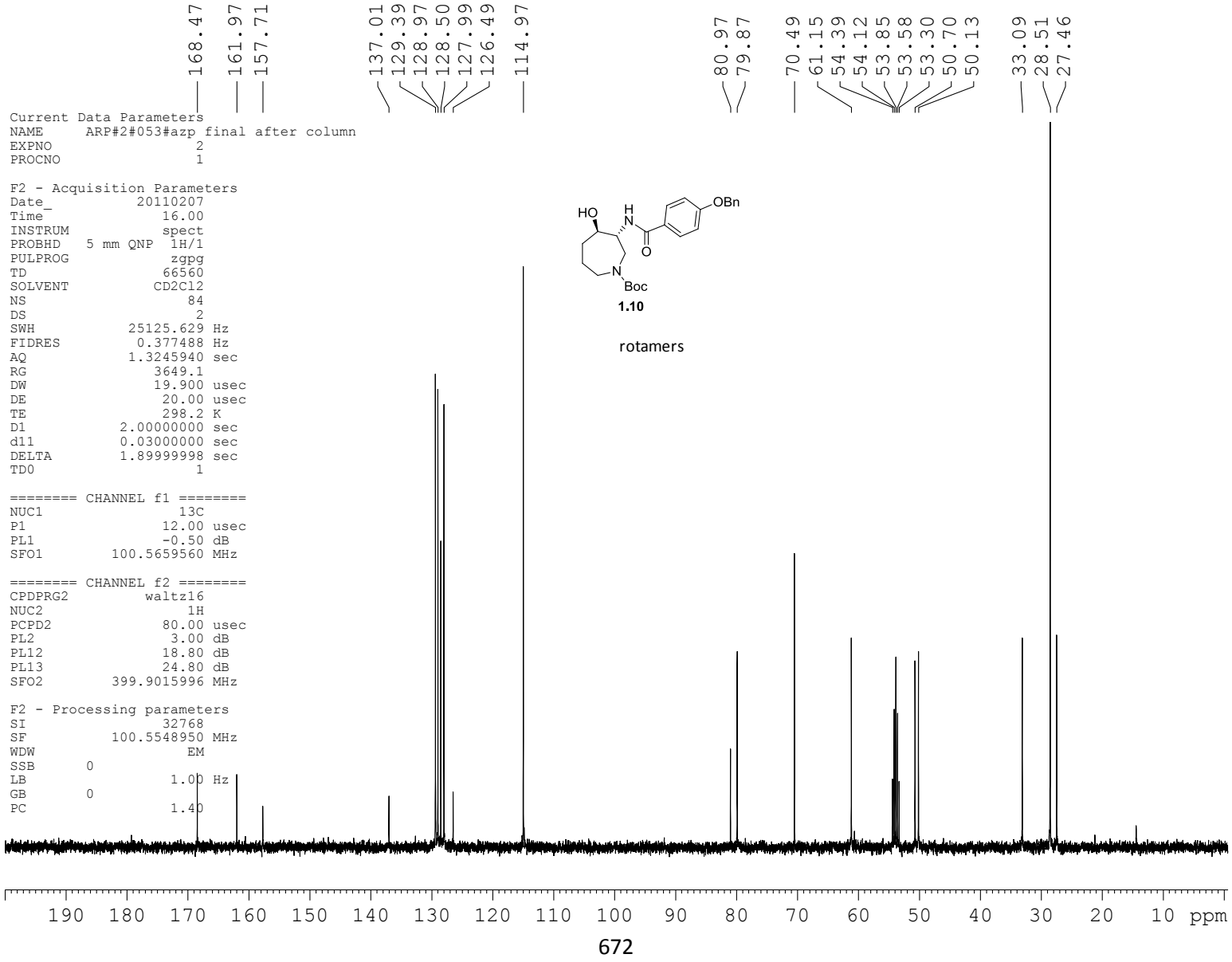

10.34
7.39
7.37
7.35
7.32
7.26
7.24
7.23
7.20
7.20
7.18
7.16
7.16
7.13
7.11
7.06
6.99
6.97
6.92
6.90
6.85
6.84
6.83
5.20
4.86
4.76
4.70
1.56
OBn
O
CO2Bn
OHC
OBn
OBn
6.14
Current Data Parameters
NAME arp553
EXPNO 1
PROCNO 1
F2 - Acquisition Parameters
Date_ 20120531
Time 9.05
INSTRUM spect
PROBHD 5 mm QNP 1H/1
PULPROG zg30
TD 32768
SOLVENT CDCl3
NS 16
DS 0
SWH 5995.204 Hz
FIDRES 0.182959 Hz
AQ 2.7329011 sec
RG 181
DW 83.400 usec
DE 20.00 usec
TE 298.2 K
D1 2.00000000 sec
TD0 1
======== CHANNEL f1 ========
NUC1 1H
P1 13.50 usec
PL1 3.00 dB
SFO1 399.9023994 MHz
F2 - Processing parameters
SI 32768
SF 399.9000132 MHz
WDW no
SSB 0
LB 0 Hz
GB 0
PC 1.00
11
10
9
8
7
6
5
4
3
2
1
ppm
0.93
19.07
1.12
1.08
2.13
2.06
2.00
2.07
2.20
2.00

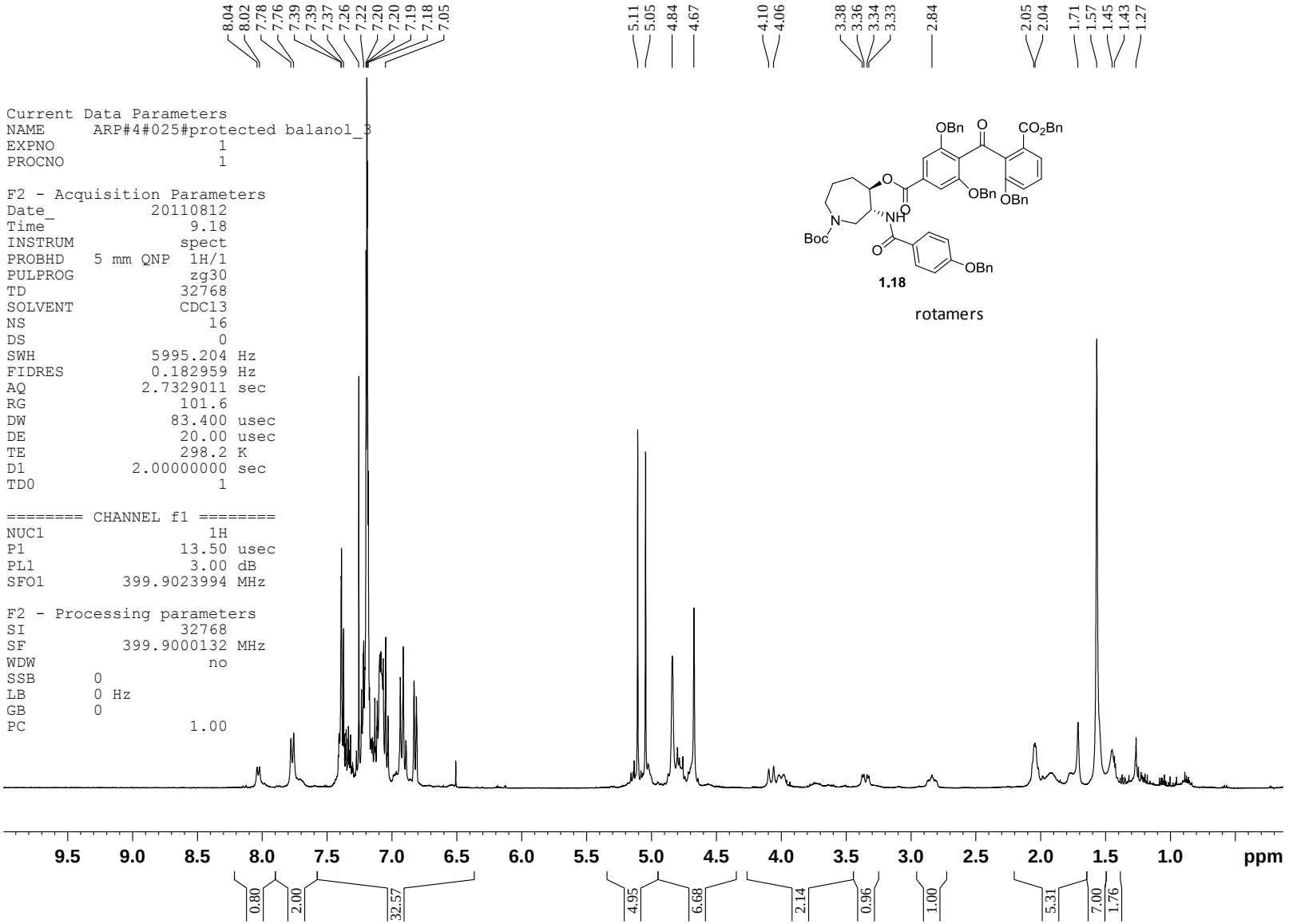

190.46
189.64
170.99
170.96
170.93
168.44
157.54
156.11
154.68
137.01
136.01
135.78
135.22
134.88
134.07
132.56
132.30
129.59
128.86
128.81
128.71
128.62
128.48
128.36
128.31
127.76
125.85
122.19
115.17
107.44
77.75
77.43
77.12
76.86
71.29
70.97
67.80
Current Data Parameters
NAME arp553
EXPNO 2
PROCNO 1
F2 - Acquisition Parameters
Date_ 20120531
Time 9.15
INSTRUM spect
PROBHD 5 mm QNP 1H/1
PULPROG zgpg
TD 66560
SOLVENT CDCl3
NS 257
DS 2
SWH 25125.629 Hz
FIDRES 0.377488 Hz
AQ 1.3245940 sec
RG 3649.1
DW 19.900 usec
DE 20.00 usec
TE 298.2 K
D1 2.00000000 sec
d11 0.03000000 sec
DELTA 1.89999998 sec
TD0 1
======== CHANNEL f1 ========
NUC1 13C
P1 12.00 usec
PL1 -0.50 dB
SFO1 100.5659560 MHz
======== CHANNEL f2 ========
CPDPRG2 waltz16
NUC2 1H
PCPD2 80.00 usec
PL2 3.00 dB
PL12 18.80 dB
PL13 24.80 dB
SFO2 399.9015996 MHz
F2 - Processing parameters
SI 32768
SF 100.5548950 MHz
WDW EM
SSB 0
GB 0
PC 1.40
OBn
O
CO2Bn
OHC
OBn
OBn
6.14
190 180 170 160 150 140 130 120 110 100 90 80 70 60 50 40 30 20 10 ppm

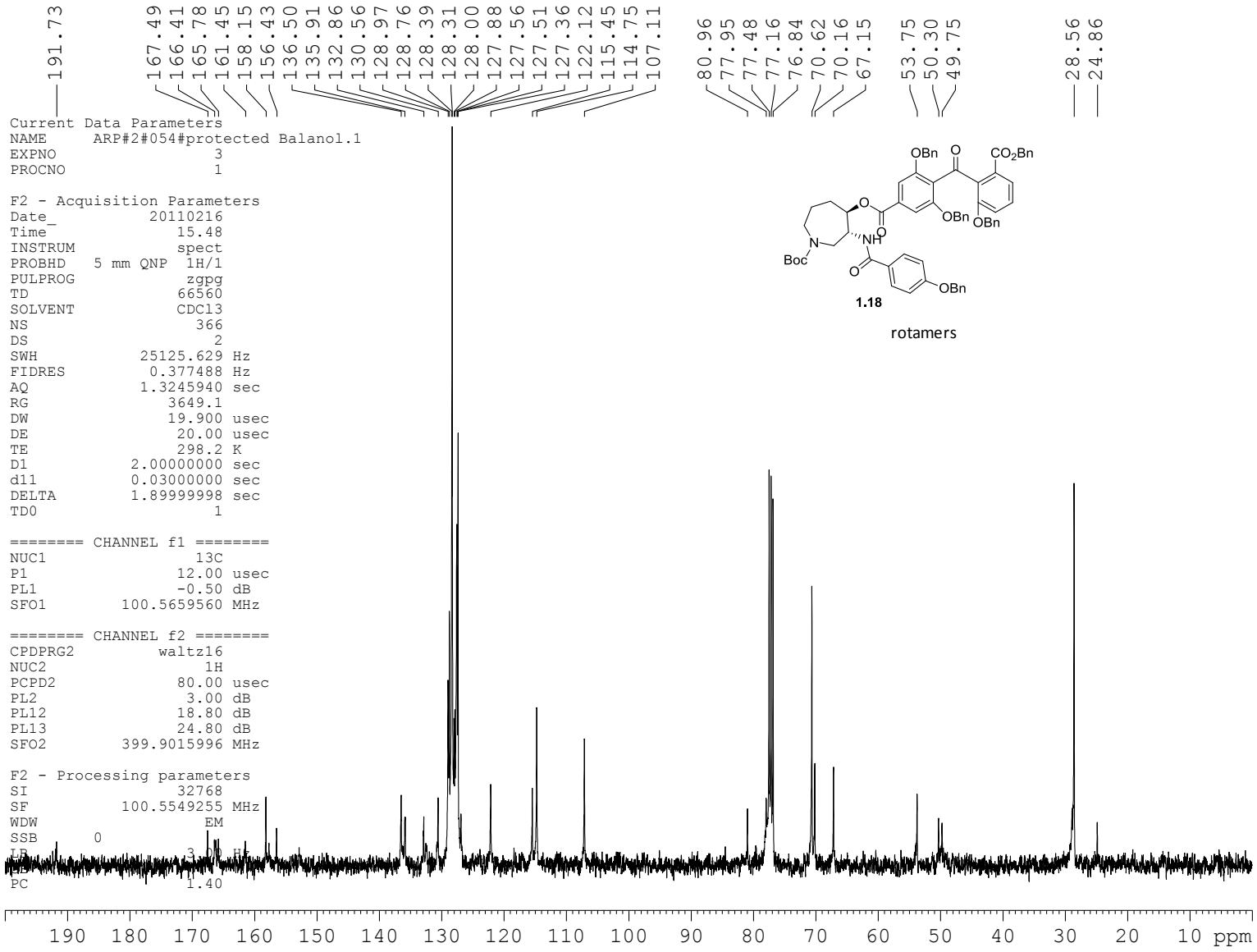

7.32
7.30
7.28
7.24
7.24
7.23
7.22
7.22
7.21
7.20
7.20
7.19
7.18
7.14
7.12
7.10
7.07
7.06
7.06
7.05
6.96
6.96
6.94
6.85
6.83
5.13
4.79
4.70
OBn
O
CO2Bn
HO2C
OBn
OBn
1.28
Current Data Parameters
NAME A-benzophenone-final acid
EXPNO 1
PROCNO 1
F2 - Acquisition Parameters
Date_ 20120625
Time 11.15
INSTRUM spect
PROBHD 5 mm QNP 1H/1
PULPROG zg30
TD 32768
SOLVENT CDCl3
NS 16
DS 0
SWH 5995.204 Hz
FIDRES 0.182959 Hz
AQ 2.7329011 sec
RG 256
DW 83.400 usec
DE 20.00 usec
TE 296.2 K
D1 2.00000000 sec
TD0 1
======== CHANNEL f1 ========
NUC1 1H
P1 13.50 usec
PL1 3.00 dB
SFO1 399.9023994 MHz
F2 - Processing parameters
SI 32768
SF 399.9000132 MHz
WDW no
SSB 0
LB 0 Hz
GB 0
PC 1.00
9.5
9.0
8.5
8.0
7.5
7.0
6.5
6.0
5.5
5.0
4.5
4.0
3.5
3.0
2.5
2.0
1.5
1.0
ppm
15.93
2.49
4.17
1.14
2.07
2.00
3.87
2.01

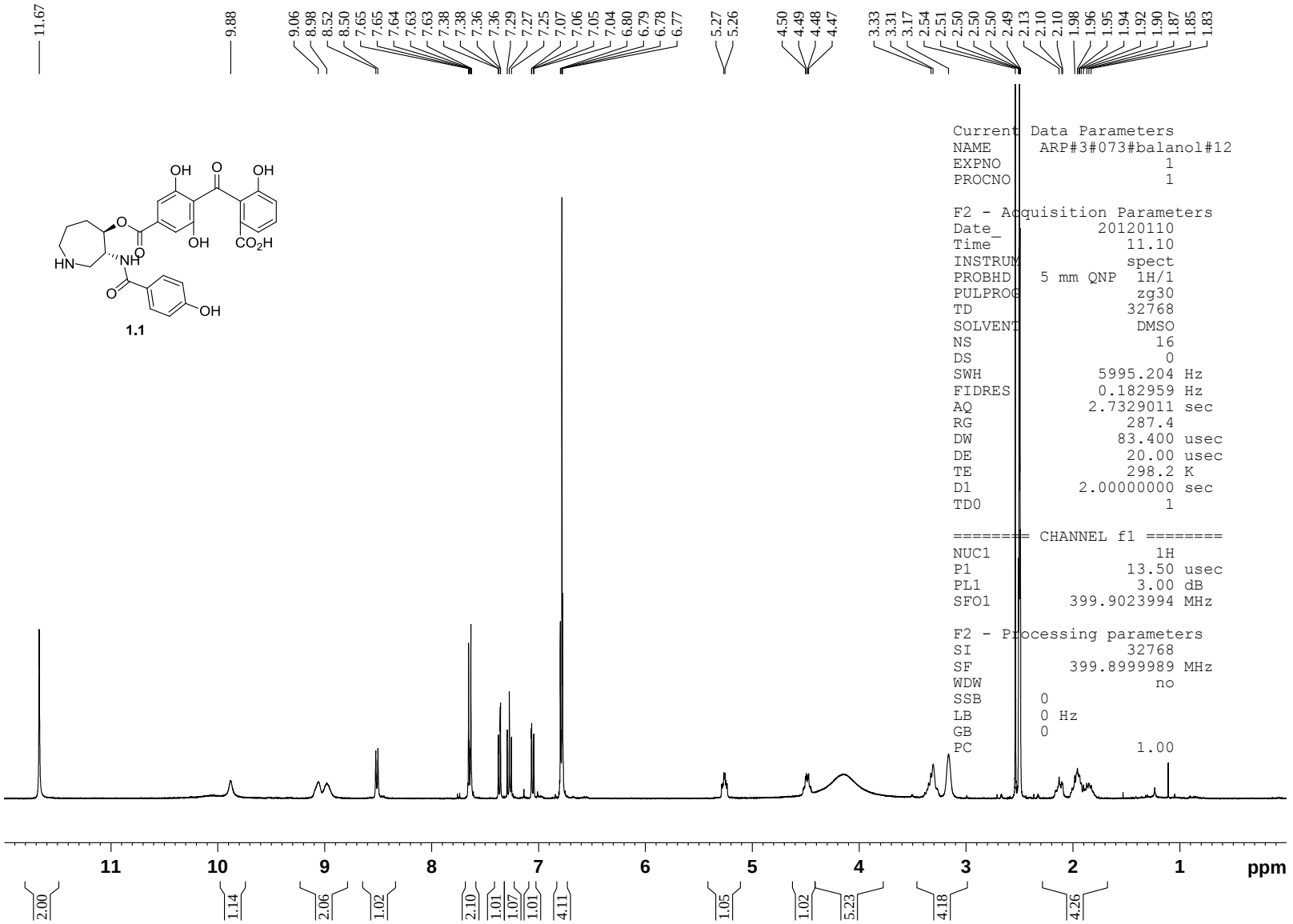

191.73
170.83
167.65
158.00
156.64
136.19
135.92
135.72
133.26
131.91
131.72
130.94
128.49
128.40
128.09
127.78
127.36
124.85
122.18
115.34
107.35
77.48
77.16
76.85
70.75
70.56
67.29
Current Data Parameters
NAME A-benzophenone-final acid
EXPNO 2
PROCNO 1
F2 - Acquisition Parameters
Date_ 20120625
Time 11.27
INSTRUM spect
PROBHD 5 mm QNP 1H/1
PULPROG zgpg
TD 66560
SOLVENT CDCl3
NS 301
DS 2
SWH 25125.629 Hz
FIDRES 0.377488 Hz
AQ 1.3245940 sec
RG 3251
DW 19.900 usec
DE 20.00 usec
TE 296.2 K
D1 2.00000000 sec
d11 0.03000000 sec
DELTA 1.89999998 sec
TD0 1
======== CHANNEL f1 ========
NUC1 13C
P1 12.00 usec
PL1 -0.50 dB
SFO1 100.5659560 MHz
======== CHANNEL f2 ========
CPDPRG2 waltz16
NUC2 1H
PCPD2 80.00 usec
PL2 3.00 dB
PL12 18.80 dB
PL13 24.80 dB
SFO2 399.9015996 MHz
F2 - Processing parameters
SI 32768
SF 100.5549220 MHz
WDW EM
SSB 0
LB 0
GB 0
PC 1.40
OBn
O
CO2Bn
HO2C
OBn
OBn
1.28
190
180
170
160
150
140
130
120
110
100
90
80
70
60
50
40
30
20
ppm

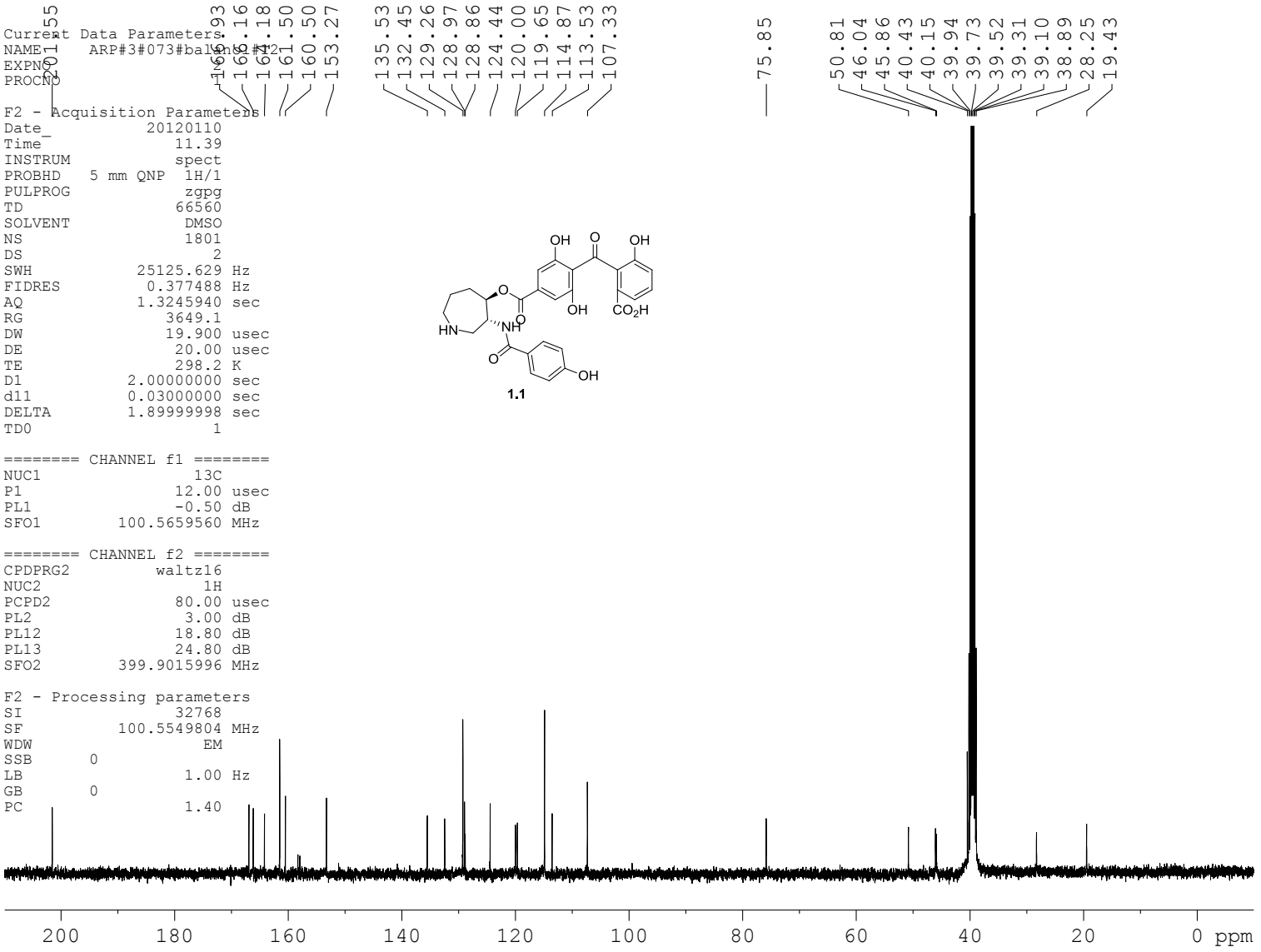

8.97
8.95
7.91
7.89
7.48
7.46
7.44
7.09
7.07
5.16
4.10
4.06
3.79
3.34
2.78
1.91
1.89
1.72
1.71
1.70
1.69
1.53
HO
H
N
O
OBn
N
Boc
1.10
rotamers
Current Data Parameters
NAME ARP#2#053#azp final
EXPNO 1
PROCNO 1
F2 - Acquisition Parameters
Date_ 20110207
Time 15.52
INSTRUM spect
PROBHD 5 mm QNP 1H/1
PULPROG zg30
TD 32768
SOLVENT CD2Cl2
NS 16
DS 0
SWH 5995.204 Hz
FIDRES 0.182959 Hz
AQ 2.7329011 sec
RG 50.8
DW 83.400 usec
DE 20.00 usec
TE 298.2 K
D1 2.00000000 sec
TD0 1
======== CHANNEL f1 ========
NUC1 1H
P1 13.50 usec
PL1 3.00 dB
SFO1 399.9023994 MHz
F2 - Processing parameters
SI 32768
SF 399.9000027 MHz
WDW no
SSB 0
LB 0 Hz
GB 0
PC 1.00
9.5
9.0
8.5
8.0
7.5
7.0
6.5
6.0
5.5
5.0
4.5
4.0
3.5
3.0
2.5
2.0
1.5
1.0
0.5
ppm
1.01
2.12
5.03
2.01
2.28
3.42
1.16
0.98
0.99
4.02
9.45

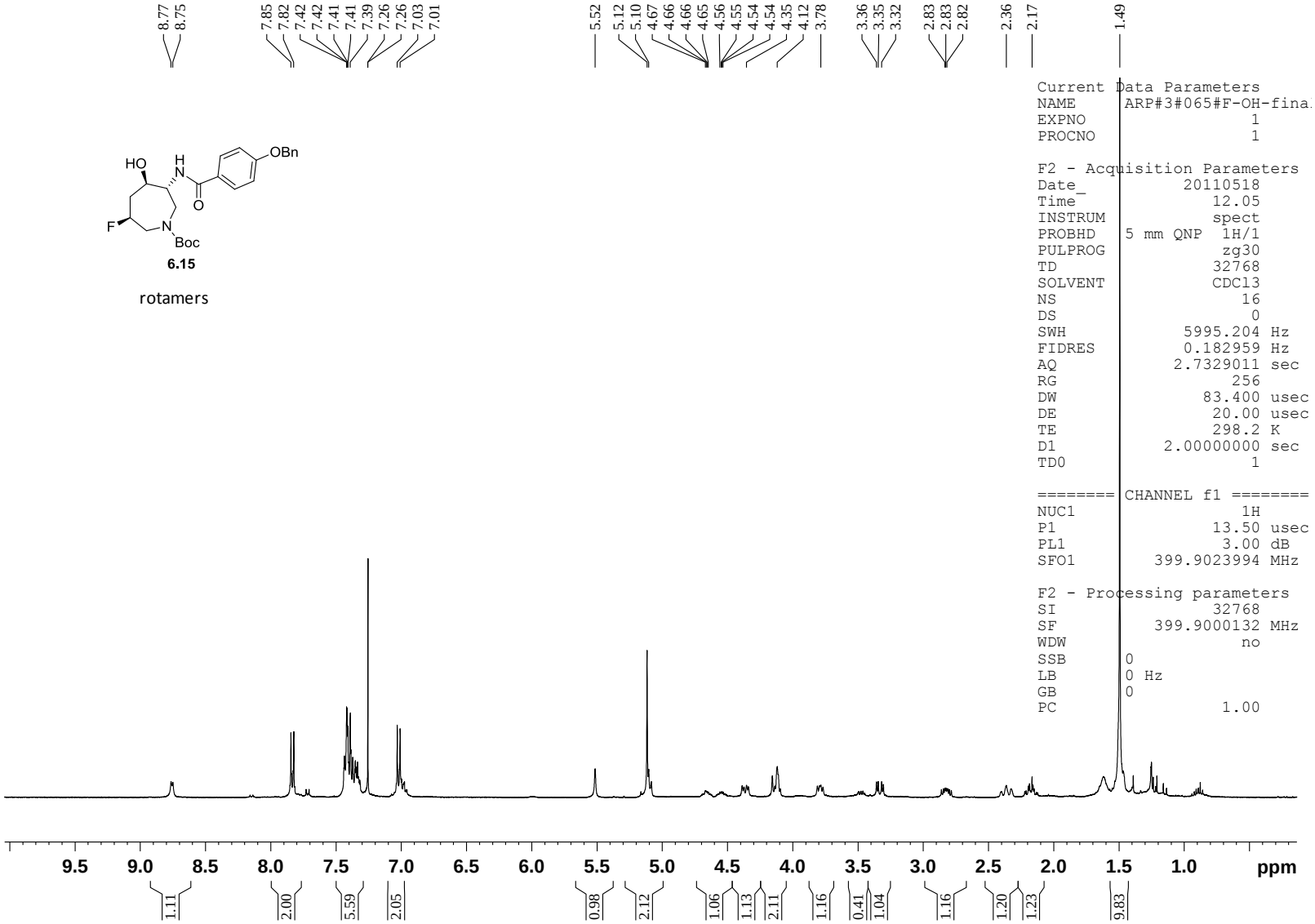

168.47
161.97
157.71
137.01
129.39
128.97
128.50
127.99
126.49
114.97
80.97
79.87
70.49
61.15
54.39
54.12
53.85
53.58
53.30
50.70
50.13
33.09
28.51
27.46
Current Data Parameters
NAME ARP#2#053#azp final after column
EXPNO 2
PROCNO 1
F2 - Acquisition Parameters
Date_ 20110207
Time 16.00
INSTRUM spect
PROBHD 5 mm QNP 1H/1
PULPROG zgpg
TD 66560
SOLVENT CD2Cl2
NS 84
DS 2
SWH 25125.629 Hz
FIDRES 0.377488 Hz
AQ 1.3245940 sec
RG 3649.1
DW 19.900 usec
DE 20.00 usec
TE 298.2 K
D1 2.00000000 sec
d11 0.03000000 sec
DELTA 1.89999998 sec
TD0 1
======== CHANNEL f1 ========
NUC1 13C
P1 12.00 usec
PL1 -0.50 dB
SFO1 100.5659560 MHz
======== CHANNEL f2 ========
CPDPRG2 waltz16
NUC2 1H
PCPD2 80.00 usec
PL2 3.00 dB
PL12 18.80 dB
PL13 24.80 dB
SFO2 399.9015996 MHz
F2 - Processing parameters
SI 32768
SF 100.5548950 MHz
WDW EM
SSB 0
LB 1.00 Hz
GB 0
PC 1.40
HO
N
H
O
OBn
N
Boc
1.10
rotamers
190 180 170 160 150 140 130 120 110 100 90 80 70 60 50 40 30 20 10 ppm

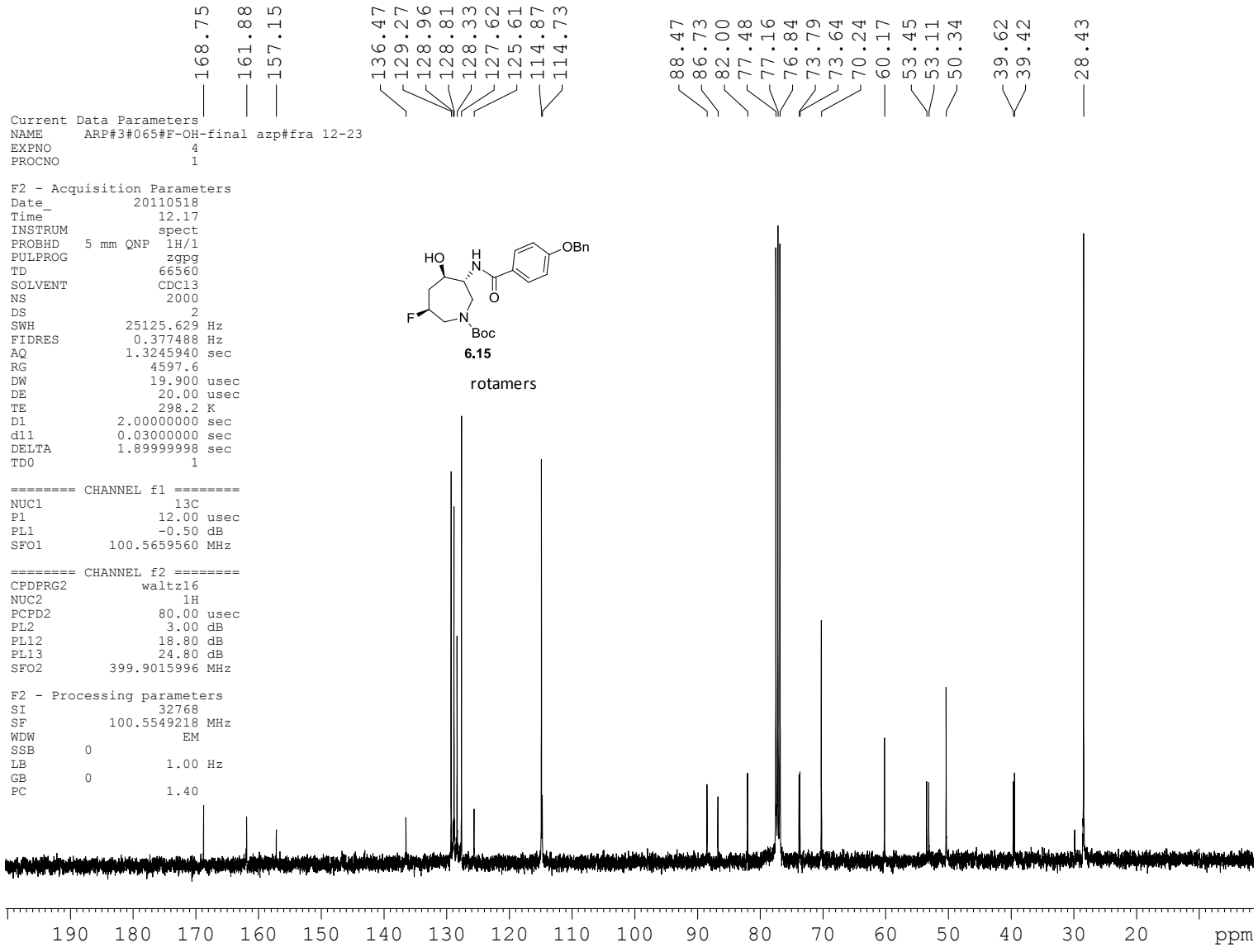

8.04
8.02
7.78
7.76
7.39
7.39
7.37
7.26
7.22
7.20
7.20
7.19
7.18
7.05
5.11
5.05
4.84
4.67
4.10
4.06
3.38
3.36
3.34
3.33
2.84
2.05
2.04
1.71
1.57
1.45
1.43
1.27
Current Data Parameters
NAME ARP#4#025#protected balanol_3
EXPNO 1
PROCNO 1
F2 - Acquisition Parameters
Date_ 20110812
Time 9.18
INSTRUM spect
PROBHD 5 mm QNP 1H/1
PULPROG zg30
TD 32768
SOLVENT CDCl3
NS 16
DS 0
SWH 5995.204 Hz
FIDRES 0.182959 Hz
AQ 2.7329011 sec
RG 101.6
DW 83.400 usec
DE 20.00 usec
TE 298.2 K
D1 2.00000000 sec
TD0 1
======== CHANNEL f1 ========
NUC1 1H
P1 13.50 usec
PL1 3.00 dB
SFO1 399.9023994 MHz
F2 - Processing parameters
SI 32768
SF 399.9000132 MHz
WDW no
SSB 0
LB 0 Hz
GB 0
PC 1.00
OBn
O
CO2Bn
OBn
OBn
O
O
N
Boc
NH
O
OBn
1.18
rotamers
9.5
9.0
8.5
8.0
7.5
7.0
6.5
6.0
5.5
5.0
4.5
4.0
3.5
3.0
2.5
2.0
1.5
1.0
ppm
0.80
2.00
32.57
4.95
6.68
2.14
0.96
1.00
5.31
7.00
1.76

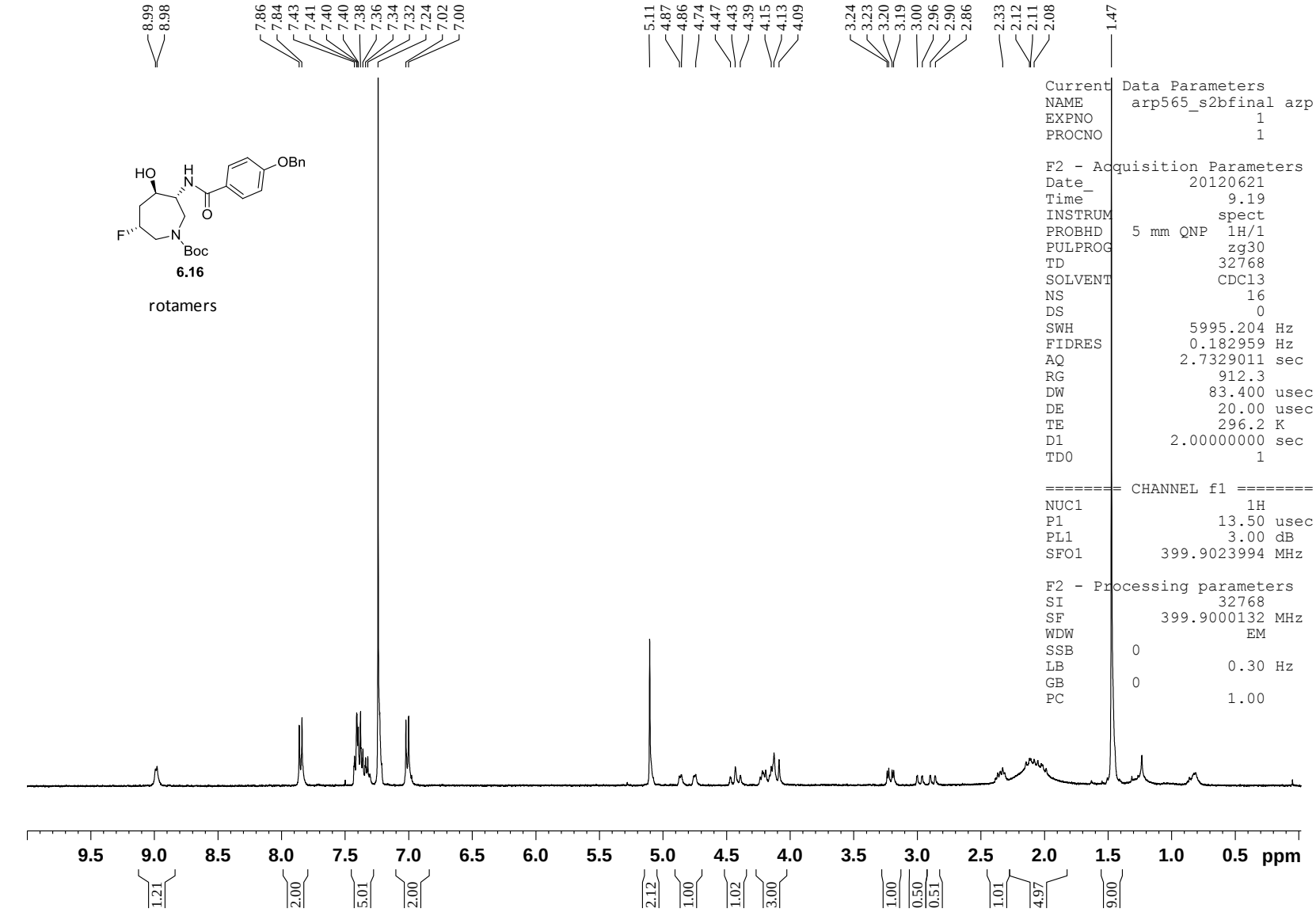

191.73
167.49
166.41
165.78
161.45
158.15
156.43
136.50
135.91
132.86
130.56
128.97
128.76
128.39
128.31
128.00
127.88
127.56
127.51
127.36
122.12
115.45
114.75
107.11
80.96
77.95
77.48
77.16
76.84
70.62
70.16
67.15
53.75
50.30
49.75
28.56
24.86
Current Data Parameters
NAME ARP#2#054#protected Balanol1.1
EXPNO 3
PROCNO 1
F2 - Acquisition Parameters
Date_ 20110216
Time 15.48
INSTRUM spect
PROBHD 5 mm QNP 1H/1
PULPROG zgpg
TD 66560
SOLVENT CDCl3
NS 366
DS 2
SWH 25125.629 Hz
FIDRES 0.377488 Hz
AQ 1.3245940 sec
RG 3649.1
DW 19.900 usec
DE 20.00 usec
TE 298.2 K
D1 2.00000000 sec
d11 0.03000000 sec
DELTA 1.89999998 sec
TD0 1
======== CHANNEL f1 ========
NUC1 13C
P1 12.00 usec
PL1 -0.50 dB
SFO1 100.5659560 MHz
======== CHANNEL f2 ========
CPDPRG2 waltz16
NUC2 1H
PCPD2 80.00 usec
PL2 3.00 dB
PL12 18.80 dB
PL13 24.80 dB
SFO2 399.9015996 MHz
F2 - Processing parameters
SI 32768
SF 100.5549255 MHz
WDW EM
SSB 0
LB 3.00 Hz
GB 0
PC 1.40
OBn
O
CO2Bn
OBn
OBn
O
O
NH
N
Boc
O
OBn
1.18
rotamers
190 180 170 160 150 140 130 120 110 100 90 80 70 60 50 40 30 20 10 ppm

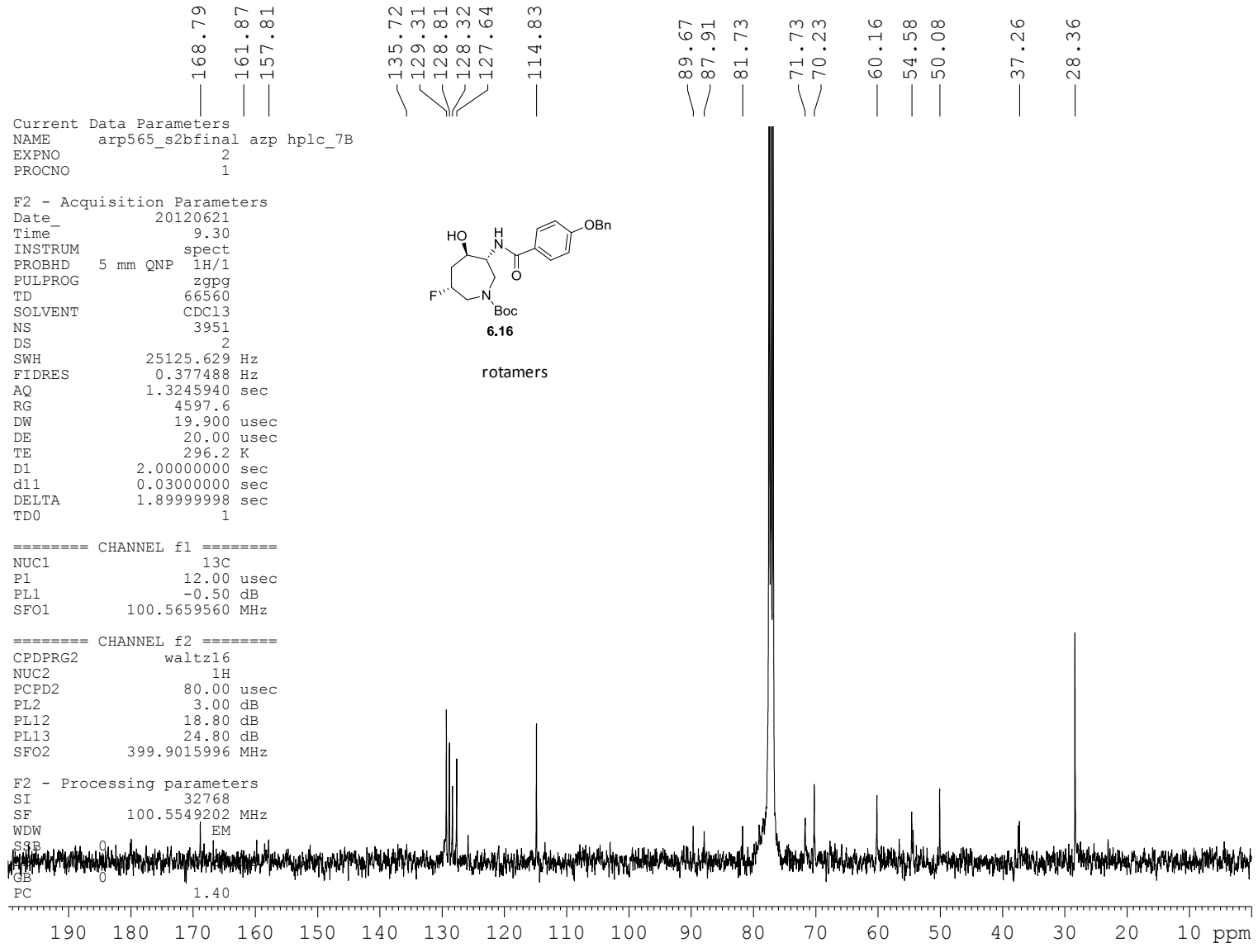

11.67
9.88
9.06
8.98
8.52
8.50
7.65
7.64
7.63
7.63
7.38
7.38
7.36
7.36
7.29
7.27
7.25
7.07
7.06
7.05
7.04
6.80
6.79
6.78
6.77
5.27
5.26
4.50
4.49
4.48
4.47
3.33
3.31
3.17
2.54
2.51
2.50
2.50
2.50
2.49
2.13
2.10
2.10
1.98
1.96
1.95
1.94
1.92
1.90
1.87
1.85
1.83
OH
O
OH
OH
CO2H
O
HN
NH
O
OH
1.1
Current Data Parameters
NAME ARP#3#073#balanol#12
EXPNO 1
PROCNO 1
F2 - Acquisition Parameters
Date_ 20120110
Time 11.10
INSTRUM spect
PROBHD 5 mm QNP 1H/1
PULPROG zg30
TD 32768
SOLVENT DMSO
NS 16
DS 0
SWH 5995.204 Hz
FIDRES 0.182959 Hz
AQ 2.7329011 sec
RG 287.4
DW 83.400 usec
DE 20.00 usec
TE 298.2 K
D1 2.00000000 sec
TD0 1
======== CHANNEL f1 ========
NUC1 1H
P1 13.50 usec
PL1 3.00 dB
SFO1 399.9023994 MHz
F2 - Processing parameters
SI 32768
SF 399.8999989 MHz
WDW no
SSB 0
LB 0 Hz
GB 0
PC 1.00
11
10
9
8
7
6
5
4
3
2
1
ppm
2.00
1.14
2.06
1.02
2.10
1.01
1.07
1.01
4.11
1.05
1.02
5.23
4.18
4.26

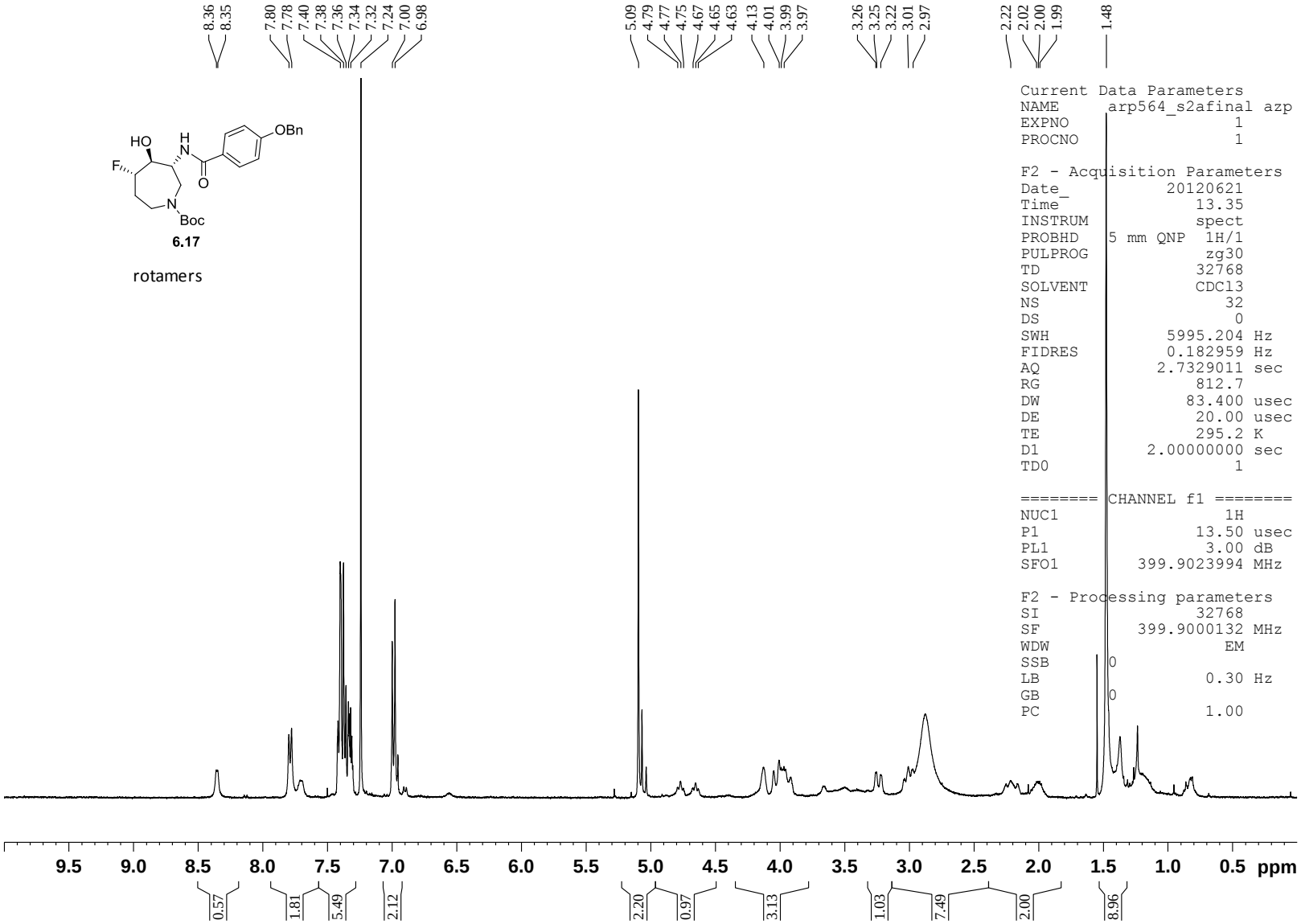

Current Data Parameters
NAME ARP#3#073#balsa#12
EXPNO 1
PROCNO 1
F2 - Acquisition Parameters
Date_ 20120110
Time 11.39
INSTRUM spect
PROBHD 5 mm QNP 1H/1
PULPROG zgpg
TD 66560
SOLVENT DMSO
NS 1801
DS 2
SWH 25125.629 Hz
FIDRES 0.377488 Hz
AQ 1.3245940 sec
RG 3649.1
DW 19.900 usec
DE 20.00 usec
TE 298.2 K
D1 2.00000000 sec
d11 0.03000000 sec
DELTA 1.89999998 sec
TD0 1
======== CHANNEL f1 ========
NUC1 13C
P1 12.00 usec
PL1 -0.50 dB
SFO1 100.5659560 MHz
======== CHANNEL f2 ========
CPDPRG2 waltz16
NUC2 1H
PCPD2 80.00 usec
PL2 3.00 dB
PL12 18.80 dB
PL13 24.80 dB
SFO2 399.9015996 MHz
F2 - Processing parameters
SI 32768
SF 100.5549804 MHz
WDW EM
SSB 0
LB 1.00 Hz
GB 0
PC 1.40
169.93
168.16
167.18
161.50
160.50
153.27
135.53
132.45
129.26
128.97
128.86
124.44
120.00
119.65
114.87
113.53
107.33
75.85
50.81
46.04
45.86
40.43
40.15
39.94
39.73
39.52
39.31
39.10
38.89
28.25
19.43
1.1
200
180
160
140
120
100
80
60
40
20
0 ppm

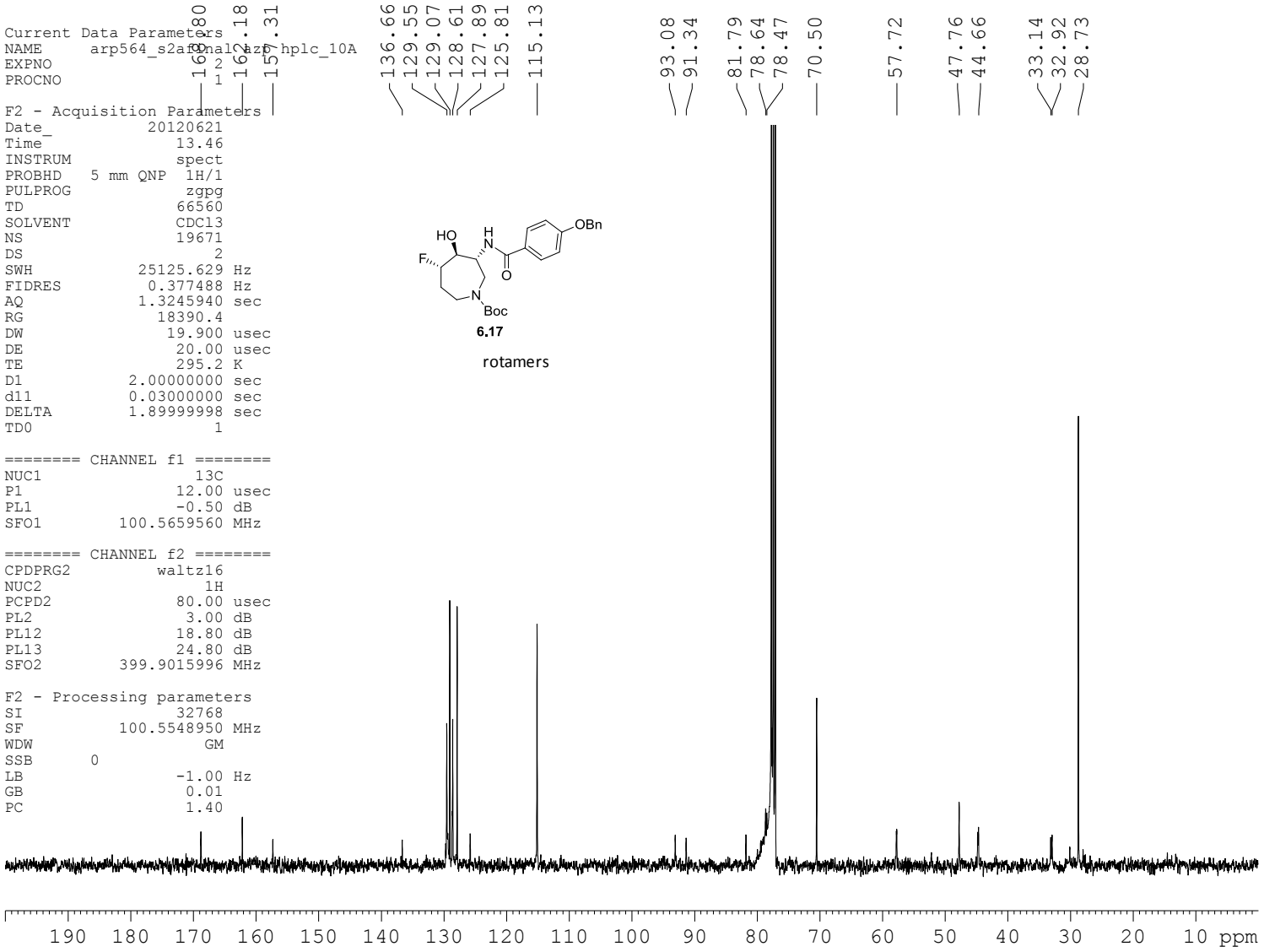

8.77
8.75
7.85
7.82
7.42
7.42
7.41
7.41
7.39
7.26
7.26
7.03
7.01
5.52
5.12
5.10
4.67
4.66
4.66
4.65
4.56
4.55
4.54
4.54
4.35
4.12
3.78
3.36
3.35
3.32
2.83
2.83
2.82
2.36
2.17
1.49
HO
H
N
OBn
O
F
N
Boc
6.15
rotamers
Current Data Parameters
NAME ARP#3#065#F-OH-fina
EXPNO 1
PROCNO 1
F2 - Acquisition Parameters
Date_ 20110518
Time 12.05
INSTRUM spect
PROBHD 5 mm QNP 1H/1
PULPROG zg30
TD 32768
SOLVENT CDCl3
NS 16
DS 0
SWH 5995.204 Hz
FIDRES 0.182959 Hz
AQ 2.7329011 sec
RG 256
DW 83.400 usec
DE 20.00 usec
TE 298.2 K
D1 2.00000000 sec
TD0 1
======== CHANNEL f1 ========
NUC1 1H
P1 13.50 usec
PL1 3.00 dB
SFO1 399.9023994 MHz
F2 - Processing parameters
SI 32768
SF 399.9000132 MHz
WDW no
SSB 0
LB 0 Hz
GB 0
PC 1.00
9.5
9.0
8.5
8.0
7.5
7.0
6.5
6.0
5.5
5.0
4.5
4.0
3.5
3.0
2.5
2.0
1.5
1.0
ppm
1.11
2.00
5.59
2.05
0.98
2.12
1.06
1.13
2.11
1.16
0.41
1.04
1.16
1.20
1.23
9.83

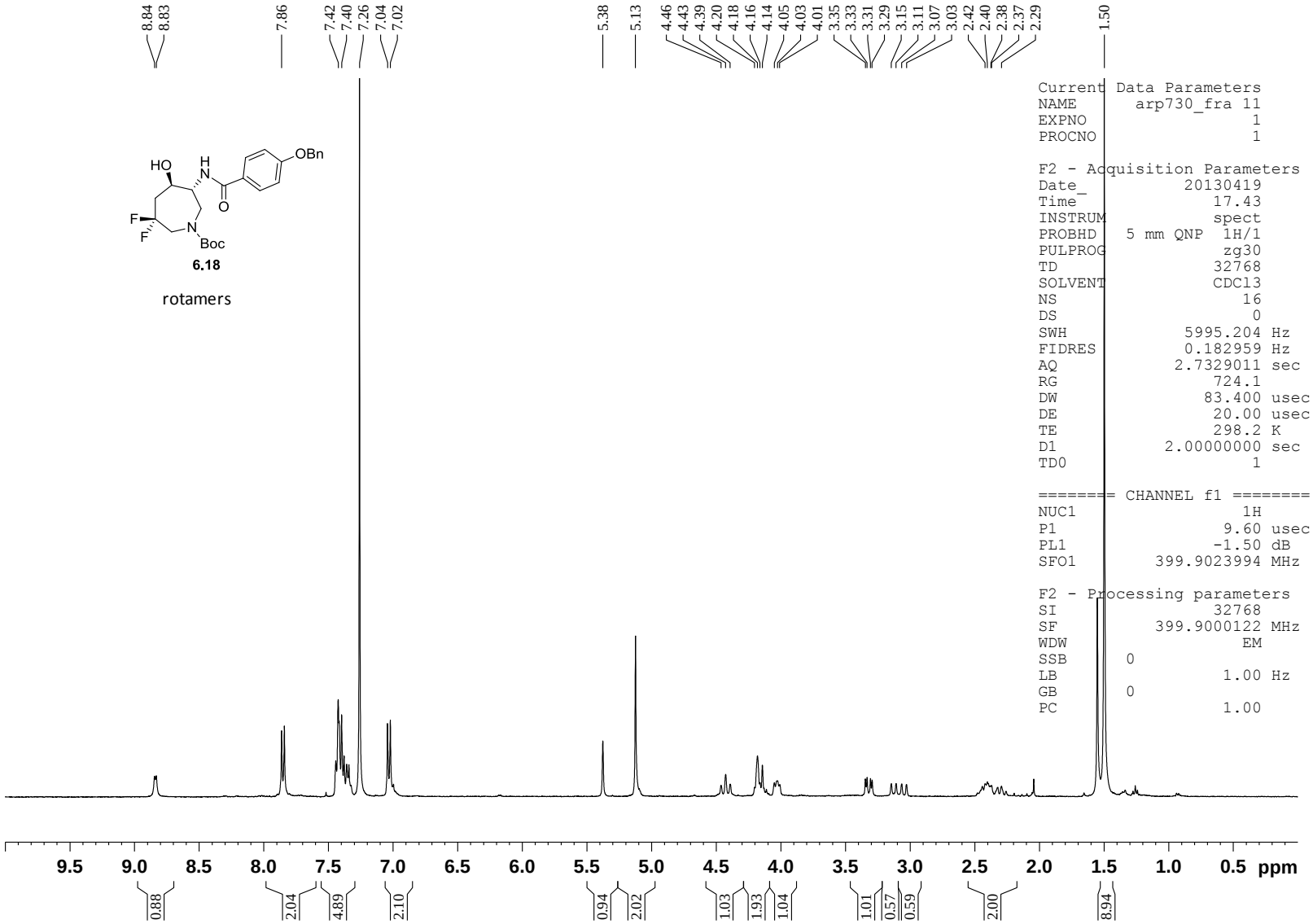

168.75
161.88
157.15
136.47
129.27
128.96
128.81
128.33
127.62
125.61
114.87
114.73
88.47
86.73
82.00
77.48
77.16
76.84
73.79
73.64
70.24
60.17
53.45
53.11
50.34
39.62
39.42
28.43
Current Data Parameters
NAME ARP#3#065#F-OH-final azp#fra 12-23
EXPNO 4
PROCNO 1
F2 - Acquisition Parameters
Date_ 20110518
Time 12.17
INSTRUM spect
PROBHD 5 mm QNP 1H/1
PULPROG zgpg
TD 66560
SOLVENT CDCl3
NS 2000
DS 2
SWH 25125.629 Hz
FIDRES 0.377488 Hz
AQ 1.3245940 sec
RG 4597.6
DW 19.900 usec
DE 20.00 usec
TE 298.2 K
D1 2.00000000 sec
d11 0.03000000 sec
DELTA 1.89999998 sec
TD0 1
======== CHANNEL f1 ========
NUC1 13C
P1 12.00 usec
PL1 -0.50 dB
SFO1 100.5659560 MHz
======== CHANNEL f2 ========
CPDPRG2 waltz16
NUC2 1H
PCPD2 80.00 usec
PL2 3.00 dB
PL12 18.80 dB
PL13 24.80 dB
SFO2 399.9015996 MHz
F2 - Processing parameters
SI 32768
SF 100.5549218 MHz
WDW EM
SSB 0
LB 1.00 Hz
GB 0
PC 1.40
HO
H
N
OBn
O
F
N
Boc
6.15
rotamers
190 180 170 160 150 140 130 120 110 100 90 80 70 60 50 40 30 20 ppm

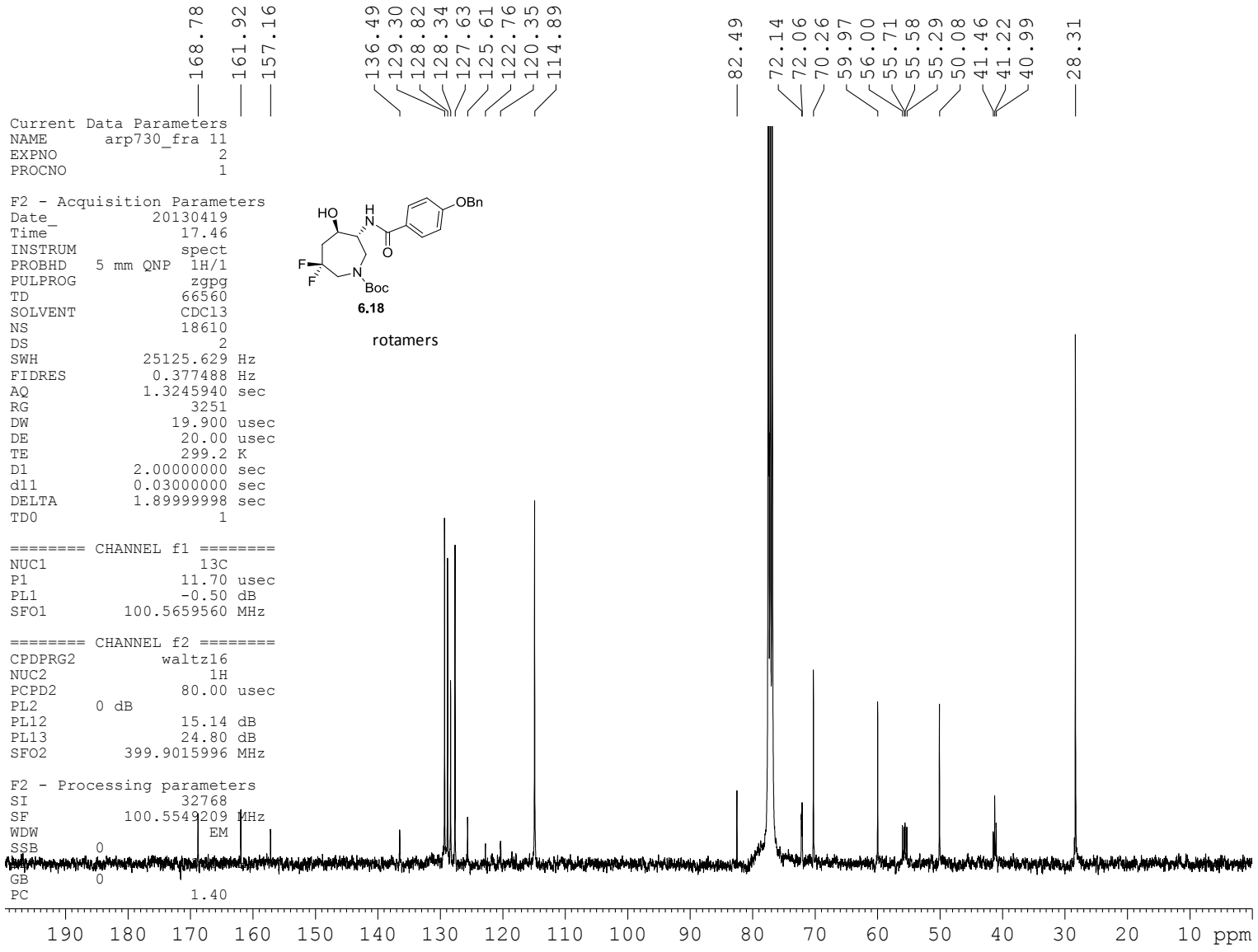

8.99
8.98
7.86
7.84
7.43
7.41
7.40
7.40
7.38
7.36
7.34
7.32
7.24
7.02
7.00
5.11
4.87
4.86
4.74
4.47
4.43
4.39
4.15
4.13
4.09
3.24
3.23
3.20
3.19
3.00
2.96
2.90
2.86
2.33
2.12
2.11
2.08
1.47
HO
H
N
O
OBn
F
N
Boc
6.16
rotamers
Current Data Parameters
NAME arp565_s2bfinal azp
EXPNO 1
PROCNO 1
F2 - Acquisition Parameters
Date_ 20120621
Time 9.19
INSTRUM spect
PROBHD 5 mm QNP 1H/1
PULPROG zg30
TD 32768
SOLVENT CDCl3
NS 16
DS 0
SWH 5995.204 Hz
FIDRES 0.182959 Hz
AQ 2.7329011 sec
RG 912.3
DW 83.400 usec
DE 20.00 usec
TE 296.2 K
D1 2.00000000 sec
TD0 1
======== CHANNEL f1 ========
NUC1 1H
P1 13.50 usec
PL1 3.00 dB
SFO1 399.9023994 MHz
F2 - Processing parameters
SI 32768
SF 399.9000132 MHz
WDW EM
SSB 0
LB 0.30 Hz
GB 0
PC 1.00
9.5
9.0
8.5
8.0
7.5
7.0
6.5
6.0
5.5
5.0
4.5
4.0
3.5
3.0
2.5
2.0
1.5
1.0
0.5
ppm
1.21
2.00
5.01
2.00
2.12
1.00
1.02
3.00
1.00
0.50
0.51
1.01
4.97
9.00

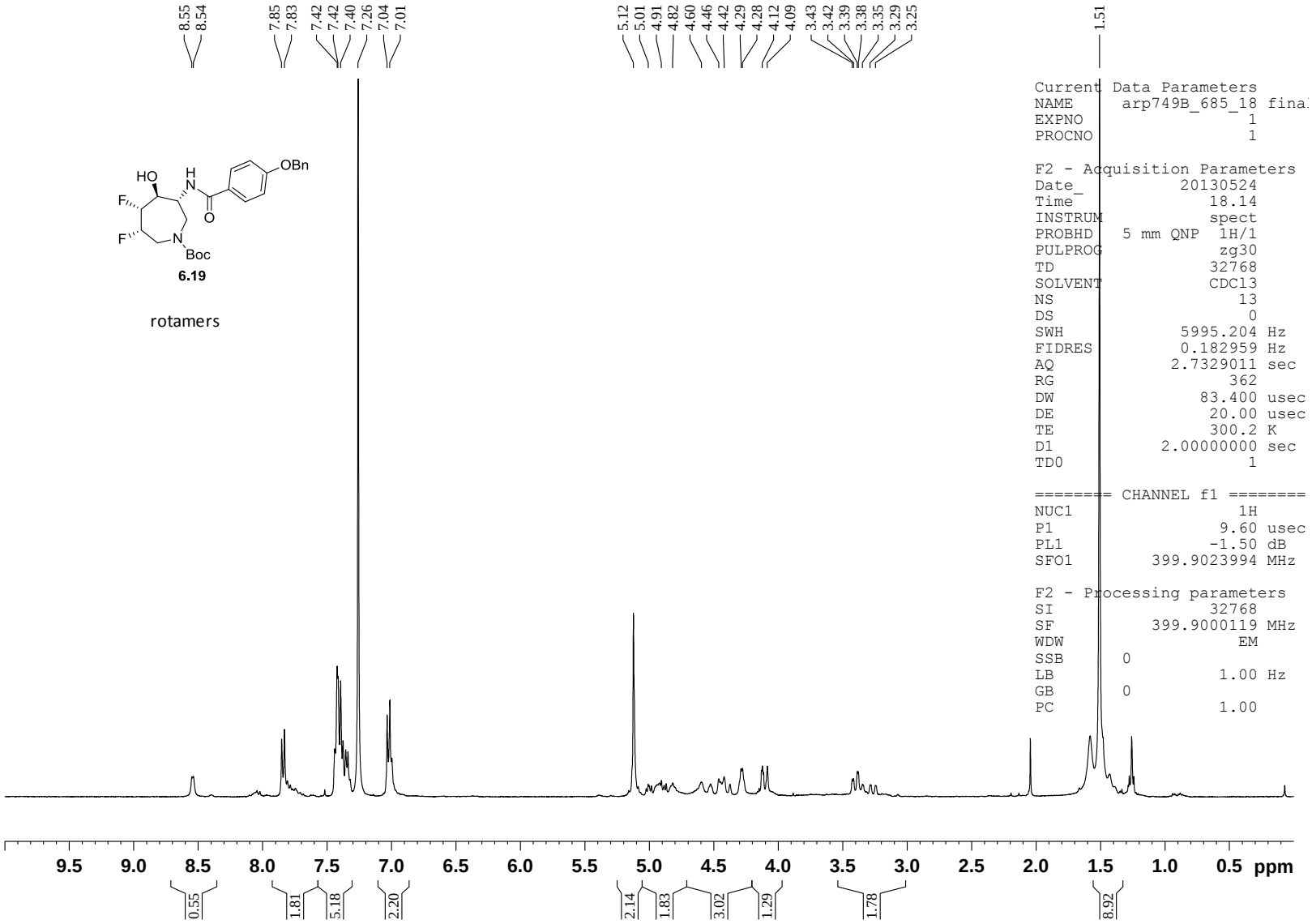

168.79
161.87
157.81
135.72
129.31
128.81
128.32
127.64
114.83
89.67
87.91
81.73
71.73
70.23
60.16
54.58
50.08
37.26
28.36
Current Data Parameters
NAME arp565_s2bfinal azp hplc_7B
EXPNO 2
PROCNO 1
F2 - Acquisition Parameters
Date_ 20120621
Time 9.30
INSTRUM spect
PROBHD 5 mm QNP 1H/1
PULPROG zgpg
TD 66560
SOLVENT CDCl3
NS 3951
DS 2
SWH 25125.629 Hz
FIDRES 0.377488 Hz
AQ 1.3245940 sec
RG 4597.6
DW 19.900 usec
DE 20.00 usec
TE 296.2 K
D1 2.00000000 sec
d11 0.03000000 sec
DELTA 1.89999998 sec
TD0 1
======== CHANNEL f1 ========
NUC1 13C
P1 12.00 usec
PL1 -0.50 dB
SFO1 100.5659560 MHz
======== CHANNEL f2 ========
CPDPRG2 waltz16
NUC2 1H
PCPD2 80.00 usec
PL2 3.00 dB
PL12 18.80 dB
PL13 24.80 dB
SFO2 399.9015996 MHz
F2 - Processing parameters
SI 32768
SF 100.5549202 MHz
WDW EM
SSB 0
LB 1.00
GB 0
PC 1.40
HO
H
N
O
OBn
F
N
Boc
6.16
rotamers
190 180 170 160 150 140 130 120 110 100 90 80 70 60 50 40 30 20 10 ppm

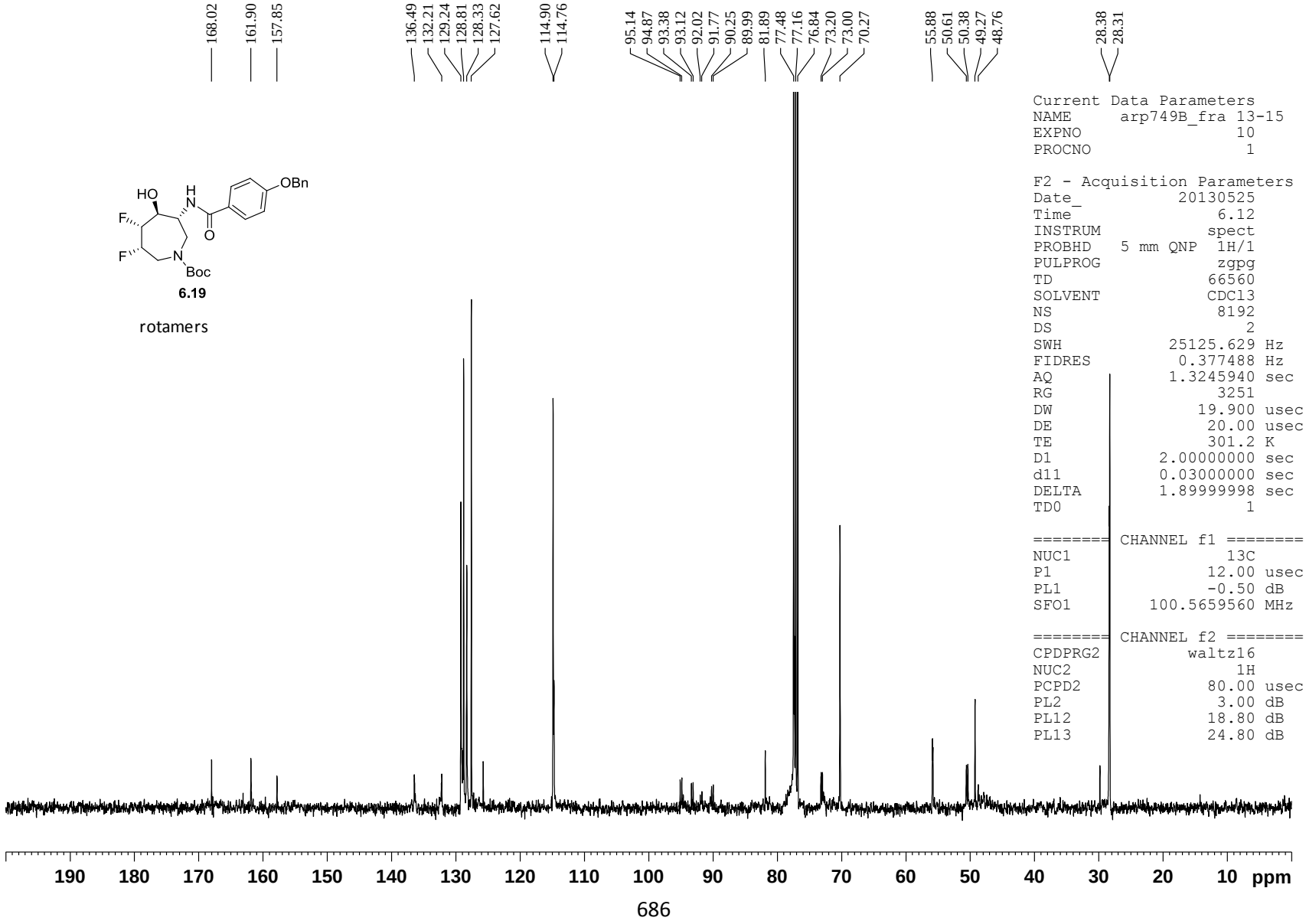

8.36
8.35
7.80
7.78
7.40
7.38
7.36
7.34
7.32
7.24
7.00
6.98
5.09
4.79
4.77
4.75
4.67
4.65
4.63
4.13
4.01
3.99
3.97
3.26
3.25
3.22
3.01
2.97
2.22
2.02
2.00
1.99
1.48
HO
H
N
OBn
F
O
N
Boc
6.17
rotamers
Current Data Parameters
NAME arp564_s2afinal azp
EXPNO 1
PROCNO 1
F2 - Acquisition Parameters
Date_ 20120621
Time 13.35
INSTRUM spect
PROBHD 5 mm QNP 1H/1
PULPROG zg30
TD 32768
SOLVENT CDCl3
NS 32
DS 0
SWH 5995.204 Hz
FIDRES 0.182959 Hz
AQ 2.7329011 sec
RG 812.7
DW 83.400 usec
DE 20.00 usec
TE 295.2 K
D1 2.00000000 sec
TD0 1
======== CHANNEL f1 ========
NUC1 1H
P1 13.50 usec
PL1 3.00 dB
SFO1 399.9023994 MHz
F2 - Processing parameters
SI 32768
SF 399.9000132 MHz
WDW EM
SSB 0
LB 0.30 Hz
GB 0
PC 1.00
9.5
9.0
8.5
8.0
7.5
7.0
6.5
6.0
5.5
5.0
4.5
4.0
3.5
3.0
2.5
2.0
1.5
1.0
0.5
ppm
0.57
1.81
5.49
2.12
2.20
0.97
3.13
1.03
7.49
2.00
8.96

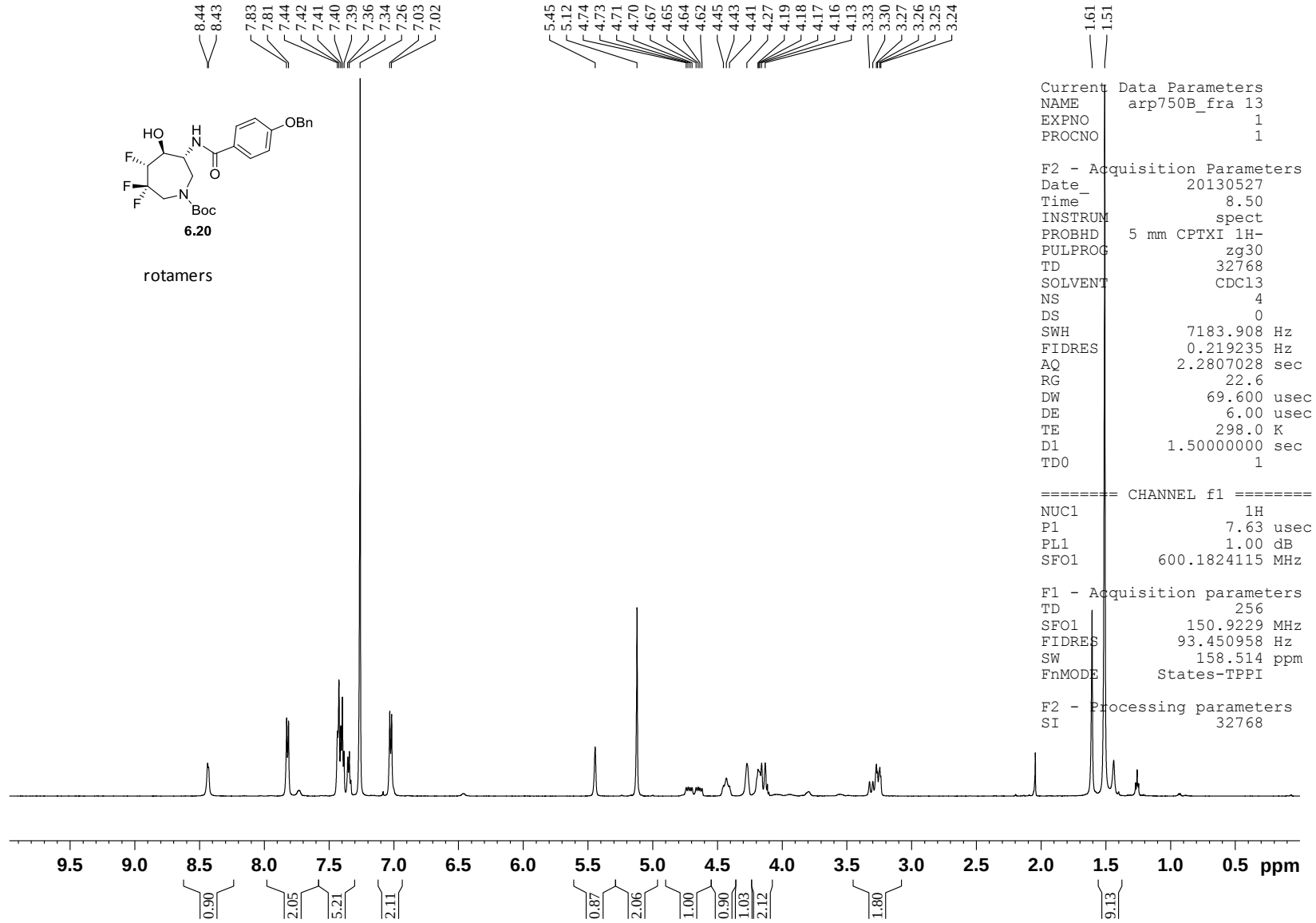

Current Data Parameters
NAME arp564_s2aminal4azp_hplc_10A
EXPNO 2
PROCNO 1
F2 - Acquisition Parameters
Date_ 20120621
Time 13.46
INSTRUM spect
PROBHD 5 mm QNP 1H/1
PULPROG zgpg
TD 66560
SOLVENT CDCl3
NS 19671
DS 2
SWH 25125.629 Hz
FIDRES 0.377488 Hz
AQ 1.3245940 sec
RG 18390.4
DW 19.900 usec
DE 20.00 usec
TE 295.2 K
D1 2.00000000 sec
d11 0.03000000 sec
DELTA 1.89999998 sec
TD0 1
======== CHANNEL f1 ========
NUC1 13C
P1 12.00 usec
PL1 -0.50 dB
SFO1 100.5659560 MHz
======== CHANNEL f2 ========
CPDPRG2 waltz16
NUC2 1H
PCPD2 80.00 usec
PL2 3.00 dB
PL12 18.80 dB
PL13 24.80 dB
SFO2 399.9015996 MHz
F2 - Processing parameters
SI 32768
SF 100.5548950 MHz
WDW GM
SSB 0
LB -1.00 Hz
GB 0.01
PC 1.40
169.80
164.18
157.31
136.66
129.55
129.07
128.61
127.89
125.81
115.13
93.08
91.34
81.79
78.64
78.47
70.50
57.72
47.76
44.66
33.14
32.92
28.73
HO
F
N
H
O
OBn
N
Boc
6.17
rotamers
190 180 170 160 150 140 130 120 110 100 90 80 70 60 50 40 30 20 10 ppm

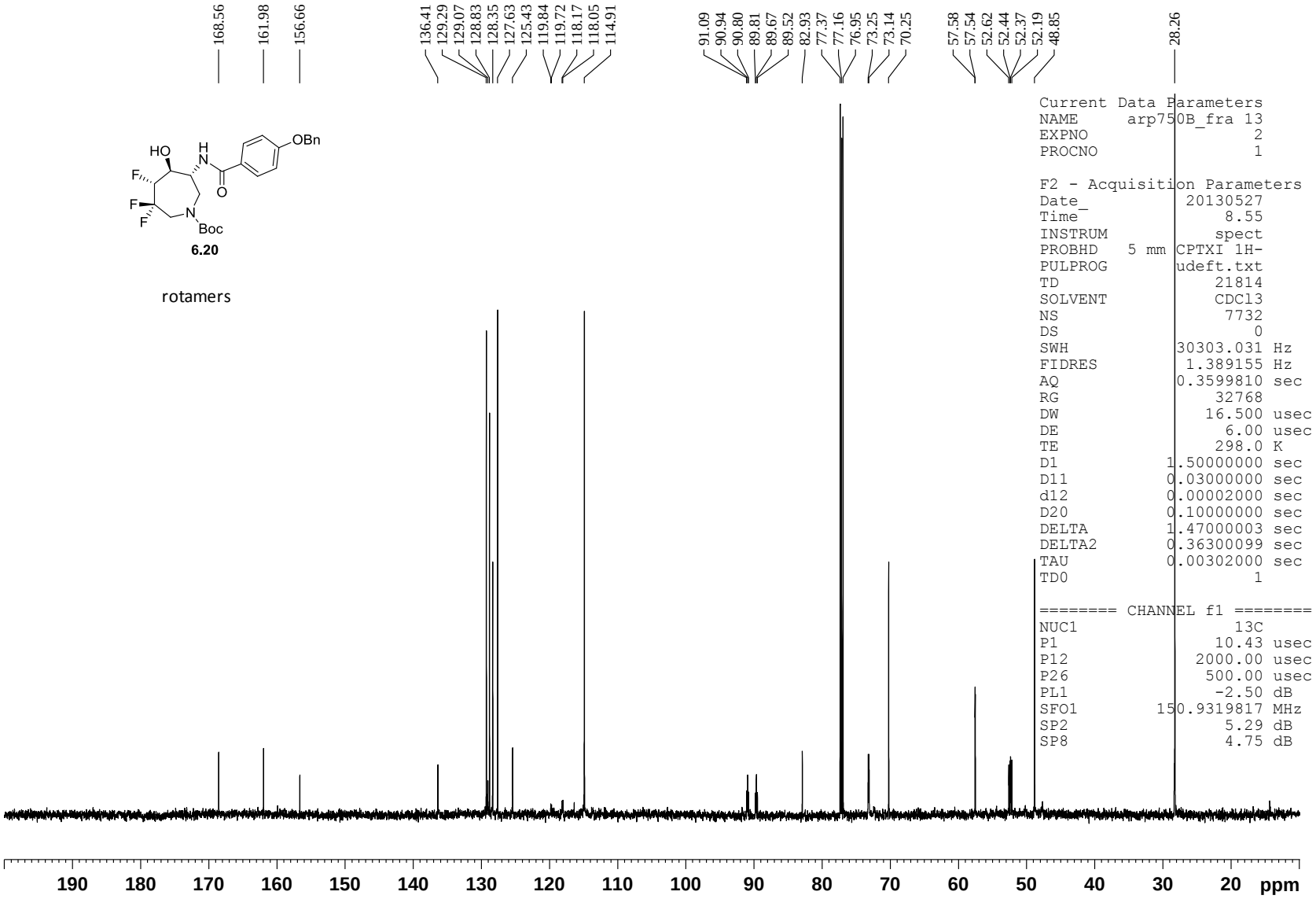

8.84
8.83
7.86
7.42
7.40
7.26
7.04
7.02
5.38
5.13
4.46
4.43
4.39
4.20
4.18
4.16
4.14
4.05
4.03
4.01
3.35
3.33
3.31
3.29
3.15
3.11
3.07
3.03
2.42
2.40
2.38
2.37
2.29
1.50
HO
H
N
OBn
O
F
F
N
Boc
6.18
rotamers
Current Data Parameters
NAME arp730_fra 11
EXPNO 1
PROCNO 1
F2 - Acquisition Parameters
Date_ 20130419
Time 17.43
INSTRUM spect
PROBHD 5 mm QNP 1H/1
PULPROG zg30
TD 32768
SOLVENT CDCl3
NS 16
DS 0
SWH 5995.204 Hz
FIDRES 0.182959 Hz
AQ 2.7329011 sec
RG 724.1
DW 83.400 usec
DE 20.00 usec
TE 298.2 K
D1 2.00000000 sec
TD0 1
======== CHANNEL f1 ========
NUC1 1H
P1 9.60 usec
PL1 -1.50 dB
SFO1 399.9023994 MHz
F2 - Processing parameters
SI 32768
SF 399.9000122 MHz
WDW EM
SSB 0
LB 1.00 Hz
GB 0
PC 1.00
9.5
9.0
8.5
8.0
7.5
7.0
6.5
6.0
5.5
5.0
4.5
4.0
3.5
3.0
2.5
2.0
1.5
1.0
0.5
ppm
0.88
2.04
4.89
2.10
0.94
2.02
1.03
1.93
1.04
1.01
0.57
0.59
2.00
8.94

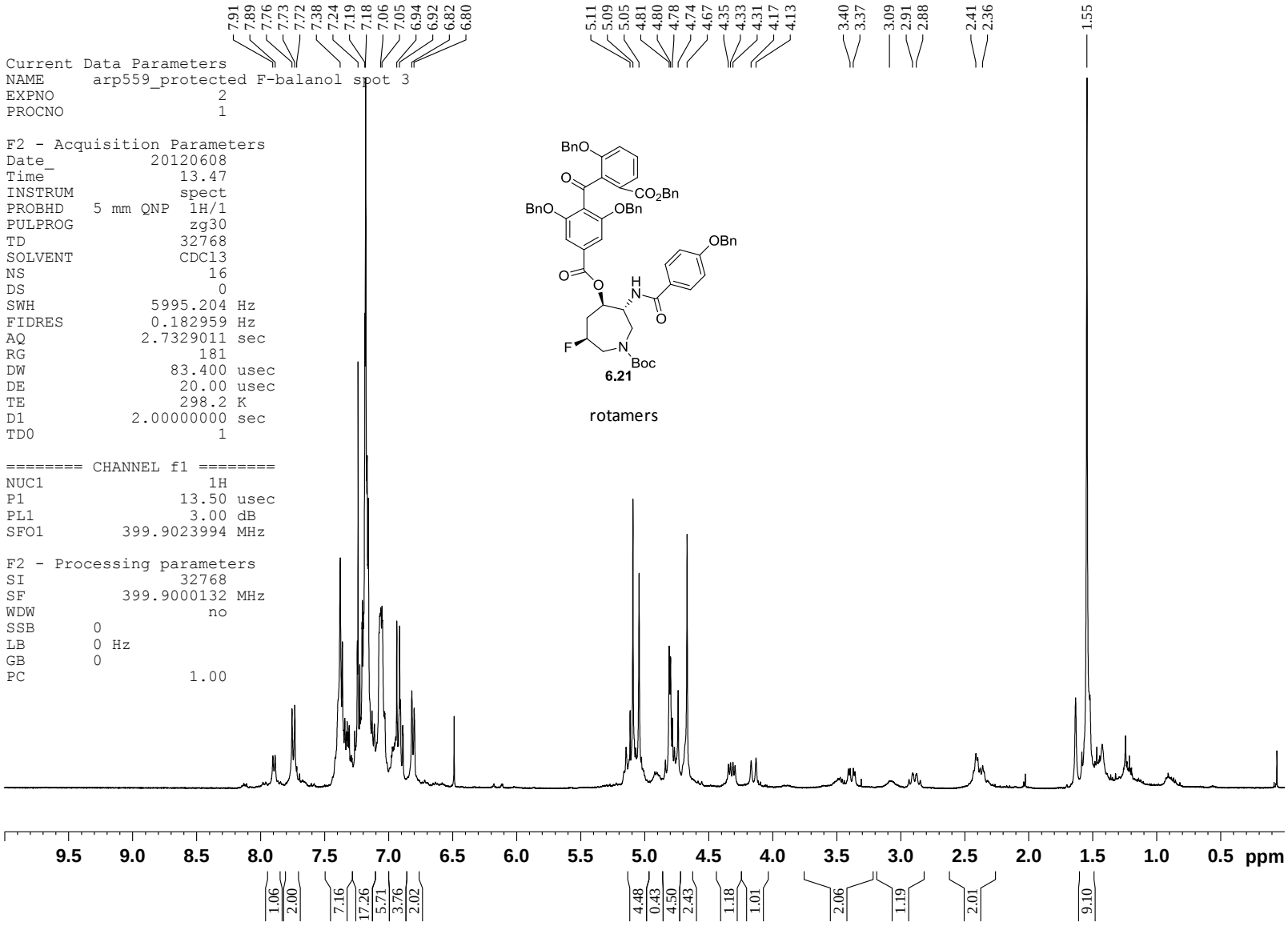

168.78
161.92
157.16
136.49
129.30
128.82
128.34
127.63
125.61
122.76
120.35
114.89
82.49
72.14
72.06
70.26
59.97
56.00
55.71
55.58
55.29
50.08
41.46
41.22
40.99
28.31
Current Data Parameters
NAME arp730_fra 11
EXPNO 2
PROCNO 1
F2 - Acquisition Parameters
Date_ 20130419
Time 17.46
INSTRUM spect
PROBHD 5 mm QNP 1H/1
PULPROG zgpg
TD 66560
SOLVENT CDCl3
NS 18610
DS 2
SWH 25125.629 Hz
FIDRES 0.377488 Hz
AQ 1.3245940 sec
RG 3251
DW 19.900 usec
DE 20.00 usec
TE 299.2 K
D1 2.00000000 sec
d11 0.03000000 sec
DELTA 1.89999998 sec
TD0 1
======== CHANNEL f1 ========
NUC1 13C
P1 11.70 usec
PL1 -0.50 dB
SFO1 100.5659560 MHz
======== CHANNEL f2 ========
CPDPRG2 waltz16
NUC2 1H
PCPD2 80.00 usec
PL2 0 dB
PL12 15.14 dB
PL13 24.80 dB
SFO2 399.9015996 MHz
F2 - Processing parameters
SI 32768
SF 100.5549209 MHz
WDW EM
SSB 0
LB 0
GB 0
PC 1.40
HO
H
N
O
OBn
F
F
N
Boc
6.18
rotamers
190 180 170 160 150 140 130 120 110 100 90 80 70 60 50 40 30 20 10 ppm

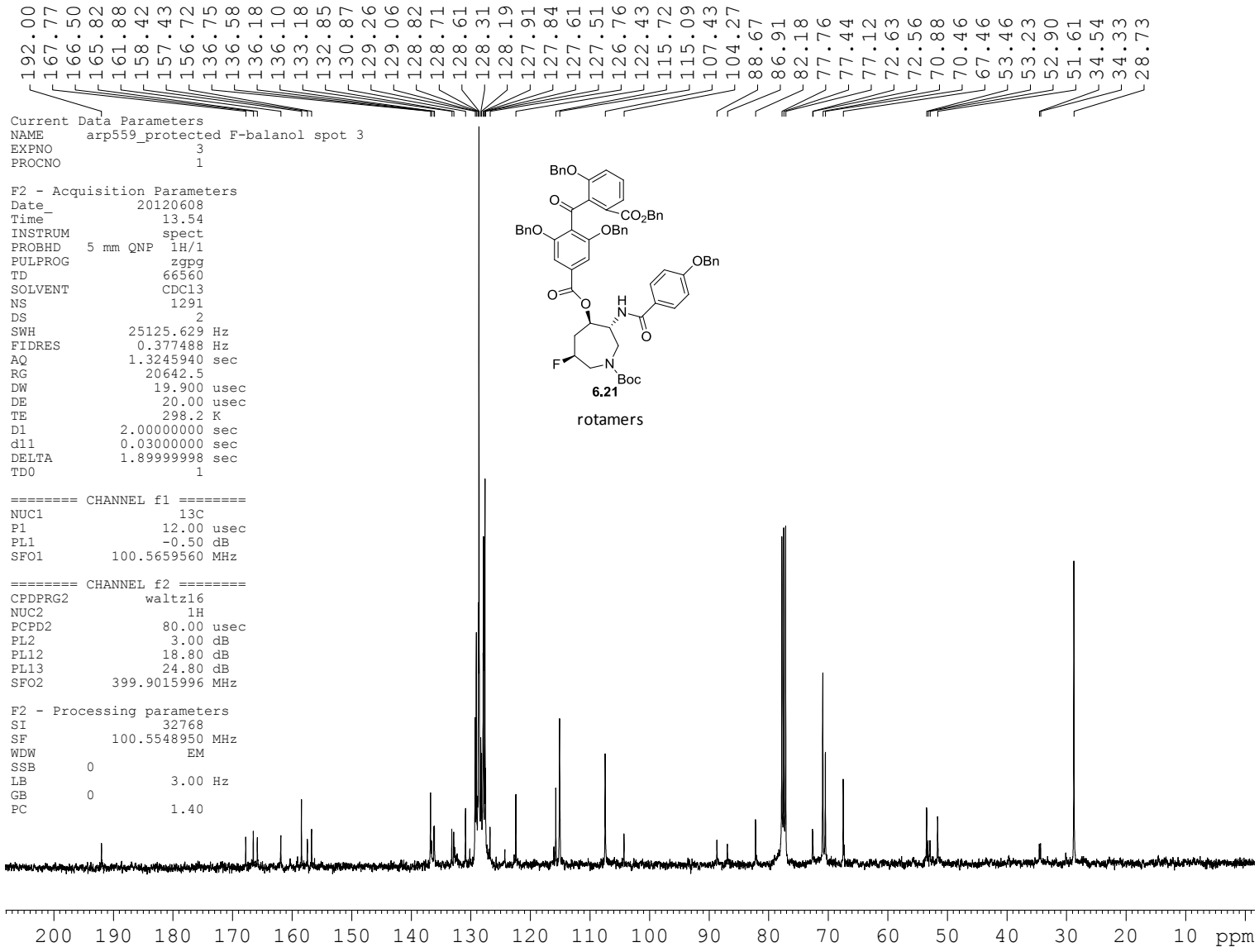

8.55
8.54
7.85
7.83
7.42
7.42
7.40
7.26
7.04
7.01
5.12
5.01
4.91
4.82
4.60
4.46
4.42
4.29
4.28
4.12
4.09
3.43
3.42
3.39
3.38
3.35
3.29
3.25
1.51
HO
H
N
OBn
F
O
F
N
Boc
6.19
rotamers
Current Data Parameters
NAME arp749B_685_18 fina
EXPNO 1
PROCNO 1
F2 - Acquisition Parameters
Date_ 20130524
Time 18.14
INSTRUM spect
PROBHD 5 mm QNP 1H/1
PULPROG zg30
TD 32768
SOLVENT CDC13
NS 13
DS 0
SWH 5995.204 Hz
FIDRES 0.182959 Hz
AQ 2.7329011 sec
RG 362
DW 83.400 usec
DE 20.00 usec
TE 300.2 K
D1 2.00000000 sec
TD0 1
======== CHANNEL f1 ========
NUC1 1H
P1 9.60 usec
PL1 -1.50 dB
SFO1 399.9023994 MHz
F2 - Processing parameters
SI 32768
SF 399.9000119 MHz
WDW EM
SSB 0
LB 1.00 Hz
GB 0
PC 1.00
9.5
9.0
8.5
8.0
7.5
7.0
6.5
6.0
5.5
5.0
4.5
4.0
3.5
3.0
2.5
2.0
1.5
1.0
0.5
ppm
0.55
1.81
5.18
2.20
2.14
1.83
3.02
1.29
1.78
8.92

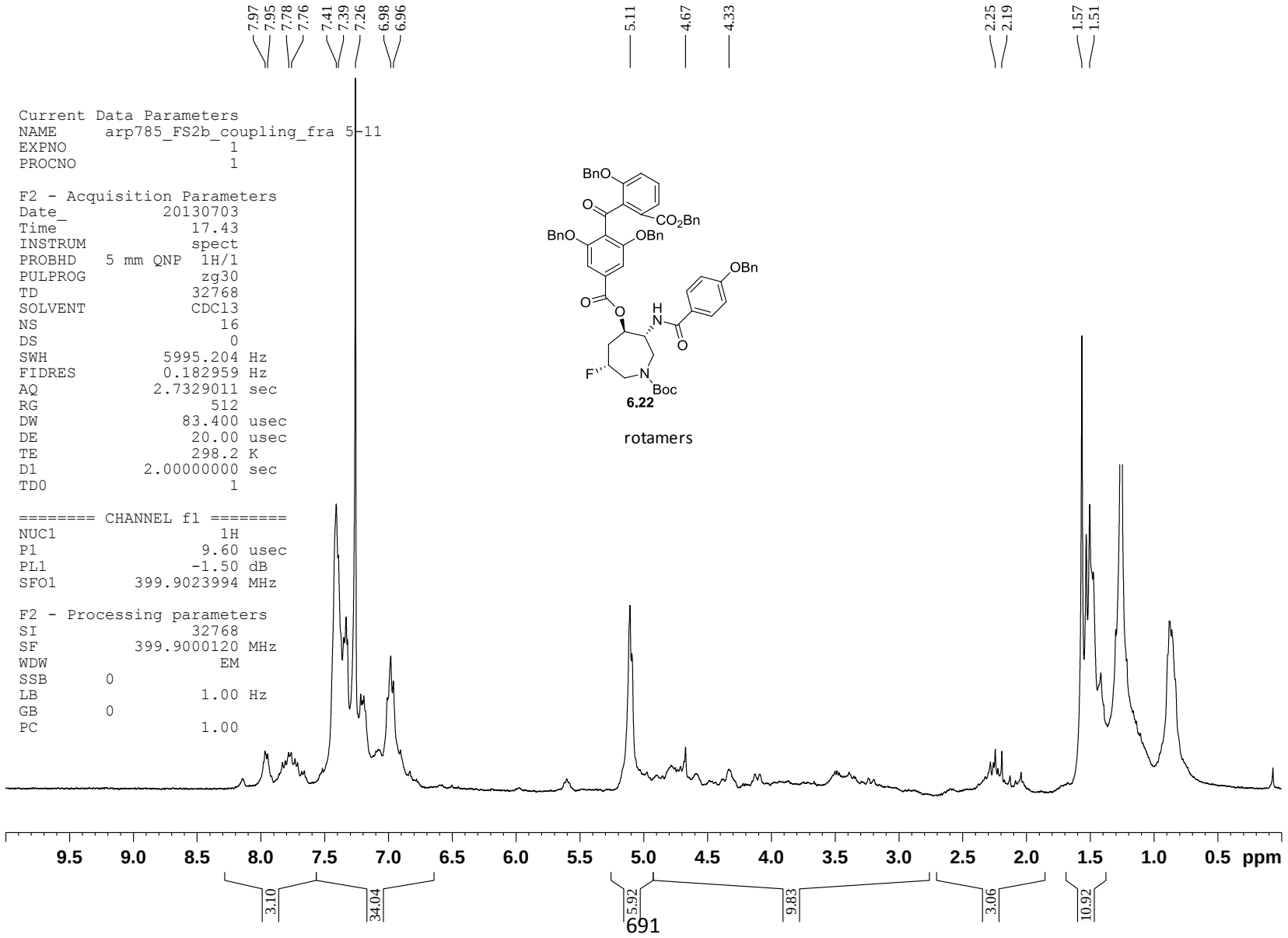

168.02
161.90
157.85
136.49
132.21
129.24
128.81
128.33
127.62
114.90
114.76
95.14
94.87
93.38
93.12
92.02
91.77
90.25
89.99
81.89
77.48
77.16
76.84
73.20
73.00
70.27
55.88
50.61
50.38
49.27
48.76
28.38
28.31
HO
H
N
OBn
F
O
F
N
Boc
6.19
rotamers
Current Data Parameters
NAME arp749B_fra 13-15
EXPNO 10
PROCNO 1
F2 - Acquisition Parameters
Date_ 20130525
Time 6.12
INSTRUM spect
PROBHD 5 mm QNP 1H/1
PULPROG zgpg
TD 66560
SOLVENT CDCl3
NS 8192
DS 2
SWH 25125.629 Hz
FIDRES 0.377488 Hz
AQ 1.3245940 sec
RG 3251
DW 19.900 usec
DE 20.00 usec
TE 301.2 K
D1 2.00000000 sec
d11 0.03000000 sec
DELTA 1.89999998 sec
TD0 1
======== CHANNEL f1 ========
NUC1 13C
P1 12.00 usec
PL1 -0.50 dB
SFO1 100.5659560 MHz
======== CHANNEL f2 ========
CPDPRG2 waltz16
NUC2 1H
PCPD2 80.00 usec
PL2 3.00 dB
PL12 18.80 dB
PL13 24.80 dB
190 180 170 160 150 140 130 120 110 100 90 80 70 60 50 40 30 20 10 ppm

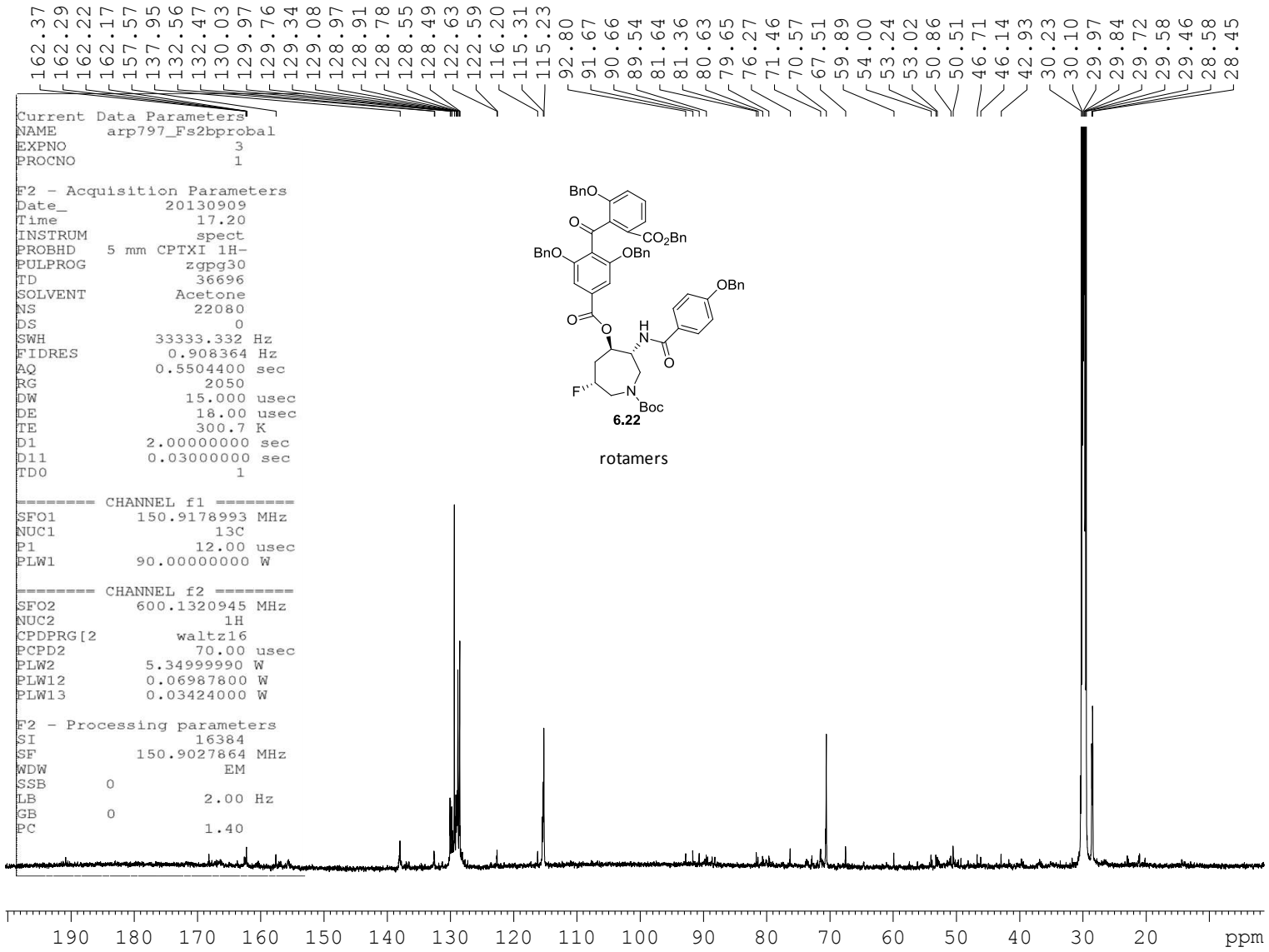

8.44
8.43
7.83
7.81
7.44
7.42
7.41
7.40
7.39
7.36
7.34
7.26
7.03
7.02
5.45
5.12
4.74
4.73
4.71
4.70
4.67
4.65
4.64
4.62
4.45
4.43
4.41
4.27
4.19
4.18
4.17
4.16
4.13
3.33
3.30
3.27
3.26
3.25
3.24
1.61
1.51
HO
H
N
OBn
F
F
F
N
Boc
O
6.20
rotamers
Current Data Parameters
NAME arp750B_fra 13
EXPNO 1
PROCNO 1
F2 - Acquisition Parameters
Date_ 20130527
Time 8.50
INSTRUM spect
PROBHD 5 mm CPTXI 1H-
PULPROG zg30
TD 32768
SOLVENT CDCl3
NS 4
DS 0
SWH 7183.908 Hz
FIDRES 0.219235 Hz
AQ 2.2807028 sec
RG 22.6
DW 69.600 usec
DE 6.00 usec
TE 298.0 K
D1 1.50000000 sec
TD0 1
======== CHANNEL f1 ========
NUC1 1H
P1 7.63 usec
PL1 1.00 dB
SFO1 600.1824115 MHz
F1 - Acquisition parameters
TD 256
SFO1 150.9229 MHz
FIDRES 93.450958 Hz
SW 158.514 ppm
FnMODE States-TPPI
F2 - Processing parameters
SI 32768
9.5
9.0
8.5
8.0
7.5
7.0
6.5
6.0
5.5
5.0
4.5
4.0
3.5
3.0
2.5
2.0
1.5
1.0
0.5
ppm
0.90
2.05
5.21
2.11
0.87
2.06
1.00
0.90
1.03
2.12
1.80
9.13

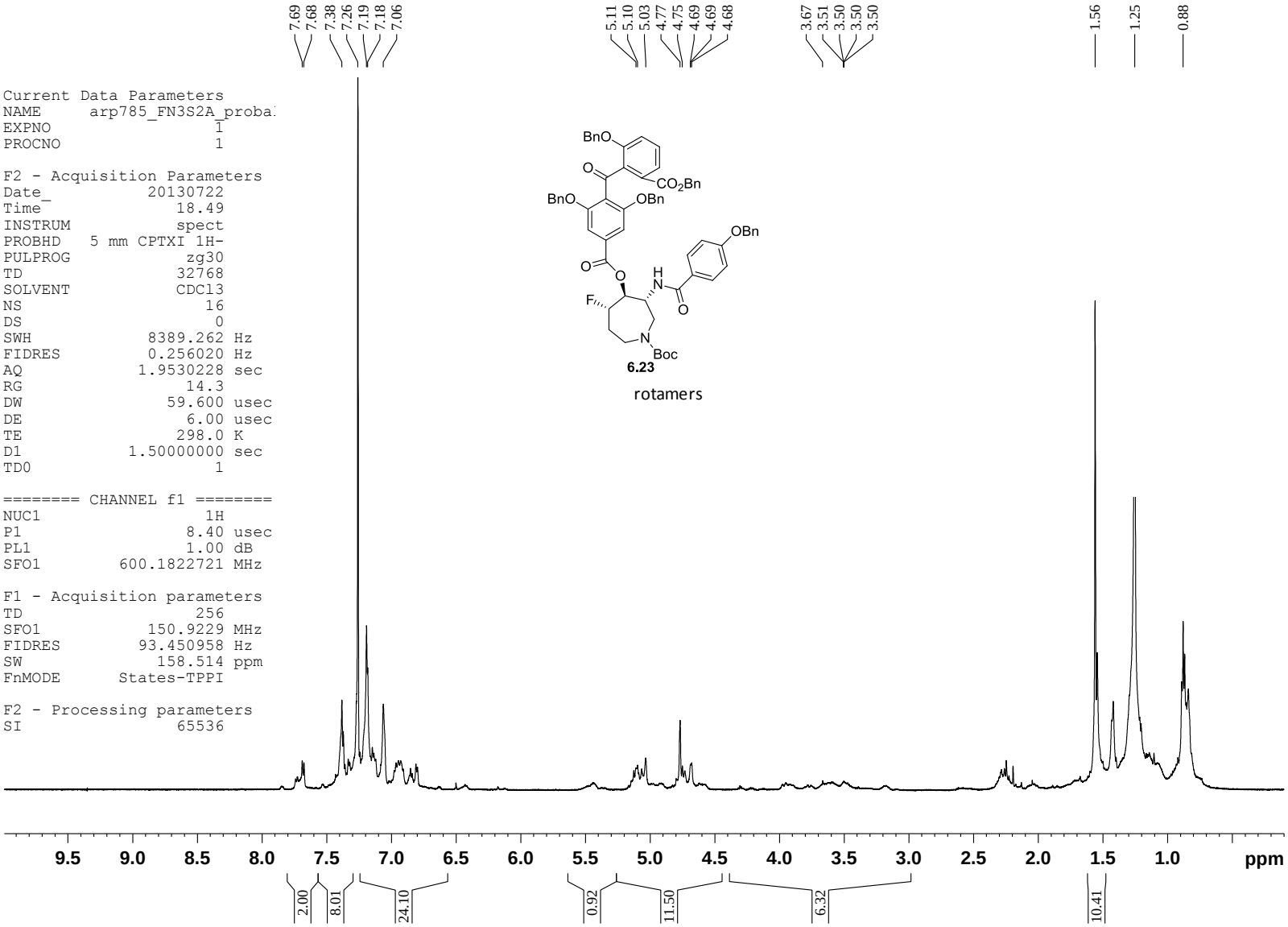

168.56
161.98
156.66
136.41
129.29
129.07
128.83
128.35
127.63
125.43
119.84
119.72
118.17
118.05
114.91
91.09
90.94
90.80
89.81
89.67
89.52
82.93
77.37
77.16
76.95
73.25
73.14
70.25
57.58
57.54
52.62
52.44
52.37
52.19
48.85
28.26
HO
H
N
OBn
F
F
F
N
O
Boc
6.20
rotamers
Current Data Parameters
NAME arp750B_fra 13
EXPNO 2
PROCNO 1
F2 - Acquisition Parameters
Date_ 20130527
Time_ 8.55
INSTRUM spect
PROBHD 5 mm CPTXI 1H-
PULPROG udeft.txt
TD 21814
SOLVENT CDCl3
NS 7732
DS 0
SWH 30303.031 Hz
FIDRES 1.389155 Hz
AQ 0.3599810 sec
RG 32768
DW 16.500 usec
DE 6.00 usec
TE 298.0 K
D1 1.50000000 sec
D11 0.03000000 sec
d12 0.00002000 sec
D20 0.10000000 sec
DELTA 1.47000003 sec
DELTA2 0.36300099 sec
TAU 0.00302000 sec
TD0 1
======== CHANNEL f1 ========
NUC1 13C
P1 10.43 usec
P12 2000.00 usec
P26 500.00 usec
PL1 -2.50 dB
SFO1 150.9319817 MHz
SP2 5.29 dB
SP8 4.75 dB
190
180
170
160
150
140
130
120
110
100
90
80
70
60
50
40
30
20
ppm

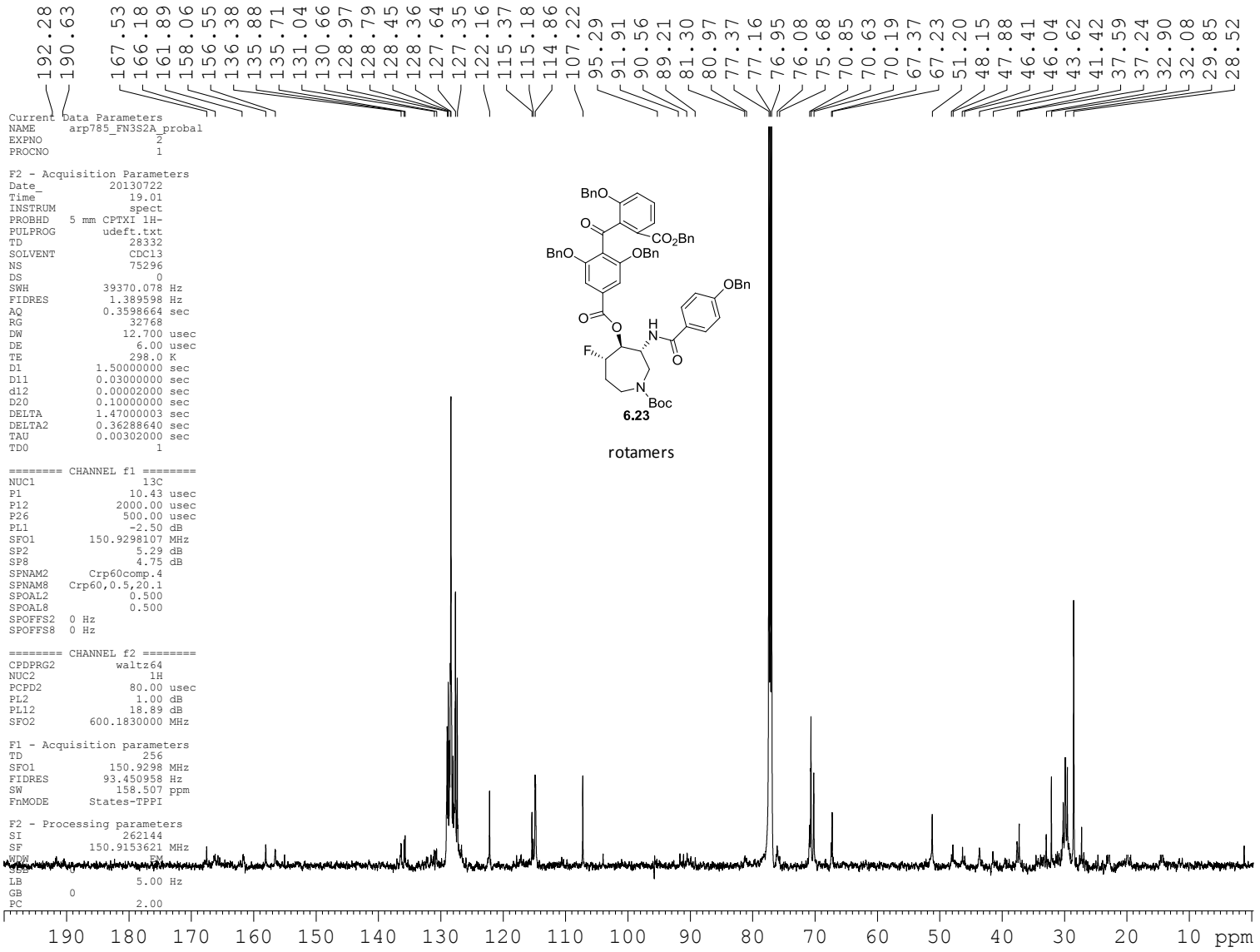

Current Data Parameters
NAME arp559_protected F-balanol spot 3
EXPNO 2
PROCNO 1
F2 - Acquisition Parameters
Date_ 20120608
Time 13.47
INSTRUM spect
PROBHD 5 mm QNP 1H/1
PULPROG zg30
TD 32768
SOLVENT CDCl3
NS 16
DS 0
SWH 5995.204 Hz
FIDRES 0.182959 Hz
AQ 2.7329011 sec
RG 181
DW 83.400 usec
DE 20.00 usec
TE 298.2 K
D1 2.00000000 sec
TD0 1
======== CHANNEL f1 ========
NUC1 1H
P1 13.50 usec
PL1 3.00 dB
SFO1 399.9023994 MHz
F2 - Processing parameters
SI 32768
SF 399.9000132 MHz
WDW no
SSB 0
LB 0 Hz
GB 0
PC 1.00
7.91 7.89 7.76 7.73 7.72 7.38 7.24 7.19 7.18 7.06 7.05 6.94 6.92 6.82 6.80
5.11 5.09 5.05 4.81 4.80 4.78 4.74 4.67 4.35 4.33 4.31 4.17 4.13
3.40 3.37 3.09 2.91 2.88 2.41 2.36 1.55
BnO
CO2Bn
OBn
OBn
F
Boc
6.21
rotamers
9.5 9.0 8.5 8.0 7.5 7.0 6.5 6.0 5.5 5.0 4.5 4.0 3.5 3.0 2.5 2.0 1.5 1.0 0.5 ppm
1.06 2.00 7.16 17.26 5.71 3.76 2.02 4.48 0.43 4.50 2.43 1.18 1.01 2.06 1.19 2.01 9.10

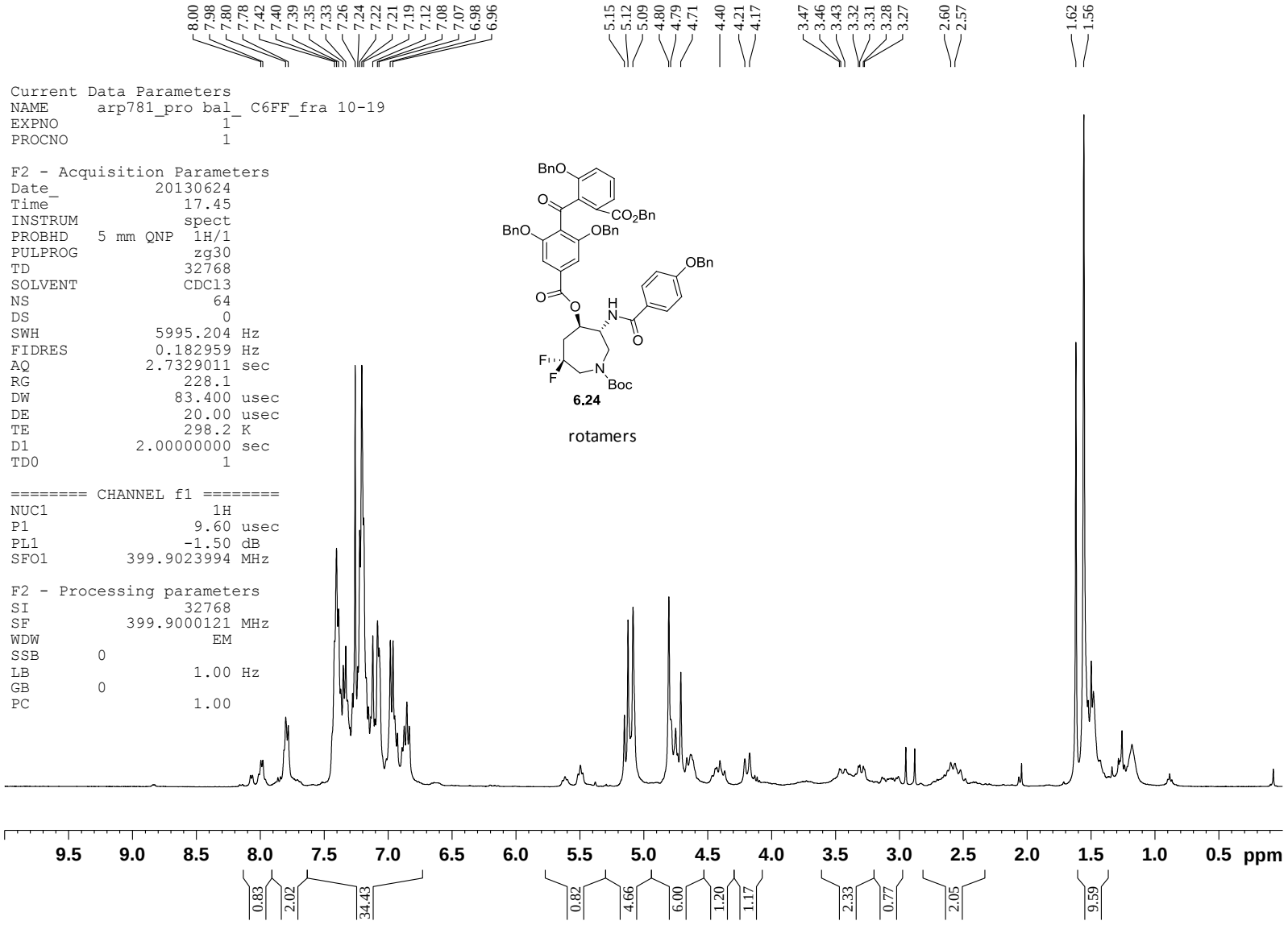

192.00
167.77
166.50
165.82
161.88
158.42
157.43
156.72
136.75
136.58
136.18
136.10
133.18
132.85
130.87
129.26
129.06
128.82
128.71
128.61
128.31
128.19
127.91
127.84
127.61
127.51
126.76
122.43
115.72
115.09
107.43
104.27
88.67
86.91
82.18
77.76
77.44
77.12
72.63
72.56
70.88
70.46
67.46
53.46
53.23
52.90
51.61
34.54
34.33
28.73
Current Data Parameters
NAME arp559_protected F-balanol spot 3
EXPNO 3
PROCNO 1
F2 - Acquisition Parameters
Date_ 20120608
Time 13.54
INSTRUM spect
PROBHD 5 mm QNP 1H/1
PULPROG zgpg
TD 66560
SOLVENT CDCl3
NS 1291
DS 2
SWH 25125.629 Hz
FIDRES 0.377488 Hz
AQ 1.3245940 sec
RG 20642.5
DW 19.900 usec
DE 20.00 usec
TE 298.2 K
D1 2.00000000 sec
d11 0.03000000 sec
DELTA 1.89999998 sec
TD0 1
======== CHANNEL f1 ========
NUC1 13C
P1 12.00 usec
PL1 -0.50 dB
SFO1 100.5659560 MHz
======== CHANNEL f2 ========
CPDPRG2 waltz16
NUC2 1H
PCPD2 80.00 usec
PL2 3.00 dB
PL12 18.80 dB
PL13 24.80 dB
SFO2 399.9015996 MHz
F2 - Processing parameters
SI 32768
SF 100.5548950 MHz
WDW EM
SSB 0
LB 3.00 Hz
GB 0
PC 1.40
BnO
CO2Bn
OBn
OBn
H
N
O
F
N
Boc
6.21
rotamers
200 190 180 170 160 150 140 130 120 110 100 90 80 70 60 50 40 30 20 10 ppm

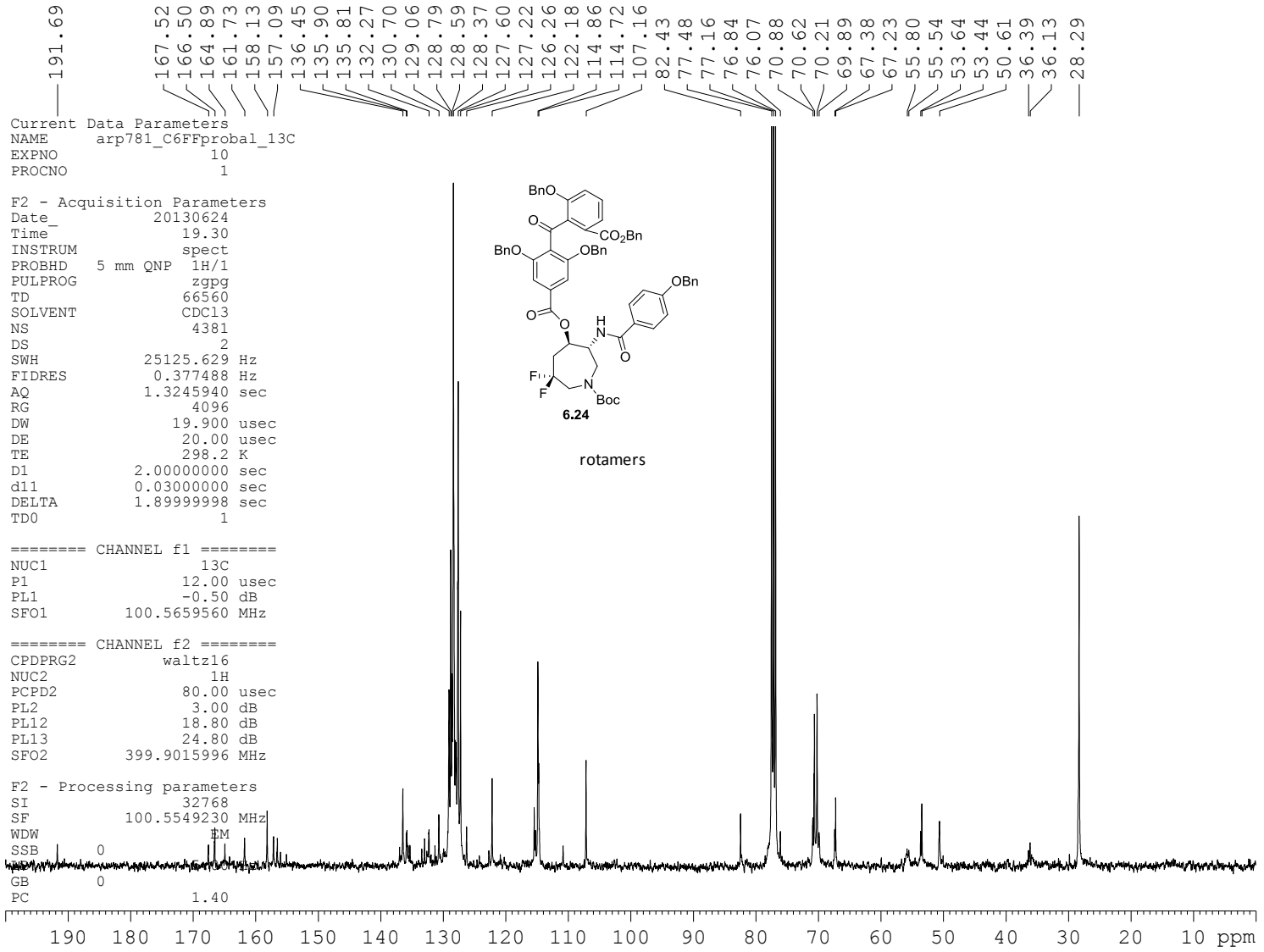

7.97
7.95
7.78
7.76
7.41
7.39
7.26
6.98
6.96
5.11
4.67
4.33
2.25
2.19
1.57
1.51
Current Data Parameters
NAME arp785_FS2b_coupling_fra 5-11
EXPNO 1
PROCNO 1
F2 - Acquisition Parameters
Date_ 20130703
Time 17.43
INSTRUM spect
PROBHD 5 mm QNP 1H/1
PULPROG zg30
TD 32768
SOLVENT CDCl3
NS 16
DS 0
SWH 5995.204 Hz
FIDRES 0.182959 Hz
AQ 2.7329011 sec
RG 512
DW 83.400 usec
DE 20.00 usec
TE 298.2 K
D1 2.00000000 sec
TD0 1
======== CHANNEL f1 ========
NUC1 1H
P1 9.60 usec
PL1 -1.50 dB
SFO1 399.9023994 MHz
F2 - Processing parameters
SI 32768
SF 399.9000120 MHz
WDW EM
SSB 0
LB 1.00 Hz
GB 0
PC 1.00
BnO
CO2Bn
OBn
OBn
H
N
O
F
N
Boc
6.22
rotamers
9.5
9.0
8.5
8.0
7.5
7.0
6.5
6.0
5.5
5.0
4.5
4.0
3.5
3.0
2.5
2.0
1.5
1.0
0.5
ppm
3.10
34.04
5.92
9.83
3.06
10.92

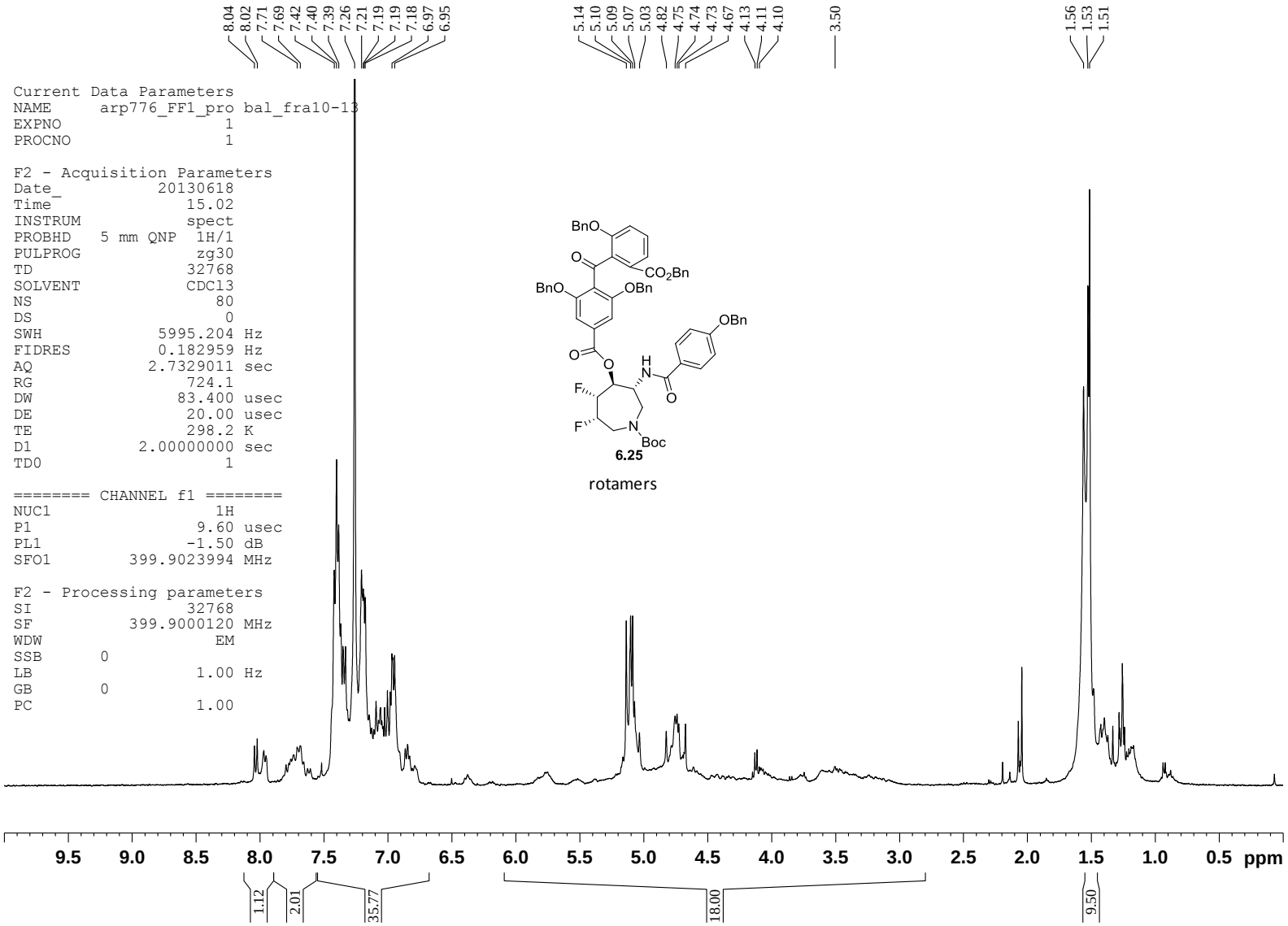

162.37 162.29 162.22 162.17 157.57 137.95 132.56 132.47 130.03 129.97 129.76 129.34 129.08 128.97 128.91 128.78 128.55 128.49 122.63 122.59 116.20 115.31 115.23
92.80 91.67 90.66 89.54 81.64 81.36 80.63 79.65 76.27 71.46 70.57 67.51 59.89 54.00 53.24 53.02 50.86 50.51 46.71 46.14 42.93 30.23 30.10 29.97 29.84 29.72 29.58 29.46 28.58 28.45
Current Data Parameters
NAME arp797_Fs2bprobal
EXPNO 3
PROCNO 1
F2 - Acquisition Parameters
Date_ 20130909
Time 17.20
INSTRUM spect
PROBHD 5 mm CPTXI 1H-
PULPROG zgpg30
TD 36696
SOLVENT Acetone
NS 22080
DS 0
SWH 33333.332 Hz
FIDRES 0.908364 Hz
AQ 0.5504400 sec
RG 2050
DW 15.000 usec
DE 18.00 usec
TE 300.7 K
D1 2.00000000 sec
D11 0.03000000 sec
TD0 1
======== CHANNEL f1 ========
SFO1 150.9178993 MHz
NUC1 13C
P1 12.00 usec
PLW1 90.00000000 W
======== CHANNEL f2 ========
SFO2 600.1320945 MHz
NUC2 1H
CPDPRG[2 waltz16
PCPD2 70.00 usec
PLW2 5.34999990 W
PLW12 0.06987800 W
PLW13 0.03424000 W
F2 - Processing parameters
SI 16384
SF 150.9027864 MHz
WDW EM
SSB 0
LB 2.00 Hz
GB 0
PC 1.40
BnO
CO2Bn
OBn
OBn
F
N
Boc
6.22
rotamers
190 180 170 160 150 140 130 120 110 100 90 80 70 60 50 40 30 20 ppm

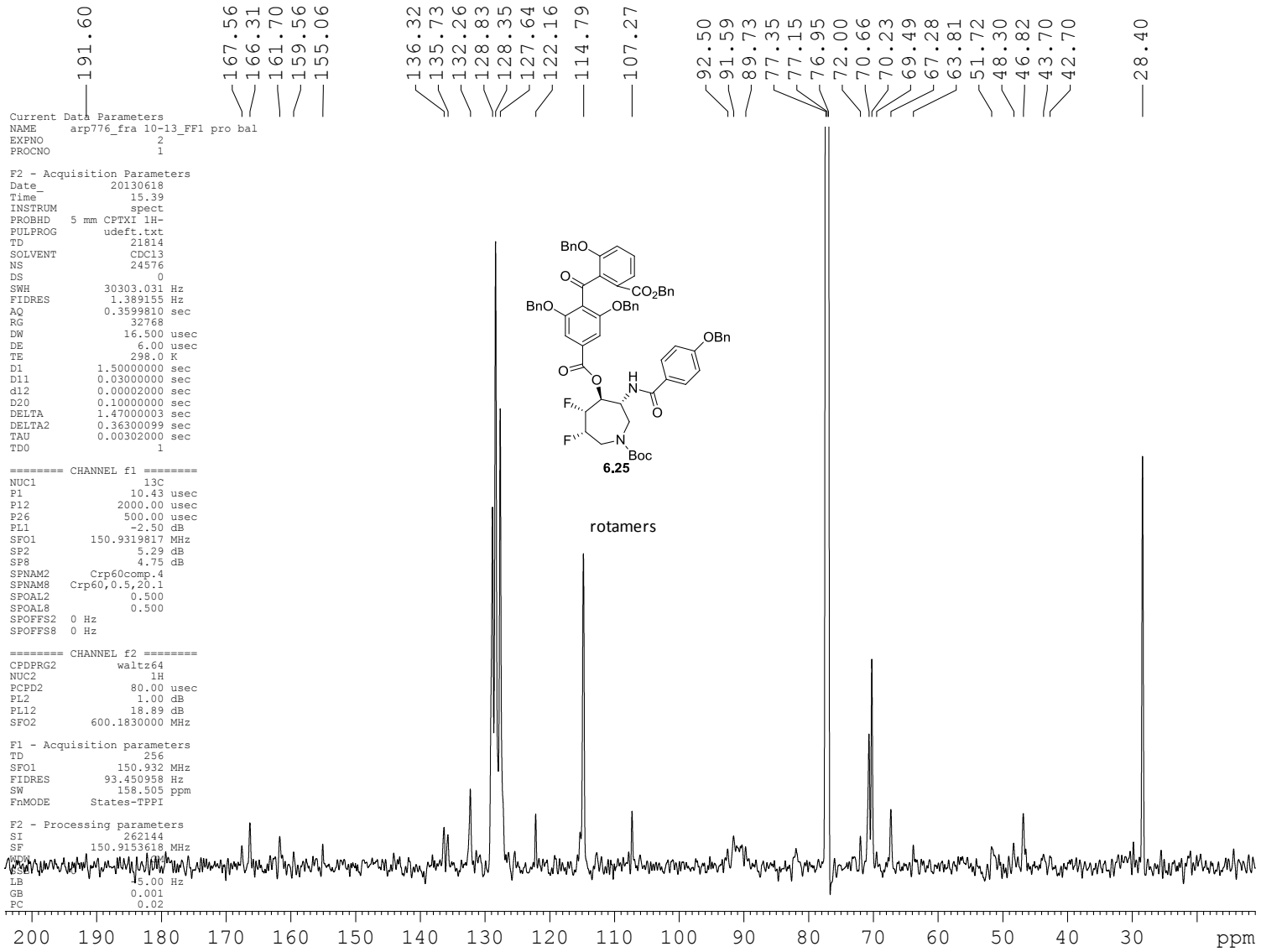

7.69
7.68
7.38
7.26
7.19
7.18
7.06
5.11
5.10
5.03
4.77
4.75
4.69
4.69
4.68
3.67
3.51
3.50
3.50
3.50
1.56
1.25
0.88
Current Data Parameters
NAME arp785_FN3S2A_proba
EXPNO 1
PROCNO 1
F2 - Acquisition Parameters
Date_ 20130722
Time 18.49
INSTRUM spect
PROBHD 5 mm CPTXI 1H-
PULPROG zg30
TD 32768
SOLVENT CDCl3
NS 16
DS 0
SWH 8389.262 Hz
FIDRES 0.256020 Hz
AQ 1.9530228 sec
RG 14.3
DW 59.600 usec
DE 6.00 usec
TE 298.0 K
D1 1.50000000 sec
TD0 1
======== CHANNEL f1 ========
NUC1 1H
P1 8.40 usec
PL1 1.00 dB
SFO1 600.1822721 MHz
F1 - Acquisition parameters
TD 256
SFO1 150.9229 MHz
FIDRES 93.450958 Hz
SW 158.514 ppm
FnMODE States-TPPI
F2 - Processing parameters
SI 65536
BnO
O
CO2Bn
BnO
OBn
OBn
O
O
H
N
F
O
N
Boc
6.23
rotamers
9.5
9.0
8.5
8.0
7.5
7.0
6.5
6.0
5.5
5.0
4.5
4.0
3.5
3.0
2.5
2.0
1.5
1.0
ppm
2.00
8.01
24.10
0.92
11.50
6.32
10.41

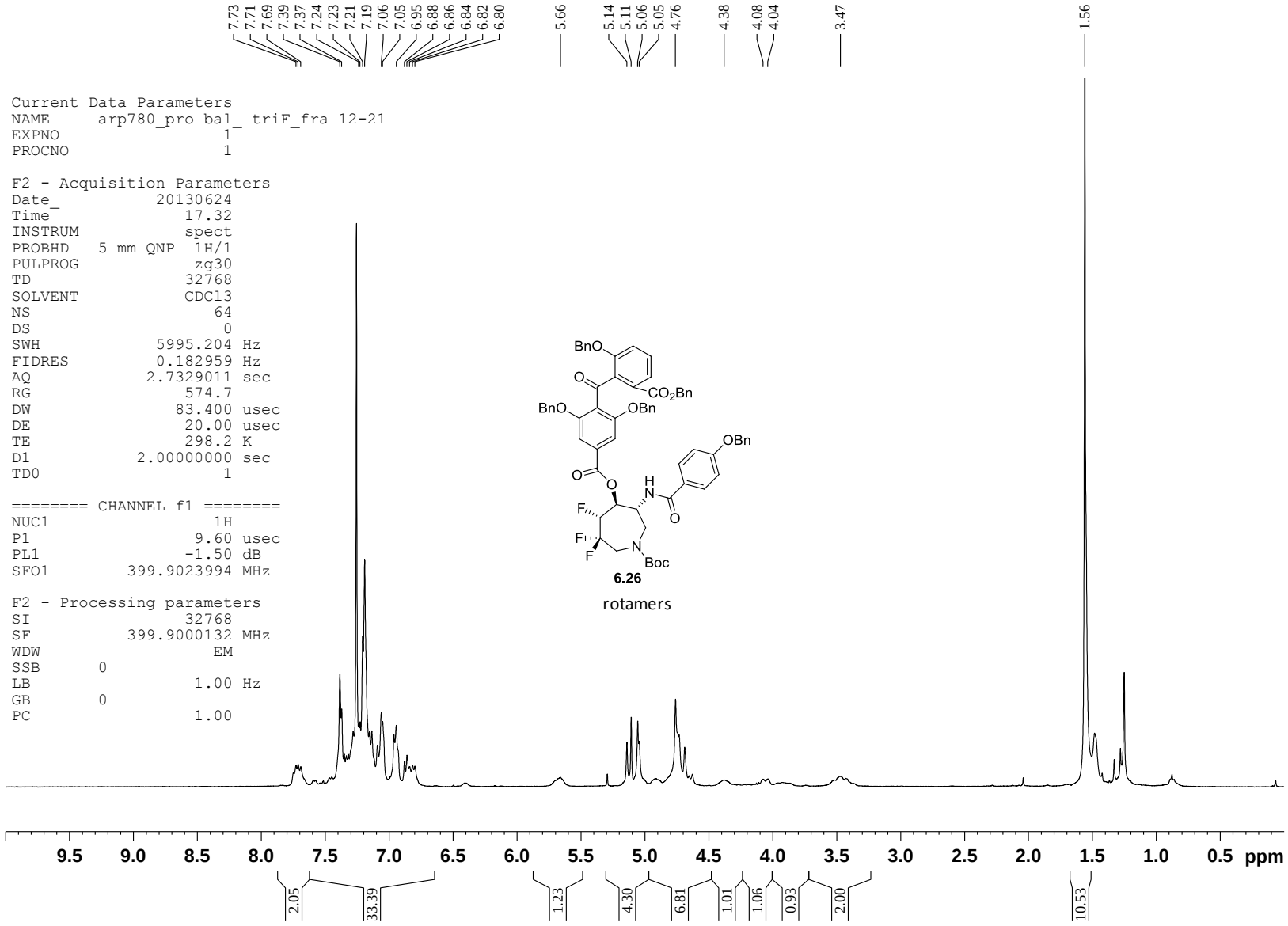

192.28
190.63
167.53
166.18
161.89
158.06
156.55
136.38
135.88
135.71
131.04
130.66
128.97
128.79
128.45
128.36
127.64
127.35
122.16
115.37
115.18
114.86
107.22
95.29
91.91
90.56
89.21
81.30
80.97
77.37
77.16
76.95
76.08
75.68
70.85
70.63
70.19
67.37
67.23
51.20
48.15
47.88
46.41
46.04
43.62
41.42
37.59
37.24
32.90
32.08
29.85
28.52
Current Data Parameters
NAME arp785_FN3S2A_proba1
EXPNO 2
PROCNO 1
F2 - Acquisition Parameters
Date_ 20130722
Time 19.01
INSTRUM spect
PROBHD 5 mm CPTXI 1H-
PULPROG udeft.txt
TD 28332
SOLVENT CDC13
NS 75296
DS 0
SWH 39370.078 Hz
FIDRES 1.389598 Hz
AQ 0.3598664 sec
RG 32768
DW 12.700 usec
DE 6.00 usec
TE 298.0 K
D1 1.50000000 sec
D11 0.03000000 sec
d12 0.00002000 sec
D20 0.10000000 sec
DELTA 1.47000003 sec
DELTA2 0.36288640 sec
TAU 0.00302000 sec
TD0 1
======== CHANNEL f1 ========
NUC1 13C
P1 10.43 usec
P12 2000.00 usec
P26 500.00 usec
PL1 -2.50 dB
SFO1 150.9298107 MHz
SP2 5.29 dB
SP8 4.75 dB
SPNAM2 Crp60comp.4
SPNAM8 Crp60,0.5,20.1
SPOAL2 0.500
SPOAL8 0.500
SPOFFS2 0 Hz
SPOFFS8 0 Hz
======== CHANNEL f2 ========
CPDPRG2 waltz64
NUC2 1H
PCPD2 80.00 usec
PL2 1.00 dB
PL12 18.89 dB
SFO2 600.1830000 MHz
F1 - Acquisition parameters
TD 256
SFO1 150.9298 MHz
FIDRES 93.450958 Hz
SW 158.507 ppm
FnMODE States-TPPI
F2 - Processing parameters
SI 262144
SF 150.9153621 MHz
WDW EM
SSB 0
LB 5.00 Hz
GB 0
PC 2.00
BnO
O
CO2Bn
BnO
OBn
OBn
O
O
H
N
F
O
N
Boc
6.23
rotamers
190 180 170 160 150 140 130 120 110 100 90 80 70 60 50 40 30 20 10 ppm

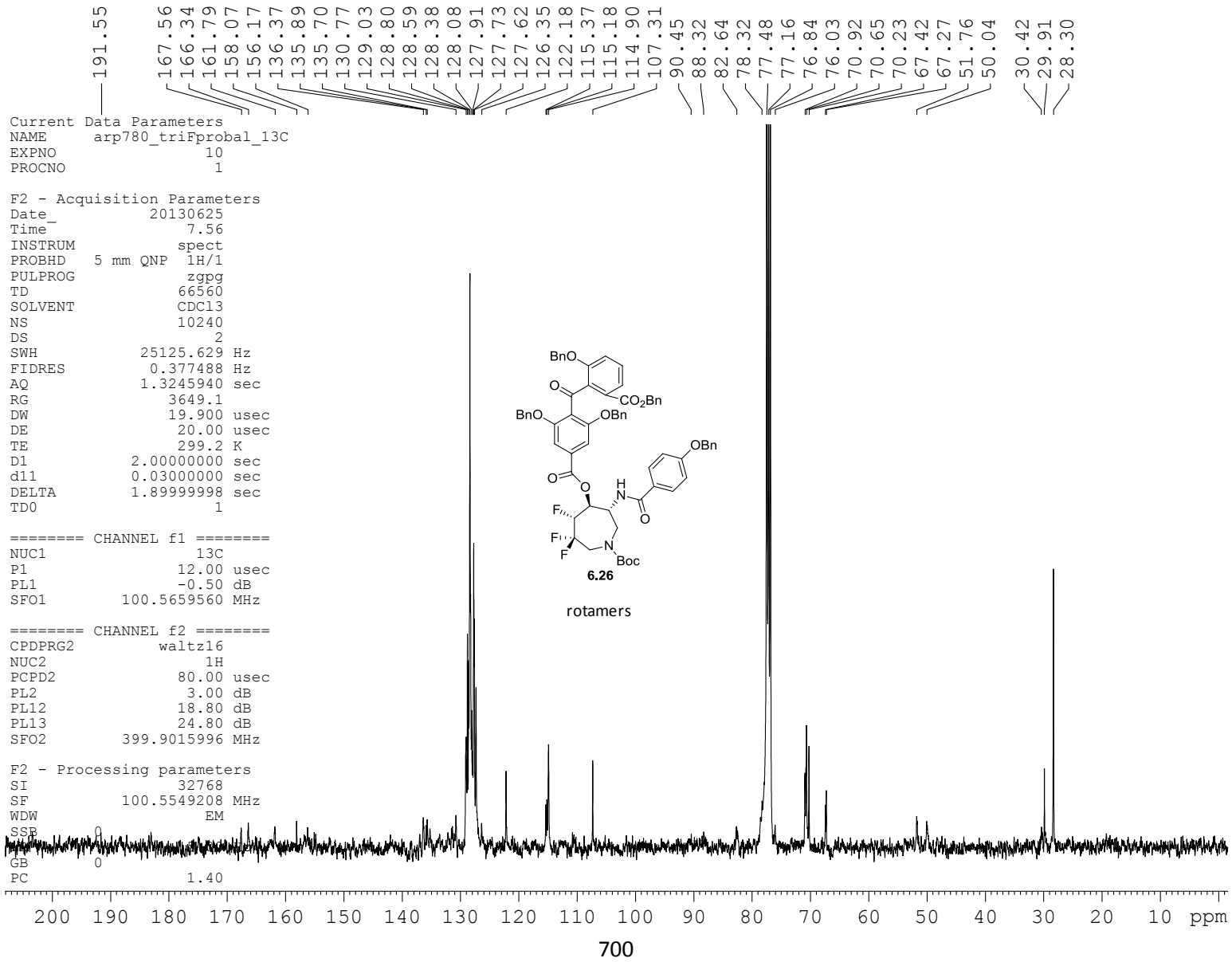

8.00
7.98
7.80
7.78
7.42
7.40
7.39
7.35
7.33
7.26
7.24
7.22
7.21
7.19
7.12
7.08
7.07
6.98
6.96
5.15
5.12
5.09
4.80
4.79
4.71
4.40
4.21
4.17
3.47
3.46
3.43
3.32
3.31
3.28
3.27
2.60
2.57
1.62
1.56
Current Data Parameters
NAME arp781_pro bal_ C6FF_fra 10-19
EXPNO 1
PROCNO 1
F2 - Acquisition Parameters
Date_ 20130624
Time 17.45
INSTRUM spect
PROBHD 5 mm QNP 1H/1
PULPROG zg30
TD 32768
SOLVENT CDCl3
NS 64
DS 0
SWH 5995.204 Hz
FIDRES 0.182959 Hz
AQ 2.7329011 sec
RG 228.1
DW 83.400 usec
DE 20.00 usec
TE 298.2 K
D1 2.00000000 sec
TD0 1
======== CHANNEL f1 ========
NUC1 1H
P1 9.60 usec
PL1 -1.50 dB
SFO1 399.9023994 MHz
F2 - Processing parameters
SI 32768
SF 399.9000121 MHz
WDW EM
SSB 0
LB 1.00 Hz
GB 0
PC 1.00
BnO
O
CO2Bn
BnO
OBn
OBn
O
O
H
N
O
F
F
N
Boc
6.24
rotamers
9.5
9.0
8.5
8.0
7.5
7.0
6.5
6.0
5.5
5.0
4.5
4.0
3.5
3.0
2.5
2.0
1.5
1.0
0.5
ppm
0.83
2.02
34.43
0.82
4.66
6.00
1.20
1.17
2.33
0.77
2.05
9.59

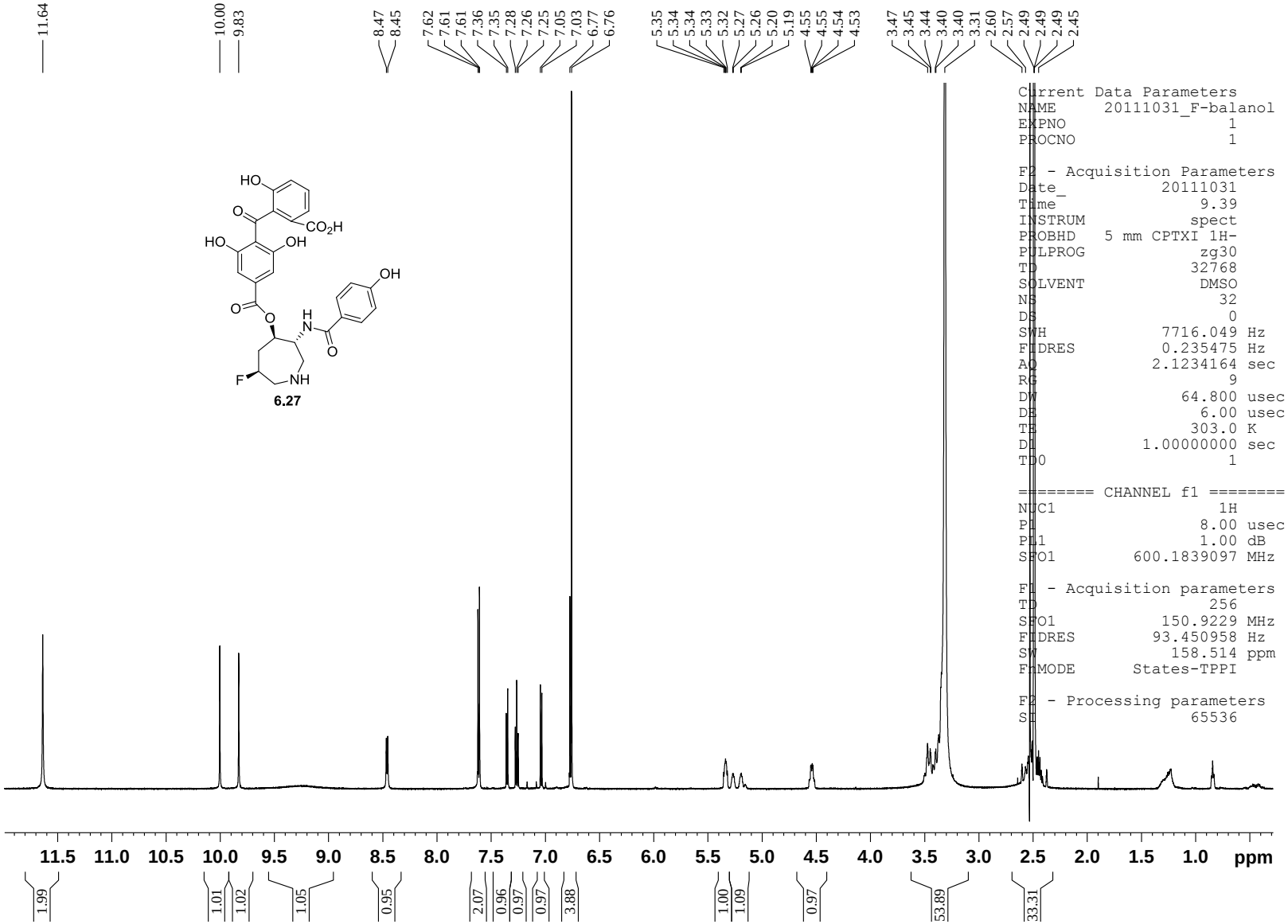

191.69
167.52
166.50
164.89
161.73
158.13
157.09
136.45
135.90
135.81
132.27
130.70
129.06
128.79
128.59
128.37
127.60
127.22
126.26
122.18
114.86
114.72
107.16
82.43
77.48
77.16
76.84
76.07
70.88
70.62
70.21
69.89
67.38
67.23
55.80
55.54
53.64
53.44
50.61
36.39
36.13
28.29
Current Data Parameters
NAME arp781_C6FFprobal_13C
EXPNO 10
PROCNO 1
F2 - Acquisition Parameters
Date_ 20130624
Time 19.30
INSTRUM spect
PROBHD 5 mm QNP 1H/1
PULPROG zgpg
TD 66560
SOLVENT CDCl3
NS 4381
DS 2
SWH 25125.629 Hz
FIDRES 0.377488 Hz
AQ 1.3245940 sec
RG 4096
DW 19.900 usec
DE 20.00 usec
TE 298.2 K
D1 2.00000000 sec
d11 0.03000000 sec
DELTA 1.89999998 sec
TD0 1
======== CHANNEL f1 ========
NUC1 13C
P1 12.00 usec
PL1 -0.50 dB
SFO1 100.5659560 MHz
======== CHANNEL f2 ========
CPDPRG2 waltz16
NUC2 1H
PCPD2 80.00 usec
PL2 3.00 dB
PL12 18.80 dB
PL13 24.80 dB
SFO2 399.9015996 MHz
F2 - Processing parameters
SI 32768
SF 100.5549230 MHz
WDW EM
SSB 0
GB 0
PC 1.40
BnO
CO2Bn
OBn
OBn
OBn
H
N
O
F
F
N
Boc
6.24
rotamers
190 180 170 160 150 140 130 120 110 100 90 80 70 60 50 40 30 20 10 ppm

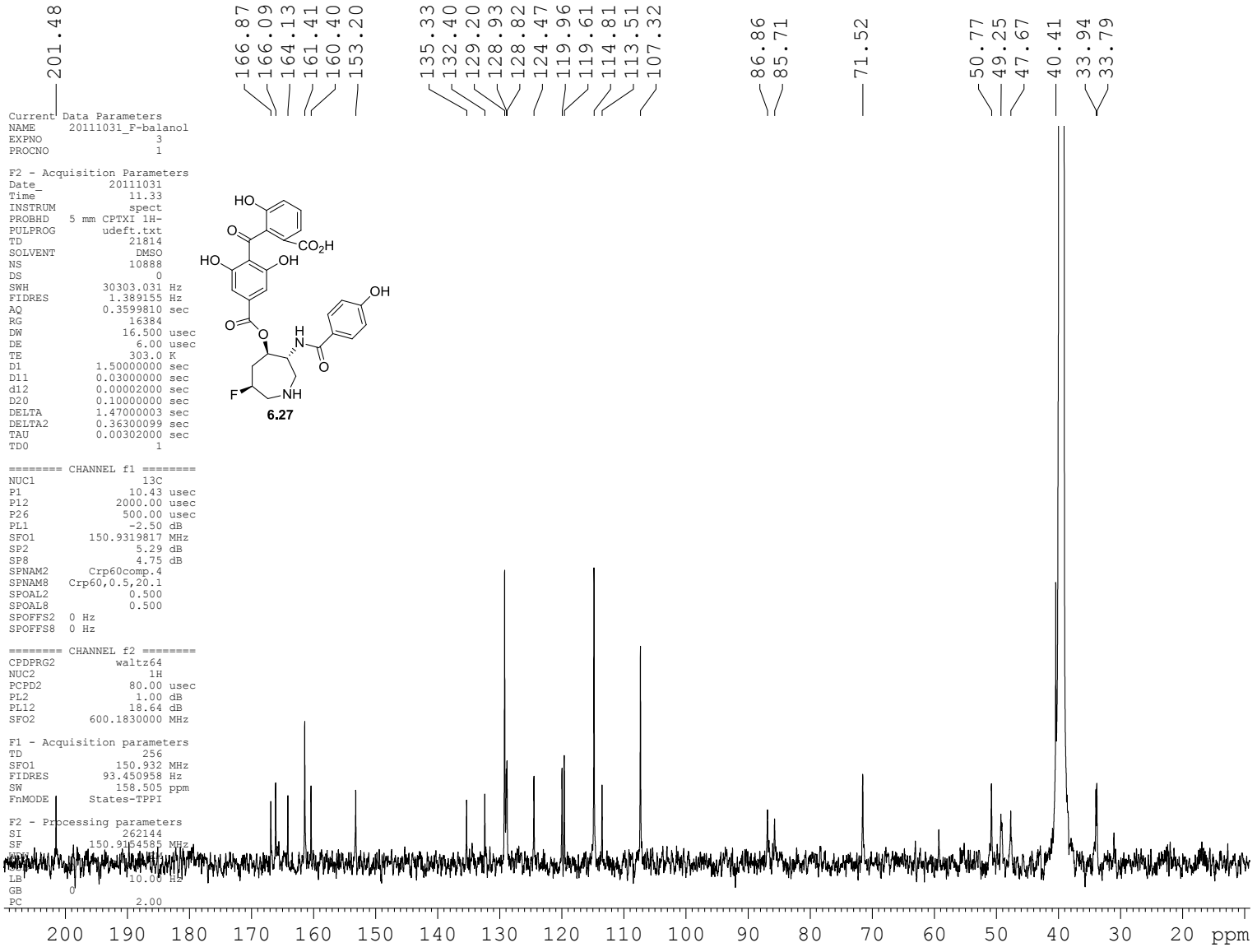

8.04
8.02
7.71
7.69
7.42
7.40
7.39
7.26
7.21
7.19
7.19
7.18
6.97
6.95
5.14
5.10
5.09
5.07
5.03
4.82
4.75
4.74
4.73
4.67
4.13
4.11
4.10
3.50
1.56
1.53
1.51
Current Data Parameters
NAME arp776_FF1_pro bal_fra10-13
EXPNO 1
PROCNO 1
F2 - Acquisition Parameters
Date_ 20130618
Time 15.02
INSTRUM spect
PROBHD 5 mm QNP 1H/1
PULPROG zg30
TD 32768
SOLVENT CDC13
NS 80
DS 0
SWH 5995.204 Hz
FIDRES 0.182959 Hz
AQ 2.7329011 sec
RG 724.1
DW 83.400 usec
DE 20.00 usec
TE 298.2 K
D1 2.00000000 sec
TD0 1
======== CHANNEL f1 ========
NUC1 1H
P1 9.60 usec
PL1 -1.50 dB
SFO1 399.9023994 MHz
F2 - Processing parameters
SI 32768
SF 399.9000120 MHz
WDW EM
SSB 0
LB 1.00 Hz
GB 0
PC 1.00
BnO
CO2Bn
OBn
F
N
Boc
6.25
rotamers
9.5
9.0
8.5
8.0
7.5
7.0
6.5
6.0
5.5
5.0
4.5
4.0
3.5
3.0
2.5
2.0
1.5
1.0
0.5
ppm
1.12
2.01
35.77
18.00
9.50

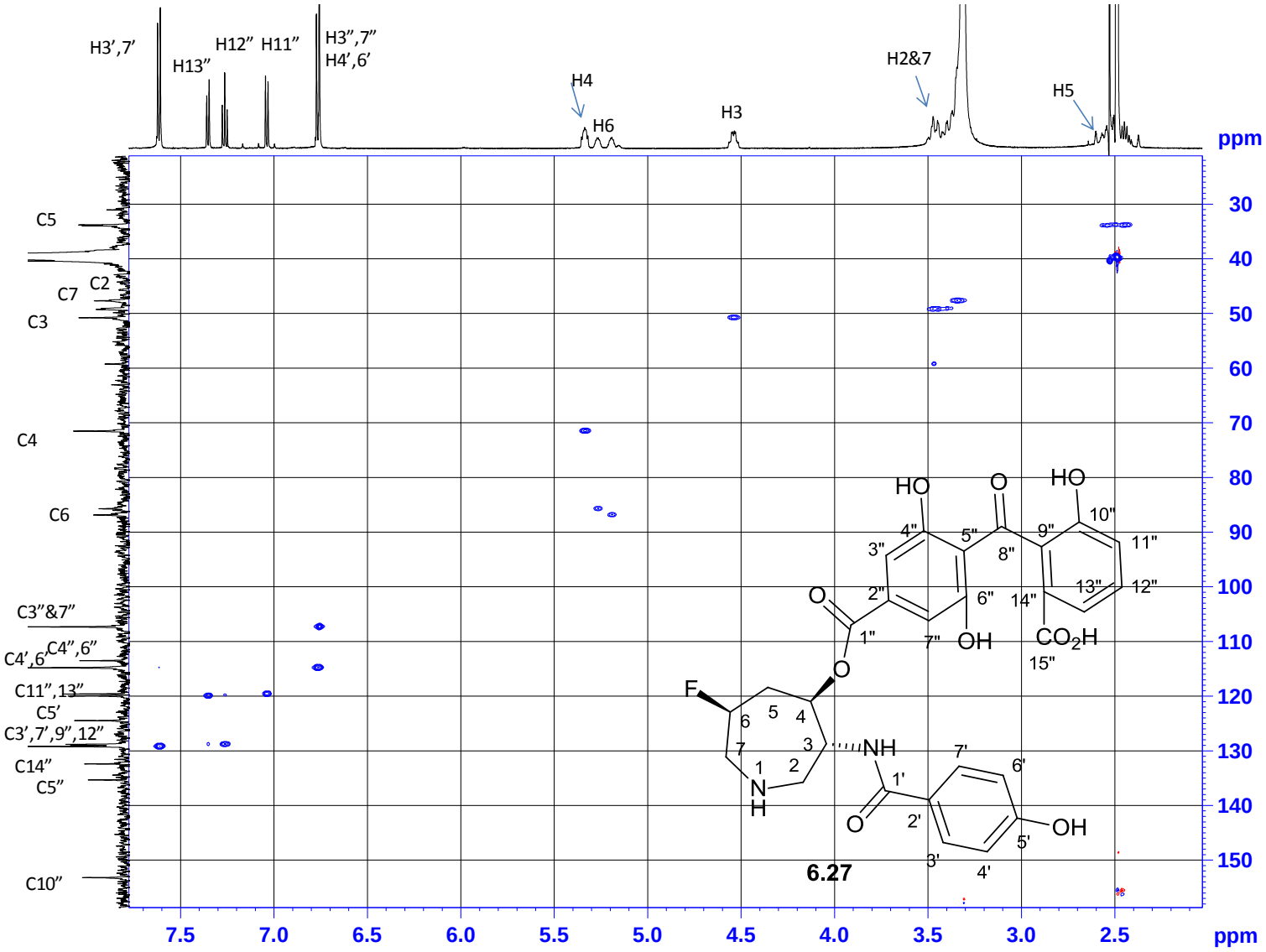

191.60
167.56
166.31
161.70
159.56
155.06
136.32
135.73
132.26
128.83
128.35
127.64
122.16
114.79
107.27
92.50
91.59
89.73
77.35
77.15
76.95
72.00
70.66
70.23
69.49
67.28
63.81
51.72
48.30
46.82
43.70
42.70
28.40
Current Data Parameters
NAME arp776_fra 10-13_FF1 pro bal
EXPNO 2
PROCNO 1
F2 - Acquisition Parameters
Date_ 20130618
Time 15.39
INSTRUM spect
PROBHD 5 mm CPTXI 1H-
PULPROG udeft.txt
TD 21814
SOLVENT CDCl3
NS 24576
DS 0
SWH 30303.031 Hz
FIDRES 1.389155 Hz
AQ 0.3599810 sec
RG 32768
DW 16.500 usec
DE 6.00 usec
TE 298.0 K
D1 1.50000000 sec
D11 0.03000000 sec
d12 0.00002000 sec
D20 0.10000000 sec
DELTA 1.47000003 sec
DELTA2 0.36300099 sec
TAU 0.00302000 sec
TD0 1
======== CHANNEL f1 ========
NUC1 13C
P1 10.43 usec
P12 2000.00 usec
P26 500.00 usec
PL1 -2.50 dB
SFO1 150.9319817 MHz
SP2 5.29 dB
SP8 4.75 dB
SPNAM2 Crp60comp.4
SPNAM8 Crp60,0.5,20.1
SPOAL2 0.500
SPOAL8 0.500
SPOFFS2 0 Hz
SPOFFS8 0 Hz
======== CHANNEL f2 ========
CPDPRG2 waltz64
NUC2 1H
PCPD2 80.00 usec
PL2 1.00 dB
PL12 18.89 dB
SFO2 600.1830000 MHz
F1 - Acquisition parameters
TD 256
SFO1 150.932 MHz
FIDRES 93.450958 Hz
SW 158.505 ppm
FnMODE States-TPPI
F2 - Processing parameters
SI 262144
SF 150.9153618 MHz
WDW EM
SSB 1
LB 5.00 Hz
GB 0.001
PC 0.02
BnO
CO2Bn
OBn
OBn
F
F
N
Boc
6.25
rotamers
200
190
180
170
160
150
140
130
120
110
100
90
80
70
60
50
40
30
ppm

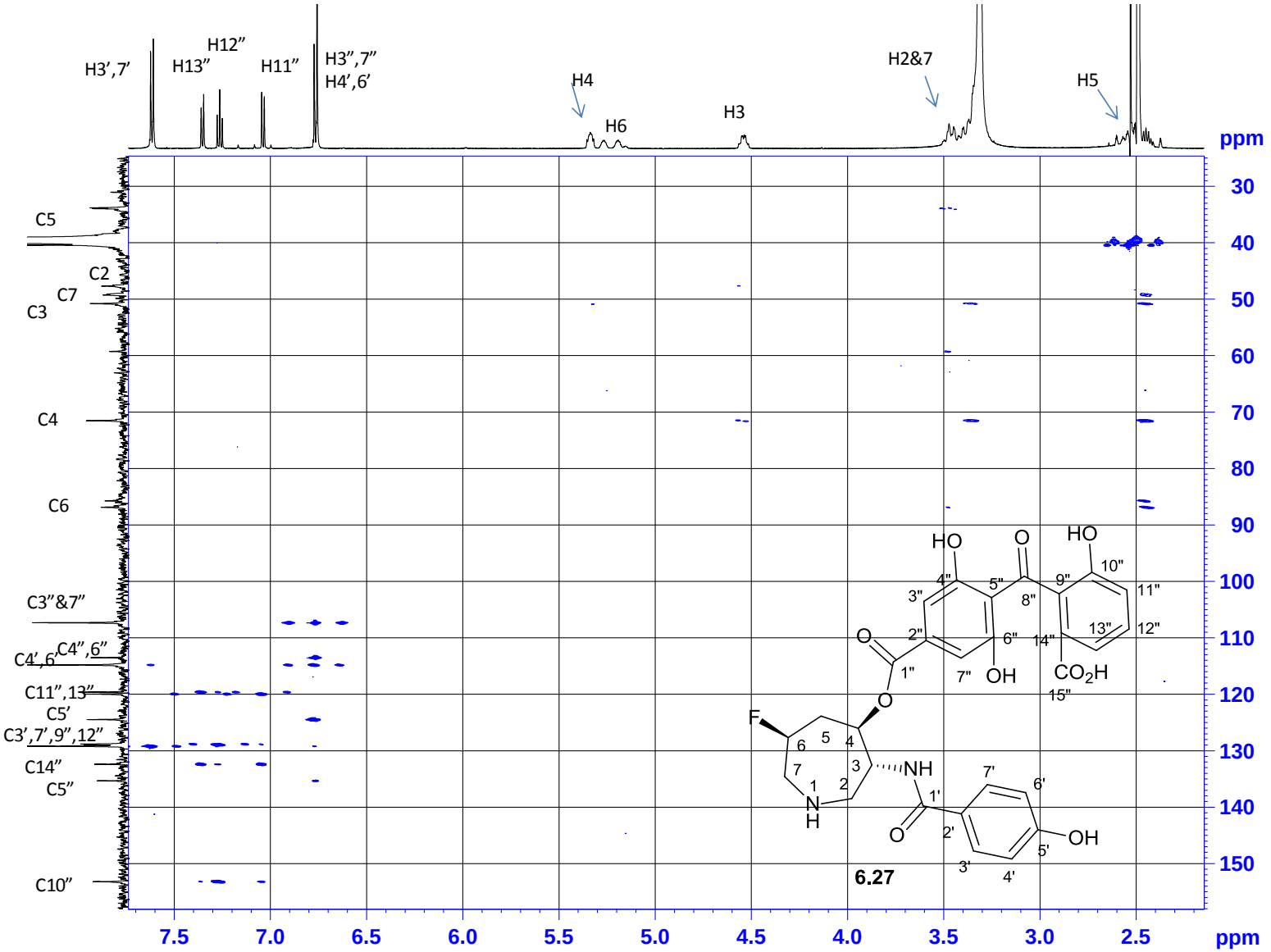

7.73
7.71
7.69
7.39
7.37
7.24
7.23
7.21
7.19
7.06
7.05
6.95
6.88
6.86
6.84
6.82
6.80
5.66
5.14
5.11
5.06
5.05
4.76
4.38
4.08
4.04
3.47
1.56
Current Data Parameters
NAME arp780_pro bal_ triF_fra 12-21
EXPNO 1
PROCNO 1
F2 - Acquisition Parameters
Date_ 20130624
Time 17.32
INSTRUM spect
PROBHD 5 mm QNP 1H/1
PULPROG zg30
TD 32768
SOLVENT CDCl3
NS 64
DS 0
SWH 5995.204 Hz
FIDRES 0.182959 Hz
AQ 2.7329011 sec
RG 574.7
DW 83.400 usec
DE 20.00 usec
TE 298.2 K
D1 2.00000000 sec
TD0 1
======== CHANNEL f1 ========
NUC1 1H
P1 9.60 usec
PL1 -1.50 dB
SFO1 399.9023994 MHz
F2 - Processing parameters
SI 32768
SF 399.9000132 MHz
WDW EM
SSB 0
LB 1.00 Hz
GB 0
PC 1.00
BnO
O
CO2Bn
BnO
OBn
OBn
O
O
H
N
O
F
F
F
N
Boc
6.26
rotamers
9.5
9.0
8.5
8.0
7.5
7.0
6.5
6.0
5.5
5.0
4.5
4.0
3.5
3.0
2.5
2.0
1.5
1.0
0.5
ppm
2.05
33.39
1.23
4.30
6.81
1.01
1.06
0.93
2.00
10.53

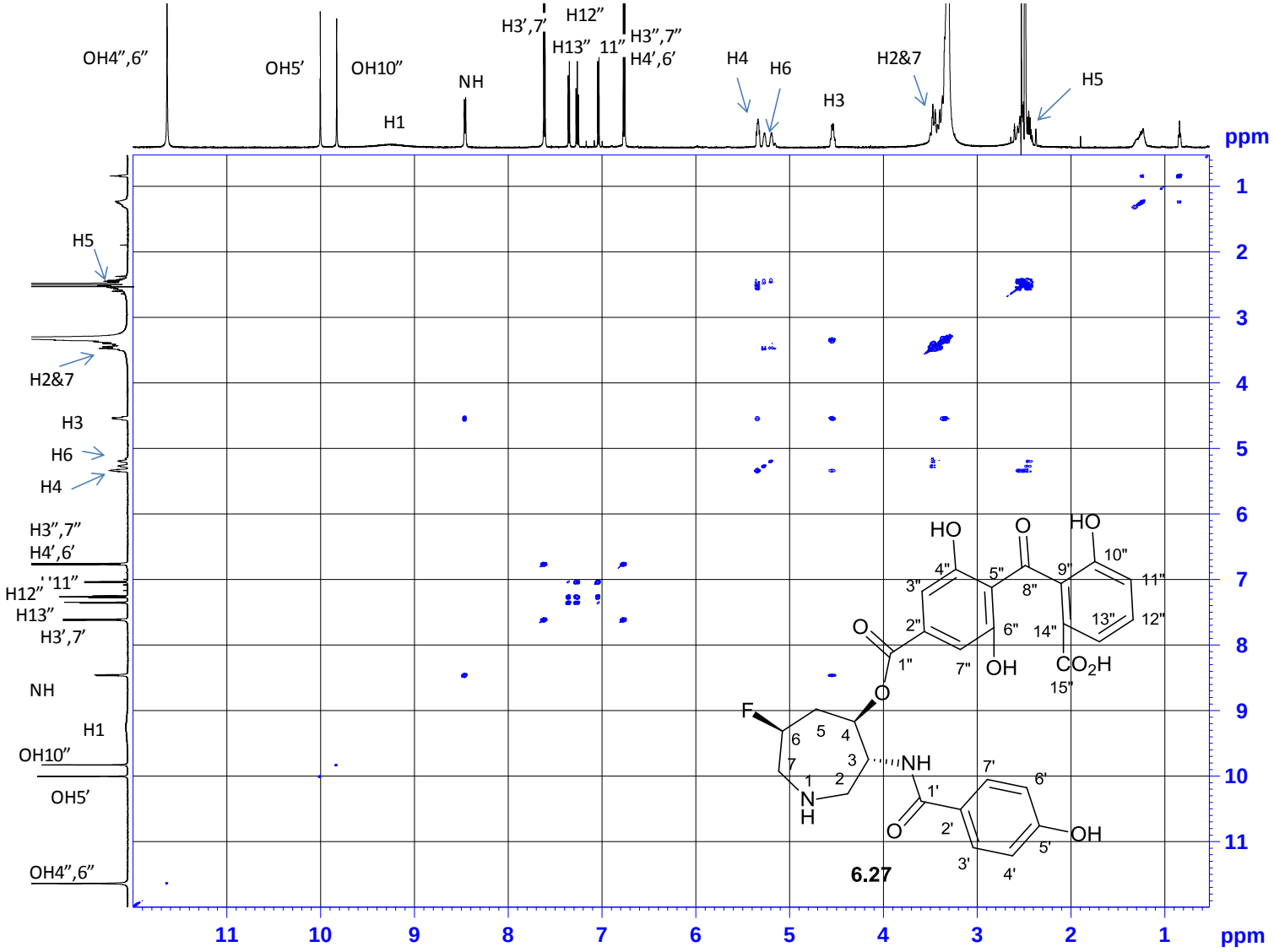

191.55
167.56
166.34
161.79
158.07
156.17
136.37
135.89
135.70
130.77
129.03
128.80
128.59
128.38
128.08
127.91
127.73
127.62
126.35
122.18
115.37
115.18
114.90
107.31
90.45
88.32
82.64
78.32
77.48
77.16
76.84
76.03
70.92
70.65
70.23
67.42
67.27
51.76
50.04
30.42
29.91
28.30
Current Data Parameters
NAME arp780_triFprobal_13C
EXPNO 10
PROCNO 1
F2 - Acquisition Parameters
Date_ 20130625
Time 7.56
INSTRUM spect
PROBHD 5 mm QNP 1H/1
PULPROG zgpg
TD 66560
SOLVENT CDCl3
NS 10240
DS 2
SWH 25125.629 Hz
FIDRES 0.377488 Hz
AQ 1.3245940 sec
RG 3649.1
DW 19.900 usec
DE 20.00 usec
TE 299.2 K
D1 2.00000000 sec
d11 0.03000000 sec
DELTA 1.89999998 sec
TD0 1
======== CHANNEL f1 ========
NUC1 13C
P1 12.00 usec
PL1 -0.50 dB
SFO1 100.5659560 MHz
======== CHANNEL f2 ========
CPDPRG2 waltz16
NUC2 1H
PCPD2 80.00 usec
PL2 3.00 dB
PL12 18.80 dB
PL13 24.80 dB
SFO2 399.9015996 MHz
F2 - Processing parameters
SI 32768
SF 100.5549208 MHz
WDW EM
SSB 0
LB 0
GB 0
PC 1.40
BnO
CO2Bn
OBn
OBn
F
F
F
N
Boc
H
N
O
6.26
rotamers
200 190 180 170 160 150 140 130 120 110 100 90 80 70 60 50 40 30 20 10 ppm

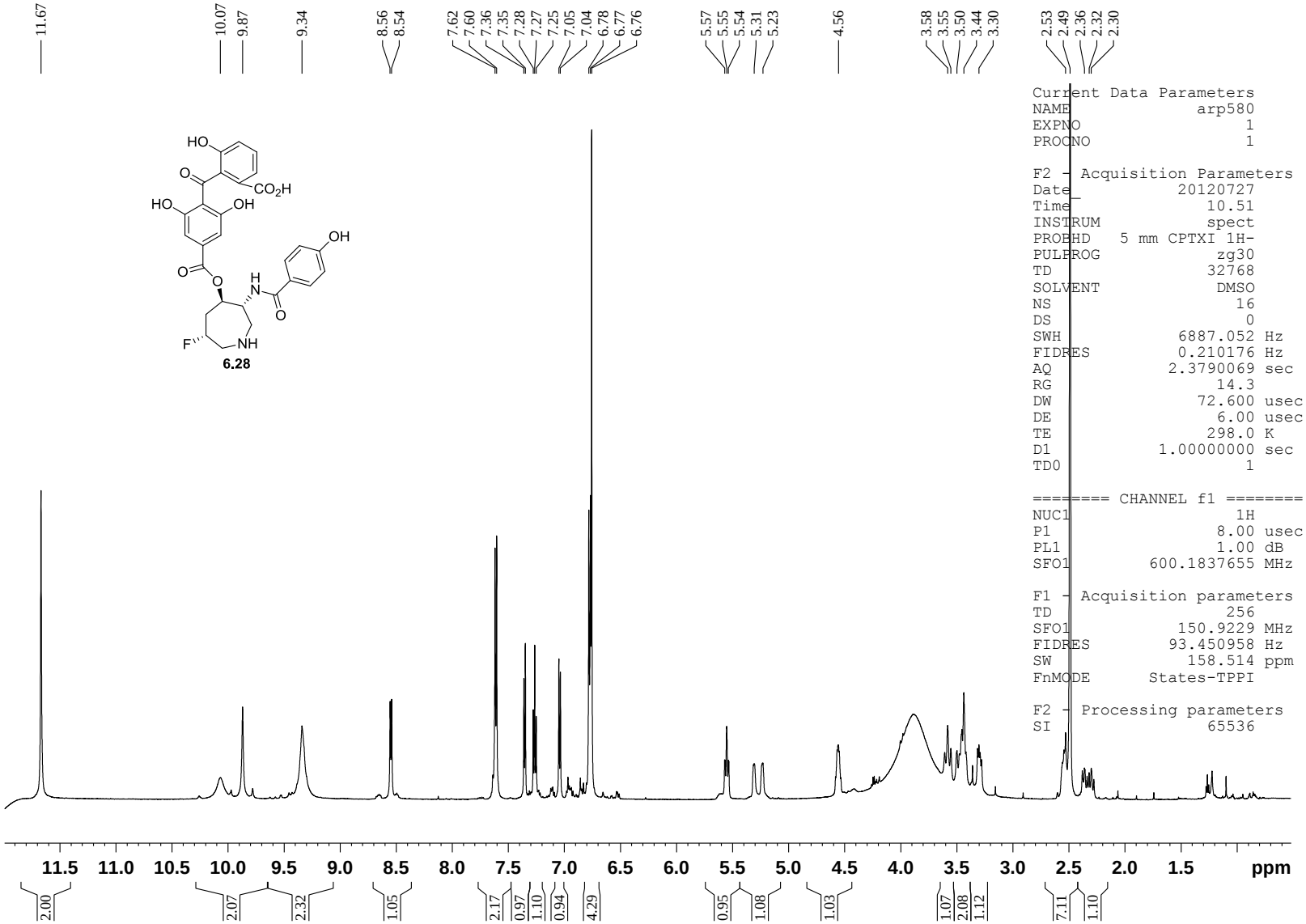

11.64
10.00
9.83
8.47
8.45
7.62
7.61
7.61
7.36
7.35
7.28
7.26
7.25
7.05
7.03
6.77
6.76
5.35
5.34
5.34
5.33
5.32
5.27
5.26
5.20
5.19
4.55
4.55
4.54
4.53
3.47
3.45
3.44
3.40
3.40
3.31
2.60
2.57
2.49
2.49
2.49
2.45
HO
O
CO2H
HO
OH
OH
O
O
H
N
O
F
NH
6.27
Current Data Parameters
NAME 20111031_F-balanol
EXPNO 1
PROCNO 1
F2 - Acquisition Parameters
Date_ 20111031
Time 9.39
INSTRUM spect
PROBHD 5 mm CPTXI 1H-
PULPROG zg30
TD 32768
SOLVENT DMSO
NS 32
DS 0
SWH 7716.049 Hz
FIDRES 0.235475 Hz
AQ 2.1234164 sec
RG 9
DW 64.800 usec
DE 6.00 usec
TE 303.0 K
D1 1.00000000 sec
TD0 1
======== CHANNEL f1 ========
NUC1 1H
P1 8.00 usec
PL1 1.00 dB
SFO1 600.1839097 MHz
F1 - Acquisition parameters
TD 256
SFO1 150.9229 MHz
FIDRES 93.450958 Hz
SW 158.514 ppm
FnMODE States-TPPI
F2 - Processing parameters
SI 65536
11.5
11.0
10.5
10.0
9.5
9.0
8.5
8.0
7.5
7.0
6.5
6.0
5.5
5.0
4.5
4.0
3.5
3.0
2.5
2.0
1.5
1.0
ppm
1.99
1.01
1.02
1.05
0.95
2.07
0.96
0.97
0.97
3.88
1.00
1.09
0.97
53.89
33.31

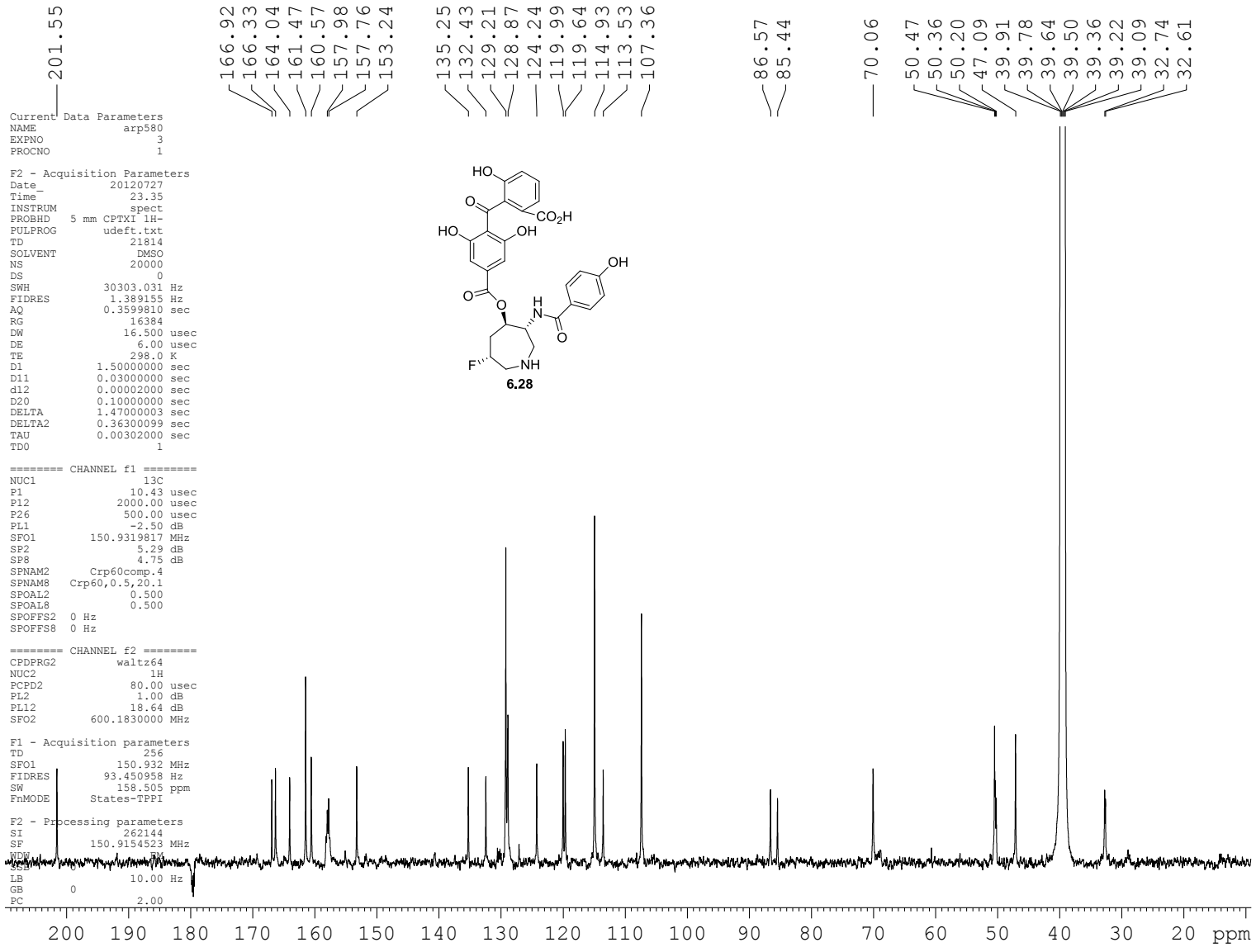

201.48
166.87
166.09
164.13
161.41
160.40
153.20
135.33
132.40
129.20
128.93
128.82
124.47
119.96
119.61
114.81
113.51
107.32
86.86
85.71
71.52
50.77
49.25
47.67
40.41
33.94
33.79
Current Data Parameters
NAME 20111031_F-balanol
EXPNO 3
PROCNO 1
F2 - Acquisition Parameters
Date_ 20111031
Time 11.33
INSTRUM spect
PROBHD 5 mm CPTXI 1H-
PULPROG udeft.txt
TD 21814
SOLVENT DMSO
NS 10888
DS 0
SWH 30303.031 Hz
FIDRES 1.389155 Hz
AQ 0.3599810 sec
RG 16384
DW 16.500 usec
DE 6.00 usec
TE 303.0 K
D1 1.50000000 sec
D11 0.03000000 sec
d12 0.00002000 sec
D20 0.10000000 sec
DELTA 1.47000003 sec
DELTA2 0.36300099 sec
TAU 0.00302000 sec
TD0 1
======== CHANNEL f1 ========
NUC1 13C
P1 10.43 usec
P12 2000.00 usec
P26 500.00 usec
PL1 -2.50 dB
SFO1 150.9319817 MHz
SP2 5.29 dB
SP8 4.75 dB
SPNAM2 Crp60comp.4
SPNAM8 Crp60,0.5,20.1
SPOAL2 0.500
SPOAL8 0.500
SPOFFS2 0 Hz
SPOFFS8 0 Hz
======== CHANNEL f2 ========
CPDPRG2 waltz64
NUC2 1H
PCPD2 80.00 usec
PL2 1.00 dB
PL12 18.64 dB
SFO2 600.1830000 MHz
F1 - Acquisition parameters
TD 256
SFO1 150.932 MHz
FIDRES 93.450958 Hz
SW 158.505 ppm
FnMODE States-TPPI
F2 - Processing parameters
SI 262144
SF 150.9164585 MHz
LB 10.00 Hz
GB 0
PC 2.00
HO
O
CO2H
HO
OH
OH
O
O
H
N
O
F
NH
6.27
200 190 180 170 160 150 140 130 120 110 100 90 80 70 60 50 40 30 20 ppm

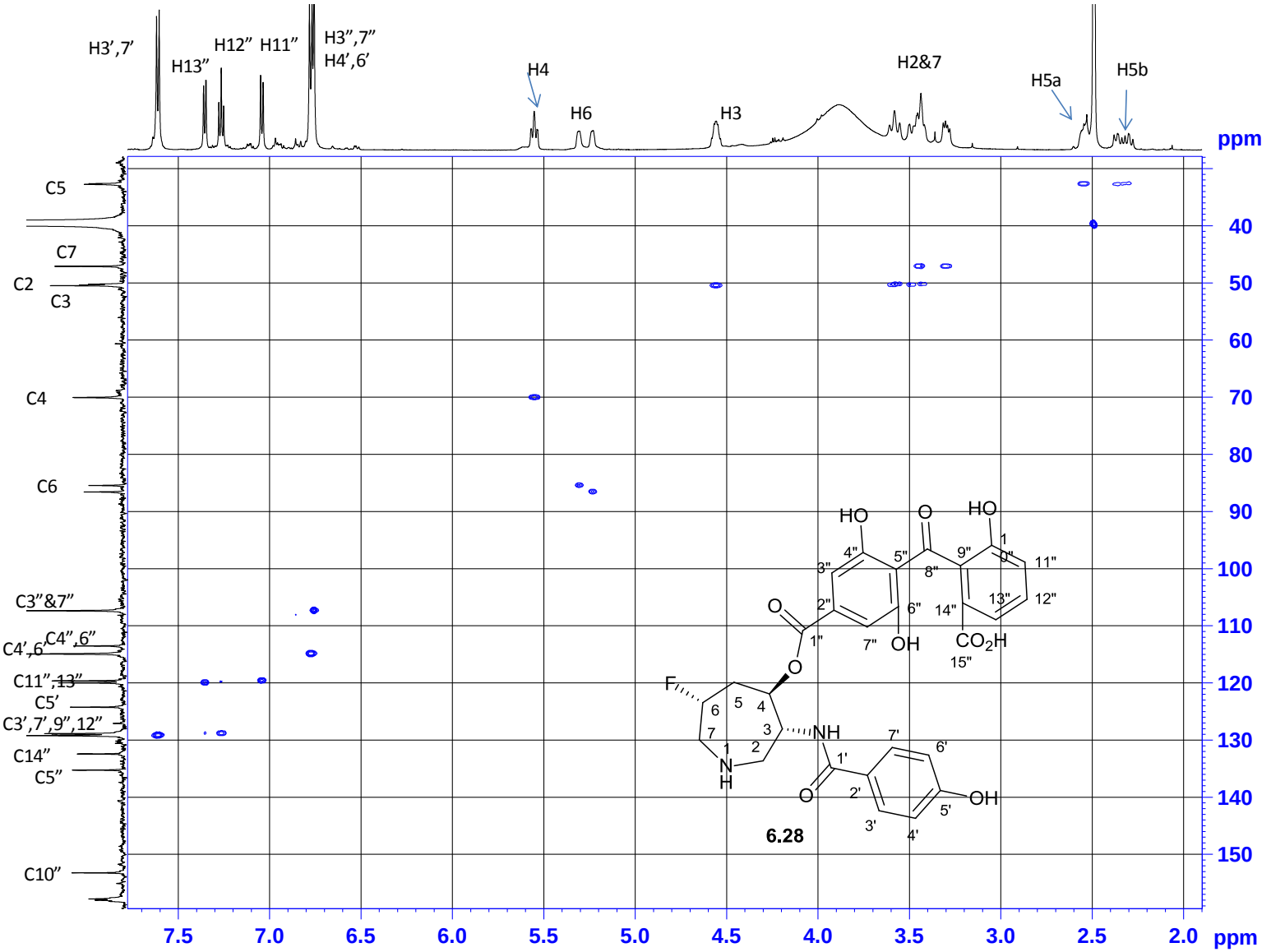

H3',7'
H13"
H12"
H11"
H3",7"
H4',6'
H4
H6
H3
H2&7
H5
ppm
C5
C7
C2
C3
C4
C6
C3"&7"
C4',6'
C4",6"
C11",13"
C5'
C3',7',9",12"
C14"
C5"
C10"
7.5
7.0
6.5
6.0
5.5
5.0
4.5
4.0
3.5
3.0
2.5
ppm
6.27

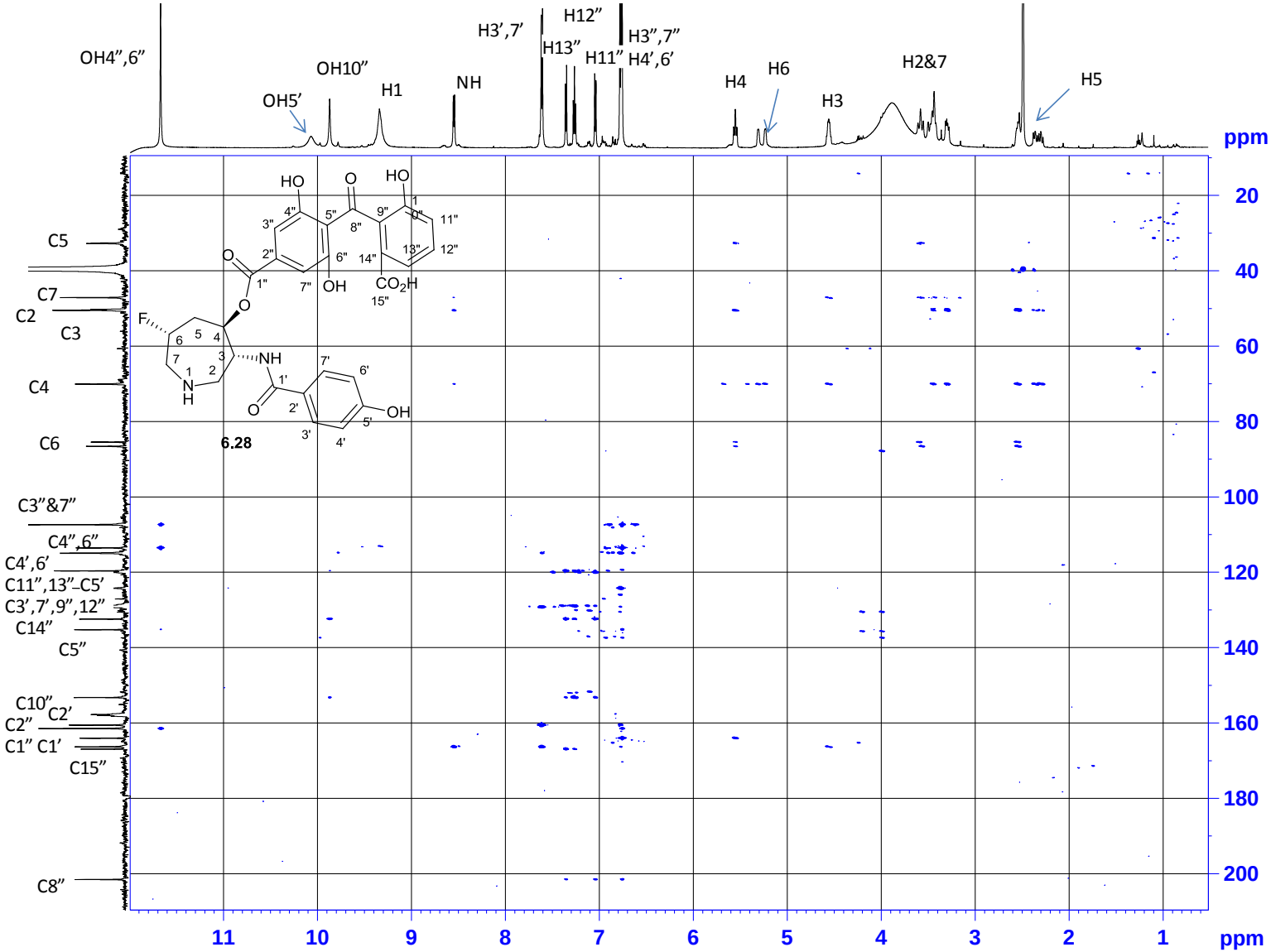

H3′,7′
H12″
H13″
H11″
H3″,7″
H4′,6′
H4
H6
H3
H2&7
H5
ppm
C5
C2
C7
C3
C4
C6
C3″&7″
C4′,6′
C4″,6″
C11″,13″
C5′
C3′,7′,9″,12″
C14″
C5″
C10″
7.5
7.0
6.5
6.0
5.5
5.0
4.5
4.0
3.5
3.0
2.5
ppm
6.27

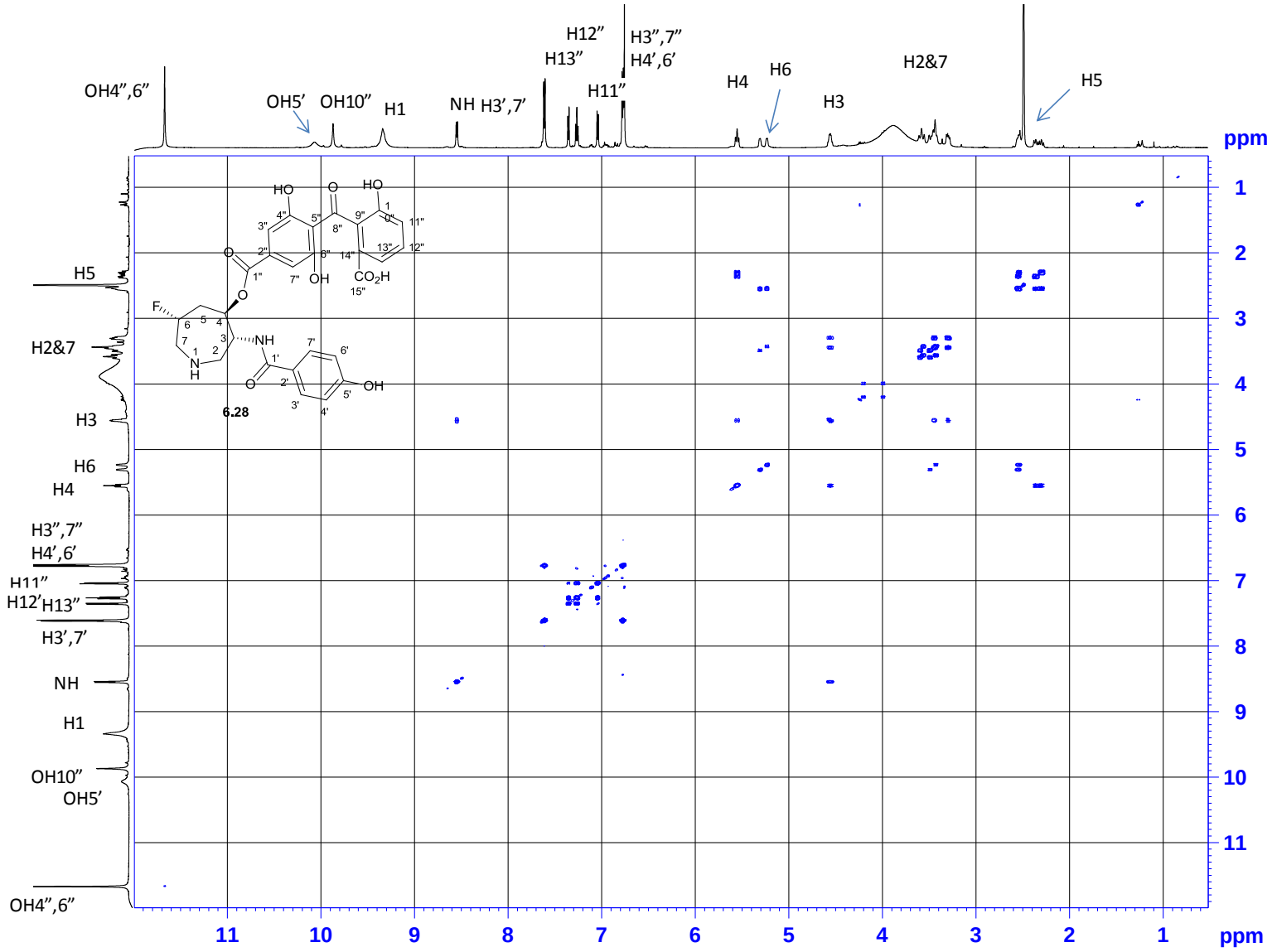

OH4",6"
OH5'
OH10"
H1
NH
H3',7'
H12"
H13"
11"
H3",7"
H4',6'
H4
H6
H3
H2&7
H5
ppm
1
2
3
4
5
6
7
8
9
10
11
H5
H2&7
H3
H6
H4
H3",7"
H4',6'
H12"
11"
H13"
H3',7'
NH
H1
OH10"
OH5'
OH4",6"
HO
O
HO
10"
11"
4"
5"
8"
9"
3"
2"
6"
14"
13"
12"
1"
7"
OH
CO2H
15"
F
6
5
4
7
3
NH
1
2
N
H
7'
6'
1'
2'
O
OH
5'
3'
4'
6.27
11
10
9
8
7
6
5
4
3
2
1
ppm

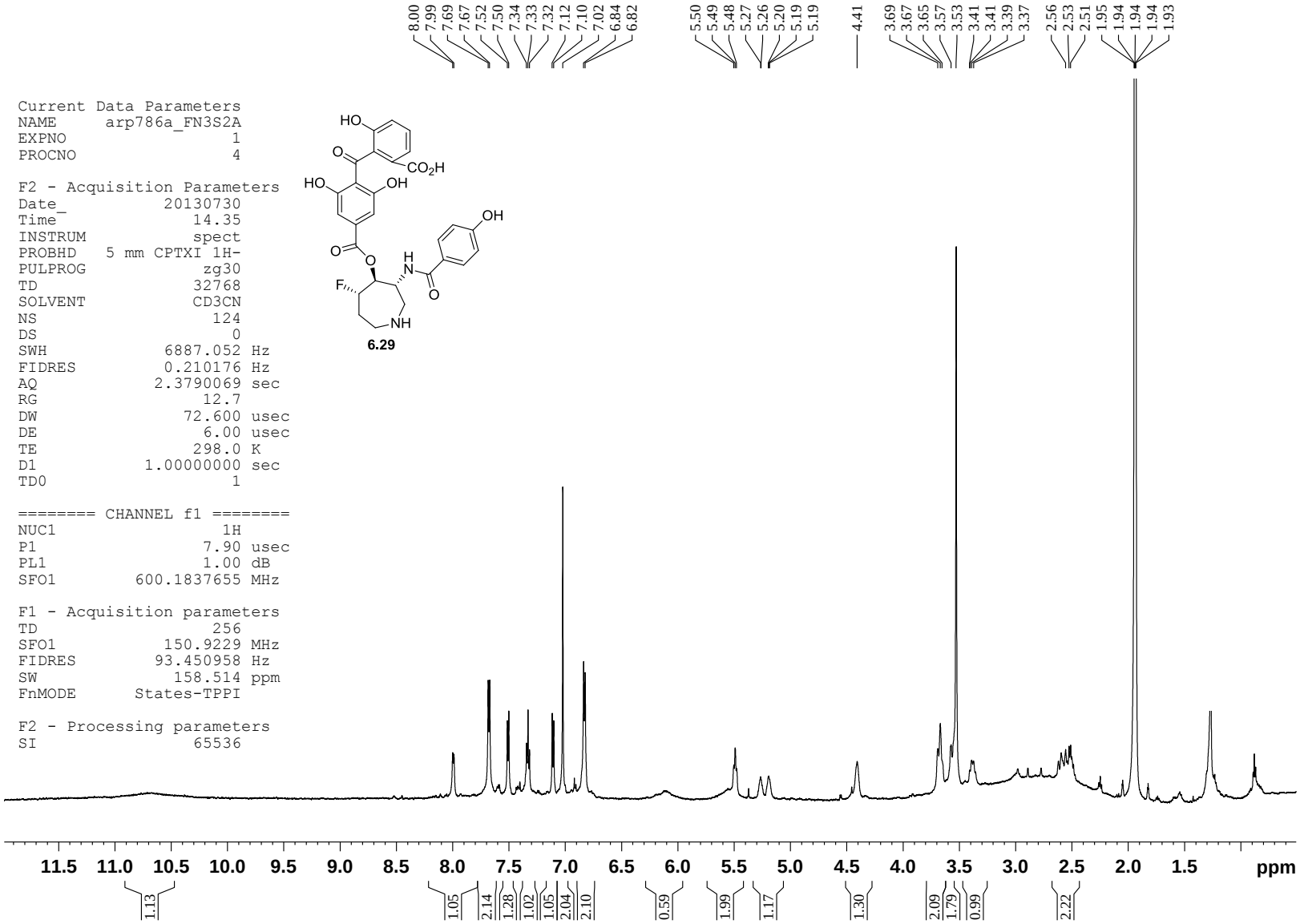

11.67
10.07
9.87
9.34
8.56
8.54
7.62
7.60
7.36
7.35
7.28
7.27
7.25
7.05
7.04
6.78
6.77
6.76
5.57
5.55
5.54
5.31
5.23
4.56
3.58
3.55
3.50
3.44
3.30
2.53
2.49
2.36
2.32
2.30
HO
O
CO2H
HO
OH
OH
O
O
H
N
O
F
NH
6.28
Current Data Parameters
NAME arp580
EXPNO 1
PROCNO 1
F2 - Acquisition Parameters
Date 20120727
Time 10.51
INSTRUM spect
PROBHD 5 mm CPTXI 1H-
PULPROG zg30
TD 32768
SOLVENT DMSO
NS 16
DS 0
SWH 6887.052 Hz
FIDRES 0.210176 Hz
AQ 2.3790069 sec
RG 14.3
DW 72.600 usec
DE 6.00 usec
TE 298.0 K
D1 1.00000000 sec
TD0 1
======== CHANNEL f1 ========
NUC1 1H
P1 8.00 usec
PL1 1.00 dB
SFO1 600.1837655 MHz
F1 - Acquisition parameters
TD 256
SFO1 150.9229 MHz
FIDRES 93.450958 Hz
SW 158.514 ppm
FnMODE States-TPPI
F2 - Processing parameters
SI 65536
11.5 11.0 10.5 10.0 9.5 9.0 8.5 8.0 7.5 7.0 6.5 6.0 5.5 5.0 4.5 4.0 3.5 3.0 2.5 2.0 1.5 ppm
2.00
2.07
2.32
1.05
2.17
0.97
1.10
0.94
4.29
0.95
1.08
1.03
1.07
2.08
1.12
7.11
1.10

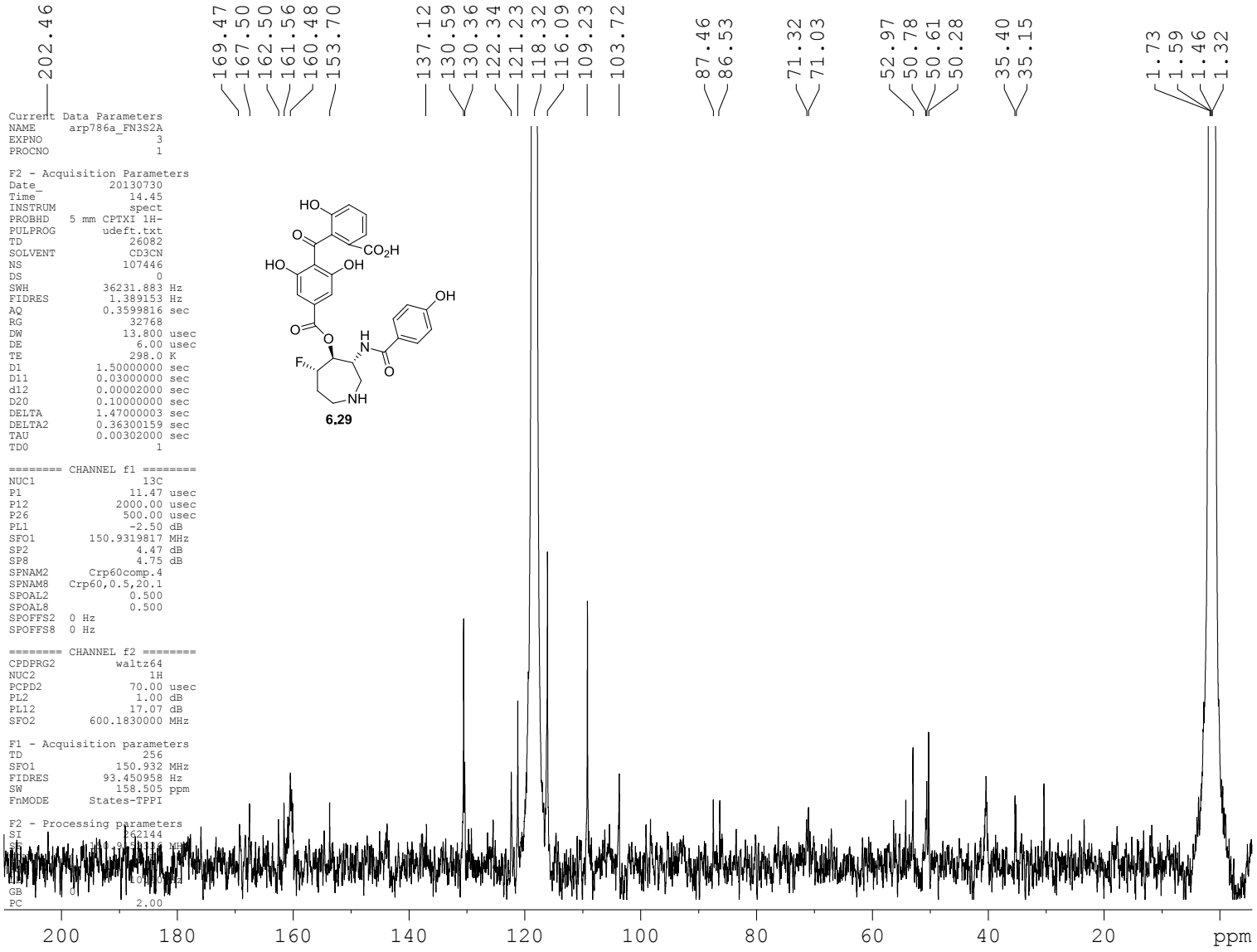

201.55
166.92
166.33
164.04
161.47
160.57
157.98
157.76
153.24
135.25
132.43
129.21
128.87
124.24
119.99
119.64
114.93
113.53
107.36
86.57
85.44
70.06
50.47
50.36
50.20
47.09
39.91
39.78
39.64
39.50
39.36
39.22
39.09
32.74
32.61
Current Data Parameters
NAME arp580
EXPNO 3
PROCNO 1
F2 - Acquisition Parameters
Date_ 20120727
Time 23.35
INSTRUM spect
PROBHD 5 mm CPTXI 1H-
PULPROG udeft.txt
TD 21814
SOLVENT DMSO
NS 20000
DS 0
SWH 30303.031 Hz
FIDRES 1.389155 Hz
AQ 0.3599810 sec
RG 16384
DW 16.500 usec
DE 6.00 usec
TE 298.0 K
D1 1.50000000 sec
D11 0.03000000 sec
d12 0.00002000 sec
D20 0.10000000 sec
DELTA 1.47000003 sec
DELTA2 0.36300099 sec
TAU 0.00302000 sec
TD0 1
======== CHANNEL f1 ========
NUC1 13C
P1 10.43 usec
P12 2000.00 usec
P26 500.00 usec
PL1 -2.50 dB
SFO1 150.9319817 MHz
SP2 5.29 dB
SP8 4.75 dB
SPNAM2 Crp60comp.4
SPNAM8 Crp60,0.5,20.1
SPOAL2 0.500
SPOAL8 0.500
SPOFFS2 0 Hz
SPOFFS8 0 Hz
======== CHANNEL f2 ========
CPDPRG2 waltz64
NUC2 1H
PCPD2 80.00 usec
PL2 1.00 dB
PL12 18.64 dB
SFO2 600.1830000 MHz
F1 - Acquisition parameters
TD 256
SFO1 150.932 MHz
FIDRES 93.450958 Hz
SW 158.505 ppm
FnMODE States-TPPI
F2 - Processing parameters
SI 262144
SF 150.9154523 MHz
WDW EM
SSB 0
LB 10.00 Hz
GB 0
PC 2.00
HO
O
CO2H
HO
OH
OH
O
O
H
N
O
F
NH
6.28
200 190 180 170 160 150 140 130 120 110 100 90 80 70 60 50 40 30 20 ppm


H3',7'
H13"
H12"
H11"
H3",7"
H4',6'
H4
H6
H3
H2&7
H5a
H5b
ppm
C5
C7
C2
C3
C4
C6
C3"&7"
C4',6'
C4",6"
C11",13"
C5'
C3',7',9",12"
C14"
C5"
C10"
7.5
7.0
6.5
6.0
5.5
5.0
4.5
4.0
3.5
3.0
2.5
2.0
ppm
40
50
60
70
80
90
100
110
120
130
140
150
HO
O
HO
OH
CO2H
F
NH
N
H
6.28


OH4″,6″
OH5′
OH10″
H1
NH
H3′,7′
H12″
H13″
H11″
H3″,7″
H4′,6′
H4
H6
H3
H2&7
H5
ppm
C5
C7
C2
C3
C4
C6
C3″&7″
C4″,6″
C4′,6′
C11″,13″–C5′
C3′,7′,9″,12″
C14″
C5″
C10″
C2′
C2″
C1″ C1′
C15″
C8″
6.28
11
10
9
8
7
6
5
4
3
2
1
ppm
20
40
60
80
100
120
140
160
180
200


OH4″,6″
OH5′
OH10″
H1
NH
H3′,7′
H12″
H13″
H11″
H3″,7″
H4′,6′
H4
H6
H3
H2&7
H5
ppm
6.28
11
10
9
8
7
6
5
4
3
2
1
ppm


8.00
7.99
7.69
7.67
7.52
7.50
7.34
7.33
7.32
7.12
7.10
7.02
6.84
6.82
5.50
5.49
5.48
5.27
5.26
5.20
5.19
5.19
4.41
3.69
3.67
3.65
3.57
3.53
3.41
3.41
3.39
3.37
2.56
2.53
2.51
1.95
1.94
1.94
1.94
1.93
Current Data Parameters
NAME arp786a_FN3S2A
EXPNO 1
PROCNO 4
F2 - Acquisition Parameters
Date_ 20130730
Time 14.35
INSTRUM spect
PROBHD 5 mm CPTXI 1H-
PULPROG zg30
TD 32768
SOLVENT CD3CN
NS 124
DS 0
SWH 6887.052 Hz
FIDRES 0.210176 Hz
AQ 2.3790069 sec
RG 12.7
DW 72.600 usec
DE 6.00 usec
TE 298.0 K
D1 1.00000000 sec
TD0 1
======== CHANNEL f1 ========
NUC1 1H
P1 7.90 usec
PL1 1.00 dB
SFO1 600.1837655 MHz
F1 - Acquisition parameters
TD 256
SFO1 150.9229 MHz
FIDRES 93.450958 Hz
SW 158.514 ppm
FnMODE States-TPPI
F2 - Processing parameters
SI 65536
HO
O
CO2H
HO
OH
OH
O
O
H
N
O
F
NH
6.29
11.5
11.0
10.5
10.0
9.5
9.0
8.5
8.0
7.5
7.0
6.5
6.0
5.5
5.0
4.5
4.0
3.5
3.0
2.5
2.0
1.5
ppm
1.13
1.05
2.14
1.28
1.02
1.05
2.04
2.10
0.59
1.99
1.17
1.30
2.09
1.79
0.99
2.22



Current Data Parameters
NAME arp786a_FN3S2A
EXPNO 3
PROCNO 1

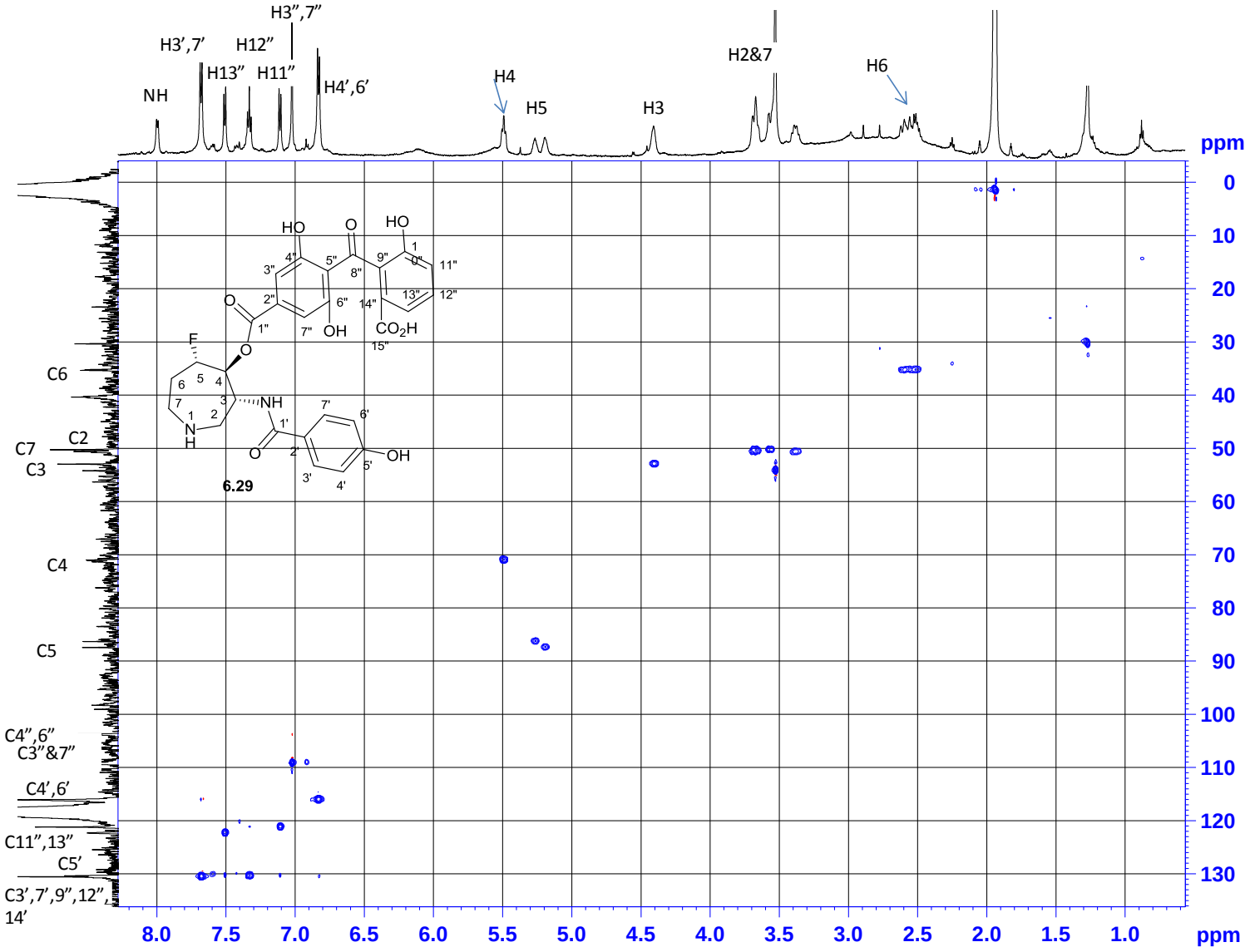
F2 - Acquisition Parameters
Date_ 20130730
Time 14.45
INSTRUM spect
PROBHD 5 mm CPTXI 1H-
PULPROG udeft.txt
TD 26082
SOLVENT CD3CN
NS 107446
DS 0
SWH 36231.883 Hz
FIDRES 1.389153 Hz
AQ 0.3599816 sec
RG 32768
DW 13.800 usec
DE 6.00 usec
TE 298.0 K
D1 1.50000000 sec
D11 0.03000000 sec
d12 0.00002000 sec
D20 0.10000000 sec
DELTA 1.47000003 sec
DELTA2 0.36300159 sec
TAU 0.00302000 sec
TD0 1

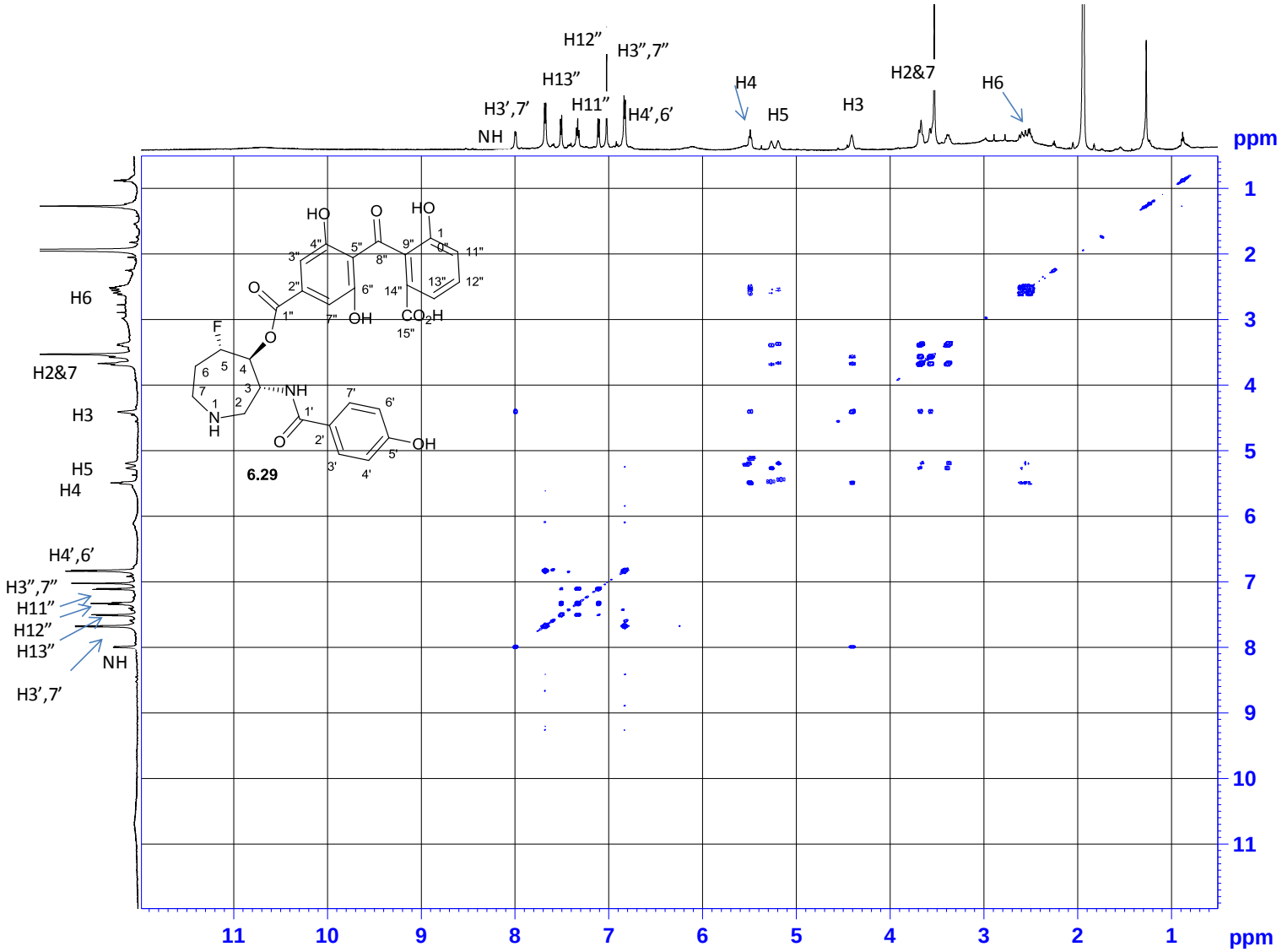
======== CHANNEL f1 ========
NUC1 13C
P1 11.47 usec
P12 2000.00 usec
P26 500.00 usec
PL1 -2.50 dB
SFO1 150.9319817 MHz
SP2 4.47 dB
SP8 4.75 dB
SPNAM2 Crp60comp.4
SPNAM8 Crp60,0.5,20.1
SPOAL2 0.500
SPOAL8 0.500
SPOFFS2 0 Hz
SPOFFS8 0 Hz

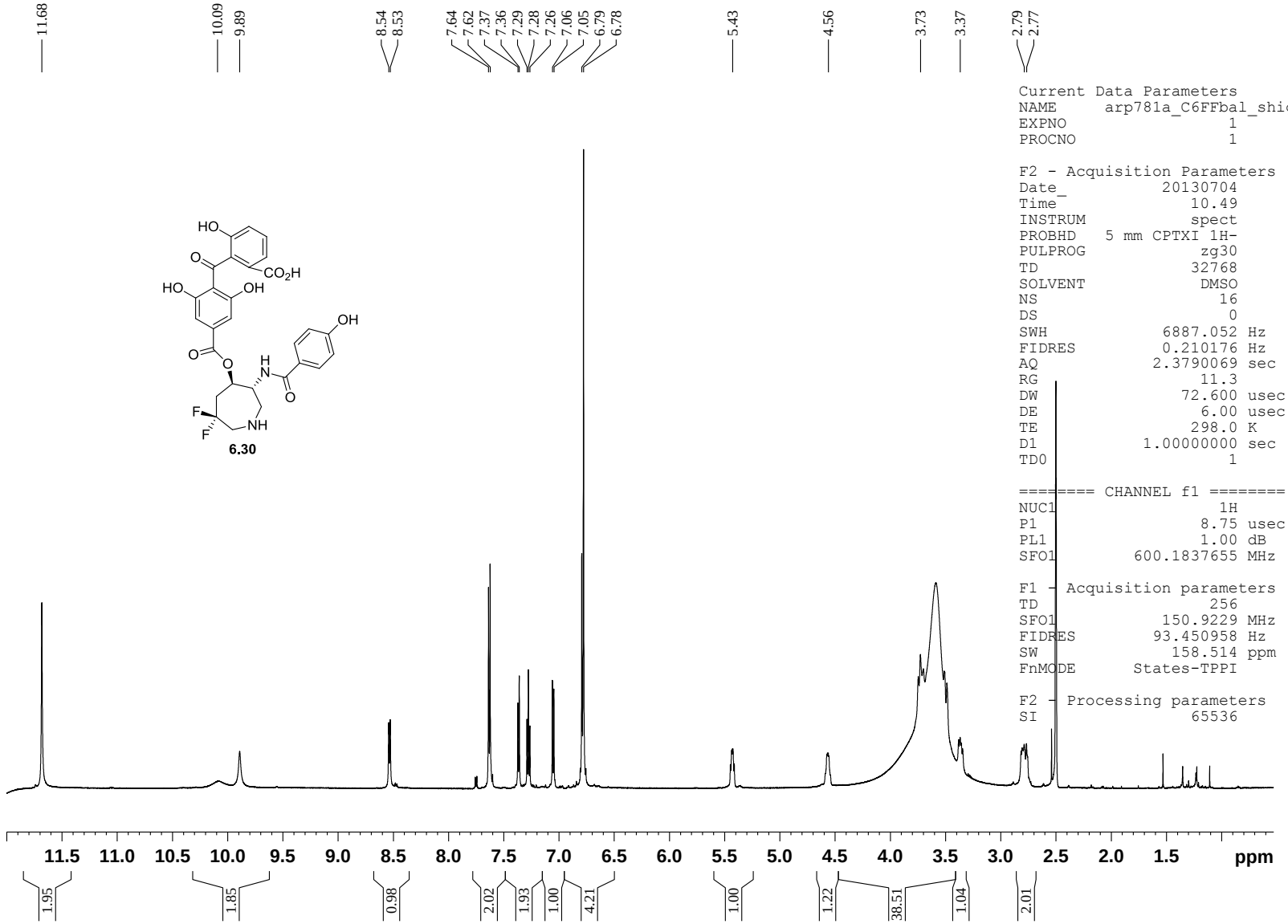
======== CHANNEL f2 ========
CPDPRG2 waltz64
NUC2 1H
PCPD2 70.00 usec
PL2 1.00 dB
PL12 17.07 dB
SFO2 600.1830000 MHz

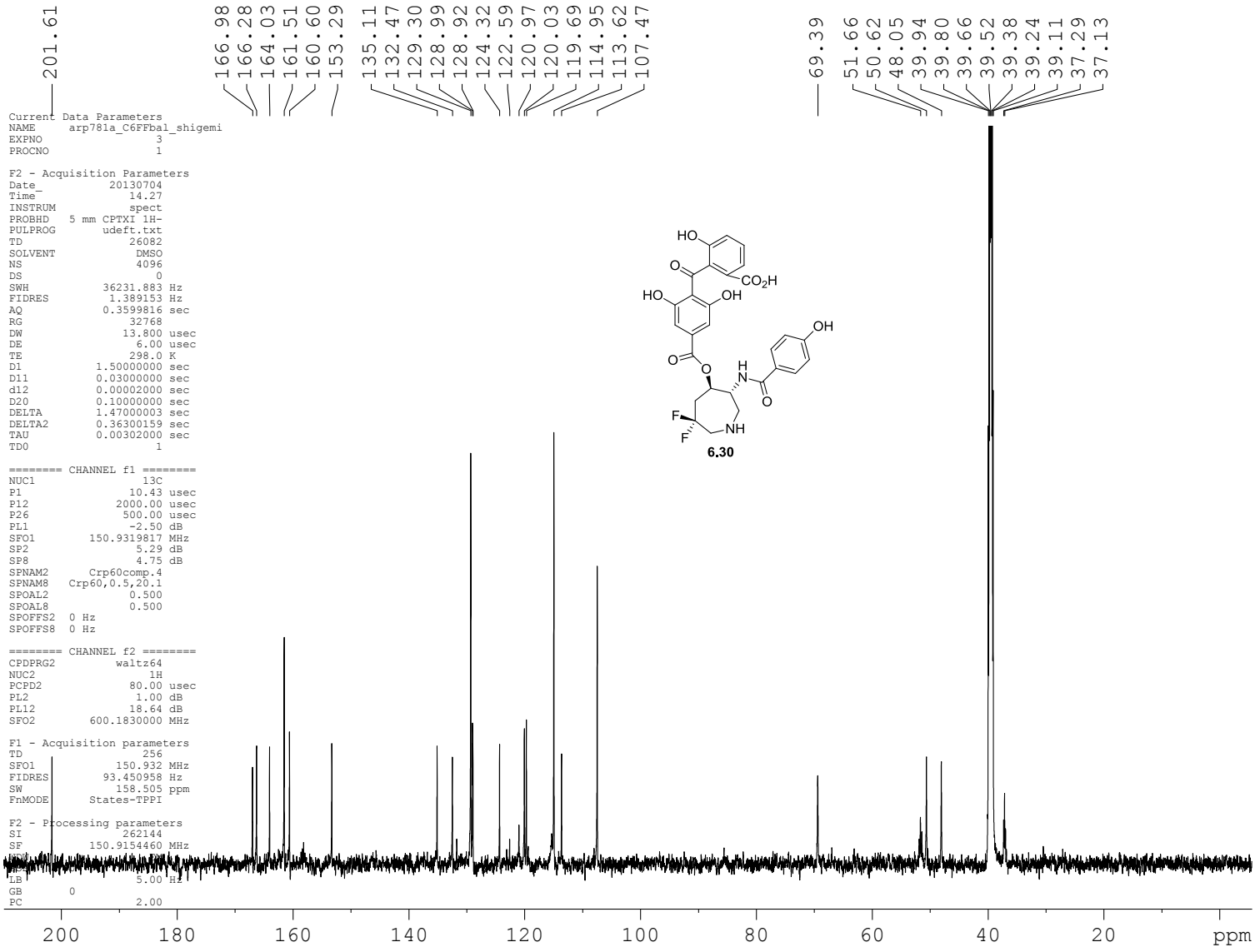
F1 - Acquisition parameters
TD 256
SFO1 150.932 MHz
FIDRES 93.450958 Hz
SW 158.505 ppm
FnMODE States-TPPI

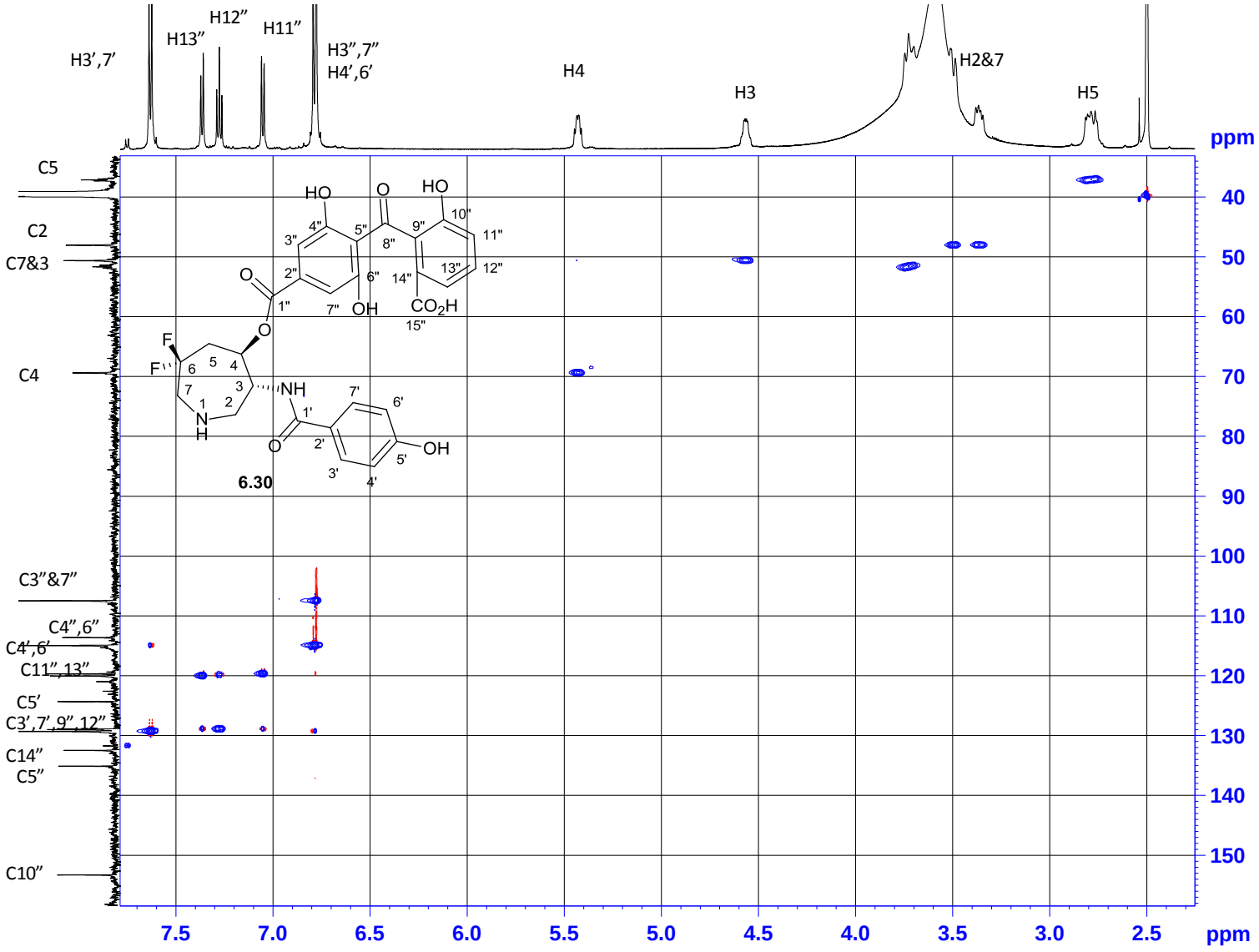
F2 - Processing parameters
SI 262144
SF 150.9319816 MHz
WDW EM
SSB 0
LB 1.00 Hz
GB 0
PC 2.00

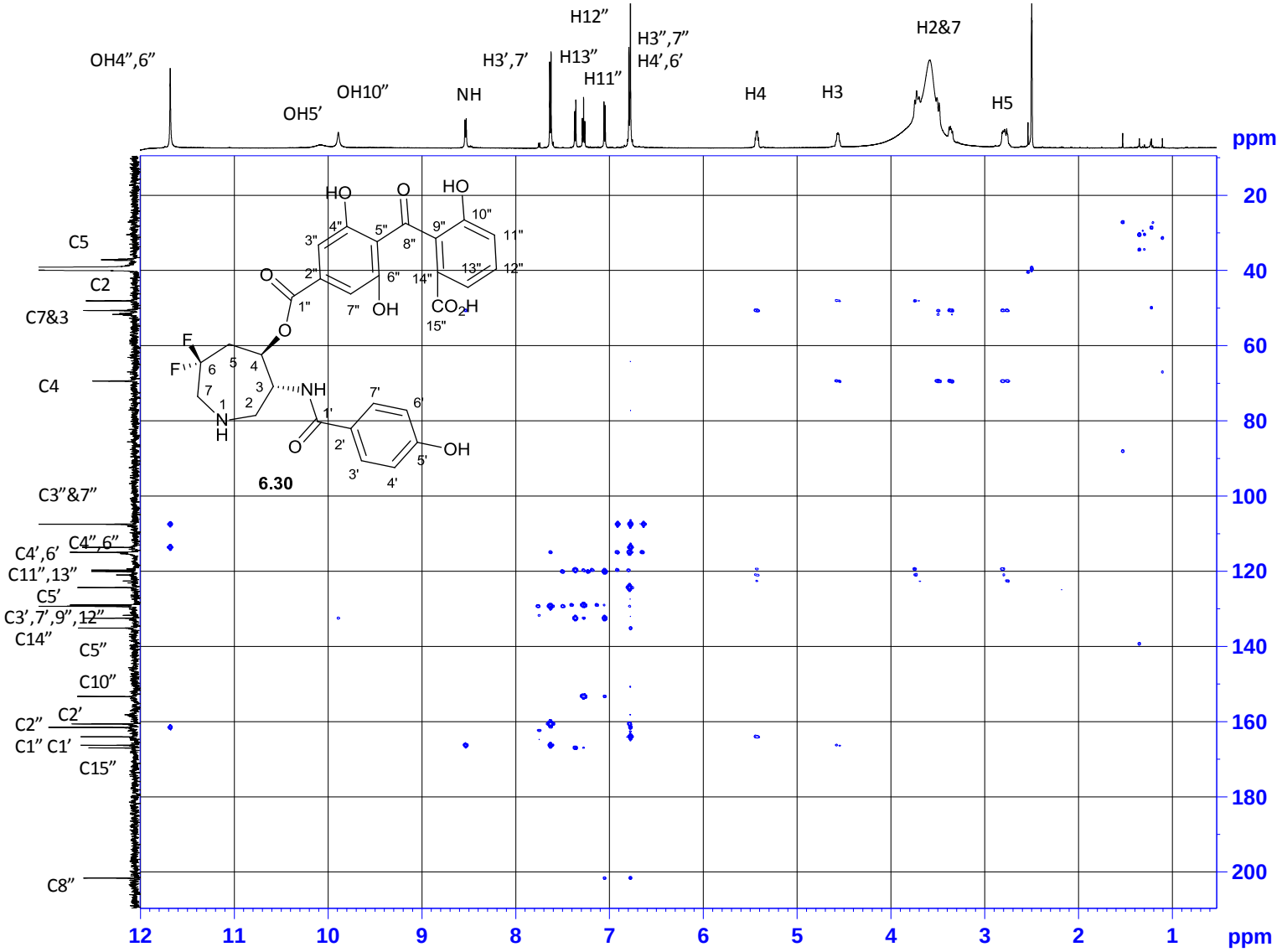

H3″,7″
H3′,7′
H12″
H13″
H11″
H4′,6′
NH
H4
H5
H3
H2&7
H6
ppm
0
10
20
30
40
50
60
70
80
90
100
110
120
130
C6
C2
C7
C3
C4
C5
C4″,6″
C3″&7″
C4′,6′
C11″,13″
C5′
C3′,7′,9″,12″,14′
6.29
8.0
7.5
7.0
6.5
6.0
5.5
5.0
4.5
4.0
3.5
3.0
2.5
2.0
1.5
1.0
ppm

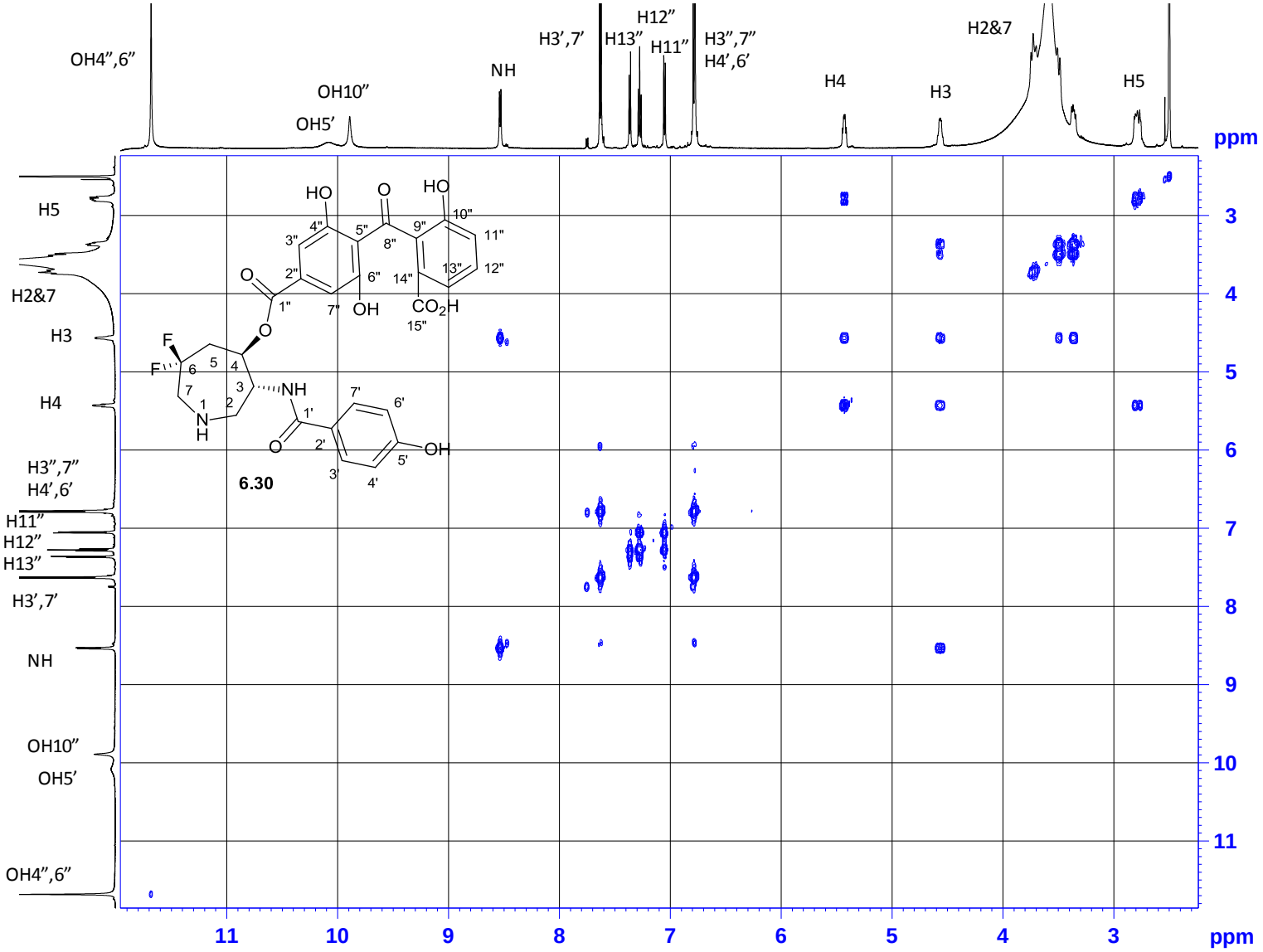

H12”
H3”,7”
H13”
H11”
H4’,6’
H3’,7’
NH
H4
H5
H3
H2&7
H6
ppm
HO
O
HO
F
NH
OH
6.29
H6
H2&7
H3
H5
H4
H4’,6’
H3”,7”
H11”
H12”
H13”
NH
H3’,7’
11
10
9
8
7
6
5
4
3
2
1
ppm

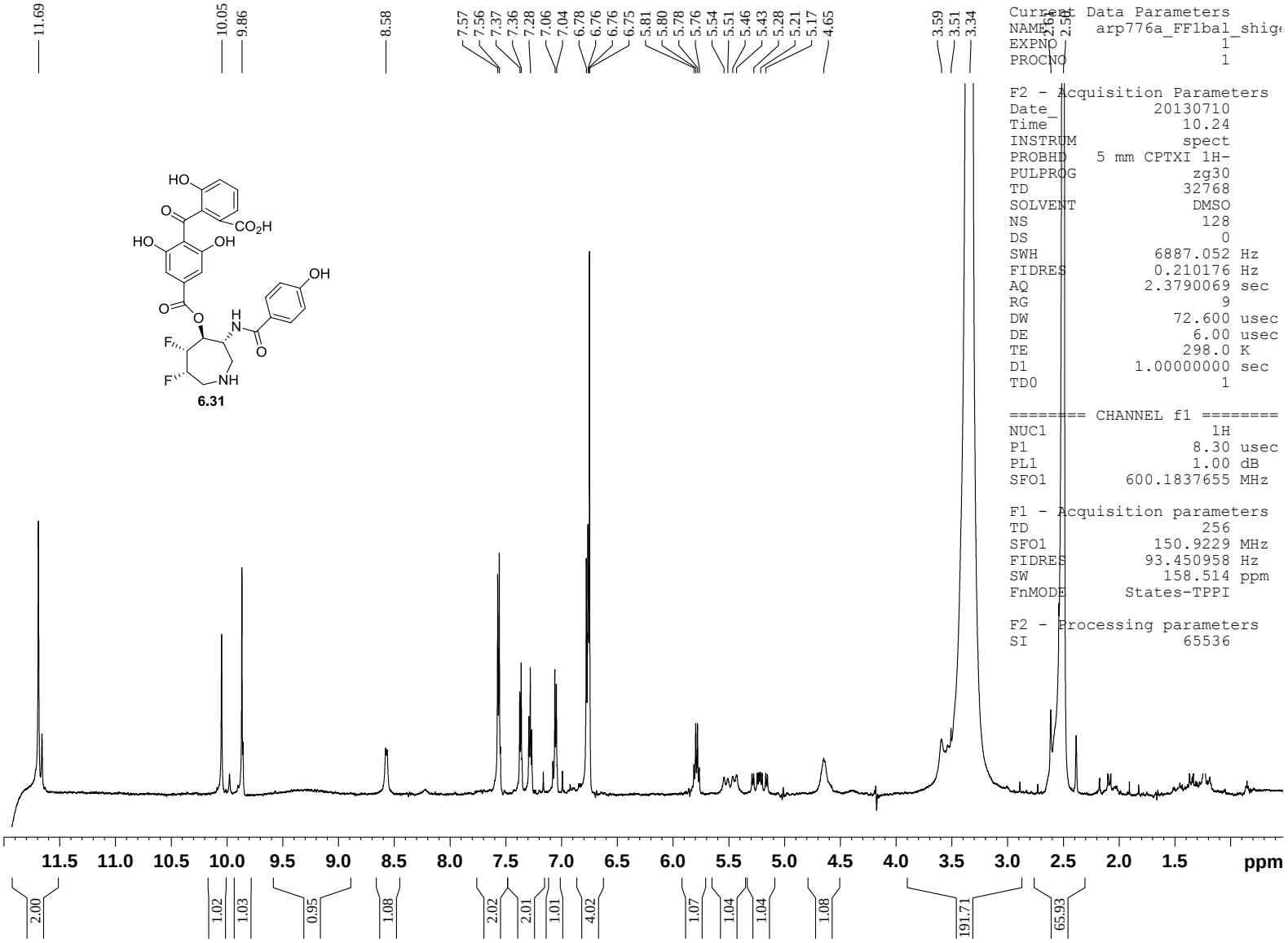

11.68
10.09
9.89
8.54
8.53
7.64
7.62
7.37
7.36
7.29
7.28
7.26
7.06
7.05
6.79
6.78
5.43
4.56
3.73
3.37
2.79
2.77
HO
O
CO2H
HO
OH
OH
O
O
H
N
O
F
F
NH
6.30
Current Data Parameters
NAME arp781a_C6FFbal_shi
EXPNO 1
PROCNO 1
F2 - Acquisition Parameters
Date_ 20130704
Time 10.49
INSTRUM spect
PROBHD 5 mm CPTXI 1H-
PULPROG zg30
TD 32768
SOLVENT DMSO
NS 16
DS 0
SWH 6887.052 Hz
FIDRES 0.210176 Hz
AQ 2.3790069 sec
RG 11.3
DW 72.600 usec
DE 6.00 usec
TE 298.0 K
D1 1.00000000 sec
TD0 1
======== CHANNEL f1 ========
NUC1 1H
P1 8.75 usec
PL1 1.00 dB
SFO1 600.1837655 MHz
F1 - Acquisition parameters
TD 256
SFO1 150.9229 MHz
FIDRES 93.450958 Hz
SW 158.514 ppm
FnMODE States-TPPI
F2 - Processing parameters
SI 65536
11.5
11.0
10.5
10.0
9.5
9.0
8.5
8.0
7.5
7.0
6.5
6.0
5.5
5.0
4.5
4.0
3.5
3.0
2.5
2.0
1.5
ppm
1.95
1.85
0.98
2.02
1.93
1.00
4.21
1.00
1.22
38.51
1.04
2.01

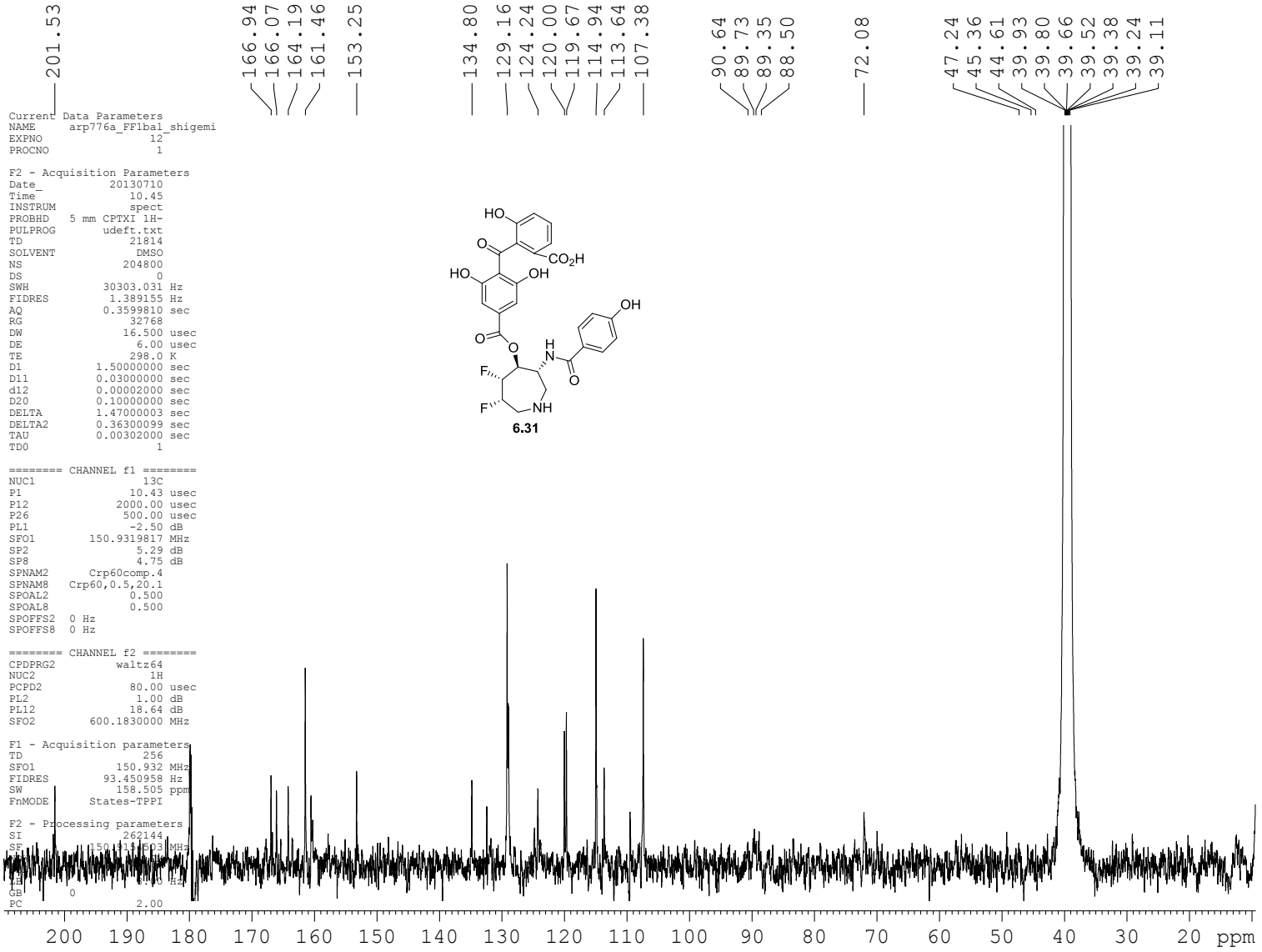

201.61
166.98
166.28
164.03
161.51
160.60
153.29
135.11
132.47
129.30
128.99
128.92
124.32
122.59
120.97
120.03
119.69
114.95
113.62
107.47
69.39
51.66
50.62
48.05
39.94
39.80
39.66
39.52
39.38
39.24
39.11
37.29
37.13
Current Data Parameters
NAME arp781a_C6FFbal_shigemi
EXPNO 3
PROCNO 1
F2 - Acquisition Parameters
Date_ 20130704
Time 14.27
INSTRUM spect
PROBHD 5 mm CPTXI 1H-
PULPROG udeft.txt
TD 26082
SOLVENT DMSO
NS 4096
DS 0
SWH 36231.883 Hz
FIDRES 1.389153 Hz
AQ 0.3599816 sec
RG 32768
DW 13.800 usec
DE 6.00 usec
TE 298.0 K
D1 1.50000000 sec
D11 0.03000000 sec
d12 0.00002000 sec
D20 0.10000000 sec
DELTA 1.47000003 sec
DELTA2 0.36300159 sec
TAU 0.00302000 sec
TD0 1
======== CHANNEL f1 ========
NUC1 13C
P1 10.43 usec
P12 2000.00 usec
P26 500.00 usec
PL1 -2.50 dB
SFO1 150.9319817 MHz
SP2 5.29 dB
SP8 4.75 dB
SPNAM2 Crp60comp.4
SPNAM8 Crp60,0.5,20.1
SPOAL2 0.500
SPOAL8 0.500
SPOFFS2 0 Hz
SPOFFS8 0 Hz
======== CHANNEL f2 ========
CPDPRG2 waltz64
NUC2 1H
PCPD2 80.00 usec
PL2 1.00 dB
PL12 18.64 dB
SFO2 600.1830000 MHz
F1 - Acquisition parameters
TD 256
SFO1 150.932 MHz
FIDRES 93.450958 Hz
SW 158.505 ppm
FnMODE States-TPPI
F2 - Processing parameters
SI 262144
SF 150.9154460 MHz
WDW EM
SSB 0
LB 5.00 Hz
GB 0
PC 2.00
HO
O
CO2H
HO
OH
OH
O
O
H
N
O
F
F
NH
6.30
200
180
160
140
120
100
80
60
40
20
ppm

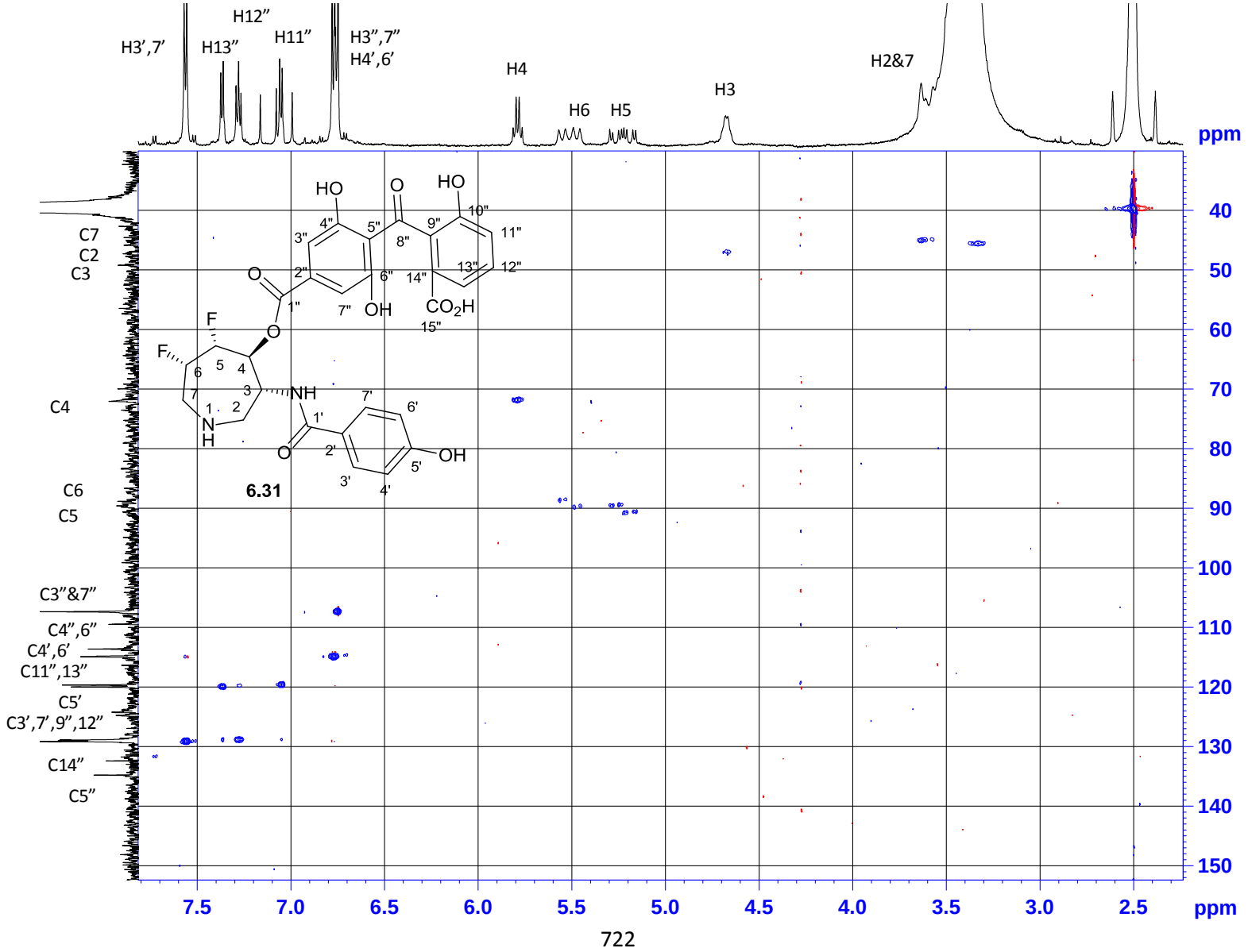

H3',7'
H13"
H12"
H11"
H3",7"
H4',6'
H4
H3
H2&7
H5
ppm
C5
C2
C7&3
C4
C3"&7"
C4",6"
C4',6'
C11",13"
C5'
C3',7',9",12"
C14"
C5"
C10"
6.30
7.5
7.0
6.5
6.0
5.5
5.0
4.5
4.0
3.5
3.0
2.5
ppm

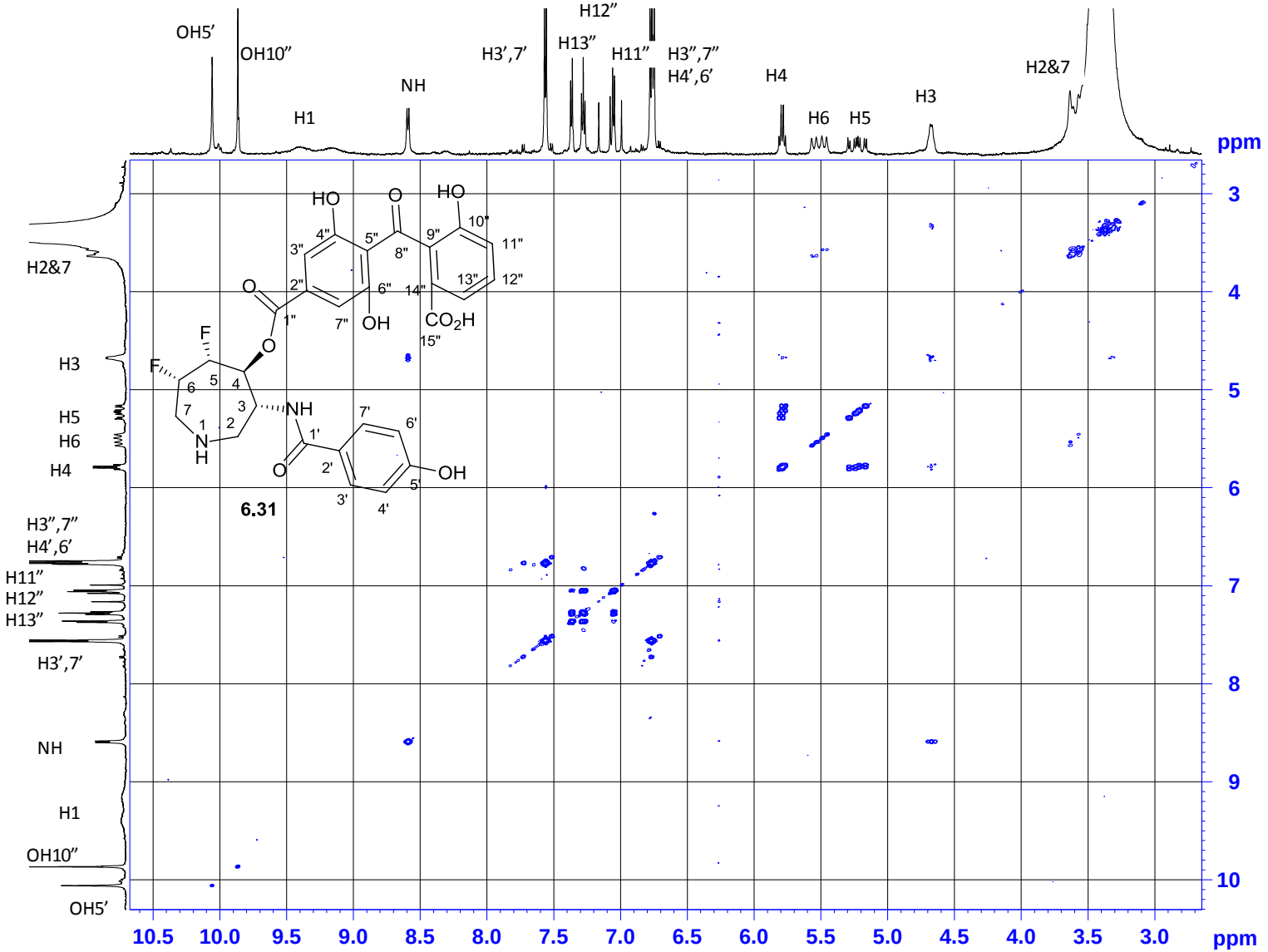

OH4”,6”
OH5’
OH10”
NH
H3’,7’
H12”
H13”
H11”
H3”,7”
H4’,6’
H4
H3
H2&7
H5
ppm
C5
C2
C7&3
C4
C3”&7”
C4”,6”
C4’,6’
C11”,13”
C5’
C3’,7’,9”,12”
C14”
C5”
C10”
C2’
C2”
C1” C1’
C15”
C8”
6.30
12
11
10
9
8
7
6
5
4
3
2
1
ppm

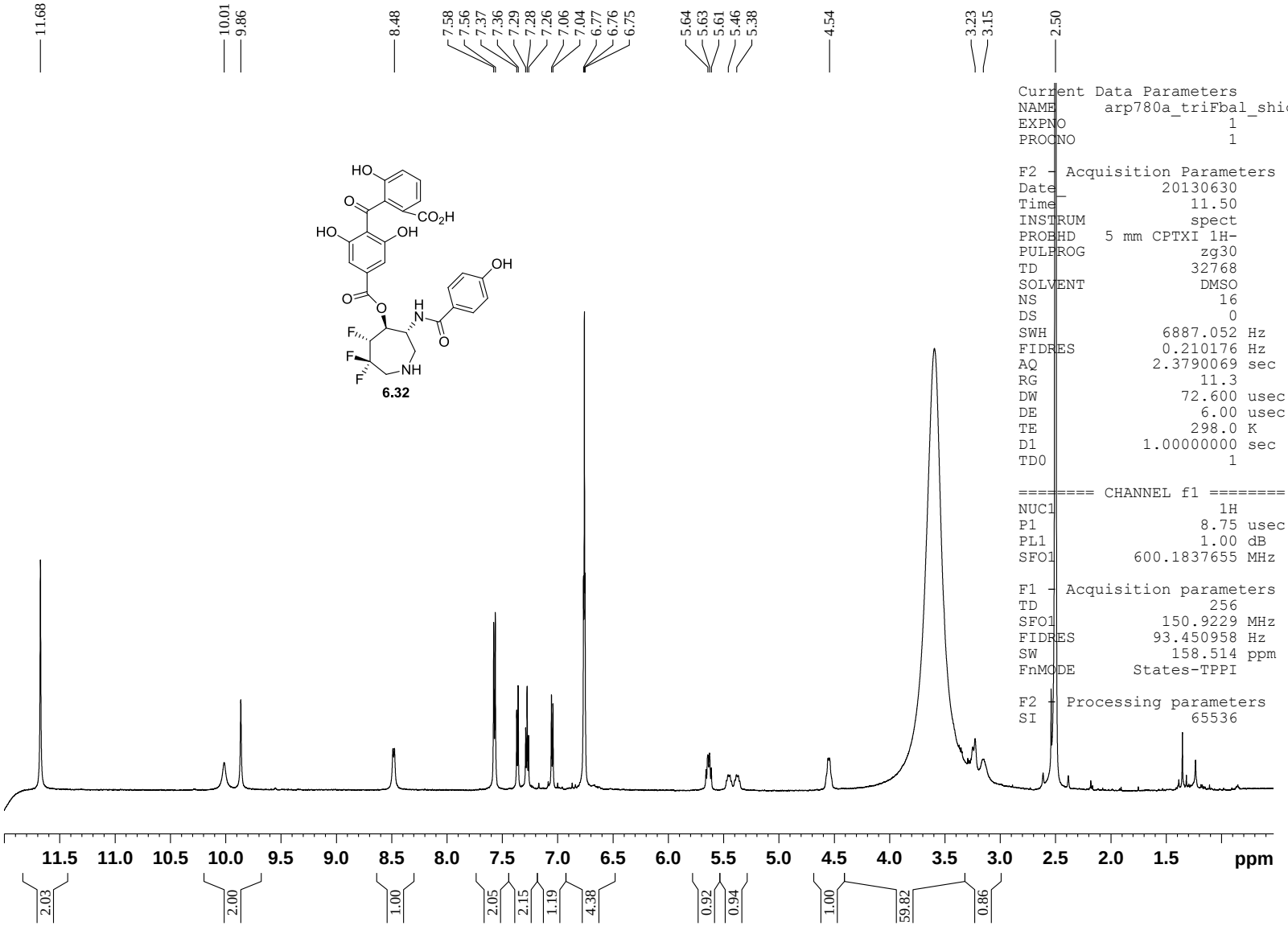

OH4”,6”
OH10”
OH5’
NH
H3’,7’
H12”
H13”
H11”
H3”,7”
H4’,6’
H4
H3
H2&7
H5
ppm
6.30
11
10
9
8
7
6
5
4
3
ppm

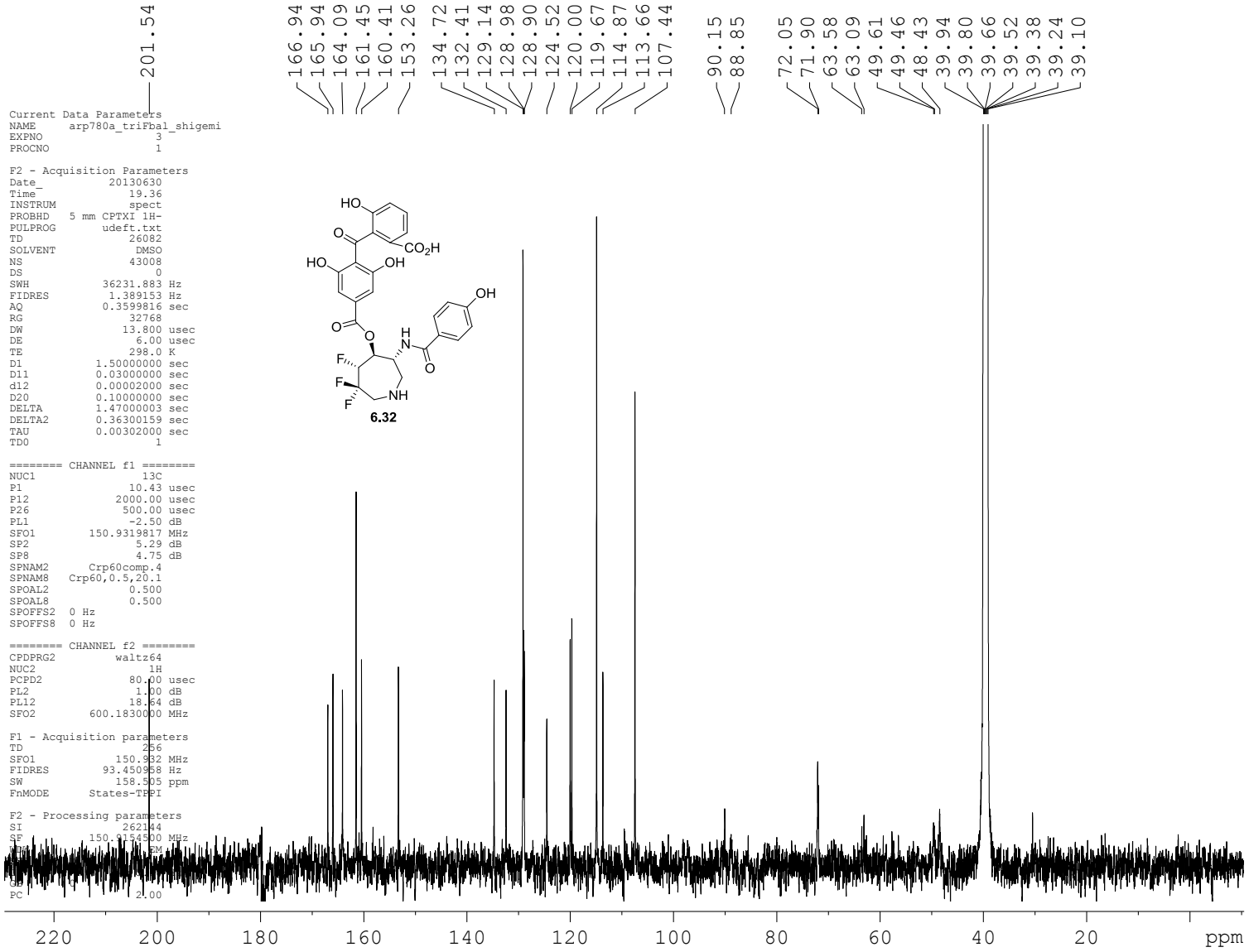

11.69
10.05
9.86
8.58
7.57
7.56
7.37
7.36
7.28
7.06
7.04
6.78
6.76
6.76
6.75
5.81
5.80
5.78
5.76
5.54
5.51
5.46
5.43
5.28
5.21
5.17
4.65
3.59
3.51
3.34
2.61
2.58
HO
O
CO2H
HO
OH
OH
O
O
H
N
O
F
F
NH
6.31
Current Data Parameters
NAME arp776a_FF1bal_shig
EXPNO 1
PROCNO 1
F2 - Acquisition Parameters
Date_ 20130710
Time 10.24
INSTRUM spect
PROBHD 5 mm CPTXI 1H-
PULPROG zg30
TD 32768
SOLVENT DMSO
NS 128
DS 0
SWH 6887.052 Hz
FIDRES 0.210176 Hz
AQ 2.3790069 sec
RG 9
DW 72.600 usec
DE 6.00 usec
TE 298.0 K
D1 1.00000000 sec
TD0 1
======== CHANNEL f1 ========
NUC1 1H
P1 8.30 usec
PL1 1.00 dB
SFO1 600.1837655 MHz
F1 - Acquisition parameters
TD 256
SFO1 150.9229 MHz
FIDRES 93.450958 Hz
SW 158.514 ppm
FnMODE States-TPPI
F2 - Processing parameters
SI 65536
11.5
11.0
10.5
10.0
9.5
9.0
8.5
8.0
7.5
7.0
6.5
6.0
5.5
5.0
4.5
4.0
3.5
3.0
2.5
2.0
1.5
ppm
2.00
1.02
1.03
0.95
1.08
2.02
2.01
1.01
4.02
1.07
1.04
1.04
1.08
191.71
65.93

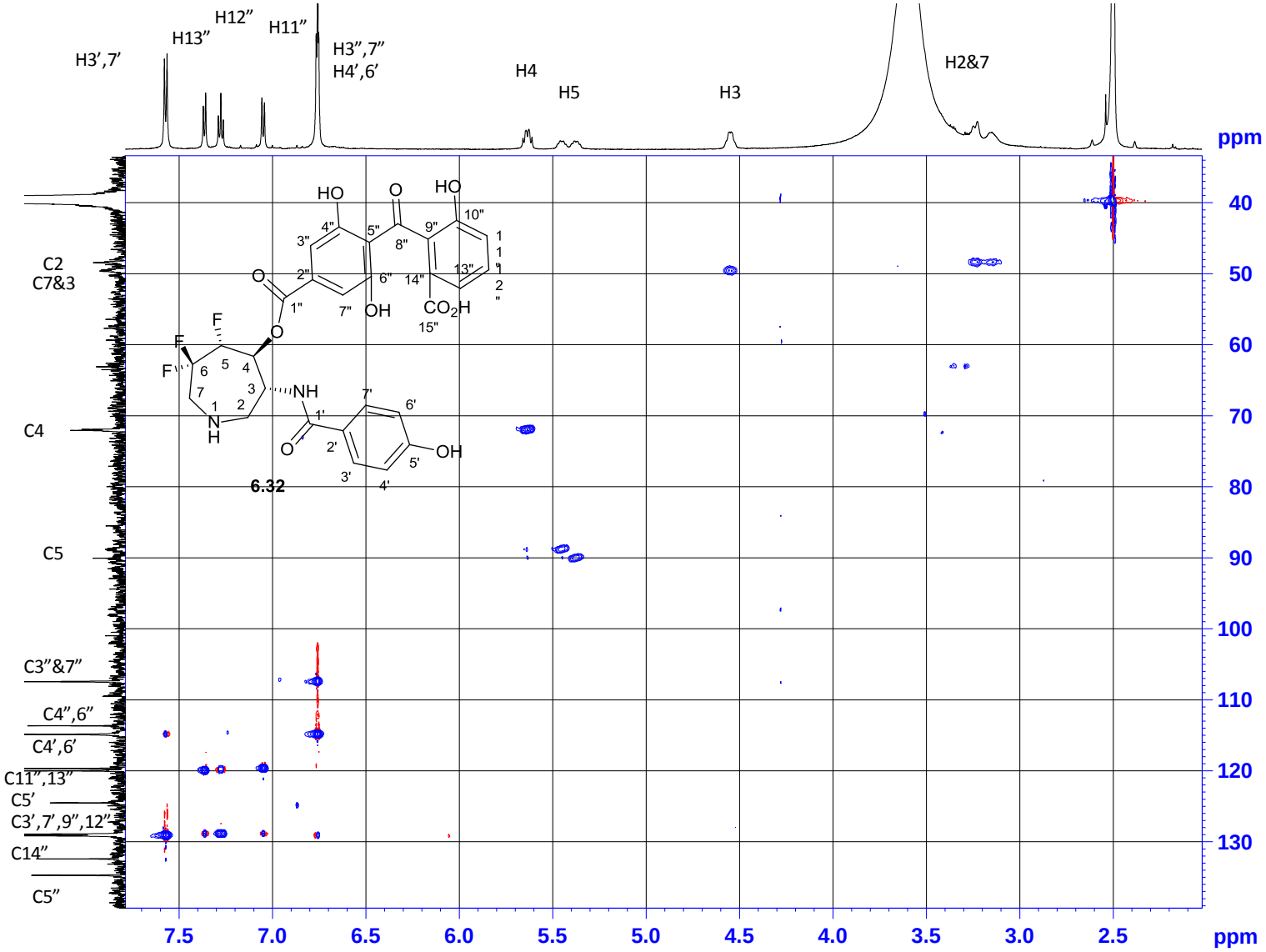

201.53
166.94
166.07
164.19
161.46
153.25
134.80
129.16
124.24
120.00
119.67
114.94
113.64
107.38
90.64
89.73
89.35
88.50
72.08
47.24
45.36
44.61
39.93
39.80
39.66
39.52
39.38
39.24
39.11
Current Data Parameters
NAME arp776a_FF1bal_shigemi
EXPNO 12
PROCNO 1
F2 - Acquisition Parameters
Date_ 20130710
Time 10.45
INSTRUM spect
PROBHD 5 mm CPTXI 1H-
PULPROG udeft.txt
TD 21814
SOLVENT DMSO
NS 204800
DS 0
SWH 30303.031 Hz
FIDRES 1.389155 Hz
AQ 0.3599810 sec
RG 32768
DW 16.500 usec
DE 6.00 usec
TE 298.0 K
D1 1.50000000 sec
D11 0.03000000 sec
d12 0.00002000 sec
D20 0.10000000 sec
DELTA 1.47000003 sec
DELTA2 0.36300099 sec
TAU 0.00302000 sec
TD0 1
======== CHANNEL f1 ========
NUC1 13C
P1 10.43 usec
P12 2000.00 usec
P26 500.00 usec
PL1 -2.50 dB
SFO1 150.9319817 MHz
SP2 5.29 dB
SP8 4.75 dB
SPNAM2 Crp60comp.4
SPNAM8 Crp60,0.5,20.1
SPOAL2 0.500
SPOAL8 0.500
SPOFFS2 0 Hz
SPOFFS8 0 Hz
======== CHANNEL f2 ========
CPDPRG2 waltz64
NUC2 1H
PCPD2 80.00 usec
PL2 1.00 dB
PL12 18.64 dB
SFO2 600.1830000 MHz
F1 - Acquisition parameters
TD 256
SFO1 150.932 MHz
FIDRES 93.450958 Hz
SW 158.505 ppm
FnMODE States-TPPI
F2 - Processing parameters
SI 262144
SF 150.1311605 MHz
WDW EM
SSB 0
LB 1.00 Hz
GB 0
PC 2.00
HO
O
CO2H
HO
OH
OH
O
O
H
N
O
F
F
NH
6.31
200 190 180 170 160 150 140 130 120 110 100 90 80 70 60 50 40 30 20 ppm

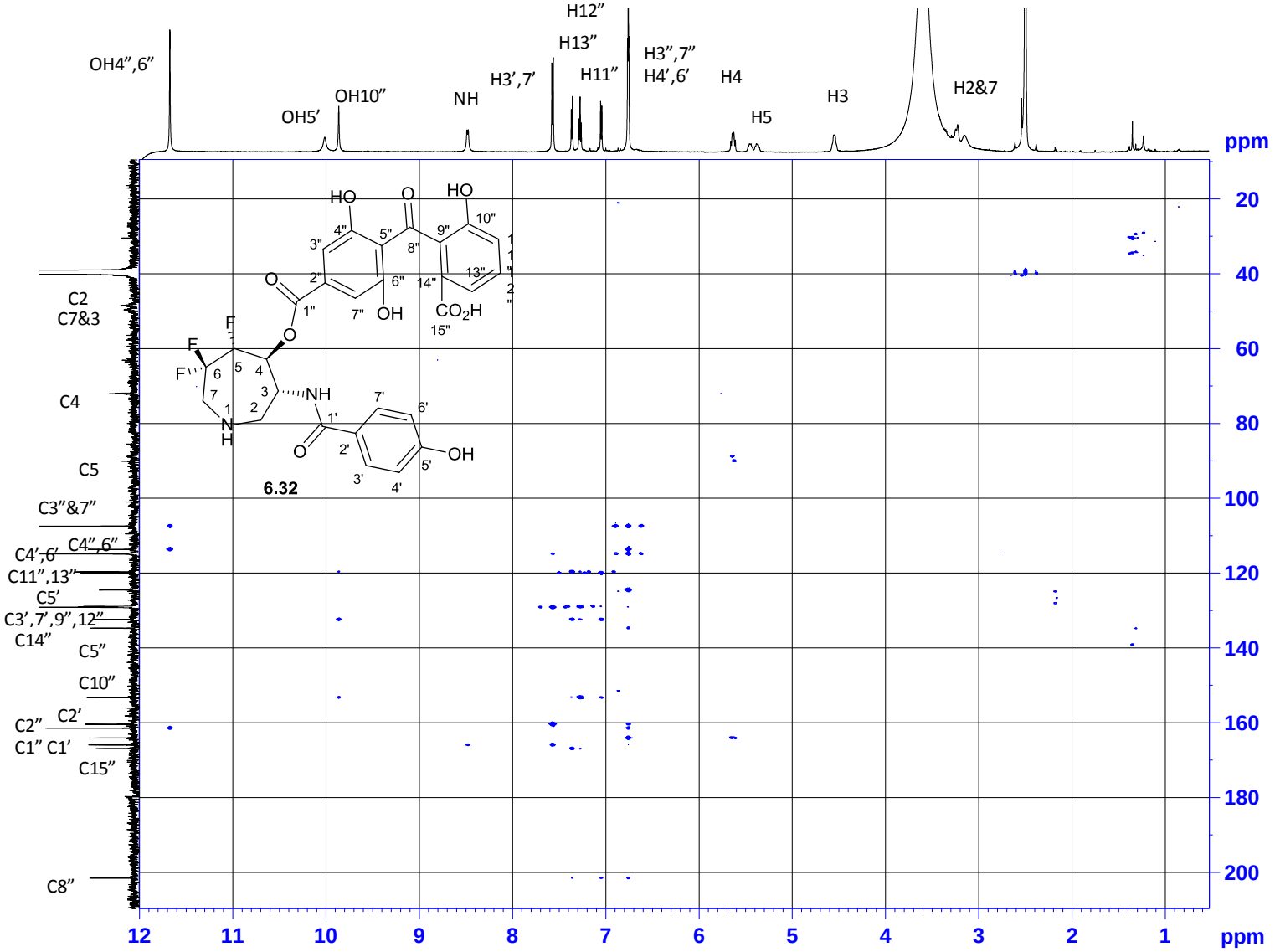

H3',7'
H13"
H12"
H11"
H3",7"
H4',6'
H4
H6
H5
H3
H2&7
ppm
C7
C2
C3
C4
C6
C5
C3"&7"
C4",6"
C4',6'
C11",13"
C5'
C3',7',9",12"
C14"
C5"
6.31
7.5
7.0
6.5
6.0
5.5
5.0
4.5
4.0
3.5
3.0
2.5
ppm

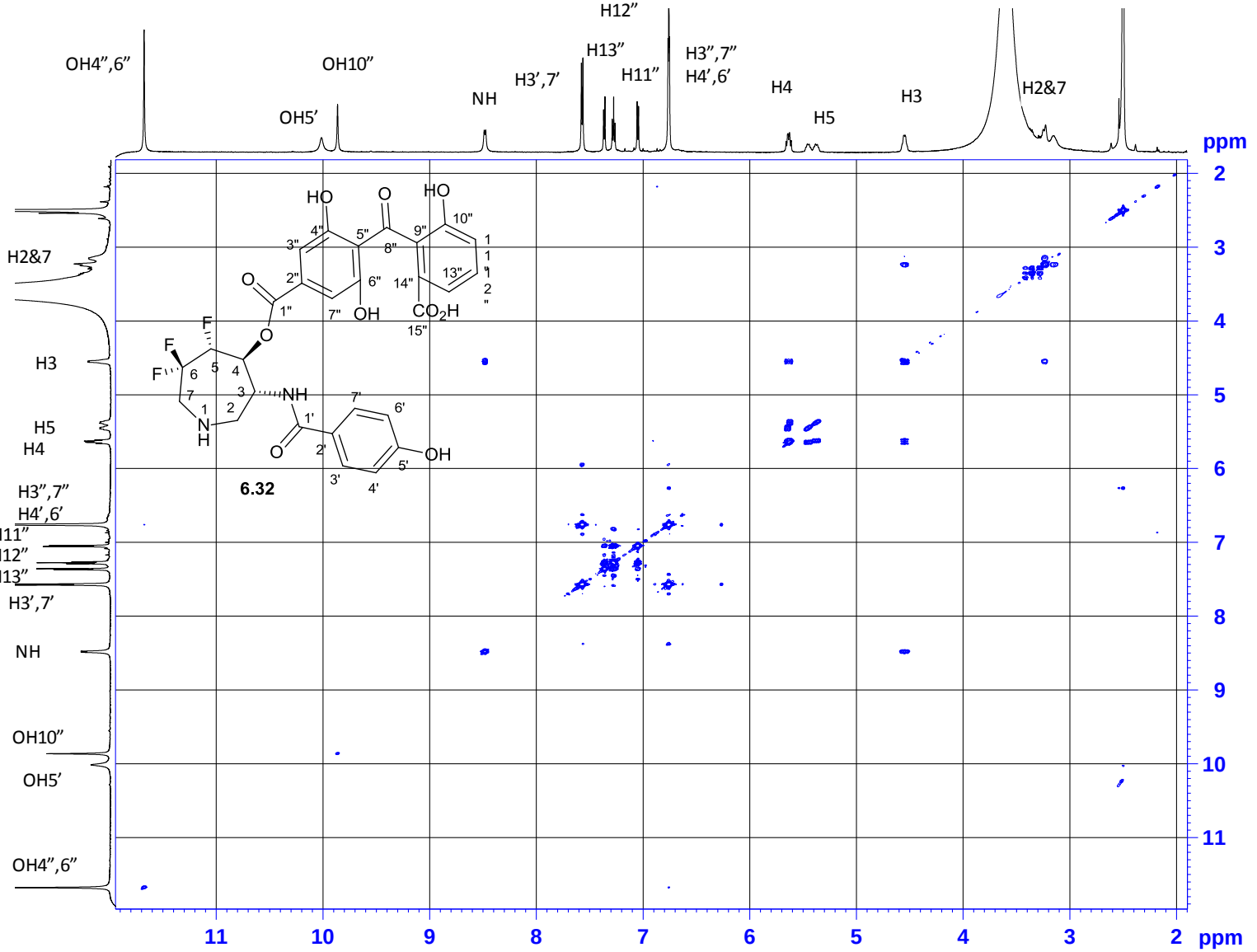

OH5′
OH10″
H1
NH
H3′,7′
H12″
H13″
H11″
H3″,7″
H4′,6′
H4
H6
H5
H3
H2&7
ppm
H2&7
H3
H5
H6
H4
H3″,7″
H4′,6′
H11″
H12″
H13″
H3′,7′
NH
H1
OH10″
OH5′
6.31
10.5
10.0
9.5
9.0
8.5
8.0
7.5
7.0
6.5
6.0
5.5
5.0
4.5
4.0
3.5
3.0
ppm


11.68
10.01
9.86
8.48
7.58
7.56
7.37
7.36
7.29
7.28
7.26
7.06
7.04
6.77
6.76
6.75
5.64
5.63
5.61
5.46
5.38
4.54
3.23
3.15
2.50
HO
O
CO2H
HO
OH
OH
O
O
H
N
O
F
F
F
NH
6.32
Current Data Parameters
NAME arp780a_triFbal_shi
EXPNO 1
PROCNO 1
F2 - Acquisition Parameters
Date_ 20130630
Time 11.50
INSTRUM spect
PROBHD 5 mm CPTXI 1H-
PULPROG zg30
TD 32768
SOLVENT DMSO
NS 16
DS 0
SWH 6887.052 Hz
FIDRES 0.210176 Hz
AQ 2.3790069 sec
RG 11.3
DW 72.600 usec
DE 6.00 usec
TE 298.0 K
D1 1.00000000 sec
TD0 1
======== CHANNEL f1 ========
NUC1 1H
P1 8.75 usec
PL1 1.00 dB
SFO1 600.1837655 MHz
F1 - Acquisition parameters
TD 256
SFO1 150.9229 MHz
FIDRES 93.450958 Hz
SW 158.514 ppm
FnMODE States-TPPI
F2 - Processing parameters
SI 65536
11.5
11.0
10.5
10.0
9.5
9.0
8.5
8.0
7.5
7.0
6.5
6.0
5.5
5.0
4.5
4.0
3.5
3.0
2.5
2.0
1.5
ppm
2.03
2.00
1.00
2.05
2.15
1.19
4.38
0.92
0.94
1.00
59.82
0.86


201.54
166.94
165.94
164.09
161.45
160.41
153.26
134.72
132.41
129.14
128.98
128.90
124.52
120.00
119.67
114.87
113.66
107.44
90.15
88.85
72.05
71.90
63.58
63.09
49.61
49.46
48.43
39.94
39.80
39.66
39.52
39.38
39.24
39.10
Current Data Parameters
NAME arp780a_triFbal_shigemi
EXPNO 3
PROCNO 1
F2 - Acquisition Parameters
Date_ 20130630
Time 19.36
INSTRUM spect
PROBHD 5 mm CPTXI 1H-
PULPROG udeft.txt
TD 26082
SOLVENT DMSO
NS 43008
DS 0
SWH 36231.883 Hz
FIDRES 1.389153 Hz
AQ 0.3599816 sec
RG 32768
DW 13.800 usec
DE 6.00 usec
TE 298.0 K
D1 1.50000000 sec
D11 0.03000000 sec
d12 0.00002000 sec
D20 0.10000000 sec
DELTA 1.47000003 sec
DELTA2 0.36300159 sec
TAU 0.00302000 sec
TD0 1
======== CHANNEL f1 ========
NUC1 13C
P1 10.43 usec
P12 2000.00 usec
P26 500.00 usec
PL1 -2.50 dB
SFO1 150.9319817 MHz
SP2 5.29 dB
SP8 4.75 dB
SPNAM2 Crp60comp.4
SPNAM8 Crp60,0.5,20.1
SPOAL2 0.500
SPOAL8 0.500
SPOFFS2 0 Hz
SPOFFS8 0 Hz
======== CHANNEL f2 ========
CPDPRG2 waltz64
NUC2 1H
PCPD2 80.00 usec
PL2 1.00 dB
PL12 18.64 dB
SFO2 600.1830000 MHz
F1 - Acquisition parameters
TD 256
SFO1 150.932 MHz
FIDRES 93.450958 Hz
SW 158.505 ppm
FnMODE States-TPPI
F2 - Processing parameters
SI 262144
SF 150.9154500 MHz
WDW EM
GB
PC 2.00
HO
O
CO2H
HO
OH
OH
O
O
H
N
O
F
F
F
NH
6.32
220
200
180
160
140
120
100
80
60
40
20
ppm


H3',7'
H13"
H12"
H11"
H3",7"
H4',6'
H4
H5
H3
H2&7
ppm
C2
C7&3
C4
C5
C3"&7"
C4",6"
C4',6'
C11",13"
C5'
C3',7',9",12"
C14"
C5"
6.32
7.5
7.0
6.5
6.0
5.5
5.0
4.5
4.0
3.5
3.0
2.5
ppm


OH4″,6″
OH5′
OH10″
NH
H3′,7′
H12″
H13″
H11″
H3″,7″
H4′,6′
H4
H5
H3
H2&7
ppm
C2
C7&3
C4
C5
C3″&7″
C4″,6″
C4′,6′
C11″,13″
C5′
C3′,7′,9″,12″
C14″
C5″
C10″
C2′
C2″
C1″ C1′
C15″
C8″
6.32
12
11
10
9
8
7
6
5
4
3
2
1
ppm


OH4”,6”
OH10”
OH5’
NH
H3’,7’
H12”
H13”
H11”
H3”,7”
H4’,6’
H4
H5
H3
H2&7
ppm
6.32
11
10
9
8
7
6
5
4
3
2
ppm

Binding assays supporting information:

The nomenclature shown on the binding curves for the molecules tested can be correlated to the compound numbering in chapter 6 as follows:

ARP1 = (−)–balanol (**1.1**)

ARP2 = **6.27**

ARP3 = **6.28**

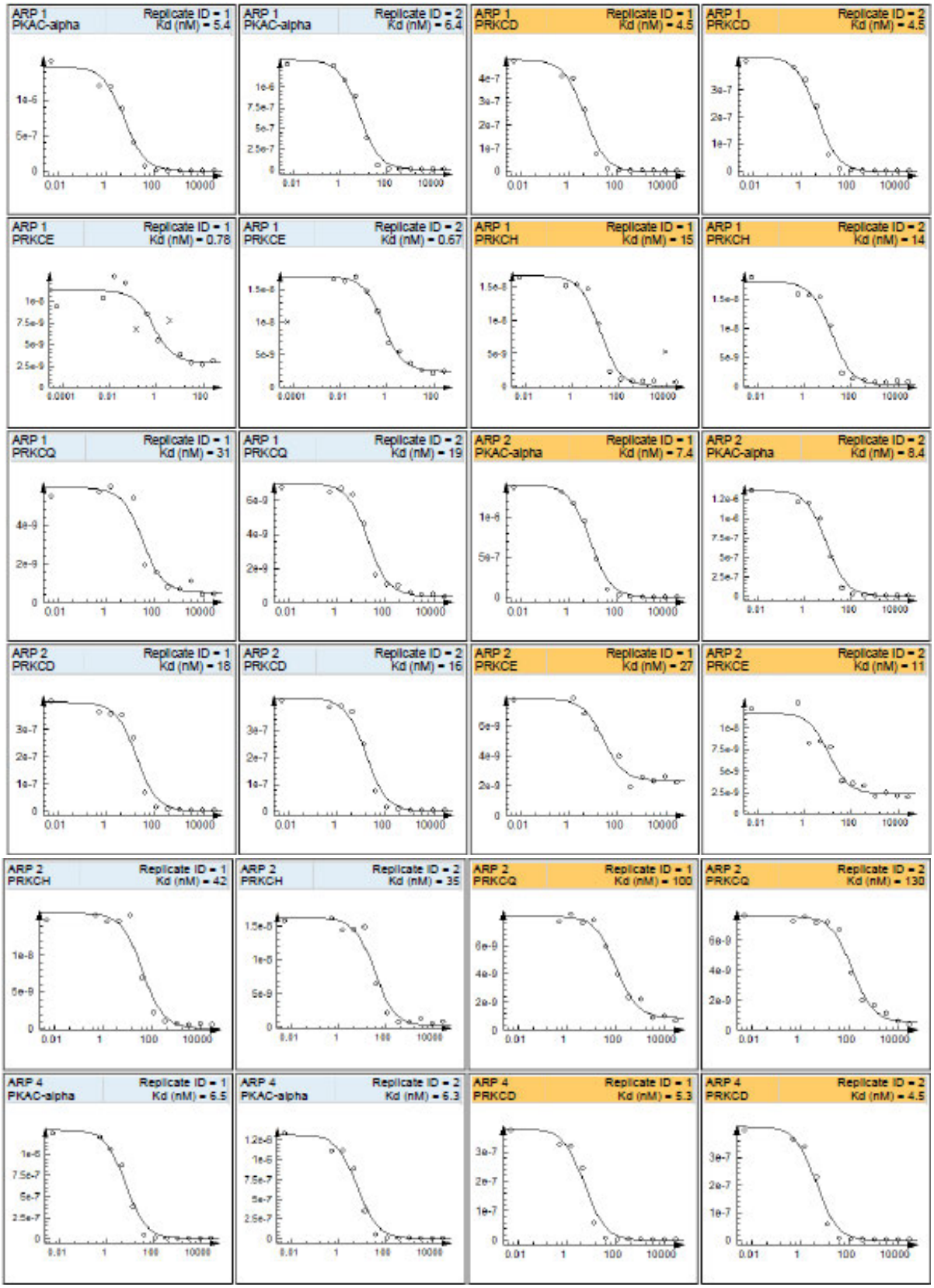
ARP4 = **6.29**

June13_ARP30 = **6.30**

June13_ARP28 = **6.31**

June13_ARP31 = **6.32**

Following are the binding curve images for (−)–balanol (**1.1**) and analogues **6.27**–**6.32**. The amount of kinase measured by qPCR (Signal; y-axis) was plotted against the corresponding compound concentration in nM in log10 scale (x-axis). Data points marked with an "x" were not used for K_d determination.


ARP 1
PKAC-alpha
Replicate ID = 1
Kd (nM) = 5.4
ARP 1
PKAC-alpha
Replicate ID = 2
Kd (nM) = 6.4
ARP 1
PRKCD
Replicate ID = 1
Kd (nM) = 4.5
ARP 1
PRKCD
Replicate ID = 2
Kd (nM) = 4.5
ARP 1
PRKCE
Replicate ID = 1
Kd (nM) = 0.78
ARP 1
PRKCE
Replicate ID = 2
Kd (nM) = 0.67
ARP 1
PRKCH
Replicate ID = 1
Kd (nM) = 15
ARP 1
PRKCH
Replicate ID = 2
Kd (nM) = 14
ARP 1
PRKCQ
Replicate ID = 1
Kd (nM) = 31
ARP 1
PRKCQ
Replicate ID = 2
Kd (nM) = 19
ARP 2
PKAC-alpha
Replicate ID = 1
Kd (nM) = 7.4
ARP 2
PKAC-alpha
Replicate ID = 2
Kd (nM) = 8.4
ARP 2
PRKCD
Replicate ID = 1
Kd (nM) = 18
ARP 2
PRKCD
Replicate ID = 2
Kd (nM) = 16
ARP 2
PRKCE
Replicate ID = 1
Kd (nM) = 27
ARP 2
PRKCE
Replicate ID = 2
Kd (nM) = 11
ARP 2
PRKCH
Replicate ID = 1
Kd (nM) = 42
ARP 2
PRKCH
Replicate ID = 2
Kd (nM) = 35
ARP 2
PRKCQ
Replicate ID = 1
Kd (nM) = 100
ARP 2
PRKCQ
Replicate ID = 2
Kd (nM) = 130
ARP 4
PKAC-alpha
Replicate ID = 1
Kd (nM) = 6.5
ARP 4
PKAC-alpha
Replicate ID = 2
Kd (nM) = 6.3
ARP 4
PRKCD
Replicate ID = 1
Kd (nM) = 5.3
ARP 4
PRKCD
Replicate ID = 2
Kd (nM) = 4.5

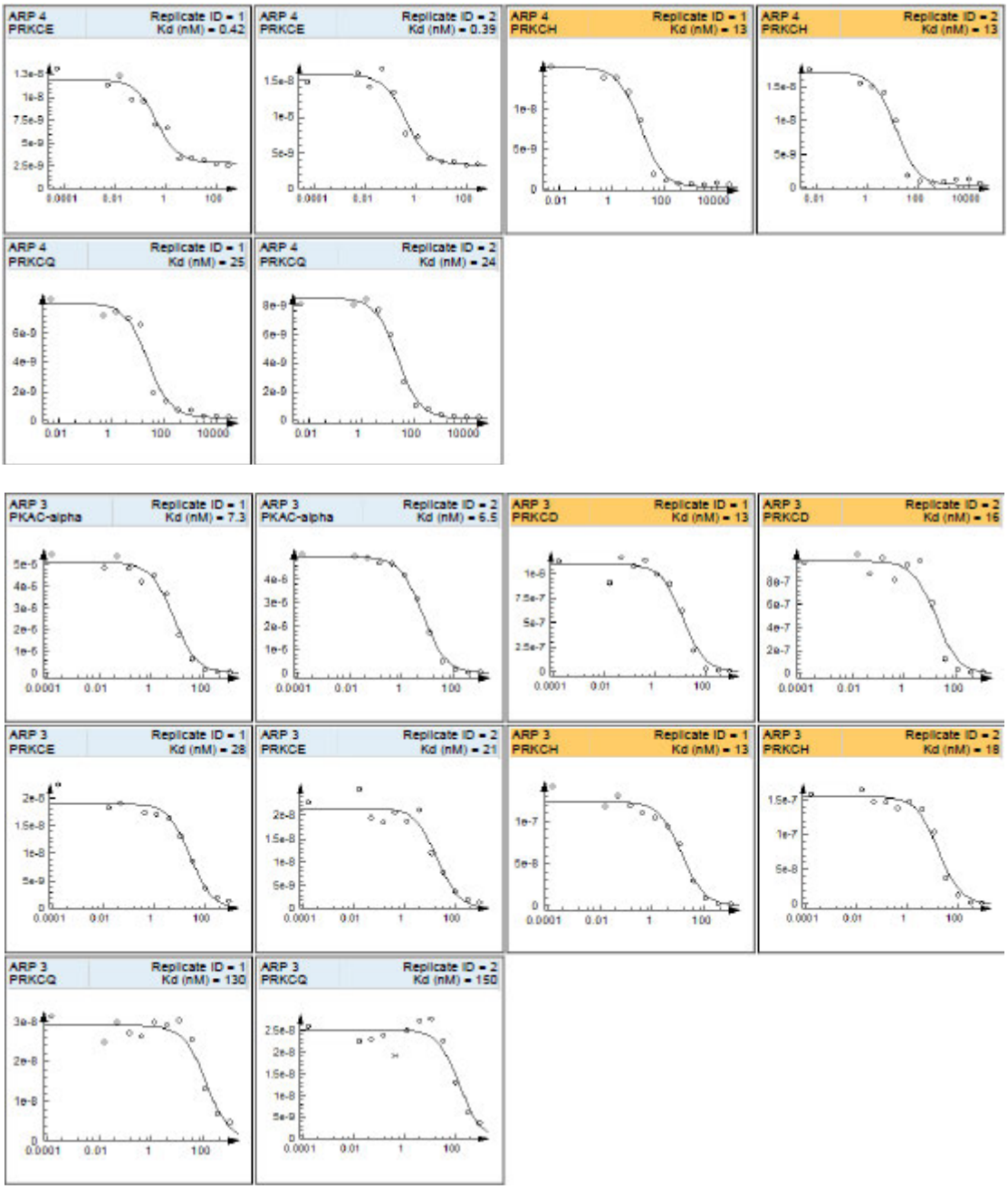
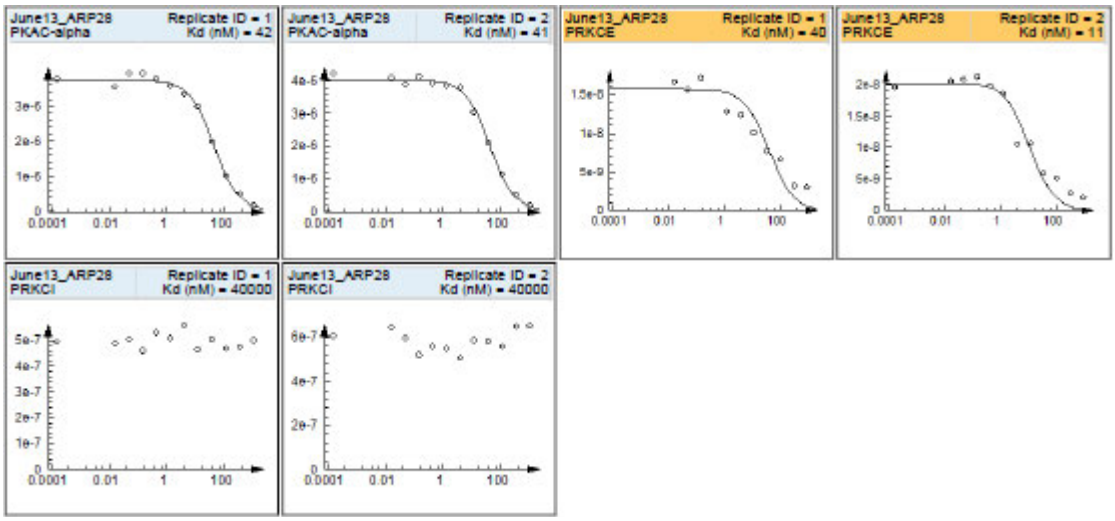
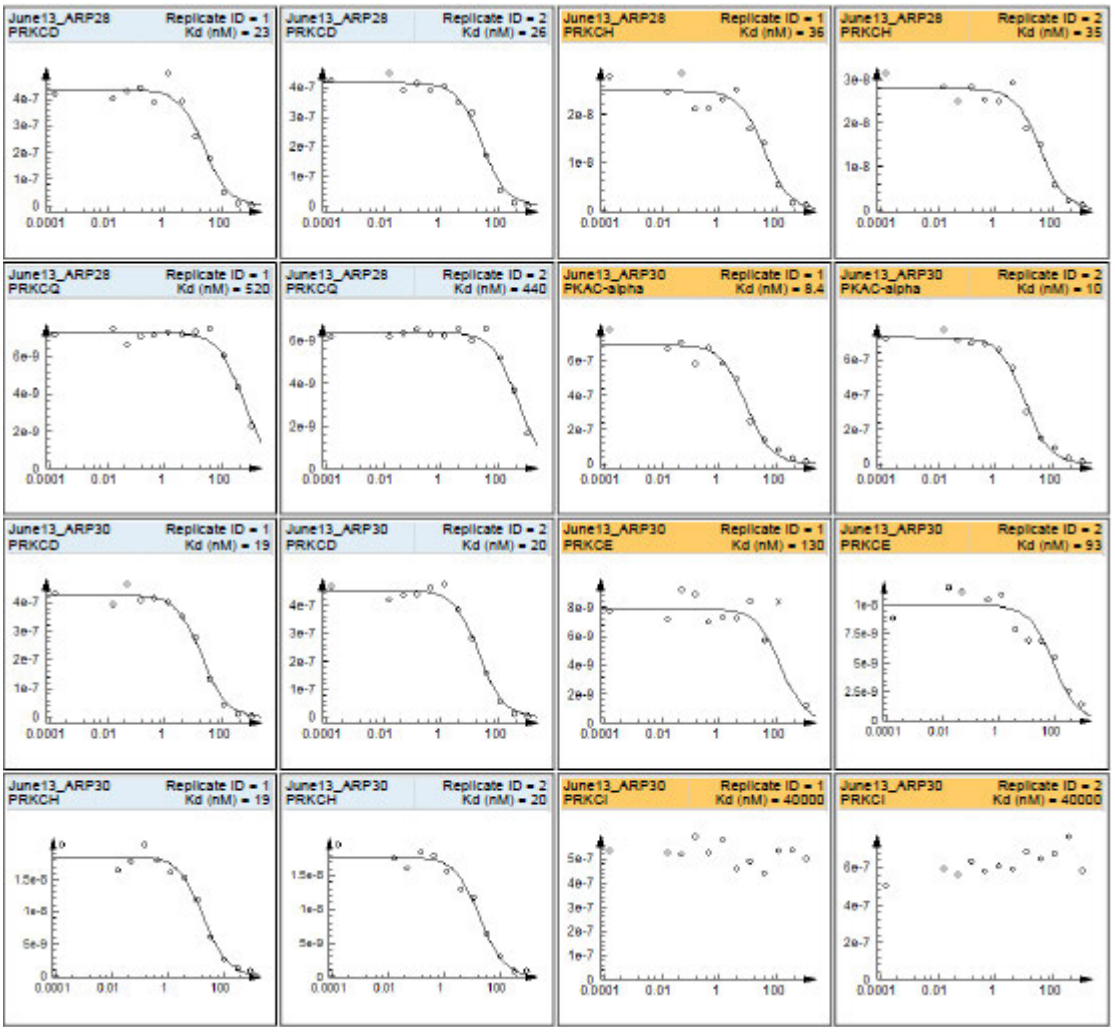


Figure E1: Binding curve images for balanol, **6.27**–**6.29**


June13_ARP28
PKAC-alpha
Replicate ID = 1
Kd (nM) = 42
June13_ARP28
PKAC-alpha
Replicate ID = 2
Kd (nM) = 41
June13_ARP28
PRKCE
Replicate ID = 1
Kd (nM) = 40
June13_ARP28
PRKCE
Replicate ID = 2
Kd (nM) = 11
June13_ARP28
PRKCI
Replicate ID = 1
Kd (nM) = 40000
June13_ARP28
PRKCI
Replicate ID = 2
Kd (nM) = 40000


June13_ARP28
PRKCD
Replicate ID = 1
Kd (nM) = 23
June13_ARP28
PRKCD
Replicate ID = 2
Kd (nM) = 26
June13_ARP28
PRKCH
Replicate ID = 1
Kd (nM) = 36
June13_ARP28
PRKCH
Replicate ID = 2
Kd (nM) = 35
June13_ARP28
PRKCQ
Replicate ID = 1
Kd (nM) = 520
June13_ARP28
PRKCQ
Replicate ID = 2
Kd (nM) = 440
June13_ARP30
PKAC-alpha
Replicate ID = 1
Kd (nM) = 8.4
June13_ARP30
PKAC-alpha
Replicate ID = 2
Kd (nM) = 10
June13_ARP30
PRKCD
Replicate ID = 1
Kd (nM) = 19
June13_ARP30
PRKCD
Replicate ID = 2
Kd (nM) = 20
June13_ARP30
PRKCE
Replicate ID = 1
Kd (nM) = 130
June13_ARP30
PRKCE
Replicate ID = 2
Kd (nM) = 93
June13_ARP30
PRKCH
Replicate ID = 1
Kd (nM) = 19
June13_ARP30
PRKCH
Replicate ID = 2
Kd (nM) = 20
June13_ARP30
PRKCI
Replicate ID = 1
Kd (nM) = 40000
June13_ARP30
PRKCI
Replicate ID = 2
Kd (nM) = 40000

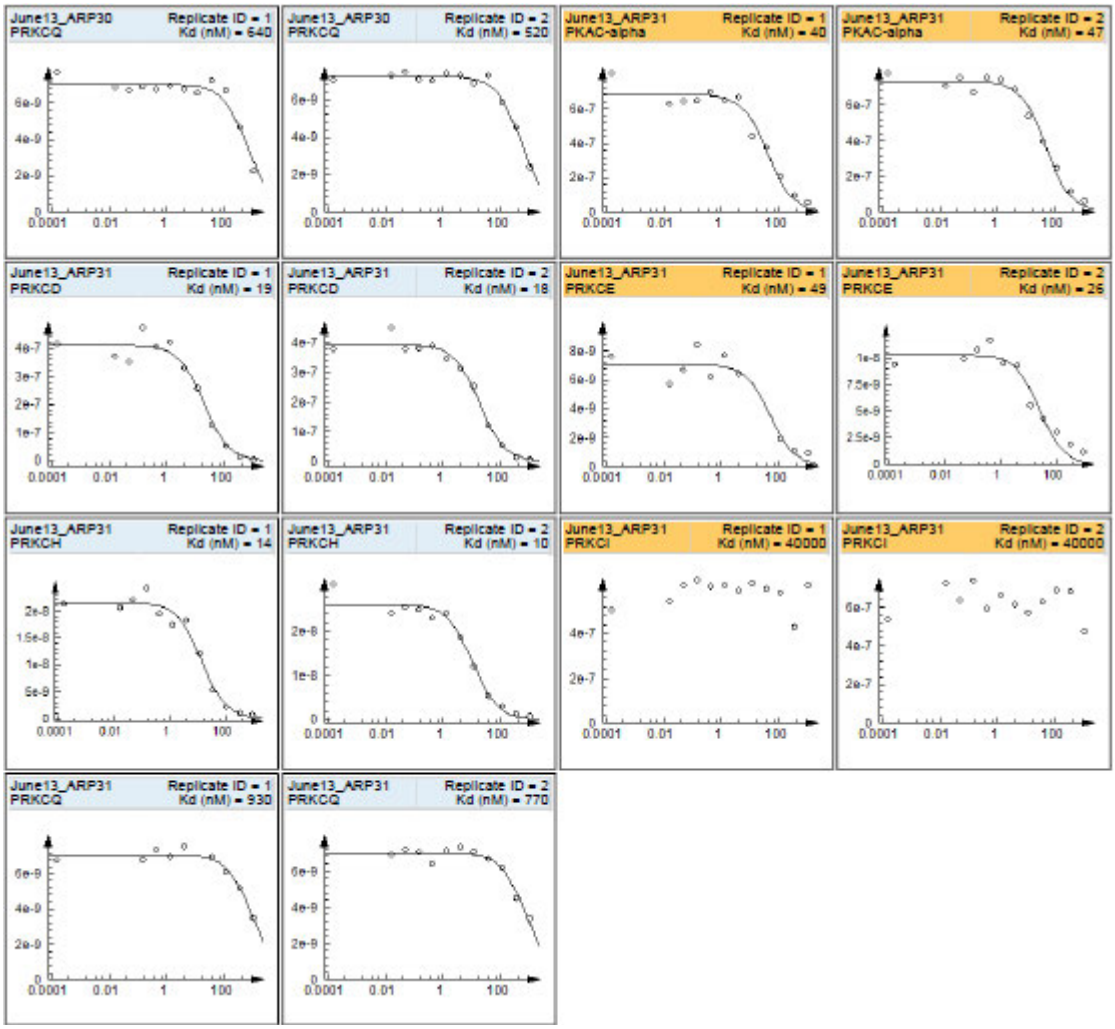


Figure E2: Binding curve images for **6.30**–**6.32**